frontiers | Research Topics

Inflammation and fibrosis in the gastrointestinal tract and liver: Mechanisms and targets

Edited by
Ralf Weiskirchen, Dario Sorrentino and Wolfgang Richard Stremmel

Published in
Frontiers in Pharmacology



FRONTIERS EBOOK COPYRIGHT STATEMENT

The copyright in the text of individual articles in this ebook is the property of their respective authors or their respective institutions or funders. The copyright in graphics and images within each article may be subject to copyright of other parties. In both cases this is subject to a license granted to Frontiers.

The compilation of articles constituting this ebook is the property of Frontiers.

Each article within this ebook, and the ebook itself, are published under the most recent version of the Creative Commons CC-BY licence. The version current at the date of publication of this ebook is CC-BY 4.0. If the CC-BY licence is updated, the licence granted by Frontiers is automatically updated to the new version.

When exercising any right under the CC-BY licence, Frontiers must be attributed as the original publisher of the article or ebook, as applicable.

Authors have the responsibility of ensuring that any graphics or other materials which are the property of others may be included in the CC-BY licence, but this should be checked before relying on the CC-BY licence to reproduce those materials. Any copyright notices relating to those materials must be complied with.

Copyright and source acknowledgement notices may not be removed and must be displayed in any copy, derivative work or partial copy which includes the elements in question.

All copyright, and all rights therein, are protected by national and international copyright laws. The above represents a summary only. For further information please read Frontiers' Conditions for Website Use and Copyright Statement, and the applicable CC-BY licence.

ISSN 1664-8714
ISBN 978-2-88971-626-5
DOI 10.3389/978-2-88971-626-5

About Frontiers

Frontiers is more than just an open access publisher of scholarly articles: it is a pioneering approach to the world of academia, radically improving the way scholarly research is managed. The grand vision of Frontiers is a world where all people have an equal opportunity to seek, share and generate knowledge. Frontiers provides immediate and permanent online open access to all its publications, but this alone is not enough to realize our grand goals.

Frontiers journal series

The Frontiers journal series is a multi-tier and interdisciplinary set of open-access, online journals, promising a paradigm shift from the current review, selection and dissemination processes in academic publishing. All Frontiers journals are driven by researchers for researchers; therefore, they constitute a service to the scholarly community. At the same time, the *Frontiers journal series* operates on a revolutionary invention, the tiered publishing system, initially addressing specific communities of scholars, and gradually climbing up to broader public understanding, thus serving the interests of the lay society, too.

Dedication to quality

Each Frontiers article is a landmark of the highest quality, thanks to genuinely collaborative interactions between authors and review editors, who include some of the world's best academicians. Research must be certified by peers before entering a stream of knowledge that may eventually reach the public - and shape society; therefore, Frontiers only applies the most rigorous and unbiased reviews. Frontiers revolutionizes research publishing by freely delivering the most outstanding research, evaluated with no bias from both the academic and social point of view. By applying the most advanced information technologies, Frontiers is catapulting scholarly publishing into a new generation.

What are Frontiers Research Topics?

Frontiers Research Topics are very popular trademarks of the *Frontiers journals series*: they are collections of at least ten articles, all centered on a particular subject. With their unique mix of varied contributions from Original Research to Review Articles, Frontiers Research Topics unify the most influential researchers, the latest key findings and historical advances in a hot research area.

Find out more on how to host your own Frontiers Research Topic or contribute to one as an author by contacting the Frontiers editorial office: frontiersin.org/about/contact

Inflammation and fibrosis in the gastrointestinal tract and liver: Mechanisms and targets

Topic editors

Ralf Weiskirchen — RWTH Aachen University, Germany

Dario Sorrentino — School of Medicine, Virginia Tech Carilion, United States

Wolfgang Richard Stremmel — Medical Center Baden-Baden, Germany

Citation

Weiskirchen, R., Sorrentino, D., Stremmel, W. R., eds. (2023). *Inflammation and fibrosis in the gastrointestinal tract and liver: Mechanisms and targets*. Lausanne: Frontiers Media SA. doi: 10.3389/978-2-88971-626-5

Table of contents

07 Editorial: Inflammation and Fibrosis in the Gastrointestinal Tract and Liver: Mechanisms and Targets
Ralf Weiskirchen, Dario Sorrentino and Wolfgang R. Stremmel

11 UPLC-Q-TOF/MS-Based Serum and Urine Metabonomics Study on the Ameliorative Effects of Palmatine on *Helicobacter pylori*–Induced Chronic Atrophic Gastritis
Xing Chen, Jianzhong Zhang, Ruilin Wang, Honghong Liu, Chunmei Bao, Shihua Wu, Jianxia Wen, Tao Yang, Ying Wei, Sichen Ren, Yuling Tong and Yanling Zhao

27 Intrahepatic T_H17/T_{Reg} Cells in Homeostasis and Disease—It's All About the Balance
Hannah K. Drescher, Lea M. Bartsch, Sabine Weiskirchen and Ralf Weiskirchen

46 Rutaecarpine Ameliorates Ethanol-Induced Gastric Mucosal Injury in Mice by Modulating Genes Related to Inflammation, Oxidative Stress and Apoptosis
Sichen Ren, Ying Wei, Ruilin Wang, Shizhang Wei, Jianxia Wen, Tao Yang, Xing Chen, Shihua Wu, Manyi Jing, Haotian Li, Min Wang and Yanling Zhao

59 Hepatoprotective Effect and Molecular Mechanisms of Hengshun Aromatic Vinegar on Non-Alcoholic Fatty Liver Disease
Shenghu Zhu, Linshu Guan, Xuemei Tan, Guoquan Li, Changjie Sun, Meng Gao, Bao Zhang and Lina Xu

72 Intestinal Epithelial Cell-Derived Extracellular Vesicles Modulate Hepatic Injury via the Gut-Liver Axis During Acute Alcohol Injury
Arantza Lamas-Paz, Laura Morán, Jin Peng, Beatriz Salinas, Nuria López-Alcántara, Svenja Sydor, Ramiro Vilchez-Vargas, Iris Asensio, Fengjie Hao, Kang Zheng, Beatriz Martín-Adrados, Laura Moreno, Angel Cogolludo, Manuel Gómez del Moral, Lars Bechmann, Eduardo Martínez-Naves, Javier Vaquero, Rafael Bañares, Yulia A. Nevzorova and Francisco Javier Cubero

87 Carveol a Naturally-Derived Potent and Emerging Nrf2 Activator Protects Against Acetaminophen-Induced Hepatotoxicity
Zaif Ur Rahman, Lina Tariq Al Kury, Abdullah Alattar, Zhen Tan, Reem Alshaman, Imran Malik, Haroon Badshah, Zia Uddin, Atif Ali Khan Khalil, Naveed Muhammad, Saifullah Khan, Amjad Ali, Fawad Ali Shah, Jing Bo Li and Shupeng Li

102 Rapamycin is Effective for Upper but not for Lower Gastrointestinal Crohn's Disease-Related Stricture: A Pilot Study
Min Zhong, Bota Cui, Jie Xiang, Xia Wu, Quan Wen, Qianqian Li and Faming Zhang

108 Fructose and Non-Alcoholic Steatohepatitis
Elke Roeb and Ralf Weiskirchen

119 Inhibition of 5-Lipoxygenase in Hepatic Stellate Cells Alleviates Liver Fibrosis
Shiyun Pu, Yanping Li, Qinhui Liu, Xu Zhang, Lei Chen, Rui Li, Jinhang Zhang, Tong Wu, Qin Tang, Xuping Yang, Zijing Zhang, Ya Huang, Jiangying Kuang, Hong Li, Min Zou, Wei Jiang and Jinhan He

133 Targeting Certain Interleukins as Novel Treatment Options for Liver Fibrosis
Su Yeon An, Anca D. Petrescu and Sharon DeMorrow

144 The Placebo and Nocebo Responses in Clinical Trials in Inflammatory Bowel Diseases
Paul Enck and Sibylle Klosterhalfen

152 An Update for Pharmacologists on New Treatment Options for Inflammatory Bowel Disease: The Clinicians' Perspective
Carsten Schmidt, Philip C. Grunert and Andreas Stallmach

162 Development and Validation of an Interleukin-6 Nomogram to Predict Primary Non-response to Infliximab in Crohn's Disease Patients
Yueying Chen, Hanyang Li, Qi Feng and Jun Shen

171 Novel and Emerging Therapies for Inflammatory Bowel Disease
Badr Al-Bawardy, Raina Shivashankar and Deborah D. Proctor

187 Targeting Gremlin 1 Prevents Intestinal Fibrosis Progression by Inhibiting the Fatty Acid Oxidation of Fibroblast Cells
Yang Yang, Qi-Shan Zeng, Min Zou, Jian Zeng, Jiao Nie, DongFeng Chen and Hua-Tian Gan

200 Ultrasonographic Evaluation of Intestinal Fibrosis and Inflammation in Crohn's Disease. The State of the Art
Francesca Ferretti, Rosanna Cannatelli, Sandro Ardizzone, Jeanette A. Maier and Giovanni Maconi

212 *Cichorium pumilum* Jacq Extract Inhibits LPS-Induced Inflammation via MAPK Signaling Pathway and Protects Rats From Hepatic Fibrosis Caused by Abnormalities in the Gut-Liver Axis
Chang Han, Xi Wu, Nan Zou, Yunsheng Zhang, Jinqi Yuan, Yuefeng Gao, Wen Chen, Jia Yao, Cong Li, Jinqiu Hou and Dongmei Qin

228 Cellular Mechanisms of Liver Fibrosis
Pragyan Acharya, Komal Chouhan, Sabine Weiskirchen and Ralf Weiskirchen

256 Antisense Tissue Factor Oligodeoxynucleotides Protected Diethyl Nitrosamine/Carbon Tetrachloride-Induced Liver Fibrosis Through Toll Like Receptor4-Tissue Factor-Protease Activated Receptor1 Pathway
Maha M. Shouman, Rania M. Abdelsalam, Mahmoud M. Tawfick, Sanaa A. Kenawy and Mona M. El-Naa

271 Salidroside Inhibits CCl_4-Induced Liver Fibrosis in Mice by Reducing Activation and Migration of HSC Induced by Liver Sinusoidal Endothelial Cell-Derived Exosomal SphK1
Qiannan Ye, Yang Zhou, Changqing Zhao, Lieming Xu and Jian Ping

285 Dapagliflozin Alleviates Hepatic Steatosis by Restoring Autophagy via the AMPK-mTOR Pathway
Liuran Li, Qinghua Li, Wenbin Huang, Yibing Han, Huiting Tan, Min An, Qianru Xiang, Rui Zhou, Li Yang and Yanzhen Cheng

295 Exosomes in Intestinal Inflammation
Kanchana K. Ayyar and Alan C. Moss

311 Noncanonical NF-κB Signaling Upregulation in Inflammatory Bowel Disease Patients is Associated With Loss of Response to Anti-TNF Agents
Vu Q. Nguyen, Kristin Eden, Holly A. Morrison, Megan B. Sammons, Kristin K. Knight, Siena Sorrentino, Rebecca M. Brock, Douglas J. Grider, Irving C. Allen and Dario Sorrentino

320 Kaempferol Alleviates Steatosis and Inflammation During Early Non-Alcoholic Steatohepatitis Associated With Liver X Receptor α-Lysophosphatidylcholine Acyltransferase 3 Signaling Pathway
Hongjiao Xiang, Mingmei Shao, Yifei Lu, Junmin Wang, Tao Wu and Guang Ji

335 Bicyclol Alleviates Signs of BDL-Induced Cholestasis by Regulating Bile Acids and Autophagy-Mediated HMGB1/p62/Nrf2 Pathway
Jingwen Zhao, Maojuan Ran, Ting Yang, Liwei Chen, Peixu Ji, Xiuxiu Xu, Lu Zhang, Siyuan Sun, Xin Liu, Simin Zhou, Lu Zhou and Jie Zhang

349 A Retinoid X Receptor Agonist Directed to the Large Intestine Ameliorates T-Cell-Mediated Colitis in Mice
Ryohtaroh Matsumoto, Daisuke Takahashi, Masaki Watanabe, Shunsuke Nakatani, Yuta Takamura, Yuji Kurosaki, Hiroki Kakuta and Koji Hase

360 AICAR, an AMP-Activated Protein Kinase Activator, Ameliorates Acute Pancreatitis-Associated Liver Injury Partially Through Nrf2-Mediated Antioxidant Effects and Inhibition of NLRP3 Inflammasome Activation
Lijun Kong, Hewei Zhang, Chaosheng Lu, Keqing Shi, Hongjian Huang, Yushu Zheng, Yongqiang Wang, Dan Wang, Hongwei Wang and Wei Huang

377 Metformin Exerts Anti-inflammatory and Mucus Barrier Protective Effects by Enriching Akkermansia muciniphila in Mice With Ulcerative Colitis
Haoran Ke, Fang Li, Wenlin Deng, Zitong Li, Siqi Wang, Pinjing Lv and Ye Chen

394 The Effects of Vitamin D Supplementation on Anthropometric and Biochemical Indices in Patients With Non-alcoholic Fatty Liver Disease: A Systematic Review and Meta-analysis
Shahla Rezaei, Reza Tabrizi, Peyman Nowrouzi-Sohrabi, Mohammad Jalali, Mojtaba Shabani-Borujeni, Shayan Modaresi, Maryam Gholamalizadeh and Saeid Doaei

408 Inflammatory-Dependent Bidirectional Effect of Bile Acids on NLRP3 Inflammasome and Its Role in Ameliorating CPT-11-Induced Colitis
Chuyao Liao, Di Wang, Siyuan Qin, Ying Zhang, Jie Chen, Ruijie Xu, Fengguo Xu and Pei Zhang

frontiers in Pharmacology

EDITORIAL
published: 24 September 2021
doi: 10.3389/fphar.2021.773228

Editorial: Inflammation and Fibrosis in the Gastrointestinal Tract and Liver: Mechanisms and Targets

Ralf Weiskirchen[1]*, *Dario Sorrentino*[2†] and *Wolfgang R. Stremmel*[3]

[1]Institute for Molecular Pathobiochemistry, Experimental Gene Therapy and Clinical Chemistry (IFMPEGKC), RWTH University Hospital Aachen, Aachen, Germany, [2]IBD Center, Division of Gastroenterology, Virginia Tech Carilion School of Medicine, Roanoke, VA, United States, [3]Practice for Internal Medicine, Baden-Baden, Germany

Keywords: liver, gastrointestinal tract, IBD, inflammation, fibrosis, therapy

Editorial on the Research Topic

Inflammation and Fibrosis in the Gastrointestinal Tract and Liver: Mechanisms and Targets

INTRODUCTION

Inflammation of the gastrointestinal tract and liver can be caused by a variety of factors including genetic diseases, immune mediated conditions, environmentally induced reactions, toxic exposure, tissue injury, abnormalities in the gut-liver axis, and general infectious diseases. The consequence of inflammation is wound healing following fibrous tissue repair and regeneration. Although it occurs in all organs, each organ shows a specific pattern of reactivity.

In this Research Topic, leading experts from the field of Gastroenterology and Hepatology share new findings and current concepts in the pathogenesis and management of inflammation and fibrosis in the gastrointestinal tract and liver. In total about 200 basic scientists and clinicians from eight countries (China, Egypt, Germany, India, Japan, Spain, Italy, and USA) contributed 28 originals or review articles about current perspectives and findings in corresponding diseases. These articles cover a wide range of aspects in the pathogenesis of liver inflammation and fibrosis, gastrointestinal disease, and inflammatory bowel disease (IBD). The contributions show that these fascinating fields have made conceptual advances that in the near future will hopefully lead to novel treatment options.

LIVER INFLAMMATION AND FIBROSIS

An et al. discuss the main roles of interleukins (ILs) in the context of hepatic inflammation and how this knowledge can be used for the development of therapeutic drugs. In particular, they highlight the dynamics by which interleukins mediate the cross-talk between hepatic cells during liver inflammation and injury. It becomes clear that abrogating IL signaling might prevent the progression of hepatic fibrogenesis in the early stages of liver injury. However, as the authors discuss there are some practical problems that need to be addressed to move IL-targeted therapies from the experimental stage to the clinical setting.

In an experimental animal study, Han et al. investigated the impact of a traditional medicinal herbal extract derived from Chicory (*Cichorium pumilum Jacq*) in a rat model of liver fibrosis induced by chronic colitis. The authors demonstrate that this herb can promote probiotic growth and prevent liver fibrosis. In addition, the authors demonstrate that Lactucin that is one of the bitter

OPEN ACCESS

Edited by and reviewed by:
Angelo A. Izzo,
University of Naples Federico II, Italy

***Correspondence:**
Ralf Weiskirchen
rweiskirchen@ukaachen.de

†***Deceased***

Specialty section:
This article was submitted to Gastrointestinal and Hepatic Pharmacology, a section of the journal Frontiers in Pharmacology

Received: *09 September 2021*
Accepted: *13 September 2021*
Published: *24 September 2021*

Citation:
Weiskirchen R, Sorrentino D and Stremmel WR (2021) Editorial: Inflammation and Fibrosis in the Gastrointestinal Tract and Liver: Mechanisms and Targets. Front. Pharmacol. 12:773228. doi: 10.3389/fphar.2021.773228

tasting sesquiterpene lactone of Chicory is able to inhibit lipopolysaccharide-induced inflammatory responses *in vitro* and activation of the Mitogen-activated protein kinase and Akt signaling. Therefore, the authors proposed Lactucin as one of the most significant anti-inflammatory compounds in Chicory extracts.

Another compound boosting endogenous antioxidant mechanisms in the context of acetaminophen (APAP)-induced liver damage was identified by Rahman et al. In their study, the authors provide evidence that carveol improves liver detriments and liver metabolic deficits in mice subjected to APAP, while the nuclear factor erythroid 2-related factor 2 (Nrf2) inhibitor all-trans retinoic acid exaggerated APAP toxicity. Mechanistically, the authors found that carveol treatment increases *Nrf2* expression that combats various reactive oxygen species and other stress kinases. Additional, comprehensible *in-silico* docking studies showed that carveol might have an affinity to the active catalytic pockets of COX-2, HO-1, IL-1, NF-κB, iNOS, Nrf2 and TNF-α that all impact inflammation.

The *Nrf2* pathway was also investigated in an experiment study by Zhao et al., who analyzed the effect of bicyclol in cholestatic mice caused by bile duct ligation. Interestingly, it was found that bicyclol acts as a significant hepatoprotective agent that attenuates liver damage by increasing the levels of hydropholic bile acids such as α-muricholic acid (MCA) and β-MCA. Moreover, bicyclol promoted autophagy and activated *Nrf2* expression and antioxidant downstream genes.

Pu et al. provide evidence that the 5-lipoxygenase (5-LO) that catalyzes the oxidation of essential fatty acid substrates into inflammatory leukotrienes is a key enzyme involved in mediating hepatic fibrosis. The authors could show that genetic ablation or pharmacological inhibition of 5-LO is therapeutically beneficial to block hepatic fibrosis *in vitro* and *in vivo*. In line, patients suffering from non-alcoholic steatohepatitis and liver fibrosis showed elevated levels of 5-LO suggesting that strategies to target 5-LO may offer new therapeutic avenues.

A new network in the pathogenesis of hepatic fibrosis was introduced by Shouman et al. They evaluated antisense oligonucleotides directed against the tissue factor in rats in which liver fibrosis were induced by a single administration of Diethylnitrosamine followed by repeated doses of carbon tetrachloride once weekly for 6 weeks. The authors could demonstrate that the blockage of tissue factor expression resulted in a significant downregulation of the protease-activated receptor 1 (PAR1) and toll-like receptor 4 (TLR4) that are both critical drivers in hepatic inflammation and fibrosis.

Roeb and Weiskirchen summarized findings from a selective literature search on topics related to non-alcoholic fatty liver disease (NAFLD), fructose and fibrosis. The study showed that the rate of overweight and obesity is significantly higher in adult and pediatric patients suffering from non-alcoholic steatohepatitis (NASH). Although it is presently not known whether this is due to an excess of energy or the particular metabolism of fructose, the authors suggest that reduction in sugar consumption in conjunction with avoidance of foods enriched in saturated fats and weight loss is recommended for NAFLD and NASH patients.

Xiang et al. analyzed the effects of kaempferol on the liver X receptor α (LXRα)/lysophosphatidylcholine acyltransferase 3 (LPCAT3) pathway in livers of mice fed a high fat diet inducing NASH. They could show that this natural flavonol reduces endoplasmic reticulum stress and inflammation as assessed *in vitro* and *in vivo* by reduced expression of LXRα, LPCAT3 and genes involved in the initiation or execution of endoplasmic reticulum stress. Based on their results the authors conclude that the LXRα/LPCAT network offers new potential targets for NASH treatment.

Acharya et al. summarized recent aspects in the understanding of hepatic fibrosis including relevant disease-associated pathways, cellular and molecular drivers of fibrogenesis, and how this knowledge can be translated into therapy of respective disease. The review shows that hepatic fibrogenesis is a highly complex and orchestrated process that offers many therapeutic opportunities for impeding or reversing this disease process.

The sodium-glucose cotransporter two inhibitor dapaglifloxin was shown by Li et al. ameliorates hepatic steatosis by decreasing the *de novo* lipogenesis enzyme acetyl-CoA carboxylase 1 (ACC1), increasing the fatty oxidation enzyme acyl-CoA oxidase 1 (ACOX1), and inducing autophagy via the AMPK-mTOR pathway. This may be in future used as therapeutic approach to treat NAFLD by a functional mechanism.

The group of Ye et al. showed that Salidroside inhibits carbon tetrachloride-induced liver fibrosis in mice by suppression of JNK activation and modulating the sphingosine kinase 1/sphingosine-1-phosphate signaling pathway for inhibition of Akt. This reduces activation and migration of hepatic stellate cells (HSC) as the executive players in fibrosis. Salidroside alleviates by this mechanism liver injury, hepatocyte apoptosis and consequently liver fibrosis.

A review article by Drescher et al. discusses developmental differences between individual immune cells and their role in health and disease, with a focus on liver diseases. They summarized findings showing there exists a fragile balance between T helper 17 (T_H17) and regulatory T cells (T_{Reg}) that is critical in maintaining immune homeostasis during acute and chronic inflammation.

Zhu et al. focused on Hengshun aromatic vinegar as a food additive to improve NAFLD. It improved cell viability and attenuated cell damage. Serum levels of triglycerides, transaminases (ALT, AST) and malondialdehyde (MDA) dropped. Inflammation and lipogenesis were reduced by interference with metabolic key regulators, i.e. by enhancing silent information regulator of transcription 1 (Sirt1). Thus, it represents a new assistant strategy to fight NAFLD.

Kong et al. investigated the role of the AMP analog 5-aminoimidazole-4-carboxamide (AICAR) which acts as an activator of the AMP-kinase (AMPK) on the pathogenesis of acute pancreatitis-associated liver injury (PALI). In a rat model of sodium taurocholate-induced acute pancreatitis, they found that AICAR attenuated PALI and restored liver function. Moreover, the compound activated the AMPK/Nrf2 signaling pathway, while the AMPK inhibitor Compound C aggravated PALI. In Nrf2 null mice, the effect

of AICAR on alleviation of liver injury was significantly weakened suggesting that AICAR protects against PALI by interfering with *Nrf2*-triggered processes.

GASTROINTESTINAL TRACT

Lamas-Paz et al. identified a novel mechanism that triggers acute alcoholic hepatic injury in the context of the gut-liver axis. The authors could demonstrate mice subjected to acute alcohol injury develop significant alterations in the gut microbiota and in intestinal epithelial barrier function. Interestingly, these alterations are triggered by yet unknown mediators released from extracellular vesicles produced by intestinal epithelial cells provoking deleterious effects on hepatocyte viability and steatosis.

A thematically related study by Ren et al. demonstrated that the COX-2 inhibitor rutaecaprine has gastroprotective effects on ethanol-induced acute gastric mucosal injury in mice. In the respective model, rutaecaprine augmented cellular antioxidant capacity, most likely by triggering antioxidant and anti-apoptosis defense capacities that results in inhibition of the inflammatory acting NF-κB, pathway.

Chen et al. performed an ultra-high performance liquid chromatography-quadrupole time-of-flight mass spectrometry (UPLC-Q-TOF/MS)-based study to investigate the ameliorative effects of palmatine on *Heliobacter pylori*-induced chronic atrophic gastritis in rats using serum and urine metabolomics. Interestingly, this alkaloid attenuated pathological damage and inflammation and improved integrity of the gastric mucosal epithelial barrier. Mechanistically, the authors suggested that the therapeutic effects of palmatine are majorly attributable to its capacity to impact the metabolism of taurine, subtaurine, glycerol phospholipid and the mutual transformation of pentose and glucoronide.

Yang et al. found that Gremlin 1 (GREM1) is significantly increased in mouse fibrotic colon. In their original study, the authors demonstrated that GREM1 promoted the proliferations and activation of intestinal fibroblasts by activating the VEGFR2 receptor and triggering fatty acid oxidation. In line with these findings, the authors could block intestinal fibrosis progression *in vivo* by blocking the GREM1-VEGFR2 axis.

INFLAMMATORY BOWEL DISEASE

Enck and Klosterhalfen addressed the interesting question why in trials of irritable bowel syndrome (IBS) and IBD the placebo rates are remarkably high. Based on a meta-analysis, they report that the spontaneous improvement accounts for 50% of the placebo effect. Moreover, nocebo effects are easily detectable in randomized control trials (RCTs), whereas adverse events are difficult to see in respective reports.

Chen Y et al. developed a novel prediction model useful to estimate the risk of primary non-response rate to infliximab therapy and select the optimal treatment for individual patients suffering from Crohn's disease. In their retrospective study including 322 Crohn's disease patients and data from the Gene Expression Omnibus (GEO) database, the authors performed and intensive bioinformatics analysis and provide evidence that IL-6 is a good predictive factor for risk assessment.

Schmidt et al. evaluated the clinical efficacy of tumor necrosis factor antibodies on chronic IBD outcome. In total one third of the patients do not respond and in many cases drug efficacy is lost over time. Contraindications, adverse events and intolerance have to be considered when these biologicals are administered. This overview of new therapeutic approaches with novel biologicals is helpful for clinicians treating IBD.

The group of Zhong et al. showed that the serine-threonine kinase inhibitor rapamycin is effective in the treatment of upper gastrointestinal Crohn's disease-related stricture formation, but has no effect in lower gastrointestinal Crohn's disease. The drug was recently shown to reduce intestinal fibrosis by inhibiting CX3Cr1-mTOR-induced autophagy in mononuclear phagocytes and upregulating the IL-23/IL-22 axis. This was now evaluated by a Gastrointestinal obstruction symptoms score and diet score, which both showed improvement in upper gastrointestinal Crohn's disease, but not in lower gut stricture disease. Adverse events were recorded in 40% of the patients, mostly mouth ulcers. However, no death or serious opportunistic infections were observed. This therapy may avoid surgical or endoscopic interventions. These promising results should now be confirmed in randomized trials with larger numbers of patients.

Al-Bawardy et al. highlighted the relevance of continued development of new therapeutic strategies and modifications of existing therapies to improve the outcome of IBD. In particular, they suggested small molecule inhibitors targeting the Janus kinase or the sphingosine-1-phosphate receptor that both critically contribute to the pathogenesis of IBD as promising therapeutic targets. Most important is that most of these agents can be administered orally and have a favorable safety profile compared to established anti-TNF agents.

Ayyar and Moss summarized the actual knowledge on extracellular vesicles including exosomes in intestinal inflammation. The compiled information illustrates that exosomes in particular and extracellular vesicles in general are capable of modulating gene expression and cellular functions, thereby critically impacting inflammation, immune responses, and composition of gut microbiota. As such these vesicles might be suitable biomarkers of IBD and molecular structures for therapeutic targeting specific cargos to the inflamed gastrointestinal tract.

Ferretti et al. provide an update on current sonographic methods to discriminate inflammation and fibrosis in Crohn's disease, mainly focusing on studies investigating pathological features or the response to treatment as direct and indirect reference parameters. In their contribution, the authors highlight strengths and weaknesses of individual ultrasound methods and conclude that despite the promising results obtained with novel sonographic techniques such as contrast-enhanced ultrasound (CEUS) and sonoelastrography, several limitations must be addressed before using these techniques in routine clinical practice and trials.

Matsumoto et al. investigated potential therapeutic effects of the RXR agonist Net-3IB that was previously developed in their team in an experimental model of colitis induced through the adoptive transfer of $CD45RB^{high}CD4^{+}$ cells. The authors showed

that Net-3IB ameliorates colitis by inhibiting both the expansion of Th1 cells and the activation of inflammatory macrophages locally in the colon. Thus, the small molecule inhibitor appears to be a promising candidate for the treatment of IBD.

Ke and colleagues addressed the question whether the anti-inflammatory effect of metformin in the intestine is due to a change of the microbiota. They examined this in the experimental colitis model of dextran sulfate sodium (DSS)-induced ulcerative colitis. Indeed the inflammation was attenuated by metformin. An increased expression of mucin 2 was noted. The gut microbiota changed under metformin by increasing protective *Lactobacillus* and *Akkermansia species*. With antibiotic exposure the anti-inflammatory and mucus-protecting effect of metformin was abolished. It is concluded that metformin-induced changes of the microbiota are therapeutically effective in ulcerative colitis.

The study by Nguyen et al. demonstrates the importance of the noncanonical NF-κB signaling pathway in IBD patients. In their study, the authors analyzed the expression of 88 target genes known to be associated with noncanonical NF-κB signaling in biopsy specimens that were collected during colonoscopy. Importantly, the expression of a number of genes was associated with increased gastrointestinal inflammation and in particular in patients unresponsive to anti-TNF agents. Although the study is based on a relatively small sample size, the study suggests that the noncanonical NF-κB signaling is an understudied pathway that critically impacts the pathogenesis of IBD.

All these 28 articles show that inflammation and fibrosis of the gastrointestinal tract and liver are complex problems. Currently, there are a number of real breakthroughs in this research area, but of course scientists and clinicians are still at the beginning in the identification of suitable therapeutic targets. Since the frequency of these malignancies and their complications currently increase dramatically, new strategies anti-inflammatory and anti-fibrotic therapies are urgently needed.

AUTHOR CONTRIBUTIONS

All authors contributed equally to the review and editorial process for this article Research Topic.

ACKNOWLEDGMENTS

The authors are grateful to all authors that have provided excellent contributions to this Research Topic and the kind support of the Editorial office team of Frontiers that helped to arrange a strict review process and assisted to enable reliable correspondence with the authors. Moreover, we acknowledge the excellent and efficient work of the expert reviewers who reviewed submissions in a timely, fair, and constructive manner. In addition, we like to thank Drs. Leo A. van Grunsven (Vrije University Brussel, Belgium), Stefano Fiorucci (University of Perugia, Italy), Luca Antonioli (University of Pisa, Italy), and Barbara Romano (University of Naples Federico II, Italy), who edited contributions in which we had conflicts of interest.

Conflict of Interest: The authors declare that the research was conducted in the absence of any commercial or financial relationships that could be construed as a potential conflict of interest.

Publisher's Note: All claims expressed in this article are solely those of the authors and do not necessarily represent those of their affiliated organizations, or those of the publisher, the editors, and the reviewers. Any product that may be evaluated in this article, or claim that may be made by its manufacturer, is not guaranteed or endorsed by the publisher.

Copyright © 2021 Weiskirchen, Sorrentino and Stremmel. This is an open-access article distributed under the terms of the Creative Commons Attribution License (CC BY). The use, distribution or reproduction in other forums is permitted, provided the original author(s) and the copyright owner(s) are credited and that the original publication in this journal is cited, in accordance with accepted academic practice. No use, distribution or reproduction is permitted which does not comply with these terms.

frontiers in Pharmacology

ORIGINAL RESEARCH
published: 15 September 2020
doi: 10.3389/fphar.2020.586954

UPLC-Q-TOF/MS-Based Serum and Urine Metabonomics Study on the Ameliorative Effects of Palmatine on *Helicobacter pylori*–Induced Chronic Atrophic Gastritis

Xing Chen[1,2], *Jianzhong Zhang*[3], *Ruilin Wang*[4], *Honghong Liu*[4], *Chunmei Bao*[5], *Shihua Wu*[1,2], *Jianxia Wen*[1,2], *Tao Yang*[1,2], *Ying Wei*[1,2], *Sichen Ren*[1,2], *Yuling Tong*[1,2] *and Yanling Zhao*[1*]

[1] Department of Pharmacy, Fifth Medical Center of PLA General Hospital, Beijing, China, [2] College of Pharmacy, Chengdu University of Traditional Chinese Medicine, Chengdu, China, [3] Center of Disease Control and Prevention, National Institute for Communicable Disease Control and Prevention, Beijing, China, [4] Integrative Medical Center, Fifth Medical Center of PLA General Hospital, Beijing, China, [5] Division of Clinical Microbiology, Fifth Medical Center of PLA General Hospital, Beijing, China

OPEN ACCESS

Edited by:
Ralf Weiskirchen,
RWTH Aachen University, Germany

Reviewed by:
Wirginia Kukuła-Koch,
Medical University of Lublin, Poland
Yanxiang Wang,
Chinese Academy of Medical Sciences, China

***Correspondence:**
Yanling Zhao
zhaoyl2855@126.com

Specialty section:
This article was submitted to Gastrointestinal and Hepatic Pharmacology, a section of the journal Frontiers in Pharmacology

Received: *24 July 2020*
Accepted: *27 August 2020*
Published: *15 September 2020*

Citation:
Chen X, Zhang J, Wang R, Liu H, Bao C, Wu S, Wen J, Yang T, Wei Y, Ren S, Tong Y and Zhao Y (2020) UPLC-Q-TOF/MS-Based Serum and Urine Metabonomics Study on the Ameliorative Effects of Palmatine on Helicobacter pylori–Induced Chronic Atrophic Gastritis. Front. Pharmacol. 11:586954. doi: 10.3389/fphar.2020.586954

Objective: The main objective of this study was to investigate the ameliorative effects of Palmatine (Pal) on *Helicobacter pylori* (*H. pylori*) induced chronic atrophic gastritis (CAG)

Method: Body function, serum biochemical indicators and histopathology were used to evaluate the pharmacodynamics of Pal on CAG rats. The target genes expression levels were verified and assessed by RT-PCR and immunohistochemistry (IHC). Moreover, UPLC-Q-TOF/MS analysis based on urine and serum was performed to identify the potential metabolites in the pathological process of CAG induced by *H. pylori*. Metabolic pathway analysis was performed to elucidate the metabolic network associated with Pal treatment of CAG.

Results: Pal (10, 20, 40 mg/kg/day) significantly restored the body function of CAG rats, reduced the serum biochemical indicators, and maintained the integrity of the gastric mucosal epithelial barrier while alleviated gastric histological damage. Metabolomics analysis shows that the therapeutic effect of Pal on CAG involves 10 metabolites and 10 metabolic pathways, of which the Taurine and hypotaurine metabolism, Glycerophospholipid metabolism and Pentose and glucuronate interconversions are closely related to the gastrointestinal protection of Pal, and these metabolic pathways crosstalk with each other due to the internet hub of citric acid cycle.

Conclusions: Metabolomics was used for the first time to identify potential biomarkers of CAG and to illuminate the therapeutic mechanism of Pal on CAG induced by *H. pylori*. The results provided a new insight for further research on CAG treatment.

Keywords: palmatine, *Helicobacter pylori*, chronic atrophic gastritis, metabolomics, molecular mechanisms

INTRODUCTION

Chronic atrophic gastritis (CAG) is a common disease of the digestive system which is considered a precursor condition for gastric cancer (GC). The rate of CAG progression to GC was as high as 2% per year during a 16 years of follow-up report (Lahner et al., 2015). It is understood that GC ranks fourth in the global incidence of various cancers worldwide and is the second cause of cancer-related deaths (Topi et al., 2020). *Helicobacter pylori* (*H. pylori*) is an obligate pathogen in the stomach, and the persistent inflammatory response caused by colonization is the strongest single risk factor for GC (Schulz et al., 2019). It has been recognized by the World Health Organization as a "definite carcinogen" since 1994, and the evidence for its role in gastric cancer (GC) development was expanded and updated in 2012 (Crafa et al., 2018). The risk of carcinogenic risk is closely related to the strain-specific bacterial components, host immune responses and effective drug intervention. Therefore, while focusing on the prevention of gastric cancer risk in people with *H. pylori* infection, delineating the drug treatment and mechanisms for gastric inflammation has profound significance for greatly reducing the incidence of CAG and GC.

Palmatine (Pal, **Figure 2A**) is an isoquinoline alkaloid from *Coptidis rhizoma* (Huanglian in Chinese), and is classified as an anti-inflammatory drug in Chinese Pharmacopeia (Tarabasz and Kukula-Koch, 2020). It can be used to relieve bacterial dysentery, gynecological inflammation and urinary tract-related surgical infections on clinic (Yokozawa et al., 2005; Wang et al., 2017). It has been the subject of scientific interest in recent years due to its multiple antibacterial, antiviral, and gastrointestinal protection biological activities (Li et al., 2018; Chen et al., 2020). However, the largely potential anti-gastritis mechanism of Pal remain unknown, and whether Pal can be safely and effectively used in clinical still needs more investigation.

Recently, omics techniques, such as transcriptomics, proteomics, and metabolomics have been widely used to identify potential disease markers and elucidate biologically related mechanisms. Metabolite profiling provides a clearer explanation of the relationship between drug efficacy, pharmacological effects, and metabolic pathways by analyzing specific biomarkers during disease and drug treatment. It has shown great potential in many life science fields, such as toxicology, disease diagnosis, drug mechanism research and natural product discovery (Wang et al., 2011). Previous studies have shown that *H. pylori* infection causes various metabolic alterations at lesional sites associated with disease transformation attribution. (Nishiumi et al., 2017). To the best of our knowledge, although the metabolites of Pal *in vivo* have been analyzed for quality evaluation or pharmacological activity (Wang et al., 2017), the analysis of Pal and its metabolitesmetabolite changes in *H. pylori*–induced gastritis individuals is currently lacking.

All the considerations above prompted the application of metabolomics to comprehensively explore the gastrointestinal toxicity of Pal and its protective effect on *H. pylori*–induced CAG. In this study, serum biochemical indicators and pathological observations were used to evaluate theameliorative effect of Pal on CAG. UPLC-Q-TOF/MS metabolomics research was applied to obtain and analyze the changes of different metabolites in urine and serum during Pal therapy (**Figure 1**). Finally, it systematically clarified the modulatory properties of Pal on *H. pylori*–induced CAG, and further confirmed the feasibility of Pal for treatment of *H. pylori*–induced CAG.

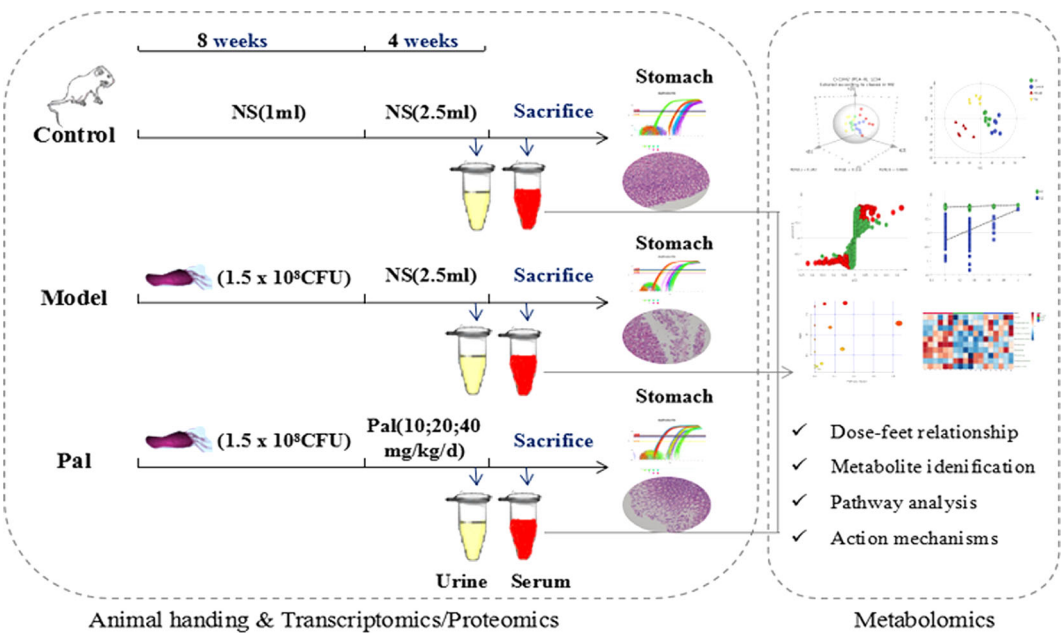


FIGURE 1 | Scheme of the study.

MATERIALS AND METHODS

Chemicals and Reagents

Pal standard ($C_{21}H_{25}NO_4$, purity > 90%, Cat. No.10605-02-4) was purchased from Chroma Biotechnology Co. Ltd (Chengdu, China). Dissolved it into normal saline (NS 0.9%) and diluted to the corresponding concentration for later use.

H. pylori Strains and Growth Condition

H. pylori strain was kindly provided by Prof. Jianzhong which was isolated from CAG patient (No. ZCDC111001). Columbia agar plats (Thermo Fisher Scientific Co., Ltd., Beijing, China) was used for bacterial propagation and shake for 48–72 h under the microaerobic conditions (6% O2, 7.2% CO2, 7.1% H2, 79.7% N2) of Low Oxygen Cell Culture Jar (UNITECH Co., Ltd., Guangzhou, China).

Animals

Male Sprague Dawley (SD) rats (180 ± 20 g) were purchased from Sibeifu Biotechnology Co., Ltd. (Permission No. SCXK (jing) 2016-0002, Beijing, China). Rats were adapted the specific environment (humidity: 55% ± 5%, temperature: 25°C ± 0.5°C and 12-h/12-h light/dark cycle) and given sufficient sterile food and water for 2 weeks. All experimental procedures have been reviewed and approved by the Animal Ethical and Experimental Committee of the Fifth Medical Center of PLA General Hospital (Approval ID: IACUC-2018-010) and strictly implemented in accordance with the "Guide for the Care and Use of Laboratory Animals" (https://grants.nih.gov/grants/olaw/guide-for-the-care-and-use-of-laboratory-animals.pdf).

Induction of CAG

CAG model was induced by *H. pylori* as previously described (Werawatganon, 2014). Live bacteria were collected and adjusted to 1.5×10^8 colony forming units (CFU)/ml with normal saline (NS). Rats were administered with *H. pylori* strains at 1 day intervals to induce CAG model. Hematoxylin and eosin (H & E) staining and a rapid urease kit were used to evaluate the inflammation of stomach tissue at 8 weeks of infection. After CAG model was successfully duplicated, animals were randomly assigned into five groups (n = 6/group): Control group, Model group, Pal group (PalL PalM, PalH = 10, 20, 40 mg/kg/day) respectively. A normal diet was maintained during the 4 weeks of Pal treatment. In this study, the doses of Pal was referenced to previous experiments (Jung et al., 2014).

Sample Collection and Preparation

At the end of the experiment, each rat was put into a metabolic cage (1 per cage) to collect 24-h urine and then sacrificed rats to obtain blood from aorta abdominalis.

Collected the gastric tissue and cut along the large curvature of the stomach, soaked in 10% neutral formalin buffer and embedded in paraffin to observe the pathological changes. The blood was centrifuged at 3.5×10^3 rpm for 12 min to separate the serum and transferred to −8°C for storage before biochemical parameters and metabolomics analysis.

Histopathological Analysis

Cuted 3–5μm thick paraffin slice of stomach tissue. H & E staining was performed for highlighting the pathological damage and inflammation of stomach tissues. The test result was observed with a light microscope (200 ×, 400 × magnifications).

Measurement of Cytokine Concentrations

Serum was stored at −80°C before to cytokine determination. The levels of Pepsinogen I (PG I), Pepsinogen II (PG II), Gastrin17 (G-17) and Ghrelin were quantified by ELISA kits (MLBIO biotechnology Co., Ltd., Shanghai, China) according to the protocols provided by the manufacturer. Synergy H1 Hybrid Reader (Biotek, Winooski, VT, USA) was used to measure the absorbance at 450 nm.

Quantitative RT-PCR

Total RNA was extracted from stomach tissues by using Trizol reagent (Nordic Bioscience, Beijing, China) and then converted into cDNA by reverse transcription kit (Promega, Madison, USA). RT-PCR was selected SYBR Green PCR Master Mix (Nordic Bioscience, Beijing, China) and executed on QuantSTUDIO TM 6 Flex System (Applied Biosystems, Foster City, CA, USA). The level of mRNA was normalized to GAPDH expression based on $2^{-\Delta\Delta CT}$ method. The primers sequences of IFN-γ, Ghrelin, Epithelial cadherin (E-Cadherin), Desmoglein 2 (DSG 2), Zonula occludens-1 (ZO-1) and Mucin 1(Muc1) were listed in **Table 1**.

Immunohistochemistry/ Immunofluorescence

Paraffin sections of stomach tissues were stained with anti-E-Cadherin, anti-DSG 2, anti-ZO-1, anti-Muc1 Ab (**Table 2**) for IHC/immunofluorescence (IF), and lastly examined using NIS Elements Imaging Software Version 4.0 (Olympus, Japan).

TABLE 1 | Primers sequences.

Gene	Forward primer	Reverse primer
Rat IFN-γ	ACAACCCACAGATCCAGCACAAAG	GCTTCCTTAGGCTAGATTCTGGTGAC
Rat Ghrelin	CCAGAAAGCCCAGCAGAGAAAGG	ACATCGAAGGGAGCATTGAACCTG
Rat E-Cadherin	CCTACAATGCTGCCATCGCCTAC	GGGTAACTCTCTCGGTCCAGTCC
Rat Dsg2	CGGAGTGTCTGTGCGGATGC	GGCTGGTCAATGATGGAGAAGGTG
Rat ZO-1	CGCAGCCAGTTCAAACAAAGTTCC	GCAACATCAGCAATCGGTCCAAAG
Rat Muc1	GCCCATCTCTCCCACCATCCC	GGAAGACCGCTGTGCTGTAGTAAG

TABLE 2 | Antibodies and other reagents.

Antibodies	Dilution rate	Manufacturers	Cat.No.
For IHC			
Rabbit anti-Rat Desmoglein2/ DSG2	1/250–1/500	Abcam	ab150372
Rabbit anti-Rat ZO-1 tight junction	1/500	Abcam	ab221547
Rabbit anti-Rat E-Cadherin	1:50–1:200	Cell signaling technology	14472
For IF			
Rabbit anti-Rat Muc1	1/500	Abcam	ab45167

Metabolic Profiling

The serum and urine samples were thawed at room temperature prior to analysis. Added three times methanol to serum or urine and centrifuged at 12,000 rpm for 12 min to precipitate the protein. Collected the supernatant filtrate with nylon filter. Ten microliter of each sample was mixed to prepare quality control (QC), and the remaining samples were used for UPLC-Q-TOF/MS testing.

An Agilent 1290 series UHPLC system (Agilent Technologies, Santa Clara, CA, USA) system was used for serum and urine metabolic profiling analysis. ZORBOX RRHD C18 analytical column (2.1 mm × 100 mm, 1.8 μm., Agilent Technologies, Santa Clara, CA, USA) was used for sample separation at 30°C. The injection volume was 4 μl and flow rate was 0.30ml/min. Solvent A (0.1% formic acid in acetonitrile) and solvent B (0.1% formic acid in water) were mixed into a gradient mobile phase under a 25-min gradient program: 0–1.0 min (95% A); 1.0–9.0 min (95%–60% A); 9.0–19.0 min (60%–10%); 19.0–21.0 min (10%–0% A); 21.0–25.0 min (100% B). Each sample is injected only once, a QC sample and a blank were injected after every 10 samples to ensure the stability and repeatability of the system. Both positive and negative mode electrospray ionization sources (ESI) were used (Electrospray capillary voltage: 4.0kV in ESI+ and 3.5 kV in ESI-; Mass range: 50 to 1,200 m/z; Gas flow:13 L/min; Nebulizer: 20 psi; Sheath gas temperature: 275°C; Sheath gas flow: 12 L/min; Nozzle voltage: 2,000V) in this study.

Data Extraction and Multivariate Analysis

Sample data was extracted by using MassHunter Profinder software (version B.06.00; Agilent, Santa Clara, CA, USA) for analysis and comparison. Data was normalized with MetaboAnalyst 4.0 and then SIMCA-P V14.1 (Umetrics, Umea, Sweden) was used for principal component analysis (PCA) and orthogonal-partial least squares-discriminant analysis (OPLS-DA). The potential biomarkers were identified based on precise molecular weight in the Human Metabolome Database (HMDB) and METLIN (http://metlin.scripps.edu/) database. MetaboAnalyst 4.0 (http://www.metaboanalyst.ca/) was visualized enrichment pathway of potential markers.

Statistical Analysis

Statistical analysis was performed by SPSS 20.0 software program (Chicago, IL, USA) using one-way ANOVA followed by t-test. GraphPad Prism software (version 6.02; Inc., San Diego, USA) was used to visualize the results. $P < 0.05$ was considered statistically significant.

RESULTS

Pal Attenuated Pathological Damage and Inflammation in H. pylori–Induced CAG

During *H. pylori* infection, rats infected with *H. pylori* developed symptoms of inappetence, diarrhea, and the weight gain trend of the model group was markedly slower than control group during the whole experiment (**Figure 2B**). In addition, the positive results of the rapid urease kit proved the reliability of the model (**Figure 2C**). The pathological result showed that the epithelial cells of gastric mucosa in control group were arranged neatly without shedding, and the morphology of submucosal was normal; model group was characterized by thin mucosa and partial mucosa shedding, submucosal edema and eosinophil infiltration in the stomach, atrophy of glands at the junction of the anterior and posterior stomach and reduction of inherent glands (**Figure 2D**). Those changes were similar to CAG patients caused by *H. pylori* in clinic. After 4 weeks of Pal intervention, the body weight of CAG rats gradually recovered, and the pathological gastric mucosal damage was significantly reduced (**Figure 2D**), suggesting that Pal had a significant protective effect on CAG induced by *H. pylori*.

Pal Improved Biomarkers in Serum of H. pylori–Induced CAG

To clarify the activities of several specific markers of *H. pylori*–induced CAG rats, the serum supernatant levels of serum PG I, PG II, and G-17 were estimated. As showed in **Figure 3**, PG I, PG II, PG I/PG II, and G-17 decreased markedly in *H. pylori*–induced model group compared to control group. Conversely, PG I, PG II, and G-17 significantly increased after Pal administration, and the above biomarkers in the PalH group maintained higher levels compared with the PalL group (**Figures 3A–D**). In addition, Pal reversed the decrease in the ratio of PG I/PG II induced by *H. pylori* in the model group, which was more obvious in PalH group (**Figure 3C**). Altogether, these results *in vivo* implied that the activities of several specific markers, including PG I, PG II, and G-17, and the ratio of PG I/PG II, could get dose-dependently improved by Pal intervention.

Pal Relieved the Release Disorder of Ghrelin by Inhibiting IFN-γ

To test whether the CAG rat model induced by *H. pylori* was IFN-γ associated inflammation and would further change the expression of ghrelin, the expression of IFN-γ and ghrelin in stomach and serum were evaluated by RT-PCR and ELISA respectively. Results were presented in **Figure 4**. Evidently, the significant increase of IFN-γ expression in stomach of *H. pylori* infected rats was accompanied by a decrease in the expression of ghrelin, while the concentration of ghrelin in serum was also significantly reduced (**Figures 4A–C**). Accordingly, these

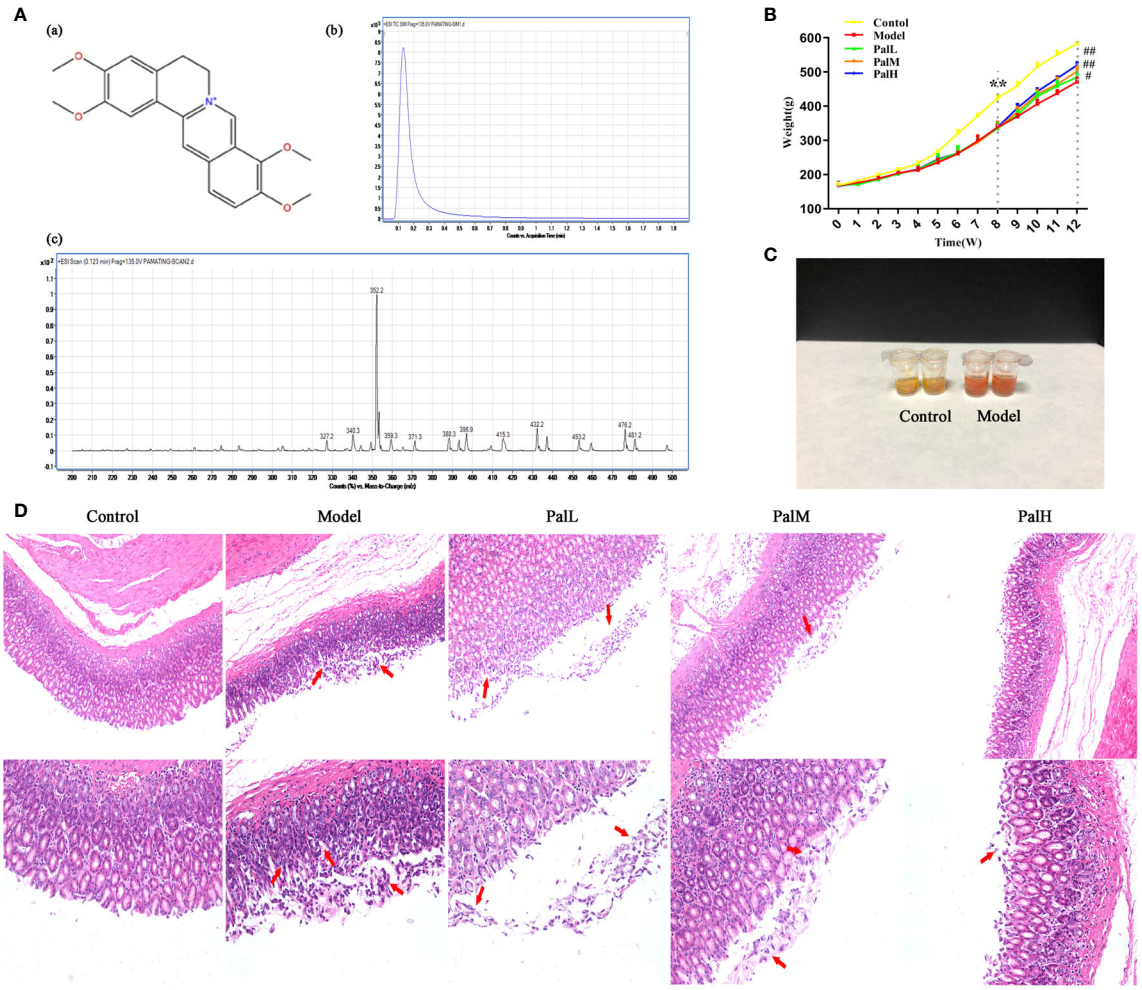


FIGURE 2 | Pal attenuated pathological damage and inflammation in *H. pylori*–induced chronic atrophic gastritis (CAG). **(A)** Chemical structure (a), TIC (b) and Scan (c) chromatogram of Pal. **(B)** Weight of SD rats (n=6). **(C)** Rapid urease test of stomach tissues. **(D)** Morphology and hematoxylin and eosin (H & E) staining of rats stomach (200 × and 400 × magnification). $^{**}P < 0.01$ vs control group. $^{\#}P < 0.05$ and $^{\#\#}P < 0.01$ vs model group. PalL (10 mg/kg); PalM: (20 mg/kg); PalH: (40 mg/kg).

findings indicated that IFN-γ inflammatory response and impaired production of ghrelin in the stomach are associated with CAG induced by *H. pylori*, which ultimately leads to a decrease in the concentration of serum ghrelin (**Figure 4D**). However, Pal could dose-dependently reduced the level of IFN-γ gene and alleviated the release of ghrelin. Consequently, the above results suggested that Pal could restore ghrelin expression by inhibiting IFN-γ and had anti-inflammatory properties in CAG induced by *H. pylori*.

Pal Protected Mucosal Integrity by Modulating Epithelial Junctions and Mucins

To further evaluated the protective effect of Pal on the gastric mucosa of CAG rats induced by *H. pylori*, the mRNA expression of ZO-1, E-cadherin, DSG2, Muc1 were detected using RT-PCR. The results show that the expression of the above mentioned mRNA in the model group was significantly downregulated compared with the control group. However, Pal significantly reversed the inhibitory effect of *H. pylori* (**Figures 5A–D**).

Subsequently, the protein expression of ZO-1, E-cadherin, DSG2, Muc1 were measured to evaluate the integrity on gastric mucosa epithelium. The results showed that all proteins were reduced in model group, indicating that the gastric mucosa epithelium structure was disrupted. In contrast, Pal promoted the expression of ZO-1, E-cadherin, DSG2 and increased the fluorescence intensity of Muc1, and there was a statistically significant difference between the PalH group and the model group (**Figures 5E, F**). Therefore, Pal could protect mucosal integrity by modulating epithelial junctions and mucins, and PalH group was selected for subsequent metabolomics analysis.

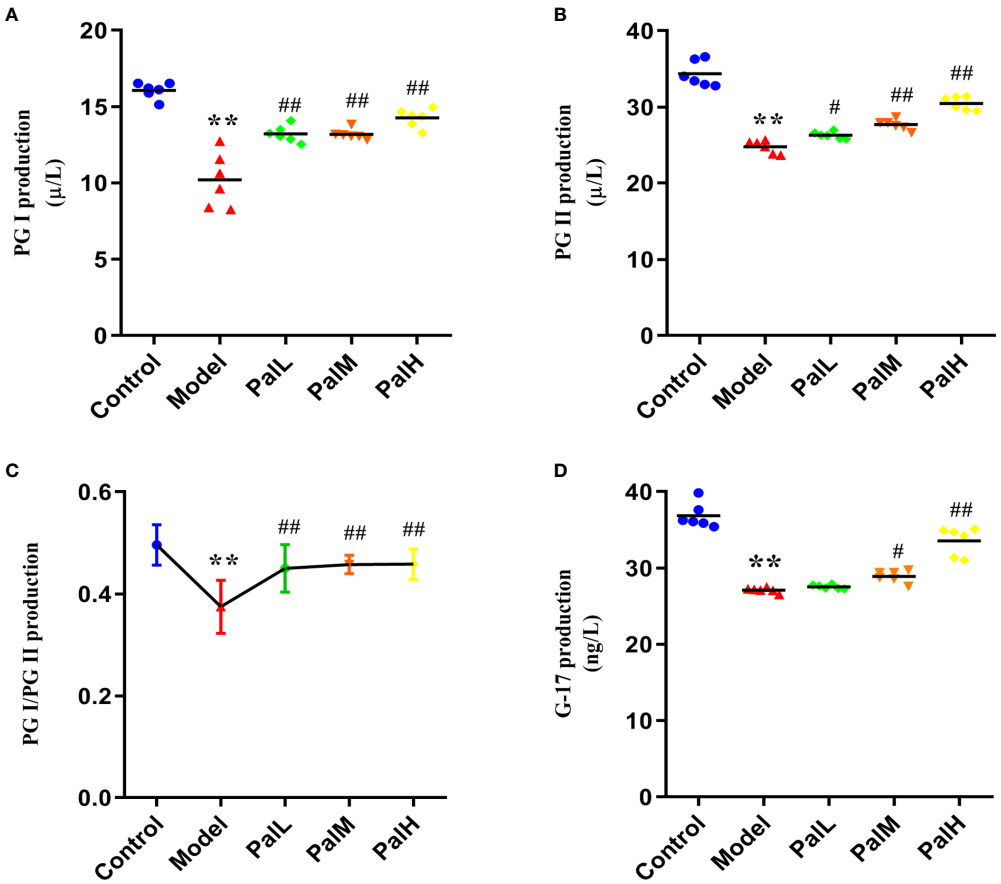


FIGURE 3 | Pal improves biomarkers in serum of *H. pylori*–induced chronic atrophic gastritis (CAG). **(A–D)** PG I **(A)**, PG II **(B)**, PG I/PG II **(C)**, and G-17 **(D)** production in serum was measured by ELISA (n=6). $^{**}P < 0.01$ vs control group. $^{\#}P < 0.05$ and $^{\#\#}P < 0.01$ vs model group. PalL (10 mg/kg); PalM: (20 mg/kg); PalH: (40 mg/kg).

Serum Metabolomics Analysis

PCA is an unsupervised pattern recognition approach used to reduce the dimension of UPLC-MS data and to disclose intrinsic clustering of samples. In this study, PCA was used to summarize and distinguish the metabolic phenotypes and metabolites between control, model, and PalH group in both ESI+ and ESI- models. QC can confirm whether the systematic error of the experiment is within the controllable range. The cluster analysis of QC suggested that the method was stability and repeatability. The PCA score plots showed that clear separations were observed among the clusters of the control, model and PalH group in both ESI+ and ESI− modes (**Figure 6**), which indicated *H. pylori*–induced remarkable changes in serum endogenous metabolites and Pal could restore the metabolic profiling of serum in CAG rats. The R^2X of ESI+ and ESI− PCA models confirmed the credibility of these two models. Thus, the CAG model was successful, and could be used to explore the effects of Pal on CAG induced by *H. pylori*. Subsequently, Summarized the influence of variables on the model according to the corresponding loading scores plots from PCA, multivariate analysis was used to explore specific differential metabolites.

The differential metabolites from control vs model group and model vs PalH group were identified in OPLS-DA mode respectively. The relevant parameter of OPLS-DA model and permutation tests (n=100) demonstrated that the modes had good predictive capabilities. Obvious classifications were observed among control, model and PalH groups in both of ESI+ and ESI- modes. Metabolites that meet a threshold of VIP ≥ 1.0 and | *P* (corr) | ≥ 0.58 in the corresponding S-plot were considered potential candidates (**Figure 7**). Combined the potential candidates obtained in ESI+ and ESI−. Based on ANOVA analysis ($P < 0.05$), candidates with significant changes were identified as biomarkers in the METLIN and Metaboanalyst databases. Finally, three biomarkers were screened in serum, and relevant information and variation trends between groups were listed in **Table 3** and **Figure 8**.

Urine Metabolomics Analysis

To further explored the overall metabolism in the urine of the CAG, PCA approach was applied to distinguish the metabolic phenotypes and metabolites between control, model, and PalH

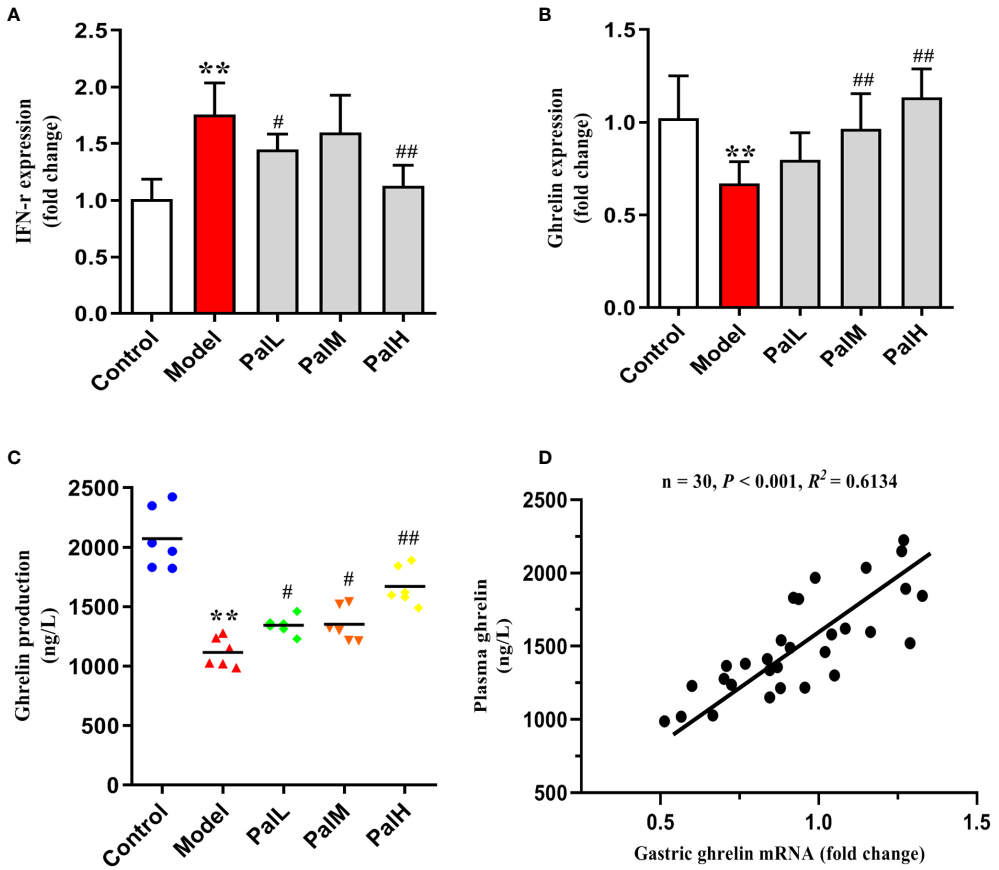


FIGURE 4 | Pal relieved the release disorder of ghrelin by inhibiting IFN-γ. **(A, B)** IFN-γ and ghrelin mRNA in gastric mucosa were analyzed by RT-PCR (n=6). **(C)** ghrelin production in serum was measured by ELISA (n=6). **(D)** Pearson correlation coefficient analysis of ghrelin expression in gastric mucosa and serum. $^{**}P < 0.01$ vs control group. $^{\#}P < 0.05$ and $^{\#\#}P < 0.01$ vs model group. PalL (10 mg/kg); PalM: (20 mg/kg); PalH: (40 mg/kg).

groups. The R^2X of ESI+ and ESI– in PCA models confirmed the reliability of these two models. The PCA score plots indicated remarkable changes of endogenous metabolites in urine induced by *H. pylori* and Pal could restore the metabolic profiling of urine in CAG rats (**Figure 9**).

OPLS-DA score plots showed that the metabolic profile of the model group deviated from control group, and PalH group in both of ESI+ and ESI- modes, suggesting that significant biochemical changes were induced by CAG. The relevant parameter of OPLS-DA mode and permutation tests (n = 100) demonstrated that the modes had good explanatory and predictive capabilities (**Figure 10**). Combined the potential candidates obtained in ESI+ and ESI-, and further determined biomarkers by using ANOVA analysis. Finally, the seven biomarkers in urine were summarized. **Table 3** and **Figure 8** listed the corresponding formulations, quality (m/z), retention time and change trend of each group.

Pathway Analysis of Pal Treatment

The hierarchical cluster analysis heatmap generated according to the relative concentration of metabolic markers in serum and urine can intuitively displayed the differences in metabolic profiles between different samples (**Figure 11A**). Metabo Analyst 4.0 was performed for pathway analysis to visualize the affected metabolic pathways in CAG rats. As shown in **Table 4** and **Figure 11**, Taurine and hypotaurine metabolism, Glycerophospholipid metabolism, Pentose and glucuronate interconversions were considered as the crucial signaling pathways in CAG and Pal treatment. In addition, the related metabolic pathways crosstalk with each other by the citric acid (TCA) cycle. The match status, *P* value, log(P) and impact of each pathway were listed in **Table 4**.

DISCUSSION

Huang Lian has been applied to endocrine system and gastrointestinal diseases in clinic for thousands of years (Zou et al., 2017; Ma et al., 2019). More and more studies regarding the effects of the active ingredients in HuangLian on gastrointestinal diseases is available. Previous studies have shown that Pal and

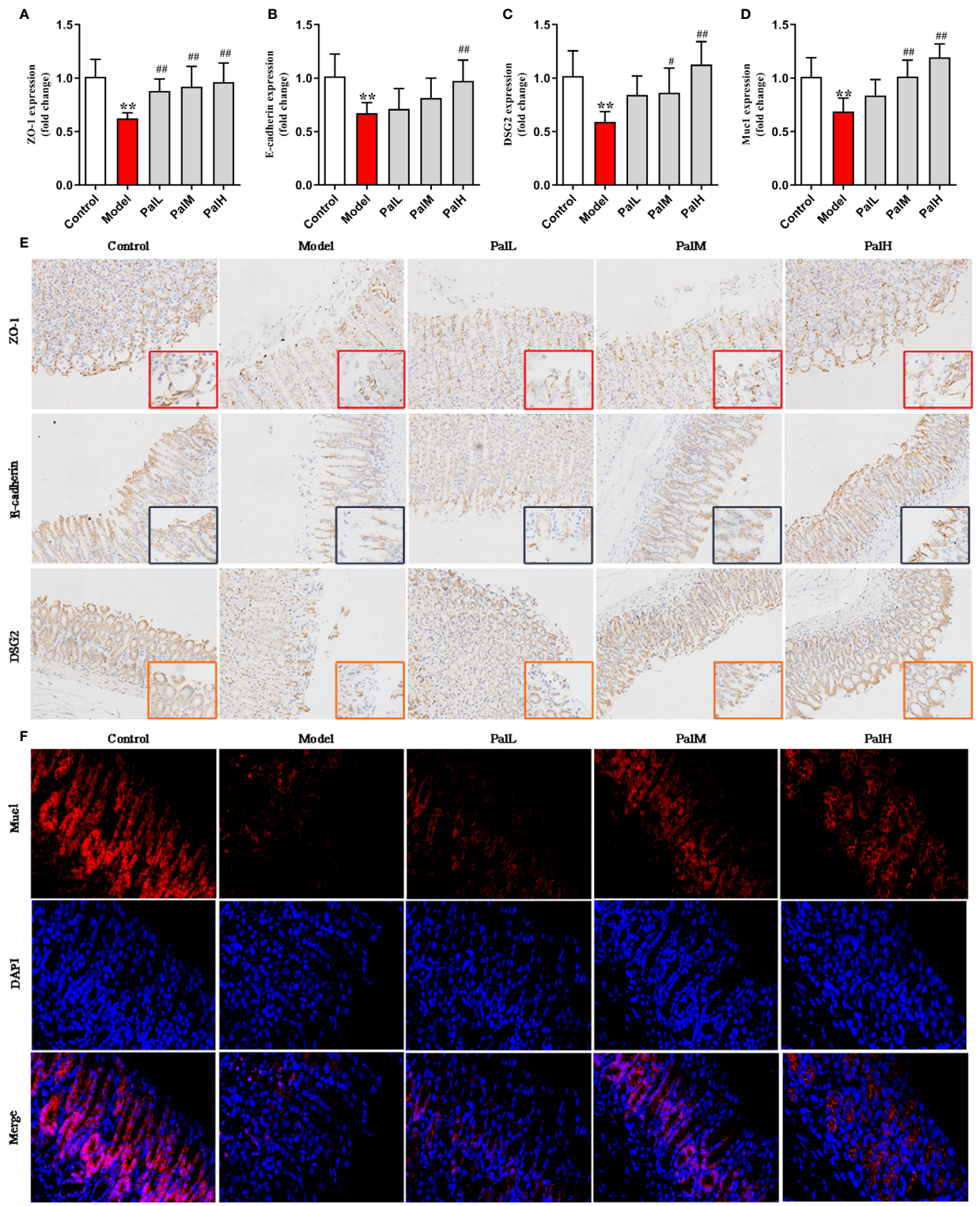


FIGURE 5 | Pal protected mucosal integrity by modulating epithelial junctions and mucins. **(A–D)** ZO-1 **(A)**, E-cadherin **(B)**, Desmoglein 2 (DSG 2) **(C)** and Muc1 **(D)** mRNA in gastric mucosa were analyzed by RT-PCR (n=6). **(E)** Representative immunohistochemical staining images in gastric mucosa showing ZO-1, E-cadherin, DSG2 expressing (200 × and 400 × magnification). **(F)** Representative immunofluorescence staining images in gastric mucosa showing Muc1 expressing (400 × magnification). $^{**}P < 0.01$ vs control group. $^{\#}P < 0.05$ and $^{\#\#}P < 0.01$ vs model group. PalL (10 mg/kg); PalM: (20 mg/kg); PalH: (40 mg/kg).

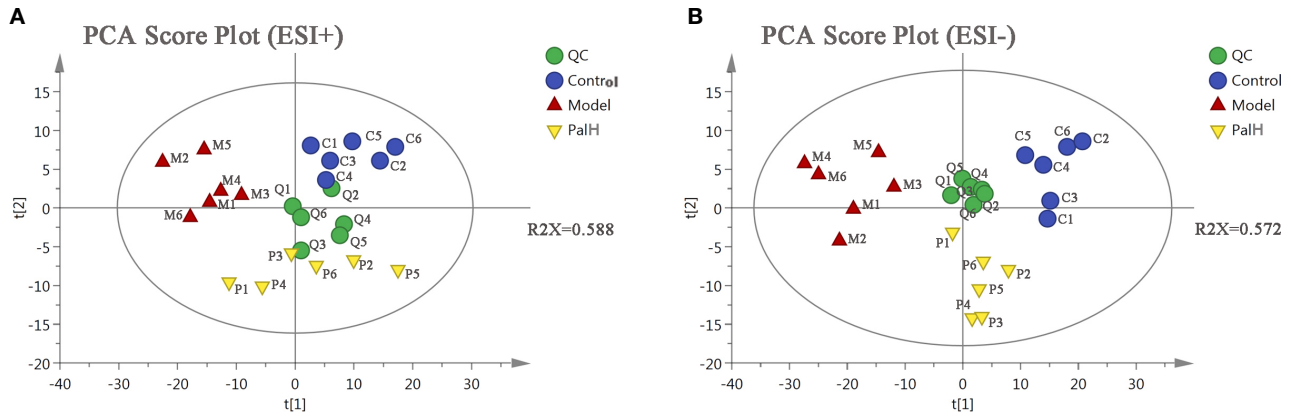


FIGURE 6 | The principal component analysis (PCA) score plot of serum metabolomics analysis. **(A)** ESI+ model. **(B)** ESI- model. PalH: (40 mg/kg).

berberine inhibited the proliferation of gastric cancer cells (MGC803) in a dose-dependent manner and the inhibitory effect more significantly in combination with berberine (Zhao and Zhang, 2011). Jung J et al. demonstrated the antibacterial activity of Pal and its protective effect on gastric injury through the *H. pylori* colony formation experiment and the hydrochloric acid/ethanol induced gastric ulcer model, and the efficacy is better than berberine (Jung et al., 2014). Moreover, Pal was confirmed to have a clear antibacterial activity against *H. pylori* in a molecular docking simulation experiment (Zhou et al., 2017). Therefore, Pal is considered to be a promising non-antibiotic drug candidate for the treatment of *H. pylori*–induced CAG.

H. pylori–induced gastritis is one of the optimized models used to study CAG. As in humans, weight loss, inappetence, diarrhea, and pathological changes in rats are usually consistent symptoms of CAG (Kishikawa et al., 2020). Given that the intractable characteristic and high morbidity of CAG, UPLC-Q-TOF/MS method based on serum combined with urin metabolomics was firstly investigated in this study to clarify the protective effect of Pal on CAG and attempted to clarify the mechanisms of action.

Gastric infections due to *H. pylori* overgrowth are associated with reduced fundic ghrelin and G-17 expression and increased IFN-γ production (Strickertsson et al., 2011). Ghrelin plays an essential role in the mechanism of gastric mucosal defense, the reduction of ghrelin production in the fundic is the main reason for the decrease of serum ghrelin concentration, and it is closely related to the ratio of PG I/PG II, in which the PG I/PG II < 3 is considered a reliable sign of severe atrophic gastritis. PG I is secreted only by secretory glands of the corpus mucosa, PG II is synthesized by gastric antrum and duodenum, and G-17 is only expressed by G cells of the antral mucosa. Thus the combination of the results of the PG I, PG II, PG I/PG II and G-17 test can more comprehensively and accurately detect the presence of CAG (Osawa et al., 2005; Zagari et al., 2017). In this study, the model group had high levels of pro-inflammatory cytokines IFN-γ, low levels of ghrelin, G-17, PG I, PG II, and PGI/PGII ratios. However, the levels of biomarkers and proinflammatory cytokines was decreased in Pal treatment revealed that Pal could effectively ameliorate CAG triggered by *H. pylori*.

CAG induced by *H. pylori* is triggered by the destruction of gastric mucosal epithelial barrier function, which further leads to excessive response of immune cells to microbiota. The gastrointestinal mucosa can protect the digestive tract from harmful substances and is an important barrier to maintain environmental stability in the digestive tract (Zhang et al., 2014). This mucosal barrier is predominantly composed of apical junctional complex (AJC) and mucins. AJC include tight junctions (TJs), adherens junctions (AJs) and desmosomes. Muc1 is a prototypical member of the membrane bound mucin subfamily. In this study, the expression and distribution of TJ proteins (ZO-1), AJ proteins (E-cadherin), desmosome protein (DSG2), and Muc1 in gastrointestinal epithelial cells infected with *H. pylori* were systematically investigated. The mRNA and protein expression of AJC and Muc1 were significantly downregulated in the model group, suggesting that *H pylori* breached the mucosal layer and increased the permeability of gastric mucosa. However, Pal promoted the mRNA and protein expression of AJC and Muc1, indicating that Pal could protect the gastric mucosal barrier from the *H.pylori* elicited epithelial structural damage by increasing mucin synthesis and improving epithelial AJC.

Subsequently, UPLC-Q-TOF/MS metabolomic analysis was used to determine the fingerprints of serum and urine metabolic characteristics of GCA rats. PCA and OPLS-DA model showed sufficient sensitivity and specificity to distinguish model from control group. The significant difference between the PalH and model group suggested Pal protected CAG by reversing potential metabolites to normal levels. Meanwhile, the biological function and relevant pathway were identified by HMDB and MetaboAnalyst platform to elucidate the underlying mechanism. 10 related endogenous metabolites were selected as potential biomarkers which were associated with Taurine and hypotaurine metabolism,

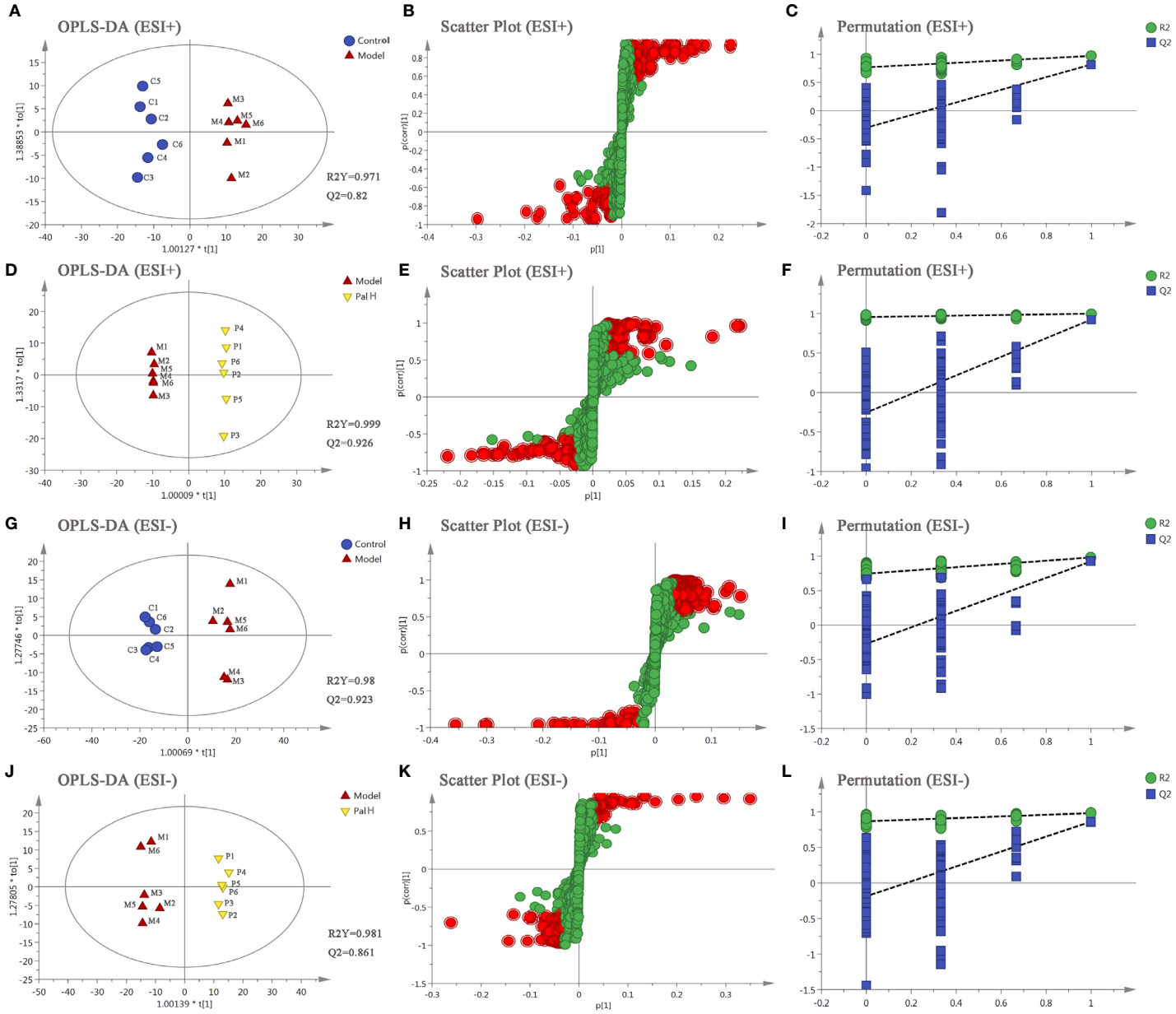


FIGURE 7 | The orthogonal-partial least squares-discriminant analysis (OPLS-DA) score plots, S-plots and 100-permutation test of serum metabolomics analysis. **(A–F)** ESI+ model. **(G–L)** ESI- model. PalH: (40 mg/kg).

TABLE 3 | Identified metabolites of serum and urine.

No	Source	Compound name	Formula	Query mass	Monoisotopic_mass	R.T. (min)	Pathway
1	Serum (ESI+)	Phosphatidylcholine	$C_{46}H_{82}NO_7P$	792.5951	791.5829	7.14	Glycerophospholipid metabolism
2	Serum (ESI-)	LysoPC(16:0/0:0)	$C_{24}H_{50}NO_7P$	496.3396	495.3325	15.35	Glycerophospholipid metabolism
3		Taurine	$C_2H_7NO_3S$	124.0073	125.0147	0.89	Taurine and hypotaurine metabolism; Primary bile acid biosynthesis
4	Urine(ESI +)	Glycerylphosphorylethanolamine	$C_5H_{14}NO_6P$	216.0631	215.0559	5.51	Glycerophospholipid metabolism
5		Pyridoxamine	$C_8H_{12}N_2O_2$	169.0971	168.0898	2.35	Vitamin B6 metabolism
6		Pantetheine	$C_{11}H_{22}N_2O_4S$	279.1318	278.1300	5.39	Pantothenate and CoA biosynthesis
7		Pantothenate	$C_9H_{17}NO_5$	220.1172	219.1107	2.91	Pantothenate and CoA biosynthesis
8		S-Adenosylmethioninamine	$C_{14}H_{23}N_6O_3S$	355.1565	355.1552	0.85	Cysteine and methionine metabolism; Arginine and proline metabolism
9	Urine (ESI-)	β-D-Glucuronoside	$C_{14}H_{18}O_7$	297.0975	298.1053	2.65	Pentose and glucuronate interconversions
10		Oxalosuccinate	$C_6H_6O_7$	189.0038	190.0114	2.72	Citrate cycle (TCA cycle)

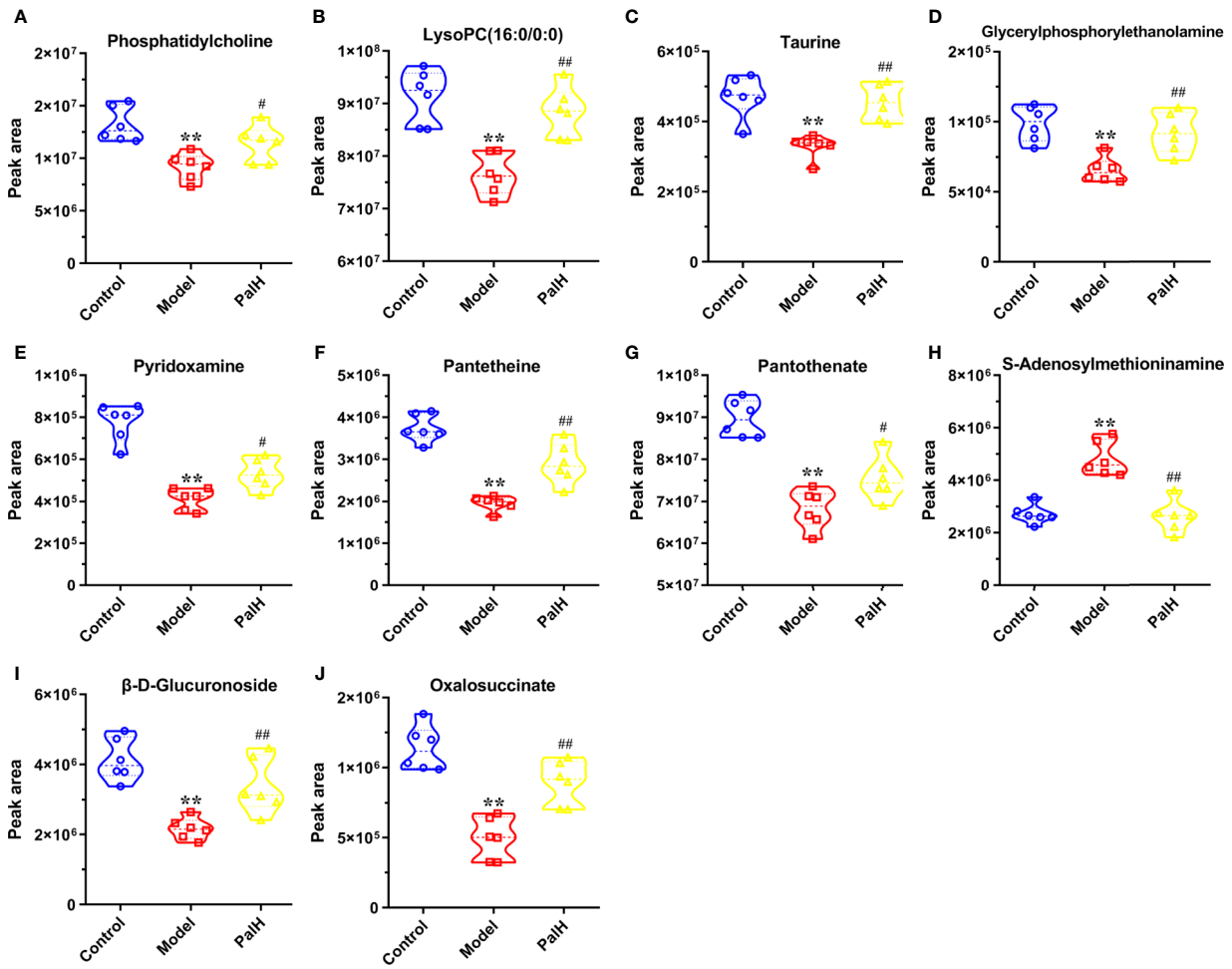


FIGURE 8 | Potential metabolites changes in *H. pylori* - induced CAG with PalH treatment. **(A)** Phosphatidylcholine. **(B)** LysoPC(16:0/0:0). **(C)** Taurine. **(D)** Glycerylphosphorylethanolamine. **(E)** Pyridoxamine. **(F)** Pantetheine. **(G)** Pantothenate. **(H)** S-Adenosylmethioninamine. **(I)** β-D-Glucuronoside. **(J)** Oxalosuccinate. $^{**}P < 0.01$ vs control group. $^{\#}P < 0.05$ and $^{\#\#}P < 0.01$ vs model group. PalH: (40mg / kg).

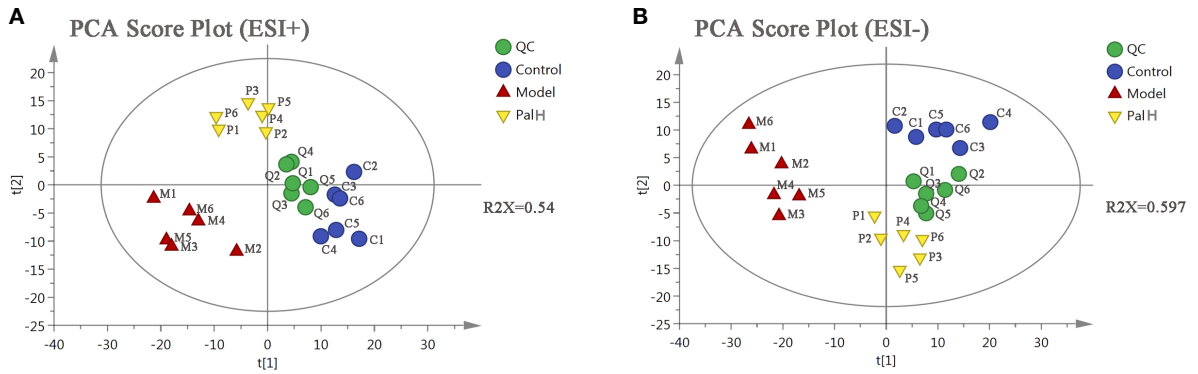


FIGURE 9 | The principal component analysis (PCA) score plot of urine metabolomics analysis. **(A)** ESI+ model. **(B)** ESI- model. PalH: (40 mg/kg).

Glycerophospholipid metabolism, Pentose and glucuronate interconversions, Vitamin B6 metabolism, Pantothenate and CoA biosynthesis, Cysteine and methionine metabolism, Primary bile acid biosynthesis, Arginine and proline metabolism, TCA cycle.

According to the influence value threshold of 0.10, Taurine and hypotaurine metabolism, Glycerophospholipid metabolism, Pentose and glucuronate interconversions are selected as the most relevant pathways. Numerous studies have proved that the disorders of Taurine metabolism play a pivotal pathogenetic role in the initiation and progression of gastrointestinal diseases (Gu et al., 2020). Taurine has been well recognized as an antioxidant both *in vitro* and *in vivo*, and high concentrations of taurine probably contribute to the protection of gastric mucosa from oxidative stress. *H. pylori* infection leads to a decrease in taurine in model rats, indicating that the antioxidant activity decreased in the course of CAG. Glycerophospholipid metabolism was continually disturbed during CAG which has been demonstrated to be closely associated with the immune response. Glycerophospholipid levels are significantly reduced in GCA patients, indicated the disease related dysfunction in glycerophospholipid metabolism (Sun et al., 2020). As one of the subcategories of carbohydrate metabolism, Pentose and glucuronate interconversions is the basis for providing more carbohydrates to the gastrointestinal tract to resist the more complex environment caused by *H. pylori*. In this study, immune dysfunction and energy metabolism disorders together provide a favorable environment for the colonization of *H. pylori*. Pal has a significant callback function on related biomarkers, which may help to improve the CAG induced by *H. pylori*.

Vitamin B6 (VB6) metabolism is necessary to maintain normal physiological functions *in vivo*. Studies have shown that VB6 participates in cellular and humoral immunity during the process of immune response. VB6 deficiency can cause a decline in immunity and affect the expression of certain inflammatory factors (IFN-γ, IL-8), and plays an important role in inflammation caused by gastrointestinal injury (Zhou et al., 2019). As a multifactorial disease, gastrointestinal diseases is ultimately caused by the imbalance between acid secretion and cytoprotective factors. Pantothenate and Pantetheine are important metabolite of Pantothenate and CoA biosynthesis, which are significantly reduced metabolites in gastric ulcers, suggesting Pantothenate and CoA biosynthesis was closely related to the progress of gastrointestinal diseases (Farrokhi et al., 2019). The balance of amino acid metabolism often determines the progression of the disease. In this study, CAG caused an increase in S-adenosylmethionine indicated the imbalance of Cysteine and methionine metabolism and Arginine and proline metabolism. Arginine and proline are considered as potential plasma biomarkers of gastric injury, which can monitor various physiological and pathological conditions of the gastrointestinal tract in real time (Shin et al., 2019). High levels of amino acids is a nutritional requirements for growth of *H. pylori* (Nedenskov, 1994). Turning to another obviously affected amino acid, taurine also affects Primary bile acid biosynthesis. The synthesis and secretion of bile acids are blocked resulting in excessive bacterial growth and impaired epithelial barrier function (AJC and Mcu1), further promoting bacterial transmembrane invasion. It was worth noting that, similar to previous studies, the TCA cycle was down-regulated in this study (Nishiumi et al., 2017). As a critical metabolic checkpoint in the pathological environment, TCA cycle drives a variety of important metabolic pathways and eventually forms a closely related interactive network.

In summary, Pal could reverse the metabolic disorder caused by CAG induced by *H. pylori*, destroy the favorable conditions of *H. pylori* colonization, maintain the gastric mucosal epithelial barrier, restore the immune function of the body, and effectively curb the rapid development of CAG (**Figure 11C**).

CONCLUSION

This study was the first to systematically explore the efficacy and molecular mechanism of Pal in the treatment of CAG induced by *H. pylori* based on serum and urine metabolomics. The results

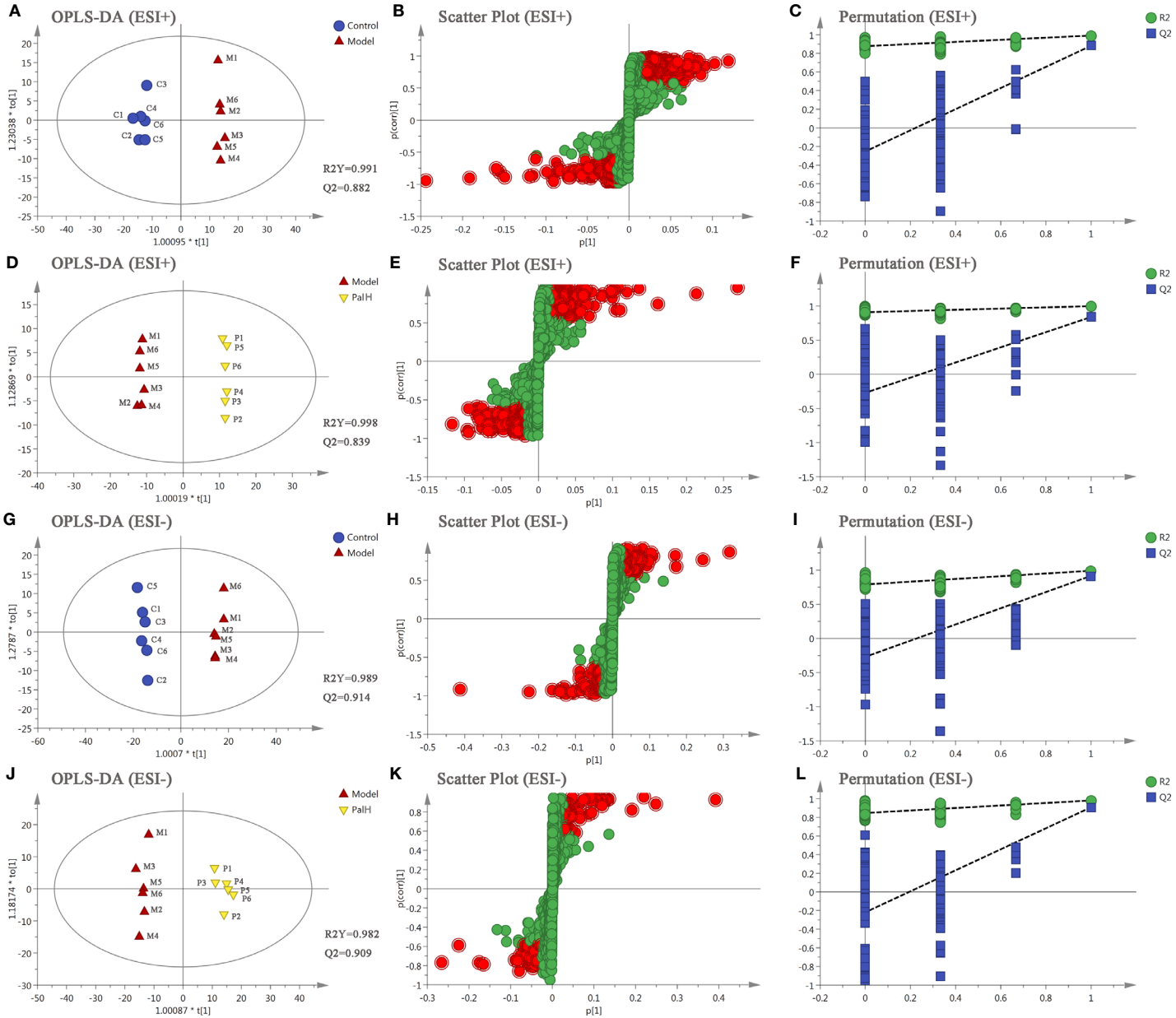


FIGURE 10 | The orthogonal-partial least squares-discriminant analysis (OPLS-DA) score plots, S-plots and 100-permutation test of serum metabolomics analysis. **(A–F)** ESI+ model. **(G–L)** ESI- model. PalH: (40 mg/kg).

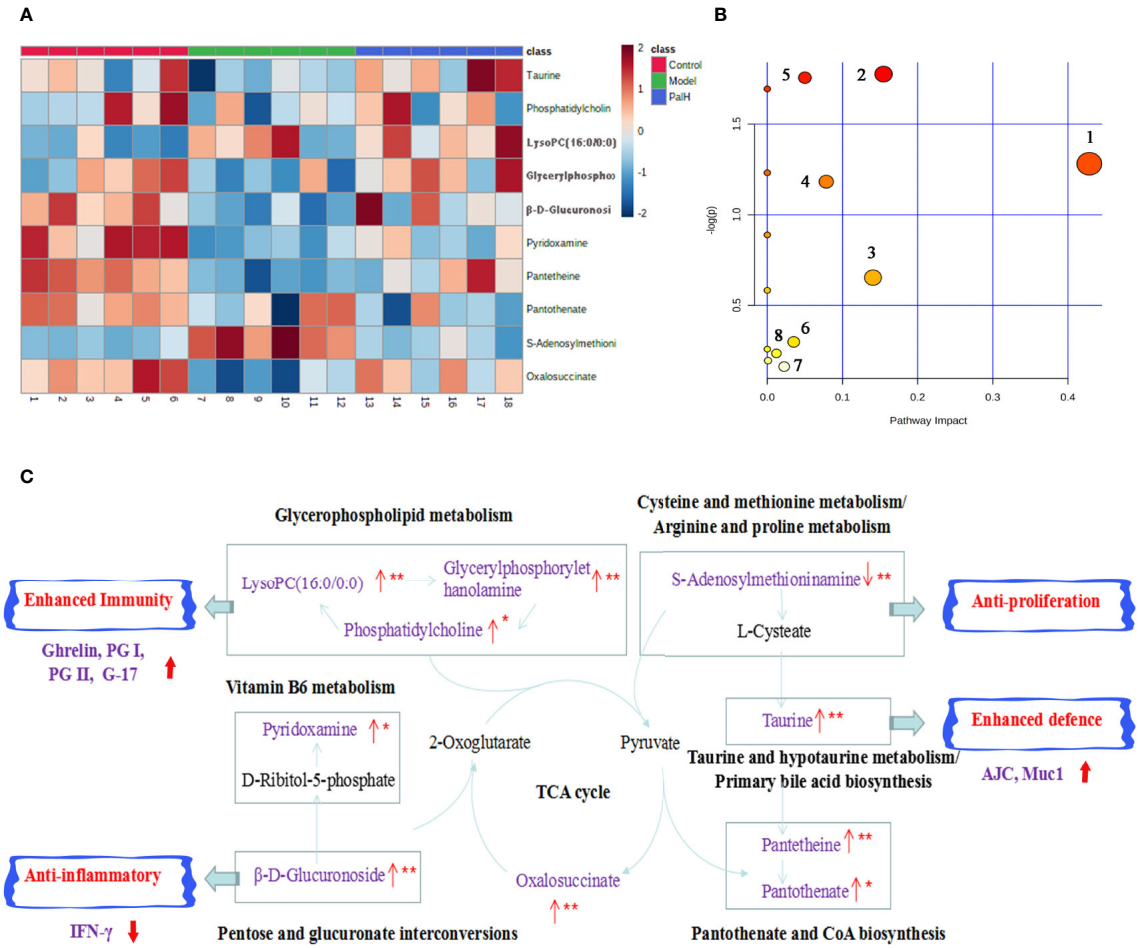


FIGURE 11 | Pathway analysis of Pal treatment. **(A)** The heatmap of 10 potential metabolites. **(B)** Metabolomic pathway construction of the metabolic pathways involved in the effects of Pal on chronic atrophic gastritis (CAG). **(C)** Signaling networks associated with the differentially expressed metabolic pathways. Red represents the detected metabolite.

TABLE 4 | Results of integrating enrichment analysis of biomarkers with MetaboAnalyst 4.0.

No	Pathway	Match status	Raw *p*	– log(p)	Impact
1	Taurine and hypotaurine metabolism	1/8	0.27773	1.2811	0.42857
2	Glycerophospholipid metabolism	3/36	0.16941	1.7754	0.15471
3	Pentose and glucuronate interconversions	1/18	0.52028	0.65339	0.14062
4	Vitamin B6 metabolism	1/9	0.3066	1.1822	0.07843
5	Pantothenate and CoA biosynthesis	2/19	0.1728	1.7556	0.05
6	Cysteine and methionine metabolism	1/33	0.7417	0.29881	0.03514
7	Primary bile acid biosynthesis	1/46	0.84974	0.16283	0.02239
8	Arginine and proline metabolism	1/38	0.79016	0.23552	0.01212
9	Citrate cycle (TCA cycle)	1/20	0.18215	1.7029	0.00

showed that the metabolism of taurine and subtaurine, the metabolism of glycerol phospholipid and the mutual transformation of pentose and glucuronide played a dominant role in the Pal treatment of *H. pylori*–induced CAG. The selected metabolites and metabolic pathways might be served as potential drug targets for CAG diagnosis and treatment, which is of great significance for the development of Pal-related drugs for the treatment of CAG.

DATA AVAILABILITY STATEMENT

The raw data supporting the conclusions of this article will be made available by the authors, without undue reservation, to any qualified researcher.

ETHICS STATEMENT

The animal study was reviewed and approved by Fifth Medical Center of PLA General Hospital (Approval ID: IACUC-2018-010).

AUTHOR CONTRIBUTIONS

All authors contributed to the article and approved the submitted version. Conceptualization: XC. Methodology: JZ, RW, HL, CB. Investigation: SW, JW, TY, YW, SR, YT. Writing—original draft: XC. Writing—review and editing: XC. Funding acquisition: YZ.

ACKNOWLEDGMENTS

The authors appreciate the financial support of the National key Research and Development Program (No.2018YFC1704500).

REFERENCES

Chen, X., Wang, R. L., Bao, C. M., Zhang, J. Z., Zhang, J. L., Li, R. S., et al. (2020). Palmatine ameliorates Helicobacter pylori-induced chronic atrophic gastritis by inhibiting MMP-10 through ADAM17/EGFR. *Eur. J. Pharmacol.* 882:173267. doi: 10.1016/j.ejphar.2020.173267

Crafa, P., Russo, M., Miraglia, C., Barchi, A., Moccia, F., Nouvenne, A., et al. (2018). From Sidney to OLGA: an overview of atrophic gastritis. *Acta BioMed.* 89, 93–99. doi: 10.23750/abm.v89i8-S.7946

Farrokhi, Y. R., Amiri-Dashatan, N., Koushki, M., Dadpay, M., and Goshadrou, F. (2019). A Metabolomic Study to Identify Potential Tissue Biomarkers for Indomethacin-Induced Gastric Ulcer in Rats. *Avicenna J. Med. Biotechnol.* 11 (4), 299–307.

Gu, J. P., Huang, C. H., Hu, X. M., Xia, J. M., Shao, W., and Lin, D. H. (2020). Nuclear magnetic resonance-based tissue metabolomic analysis clarifies molecular mechanisms of gastric carcinogenesis. *Cancer Sci.* 111 (9), 3195–3209. doi: 10.1111/cas.14443

Jung, J., Choi, J. S., and Jeong, C. S. (2014). Inhibitory Activities of Palmatine from Coptis chinensis Against Helicobactor pylori and Gastric Damage. *Toxicol. Res.* 30, 45–48. doi: 10.5487/TR.2014.30.1.045

Kishikawa, H., Ojiro, K., Nakamura, K., Katayama, T., Arahata, K., Takarabe, S., et al. (2020). Previous Helicobacter pylori infection-induced atrophic gastritis: A distinct disease entity in an understudied population without a history of eradication. *Helicobacter* 25 (1), e12669. doi: 10.1111/hel.12669

Lahner, E., Esposito, G., Pilozzi, E., Purchiaroni, F., Corleto, V. D., Di, G. E., et al. (2015). Occurrence of gastric cancer and carcinoids in atrophic gastritis during prospective long-term follow up. *Scand. J. Gastroenterol.* 50 (7), 856–865. doi: 10.3109/00365521.2015.1010570

Li, C., Huang, P., Wong, K., Xu, Y. F., Tan, L. H., Chen, H. B., et al. (2018). Coptisine-induced inhibition of Helicobacter pylori: elucidation of specific mechanisms by probing urease active site and its maturation process. *J. Enzyme Inhib. Med. Chem.* 33, 1362–1375. doi: 10.1080/14756366.2018.1501044

Ma, H., He, K., Zhu, J. W., Li, X. G., and Ye, X. L. (2019). The anti-hyperglycemia effects of Rhizoma Coptidis alkaloids: A systematic review of modern pharmacological studies of the traditional herbal medicine. *Fitoterapia* 134, 210–220. doi: 10.1016/j.fitote.2019.03.003

Nedenskov, P. (1994). Nutritional requirements for growth of Helicobacter pylori. *Appl. Environ. Microbiol.* 60 (9), 3450–3453. doi: 10.1128/AEM.60.9.3450-3453.1994

Nishiumi, S., Yoshida, M., and Azuma, T. (2017). Alterations in metabolic pathways in stomach of mice infected with Helicobacter pylori. *Microb. Pathog.* 109, 78–85. doi: 10.1016/j.micpath.2017.05.027

Osawa, H., Nakazato, M., Date, Y., Kita, H., Ohnishi, H., Ueno, H., et al. (2005). Impaired production of gastric ghrelin in chronic gastritis associated with Helicobacter pylori. *J. Clin. Endocrinol. Metab.* 90 (1), 10–16. doi: 10.1210/jc.2004-1330

Schulz, C., Schütte, K., Mayerle, J., and Malfertheiner, P. (2019). Helicobacter pyloriThe role of the gastric bacterial microbiome in gastric cancer: and beyond. *Therap. Adv. Gastroenterol.* 12:1756284819894062. doi: 10.1177/1756284819894062

Shin, S. Y., Jeong, H. M., Chung, S. E., Kim, T. H., Thapa, S. K., Lee, D. Y., et al. (2019). Simultaneous analysis of acetylcarnitine, proline, hydroxyproline, citrulline, and arginine as potential plasma biomarkers to evaluate NSAIDs-induced gastric injury by liquid chromatography-tandem mass spectrometry. *J. Pharm. BioMed. Anal.* 165, 101–111. doi: 10.1016/j.jpba.2018.11.051

Strickertsson, J. A., Døssing, K. B., Aabakke, A. J., Nilsson, H. O., Hansen, T. V., Knigge, U., et al. (2011). Interferon-γ inhibits ghrelin expression and secretion via a somatostatin-mediated mechanism. *World J. Gastroenterol.* 17 (26), 3117–3125. doi: 10.3748/wjg.v17.i26.3117

Sun, Y. F., Li, S. S., Li, J., Xiao, X., Hua, Z. L., Wang, X., et al. (2020). A clinical metabolomics-based biomarker signature as an approach for early diagnosis of gastric cardia adenocarcinoma. *Oncol. Lett.* 19 (1), 681–690. doi: 10.3892/ol.2019.11173

Tarabasz, D., and Kukula-Koch, W. (2020). Palmatine: A review of pharmacological properties and pharmacokinetics. *Phytother. Res.* 34 (1), 33–50. doi: 10.1002/ptr.6504

Topi, S., Santacroce, L., Bottalico, L., Ballini, A., Inchingolo, A. D., Dipalma, G., et al. (2020). Gastric Cancer in History: A Perspective Interdisciplinary Study. *Cancers (Basel)* 12 (2), 264. doi: 10.3390/cancers12020264

Wang, X., Sun, H., Zhang, A., Sun, W., Wang, P., and Wang, Z. (2011). Potential role of metabolomics approaches in the area of traditional Chinese medicine: as pillars of the bridge between Chinese and Western medicine. *J. Pharm. BioMed. Anal.* 55, 859–868. doi: 10.1016/j.jpba.2011.01.042

Wang, L., Wang, X., Zhang, S. L., Zhu, X. M., Liu, Y. Q., Song, Z. J., et al. (2017). Gastroprotective effect of palmatine against acetic acid-induced gastric ulcers in rats. *J. Natural Med.* 71 (1), 257–264. doi: 10.1007/s11418-016-1057-2

Wang, K., Chai, L. W., Ding, L. Q., and Qiu, F. (2017). Identification of metabolites of palmatine in rats after oral administration using ultra-high-performance liquid chromatography/quadrupole time-of-flight mass spectrometry. *Rapid Commun. Mass Spectrom.* 31, 523–537. doi: 10.1002/rcm.7819

Werawatganon, D. (2014). Simple animal model of Helicobacter pylori infection. *World J. Gastroenterol.* 20, 6420–6424. doi: 10.3748/wjg.v20.i21.642

Yokozawa, T., Satoh, A., Cho, E. J., Kashiwada, Y., and Ikeshiro, Y. (2005). Protective role of *Coptidis Rhizoma* alkaloids against peroxynitrite-induced damage to renal tubular epithelial cells. *J. Pharm. Pharmacol.* 57, 367–374. doi: 10.1211/0022357055470

Zagari, R. M., Rabitti, S., Greenwood, D. C., Eusebi, L. H., Vestito, A., and Bazzoli, F. (2017). Systematic review with meta-analysis: diagnostic performance of the combination of pepsinogen, gastrin-17 and anti-Helicobacter pylori antibodies serum assays for the diagnosis of atrophic gastritis. *Aliment. Pharmacol. Ther.* 46 (7), 657–667. doi: 10.1111/apt.14248

Zhang, C., Zhang, H. Y., Yu, L., and Cao, Y. (2014). Helicobacter pylori dwelling on the apical surface of gastrointestinal epithelium damages the mucosal barrier through direct contact. *Helicobacter* 19 (5), 330–342. doi: 10.1111/hel.12138

Zhao, W., and Zhang, X. Z. (2011). Inhibitory effect of Palmatine and berberine on the proliferation of HUMAN gastric cancer cell MGC803. *Life Sci. Instrum.* 9 (02), 44–47.

Zhou, J. T., Li, C.-L., Tan, L. H., Xu, Y. F., Liu, Y. H., Mo, Z. Z., et al. (2017). Inhibition of Helicobacter pylori and Its Associated Urease by Palmatine: Investigation on the Potential Mechanism. *PLoS One* 12, e0168944. doi: 10.1371/journal.pone.0168944

Zhou, J., Yao, N., Wang, S. X., An, D. C., Cao, K., Wei, J. L., et al. (2019). Fructus Gardeniae-induced gastrointestinal injury was associated with the inflammatory response mediated by the disturbance of vitamin B6, phenylalanine, arachidonic acid, taurine and hypotaurine metabolism. *J. Ethnopharmacol.* 235, 47–55. doi: 10.1016/j.jep.2019.01.041

Zou, K., Li, Z., Zhang, Y., Zhang, H. Y., Li, B., Zhu, W. L., et al. (2017). Advances in the study of berberine and its derivatives: a focus on anti-inflammatory and anti-tumor effects in the digestive system. *Acta Pharmacol. Sin.* 38, 157–167. doi: 10.1038/aps.2016.125

Conflict of Interest: The authors declare that the research was conducted in the absence of any commercial or financial relationships that could be construed as a potential conflict of interest.

Copyright © 2020 Chen, Zhang, Wang, Liu, Bao, Wu, Wen, Yang, Wei, Ren, Tong and Zhao. This is an open-access article distributed under the terms of the Creative Commons Attribution License (CC BY). The use, distribution or reproduction in other forums is permitted, provided the original author(s) and the copyright owner(s) are credited and that the original publication in this journal is cited, in accordance with accepted academic practice. No use, distribution or reproduction is permitted which does not comply with these terms.

frontiers in Pharmacology

REVIEW
published: 02 October 2020
doi: 10.3389/fphar.2020.588436

Intrahepatic T_H17/T_{Reg} Cells in Homeostasis and Disease—It's All About the Balance

Hannah K. Drescher[1*†], *Lea M. Bartsch*[1*†], *Sabine Weiskirchen*[2] *and Ralf Weiskirchen*[2]

[1] Division of Gastroenterology, Massachusetts General Hospital and Harvard Medical School, Boston, MA, United States, [2] Institute of Molecular Pathobiochemistry, Experimental Gene Therapy and Clinical Chemistry (IFMPEGKC), University Hospital, RWTH Aachen, Aachen, Germany

Both acute and chronic hepatic inflammation likely result from an imbalance in the T_H1/T_H2 cell response and can lead to liver fibrosis and end-stage liver disease. More recently, a novel CD4+ T helper cell subset was described, characterized by the production of IL-17 and IL-22. These T_H17 cells 50were predominantly implicated in host defense against infections and in autoimmune diseases. Interestingly, studies over the last 10 years revealed that the development of T_H17 cells favors pro-inflammatory responses in almost all tissues and there is a reciprocal relationship between T_H17 and T_{Reg} cells. The balance between $T_H17$and T_{Reg} cells is critical for immune reactions, especially in injured liver tissue and the return to immune homeostasis. The pathogenic contribution of T_H17 and T_{Reg} cells in autoimmunity, acute infection, and chronic liver injury is diverse and varies among disease etiologies. Understanding the mechanisms underlying T_H17 cell development, recruitment, and maintenance, along with the suppression of T_{Reg} cells, will inform the development of new therapeutic strategies in liver diseases. Active manipulation of the balance between pathogenic and regulatory processes in the liver may assist in the restoration of homeostasis, especially in hepatic inflammation.

Keywords: T_H17 cells, T_{Reg} cells, T_H17/T_{Reg} balance, liver, autoimmune diseases, viral infection

OPEN ACCESS

Edited by:
Stefano Fiorucci,
University of Perugia, Italy

Reviewed by:
Michele Biagioli,
University of Perugia, Italy
Jae-Sung Kim,
Washington University in St. Louis, United States

****Correspondence:***
Hannah K. Drescher
hdrescher@mgh.harvard.edu
Lea M. Bartsch
lbartsch1@mgh.harvard.edu

[†]These authors have contributed equally to this work

Specialty section:
This article was submitted to Gastrointestinal and Hepatic Pharmacology, a section of the journal Frontiers in Pharmacology

Received: *28 July 2020*
Accepted: *15 September 2020*
Published: *02 October 2020*

Citation:
Drescher HK, Bartsch LM, Weiskirchen S and Weiskirchen R (2020) Intrahepatic T_H17/T_{Reg} Cells in Homeostasis and Disease—It's All About the Balance. Front. Pharmacol. 11:588436. doi: 10.3389/fphar.2020.588436

INTRODUCTION

CD4 T cells play a central role in mediating the host immune response to pathogens and in autoimmunity, cancer, and chronic inflammation. They maintain and enhance CD8 T cell responses, interact with B cells to induce antibody development, regulate the function of monocytes/macrophages, and orchestrate the immune response to pathogens. CD4+ T cells also modulate immune homeostasis by suppressing pro-inflammatory immune responses, build immunologic memory, and control autoimmunity (Zhu et al., 2010). These functions are achieved through the differentiation of naïve CD4+ T cells into subsets of effector, memory, and regulatory T cells.

T cell activation and differentiation rely on different stimuli, and differentiation is initiated by a cognate antigen presented by specialized antigen-presenting cells (APCs) or other immune cells. Fragmented antigens are presented on major histocompatibility complex 2 (MHC-2) molecules and

recognized by the T cell receptor (TCR). Various co-stimulatory receptors and cytokines are essential for T cell activation and determine the direction of T cell differentiation.

Distinct subpopulations of CD4 T cells originating from a common precursor were first described in 1986: in mouse T cell clones, Mosmann and Coffman found that two types of T helper cells could be distinguished by their cytokine production, lymphokine activity, and transcription factor and surface marker expression (Mosmann et al., 1986). The authors defined type 1 T helper cells (T_H1) by their secretion of interferon-γ (IFN-γ), interleukin-2 (IL-2) and tumor necrosis factor-α (TNF-α). Type 2 T helper cells (T_H2) were characterized by the expression of IL-4, IL-5, and IL-13. Interestingly, the cytokines secreted by each mature T helper cell subset directly antagonize the development and differentiation of the corresponding opposite T helper cell subtype, thereby sustaining lineage-specific immune responses.

This profile has since been refined. Intensive studies of the complex cytokine milieu and transcription factor networks involved in the differentiation of CD4 T helper cell subsets originating from the same naïve CD4 T cell precursor identified many more T helper cell subsets. The potentially distinct T cell lineages include not only T_H1, T_H2, T_H17, and peripheral regulatory T cells (pT_{Reg}) cells, but also T_H9, T_H22, regulatory type 1 (Tr1), and follicular helper T cells (T_{FH}) (Saravia et al., 2019). CD4+ T cell lineages are now understood to be a plastic and flexible network. One CD4+ subset cannot differentiate from only one distinct precursor cell, but rather differentiates from different subsets depending on the environmental milieu (**Figure 1**).

In this review, we discuss developmental differences between T_H17 and T_{Reg} cells and their roles in health and disease, with a focus on liver disease. The fragile balance between these two cell types was recently found to play a crucial role in maintaining immune homeostasis. A shift of this balance drives pro-inflammatory immune responses, especially in chronic inflammatory diseases, cancer and autoimmunity. Here, we highlight the intrahepatic effects of this balance in acute and chronic inflammation as well as in liver cancer and autoimmunity.

T_H17 CELLS IN HEALTH AND DISEASE

A T helper cell subset of IL-17 producing T_H17 cells defends against fungal and extracellular bacterial infection and are integral in tissue inflammation and autoimmune diseases (Tesmer et al., 2008). While it was first believed that these cells are an inflammatory subset within the T_H1 lineage, it was later determined that T_H17 cells are an independent T helper cell lineage (Aarvak et al., 1999).

T_H17 Cell Development

The discovery of a new T helper cell subset with pro-inflammatory properties, referred to as T_H17 cells because of their expression of IL-17A, revolutionized the understanding of the adaptive immune system in the early 2000s (Park et al., 2005). T_H17 cell differentiation in secondary lymphoid organs

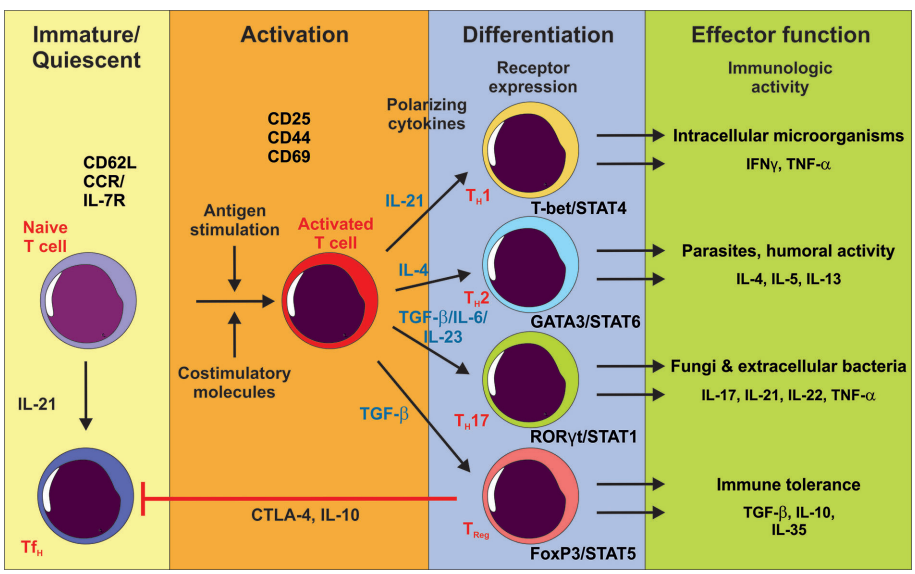


FIGURE 1 | After activation of the T cell receptor by antigen stimulation and co-stimulation, immature CD4+ naïve T cells proliferate and can differentiate into different effector T cells depending on the cytokine milieu. IL-21 stimulation promotes the T_H1 subpopulation accompanied with T-bet/STAT4 expression and effector function against intracellular pathogens. T_H2 cell populations develop after IL-4 stimulation with GATA3/STAT6 upregulation and supporting anti-parasite immune response and humoral activity. TGF-β in the presence of pro-inflammatory cytokines promotes T_H17 cell differentiation. T_H17 cells support the immune response against fungi and extracellular bacteria, whereas T_{Reg} cells have an immune tolerant function by producing anti-inflammatory cytokines and inhibiting T_{FH} function. Although these specific cytokines are important for CD4+ T cell subpopulation development, the differentiation is a plastic and flexible network.

depends on an inflammatory cytokine milieu consisting of IL-23, TGF-β, IL-6, IL-1β, and IL-21 to activate the expression of the lineage-specific transcription factor RORγt, fostering T_H17 cell generation. The role of RORγt was described by Ivanov et al. in 2006, who found this transcription factor to be expressed by IL-17 producing T helper cells in the lamina propria; in RORγt-deficient mice, IL-17+ cells were absent (Ivanov et al., 2006).

T_H17 cells expand in the periphery and at the tissue site of inflammation and secrete a distinct group of effector molecules such as IL-17A, IL-17F, IL-21, IL-22, and IL-6 and express IL-23 receptor (IL-23R) on their surface (Bettelli et al., 2006; Mangan et al., 2006). Human T_H17 cells originate from a CD161+ (the human equivalent to NK1.1) precursor in the thymus and umbilical cord blood and express CCR4 and CCR6 but not CXCR3 (Cosmi et al., 2008; Maggi et al., 2010).

Autocrine- and paracrine-derived TGF-β plays an interesting role during T_H17 cell polarization. During the induction of RORγt expression, TGF-β synergizes with IL-6. TGF-β and IL-6 typically have opposing effects, but in this setting these proteins amplify the maturation of T_H17 cells. In an autocrine amplification loop, TGF-β is further able to synergize with IL-21, which is predominantly produced by T_H17 cells. This synergy promotes and enhances T_H17 cell differentiation and pro-inflammatory immune responses (Gutcher et al., 2011). High concentrations of TGF-β in the absence of pro-inflammatory cytokines can lead to the inhibition of RORγt expression.

TGF-β can also induce the surface expression of IL-23R on differentiating T_H17 cells, along with IL-6/IL-21, making the cells responsive to the inflammatory cytokine IL-23. IL-23 is a member of the IL-12 cytokine family and is mainly produced by APCs. It enhances the activation of STAT3, which together with RORγt stabilizes T_H17 cell function. Therefore, IL-23 is not only important for T_H17 cell generation and thereby the activation and maintenance of inflammatory responses at the tissue site of inflammation, but also promotes persistent chronic inflammation by supporting the proliferation of T_H17 cells within the activated memory T cell pool (Aggarwal et al., 2003; Zhou et al., 2007; McGeachy et al., 2009).

In 2007, McGeachy et al. and Korn et al. described "classical" and "alternative" modes of T_H17 cell activation that were further supported by a study from Ghoreschi et al. in 2010 (Korn et al., 2007; McGeachy et al., 2007; Ghoreschi et al., 2010). The different modes are driven by the availability of IL-23 and TGF-β. "Classical" T_H17 cells, which arise from naïve CD4 T cells in the presence of TGF-β and IL-6 and the relative lack of IL-23, act through nonpathogenic expression of IL-10. Absence of expression of the TGF-β RII prevents the formation of T_H17 cells that mediate the development of experimental autoimmune encephalomyelitis (EAE) (Veldhoen et al., 2006). The idea of a nonpathogenic T_H17 cell subtype is further underlined by the fact that in homeostasis, T_H17 cells are present in the intestine without detrimental effects. "Alternative" T_H17 cells mature in the presence of IL-23 and are the pathogenic T_H17 subtype. Overall, the development of T_H17 cells is driven by a complex equilibrium of cytokine milieu, which influences many fine-tuning processes and a spectrum of effector functions.

The secretion of cytokines from either terminally differentiated T_H1 (IFN-γ) or T_H2 (IL-4) cells antagonizes the expansion of other T helper cell subtypes to sustain a lineage-specific immune response during infection. The differentiation of T_H17 cells is negatively regulated by IFN-γ and IL-4 *via* the inhibition of IL-23 and by T_{Reg} cells *via* retinoic acid and IL-2. Opposingly, IL-17 and IL-23 hamper the development of T_H1 cells (Harrington et al., 2005; Nakae et al., 2007). Interestingly, another IFN-γ and IL-4 independent pathway controls the development of T_H17 cells. This process is driven by an additional member of the IL-12 family, IL-27. Like IL-12 and IL-23, IL-27 is secreted by APCs and acts independently of IFN-γR, IL-6R, and T-Bet but requires STAT1. Batten et al. and Stumhofer et al. found that a lack of IL-27 signaling lead to an increase in T_H17 cells in autoimmune encephalomyelitis and chronic encephalitis (Batten et al., 2006; Stumhofer et al., 2006).

Unlike T_H1 and T_H2 cells, T_H17 cells have an unstable cytokine memory and convey a surprising capacity of late-stage plasticity in their polarization status to adapt to a changing microenvironment. Because T_H17 cells express low levels of IL-12R, they influence a phenotype shift after IL-12 stimulation that downregulates IL-17 and makes the cells susceptible to polarizing into a T_H1-, but not a T_H2-, like phenotype (Lee et al., 2009). This plasticity and the synergy between T_H1 and T_H17 cells is important for host defense mechanisms, as shown in a mouse model of *Mycobacterium tuberculosis* infection in which an early T_H17 immune response recruited T_H1 cells to the site of inflammation and promoted the development of T cell memory (Khader et al., 2007). It can also be a driving mechanism in autoimmunity and cancer.

T_H17 Cells in Host Defense and Autoimmunity

Until 1996, it was assumed that autoimmune diseases are the consequence of a dysregulation of T_H1 responses. A study by Ferber et al. showed that loss of IFN-γ did not prevent the development of EAE but rather worsened disease progression (Ferber et al., 1996). Based on those findings, Oppmann and colleagues described IL-23 as new cytokine secreted by dendritic cells (DCs) that can induce the production of IFN-γ and IL-17 (Oppmann et al., 2000). Antibody-mediated blockade of IL-23 and generation of IL-23 deficient mice highlighted its involvement in the development of Crohn's disease, psoriasis, EAE, and collagen-induced arthritis and the experimental animals either showed delayed and reduced disease severity or never developed autoimmune disease (Cua et al., 2003; Murphy et al., 2003; Mannon et al., 2004; Krueger et al., 2007). Clinical trials using monoclonal antibodies interfering with IL-12 and IL-23, such as ustekinumab, showed promising results in the improvement of psoriasis and psoriatic arthritis symptoms. In chronic ulcerative colitis patients, blockade of the interaction of IL-12 and IL-23 and their specific receptors on T_H1 and T_H17 cells also showed beneficial effects (Sands et al., 2019). Other antibodies, such as secukinumab, specifically targeting IL-17A were also highly effective in psoriasis patients (Sanford and McKeage, 2015).

Additionally, blockade of IL-17 or the loss of the regulatory mediators RORγt and IL-6 resulted in comparable outcomes ***via*** a lack of infiltration of T_H17 cells into the tissue sites of inflammation, pointing to a crucial role for these cells in the development and progression of autoimmune diseases. Finally, experiments performing an adoptive transfer of T_H17 cells clearly showed that these cells, but not T_H1 cells, modulate autoimmune conditions in mice. This finding was supported in human patients with multiple sclerosis, rheumatoid arthritis, and psoriasis, in whom increased levels of IL-17 and IL-23 were observed (Ziolkowska et al., 2000; Cho et al., 2004; Vaknin-Dembinsky et al., 2006). Although an increasing body of evidence points to a dominant role of T_H17 cells as inducers of autoimmunity, it is important to note that T_H1 cells are also crucial in the development of autoimmunity. Each target tissue of inflammation actively participates in the formation of a site-specific cytokine milieu through its cellular composition.

The gut is an especially interesting organ to investigate the plasticity of T_H17 cells. In homeostasis, the intestine is the primary site of T_H17 cell differentiation, and the gut microbiota heavily influences its regulation. The TCR of intestinal T_H17 cells has a distinct specificity for antigens coming from segmented filamentous bacteria, suggesting that these bacteria are critical for the induction of gut-resident T_H17 maturation (Huber et al., 2012). The function of these cells under non-pathogenic conditions is to protect against microbial invasion and maintain intestinal barrier function as well as to maintain other barrier sites of the body such as the lung epithelium or the skin. Non-pathogenic characteristics of these cells can specifically be found in the small intestine, where they limit inflammation in response to bacterial or parasitic infections ***via*** the secretion of IL-10. The fragile and complexly controlled phenotype of T_H17 cells can easily shift to an activated state in which cells attain pathogenicity and induce tissue inflammation that often leads to autoimmunity in the intestine and in other distant organs (Wu et al., 2010). In Peyer's Patches, T_H17 cells transition into a phenotype similar to T_{FH} cells producing IL-21 and Bcl-6 that can induce the production of IgA antibodies by germinal center B cells (Hirota et al., 2013). Upon bacterial infection in the colon, T_H17 cells can transform into cells producing IL-17 and IFN-γ simultaneously in an IL-23 dependent manner and further develop into a TH1-like cell type. Transferring this cell type can lead to a T_H17/T_H1 cell-induced transfer-colitis (Morrison et al., 2013; Harbour et al., 2015).

In humans, T cells expressing IL-17 and IFN-γ were found in peripheral blood and the gut lamina propria of patients with inflammatory bowel disease (Globig et al., 2014). T_H17/T_H1 cells are present at the organ site of inflammatory responses in different models of autoimmune diseases, such as in the colon in chronic colitis or as revealed by single-cell RNA-sequencing analysis in experimental autoimmune encephalitis (EAE), which serves as model for human multiple sclerosis (Neurath et al., 2002; Gaublomme et al., 2015). Hirota and colleagues demonstrated that these cells derive from T_H17 rather than from T_H1 cells (Hirota et al., 2011). This was further supported by a study from Bettelli **et al.** who showed that animals deficient for the transcription factor T-bet were protected against the development of EAE (Bettelli et al., 2004).

These findings suggest that T cells expressing IL-17 and IFN-γ, also known as double producers, are highly pathogenic and predominantly involved in autoimmune diseases and tissue inflammation. However, it is not fully understood whether the production of IFN-γ by T_H17 cells serves to limit T_H17 cell-induced inflammation or rather promotes inflammation.

REGULATORY T CELLS (T_{REG}) IN HEALTH AND DISEASE

T_{Reg} Development

Regulatory T cells (T_{Reg}) balance host defense against foreign pathogens, foster immune tolerance, and orchestrate immune homeostasis. The two main T_{Reg} subsets are natural T_{Reg} cells (nT_{Reg}), which provide central tolerance against self-antigens, and peripheral T_{Reg} cells (pTReg), which develop extrathymically from conventional T cells and recognize non-self-antigens (Sakaguchi, 2004). T cells maintain peripheral tolerance by regulating inflammatory responses against the microbiota, commensals, and pathogens (Hadis et al., 2011; Lathrop et al., 2011) (**Figure 2**).

Natural T_{Reg} Development

nT_{Regs} develop during the neonatal period during thymocyte maturation (Liston et al., 2008). Stable nT_{Reg} development requires a complex network of antigen presenting cells (APCs) and 1) TCR-dependent recognition of self-antigens, 2) cytokine stimulation (IL-2, IL-15, and IL-7), and 3) other costimulatory signals (Bayer et al., 2005). The TCR repertoire of nT_{Reg} cells varies from the effector T cell repertoire with only minor overlap (Wong et al., 2007). The recognition affinity of self-antigens by nT_{Reg} cells is crucial for nT_{Reg} development and must fall between positive and negative selection (Maloy and Powrie, 2001). In addition to affinity to the MHC self-antigen complex, the expression level on the APC is important for optimal nT_{Reg} maturation. Cytokine stimulation by IL-2, IL-15, and IL-7 promote nT_{Reg} development, function, and homeostasis (Vang et al., 2008). Costimulatory signals through CD28 stimulation are also essential to maintain nT_{Reg} survival and to avoid defective nT_{Reg} development (Tai et al., 2005). Thus, costimulatory signals function as expansion, rather than as selective, signals.

During thymic differentiation of nT_{Reg} cells, immature single-positive CD4+ T cells express the IL-2 receptor α chain (CD25) (Setoguchi et al., 2005). CD25 has high IL-2 affinity, is continuously expressed on T_{Reg} cells, and benefits T_{Reg} responsiveness in comparison to effector cells when IL-2 concentrations are low. CD25 deficiency is related to defective T_{Reg} development, function, and an imbalanced immune system (Goudy et al., 2013). After differentiation, nT_{Reg} cells stabilize their lineage specific transcription factor forkhead box protein 3 (FOXP3) and gain suppressive functions (Fontenot et al., 2017).

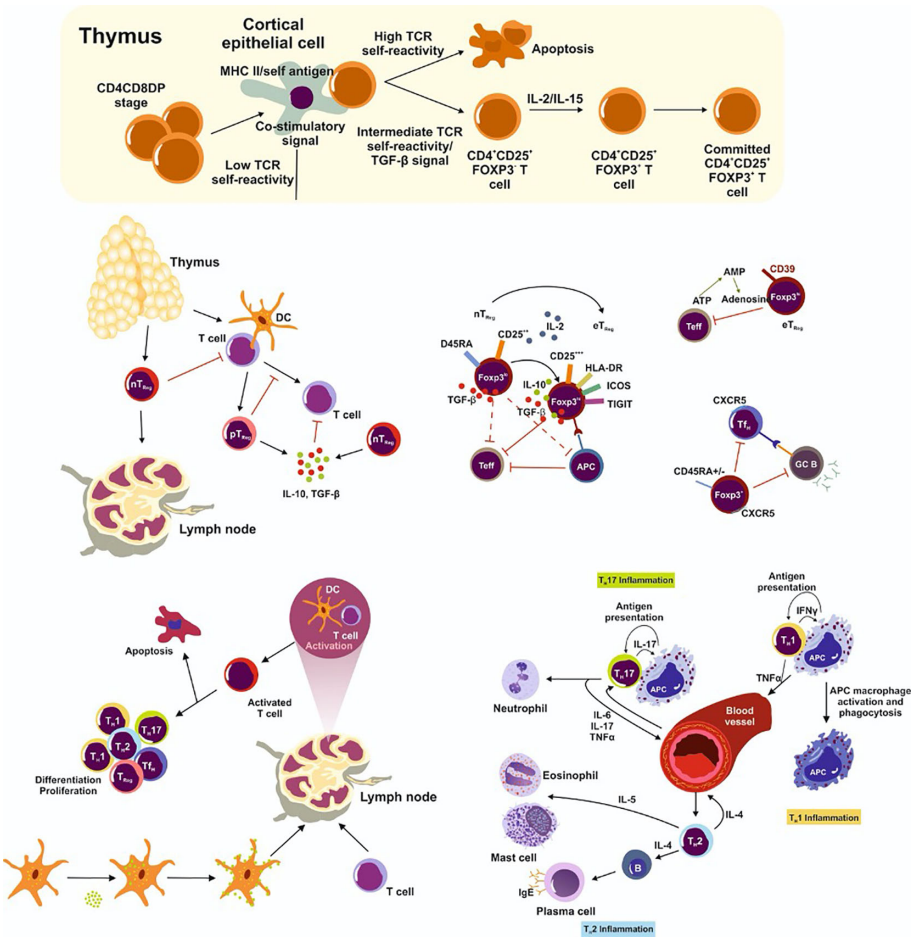


FIGURE 2 | Natural T_{Reg} cells (nT_{Reg}) maturate in the thymus. Their development requires the interplay of TCR-dependent recognition of self-antigen, a specific cytokine milieu (including TGF-β, IL-2, IL-7, IL-15) and the presence of co-stimulatory factors. They then infiltrate into the periphery. In the lymph node, T cells encounter a specific antigen from antigen presenting cells and become activated. Depending on the strength of the TCR binding and the presence or absence of co-stimulatory factors, cells either differentiate and proliferate into effector cells or undergo apoptosis. Peripheral T_{Reg} (pT_{Reg}) cells develop predominately in the periphery from naïve CD4+ T cells. However, nT_{Reg} and pT_{Reg} cells share the lineage markers CD25 and FoxP3 which are highly expressed in effector T_{Reg} cells (eT_{Reg}). eT_{Reg} cells suppress antigen presenting cells (APC) and effector T cells (T_{eff}) and are thereby very efficient in inhibiting the pro-inflammatory immune response. Furthermore, T_{Reg} cells express CD39 on the cell surface to convert extracellular ATP (eATP) to adenosine and prevent a pro-inflammatory immune response. Follicular helper T (T_{FH}) cells suppress the germinal center B cell reaction. Importantly, T_{Regs} also inhibit T_{eff} in the circulation. T_H17 cells secret pro-inflammatory cytokines and attract neutrophils to the inflammation site, while T_H1 cells promote macrophage development and function and T_H2 cells lead to plasma, eosinophil, and mast cell differentiation and generate a pro-inflammatory immune response.

They further exhibit a specific CpG hypomethylation at three conserved non-coding DNA sequences (CNS) at the FOXP3 promotor, influencing the overall transcriptional activity of the cell (Toker et al., 2013). These epigenetic modifications are obligatory for T_{Reg} lineage stability, because they influence the activity of central signaling pathways like NF-κB, NFAT, STAT5, mTOR, and the binding of transcription factors to the FOXP3 promotor (Zheng et al., 2010). Further, T_{Reg}-specific demethylation regions (TSDRs) contribute to a specific demethylation signature abundant in T_{Reg} function-defining genes (e.g., CTLA-4, IL-2RA, IKzf4) which regulate the overall transcriptional activity, development, and function of T_{Reg} cells.

Although FOXP3 is interrelated with T_{Reg} function, its expression is not exclusive for T_{Reg} cells as it can be transiently upregulated in activated T cells and likewise several T_{Reg} specific genes are FOXP3 independent. However, FOXP3 is necessary but not sufficient to induce T_{Reg} cells (Hill et al., 2007).

Peripheral T_{Reg} Development

In contrast to nT_{Reg} cells, pT_{Reg} cells develop in the peripheral tissue from naïve CD4+ T cells across the lifespan of an individual. pT_{Reg} cells also have a slightly different TCR repertoire and prevent an overwhelming immune response from occurring in response to microbiota, commensals, and pathogens (Hadis et al., 2011; Lathrop et al., 2011). pT_{Reg} and nT_{Reg} cells share the expression of the lineage defining molecules CD25 and FOXP3. Although, the frequency of pT_{Reg} cells is low, their percentage can be enriched in different tissues under

inflammatory conditions (Curotto de Lafaille et al., 2008). Like nT_{Reg} cells, the promotion of pT_{Reg} differentiation is driven by TCR signaling, TGF-β, and IL-2 and costimulatory signals (Chen et al., 2003). The importance of TGF-β signaling was demonstrated in mice, when TGF-β deficiency prevented pT_{Reg} differentiation and FOXP3 stabilization (Marie et al., 2005) suggesting that specific demethylation at the FOXP3 promotor is important for pT_{Reg} differentiation, function, and lineage stability (Takimoto et al., 2010).

pT_{Reg} development can differ by tissue. The process is highly induced in the intestine because of the special immune demands at this site. Primarily, mucosal DCs support pT_{Reg} development by producing TGF-β and retinoic acid (Coombes et al., 2007). The latter supports FOXP3 stabilization by CNS1 (Mucida et al., 2009). In addition, pT_{Reg} differentiation is enhanced by metabolites produced by the microbiota in the intestine, along with chromatin structure and FOXP3 stabilization facilitated by short chain fatty acids (Arpaia et al., 2013). Fascinatingly, a high percentage of the pT_{Reg} population in the intestine co-expresses RORγt and FOXP3 while preserving the overall epigenetic and genetic signature and function of T_{Reg} cells (Yang et al., 2016).

The peripheral FOXP3+ cell population is very heterogenous and can be divided into different subpopulations according to FOXP3, CD25, and CD45RA expression profiles reflecting their activation, cytokine expression, and manifestation of epigenetic changes. $CD45RA^{+}FOXP3^{low}CD25^{low}$ are defined as resting or naïve T_{Reg} cells. $CD45RA^{-}FOXP3^{high}CD25^{high}$ are described as effector T_{Reg} cells (eT_{Reg}), and $CD45RA^{-}FOXP3^{low}CD25^{low}$ cells are non T_{Reg} cells and represent activated conventional T cells. The $CD45RA^{+}FOXP3^{low}CD25^{low}$ subpopulation is further characterized by the expression of naïve T cell markers, the majority of which express CD31, a thymic emigrant marker, and the TSDR is widely conserved. The $CD45RA^{-}FOXP3^{high}CD25^{high}$ subpopulation, in contrast, exhibits a highly suppressive and proliferative capacity and is profoundly demethylated (Miyara et al., 2009).

The Role of T_{Reg} Cells in Immune Homeostasis and Inflammation

T_{Reg} cells balance the immune response in homeostasis and inflammation. These cells orchestrate the immune response of effector T cells (T_{eff}) and initiate anti-inflammatory mechanisms.

Basic Mechanism of T_{Reg} Function

T_{Reg} cells influence the immune response by producing anti-inflammatory cytokines such as IL-10 and TGF-β. IL-10 has a potent immunosuppressive function by inhibiting the production of pro-inflammatory chemokines and cytokines and establishing immune balance in response to a pathogen, autoimmune disease, and allergy (O'Garra et al., 2004). IL-10 directly inhibits co-stimulation ***via*** CD28 and ICOS and indirectly by the downregulation of co-stimulatory molecules on APCs (Taylor et al., 2007). In addition, IL-10 produced by T_{Reg} cells orchestrates antibody production in allergies from IgE toward IgG4. IgG4 and IL-10 production is upregulated in a course of allergen-specific immunotherapies and inhibits IgE-mediated anaphylaxis (Epp et al., 2018).

Interestingly, T_{Regs} producing TGF-β may not be required for complete T_{Reg} function and influence overall T_{Reg} differentiation (Piccirillo, 2008). Numerous studies revealed the importance of TGF-β mediated T_{Reg} function and the upregulation of TGF-β to amend their suppressive function. TGF-β represses the cytolytic function of effector CD8+ cells by downregulating cytolytic genes (e.g., Fas ligand, perforin, granzyme A, B and IFN-γ) in autoimmune diseases and cancer (Thomas and Massague, 2005). In addition, TGF-β produced by T_{Reg} cells inhibits natural killer cell function and contributes to the overall anti-inflammatory effects of TGF-β (Cortez et al., 2017). Furthermore, T_{Reg}-mediated TGF-β can suppress naïve T cell activation and differentiation and can function as a self-regulating stimulus to maintain T_{Reg} development (Tran, 2012). Although the role of TGF-β in direct suppressive T_{Reg} function remains controversial, this cytokine seems important but not obligatory.

Another anti-inflammatory cytokine that complements the inhibitory repertoire of T_{Reg} cells is IL-35. IL-35 plays a suppressive role in autoimmune diseases, allergies, and cancer models. In addition to T_{Reg} cells, IL-35 is secreted by B_{Reg} cells and CD8+ cells. Thus, this cytokine prevents effector T cell expansion, cytokine production, and T_H17 differentiation (Collison et al., 2007; Niedbala et al., 2007). IL-35 also supports T_{Reg} and B_{Reg} expansion and activation by influencing the immune response in autoimmunity (Dambuza et al., 2017). In sum, cytokines fundamentally contribute to suppressive T_{Reg} function.

T_{Reg} cells express various inhibitory receptors on the cell surface. One of the most important and well-studied inhibitory receptors is the cytotoxic T lymphocyte antigen-4 (CTLA-4), which is functionally and structurally related to CD28 and can bind B7 with a 50–100-fold higher affinity. CTLA-4 is upregulated in activated and exhausted T cells but continuously expressed on T_{Reg} cells and supports their inhibitory function. By binding to B7, CTLA-4 inhibits T cell activation, proliferation, and cytokine production including IL-2 (Krummel and Allison, 1996). CTLA-4 further leads to the removal of costimulatory receptors on APCs (Sansom, 2015). A defect in CTLA-4 function, for example by non-sense mutation in the gene encoding CTLA-4, leads to defective T_{Reg} function and is accompanied by complex autoimmune disorder and immunodeficiency in humans. Interestingly, patients had a higher T_{Reg} abundancy but decreased CTLA-4 expression on the T_{Reg} cell surface. Patients with the inherited heterozygous loss of function mutation develop systemic autoimmune disorders like type 1 diabetes, autoimmune thyroid disease, systemic lupus erythematosus, and inflammatory bowel disease (Kuehn et al., 2014; Schubert et al., 2014).

T_{Reg} cells also express the inhibitory receptors programmed cell death protein 1 (PD-1) and lymphocyte-activation gene function 3 (LAG-3). PD-1 and FOXP3 work collaboratively to maintain immune tolerance, with PD-1 important to maintaining the activation balance between effector T cells and T_{Reg} cells (Zhang B. et al., 2016). In a course of anti-PD-1 therapy in cancer, PD-1+ T_{Reg} cells were amplified and mediated cancer growth (Kamada et al., 2019). LAG-3 contributes to immunosuppressive T_{Reg} function in a tumor environment and promotes maternal tolerance during pregnancy (Camisaschi

et al., 2010; Zhang and Sun, 2020). Hence, LAG-3 inhibits DC maturation and function. Thus, inhibitory receptors play a fundamental role in T_{Reg} function but remain poorly understood.

In addition to cytokines and inhibitory receptors, T_{Reg} cells use metabolic disruption to influence the immune response. IL-2 is one of the most important cytokines for T cell expansion and is mandatory for T_{Reg} function and differentiation (Davidson et al., 2007). T_{Reg} cells express the high-affinity IL-2 receptor CD25 on their surface and could have a metabolic advantage in comparison to effector T cells, especially in a milieu where the IL-2 concentration is low. Accordingly, cytokine deprivation by T_{Reg} cells induced apoptosis in effector T cells (Pandiyan et al., 2007). In contrast, IL-2 consumption was not required for T_{Reg} suppression (Oberle et al., 2007). Nevertheless, modern low-dose IL-2 therapies in various diseases could demonstrate a preferential T_{Reg} expansion and thereby have a positive effect on patient outcome (Hartemann et al., 2013; Matsuoka et al., 2013; He et al., 2016).

T_{Reg} cells use the membrane-bound ectonucleotidases CD73 and CD39 to generate adenosine from extracellular ATP to influence the immune response. Extracellular ATP usually promotes inflammation, whereas adenosine leads to anti-inflammatory effects. CD39 is abundant on T_{Reg} cells, whereas CD73 is intracellularly enriched in human T_{Reg} cells and upregulated after T_{Reg} activation (Schuler et al., 2014). T_{Reg} cells are sensitive to extracellular ATP, and the upregulation of CD39 is accompanied by remission of inflammatory bowel disease (Gibson et al., 2015). Thus, CD39 signaling is primarily a mechanism to suppress T_H17 function and development. Adenosine leads to CTLA-4 and PD-1 upregulation in T_{Reg} cells and promotes T_{Reg} suppression of DC function (Ring et al., 2015).

The first indication that cytolytic mechanisms play a role in T_{Reg} function came from studies of granzyme B. In particular, granzyme B is upregulated in activated T_{Reg} cells and mediates suppression of B cell function, and granzyme B deficiency reduces T_{Reg} suppression. Granzyme B-expressing T_{Reg} cells are enriched in human colorectal cancer and potent suppressors of effector T cells. Further, T_{Reg} cells protect themselves from granzyme B-mediated killing by upregulating serine protease inhibitor 6 (Azzi et al., 2013; Sun et al., 2020).

T_{Reg} Function in Autoimmunity

Defects in molecules important for T_{Reg} function can lead to autoimmune diseases, underlying the importance of T_{Reg} effector proteins in pathophysiology. For example, the inherited IPEX syndrome (X-linked autoimmune syndrome immunodysregulation polyendocrinopathy enteropathy X-linked) is caused by different loss of function mutations in the FOXP3 gene. These defects can further lead to the development of autoimmune diseases like diabetes type 1, autoimmune colitis, or hepatitis (Le Bras and Geha, 2006). IL-2RA mutations cause a phenotype similar to IPEX syndrome and CD25 deficiency can increase the vulnerability to viral infection (Goudy et al., 2013). In addition to these monogenetic T_{Reg} diseases, T_{Reg} dysfunction appears in other immune deficient syndromes. Autoimmune diseases like type 1 diabetes, multiple sclerosis, systemic lupus erythematosus, myasthenia gravis, and rheumatoid arthritis are associated with altered T_{Reg} quantity or quality (Wakabayashi et al., 2006; Lapierre et al., 2013).

The direction of T_{Reg} alteration is controversial. Different studies show either an increase or decrease in T_{Reg} cell numbers based on the stage of the disease and the heterogeneous use of T_{Reg}-defining molecules. In addition, as explained above, T_{Reg} defining molecules can be upregulated after general T cell activation in humans (Pillai et al., 2007). Nevertheless, T_{Reg} cells are an important target for therapy of autoimmune diseases and remission can partly reverse the defective T_{Reg} function (Hartemann et al., 2013; Humrich et al., 2015; Rosenzwajg et al., 2015; He et al., 2016). Treatment with tocilizumab in patients with rheumatoid arthritis, for example, increased T_{Reg} frequency and restored T_{Reg} function (Kikuchi et al., 2015). Another therapeutic approach is the adoptive transfer of ***in vitro***-expanded T_{Reg} cells. This strategy was beneficial in mouse models and is now being tested in humans (Morgan et al., 2005; Mathew et al., 2018).

Tumor tissue is especially challenging for the immune system. T_{Reg} cells impair the immune response against tumor antigens by effector T cells that evolve from potential self-reactive cells. In general, a T_{Reg}-enriched tumor tissue with decreased abundancy of CD8+ cells is associated with poor prognosis, metastasis, and reduced survival (Mougiakakos et al., 2010). Tumor-infiltrating T_{Reg} cells are primarily effector T_{Reg} cells (CD45RA-FOXP3highCD25high), which are active and proliferative. Furthermore, these cells differ in the expression of activation markers, T_{Reg} markers, and inhibitory receptors on their cell surface. Tumor-infiltrating T_{Reg} cells also express several chemokine receptors such as CCR4 and CCR8 (De Simone et al., 2016). In the tumor, T_{Reg} cells interact with immune cells, cancer cells, and fibroblasts to influence tumor immunity. Tumor-associated fibroblasts promote tumor progression and positively regulate T_{Reg} function and frequency (Kato et al., 2018). Furthermore, T_{Reg} cells and cancer cells bidirectionally support their growth and function. Immunosuppressive T_{Reg} function enables tumor progression, while cancer cells secrete TGF-β, IDO, and COX-2 to promote T_{Reg} trafficking and differentiation (Costa et al., 2018). Adenosine is produced by cancer cells and T_{Reg} cells and functions as a mediator, encouraging cancer cell growth, angiogenesis, and metastasis (Chimote et al., 2018). In addition to cancer cell effects, T_{Reg} cells have a tremendous impact on tumor-infiltrating immune cells. They reciprocally promote nonclassical monocytes, B_{Reg} differentiation, and MDSCs trafficking to create an immunosuppressive cell composition. Furthermore, T_{Reg} cells inhibit proinflammatory immune cells such as NK cells and cytotoxic lymphocytes to prevent an effective anti-tumor immune response (Chang et al., 2016; Sarhan et al., 2018). Modern immunotherapies use anti-CTLA-4 and anti-PD-1, which mainly target the T_{Reg} immune response (Ha et al., 2019).

An important cell subpopulation that balances the immune response in the course of pathogen infection and vaccination are follicular regulatory T cells (T_{FR}). T_{FR} cells affect the humoral immune response by influencing B cell maturation in the germinal center (GC). During this process, B cells undergo

somatic hypermutation to establish a high affinity and effective humoral immune response. This development is supported by T_{FH} cells and is tightly regulated by T_{FR} to prevent autoimmunity and an imbalanced immune response (Wollenberg et al., 2011). T_{FR} influence T_{FH} frequency and function and in addition B cells directly by inhibiting their activation. Interestingly, T_{FR} express a distinct TCR repertoire for foreign antigens and potential self-antigens. T_{FR} resemble T_{FH} cells in CXCR5, ICOS, and BCL-6 expression but T_{FR} also express CD28, FOXP3, and Blimp1 (Chung et al., 2011). T_{FR} cells differentiate from CD25 +FOXP3+ cells and function as an effector T_{Reg} subpopulation (Linterman et al., 2011). CTLA-4 is the most important mode of T_{FR}-mediated immune cell regulation, but PD-1 also contributes to full T_{FR} function (Sage et al., 2014). T_{FR} and T_{FH} influence one another reciprocally, and the interaction can be influenced by the microenvironment. In a recently published study, different adjuvants balanced T_{FR} frequency and function during vaccination (Bartsch et al., 2020). The T_{FR} function was affected by IL-6 signaling and the altered T_{FR} cell frequency influenced antibody glycosylation and the overall humoral immune response (Bartsch et al., 2020).

In addition to the GC reaction, T_{FR} can be detected in the blood even at low frequency. Circulating T_{FR} cells have a memory-like phenotype and fine tune the secondary response to an antigen by influencing reactivation of DCs to GC and cytokine production, antibody class-switching, and B cell activation (Sage et al., 2014). T_{FR} dysfunction can be associated with autoimmune diseases, graft versus host reactions, and allergies (He et al., 2013). Overall, T_{Reg} cells play an important role in orchestrating the immune response in health and disease.

THE T_H17/T_{REG} CELL BALANCE IN THE LIVER

The liver is an immunogenetic organ exposed to a variety of antigens and pathogens from the digestive tract and is essential to building an effective immune response. Interestingly, and in contrast to the blood, the CD4/CD8 ratio is reversed in the liver (Doherty and O'Farrelly, 2000). The liver is naturally enriched with innate immune cells, namely, macrophages (Kupffer cells), natural killer (NK) cells, and NK T cells. Especially during fibrogenesis, infiltrating monocytes are important for continuous inflammation and the activation of extracellular matrix producing hepatic stellate cells (HSCs). The adaptive immune system also plays a critical role in these processes. The intrahepatic T_{Reg} frequency can differ from 1% to 5% among all intrahepatic lymphocytes (Oo et al., 2012). The expression of IL-17RA was observed on parenchymal and non-parenchymal cells including hepatocytes, HSCs, Kupffer cells, and endothelial cells, all of which exacerbate inflammatory reactions upon injury. In two different mouse models of hepatic fibrosis (bile duct ligation and carbon tetrachloride), the deletion of IL-17A, IL-23, and IL-17RA inhibited HSC activation and fibrosis development. This finding implies a direct functional link between IL-17A mediated stimulation of HSCs by activation of STAT3-dependent signaling (Meng et al., 2012). Further, isolation experiments in primary liver-resident cells revealed IL-17 production and IL-17 signal transmission by almost all liver-resident cell types. Kupffer cells especially express high levels of IL-17 and show significant upregulation of IL-17 and IL-1β upon stimulation. mRNA expression of IL-17RA and IL-17RC could additionally be found in hepatocytes, Kupffer cells, HSCs, and liver endothelial cells. Despite IL-17RA expression, hepatocytes and liver endothelial cells do not express IL-17 themselves (Zenewicz et al., 2007). Another study using a cell transplantation model pointed to a direct interaction between HSCs and T_{Reg} cells. Jiang et al. found that upon transplantation, HSCs in allogeneic recipients convey the selective expansion of $CD4^+CD25^+FoxP3^+$ cells in an IL-2-dependent fashion to protect parenchymal cells from rejection (Jiang et al., 2008).

In contrast, CD4+ and CD8+ T cells, NK T cells, γδT cells, neutrophils, and macrophages do express IL-17 in the liver. The equilibrium of T_H17 and T_{Reg} cells is regulated not only by differentiation but also at the epigenetic level. Interestingly, recent studies show that in the presence of IL-1β, IL-2, IL-21, and IL-23, IL-17 producing cells can also develop from T_{Reg} cells due to a differentiation switch that removes their suppressive function (Koenen et al., 2008; Deknuydt et al., 2009).

T_{Reg} and T_H17 cells are also often significantly increased in chronic inflammatory liver diseases and are important to balance the persisting pro-inflammatory immune response. Interestingly, a reciprocal relationship between T_H17 and T_{Reg} cells exists in their differentiation as in their effector function (**Figure 3**).

T_{Reg} and T_{H17} cells can co-express the lineage defining transcription factors RORγt and FOXP3. Environmental conditions such as the tissue-specific cytokine milieu at the site of infection can influence this expression and influence the balance by fostering either T_{Reg} or T_H17 cell development by simultaneous inhibition of the other cell type. TGF-β, for example, is required for the differentiation of both subsets; the absence or presence of proinflammatory cytokines defines whether a T_H17 or T_{Reg} cell develops (Yang et al., 2008; Hammerich et al., 2011). In contrast, T_H17 cells express IL-10 receptor α, which can convey a T_{Reg}-induced decrease in T_H17 cells in an IL-10-dependent manner (Huber et al., 2011). Recent studies point to a delicate balance between T_H17 and T_{Reg} cells crucial to maintaining tissue homeostasis. In addition to IL-6, other factors such as retinoic acid, rapamycin, or cytokines (e.g., IL-2 and IL-27) influence this balance significantly. T_{Reg} cells are assigned a decisive role in hepatic immunity. Results obtained in mouse models of acute and chronic liver disease also point to a major involvement of T_H17 and T_{Reg} cells in a variety of human inflammatory liver diseases. For example, in a cancer milieu, glucose consumption by tumor cells preferentially promotes T_{Reg} differentiation and decreases T_H17 cell development thereby supporting the immune escape strategy of tumor cells. Another important ubiquitous environmental condition during chronic and acute infection is hypoxia. Hypoxia can induce the hypoxia inducible factor 1α (HIF-1α) as an adaptive mechanism of the cells to low oxygen concentration. HIF-1α stabilization supports RORγt and IL-17 production while targeting FOXP3 to

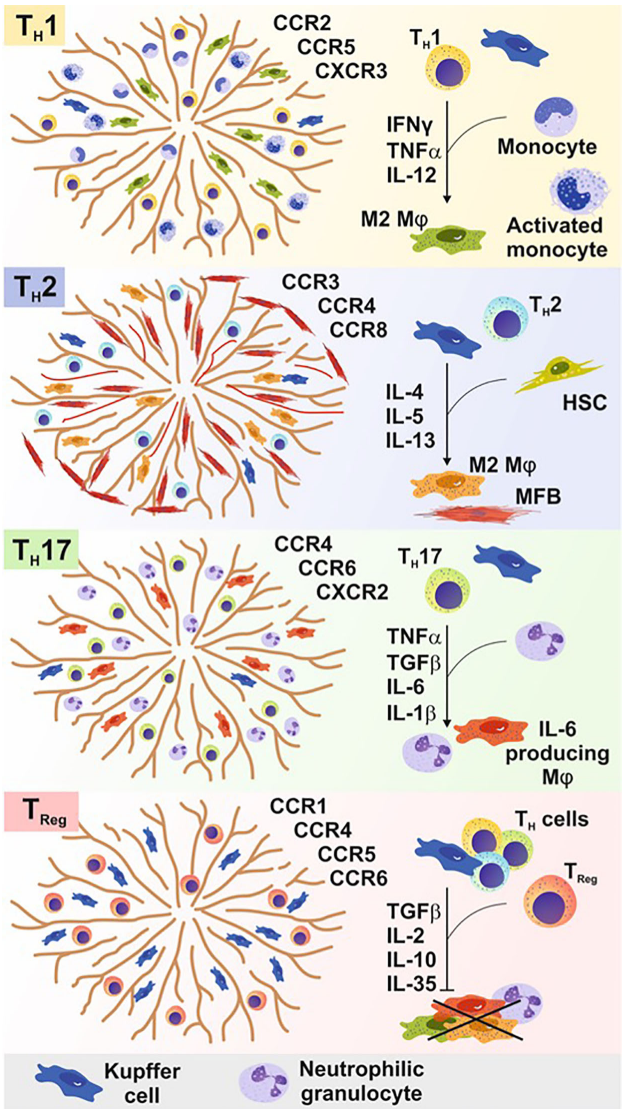


FIGURE 3 | In acute and chronic liver diseases, T cells are crucial to either initiate, maintain, or terminate pro-inflammatory immune responses. Different T cell subpopulations develop, expand, and function based on a distinct cytokine milieu influenced by the presence of different types of immune cells. Different CD4+ cells recognize certain chemokine receptors within the liver and are thereby attracted by different cell types and stimuli to infiltrate the liver tissue. The differentiation of these subsets requires a specific cytokine milieu generated by non-parenchymal cells (e.g. monocytes) or parenchymal cells [e.g., hepatic stellate cells (HSCs)]. T_H1 cell cells promote alternatively activated macrophage development (M2), whereas T_H2 cells additionally promote liver myofibroblast (MFB) activation. T_H17 cells leads to the recruitment of neutrophils, granulocytes, and macrophages to the site of inflammation to induce and sustain a pro-inflammatory immune response. Regulatory T (T_{Reg}) cells and follicular T (T_{FH}) cells prevent the pro-inflammatory immune response of several parenchymal and non-parenchymal cells within the liver tissue in course of an inflammatory immune response.

proteasomal degradation. Manipulation of the balance between pathogenic and regulatory processes in the liver are believed to allow the focused restoration of homeostasis especially during hepatic inflammation.

The detailed analysis of T_H17 cells in human liver remains difficult because the cell frequency is low and cells can only be analyzed after their ***in vitro*** activation with phorbol 12-myristate 13-acetate (PMA) and ionomycin. This ***in vitro*** activation is interesting but must be critically considered because the extent to which it reflects the ***in vivo*** situation and cell status upon isolation is unknown.

Autoimmune Diseases

One example of specific immune change in the liver is autoimmune hepatitis (AIH). Although the cause of AIH is not fully understood, T cell mediated liver tissue destruction is involved and AIH could be associated with genetic and environmental alterations. AIH leads to chronic liver inflammation, circulating autoantibodies, and elevated liver enzymes (Tait et al., 1989). Zhao et al. showed that patients with AIH have increased serum levels of IL-17 and IL-23 together with an increased frequency of T_H17 cells in the liver compared to controls. Furthermore, the frequency and function of T_{Reg} cells in the blood was decreased (Ferri et al., 2010). By analyzing the T cell composition in the liver, it was demonstrated that the total T_{Reg} number was not altered in AIH patients. In contrast, these patients displayed higher hepatic expression of the T_H17-related cytokines IL-17, IL-23, IL-6, and RORγt. *In vitro* experiments showed that IL-17 induces IL-6 *via* MAPK signaling in hepatocytes, which in turn stimulates T_H17 cell differentiation and infiltration in a positive feedback loop (Zhao et al., 2011). These results are supported by a retrospective study of 100 AIH patients. In addition to elevated serum levels of IL-17, IL-6, IL-21, and TNF-α, an increased frequency of T_H17 cells was observed. Pro-inflammatory cytokines were positively correlated with liver injury, whereas IL-10 was negatively regulated with autoantibodies (An, 2019). Likewise, T_{Reg} cells from AIH patients had decreased CD39 expression and functionally failed to prevent T_H17 accumulation mediated by extracellular ATP (Grant et al., 2014). Remission in AIH patients was associated with restored T cell balance, and the infusion of ex vivo expanded T_{Reg} cells was beneficial in a murine model (Lapierre et al., 2013). In sum, the balance of T_{Reg} and T_H17 composition at the site of inflammation and T_{Reg} function is critical in AIH pathomechanisms.

Primary biliary cirrhosis (PBC) is a chronic cholestatic liver disease characterized by the loss of immune self-tolerance leading to the chronic injury of biliary epithelial cells. Ninety percent of affected patients are women older than 40 years. The importance of the T_H17/T_{Reg} balance in disease progression of primary biliary cirrhosis (PBC) is evident when considering that a knockout for CD25 (IL-2Rα) in mice serves as an animal model for this disease. Mice spontaneously develop autoantibodies caused by a loss of function of T_{Reg} cells and acquire biliary duct damage similar to that observed in PBC patients (Wakabayashi et al., 2006). Deficiency of functional T_{Reg} cells leads to elevated T_H17 cell numbers in the liver and elevated IL-17 levels in these mice compared to wildtype controls. A possible explanation might be the missing repressive function of IL-2 during T_H17 cell differentiation. In line with the results obtained in mice, patients suffering from liver fibrosis due to PBC show a higher frequency of T_H17 cells in blood than healthy control

patients. Liver biopsy samples of PBC patients point to a dislocation of these cells around the portal tracts (Shi et al., 2015). Patients with cirrhosis secondary to PBC displayed an even higher infiltration of T_H17 cells into liver tissue (Tan et al., 2013). However, the exact mechanisms that cause an induction of T_H17 cells in livers of IL-2RA knockout animals remain elusive.

Primary sclerosing cholangitis (PSC) is another chronic-inflammatory liver disease with an unknown pathogenesis. Similar to PBC, PSC can lead to liver fibrosis and obliteration of intra-and extrahepatic bile ducts. PSC is often associated with chronic ulcerative colitis, and there is no effective treatment (Hirschfield et al., 2013). Patients with also have a decreased peripheral T_{Reg} frequency with epigenetic changes. Furthermore, a decrease in T_{Reg} numbers was associated with an IL-2RA gene polymorphism and lead to reduced T_{Reg} function (Sebode et al., 2014), (**Figure 4**).

Acute Liver Injury

Mouse models of acute liver injury were used to further investigate the role of T_H17 cells in the liver. In the concanavalin A- (ConA-) model of acute T cell induced hepatitis, IL-1- deficient animals were challenged and knockout mice developed less severe injury with higher T_{Reg} numbers compared to wildtype mice (Nagata et al., 2008). However, these results are controversial; another study found in the same model that IL-17-deficient mice seemed to develop a comparable level of liver injury after ConA-treatment (Zenewicz et al., 2007). In another interesting mouse model of drug-induced liver injury (halothane injection intraperitoneally), mice had increased serum levels of IL-17. After the administration of an IL-17 neutralizing antibody serum, liver enzymes AST and ALT had significantly decreased levels, with a downregulation of inflammatory cytokines such as TNF-α. These beneficial effects could be directly reversed by the application of recombinant IL-17 (Kobayashi et al., 2009).

Viral Infection

The T_{Reg}/T_H17 balance is essential for an effective immune response and at the same time preventing excessive liver injury during viral infection. Thus, the liver is affected by several viruses, and some of them lead to persistent infection and can cause liver cirrhosis, organ failure, and cancer. During acute hepatitis A virus (HAV) infection, serum IL-17 levels are correlated with liver injury, and liver resident and circulating T_{Reg} frequencies are negatively linked to elevation of ALT and AST (Choi et al., 2015).

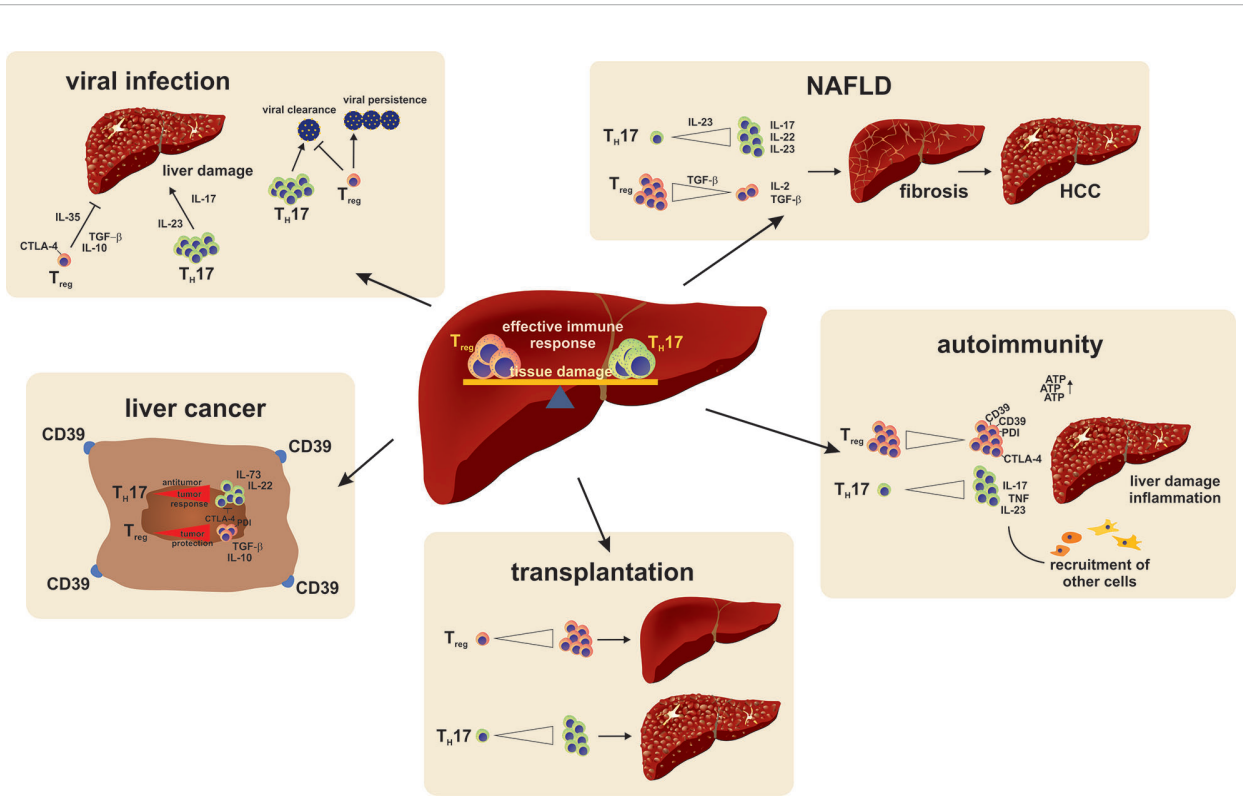


FIGURE 4 | A reciprocal relationship exists between T_H17 and T_{Reg} cells. Their balance is found to be important in the persistence or recovery from liver injury. A shift of the balance to a more dominant T_H17 cell response favors pro-inflammatory reactions and persisting damage. In viral infections, T_H17 are especially important for viral clearance but at the same time cause liver damage. T_{Reg} cell on the other hand prevent liver damage but also trigger viral persistence by strengthening the anti-inflammatory immune response. An imbalance of the T_H17/T_{Reg} milieu to a dominant T_H17 cell response favors disease development and progression in NAFLD. In autoimmune diseases a T_{Reg} cell responses have beneficial effects in regards to self-tolerance, restore immune homeostasis and are even proposed as a treatment option in acute and chronic transplant rejection reactions. In a tumor environment T_{Reg} cells support tumor cells from being targeted by the immune system and hence promote tumor growth and metastasis.

The major problem in persistent viral infection is a failure of the T cell response involving T cell exhaustion due to persistent antigen presentation. T_{Reg} cells also play a role in the immunopathology of persistent viral infection. It was demonstrated that liver sinusoidal endothelial cells (LSEC) are potent enough to promote T_{Reg} differentiation by the continuous induction of FOXP3 in conventional T cells, although all liver cells were able to induce T_{Reg} differentiation. T_{Reg} stabilization did not require inflammation but did require TGF-β, which is abundant on the LSEC cell membrane. Experimentally, LSEC-induced T_{Reg} cells expressed FOXP3 and had efficient inhibitory functions on effector T cells *in vitro* and *in vivo* (Carambia et al., 2014). Antigen presentation on LSECs and thereby an early T_{Reg} development in a course of sub-infectious viral infection of hepatotropic viruses, e.g., chronic hepatitis C virus (HCV), can support ineffective virus clearance and chronic infection (Park et al., 2013). In contrast, virus-specific T_H17 cells were correlated with liver injury and inflammation, but T_H17 quantity could not be linked to effective viral clearance. Furthermore, IL-23 and IL-17 levels in HCV-infected patients were elevated, and IL-23 therapy was reported to modulate the antiviral response by preferentially promoting T_H17 immune cells (Meng et al., 2016). In a course of HCV infection, T_{Reg} cells were mainly found in necro-inflammatory liver areas to inhibit the effector CD8 T cell response, which is the main cause of liver damage in HCV and hepatitis B virus (HBV) infection. Isolated T_{Reg} cells from HCV-infected patients suppressed virus-specific CD8+ cells, whereas the depletion of T_{Reg} cells increased their proliferation. Furthermore, TCR analysis demonstrated that the effective T_{Reg} population during chronic HCV infection is heterogeneous and consists of nT_{Reg} and pT_{Reg} cells (Losikoff et al., 2012). In comparing the T_{Reg} cells of patients who spontaneously resolved the infection and patients with persistent infection, core virus-specific T_{Reg} cells were primarily found in patients with chronic HCV infection. They inhibit the virus-specific T cell response by producing IL-10 and IL-35 (Langhans et al., 2010). Furthermore, several studies investigated a positive correlation between T_{Reg} quantity and function with chronic HCV progression (Cabrera et al., 2004; Ebinuma et al., 2008). T_H17 cells on the other hand are enriched in livers of patients with chronic HCV infection mainly driven by Tim-3, which leads to a differential regulation of IL-12 and IL-23 (Wang et al., 2013).

The T_{Reg}/T_H17 balance also plays an important role in chronic HBV infection. T_{Reg} cells inhibit the antiviral response of effector T cells (Yan et al., 2014). The frequency of circulating T_{Reg} cells is differently described in chronic HBV infection, but there are some indications that the T_{Reg} frequency is increased in severe chronic HBV infection. Furthermore, T_{Reg} frequencies could be positively correlated with viral load, HBeAg (Hepatitis B envelope Antigen), and HBsAg (Hepatitis B surface Antigen) (Manigold and Racanelli, 2007; TrehanPati et al., 2011). Patients with a predominant T_H17 response have high plasma viral loads. Especially in HBV infection and HBV-induced cirrhosis, IL-17+ cells increase with cirrhosis stage and the HBcAg (Hepatitis B core Antigen) mediates T_H17 cell responses by an IL-17R-induced activation of monocytes/macrophages. This effect leads to the production of elevated levels of pro-inflammatory cytokines such as IL-6, TNF-α, IL-12, and IL-23 (Sun et al., 2012). Further, the elevation of T_{Reg} and T_{FR} cells in chronically HBV infected patients associated with elevated IL-10 and TGF-β levels in comparison to healthy individuals (Liu et al., 2020). T_{Reg} differentiation was thereby promoted by TGF-β production of hepatic stellate cells and activation of Notch signaling during chronic inflammation. In a course of antiviral response, T_H17 cells increased in quantity accompanied with an increase in viral load (Ichikawa et al., 2011; Yan et al., 2014). In addition, in course of antiviral therapy, PD-1 expression decreased on T_H17 cells and other effector T cells, indicating an improved T cell exhaustion; however, PD-1 was not present on T_{Reg} cells (Wei et al., 2013). The T_H17/T_{Reg} balance is critical in the development of liver cirrhosis in chronically-infected patients. An imbalance in T_H17/T_{Reg} cells was thereby an independent predictive factor for decompensated liver cirrhosis (Lan et al., 2019). In addition, Yang et al. demonstrated that IL-35 is responsible to balance the T_{Reg} and T_H17 balance in acute and chronic HBV infection by preferentially increasing virus-specific T_{Reg} cells and the prevention of T_H17 cell differentiation (Yang et al., 2019). In conclusion, T_{Reg} and T_H17 cells contribute to the immune response during viral liver infection and the optimal balance is important for an effective antiviral immune response and prevention of complications (**Figure 4**).

Alcoholic and Nonalcoholic Steatohepatitis (ASH and NASH)

Patients with alcoholic steatohepatitis (ASH) show a direct correlation between the severity of inflammation and the amount of liver damage. The degradation of ethanol mediated by cytochrome P450 2E1 (CYP2E1) is associated with various inflammatory responses within the liver. The immune response leads to the production of reactive oxygen species (ROS) and TNF-α and the infiltration of immune cells. T cells infiltrating into the liver secrete high levels of pro-inflammatory cytokines, thereby attracting neutrophils to the tissue site of inflammation. Neutrophil recruitment could be closely linked to the prominence of T_H17 cells. This in turn leads to increased IL-17 serum levels in ASH patients, which could be directly linked to progressive liver damage. Further, the number of T_{Reg} cells decreases in the blood of these patients (Lemmers et al., 2009).

Nonalcoholic steatohepatitis (NASH) is related to metabolic syndrome. This condition has become the most common cause of chronic liver disease and will likely be the main cause for liver transplantations within the next decade (Younossi et al., 2019). Patients with non-alcoholic fatty liver disease (NAFLD) have a high risk to progress from simple steatosis to more advanced disease stages such as NASH, cirrhosis, and hepatocellular cancer (HCC). The exact mechanisms of the pathogenesis of NASH are poorly understood. However, the role of the activation of the adaptive immune system *via* a T_H17-mediated immune responses is becoming evident.

Targeting the balance between T_H17 and T_{Reg} cells is a relatively new approach and currently topic of many research studies. The lack of available human tissue samples makes it difficult to investigate this as a potential new treatment option.

Nevertheless, recent studies in mice and few data from humans indicate a decisive role of CD4+ T cells in the progression from NAFLD to NASH up to HCC development (Hammerich et al., 2011; Rau et al., 2016). A key mechanism within this process is a strong infiltration of neutrophils together with an increased IL-6 signaling and T_H17 accumulation (Hubscher, 2006). This further leads to a depolarization of the intrahepatic CD4+ cell response to a more T_H17 cell-driven reaction; at the same time, T_{Reg} cell activity is suppressed (Gomes et al., 2016; Rau et al., 2016). Although the total T_{Reg} number of circulating and intrahepatic T_{Reg} cells is not altered, the overall T_H17/T_{Reg} balance is shifted to a more dominant pro-inflammatory immune response.

The majority of data on T_H17 cells in NASH is limited to mice. Different mouse models for diet-induced nonalcoholic steatohepatitis, such as the methionine-choline deficient-diet (MCD-diet) and the widely used high fat diet (HFD) model, can lead to steatohepatitis and subsequent fibrosis. Disease development and progression in these models is accompanied with an increase in T_{Reg} cell numbers at early disease stages in which only steatosis is present, and shifts significantly to a more dominant T_H17 cell-driven response at later time points when steatohepatitis and beginning fibrosis are present. In the liver fibrosis CCL4 mouse model, increased IL-17 levels led to an elevated collagen1α1 expression in HSCs triggered by STAT3 signaling (Meng et al., 2012). Gomes et al. showed in 2016 that the excess of nutrients leads to the expression of the factor unconventional prefoldin RPB5 interactor (URI) in liver of mice treated with different steatohepatitis-inducing diets. URI promoted HCC development *via* a shift of the CD4+ T cell composition during NASH and NASH-HCC development. The overexpression of human URI in mouse hepatocytes led to spontaneous development of steatohepatitis, which could be strengthened by feeding steatohepatitis-inducing diets (CD-HFD) or MCD. Disease was accompanied by increased IL-17 and T_H17 cells in blood and liver. Mice with a heterozygous, hepatocyte-specific deficiency for URI were protected from the development of steatohepatitis together with decreased numbers of T_H17 cells. Inhibiting the differentiation of T_H17 cells through the blockade of RORγt lead to an improved in lipid metabolism, insulin resistance, and HCC development. The application of recombinant IL-17 in wildtype mice induced steatohepatitis, the infiltration of neutrophils to white adipose tissue, and led to an increased number of T_H17 cells.

Interestingly, data from human NASH patients correlated with the expression of URI with high IL-17 levels and hepatic steatosis (Gomes et al., 2016). Another study points to overall diminished CD4+ T cell numbers in NASH, and that this reduction is an essential factor in the progression from NASH to HCC development (Ma et al., 2016). The observed changes in the T helper cell profile during NASH development can be caused either by a depolarization of CD4+ T cells to a T_H17 cell phenotype, or by a relative shift of the CD4+ T cell composition in the liver due to depletion of other T helper cell subsets, or driven by an altered infiltration of distinct CD4+ T cell subsets.

A study from Rau et al. in 2016 showed that the progression from NAFLD to NASH is directly correlated with an increased frequency in T_H17 cells in blood and liver of NAFLD and NASH patients together with an altered T_H17/T_{Reg} balance depicted by an increased T_H17/T_{Reg} cell ratio in both compartments (Rau et al., 2016). In visceral adipose tissue and subcutaneous adipose tissue of morbid obese patients, an increase in the mRNA expression of IL-17 was found compared to normal weight patients. The same patients also showed increased numbers of T_H17 cells in both adipose tissues and peripheral blood mononuclear cells (PBMCs), while T_{Reg} cell numbers were decreased due to impaired survival of these cells (McLaughlin et al., 2014). A recent study published in April 2020 further points to the direct relationship between liver and adipose tissue in regulating the T_H17/T_{Reg} balance. Van Herck and colleagues demonstrated that mice fed a high-fat high-fructose diet displayed an increase in T_H17 cells in both compartments, with a simultaneous decrease in T_{Reg} cells. After removing the steatohepatitis-inducing diet, the disruption in the T_H17/T_{Reg} balance persisted. The administration of an IL-17 neutralizing antibody subsequently decreased the pro-inflammatory immune response in the liver (Van Herck et al., 2020). NASH is further closely related to the development of HCC. The involvement of TH17 cells in tumor formation and patient survival was recently described as influencing the prevention of apoptosis in tumor cells induced by T_H17 cells due to IL-17 promoting angiogenesis and an IL-23 driven tumor growth (Langowski et al., 2006; Zhang et al., 2009). Understanding the role of T_H17/T_{Reg} balance and targeting it therapeutically is an interesting approach for the treatment of NASH (**Figure 4**).

Liver Fibrosis and Hepatocellular Carcinoma

Chronic liver disease changes and impairs organ structure and function. Liver disease leads to tissue replacement and scaring subsequently leading to liver fibroses and cirrhosis. Several studies describe the importance of T_H17 and T_{Reg} cells in this process. Although the exact role of T_{Reg} cells in liver fibrogenesis is not fully understood, T_{Reg} cells support liver fibrosis by influencing metalloproteinases activation (Zhang X. et al., 2016). T_H17 cells further signal on non-lymphoid cells such as endothelial cells, fibroblasts, and keratinocytes inducing the production of inflammatory cytokines such as IL-6, GM-CSF, IL-1, TGF-β, TNF-α, and MCP-1 to attract immune cells thereby promoting pro-inflammatory immune responses. IL-17 receptor signaling further activates the expression of antimicrobial peptides and matrix metalloproteinases, whereas the latter are important for the degradation of scar tissue during infection (Bettelli et al., 2008). In patients with more severe liver cirrhosis, an increased frequency of circulating T_{Reg} cells, but a decreased T_{Reg}/T_H17 ratio was positively correlated with disease progression (Li et al., 2012). More particularly, the abundant expression of TGF-β and IL-6 in the liver, which both favor the differentiation of T_H17 cells, points to a major contribution of these cells during this process. Liver cirrhosis is one of the major risk factors for the development of HCC. Thus, 80%–90% of HCC develop in the course of chronic inflammation (Refolo et al., 2020). HCC is associated with a poor prognosis, is hard to detect, is aggressive, and has limited therapeutic options. T_{Reg} and T_H17 cells were increased in tumor tissue in comparison to the surrounding liver tissue. Not only high

intra-tumoral T_{Reg} frequencies and a decreased T_H17 quantity but also CD39 expressed by tumor cells and T_{Reg} cells facilitated HCC growth, metastasis, and poor prognosis by mainly affecting T_H17 function and differentiation (Bettini et al., 2012). T_{Reg} cell depletion, however, negatively influenced HCC growth (Cany et al., 2011). Interestingly, high IL-17 and IL-17R expression in the tumor tissue and elevated circulating T_H17 cells are also associated with poor survival and early HCC recurrence. Sorafenib is currently used in HCC treatment and targets varies kinases expressed in T_{Reg} cells. This therapy negatively affects the T_{Reg} frequency, which can be correlated to overall improved survival (Voron et al., 2014). To improve the overall survival of HCC patients, new therapeutic approaches are essential. A defect in T cell function is described and immunotherapies are potential effective treatment strategies. One possibility could be checkpoint inhibition. PD-1 upregulation for example can be detected in circulating T_{Reg} cells in HCC patients, supporting the overall immune dysregulation. Therefore, anti PD-1 is a promising strategy. This therapy reverses the T_{Reg} mediated inhibition of T_H17 cells and other effector T cells (Langhans et al., 2010) (**Figure 4**).

Liver Transplantation

Liver transplantation is in many cases the only possibility to cure end-stage liver disease. The short-term outcome has significantly improved, but chronic organ rejection and the side effects of immunosuppressive therapy remain a concern. The optimal immunosuppressive treatment to prevent organ rejection and toxicity and at the same time avoid opportunistic infections must be tightly balanced and will vary between individuals. The state of optimal immunotherapy, called operational tolerance, is difficult to achieve, and most patients require a life-long therapy with numerous side effects. Thus, new therapeutic approaches following liver transplantation are urgently needed.

T_{Reg} cells play a leading role in averting the cause of graft-versus-host disease (GvHD) which leads to organ rejection. T_{Reg}/T_H17 balance plays a fundamental role in rejection pathogenesis (Wang et al., 2019), and T_H17 cells were found to be elevated during acute and chronic organ rejection. In addition, the pro-inflammatory cytokine milieu during organ rejection can induce RORγt and IL-17 expression in T_{Reg} cells. Thus, T_{Reg} cells seem to contribute to organ rejection. Indeed, an early decrease in T_{Reg} frequency is a risk factor for suspected acute and biopsy proven acute rejection (Han et al., 2020). In addition, CD39 expression in the transplanted liver tissue influences the T_{Reg} and T_H17 immune response and thereby organ rejection and GvHD (Yoshida et al., 2015). Adoptive T_{Reg} transfer was protective in mice, and currently several clinical trials are testing the efficiency and safety in humans (Romano et al., 2017). Another study tested the T_{Reg} therapy in patients 6–12 months after liver transplantation and demonstrated an increase in circulating T_{Reg} cells and reduced anti-donor T cell response (Sanchez-Fueyo et al., 2020). Although the long-term effects are not evaluated, T_{Reg} therapy could be a promising therapeutic approach. In contrast to the beneficial effects, in transplant patients with HCV infection, early high levels of T_{Reg} cells and T_H1 cells after liver transplantation are associated with severe recurrent HCV infection (Ghazal et al., 2019).

In addition to T cell-mediated organ rejection, danger associated molecular patterns (DAMPs) play an important role in triggering sterile inflammation in the liver after organ transplantation. Sterile inflammation could be detected in different solid organs after implantation, and sterile inflammation influences the transplant tolerance and chronic rejection. A recently published study described the correlation between elevated DAMPs and acute postoperative multi-organ dysfunction (Nagakawa et al., 2020). In sum, several studies implicate the contribution of sterile inflammation in acute and chronic organ rejection and are reviewed elsewhere (Braza et al., 2016) (**Figure 4**).

CONCLUSION

T_H17 and T_{Reg} cells are essential in orchestrating the intrahepatic immune response in health and disease. Under homeostatic conditions their balance must be tightly regulated to have an effective immune response and to prevent tissue damage. In the course of several diseases, their balance is shifted. Especially in the liver, the T_H17/T_{Reg} response is tremendously important. An overwhelming T_H17 response, for example in NASH, can promote the inflammatory state of disease and is associated with disease progression. On the other hand, T_{Reg} cells prevent the anti-tumoral immune response in HCC and promote metastasis and cancer growth. Furthermore, both cell subsets can be beneficial in different liver diseases settings. Thus, T_H17 cells are necessary for effective pathogen clearance in the liver and T_{Reg} cells are important to coordinate the immune response in autoimmunity and after liver transplantation. Most of the findings on the role of T_H17 and T_{Reg} cells were generated in mice. The importance of investigating their influence in humans is highlighted in several disease settings. Many studies demonstrate the necessity of investigating the function and quantity of these cells in liver tissue specifically, as circulating cells may not reflect intrahepatic conditions. In addition to altered function and quantities in liver diseases, T_H17/T_{Reg} cell balance could be a therapeutic target in disease settings.

Future studies should investigate the function of T_H17 and T_{Reg} cells in liver tissue and review their balance. Furthermore, different signals that might influence T_H17/T_{Reg} cells, especially in the liver, must be analyzed to fully understand the liver-specific pathomechanism and to inform a liver-specific therapy.

AUTHOR CONTRIBUTIONS

Conceptualization: HD and LB. Writing—original draft preparation: HD, LB, and RW. Visualization: SW. funding acquisition: HD, LB, and RW. All authors contributed to the article and approved the submitted version.

FUNDING

The research was funded by the German Research Foundation (RW: SFB/TRR57, HD: DR 1161/1-1 LB: BA 7175/1-1).

REFERENCES

Aarvak, T., Chabaud, M., Miossec, P., and Natvig, J. B. (1999). IL-17 is produced by some proinflammatory Th1/Th0 cells but not by Th2 cells. *J. Immunol.* 162 (3), 1246–1251.

Aggarwal, S., Ghilardi, N., Xie, M. H., de Sauvage, F. J., and Gurney, A. L. (2003). Interleukin-23 promotes a distinct CD4 T cell activation state characterized by the production of interleukin-17. *J. Biol. Chem.* 278 (3), 1910–1914. doi: 10.1074/jbc.M207577200

An, J. (2019). Expression and significance of Th17 cells and related factors in patients with autoimmune hepatitis. *Comb. Chem. High Throughput Screen* 22 (4), 232–237. doi: 10.2174/1386207322666190402160455

Arpaia, N., Campbell, C., Fan, X., Dikiy, S., van der Veeken, J., deRoos, P., et al. (2013). Metabolites produced by commensal bacteria promote peripheral regulatory T-cell generation. *Nature* 504 (7480), 451–455. doi: 10.1038/nature12726

Azzi, J., Skartsis, N., Mounayar, M., Magee, C. N., Batal, I., Ting, C., et al. (2013). Serine protease inhibitor 6 plays a critical role in protecting murine granzyme B-producing regulatory T cells. *J. Immunol.* 191 (5), 2319–2327. doi: 10.4049/jimmunol.1300851

Bartsch, Y. C., Eschweiler, S., Leliavski, A., Lunding, H. B., Wagt, S., Petry, J., et al. (2020). IgG Fc sialylation is regulated during the germinal center reaction upon immunization with different adjuvants. *J. Allergy Clin. Immunol.* 146 (3), 652–666.e11. doi: 10.1016/j.jaci.2020.04.059

Batten, M., Li, J., Yi, S., Kljavin, N. M., Danilenko, D. M., Lucas, S., et al. (2006). Interleukin 27 limits autoimmune encephalomyelitis by suppressing the development of interleukin 17-producing T cells. *Nat. Immunol.* 7 (9), 929–936. doi: 10.1038/ni1375

Bayer, A. L., Yu, A., Adeegbe, D., and Malek, T. R. (2005). Essential role for interleukin-2 for CD4(+)CD25(+) T regulatory cell development during the neonatal period. *J. Exp. Med.* 201 (5), 769–777. doi: 10.1084/jem.20041179

Bettelli, E., Sullivan, B., Szabo, S. J., Sobel, R. A., Glimcher, L. H., and Kuchroo, V. K. (2004). Loss of T-bet, but not STAT1, prevents the development of experimental autoimmune encephalomyelitis. *J. Exp. Med.* 200 (1), 79–87. doi: 10.1084/jem.20031819

Bettelli, E., Carrier, Y., Gao, W., Korn, T., Strom, T. B., Oukka, M., et al. (2006). Reciprocal developmental pathways for the generation of pathogenic effector TH17 and regulatory T cells. *Nature* 441 (7090), 235–238. doi: 10.1038/nature04753

Bettelli, E., Korn, T., Oukka, M., and Kuchroo, V. K. (2008). Induction and effector functions of T(H)17 cells. *Nature* 453 (7198), 1051–1057. doi: 10.1038/nature07036

Bettini, M., Castellaw, A. H., Lennon, G. P., Burton, A. R., and Vignali, D. A. (2012). Prevention of autoimmune diabetes by ectopic pancreatic beta-cell expression of interleukin-35. *Diabetes* 61 (6), 1519–1526. doi: 10.2337/db11-0784

Braza, F., Brouard, S., Chadban, S., and Goldstein, D. R. (2016). Role of TLRs and DAMPs in allograft inflammation and transplant outcomes. *Nat. Rev. Nephrol.* 12 (5), 281–290. doi: 10.1038/nrneph.2016.41

Cabrera, R., Tu, Z., Xu, Y., Firpi, R. J., Rosen, H. R., Liu, C., et al. (2004). An immunomodulatory role for CD4(+)CD25(+) regulatory T lymphocytes in hepatitis C virus infection. *Hepatology* 40 (5), 1062–1071. doi: 10.1002/hep.20454

Camisaschi, C., Casati, C., Rini, F., Perego, M., De Filippo, A., Triebel, F., et al. (2010). LAG-3 expression defines a subset of CD4(+)CD25(high)Foxp3(+) regulatory T cells that are expanded at tumor sites. *J. Immunol.* 184 (11), 6545–6551. doi: 10.4049/jimmunol.0903879

Cany, J., Tran, L., Gauttier, V., Judor, J. P., Vassaux, G., Ferry, N., et al. (2011). Immunotherapy of hepatocellular carcinoma: is there a place for regulatory T-lymphocyte depletion? *Immunotherapy* 3 (4 Suppl), 32–34. doi: 10.2217/imt.11.29

Carambia, A., Freund, B., Schwinge, D., Heine, M., Laschtowitz, A., Huber, S., et al. (2014). TGF-beta-dependent induction of CD4(+)CD25(+)Foxp3(+) Tregs by liver sinusoidal endothelial cells. *J. Hepatol.* 61 (3), 594–599. doi: 10.1016/j.jhep.2014.04.027

Chang, A. L., Miska, J., Wainwright, D. A., Dey, M., Rivetta, C. V., Yu, D., et al. (2016). CCL2 Produced by the glioma microenvironment is essential for the recruitment of regulatory T cells and myeloid-derived suppressor cells. *Cancer Res.* 76 (19), 5671–5682. doi: 10.1158/0008-5472.CAN-16-0144

Chen, W., Jin, W., Hardegen, N., Lei, K. J., Li, L., Marinos, N., et al. (2003). Conversion of peripheral CD4+CD25- naive T cells to CD4+CD25+ regulatory T cells by TGF-beta induction of transcription factor Foxp3. *J. Exp. Med.* 198 (12), 1875–1886. doi: 10.1084/jem.20030152

Chimote, A. A., Balajthy, A., Arnold, M. J., Newton, H. S., Hajdu, P., Qualtieri, J., et al. (2018). A defect in KCa3.1 channel activity limits the ability of CD8(+) T cells from cancer patients to infiltrate an adenosine-rich microenvironment. *Sci. Signal* 11 (527), eaaq1616. doi: 10.1126/scisignal.aaq1616

Cho, M. L., Yoon, C. H., Hwang, S. Y., Park, M. K., Min, S. Y., Lee, S. H., et al. (2004). Effector function of type II collagen-stimulated T cells from rheumatoid arthritis patients: cross-talk between T cells and synovial fibroblasts. *Arthritis Rheum.* 50 (3), 776–784. doi: 10.1002/art.20106

Choi, Y. S., Lee, J., Lee, H. W., Chang, D. Y., Sung, P. S., Jung, M. K., et al. (2015). Liver injury in acute hepatitis A is associated with decreased frequency of regulatory T cells caused by Fas-mediated apoptosis. *Gut* 64 (8), 1303–1313. doi: 10.1136/gutjnl-2013-306213

Chung, Y., Tanaka, S., Chu, F., Nurieva, R.II, Martinez, G. J., Rawal, S., et al. (2011). Follicular regulatory T cells expressing Foxp3 and Bcl-6 suppress germinal center reactions. *Nat. Med.* 17 (8), 983–988. doi: 10.1038/nm.2426

Collison, L. W., Workman, C. J., Kuo, T. T., Boyd, K., Wang, Y., Vignali, K. M., et al. (2007). The inhibitory cytokine IL-35 contributes to regulatory T-cell function. *Nature* 450 (7169), 566–569. doi: 10.1038/nature06306

Coombes, J. L., Siddiqui, K. R., Arancibia-Carcamo, C. V., Hall, J., Sun, C. M., Belkaid, Y., et al. (2007). A functionally specialized population of mucosal CD103+ DCs induces Foxp3+ regulatory T cells via a TGF-beta and retinoic acid-dependent mechanism. *J. Exp. Med.* 204 (8), 1757–1764. doi: 10.1084/jem.20070590

Cortez, V. S., Ulland, T. K., Cervantes-Barragan, L., Bando, J. K., Robinette, M. L., Wang, Q., et al. (2017). SMAD4 impedes the conversion of NK cells into ILC1-like cells by curtailing non-canonical TGF-beta signaling. *Nat. Immunol.* 18 (9), 995–1003. doi: 10.1038/ni.3809

Cosmi, L., De Palma, R., Santarlasci, V., Maggi, L., Capone, M., Frosali, F., et al. (2008). Human interleukin 17-producing cells originate from a CD161+CD4+ T cell precursor. *J. Exp. Med.* 205 (8), 1903–1916. doi: 10.1084/jem.20080397

Costa, A., Kieffer, Y., Scholer-Dahirel, A., Pelon, F., Bourachot, B., Cardon, M., et al. (2018). Fibroblast heterogeneity and immunosuppressive environment in human breast cancer. *Cancer Cell* 33 (3), 463–479 e410. doi: 10.1016/j.ccell.2018.01.011

Cua, D. J., Sherlock, J., Chen, Y., Murphy, C. A., Joyce, B., Seymour, B., et al. (2003). Interleukin-23 rather than interleukin-12 is the critical cytokine for autoimmune inflammation of the brain. *Nature* 421 (6924), 744–748. doi: 10.1038/nature01355

Curotto de Lafaille, M. A., Kutchukhidze, N., Shen, S., Ding, Y., Yee, H., and Lafaille, J. J. (2008). Adaptive Foxp3+ regulatory T cell-dependent and -independent control of allergic inflammation. *Immunity* 29 (1), 114–126. doi: 10.1016/j.immuni.2008.05.010

Dambuza, I. M., He, C., Choi, J. K., Yu, C. R., Wang, R., Mattapallil, M. J., et al. (2017). IL-12p35 induces expansion of IL-10 and IL-35-expressing regulatory B cells and ameliorates autoimmune disease. *Nat. Commun.* 8 (1), 719. doi: 10.1038/s41467-017-00838-4

Davidson, T. S., DiPaolo, R. J., Andersson, J., and Shevach, E. M. (2007). Cutting Edge: IL-2 is essential for TGF-beta-mediated induction of Foxp3+ T regulatory cells. *J. Immunol.* 178 (7), 4022–4026. doi: 10.4049/jimmunol.178.7.4022

De Simone, M., Arrigoni, A., Rossetti, G., Gruarin, P., Ranzani, V., Politano, C., et al. (2016). Transcriptional landscape of human tissue lymphocytes unveils uniqueness of tumor-infiltrating T regulatory cells. *Immunity* 45 (5), 1135–1147. doi: 10.1016/j.immuni.2016.10.021

Deknuydt, F., Bioley, G., Valmori, D., and Ayyoub, M. (2009). IL-1beta and IL-2 convert human Treg into T(H)17 cells. *Clin. Immunol.* 131 (2), 298–307. doi: 10.1016/j.clim.2008.12.008

Doherty, D. G., and O'Farrelly, C. (2000). Innate and adaptive lymphoid cells in the human liver. *Immunol. Rev.* 174, 5–20. doi: 10.1034/j.1600-0528.2002.017416.x

Ebinuma, H., Nakamoto, N., Li, Y., Price, D. A., Gostick, E., Levine, B. L., et al. (2008). Identification and in vitro expansion of functional antigen-specific

CD25+ FoxP3+ regulatory T cells in hepatitis C virus infection. *J. Virol.* 82 (10), 5043–5053. doi: 10.1128/JVI.01548-07

Epp, A., Hobusch, J., Bartsch, Y. C., Petry, J., Lilienthal, G. M., Koeleman, C. A. M., et al. (2018). Sialylation of IgG antibodies inhibits IgG-mediated allergic reactions. *J. Allergy Clin. Immunol.* 141 (1), 399–402 e398. doi: 10.1016/j.jaci.2017.06.021

Ferber, I. A., Brocke, S., Taylor-Edwards, C., Ridgway, W., Dinisco, C., Steinman, L., et al. (1996). Mice with a disrupted IFN-gamma gene are susceptible to the induction of experimental autoimmune encephalomyelitis (EAE). *J. Immunol.* 156 (1), 5–7.

Ferri, S., Longhi, M. S., De Molo, C., Lalanne, C., Muratori, P., Granito, A., et al. (2010). A multifaceted imbalance of T cells with regulatory function characterizes type 1 autoimmune hepatitis. *Hepatology* 52 (3), 999–1007. doi: 10.1002/hep.23792

Fontenot, J. D., Gavin, M. A., and Rudensky, A. Y. (2017). Pillars article: Foxp3 programs the development and function of CD4+CD25+ regulatory T cells. *Nat. Immunol.* 2003. 4, 330–336. *J. Immunol.* 198 (3), 986–992. doi: 10.1038/ni904

Gaublomme, J. T., Yosef, N., Lee, Y., Gertner, R. S., Yang, L. V., Wu, C., et al. (2015). Single-cell genomics unveils critical regulators of Th17 cell pathogenicity. *Cell* 163 (6), 1400–1412. doi: 10.1016/j.cell.2015.11.009

Ghazal, K., Morales, O., Barjon, C., Dahlqvist, G., Aoudjehane, L., Ouaguia, L., et al. (2019). Early high levels of regulatory T cells and T helper 1 may predict the progression of recurrent hepatitis C after liver transplantation. *Clin. Res. Hepatol. Gastroenterol.* 43 (3), 273–281. doi: 10.1016/j.clinre.2018.10.005

Ghoreschi, K., Laurence, A., Yang, X. P., Tato, C. M., McGeachy, M. J., Konkel, J. E., et al. (2010). Generation of pathogenic T(H)17 cells in the absence of TGF-beta signalling. *Nature* 467 (7318), 967–971. doi: 10.1038/nature09447

Gibson, D. J., Elliott, L., McDermott, E., Tosetto, M., Keegan, D., Byrne, K., et al. (2015). Heightened expression of CD39 by regulatory T lymphocytes Is associated with therapeutic remission in inflammatory bowel disease. *Inflammation Bowel. Dis.* 21 (12), 2806–2814. doi: 10.1097/MIB.0000000000000566

Globig, A. M., Hennecke, N., Martin, B., Seidl, M., Ruf, G., Hasselblatt, P., et al. (2014). Comprehensive intestinal T helper cell profiling reveals specific accumulation of IFN-gamma+IL-17+coproducing CD4+ T cells in active inflammatory bowel disease. *Inflammation Bowel. Dis.* 20 (12), 2321–2329. doi: 10.1097/MIB.0000000000000210

Gomes, A. L., Teijeiro, A., Buren, S., Tummala, K. S., Yilmaz, M., Waisman, A., et al. (2016). Metabolic inflammation-associated IL-17A causes non-alcoholic steatohepatitis and hepatocellular carcinoma. *Cancer Cell* 30 (1), 161–175. doi: 10.1016/j.ccell.2016.05.020

Goudy, K., Aydin, D., Barzaghi, F., Gambineri, E., Vignoli, M., Ciullini Mannurita, S., et al. (2013). Human IL2RA null mutation mediates immunodeficiency with lymphoproliferation and autoimmunity. *Clin. Immunol.* 146 (3), 248–261. doi: 10.1016/j.clim.2013.01.004

Grant, C. R., Liberal, R., Holder, B. S., Cardone, J., Ma, Y., Robson, S. C., et al. (2014). Dysfunctional CD39(POS) regulatory T cells and aberrant control of T-helper type 17 cells in autoimmune hepatitis. *Hepatology* 59 (3), 1007–1015. doi: 10.1002/hep.26583

Gutcher, I., Donkor, M. K., Ma, Q., Rudensky, A. Y., Flavell, R. A., and Li, M. O. (2011). Autocrine transforming growth factor-beta1 promotes in vivo Th17 cell differentiation. *Immunity* 34 (3), 396–408. doi: 10.1016/j.immuni.2011.03.005

Ha, D., Tanaka, A., Kibayashi, T., Tanemura, A., Sugiyama, D., Wing, J. B., et al. (2019). Differential control of human Treg and effector T cells in tumor immunity by Fc-engineered anti-CTLA-4 antibody. *Proc. Natl. Acad. Sci. U.S.A.* 116 (2), 609–618. doi: 10.1073/pnas.1812186116

Hadis, U., Wahl, B., Schulz, O., Hardtke-Wolenski, M., Schippers, A., Wagner, N., et al. (2011). Intestinal tolerance requires gut homing and expansion of FoxP3+ regulatory T cells in the lamina propria. *Immunity* 34 (2), 237–246. doi: 10.1016/j.immuni.2011.01.016

Hammerich, L., Heymann, F., and Tacke, F. (2011). Role of IL-17 and Th17 cells in liver diseases. *Clin. Dev. Immunol.* 2011, 345803. doi: 10.1155/2011/345803

Han, J. W., Joo, D. J., Kim, J. H., Rha, M. S., Koh, J. Y., Park, H. J., et al. (2020). Early reduction of regulatory T cells is associated with acute rejection in liver transplantation under tacrolimus-based immunosuppression with basiliximab induction. *Am. J. Transplant.* 20 (8), 2058–2069. doi: 10.1111/ajt.15789

Harbour, S. N., Maynard, C. L., Zindl, C. L., Schoeb, T. R., and Weaver, C. T. (2015). Th17 cells give rise to Th1 cells that are required for the pathogenesis of colitis. *Proc. Natl. Acad. Sci. U.S.A.* 112 (22), 7061–7066. doi: 10.1073/pnas.1415675112

Harrington, L. E., Hatton, R. D., Mangan, P. R., Turner, H., Murphy, T. L., Murphy, K. M., et al. (2005). Interleukin 17-producing CD4+ effector T cells develop via a lineage distinct from the T helper type 1 and 2 lineages. *Nat. Immunol.* 6 (11), 1123–1132. doi: 10.1038/ni1254

Hartemann, A., Bensimon, G., Payan, C. A., Jacqueminet, S., Bourron, O., Nicolas, N., et al. (2013). Low-dose interleukin 2 in patients with type 1 diabetes: a phase 1/2 randomised, double-blind, placebo-controlled trial. *Lancet Diabetes Endocrinol.* 1 (4), 295–305. doi: 10.1016/S2213-8587(13)70113-X

He, J. S., Meyer-Hermann, M., Xiangying, D., Zuan, L. Y., Jones, L. A., Ramakrishna, L., et al. (2013). The distinctive germinal center phase of IgE+ B lymphocytes limits their contribution to the classical memory response. *J. Exp. Med.* 210 (12), 2755–2771. doi: 10.1084/jem.20131539

He, J., Zhang, X., Wei, Y., Sun, X., Chen, Y., Deng, J., et al. (2016). Low-dose interleukin-2 treatment selectively modulates CD4(+) T cell subsets in patients with systemic lupus erythematosus. *Nat. Med.* 22 (9), 991–993. doi: 10.1038/nm.4148

Hill, J. A., Feuerer, M., Tash, K., Haxhinasto, S., Perez, J., Melamed, R., et al. (2007). Foxp3 transcription-factor-dependent and -independent regulation of the regulatory T cell transcriptional signature. *Immunity* 27 (5), 786–800. doi: 10.1016/j.immuni.2007.09.010

Hirota, K., Duarte, J. H., Veldhoen, M., Hornsby, E., Li, Y., Cua, D. J., et al. (2011). Fate mapping of IL-17-producing T cells in inflammatory responses. *Nat. Immunol.* 12 (3), 255–263. doi: 10.1038/ni.1993

Hirota, K., Turner, J. E., Villa, M., Duarte, J. H., Demengeot, J., Steinmetz, O. M., et al. (2013). Plasticity of Th17 cells in Peyer's patches is responsible for the induction of T cell-dependent IgA responses. *Nat. Immunol.* 14 (4), 372–379. doi: 10.1038/ni.2552

Hirschfield, G. M., Karlsen, T. H., Lindor, K. D., and Adams, D. H. (2013). Primary sclerosing cholangitis. *Lancet* 382 (9904), 1587–1599. doi: 10.1016/S0140-6736(13)60096-3

Huber, S., Gagliani, N., Esplugues, E., O'Connor, W. Jr., Huber, F. J., Chaudhry, A., et al. (2011). Th17 cells express interleukin-10 receptor and are controlled by Foxp3(-) and Foxp3+ regulatory CD4+ T cells in an interleukin-10-dependent manner. *Immunity* 34 (4), 554–565. doi: 10.1016/j.immuni.2011.01.020

Huber, S., Gagliani, N., and Flavell, R. A. (2012). Life, death, and miracles: Th17 cells in the intestine. *Eur. J. Immunol.* 42 (9), 2238–2245. doi: 10.1002/eji.201242619

Hubscher, S. G. (2006). Histological assessment of non-alcoholic fatty liver disease. *Histopathology* 49 (5), 450–465. doi: 10.1111/j.1365-2559.2006.02416.x

Humrich, J. Y., von Spee-Mayer, C., Siegert, E., Alexander, T., Hiepe, F., Radbruch, A., et al. (2015). Rapid induction of clinical remission by low-dose interleukin-2 in a patient with refractory SLE. *Ann. Rheum. Dis.* 74 (4), 791–792. doi: 10.1136/annrheumdis-2014-206506

Ichikawa, S., Mucida, D., Tyznik, A. J., Kronenberg, M., and Cheroutre, H. (2011). Hepatic stellate cells function as regulatory bystanders. *J. Immunol.* 186 (10), 5549–5555. doi: 10.4049/jimmunol.1003917

Ivanov, I. I., McKenzie, B. S., Zhou, L., Tadokoro, C. E., Lepelley, A., Lafaille, J. J., et al. (2006). The orphan nuclear receptor RORgammat directs the differentiation program of proinflammatory IL-17+ T helper cells. *Cell* 126 (6), 1121–1133. doi: 10.1016/j.cell.2006.07.035

Jiang, G., Yang, H. R., Wang, L., Wildey, G. M., Fung, J., Qian, S., et al. (2008). Hepatic stellate cells preferentially expand allogeneic CD4+ CD25+ FoxP3+ regulatory T cells in an IL-2-dependent manner. *Transplantation* 86 (11), 1492–1502. doi: 10.1097/TP.0b013e31818bfd13

Kamada, T., Togashi, Y., Tay, C., Ha, D., Sasaki, A., Nakamura, Y., et al. (2019). PD-1(+) regulatory T cells amplified by PD-1 blockade promote hyperprogression of cancer. *Proc. Natl. Acad. Sci. U.S.A.* 116 (20), 9999–10008. doi: 10.1073/pnas.1822001116

Kato, T., Noma, K., Ohara, T., Kashima, H., Katsura, Y., Sato, H., et al. (2018). Cancer-associated fibroblasts affect intratumoral CD8(+) and FoxP3(+) T cells via IL6 in the tumor microenvironment. *Clin. Cancer Res.* 24 (19), 4820–4833. doi: 10.1158/1078-0432.CCR-18-0205

Khader, S. A., Bell, G. K., Pearl, J. E., Fountain, J. J., Rangel-Moreno, J., Cilley, G. E., et al. (2007). IL-23 and IL-17 in the establishment of protective pulmonary

CD4+ T cell responses after vaccination and during Mycobacterium tuberculosis challenge. *Nat. Immunol.* 8 (4), 369–377. doi: 10.1038/ni1449

Kikuchi, J., Hashizume, M., Kaneko, Y., Yoshimoto, K., Nishina, N., and Takeuchi, T. (2015). Peripheral blood CD4(+)CD25(+)CD127(low) regulatory T cells are significantly increased by tocilizumab treatment in patients with rheumatoid arthritis: increase in regulatory T cells correlates with clinical response. *Arthritis Res. Ther.* 17, 10. doi: 10.1186/s13075-015-0526-4

Kobayashi, E., Kobayashi, M., Tsuneyama, K., Fukami, T., Nakajima, M., and Yokoi, T. (2009). Halothane-induced liver injury is mediated by interleukin-17 in mice. *Toxicol. Sci.* 111 (2), 302–310. doi: 10.1093/toxsci/kfp165

Koenen, H. J., Smeets, R. L., Vink, P. M., van Rijssen, E., Boots, A. M., and Joosten, I. (2008). Human CD25highFoxp3pos regulatory T cells differentiate into IL-17-producing cells. *Blood* 112 (6), 2340–2352. doi: 10.1182/blood-2008-01-133967

Korn, T., Bettelli, E., Gao, W., Awasthi, A., Jager, A., Strom, T. B., et al. (2007). IL-21 initiates an alternative pathway to induce proinflammatory T(H)17 cells. *Nature* 448 (7152), 484–487. doi: 10.1038/nature05970

Krueger, G. G., Langley, R. G., Leonardi, C., Yeilding, N., Guzzo, C., Wang, Y., et al. (2007). A human interleukin-12/23 monoclonal antibody for the treatment of psoriasis. *N. Engl. J. Med.* 356 (6), 580–592. doi: 10.1056/NEJMoa062382

Krummel, M. F., and Allison, J. P. (1996). CTLA-4 engagement inhibits IL-2 accumulation and cell cycle progression upon activation of resting T cells. *J. Exp. Med.* 183 (6), 2533–2540. doi: 10.1084/jem.183.6.2533

Kuehn, H. S., Ouyang, W., Lo, B., Deenick, E. K., Niemela, J. E., Avery, D. T., et al. (2014). Immune dysregulation in human subjects with heterozygous germline mutations in CTLA4. *Science* 345 (6204), 1623–1627. doi: 10.1126/science.1255904

Lan, Y. T., Wang, Z. L., Tian, P., Gong, X. N., Fan, Y. C., and Wang, K. (2019). Treg/Th17 imbalance and its clinical significance in patients with hepatitis B-associated liver cirrhosis. *Diagn. Pathol.* 14 (1), 114. doi: 10.1186/s13000-019-0891-4

Langhans, B., Braunschweiger, I., Arndt, S., Schulte, W., Satoguina, J., Layland, L. E., et al. (2010). Core-specific adaptive regulatory T-cells in different outcomes of hepatitis C. *Clin. Sci. (Lond)* 119 (2), 97–109. doi: 10.1042/CS20090661

Langowski, J. L., Zhang, X., Wu, L., Mattson, J. D., Chen, T., Smith, K., et al. (2006). IL-23 promotes tumour incidence and growth. *Nature* 442 (7101), 461–465. doi: 10.1038/nature04808

Lapierre, P., Beland, K., Yang, R., and Alvarez, F. (2013). Adoptive transfer of ex vivo expanded regulatory T cells in an autoimmune hepatitis murine model restores peripheral tolerance. *Hepatology* 57 (1), 217–227. doi: 10.1002/hep.26023

Lathrop, S. K., Bloom, S. M., Rao, S. M., Nutsch, K., Lio, C. W., Santacruz, N., et al. (2011). Peripheral education of the immune system by colonic commensal microbiota. *Nature* 478 (7368), 250–254. doi: 10.1038/nature10434

Le Bras, S., and Geha, R. S. (2006). IPEX and the role of Foxp3 in the development and function of human Tregs. *J. Clin. Invest.* 116 (6), 1473–1475. doi: 10.1172/JCI28880

Lee, Y. K., Turner, H., Maynard, C. L., Oliver, J. R., Chen, D., Elson, C. O., et al. (2009). Late developmental plasticity in the T helper 17 lineage. *Immunity* 30 (1), 92–107. doi: 10.1016/j.immuni.2008.11.005

Lemmers, A., Moreno, C., Gustot, T., Marechal, R., Degre, D., Demetter, P., et al. (2009). The interleukin-17 pathway is involved in human alcoholic liver disease. *Hepatology* 49 (2), 646–657. doi: 10.1002/hep.22680

Li, J., Qiu, S. J., She, W. M., Wang, F. P., Gao, H., Li, L., et al. (2012). Significance of the balance between regulatory T (Treg) and T helper 17 (Th17) cells during hepatitis B virus related liver fibrosis. *PloS One* 7 (6), e39307. doi: 10.1371/journal.pone.0039307

Linterman, M. A., Pierson, W., Lee, S. K., Kallies, A., Kawamoto, S., Rayner, T. F., et al. (2011). Foxp3+ follicular regulatory T cells control the germinal center response. *Nat. Med.* 17 (8), 975–982. doi: 10.1038/nm.2425

Liston, A., Nutsch, K. M., Farr, A. G., Lund, J. M., Rasmussen, J. P., Koni, P. A., et al. (2008). Differentiation of regulatory Foxp3+ T cells in the thymic cortex. *Proc. Natl. Acad. Sci. U. S. A.* 105 (33), 11903–11908. doi: 10.1073/pnas.0801506105

Liu, C., Xu, L., Xia, C., Long, Y., Liu, C., Lu, S., et al. (2020). Increased proportion of functional subpopulations in circulating regulatory T cells in patients with chronic hepatitis B. *Hepatol. Res.* 50 (4), 439–452. doi: 10.1111/hepr.13472

Losikoff, P. T., Self, A. A., and Gregory, S. H. (2012). Dendritic cells, regulatory T cells and the pathogenesis of chronic hepatitis C. *Virulence* 3 (7), 610–620. doi: 10.4161/viru.21823

Ma, C., Kesarwala, A. H., Eggert, T., Medina-Echeverz, J., Kleiner, D. E., Jin, P., et al. (2016). NAFLD causes selective CD4(+) T lymphocyte loss and promotes hepatocarcinogenesis. *Nature* 531 (7593), 253–257. doi: 10.1038/nature16969

Maggi, L., Santarlasci, V., Capone, M., Peired, A., Frosali, F., Crome, S. Q., et al. (2010). CD161 is a marker of all human IL-17-producing T-cell subsets and is induced by RORC. *Eur. J. Immunol.* 40 (8), 2174–2181. doi: 10.1002/eji.200940257

Maloy, K. J., and Powrie, F. (2001). Regulatory T cells in the control of immune pathology. *Nat. Immunol.* 2 (9), 816–822. doi: 10.1038/ni0901-816

Mangan, P. R., Harrington, L. E., O'Quinn, D. B., Helms, W. S., Bullard, D. C., Elson, C. O., et al. (2006). Transforming growth factor-beta induces development of the T(H)17 lineage. *Nature* 441 (7090), 231–234. doi: 10.1038/nature04754

Manigold, T., and Racanelli, V. (2007). T-cell regulation by CD4 regulatory T cells during hepatitis B and C virus infections: facts and controversies. *Lancet Infect. Dis.* 7 (12), 804–813. doi: 10.1016/S1473-3099(07)70289-X

Mannon, P. J., Fuss, I. J., Mayer, L., Elson, C. O., Sandborn, W. J., Present, D., et al. (2004). Anti-interleukin-12 antibody for active Crohn's disease. *N. Engl. J. Med.* 351 (20), 2069–2079. doi: 10.1056/NEJMoa033402

Marie, J. C., Letterio, J. J., Gavin, M., and Rudensky, A. Y. (2005). TGF-beta1 maintains suppressor function and Foxp3 expression in CD4+CD25+ regulatory T cells. *J. Exp. Med.* 201 (7), 1061–1067. doi: 10.1084/jem.20042276

Mathew, J. M., V. J, H., LeFever, A., Konieczna, I., Stratton, C., He, J., et al. (2018). A phase I clinical trial with ex vivo expanded recipient regulatory T cells in living donor kidney transplants. *Sci. Rep.* 8 (1), 7428. doi: 10.1038/s41598-018-25574-7

Matsuoka, K., Koreth, J., Kim, H. T., Bascug, G., McDonough, S., Kawano, Y., et al. (2013). Low-dose interleukin-2 therapy restores regulatory T cell homeostasis in patients with chronic graft-versus-host disease. *Sci. Transl. Med.* 5 (179), 179ra143. doi: 10.1126/scitranslmed.3005265

McGeachy, M. J., Bak-Jensen, K. S., Chen, Y., Tato, C. M., Blumenschein, W., McClanahan, T., et al. (2007). TGF-beta and IL-6 drive the production of IL-17 and IL-10 by T cells and restrain T(H)-17 cell-mediated pathology. *Nat. Immunol.* 8 (12), 1390–1397. doi: 10.1038/ni1539

McGeachy, M. J., Chen, Y., Tato, C. M., Laurence, A., Joyce-Shaikh, B., Blumenschein, W. M., et al. (2009). The interleukin 23 receptor is essential for the terminal differentiation of interleukin 17-producing effector T helper cells in vivo. *Nat. Immunol.* 10 (3), 314–324. doi: 10.1038/ni.1698

McLaughlin, T., Liu, L. F., Lamendola, C., Shen, L., Morton, J., Rivas, H., et al. (2014). T-cell profile in adipose tissue is associated with insulin resistance and systemic inflammation in humans. *Arterioscler. Thromb. Vasc. Biol.* 34 (12), 2637–2643. doi: 10.1161/ATVBAHA.114.304636

Meng, F., Wang, K., Aoyama, T., Grivennikov, S. I., Paik, Y., Scholten, D., et al. (2012). Interleukin-17 signaling in inflammatory, Kupffer cells, and hepatic stellate cells exacerbates liver fibrosis in mice. *Gastroenterology* 143 (3), 765–776.e3. doi: 10.1053/j.gastro.2012.05.049

Meng, P., Zhao, S., Niu, X., Fu, N., Su, S., Wang, R., et al. (2016). Involvement of the interleukin-23/interleukin-17 axis in chronic hepatitis C virus infection and its treatment responses. *Int. J. Mol. Sci.* 17 (11). doi: 10.3390/ijms17071070

Miyara, M., Yoshioka, Y., Kitoh, A., Shima, T., Wing, K., Niwa, A., et al. (2009). Functional delineation and differentiation dynamics of human CD4+ T cells expressing the FoxP3 transcription factor. *Immunity* 30 (6), 899–911. doi: 10.1016/j.immuni.2009.03.019

Morgan, M. E., Flierman, R., van Duivenvoorde, L. M., Witteveen, H. J., van Ewijk, W., van Laar, J. M., et al. (2005). Effective treatment of collagen-induced arthritis by adoptive transfer of CD25+ regulatory T cells. *Arthritis Rheum.* 52 (7), 2212–2221. doi: 10.1002/art.21195

Morrison, P. J., Bending, D., Fouser, L. A., Wright, J. F., Stockinger, B., Cooke, A., et al. (2013). Th17-cell plasticity in Helicobacter hepaticus-induced intestinal inflammation. *Mucosal. Immunol.* 6 (6), 1143–1156. doi: 10.1038/mi.2013.11

Mosmann, T. R., Cherwinski, H., Bond, M. W., Giedlin, M. A., and Coffman, R. L. (1986). Two types of murine helper T cell clone. I. Definition according to profiles of lymphokine activities and secreted proteins. *J. Immunol.* 136 (7), 2348–2357.

Mougiakakos, D., Johansson, C. C., Trocme, E., All-Ericsson, C., Economou, M. A., Larsson, O., et al. (2010). Intratumoral forkhead box P3-positive regulatory T cells predict poor survival in cyclooxygenase-2-positive uveal melanoma. *Cancer* 116 (9), 2224–2233. doi: 10.1002/cncr.24999

Mucida, D., Pino-Lagos, K., Kim, G., Nowak, E., Benson, M. J., Kronenberg, M., et al. (2009). Retinoic acid can directly promote TGF-beta-mediated Foxp3(+) Treg cell conversion of naive T cells. *Immunity* 30 (4), 471–472; author reply 472-473. doi: 10.1016/j.immuni.2009.03.008

Murphy, C. A., Langrish, C. L., Chen, Y., Blumenschein, W., McClanahan, T., Kastelein, R. A., et al. (2003). Divergent pro- and antiinflammatory roles for IL-23 and IL-12 in joint autoimmune inflammation. *J. Exp. Med.* 198 (12), 1951–1957. doi: 10.1084/jem.20030896

Nagakawa, K., Soyama, A., Hidaka, M., Adachi, T., Ono, S., Hara, T., et al. (2020). Elevated plasma levels of mitochondria-derived damage-associated molecular patterns during liver transplantation: predictors for postoperative multi-organ dysfunction syndrome. *Tohoku J. Exp. Med.* 250 (2), 87–93. doi: 10.1620/tjem.250.87

Nagata, T., McKinley, L., Peschon, J. J., Alcorn, J. F., Aujla, S. J., and Kolls, J. K. (2008). Requirement of IL-17RA in Con A induced hepatitis and negative regulation of IL-17 production in mouse T cells. *J. Immunol.* 181 (11), 7473–7479. doi: 10.4049/jimmunol.181.11.7473

Nakae, S., Iwakura, Y., Suto, H., and Galli, S. J. (2007). Phenotypic differences between Th1 and Th17 cells and negative regulation of Th1 cell differentiation by IL-17. *J. Leukoc. Biol.* 81 (5), 1258–1268. doi: 10.1189/jlb.1006610

Neurath, M. F., Weigmann, B., Finotto, S., Glickman, J., Nieuwenhuis, E., Iijima, H., et al. (2002). The transcription factor T-bet regulates mucosal T cell activation in experimental colitis and Crohn's disease. *J. Exp. Med.* 195 (9), 1129–1143. doi: 10.1084/jem.20011956

Niedbala, W., Wei, X. Q., Cai, B., Hueber, A. J., Leung, B. P., McInnes, I. B., et al. (2007). IL-35 is a novel cytokine with therapeutic effects against collagen-induced arthritis through the expansion of regulatory T cells and suppression of Th17 cells. *Eur. J. Immunol.* 37 (11), 3021–3029. doi: 10.1002/eji.200737810

Oberle, N., Eberhardt, N., Falk, C. S., Krammer, P. H., and Suri-Payer, E. (2007). Rapid suppression of cytokine transcription in human CD4+CD25 T cells by CD4+Foxp3+ regulatory T cells: independence of IL-2 consumption, TGF-beta, and various inhibitors of TCR signaling. *J. Immunol.* 179 (6), 3578–3587. doi: 10.4049/jimmunol.179.6.3578

Oo, Y. H., Banz, V., Kavanagh, D., Liaskou, E., Withers, D. R., Humphreys, E., et al. (2012). CXCR3-dependent recruitment and CCR6-mediated positioning of Th-17 cells in the inflamed liver. *J. Hepatol.* 57 (5), 1044–1051. doi: 10.1016/j.jhep.2012.07.008

Oppmann, B., Lesley, R., Blom, B., Timans, J. C., Xu, Y., Hunte, B., et al. (2000). Novel p19 protein engages IL-12p40 to form a cytokine, IL-23, with biological activities similar as well as distinct from IL-12. *Immunity* 13 (5), 715–725. doi: 10.1016/S1074-7613(00)00070-4

O'Garra, A., Vieira, P. L., Vieira, P., and Goldfeld, A. E. (2004). IL-10-producing and naturally occurring CD4+ Tregs: limiting collateral damage. *J. Clin. Invest.* 114 (10), 1372–1378. doi: 10.1172/JCI23215

Pandiyan, P., Zheng, L., Ishihara, S., Reed, J., and Lenardo, M. J. (2007). CD4+CD25+Foxp3+ regulatory T cells induce cytokine deprivation-mediated apoptosis of effector CD4+ T cells. *Nat. Immunol.* 8 (12), 1353–1362. doi: 10.1038/ni1536

Park, H., Li, Z., Yang, X. O., Chang, S. H., Nurieva, R., Wang, Y. H., et al. (2005). A distinct lineage of CD4 T cells regulates tissue inflammation by producing interleukin 17. *Nat. Immunol.* 6 (11), 1133–1141. doi: 10.1038/ni1261

Park, S. H., Veerapu, N. S., Shin, E. C., Biancotto, A., McCoy, J. P., Capone, S., et al. (2013). Subinfectious hepatitis C virus exposures suppress T cell responses against subsequent acute infection. *Nat. Med.* 19 (12), 1638–1642. doi: 10.1038/nm.3408

Piccirillo, C. A. (2008). Regulatory T cells in health and disease. *Cytokine* 43 (3), 395–401. doi: 10.1016/j.cyto.2008.07.469

Pillai, V., Ortega, S. B., Wang, C. K., and Karandikar, N. J. (2007). Transient regulatory T-cells: a state attained by all activated human T-cells. *Clin. Immunol.* 123 (1), 18–29. doi: 10.1016/j.clim.2006.10.014

Rau, M., Schilling, A. K., Meertens, J., Hering, I., Weiss, J., Jurowich, C., et al. (2016). Progression from nonalcoholic fatty liver to nonalcoholic steatohepatitis is marked by a higher frequency of Th17 cells in the liver and an increased Th17/resting regulatory T cell ratio in peripheral blood and in the liver. *J. Immunol.* 196 (1), 97–105. doi: 10.4049/jimmunol.1501175

Refolo, M. G., Messa, C., Guerra, V., Carr, B. I., and D'Alessandro, R. (2020). Inflammatory Mechanisms of HCC Development. *Cancers (Basel)* 12 (3), 641. doi: 10.3390/cancers12030641

Ring, S., Pushkarevskaya, A., Schild, H., Probst, H. C., Jendrossek, V., Wirsdorfer, F., et al. (2015). Regulatory T cell-derived adenosine induces dendritic cell migration through the Epac-Rap1 pathway. *J. Immunol.* 194 (8), 3735–3744. doi: 10.4049/jimmunol.1401434

Romano, M., Tung, S. L., Smyth, L. A., and Lombardi, G. (2017). Treg therapy in transplantation: a general overview. *Transpl. Int.* 30 (8), 745–753. doi: 10.1111/tri.12909

Rosenzwajg, M., Churlaud, G., Mallone, R., Six, A., Derian, N., Chaara, W., et al. (2015). Low-dose interleukin-2 fosters a dose-dependent regulatory T cell tuned milieu in T1D patients. *J. Autoimmun.* 58, 48–58. doi: 10.1016/j.jaut.2015.01.001

Sage, P. T., Paterson, A. M., Lovitch, S. B., and Sharpe, A. H. (2014). The coinhibitory receptor CTLA-4 controls B cell responses by modulating T follicular helper, T follicular regulatory, and T regulatory cells. *Immunity* 41 (6), 1026–1039. doi: 10.1016/j.immuni.2014.12.005

Sakaguchi, S. (2004). Naturally arising CD4+ regulatory t cells for immunologic self-tolerance and negative control of immune responses. *Annu. Rev. Immunol.* 22, 531–562. doi: 10.1146/annurev.immunol.21.120601.141122

Sanchez-Fueyo, A., Whitehouse, G., Grageda, N., Cramp, M. E., Lim, T. Y., Romano, M., et al. (2020). Applicability, safety, and biological activity of regulatory T cell therapy in liver transplantation. *Am. J. Transplant.* 20 (4), 1125–1136. doi: 10.1111/ajt.15700

Sands, B. E., Sandborn, W. J., Panaccione, R., O'Brien, C. D., Zhang, H., Johanns, J., et al. (2019). Ustekinumab as induction and maintenance therapy for ulcerative colitis. *N. Engl. J. Med.* 381 (13), 1201–1214. doi: 10.1056/NEJMoa1900750

Sanford, M., and McKeage, K. (2015). Secukinumab: first global approval. *Drugs* 75 (3), 329–338. doi: 10.1007/s40265-015-0359-0

Sansom, D. M. (2015). IMMUNOLOGY. Moving CTLA-4 from the trash to recycling. *Science* 349 (6246), 377–378. doi: 10.1126/science.aac7888

Saravia, J., Chapman, N. M., and Chi, H. (2019). Helper T cell differentiation. *Cell Mol. Immunol.* 16 (7), 634–643. doi: 10.1038/s41423-019-0220-6

Sarhan, D., Hippen, K. L., Lemire, A., Hying, S., Luo, X., Lenvik, T., et al. (2018). Adaptive NK cells resist regulatory T-cell suppression driven by IL37. *Cancer Immunol. Res.* 6 (7), 766–775. doi: 10.1158/2326-6066.CIR-17-0498

Schubert, D., Bode, C., Kenefeck, R., Hou, T. Z., Wing, J. B., Kennedy, A., et al. (2014). Autosomal dominant immune dysregulation syndrome in humans with CTLA4 mutations. *Nat. Med.* 20 (12), 1410–1416. doi: 10.1038/nm.3746

Schuler, P. J., Saze, Z., Hong, C. S., Muller, L., Gillespie, D. G., Cheng, D., et al. (2014). Human CD4+ CD39+ regulatory T cells produce adenosine upon co-expression of surface CD73 or contact with CD73+ exosomes or CD73+ cells. *Clin. Exp. Immunol.* 177 (2), 531–543. doi: 10.1111/cei.12354

Sebode, M., Peiseler, M., Franke, B., Schwinge, D., Schoknecht, T., Wortmann, F., et al. (2014). Reduced FOXP3(+) regulatory T cells in patients with primary sclerosing cholangitis are associated with IL2RA gene polymorphisms. *J. Hepatol.* 60 (5), 1010–1016. doi: 10.1016/j.jhep.2013.12.027

Setoguchi, R., Hori, S., Takahashi, T., and Sakaguchi, S. (2005). Homeostatic maintenance of natural Foxp3(+) CD25(+) CD4(+) regulatory T cells by interleukin (IL)-2 and induction of autoimmune disease by IL-2 neutralization. *J. Exp. Med.* 201 (5), 723–735. doi: 10.1084/jem.20041982

Shi, T., Zhang, T., Zhang, L., Yang, Y., Zhang, H., and Zhang, F. (2015). The distribution and the fibrotic role of elevated inflammatory Th17 cells in patients with primary biliary cirrhosis. *Med. (Baltimore)* 94 (44), e1888. doi: 10.1097/MD.0000000000001888

Stumhofer, J. S., Laurence, A., Wilson, E. H., Huang, E., Tato, C. M., Johnson, L. M., et al. (2006). Interleukin 27 negatively regulates the development of interleukin 17-producing T helper cells during chronic inflammation of the central nervous system. *Nat. Immunol.* 7 (9), 937–945. doi: 10.1038/ni1376

Sun, H. Q., Zhang, J. Y., Zhang, H., Zou, Z. S., Wang, F. S., and Jia, J. H. (2012). Increased Th17 cells contribute to disease progression in patients with HBV-associated liver cirrhosis. *J. Viral. Hepat.* 19 (6), 396–403. doi: 10.1111/j.1365-2893.2011.01561.x

Sun, B., Liu, M., Cui, M., and Li, T. (2020). Granzyme B-expressing treg cells are enriched in colorectal cancer and present the potential to eliminate autologous T conventional cells. *Immunol. Lett.* 217, 7–14. doi: 10.1016/j.imlet.2019.10.007

Tai, X., Cowan, M., Feigenbaum, L., and Singer, A. (2005). CD28 costimulation of developing thymocytes induces Foxp3 expression and regulatory T cell differentiation independently of interleukin 2. *Nat. Immunol.* 6 (2), 152–162. doi: 10.1038/ni1160

Tait, B., Mackay, I. R., Board, P., Coggan, M., Emery, P., and Eckardt, G. (1989). HLA A1, B8, DR3 extended haplotypes in autoimmune chronic hepatitis. *Gastroenterology* 97 (2), 479–481. doi: 10.1016/0016-5085(89)90088-7

Takimoto, T., Wakabayashi, Y., Sekiya, T., Inoue, N., Morita, R., Ichiyama, K., et al. (2010). Smad2 and Smad3 are redundantly essential for the TGF-beta-mediated regulation of regulatory T plasticity and Th1 development. *J. Immunol.* 185 (2), 842–855. doi: 10.4049/jimmunol.0904100

Tan, Z., Qian, X., Jiang, R., Liu, Q., Wang, Y., Chen, C., et al. (2013). IL-17A plays a critical role in the pathogenesis of liver fibrosis through hepatic stellate cell activation. *J. Immunol.* 191 (4), 1835–1844. doi: 10.4049/jimmunol.1203013

Taylor, A., Akdis, M., Joss, A., Akkoc, T., Wenig, R., Colonna, M., et al. (2007). IL-10 inhibits CD28 and ICOS costimulations of T cells via src homology 2 domain-containing protein tyrosine phosphatase 1. *J. Allergy Clin. Immunol.* 120 (1), 76–83. doi: 10.1016/j.jaci.2007.04.004

Tesmer, L. A., Lundy, S. K., Sarkar, S., and Fox, D. A. (2008). Th17 cells in human disease. *Immunol. Rev.* 223, 87–113. doi: 10.1111/j.1600-065X.2008.00628.x

Thomas, D. A., and Massague, J. (2005). TGF-beta directly targets cytotoxic T cell functions during tumor evasion of immune surveillance. *Cancer Cell* 8 (5), 369–380. doi: 10.1016/j.ccr.2005.10.012

Toker, A., Engelbert, D., Garg, G., Polansky, J. K., Floess, S., Miyao, T., et al. (2013). Active demethylation of the Foxp3 locus leads to the generation of stable regulatory T cells within the thymus. *J. Immunol.* 190 (7), 3180–3188. doi: 10.4049/jimmunol.1203473

Tran, D. Q. (2012). TGF-beta: the sword, the wand, and the shield of FOXP3(+) regulatory T cells. *J. Mol. Cell Biol.* 4 (1), 29–37. doi: 10.1093/jmcb/mjr033

TrehanPati, N., Kotillil, S., Hissar, S. S., Shrivastava, S., Khanam, A., Sukriti, S., et al. (2011). Circulating Tregs correlate with viral load reduction in chronic HBV-treated patients with tenofovir disoproxil fumarate. *J. Clin. Immunol.* 31 (3), 509–520. doi: 10.1007/s10875-011-9509-7

Vaknin-Dembinsky, A., Balashov, K., and Weiner, H. L. (2006). IL-23 is increased in dendritic cells in multiple sclerosis and down-regulation of IL-23 by antisense oligos increases dendritic cell IL-10 production. *J. Immunol.* 176 (12), 7768–7774. doi: 10.4049/jimmunol.176.12.7768

Van Herck, M. A., Vonghia, L., Kwanten, W. J., Jule, Y., Vanwolleghem, T., Ebo, D., et al. (2020). Diet reversal and immune modulation show key role for liver and adipose tissue T cells in murine non-alcoholic steatohepatitis. *Cell Mol. Gastroenterol. Hepatol.* 10 (3), 467–490. doi: 10.1016/j.jcmgh.2020.04.010

Vang, K. B., Yang, J., Mahmud, S. A., Burchill, M. A., Vegoe, A. L., and Farrar, M. A. (2008). IL-2, -7, and -15, but not thymic stromal lymphopoeitin, redundantly govern CD4+Foxp3+ regulatory T cell development. *J. Immunol.* 181 (5), 3285–3290. doi: 10.4049/jimmunol.181.5.3285

Veldhoen, M., Hocking, R. J., Flavell, R. A., and Stockinger, B. (2006). Signals mediated by transforming growth factor-beta initiate autoimmune encephalomyelitis, but chronic inflammation is needed to sustain disease. *Nat. Immunol.* 7 (11), 1151–1156. doi: 10.1038/ni1391

Voron, T., Marcheteau, E., Pernot, S., Colussi, O., Tartour, E., Taieb, J., et al. (2014). Control of the immune response by pro-angiogenic factors. *Front. Oncol.* 4, 70. doi: 10.3389/fonc.2014.00070

Wakabayashi, K., Lian, Z. X., Moritoki, Y., Lan, R. Y., Tsuneyama, K., Chuang, Y. H., et al. (2006). IL-2 receptor alpha(-/-) mice and the development of primary biliary cirrhosis. *Hepatology* 44 (5), 1240–1249. doi: 10.1002/hep.21385

Wang, J. M., Shi, L., Ma, C. J., Ji, X. J., Ying, R. S., Wu, X. Y., et al. (2013). Differential regulation of interleukin-12 (IL-12)/IL-23 by Tim-3 drives T(H)17 cell development during hepatitis C virus infection. *J. Virol.* 87 (8), 4372–4383. doi: 10.1128/JVI.03376-12

Wang, K., Song, Z. L., Wu, B., Zhou, C. L., Liu, W., and Gao, W. (2019). The T-helper cells 17 instead of Tregs play the key role in acute rejection after pediatric liver transplantation. *Pediatr. Transplant.* 23 (3), e13363. doi: 10.1111/petr.13363

Wei, F., Zhong, S., Ma, Z., Kong, H., Medvec, A., Ahmed, R., et al. (2013). Strength of PD-1 signaling differentially affects T-cell effector functions. *Proc. Natl. Acad. Sci. U.S.A.* 110 (27), E2480–E2489. doi: 10.1073/pnas.1305394110

Wollenberg, I., Agua-Doce, A., Hernandez, A., Almeida, C., Oliveira, V. G., Faro, J., et al. (2011). Regulation of the germinal center reaction by Foxp3+ follicular regulatory T cells. *J. Immunol.* 187 (9), 4553–4560. doi: 10.4049/jimmunol.1101328

Wong, J., Obst, R., Correia-Neves, M., Losyev, G., Mathis, D., and Benoist, C. (2007). Adaptation of TCR repertoires to self-peptides in regulatory and nonregulatory CD4+ T cells. *J. Immunol.* 178 (11), 7032–7041. doi: 10.4049/jimmunol.178.11.7032

Wu, H. J., Ivanov, I. I., Darce, J., Hattori, K., Shima, T., Umesaki, Y., et al. (2010). Gut-residing segmented filamentous bacteria drive autoimmune arthritis via T helper 17 cells. *Immunity* 32 (6), 815–827. doi: 10.1016/j.immuni.2010.06.001

Yan, Z., Zhou, J., Zhang, M., Fu, X., Wu, Y., and Wang, Y. (2014). Telbivudine decreases proportion of peripheral blood CD4+CD25+CD127low T cells in parallel with inhibiting hepatitis B virus DNA. *Mol. Med. Rep.* 9 (5), 2024–2030. doi: 10.3892/mmr.2014.2042

Yang, X. O., Nurieva, R., Martinez, G. J., Kang, H. S., Chung, Y., Pappu, B. P., et al. (2008). Molecular antagonism and plasticity of regulatory and inflammatory T cell programs. *Immunity* 29 (1), 44–56. doi: 10.1016/j.immuni.2008.05.007

Yang, B. H., Hagemann, S., Mamareli, P., Lauer, U., Hoffmann, U., Beckstette, M., et al. (2016). Foxp3(+) T cells expressing RORgammat represent a stable regulatory T-cell effector lineage with enhanced suppressive capacity during intestinal inflammation. *Mucosal. Immunol.* 9 (2), 444–457. doi: 10.1038/mi.2015.74

Yang, L., Jia, S., Shao, X., Liu, S., Zhang, Q., Song, J., et al. (2019). Interleukin-35 modulates the balance between viral specific CD4(+)CD25(+)CD127(dim/-) regulatory T cells and T helper 17 cells in chronic hepatitis B virus infection. *Virol. J.* 16 (1), 48. doi: 10.1186/s12985-019-1158-0

Yoshida, O., Dou, L., Kimura, S., Yokota, S., Isse, K., Robson, S. C., et al. (2015). CD39 deficiency in murine liver allografts promotes inflammatory injury and immune-mediated rejection. *Transpl. Immunol.* 32 (2), 76–83. doi: 10.1016/j.trim.2015.01.003

Younossi, Z., Tacke, F., Arrese, M., Chander Sharma, B., Mostafa, I., Bugianesi, E., et al. (2019). Global Perspectives on Nonalcoholic Fatty Liver Disease and Nonalcoholic Steatohepatitis. *Hepatology* 69 (6), 2672–2682. doi: 10.1002/hep.30251

Zenewicz, L. A., Yancopoulos, G. D., Valenzuela, D. M., Murphy, A. J., Karow, M., and Flavell, R. A. (2007). Interleukin-22 but not interleukin-17 provides protection to hepatocytes during acute liver inflammation. *Immunity* 27 (4), 647–659. doi: 10.1016/j.immuni.2007.07.023

Zhang, Y. H., and Sun, H. X. (2020). Immune checkpoint molecules in pregnancy: Focus on regulatory T cells. *Eur. J. Immunol.* 50 (2), 160–169. doi: 10.1002/eji.201948382

Zhang, J. P., Yan, J., Xu, J., Pang, X. H., Chen, M. S., Li, L., et al. (2009). Increased intratumoral IL-17-producing cells correlate with poor survival in hepatocellular carcinoma patients. *J. Hepatol.* 50 (5), 980–989. doi: 10.1016/j.jhep.2008.12.033

Zhang, B., Chikuma, S., Hori, S., Fagarasan, S., and Honjo, T. (2016). Nonoverlapping roles of PD-1 and FoxP3 in maintaining immune tolerance in a novel autoimmune pancreatitis mouse model. *Proc. Natl. Acad. Sci. U.S.A.* 113 (30), 8490–8495. doi: 10.1073/pnas.1608873113

Zhang, X., Feng, M., Liu, X., Bai, L., Kong, M., Chen, Y., et al. (2016). Persistence of cirrhosis is maintained by intrahepatic regulatory T cells that inhibit fibrosis resolution by regulating the balance of tissue inhibitors of metalloproteinases and matrix metalloproteinases. *Transl. Res.* 169, 67–79 e61-62. doi: 10.1016/j.trsl.2015.10.008

Zhao, L., Tang, Y., You, Z., Wang, Q., Liang, S., Han, X., et al. (2011). Interleukin-17 contributes to the pathogenesis of autoimmune hepatitis through inducing hepatic interleukin-6 expression. *PloS One* 6 (4), e18909. doi: 10.1371/journal.pone.0018909

Zheng, Y., Josefowicz, S., Chaudhry, A., Peng, X. P., Forbush, K., and Rudensky, A. Y. (2010). Role of conserved non-coding DNA elements in the Foxp3 gene in regulatory T-cell fate. *Nature* 463 (7282), 808–812. doi: 10.1038/nature08750

Zhou, L., Ivanov, I. I., Spolski, R., Min, R., Shenderov, K., Egawa, T., et al. (2007). IL-6 programs T(H)-17 cell differentiation by promoting sequential

engagement of the IL-21 and IL-23 pathways. *Nat. Immunol.* 8 (9), 967–974. doi: 10.1038/ni1488

Zhu, J., Yamane, H., and Paul, W. E. (2010). Differentiation of effector CD4 T cell populations (*). *Annu. Rev. Immunol.* 28, 445–489. doi: 10.1146/annurev-immunol-030409-101212

Ziolkowska, M., Koc, A., Luszczykiewicz, G., Ksiezopolska-Pietrzak, K., Klimczak, E., Chwalinska-Sadowska, H., et al. (2000). High levels of IL-17 in rheumatoid arthritis patients: IL-15 triggers in vitro IL-17 production via cyclosporin A-sensitive mechanism. *J. Immunol.* 164 (5), 2832–2838. doi: 10.4049/jimmunol.164.5.2832

Conflict of Interest: The authors declare that the research was conducted in the absence of any commercial or financial relationships that could be construed as a potential conflict of interest.

Copyright © 2020 Drescher, Bartsch, Weiskirchen and Weiskirchen. This is an open-access article distributed under the terms of the Creative Commons Attribution License (CC BY). The use, distribution or reproduction in other forums is permitted, provided the original author(s) and the copyright owner(s) are credited and that the original publication in this journal is cited, in accordance with accepted academic practice. No use, distribution or reproduction is permitted which does not comply with these terms.

frontiers in Pharmacology

ORIGINAL RESEARCH
published: 26 November 2020
doi: 10.3389/fphar.2020.600295

Rutaecarpine Ameliorates Ethanol-Induced Gastric Mucosal Injury in Mice by Modulating Genes Related to Inflammation, Oxidative Stress and Apoptosis

*Sichen Ren[1,2], Ying Wei[1,2], Ruilin Wang[3], Shizhang Wei[1,2], Jianxia Wen[1,2], Tao Yang[2,4], Xing Chen[1,2], Shihua Wu[1,2], Manyi Jing[2], Haotian Li[2], Min Wang[2] and Yanling Zhao[2]**

[1]School of Pharmacy, Chengdu University of Traditional Chinese Medicine, Chengdu, China, [2]Department of Pharmacy, The Fifth Medical Center of Chinese PLA General Hospital, Beijing, China, [3]Integrative Medical Center, The Fifth Medical Center of Chinese PLA General Hospital, Beijing, China, [4]School of Clinical Medicine, Chengdu University of Traditional Chinese Medicine, Chengdu, China

OPEN ACCESS

Edited by:
Ralf Weiskirchen,
RWTH Aachen University, Germany

Reviewed by:
Sun Young Park,
Pusan National University, South Korea
Ahmed Esmat Abdel Moneim,
Helwan University, Egypt

***Correspondence:**
Yanling Zhao
zhaoyl2855@126.com

Specialty section:
This article was submitted to Gastrointestinal and Hepatic Pharmacology, a section of the journal Frontiers in Pharmacology

Received: 29 August 2020
Accepted: 20 October 2020
Published: 26 November 2020

Citation:
Ren S, Wei Y, Wang R, Wei S, Wen J, Yang T, Chen X, Wu S, Jing M, Li H, Wang M and Zhao Y (2020) Rutaecarpine Ameliorates Ethanol-Induced Gastric Mucosal Injury in Mice by Modulating Genes Related to Inflammation, Oxidative Stress and Apoptosis. Front. Pharmacol. 11:600295. doi: 10.3389/fphar.2020.600295

Background: Rutaecarpine (RUT), a major quinazolino carboline alkaloid compound from the dry unripe fruit *Tetradium ruticarpum* (A. Juss.) T. G. Hartley, has various pharmacological effects. The aim of this present study was to investigate the potential gastroprotective effect of rutaecarpine on ethanol-induced acute gastric mucosal injury in mice and associated molecular mechanisms, such as activating Nrf2 and Bcl-2 via PI3K/AKT signaling pathway and inhibiting NF-κB.

Methods: Gastric ulcer index and histopathology was carried out to determine the efficacy of RUT in gastric ulceration, and the content of SOD, GSH in serum and CAT, MDA, MPO, TNF-α, IL-6, IL-1β in tissue were measured by kits. Besides, in order to illustrate the potential inflammatory, oxidative, and apoptotic perturbations, the mRNA levels of NF-κB p65, PI3K, AKT, Nrf2, Nqo1, HO-1, Bcl-2 and Bax were analyzed. In addition, the protein expression of NF-κB p65 and Nrf2 in cytoplasm and nucleus, AKT, p-AKT, Bcl-2 Bax and Caspase 3 were analyzed for further verification. Finally, immunofluorescence analysis was performed to further verify nuclear translocation of NF-κB p65.

Results: Current data strongly demonstrated that RUT alleviated the gross gastric damage, ulcer index and the histopathology damage caused by ethanol. RUT inhibited the expression and nuclear translocation of NF-κB p65 and the expression of its downstream signals, such as TNF-α, IL-6, IL-1β and MPO. Immunofluorescence analysis also verifies the result. In the context of oxidative stress, RUT improved the antioxidant milieu by remarkably upregulating the expression Nqo1 and HO-1 with activating Nrf2, and could remarkably upregulate antioxidant SOD, GSH, CAT and downregulate levels of MDA. Additionally, RUT activate the expression of Bcl-2 and inhibited the expression of downstream signals Bax and Caspase 3 to promote gastric cellular survival. These were confirmed by RUT activation of the PI3K/AKT pathway manifested by enhanced expression of PI3K and promotion of AKT phosphorylation.

Conclusion: Taken together, these results strongly demonstrated that RUT exerted a gastroprotective effect against gastric mucosal injury induced by ethanol. The underlying mechanism might be associated with the improvement of anti-inflammatory, anti-oxidation and anti-apoptosis system.

Keywords: rutaecarpine, ethanol, gastric mucosal injury, anti-inflammation, anti-oxidation, anti-apoptosis

INTRODUCTION

Gastric ulcer (GU) is a common multifactorial gastrointestinal disease worldwide, affecting the quality of life of millions of patients. According to the survey, 20–60 people out of every 100,000 population suffer from GUs, accounting for 5–10% of the world's mortality (Sung et al., 2010). Under normal physiological conditions, the mucosa maintains its integrity through defense, thus maintaining the gastric epithelial barrier and blood flow, as well as the presence of protective factors such as mucus, prostaglandins, bicarbonate, heat shock protein (HSP) and growth factors. Mucosal damage may occur when the toxic factors such as gastric acid, pepsin, bile acid, ethanol, *Helicobacter pylori* and nonsteroidal anti-inflammatory drugs (NSAIDs) invade and exceed the defense function load of gastric mucosa (Guth et al., 1979; Lee et al., 2017; Khan et al., 2018). Some other factors, such as inadequate dietary habits, excessive ethanol consumption, cigarette smoking, stress and hereditary predisposition, also may lead to the development of GU (Søreide et al., 2015; Jeon et al., 2020). Yet, the clinical treatment for the disease focuses on the use of antisecretory drugs such as H2 receptor antagonist (cimetidine) or proton pump inhibitors (omeprazole), antibiotics (clarithromycin), antacids (aluminum hydroxide), prostaglandin analogues and mucosal protective agents (bismuth) currently (Wallace, 2008). Although the use of these drug is associated with the problem of reoccurrence of GU and several undesirable side effects, the usage is still on the rise, which brings more risks (Piao et al., 2018). Therefore, the search for alternative drugs or natural resources has attracted many scholars.

With the deepening of the research on natural drugs, the characteristics of some natural drugs with rich sources and less side effects have been recognized. Rutaecarpine (RUT, **Figure 1**), a major quinazolino carboline alkaloid compound from the dry unripe fruit (named "Wu-Chu-Yu" in China) of *Tetradium ruticarpum* (A. Juss.) T. G. Hartley. It is a longstanding and multipurpose Chinese medicine traditionally used for the treatment of abdominal pain, vomiting and pyresis (Zhao et al., 2015). As one of the main active components of "Wu-Chu-Yu", RUT has a wide range of biological and pharmacological effects, such as diuresis, perspiration, uterotonic action, cardiovascular protection, improving brain function, protecting gastric mucosa, anti-inflammatory and anti-oxidation, and its pharmacological mechanism involves a variety of biological targets (Jia et al., 2010; Tian et al., 2019). Several *in vitro* studies acknowledged positive effect of RUT in peritoneal resident macrophages (Li et al., 2019), monocytes (Liu et al., 2016), osteoclast (Fukuma et al., 2018), HepG2 cells (Jin et al., 2017; Surbala et al., 2020) and Hepa-1c1c7 cells (Lee et al., 2012). Meanwhile, RUT has shown versatile beneficial effects on several experimental models, such as colitis (Zhang et al., 2020), atherosclerosis (Luo et al., 2020), cerebral ischemia-reperfusion (Han et al., 2019), hypertension (Ma et al., 2019), Acute kidney injury (Liu et al., 2020a; Liu et al., 2020b), type 2 diabetic (Surbala et al., 2020), Alzheimer's disease (Ahmad et al., 2020; Huang et al., 2020) and so on. Notably, RUT exerted definite anti-inflammatory, anti-oxidation and anti-apoptosis effects in several experimental pathology with the signaling of NF-κB, Nrf2/HO-1, Bcl-2/Bax pathways (Jin et al., 2017; Li et al., 2019a; Li et al., 2019b; Han et al., 2019). Yet, few reports focused on the effect of RUT on the ethanol-induced gastric ulcer based on above pathways. Hence, the aim of the current study was to investigate the ameliorative activity of RUT on ethanol-induced gastric ulcer and explore its underlying mechanisms.

MATERIALS AND METHODS

Reagents

In this study, RUT (pure: ≥98%) were purchased from Chengdu Chroma-Biotechnology Company (Chengdu, China). As the positive control, omeprazole (OME) was supplied by AstraZeneca Research-based Biopharmaceutical Company (Sweden). Biochemical indicator kits for SOD (Cat.No.: A001-3-2), GSH (Cat.No.: A006-2-1), CAT (Cat.No.: A007-1-1), MDA (Cat.No.: A003-1-1) and MPO (Cat.No.: A044-1-1) were provided by the Nanjing Jiancheng Bioengineering Institute (Nanjing, China) and enzyme-linked immune sorbent assay (ELISA) kits for TNF-α (Cat.No.: ml002293), IL-6 (Cat.No.: ml002293) and IL-1β (Cat.No.: ml063132) were provided by Shanghai enzyme linked biology Co., Ltd. (Shanghai, China). All antibodies were provided by Cell Signaling Technology, Inc. (Danvers, MA, United States), Abcam plc. (Cambridge, United Kingdom) or Proteintech Group, Inc. (Rosemont, IL, USA), and the specific information is shown in **Table 1**. All other experimental supplies were purchased from commercial sources.

Animals and Treatments

A total of 50 male specific pathogen-free (SPF) KM mice weighting 20 ± 2 g were obtained from SPF (Beijing) Biotechnology Co., Ltd. (Permission No. SCXK-(A) 2012-0004). All the animals were maintained in the same temperature (25 ± 2°C) and lighting (12:12 h light:dark cycle) conditions for 1 w and provided with water and standard chow ad libitum. All experimental procedures were approved by the Animal Experiment Committee of Fifth Medical Centre, General Hospital of Chinese People's Liberation Army, and carried out in accordance with the guidelines of the Council on Animal Care of Academia Sinica.

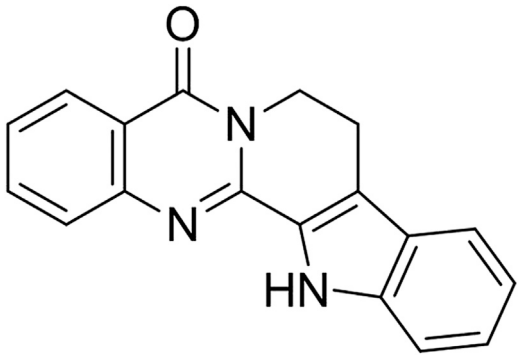


FIGURE 1 | The chemical structure of rutaecarpine.

All the animals were randomly assigned five groups with ten mice in each group. RUT and OME were prepared as a stock solution in 0.5% carboxymethyl cellulose sodium (CMC-Na) and diluted to the appropriate dosage or concentration. In the first 3 days, RUT of 450 and 900 μg/kg were administered intragastrically to RUT low dose group and RUT high dose group, respectively. OME group were administered omeprazole 20 mg/kg, while normal control group and model group were given the vehicle (0.5% CMC-Na). On the third day, 2 h after each group administration, normal control group received normal saline while other groups intragastrically received ethanol (10 ml/kg) instead. The animals were deprived of food for 24 h before the experiments but allowed free access to water and placed in wire cages to avoid interference from litter and feces. Finally, the animals were sacrificed after 2 h and their serum and gastric tissues were harvested for the further studies.

Macroscopic Assessment of Mucosal Lesions

Stomachs were removed and expanded along the larger curvature and rinsed thoroughly in saline solution. Then two observers who unaware of the treatment measured the lesion size with a vernier caliper and a magnifying glass, and calculated the ulcer index (UI) according to the Guth standard (Guth et al., 1979): no lesion (score 0), epithelial lesion or the lesion <1 mm (score 1), 1 mm ≤ lesion < 2 mm (score 2), 2 mm ≤ lesion <3 mm (score 3), 3 mm ≤ lesion <4 mm (score 4), 4 mm ≤ lesion (score segmentally), and twice for width > 1 mm. The scores were relative values, and the average UI of each group was obtained by dividing the total scores by the number of animals. The inhibition effect (%) of each protective material was calculated by using the following formula:

$$\text{Ulcer inhibition}\% = (\text{UI in model} - \text{UI in test}) \times 100/\text{UI in model}$$

Histological Analysis

Gastric tissues were excised and fixed in 10% buffered formalin for more than 48 h. After dehydrating in gradient alcohol and embedding in paraffin, three or four paraffin-embedded sections (4–5 μm thick) were prepared and stained with hematoxylin and eosin (H&E) for histological evaluation. Then the pathological changes in the gastric tissues were observed under a Nikon microscope (Nikon Instruments Inc., Japan) and analyzed by NIS-Elements (version F 4.0, Japan) software.

TABLE 1 | Antibodies information.

Antibodies	Dilution	Manufacturers	Cat. No.
For western blot analysis			
Rabbit anti-NF-κB p65	1:1,000	Cell signaling technology	8242T
Rabbit Anti-Nrf2	1:1,000	Proteintech	16396-1-AP
Rabbit anti-Bcl-2	1:1,000	Cell signaling technology	3498T
Rabbit anti-Bax	1:1,000	Cell signaling technology	2772T
Rabbit anti-cleaved Caspase-3	1:5,000	Abcam	ab214430
Rabbit Anti-AKT	1:1,000	Proteintech	10176-2-AP
Mouse Anti-pAKT	1:5,000	Proteintech	66444-1-Ig
Rabbit Anti-GAPDH	1:10000	Proteintech	10494-1-AP
Rabbit anti-histone H3	1:2000	Cell signaling technology	4499T
For immunofluorescence analysis			
Rabbit anti-NF-κB p65	1:500	Cell signaling technology	8242T

Determinations of GSH, SOD, CAT, MDA, MPO, TNF-α, IL-6, IL-1β Levels

Blood samples were collected and centrifuged at 3,000 rpm for 10 min, and then the serum samples were stored at −80°C until analysis. Gastric tissues were homogenized with cold saline and centrifuged at 12,000 rpm at 4°C for 10 min, and the supernatant of the homogenate was collected and stored at −80°C. The serum levels of SOD, GSH and the tissue levels of CAT, MDA, MPO, TNF-α, IL-6, IL-1β were measured (Liu et al., 2010; Yang et al., 2019). In brief, according to the manufacturer's protocols, the level of SOD were tested by water-soluble tetrazolium-1 (WST-1) method, the final color was read at 450 nm. Then we used ammonium molybdate method to measure the change of CAT at 405 nm and the protein level was detected by BCA Protein Assay kit (Beijing Solarbio Science & Technology Co., Ltd. Beijing, China), because ammonium molybdate can stop decomposition of H_2O_2 by CAT and form a yellow complex with remaining H_2O_2. Based on the principle that GSH can react with dithiodinitrobenzoic acid (DTNB), we quantitatively determined the content of GSH in serum by colorimetry at 405 nm. Additionally, the MDA activity were detected by thiobarbituric acid (TBA) method, the final color was detected at 450, 532, and 600 nm. According to the capability of MPO contained in neutrophils to reduce the hydrogen peroxide, we quantitatively detected the content of MPO at 460 nm to determine the number of neutrophils. For TNF-α, IL-6, IL-1β, we used enzyme-linked immune sorbent assay (ELISA) to implement. The detection operations of all these experiments

TABLE 2 | Primers sequences for RT-PCR.

Gene	Sense primer (5′-3′)	Antisense primer (5′-3′)
NF-κB p65	TCCAGGCTCCTGTTCGAGTCTC	CGGTGGCGATCATCTGTGTCTG
PI3K	CTGAGAACGCCACCGCCTTG	TCCACCACGACTTGACACATTAGC
Nrf2	GTAGATGACCATGAGTCGCTTGCC	CTTGCTCCATGTCCTGCTCTATGC
Nqo1	AGGCTGCTGTAGAGGCTCTGAAG	GCTCAGGCGTCCTTCCTTATATGC
HO-1	ACCGCCTTCCTGCTCAACATTG	CTCTGACGAAGTGACGCCATCTG
Bcl-2	TCCTTCCAGCCTGAGAGCAACC	TCACGACGGTAGCGACGAGAG
Bax	CGTGAGCGGCTGCTTGTCTG	ATGGTGAGCGAGGCGGTGAG
β-actin	ATCACTATTGGCAACGAGCGGTTC	CAGCACTGTGTTGGCATAGAGGTC

were carried out on Synergy Hybrid Reader (Biotek, Winooski, VT, United States).

Quantitative RT-PCR Analyses

The mRNA expressions of NF-κB, PI3K, Nrf2, Nqo1, HO-1, Bcl-2, and Bax in the gastric tissue were detected by quantitative reverse transcription polymerase chain reaction (RT-PCR). According to the manufacturer's protocol, total RNA was isolated from about 40 mg frozen gastric tissues of each group using Trizol reagent (Life Technologies, CA, United States). The RNA concentration was measured at 260 and 280 nm on a spectrophotometer (Purity (A260/A280) was considered qualified within the threshold of 1.8–2.2). Hereafter, RNA (2 μg) was reverse-transcribed using a RevertAid First Strand cNDA Synthesis Kit (Thermo Fisher Scientific, MA, United States). The program setting was: incubate for 5 min at 25°C followed by 60 min at 42°C and terminate the reaction by heating at 70°C for 5 min, and the obtained cDNA was stored at −20°C for subsequent PCR reactions. At last, 2 μL cDNA and SYBR™ Select Master Mix (Applied Biosystem, CA, United States) was used and then PCR amplification was carried out by ABI 7500 Real Time PCR machine (Applied Biosystems Inc., Carlsbad, CA, United States), running 45 cycles at 95°C for 5 s and 60°C for 60 s. The method recommended in Minimum Information for the Publication of Quantitative Real-Time PCR Experiments (MIQE) was strictly followed (Bustin et al., 2009). The data was calculated through $2^{-\triangle\triangle CT}$ method with β-actin as an endogenous reference. **Table 2** listed the primers used in this study.

Western Blot Analysis

Mice gastric tissue (50 mg) was homogenized and lysed in ice-cold radio immunoprecipitation assay (RIPA) lysis buffer containing 1% phenylmethylsulfonyl fluoride (PMSF), phosphatase inhibitor and protease inhibitor cocktail. Subsequently, the samples were centrifuged at 10,000 g and 4°C for 10 min. After centrifugation, the supernatant was collected and subjected to BCA Protein Assay kit (Beijing Solarbio Science & Technology Co., Ltd. Beijing, China) to measure protein concentration. In addition, nuclear and cytoplasmic extraction were performed using a nuclear extraction kit (Beijing Solarbio Science & Technology Co., Ltd., Beijing, China) to detect the presence of NF-κB and Nrf2 in nuclear and cytoplasmic proteins. Specifically, according to the manufacturer's instructions, 20 mg gastric tissue homogenate was vortexed at high speed for 15 s in 100 μl cytoplasmic protein extraction reagent containing 1% PMSF and then ice bath for 10 min. Subsequently, the samples were vortexed again for 10 s and centrifuge at 15,000 g at 4°C for 10 min. The resulting supernatant was cytoplasmic protein, whereas the precipitate was nuclear protein. Later, the supernatant was separated completely and 50 ul nuclear protein extraction reagent was added into the nuclear protein. The supernatant containing nucleoprotein was obtained by the same method. Similarly, their protein concentration was determined by BCA Protein Assay kit. The samples were denatured with reducing Laemmli SDS sample buffer and soaked in water at 95°C for 5 min. For Western blot analysis, the same amount of protein from all lysates of each sample was separated by 10–12% sodium dodecyl sulfate-polyacrylamide gel electrophoresis (SDS-PAGE), and then transferred onto the polyvinylidene fluoride (PVDF) membranes. Then immunodetection was carried out using corresponding primary antibodies (**Table 1**) in a solution of 5% bovine serum albumin (BSA), Tris-buffered saline (TBS), and 0.05% Tween 20 overnight at 4°C after blocked in BSA at room temperature for 2 h. GAPDH was used as the control for total and cytosolic protein extract, while Histone H3 was the control for nuclear protein extract. After incubation with the appropriate secondary antibodies at room temperature for 2 h, the membranes were washed 3 times in TBST (TBS with Tween 20), and the immunoreactive protein was measured using a chemiluminescence system. All Western blot studies were repeated three times.

Immunofluorescence Analysis

In order to further verify that RUT reversed ethanol-induced NF-κB translocation from the cytoplasm to the nucleus, immunofluorescence analysis was performed. After deparaffinization and dehydration in gradient alcohol, gastric tissue paraffin sections were placed in ethylenediaminetetraacetic acid (EDTA) for antigen retrieval. Then the sections were washed three times with phosphate-buffered saline (PBS) and blocked with 1% BSA for 30 min at room temperature. Subsequently, sections were incubated with anti-NF-κB p65 antibody (1:500, **Table 1**) in a solution of 5% BSA and PBS at 4°C overnight in a damp box. After washed three times the next day, the sections were incubated with the appropriate secondary antibody for 1 h at room temperature. Later, 4,6-diamidino-2-phenylindole (DAPI) was used to stain nuclei and images were taken with a confocal microscope (NIKON Eclipse C1, Nikon Instruments Inc., Japan)

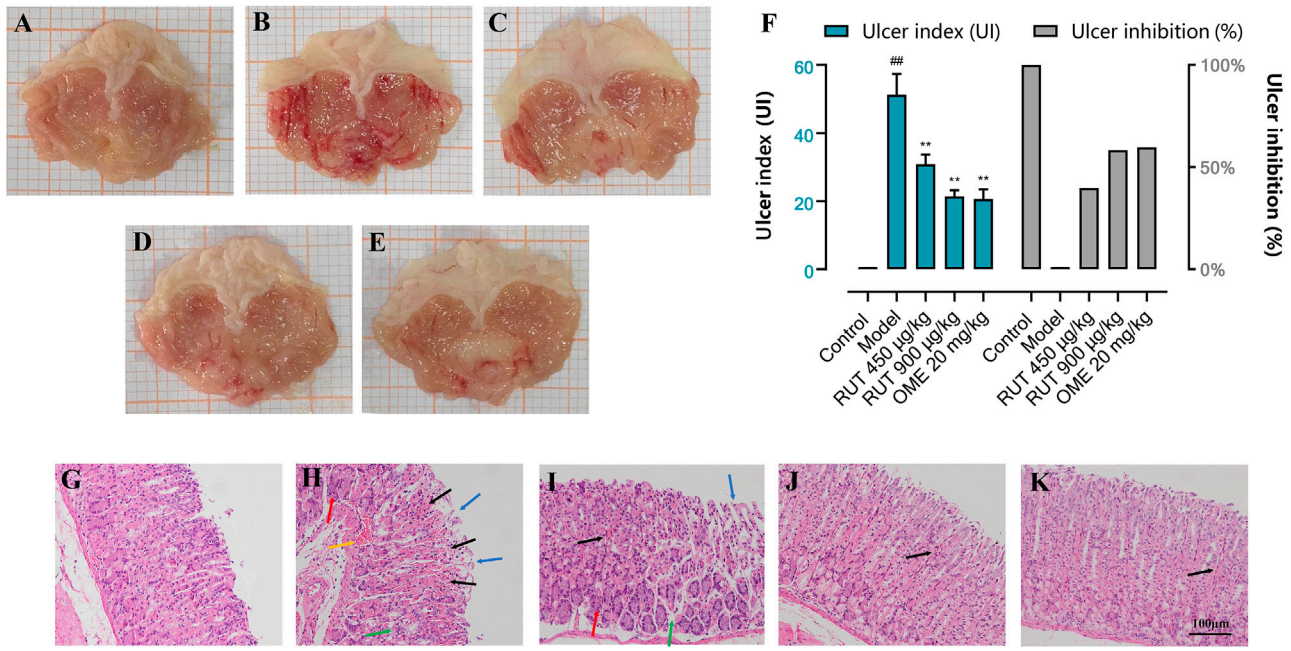


FIGURE 2 | Effect of RUT on ethanol-induced gastric mucosa injury in mice in different groups. Note: **(A–E)** Macroscopic representative images; **(F)** Ulcer index and ulcer inhibition; **(G–K)** Microscopic representative images (H&E stained, ×200 magnification; Scare bar: 100 μm. Blue →: loss of gastric epithelial cells; Black →: hemorrhagic injury; Yellow →: vascular congestion; Green →: edema; Red →: inflammatory cells infiltration). **(A,G)** Normal control group; **(B,H)** Model group; **(C,I)** RUT 450 μg/kg group; **(D,J)** RUT 900 μg/kg group; **(E,K)** OME 20 mg/kg group. Values are expressed as mean ± SD (n = 8). #$p < 0.05$ and ##$p < 0.01$ when compared with the control group. *$p < 0.05$ and **$p < 0.01$ when compared with the model group.

and analyzed by NIKON DS-U3 (Nikon Instruments Inc., Japan). Finally, we use Image-Pro Plus (version 6.0, Media Cybemetics, INC., Rockville, MD, United States) to measure and inregrate the optical density and total per area for a statistical analysis of Immunofluorescence staining.

Statistical Analysis

The experimental data were expressed as mean ± standard deviation (SD), and analyzed with the SPSS software program (Version 24.0, SPSS Inc., Chicago, IL, United States). Differences between groups were evaluated by one-way analysis of variance (ANOVA). Statistical analysis was performed using the GraphPad Prism Software (Version 8.0.1, California, United States). A value of $p < 0.05$ was considered statistically significant, and a value of $p < 0.01$ was considered highly significant.

RESULTS

Effect of RUT on Gross Evaluation of the Gastric Mucasa in Mice

Acute gastric mucosal injury was induced by intragastric administration of absolute ethanol. **Figure 2** shows that no visible lesions developed in the normal control group. The RUT groups or OME group showed extensively reduced gastric injury compared with the model group, which showed severe gastric mucosal damage appearing as glandular area hyperemia, mucosal edema accompanied by dot and linear hemorrhage necrosis.

Then, in order to reflect the effect of RUT on ethanol stimulation, we used the Guth standard to quantitatively assess the gastric lesions and calculate ulcer inhibition rate. As shown in **Figure 2F**, the model group indicated by an average UI of 51.25 ± 6.09 ($p < 0.01$). However, pre-treatment with RUT at doses of 450 and 900 μg/kg or omeprazole (20 mg/kg) produced a significant reduction in the percentage of UI (by 39.76, 58.28 and 59.75%, respectively) when compared to the model group ($p < 0.01$).

Effect of Rutaecarpine on Histopathological Assessment of Gastric Damage

In order to evaluate the protective effect of RUT on the stomach in microscopic conditions, we conducted histopathological analysis. **Figures 2G–K** shows the histopathological alterations in gastric specimens of different experimental groups. The normal control group showed normal histological structures of the mucosa, submucosa as well as the muscularis. Serious damage of gastric mucosa was found in the submucosa of the model group, and the superficial gastric epithelium was disrupted and exfoliated. Moreover, vascular congestion, edema and inflammatory cells infiltration were also observed. It was clear that the gastric mucosa damages were attenuated with omeprazole or RUT demonstrated by the integrity of superficial gastric epithelium and improvement of

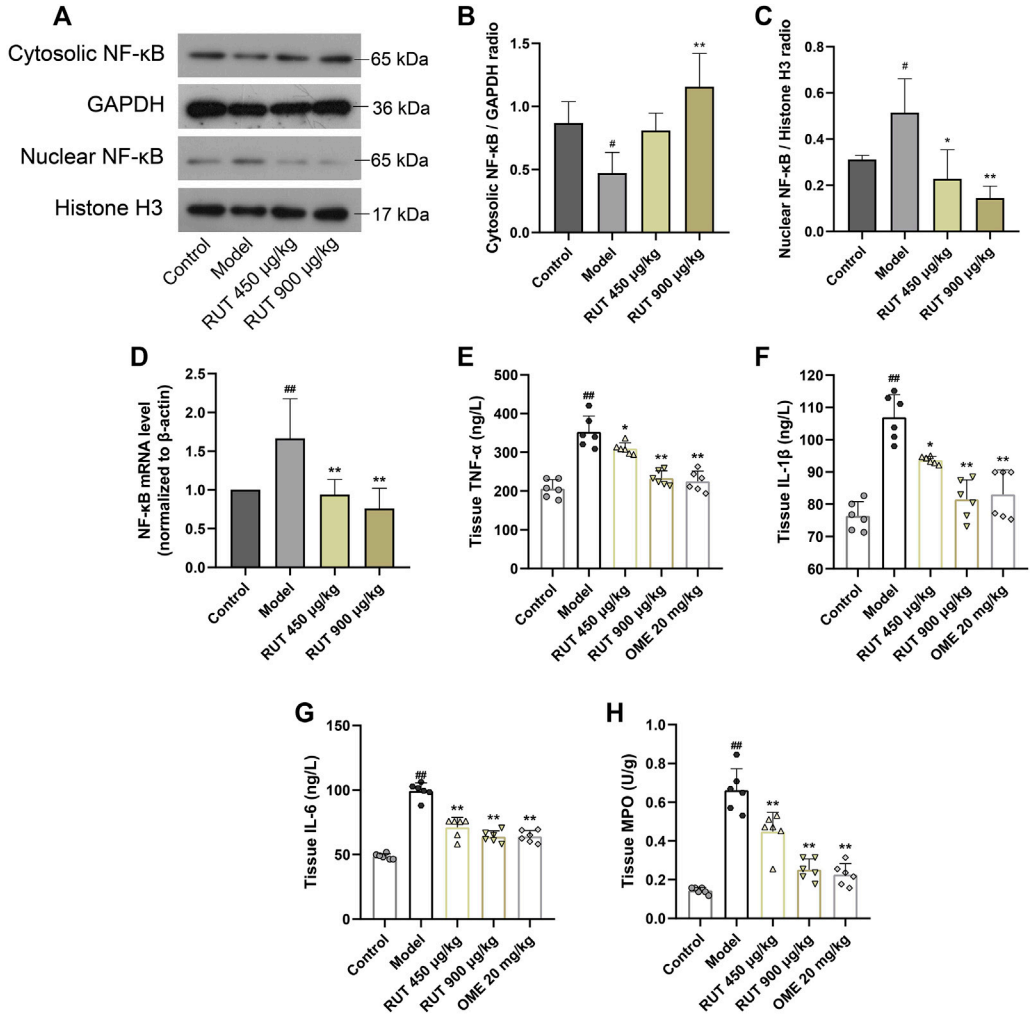


FIGURE 3 | Effect of RUT on inflammatory factors levels in gastric damage induced by ethanol. Note: **(A)** Western blot images of cytosolic and nuclear NF-κB p65; **(B)** Cytosolic NF-κB p65 protein level; **(C)** Nuclear NF-κB p65 protein level; **(D)** NF-κB p65 mRNA level; **(E)** Tissue TNF-α level; **(F)** Tissue IL-1β level; **(G)** Tissue IL-6 level; **(H)** Tissue MPO level. Values are expressed as mean ± SD (n = 6). #$p < 0.05$ and ##$p < 0.01$ when compared with the control group. *$p < 0.05$ and **$p < 0.01$ when compared with the model group.

hemorrhagic injury, edema and inflammatory infiltration Notably, the pretreatment of mice with 900 μg/kg of RUT conferred the most gastroprotection.

Effect of Rutaecarpine on Gastric NF-κB Activation and Its Downstream Inflammatory Cytokines Levels

Next, we assessed the variation of inflammatory factors in gastric mucosa aiming at exploring the intervene of RUT on inflammation. As revealed in **Figure 3**, the inflammatory disturbances were evaluated by monitoring the NF-κB nuclear translocation and alterations in its downstream signals. In terms of results, ethanol intake leaded to a sharp increase in NF-κB expression and nuclear translocation compared with control group (**Figures 3A–D**). Meanwhile, it also upregulated the level of some proinflammatory cytokines, such as TNF-α, IL-1β, IL-6 as well as MPO (**Figures 3E–H**). While performance of RUT pretreatment attenuated the expression and nuclear translocation of NF-κB. In addition, RUT reversed the level of TNF-α, IL-1β, IL-6 and MPO effectively, which is consistent with the results after OME processing. We also additionally used immunofluorescence to analyze the nuclear translocation of NF-κB, and the result also verified the previous results (**Figure 4**). All of which prove that the anti-inflammatory effect of RUT can relieve gastric mucosal damage.

Effect of Rutaecarpine on Ethanol-Triggered Oxidative Stress and Antioxidant Enzumes Activity

Then, we explored the stimulation of oxidative stress in the gastric mucosa by monitoring changes in antioxidants and lipid peroxidation levels. Exposure to ethanol presented a high level

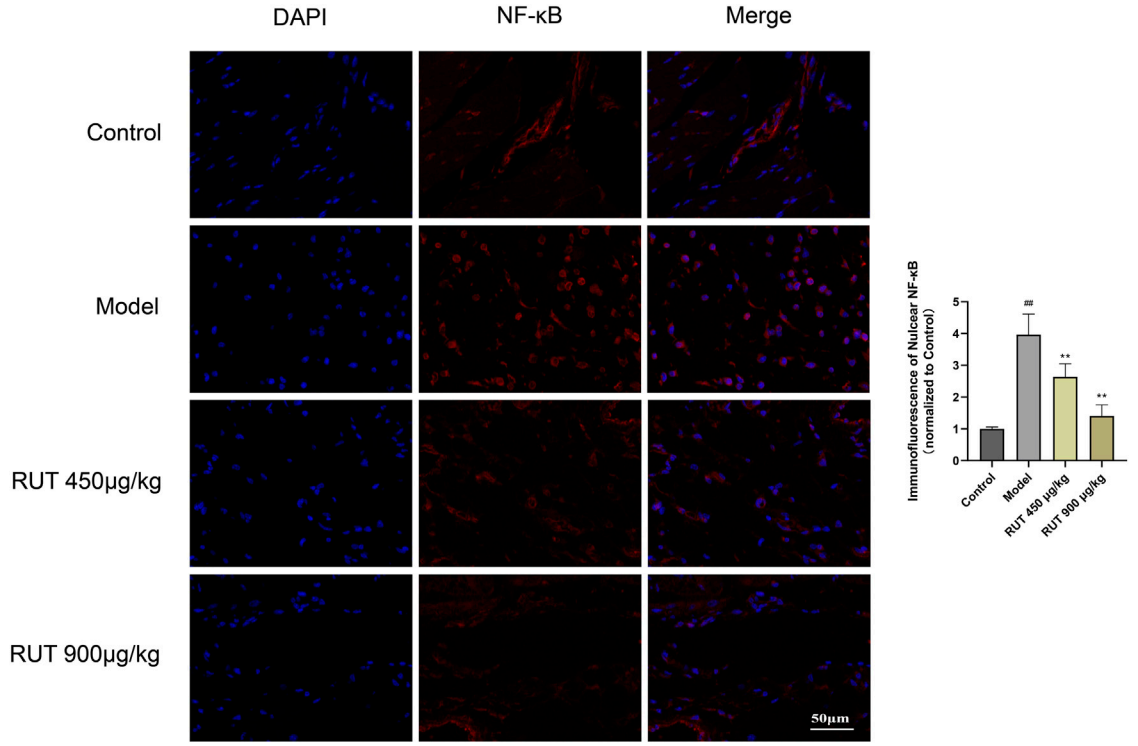


FIGURE 4 | Immunofluorescence analysis for the effect of RUT on NF-κB nuclear translocation (IF ×400 magnification; Scare bar: 50 μm; n = 3).

of lipid peroxidation, which was indicated by the increase of MDA (**Figure 5I**). In addition, the intake of ethanol significantly inhibited the activity and nuclear translocation of the antioxidant element Nrf2 (**Figures 5A–D**), accompanied by a decrease in its downstream signals levels, such as Nqo1, HO-1, SOD, CAT and GSH (**Figures 5E–H**), of which the levels of SOD, CAT and GSH were the same as those after OME treatment. RUT obviously offsets these oxidation distortions as proved by the reversal of the levels of these factors. Therefore, these results indicated that the involvement of RUT antioxidation activity for the restoration of gastric damages partly.

Effect of Rutaecarpine on Apoptosis Factors Levels and PI3K/AKT Pathway

At last, for effect of RUT on apoptosis, we measured the production of apoptotic signals and the activation of the PI3K/AKT pathway. It could be clearly observed that ethanol triggered gastric apoptosis as proved by the pronounced reduction in the level of Bcl-2 (**Figures 6A–C**) and the increase in the level of Bax (**Figures 6A,D,E**), and Caspase 3 (**Figures 6A,F**) when compared with the normal control group. In addition, ethanol inhibited the activity of PI3K/AKT pathway significantly. It is worth noting that RUT counteracted these mutations as demonstrated by the decline of Bax and restoration of Bcl-2. And Caspase 3 maintained its previous level after OME treatment. Besides, RUT restored the mRNA expression of PI3K and protein expression of pAKT. These results demonstrate that RUT plays a considerable role in ameliorating the apoptosis situation in gastric mucosa and activating PI3K/AKT pathway, which is implicated in RUT gastroprotective effects.

DISCUSSION

GU is a multifactorial gastrointestinal disease, of which alcohol is the biggest contributing factor (Das and Banerjee, 1993). In this previous study, due to the functional and anatomical similarity to the human stomach, the mice were chosen as the model and administered ethanol intragastrically to simulate human GUs caused by excessive drinking. Additionally, in several frequently used models, such as ethanol, pylorus ligation, non-steroidal anti-inflammatory drugs (NSAIDs) and stress-induced GU, the ethanol model is one of the widely used experimental models, which is similar to lots of characteristics of human acute peptic ulcer disease (Deding et al., 2016; Li et al., 2018). However, the mechanism of ethanol damage to gastric mucosa is not completely clear. Previous studies have shown that it is related to the direct damage of gastric epithelial cells (Zhao et al., 2009) and mucus layer (da Silva et al., 2018), or the indirect damage such as the influence of gastric mucosal hemodynamics (Kawano and Tsuji, 2020), infiltration of leukocytes and ensued inflammatory (Li et al., 2017) and oxidative stress (Loguercio et al., 2009; Salaspuro, 2011) and apoptosis distortion (Arab et al., 2019). Thus, this present study focused on the forthputting of

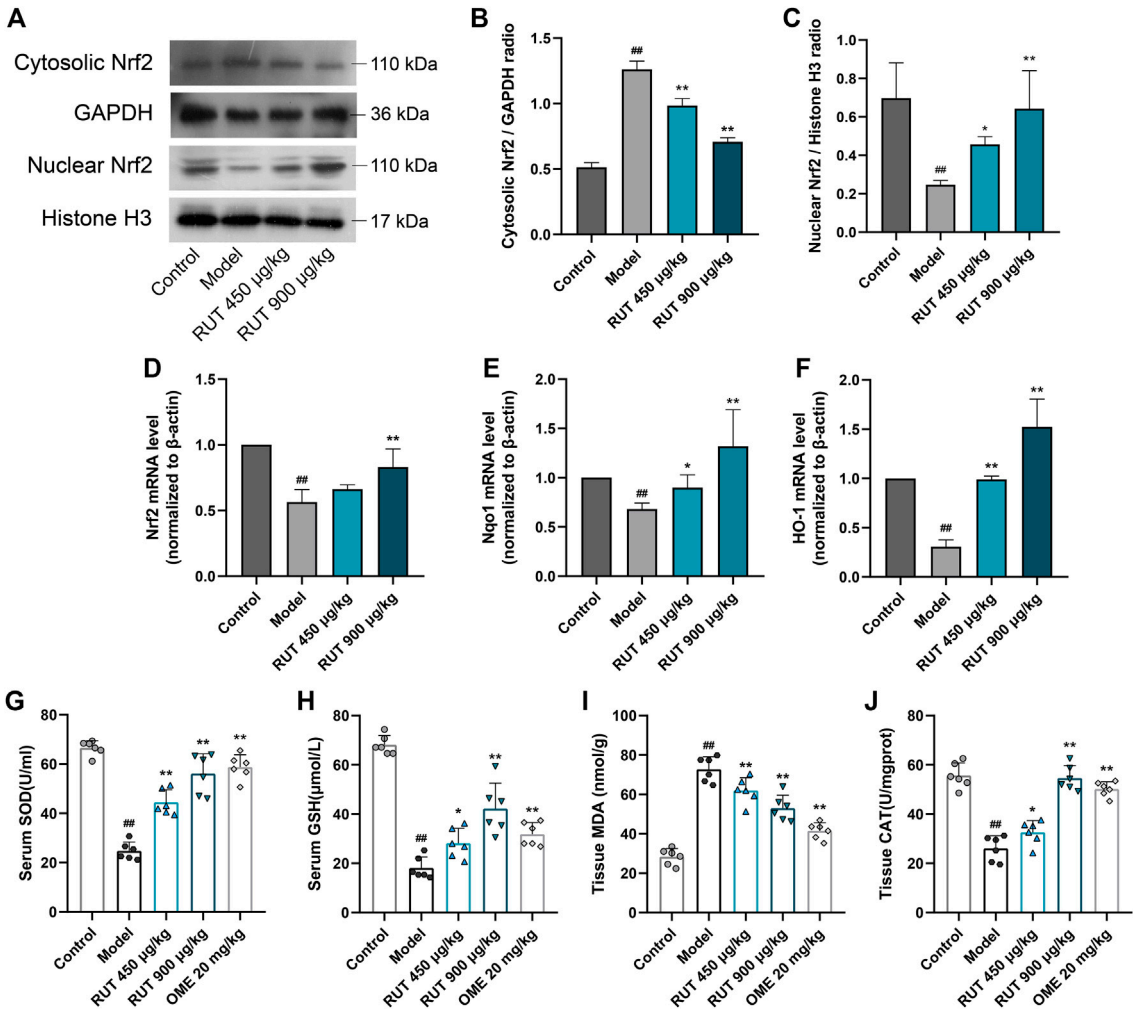


FIGURE 5 | Effect of RUT on oxidative stress factors levels in gastric damage induced by ethanol. Note: **(A)** Western blot images of cytosolic and nuclear Nrf2; **(B)** Cytosolic Nrf2 protein level; **(C)** Nuclear Nrf2 protein level; **(D)** Nrf2 mRNA level; **(E)** Nqo1 mRNA level; **(F)** HO-1 mRNA level; **(G)** Serum SOD level; **(H)** Serum GSH level; **(I)** Tissue MDA level. Values are expressed as mean ± SD (n = 6). #$p < 0.05$ and ##$p < 0.01$ when compared with the control group. *$p < 0.05$ and **$p < 0.01$ when compared with the model group.

RUT to treat ethanol-induced gastric injury through anti-inflammatory, anti-oxidation and anti-apoptosis.

In term of our results, ethanol intake could trigger severe inflammation in stomach, accompanied by activation of the NF-κB pathway and up-regulation of its downstream signal, such as TNF-a, IL-1B, IL-6 and MPO. These findings are in line with previous researches (Raish et al., 2018; Yeo et al., 2018;). In fact, NF-κB is expressed in almost all cells and performs a nonnegligible role in the pathogenesis of GU. Four transcript variants encoding different isoforms have been found including NF-κB p65/p105/p50/p52. In this article, we detected NF-κB p65 due to its contribution to inflammation. Many pro-inflammatory stimuli and ROS can lead to the activation of NF-κB through the phosphorylation of inhibitors of κB (IκBs) by the IκB kinase (IKK) complex (Akanda et al., 2018; Chen et al., 2001; Arab et al., 2019). Afterwards, free NF-κB translocates into the nucleus and consequently results in the transcriptional activation of a variety of pro-inflammatory mediators, such as TNF-α, IL-1β and IL-6 and MPO (Mitsuyama et al., 2006). Interestingly, RUT mitigated the gastric damage by inhibiting the NF-κB pathway, and then suppressed downstream proinflammatory elements. These correlates were consistent with mitigation of leukocyte infiltration. It is undoubtedly an efficacious strategy for the treatment of GU to ameliorate the aberration of these inflammatory pathological factors. In fact, RUT has pronounced anti-inflammatory capabilities in a variety of disease models according to the reports (Li et al., 2019a; Li et al., 2019b; Luo et al., 2020), which also corroborates our results from the side.

It is familiar that in addition to inflammation, the excessive generation of ROS also affects oxidative stress, which leads to altering the endogenous antioxidant defense system, including SOD and GSH (Arunachalam et al., 2019). The main source of ROS in ethanol-damaged gastric tissue is infiltration of activated

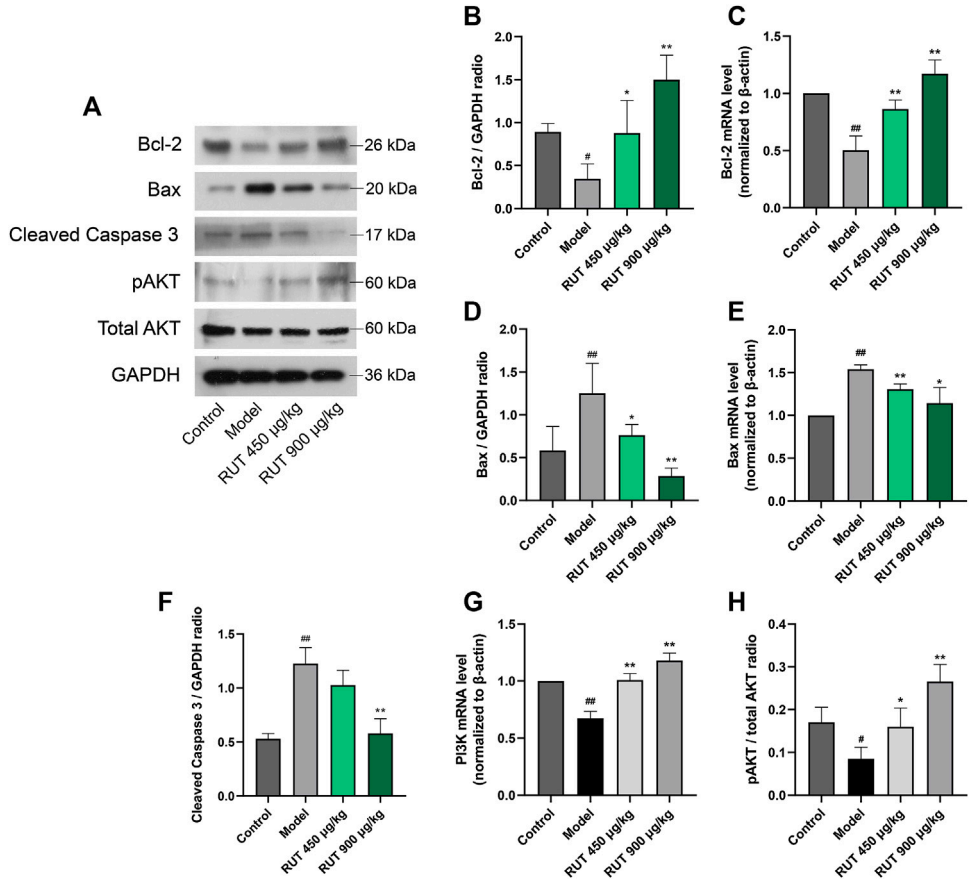


FIGURE 6 | Effect of RUT on apoptosis factors levels and PI3K pathway in gastric damage induced by ethanol. Note: **(A)** Western blot images of Bcl-2, Bax, pAKT and total AKT; **(B)** Bcl-2 protein level; **(C)** Bcl-2 mRNA level; **(D)** Bax protein level; **(E)** Bax mRNA level; **(F)** Tissue Caspase 9 level; **(G)** Caspase 3 mRNA level; **(H)** Tissue Caspase 3 level; **(I)** PI3K mRNA level. **(J)** pAKT protein level; Values are expressed as mean ± SD (n = 6). #$p < 0.05$ and ##$p < 0.01$ when compared with the control group. *$p < 0.05$ and **$p < 0.01$ when compared with the model group.

neutrophils, which MPO is a crucial indicator of neutrophil infiltration in ulcer-induced injuries (Arab et al., 2015; Paulrayer et al., 2017). Lipid peroxidation is consequence of ROS reaction against cell membrane and produces significant levels of MDA, which leads to oxidative gastric damage (Yu et al., 2017). The present findings indicated that the application of ethanol indulged MDA and significantly inhibited the production of the Nrf2. These changes prevented transcription factor Nrf2 from serving as a sensor to regulate the expression of antioxidant enzymes (HO-1 and Nqo1) driven by antioxidant response elements (ARE) in response to oxidative stimulation. The observations were consistent with previous researches (Nguyen et al., 2009; Itoh et al., 2010). Interestingly, our results show that RUT remarkably reverses the redox induced by ethanol. A good explanation for inhibiting oxidative stress was the observed remission of neutrophil infiltration and the decrease of membrane lipid peroxidation level. Ample evidence demonstrated the antioxidants plays a central role in process of GU (Kwiecien et al., 2002; Raish et al., 2018; Mohan, et al., 2020). Our data validated the restoration of Nrf2 along with the prototypical Nrf2 target genes (HO-1 and Nqo1) and the replenish of crucial antioxidation elements (SOD, CAT and GSH) in the wake of RUT treatment. All of data suggest the potential prospects of RUT in treating GU through anti-oxidation.

Numerous studies demonstrated that apoptosis also goes hand in hand with the occurrence of GU, and the continuous excessive production of apoptosis will destroy the integrity of gastric mucosa and eventually induce gastric mucosa dysfunction (Liu et al., 2020). Mechanistically, our data indicated ethanol intake made the anti-apoptosis gene Bcl-2 down-regulated markedly driven by ROS and pro-inflammatory signals. In this circumstance, the restriction to the apoptotic protein Bax was limited, which in turn leaded to the mitochondrial escape of cytochrome C and subsequently activated Caspase 9 and Caspase 3. This is consistent with previous studies (Raish et al., 2018; Xie et al., 2020). After receiving RUT, it could be clearly observed that the anti-apoptosis capacity of gastric mucosa was enhanced, manifested in the recovery of BCL-2 level and the control of Bax and Caspase 3. Actually, previous studies have demonstrated the latent anti-apoptosis activity (Li et al., 2019a; Li et al., 2019b; Han et al., 2019). And our data strongly indicated that RUT could partly participate in the palliation of the damage caused by ethanol though anti-apoptosis.

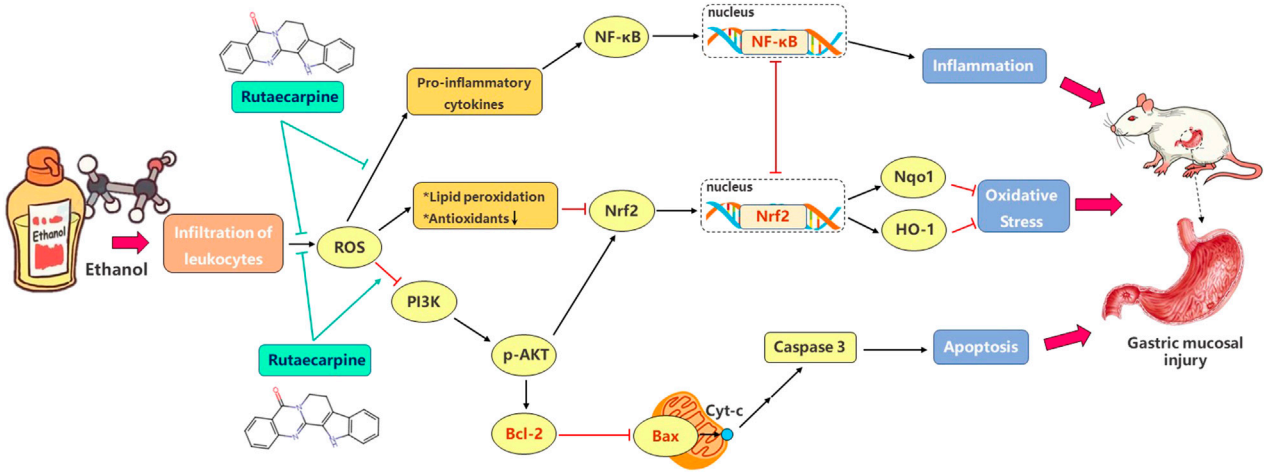


FIGURE 7 | Schematic diagram of signal pathway that mediates ethanol-induced gastric mucosal injury and the ameliorative effects of RUT on mice. (→: activate; ⊣: inhibit).

The present findings also revealed that ethanol inhibited PI3K/AKT pathway, which is consistent with previous literature (Zhang et al., 2019). In fact, the activation of PI3K/AKT pathway is essential for cell resistance to oxidation and apoptosis (Arab et al., 2019; Cao et al., 2020). Our data suggest that the activation of AKT phosphorylation promoted by RUT was associated with the Nrf2 and Bcl-2 up-regulation and in turn to the down-regulation of Bax.

In summary, inflammation, oxidative stress and apoptosis are closely related to the occurrence of GU. The excessive production of ROS released inflammation and apoptosis signals, and inhibited antioxidant elements to promote the continuous production of oxidative stress. Our findings clearly revealed that RUT augments cellular anti-inflammation, antioxidant and anti-apoptosis defense capacities, thereby protecting cells from ethanol damage. The potential mechanism seems to be related to the induction of antioxidant and anti-apoptosis enzymes synthesis by activating Nrf2 and Bcl-2 through PI3K/AKT-dependent pathway, and to the inhibition of NFKB pathway and inflammation signals. **Figure 7** showed their complex relationship. These findings indicate that RUT might be a potential therapeutic agent for GU.

DATA AVAILABILITY STATEMENT

The original contributions presented in the study are included in the article/supplementary material, further inquiries can be directed to the corresponding author.

AUTHOR CONTRIBUTIONS

SR and YZ conceived the project and wrote the manuscript. SR performed main part of the experiments, with contributions from YW, RW, SW, and JW. TY, XC, SW, MJ, HL, and MW contributed to the data collection and analysis. YZ participated in the project design as well as manuscript draft preparation and revision. All authors read and approved the final manuscript.

ACKNOWLEDGMENTS

This research was financially supported by the National Key Research and Development Program (No. 2018YFC1704500).

REFERENCES

Ahmad, S. S., Sinha, M., Ahmad, K., Khalid, M., and Choi, I. (2020). Study of Caspase 8 inhibition for the management of Alzheimer's disease: a molecular docking and dynamics simulation. *Molecules* 25 (9), 2071. doi:10.3390/molecules25092071

Akanda, M. R., Kim, I. S., Ahn, D., Tae, H. J., Nam, H. H., Choo, B. K., et al. (2018). Anti-inflammatory and gastroprotective roles of Rabdosia inflexa through downregulation of pro-inflammatory cytokines and MAPK/NF-κB signaling pathways. *Int. J. Mol. Sci.* 19 (2), 584. doi:10.3390/ijms19020584

Arab, H. H., Salama, S. A., Omar, H. A., Arafa, e., and Maghrabi, I. A. (2015). Diosmin protects against ethanol-induced gastric injury in rats: novel anti-ulcer actions. *PloS One* 10 (3), e0122417. doi:10.1371/journal.pone.0122417

Arab, H. H., Salama, S. A., Eid, A. H., Kabel, A. M., and Shahin, N. N. (2019). Targeting MAPKs, NF-κB, and PI3K/AKT pathways by methyl palmitate ameliorates ethanol-induced gastric mucosal injury in rats. *J. Cell. Physiol.* 234 (12), 22424–22438. doi:10.1002/jcp.28807

Arunachalam, K., Damazo, A. S., Pavan, E., Oliveira, D. M., Figueiredo, F. F., Machado, M., et al. (2019). Cochlospermum regium (Mart. ex Schrank) Pilg.: evaluation of chemical profile, gastroprotective activity and mechanism of action of hydroethanolic extract of its xylopodium in acute and chronic experimental models. *J. Ethnopharmacol.* 233, 101–114. doi:10.1016/j.jep.2019.01.002

Bustin, S. A., Benes, V., Garson, J. A., Hellemans, J., Huggett, J., Kubista, M., et al. (2009). The MIQE guidelines: minimum information for publication of quantitative real-time PCR experiments. *Clin. Chem.* 55 (4), 611–622. doi:10.1373/clinchem.2008.112797

Cao, W. Q., Zhai, X. Q., Ma, J. W., Fu, X. Q., Zhao, B. S., Zhang, P., et al. (2020). Natural borneol sensitizes human glioma cells to cisplatin-induced apoptosis by triggering ROS-mediated oxidative damage and regulation of MAPKs and PI3K/AKT pathway. *Pharm. Biol.* 58 (1), 72–79. doi:10.1080/13880209.2019.1703756

Chen, F., Castranova, V., and Shi, X. (2001). New insights into the role of nuclear factor-kappaB in cell growth regulation. *Am. J. Pathol.* 159 (2), 387–397. doi:10.1016/s0002-9440(10)61708-7

da Silva, D. M., Martins, J., de Oliveira, D. R., Florentino, I. F., da Silva, D., Dos Santos, F., et al. (2018). Effect of allantoin on experimentally induced gastric ulcers: pathways of gastroprotection. *Eur. J. Pharmacol.* 821, 68–78. doi:10.1016/j.ejphar.2017.12.052

Das, D. and Banerjee, R. K. (1993). Effect of stress on the antioxidant enzymes and gastric ulceration. *Mol. Cell. Biochem.* 125 (2), 115–125. doi:10.1007/BF00936440

Deding, U., Ejlskov, L., Grabas, M. P., Nielsen, B. J., Torp-Pedersen, C., and Bøggild, H. (2016). Perceived stress as a risk factor for peptic ulcers: a register-based cohort study. *BMC Gastroenterol.* 16 (1), 140. doi:10.1186/s12876-016-0554-9

Fukuma, Y., Sakai, E., Komaki, S., Nishishita, K., Okamoto, K., and Tsukuba, T. (2018). Rutaecarpine attenuates osteoclastogenesis by impairing macrophage colony stimulating factor and receptor activator of nuclear factor κ-B ligand-stimulated signalling pathways. *Clin. Exp. Pharmacol. Physiol.* 45 (8), 863–865. doi:10.1111/1440-1681.12941

Guth, P. H., Aures, D., and Paulsen, G. (1979). Topical aspirin plus HCl gastric lesions in the rat. Cytoprotective effect of prostaglandin, cimetidine, and probanthine. *Gastroenterology* 76 (1), 88–93. doi:10.1016/s0016-5085(79)80133-x

Han, M., Hu, L., and Chen, Y. (2019). Rutaecarpine may improve neuronal injury, inhibits apoptosis, inflammation and oxidative stress by regulating the expression of ERK1/2 and Nrf2/HO-1 pathway in rats with cerebral ischemia-reperfusion injury. *Drug Des. Dev. Ther.* 13, 2923–2931. doi:10.2147/DDDT.S216156

Huang, X. F., Dong, Y. H., Wang, J. H., Ke, H. M., Song, G. Q., and Xu, D. F. (2020). Novel PDE5 inhibitors derived from rutaecarpine for the treatment of Alzheimer's disease. *Bioorg. Med. Chem. Lett.* 30 (9), 127097. doi:10.1016/j.bmcl.2020.127097

Itoh, K., Mimura, J., and Yamamoto, M. (2010). Discovery of the negative regulator of Nrf2, Keap1: a historical overview. *Antioxid. Redox signal.* 13 (11), 1665–1678. doi:10.1089/ars.2010.3222

Jeon, D. B., Shin, H. G., Lee, B. W., Jeong, S. H., Kim, J. H., Ha, J. H., et al. (2020). Effect of heat-killed *Enterococcus faecalis* EF-2001 on ethanol-induced acute gastric injury in mice: protective effect of EF-2001 on acute gastric ulcer. *Hum. Exp. Toxicol.* 39 (5), 721–733. doi:10.1177/0960327119899987

Jia, S. j., and Hu, C. P. (2010). Pharmacological effects of rutaecarpine as a cardiovascular protective agent. *Molecules* 15: 1873–81. doi:10.3390/molecules15031873

Jin, S. W., Hwang, Y. P., Choi, C. Y., Kim, H. G., Kim, S. J., Kim, Y., et al. (2017). Protective effect of rutaecarpine against t-BHP-induced hepatotoxicity by upregulating antioxidant enzymes via the CaMKII-AKT and Nrf2/ARE pathways. *Food Chem. Toxicol.* 100, 138–148. doi:10.1016/j.fct.2016.12.031

Kawano, S. and Tsuji, S. (2000). Role of mucosal blood flow: a conceptional review in gastric mucosal injury and protection. *J. Gastroenterol. Hepatol.* 15 (Suppl. l), D1–D6. doi:10.1046/j.1440-1746.2000.02142.x

Khan, M., Khundmiri, S., Khundmiri, S. R., Al-Sanea, M. M., and Mok, P. L. (2018). Fruit-Derived polysaccharides and terpenoids: recent update on the gastroprotective effects and mechanisms. *Front. Pharmacol.* 9, 569. doi:10.3389/fphar.2018.00569

Kwiecień, S., Brzozowski, T., and Konturek, S. J. (2002). Effects of reactive oxygen species action on gastric mucosa in various models of mucosal injury. *J. Physiol. Pharmacol.* 53 (1), 39–50.

Lee, S. J., Ahn, H., Nam, K. W., Kim, K. H., and Mar, W. (2012). Effects of rutaecarpine on hydrogen peroxide-induced apoptosis in murine hepa-1c1c7 cells. *Biomol. Ther.* 20 (5), 487–491. doi:10.4062/biomolther.2012.20.5.487

Lee, Y. B., Yu, J., Choi, H. H., Jeon, B. S., Kim, H. K., Kim, S. W., et al. (2017). The association between peptic ulcer diseases and mental health problems: a population-based study: a STROBE compliant article. *Medicine* 96 (34), e7828. doi:10.1097/MD.0000000000007828

Li, W., Wang, Y., Wang, X., Zhang, H., He, Z., Zhi, W., et al. (2017). Gastroprotective effect of esculin on ethanol-induced gastric lesion in mice. *Fundam. Clin. Pharmacol.* 31 (2), 174–184. doi:10.1111/fcp.12255

Li, Q., Hu, X., Xuan, Y., Ying, J., Fei, Y., Rong, J., et al. (2018). Kaempferol protects ethanol-induced gastric ulcers in mice via pro-inflammatory cytokines and NO. *Acta Biochim. Biophys. Sin.* 50 (3), 246–253. doi:10.1093/abbs/gmy002

Li, Y., Zhang, G., Chen, M., Tong, M., Zhao, M., Tang, F., et al. (2019a). Rutaecarpine inhibited imiquimod-induced psoriasis-like dermatitis via inhibiting the NF-κB and TLR7 pathways in mice. *Biomed. Pharmacother.* 109, 1876–1883. doi:10.1016/j.biopha.2018.10.062

Li, Z., Yang, M., Peng, Y., Gao, M., and Yang, B. (2019b). Rutaecarpine ameliorated sepsis-induced peritoneal resident macrophages apoptosis and inflammation responses. *Life Sci.* 228, 11–20. doi:10.1016/j.lfs.2019.01.038

Liu, S. H., Ma, K., Xu, X. R., and Xu, B. (2010). A single dose of carbon monoxide intraperitoneal administration protects rat intestine from injury induced by lipopolysaccharide. *Cell Stress Chaperones*, 15 (5), 717–727. doi:10.1007/s12192-010-0183-0

Liu, R., Hao, Y. T., Zhu, N., Liu, X. R., Kang, J. W., Mao, R. X., et al. (2020a). The gastroprotective effect of small molecule oligopeptides isolated from Walnut (*Juglans regia* L.) against ethanol-induced gastric mucosal injury in rats. *Nutrients* 12 (4), 1138. doi:10.3390/nu12041138

Liu, X. Q., Jin, J., Li, Z., Jiang, L., Dong, Y. H., Cai, Y. T., et al. (2020b). Rutaecarpine derivative Cpd-6c alleviates acute kidney injury by targeting PDE4B, a key enzyme mediating inflammation in cisplatin nephropathy. *Biochem. Pharmacol.* 180, 114132. doi:10.1016/j.bcp.2020.114132

Liu, Y., Fu, Y. Q., Peng, W. J., Yu, Y. R., Wu, Y. S., Yan, H., et al. (2016). Rutaecarpine reverses the altered Connexin expression pattern induced by oxidized low-density Lipoprotein in monocytes. *J. Cardiovasc. Pharmacol.* 67 (6), 519–525. doi:10.1097/FJC.0000000000000372

Loguercio, C., Tuccillo, C., Federico, A., Fogliano, V., Del Vecchio Blanco, C., and Romano, M. (2009). Alcoholic beverages and gastric epithelial cell viability: effect on oxidative stress-induced damage. *J. Physiol. Pharmacol.* 60 (Suppl. 7), 87–92. PMID: 20388950. Available at: https://pubmed.ncbi.nlm.nih.gov/20388950/

Luo, J., Wang, X., Jiang, X., Liu, C., Li, Y., Han, X., et al. (2020). Rutaecarpine derivative R3 attenuates atherosclerosis via inhibiting NLRP3 inflammasome-related inflammation and modulating cholesterol transport. *FASEB J.* 34 (1), 1398–1411. doi:10.1096/fj.201900903RRR

Ma, J., Chen, L., Fan, J., Cao, W., Zeng, G., Wang, Y., et al. (2019). Dual-targeting Rutaecarpine-NO donor hybrids as novel anti-hypertensive agents by promoting release of CGRP. *Eur. J. Med. Chem.* 168, 146–153. doi:10.1016/j.ejmech.2019.02.037

Mitsuyama, K., Tsuruta, O., Matsui, Y., Harada, K., Tomiyasu, N., Suzuki, A., et al. (2006). Activation of c-Jun N-terminal kinase (JNK) signalling in experimentally induced gastric lesions in rats. *Clin. Exp. Immunol.* 143 (1), 24–29. doi:10.1111/j.1365-2249.2005.02959.x

Mohan, S., Hobani, Y. H., Shaheen, E., Abou-Elhamd, A. S., Abdelhaleem, A., Alhazmi, H. A., et al. (2020). Ameliorative effect of Boesenbergin A, a chalcone isolated from *Boesenbergia rotunda* (Fingerroot) on oxidative stress and inflammation in ethanol-induced gastric ulcer *in vivo*. *J. Ethnopharmacol.* 261, 113104. doi:10.1016/j.jep.2020.113104

Nguyen, T., Nioi, P., and Pickett, C. B. (2009). The Nrf2-antioxidant response element signaling pathway and its activation by oxidative stress. *J. Biol. Chem.* 284 (20), 13291–13295. doi:10.1074/jbc.r900010200

Paulrayer, A., Adithan, A., Lee, J. H., Moon, K. H., Kim, D. G., Im, S. Y., et al. (2017). Aronia melanocarpa (Black Chokeberry) reduces ethanol-induced gastric damage via regulation of HSP-70, NF-κB, and MCP-1 signaling. *Int. J. Mol. Sci.* 18 (6), 1195. doi:10.3390/ijms18061195

Piao, X., Li, S., Sui, X., Guo, L., Liu, X., Li, H., et al. (2018). 1-Deoxynojirimycin (DNJ) ameliorates indomethacin-induced gastric ulcer in mice by affecting NF-kappaB signaling pathway. *Front. Pharmacol.* 9, 372. doi:10.3389/fphar.2018.00372

Raish, M., Ahmad, A., Ansari, M. A., Alkharfy, K. M., Aljenoobi, F. I., Jan, B. L., et al. (2018). Momordica charantia polysaccharides ameliorate oxidative stress, inflammation, and apoptosis in ethanol-induced gastritis in mucosa through NF-kB signaling pathway inhibition. *Int. J. Biol. Macromol.* 111, 193–199. doi:10.1016/j.ijbiomac.2018.01.008

Salaspuro, M. (2011). Acetaldehyde and gastric cancer. *J. Dig. Dis.* 12 (2), 51–59. doi:10.1111/j.1751-2980.2011.00480.x

Søreide, K., Thorsen, K., Harrison, E. M., Bingener, J., Møller, M. H., Ohene-Yeboah, M., et al. (2015). Perforated peptic ulcer. *Lancet* 386 (10000), 1288–1298. doi:10.1016/s0140-6736(15)00276-7 |

Sung, J. J., Tsoi, K. K., Ma, T. K., Yung, M. Y., Lau, J. Y., and Chiu, P. W. (2010). Causes of mortality in patients with peptic ulcer bleeding: a prospective cohort study of 10,428 cases. *Am. J. Gastroenterol.* 105 (1), 84–89. doi:10.1038/ajg.2009.507

Surbala, L., Singh, C. B., Devi, R. V., and Singh, O. J. (2020). Rutaecarpine exhibits anti-diabetic potential in high fat diet-multiple low dose streptozotocin induced type 2 diabetic mice and *in vitro* by modulating hepatic glucose homeostasis. *J. Pharmacol. Sci.* 143 (4), 307–314. doi:10.1016/j.jphs.2020.04.008

Tian, K. M., Li, J. J., and Xu, S. W. (2019). Rutaecarpine: a promising cardiovascular protective alkaloid from Evodia rutaecarpa (Wu Zhu Yu). *Pharmacol. Res.* 141, 541–550. doi:10.1016/j.phrs.2018.12.019

Wallace, J. L. (2008). Prostaglandins, NSAIDs, and gastric mucosal protection: why doesn't the stomach digest itself?. *Physiol. Rev.* 88 (4), 1547–1565. doi:10.1152/physrev.00004.2008

Xie, L., Guo, Y. L., Chen, Y. R., Zhang, L. Y., Wang, Z. C., Zhang, T., et al. (2020). A potential drug combination of omeprazole and patchouli alcohol significantly normalizes oxidative stress and inflammatory responses against gastric ulcer in ethanol-induced rat model. *Int. Immunopharmacol.* 85, 106660. doi:10.1016/j.intimp.2020.106660

Yang, S., Wang, H., Yang, Y., Wang, R., Wang, Y., Wu, C., et al. (2019). Baicalein administered in the subacute phase ameliorates ischemia-reperfusion-induced brain injury by reducing neuroinflammation and neuronal damage. *Biomed. Pharmacother.* 117, 109102. doi:10.1016/j.biopha.2019.109102

Yeo, D., Hwang, S. J., Kim, W. J., Youn, H. J., and Lee, H. J. (2018). The aqueous extract from Artemisia capillaris inhibits acute gastric mucosal injury by inhibition of ROS and NF-kB. *Biomed. Pharmacother.* 99, 681–687. doi:10.1016/j.biopha.2018.01.118

Yu, T., Yang, Y., Kwak, Y. S., Song, G. G., Kim, M. Y., Rhee, M. H., et al. (2017). Ginsenoside Rc from Panax ginseng exerts anti-inflammatory activity by targeting TANK-binding kinase 1/interferon regulatory factor-3 and p38/ATF-2. *J. Ginseng Res.* 41 (2), 127–133. doi:10.1016/j.jgr.2016.02.001

Zhang, Z., Wen, H., Weng, J., Feng, L., Liu, H., Hu, X., et al. (2019). Silencing of EPCAM suppresses hepatic fibrosis and hepatic stellate cell proliferation in mice with alcoholic hepatitis via the PI3K/AKT/mTOR signaling pathway. *Cell Cycle* 18 (18), 2239–2254. doi:10.1080/15384101.2019.1642067

Zhang, Y., Yan, T., Sun, D., Xie, C., Wang, T., Liu, X., et al. (2020). Rutaecarpine inhibits KEAP1-NRF2 interaction to activate NRF2 and ameliorate dextran sulfate sodium-induced colitis. *Free Radic. Biol. Med.* 148, 33–41. doi:10.1093/abbs/gmp014

Zhao, W., Zhu, F., Shen, W., Fu, A., Zheng, L., Yan, Z., et al. (2009). Protective effects of DIDS against ethanol-induced gastric mucosal injury in rats. *Acta Biochim. Biophys. Sin.* 41 (4), 301–308. doi:10.1093/abbs/gmp014

Zhao, Z., Gong, S., Wang, S., and Ma, C. (2015). Effect and mechanism of evodiamine against ethanol-induced gastric ulcer in mice by suppressing Rho/NF-кБ оатжхачћ *Int. Immunopharmacol.* 28 (1), 588–595. doi:10.1016/j.intimp.2015.07.030

Conflict of Interest: The authors declare that the research was conducted in the absence of any commercial or financial relationships that could be construed as a potential conflict of interest.

Copyright © 2020 Ren, Wei, Wang, Wei, Wen, Yang, Chen, Wu, Jing, Li, Wang and Zhao. This is an open-access article distributed under the terms of the Creative Commons Attribution License (CC BY). The use, distribution or reproduction in other forums is permitted, provided the original author(s) and the copyright owner(s) are credited and that the original publication in this journal is cited, in accordance with accepted academic practice. No use, distribution or reproduction is permitted which does not comply with these terms.

Glossary

GU gastric ulcer

RUT rutaecarpine

OME omeprazole

UI ulcer index

NF-κB nuclear factor κB

TNF-α tumor necrosis factor-α

IL-1β interleukin-1β

IL-6 interleukin-6

MPO myeloperoxidase

DAPI 4,6-diamidino-2-phenylindole

Nrf2 nuclear factor erythroid 2-related factor 2

Nqo1 NAD(P)H/quinone oxidoreductase 1

HO-1 heme oxygenase-1

SOD superoxide dismutase

GSH glutathione

CAT catalase

MDA malondialdehyde

Bcl-2 B cell lymphoma-2 expression

Bax Bcl-2 associated x

Cyt C cytochrome C

pAKT phospho protein kinase B

PI3K phosphatidylinositol 3-kinase

frontiers in Pharmacology

ORIGINAL RESEARCH
published: 04 December 2020
doi: 10.3389/fphar.2020.585582

Hepatoprotective Effect and Molecular Mechanisms of Hengshun Aromatic Vinegar on Non-Alcoholic Fatty Liver Disease

Shenghu Zhu[1†], Linshu Guan[2†], Xuemei Tan[2], Guoquan Li[1], Changjie Sun[2], Meng Gao[2], Bao Zhang[1] and Lina Xu[2,3]**

[1]Jiangsu Hengshun Vinegar Industry Co., Ltd., Zhenjiang, China, [2]College of Pharmacy, Dalian Medical University, Dalian, China, [3]Key Laboratory for Basic and Applied Research on Pharmacodynamic Substances of Traditional Chinese Medicine of Liaoning Province, Dalian Medical University, Dalian, China

OPEN ACCESS

Edited by:
Wolfgang Richard Stremmel, Other, Baden-Baden, Germany

Reviewed by:
Binan Lu, Minzu University of China, China
Shasha Song, Huazhong University of Science and Technology, China

***Correspondence:**
Bao Zhang
zhangbao_nng@163.com
Lina Xu
xulina627@163.com

†These authors have contributed equally to this work and share first authorship

Specialty section:
This article was submitted to Gastrointestinal and Hepatic Pharmacology, a section of the journal Frontiers in Pharmacology

Received: *21 July 2020*
Accepted: *09 November 2020*
Published: *04 December 2020*

Citation:
Zhu S, Guan L, Tan X, Li G, Sun C, Gao M, Zhang B and Xu L (2020) Hepatoprotective Effect and Molecular Mechanisms of Hengshun Aromatic Vinegar on Non-Alcoholic Fatty Liver Disease. Front. Pharmacol. 11:585582. doi: 10.3389/fphar.2020.585582

Aromatic vinegar with abundant bioactive components can be used as a food additive to assist the treatment of various diseases. However, its effect on non-alcoholic fatty liver disease (NAFLD) is still unknown. The purpose of this study was to investigate the mechanism of Hengshun aromatic vinegar in preventing NAFLD *in vivo* and *in vitro*. Aromatic vinegar treatment was applied to rats fed with a high-fat diet (HFD) and HepG2 cells challenged with palmitic acid (PA). Our results showed that aromatic vinegar markedly improved cell viabilities and attenuated cell damage *in vitro*. The levels of TC, TG, FFA, AST, ALT, and malondialdehyde (MDA) in HFD-induced rats were significantly decreased by aromatic vinegar. Mechanism investigation revealed that aromatic vinegar markedly up-regulated the level of silent information regulator of transcription 1 (Sirt1), and thereby inhibited inflammation of the pathway through down-regulating the expressions of high mobility group box 1, toll-likereceptor-4, nuclear transcription factor-κB, tumor necrosis factor receptor-associated factor-6, and inflammatory factors. Aromatic vinegar simultaneously increased the expression of farnesoid X receptor and suppressed expressions of lipogenesis related proteins, including fatty acid synthase, acetyl-CoA carboxylase-1, sterol regulatory element binding transcription factor 1, and stearoyl-CoA desaturase-1. These results were further validated by knockdown of Sirt1 using siRNAs silencing *in vitro*. In conclusion, Hengshun aromatic vinegar showed protective effects against NAFLD by enhancing the activity of SIRT1 and thereby inhibiting lipogenesis and inflammation pathways, which is expected to become a new assistant strategy for NAFLD therapy in the future.

Keywords: non-alcoholic fatty liver disease, aromatic vinegar, inflammation, lipid metabolism, silent information regulator of transcription 1

INTRODUCTION

Non-alcoholic fatty liver disease (NAFLD) is a clinicopathological syndrome characterized by excessive fatty deposition of hepatocytes, excluding alcohol and other well-defined liver damage factors. It is strongly associated with dyslipidemia, obesity, hypertension, and insulin resistance (Dowman et al., 2011). NAFLD encompasses a series of pathological changes ranging from simple

hepatic lipid accumulation (steatosis) to non-alcoholic steatohepatitis (NASH) accompanied by inflammation and varying degrees of fibrosis (Soares e Silva et al., 2015). What is more serious is that NAFLD may even develop into eventual cirrhosis, hepatocellular carcinoma, and death related to liver disease (Farrell and Larter, 2006). In 2016, the global prevalence of NAFLD was about 25%, with the highest rates in South America and the Middle East and the lowest in Africa (Younossi et al., 2016). Statistics showed an upward trend in global morbidity, with an estimated increase of 3.6 million cases per year. It is estimated that the overall prevalence of NAFLD among adults will reach 33.5% by 2030 (Estes et al., 2018). Therefore, NAFLD has become an increasingly serious public health problem due to its rising incidence whether in developed or semi-developed countries.

Due to the occult nature of the disease, the specific pathogenesis of NAFLD is still unclear, and it is believed that NAFLD is affected by a variety of factors. At present, the "two-hit" hypothesis on the pathogenesis of NAFLD has been widely summarized and provides a profound theoretical basis for a series of subsequent studies (Basaranoglu et al., 2013). In the development of NAFLD, the "first hit" refers primarily to the abnormal accumulation of triglyceride (TG) in hepatocytes which has been confirmed to be associated with excessive lipid intake and insulin resistance (IR) (Bugianesi et al., 2010). Based on the first attack, the accumulation of lipids in hepatocytes destroys the oxidative capacity of mitochondria, leading to an increase in the number of reactive oxygen species involved in the re-reaction. Under the combined action of multiple cytokines, such mitochondrial oxidative stress ultimately leads to the "second hit" of NAFLD. It may trigger inflammation, fibrosis, and even hepatocytes apoptosis, ultimately causing end-stage liver disease (Rolo et al., 2012; Xia et al., 2019). Accordingly, we conclude that targeting the regulation of blood lipids and inflammatory responses will play an important role in the treatment of NAFLD.

At present, there is no effective treatment method for NAFLD, and commonly accepted treatment strategies mainly include weight loss, dietary changes, and physical exercise. With the widespread prevalence of NAFLD, people pay more and more attention to dietary changes as a preventive measure and therapeutic strategy for the disease. Studies have shown that Patchouli alcohol, a kind of medicinal food in Asian countries, has a protective effect against NAFLD by altering the metabolism (Wu et al., 2019). Other studies have indicated that tomato juice intake reduces triglycerides and cholesterol levels in the liver and serum, as well as the degree of hepatic steatosis (García-Alonso et al., 2017). Therefore, consumption of tomato juice or its extracts can improve the metabolic patterns of NAFLD induced by a high-fat diet (HFD). In addition, spinach can alleviate HFD-induced obesity, through increasing the number of Lactobacillus counts, lowering fasting blood glucose and total LDL-cholesterol, and preventing excessive cholesterol accumulation in the liver (Elvira-Torales et al., 2019).

Vinegar is a kind of fermented acidic liquid food, which is used as a condiment in cuisine. Previous studies have indicated that vinegar supplementation has a positive effect on the prevention of cardiovascular diseases, ulcerative colitis (UC), the recurrence of kidney stones, and that it can regulate blood glucose and blood pressure (Jing et al., 2015; Shen et al., 2016; Zhu et al., 2019). Moreover, dietary vinegar plays a certain role in reducing body weight, visceral and subcutaneous fat, and regulating lipid metabolism, it also has functional properties including antibacterial effects, antioxidation, control of blood glucose, anticancer properties and so on (Kondo et al., 2009; Budak et al., 2014; Chen et al., 2016). A recent study demonstrated that synthetic acetic acid vinegar and Nipa vinegar had weight loss and anti-inflammatory effects on mice maintaining a HFD (Beh et al., 2017). However, the effect and molecular mechanism of aromatic vinegar on NAFLD remains unclear. Therefore, we conducted the following studies to investigate the hypolipidemic and hepatoprotective effects of Hengshun aromatic vinegar on NAFLD rats induced by a HFD and HepG2 cells induced by palmitic acid (PA) and elucidate the underlying molecular mechanism.

MATERIALS AND METHODS

Chemicals and Materials

Hengshun aromatic vinegar was obtained from Jiangsu Hengshun Vinegar Industry Co., Ltd. (Zhenjiang, China). Dulbecco's Modified Eagle's medium (DMEM) and fetal bovine serum (FBS) were purchased from Gibco (California, United States). Oil Red O staining kit, 3-(4,5-Dimethylthiazol-2-yl)-2,5-diphenyltetrazolium bromide (MTT), PA, and simvastatin were supplied by Solarbio Science and Technology Co., Ltd. (Beijing, China). Total cholesterol (TC), TG, alanine aminotransferase (ALT), aspartate amino-transferase (AST), free fatty acids (FFA), and malondialdehyde (MDA) detection kits were obtained from Nanjing Jiancheng Institute of Biotechnology (Nanjing, China). The tissue protein extraction kit was purchased from KEYGEN Biotech (Nanjing, China). Enhanced bicinchoninic acid (BCA) protein assay kit was purchased from Beyotime Institute of Biotechnology (Jiangsu, China). TransZolTM, TransScript All-in-One First-Strand cDNA Synthesis SuperMix for qPCR, TransStart Top Green qPCR SuperMix, protein marker, EasySee Western blot kit were purchased from TransGen Biotech (Beijing, China). silent information regulator of transcription 1 (Sirt1) SiRNA (Sequences, sense: 5′-GGAGAUGAUCAAGAGGCAATT-3′, antisense: 5′-UUGCCUCUUGAUCAUCUCCTT-3′) was designed and obtained from GenePharma Co., Ltd. (Shanghai, China). Lipofectamine2000 reagent was purchased from Thermo Fisher Scientific (Waltham, America).

Cell Culture

HepG2 cells were purchased from the Shanghai Institute of Biochemistry and Cell Biology (Shanghai, China) and cultured in DMEM medium supplemented with 10% FBS in a humidified environment containing 5% CO_2 and 95% O_2 at 37°C.

Cytotoxicity of Aromatic Vinegar

HepG2 cells were seeded into 96-well plates at a density of 5×10^4 cells/well overnight, and treated with various concentrations of

aromatic vinegar (0.125, 0.25, 0.5, 1, 1.5, 2, 3, and 4%) for 12, 24 and 36 h, respectively, and then the toxicity of the compound was assayed through the MTT method. A total of 10 μl MTT solution (5 mg/ml) was added to each well and incubated for 4 h, and then the formazan crystals were dissolved by 150 μl of DMSO. The absorbance of the specimen was quantified at 490 nm by a microplate reader (Thermo Fisher Scientific, MA, United States), and cell viabilities were calculated.

Palmitic Acid Induced Injury in HepG2 Cells

A series of working dilutions of PA were prepared in a serum-free DMEM medium. HepG2 cells were seeded into 96-well plates at a density of 5×10^4 cells/well overnight, and then treated with various concentrations (0.1, 0.2, 0.3, 0.4, 0.5, 0.6, 0.8 and 1.0 mmol/L) of PA for 12, 24 and 36 h. Cell viabilities were detected using the MTT method as described above and a suitable concentration of PA (0.3 mmol/L) was optimized.

HepG2 cells (5×10^4 cells/well) were seeded into 96-well plates and incubated overnight. The cells in treatment groups were pretreated with aromatic vinegar at concentrations of 0.5, 1, and 1.5% for 24 h, and then treated with 0.3 mmol/L of PA for 24 h. Cells in the control group were cultured in serum-free DMEM medium under normal conditions for 48 h, and those for the model group were treated with 0.3 mmol/l of PA for 24 h. Finally, the viability of cell was determined with the MTT method as described above.

Animals and Treatment

Seventy male Sprague-Dawley (SD) rats, weighing 180–220 g, were obtained from Liaoning Changsheng Biotechnology (SYXK (Liao) 2018-0007). The rats were kept under the controlled condition with constant temperature (23 ± 2°C), relative humidity (55% ± 5%), a 12 h light/dark cycle, and free access to water and food.

After 1 week of acclimatization, the rats were randomly divided into seven groups (n = 10), including the control group, the aromatic vinegar control group, the model group, the aromatic vinegar-treated groups (2.50, 1.25, 0.83 ml/kg aromatic vinegar), and the positive control group (4 mg/kg simvastatin). Normal saline was intragastrically administrated to the rats in the control and model group, and Hengshun aromatic vinegar and simvastatin were given to the treated animals once daily for 9 weeks. During this period, rats in the control and aromatic vinegar control group were fed a normal chow diet, while rats in other groups were fed a (HFD, consisting of 10% fat, 20% sucrose, 2.5% cholesterol, 1% cholate, 1% egg, 30% bean sprout and 35.5% chow diet) (Qin et al., 2018; Tang et al., 2018). Finally, the animals were sacrificed after an overnight fast, and serum samples were extracted from blood samples, centrifuged (3,500 rpm, 4°C) for 10 min and stored at −20°C until detection. The liver tissues were rapidly collected and stored at −80°C for other assays.

Biochemical Assay

The levels of AST, ALT, TC, TG, and FFA in serum, and MDA in the liver tissue were determined using the detection kits based on the manufacturer's instructions.

H&E and Oil Red O Staining

In vivo experiments, liver tissues were fixed in 10% polyoxymethylene solution, processed by standard histological procedures, and ultimately embedded in paraffin wax. Then, the tissues were sectioned into 5-μm slices, which were stained with H&E. To evaluate lipid droplets in the liver, the frozen liver sections were stained with Oil Red O. In vitro experiments, HepG2 cells were treated with vinegar for 24 h and then the PA model was established for 24 h. After washing with PBS for 3 times, the cells were fixed with 10% paraformaldehyde solution for 30 min, and then stained with Oil Red O for 30 min finally washed with 60% isopropanol and PBS in sequence. Eventually, images of the stained sections and cells were obtained using a light microscope (NIKON, Tokyo, Japan).

Immunofluorescence Assay

The paraffin sections of the liver were dewaxed twice with xylene for 15 min each time and rehydrated with different concentrations of alcohol (100, 90, 80, 70, and 60%) for 5 min. We then treated them with citrate buffer (pH = 6.0) in boiling water for 15 min for thermal repair. The deparaffinized liver tissue sections were incubated with rabbit anti-Sirt1, anti-farnesoid X receptor (FXR), or anti-high mobility group box 1 (HMGB1) (1:70, dilution) antibodies in a humidified box at 4°C overnight. After washing with PBS three times, the sections were incubated with a fluorescein-labeled secondary antibody for 1 h at 37°C. Eventually, the immunostained samples were imaged by fluorescence microscopy (Olympus, Tokyo, Japan).

Real-Time PCR Assay

Total RNA samples were obtained from HepG2 cells and liver tissues using RNAiso Plus reagent following the manufacturer's protocol. After purity determination, cDNA was synthesized using a PrimeScript® RT reagent Kit with a TC-512 PCR system (TECHNE, United Kingdom). The levels of mRNA were performed by using real-time PCR with SYBR® PremixEx Taq TM II (Tli RNaseH Plus) in an ABI 7500 Real Time PCR System (Applied Biosystems, United States). The forward (F) and reverse (R) primers for the tested genes are listed in **Table 1**. Among the data from each sample, the Ct value of the target genes was normalized to that of GAPDH. The relative quantification of mRNAs was calculated using the $2^{-\triangle\triangle Ct}$ method.

Western Blotting Assay

Total protein samples from the liver tissues of rats and cells were extracted using a protein extraction kit and the protein content was determined by BCA Kit. Then, the proteins were loaded onto the SDS-PAGE gel (8–12%), separated electrophoretically, and transferred to PVDF membranes (Millipore, Massachusetts, United States). After being blocked with 5% dried skim milk for 3 h, the membranes were incubated with appropriate primary antibodies overnight at 4°C. The blots were then incubated with the goat anti-rabbit IgG-horseradish peroxidase-conjugated secondary antibody for 3 h. Protein expressions were detected by the enhanced chemiluminescence (ECL) method and the images were obtained by Bio-Spectrum Gel Imaging System (UVP, Upland, CA, United States). The intensity values of the

TABLE 1 | The primer sequences used for real-time PCR assay.

Genes	Forward primer (5′-3′)	Reverse primer (5′-3′)
Rats GAPDH	GGCACAGTCAAGGCTGAGAATG	ATGGTGGTGAAGACGCCAGTA
IL-1β	CCCTGAACTCAACTGTGAAATAGCA	CCCAAGTCAAGGGCTTGGAA
IL-6	ATTGTATGAACAGCGATGATGCAC	CCAGGTAGAAACGGAACTCCAGA
TNF-α	TCAGTTCCATGGCCCAGAC	GTTGTCTTTGAGATCCATGCCATT
Human GAPDH	GCACCGTCAAGGCTGAGAAC	TGGTGAAGACGCCAGTGGA
IL-1β	CTGAGCACCTTCTTTCCCTTCA	TGGACCAGACATCACCAAGCT
IL-6	TGGCTGAAAAAGATGGATGCT	TCTGCACAGCTCTGGCTTGT
TNF-α	TGTAGCCCATGTTGTAGCAAACC	GAGGACCTGGGAGTAGATGAGGTA

TNF-α, tumor necrosis factor-α; IL-1β, interleukin-1β; IL-6, interleukin-6.

relative protein levels were normalized with GAPDH as an internal control.

Silent Information Regulator of Transcription 1 siRNA Treatment

HepG2 cells were cultured for approximately 24 h to 70–80% confluence in six-well plates. The cells were then transfected with Sirt1-targeted siRNA or empty vector plasmid (negative control, NC) using lipofectamine2000 reagent according to the manufacturer's protocol. After transfection for 6 h, the medium was replaced with a complete medium. When the cells reached the appropriate density, they were exposed to aromatic vinegar (1.5%) for 24 h and treated with PA (0.3 mmol/l) for an additional 24 h. Then, the cells were collected for further experiments.

Statistical Analysis

All data were expressed as the mean ± SD. Statistical analysis was performed using GraphPad Prism 5.0 software (San Diego, CA, United States). Significant differences among multiple groups were analyzed by a one-way ANOVA test followed by the Newman-Keuls test when comparing multiple independent groups. An unpaired t-test was carried out in the comparison two different groups. The results were considered to be statistically significant at $p < 0.05$. The data and statistical analysis were in accordance with standard recommendations for pharmacological experiment design and analysis.

RESULTS

Aromatic Vinegar Attenuates Palmitic Acid-Induced Damage in HepG2 Cells

The results indicate that when the concentration of aromatic vinegar was higher than 1.5%, aromatic vinegar induced cell damage in HepG2 cells (**Figure 1A**). When the concentration of aromatic vinegar was less than 1.5%, the viability of HepG2 cells has no significant difference compared with the control group, indicating that aromatic vinegar was safe for HepG2 cells under the treatment conditions. Therefore, aromatic vinegar at

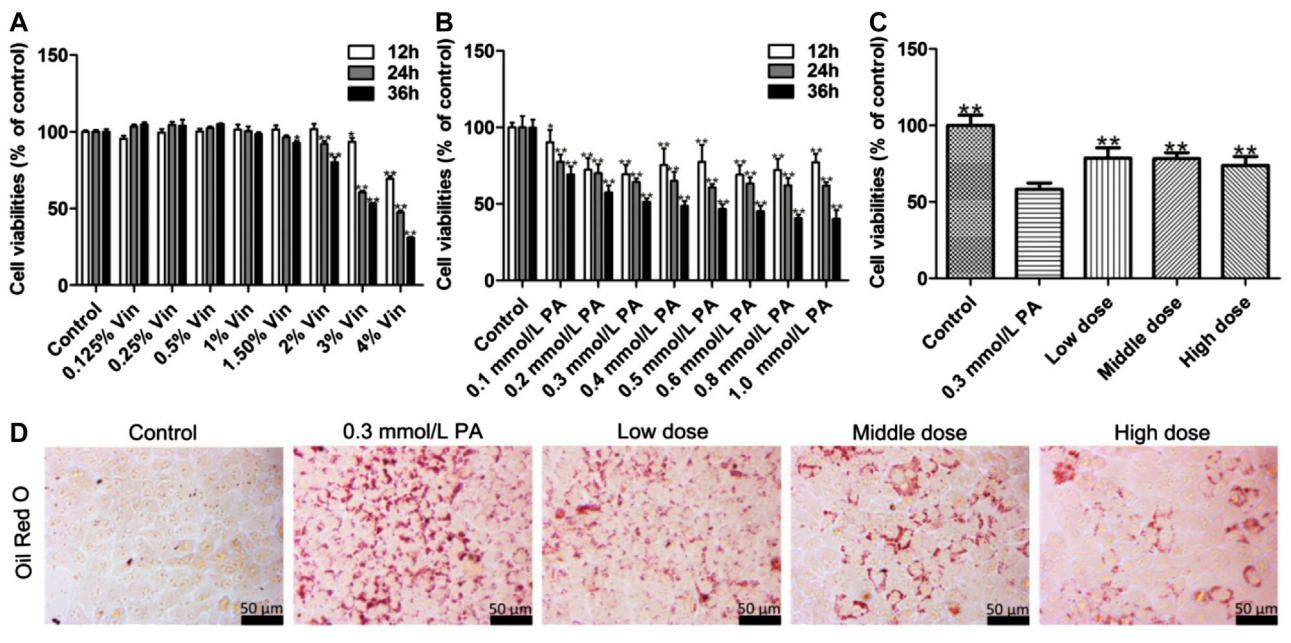


FIGURE 1 | Protective effects of aromatic vinegar on palmitic acid (PA)-induced damage in HepG2 cells. **(A)** Cytotoxicity of aromatic vinegar (Vin) on HepG2 cells; **(B)** Effects of PA on cell viability; **(C)** Effects of aromatic vinegar attenuated on PA-induced cell damage; **(D)** Effects of aromatic vinegar on Oil Red O staining in HepG2 cells (×400 magnification; Scale bar = 50 μm). Values are expressed as the mean ± SD (n = 5). $^{*}p < 0.05$, $^{**}p < 0.01$ compared with model groups.

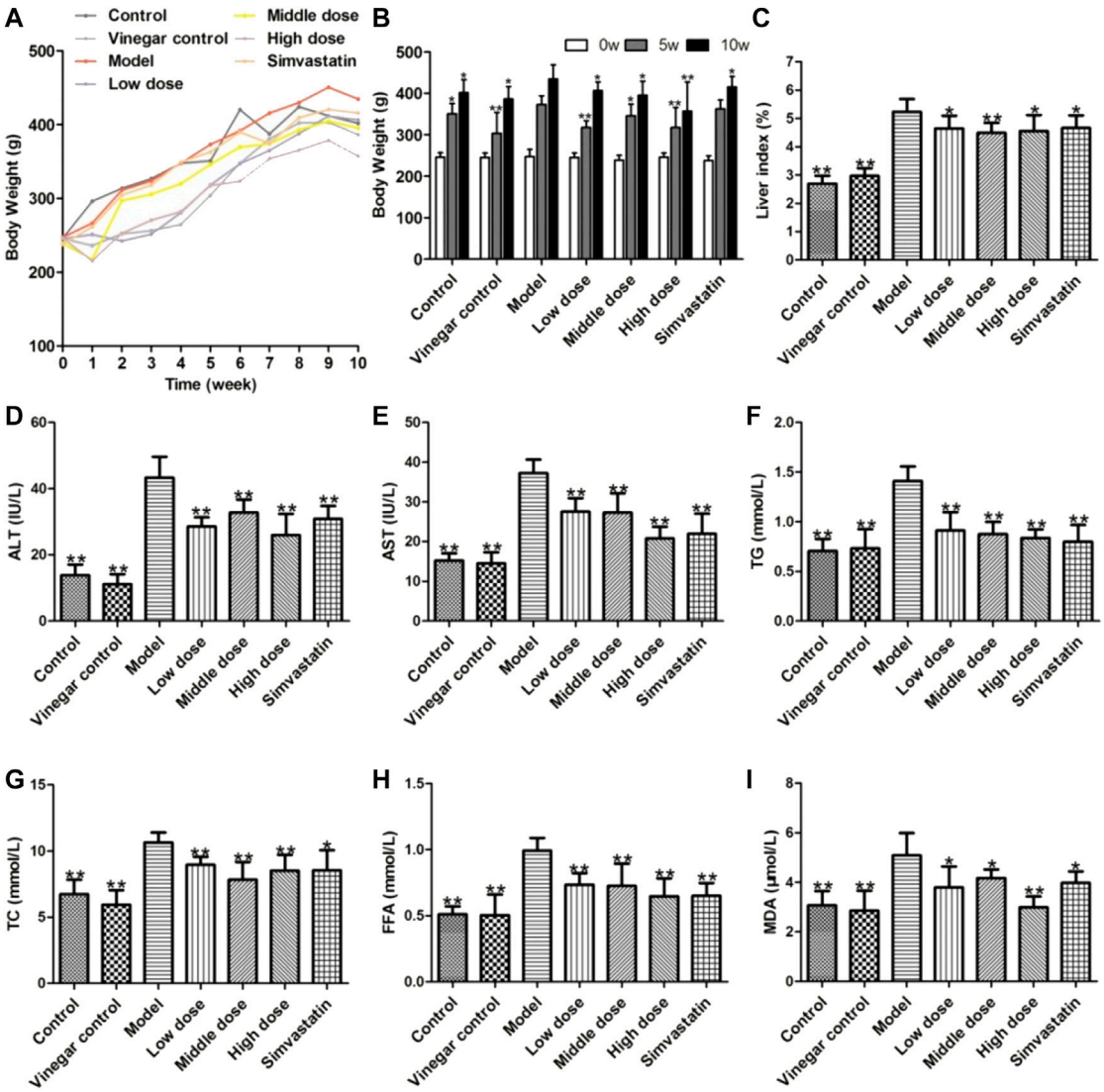


FIGURE 2 | Effects of aromatic vinegar on biochemical indexes of rats. **(A,B)** Effect of aromatic vinegar on body weight **(C)** Effects of aromatic vinegar on the ratio of liver to body weight (%); **(D–I)** Effects of aromatic vinegar on the levels of alanine transaminase (ALT), aspartate transaminase (AST), TG, total cholesterol (TC), and free fatty acid (FFA) in serum and malondialdehyde (MDA) in liver tissue. Values are expressed as the mean ± SD (n = 8). *$p < 0.05$, **$p < 0.01$ compared with model groups.

concentrations of 0.5, 1, and 1.5% for 24 h were selected to protect HepG2 cells against PA-induced injury.

According to the results, the suitable concentration and treatment time of PA *in vitro* experiments were optimized. As shown in **Figure 1B**, compared with control groups, the viability rates of HepG2 cells were significantly decreased by 0.1–1.0 mmol/L PA treatment, which was decreased to 64.31% by 0.3 mmol/L of PA treatment for 24 h. Therefore, HepG2 cells were treated with 0.3 mmol/L PA for 24 h to establish the injury model.

In treatment groups, HepG2 cells were pretreated with aromatic vinegar at the concentrations of 0.5, 1, and 1.5% for 24 h, and then treated with 0.3 mmol/L of PA for 24 h. Subsequently, the results showed that aromatic vinegar pretreatment can significantly reverse the PA-induced cell damage and has an obvious protective effect on cells in a dose-dependent manner (**Figure 1C**).

As shown in **Figure 1D**, Oil Red O staining indicated that a large number of lipid droplet accumulations were observed in HepG2 cells after PA modeling, while aromatic vinegar treatment groups improved PA-induced lipid droplet accumulation compared with the model group.

Effects of Aromatic Vinegar on Body Weight and Biochemical Indexes in Rats With Non-Alcoholic Fatty Liver Disease

The body weights of each group of rats were measured weekly. As shown in **Figures 2A**,**B**, the body weight of rats increased in each group after 10 weeks of feeding, while it was significantly

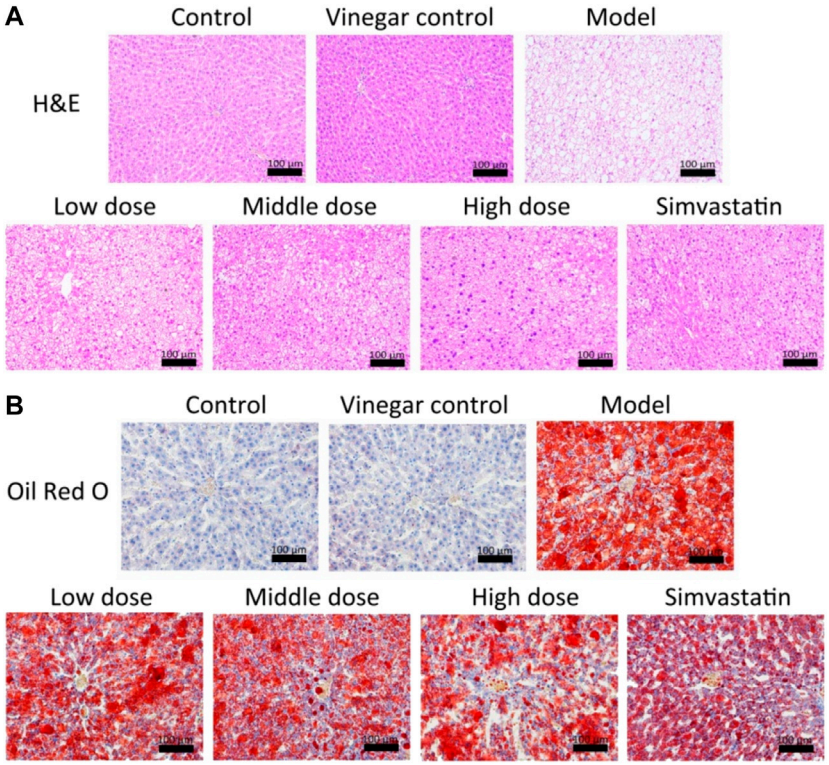


FIGURE 3 | Effects of aromatic vinegar against non-alcoholic fatty liver disease in rats based on staining. **(A)** Effects of aromatic vinegar on HE staining images of liver tissues in rats (×200 magnification); **(B)** Effects of aromatic vinegar on Oil Red O staining images of liver tissues in rats (×200 magnification). Scale bar = 100 μm. Values are expressed as the mean ± SD. $^{*}p < 0.05$, $^{**}p < 0.01$ compared with model groups.

improved in the aromatic vinegar and simvastatin administration groups compared with that of the model group. Similarly, the ratios of liver to body weight in aromatic vinegar groups and the simvastatin group were dramatically decreased compared with the model group (**Figure 2C**).

AST and ALT are specific aminotransferases in the liver, and their levels increase when the liver is damaged. As shown in **Figures 2D**,**E**, the levels of serum ALT and AST were significantly increased in the model group, while aromatic vinegar and simvastatin could markedly reduce these levels. Therefore, we concluded that feeding a HFD can cause liver damage in rats, while aromatic vinegar or simvastatin treatment can ameliorate liver damage. Similar results were shown in **Figures 2F**,**G**,**H**, the TG, TC, and FFA levels significantly increased in rats fed a HFD compared with the control group, while those were significantly reduced in aromatic vinegar groups. Moreover, as shown in **Figure 2I**, aromatic vinegar significantly reduced the MDA level in liver tissue compared with the model group. These data indicated that aromatic vinegar can ameliorate obesity and dyslipidaemia induced by a HFD, and significantly alleviate NAFLD via suppressing oxidative stress.

Effect of Aromatic Vinegar on Liver Pathology

H&E staining showed that livers had an intact lobular architecture with a clear central vein and radiation line, and the cell cord is arranged neatly in the control group and vinegar control group. A large number of fat vacuoles and inflammatory cell infiltration appeared in the liver tissues of the model group, while aromatic vinegar and simvastatin administration significantly improved this condition (**Figure 3A**). In addition, compared with the control group, lipid droplets increased significantly in the HFD induced model, while administration groups significantly improved lipid accumulation in a dose-dependent way (**Figure 3B**). Oil Red O staining further showed that aromatic vinegar could inhibit excessive lipid accumulation in the liver. These data indicated that aromatic vinegar had a good effect on protecting the liver and reducing lipid.

Aromatic Vinegar Activates Silent Information Regulator of Transcription 1 Pathway to Regulate Hepatic Lipid Synthesis and Inflammation *In Vitro* and *In Vivo*

As shown in **Figures 4A**,**B**, the expression levels of SIRT1, FXR and HMGB1 in HepG2 cells and the liver tissues of rats were assessed by western blotting assay. The results indicated that the expression levels of SIRT1 and FXR were significantly down-regulated, and the level of HMGB1 was markedly up-regulated compared with control groups in vitro and in vivo. However,

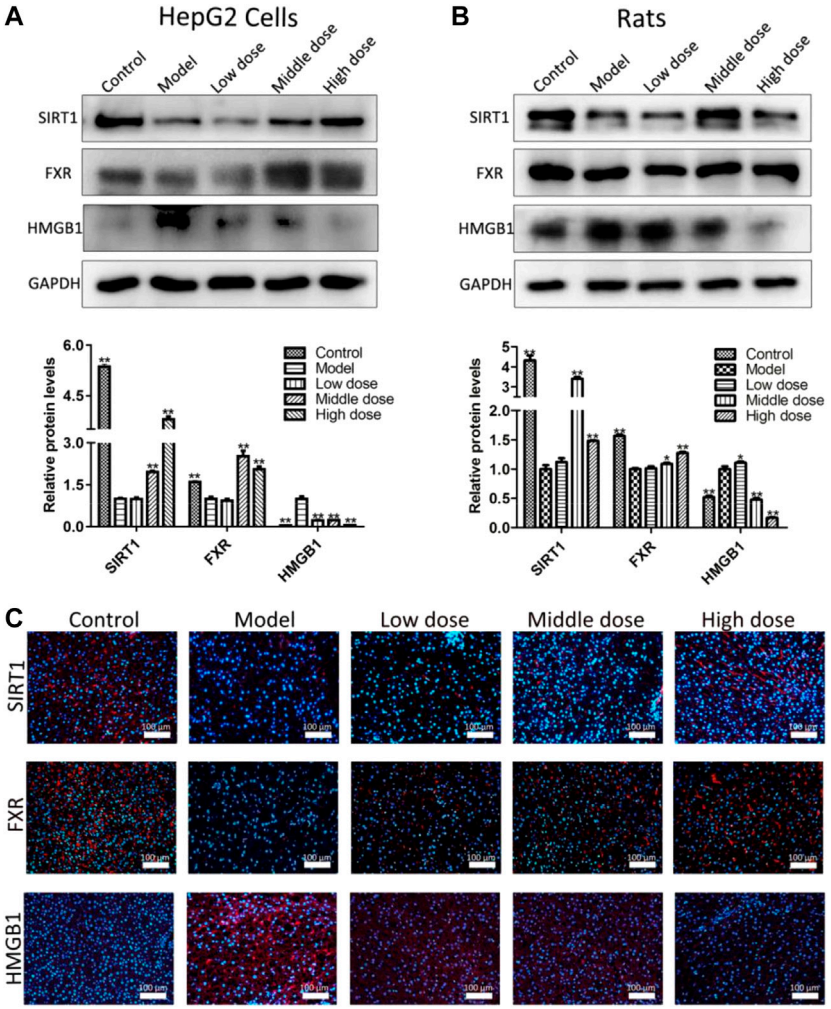


FIGURE 4 | Aromatic vinegar activates the silent information regulator of transcription 1 pathway *in vitro* and *in vivo*. **(A)** Effects of aromatic vinegar on the expression levels of SIRT1, farnesoid X receptor (FXR) and high mobility group box 1 (HMGB1) *in vitro*; **(B)** Effects of aromatic vinegar on the expression levels of SIRT1, FXR and HMGB1 *in vivo*; **(C)** Effects of aromatic vinegar on SIRT1, FXR and HMGB1 levels based on immunofluorescence staining *in vivo* (×200 magnification). Scale bar = 100 μm. Values are expressed as the mean ± SD (n = 3). $^{*}p < 0.05$, $^{**}p < 0.01$ compared with model groups.

compared with model groups, aromatic vinegar significantly increased the expression levels of SIRT1 and FXR, and decreased the levels of HMGB1.

As shown in **Figure 4C**, the results indicate that the levels of SIRT1 and FXR-positive cells were substantially increased, and HMGB1-positive areas were obviously decreased in liver tissues by aromatic vinegar compared with the control groups based on immunofluorescence assays. These results indicated that aromatic vinegar activated the SIRT1 pathway, and then affected the expression levels of FXR and HMGB1.

Aromatic Vinegar Ameliorates Lipid Metabolism *In Vitro* and *In Vivo*

The results in **Figure 5** show that aromatic vinegar markedly down-regulated the expression levels of proteins and genes associated with lipogenesis compared with the model groups *in vitro* and *in vivo*, including sterol regulatory element binding transcription factor 1 (SREBP1), fatty acid synthase (FASN), acetyl-CoA carboxylase-1 (ACC1) and stearoyl-CoA desaturase-1 (SCD1). The data indicated that aromatic vinegar could play an anti-NAFLD role by regulating lipid metabolism related proteins.

Aromatic Vinegar Attenuates Inflammation *In Vitro* and *In Vivo*

As shown in **Figures 6A**,**B**, compared with control groups, the protein levels of toll-like receptor-4 (TLR4), nuclear transcription factor-κB (NF-κB) and tumor necrosis factor receptor-associated factor-6 (TRAF6) were all significantly increased, while the expression of which was significantly reversed by administrating aromatic vinegar *in vitro* and *in vivo*. As shown in **Figures 6C**,**D**, *in vitro* and *in vivo*, increased mRNA

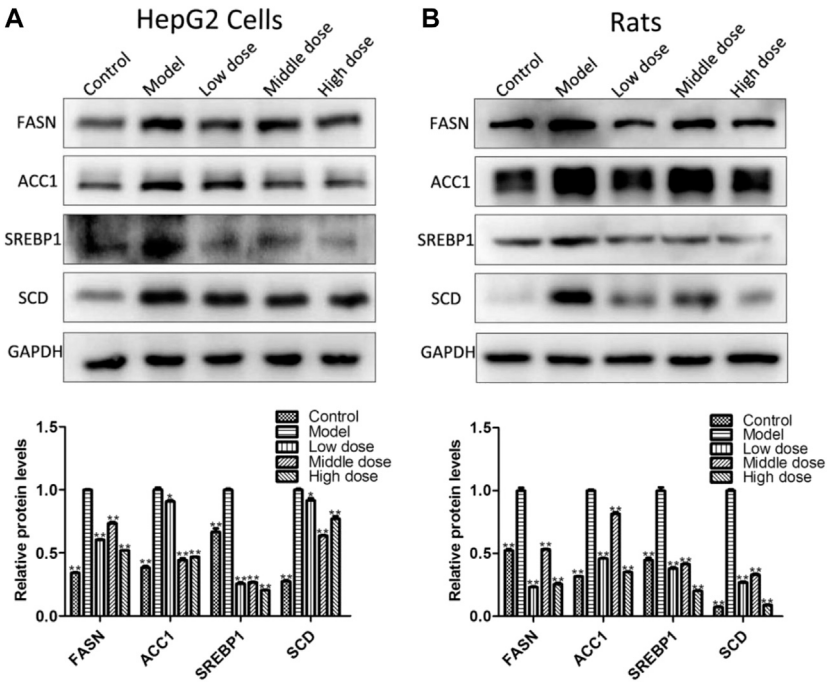


FIGURE 5 | Effect of aromatic vinegar on the levels of some proteins related to lipid metabolism. **(A)** Effects of aromatic vinegar on the protein levels of fatty acid synthase (FASN), acetyl-CoA carboxylase-1 (ACC1), sterol regulatory element binding transcription factor 1 (SREBP1) and stearoyl-CoA desaturase-1 (SCD) *in vitro*; **(B)** Effects of aromatic vinegar on the protein levels of FASN, ACC1, SREBP1 and SCD *in vivo*. Values are expressed as the mean ± SD (n = 3). $^{*}p < 0.05$, $^{**}p < 0.01$ compared with model groups.

levels of tumor necrosis factor-α (TNF-α), interleukin-1β (IL-1β) and interleukin-6 (IL-6) were observed in the model groups, which were markedly decreased by aromatic vinegar. These results indicated that aromatic vinegar delayed NAFLD through ameliorating inflammation.

Effect of Aromatic Vinegar on Lipid Metabolism and Inflammation After Transfecting Silent Information Regulator of Transcription 1 SiRNA *In Vitro*

To further determine the effect of aromatic vinegar on SIRT1 pathway, HepG2 cells were transfected with SIRT1 siRNA and pretreated with aromatic vinegar for 24 h before other tests. As shown in **Figure 7A**, transfecting SIRT1 siRNA aggravated PA-induced injury compared with the group transfected with negtive control siRNA. In addition, the protein levels of SIRT1 and FXR were markedly increased, and HMGB1 was markedly decreased in aromatic vinegar-treated groups after transfection. Obviously, SIRT1 siRNA reduced the protective effect of aromatic vinegar on PA-induced injury. What's more, SIRT1 siRNA blocked the effects of aromatic vinegar on the mRNA levels of IL-1β, IL-6 and TNF-α (**Figure 7B**). Based on the Oil Red O staining shown in **Figure 7C**, aromatic vinegar treatment groups obviously improved PA-induced lipid droplet accumulation with or without SIRT1 siRNA. These results further strongly demonstrated that the regulatory effect of aromatic vinegar on lipid metabolism and inflammation was achieved through regulation of the SIRT1/FXR and SIRT1/HMGB1 signal pathways.

DISCUSSION

NAFLD is a type of acquired metabolic stress liver injury, which is closely related to insulin resistance and genetic susceptibility (Cheung and Sanyal, 2010). With the epidemic trend of obesity caused by unhealthy diet, the prevalence of NAFLD are rising worldwide, and NAFLD has become the main cause of chronic liver disease in developed countries (Safari and Gérard, 2019; Stefan et al., 2019). NAFLD is a major global health issue that deserves close attention. The pathogenesis of NAFLD is a complex process, in which the occurrence of hepatic lipotoxicity may further lead to mitochondrial dysfunction, thereby activating inflammatory responses (Zhang et al., 2018). The liver provides a central store for excessive lipid accumulation (Chung et al., 2017). NAFLD is characterized primarily by fatty deposition of hepatocytes, which accounts for more than 5% of the liver weight (Gong et al., 2017). As is known to all, Hengshun aromatic vinegar is one of the most famous traditional fermented vinegars in China, and is generally produced from glutinous rice, wheat bran, and rice hulls through a unique solid layered fermentation process (Xu et al., 2011a). It has the characteristics of "color, fragrance, acid, alcohol, thick," and has a strong taste that is sour and not astringent, fragrant and slightly sweet, colory and strong taste. Although there is no

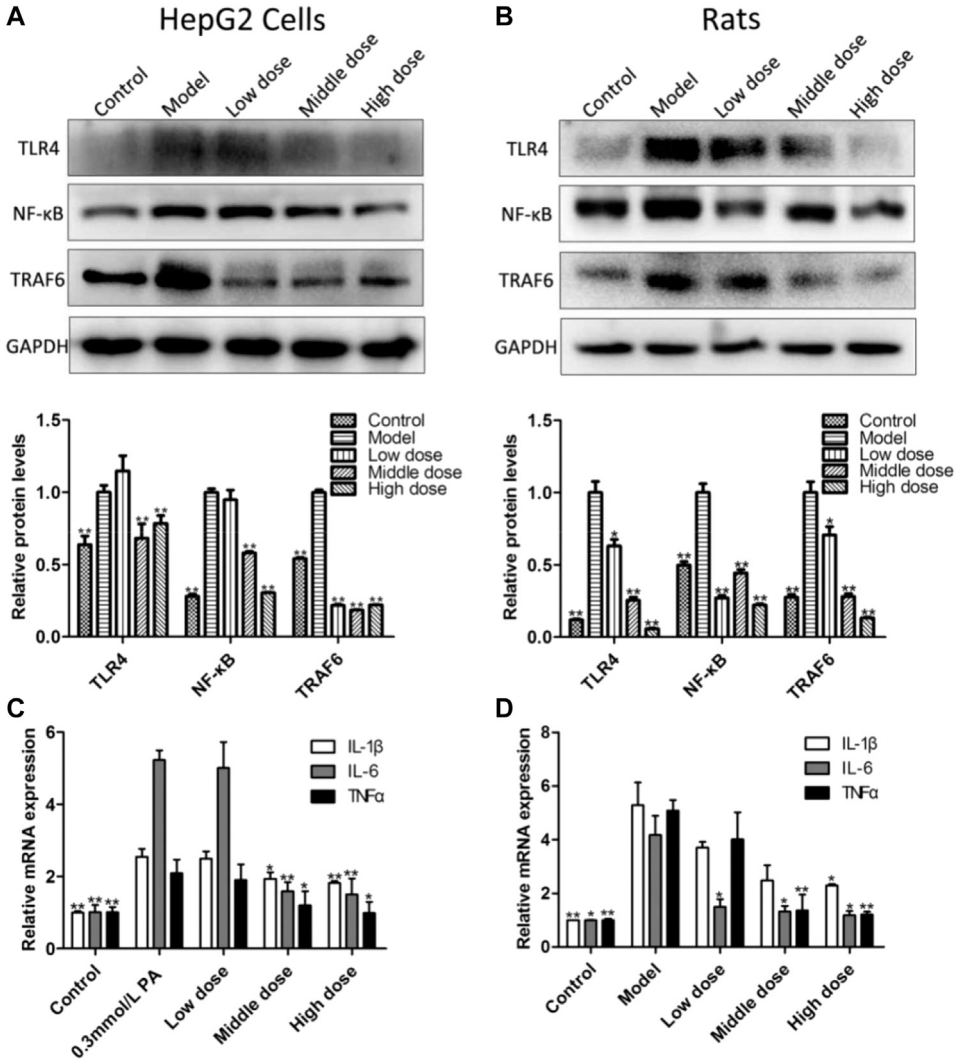


FIGURE 6 | Effect of aromatic vinegar on the levels of some proteins related to inflammation and inflammatory mediators. **(A)** Effects of aromatic vinegar on the protein levels of toll-likereceptor-4 (TLR4), nuclear transcription factor-κB (NF-κB) and tumor necrosis factor receptor-associated factor-6 (TRAF6) *in vitro*; **(B)** Effects of aromatic vinegar on the protein levels of TLR4, NF-κB and TRAF6 *in vivo*; **(C)** Effects of aromatic vinegar on the mRNA levels of tumor necrosis factor-α (TNF-α), interleukin-1β (IL-1β) and interleukin-6 (IL-6) *in vitro*; **(D)** Effects of aromatic vinegar on the mRNA levels of TNF-α, IL-1β and IL-6 *in vivo*. Values are expressed as the mean ± SD (n = 3). $^{*}p < 0.05$, $^{**}p < 0.01$ compared with model groups.

accurate formulation for aromatic vinegar, it has a hundred years of mature, reliable production technology and quality control. What's more, Chinese literature has found that Hengshun aromatic vinegar contains 88.09% water and volatile matter and 11.91% solid matter (w/v), and is rich in organic acids, sugar, protein, amino acids and other aromatic ingredients, which largely affect its taste characteristics and organoleptic quality (Zhao et al., 2018). The effective components in it are relatively abundant and stable through the fingerprint analysis and amino acid analysis. During the brewing process, aromatic vinegar produces many bioactive compounds, such as organic acids, amino acids and phenolic compounds, which play important roles in antioxidant activities (Zhang et al., 2019). In addition, polyphenols, flavonoids, and melanoidins were found in Hengshun aromatic vinegar, which play crucial roles in diseases prevention and contribute benefits to human health (Zhao et al., 2018; Duan et al., 2019). Studies have also showed that the alkylpyrazine named ligustrazine was found as a bioactive compound in Hengshun aromatic vinegar, which has the health effects such as reducing blood pressure, promoting blood circulation and removing stasis, improving coronary heart disease, thrombolytic therapy and liver protection (Xu et al., 2011b; Chen et al., 2019). In the present study, PA-induced HepG2 cells and HFD-induced SD rats were used as NAFLD models *in vitro* and *in vivo* to investigate the pharmacodynamic actions and molecular mechanism of Hengshun aromatic vinegar. Aromatic vinegar showed significant effects against NAFLD due to the evidences with

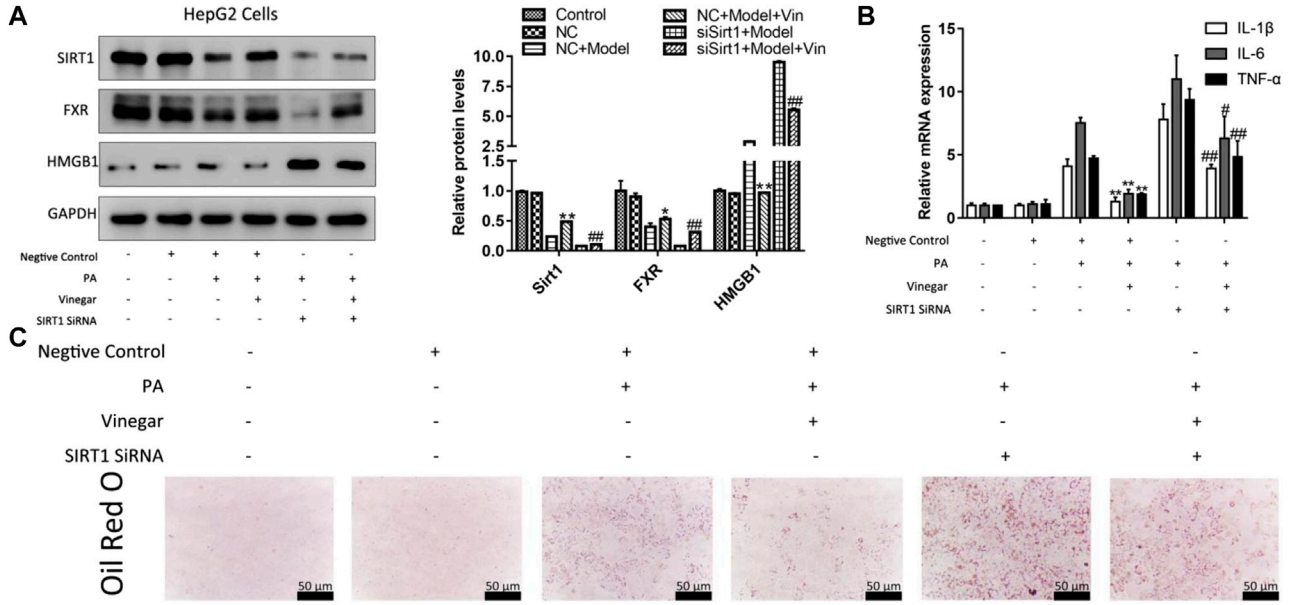


FIGURE 7 | Effffect of aromatic vinegar on silent information regulator of transcription 1 (SIRT1)/FXR and SIRT1/high mobility group box 1 (HMGB1) pathway in HepG2 cells transfected with SIRT1 siRNA. **(A)** The protein levels of SIRT1, FXR and HMGB1; **(B)** The mRNA levels of interleukin-1β (IL-1β), interleukin-6 (IL-6) and TNF-α; **(C)** Oil Red O staining (×400 magnification; Scale bar = 50 μm). Values are expressed as the mean ± SD (n = 3). $^{*}p < 0.05$, $^{**}p < 0.01$ compared with model group transfected with negtive control siRNA (NC + Model); $\#p < 0.05$, $\#p < 0.01$ compared with model group transfected with SIRT1 siRNA (siSirt1 + Model).

the decreased levels of AST, ALT, TC, TG, FFA and MDA, and the alleviation of histopathological changes.

SIRT1, a nonamide adenine dinucleotide (NAD^+)-dependent protein deacetylase, acts as an important modulator of metabolic pathways and plays a critical role in the pathophysiology of many metabolic diseases. It's a member of silent information regulator 2 family, which are a group of proteins with either histone deacetylase or mono-ADP-ribosyltransferase activity (Colak et al., 2011). In recent years, studies have shown that SIRT1 with an extensive spectrum of biological functions plays an important role in the regulation related to metabolism, cell survival and apoptosis (Silva and Wahlestedt, 2010). In addition, it has been found that the pathophysiological mechanism of NAFLD may be affected by the activation of SIRT1 (Colak et al., 2014). Studies have shown that dioscin regulated lipid metabolism through SIRT1/AMPK signal pathway and significantly prevented NAFLD (Yao et al., 2018). Similarly, it has also been reported that celastrol ameliorated NAFLD by SIRT1 pathway, which had an important role in improving liver metabolic injury induced by HFD (Zhang et al., 2016). In this study, we did find the result that the expression of SIRT1 was down-regulated in model group, which was consistent with SIRT1 expression in other studies. Moreover, our SIRT1 siRNA experimental results proved that the main target of aromatic vinegar was SIRT1. It attenuated NAFLD by activating the SIRT1 pathway to regulate liver lipid metabolism and inflammation *in vitro* and *in vivo*.

As a key regulator of hepatic metabolic homeostasis, hepatic SIRT1 acts as an endogenous activator of its downstream protein FXR in hepatocytes (Yang et al., 2017). FXR, a member of the nuclear receptor super family of ligand-activated transcription factors, has recently been demonstrated to play a key role in the molecular mechanism of regulating lipid glucose homeostasis (Nie et al., 2017). At the same time, FXR is the primary nuclear receptor for bile acids and plays an important role in bile acid homeostasis (Yang et al., 2017). In addition, FXR is a crucial target protein downstream of SIRT1, which plays a connecting role after being regulated by SIRT1. Generally speaking, hepatic FXR regulates lipid homeostasis through a variety of mechanisms, including reducing fatty acid synthesis, decreasing fatty acid uptake, and increasing β-oxidation (Cave et al., 2016). Celastrol has a protective effect on cholestatic liver injury by regulating SIRT1/FXR pathway (Zhao et al., 2019). Other research revealed that imperatorin exerts the protective effect against hepatotoxicity induced by excessive acetaminophen similarly by stimulating the SIRT1/FXR pathway (Gao et al., 2020). Moreover, studies have showed that NAFLD may be mitigated through the regulation of SIRT1/FXR signaling pathway (Han et al., 2019). Through the activation of FXR, a major adipogenic regulator called SREBP1 will be regulated and further reduced the protein levels of FASN, ACC1 and SCD in its downstream which are related to lipogenesis (Dong et al., 2019). Consistent with other research results, we found that FXR regulated by SIRT1 activates downstream protein SREBP1, which affects the protein levels of FASN, ACC1 and SCD, thereby reducing adipogenesis (**Figure 8**). Our results indicated that aromatic vinegar could alleviate NAFLD by reducing lipogenesis through SIRT1/FXR signaling pathway. What's more, the SIRT1 siRNA experimental results also confirmed this conclusion.

It has been confirmed that SIRT1 not only regulates FXR, but also activates HMGB1, a key inflammatory mediator in the inflammatory

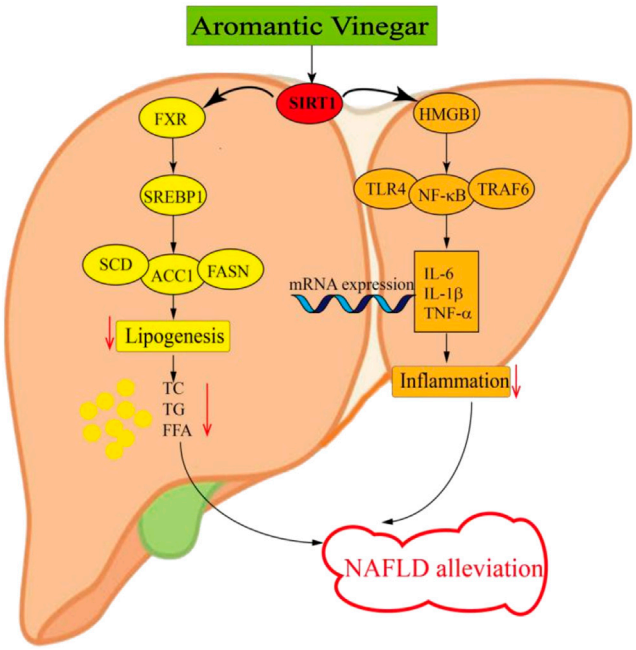


FIGURE 8 | Schematic diagram of the anti-lipid metabolism and anti-inflammatory effect of Hengshun aromatic vinegar.

signaling pathway (Qi et al., 2017). Recent study has demonstrated that SIRT1 is a key factor in the negative regulation of HMGB1, whose release is regulated by SIRT1 acetylation mediated direct interaction (Hwang et al., 2015). It has been reported that SIRT1 induces HMGB1 expression, thereby modulating ovarian cancer behaviors (Jiang et al., 2018). Le K et al. have demonstrated that resveratrol plays a neuroprotective role in neonatal hypoxic-ischemic brain injury by activating SIRT1 to inhibit HMGB1 signaling (Le et al., 2019). Moreover, The SIRT1/HMGB1 pathway has been proved to be an important target for inhibiting of NAFLD inflammation (Zeng et al., 2015). HMGB1, ubiquitously and highly expressed in hepatocytes, is a critical chromosomal non-histone protein that can regulate DNA structure. As we all know, it plays a pivotal role in the initiation and maintenance inflammation responses, which is a key process that takes place in ordinary liver diseases such as NAFLD (Khambu et al., 2019). The inflammation responses during NAFLD may be the result of stress, damage and cell death of hepatocytes caused by lipid, and such lipotoxicity further leads to the release of HMGB1 (Ibrahim et al., 2018). The downstream inflammation-related proteins such as TLR4, TRAF6 and NF-κB are activated due to the release of HMGB1 (Li et al., 2011; Lan et al., 2017). Researches have shown that liver inflammation is caused by pro-inflammatory cytokines and chemokines generated by adipocytes, lipid-laden hepatocytes and hepatic macrophages (Manne et al., 2018). NF-κB, activated by HMGB1, acts as a major transcriptional regulator regulating inflammation and cell death during the development of NAFLD (Jiang et al., 2019). After NF-κB activation, it is transferred from the cytoplasm to the nucleus, releasing a great deal of inflammatory factors. The alteration of NF-κB activity can affect the expression of hepatic pro-inflammatory cytokines, such as IL-1β, IL-6 and TNF-α, and the excessive production of which may lead to inflammatory reaction (Gäbele et al., 2009). In the present study, we obtained the following results that SIRT1 induced the release of HMGB1, which regulated the downstream inflammation-related proteins TLR4, TRAF6, and NF-κB. After activation, NF-κB released a large number of inflammatory factors including IL-1β, IL-6, and TNF-α (**Figure 8**). These results supported the view that aromatic vinegar played a critical role in relieving NAFLD by regulating inflammation through SIRT1/HMGB1 signaling pathway. In addition, the experimental results of SIRT1 siRNA also confirmed this conclusion.

There are some shortages in the current study. The anti-NAFLD effects of aromatic vinegar were evaluated only in cell and rats model, which needs to be further evaluated in clinical studies. It has been reported in Chinese journal that Hengshun aromatic vinegar concentrate, extract and its different molecular weight components could inhibit the oxidative modification of human low density lipoprotein. It provids the possibility for the clinical application of aromatic vinegar in treating NAFLD combined with our findings in this study. As flavoring, aromatic vinegar is difficult to be developed into a medicine for the treatment of diseases. Previous studies have suggested that osteoporosis was alleviated in rats by consumption of aromatic vinegar alone or in combination with calcium salt (Yu et al., 2020). Consequently, it will be a direction in the future that aromatic vinegar could be developed as a clinical adjunctive therapy to alleviate NAFLD and further studies could investigate the combination effect of Hengshun aromatic vinegar with other medicines.

CONCLUSION

Our study demonstrated that Hengshun aromatic vinegar showed valid effects against NAFLD via regulating lipid metabolism and inflammation by targeting SIRT1. This study provided new evidence for the recommendation that Hengshun aromatic vinegar can be used as an adjuvant strategy for the therapy and health care of NAFLD.

DATA AVAILABILITY STATEMENT

The raw data supporting the conclusions of this article will be made available by the authors, without undue reservation, to any qualified researcher.

ETHICS STATEMENT

The animal study was reviewed and approved by Animal Research Committee of Dalian Medical University.

AUTHOR CONTRIBUTIONS

Data curation, LX; Funding acquisition, GL; Methodology, SZ and LG; Project administration and resources, BZ; Software,

MG; Validation, LG, XT, and CS; Writing – original draft, LG and LX; Writing – review and editing, LX. SZ and LG contributed same work to this paper and they are the co-first authors.

FUNDING

This work was financially supported by the Key Research and Development Project of Zhenjiang, China (ZD2019001).

REFERENCES

Basaranoglu, M., Basaranoglu, G., and Sentürk, H. (2013). From fatty liver to fibrosis: a tale of "second hit". *World J. Gastroenterol* 19, 1158–1165. doi:10.3748/wjg.v19.i8.1158

Beh, B. K., Mohamad, N. E., Yeap, S. K., Ky, H., Boo, S. Y., Chua, J. Y. H., et al. (2017). Anti-obesity and anti-inflammatory effects of synthetic acetic acid vinegar and Nipa vinegar on high-fat-diet-induced obese mice. *Sci. Rep.* 7, 6664. doi:10.1038/s41598-017-06235-7

Budak, N. H., Aykin, E., Seydim, A. C., Greene, A. K., and Guzel-Seydim, Z. B. (2014). Functional properties of vinegar. *J. Food Sci.* 79, R757–R764. doi:10.1111/1750-3841.12434

Bugianesi, E., Moscatiello, S., Ciaravella, M. F., and Marchesini, G. (2010). Insulin resistance in nonalcoholic fatty liver disease. *Curr. Pharm. Des.* 16, 1941–1951. doi:10.2174/138161210791208875

Cave, M. C., Clair, H. B., Hardesty, J. E., Falkner, K. C., Feng, W., Clark, B. J., et al. (2016). Nuclear receptors and nonalcoholic fatty liver disease. *Biochim. Biophys. Acta* 1859, 1083–1099. doi:10.1016/j.bbagrm.2016.03.002

Chen, B., Ma, Y., Xue, X., Wei, J., Hu, G., and Lin, Y. (2019). Tetramethylpyrazine reduces inflammation in the livers of mice fed a high fat diet. *Mol. Med. Rep.* 19, 2561–2568. doi:10.3892/mmr.2019.9928

Chen, H., Chen, T., Giudici, P., and Chen, F. (2016). Vinegar functions on health: Constituents, sources, and formation mechanisms. *Compr. Rev. Food Sci. Food Saf.* 15, 1124–1138. doi:10.1111/1541-4337.12228

Cheung, O. and Sanyal, A. J. (2010). Recent advances in nonalcoholic fatty liver disease. *Curr. Opin. Gastroenterol.* 26, 202–208. doi:10.1097/MOG.0b013e328337b0c4

Chung, K. W., Kim, K. M., Choi, Y. J., An, H. J., Lee, B., Kim, D. H., et al. (2017). The critical role played by endotoxin-induced liver autophagy in the maintenance of lipid metabolism during sepsis. *Autophagy* 13, 1113–1129. doi:10.1080/15548627.2017.1319040

Colak, Y., Ozturk, O., Senates, E., Tuncer, I., Yorulmaz, E., Adali, G., et al. (2011). SIRT1 as a potential therapeutic target for treatment of nonalcoholic fatty liver disease. *Med. Sci. Mon. Int. Med. J. Exp. Clin. Res.* 17, HY5. doi:10.12659/msm.881749

Colak, Y., Yesil, A., Mutlu, H. H., Caklili, O. T., Ulasoglu, C., Senates, E., et al. (2014). A potential treatment of non-alcoholic fatty liver disease with SIRT1 activators. *J. Gastrointestin. Liver Dis.* 23, 311–319. doi:10.15403/jgld.2014.1121.233.yck

Dong, R., Yang, X., Wang, C., Liu, K., Liu, Z., Ma, X., et al. (2019). Yangonin protects against non-alcoholic fatty liver disease through farnesoid X receptor. *Phytomedicine* 53, 134–142. doi:10.1016/j.phymed.2018.09.006

Dowman, J. K., Armstrong, M. J., Tomlinson, J. W., and Newsome, P. N. (2011). Current therapeutic strategies in non-alcoholic fatty liver disease. *Diabetes Obes. Metabol.* 13, 692–702. doi:10.1111/j.1463-1326.2011.01403.x

Duan, W., Xia, T., Zhang, B., Li, S., Zhang, C., Zhao, C., et al. (2019). Changes of physicochemical, bioactive compounds and antioxidant capacity during the brewing process of zhenjiang aromatic vinegar. *Molecules* 24, 3935. doi:10.3390/molecules24213935

Elvira-Torales, L. I., Periago, M. J., González-Barrio, R., Hidalgo, N., Navarro-González, I., Gómez-Gallego, C., et al. (2019). Spinach consumption ameliorates the gut microbiota and dislipaemia in rats with diet-induced non-alcoholic fatty liver disease (NAFLD). *Food Funct.* 10, 2148–2160. doi:10.1039/c8fo01630e

Estes, C., Razavi, H., Loomba, R., Younossi, Z., and Sanyal, A. J. (2018). Modeling the epidemic of nonalcoholic fatty liver disease demonstrates an exponential increase in burden of disease. *Hepatology* 67, 123–133. doi:10.1002/hep.29466

Farrell, G. C. and Larter, C. Z. (2006). Nonalcoholic fatty liver disease: from steatosis to cirrhosis. *Hepatology* 43, S99–S112. doi:10.1002/hep.20973

Gäbele, E., Froh, M., Arteel, G. E., Uesugi, T., Hellerbrand, C., Schölmerich, J., et al. (2009). TNFα is required for cholestasis-induced liver fibrosis in the mouse. *Biochem. Biophys. Res. Commun.* 378, 348–353. doi:10.1016/j.bbrc.2008.10.155

Gao, Z., Zhang, J., Wei, L., Yang, X., Zhang, Y., Cheng, B., et al. (2020). The protective effects of imperatorin on acetaminophen overdose-induced Acute liver injury. *Oxidat. Med. Cell Longev.* 2020, 1. doi:10.1155/2020/8026838

García-Alonso, F. J., González-Barrio, R., Martín-Pozuelo, G., Hidalgo, N., Navarro-González, I., Masuero, D., et al. (2017). A study of the prebiotic-like effects of tomato juice consumption in rats with diet-induced non-alcoholic fatty liver disease (NAFLD). *Food Funct.* 8, 3542–3552. doi:10.1039/c7fo00393e

Gong, Z., Tas, E., Yakar, S., and Muzumdar, R. (2017). Hepatic lipid metabolism and non-alcoholic fatty liver disease in aging. *Mol. Cell. Endocrinol.* 455, 115–130. doi:10.1016/j.mce.2016.12.022

Han, X., Cui, Z.-Y., Song, J., Piao, H.-Q., Lian, L.-H., Hou, L.-S., et al. (2019). Acanthoic acid modulates lipogenesis in nonalcoholic fatty liver disease via FXR/LXRs-dependent manner. *Chem. Biol. Interact.* 311, 108794. doi:10.1016/j.cbi.2019.108794

Hwang, J. S., Choi, H. S., Ham, S. A., Yoo, T., Lee, W. J., Paek, K. S., et al. (2015). Deacetylation-mediated interaction of SIRT1-HMGB1 improves survival in a mouse model of endotoxemia. *Sci. Rep.* 5, 15971. doi:10.1038/srep15971

Ibrahim, S. H., Hirsova, P., and Gores, G. J. (2018). Non-alcoholic steatohepatitis pathogenesis: sublethal hepatocyte injury as a driver of liver inflammation. *Gut* 67, 963–972. doi:10.1136/gutjnl-2017-315691

Jiang, J., Yan, L., Shi, Z., Wang, L., Shan, L., and Efferth, T. (2019). Hepatoprotective and anti-inflammatory effects of total flavonoids of Qu Zhi Ke (peel of Citrus changshan-huyou) on non-alcoholic fatty liver disease in rats via modulation of NF-κB and MAPKs. *Phytomedicine* 64, 153082. doi:10.1016/j.phymed.2019.153082

Jiang, W., Jiang, P., Yang, R., and Liu, D. F. (2018). Functional role of SIRT1-induced HMGB1 expression and acetylation in migration, invasion and angiogenesis of ovarian cancer. *Eur. Rev. Med. Pharmacol. Sci.* 22, 4431–4439. doi:10.26355/eurrev_201807_15494

Jing, L., Yanyan, Z., and Junfeng, F. (2015). Acetic acid in aged vinegar affects molecular targets for thrombus disease management. *Food Funct.* 6, 2845–2853. doi:10.1039/c5fo00327j

Khambu, B., Yan, S., Huda, N., and Yin, X.-M. (2019). Role of high-mobility group box-1 in liver pathogenesis. *Int. J. Mol. Sci.* 20, 5314. doi:10.3390/ijms20215314

Kondo, T., Kishi, M., Fushimi, T., Ugajin, S., and Kaga, T. (2009). Vinegar intake reduces body weight, body fat mass, and serum triglyceride levels in obese Japanese subjects. *Biosci. Biotechnol. Biochem.* 73, 1837–1843. doi:10.1271/bbb.90231

Lan, K.-C., Chao, S.-C., Wu, H.-Y., Chiang, C.-L., Wang, C.-C., Liu, S.-H., et al. (2017). Salidroside ameliorates sepsis-induced acute lung injury and mortality via downregulating NF-κB and HMGB1 pathways through the upregulation of SIRT1. *Sci. Rep.* 7, 12026. doi:10.1038/s41598-017-12285-8

Le, K., Chibaatar Daliv, E., Wu, S., Qian, F., Ali, A. I., Yu, D., et al. (2019). SIRT1-regulated HMGB1 release is partially involved in TLR4 signal transduction: a possible anti-neuroinflammatory mechanism of resveratrol in neonatal hypoxic-ischemic brain injury. *Int. Immunopharm.* 75, 105779. doi:10.1016/j.intimp.2019.105779

Li, L., Chen, L., Hu, L., Liu, Y., Sun, H.-Y., Tang, J., et al. (2011). Nuclear factor high-mobility group box1 mediating the activation of toll-like receptor 4 signaling in hepatocytes in the early stage of nonalcoholic fatty liver disease in mice. *Hepatology* 54, 1620–1630. doi:10.1002/hep.24552

Manne, V., Handa, P., and Kowdley, K. V. (2018). Pathophysiology of nonalcoholic fatty liver disease/nonalcoholic steatohepatitis. *Clin. Liver Dis.* 22, 23–37. doi:10.1016/j.cld.2017.08.007

Nie, H., Song, C., Wang, D., Cui, S., Ren, T., Cao, Z., et al. (2017). MicroRNA-194 inhibition improves dietary-induced non-alcoholic fatty liver disease in mice through targeting on FXR. *Biochim. Biophys. Acta* 1863, 3087–3094. doi:10.1016/j.bbadis.2017.09.020

Qi, Z., Zhang, Y., Qi, S., Ling, L., Gui, L., Yan, L., et al. (2017). Salidroside inhibits HMGB1 acetylation and release through upregulation of SirT1 during inflammation. *Oxidat. Med. Cell Longev.* 2017, 1. doi:10.1155/2017/9821543

Qin, G., Ma, J., Huang, Q., Yin, H., Han, J., Li, M., et al.. (2018). Isoquercetin improves hepatic lipid accumulation by activating AMPK pathway and suppressing TGF-β signaling on an HFD-induced nonalcoholic fatty liver disease rat model. *Int. J. Mol. Sci.* 19, 4126. doi:10.3390/ijms19124126

Rolo, A. P., Teodoro, J. S., and Palmeira, C. M. (2012). Role of oxidative stress in the pathogenesis of nonalcoholic steatohepatitis. *Free Radic. Biol. Med.* 52, 59–69. doi:10.1016/j.freeradbiomed.2011.10.003

Safari, Z. and Gérard, P. (2019). The links between the gut microbiome and non-alcoholic fatty liver disease (NAFLD). *Cell. Mol. Life Sci.* 76, 1541–1558. doi:10.1007/s00018-019-03011-w

Shen, F., Feng, J., Wang, X., Qi, Z., Shi, X., An, Y., et al. (2016). Vinegar treatment prevents the development of murine experimental colitis via inhibition of inflammation and apoptosis. *J. Agric. Food Chem.* 64, 1111–1121. doi:10.1021/acs.jafc.5b05415

Silva, J. P. and Wahlestedt, C. (2010). Role of Sirtuin 1 in metabolic regulation. *Drug Discov. Today* 15, 781–791. doi:10.1016/j.drudis.2010.07.001

Soares e Silva, A. K., de Oliveira Cipriano Torres, D., dos Santos Gomes, F. O., dos Santos Silva, B., Lima Ribeiro, E., Costa Oliveira, A., et al. (2015). LPSF/GQ-02 inhibits the development of hepatic steatosis and inflammation in a mouse model of non-alcoholic fatty liver disease (NAFLD). *PLoS One* 10, e0123787. doi:10.1371/journal.pone.0123787

Stefan, N., Häring, H.-U., and Cusi, K. (2019). Non-alcoholic fatty liver disease: causes, diagnosis, cardiometabolic consequences, and treatment strategies. *Lancet Diabetes Endocrinol.* 7, 313–324. doi:10.1016/S2213-8587(18)30154-2

Tang, W., Yao, X., Xia, F., Yang, M., Chen, Z., Zhou, B., et al. (2018). Modulation of the gut microbiota in rats by hugan qingzhi tablets during the treatment of high-fat-diet-induced nonalcoholic fatty liver disease. *Oxidat. Med. Cell Longev.* 2018, 1. doi:10.1155/2018/7261619

Wu, X., Xu, N., Li, M., Huang, Q., Wu, J., Gan, Y., et al. (2019). Protective effect of patchouli alcohol against high-fat diet induced hepatic steatosis by alleviating endoplasmic reticulum stress and regulating VLDL metabolism in rats. *Front. Pharmacol.* 10, 1134. doi:10.3389/fphar.2019.01134

Xia, H., Zhu, X., Zhang, X., Jiang, H., Li, B., Wang, Z., et al. (2019). Alpha-naphthoflavone attenuates non-alcoholic fatty liver disease in oleic acid-treated HepG2 hepatocytes and in high fat diet-fed mice. *Biomed. Pharmacother.* 118, 109287. doi:10.1016/j.biopha.2019.109287

Xu, W., Huang, Z., Zhang, X., Li, Q., Lu, Z., Shi, J., et al. (2011a). Monitoring the microbial community during solid-state acetic acid fermentation of Zhenjiang aromatic vinegar. *Food Microbiol.* 28, 1175–1181. doi:10.1016/j.fm.2011.03.011

Xu, W., Xu, Q., Chen, J., Lu, Z., Xia, R., Li, G., et al. (2011b). Ligustrazine formation in Zhenjiang aromatic vinegar: changes during fermentation and storing process. *J. Sci. Food Agric.* 91, 1612–1617. doi:10.1002/jsfa.4356

Yang, J., Sun, L., Wang, L., Hassan, H. M., Wang, X., Hylemon, P. B., et al. (2017). Activation of SIRT1/FXR signaling pathway attenuates triptolide-induced hepatotoxicity in rats. *Front. Pharmacol.* 8, 260. doi:10.3389/fphar.2017.00260

Yao, H., Tao, X., Xu, L., Qi, Y., Yin, L., Han, X., et al. (2018). Dioscin alleviates non-alcoholic fatty liver disease through adjusting lipid metabolism via SIRT1/AMPK signaling pathway. *Pharmacol. Res.* 131, 51–60. doi:10.1016/j.phrs.2018.03.017

Younossi, Z. M., Koenig, A. B., Abdelatif, D., Fazel, Y., Henry, L., and Wymer, M. (2016). Global epidemiology of nonalcoholic fatty liver disease-meta-analytic assessment of prevalence, incidence, and outcomes. *Hepatology* 64, 73–84. doi:10.1002/hep.28431

Yu, Y., Zhang, Z., Zhang, B., Zeng, Y., Li, X., Ji, H., et al. (2020). Implication of vinegar alone or in combination with caltrate in a rat osteoporosis model induced by a low calcium diet and retinoic acid. *Chin. Tradit. Med. J.* 3, 1–8.

Zeng, W., Shan, W., Gao, L., Gao, D., Hu, Y., Wang, G., et al. (2015). Inhibition of HMGB1 release via salvianolic acid B-mediated SIRT1 up-regulation protects rats against non-alcoholic fatty liver disease. *Sci. Rep.* 5, 16013. doi:10.1038/srep16013

Zhang, B., Xia, T., Duan, W., Zhang, Z., Li, Y., Fang, B., et al. (2019). Effects of organic acids, amino acids and phenolic compounds on antioxidant characteristic of Zhenjiang aromatic vinegar. *Molecules* 24, 3799. doi:10.3390/molecules24203799

Zhang, X., Ji, X., Wang, Q., and Li, J. Z. (2018). New insight into inter-organ crosstalk contributing to the pathogenesis of non-alcoholic fatty liver disease (NAFLD). *Protein Cell* 9, 164–177. doi:10.1007/s13238-017-0436-0

Zhang, Y., Geng, C., Liu, X., Li, M., Gao, M., Liu, X., et al. (2017). Celastrol ameliorates liver metabolic damage caused by a high-fat diet through SIRT1. *Mol. Metabol.* 6, 138–147. doi:10.1016/j.molmet.2016.11.002

Zhao, C., Xia, T., Du, P., Duan, W., Zhang, B., Zhang, J., et al. 2018). Chemical composition and antioxidant characteristic of traditional and industrial Zhenjiang aromatic vinegars during the aging process. *Molecules* 23, 2949. doi:10.3390/molecules23112949

Zhao, Q., Liu, F., Cheng, Y., Xiao, X.-R., Hu, D.-D., Tang, Y.-M., et al. (2019). Celastrol protects from cholestatic liver injury through modulation of SIRT1-FXR signaling. *Mol. Cell. Proteomics* 18, 520–533. doi:10.1074/mcp.RA118.000817

Zhu, W., Liu, Y., Lan, Y., Li, X., Luo, L., Duan, X., et al. (2019). Dietary vinegar prevents kidney stone recurrence via epigenetic regulations. *EBioMedicine* 45, 231–250. doi:10.1016/j.ebiom.2019.06.004

Conflict of Interest: Authors SZ, GL, and BZ were employed by the company "Jiangsu Hengshun Vinegar Industry Co., Ltd." (Zhenjiang, China).

The remaining authors declare that the research was conducted in the absence of any commercial or financial relationships that could be construed as a potential conflict of interest.

Copyright © 2020 Zhu, Guan, Tan, Li, Gao, Zhang and Xu. This is an open-access article distributed under the terms of the Creative Commons Attribution License (CC BY). The use, distribution or reproduction in other forums is permitted, provided the original author(s) and the copyright owner(s) are credited and that the original publication in this journal is cited, in accordance with accepted academic practice. No use, distribution or reproduction is permitted which does not comply with these terms.

frontiers in Pharmacology

ORIGINAL RESEARCH
published: 21 December 2020
doi: 10.3389/fphar.2020.603771

Intestinal Epithelial Cell-Derived Extracellular Vesicles Modulate Hepatic Injury via the Gut-Liver Axis During Acute Alcohol Injury

Arantza Lamas-Paz[1,2†], Laura Morán[1,3†], Jin Peng[4†], Beatriz Salinas[3,5,6,7], Nuria López-Alcántara[1], Svenja Sydor[8], Ramiro Vilchez-Vargas[9], Iris Asensio[3,10], Fengjie Hao[1,2,11], Kang Zheng[1,2,12], Beatriz Martín-Adrados[1,2], Laura Moreno[8,13], Angel Cogolludo[8,13], Manuel Gómez del Moral[2,14], Lars Bechmann[8], Eduardo Martínez-Naves[1,2], Javier Vaquero[3,10], Rafael Bañares[3,10], Yulia A. Nevzorova[1,2,15‡] and Francisco Javier Cubero[1,2‡]*

[1]Department of Immunology, Ophthalmology and ENT, Complutense University School of Medicine, Madrid, Spain, [2]12 de Octubre Health Research Institute (imas12), Madrid, Spain, [3]Servicio de Aparato Digestivo del Hospital General Universitario Gregorio Marañón, Instituto de Investigación Sanitaria Gregorio Marañón (IiSGM), Madrid, Spain, [4]Department of Hepatobiliary Surgery, Nanjing Drum Tower Hospital, The Affiliated Hospital of Nanjing University Medical School, Nanjing, China, [5]Centro Nacional de Investigaciones Cardiovasculares Carlos III, Madrid, Spain, [6]Bioengineering and Aerospace Engineering Department, Universidad Carlos III de Madrid, Madrid, Spain, [7]Centro de Investigación Biomédico en Red de Salud Mental (CIBERSAM), Madrid, Spain, [8]Department of Internal Medicine, University Hospital Knappschaftskrankenhaus, Ruhr-University Bochum, Bochum, Germany, [9]Department of Gastroenterology, Hepatology, and Infectious Diseases, Otto von Guericke University Hospital Magdeburg, Magdeburg, Germany, [10]Centre for Biomedical Research, Network on Liver and Digestive Diseases (CIBEREHD), Madrid, Spain, [11]Department of General Surgery, Hepatobiliary Surgery, Ruijin Hospital, Shanghai Jiao Tong University School of Medicine, Shanghai, China, [12]Department of Anesthesiology, Zhongda Hospital, School of Medicine, Southeast University, Nanjing, China, [13]Department of Pharmacology and Toxicology, Complutense University School of Medicine and Centre for Biomedical Research, Network on Respiratory Diseases (CIBERES), Madrid, Spain, [14]Department of Cell Biology, Complutense University School of Medicine, Madrid, Spain, [15]Department of Internal Medicine III, University Hospital RWTH Aachen, Aachen, Germany

OPEN ACCESS

Edited by:
Ralf Weiskirchen, RWTH Aachen University, Germany

Reviewed by:
Laura E. Nagy, Cleveland Clinic, United States
Paramananda Saikia, Cleveland Clinic, United States
Chaoxin Man, Northeast Agricultural University, China

***Correspondence:**
Francisco Javier Cubero
fcubero@ucm.es

[†]These authors have contributed equally to this work and share first authorship
[‡]These authors have contributed equally to this work and share senior authorship

Specialty section:
This article was submitted to Gastrointestinal and Hepatic Pharmacology, a section of the journal Frontiers in Pharmacology

Received: *07 September 2020*
Accepted: *05 October 2020*
Published: *21 December 2020*

Citation:
Lamas-Paz A, Morán L, Peng J, Salinas B, López-Alcántara N, Sydor S, Vilchez-Vargas R, Asensio I, Hao F, Zheng K, Martín-Adrados B, Moreno L, Cogolludo A, Gómez del Moral M, Bechmann L, Martínez-Naves E, Vaquero J, Bañares R, Nevzorova YA and Cubero FJ (2020) Intestinal Epithelial Cell-Derived Extracellular Vesicles Modulate Hepatic Injury via the Gut-Liver Axis During Acute

Binge drinking, i.e., heavy episodic drinking in a short time, has recently become an alarming societal problem with negative health impact. However, the harmful effects of acute alcohol injury in the gut-liver axis remain elusive. Hence, we focused on the physiological and pathological changes and the underlying mechanisms of experimental binge drinking in the context of the gut-liver axis. Eight-week-old mice with a C57BL/6 background received a single dose (p.o.) of ethanol (EtOH) [6 g/kg b.w.] as a preclinical model of acute alcohol injury. Controls received a single dose of PBS. Mice were sacrificed 8 h later. In parallel, HepaRGs and Caco-2 cells, human cell lines of differentiated hepatocytes and intestinal epithelial cells intestinal epithelial cells (IECs), respectively, were challenged in the presence or absence of EtOH [0–100 mM]. Extracellular vesicles (EVs) isolated by ultracentrifugation from culture media of IECs were added to hepatocyte cell cultures. Increased intestinal permeability, loss of

Abbreviations: ADH, alcohol dehydrogenase; ALDH, aldehyde dehydrogenase; BAC, blood alcohol concentration; DLS, dynamic light scattering; EtOH, ethanol; EVs, extracellular vesicles; H&E, hematoxylin and eosin; IF, immunofluorescence; IECs, intestinal epithelial cells; IL-1β, interleukin-1β; KCs, Kupffer cells; LPS, lipopolysaccharides; LW/BW, liver weight vs. body weight; NTA, nanoparticle tracking analysis; ORO, oil red O; qRT-PCR, quantitative real-time PCR; Srebp-1, sterol regulatory binding protein-1; Tnf-α, tumor necrosis factor-alpha; TJs, tight junctions; Tlr-4, toll-like receptor-4; ZO-1, zone occludens-1.

zonula occludens-1 (ZO-1) and MUCIN-2 expression, and alterations in microbiota—increased *Lactobacillus* and decreased Lachnospiraceae species—were found in the large intestine of mice exposed to EtOH. Increased TUNEL-positive cells, infiltration of CD11b-positive immune cells, pro-inflammatory cytokines (e.g., *tlr4*, *tnf*, *il1β*), and markers of lipid accumulation (Oil Red O, *srbep1*) were evident in livers of mice exposed to EtOH, particularly in females. *In vitro* experiments indicated that EVs released by IECs in response to ethanol exerted a deleterious effect on hepatocyte viability and lipid accumulation. Overall, our data identified a novel mechanism responsible for driving hepatic injury in the gut-liver axis, opening novel avenues for therapy.

Keywords: hepatocytes, intestinal epithelial cells, extracellular vesicles, alcohol (EtOH), gut-liver axis

INTRODUCTION

Alcohol abuse is a leading cause of liver-related morbidity and mortality, which has become a global problem due to the financial burden on society and the healthcare system (Dolganiuc and Szabo, 2009; Gao and Bataller, 2011). While the adverse effects of long-term chronic alcohol abuse have been widely studied, the underlying mechanisms of short-term binge and sporadic drinking, also termed acute alcohol-derived tissue injury, remain elusive.

Binge drinking refers to an excessive consumption of large amounts of alcohol in a very short period of time, in which increases the blood alcohol concentration (BAC) levels to at least 0.08 g/dl (Ventura-Cots et al., 2017). The National Institute on Alcohol Abuse and Alcoholism defines binge drinking as a consume of four (women) or five (men) standard drinks per day within 2 h at least once during Binge drinking refers to excessive consumption of large amounts of alcohol in a short period of time, in which the (BAC) levels increase to at least 0.08 g/dl (Ventura-Cots et al., 2017). The National Institute on Alcohol Abuse and Alcoholism defines binge drinking as the consumption of four (women) or five (men) standard drinks per day within 2 h at least once during the past 30 days (Ventura-Cots et al., 2017). However, the standard drink varies significantly from country to country from 7.9 g of alcohol in the United Kingdom to 14 g in the United States or 19.75 g in Japan (Dolganiuc and Szabo, 2009).

Noticeably, the rate of alcohol absorption depends on several factors, including the amount and concentration of alcohol ingested and physiological factors determined by gender (Cederbaum, 2012; Kim et al., 2015; Griswold et al., 2018). Furthermore, sex differences such as body fat, body water, levels of alcohol dehydrogenase (ADH), and hormones affect the hepatic metabolism of alcohol (Gill, 2000; Naugler et al., 2007; Griswold et al., 2018; Lamas-Paz et al., 2018).

Upon acute alcohol injury, alterations of the intestinal epithelial barrier occur at multiple levels including tight junctions (TJs), between gut epithelial cells, production of mucin, recruitment and activation of inflammatory cells to the intestinal wall. In addition, the composition of the gut microbiome changes as a result of alcohol consumption. These result in increased translocation of microbial product from the gut to the liver via the portal circulation. Besides increased levels of lipopolysaccharides, other microbial components may also reach the liver where in the liver sinusoids Kupffer cells and other recruited immune cells become activated and produce large amounts of pro-inflammatory cytokines (e.g., TNF, IL-1β), which further increase gut permeability, thus fueling inflammation in the gut and favoring the development of liver disease (Szabo, 2015; Gao et al., 2019).

Emerging evidence showed that EVs are important contributors to the coordinated signaling events between the gut and the liver (Bui et al., 2018), a bidirectional axis linking the biliary tract, the portal vein, and the systemic circulation (Tripathi et al., 2018).

In the present study, we aimed to evaluate the underlying mechanisms driving acute alcohol injury *in vitro* and in female and male mice in the context of the gut-liver axis.

MATERIALS AND METHODS

Cell Culture and Cell Viability

HepaRG cells (BioPredict International, Rennes, France) were seeded following the supplier's protocol, and Caco-2 cells, a human intestinal cell line widely used as a model of the intestinal barrier, were cultured in Dulbecco's modified Eagle's medium (Gibco, Rockville, MD) containing 20% heat-inactivated FBS, 1% penicillin/streptomycin, and 2 mM L-glutamine (ICN Pharmaceuticals, Costa Mesa, CA). Once HepaRGs or Caco-2 cells reached approximately 85% confluence, starving was performed for 4 h, and cells were challenged with EtOH [0–100 mM] (Panreac AppliChem, Darmstadt, Germany) for another 24 h. Cells were kept at 37°C in an atmosphere with 5% CO_2. Pictures of cells were taken in an optical microscope (DMIL LED, Leica, Wetzlar, Germany) connected to a camera (Leica MC170HD, Leica). Cell viability was determined by CCK8 (Merck, Munich, Germany) following the manufacturer's instructions. After fixing the cells with 4% PFA, cell death and lipid accumulation were tested by TUNEL (Roche, Rotkreuz, Switzerland) and oil red O (ORO) (Merck), respectively, as previously described (Cubero et al., 2015; Liao et al., 2019).

Animal Model of Acute Alcohol Injury

Healthy C57BL/6J mice purchased from ENVIGO (Valencia, Spain) were bred and maintained in the Animal Facility of the Faculty of Biology at UCM, Madrid, in a temperature-controlled room with 12 h light/dark cycles and allowed food and water *ad libitum*. For our study, we used female and male 8 week-old mice.

Animal studies were approved by the local authority (Consejería de Medio Ambiente, Administración Local y Ordenación del Territorio; PROEX-154/16).

Acute alcohol injury was performed by oral gavage. Briefly, mice (n = 8–10/group) were fasted overnight for 12 h. In the morning, they were fed with a dose of 30% EtOH (gavage of 6 g/kg b.w.) (Pruett et al., 2020) using a gavage needle (Kent Scientific, Torrington, CT). Mice fed with PBS instead of EtOH served as controls. All animals were sacrificed at 8 h after the EtOH challenge using an overdose of isoflurane (Solvet, Segovia, Spain) inhalation.

Intestinal Permeability *In Vivo*

Isothiocyanate conjugated dextran (FITC-dextran, molecular mass 4.0 kDa) (TdBCons, Uppsala, Sweden) was dissolved in PBS at a concentration of 200 mg/ml and administrated to 12 h fasted mice (10 ml/kg body weight) using a gavage needle (Kent Scientific). After 4 h, mice were sacrificed by an overdose of isoflurane (Solvet) inhalation. Concentration of FITC was determined in serum by fluorometry with an excitation of 485 nm and an emission wavelength of 528 nm using serially diluted FITC-dextran (0, 125, 250, 500, 1,000, 2,000, 4,000, 6,000, 8,000, 10,000 ng/ml) as standards.

Histological and Morphological Analyses

Livers from mice were harvested, fixed with 4% PFA, and embedded in paraffin for histological evaluation using hematoxylin and eosin (H&E), performed by Dr Juana Flores, an experienced pathologist (School of Veterinary, UCM). Photomicrographs of stained sections were randomly taken in a ×20 magnification in an optical microscope (Nikon Eclipse Ci, Tokyo, Japan), and ORO-positive areas were quantified using free NIH Image/J software (National Institutes of Health, Bethesda, MD).

Immunofluorescence Staining

Liver and colon from each mouse were preserved in cassettes in Tissue-Tek (Sakura Finetek U.S.A, Torrance, CA) at −80 C. Immunostainings for ZO-1 (Invitrogen, Paisley, FL), MUCIN-2 (Santa Cruz, Dallas, TX), TUNEL (Roche), and CD11b (BD, Madrid, Spain) were performed as previously described (Liao et al., 2019). Anti-mouse and anti-rabbit Alexa Fluor 488 (Invitrogen) were used as secondary antibodies.

Quantitative Real-Time Polymerase Chain Reaction

Total RNA was purified from liver tissue using Trizol reagent (Invitrogen). Total RNA [1 µg] was used to synthesize cDNA using Super Script first Stand Synthesis System (Invitrogen) and was resuspended in 100 µl of RNAse-free water (Merck). Quantitative real-time PCR was performed using SYBR Green Reagent (Invitrogen) by the Genomics and Proteomics Facility (School of Biology, UCM). The mRNA expression of *il1β*, *Srebp1*, *Tlr4*, *Tnf*, and *Gapdh* expression was studied (**Supplementary Table S1**). Relative gene expression was normalized to the expression of *Gapdh*. Primer sequences are provided upon request.

Microbiota Analysis

DNA was extracted from foecal content as previously described (Sydor et al., 2020). All samples were resampled to the minimum sequencing depth of 17719 reads using phyloseq package (Mcmurdie and Holmes, 2013) and returning 2,167 phylotypes (**Supplementary Figure S2**).

Biochemical Measurements

Serum transaminases in blood and cell's supernatant were analyzed in the Central Laboratory Facility at the Gregorio Marañón Research Health Institute at Madrid (iISGM) using automated analyzers. For the evaluation of intrahepatic triglycerides, liver samples were homogenized in a specific Tris buffer (10 mM Tris, 2 mM EDTA, 0.25 M sucrose, and pH 7.5) and successively processed using a commercial colorimetric kit (Human Diagnostics, Wiesbaden), according to the manufacturer's instructions.

Isolation of Extracellular Vesicles

For *in vivo* experiments, blood from the cava vein was collected in 1.1 ml serum gel polypropylene microtubes (Sarstedt, Barcelona). Serum was obtained by centrifugation at 12,000 *g* for 10 min at 4°C. Serum was then centrifuged using a Microliter Centrifuge Z233 MK-2 (Hermle, Wehingen, Germany) at 10,000 *g* during 30 min. Then, the supernatant was ultracentrifuged twice at 100,000 *g* using a Hitachi micro ultracentrifuge CS150FNX (Hitachi, Tokyo, Japan) with an S5AA2 rotor in 1.5 ml Eppendorf tubes (Fisher Scientific, Madrid, Spain) during 75 min each. Finally, the pellet containing EVs was resuspended in 50 µl of PBS. Samples were measured by dynamic light scattering (Malvern Instruments, United Kingdom). Next, recollected samples were filtered through 0.44 µm filters, and the obtained sample was diluted 1:10 for nanoparticle tracking analysis (NTA).

For *in vitro* tests, supernatants were collected from cultures of Caco-2 and HepaRG cells treated with EtOH [0–100 mM]. EVs were isolated from supernatants using ultracentrifugation. Briefly, the culture supernatant was centrifuged at 2,000 *g* and 10,000 *g* for 20 and 30 min, respectively, to remove cellular debris and larger vesicles. The resultant supernatant was ultracentrifuged twice at 100,000 *g* for 75 min. The pellet was resuspended in 50 µl of PBS and stored at −80°C. Free EVs medium was prepared by ultracentrifugation of 10% FBS for 16 h on a Hitachi micro ultracentrifuge CS150FNX (Hitachi, Japan).

Experiments With Extracellular Vesicles

HepaRG cells were cultured with EVs isolated from the supernatant of Caco-2 cells previously treated with EtOH [0–100 mM] and diluted into EVs-free medium. Controls were challenged with EVs-free medium. Twenty-four hours later, cells were washed and fixed with 4% PFA. Cell viability, cell death, and lipid deposition were then evaluated.

Nanoparticle Tracking Analysis

The number and size of EVs were quantified and characterized using NTA with the Nanosight NS300 instrument equipped with a 405 nm green laser and an sCMOS high sensitivity camera with NTA (Malvern Instruments). Particles were recorded in five different 60-s videos. The data were analyzed using NTA software SOPs v3.4, following the manufacturer's instructions.

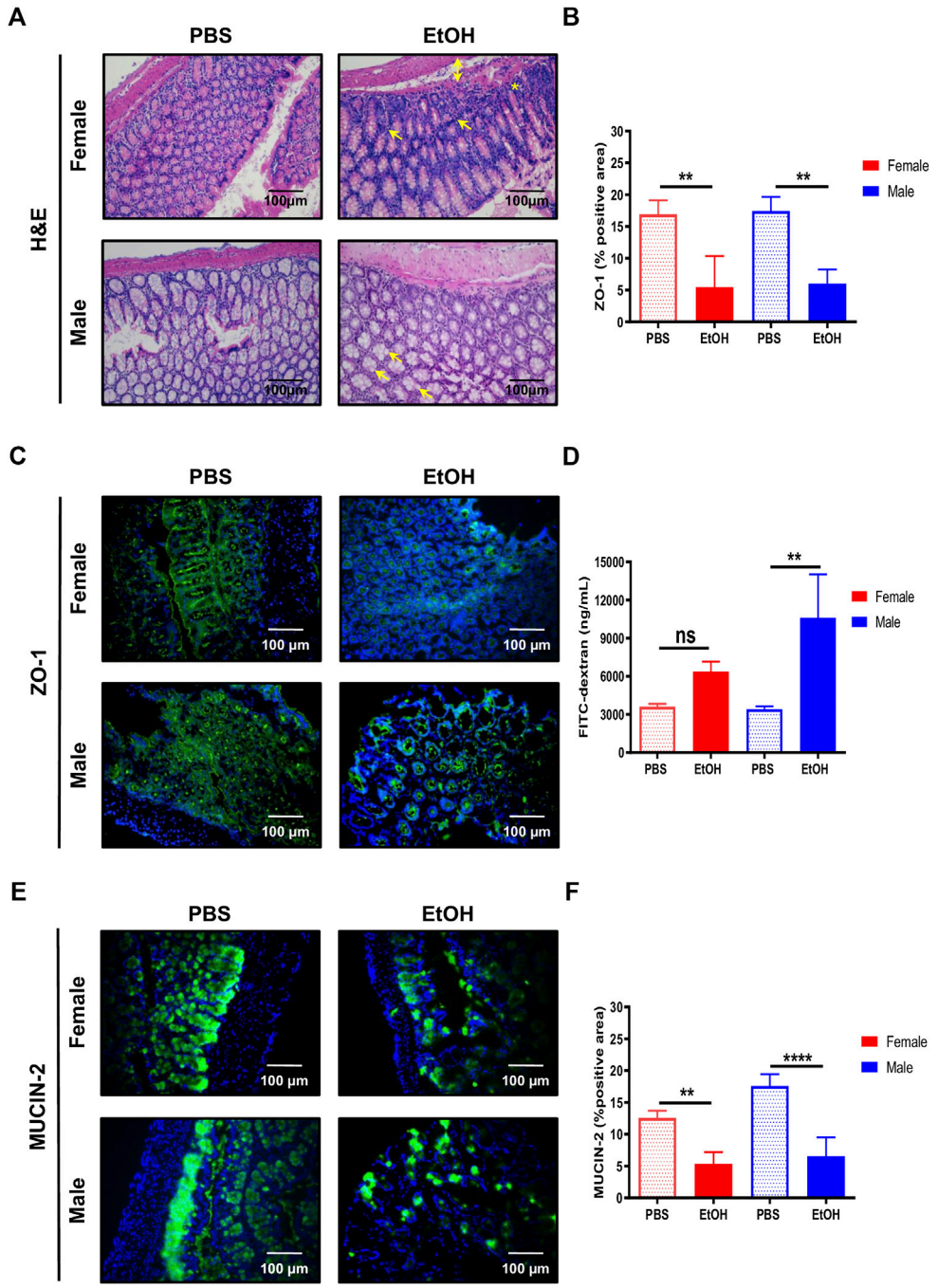


FIGURE 1 | Acute alcohol injury disrupts the gut intestinal barrier in female and male mice. **(A)** Representative H&E staining was performed in paraffin colon sections of female and male mice treated with EtOH [6 g/kg] or PBS (n = 5–7/group). **(B)** Quantification of the ZO-1 positive area was performed and graphed (n = 4/group). **(C)** ZO-1 immunofluorescence staining was performed in colons of male and female mice. **(D)** FITC-dextran levels in serum from female and male mice was quantified as a measure of intestinal permeability (n = 3–4/group). **(E)** MUCIN-2 immunofluorescence staining was performed in colons of female and male mice. **(F)** Quantification of the MUCIN-2 positive area was done and graphed (n = 4–5/group; $^{**}p < 0.01$, $^{****}p < 0.0001$). In female mice, arrows mark mixed inflammation; double arrow, oedema in submucosa and a star, degeneration of crypt basal cells. In male mice, arrows mark mild hypertrophy in Goblet cells.

Statistical Analysis

All statistical analyses consisted of One-Way ANOVA followed by Tukey post-hoc test using GraphPad Prism version 8.0 software (San Diego, CA). A $p < 0.05$ was considered statistically significant. Data were expressed as mean ± SD of the mean (SEM).

RESULT

Experimental Acute Alcohol Injury Induces Gut Dysbiosis

The gut mucosa is particularly susceptible to alcohol-induced tissue injury (Molina and Nelson, 2018). Thus, we first focused on evaluating the impact of binge alcohol drinking via the circulatory system in the large intestine. Histopathological evaluation of experimental acute alcohol injury revealed mixed inflammation in the colon, oedema in the submucosa, and cellular degeneration of crypt basal cells in colons of female mice exposed to acute alcohol injury (**Figure 1A**). In contrast, male-EtOH treated colon displayed mild hypertrophy in Goblet cells (**Figure 1A**). No relevant findings were observed in mice challenged with PBS (**Figure 1A**).

Since acute alcohol exposure induces gut permeability by disrupting not only the epithelial cells, but also the space between them that is controlled by (TJs) (Fanning and Anderson, 2009), we next evaluated whether changes in intestinal TJs that result in leaky gut occurred during experimental acute alcohol injury in female and male mice. Interestingly, the expression of zonula occludens-1 (ZO-1) was significantly decreased in colons of female and, to a bigger extent, of male mice, compared with PBS-fed animals (**Figures 1B,C**).

Next, we used the FITC-dextran gavage method to determine the impact of acute alcohol injury on intestinal permeability *in vivo*. Compared with PBS-treated animals, intestinal permeability tended to increase in female mice and was significantly increased in male mice exposed to EtOH (**Figure 1D**). Altogether, these results indicated that experimental acute alcohol injury increased intestinal permeability in mice.

The intestinal mucous layer prevents direct contact between the intestinal epithelium and bacteria by avoiding its way through. The major component of the intestinal mucous layer is MUCIN-2, which is secreted by Goblet cells (Van Der Sluis et al., 2006). Immunofluorescent staining of MUCIN-2 revealed thinner layers in the large intestine of EtOH-treated female and, to a bigger extent, male mice, compared with PBS-treated animals (**Figures 1E,F**).

Characterization of Changes in Gut Microbiota During Acute Alcohol Injury

Overwhelming evidence has shown that changes in the intestinal microbiome might contribute to alcohol-associated intestinal inflammation and permeability (Sarin et al., 2019). Therefore, foecal microbiota from all experimental groups was analyzed (**Supplementary Figures S1A,B**). No difference in gut microbiota composition was found between female or male mice treated with either PBS or EtOH (p value = 0.049). Principal coordinates analysis (**Supplementary Figure S1A**) revealed that six phylotypes, four of them belonging to the phylum Firmicutes, trended to increase under acute ethanol consumption. On the contrary, 12 phylotypes, seven belonging also to Firmicutes, trended to diminished in EtOH-treated mice. Especially Phy1 and Phy5 (both belonging to the family Erysipelotrichaceae) together with Phy2 (*Lactobacillus* sp.) were observed in more abundance in EtOH-treated mice, while Phy3 (*Turicibacter* sp.), Phy7 (*Bifidobacterium pseudolongum*), and Phy9 (*Lactobacillus johnosonii* or *acidophilus*) were observed in less abundances in EtOH-treated mice (**Supplementary Figure S1B**). Mann-Whitney test detected statistically significant differences between EtOH-treated and PBS-treated mice in three phylotypes. Phy2 (p value = 0.006) and Phy5 (p value = 0.006), both belonging to *Lactobacillus* sp., increased the relative abundance in EtOH-treated mice, while Phy63 (p value = 0.03), belonging to Lachnospiraceae, diminished in EtOH-treated mice.

Altogether, these results suggest that experimental acute alcohol-derived tissue injury triggers gut dysbiosis.

Steatosis and Inflammation Induced by Acute Alcohol Injury Is More Pronounced in Female Mice

The disruption of the intestinal barrier during alcohol exposure is related to liver injury (Sambrotta et al., 2014; Roychowdhury et al., 2019). Since experimental binge EtOH exposure impaired intestinal barrier integrity, we subsequently investigated the effects of acute alcohol injury on the liver. Light microscopy revealed normal lobular architecture with sinusoidal hepatic cords and typical liver architecture in PBS-treated mice (**Figure 2A**). In contrast, the structure of the hepatic lobules was disordered in mice with acute alcohol injury, with noticeable swelling around the central vein. The cytoplasm was translucent, exhibiting ballooning degeneration, some extent of hepatocellular necrosis, and visible inflammatory cell infiltration ($CD11b^+$ cells). Interestingly, female livers exhibited extensive degeneration of hepatocytes (eosinophil cytoplasm) and nuclear lysis (**Figure 2A**). In line with these data, the LW/BW ratio of EtOH-treated female mice was significantly higher compared with PBS-treated mice (**Figure 2B; Supplementary Figure S2A,B**).

Next, serum markers of liver damage were evaluated. ALT levels were increased in male EtOH-treated mice compared with female or vehicle-treated mice (**Figure 2C**). ALP–a marker of cholestasis–was elevated in male mice after acute alcohol injury, while a tendency toward increased ALP was observed in female mice compared with PBS-treated animals (**Figure 2D**). Alcohol triggers hepatocyte cell death; thus, we investigated cell death in the liver using TUNEL. The percentage of TUNEL-positive cells increased after acute alcohol injury in female livers and, to a lesser extent, in male mice. In contrast, no relevant cell death was found in PBS-treated mice (**Figures 2E,F**).

Ethanol is metabolized in the liver by hepatocytes, being a primary inducer of liver injury and hepatic steatosis (Diehl et al., 1988; Ji et al., 2006; Kwon et al., 2014; Steiner and Lang, 2017). The staining of neutral lipids with ORO staining indicated an increase of lipid accumulation in livers of female and, to a lesser extent, of male mice, challenged with experimental acute alcohol injury (**Figures 3A,B**). Moreover, quantification of hepatic triglycerides showed an increase in both female and male animals, and activation of srebp-1, associated with increased

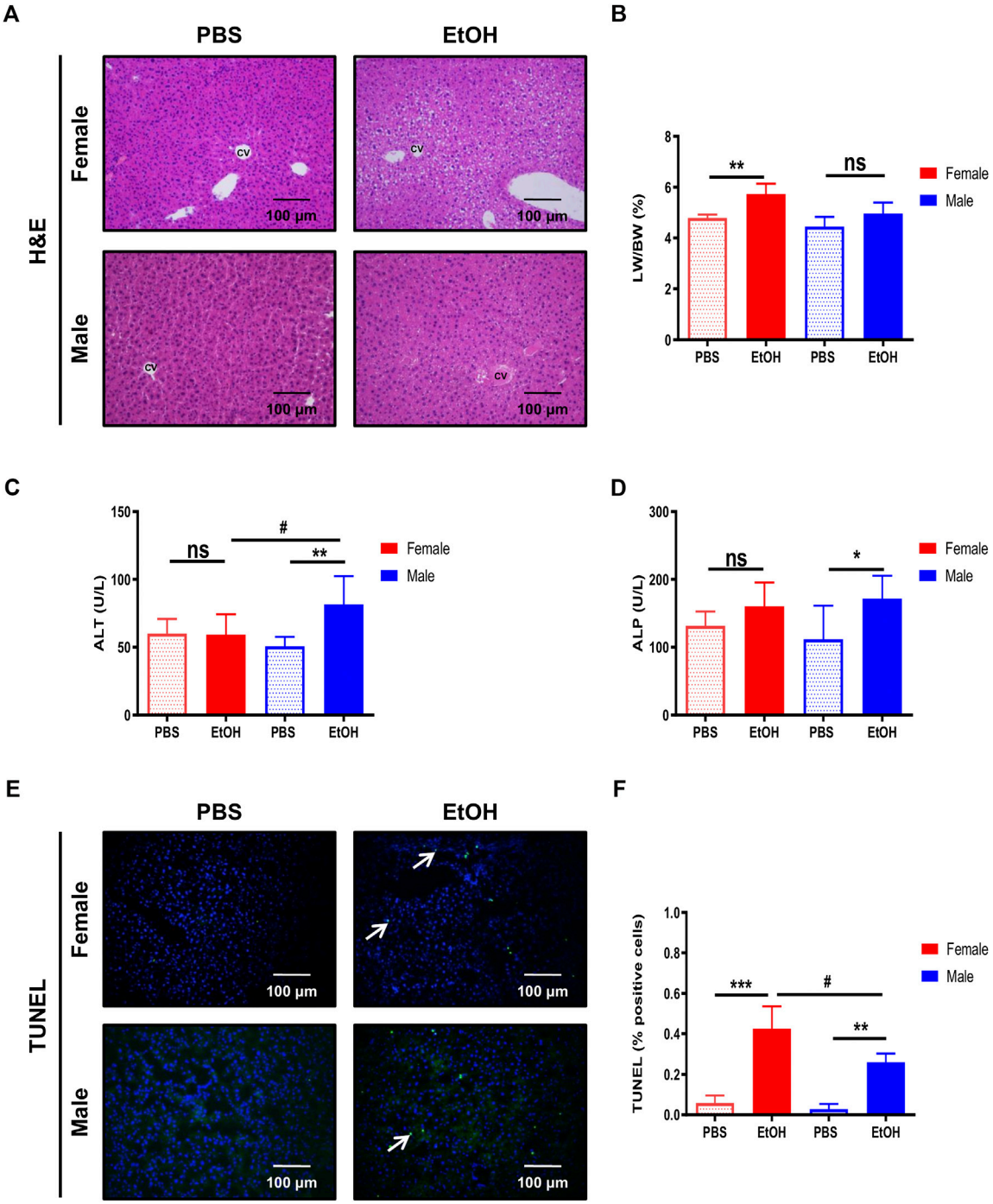


FIGURE 2 | Binge ethanol exposure to mice causes changes in liver architecture and cell death. **(A)** H&E staining in female and male mice treated with EtOH [6 g/kg] or PBS performed in paraffin liver sections (n = 6–8/group). **(B)** Liver-to-body weight (LW/BW) ratio in female and male mice after acute alcohol injury (n = 5–8/group). Serum **(C)** ALT and **(D)** ALP levels in female and male mice (n = 7–8/group). **(E)** TUNEL staining was performed in liver cryosections of female and male mice. **(F)** Quantification of TUNEL positive cells was done and graphed (n = 3/group;$^{*}p < 0.05$, $^{***}p < 0.001$, $^{\#}p < 0.05$).

expression of lipogenic genes, was also induced by EtOH predominantly in female mice (**Figures 3C,D**).

Since immune infiltration and inflammation are characteristic of alcohol-induced liver injury, quantification of CD11b-positive cells and markers of inflammation, including *tnf-α*, *il1β*, and *tlr4*, were also evaluated. The number of CD11b positive cells was increased in female livers (**Figure 3E**), in agreement with the upregulation of mRNA transcripts for *tnf-α*, *il1β*, and *tlr4* observed in female mice (**Figures 3F–H**). In summary, our data suggest that female mice are more sensitive to liver injury

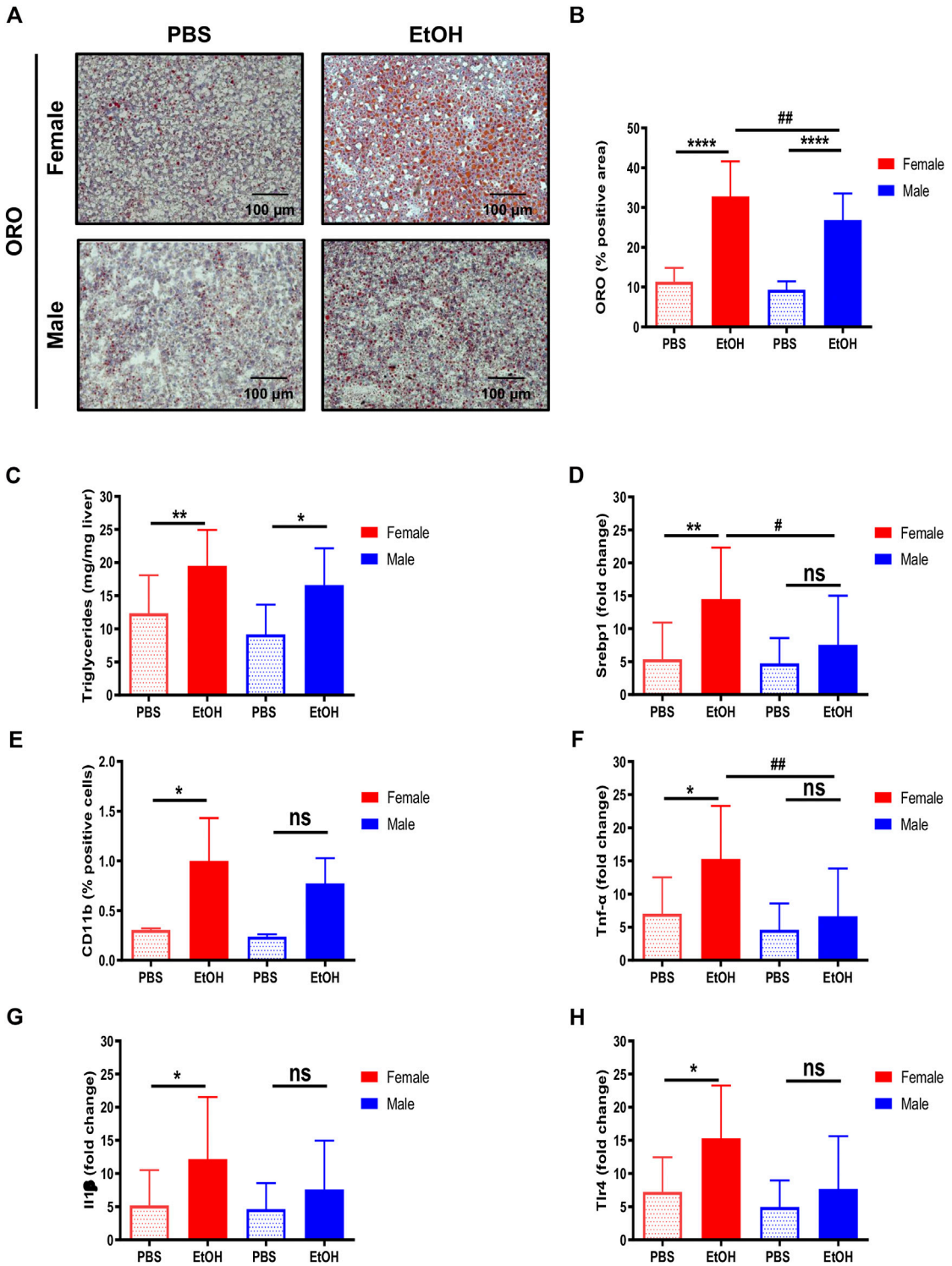


FIGURE 3 | Hepatic lipid accumulation and inflammation are characteristic of female mice. **(A)** ORO staining performed in liver cryosection of female and male C57BL/6J mice treated with EtOH [6 g/kg] or PBS. **(B)** Quantification of lipid droplets by ORO positive area was done and graphed (n = 5–6/group). **(C)** Quantification of hepatic triglycerides was done and graphed (n = 8/group). **(D)** *Srbp-1* mRNA expression was determined by qPCR and normalized to the amount of GAPDH in the liver of female and male mice (n = 5–8/group). **(E)** Quantification of CD11b positive cells was done and graphed (n = 3/group). **(F)** *Tnf-α*, **(G)** *Il1β*, and **(H)** *Tlr4* mRNA expression determined by qPCR and normalized to the amount of *gapdh* in liver of female and male mice (n = 4–10/group; $^{*}p < 0.05$, $^{****}p < 0.0001$, $^{\#}p < 0.05$, $^{\#\#}p < 0.01$).

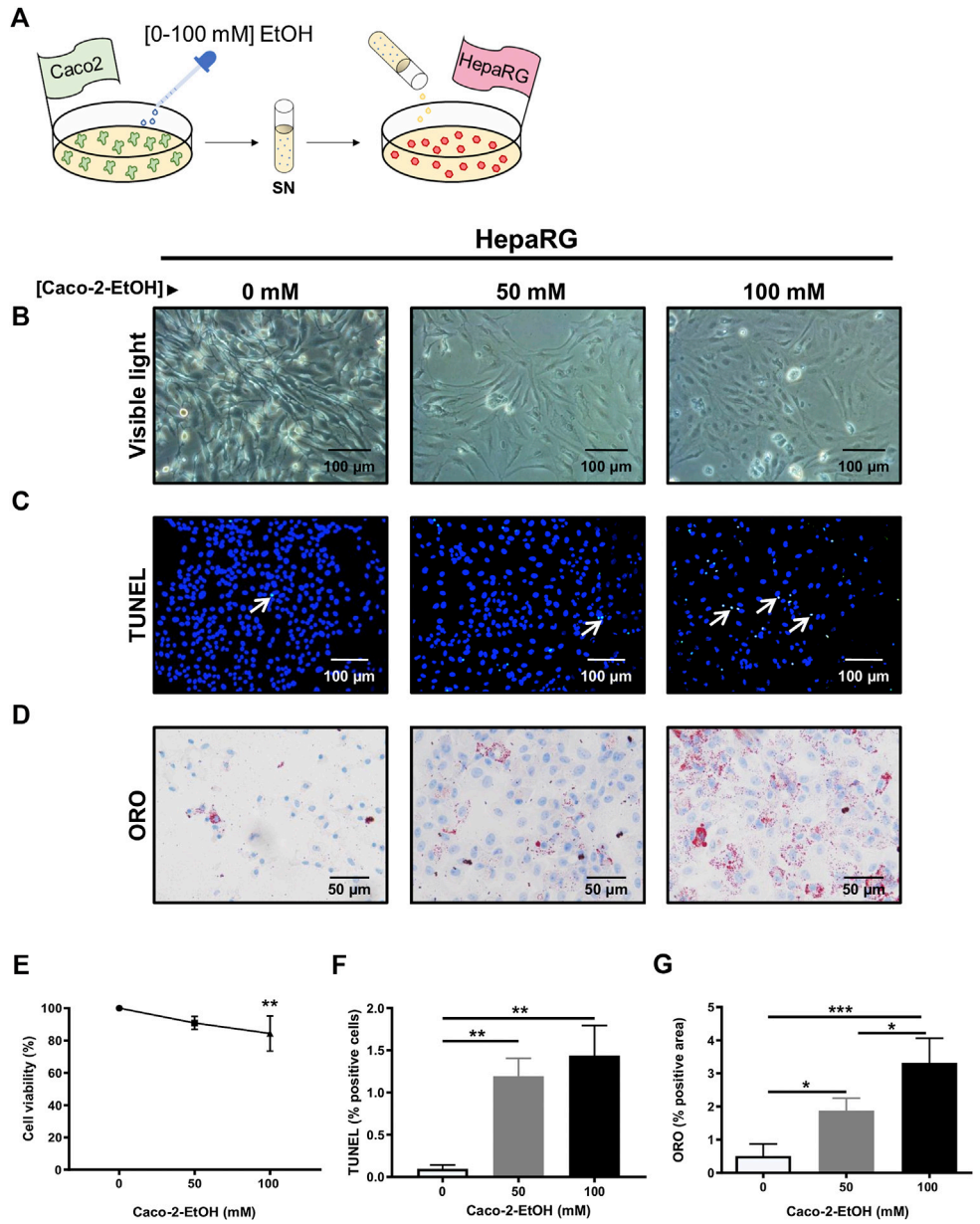


FIGURE 4 | HepaRG cells challenged with supernatant from EtOH-treated Caco-2 cells displayed exacerbated cell damage. **(A)** Experimental *in vitro* model of the effect of acute alcohol injury on intestinal epithelial permeability and on liver injury: cultures of HepaRG cells were exposed to the supernatant from Caco-2 cells that had been previously treated with different concentrations of EtOH [0–100 mM]. **(B)** HepaRG cells exposed to the supernatant of Caco-2 cells treated with EtOH [0–100 mM] showed by visible light (n = 4/group). **(C)** TUNEL staining was performed in HepaRG cells exposed to the supernatant of Caco-2 cells treated with EtOH [0–100 mM]. **(D)** Oil Red O (ORO) staining was performed in HepaRG cells exposed to the supernatant of Caco-2 cells treated with EtOH [0–100 mM]. **(E)** Cell viability of HepaRG cells challenged with supernatant from EtOH-treated Caco-2 cells determined by CCK8 (n = 6/group). **(F)** Quantification of TUNEL positive cells HepaRG cells exposed to supernatant from EtOH-treated Caco-2 cells (n = 3/group). **(G)** Quantification of lipid droplets by ORO positive area in HepaRG cells exposed to supernatant from EtOH-treated Caco-2 cells (%) (n = 3–4/group; $^{*}p < 0.05$, $^{***}p < 0.001$).

due to acute alcohol injury in terms of steatosis and inflammation.

Assessment of Acute Alcohol Injury-Derived Damage in an *In Vitro* Model

In order to reproduce an *in vitro* model of the intestinal epithelial barrier, Caco-2 cells were plated and regularly monitored visually using a light microscope. First, Caco-2 cells were challenged with EtOH [0–100 mM], which caused cytoplasmic retractions, cell shrinkage, and cell death. High EtOH concentrations evidenced loss of cell-cell contact and detachment after 24 h EtOH exposure as observed under the visible light (**Supplementary Figure S3A,B**). Cell viability tested by CCK8 showed decreased cell viability along with increasing concentrations of EtOH (**Supplementary Figure**

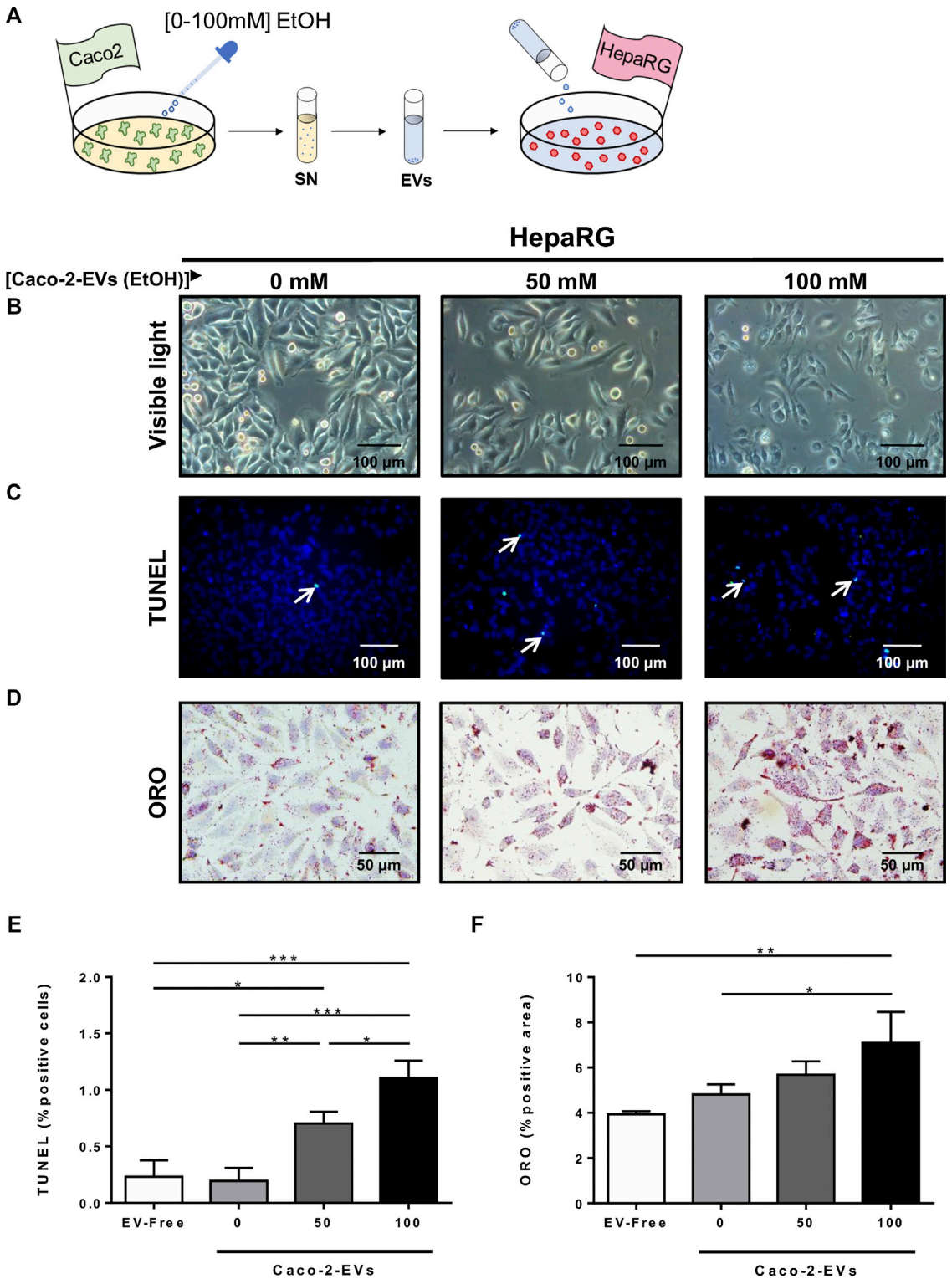


FIGURE 5 | Extracellular vesicles released from IECs trigger hepatocyte cell damage *in vitro*. **(A)** Cultures of HepaRG cells were treated with EVs isolated by ultracentrifugation from the supernatant of Caco-2 cells previously exposed to different concentrations of EtOH [0–100 mM]. **(B)** Morphology analysis of HepaRG cells by visible light. **(C)** TUNEL staining was performed in HepG2 cells exposed to EVs from EtOH-pretreated Caco-2-cells. **(D)** ORO staining performed in HepaRG cells challenged with EVs from EtOH-pretreated Caco-2-cells. **(E)** Quantification of TUNEL positive HepaRG cells after challenge with EVs isolated from the supernatant of Caco-2 cells previously treated with different concentrations of EtOH [0–100 mM] (n = 3/group). **(F)** Quantification of lipid droplets by ORO positive area in HepaRG cells challenged with EVs isolated from the supernatant of Caco-2 cells previously treated with different concentrations of EtOH [0–100 mM] (n = 3/group; $^{*}p < 0.05$, $^{***}p < 0.001$).

S3C). These data were corroborated using TUNEL staining, which also showed an elevation of the number of Caco-2 TUNEL-positive cells with increasing concentrations of alcohol (**Supplementary Figure S3B,D**).

As an *in vitro* model of hepatocytes, we also used the well-characterized HepaRG hepatocyte human cell line to understand the effect of alcohol exposure in the liver. HepaRG cells were challenged by exposure to EtOH [0–100]. The loss of cell architecture was evident with a concentration of 50 mM EtOH (**Supplementary Figure S3A**). Cell viability assay revealed a decrease of alive cells proportionally associated with increasing concentrations of EtOH (**Supplementary Figure S3B,C**). Moreover, TUNEL staining also confirmed that the number of dead HepaRG cells increased after exposure to EtOH (**Supplementary Figures S3D**). Besides, lipid deposition evaluated by ORO staining showed higher lipid accumulation with increasing EtOH concentrations (**Supplementary Figures S3C,F**).

Intestinal Epithelial Cells Secrete Factors That Modulate Hepatocyte Injury During Acute Alcohol Injury

To replicate the effect of acute ethanol-derived injury on intestinal epithelial permeability and its impact on liver cell injury, 85% confluent HepaRG cells cultured in 12-well plates were challenged with 1 ml of supernatant from Caco-2 cells treated with EtOH [0–100 mM] (**Figure 4A**). The viability of HepaRG cells decreased at the higher concentrations of EtOH in the Caco-2 supernatant (**Figures 4B,E**), and these data correlated with the percentage of TUNEL positive cells (**Figures 4C,F**). Increased lipid accumulation, as assessed by ORO staining, was also found in HepaRG cells challenged with the supernatant of EtOH-treated Caco-2 cells (**Figures 4D,G**). These data indicate that the release of mediators from (IECs) might be responsible for hepatocyte injury during acute alcohol injury.

Extracellular Vesicles Released From Intestinal Epithelial Cells Trigger Hepatocyte Damage *In Vitro*

It has been well-documented that the release of EVs, produced under pathological conditions, might be responsible for cell damage. To understand whether the release of EVs by IECs might trigger liver damage during acute alcohol injury, we tested this hypothesis by isolating EVs from our *in vitro* model of the intestinal epithelial barrier.

Cell cultures of differentiated hepatocytes were exposed to EVs treated with EtOH [0–100 mM] (**Figure 5A**). HepaRG cells changed the morphology and lost the polarity when challenged with EVs from EtOH-pretreated Caco-2 cells (**Figure 5B**).

Concomitant with these changes, the cell viability of HepaRG cells decreased, as observed by the increase of positive TUNEL cells after *in vitro* acute alcohol injury (**Figures 5C,E**). Next, we measured lipid deposition in hepatocytes in response to EVs released by EtOH-pretreated Caco-2 cells. Interestingly, EVs from EtOH-pretreated Caco-2 cells caused an increase in lipid deposition of differentiated hepatocytes (**Figures 5D,F**), suggesting a possible role for EVs released by IECs in liver damage during acute alcohol injury.

Characterization of Extracellular Vesicles During Acute Alcohol Injury *In Vitro* and *In Vivo*

EVs were isolated from the supernatant of Caco-2 cells exposed to EtOH [0–100 mM] and from serum extracted from the portal vein of mice challenged to experimental acute alcohol injury, respectively, using a sequential ultracentrifugation method. Dynamic Light Scattering analysis showed the size distribution by intensity, confirming the existence of different populations of EVs (**Supplementary Table S2**), and NTA validated the morphology, size, and concentration of EVs in the diverse experimental groups (**Figure 6** and **Supplementary Figures S5B–D**). Although the concentration of particles was significantly increased to $2.34\ E^9 \pm 1.14\ E^8$ and $2.9\ E^9 \pm 5.82\ E^8$ particles/ml in the supernatant of Caco-2 cells exposed to 50 and 100 mM EtOH, respectively, compared with the control group $1.17\ E^9 \pm 2.31\ E^8$ (**Figure 6A**), no differences were found in the size of EVs upon EtOH exposure (**Figure 6B**).

Next, we measured the number of particles in serum extracted from mice subjected to experimental acute alcohol injury. While no differences were found in the number of particles/ml between PBS and EtOH-treated animals, the concentration of particles was $1.12\ E^9 \pm 1.40\ E^8$ and $1.59\ E^9 \pm 2.00\ E^8$ in EtOH-fed male and female mice, respectively, compared with PBS-injected male and female mice $1.30\ E^9 \pm 1.61\ E^8$ and $1.80\ E^9 \pm 3.99\ E^8$. These results might indicate a tendency toward a reduced particle concentration in male animals after acute alcohol exposure (**Figure 6C**). NTA showed mean particle size of 90 nm in serum samples consistent with the size of exosomes (**Figure 6D**).

DISCUSSION

Scientific research on alcohol abuse has traditionally focused on the mechanisms of chronic toxicity, given its financial burden and societal costs. More recently, acute alcohol injury has emerged as a social problem since binge drinking is alarmingly increasing both in women and in men (Dolganiuc and Szabo, 2009; Mcketta and Keyes, 2019). However, the mechanisms by which acute alcohol injury affects human health are not fully understood. Thus, there is a need for preclinical and translational studies focused on the effects of binge alcohol drinking.

In the present study, we first used a suitable *in vivo* model for assessing the effects of a single binge episode by administering 6 g/kg b.w. of EtOH to mice, based on previous studies (Carson and Pruett, 1996).

Intestinal barrier function is key to preventing the alcohol-induced inflammation locally and systemically. Goblet cells in the intestinal epithelium produce protective trefoil factors and mucins, which are abundantly core glycosylated and either localized to the cell membrane or secreted into the lumen to form the mucous layer (Shao et al., 2018). Decreased expression

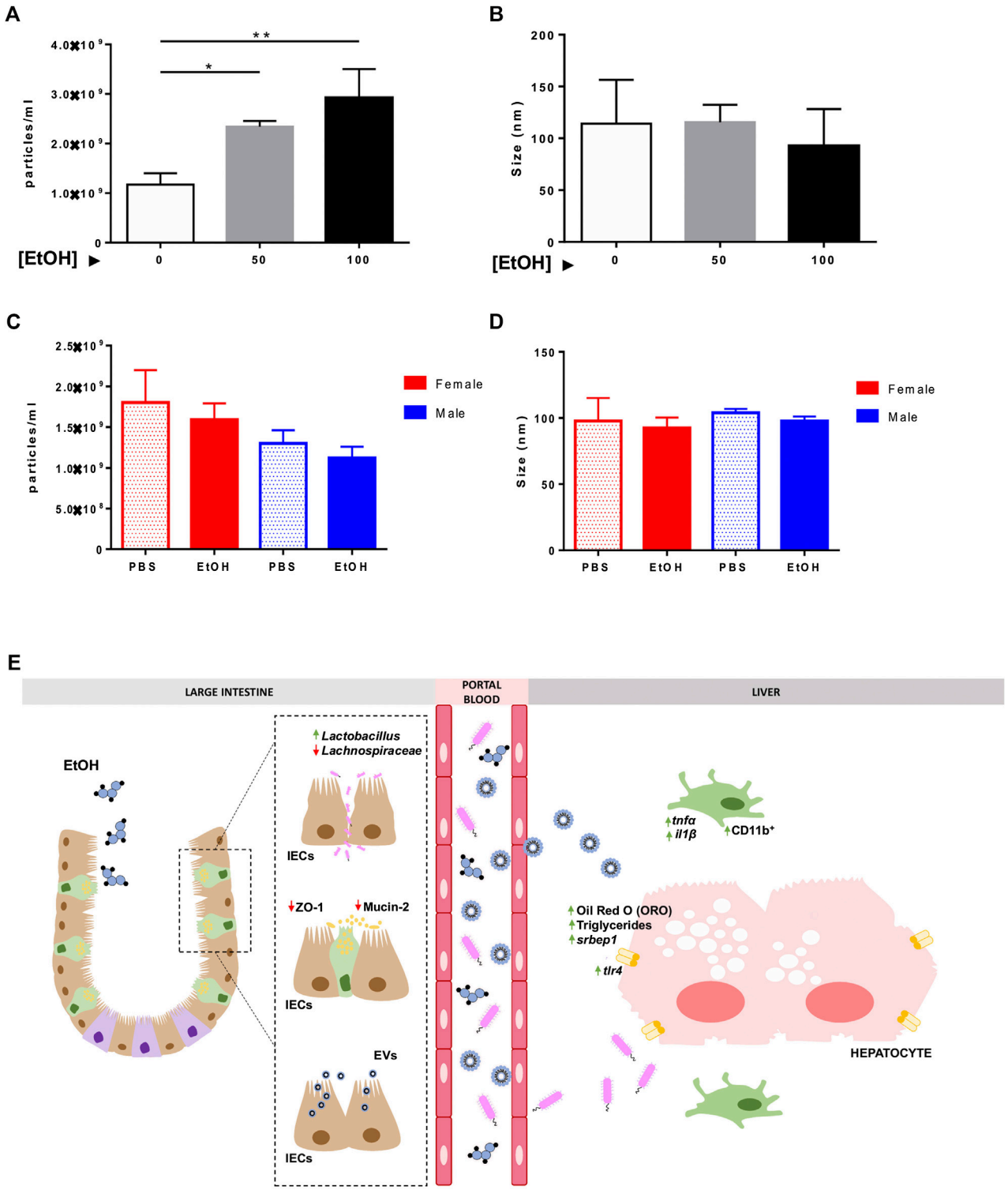


FIGURE 6 | Characterization of extracellular vesicles *in vitro* and *in vivo*. Isolated EVs from the supernatant of Caco-2 cells challenged with different concentrations of EtOH [0–100 mM] were measured by NTA, and **(A)** particles/ml and **(B)** size of EVs were represented. Isolated EVs were extracted from the serum of female and male mice treated with EtOH or PBS, and they were analyzed using NTA. **(C)** Particles/ml and **(D)** size of EVs were graphed (n = 3/group; $^{*}p < 0.05$, $^{**}p < 0.01$). **(E)** Schematic representation of the pathophysiological events that occur during acute alcohol exposure. Acute alcohol ingestion triggers damage to the intestinal epithelial barrier. Increased FITC-Dextran, disruption in tight junctions (ZO-1), and loss of mucosa (MUCIN-2) and alteration of the gut microbiota (increased *Lactobacillus* and decreased Lachnospiraceae) indicate damage to the intestinal epithelial barrier and gut dysbiosis. Translocation of microbial bacterial products through the leaky gut causes overexpression of *tlr4* and intestinal-derived inflammation in the liver–presence of CD11b-positive cells, *tnf-α*, and *il1β*, and mild steatosis and lipid accumulation. Our *in vitro* experiments suggest that ethanol triggers the release of EVs by intestinal epithelial cells (IECs), which exert a deleterious effect on hepatocyte viability and lipid accumulation.

of MUCIN-2 protein in the large intestine of female and male mice was observed after acute alcohol exposure. Interestingly, *mucin-2* knockout mice are protected against alcohol feeding-induced dysbiosis (Hartmann et al., 2013), likely due to higher expression of antimicrobial peptides.

Additionally, paracellular permeability in the intestinal epithelium sealed by TJs (Shao et al., 2018) was disrupted in the colon of EtOH-treated female and male mice, in which the loss of ZO-1 was characteristic. These results are in agreement with previous observations reporting that chronic-binge ethanol feeding impaired intestinal TJs (Cresci et al., 2017). Moreover, occludin deficiency increases susceptibility to EOH-induced mucosal dysfunction and liver damage in mice (Mir et al., 2016).

Alcohol ingestion causes intestinal bacterial overgrowth and changes in microbial composition in preclinical models as well as in patients with alcohol use disorder (Sarin et al., 2019). In our study, one alcohol binge increased the *Lactobacillus* phylum and decreased the Lachnospiraceae family. A decrease in *Lactobacillus* species and Lachnospiraceae family has been reported in alcohol consumption/feeding and alcoholic cirrhosis (Bajaj et al., 2012; Sarin et al., 2019). However, *Lactobacillus* species are increased in hepatic steatosis (Jang et al., 2019), which was observed in acute alcohol injury-exposed animals, and bacterial microbiota also change with the progression of alcoholic liver disease. Moreover, in a similar preclinical model that used a lower EtOH dosage (3 g/kg b.w.), Chen and colleagues (2016) reported no changes in intestinal microbiota and relative abundance of *Lactobacillus* and Firmicutes. Moreover, it is very likely that *Lactobacillus* elevation acts to counteract lipid metabolism imbalance as previously reported (Martin et al., 2008). Overall, these data suggest that alterations to the gut mucus layer, together with intestinal hyperpermeability and bacterial overgrowth, trigger bacterial translocation. Therefore, microbial products that reach the liver might contribute to hepatic injury during acute alcohol exposure.

Hepatic steatosis develops acutely in most individuals that consume even moderate amounts of alcohol. Steatosis changes are also seen in rodent models of binge drinking (Massey and Arteel, 2012). Although steatosis is an inert pathology *per se*, it sensitizes the liver to injury caused by a second insult. Binge drinking is a major risk factor for advanced liver disease (Ventura-Cots et al., 2017). Ethanol-treated mice displayed increased hepatic lipid accumulation, and this effect was more noticeable in female animals. This phenomenon was associated with increased immune infiltration (CD11b putative macrophages) and pro-inflammatory mediators of hepatic inflammation (e.g., *tnf-α*, *il1β*), which contribute to alcohol-related liver injury (Kawaratani et al., 2013; Bala et al., 2014; Rocco et al., 2014; Cresci et al., 2017).

Ethanol pre-exposure can prime Kupffer cells to lipopolysaccharides stimulation, resulting in enhanced *tnf-α* release, and binge drinking can impair the immune response via alteration of *tlr4* signaling (Massey and Arteel, 2012; Bala et al., 2014), as observed in our acute alcohol injury model. Moreover, our data demonstrated a significant increase in cell death in EtOH-treated mice, corroborated by elevated serum markers of liver injury (e.g., ALT). In agreement with other publications (Wagnerberger et al., 2013; Cresci et al., 2017), the more pronounced liver damage observed after acute alcohol injury in the liver of female mice may result from increased activation of TLR4-dependent signaling in this gender. However, in-depth studies need to be performed to shed light on the activation of specific molecular mechanisms that might be sex-dependent in the gut-liver axis.

Gender-related differences in total liver (ADH) and aldehyde dehydrogenase activity among different animal species have been observed in many studies. The differential liver injury between female and male animals could be explained by various factors, including the lower activity of class I and II ADH isoenzymes in females (Chrostek et al., 2003). This difference could help explain the fact that after men and women ingest the same dose of alcohol, women have higher BAC levels and increased injury. Corrao and colleagues (1998) reported that the same amount of average alcohol consumption was related to a higher risk of liver cirrhosis in women than in men. In contrast, women displayed slower gastric metabolism. Additionally, the levels of hormones, such as estrogen, might also influence several of the above factors (Wagnerberger et al., 2013).

Next, we sought to mechanistically approach the pathomechanisms underlying acute alcohol injury in the context of the gut-liver axis by modeling our experimental model *in vitro*. First, the effects of EtOH were assessed in Caco-2 cells, a human cell line of IECs. Concomitant with Wang's study (Wang et al., 2014), acute alcohol injury in culture decreased cell viability and exacerbated cell death, even though our results were collected 24 h after challenge (Dolganiuc and Szabo, 2009). Furthermore, EtOH caused changes in cell death and lipid deposition in HepaRGs, a human hepatoma cell line, in a dose-dependent manner, data that agree with previous publications (Tuoi Do et al., 2011). However, these authors observed that exposure to 100 mM ethanol significantly raised caspase 3/7 activity between 48 and 72 h, suggesting that apoptosis might occur later in time in culture. However, *in vivo*, we observed TUNEL-related cell death 8 h after acute ethanol injury. Others reported maximal apoptotic rate levels 4 h after ethanol exposure but TUNEL-positivity from 1 to 9 h (Yun et al., 2014), which might be increased levels of expression of CYP2E1 at these times after acute ethanol-derived tissue injury.

Accumulating evidence supports a role for EVs in regulating hepatic function. The gut-liver axis communication was modeled *in vitro* by challenging HepaRG cells with supernatant of Caco-2 cells. Human HepaRG hepatocytes treated with the supernatant of EtOH-pretreated Caco-2 cells dramatically changed their morphology, increased cell death, and accumulated lipids, as it occurs *in vivo*. This set of results suggested that the release of mediators by IECs may play a crucial role in the initiation and development of liver injury, and thus hepatocyte might uptake EVs as observed in models of viral hepatitis, partial hepatectomy and ischemia-reperfusion injury (Hirsova et al., 2016).

Recent studies pointed to a defined group of biological nanovesicles, namely exosomes or extracellular vesicles, as a

key player in modulating the deleterious effects of alcohol in different tissues (Eguchi and Feldstein, 2018). Since our data indicated that EVs might be potential communicating tools in the gut-liver axis, we performed an *in vitro* model whereby EVs secreted by IECs (Caco-2 cells) in response to EtOH were added to HepaRG hepatocytes. EtOH significantly increased the number of nanoparticles released by Caco-2 cells, which were challenged to HepaRG cells. Decreased cell viability and high lipid accumulation were observed in this cell line of human hepatocytes, concomitant with our *in vivo* results.

In parallel, EVs isolated from portal blood of EtOH- and PBS-treated mice were collected and characterized. Our goal was to demonstrate that EVs released specifically by IECs can be used as potential biomarkers of acute alcohol injury. Our data showed a mean size of 90 nm in serum samples consistent with the size of EVs. However, hepatocytes also release EVs that are detected in blood as well, as previously reported (Eguchi et al., 2017), suggesting that the gut-liver axis is a bidirectional communication pathway.

Our results show that mice develop alterations in the gut-liver axis in response to experimental acute alcohol injury. Overall, alterations in the intestinal epithelial barrier associated with increased permeability, a thinner mucous protective layer, and changes in gut microbiota were evident. Interestingly, female mice were more prone to hepatic injury in response to a single binge episode, specifically in markers of steatosis and inflammation. Moreover, we showed that the release of mediators by IECs might have an impact on liver cells during acute alcohol injury, and demonstrated the presence and the effects of EVs both *in vivo* and *in vitro* (**Figure 6E**). These findings further deepen in the mechanisms triggered by acute alcohol exposure and open new therapeutic windows.

DATA AVAILABILITY STATEMENT

The datasets generated for this study can be found in ENA, Accession No. PRJEB40638.

ETHICS STATEMENT

Animal studies were approved by the Consejería de Medio Ambiente, Administración Local y Ordenación del Territorio (PROEX-154/16).

AUTHOR CONTRIBUTIONS

AL-P and LM carried out the experiments and drafted the manuscript. JP provided funds for the study. NL-A, FH, and KZ performed experiments. SS, RV-V, and LB performed the microbiota studies. YN contributed to the intellectual work and provided experimental techniques. BM-A, LM-G, and AC contributed with the extracellular vesicles characterization. IA, MG, JV, RB, BM-A, and EM-N conducted experiments and/or provided pivotal intellectual and YN and FJ supervised, and analyzed the experiments, provided the funding and drafted the manuscript

FUNDING

This work was supported by the MINECO Retos SAF2016-78711, SAF2017-87919-R, EXOHEP-CM S2017/BMD-3727, NanoLiver-CM Y2018/NMT-4949, ERAB Ref. EA 18/14, AMMF 2018/117, UCM-25-2019 and COST Action CA17112, the German Research Foundation (SFB/TRR57/P04, SFB 1382-403224013/A02, and DFG NE 2128/2-1). FC and YN are Ramón y Cajal Researchers RYC-2014-15242 and RYC-2015-17438. FC is a Gilead Liver Research 2018. KZ is a recipient of a Chinese Scholarship Council (CSC). BK20170127 from the Natural Science Foundation of Jiangsu Province to JP

SUPPLEMENTARY MATERIAL

The Supplementary Material for this article can be found online at: https://www.frontiersin.org/articles/10.3389/fphar.2020.603771/full#supplementary-material

REFERENCES

Bajaj, J. S., Ridlon, J. M., Hylemon, P. B., Thacker, L. R., Heuman, D. M., Smith, S., et al. (2012). Linkage of gut microbiome with cognition in hepatic encephalopathy. *Am. J. Physiol. Gastrointest. Liver Physiol.* 302, G168–G175. doi:10.1152/ajpgi.00190.2011

Bala, S., Marcos, M., Gattu, A., Catalano, D., and Szabo, G. (2014). Acute binge drinking increases serum endotoxin and bacterial DNA levels in healthy individuals. *PloS One* 9, e96864. doi:10.1371/journal.pone.0096864

Bui, T. M., Mascarenhas, L. A., and Sumagin, R. (2018). Extracellular vesicles regulate immune responses and cellular function in intestinal inflammation and repair. *Tissue Barriers* 6, e1431038. doi:10.1080/21688370.2018.1431038

Carson, E. J., and Pruett, S. B. (1996). Development and characterization of a binge drinking model in mice for evaluation of the immunological effects of ethanol. *Alcohol Clin. Exp. Res.* 20, 132–138. doi:10.1111/j.1530-0277.1996.tb01055.x

Cederbaum, A. I. (2012). Alcohol metabolism. *Clin. Liver Dis.* 16, 667–685. doi:10.1016/j.cld.2012.08.002

Chen, P., Miyamoto, Y., Mazagova, M., Lee, K.-C., Eckmann, L., and Schnabl, B. (2016). Microbiota and alcoholic liver disease. *Alcohol Clin. Exp. Res.* 40, 1791–1792. doi:10.1111/acer.13129

Chrostek, L., Jelski, W., Szmitkowski, M., and Puchalski, Z. (2003). Gender-related differences in hepatic activity of alcohol dehydrogenase isoenzymes and aldehyde dehydrogenase in humans. *J. Clin. Lab. Anal.* 17, 93–96. doi:10.1002/jcla.10076

Corrao, G., Bagnardi, V., Zambon, A., and Torchio, P. (1998). Meta-analysis of alcohol intake in relation to risk of liver cirrhosis. *Alcohol Alcohol.* 33, 381–392. doi:10.1093/oxfordjournals.alcalc.a008408

Cresci, G. A., Glueck, B., Mcmullen, M. R., Xin, W., Allende, D., and Nagy, L. E. (2017). Prophylactic tributyrin treatment mitigates chronic-binge ethanol-induced intestinal barrier and liver injury. *J. Gastroenterol. Hepatol.* 32, 1587–1597. doi:10.1111/jgh.13731

Cubero, F. J., Zhao, G., Nevzorova, Y. A., Hatting, M., Al Masaoudi, M., Verdier, J., et al. (2015). Haematopoietic cell-derived Jnk1 is crucial for chronic

inflammation and carcinogenesis in an experimental model of liver injury. *J. Hepatol.* 62, 140–149. doi:10.1016/j.jhep.2014.08.029

Diehl, A. M., Goodman, Z., and Ishak, K. G. (1988). Alcohollike liver disease in nonalcoholics. *Gastroenterology* 95, 1056–1062. doi:10.1016/0016-5085(88)90183-7

Dolganiuc, A., and Szabo, G. (2009). *In vitro* and *in vivo* models of acute alcohol exposure. *World J. Gastroenterol.* 15, 1168–1177. doi:10.3748/wjg.15.1168

Eguchi, A., and Feldstein, A. E. (2018). Extracellular vesicles in non-alcoholic and alcoholic fatty liver diseases. *Liver Res.* 2, 30–34. doi:10.1016/j.livres.2018.01.001

Eguchi, A., Lazaro, R. G., Wang, J., Kim, J., Povero, D., Willliams, B., et al. (2017). Extracellular vesicles released by hepatocytes from gastric infusion model of alcoholic liver disease contain a MicroRNA barcode that can be detected in blood. *Hepatology* 65, 475–490. doi:10.1002/hep.28838

Fanning, A. S., and Anderson, J. M. (2009). Zonula occludens-1 and -2 are cytosolic scaffolds that regulate the assembly of cellular junctions. *Ann. N. Y. Acad. Sci.* 1165, 113–120. doi:10.1111/j.1749-6632.2009.04440.x

Gao, B., Ahmad, M. F., Nagy, L. E., and Tsukamoto, H. (2019). Inflammatory pathways in alcoholic steatohepatitis. *J. Hepatol.* 70, 249–259. doi:10.1016/j.jhep.2018.10.023

Gao, B., and Bataller, R. (2011). Alcoholic liver disease: pathogenesis and new therapeutic targets. *Gastroenterology* 141, 1572–1585. doi:10.1053/j.gastro.2011.09.002

Gill, J. (2000). The effects of moderate alcohol consumption on female hormone levels and reproductive function. *Alcohol Alcohol.* 35, 417–423. doi:10.1093/alcalc/35.5.417

Griswold, M. G., Fullman, N., Hawley, C., Arian, N., Zimsen, S. R. M., Tymeson, H. D., et al. (2018). Alcohol use and burden for 195 countries and territories, 1990–2016: a systematic analysis for the Global Burden of Disease Study 2016. *Lancet* 392, 1015–1035. doi:10.1016/s0140-6736(18)31310-2

Hartmann, P., Chen, P., Wang, H. J., Wang, L., Mccole, D. F., Brandl, K., et al. (2013). Deficiency of intestinal mucin-2 ameliorates experimental alcoholic liver disease in mice. *Hepatology* 58, 108–119. doi:10.1002/hep.26321

Hirsova, P., Ibrahim, S. H., Verma, V. K., Morton, L. A., Shah, V. H., Larusso, N. F., et al. (2016). Extracellular vesicles in liver pathobiology: small particles with big impact. *Hepatology* 64, 2219–2233. doi:10.1002/hep.28814

Jang, H. R., Park, H.-J., Kang, D., Chung, H., Nam, M. H., Lee, Y., et al. (2019). A protective mechanism of probiotic *Lactobacillus* against hepatic steatosis via reducing host intestinal fatty acid absorption. *Exp. Mol. Med.* 51, 1–14. doi:10.1038/s12276-019-0293-4

Ji, C., Chan, C., and Kaplowitz, N. (2006). Predominant role of sterol response element binding proteins (SREBP) lipogenic pathways in hepatic steatosis in the murine intragastric ethanol feeding model. *J. Hepatol.* 45, 717–724. doi:10.1016/j.jhep.2006.05.009

Kawaratani, H., Tsujimoto, T., Douhara, A., Takaya, H., Moriya, K., Namisaki, T., et al. (2013). The effect of inflammatory cytokines in alcoholic liver disease. *Mediat. Inflamm.* 2013, 495156. doi:10.1155/2013/495156

Kim, I. H., Kisseleva, T., and Brenner, D. A. (2015). Aging and liver disease. *Curr. Opin. Gastroenterol.* 31, 184–191. doi:10.1097/mog.0000000000000176

Kwon, H.-J., Won, Y.-S., Park, O., Chang, B., Duryee, M. J., Thiele, G. E., et al. (2014). Aldehyde dehydrogenase 2 deficiency ameliorates alcoholic fatty liver but worsens liver inflammation and fibrosis in mice. *Hepatology* 60, 146–157. doi:10.1002/hep.27036

Lamas-Paz, A., Hao, F., Nelson, L. J., Vázquez, M. T., Canals, S., Moral, M. G. d., et al. (2018). Alcoholic liver disease: utility of animal models. *World J. Gastroenterol.* 24, 5063–5075. doi:10.3748/wjg.v24.i45.5063

Liao, L., Schneider, K. M., Galvez, E. J. C., Frissen, M., Marschall, H.-U., Su, H., et al. (2019). Intestinal dysbiosis augments liver disease progression via NLRP3 in a murine model of primary sclerosing cholangitis. *Gut* 68, 1477–1492. doi:10.1136/gutjnl-2018-316670

Martin, F. P. J., Wang, Y., Sprenger, N., Yap, I. K. S., Lundstedt, T., Lek, P., et al. (2008). Probiotic modulation of symbiotic gut microbial-host metabolic interactions in a humanized microbiome mouse model. *Mol. Syst. Biol.* 4, 157. doi:10.1038/msb4100190

Massey, V. L., and Arteel, G. E. (2012). Acute alcohol-induced liver injury. *Front. Physiol.* 3, 193. doi:10.3389/fphys.2012.00193

Mcketta, S., and Keyes, K. M. (2019). Heavy and binge alcohol drinking and parenting status in the United States from 2006 to 2018: an analysis of nationally representative cross-sectional surveys. *PLoS Med.* 16, e1002954. doi:10.1371/journal.pmed.1002954

Mcmurdie, P. J., and Holmes, S. (2013). phyloseq: an R package for reproducible interactive analysis and graphics of microbiome census data. *PLoS One* 8, e61217. doi:10.1371/journal.pone.0061217

Mir, H., Meena, A. S., Chaudhry, K. K., Shukla, P. K., Gangwar, R., Manda, B., et al. (2016). Occludin deficiency promotes ethanol-induced disruption of colonic epithelial junctions, gut barrier dysfunction and liver damage in mice. *Biochim. Biophys. Acta Gen. Subj.* 1860, 765–774. doi:10.1016/j.bbagen.2015.12.013

Molina, P. E., and Nelson, S. (2018). Binge drinking's effects on the body. Alcohol research: current reviews vol. 39 (1) (2018):99–109. PMC6104963 PMID: 30557153 ISSN 2168-3492

Naugler, W. E., Sakurai, T., Kim, S., Maeda, S., Kim, K., Elsharkawy, A. M., et al. (2007). Gender disparity in liver cancer due to sex differences in MyD88-dependent IL-6 production. *Science* 317, 121–124. doi:10.1126/science.1140485

Pruett, S., Tan, W., Howell, G. E., 3rd, and Nanduri, B. (2020). Dosage scaling of alcohol in binge exposure models in mice: an empirical assessment of the relationship between dose, alcohol exposure, and peak blood concentrations in humans and mice. *Alcohol* 89, 9–17. doi:10.1016/j.alcohol.2020.03.011

Rocco, A., Compare, D., Angrisani, D., Sanduzzi Zamparelli, M., and Nardone, G. (2014). Alcoholic disease: liver and beyond. *World J. Gastroenterol.* 20, 14652–14659. doi:10.3748/wjg.v20.i40.14652

Roychowdhury, S., Glueck, B., Han, Y., Mohammad, M. A., and Cresci, G. A. M. (2019). A designer synbiotic attenuates chronic-binge ethanol-induced gut-liver injury in mice. *Nutrients* 11, 97. doi:10.3390/nu11010097

Sambrotta, M., Strautnieks, S., Papouli, E., Rushton, P., Clark, B. E., Parry, D. A., et al. (2014). Mutations in TJP2 cause progressive cholestatic liver disease. *Nat. Genet.* 46, 326–328. doi:10.1038/ng.2918

Sarin, S. K., Pande, A., and Schnabl, B. (2019). Microbiome as a therapeutic target in alcohol-related liver disease. *J. Hepatol.* 70, 260–272. doi:10.1016/j.jhep.2018.10.019

Shao, T., Zhao, C., Li, F., Gu, Z., Liu, L., Zhang, L., et al. (2018). Intestinal HIF-1α deletion exacerbates alcoholic liver disease by inducing intestinal dysbiosis and barrier dysfunction. *J. Hepatol.* 69, 886–895. doi:10.1016/j.jhep.2018.05.021

Steiner, J. L., and Lang, C. H. (2017). Alcohol, adipose tissue and lipid dysregulation. *Biomolecules* 7, 16. doi:10.3390/biom7010016

Sydor, S., Best, J., Messerschmidt, I., Manka, P., Vilchez-Vargas, R., Brodesser, S., et al. (2020). Altered microbiota diversity and bile acid signaling in cirrhotic and noncirrhotic NASH-HCC. *Clin. Transl. Gastroenterol.* 11, e00131. doi:10.14309/ctg.0000000000000131

Szabo, G. (2015). Gut-liver axis in alcoholic liver disease. *Gastroenterology* 148, 30–36. doi:10.1053/j.gastro.2014.10.042

Tripathi, A., Debelius, J., Brenner, D. A., Karin, M., Loomba, R., Schnabl, B., et al. (2018). The gut-liver axis and the intersection with the microbiome. *Nat. Rev. Gastroenterol. Hepatol.* 15, 397–411. doi:10.1038/s41575-018-0011-z

Tuoi Do, T. H., Gaboriau, F., Ropert, M., Moirand, R., Cannie, I., Brissot, P., et al. (2011). Ethanol effect on cell proliferation in the human hepatoma HepaRG cell line: relationship with iron metabolism. *Alcohol Clin. Exp. Res.* 35, 408–419. doi:10.1111/j.1530-0277.2010.01358.x

Van Der Sluis, M., De Koning, B. A. E., De Bruijn, A. C. J. M., Velcich, A., Meijerink, J. P. P., Van Goudoever, J. B., et al. (2006). Muc2-deficient mice spontaneously develop colitis, indicating that MUC2 is critical for colonic protection. *Gastroenterology* 131, 117–129. doi:10.1053/j.gastro.2006.04.020

Ventura-Cots, M., Watts, A. E., and Bataller, R. (2017). Binge drinking as a risk factor for advanced alcoholic liver disease. *Liver Int.* 37, 1281–1283. doi:10.1111/liv.13482

Wagnerberger, S., Fiederlein, L., Kanuri, G., Stahl, C., Millonig, G., Mueller, S., et al. (2013). Sex-specific differences in the development of acute alcohol-induced liver steatosis in mice. *Alcohol Alcohol.* 48, 648–656. doi:10.1093/alcalc/agt138

Wang, Y., Tong, J., Chang, B., Wang, B., Zhang, D., and Wang, B. (2014). Effects of alcohol on intestinal epithelial barrier permeability and expression of tight junction-associated proteins. *Mol. Med. Rep.* 9, 2352–2356. doi:10.3892/mmr.2014.2126

Yun, J.-W., Son, M.-J., Abdelmegeed, M. A., Banerjee, A., Morgan, T. R., Yoo, S.-H., et al. (2014). Binge alcohol promotes hypoxic liver injury through a CYP2E1-HIF-1α-dependent apoptosis pathway in mice and humans. *Free Radic. Biol. Med.* 77, 183–194. doi:10.1016/j.freeradbiomed.2014.08.030

Conflict of Interest: The authors declare that the research was conducted in the absence of any commercial or financial relationships that could be construed as a potential conflict of interest.

Copyright © 2020 Lamas-Paz, Morán, Peng, Salinas, López-Alcántara, Sydor, Vilchez-Vargas, Asensio, Hao, Zheng, Martín-Adrados, Moreno, Cogolludo, Gómez del Moral, Bechmann, Martínez-Naves, Vaquero, Bañares, Nevzorova and Cubero. This is an open-access article distributed under the terms of the Creative Commons Attribution License (CC BY). The use, distribution or reproduction in other forums is permitted, provided the original author(s) and the copyright owner(s) are credited and that the original publication in this journal is cited, in accordance with accepted academic practice. No use, distribution or reproduction is permitted which does not comply with these terms.

frontiers in Pharmacology

ORIGINAL RESEARCH
published: 28 January 2021
doi: 10.3389/fphar.2020.621538

Carveol a Naturally-Derived Potent and Emerging Nrf2 Activator Protects Against Acetaminophen-Induced Hepatotoxicity

Zaif Ur Rahman[1,2], Lina Tariq Al Kury[3], Abdullah Alattar[4], Zhen Tan[1], Reem Alshaman[4], Imran Malik[5], Haroon Badshah[2], Zia Uddin[6], Atif Ali Khan Khalil[7], Naveed Muhammad[2], Saifullah Khan[8], Amjad Ali[9], Fawad Ali Shah[5], Jing Bo Li[1]* and Shupeng Li[10]**

[1]Shenzhen University Clinical Research Center for Neurological Diseases, Health Management Center, Shenzhen University General Hospital, Shenzhen University Clinical Medical Academy, Shenzhen University, Shenzhen, China, [2]Department of Pharmacy, Abdul Wali Khan University, Khyber Pakhtunkhwa, Pakistan, [3]College of Natural and Health Sciences, Zayed University, Abu Dhabi, United Arab Emirates, [4]Department of Pharmacology and Toxicology, Faculty of Pharmacy, University of Tabuk, Tabuk, Saudi Arabia, [5]Riphah Institute of Pharmaceutical Sciences, Riphah International University, Islamabad, Pakistan, [6]Department of Pharmacy, COMSATS University Islamabad, Abbottabad Campus, Abbottabad, Pakistan, [7]Department of Biological Sciences, National University of Medical Sciences, Rawalpindi, Pakistan, [8]Department of Microbiology and Biotechnology, Abasyn University Peshawar, Khyber Pakhtunkhwa, Pakistan, [9]Department of Botany, University of Malakand, Khyber Pakhtunkhwa, Pakistan, [10]State Key Laboratory of Oncogenomics, School of Chemical Biology and Biotechnology, Shenzhen Graduate School, Peking University, Shenzhen, China

OPEN ACCESS

Edited by:
Ralf Weiskirchen, RWTH Aachen University, Germany

Reviewed by:
Kala Kumar Bharani, P. V. Narsimha Rao Telangana Veterinary University, India
Wei Chen, Stanford University, United States

***Correspondence:**
Fawad Ali Shah
fawad.shah@riphah.edu
Shupeng Li
lisp@pkusz.edu.cn
Jing Bo Li
lijb_003@163.com

Specialty section:
This article was submitted to Gastrointestinal and Hepatic Pharmacology, a section of the journal Frontiers in Pharmacology

Received: *26 October 2020*
Accepted: *23 December 2020*
Published: *28 January 2021*

Citation:
Rahman ZU, Al Kury LT, Alattar A, Tan Z, Alshaman R, Malik I, Badshah H, Uddin Z, Khan Khalil AA, Muhammad N, Khan S, Ali A, Shah FA, Li JB and Li S (2021) Carveol a Naturally-Derived Potent and Emerging Nrf2 Activator Protects Against Acetaminophen-Induced Hepatotoxicity. Front. Pharmacol. 11:621538. doi: 10.3389/fphar.2020.621538

Acetaminophen (N-acetyl p-aminophenol or APAP) is used worldwide for its antipyretic and anti-inflammatory potential. However, APAP overdose sometimes causes severe liver damage. In this study, we elucidated the protective effects of carveol in liver injury, using molecular and *in silico* approaches. Male BALB/c mice were divided into two experimental cohorts, to identify the best dose and to further assess the role of carveol in the nuclear factor E2-related factor; nuclear factor erythroid 2; p45-related factor 2 (Nrf2) pathway. The results demonstrated that carveol significantly modulated the detrimental effects of APAP by boosting endogenous antioxidant mechanisms, such as nuclear translocation of Nrf2 gene, a master regulator of the downstream antioxidant machinery. Furthermore, an inhibitor of Nrf2, called all-trans retinoic acid (ATRA), was used, which exaggerated APAP toxicity, in addition to abrogating the protective effects of carveol; this effect was accompanied by overexpression of inflammatory mediators and liver = 2ltoxicity biomarkers. To further support our notion, we performed virtual docking of carveol with Nrf2-keap1 target, and the resultant drug-protein interactions validated the *in vivo* findings. Together, our findings suggest that carveol could activate the endogenous master antioxidant Nrf2, which further regulates the expression of downstream antioxidants, eventually ameliorating the APAP-induced inflammation and oxidative stress.

Keywords: acetaminophen, carveol, hepatotoxicity, anti-inflammatory, Nrf2 pathway

INTRODUCTION

Liver diseases are associated with an increased number of disability cases, and approximately 50 million liver-associated morbidity and mortality reports are documented each year (Gorrell, 2005). Because of the persistent and continuous involvement of the liver in metabolic processes, the accumulation of free radicals overwhelms the natural defense system, making the liver one of the

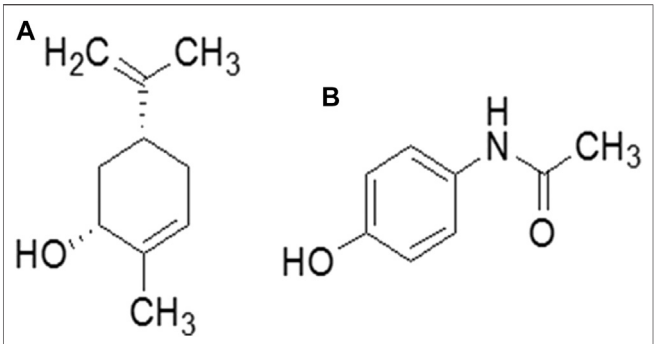


Figure 1 | Chemical structure of **(A)** carveol and **(B)** paracetamol.

most vulnerable organ. These free radicals are the prominent cause of oxidative stress-induced thiol depletion and lipid peroxidation, which subsequently trigger toxic cascading events and eventually lead to various hepatic pathologies, such as cirrhosis and acute or chronic hepatitis (Abo-Haded et al., 2017).

Paracetamol (acetaminophen, N-acetyl p-aminophenol, or APAP) is a non-prescription drug with both analgesic and antipyretic activities, and this drug is included in several preparations, either as a single moiety or in combination (Ghaffar and Tadvi, 2014). It has a large therapeutic window and is generally safe; however, when abused in large doses, it leads to severe hepatic necrosis and hepatic failure (Al-Fartosi et al., 2011). Currently, paracetamol is considered the chief causative agent of acute liver failure due to accidental overdose, which requires a liver transplant in some extreme cases (Gopal et al., 2011; Du et al., 2016). At a high dose, APAP is metabolized to glucuronic acid or sulfate conjugates (Sharma et al., 2016) and is transformed into the pro-reactive cytotoxic intermediate N-acetyl-phenzoquinoneimine (NAPQI), which is responsible for oxidative stress and intracellular glutathione (GSH) depletion (Shah et al., 2014; Hellerbrand et al., 2017; Zai et al., 2018). The covalent binding of NAPQI to mitochondria initiates cascading pathological processes, such as free radical formation and peroxynitrite accumulation, further supplemented by the release of pro-inflammatory cytokines and mediators, all of which collectively exacerbate acute and chronic liver necrosis (Dalaklioglu et al., 2013; Hennig et al., 2018). Various hepatoprotective strategies have been evaluated to protect the liver from toxins. The current clinical practice recommends silymarin as a hepatoprotective supplement to cope with various liver insults, including APAP and methotrexate (MTX) (Crowell et al., 1992). The transcription factor Nrf2 is an integral part of the host cellular defense mechanism against oxidative stress and electrophilic insult. Nrf2 binds to antioxidant response elements (ARE) at the promoter site, which in turn encodes several antioxidant/phase-II detoxifying enzymes and other relevant stress-responding factors (Thompson Coon and Ernst, 2002). Previous studies have revealed the involvement of Nrf2-ARE signaling in attenuating inflammation in several pathologies, such as stroke, and other disorders (Ma and He, 2012; Ning et al., 2018). Hence, dysregulation of Nrf2 signaling results in increased susceptibility to oxidative stress and inflammatory damage. Previous studies have demonstrated that Nrf2 plays a critical role in the regulation of inflammation and oxidative stress, which are linked to the pathophysiologies of several diseases. Therefore, Nrf2 can be considered a potential pharmacological target to be investigated against various insults, including APAP.

Natural drug moieties are an attractive source of new drugs, owing to their rich antioxidant potential. Several natural drugs have hepatoprotective potential against a variety of mediators, including free radicals and inflammatory factors (James et al., 2003; Lee et al., 2006). Carveol, a monoterpene phenol, is isolated from the essential oils extracted from the plant family *Lamiaceae* or *Labiatae*, which includes the genera *Thymbra*, *Origanum*, *Corydothymus*, *Satureja*, and *Thymus* (**Figure 1**) (Pastore et al., 2003). It has long been used in traditional Chinese medicine as an antispasmodic, a carminative, and an astringent (Aleksunes et al., 2008) and has been evaluated in the treatment of indigestion and dyspepsia (Guo and White, 2016). Carveol has been demonstrated to have antioxidative, antihyperlipidemic, and anti-inflammatory activities, and ameliorate liver toxicity in a mouse model of carbon tetrachloride (Patterson et al., 2013). However, to date, the potential hepatoprotective effects of carveol against APAP have not been evaluated. Taking into consideration the pharmacological value of essential oils extracted from plant sources and the significance of new drug discovery, the current study sought to investigate whether carveol mitigates APAP-induced detrimental effects. If so, the potential underlying molecular and cellular mechanisms should be further delineated to explain the effects of carveol on hepatocellular protection. This will not only expand the understanding of the molecular cascading mechanism of cell death but will also provide some clues to unveil the therapeutic potential of carveol.

MATERIALS AND METHODS

Chemicals and Reagents

The pharmaceutical drugs (silymarin and N-acetyl para aminophenol (paracetamol CAS: 103-90-2, C8H9NO2: APAP) of HPLC grade (99%) were supplied by a local pharmaceutical manufacturer and used as raw material. All the antibodies were procured from Santa Cruz Biotechnology, United States, or Abcam, United Kingdom. Phosphate-buffered saline (PBS) tablets were used for all morphological analyses or fresh buffers were prepared for each use. The details and corresponding catalog numbers of the primary antibodies are HO-1 (SC-13691), TRX (SC-20146), Nrf2 (SC-722), COX-2 (SC-514489), p-JNK (SC-6254), TNF-α (SC-52B83), and p-NFκB (SC-271908). Other immunohistochemistry-related consumables, such as AB and C Elite kit (two vials-SC-2018) and 3,3-diaminobenzidine (DAB) (SC-216567), were also provided by Santa Cruz Biotechnology, United States. The biotin secondary antibody (ab-6789) and DPX mounting media were purchased from Abcam United Kingdom. The p-NFκB enzyme-linked immunosorbent assay (ELISA) kit (Cat # SU-B28069) and Nrf2 kit (cat. no. SU-B30429) were purchased

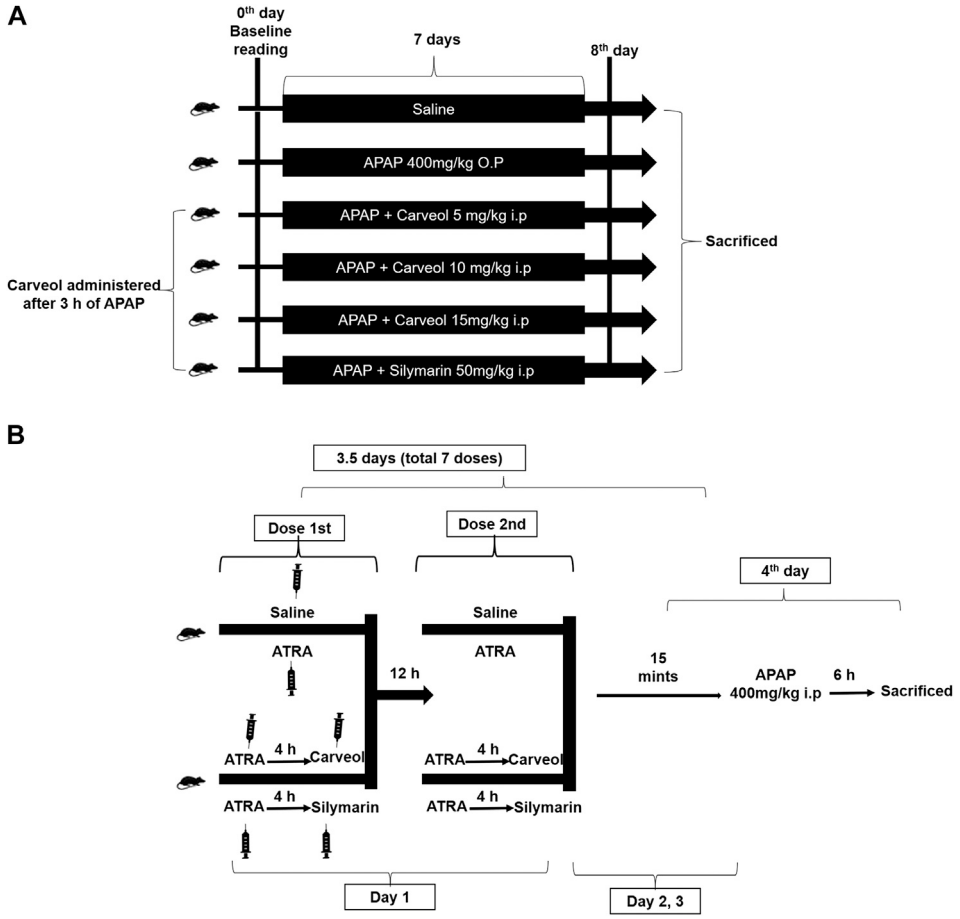


Figure 2 | Experimental design 1 **(A)**. Carveol, APAP, and silymarin were prepared in 0.9% NaCl, while ATRA was prepared in a mixture of 2% dimethyl sulfoxide and 0.9% NaCl (n = 10/group). Baseline reading was recorded at the beginning (0th day of the experiment), and mean weight and food intake were monitored during the entire experiment **(B)** Diagrammatic illustration of *in vivo* study for the Nrf2 signaling pathway. The treatment protocol was continued for 3.5 days. In all these groups, a single loading dose of paracetamol was injected (400 mg/kg, i. p.) 15 min after the last dose of ATRA or carveol or silymarin, except in the saline group. Serum samples and liver tissues were collected after 6 h of the last dose.

from Shanghai Yuchun Biotechnology, China. HO-1 (cat. No. E-EL-R0488), and TNF-α (E-EL-R0019) ELISA kits were purchased from Elabscience.

Animals and Drug Treatment

Male BLAB/c mice, weighing 30–35 g and 8–10 weeks old, were housed (three per cage) at the facility of the Riphah Institute of Pharmaceutical Sciences (RIPS), under-documented protocols (temperature: 22 ± 1 °C; humidity: 50 ± 10%). Strict laboratory protocols were followed during all experimental procedures. The animals were kept for some days at the facility before the experimental procedures, and the body weights were constantly checked every day throughout the study. Furthermore, we strictly followed the approved protocols and guidelines of the institutional research ethical committee (REC) of the Riphah Institute of Pharmaceutical Sciences (RIPS), Islamabad (Approval ID: Ref. No. REC/RIPS/2018-19/A202), which are similar to the ARRIVE guidelines, with some minor exemptions. We adopted the human endpoint criteria for euthanizing the mice if they displayed a severe sign of distress or suffering. The mice were subjected to the following experimental protocols. Two separate cohorts of animals were used for the experiments as follows:

Experimental Cohort 1

The mice treatment protocol is indicated in **Figure 2A**, and the following groups were employed. 1) Saline group: the mice received saline (0.9% NaCl) injection intraperitoneally (i. p.) for seven consecutive days, 2) APAP group: the mice received a single dose of paracetamol orally/per os (400 mg/kg, p. o.) for 7 days, 3) Three different groups of APAP + carveol: the mice received paracetamol orally for seven consecutive days, followed by a single i. p. injection of different doses of carveol, namely APAP + carveol 5 mg (5 mg/kg, i. p.); APAP + carveol 10 mg (10 mg/kg, i. p.); APAP + carveol 15 mg (15 mg/kg, i. p.), 4) APAP + silymarin group: the mice received paracetamol orally for seven consecutive days, followed by silymarin (50 mg/kg, i.p). Carveol, APAP, and silymarin were prepared in 0.9% NaCl (n = 14 per/group). At the

end of the experiment, the mice were anesthetized with xylazine and ketamine (i. p.); blood was collected via cardiac puncture and was processed for biochemical analysis. Samples from the liver were taken and frozen at −50 °C or preserved in 4% paraformaldehyde for ELISA or paraffin sectioning, respectively. Next, 4 μm thin hepatic tissue sections were made with a rotary microtome from the paraffin block, for histological analysis. Overall, three mice died during the experimental procedures, two from APAP and one from the Carveol + APAP groups, which we excluded from the experiment. The saline-treated mice survived throughout the experiments.

Experimental Cohort 2

The mice treatment protocol is indicated in **Figure 2B**, and the following groups were employed with $n = 10$/gp. 1) Saline group: the mice received saline (i. p.), 2) APAP + ATRA group: the mice received seven injections of ATRA (10 mg/kg, i. p.) at 12 h intervals, 3) APAP + ATRA + Carveol group: the mice received carveol 15 mg/kg i.p 4 h after each ATRA dose, and 4) APAP + ATRA + silymarin group: the mice received silymarin 50 mg/kg i.p 4 h after each ATRA dose. For all the groups except saline, APAP 400 mg/kg was administered (i. p.) 15 min after the last dose of ATRA (APAP + ATRA group) or carveol (APAP + ATRA + carveol) or silymarin (APAP + ATRA + silymarin). At the end of the treatment, the mice were sacrificed and samples were collected.

Hematoxylin and Eosin (H and E) Staining

Hematoxylin and eosin staining was performed according to our previous protocols (Ali et al., 2019; Ansari et al., 2019; Ullah et al., 2020). Briefly, the non-coated slides initially underwent a deparaffinization step with xylene, followed by hydration (graded ethanolic series), and finally with water. The slides were incubated in a Coplin jar containing hematoxylin to stain the nucleus. The slides were washed with water and traced for nuclear staining, using a compound microscope. The slides were then dipped in 1% HCl, 1% ammonia water, and rinsed with water. Eosin staining was then performed, the slides were subjected to dehydration, fixed in xylene, and covered with coverslips. Five images per slide were obtained using a light microscope (Olympus, Japan) at the same threshold intensity, and were later analyzed using ImageJ software to quantify the number of distorted, vacuolated, infiltrated, and surviving cells.

Liver Functional Biomarkers

Enzymes, such as AST, ALT, phosphatases, and total bilirubin (TB), were spectroscopically analyzed using an autoanalyzer (Olympus AU-2700) according to the manufacturer's instructions.

Oxidative Enzyme Analysis and Lipid Peroxidation

The non-enzymatic glutathione (GSH) level and the enzymatic glutathione S-transferase (GST) activity were determined as previously described (Ullah et al., 2020). After homogenizing liver tissue samples (cohort 1), the supernatant was collected. For the assay, the stock of 0.2 M sodium phosphate buffer was prepared as $Na_2HPO_4.2H_2O$ and NaH_2PO_4 (pH 8). For sample loading, buffer (153 μL), freshly prepared 1 mmol DTNB (40 μL), and the supernatant (6.6 μL) were sequentially mixed, and after 15 min, the absorbance of this mixture was determined using a spectrophotometer at 412 nm. A mixture of DTNB solution and phosphate buffer served as the control, whereas the buffer was used as a blank. The absorbance was calculated from the values of the absorbance of the control and the sample and expressed as μmol/mg protein. To detect GST activity (Imran et al., 2020), the stock of 0.1 M potassium phosphate buffer was prepared as $KHPO_4$ and KH_2PO_4 (at a 1:2 ratio, pH 6.5). For the assay, 1 mmol GST and 1 mmol CDNB were also prepared; then GST solution, CDNB, potassium buffer, and tissue homogenate were mixed (at a 1:1:27:1 ratio) and the optical density was determined at 340 nm. The phosphate buffer was used as a blank, and the assay mixture without homogenate was used as a control. GST activity was calculated using the extinction coefficient of the product and expressed as nmoles of CDNB conjugated/min/mg protein.

Determination of Lipid Peroxidation (LPO) in Tissue

Oxidative stress augmented the oxidation of macromolecules, such as lipids, which can be quantified by the thiobarbituric acid reactive substance (TBARS) levels. A previously reported protocol was adopted for the LPO assay, with minor changes (Imran et al., 2020). Approximately 40 μL of tissue supernatant was added to a freshly prepared solution of ferric ammonium sulfate and incubated for some time. Next, after the addition of 75 μL of thiobarbituric acid (TBA) to the mixture, the color changed, and the absorbance of the resultant mixture was immediately measured using a microplate reader (at 532 nm). The levels were expressed as nmol Tbras/min/mg protein (Iqbal et al., 2020).

Immunohistochemical Analysis

We used coated slides for immunohistochemical studies as described in a previous study (Rana et al., 2020). The slides were subjected to deparaffinization and hydration protocols as discussed for H and E. To unlock the antigenic epitopes from paraformaldehyde, proteinase K was applied to the tissue, followed by PBS rinsing. After hydration, the slides were not allowed to dry at any stage of the immunohistochemical analysis. Before blocking with normal goat serum the slides were treated with H_2O_2 to eradicate peroxidase activity. The selectivity of serum depends upon the source of the secondary antibody. After blocking for an appropriate time, primary antibodies, such as nuclear factor-κB (p-NFκB), COX2, c-Jun N-terminal kinase (p-JNK), HO-1, TNF-α, and Nrf2 (dilution 1:100, Santa Cruz Biotechnology), were applied overnight in a moistened box in the refrigerator. The following morning, the slides were removed and kept for 1 h at room temperature in a moistened chamber. After rinsing with PBS, the biotinylated secondary antibody (goat anti-mouse and goat anti-rabbit) was applied, followed by the application of ABC reagent (SCBT United States) in a

humidified chamber, and the slides were rinsed with PBS and stained with DAB. The slides were then dried, dehydrated in ascending ethanolic series, fixed in xylene, and covered with coverslips. The liver positive cells for all the primary antibodies were quantified using the ImageJ software.

Enzyme-Linked Immunosorbent Assay (ELISA)

p-NFκB, HO-1, Nrf2, and TNF-α levels were quantified using an ELISA kit as per the manufacturer's instructions (for detailed chemicals and reagents). Approximately 50 mg of the tissue sample was homogenized, using PBS (also containing PMSF as a serine inhibitor), at 15,000 RPM, followed by centrifugation and collection of the supernatant. Protein concentration in each homogenate was calculated using the BCA kit (Thermo Fisher), and the resultant protein concentration was added to each well to determine the level of the respective proteins, using an ELISA reader. The resultant picograms of cytokines per milliliter (pg/ml) were then converted pg/mg total protein).

Real-Time Polymerase Chain Reaction (RT-PCR)

Total RNA was extracted from the freshly isolated liver of mice in experimental duplicates using the TRIzol method. 20 µL of M-MuLV reverse transcriptase was used to dilute 1 µg of RNA and used this mix to synthesize cDNA with a cDNA synthesis kit (vivantis cDSK01-050 Sdn. Bhd, Malaysia). To estimate the gene expression of Nrf2 quantitatively, real-time PCR was performed using the 2X HOT SYBR Green qPCR master mix (Solar Bio cat # SR1110) and real-time Mic PCR (BioMolecular System) according to the manufacturer specifications. The sequence of the primers used for amplification was Nrf2 Forward: CCATTT ACGGAGACCCACCGCCTG and Reverse: CTCGTGTGAGAT GAGCCTCTAAGCGG and GAPDH, Forward: AGGTCGGTG TGAACGGATTTG and Reverse: TGTAGACCATGTAGTTGA GGTCA (Wakabayashi et al., 2014). The relative gene expressions of Nrf2 was determined by the 2ˆ−ΔΔCT method for real-time quantitative PCR.

Bioinformatic Studies

In silico studies were performed as previously described (Shah and Rashid, 2020). Briefly, the 3-dimensional structures of cyclooxygenase (COX2) PDB ID: IPXX, interleukin (IL-1β) PDB ID: 2MIB, PDB ID: 2TNF for TNF-α, PDB ID: 3TTI for JNK, PDB ID: ILE5 for nuclear factor-kB (NFκB), PDB ID: 1DVE for HO-1, and PDB ID: 2LZ1 for Nrf2 were downloaded from the RCSB protein data bank in Discovery Studio (DSV). Docking studies require PDB and mol2 format, for which the 3D structure of the proteins and ligand carveol were downloaded in the respective format. Both protein and ligand were loaded into the PyRx docking software, and drug-receptor interactions were evaluated by binding the energy values (E-value). The E-values further validated the best pose of the ligand in the complex, and by DSV, the best orientation and interaction were prepared and analyzed. The structure of carveol was collected from online sources.

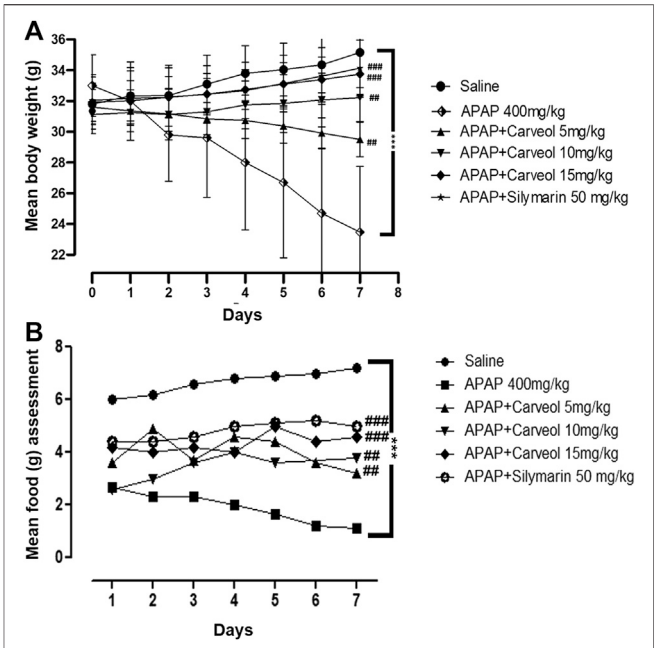


Figure 3 | Effect of carveol treatment on physical parameters, such as body weight and food intake. **(A)** Bodyweight changes **(B)** Mean food intake. The number of animals was 14/group, and the results were analyzed using a repeated two-way ANOVA test. ###$p < 0.001$, ##$p < 0.01$ compared to the APAP group, ***$p < 0.001$, compared to the saline group.

Statistical Analysis

The symbols ∗, #, $, and β were used to indicate a significant difference. * or β indicates differences compared to saline, while # to APAP and $ represents a significant difference to APAP + ATRA. All the data are expressed as mean ± SEM, and ImageJ software was used to analyze all the histological data (ImageJ 1.30; https://imagej.nih.gov/ij/). Bodyweight and food intake data were analyzed using a repeated two-way ANOVA, and the remaining data were analyzed using one-way ANOVA with Tukey's multiple comparison test as a post-hoc test.

RESULTS

Results of Experimental Design one

Effect of Carveol on Body Weight and Food Intake

Our results showed that APAP induced a dramatic and persistent loss of body weight. However, carveol prevented body weight loss in a dose-dependent manner (**Figure 3A**). Carveol, at 15 mg/kg per day, showed the most significant effect on body weight ($p < 0.001$). Bodyweight reduction could be attributed to decreased food intake, as APAP-treated mice consumed significantly less amount of food; however, carveol ameliorated this effect in a dose-dependent manner, which is comparable to that of silymarin (50 mg/kg) (**Figure 3B**, $p < 0.001$).

TABLE 1 | The protective effect of carveol on liver functional enzymes: APAP augmented the serum level of LFTs and attenuated high-density lipoprotein (HDL) level, while carveol, with respect to APAP, mitigated LFT levels and increased HDL levels.

Treatment	ALT (U/L)	AST (U/L)	TP (g/dl)	TB (mg/dl)	ALP (U/L)	Albumin (g/dl)	LDL (mg/dl)	HDL (mg/dl)
Saline	59 ± 8.71	106 ± 13.89	7.8 ± 0.30	0.33 ± 0.18	98.66 ± 15.53	4.93 ± 0.65	39 ± 5.56	78.66 ± 8.02
APAP 400 mg/kg	194.66 ± 6.02***	276.66 ± 27.02***	3.53 ± 0.40***	2.16 ± 0.30***	220.33 ± 49.44***	2.23 ± 0.30***	102.66 ± 13.05***	37.66 ± 2.51***
APAP + Carveol 5 mg/kg	164.66 ± 10.69	269.33 ± 81.5	5.7 ± 0.45##	1.23 ± .37##	177 ± 11.78	3.5 ± 36	78.66 ± 17.4	41.66 ± 3.05
APAP + Carveol 10 mg/kg	148.33 ± 11.37#	258.66 ± 36.67	5.53 ± 1.19##	1.03 ± .20##	136.66 ± 3.05##	4.23 ± .41#	64 ± 21#	52.66 ± 6.5#
APAP + Carveol 15 mg/kg	95.33 ± 7.37###	172.33 ± 14.7##	6.6 ± 0.55###	0.525 ± 0.03###	122.66 ± 8.50###	4.5 ± 0.36##	65.66 ± 17.67##	64.66 ± 7.76##
APAP + Silymarin 50 mg/kg	81.33 ± 8.50###	138.66 ± 14.22##	6.16 ± 0.40###	0.67 ± 0.29###	130 ± 16.70###	5.93 ± 0.85##	51.33 ± 9.29##	52.33 ± 2.08#

*The data are presented as means ± SEM and were analyzed using one-way ANOVA with n = 7/group. The symbols *** and ### represent $p < 0.001$ and the symbol ## represents $p < 0.01$ values of significant differences. The samples were processed from cohort 1.*

TABLE 2 | Effect of carveol on oxidative enzymes.

Treatment	GSH (μmol/mg protein)	GST (nmoles of CDNS conjugated/min/mg protein)	TBARS (nmoles Tbras/min/mg protien)
Saline	74.88 ± 13.78	25.42 ± 1.30	79.32 ± 0.70
APAP 400 mg/kg	6.30 ± 4.97***	1.78 ± 1.50***	215.58 ± 5.82***
APA + Carveol 5 mg/kg	44.4 ± 9.26#	4.67 ± 0.91	192.54 ± 2.80
APA + Carveol 10 mg/kg	54.49 ± 9.98##	8.83 ± 1.62#	167.78 ± 2.164#
APA + Carveol 15 mg/kg	62.29 ± 18.82###	14.2 ± 1.43##	131.74 ± 0.64##
APAP + Silymarin 50 mg/kg	66.68 ± 11.45###	18.20 ± 2.31##	115.83 ± 2.164##

*The symbols *** and ### represent $p < 0.001$, while the symbol ## or # represents $p < 0.01$ and $p < 0.05$, n = 7/group. The data are expressed as mean ± SEM and were analyzed using one-way ANOVA followed by Tukey's multiple comparison test. The samples were processed from cohort 1.*

Carveol Improved the Liver Detriments of APAP

Table 1 shows that APAP significantly disturbed the functional markers ($p < 0.001$), while carveol at different doses normalized the values in the APAP-administered group; carveol at 15 mg exhibited similar effects as those of silymarin.

Carveol Alleviated the Liver Metabolic Deficits Induced by APAP

The liver plays a principal role in the synthesis, storage, secretion, and catabolism of proteins, bilirubin, lipoproteins, and lipids, which represent sensitive markers during liver damage. Our results showed a significant increase in the levels of total protein (TP), albumin, and HDL, accompanied by decreased total bilirubin (TB) and low-density lipoprotein levels (**Table 1**). These results suggest that liver anabolic and catabolic functions were both severely hampered. Moreover, carveol showed a dose-dependent protective effect, which was comparable to the effects of silymarin at a dose of 15 mg/kg. Furthermore, the effect of carveol on HDL levels was more significant ($p < 0.01$) than that of the silymarin-treated group ($p < 0.05$).

Effects of Carveol on Antioxidant Enzymes

Table 2 summarizes the effects of carveol on changes in endogenous enzyme activities, following APAP treatment. APAP stimulated GSH depletion (6.30 ± 4.97), and antioxidant enzyme glutathione-S-transferase (GST) (1.78 ± 1.50) in the hepatic tissue ($p < 0.001$). Treatment with carveol at different doses attenuated the downregulation of GSH (62.29 ± 8.82) and GST (14.2 ± 1.43).

Effect of Carveol on LPO

The LPO content in the liver homogenate of the APAP group was increased to 215.58 ± 5.82, compared to that in the saline group ($p < 0.001$, **Table 2**). Carveol at 15 mg/kg dose significantly ($p < 0.01$, **Table 2**) attenuated this content (131.74 ± 0.64), an effect that could be matched to that of the silymarin group.

Carveol Protected the Liver From APAP-Induced Cellular Damage

The results of H and E staining revealed significant histopathological changes in the APAP-intoxicated animals (**Figure 4**, ###$p < 0.001$). Significant alterations were observed in the APAP group, compared to those in the saline-treated

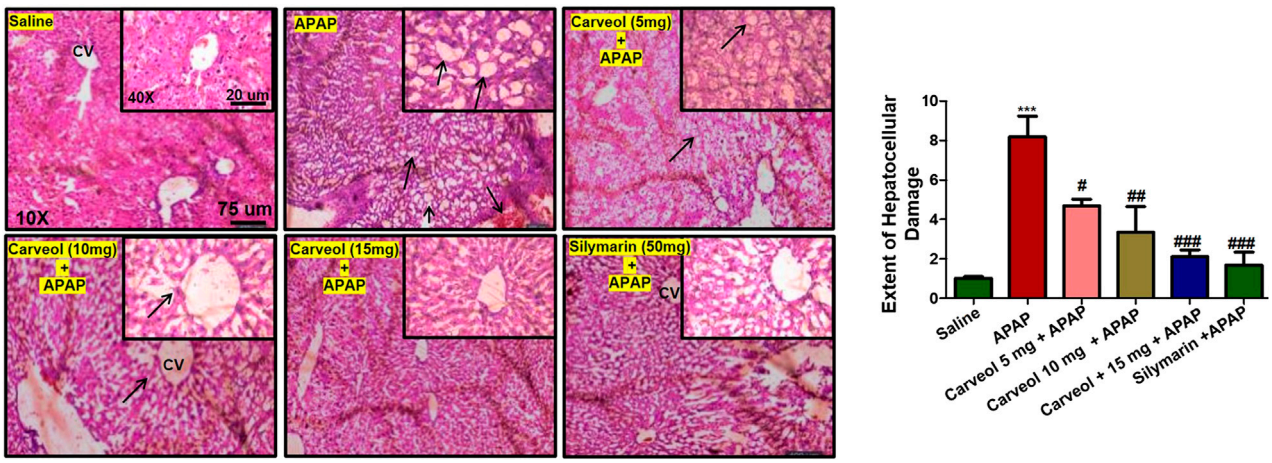


Figure 4 | Carveol restored the morphological integrity of the liver, as shown by histological examination. Liver tissue was stained with H and E (magnification, ×10 scale bar 75 μm and 40× scale bar 20 μm). The data are presented as means ± SEM and were analyzed using one-way ANOVA followed by Tukey's multiple comparison test; $n = 7$/group. The symbols *** and ### represent significant difference values of $p < 0.001$, and ## or # represent significant difference values of $p < 0.01$ or $p < 0.05$ respectively. The slides were processed from cohort 1.

TABLE 3 | Effect of carveol on histopathological scoring.

Groups	Hepatocytes necrosis	Inflammatory cells infiltration	Fatty degeneration/vacuolization
Saline	—	—	—
APAP 400 mg/kg	+++	+++	+++
APA + Carveol 5 mg/kg	+++	++	++
APA + Carveol 10 mg/kg	+	+	+
APA + Carveol 15 mg/kg	—	—	±
APAP + Silymarin 50 mg/kg	—	—	±

+++ significant, ++ high, + moderate, —nil.

animals. The saline group showed normal hepatic cell shape, and there was no vacuolization or lipid globule. Nevertheless, many aberrant morphological features, such as sinusoidal dilatation, hepatocyte degeneration with loss of lobular architecture/ hepatocyte disarray, pericentral lymphocytic infiltration, moderate steatosis/fatty degeneration, and abundant inflammatory cell infiltration, were observed in the APAP-treated groups (**Table 3**). Carveol treatment significantly reversed these histopathological abnormalities induced by APAP, in a dose-dependent manner, as revealed by the microscopic scores (Carveol histopathological score).

Effect of Carveol on APAP-Mediated Inflammatory Markers

The JNK signaling pathway mediates the stress-induced inflammatory cascade and is implicated in mitochondrial apoptosis, and its activation results in the phosphorylation of numerous transcription factors, such as AP-1, p53, Bax, and Bim. Furthermore, JNK can trigger other mediators, such as TNF-α, p-NFκB, and COX-2 (Ali A et al., 2020). To reveal the possible involvement of JNK and TNF-α, immunohistochemical staining was performed, and the results showed higher expression of these mediators in the APAP-administered group ($p < 0.001$) (**Figures 5A,B**), whereas carveol dose at 15 mg significantly reduced their hyperexpression ($p < 0.01$, **Figure 5A**, $p < 0.001$, **Figure 5B**). Moreover, COX-2 and p-NFκB expression were also evaluated, and the results showed that both were highly expressed in the APAP group ($p < 0.001$, **Figures 5C,D**). Carveol attenuated the expression of p-NFκB and TNF-α in a dose-dependent manner.

Effect of Carveol on the Nrf2 Signaling Pathway

To examine the possible effect of carveol on the Nrf2 signaling pathway, the expression of Nrf2, HO-1, and TRX was determined via immunohistochemistry (**Figure 6**). APAP activated the expression of Nrf2 (**Figure 6A**) and TRX ($p < 0.05$, **Figure 6C**) due to oxidative stress, and carveol, at 15 mg/kg, further expressed these antioxidative proteins to counteract oxidative stress ($p < 0.001$, **Figure 6A**, $p < 0.01$, **Figure 6C**). HO-1 and thioredoxin TRX exhibit similar characteristics, as both are antioxidants and eradicate reactive oxygen species, thereby protecting the cell from inflammation and apoptosis (Shah et al., 2018; Li and Liu, 2019). The effect of carveol on the thioredoxin protein level was evaluated in different

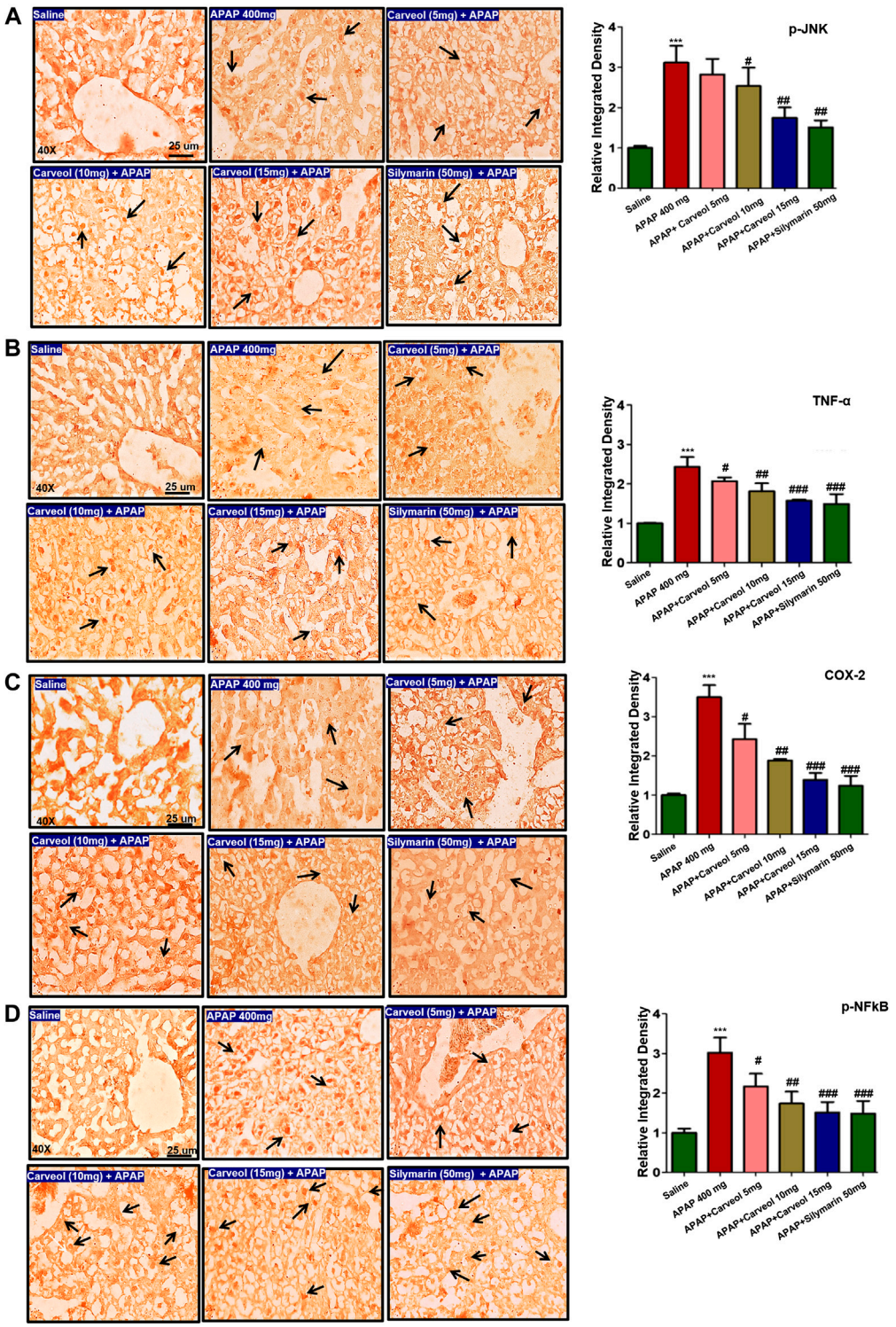


Figure 5 | Effect of carveol on inflammatory mediators. The presented images indicate immunoreactivity of **(A)** p-JNK **(B)** TNF-α **(C)** COX-2, and **(D)** p-NFκB. Scale bar = 25 μm, magnification ×40 with n = 7/group. The data presented are relative to saline and the number of experiments performed = 3. The data are presented as means ± SEM and were analyzed using one-way ANOVA followed by Tukey's multiple comparison test. The symbols *** and ### represent significant difference values of $p < 0.001$, while the symbol ## represent $p < 0.01$ values for significant differences and # represents $p < 0.05$. The slides were processed from cohort 1.

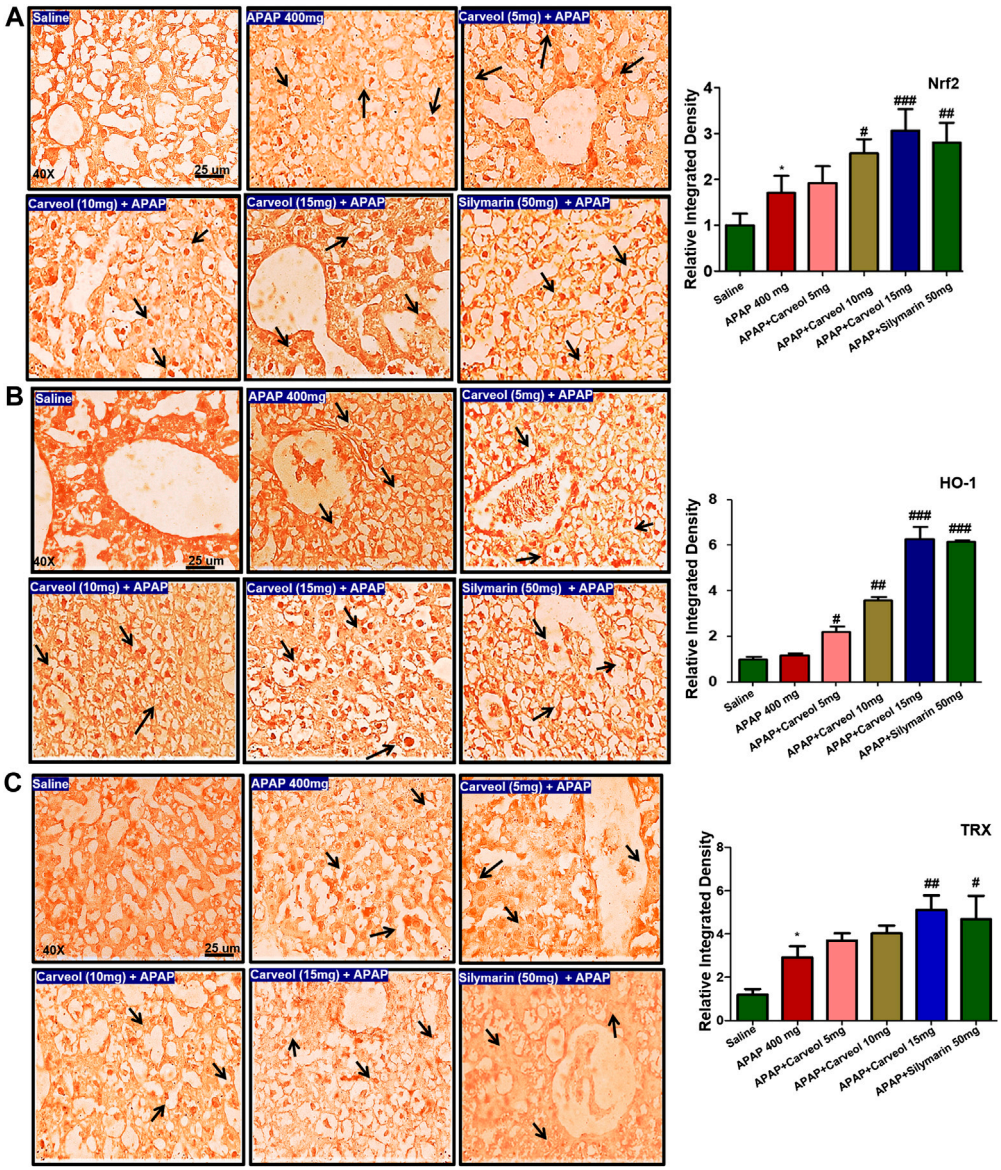


Figure 6 | Effect of carveol on immunohistochemistry expression **(A)** Nrf2 **(B)** HO-1, and **(C)** TRX with magnification ×40, and scale bar = 25 μm, *n* = 7/group. Representative histograms indicate a comparatively lower expression of **(A)** Nrf2 **(B)** HO-1, and **(C)** TRX in the APAP group than the carveol group. The data are presented as means ± SEM and were analyzed using one-way ANOVA followed by Tukey's multiple comparison test. The symbols ### represent significant difference values of $p < 0.001$, while the symbol ## represents $p < 0.01$ values of significant differences, and ∗ or # represents $p < 0.05$. # is significantly different from APAP.

experimental groups. Representative images and densitometric analysis are shown in **Figure 6**.

Results of Experimental Design 2

Carveol Enhances the Antioxidant Capacity of the Liver via the Nrf2 Signaling Pathway

To further investigate whether the antioxidative effects of carveol against APAP-induced liver injury, *in vivo*, are Nrf2-dependent, we blocked the Nrf2 effect by using ATRA at a dose of 10 mg/kg. As shown in **Figure 7A**, Nrf2 gene expression was elevated by carveol at 15 mg dose, while ATRA downregulated this expression. To further validate the hepatoprotective effect, we performed ELISA and we demonstrated similar results for Nrf2 (**Figure 7B**). The level of HO-1 was also decreased by ATRA ($p < 0.001$). Treatment with carveol at 15 mg/kg modulated the level of Nrf2 and HO-1, whereas ATRA treatment blocked the effects of carveol on Nrf2 ($p < 0.05$, **Figures 7B,C**). The expression of p-NFκB and TNF-α was also evaluated in these groups, and the results coincided with the Nrf2 findings, with hyperexpression in the ATRA + APAP group ($p < 0.001$). Moreover, carveol (15 mg/kg) attenuated the expression of p-NFκB and TNF-α in the carveol + ATRA + APAP group ($p < 0.05$, **Figure 7D**, $p < 0.001$, **Figure 7E**). The results were further validated using biochemical analysis (**Tables 4**) and H and E staining (**Figure 8**),

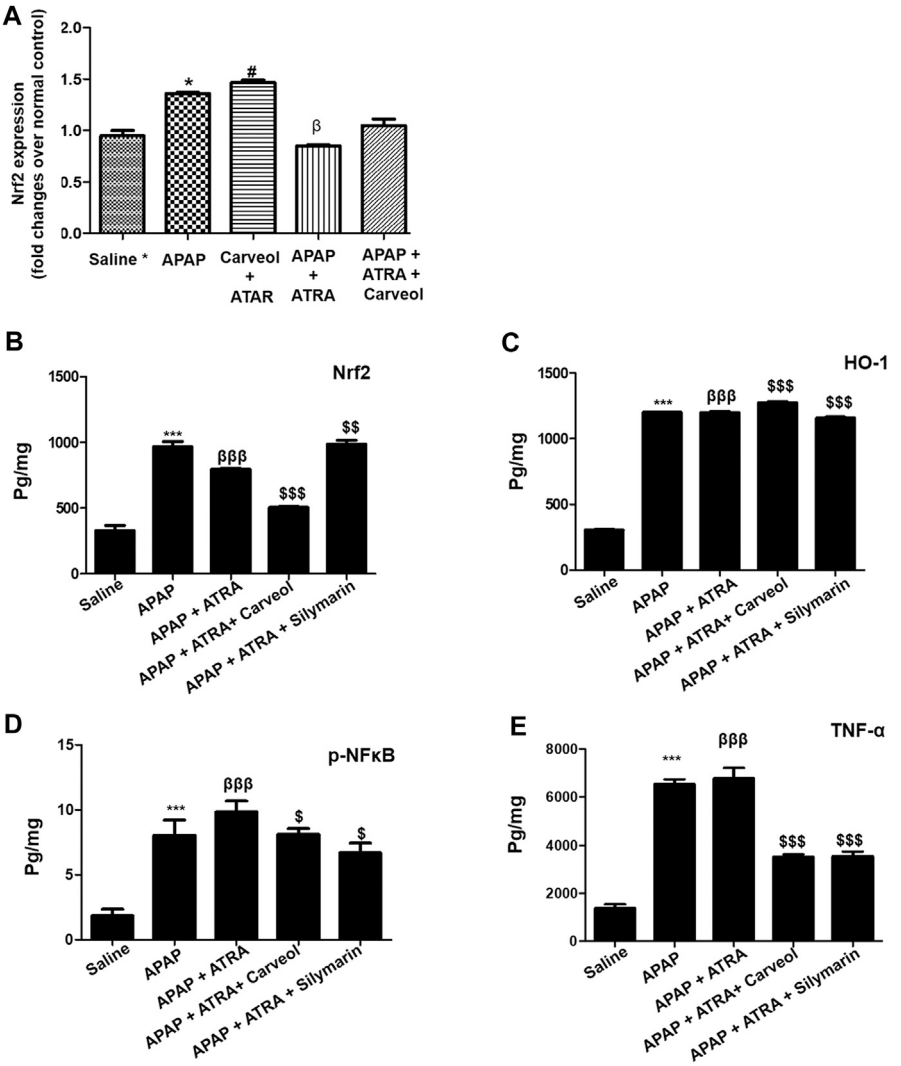


Figure 7 | Carveol produces Nrf2-dependent effects. **(A)** qPCR analysis, **(B)** Nrf2 **(C)** HO-1, **(D)** p-NFκB, and **(E)** TNF-α were quantified using ELISA. The data are expressed as mean ± SEM and were analyzed using one-way ANOVA followed by Tukey's multiple comparison test, and n = 5/group. The symbols ***, βββ and represent significant difference values of $p < 0.001$, while the symbol $ represents significant difference values of $p < 0.05$. The symbol ∗ or β represents a significant difference relative to saline, while $ represents a significant difference relative to the APAP + ATRA group. The samples were collected 6 h later, for biochemical and morphological analyses. The samples were processed from cohort 2.

TABLE 4 | ATRA abrogated the effects of carveol.

Treatment	ALT (U/L)	AST (U/L)	TP (g/dl)	ALP (U/L)	LDH (mg/dl)
Saline	67 ± 5.4	89 ± 5.32	6.8 ± 1.56	110 ± 2.7	441.33 ± 14.46
APAP 400 mg/kg + ATRA 10 mg/kg	456 ± 13.25^{βββ}	634 ± 16.35^{βββ}	2.6 ± 1.7^{ββ}	545 ± 9.89^{βββ}	3653 ± 4.03^{βββ}
APAP + ATRA + Carveol 15 mg/kg	219 ± 12.56$^{$$$}$	376 ± 3.45$^{$$$}$	5.3 ± 1.21$^{$$}$	278 ± 7.89$^{$$$}$	2162 ± 21.72$^{$$}$
APAP + ATRA + Silymarin 50 mg/kg	183 ± 14.23$^{$$$}$	312 ± 8.64$^{$$$}$	5.8 ± 2.1$^{$$}$	267 ± 5.78$^{$$$}$	2017.66 ± 25.91$^{$$}$

ATRA augmented the serum level of LFTs and attenuated the TP, while carveol significantly reduced LFT levels compared to those in the ATRA + APAP group, and increased the total protein level. The symbols βββ and $$$ represent significant difference values of p < 0.001, while the symbol $$ represents p < 0.01 values of significant differences, the symbol $ represents a significant difference relative to APAP + ATRA, while β represents a significant difference relative to the saline group. The data are expressed as means ± SEM and were analyzed using one-way ANOVA followed by Tukey's multiple comparison test, n = 5. The samples were processed from cohort 2.

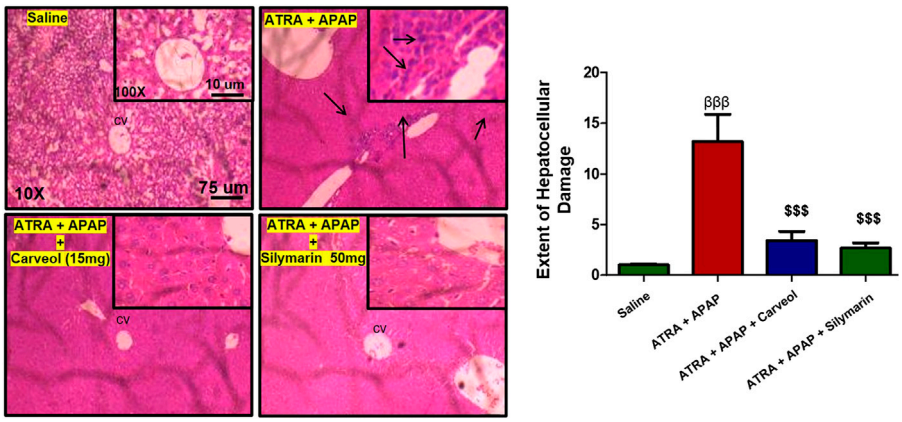


Figure 8 | Histological examination and morphological changes in liver tissues. Liver tissues stained with H and E (magnification ×10 and 40×) (n = 5/group). The necrotic cells are marked and shown by an arrow; abundant inflammatory cell infiltration can be seen in the APAP + ATRA group. The data are presented as means ± SEM and were analyzed using one-way ANOVA followed by Tukey's multiple comparison test. The symbols βββ and $$$ represent significant difference values of $p < 0.001$, the symbol β shows a significant difference relative to the saline, and the symbol $ shows a significant difference relative to the APAP + ATRA group. The slides were processed from cohort 2.

TABLE 5 | Binding energy values.

Groups	Hepatocytes necrosis	Inflammatory cells infiltration	Fatty degeneration/vacuolization
Saline	—	—	—
APAP 400 mg/kg + ATRA 10 mg/kg	+++	+++	++
APAP + ATRA + Carveol 15 mg/kg	—	—	—
APAP + ATRA + Silymarin 50 mg/kg	—	—	—

LEU, Leucine; ASP, Aspartate; ARG, Arginine; GLY, Glycine; GLU, Glutamic acid.

with amassing of inflammatory cell migration observed in the APAP + ATRA group ($p < 0.001$, **Supplementary Image S1**).

Docking Studies

Comprehensive docking studies were conducted to explore the possible targets of carveol. Cis-carveol was docked in the active catalytic pocket of COX-2, HO-1, IL-1, NFκB, inducible nitric oxide (iNOS), Nrf2, and TNF-α. **Table 5** shows the binding energies after docking analysis, and **Figure 9** shows the best pose of cis-carveol fitting to COX-2, HO-1, IL-1, NFκB, iNOS, Nrf2, and TNF-α after docking studies. The active sites of these proteins were retrieved from the literature. It was perceived that the hydroxyl group (OH-) of carveol participated in hydrogen bond formation with a protein molecule (**Figure 9**). The OH- groups of carveol, in these interactions, acted as hydrogen bond donors and the respective protein molecules were hydrogen bond acceptors. ASP-140 and ARG-136 of HO-1, LEU-80, and THR-79 of IL-1β, GLY 61 of NFκB, LEU-365 of Nrf2, and GLU-115 of TNF-α were involved in hydrogen bond interactions. In addition, non-covalent alkyl and Pi-alkyl interactions were observed, which are crucial for temporary interactions, specifically for the drug activity to be proficient in a system.

DISCUSSION

The clinical syndrome of a higher dose of APAP has long been established, and the potent natural antioxidant carveol attenuates APAP-induced detrimental outcomes in hepatic tissue; thus, this study further attested to our previously published data. We previously demonstrated that carveol treatment attenuated ischemic stroke-induced neurodegeneration, by positively affecting the Nrf2 pathway, thereby leading to a reduced infarction area (Malik et al., 2020). We demonstrated here that carveol reversed the oxidative and inflammatory cascades of APAP, possibly by triggering the Nrf2-dependent antioxidative mechanism, which is cross-linked to the pro-survival pathways (**Figure 10**). Moreover, the low energy values and relatively higher hydrogen bond formation further enhanced complex stability, as revealed through the molecular docking analysis. Additionally, previous studies have reported that targeting inflammation and oxidative stress-coupled targets could provide better therapeutic outcomes (Ali T et al., 2020; Ling et al., 2020), which opens several avenues for the use of natural drug substances.

Paracetamol is an established inducer of liver toxicity in laboratory animals, but the exact pathological mechanism for this toxicity is not well known, and several mechanisms have been

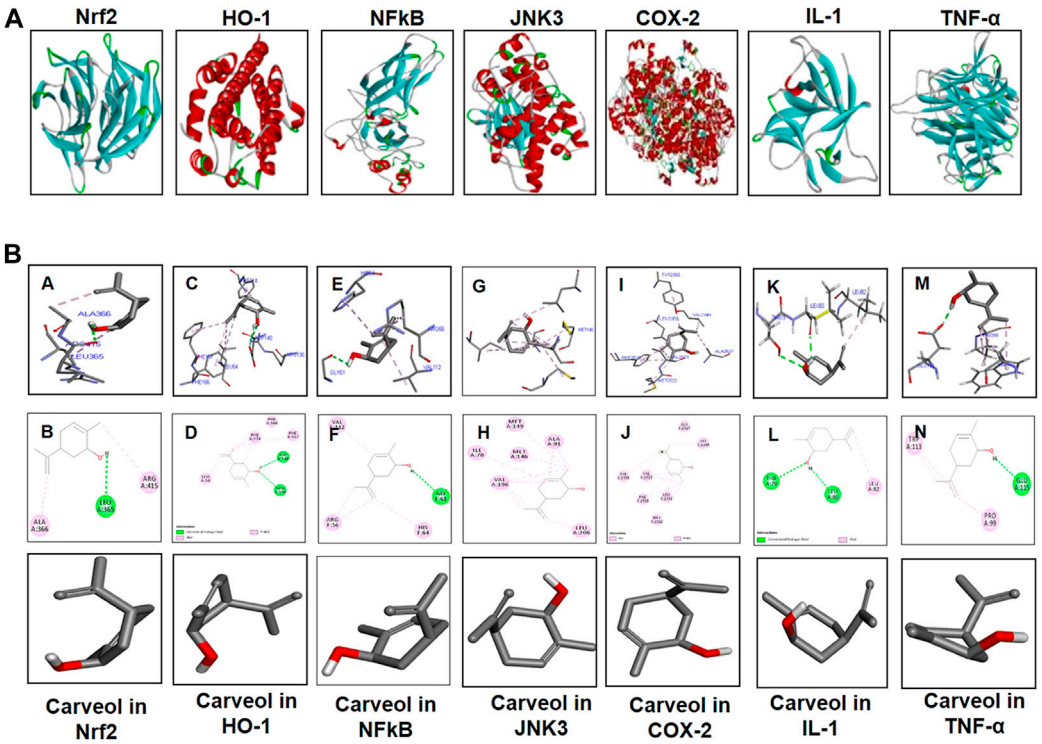


Figure 9 | Computational and docking analyses; **(A)** Tertiary structures of the proteins Nrf2, HO-1, NFκB, JNK3, COX-2, TNF-α, and IL-1β. **(B)** The docking results show the best pose of carveol that fitted to Nrf2, HO-1, NFκB, JNK3, COX-2, TNF-α, and IL-1β. The post-docking analysis was visualized using DSV in both 2D and 3D poses. The interaction between carveol and Nrf2 is shown in the panels **(A, B)**, HO-1 in the panels **(C, D)**, NFκB in the panels **(E, F)**, JNK in panels **(G, H)**, COX-2 in the panels **(I, J)**, IL-1 in the panels **(K, L)**, and TNF-α in the panels **(M, N)**. The 3D poses are shown in the panels **(A, C, E, G, I, K, M)** and the 2D in the panels **(B, D, F, H, J, L, N)**. Abbreviations: iNOS, inducible nitric oxide; TNF-α, tumor necrosis factor; IL-1β, interleukin; HO-1, heme oxygenase 1, COX-2, cyclooxygenase.

proposed. NAPQI, which is a highly reactive metabolite, is mostly attributed to this effect owing to its electrophilic nature, and it attacks several macromolecular targets (Shah et al., 2014; Sharma et al., 2016; Hellerbrand et al., 2017). The reactivity of NAPQI can be abolished by endogenous antioxidant enzymes, such as glutathione (James et al., 2003; Pastore et al., 2003; Lee et al., 2006). We observed a dose-dependent effect. Interestingly, carveol, at both doses, attenuated AST, ALT, and lactate dehydrogenase, along with favorable histological findings.

We have shown here that carveol treatment stimulates Nrf2, a key protein that combats various reactive oxygen species and other stress kinases, thereby halting necrotic and apoptotic cell death in the liver. The implications of inflammation, oxidative stress, and antioxidative mechanisms have been established previously. Our protein analysis using ELISA demonstrated that carveol alleviated the expression of different inflammatory mediators and cytokines, such as TNF-α and NFκB, which is further linked to increasing Nrf2 nuclear translocation and activation of the antioxidant machinery. Furthermore, such cascading events diminished the release of pro-inflammatory mediators and cytokines, by downregulating the NFκB signaling pathway, similar to previously reported data (Ali A et al., 2020). Nrf2 played a pivotal role in our model, as it reciprocally modulated the oxidative stress-induced inflammation. This notion was further demonstrated when ATRA treatment wore off the hepatoprotective effects of carveol and elevated the expression of the inflammatory markers. These results are consistent with other experimental models, in which Nrf2 shields against inflammation (Mohsin Alvi et al., 2020). Thus, its activation, either pharmacological or signaling cascades, rescues the tissue from the hallmarks of inflammation and oxidative stress, while its pharmacological inactivation deteriorates the pathological conditions in several other related degenerative models. Furthermore, the downstream targets of Nrf2, such as HO-1 and TRX, later mediated the protective mechanism of Nrf2. It is worth mentioning here that natural drugs are frequently reported to activate the cleavage of Nrf2-Keap1 dimer and thus allow the translocation of Nrf2 to the nucleus, to stimulate antioxidant machinery, including HO-1 and NAPDH quinine dehydrogenase-1 (NQO1), and thus provide a notable antioxidative mechanism to reverse the oxidative stress-induced inflammation (Jaiswal, 2004).

GSH, SOD, and CAT are among the first-line defense antioxidants that are important and indispensable in the defense of oxidants, particularly in the liver. SOD catalyzes the conversion of superoxide free radicals to H_2O_2 and O_2, while CAT helps in protecting against the harmful effects of superoxide and lipid peroxidation in the liver. Our results demonstrated that carveol significantly attenuated hepatic MDA, a biomarker of lipid peroxidation, and leveled the GSH, SOD, and CAT contents,

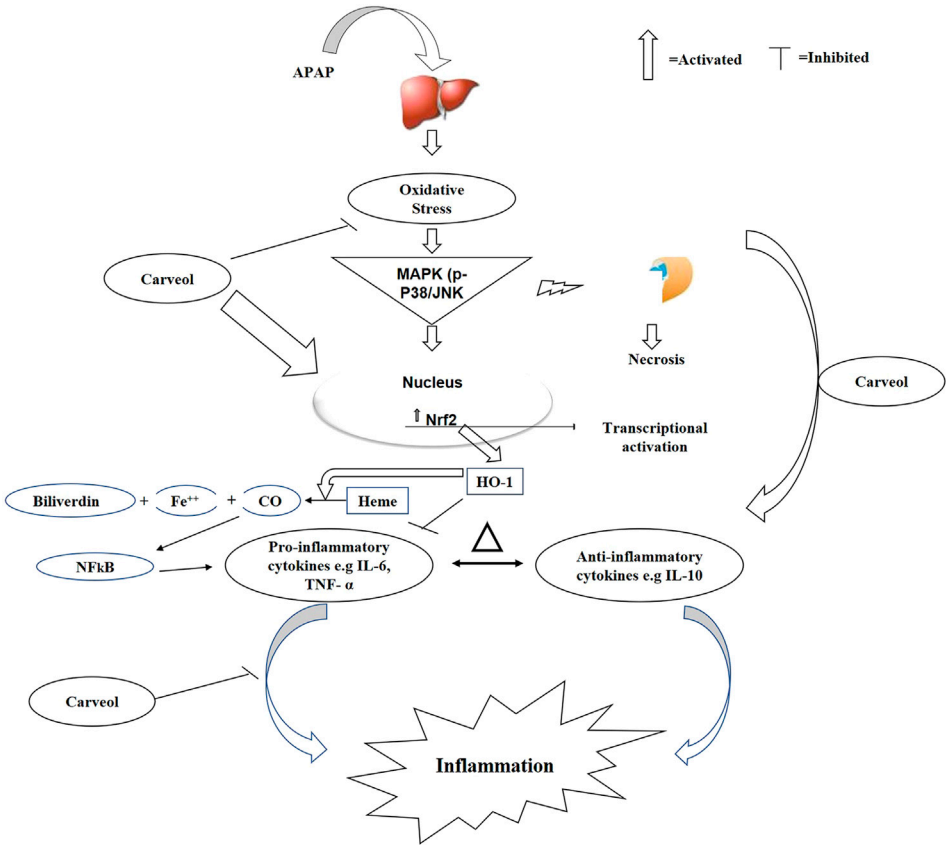


Figure 10 | The graphical representation indicates and elaborates the underlying antioxidant and anti-inflammatory mechanisms of carveol against the APAP-induced liver toxicity.

indicating a strong and complex effect of carveol in alleviating the APAP-induced oxidative stress. GSH activity is vital both for sustaining cellular homeostasis and for eliminating free radicals, such as superoxide. Furthermore, consistent studies have reported the detoxifying effect of GSH against electrophiles, such as NAPQI (Zai et al., 2018). Moreover, several protective agents act against liver insults, by normalizing GSH content. Thus, increased GSH, SOD, and CAT biosyntheses could account for the underlying mechanism of carveol against the NAPQI-induced oxidative stress and inflammation.

The Nrf2 pathway has a prominent protective role in the liver, while APAP exerts a detrimental effect on the Nrf2 pathway. A higher level of toxicity was observed in Nrf2-null mice than in wild-type mice when exposed to hepatotoxic agents (Aleksunes et al., 2008; Patterson et al., 2013; Guo and White, 2016). Previous studies on traditional Chinese drugs have shown their ability to activate Nrf2 and protect against the APAP-induced liver injury in mice. Consistent literature suggests that activation of the antioxidant machinery, such as Nrf2, could downregulate oxidative stress and the inflammatory cascade machinery, such as the NFκB pathway and cytokines (TNF-α and COX-2) (Ali A et al., 2020). The critical role of carveol in mediating the antioxidative effect of Nrf2 was further validated with the Nrf2 antagonist ATRA (Mohsin Alvi et al., 2020). ATRA administration removed the hepatoprotective effect of carveol, abolished the increased levels of Nrf2 and HO-1, and further exaggerated p-NFκB and TNF-α levels.

Several studies have documented the cross-talk between oxidative stress and the inflammation process (Al Kury et al., 2019; Al Kury et al., 2020). Therefore, drug therapeutics should be designed to subside the inflammatory process and oxidative distress, by triggering the endogenous antioxidant defense system. We also studied the expression profile of a thiol-related protein, thioredoxin (TRX), an integral enzyme in hemostatic redox reactions (Patterson et al., 2013). Carveol treatment boosted the TRX level, which further validated the antioxidant nature of carveol in APAP-induced liver injury. However, the exact mechanism of how carveol abrogated liver injury needs to be explored in detail.

APAP provokes free radical formation and subsequent pro-inflammatory mediators. Moreover, role of the JNK pathway in inflammatory cascades and cellular death has been strongly established (Ali A et al., 2020), and ROS and inflammatory cytokines can trigger JNK activation (Ali A et al., 2020; Ali T et al., 2020; Ling et al., 2020). Furthermore, the p-JNK pathway has been implicated in various animal models and human diseases (Shah et al., 2018; Li and Liu, 2019; Ali A et al., 2020; Ling et al., 2020; Malik et al., 2020), and the downregulation or

inhibition of this pathway has been found to contribute to the protective strategy (Shah et al., 2019). We observed similar activities in the APAP-intoxicated group, and carveol significantly reduced p-JNK expression. Furthermore, hepatic necrosis can be attenuated by downregulating p-NFκB expression, which may further act on the downstream COX-2 and iNOS and thus reduce ROS generation. Moreover, the expression of COX-2 and iNOS can be prevented by antagonizing p-NFκB expression (Ali A et al., 2020). Natural drug substances have significant anti-inflammatory potential, and we previously showed the inhibitory effect of carveol, polydatin, and Ginkgo biloba on NFkB, COX-2, and iNOS expression in different experimental models (Al Kury et al., 2019; Al Kury et al., 2020; Malik et al., 2020). We postulated here that carveol reduces hepatocellular necrosis by negatively modulating the expression of mitogen kinase and other inflammatory cytokines.

We performed docking analysis using the Autodock Vina program. The binding energy was evaluated for carveol and the respective proteins (**Figure 9**; **Table 5**). Different intermolecular interactive forces are vital for energetically stabilizing the drug-receptor complex. Carveol is flexibly complexed with protein targets, by establishing H-bonds and other hydrophobic interactions. Hydrogen bond formation is important for stabilization, recognition, and molecular movement (Baker and Hubbard, 1984; Desiraju and Steiner, 2001). Several studies have revealed the importance of this kind of bonding in ligand-protein complex stability, at a bond distance of 2.6Ao–3.2Ao (Glusker, 1995; Sarkhel and Desiraju, 2004; Panigrahi and Desiraju, 2007). We speculate that the formation of H-bonds between the ligand carveol and the respective protein supports the corresponding complex stability.

CONCLUSION

In summary, our *in vivo* results demonstrate that carveol could be a potent antioxidant and anti-inflammatory agent that mediates protective properties in APAP-induced liver toxicity. Furthermore, our proposed mechanism suggests that carveol may activate the master endogenous antioxidant protein Nrf2 and may be associated with the negative modulation of p-JNK and other neuroinflammatory mediators; it may, thus, offer a new therapeutic option for preventing and managing oxidative stress and inflammation in degenerative disorders.

ETHICS STATEMENT

The animal study was reviewed and approved by Research and Ethical Committee of Riphah institute of Pharmaceutical Sciences, Riphah International University Islamabad Pakistan.

AUTHOR CONTRIBUTIONS

All authors made substantial contributions to conception and design, acquisition of data, or analysis and interpretation of data; took part in drafting the article or revising it critically for important intellectual content; agreed to submit to the current journal; gave final approval of the version to be published, and agree to be accountable for all aspects of the work.

FUNDING

This work was supported by the Natural Science Foundation of Shenzhen University General Hospital Grant No: SUGH2019QD018, and the Natural Science Foundation of Shenzhen University General Hospital Grant No: SUGH2020QD015.

ACKNOWLEDGMENTS

We are thankful to Alpha Genomics (PVT) LTD., PWD branch Islamabad for providing Paid excess to qPCR analysis.

SUPPLEMENTARY MATERIAL

The Supplementary Material for this article can be found online at: https://www.frontiersin.org/articles/10.3389/fphar.2020.621538/full#supplementary-material.

REFERENCES

Abo-Haded, H. M., Elkablawy, M. A., Al-Johani, Z., Al-Ahmadi, O., and El-Agamy, D. S. (2017). Hepatoprotective effect of sitagliptin against methotrexate induced liver toxicity. *PLoS One.* 12, e0174295. doi:10.1371/journal.pone.0174295

Al Kury, L. T., Dayyan, F., Ali Shah, F., Malik, Z., Khalil, A. A. K., Alattar, A., et al. (2020). Ginkgo biloba extract protects against methotrexate-induced hepatotoxicity: a computational and pharmacological approach. *Molecules.* 25, 2540. doi:10.3390/molecules25112540

Al Kury, L. T., Zeb, A., Abidin, Z. U., Irshad, N., Malik, I., Alvi, A. M., et al. (2019). Neuroprotective effects of melatonin and celecoxib against ethanol-induced neurodegeneration: a computational and pharmacological approach. *Drug Des. Dev. Ther.* 13, 2715. doi:10.3390/molecules25112540

Al-Fartosi, K. G., Khuon, O. S., and Al-Tae, H. I. (2011). Protective role of camel's milk against paracetamol induced hepatotoxicity in male rats. *Int. J. Res. Pharm. Biomed. Sci.* 2, 1795–1799.

Aleksunes, L. M., Slitt, A. L., Maher, J. M., Augustine, L. M., Goedken, M. J., Chan, J. Y., et al. (2008). Induction of Mrp3 and Mrp4 transporters during acetaminophen hepatotoxicity is dependent on Nrf2. *Toxicol. Appl. Pharmacol.* 226, 74–83. doi:10.1016/j.taap.2007.08.022

Ali, A., Shah, F. A., Zeb, A., Malik, I., Alvi, A. M., Alkury, L. T., et al. (2020). NF-κB inhibitors attenuate MCAO induced neurodegeneration and oxidative stress—a reprofiling approach. *Front. Mol. Neurosci.* 13, 33. doi:10.3389/fnmol.2020.00033

Ali, J., Khan, A. U., Shah, F. A., Ali, H., Islam, S. U., Kim, Y. S., et al. (2019). Mucoprotective effects of Saikosaponin-A in 5-fluorouracil-induced intestinal mucositis in mice model. *Life Sci.* 239, 116888. doi:10.1016/j.lfs.2019.116888

Ali, T., Hao, Q., Ullah, N., Rahman, S. U., Shah, F. A., He, K., et al. (2020). Melatonin act as an antidepressant via attenuation of neuroinflammation by targeting Sirt1/Nrf2/HO-1 signaling. *Front. Mol. Neurosci.* 13, 96. doi:10.3389/fnmol.2020.00096

Ansari, S. F., Khan, A.-U., Qazi, N. G., Shah, F. A., and Naeem, K. (2019). *In vivo*, proteomic, and in silico investigation of sapodilla for therapeutic potential in

gastrointestinal disorders. *BioMed Res. Int.* 2019, 4921086. doi:10.1155/2019/4921086

Baker, E., and Hubbard, R. (1984). Hydrogen bonding in globular proteins. *Prog. Biophys. Mol. Biol.* 44, 97–179. doi:10.1016/0079-6107(84)90007-5

Crowell, P. L., Kennan, W. S., Haag, J. D., Ahmad, S., Vedejs, E., and Gould, M. N. (1992). Chemoprevention of mammary carcinogenesis by hydroxylated derivatives of d-limonene. *Carcinogenesis.* 13, 1261–1264. doi:10.1093/carcin/13.7.1261

Dalaklioglu, S., Genc, G., Aksoy, N., Akcit, F., and Gumuslu, S. (2013). Resveratrol ameliorates methotrexate-induced hepatotoxicity in rats via inhibition of lipid peroxidation. *Hum. Exp. Toxicol.* 32, 662–671. doi:10.1177/0960327112468178

Desiraju, G. R., and Steiner, T. (2001). *The weak hydrogen bond: in structural chemistry and biology*, Oxford, United Kingdom: Oxford University Press.

Du, K., Ramachandran, A., and Jaeschke, H. (2016). Oxidative stress during acetaminophen hepatotoxicity: sources, pathophysiological role and therapeutic potential. *Redox Biol.* 10, 148–156. doi:10.1016/j.redox.2016.10.001

Ghaffar, U., and Tadvi, N. A. (2014). Paracetamol toxicity: a review. *J Contemp Med A Dent.* 2, 12–15. doi:10.18049/jcmad/232

Glusker, J. (1995). Intermolecular interactions around functional groups in crystals: data for modeling the binding of drugs to biological macromolecules. *Acta Crystallogr., Sect. D: Biol. Crystallogr.* 51, 418–427. doi:10.1107/S0907444995003313

Gopal, K. M., Mohan, J., Meganathan, M., Sasikala, P., Gowdhaman, N., Balamurugan, K., et al. (2011). Effect of dietary fish oil (omega-3-fatty acid) against oxidative stress in isoproterenol induced myocardial injury in albino wistar rats. *Global J. Pharmacol.* 5, 4–6.

Gorrell, M. D. (2005). Dipeptidyl peptidase IV and related enzymes in cell biology and liver disorders. *Clin. Sci.* 108, 277–292. doi:10.1042/CS20040302

Guo, J. Y., and White, E. (2016). Autophagy, metabolism, and cancer. *Cold Spring Harbor Symp. Quant. Biol.* 81, 73–78. doi:10.1101/sqb.2016.81.030981

Hellerbrand, C., Schattenberg, J. M., Peterburs, P., Lechner, A., and Brignoli, R. (2017). The potential of silymarin for the treatment of hepatic disorders. *Clin. Phytosci.* 2, 7. doi:10.1186/s40816-016-0019-2

Hennig, P., Garstkiewicz, M., Grossi, S., Di Filippo, M., French, L. E., and Beer, H.-D. (2018). The crosstalk between Nrf2 and inflammasomes. *Int. J. Mol. Sci.* 19, 562. doi:10.3390/ijms19020562

Imran, M., Al Kury, L. T., Nadeem, H., Shah, F. A., Abbas, M., Naz, S., et al. (2020). Benzimidazole containing acetamide derivatives attenuate neuroinflammation and oxidative stress in ethanol-induced neurodegeneration. *Biomolecules.* 10, 108. doi:10.3390/biom10010108

Iqbal, S., Shah, F. A., Naeem, K., Nadeem, H., Sarwar, S., Ashraf, Z., et al. (2020). Succinamide derivatives ameliorate neuroinflammation and oxidative stress in Scopolamine-induced neurodegeneration. *Biomolecules.* 10, 443. doi:10.3390/biom10030443

Jaiswal, A. K. (2004). Nrf2 signaling in coordinated activation of antioxidant gene expression. *Free Radic. Biol. Med.* 36, 1199–1207. doi:10.1016/j.freeradbiomed.2004.02.074

James, L. P., Mayeux, P. R., and Hinson, J. A. (2003). Acetaminophen-induced hepatotoxicity. *Drug Metab. Dispos.* 31, 1499–1506. doi:10.1124/dmd.31.12.1499

Lee, J. I., Kang, J., and Stipanuk, M. H. (2006). Differential regulation of glutamate-cysteine ligase subunit expression and increased holoenzyme formation in response to cysteine deprivation. *Biochem. J.* 393, 181–190. doi:10.1042/BJ20051111

Li, S., and Liu, F. (2019). Polydatin attenuates neuronal loss via reducing neuroinflammation and oxidative stress in rat MCAO models. *Front. Pharmacol.* 10, 663. doi:10.3389/fphar.2019.00663

Ling, L., Alattar, A., Tan, Z., Shah, F. A., Ali, T., Alshaman, R., et al. (2020). A potent antioxidant endogenous Neurohormone melatonin, rescued MCAO by attenuating oxidative stress-associated neuroinflammation. *Front. Pharmacol.* 11, 1220. doi:10.3389/fphar.2020.01220

Ma, Q., and He, X. (2012). Molecular basis of electrophilic and oxidative defense: promises and perils of Nrf2. *Pharmacol. Rev.* 64, 1055–1081. doi:10.1124/pr.110.004333

Malik, I., Shah, F. A., Ali, T., Tan, Z., Alattar, A., Ullah, N., et al. (2020). Potent natural antioxidant carveol attenuates MCAO-stress induced oxidative, neurodegeneration by regulating the Nrf-2 pathway. *Front. Neurosci.* 14, 659. doi:10.3389/fnins.2020.00659

Mohsin Alvi, A., Tariq Al Kury, L., Umar Ijaz, M., Ali Shah, F., Tariq Khan, M., Sadiq Sheikh, A., et al. (2020). Post-treatment of Synthetic polyphenolic 1, 3, 4 oxadiazole compound A3, attenuated ischemic stroke-induced neuroinflammation and neurodegeneration. *Biomolecules.* 10, 816. doi:10.3390/biom10060816

Ning, C., Gao, X., Wang, C., Kong, Y., Liu, Z., Sun, H., et al. (2018). Ginsenoside Rg1 protects against acetaminophen-induced liver injury via activating Nrf2 signaling pathway *in vivo* and *in vitro*. *Regul. Toxicol. Pharmacol.* 98, 58–68. doi:10.1016/j.yrtph.2018.07.012

Panigrahi, S. K., and Desiraju, G. R. (2007). Strong and weak hydrogen bonds in the protein-ligand interface. *Proteins.* 67, 128–141. doi:10.1002/prot.21253

Pastore, A., Federici, G., Bertini, E., and Piemonte, F. (2003). Analysis of glutathione: implication in redox and detoxification. *Clin. Chim. Acta.* 333, 19–39. doi:10.1016/s0009-8981(03)00200-6

Patterson, A. D., Carlson, B. A., Li, F., Bonzo, J. A., Yoo, M. H., Krausz, K. W., et al. (2013). Disruption of thioredoxin reductase 1 protects mice from acute acetaminophen-induced hepatotoxicity through enhanced NRF2 activity. *Chem. Res. Toxicol.* 26, 1088–1096. doi:10.1021/tx4001013

Rana, I., Khan, N., Ansari, M. M., Shah, F. A., Din, F., Sarwar, S., et al. (2020). Solid lipid nanoparticles-mediated enhanced antidepressant activity of duloxetine in lipopolysaccharide-induced depressive model. *Colloids Surf. B Biointerfaces.* 194, 111209. doi:10.1016/j.colsurfb.2020.111209

Sarkhel, S., and Desiraju, G. R. (2004). N. H. . . O, O. H. . . ON-H...O, O-H...O, and C-H...O hydrogen bonds in protein-ligand complexes: strong and weak interactions in molecular recognitionO hydrogen bonds in protein–ligand complexes: strong and weak interactions in molecular recognition. *Proteins.* 54, 247–259. doi:10.1002/prot.10567

Shah, F.-A., Gim, S.-A., Kim, M.-O., and Koh, P.-O. (2014). Proteomic identification of proteins differentially expressed in response to resveratrol treatment in middle cerebral artery occlusion stroke model. *J. Vet. Med. Sci.* 76, 1367–1374. doi:10.1292/jvms.14-0169

Shah, F. A., Zeb, A., Ali, T., Muhammad, T., Faheem, M., Alam, S. I., et al. (2018). Identification of proteins differentially expressed in the Striatum by melatonin in a middle cerebral artery occlusion rat model-a proteomic and. *Front. Neurosci.* 12, 888. doi:10.3389/fnins.2018.00888

Shah, F. A., and Rashid, S. (2020). Conformational ensembles of non-peptide ω-conotoxin mimetics and Ca^{+} 2 ion binding to human voltage-gated N-type calcium channel Cav2. 2. *Comput. Struct. Biotechnol. J.* 18, 2357–2372. doi:10.1016/j.csbj.2020.08.027

Shah, F. A., Zeb, A., Li, S., and Al Kury, L. T. (2019). Pathological comparisons of the hippocampal changes in the transient and permeant middle cerebral artery occlusion rat models. *Front. Neurol.* 10, 1178. doi:10.3389/fneur.2019.01178

Sharma, S., Rana, S., Patial, V., Gupta, M., Bhushan, S., and Padwad, Y. (2016). Antioxidant and hepatoprotective effect of polyphenols from apple pomace extract via apoptosis inhibition and Nrf2 activation in mice. *Hum. Exp. Toxicol.* 35, 1264–1275. doi:10.1177/0960327115627689

Thompson Coon, J., and Ernst, E. (2002). Herbal medicinal products for non ulcer dyspepsia. *Aliment. Pharmacol. Ther.* 16, 1689–1699.

Ullah, U., Badshah, H., Malik, Z., Uddin, Z., Alam, M., Sarwar, S., et al. (2020). Hepatoprotective effects of melatonin and celecoxib against ethanol-induced hepatotoxicity in rats. *Immunopharmacol. Immunotoxicol.* 42, 255–263. doi:10.1080/08923973.2020.1746802

Wakabayashi, N., Skoko, J. J., Chartoumpekis, D. V., Kimura, S., Slocum, S. L., Noda, K., et al. (2014). Notch-Nrf2 axis: regulation of Nrf2 gene expression and cytoprotection by notch signaling. *Mol. Cell Biol.* 34, 653–663. doi:10.1128/MCB.01408-13

Zai, W., Chen, W., Luan, J., Fan, J., Zhang, X., Wu, Z., et al. (2018). Dihydroquercetin ameliorated acetaminophen-induced hepatic cytotoxicity via activating JAK2/STAT3 pathway and autophagy. *Appl. Microbiol. Biotechnol.* 102, 1443–1453. doi:10.1007/s00253-017-8686-6

Conflict of Interest: The authors declare that the research was conducted in the absence of any commercial or financial relationships that could be construed as a potential conflict of interest.

Copyright © 2021 Rahman, Al Kury, Alattar, Tan, Alshaman, Malik, Badshah, Uddin, Khan Khalil, Muhammad, Khan, Ali, Shah, Li and Li. This is an open-access article distributed under the terms of the Creative Commons Attribution License (CC BY). The use, distribution or reproduction in other forums is permitted, provided the original author(s) and the copyright owner(s) are credited and that the original publication in this journal is cited, in accordance with accepted academic practice. No use, distribution or reproduction is permitted which does not comply with these terms.

frontiers in Pharmacology

BRIEF RESEARCH REPORT
published: 04 February 2021
doi: 10.3389/fphar.2020.617535

Rapamycin is Effective for Upper but not for Lower Gastrointestinal Crohn's Disease-Related Stricture: A Pilot Study

Min Zhong[1,2], *Bota Cui*[1,2], *Jie Xiang*[3], *Xia Wu*[1,2], *Quan Wen*[1,2], *Qianqian Li*[1,2] *and Faming Zhang*[1,2]*

[1]*Medical Center for Digestive Diseases, The Second Affiliated Hospital of Nanjing Medical University, Nanjing, China,* [2]*Key Lab of Holistic Integrative Enterology, Nanjing Medical University, Nanjing, China,* [3]*Department of Gastroenterology, The Central Hospital of Enshi Autonomous Prefecture, Enshi, China*

Crohn's disease (CD)-related fibrotic stricture remains a clinical challenge because of no effective treatments. This study aimed to evaluate the potential efficacy of rapamycin in patients with CD-related strictures in different locations in gastrointestinal tract. A pilot prospective study on using rapamycin for CD-related stricture was performed from April 2015 to August 2020 in a single center in China. Fifteen patients were enrolled into the study. The clinical efficacy was evaluated by diet score and gastrointestinal obstruction symptoms score. Clinical responses were defined as the ability to tolerate the regular diet with vegetable fiber combined with a reduction of ≥75% in overall target score and a score of less than two points for each item. Three patients discontinued rapamycin for less than 1-month due to intolerance to adverse events, then, 12 patients received ≥1 dose of the rapamycin and provided ≥1 post-baseline target score after baseline were included for intent-to-treat (ITT) analysis. 100% (5/5) of patients with upper gastrointestinal strictures achieved clinical response after using rapamycin. However, no clinical response was observed in those patients with CD lesions in lower gastrointestinal tract. Adverse events occurred in 40% (6/15) of patients. No death or serious opportunistic infections were observed in the present study. This study firstly reported that rapamycin might be effective for CD-related stricture in the upper, but not in lower gastrointestinal tract.

Keywords: Crohn's disease, rapamycin, fibrosis, stricture, inflammatory bowel diseases, duodenum obstruction

OPEN ACCESS

Edited by:
Wolfgang Richard Stremmel, Medical Center Baden-Baden, Germany

Reviewed by:
Maria Cecilia Giron, University of Padua, Italy
Rinaldo Pellicano, Molinette Hospital, Italy

***Correspondence:**
Faming Zhang
fzhang@njmu.edu.cn

Specialty section:
This article was submitted to Gastrointestinal and Hepatic Pharmacology, a section of the journal Frontiers in Pharmacology

Received: *15 October 2020*
Accepted: *23 December 2020*
Published: *04 February 2021*

Citation:
Zhong M, Cui B, Xiang J, Wu X, Wen Q, Li Q and Zhang F (2021) Rapamycin is Effective for Upper but not for Lower Gastrointestinal Crohn's Disease-Related Stricture: A Pilot Study. Front. Pharmacol. 11:617535. doi: 10.3389/fphar.2020.617535

INTRODUCTION

Crohn's disease (CD) is a chronic relapsing inflammatory disease that can occur in any segment of the gastrointestinal tract. However, the naturally progressive disease course culminates in stricture formation (Cosnes et al., 2011), often leading to repeated bowel obstruction and surgery (Rieder et al., 2013; Singh et al., 2017). Mostly, strictures are caused by the combination of inflammation and fibrosis, and the intensity of fibrosis is almost impossible to determine (Feakins, 2020). Clinically, CD-related stenosis can be silent or symptomatic. Symptomatic stenosis may manifest as postprandial bloating, or significant intestinal obstruction, causing nausea, vomiting, and abdominal pain. Up till now, the therapy of choice for CD with fibrotic strictures, mainly

comprises endoscopic dilation endoscopic stricturotomy and surgery (Kanazawa et al., 2012; Singh et al., 2017; Shen et al., 2020), in conjunction with purely anti-inflammatory therapy. Although endoscopic dilation procedures for stricturing CD are usually technically successful, the majority of patients still required multiple sessions of endoscopic dilation, and some might develop perforation (Kanazawa et al., 2012; Singh et al., 2017). A significant number of patients have to undergo multiple surgeries, with the attendant risk of developing short bowel syndrome and intestinal failure (Rieder et al., 2013). Therefore, there is necessity to explore more effective treatments for patients with CD-related fibrotic stricture.

In recent studies, rapamycin, a serine/THR kinase inhibitor of mammalian target (mTOR), has been reported as potentially effective treatment in limited populations with refractory CD (Massey et al., 2008; Mutalib et al., 2014). Rapamycin has also been reported to inhibit the progression of kidney fibrosis (Chen et al., 2012), cardiac fibrosis (Haller et al., 2016), and pulmonary fibrosis (Xu et al., 2017). A recent study has shown that rapamycin can reduce intestinal fibrosis by inhibiting CX3Cr1+ mTOR/autophagy in mononuclear phagocytes and up-regulating the IL-23/IL-22 axis (Mathur et al., 2019). Based on the consideration on the two facts: the very low incidence of CD patients with upper gastrointestinal fibrotic stricture (Nugent et al., 1989; Van Assche et al., 2004), and the hypothesis on the local anti-fibrosis effect of rapamycin in upper section of small intestine, the present study aimed to evaluate the potential efficacy of rapamycin for patients with CD-related gastrointestinal stricture.

MATERIALS AND METHODS

Study Design and Participants

Patients with CD from the nation came to the Second Affiliated Hospital of Nanjing Medical University for seeking fecal microbiota transplantation based on automatic filtration and washing process and the related delivery, which was called as washed microbiota transplantation (WMT) (Fecal Microbiota Transplantation-standardization Study Group, 2020; Zhang et al., 2020). However, these patients with CD-related strictures were not considered for WMT, but invited to attend the present trial (NCT02675153). The study was approved by the Second Affiliated Hospital of the Nanjing Medical University Institutional Ethical Review Board (2016KY001), and written informed consent was obtained from all patients. Demographics (age, gender) and disease characteristics (disease location, duration, duration of stricture and other CD drug medications) of each patient were noted before the study.

Inclusion and Exclusion Criteria

Inclusion criteria were: (1) Patients (≥18 years of age) with a documented definite diagnosis of CD; and 2) the presence of a clinically symptomatic stricture; and 3) strictures confirmed by endoscopy (passing endoscope with difficulty) or typical image by CT enterography (CTE) or MR enterography (MRE). Patients were excluded: 1) patients who were pregnant, diagnosed with intestinal perforation, complete intestinal obstruction, any signs of dysplasia or malignancy, or use of anti-tumor necrosis factor (TNF) in the last three months; and 2) patients who were not followed up between the inception of medication and any other subsequent treatments.

Procedures and Outcome Measures

Patients were treated with rapamycin (2 mg/day, Sirolimus, Roche) and short-term enteral nutrition. Patients with colitis were also treated with 5-aminosalicylic acid (5-ASA). The intent-to-treat (ITT) population comprised all patients who received ≥1 dose of the study drug and provided ≥1 post-baseline target score after baseline.

We used a composite score considering all the essential elements including the gastrointestinal obstruction symptoms score and diet score to assess the effectiveness of treatment in clinical practice during follow-up. Response should meet the following three criteria: (a) the ability to tolerate a normal diet (vegetable fiber), with a reduction of ≥75% in overall baseline target score and sub-score ≤ 2 (**Table 1**); (b) no need for endoscopic dilation or surgery; (c) no severe adverse events or any other reasons leading to rapamycin withdrawal. The primary aim was the rate of clinical response focusing on obstruction after using rapamycin. The follow-up was at least 6 months for patients with unclear efficacy. Patients who prematurely discontinued rapamycin due to severe adverse events or who did not meet clinical response criteria after 6 months medication usage were considered treatment failure. The secondary aim was to evaluate the adverse events during medication usage in all enrolled patients. In this study, new onset of symptoms and the exacerbation of previous symptoms were recorded as adverse events. We also evaluated the primary endpoint was the rate of surgery or ED after rapamycin as the long-term treatment outcomes.

Statistical Analysis

Data were analyzed using IBM SPSS Statistics 23.0.0 (SPSS Inc., Chicago, IL, United States). Continuous variables were expressed using median and interquartile range and tested by Analysis of Variance test. Categorical data were described as number (percentages) and were tested by Chi-square analysis or Fisher's exact test. The paired data were compared using the Paired t test. $p < 0.05$ was indicative of statistical significance.

RESULTS

From April 2015 to August 2020, totally 15 patients were enrolled. The follow-up finished on December 1, 2020. The patient demographics, characteristics of CD, and previous history of drug therapy at the baseline were well balanced between the treatment groups (as shown in **Table 2**) and three of them with lesions in ileum or colon were administered oral 5-ASA simultaneously. One patient in the upper gastrointestinal group and two patients in the lower gastrointestinal group stopped to take the medication within one month because of adverse events (**Table 2**) and did not provide a post-baseline target score. Therefore, 15 patients were included in the safety

TABLE 1 | Definition of each target and scoring method in patients.

Variables	Scoring method
Abdominal pain	0: No abdominal pain
	1–2: Essentially normal
	3–5: Affecting daily life but not sleeping
	6–9: Affecting sleep
Abdominal distention	0: No abdominal distention
	1–2: Essentially normal
	3–5: Affecting daily life but not sleeping
	6–9: Affecting sleep
Diet	0: No dietary restrictions
	1–2: Essentially normal, without nausea and vomiting
	3–5: Regular diet, with nausea and vomiting
	6–8: Fluid diet and enteral nutrition, with nausea and vomiting
	9: Exclusive enteral nutrition or gastrointestinal decompression

TABLE 2 | Characteristics of the patients at baseline.

	All patients (n = 15)	Upper gastrointestinal (n = 6)	Lower gastrointestinal (n = 9)	*p* value
Age, years, median (IQR)	30 (28.5–38.5)	29 (24.3–30.8)	31 (29–39)	0.358
Male, n (%)	8 (53.3%)	4 (66.7%)	4 (44.4%)	0.608
Family history of CD, n (%)	0 (0.0%)	0 (0.0%)	0 (0.0%)	
Smoking, n (%)				0.604
Current	0 (0.0%)	0 (0.0%)	0 (0.0%)	
Ex-smoker	4 (26.7%)	1 (16.7%)	3 (33.3%)	
Never	8 (73.3%)	5 (83.3%)	6 (66.7%)	
Age at diagnosis, years, median (IQR)	25 (23–29.5)	24 (21.5–28.8)	26 (23–29)	0.852
Months from CD diagnosis to confirm the stricture, months, median (IQR)	35 (13–49)	7 (1.3–21)	46 (35–68)	0.367
Disease duration, years, median (IQR)	9 (4.5–12)	3 (3–7)	12 (10.5–12.5)	0.082
Fistulizing disease, n (%)	5 (33.3%)	2 (33.3%)	3 (33.3%)	
History of gastrointestinal surgery, n (%)	3 (20%)	0 (0.0%)	3 (33.3%)	
History of medications, n (%)				0.556
5-ASA	9 (60%)	3 (50%)	6 (66.7%)	
PPI	2 (13.3%)	2 (33.3%)	0 (0.0%)	
Immunosuppressants	9 (60%)	3e (50%)	6 (66.7%)	
Corticosteroids	8 (53.3%)	4 (66.7%)	4 (44.4%)	
Biological therapy	2 (13.3%)	1 (16.7%)	1 (11.1%)	
Adverse events				0.091
Palpation	2 (13.3%)	0 (0.0%)	2 (22.2%)	
Loss of libido	2 (13.3%)	0 (0.0%)	2 (22.2%)	
Abnormal liver enzymes	1 (6.7%)	0 (0.0%)	1 (11.1%)	
Mouth ulcer	2 (13.3%)	0 (0.0%)	2 (22.2%)	
Headache	1 (6.7%)	0 (0.0%)	1 (11.1%)	
Rash	0 (0.0%)	1 (16.7%)	2 (22.2%)	
Leukopenia	1 (6.7%)	1 (16.7%)	0 (0.0%)	

CD, Crohn's disease; 5-ASA, 5-aminosalicylic acid; PPI, proton pump inhibitors; IQR, inter quartile range.

population and 12 patients were included for in the ITT population (**Table 3**).

Response rate was 41.7% (5/12) in this study. The patients achieved response were all patients with upper gastrointestinal stricture (lesions in stomach and duodenum), but clinical failure was confirmed in all patients with lower lesions. 100% (5/5) of patients with upper gastrointestinal strictures achieved clinical response within 6 months after using rapamycin, with the mean time of 4.4 months. The overall target score of the patients decreased from the mean of 12.0 at baseline to 1.6 at 4.4 months (Paired *t* test, $p = 0.005$), with each target ≤2. By contrast, the mean score for patients with lower gastrointestinal lesions dropped to 8.7 at 6 months from 10.0 at baseline (Paired *t* test, $p = 0.022$). The adverse events as the secondary aim of the

TABLE 3 | Medications and clinical outcomes of patients.

Pt	Classification	5-ASA	Rapa duration (months)	Response (months)	HBI		Target score					
					Before	After[a]	Abdominal pain		Abdominal distention		Diet	
							Before	After[a]	Before	After[a]	Before	After[a]
1	A1, L3L4, B2	No	24	Yes (2)	2	0	0	0	5	0	5	2
2	A2, L3L4, B2	Yes	6	Yes (5)	3	0	3	0	5	0	5	0
3	A1, L4, B2	No	24	Yes (5)	2	0	0	0	0	0	6	0
4	A2, L4, B2	No	10	Yes (6)	5	1	6	0	2	0	9	1
5	A2, L4, B2	No	4	Yes (4)	3	0	0	0	5	2	9	3
6	A2, L3, B2	No	12	No	5	1	5	4	2	2	5	5
7	A2, L3, B2	Yes	11	No	5	3	5	2	1	1	6	6
8	A2, L3, B2	No	6	No	5	4	6	5	5	4	6	6
9	A2, L3, B2	Yes	6	No	5	3	3	3	3	3	3	3
10	A2, L2, B2	No	8	No	3	2	0	0	3	2	3	3
11	A2, L2, B2	No	6	No	2	2	0	0	2	2	3	3
12	A2, L3, B2	No	6	No	10	8	6	4	0	0	3	3

Rapa, Rapamycin; HBI, Harvey-Bradshaw Index; A1, ≤16 years; A2, 17–40 years; L2, colonic; L3, ileocolonic; L4, isolated upper gastrointestinal; B2, structuring; 5-ASA, 5-aminosalicylic acid.

[a]*The time that patients achieved response or received rapamycin for 6 months.*

present study occurred in six patients (6/15, 40%) (**Table 2**). No death or serious opportunistic infections were reported.

The median duration of rapamycin in patients with upper gastrointestinal stenosis was 17 (Interquartile range (IQR): 9–24) months. At a median follow-up of 49 (IQR: 42–53.5) months, three of these patients were identified to be in long-term success and have been able to completely cease medication for more than one year without relapse. One case reported clinical improvement on her obstruction in upper gastrointestinal tract after 6 months of rapamycin, but she developed rectovaginal fistula after the cessation of rapamycin for 16 months. Rapamycin was discontinued in four patients with lower gastrointestinal tract stenosis after 6 months, and three of them continued to receive rapamycin for several months of their own volition, with a median duration of 6 (IQR: 6.0–9.5) months. The median time to follow-up was 37 (IQR: 29–46) months in the lower lesions group. One patient underwent surgery 17 months after rapamycin withdrawal, while the others were treated with other immunosuppressive agents after failure of rapamycin treatment.

DISCUSSION

Treatment of CD-related stricture is a clinical challenge, especially the lesions located in upper gastrointestinal tract, and is also a high socio-economic burden due to frequent hospitalizations and surgery (Bodger et al., 2009). Despite advances in anti-inflammatory therapies in recent decades, the incidence of intestinal stenosis in CD has not changed significantly. Inflammation and fibrosis are associated, in most cases, but to different degrees. Although surgery is the choice for fibrotic stenosis, post-operative disease recurrence and re-stricture are common (Rieder et al., 2013). Endoscopic dilatation is relatively safe for patients, but the efficacy is of limited duration (Hassan et al., 2007; Taida et al., 2018). Given the current uncertainties of the medical treatment regarding the formation and progression of fibrotic strictures, new treatments are welcome.

The efficacy of mTOR inhibitors in the treatment of CD varies from studies (Massey et al., 2008; Reinisch et al., 2008; Mutalib et al., 2014). This pilot case series study explored the efficacy and safety of rapamycin in CD-related strictures. Overall, five patients (100%) with duodenum stricture achieved clinical response after rapamycin treatment, but none of patients with lower gastrointestinal stricture reported improvement. The present findings inspire us to precisely select the clinical application of rapamycin in CD-associated stenosis in duodenum or lesion close to duodenum.

In the present study, we found that Harvey-Bradshaw Index (HBI) could not accurately reflect the changes in the patients with CD-related gastrointestinal stricture. The evaluation based on clinical outcomes, including symptoms and tolerability, might be the better than using imaging changes. Therefore, the gastrointestinal symptoms and diet assessment were used for the clinical evaluation in these patients. We observed that clinical responses were only achieved in patients with upper gastrointestinal stricture by oral rapamycin, but not in patients with lower lesions. In this population, one male teenager with duodenum stricture who underwent repeated endoscopic dilation and percutaneous endoscopic gastrojejunostomy (PEG-J) for exclusive enteral nutrition, remained unresponsive for two years. After two months of treatment with rapamycin, he switched from enteral nutrition via tube to regular taking food by oral with normal diet, and the total score dropped from 10 at baseline to two at two months. He maintained clinical response to rapamycin for two years. Unfortunately, 10 months after withdrawal of rapamycin, gastroscopy revealed the progression of stenosis. Then he was treated with rapamycin again and has maintained response to date. Another patient with upper lesions took rapamycin continuously for only 6 months and developed rectovaginal fistula after stopping the medication. In view of these results, we suggest that rapamycin should be used as a long-term or maintenance therapy to achieve the best treatment response.

The enteral nutrition via tube can solve the nutritional needs of patients and relieve inflammatory bowel stricture in CD (Hu et al., 2014), but it seems not effective on fibrotic stenosis. Therefore, our results suggest that rapamycin may have a role in the treatment of fibrotic strictures. The present study showed a new treatment option for CD related strictures and further studies are expected to investigate the underlying mechanisms of this effect in the future.

An important question is whether rapamycin could prevent or delay surgery in this category of patients. We observed that 11/12 patients (91.7%) initially treated with rapamycin were surgery-free after a median follow-up of more than 3 years. The results may suggest that rapamycin has changed the natural history of the disease and is able to reverse strictures to some extent, which were thought to be non-reversible according to the Lemann Index in some patients with CD (Fiorino et al., 2015). In our study, the most common adverse event was mouth ulcer, and three patients discontinued the treatment due to adverse events within one month. However, adverse events occurred in patients after one month subsided spontaneously, indicating that the severity of adverse reactions may gradually decrease over time.

There were some limitations in the present study. The simple size was small, and the result might not be representative of the general population. In addition, the evaluation based on endoscopy or radiology was not performed for each patient. The benefits and risks of rapamycin for fibrotic strictures in long term should be assessed in randomized controlled trials.

In conclusion, although CD-related fibrotic stricture in upper gastrointestinal tract is rare, we had opportunity to enroll this specific population for this pilot study in China. We first time reported that the rapamycin should be effective in patients with CD-related fibrotic stricture in upper gastrointestinal tract, not those lesions in lower tract. Further case-control studies with appropriate sample and randomization are required to support the use of rapamycin in this specific subpopulation.

DATA AVAILABILITY STATEMENT

The original contributions presented in the study are included in the article/Supplementary Material, further inquiries can be directed to the corresponding author.

ETHICS STATEMENT

The studies involving human participants were reviewed and approved by Second Affiliated Hospital of the Nanjing Medical University Institutional Ethical Review Board (2016KY001). The patients/participants provided their written informed consent to participate in this study.

AUTHOR CONTRIBUTIONS

MZ contributed to clinical data acquisition, analyzed the data and wrote the manuscript. FZ designed the research. XW contributed to clinical data acquisition and manuscript revision. BC, JX, QL, and QW performed the clinical work.

FUNDING

This study was funded by the publicly donated Intestine Initiative Foundation; Jiangsu Provincial Medical Innovation Team (FZ); National Natural Science Foundation of China (81670495).

ACKNOWLEDGMENTS

The authors thank all the participants of the study. The authors also thank Cicilia Marcella for her kindly assistance with language improvement.

REFERENCES

Bodger, K., Kikuchi, T., and Hughes, D. (2009). Cost-effectiveness of biological therapy for Crohn's disease: markov cohort analyses incorporating United Kingdom patient-level cost data. *Aliment. Pharmacol. Ther.* 30 (3), 265–274. doi:10.1111/j.1365-2036.2009.04033.x

Chen, G., Chen, H., Wang, C., Peng, Y., Sun, L., Liu, H., et al. (2012). Rapamycin ameliorates kidney fibrosis by inhibiting the activation of mTOR signaling in interstitial macrophages and myofibroblasts. *PLoS One* 7 (3), e33626. doi:10.1371/journal.pone.0033626

Cosnes, J., Gower-Rousseau, C., Seksik, P., and Cortot, A. (2011). Epidemiology and natural history of inflammatory bowel diseases. *Gastroenterology* 140 (6), 1785–1794. doi:10.1053/j.gastro.2011.01.055

Feakins, R. M. (2020). Transmural histology scores in stricturing crohn's disease: seeking to build precision on uncertain foundations. *J. Crohns. Colitis.* 14 (6), 721–723. doi:10.1093/ecco-jcc/jjaa008

Fecal Microbiota Transplantation-standardization Study Group (2020). Nanjing consensus on methodology of washed microbiota transplantation. *Chin. Med. J.* 133 (19), 2330–2332. doi:10.1097/CM9.0000000000000954

Fiorino, G., Bonifacio, C., Allocca, M., Repici, A., Balzarini, L., Malesci, A., et al. (2015). Bowel damage as assessed by the Lemann Index is reversible on anti-TNF therapy for crohn's disease. *J. Crohns. Colitis.* 9 (8), 633–639. doi:10.1093/ecco-jcc/jjv080

Haller, S. T., Yan, Y., Drummond, C. A., Xie, J., Tian, J., Kennedy, D. J., et al. (2016). Rifamycin attenuates cardiac fibrosis in experimental uremic cardiomyopathy by reducing marinobufagenin levels and inhibiting downstream pro-fibrotic signaling. *J. Am. Heart Assoc.* 5 (10). doi:10.1161/JAHA.116.004106

Hassan, C., Zullo, A., De Francesco, V., Ierardi, E., Giustini, M., Pitidis, A., et al. (2007). Systematic review: endoscopic dilatation in Crohn's disease. *Aliment. Pharmacol. Ther.* 26, (11–12), 1457–1464. doi:10.1111/j.1365-2036.2007.03532.x

Hu, D., Ren, J., Wang, G., Li, G., Liu, S., and Yan, D. (2014). Exclusive enteral nutritional therapy can relieve inflammatory bowel stricture in Crohn's disease. *J. Clin. Gastroenterol.* 48 (9), 790–795. doi:10.1097/MCG.0000000000000041

Kanazawa, A., Yamana, T., Okamoto, K., and Sahara, R. (2012). Risk factors for postoperative intra-abdominal septic complications after bowel resection in patients with Crohn's disease. *Dis. Colon. Rectum.* 55 (9), 957–962. doi:10.1097/DCR.0b013e3182617716

Massey, D. C., Bredin, F., and Parkes, M. (2008). Use of sirolimus (rapamycin) to treat refractory Crohn's disease. *Gut* 57 (9), 1294–1296. doi:10.1136/gut.2008.157297

Mathur, R., Alam, M. M., Zhao, X. F., Liao, Y., Shen, J., Morgan, S., et al. (2019). Induction of autophagy in Cx3cr1(+) mononuclear cells limits IL-23/IL-

22 axis-mediated intestinal fibrosis. *Mucosal Immunol.* 12 (3), 612–623. doi:10.1038/s41385-019-0146-4

Mutalib, M., Borrelli, O., Blackstock, S., Kiparissi, F., Elawad, M., Shah, N., et al. (2014). The use of sirolimus (rapamycin) in the management of refractory inflammatory bowel disease in children. *J. Crohns. Colitis.* 8, (12), 1730–1734. doi:10.1016/j.crohns.2014.08.014

Nugent, F. W., and Roy, M. A. (1989). Duodenal Crohn's disease: an analysis of 89 cases. *Am. J. Gastroenterol.* 84, (3), 249–254

Reinisch, W., Panés, J., Lémann, M., Schreiber, S., Feagan, B., Schmidt, S., et al. (2008). A multicenter, randomized, double-blind trial of everolimus versus azathioprine and placebo to maintain steroid-induced remission in patients with moderate-to-severe active Crohn's disease. *Am. J. Gastroenterol.* 103 (9), 2284–2292. doi:10.1111/j.1572-0241.2008.02024.x

Rieder, F., Zimmermann, E. M., Remzi, F. H., and Sandborn, W. J. (2013). Crohn's disease complicated by strictures: a systematic review. *Gut* 62 (7), 1072–1084. doi:10.1136/gutjnl-2012-304353

Shen, B., Kochhar, G., Navaneethan, U., Farraye, F. A,, Schwartz, D. A., Iacucci, M., et al. (2020). Practical guidelines on endoscopic treatment for Crohn's disease strictures: a consensus statement from the global interventional inflammatory bowel disease group. *Lancet Gastroenterol. Hepatol.* 5 (4), 393–405. doi:10.1016/S2468-1253(19)30366-8

Singh, A., Agrawal, N., Kurada, S., Lopez, R., Kessler, H., Philpott, J., et al. (2017). Efficacy, safety, and long-term outcome of serial endoscopic balloon dilation for upper gastrointestinal crohn's disease-associated strictures-A cohort study. *J. Crohns. Colitis.* 11 (9), 1044–1051. doi:10.1093/ecco-jcc/jjx078

Taida, T., Nakagawa, T., Ohta, Y., Hamanaka, S., Okimoto, K., Saito, K., et al. (2018). Long-term outcome of endoscopic balloon dilatation for strictures in patients with crohn's disease. *Digestion* 98 (1), 26–32. doi:10.1159/000486591

Van Assche, G., Geboes, K., and Rutgeerts, P. (2004). Medical therapy for Crohn's disease strictures. *Inflamm. Bowel Dis.* 10 (1), 55–60. doi:10.1097/00054725-200401000-00009

Xu, Y., Tai, W., Qu, X., Wu, W., Li, Z., Deng, S., et al. (2017). Rifamycin protects against paraquat-induced pulmonary fibrosis: activation of Nrf2 signaling pathway. *Biochem. Biophys. Res. Commun.* 490 (2), 535–540. doi:10.1016/j.bbrc.2017.06.074

Zhang, T., Lu, G., Zhao, Z., Liu, Y., Shen, Q., Li, P., et al. (2020). Washed microbiota transplantation vs. manual fecal microbiota transplantation: clinical findings, animal studies and in vitro screening. *Protein cell* 11 (4), 251–266. doi:10.1007/s13238-019-00684-8

Conflict of Interest: Faming Zhang invented the concept of GenFMTer and transendoscopic enteral tubing and related devices. Other authors declare that the research was conducted in the absence of any commercial or financial relationships that could be construed as a potential conflict of interest.

Copyright © 2021 Zhong, Cui, Xiang, Wu, Wen, Li and Zhang. This is an open-access article distributed under the terms of the Creative Commons Attribution License (CC BY). The use, distribution or reproduction in other forums is permitted, provided the original author(s) and the copyright owner(s) are credited and that the original publication in this journal is cited, in accordance with accepted academic practice. No use, distribution or reproduction is permitted which does not comply with these terms.

frontiers in Pharmacology

REVIEW
published: 08 February 2021
doi: 10.3389/fphar.2021.634344

Fructose and Non-Alcoholic Steatohepatitis

Elke Roeb[1]* *and Ralf Weiskirchen*[2]*

[1]Department of Gastroenterology, Justus Liebig University Giessen and University Hospital Giessen, Giessen, Germany, [2]Institute of Molecular Pathobiochemistry, Experimental Gene Therapy and Clinical Chemistry (IFMPEGKC), RWTH University Hospital Aachen, Aachen, Germany

Background: The excessive consumption of free sugars is mainly responsible for the high prevalence of obesity and metabolic syndrome in industrialized countries. More and more studies indicate that fructose is involved in the pathophysiology and also in the degree of disease of non-alcoholic fatty liver disease (NAFLD). In epidemiologic studies, energy-adjusted higher fructose consumption correlates with NAFLD in overweight adults. In addition to glucose, fructose, as an equivalent component of conventional household sugar, appears to have negative metabolic effects in particular due to its exclusive hepatic metabolism. Liver-related mortality is strictly associated with the degree of fibrosis, whereas the most common cause of death in patients suffering from NAFLD and non-alcoholic steatohepatitis (NASH) are still cardiovascular diseases. In this review article, we have summarized the current state of knowledge regarding a relationship between fructose consumption, liver fibrosis and life expectancy in NASH.

Method: Selective literature search in PubMed using the keywords 'non-alcoholic fatty liver', 'fructose', and 'fibrosis' was conducted.

Results: The rate of overweight and obesity is significantly higher in both, adult and pediatric NASH patients. The consumption of free sugars is currently three times the maximum recommended amount of 10% of the energy intake. The current literature shows weight gain, negative effects on fat and carbohydrate metabolism and NASH with hypercaloric intake of fructose.

Conclusions: Excessive fructose consumption is associated with negative health consequences. Whether this is due to an excess of energy or the particular metabolism of fructose remains open with the current study situation. The urgently needed reduction in sugar consumption could be achieved through a combination of binding nutritional policy measures including taxation of sugary soft drinks. Previous studies suggest that diet-related fructose intake exceeding the amount contained in vegetables and fruits lead to an increase of hepatic lipogenesis. Thus, further studies to clarify the protective contribution of low-fructose intake to positively influence NAFLD in industrial population are urgently required.

Keywords: non-alcoholic fatty liver, obesity, diabetes, lipogenesis, sugar, fructose, inflammation, fibrosis

OPEN ACCESS

Edited by:
Leo A van Grunsven, Vrije University Brussel, Belgium

Reviewed by:
Lindsey Devisscher, Ghent University, Belgium
Pedro Miguel Rodrigues, Biodonostia Health Research Institute, Spain

***Correspondence:**
Elke Roeb
Elke.Roeb@innere.med.uni-giessen.de
Ralf Weiskirchen
rweiskirchen@ukaachen.de

Specialty section:
This article was submitted to Gastrointestinal and Hepatic Pharmacology, a section of the journal Frontiers in Pharmacology

Received: *27 November 2020*
Accepted: *07 January 2021*
Published: *08 February 2021*

Citation:
Roeb E and Weiskirchen R (2021) Fructose and Non-Alcoholic Steatohepatitis. Front. Pharmacol. 12:634344. doi: 10.3389/fphar.2021.634344

INTRODUCTION

A positive energy balance and the consumption of free sugars are particularly the basis for the development of overweight and the metabolic syndrome. Fructose as a simple sugar occurs naturally in pome fruit (in apples and pears each about 6/100 g), berries (about 7.5/100 g), in exotic fruits (pomegranate and persimmon), and in honey (about 40/100 g) as well as in synthetic honey (US Food and Drug Administration, 2018). Table sugar normally is a double sugar, which is composed of one molecule each of glucose (grape sugar) and fructose. A significant proportion of the sugar intake nowadays comes from industrially manufactured foods that contain fructose-glucose syrup (i.e., high-fructose corn syrup). The term "free sugar" describes monosaccharides (glucose, fructose) and disaccharides (sucrose, table sugar) that either occur naturally in foods such as fruit and fruit juices or are added to industrially manufactured foods and beverages (US Food and Drug Administration, 2018).

The current WHO guideline recommends that free sugar should not be more than 10% of the total energy requirement of adults and children (Guideline, 2015). With an energy demand of 2000 kcal for an average adult, this would correspond to an amount of 50 g of sugar (17 sugar cubes ≈ 12 teaspoons of household sugar ≈ 500 ml of orange juice ≈ 5 oranges). A further reduction of free sugars to 5% of the estimated guide value of the total energy consumption to diminish the risk of dental caries is recommended by the WHO with limited informative value (Guideline, 2015; Schwingshackl et al., 2020). Children have a special role with regard to sugar intake, as they have an innate, evolutionarily advantageous preference for energy-dense and sweet foods (Rabenberg and Mensink, 2013). The uptake of sugar leads to an endogenous release of opioids, an effect that is used in pediatrics for painful procedures in newborns (Stevens et al., 2016; Gibbins and Stevens, 2001).

Both, prenatally and postnatally, exposure to certain flavors through amniotic fluid and breast milk has an influence on the development of taste preferences (Mennella et al., 2001; Nehring et al., 2015). In general, breast milk seems to have a positive effect on the diversity of food accepted by children due to the greater variety of flavors compared to infant formula (Fidler Mis et al., 2017). The individual sensitivity for sweets is also influenced by genetic polymorphisms of the taste receptors. The phenomenon of “flavor learning” in childhood was taken into account within the framework of the guideline of the ESPGHAN (European Society of Paediatric Gastroenterology, Hepatology and Nutrition), which recommends a maximum sugar intake of 5% of the overall energy requirement for children aged 2–18, corresponding to 16 g sugar (4 teaspoons) in a 4 year old boy. An even lower intake is recommended for children under 2 years of age, whose taste preference appears to be influenced more better (Fidler Mis et al., 2017). The actual proportion of free sugars in total energy intake is currently 13–14% for adults and 15–17.5% for children, and is thus still well above the maximum recommended amount (Schwingshackl et al., 2020; Bagus et al., 2016; Perrar et al., 2019). Sweets (34%) and fruit juices (22%) make up the main part of the intake of free sugars in childhood, but sugar-sweetened beverages also play a role, as they hardly lead to a feeling of satiety despite their high energy density contribute (Neuenschwander-Tetri, 2013). The intake of free sugars and sugary soft drinks correlates with a low socio-economic status (Rabenberg and Mensink 2013; Richter et al., 2012). The ‘German Health Interview and Examination Survey for Children and Adolescents‘ (KiGGS) study showed that children between 3 and 17 years of age consumed an average of two glasses (1 glass = 200 ml) of sugary drinks (juices, soft drinks, etc.) per day. Assuming a sugar content of around 10 g/100 ml of drink, this corresponds to around 40 g of free sugar or 160 kcal (Rabenberg and Mensink 2013; Ventura et al., 2011).

FRUCTOSE AND NON-ALCOHOLIC FATTY LIVER DISEASE

Fructose-rich diet forms can very quickly lead to almost all basic diseases of the metabolic syndrome. (Hannou et al., 2018). This medical condition is associated with trunk obesity, arterial hypertension, high serum sugar/impaired glucose tolerance (diabetes), elevated serum triglycerides, and reduced high-density lipoproteins (**Figure 1**).

Due to its hepatic metabolism, fructose is suspected to be partly responsible for the development of non-alcoholic fatty liver disease (NAFLD). Most prandial fructose is not metabolized in the intestine but rather passes via the portal vein to the liver (Brown et al., 1997). The term NAFLD includes on the one hand the potentially reversible NAFL (non-alcoholic fatty liver), defined by a fat content of more than 5% of the hepatic parenchymal surface, as well as NASH (non-alcoholic steatohepatitis) with additional mixed-cell inflammatory infiltrates. NAFLD is etiologically closely linked to the metabolic syndrome and hyperalimentation and can lead to liver cirrhosis and/or liver cancer, especially hepatocellular carcinoma (HCC) (Roeb et al., 2015). The prevalence of NAFLD is estimated at around 26% in industrialized nations and has been characterized by a particularly significant increase in the number of cases in recent years. From 18.9% for men and 22.5% for women in 1998, the prevalence increased to 23.3% and 23.9% respectively by 2010 (Lammert et al., 2019). Fructose is the main nutrient responsible for the fatty degeneration of the liver, which can significantly lead to excess hepatic energy and, moreover, to fatty liver cells. Partly controversial retrospective data indicate higher fructose consumption in NAFLD patients and an influence on the extent of liver fibrosis (**Figure 2**) (Ouyang et al., 2008; Mosca et al., 2017; Abdelmalek et al., 2010).

Animal experiments have shown that diets enriched in fructose (70% of total energy intake) compared with a high glucose content show significant histological fatty liver disease and laboratory signs of liver cell damage (Jürgens et al., 2005; Kawasaki et al., 2009; de Castro et al., 2013). A prospective case-control study also found a connection between increased consumption of soft drinks and NAFLD (Abid et al., 2009). The enhanced intake of sugar and fructose is of great importance for the simple steatosis but also for the progression to severe forms of nonalcoholic fatty liver disease

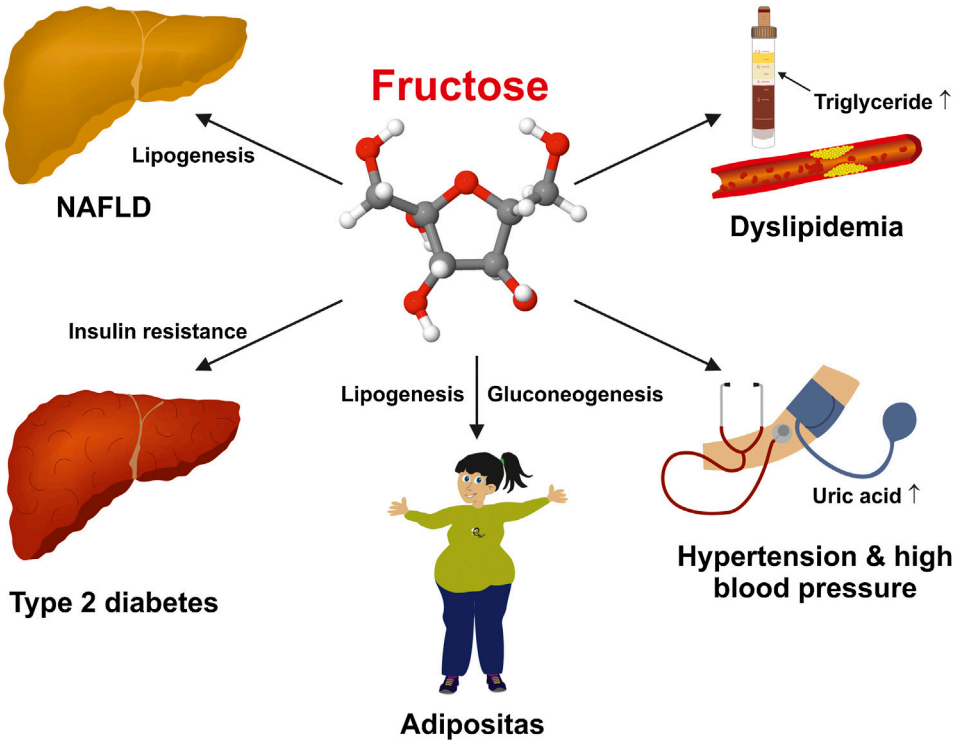


FIGURE 1 | Deleterious effects of a high fructose intake on human health. Excessive fructose consumption is a risk factor for several chronic diseases including non-alcoholic fatty liver disease (NAFLD), obesity, dyslipidemia, insulin resistance/diabetes type 2, arterial hypertension, and hyperuricemia.

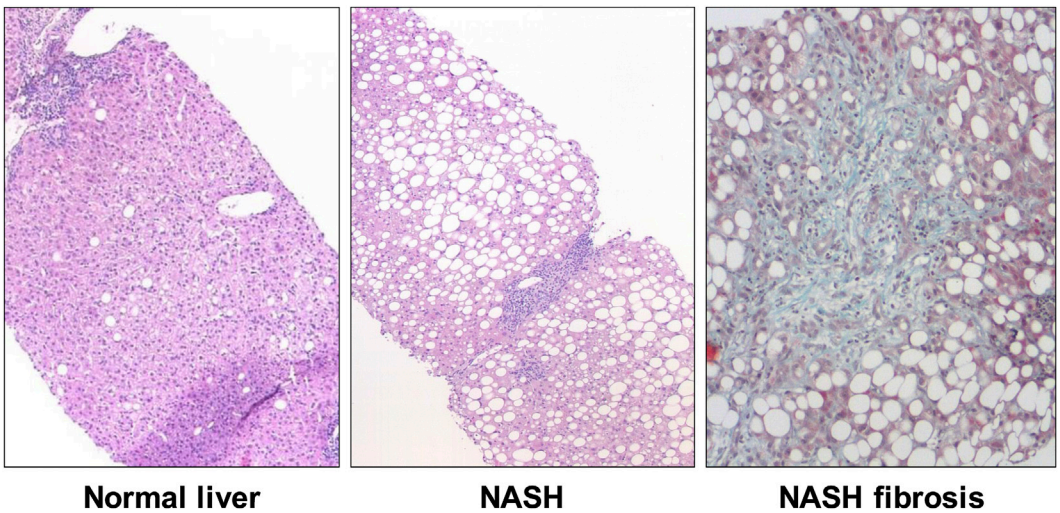


FIGURE 2 | Histopathology of nonalcoholic steatohepatitis (NASH). Compared to normal liver **(left)**, histologic features of NASH include steatosis, ballooning, and lobular inflammation **(middle)**. Although not a requirement for the histological diagnosis NASH, fibrosis is often paired with the pathological changes **(right)**.

(NAFLD), such as nonalcoholic steatohepatitis (NASH), fibrosis (NASH fibrosis), and hepatocellular carcinoma (Lim et al., 2010). The aim of the present review is a compilation of the current data that support the importance of fructose intake for the development of liver fibrosis and life expectancy in NASH.

METHODS

A selective literature search in PubMed using the keywords 'non-alcoholic fatty liver', 'fructose', and 'fibrosis' was conducted at the beginning of December 2020. Using these search teams, a total of

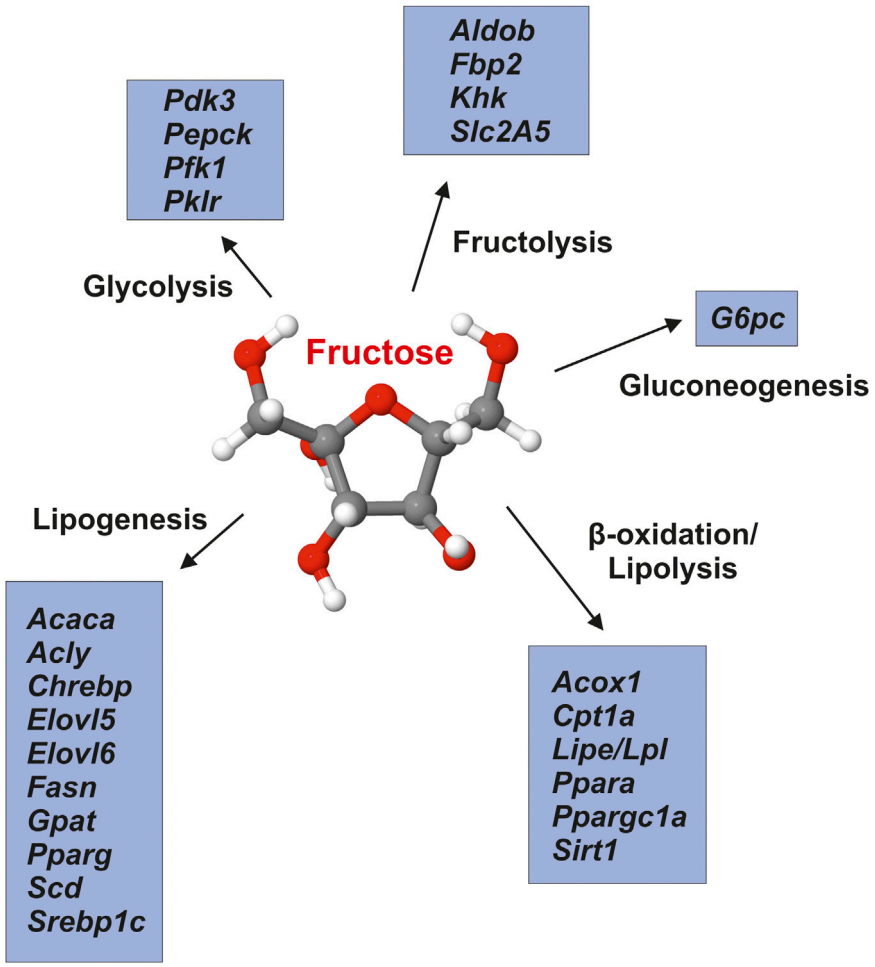


FIGURE 3 | Fructose impacts hepatic energy metabolism. Fructose modulates the expression of a large number of genes that are involved in regulation of glycolysis, lipogenesis, β-oxidation/lipolysis, fructolysis and gluconeogenesis. Gene symbols (in alphabetical order) correspond to: *Acaca*, acetyl-CoA carboxylase-α; *Acly*, ATP citrate lyase; *Acox1*, acyl-coenzyme A oxidase one; *Aldob*, aldolase B; *Chrebp*, carbohydratre response element-binding protein; *Cpt1a*, carnitine palmitoyltransferase 1 (isoform a); *Elovl5*, elongation of very long chain fatty acids-like five; *Elovl6*, elongation of very long chain fatty acids-like six; *Fasn*, fatty acid synthase; *Fbp2*, fructose-1,6-bisphosphatase two; *G6pc*, glucose-6-phosphatase; *Gpat*, glycerol-3-phosphate acyltransferase (mitochondrial); *Khk*, ketohexokinase; *Lipe/Lpl*, lipase/lipoprotein lipase; *Pdk3*, pyruvate dehydrogenase kinase, isoenzyme three; *Pepck*, phosphoenolpyruvate carboxykinase one; *Pfk1*, phosphofructokinase (muscle type); *Pklr*, pyruvate kinase (liver and red blood cell); *Ppara*, peroxisome proliferation-activated receptor-α; *Pparg*, peroxisome proliferation-activated receptor-γ; *Ppargc1a*, peroxisome proliferation-activated receptor-γ coactivator 1-α; *Scd*, stearoyl-Coa desaturase; *Sirt1*, sirtuin one; *Slc2A5*, solute carrier family 2 (facilitated glucose/fructose transporter) member five; *Srebp1c*, sterol regulatory element-binding transcription factor 1 (isoform c). Adapted from (DiStefano 2020).

135 publications were detected. After excluding pure *in vitro* trials and animal experiments, 35 publications were finally used for this review.

ASSOCIATION OF FRUCTOSE AND NON-ALCOHOLIC FATTY LIVER DISEASE

Two meta-analyses dealt with the connection between fructose consumption and fatty liver disease. In 2014 Chiu et al. as well as Chung et al. were unable to demonstrate any effect of fructose on the intrahepatocellular fat content and the alanine aminotransferase level in studies in which fructose was used in an isocaloric exchange with other carbohydrates, while the hypercaloric intake of fructose negatively affects both parameters (Chiu et al., 2014; Chung et al., 2014). The findings of these studies suggest that the study situation is sometimes controversial. However, a high fructose consumption, which is accompanied by an excess of energy, seems to be associated with increased plasma glucose and triglyceride levels and significantly contributes to hepatic steatosis (Ter Horst and Serlie 2017). The extent to which fat as a macronutrient contributes to the development of NAFLD as well as the effects of high carbohydrate intake is the subject of current research.

According to the experimental studies carried out so far, fructose acts as nutritional regulator impacting the expression of many genes engaged in fructolysis, *de novo* lipogenesis, gluconeogenesis, glycolysis, and lipolysis (e.g., fatty acid

TABLE 1 | Fructose in different foods.

Food	Glucose	Fructose
	Grams per 100 g of food	Grams per 100 g of food
Apple	3.4	6.9
Artichoke	0.8	1.7
Banana	7.4	7.2
Broccoli	0.7	1.1
Butter	0.0	0.0
Carrot	2.5	2.4
Cashew	3.0	2.9
Cauliflower	1.0	0.9
Chard	0.3	0.4
Chicken meat	0.0	0.0
Chicory	1.5	0.9
Cola	5.0	5.0
Corn	3.1	2.9
Cranberry	3.3	0.7
Cucumber	0.8	0.9
Currant red	3.5	3.8
Dates	**34.0**	**31.0**
Egg yolk	0.2	0.0
Fennel	1.5	1.3
figs	7.2	5.9
Grapes	7.3	8.2
Herring	0.0	0.0
Honey	**35.2**	**40.2**
Honeydew melon	3.9	4.2
Kale	1.2	1.4
Kiwi	5.1	5.2
Kohlrabi	1.9	1.8
lamb's lettuce	0.5	0.3
Leek	1.7	1.5
Lemon	1.2	1.1
Lentils	0.7	1.0
Mango	5.5	8.2
Milk	0.0	0.0
Oats	0.4	0.4
Orange	4.3	4.4
Papaya	2.9	3.0
Paprika red	2.7	3.0
Pasta	0.1	0.1
Peach	4.1	4.0
Peanuts	1.3	1.3
Pear	2.8	7.2
Peas	3.1	3.1
Pineapple	4.7	5.1
Plum	3.9	5.2
Pomegranate	7.9	8.5
Potato	0.5	0.4
Protein	0.4	0.0
Pumpkin	1.1	0.8
Raisins	**31.2**	**31.6**
Raspberry	2.5	3.1
Rice	0.1	0.1
Salad	0.5	0.6
Salmon	0.0	0.0
Savoy	2.0	1.8
Sunflower seeds	1.4	1.4
Sweet cherry	13	12
Tomatoes	1.2	1.5
Trout	0.0	0.0

Indicated is the total fructose and glucose content, which always includes free fructose and half the sucrose value. The values in this table are calculated from mean values according to (Souci et al., 2016).

oxidation) by mechanisms associated with transcriptome analysis and epigenetic (**Figure 3**). We suspect that these effects of fructose intake are related to the respective nutritional status and gender of the test subjects. These effects persist in spite of fructose reduction, are passed on from mothers with high fructose consumption to their offspring and might influence the hepatic fat metabolism long before obesity and insulin resistance occur (DiStefano 2020). An important regulator of cholesterol metabolism showed decreased gene expression in males from fructose-fed mothers. In accordance Liver X-receptor gene promoter methylation was increased in males from fructose-fed mothers. Thus, maternal fructose intake produces a fetal programming that influences transcription epigenetically, and both hepatic mRNA gene expression and plasma parameters of cholesterol metabolism in adult progeny (Rodrigo et al., 2018).

The association between high fructose intake and obesity has led to analyze fructose and its impact on NAFLD. The consumption of sucrose and high fructose corn syrup rose exponentially about 1,000% during 1970 and 2010 and makes up to 10% of the calories in the daily diet (Abdelmalek et al., 2010). Of 60 ultrasound-proven NAFLD patients, 80% had an excessive soft drink intake compared to 17% of healthy controls. In this same study, NAFLD subjects consumed five times more carbohydrates from soft drinks compared to controls (Abid et al., 2009). Thus, regular soft drink consumption seems to be a predictor of NAFLD and the metabolic syndrome with hypertriglyceridemia, pathological glucose tolerance in liver, weight gain, and insulin resistance (Nseir et al., 2010). High fructose concentrations were found in dates, honey, raisins, and sweet cherries as well as in cola (see **Table 1**).

In adults with NAFLD, daily fructose ingestion was associated with reduced hepatic steatosis but increased fibrosis (Abdelmalek et al., 2010). In addition, Abdelmalek et al. stated that in older patients, e.g., in adults age > or = 48 years, a daily fructose consumption was associated with histologically proven significant increased hepatic inflammation and hepatocyte ballooning. Even in healthy adult men high-fructose intake was associated with increased DNL and liver fat in healthy men fed weight-maintaining diets (Schwarz et al., 2015).

THE WAY HOW FRUCTOSE INFLUENCES NON-ALCOHOLIC FATTY LIVER DISEASE

The individual diet is highly relevant for the development of NAFLD and both, risky (e.g., fructose) and protective eatables (Mediterranean diet), have been identified, but the contribution of exorbitant calories remains crucial (Marchesini et al., 2016). Fructose metabolism in the liver is not a tightly regulated biochemical pathway in contrast to glycolysis, where the rate-limiting enzyme phosphofructokinase, is present (Nd 2019). Fructose consumption enables disturbances of metabolic pathways that might result in excessive hepatic fat accumulation. As a central organ involved in regulating energy homeostasis, the liver coordinates interactions with other organs that are critical for the maintenance of energy homeostasis. Dietary sugars such as fructose move from the small intestine

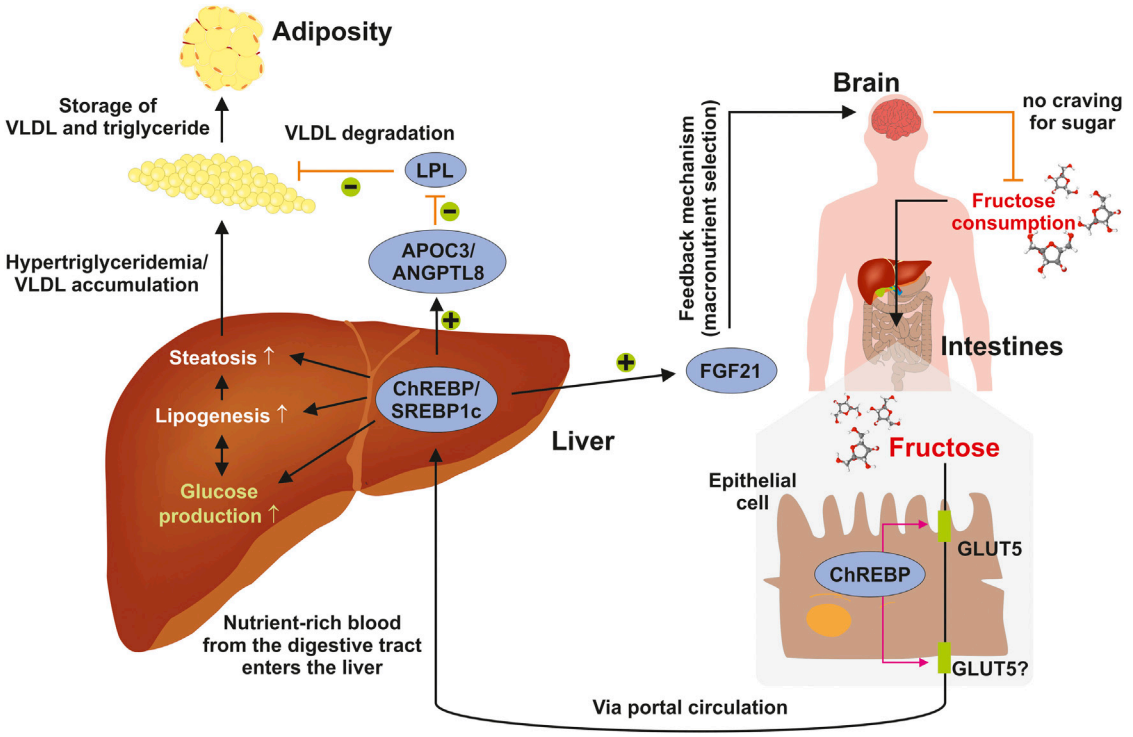


FIGURE 4 | Elevated fructose intake trigger fatty liver disease. Consumed sugar such as fructose moves from the intestinal lumen to the blood circulation through a facilitated passive transport across the apical border of enterocytes using the facilitative glucose/fructose transporter GLUT5. It is then transported into the liver through the hepatic portal vein. In the liver fructose is metabolized to glucose and drives lipid synthesis resulting in steatosis, elevated concentrations of triglycerides, and adiposity. Under physiological conditions, these processes are tightly regulated finely adjusted in crosstalk with the brain, which integrates signals impacting food intake, energy expenditure, insulin secretion, hepatic glucose production, and fatty acid metabolism. For details see text. Abbreviations used are: APOC3, apolipoprotein C-III; ANGPTL8, angiopoietin-like eight; FGF21, fibroblast growth factor 21; VLDL, very low density lipoprotein. Adapted from (Hannou et al., 2018).

into the blood circulation by means of a passive transport process throughout the apical border of enterocytes that is triggered by members of the facilitative glucose/fructose transporter (GLUT) family such as GLUT5 (Merino et al., 2019) (**Figure 4**). Thereafter, the sugar is transported toward the liver via the hepatic portal vein where it activates the production of glucose and lipid synthesis. Increased hepatic lipogenesis results in steatosis and elevated concentrations of triglycerides that on long-term give cause to adiposity. Under physiological conditions, these processes are tightly regulated. Chronic fructose consumption leads to activation of the sterol regulatory element-binding protein 1c (SREBP1c) and the carbohydrate-responsive element-binding protein (ChREBP) that in turn provokes the expression of the liver-derived hormone fibroblast growth factor 21 (FGF21) regulating energy homeostasis and protecting the liver from fructose-induced metabolic disease (Hannou et al., 2018). Moreover, ChREBP transactivates expression of the apolipoprotein C-III (APOC3) and angiopoietin-like 8 (ANGPTL8), which both lower the activation of lipoprotein lipase (LPL) and limit the clearance of very low density lipoproteins (VLDL) (Hannou et al., 2018). The metabolic activity of the liver is further modulated in crosstalk with the brain, which modulates different aspects of metabolism, including food ingestion, energy consumption, insulin secretion, glucose metabolism, and fatty acid production in adipose tissue (Roh et al., 2016).

Taken together fructose seems to functions as both, as a substrate and as an inducer of hepatic *de novo* lipogenesis (DNL) (Jegatheesan and De Bandt, 2017). Fructose absorbed from the portal blood into the liver cells is converted to fructose-1-phosphate by fructokinase and thereby activated for further metabolic steps. Fructose-1-phosphate is split into D-glyceraldehyde and dihydroxyacetone phosphate by the liver-specific fructose-1,6-diphosphate aldolase. The latter can be broken down further via the corresponding reaction of glycolysis or used for gluconeogenesis. Thus, fructose can be broken down into pyruvate more quickly than glucose since the rate-limiting reactions of glycolysis (glucokinase and phosphofructokinase reaction) are bypassed (Jegatheesan and De Bandt, 2017). By saturating the glycolytic pathway, high fructose intake might result in an accumulation of glycolysis intermediates which can be converted to glycerol-3-phosphate used in triglyceride (TG) synthesis. Excessive consumption of fructose, however, might additionally induce the deterioration of the intestinal barrier and induce inflammation (Kawabata et al., 2019). Very recently it was shown that fructose-elicited endotoxaemia activates Toll-like receptor (TLR) signaling in liver macrophages, a process that could be blocked

experimentally. To prove that hypothesis in a murine model, the restoration of barrier function was associated with reduced DNL and reduced hepatosteatosis, attenuated HCC formation and minor expression of lipogenic and inflammatory genes. In addition, an antimicrobial peptide prevented fructose-induced NAFLD (Todoric et al., 2020).

Also Lambertz et al. reviewed that fructose ingestion provokes a transformation of the gut microbiome, leading to leaky gut with enhanced permeability of the intestinal barrier, hepatic inflammation, increasing insulin resistance and - last but not least - liver fibrosis (Lambertz et al., 2017). In addition, they discuss fructose-associated changes of tight junction proteins affecting the intestinal permeability, thus resulting in an entry of bacteria and bacterial endotoxins into the blood stream. A cross-sectional epidemiological study has associated fructose uptake to the degree of hepatic fibrosis, eg fibrosis grade, in fatty liver disease. Clinical trials revealed that ingestion of fructose-containing beverages, with either fructose or sucrose, contribute to the development of NAFLD in comparison to isocaloric alternative soft drinks. In addition genetic polymorphisms increasing the uptake of glucose into lipogenic pathways are associated with NAFLD (Neuschwander-Tetri 2013). Moreover, Silbernagel et al. detected a correlation of visceral and liver fat content with cholesterol synthesis even in wholesome humans. In addition, they showed that cholesterol synthesis seems to depend on the uptake of fructose and glucose. (Silbernagel et al., 2012). However, prospective multicenter studies analyzing whether marked transformations of hepatic fat amount will influence cholesterol homeostasis are still missing.

Fructose intake increased hepatic *de novo* lipogenesis, and lipoprotein lipase activity was downregulated postprandial in humans consuming fructose in comparison with subjects consuming glucose. The authors conclude that increased *de novo* lipogenesis as well as decreased lipoprotein lipase-mediated clearance are part of the fructose-induced postprandial hypertriglyceridemia (Stanhope et al., 2009). Some years later, fructose was proposed as a key player in the formation of NAFLD (Basaranoglu et al., 2013). High-fructose corn syrup in soft drinks and other carbohydrate-sweetened beverages is a blend that is typically composed of 55% fructose, 41% glucose, and 4% complex polysaccharides. A higher intake of these beverages meaning enhanced fructose consumption has been associated with obesity, type 2 diabetes, and NAFLD in the USA. Thus, fructose provokes hepatic stress, phosphorylation of JNK and finally reduced hepatic insulin signaling (Basaranoglu et al., 2013). Moreover, it is indisputable that fructose decreases insulin sensitivity, and increases visceral adiposity in overweight/obese adults. But how does it work in lean subjects with NAFLD?

'LEAN NAFLD' SUBJECTS

The term 'lean NAFLD' quotes to liver steatosis in slim patients or patients of normal weight, according to the per region-specific body mass index (BMI). Similar to the pathogenesis of NAFLD in obese persons, fructose consumption may also be important in the development of NAFLD in leans (Kumar and Mohan, 2017). Soft drink consumption for example seems to be associated with NAFLD in the absence of conventional risk factors (Assy et al., 2008). Independent of the diagnosis metabolic syndrome, NAFLD patients displayed higher soft drink consumption in a study published by Abdi and coworkers (Abid et al., 2009). In particular the study revealed that the NAFLD patients ingested five times as much carbohydrates in soft drinks in comparison to healthy controls (40% vs. 8%, $p < 0.001$). About 7% of patients just drank one soft drink daily, over 50% consumed two to three soft drinks per day, and 38% had more than four soft drinks per day for most days within a half year. The most popular drink was Coca-Cola (regular: 32%; diet: 21%), the second most popular fruit juices (47%) (Abid et al., 2009). **Table 1** gives an overview of the fructose content of various fruits and fruit juices.

On the other hand, patients with fructose 1-phosphate aldolase B deficiency characterized by hereditary fructose intolerance also exhibit increased intrahepatic triglyceride accumulation suggesting that both the increasing concentration of fructose-1-phosphate and the derogation of β-oxidation seem to be involved in NAFLD pathogenesis. In patients with this inborn error, a higher intrahepatic triglyceride concentration with regard to controls was associated with impaired glucose tolerance. The accumulation of intermediates of fructolysis might cause intrahepatic triglyceride accumulation via impaired β-oxidation (Simons et al., 2019).

NO HINTS FOR NEGATIVE EFFECTS OF FRUCTOSE

We don't want to conceal that there are other statements to fructose consumption in men. Three review articles argue indeed against any negative effects of fructose on human health (Tappy and Lê 2010; Rippe et al., 2017; White 2013). In addition, there is no concrete evidence that fructose consumption in normal ranges has serious consequences (Tappy and Lê 2012). Whether ingestion of smaller amounts of fructose over longer time periods stimulates *de novo* lipogenesis or increases intrahepatic fat concentration has not been circumstantiated in epidemiological studies and has to be assessed (Tappy and Lê 2012).

The ingestion of fruits and vegetables seems to represent a protection for various diseases, such as type 2 diabetes. In addition fruits and vegetables were correlated with a lower risk of overall and cardiovascular disease (Wang et al., 2016). In an interventional clinical trial in order to unravel the pathogenetic mechanisms of fructose in comparison to glucose consumption Smajis et al. demonstrated that the consumption of a high dose of fructose over 8 weeks had no influence on important metabolic consequences in case of a stable energy intake, slightly lower body weight, and potentially incomplete absorption of the ingested fructose (Smajis et al., 2020). Thus, young and healthy humans

might at least for a short time period be able to compensate a higher fructose intake.

LIPOGENIC MARKERS AND TRIACYLGLYCEROL SYNTHESIS

Liver fibrosis induced by a high fructose intake was associated with increased body weight, hunger-satiety system dysregulation, increased insulin concentration, dysregulated lipid metabolism, lipoperoxidation and inflammation. In addition, enhanced levels of hepatic glucose-6-phosphate dehydrogenase (G6PD) and malic enzyme activity, the NAD(*p*)H/NAD(*p*)$^+$ ratios, the reduced glutathione concentration and increased expression of lipogenic and fibrotic markers were described. All these changes were reduced by the application of nicotinamide (Loza-Medrano et al., 2020). Specifically, nicotinamide reduced the activity and expression of G6PD and malic enzyme. This finding was associated with a reduction of the NADPH/NADP$^+$ ratios, rising GSH levels and decreased lipoperoxidation and inflammation, improving fibrosis and NASH development. The manipulation of NADPH-producing enzymes was attended by the antifibrotic, antioxidant and antilipemic effects of nicotinamide (Loza-Medrano et al., 2020).

Diacylglycerol acyltransferase (DGAT)1 and DGAT2, catalyze the final step of triglyceride synthesis (Harris et al., 2011). A recent study indicates that hepatic DGAT2 deficiency leads to a reduction of diet-induced hepatic steatosis, thus supporting the application of DGAT2 inhibitors as a therapeutic approach to ameliorate NAFLD and associated diseases (Gluchowski et al., 2019). Based on these findings, the inhibition of DGAT2 is regarded as a promising therapeutic approach for NAFLD/NASH in humans.

During cholestasis, the expression of genes encoding proteins involved in triacylglycerol (TAG) synthesis and *de novo* lipogenesis (*AGPAT1*, *GPAT1*, *MGAT1*, *DGAT1*, *DGAT2*, *FASN*, *HMGCS*1, *ACC1*, *SREBP1c*, and *PPARγ*) was downregulated (Irungbam et al., 2020). The reduced expression of *AGPAT1*, *GPAT1*, *MGAT1*, and *DGAT2* implicated that FFAs cannot be utilized for TAG synthesis. But increased free fatty acid (FFA) levels in parallel with reduction a of TAG synthesis and accumulation along with increased lipolysis during cholestasis seems to facilitate the acceleration of liver injury (Zahner et al., 2017).

INTERVENTION AND THERAPEUTIC APPROACHES IN NON-ALCOHOLIC FATTY LIVER DISEASE

Presently, there is no approved pharmacologic therapy to universally treat NAFLD. However, intensive lifestyle modifications such as drinking of unsweetened coffee and avoiding fructose corn syrup are reasonable specific dietary recommendation for patients suffering from NAFLD (Malhotra and Beaton 2015). Mediterranean diets high in vegetables, fish, nuts, grains, fruits, and olive oil enriched with unsaturated fats have been shown to beneficially effect or negatively correlate with NAFLD. In contrast, consumption of a typical Western diet, which includes soft drinks, fructose, red meat and saturated fatty acids predispose for NAFLD development (Zelber-Sagi et al., 2017). Short-term interventions by macronutrient manipulations might influence hepatic steatosis illustrating both pro- and anti-steatitic effects. In line, macronutrient manipulations that restrict uptake of carbohydrates and saturated fatty acids are reported to have efficacious effects (Stokes et al., 2019). A detailed literature review focusing on established principal has developed five key dietary recommendations including 1) traditional dietary patterns such as the Mediterranean diet, 2) limiting of excess fructose consumption and processed foods and beverages enriched in fructose, 3) replacement of dietary saturated fatty acids by long-chain omega-3 rich foods and monounsaturated fatty acids, 4) substitution of processed food, fast food, commercial bakery goods, and sweets by unprocessed or minimally processed foods that are high in fiber, including whole grains, vegetables, fruits, legumes, nuts, and seeds, and finally 5) reduction of excess alcohol consumption (George et al., 2018). Consequently, NAFLD incidence and progression is significantly reduced by improving diet quality following these guidelines. It is supposed that these benefits result from the collective effect of dietary patterns rather than from one single measure (George et al., 2018).

There is also clear evidence that regular exercise is beneficial to reduce the overall hepatic lipid content. In particular, diverse studies have shown that vigorous-intensity exercise is inversely correlated with NAFLD severity (Schon and Weiskirchen, 2016). This was particularly demonstrated in a study that enrolled more than 5,700 participants and found a dose-response relationship between physical activity and the occurrence of NAFLD (Kalathiya et al., 2015). Moreover, some clinical studies have demonstrated that short-term exercise, when conducted regularly, is already sufficient to reduce hepatocyte apoptosis in obese patients suffering from NAFLD by improving insulin sensitivity and restoration the general oxidative capacity, suggesting that active lifestyle and caloric restriction are beneficial in decreasing histological signs of fatty liver disease (Schon and Weiskirchen, 2016).

CONCLUSION

NAFLD representing a form of chronic hepatitis is one of the most important and rising causes of liver disease worldwide. Respective patients have a high frequency of metabolic comorbidities such as obesity, impaired insulin resistance and dyslipidemia. Presently, there are only limited treatment options. The current standard of care for NAFLD patients is the limitation and control of risk factors and the advice to follow recommendations for lifestyle changes. In particular, weight loss provoked by dietary restriction and regular physical exercise can be beneficial in regress of liver disease. A Mediterranean diet can significantly reduce liver fat mass even

without weight loss and is most recommended. However, there are also a substantial proportion of lean patients with NAFLD. The consumption of unsweetened coffee, reduction in fructose intake, and the avoidance of foods enriched in saturated fats are reasonable specific dietary recommendations for NAFLD and NASH patients. Sedentary activity patterns contribute as well as ingestion of low amounts of polyunsaturated fatty acid to NAFLD and metabolic syndrome. But in the case of a diverse diet, it is very difficult to emphasize the importance of one single nutrient. Thus, high-quality basic research and well-defined randomized clinical trials assessing dietary interventions that focus on liver-specific endpoints-are urgently needed as a priority.

AUTHOR CONTRIBUTIONS

All authors listed have made a substantial, direct, and intellectual contribution to the work and approved it for publication.

FUNDING

ER received grants from the German Research Foundation DFG (RO 957/10-1, RO 957/11-1), von-Behring-Roentgen Foundation (#58-0005 and #66-0008 to ER), University Medical Center Giessen and Marburg (UKGM) (#10 and #21_2013 GI to ER). RW is supported by grants from the German Research Foundation (SFB/TRR57 and WE 2554/15-1) and the Interdisciplinary Centre for Clinical Research within the Faculty of Medicine at the RWTH Aachen University (IZKF Aachen, project O3-1). The funders had no role in the design of this review or in the decision to publish it.

ACKNOWLEDGMENTS

The authors are grateful to Sabine Weiskirchen (IFMPEGKC) who prepared the figures for this review.

REFERENCES

Abdelmalek, M. F., Suzuki, A., Guy, C., Unalp-Arida, A., Colvin, R., Johnson, R. J., et al. (2010). Increased fructose consumption is associated with fibrosis severity in patients with nonalcoholic fatty liver disease. *Hepatology* 51 (6), 1961–1971. doi:10.1002/hep.23535

Abid, A., Taha, O., Nseir, W., Farah, R., Grosovski, M., and Assy, N. (2009). Soft drink consumption is associated with fatty liver disease independent of metabolic syndrome. *J. Hepatol.* 51 (5), 918–924. doi:10.1016/j.jhep.2009.05.033

Assy, N., Nasser, G., Kamayse, I., Nseir, W., Beniashvili, Z., Djibre, A., et al. (2008). Soft drink consumption linked with fatty liver in the absence of traditional risk factors. *Can. J. Gastroenterol.* 22 (10), 811–816. doi:10.1155/2008/810961

Bagus, T., Roser, S., and Watzl, B. (2016). Reformulierung von verarbeiteten lebensmitteln bewertungen und empfehlungen zur reduktion des zuckergehalts. Available at: https://www.mri.bund.de/fileadmin/MRI/Themen/Reformulierung/Reformulierung_Thema-Zucker.pdf.

Basaranoglu, M., Basaranoglu, G., Sabuncu, T., and Sentürk, H. (2013). Fructose as a key player in the development of fatty liver disease. *World J. Gastroenterol.* 19 (8), 1166–1172. doi:10.3748/wjg.v19.i8.1166

Brown, K. S., Kalinowski, S. S., Megill, J. R., Durham, S. K., and Mookhtiar, K. A. (1997). Glucokinase regulatory protein may interact with glucokinase in the hepatocyte nucleus. *Diabetes* 46 (2), 179–186. doi:10.2337/diab.46.2.179

Chiu, S., Sievenpiper, J. L., de Souza, R. J., Cozma, A. I., Mirrahimi, A., Carleton, A. J., et al. (2014). Effect of fructose on markers of non-alcoholic fatty liver disease (NAFLD): a systematic review and meta-analysis of controlled feeding trials. *Eur. J. Clin. Nutr.* 68 (4), 416–423. doi:10.1038/ejcn.2014.8

Chung, M., Ma, J., Patel, K., Berger, S., Lau, J., and Lichtenstein, A. H. (2014). Fructose, high-fructose corn syrup, sucrose, and nonalcoholic fatty liver disease or indexes of liver health: a systematic review and meta-analysis. *Am. J. Clin. Nutr.* 100 (3), 833–849. doi:10.3945/ajcn.114.086314

de Castro, U. G., dos Santos, R. A., Silva, M. E., de Lima, W. G., Campagnole-Santos, M. J., and Alzamora, A. C. (2013). Age-dependent effect of high-fructose and high-fat diets on lipid metabolism and lipid accumulation in liver and kidney of rats. *Lipids Health Dis.* 12, 136. doi:10.1186/1476-511X-12-136

DiStefano, J. K. (2020). Fructose-mediated effects on gene expression and epigenetic mechanisms associated with NAFLD pathogenesis. *Cell. Mol. Life Sci.* 77 (11), 2079–2090. doi:10.1007/s00018-019-03390-0

Fidler Mis, N., Braegger, C., Bronsky, J., Campoy, C., Domellöf, M., Embleton, N. D., et al. (2017). ESPGHAN committee on nutrition:. Sugar in infants, children and adolescents: a position paper of the European society for paediatric Gastroenterology, Hepatology and nutrition committee on nutrition. *J. Pediatr. Gastroenterol. Nutr.* 65 (6), 681–696. doi:10.1097/MPG.0000000000001733

George, E. S., Forsyth, A., Itsiopoulos, C., Nicoll, A. J., Ryan, M., Sood, S., et al. (2018). Practical dietary recommendations for the prevention and management of nonalcoholic fatty liver disease in adults. *Adv. Nutr.* 9 (1), 30–40. doi:10.1093/advances/nmx007

Gibbins, S., and Stevens, B. (2001). Mechanisms of sucrose and non-nutritive sucking in procedural pain management in infants. *Pain Res. Manag.* 6 (1), 21–28. doi:10.1155/2001/376819

Gluchowski, N. L., Gabriel, K. R., Chitraju, C., Bronson, R. T., Mejhert, N., Boland, S., et al. (2019). Hepatocyte deletion of triglyceride-synthesis enzyme acyl CoA: diacylglycerol acyltransferase 2 reduces steatosis without increasing inflammation or fibrosis in mice. *Hepatology* 70 (6), 1972–1985. doi:10.1002/hep.30765

Guideline, W. H. O. (2015). *Sugars intake for adults and children*. Geneva, Switzerland: World Health Organization.

Hannou, S. A., Haslam, D. E., McKeown, N. M., and Herman, M. A. (2018). Fructose metabolism and metabolic disease. *J. Clin. Invest.* 128 (2), 545–555. doi:10.1172/JCI96702

Harris, C. A., Haas, J. T., Streeper, R. S., Stone, S. J., Kumari, M., Yang, K., et al. (2011). DGAT enzymes are required for triacylglycerol synthesis and lipid droplets in adipocytes. *J. Lipid Res.* 52 (4), 657–667. doi:10.1194/jlr.M013003

Irungbam, K., Roderfeld, M., Glimm, H., Hempel, F., Schneider, F., Hehr, L., et al. (2020). Cholestasis impairs hepatic lipid storage via AMPK and CREB signaling in hepatitis B virus surface protein transgenic mice. *Lab. Invest.* 100 (11), 1411–1424. doi:10.1038/s41374-020-0457-9

Jegatheesan, P., and De Bandt, J. P. (2017). Fructose and NAFLD: the multifaceted aspects of fructose metabolism. *Nutrients* 9 (3), 230. doi:10.3390/nu9030230

Jürgens, H., Haass, W., Castañeda, T. R., Schürmann, A., Koebnick, C., Dombrowski, F., et al. (2005). Consuming fructose-sweetened beverages increases body adiposity in mice. *Obes. Res.* 13 (7), 1146–1156. doi:10.1038/oby.2005.136

Kalathiya, R., Aneni, E. C., Martin, S. S., Blaha, M. J., Feldman, T., Agatston, A. S., et al. (2015). Relation of physical activity to prevalence of nonalcoholic Fatty liver disease independent of cardiometabolic risk. *Am. J. Cardiol.* 115 (1), 34–39. doi:10.1016/j.amjcard.2014.09.044

Kawabata, K., Kanmura, S., Morinaga, Y., Tanaka, A., Makino, T., Fujita, T., et al. (2019). A high-fructose diet induces epithelial barrier dysfunction and exacerbates the severity of dextran sulfate sodium-induced colitis. *Int. J. Mol. Med.* 43 (3), 1487–1496. doi:10.3892/ijmm.2018.4040

Kawasaki, T., Igarashi, K., Koeda, T., Sugimoto, K., Nakagawa, K., Hayashi, S., et al. (2009). Rats fed fructose-enriched diets have characteristics of nonalcoholic hepatic steatosis. *J. Nutr.* 139 (11), 2067–2071. doi:10.3945/jn.109.105858

Kumar, R., and Mohan, S. (2017). Non-alcoholic fatty liver disease in lean subjects: characteristics and implications. *J. Clin. Transl. Hepatol.* 5 (3), 216–223. doi:10.14218/JCTH.2016.00068

Lambertz, J., Weiskirchen, S., Landert, S., and Weiskirchen, R. (2017). Fructose: A dietary sugar in crosstalk with microbiota contributing to the development and progression of non-alcoholic liver disease. *Front. Immunol.* 8, 1159. doi:10.3389/fimmu.2017.01159

Lammert, F., Lynen Jansen, P., and Lerch, M. M. (2019). *Weissbuch Gastroenterologie 2020/21: erkrankungen des Magen-Darm-Traktes, der Leber und der Bauchspeicheldrüse - gegenwart und Zukunft*. Berlin, Germany: De Gruyter.

Lim, J. S., Mietus-Snyder, M., Valente, A., Schwarz, J. M., and Lustig, R. H. (2010). The role of fructose in the pathogenesis of NAFLD and the metabolic syndrome. *Nat. Rev. Gastroenterol. Hepatol.* 7 (5), 251–264. doi:10.1038/nrgastro.2010.41

Loza-Medrano, S. S., Baiza-Gutman, L. A., Manuel-Apolinar, L., García-Macedo, R., Damasio-Santana, L., Martínez-Mar, O. A., et al. (2020). High fructose-containing drinking water-induced steatohepatitis in rats is prevented by the nicotinamide-mediated modulation of redox homeostasis and NADPH-producing enzymes. *Mol. Biol. Rep.* 47 (1), 337–351. doi:10.1007/s11033-019-05136-4

Malhotra, N., and Beaton, M. D. (2015). Management of non-alcoholic fatty liver disease in 2015. *World J. Hepatol.* 7 (30), 2962–2967. doi:10.4254/wjh.v7.i30.2962

Marchesini, G., Petta, S., and Dalle Grave, R. (2016). Diet, weight loss, and liver health in nonalcoholic fatty liver disease: pathophysiology, evidence, and practice. *Hepatology* 63 (6), 2032–2043. doi:10.1002/hep.28392

Mennella, J. A., Jagnow, C. P., and Beauchamp, G. K. (2001). Prenatal and postnatal flavor learning by human infants. *Pediatrics* 107 (6), E88. doi:10.1542/peds.107.6.e88

Merino, B., Fernández-Díaz, C. M., Cózar-Castellano, I., and Perdomo, G. (2019). Intestinal fructose and glucose metabolism in health and disease. *Nutrients* 12 (1), 94. doi:10.3390/nu12010094

Mosca, A., Nobili, V., De Vito, R., Crudele, A., Scorletti, E., Villani, A., et al. (2017). Serum uric acid concentrations and fructose consumption are independently associated with NASH in children and adolescents. *J. Hepatol.* 66 (5), 1031–1036. doi:10.1016/j.jhep.2016.12.025

Nd, A. M. (2019). Non-alcoholic fatty liver disease, an overview. *Integr. Med.* 18 (2), 42–49. https://pubmed.ncbi.nlm.nih.gov/31341444/.

Nehring, I., Kostka, T., von Kries, R., and Rehfuess, E. A. (2015). Impacts of in utero and early infant taste experiences on later taste acceptance: a systematic review. *J. Nutr.* 145 (6), 1271–1279. doi:10.3945/jn.114.203976

Neuschwander-Tetri, B. A. (2013). Carbohydrate intake and nonalcoholic fatty liver disease. *Curr. Opin. Clin. Nutr. Metab. Care* 16 (4), 446–452. doi:10.1097/MCO.0b013e328361c4d1

Nseir, W., Nassar, F., and Assy, N. (2010). Soft drinks consumption and nonalcoholic fatty liver disease. *World J. Gastroenterol.* 16 (21), 2579–2588. doi:10.3748/wjg.v16.i21.2579

Ouyang, X., Cirillo, P., Sautin, Y., McCall, S., Bruchette, J. L., Diehl, A. M., et al. (2008). Fructose consumption as a risk factor for non-alcoholic fatty liver disease. *J. Hepatol.* 48 (6), 993–999. doi:10.1016/j.jhep.2008.02.011

Perrar, I., Schadow, A. M., Schmitting, S., Buyken, A. E., and Alexy, U. (2019). Time and age trends in free sugar intake from food groups among children and adolescents between 1985 and 2016. *Nutrients* 12 (1), 20. doi:10.3390/nu12010020

Rabenberg, M., and Mensink, G. B. M. (2013). Robert Koch Institut Berlin: Limo, Saft & Co - Konsum zuckerhaltiger Getränke in Deutschland. *GBE kompakt* 4 (1), 9. doi:10.25646/3036

Richter, A., Heidemann, C., Schulze, M. B., Roosen, J., Thiele, S., and Mensink, G. B. (2012). Dietary patterns of adolescents in Germany—associations with nutrient intake and other health related lifestyle characteristics. *BMC Pediatr.* 12, 35. doi:10.1186/1471-2431-12-35

Rippe, J. M., Sievenpiper, J. L., Lê, K. A., White, J. S., Clemens, R., and Angelopoulos, T. J. (2017). What is the appropriate upper limit for added sugars consumption? *Nutr. Rev.* 75 (1), 18–36. doi:10.1093/nutrit/nuw046

Rodrigo, S., Fauste, E., de la Cuesta, M., Rodríguez, L., Álvarez-Millán, J. J., Panadero, M. I., et al. (2018). Maternal fructose induces gender-dependent changes in both LXRα promoter methylation and cholesterol metabolism in progeny. *J. Nutr. Biochem.* 61, 163–172. doi:10.1016/j.jnutbio.2018.08.011

Roeb, E., Steffen, H. M., Bantel, H., Baumann, U., Canbay, A., Demir, M., et al. (2015). S2k-Leitlinie nicht alkoholische Fettlebererkrankungen [S2k Guideline non-alcoholic fatty liver disease]. *Z. Gastroenterol.* 53 (7), 668–723. doi:10.1055/s-0035-1553193

Roh, E., Song, D. K., and Kim, M. S. (2016). Emerging role of the brain in the homeostatic regulation of energy and glucose metabolism. *Exp. Mol. Med.* 48 (3), e216. doi:10.1038/emm.2016.4

Schon, H. T., and Weiskirchen, R. (2016). Exercise-induced release of pharmacologically active substances and their relevance for therapy of hepatic injury. *Front. Pharmacol.* 7, 283. doi:10.3389/fphar.2016.00283

Schwarz, J. M., Noworolski, S. M., Wen, M. J., Dyachenko, A., Prior, J. L., Weinberg, M. E., et al. (2015). Effect of a high-fructose weight-maintaining diet on lipogenesis and liver fat. *J. Clin. Endocrinol. Metab.* 100 (6), 2434–2442. doi:10.1210/jc.2014-3678

Schwingshackl, L., Neuenschwander, M., Hoffmann, G., Buyken, A. E., and Schlesinger, S. (2020). Dietary sugars and cardiometabolic risk factors: a network meta-analysis on isocaloric substitution interventions. *Am. J. Clin. Nutr.* 111 (1), 187–196. doi:10.1093/ajcn/nqz273

Silbernagel, G., Lütjohann, D., Machann, J., Meichsner, S., Kantartzis, K., Schick, F., et al. (2012). Cholesterol synthesis is associated with hepatic lipid content and dependent on fructose/glucose intake in healthy humans. *Exp. Diabetes Res.* 2012, 361863. doi:10.1155/2012/361863

Simons, N., Debray, F. G., Schaper, N. C., Kooi, M. E., Feskens, E. J. M., Hollak, C. E. M., et al. (2019). Patients with aldolase B deficiency are characterized by increased intrahepatic triglyceride content. *J. Clin. Endocrinol. Metab.* 104 (11), 5056–5064. doi:10.1210/jc.2018-02795

Smajis, S., Gajdošík, M., Pfleger, L., Traussnigg, S., Kienbacher, C., Halilbasic, E., et al. (2020). Metabolic effects of a prolonged, very-high-dose dietary fructose challenge in healthy subjects Erratum in. *Am. J. Clin. Nutr.* 111 (2), 369–377. doi:10.1093/ajcn/nqz271

Souci, S. W., Fachmann, W., and Kraut, H. (2016). *Food consumption and nutrition tables*. Stuttgart, Germany: Medpharm GmbH Scientific Publishers.

Stanhope, K. L., Schwarz, J. M., Keim, N. L., Griffen, S. C., Bremer, A. A., Graham, J. L., et al. (2009). Consuming fructose-sweetened, not glucose-sweetened, beverages increases visceral adiposity and lipids and decreases insulin sensitivity in overweight/obese humans. *J. Clin. Invest.* 119 (5), 1322–1334. doi:10.1172/JCI37385

Stevens, B., Yamada, J., Ohlsson, A., Haliburton, S., and Shorkey, A. (2016). Sucrose for analgesia in newborn infants undergoing painful procedures. *Cochrane Database Syst. Rev.* 7 (7), CD001069. doi:10.1002/14651858.CD001069.pub5

Stokes, C. S., Lammert, F., and Krawczyk, M. (2019). Short-term dietary interventions for the management of nonalcoholic fatty liver. *Curr. Med. Chem.* 26 (19), 3483–3496. doi:10.2174/0929867324666170508144409

Tappy, L., and Lê, K. A. (2012). Does fructose consumption contribute to non-alcoholic fatty liver disease? *Clin. Res. Hepatol. Gastroenterol.* 36 (6), 554–560. doi:10.1016/j.clinre.2012.06.005

Tappy, L., and Lê, K. A. (2010). Metabolic effects of fructose and the worldwide increase in obesity. *Physiol. Rev.* 90 (1), 23–46. doi:10.1152/physrev.00019.2009

Ter Horst, K. W., and Serlie, M. J. (2017). Fructose consumption, lipogenesis, and non-alcoholic fatty liver disease. *Nutrients* 9 (9), 981. doi:10.3390/nu9090981

Todoric, J., Di Caro, G., Reibe, S., Henstridge, D. C., Green, C. R., Vrbanac, A., et al. (2020). Fructose stimulated de novo lipogenesis is promoted by inflammation. *Nat. Metab.* 2 (10), 1034–1045. doi:10.1038/s42255-020-0261-2

US Food and Drug Administration (2018). High fructose corn syrup questions and answers. Available at: https://www.fda.gov/food/food-additives-petitions/high-fructose-corn-syrup-questions-and-answers.

Ventura, E. E., Davis, J. N., and Goran, M. I. (2011). Sugar content of popular sweetened beverages based on objective laboratory analysis: focus on fructose content. *Obesity* 19 (4), 868–874. doi:10.1038/oby.2010.255

Wang, P. Y., Fang, J. C., Gao, Z. H., Zhang, C., and Xie, S. Y. (2016). Higher intake of fruits, vegetables or their fiber reduces the risk of type 2 diabetes: a meta-analysis. *J. Diabetes Investig.* 7 (1), 56–69. doi:10.1111/jdi.12376

White, J. S. (2013). Challenging the fructose hypothesis: new perspectives on fructose consumption and metabolism. *Adv. Nutr.* 4 (2), 246–256. doi:10.3945/an.112.003137

Zahner, D., Glimm, H., Matono, T., Churin, Y., Herebian, D., Mayatepek, E., et al. (2017). Hepatitis B virus surface proteins accelerate cholestatic injury and tumor progression in Abcb4-knockout mice. *Oncotarget* 8 (32), 52560–52570. doi:10.18632/oncotarget.15003

Zelber-Sagi, S., Salomone, F., and Mlynarsky, L. (2017). The Mediterranean dietary pattern as the diet of choice for non-alcoholic fatty liver disease: evidence and plausible mechanisms. *Liver Int.* 37 (7), 936–949. doi:10.1111/liv.13435

Conflict of Interest: The authors declare that the research was conducted in the absence of any commercial or financial relationships that could be construed as a potential conflict of interest.

Copyright © 2021 Roeb and Weiskirchen. This is an open-access article distributed under the terms of the Creative Commons Attribution License (CC BY). The use, distribution or reproduction in other forums is permitted, provided the original author(s) and the copyright owner(s) are credited and that the original publication in this journal is cited, in accordance with accepted academic practice. No use, distribution or reproduction is permitted which does not comply with these terms.

frontiers in Pharmacology

ORIGINAL RESEARCH
published: 18 February 2021
doi: 10.3389/fphar.2021.628583

Inhibition of 5-Lipoxygenase in Hepatic Stellate Cells Alleviates Liver Fibrosis

*Shiyun Pu[1,2†], Yanping Li[2†], Qinhui Liu[2], Xu Zhang[3], Lei Chen[1,2], Rui Li[1,2], Jinhang Zhang[1,2], Tong Wu[1,2], Qin Tang[1,2], Xuping Yang[1,2], Zijing Zhang[1,2], Ya Huang[1,2], Jiangying Kuang[1,2], Hong Li[1,2], Min Zou[1], Wei Jiang[4] and Jinhan He[1,2]**

[1]Department of Pharmacy and State Key Laboratory of Biotherapy, West China Hospital, Sichuan University, Chengdu, China, [2]Laboratory of Clinical Pharmacy and Adverse Drug Reaction, West China Hospital, Sichuan University, Chengdu, China, [3]Tianjin Key Laboratory of Metabolic Diseases and Department of Physiology, Tianjin Medical University, Tianjin, China, [4]Molecular Medicine Research Center, West China Hospital of Sichuan University, Chengdu, China

OPEN ACCESS

Edited by:
Ralf Weiskirchen,
RWTH Aachen University, Germany

Reviewed by:
Han Moshage,
University Medical Center Groningen, Netherlands
Klaas Poelstra,
University of Groningen, Netherlands
Suxian Zhao,
Third Hospital of Hebei Medical University, China
Maria De Lujan Alvarez,
CONICET Rosario, Argentina

***Correspondence:**
Jinhan He
jinhanhe@scu.edu.cn

†These authors have contributed equally to this work

Specialty section:
This article was submitted to Gastrointestinal and Hepatic Pharmacology, a section of the journal Frontiers in Pharmacology

Received: 12 November 2020
Accepted: 15 January 2021
Published: 18 February 2021

Citation:
Pu S, Li Y, Liu Q, Zhang X, Chen L, Li R, Zhang J, Wu T, Tang Q, Yang X, Zhang Z, Huang Y, Kuang J, Li H, Zou M, Jiang W and He J (2021) Inhibition of 5-Lipoxygenase in Hepatic Stellate Cells Alleviates Liver Fibrosis. Front. Pharmacol. 12:628583. doi: 10.3389/fphar.2021.628583

Background and Purpose: Activation of hepatic stellate cells (HSC) is a central driver of liver fibrosis. 5-lipoxygenase (5-LO) is the key enzyme that catalyzes arachidonic acid into leukotrienes. In this study, we examined the role of 5-LO in HSC activation and liver fibrosis.

Main Methods: Culture medium was collected from quiescent and activated HSC for target metabolomics analysis. Exogenous leukotrienes were added to culture medium to explore their effect in activating HSC. Genetic ablation of 5-LO in mice was used to study its role in liver fibrosis induced by CCl_4 and a methionine-choline-deficient (MCD) diet. Pharmacological inhibition of 5-LO in HSC was used to explore the effect of this enzyme in HSC activation and liver fibrosis.

Key Results: The secretion of LTB_4 and LTC_4 was increased in activated vs. quiescent HSC. LTB_4 and LTC_4 contributed to HSC activation by activating the extracellular signal-regulated protein kinase pathway. The expression of 5-LO was increased in activated HSC and fibrotic livers of mice. Ablation of 5-LO in primary HSC inhibited both mRNA and protein expression of fibrotic genes. *In vivo*, ablation of 5-LO markedly ameliorated the CCl_4- and MCD diet-induced liver fibrosis and liver injury. Pharmacological inhibition of 5-LO in HSC by targeted delivery of the 5-LO inhibitor zileuton suppressed HSC activation and improved CCl_4- and MCD diet-induced hepatic fibrosis and liver injury. Finally, we found increased 5-LO expression in patients with non-alcoholic steatohepatitis and liver fibrosis.

Conclusion: 5-LO may play a critical role in activating HSC; genetic ablation or pharmacological inhibition of 5-LO improved CCl_4-and MCD diet-induced liver fibrosis.

Keywords: liver fibrosis, non-alcoholic steatohepatitis, α-SMA, ERK, zileuton

Abbreviations: ALT, alanine aminotransferase; AST, aspartate aminotransferase; 5-LO, 5-lipoxygenase; 5-HPETE, 5-hydroperoxyeicosatetraenoic acid; NASH, non-alcoholic steatohepatitis; MCD diet, methionine-choline-deficient diet; MCS diet, methionine-choline-supplied diet; CCl_4, carbon tetrachloride; IL, interleukin; HSC, hepatic stellate cell; α-SMA, alpha smooth muscle actin; LTA4, leukotriene A4; LTB4, leukotriene B4; LTC4, leukotriene C_4; TIMP-1/2, tissue inhibitor of metalloproteinase 1/2; TGF-β1, transforming growth factor-β1; PAI-1, plasminogen activator inhibitor 1; Flaps, 5-LO-activating proteins; ERK, extracellular signal-regulated protein kinase; MCP-1, monocyte chemoattractant protein 1; TNF-α, tumor necrosis factor alpha.

INTRODUCTION

Liver fibrosis is a common outcome of chronic liver injury such as chronic hepatotoxicity and non-alcoholic steatohepatitis (NASH) (Yu et al., 2018). If unmanaged, liver fibrosis can advance to cirrhosis and portal hypertension and often requires liver transplantation.

Hepatic stellate cells (HSC) play a key role in the formation of hepatic fibrosis (Higashi et al., 2017). In normal liver, HSC stay quiescent (Ogawa et al., 2007). With injurious stimuli, HSC transdifferentiate from a quiescent to activated state (Puche et al., 2013), becoming proliferative and producing a high amount of α-smooth muscle actin (α-SMA) and collagens (De Minicis et al., 2008). When this extracellular matrix accumulates excessively, it causes a fibrotic outcome and scars on the liver (Wu et al., 2018). The mechanism of HSC activation is not fully understood. Several signaling pathways participate in activating HSC (Woodhoo et al., 2012). Transforming growth factor-β (TGF-β) induces the phosphorylation of Smad2/3, which in turn promotes HSC activation and regulates the expression of fibrotic genes (Feng and Derynck, 2005). Activation of extracellular signal-regulated kinase (ERK) also contributes to HSC activation (Chen et al., 2016; Xie et al., 2017).

Arachidonic acid is the precursor of biologically and clinically important eicosanoids (Harizi et al., 2008). 5-lipoxygenase (5-LO) is the key enzyme that catalyzes arachidonic acid into leukotrienes (Alexander et al., 2011). Upon activation of 5-LO-activating protein (Flap), 5-LO oxidases arachidonic acid to the unstable intermediate 5-hydroperoxyeicosatetraenoic acid (5-HPETE), which is further dehydrated to form leukotriene A4 (LTA_4) (Silverman and Drazen, 1999). LTA_4 is converted to LTB_4 via LTA_4 hydrolase enzymes or to LTC_4 via LTC_4 synthase (Hofmann and Steinhilber, 2013). Both LTB_4 and LTC_4 are inflammatory lipid mediators that have important effects on the development of allergic rhinitis, bronchial asthma and atherosclerosis (Kowal et al., 2017). Inhibiting 5-LO by an inhibitor such as zileuton or blocking the effect of leukotrienes by their receptor antagonist such as montelukast, have been clinically used for asthma treatment (De Corso et al., 2019).

Recent studies indicated that the 5-LO pathway is associated with fibrosis (Qian et al., 2015; Su et al., 2016). 5-LO is expressed in human dermal fibroblasts, synovial fibroblasts, pulmonary fibroblasts and rat adventitial fibroblasts (Lin et al., 2014; Su et al., 2016). Activation of these cells can be restrained by 5-LO inhibitors (Lin et al., 2014; Su et al., 2016). LTB_4 and LTC_4 are secreted from lung fibroblasts (Shiratori et al., 1989; Paiva et al., 2010) and contribute to the proliferation and migration of these cells (Hirata et al., 2013). However, the role of 5-LO in HSC activation and liver fibrosis remains unknown.

In this study, we first used metabolomics to reveal that LTB_4 and LTC_4 are highly secreted during the activation of HSC. Secreted LTB_4 and LTC_4 promoted HSC activation via an ERK signaling pathway. Ablation or inhibition of 5-LO could suppress HSC activation. In mouse fibrotic models, ablation or targeted inhibition of 5-LO in HSC relieved liver fibrosis and injury. Finally, we found increased expression of 5-LO in liver sections of patients with NASH and fibrosis.

MATERIALS AND METHODS

CCl_4- and Methionine-Choline–Deficient Diet-Induced Models of Liver Fibrosis

For CCl_4-induced liver fibrosis, 8-week-old C57 BL/6J (WT) and 5-lipoxygenase knockout (5-$LO^{-/-}$) mice received an intraperitoneal (i.p.) injection of CCl_4 (1 ml/kg body weight) twice a week. For MCD diet-induced liver fibrosis, WT and 5-$LO^{-/-}$ mice were fed a methionine-choline-supplied (MCS) or MCD diet (TROPHIC Animal Feed High-Tech, China) for 6 weeks. For therapeutic experiments, zileuton loaded in cRGDyK (Cyclo [Arg-Gly-Asp-$_D$Tyr-Lys])-guided liposome (RGD-Lip; 10 mg/kg) or vehicle was given by tail vein injection once every 3 days during the last 4 weeks of CCl_4 or MCD diet treatment. All mice were housed at West China Hospital, Sichuan University in accordance with the guidelines of the animal care utilization committee of the institute. Food and water were freely available to mice, except otherwise stated.

Preparation and Characterization of RGD-Lips

Liposome (Lip) were prepared by the thin-film hydration method as described (Li et al., 2019; Zhang et al., 2020). Zileuton-loaded RGD-Lips (RGD-Lip/zileuton) were prepared by adding zileuton to the lipid organic solution before the solvent evaporation. The mean particle size and zeta potential of Lip were measured by dynamic light scattering with the Zetasizer Nano ZS90 instrument (Malvern, United Kingdom). The morphology of Lip was examined by transmission electron microscopy (H-600, Hitachi, Japan) with 2% phosphotungstic acid staining.

Serum Alanine Aminotransferase and Aspartate Aminotransferase Measurement

Serum ALT and AST levels were detected by using commercial kits (BioSino Bio-Technology and Science).

Hydroxyproline Assay

An amount of 50 mg liver tissue was dissolved in acid hydrolysate in glass tube and heated in boiling water bath for 20 min. Hydroxyproline was extracted according to the manufacturer's instructions and measured by using kits (Nanjing Jiancheng Bioengineering Institute).

Histology Analysis

The left lobe of the mouse liver was removed and immediately fixed in 10% neutral-buffered formalin, embedded in paraffin, and sectioned at 4 μm. Liver sections were stained with hematoxylin and eosin (H&E). For picrosirius red staining, liver sections were incubated with 0.1% sirius red in saturated picric acid for 60 min at room temperature. The Sirus Red positive area were detected by Image J. Fibrosis was assessed by picrosirius red staining according to the Ishak fibrosis criteria (Ishak et al., 1995).

Isolation and Culture of HSC

HSC were isolated from livers of WT mice and 5-LO$^{-/-}$ mice via *in situ* collagenase perfusion and underwent differential centrifugation on Optiprep (Sigma) density gradients, as described (Kwon et al., 2014). Isolated HSC were cultured in collagen-coated dishes with DMEM supplemented with 10% fetal bovine serum and antibiotics at 37°C. The purity of HSC was >95% as determined by their typical star-like shape and abundant lipid droplets.

Measurement of Zileuton Concentration in Different Types of Liver Cells

Mice were injected with CCl_4 to cause liver fibrosis and treated with RGD-Lip/zileuton (10 mg/kg) for 4 h. Primary hepatocytes were isolated as described (Chen et al., 2019). The remaining cells were divided into three groups, fixed, perforated and stained with anti-α-SMA (HSC), anti-F4/80 (Kupffer cells) and anti-CD31 antibodies. HSC, Kupffer cells and LSECs were sorted by flow cytometry. Biliary epithelial cells were isolated as previously described (Li et al., 2019). Before extraction, cells were added to 30 μl ddH_2O and underwent repeated freezing and thawing 5 times. A 25-μl aliquot of samples was added to a 1.5-ml polypropylene tube followed by 200 μl methanol. The mixture was vortex-mixed for 5 min and centrifuged at 14,000 rpm for 10 min at room temperature. The top layer was transferred to a new 1.5 ml polypropylene tube and evaporated to vacuum dryness at 37°C. Samples were re-dissolved with 50 μl 80% methanol. The mixture was vortex-mixed for 30 s and centrifuged at 14,000 rpm for 5 min at 4 °C. The 40-μl supernatant was transferred to a 250 μl polypropylene autosampler vial and sealed with a Teflon crimp cap. Partially purified cell samples were analyzed by using LC-MS/MS.

Systematic Metabolomic Analysis of Arachidonic Acid in 5-Lipoxygenase Pathway

Serum-free supernatant from primary mouse HSC were collected in an ice bath and extracted by solid-phase extraction. The metabolomics of arachidonic acid were detected and analyzed as described (Zhang et al., 2015).

LTB_4 and LTC_4 Measurement

Serum-free primary mouse HSC were collected in an ice bath and protected from light. Samples were centrifuged (600 × g, 5 min, 4°C), and with the resulting supernatant, LTB_4 and LTC_4 levels were determined by using ELISA kits (Cayman Chemical).

Immunofluorescence Staining

Primary HSC were fixed in 4% paraformaldehyde for 15 min, incubated in 0.2% Triton X-100 1×PBS for 15 min for permeabilization of cytomembrane. Antigens in paraffin sections were repaired by microwaving in 0.01 M citrate buffer (pH = 6.0) for 15 min. Both cells and tissue samples were incubated with antibodies in 4°C for 12 h. Immunoreactive compounds were incubated in room temperature for 1 h for conjugating with fluorescence-labeling secondary antibodies. All antibodies used in these experiments are in Supplementary **Supplementary Table S1**.

Western Blot Analysis

Western blot analysis was performed as described (Chen et al., 2019). The antibodies were listed in supplementary **Supplementary Table S1**. The expression of β-tubulin was a loading control. Immunoreactive bands were visualized on nitrocellulose membranes by using fluorescence-conjugated secondary antibodies (LI-COR, United States). The relative density was calculated by the ratio of the density of the protein of interest to β-tubulin.

Real-Time PCR Analyses

Total RNA isolation and PT-PCR was performed as described (Chen et al., 2019). The primers for detected genes are in **Supplementary Table S2**.

Statistical Analysis

Experiments were repeated at least 3 times with similar results. Quantitative results are expressed as the mean ± SEM. Statistical significance was determined by Student's unpaired two-tailed *t* test or one-way ANOVA multiple comparison test as indicated in legends. $p < 0.05$ was considered statistically significant.

RESULTS

LTB_4 and LTC_4 were Enriched in Supernatant of A-HSC

To explore the potential role of lipoxygenase pathway in arachidonic acid during HSC activation, we collected cell supernatants from quiescent HSC (q-HSC) and activated HSC (a-HSC, culture activated for 7 days) (Thi Thanh Hai et al., 2018). Among metabolites identified in the lipoxygenase pathway, target metabolomics revealed that LTB_4 level was selectively increased in a-HSC (**Supplementary Figure S1**). ELISA further confirmed the increased LTB_4 level in the supernatant of a-HSC (**Figure 1A**). Consistently, the level of LTC_4, another metabolite of 5-LO, was also increased (**Figure 1B**).

LTB_4 and LTC_4 Contributed to Activating HSC via Phosphorylation of the ERK Pathway

The high level of LTB_4 and LTC_4 released by a-HSC prompted us to explore their function in activating HSC. To exclude the influence of endogenous LTB_4 and LTC_4, we isolated primary HSC from 5-LO$^{-/-}$ mice and added exogenous LTB_4 or LTC_4 to these cells for 4 days. Treatment with LTB_4 or LTC_4 significantly increased the expression of fibrotic genes including α-SMA, collagen 1a1 (Col1a1), Col3a1, Col5a1, tissue inhibitor of metalloproteinase 1 (Timp-1) and plasminogen activator inhibitor 1 (PAI-1) (**Figures 1C,D**). On immunofluorescence staining, LTB_4 and LTC_4 increased α-SMA accumulation in HSC as compared with controls (**Figure 1E**). Western blot analysis

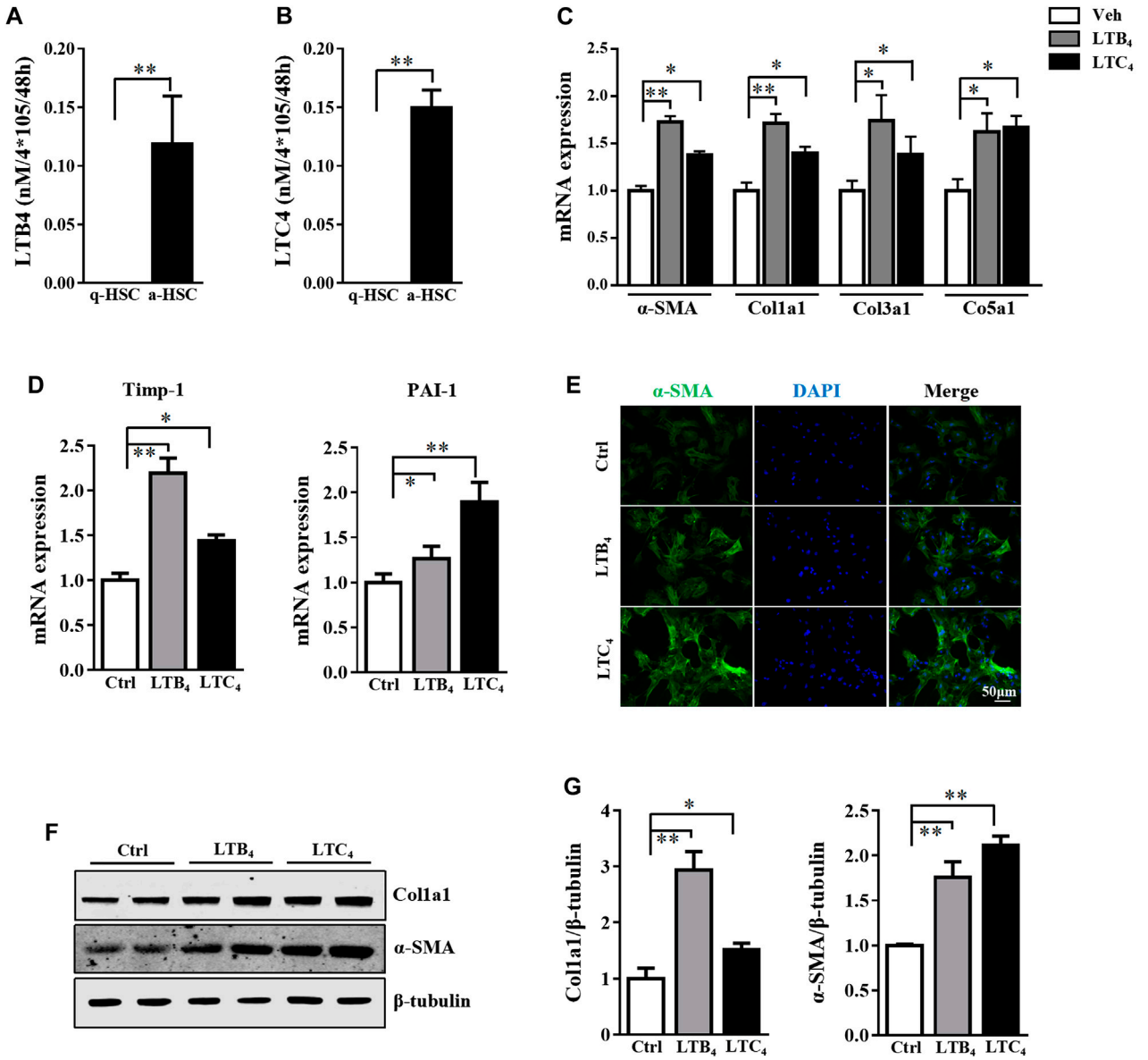


FIGURE 1 | LTB_4 and LTC_4 levels were elevated during HSC activation and promote HSC activation. **(A,B)** Primary HSC were isolated from wild-type (WT) mice and cultured for 2 days (quiescent HSC [q-HSC]) or 7 days (activated HSC [a-HSC]). ELISA detection of secretion of LTB_4 and LTC_4 in supernatant from q-HSC or a-HSC. **(C–G)** Primary HSC were isolated from 5-$LO^{-/-}$ mice and cultured in DMEM with high glucose with 10% heat-inactivated fetal bovine serum for 2 days. Cells were co-cultured with vehicle (Veh), LTB_4, or LTC_4 for 4 days. **(C,D)** qRT-PCR analysis of mRNA levels of fibrotic genes. **(E)** Immunofluorescence analysis of effect of LTB_4 or LTC_4 treatment on α-SMA expression. **(F,G)** The protein level of α-SMA and Col1a1 protein. Data are mean ± SEM, n = 5, $^*p < 0.05$, $^{**}p < 0.01$.

further confirmed that LTB_4 and LTC_4 elevated the protein levels of α-SMA and Col1a1 (**Figures 1F,G**). Therefore, LTB_4 or LTC_4 could promote HSC activation. We next explored the signaling pathway conveying the effect of LTB_4 or LTC_4. LTB_4 or LTC_4 seemed not to induce the phosphorylation of Smad2/3, a key pathway molecule for TGF-β-induced fibrosis (**Supplementary Figure S2A**). Instead, we found that LTB_4 and LTC_4 induced phosphorylation of the ERK1 signaling pathway (**Figures 2A,B**). The phosphorylation of ERK is necessary for LTB_4- and LTC_4-induced fibrosis because PD98059, a mitogen-activated protein kinase inhibitor, abolished their effects (**Figures 2C,D**; **Supplementary Figure S2B**). Other MAP kinases, according to p-p38 and p-JNK, were no change after LTB_4 or LTC_4 administration (**Supplementary Figure S2C**). Therefore, the effect of LTB4 and LTC4 on HSC may be mediated by ERK1 signaling.

5-LO was Upregulated and Promoted HSC Activation

5-LO is the key enzyme in the synthesis of LTB_4 and LTC_4 (Alexander et al., 2011). We further investigated whether the high

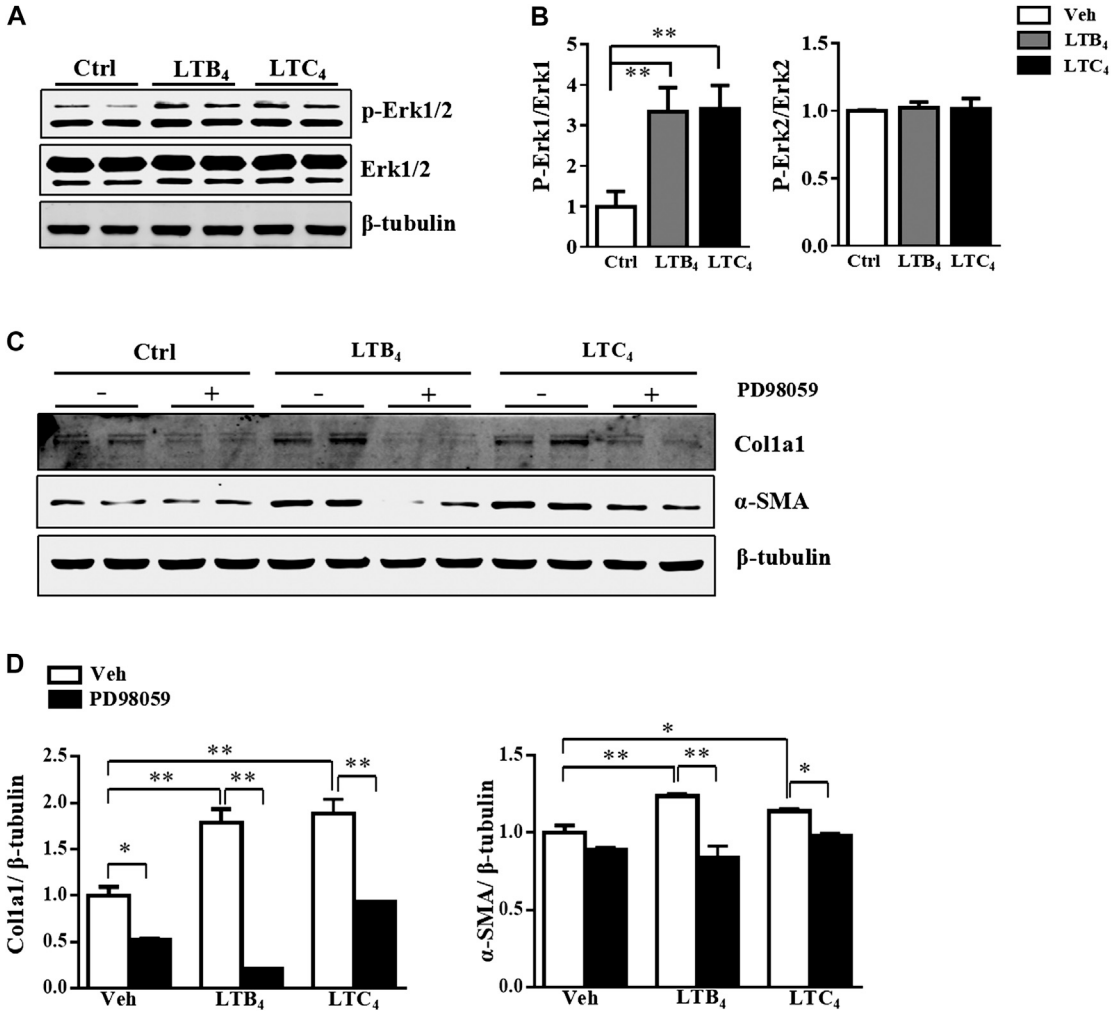


FIGURE 2 | LTB_4 and LTC_4 promote HSC activation via ERK signaling pathway. **(A,B)** The protein levels of p-ERK, t-ERK and β-tubulin in HSC after treatment with LTB_4, LTC_4 or TGF-β1 for 30 min **(C,D)** Western blot analysis of protein levels of α-SMA and Col1a1 in primary HSC isolated from 5-$LO^{-/-}$ mice and pre-treated with PD98059 before administration of LTB_4 or LTC_4. Data are mean ± SEM, n = 5, $^*p < 0.05$, $^{**}p < 0.01$.

level of LTB_4 and LTC_4 released by a-HSC resulted from the increased expression of 5-LO. The mRNA and protein levels of 5-LO were significantly upregulated in a-HSC as compared with q-HSC (**Figures 3A–C**). In contrast, the expression of Flap was not changed by HSC activation (**Figure 3B**). In CCl_4-induced liver fibrosis, 5-LO was also significantly increased along with other fibrotic genes (**Figures 3D–F**). Again, Flap expression was not significantly changed (**Figure 3E**). Liver fibrosis occurs during the progression of non-alcoholic steatohepatitis (NASH) (Nasr et al., 2018). Both the mRNA and protein levels of 5-LO were increased in an independent model of MCD diet-induced NASH (Anstee and Goldin, 2006) (**Supplementary Figures S3A–C**). These results suggest that increased 5-LO level may be responsible for the high level of LTB_4 and LTC_4 in a-HSC.

To further investigate the effect of 5-LO in HSC activation, we isolated primary HSC from wild-type and 5-$LO^{-/-}$ mice, then compared the expression of fibrotic genes after culture activation. Ablation of 5-LO significantly inhibited the expression of culture-induced fibrotic genes, such as α-SMA, Col1a1, Col3a1, Col5a1, Timp1 and PAI-1 (**Figures 4A,B**), indicating that 5-LO was involved in HSC activation. Inhibition of HSC activation was confirmed by immunofluorescent staining, which showed the expression of α-SMA less detectable in 5-$LO^{-/-}$ HSC (**Figure 4C**). Western blot analysis revealed that ablation of 5-LO suppressed α-SMA and Col1a1 expression (**Figures 4D,E**). The incubation of supernatant from WT a-HSC (WT-CM) was more effective to activate HSC than that from 5-$LO^{-/-}$ a-HSC (5-$LO^{-/-}$-CM) (**Supplementary Figures S4A,B**).

Genetic Ablation of 5-LO Ameliorated CCl_4- and MCD Diet-Induced Liver Fibrosis, Inflammation and Hepatic Injury

To explore the *in vivo* function of 5-LO in liver fibrosis, we first exposed WT and 5-$LO^{-/-}$ mice to CCl_4 twice a week for 8 weeks

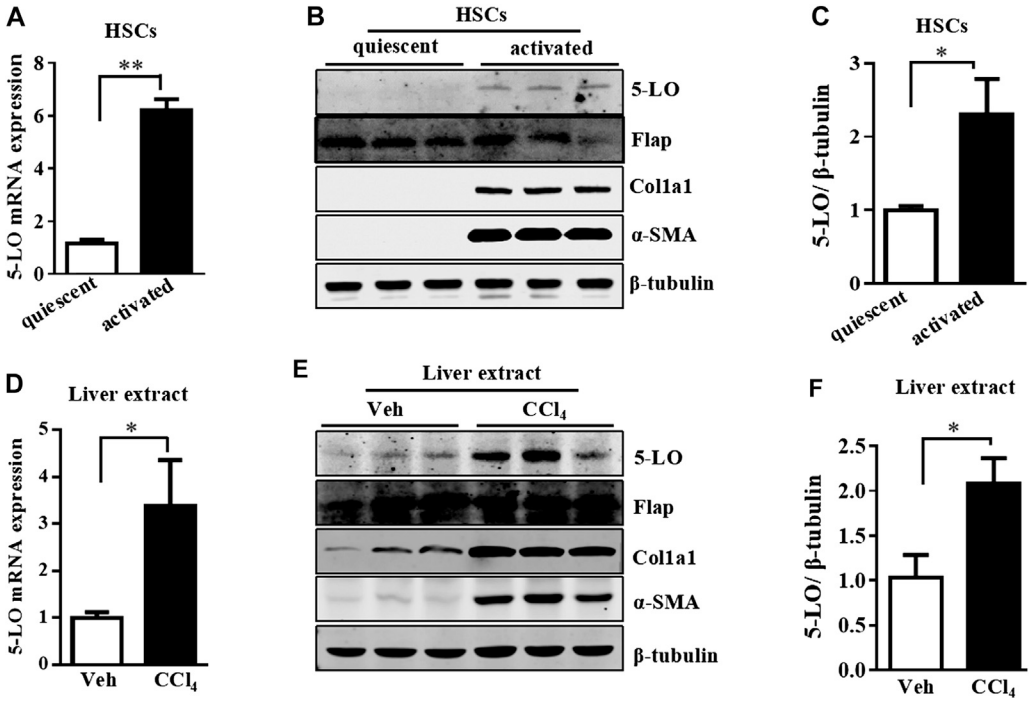


FIGURE 3 | 5-LO was upregulated in a-HSC and fibrotic livers. The mRNA and protein levels of 5-LO detected in q-HSC and a-HSC **(A–C)** and with CCl_4 treatment in mouse livers **(D–F)**. The protein levels of Flap, Col1a1, α-SMA and β-tubulin were also detected in all above groups **(B,E)**.

by intraperitoneal injection. As expected, CCl_4 caused significant hepatic fibrosis as compared with olive oil, as assessed by picrosirius red staining (**Figures 5A,B**). In contrast, 5-LO$^{-/-}$ mice showed improved liver fibrosis and decreased hepatic fibrosis scores (**Figure 5C**). Consistently, the level of hydroxyproline was significantly lower in 5-LO$^{-/-}$ than WT mice (**Figure 5D**), which suggests that 5-LO deletion conferred resistance to CCl_4-induced hepatic fibrosis. Among the fibrotic markers, α-SMA, collagens, TGF-β1, Timp-1/2 and PAI-1 were greatly suppressed in 5-LO$^{-/-}$ mice after CCl_4 treatment (**Figures 5E,F**). The protein levels of α-SMA and Col1a1 were also greatly reduced in 5-LO$^{-/-}$ mice with chronic CCl_4 injection (**Figure 5G**). CCl_4 administration showed an increasing serum levels of ALT and AST (**Supplementary Figure S5A**). However, this liver injury was significantly decreased in 5-LO$^{-/-}$ mice. Chronic liver injury accelerated the accumulation of inflammatory cells around the vessels (**Supplementary Figure S5B**). Ablation of 5-LO greatly suppressed CCl_4-induced inflammatory cell infiltration (**Supplementary Figures S5B,C**). These results were further supported by the decreased expression of inflammatory genes seen in the liver of 5-LO$^{-/-}$ mice (**Supplementary Figure S5D**).

In another independent model of MCD diet-induced NASH, collagen deposition was reduced in livers of 5-LO$^{-/-}$ mice along with decreased fibrosis scores and hydroxyproline levels (**Supplementary Figures S6A–D**). Improved liver fibrosis was further confirmed by gene expression and protein analysis. Indeed, 5-LO ablation decreased the mRNA levels of fibrotic genes (α-SMA, Col1a1, Col3a1, Col5a1, TGF-β1, Timp-1/2 and PAI-1) (**Supplementary Figures S6E,F**) and the protein levels of α-SMA and Col1a1 (**Supplementary Figures S6G,H**). 5-LO ablation was protective in MCD-diet induced liver injury, as indicated by reduced serum levels of ALT and AST and inflammation scores (**Supplementary Figures S7A–C**). Inflammation plays an important role in MCD diet-induced NASH (Locatelli et al., 2014). Consistently, the mRNA levels of inflammatory genes including tumor necrosis factor α (TNF-α), interleukin 1β (IL-1β) and monocyte chemoattractant protein 1 (Mcp-1) were decreased in 5-LO$^{/-}$ mice (**Supplementary Figure S7D**). The hepatic expression of CD68, a marker of macrophages, was also reduced (**Supplementary Figure S7D**). Therefore, 5-LO ablation ameliorated CCl_4- and MCD diet-induced hepatic fibrosis, inflammation and liver injury.

Pharmacological Inhibition of 5-LO by Targeted Delivery Suppressed HSC Activation

The protective effect of 5-LO ablation prompted us to explore whether pharmacological inhibition of 5-LO would have a similar effect in restraining the activation of primary HSC. We used an HSC-specific drug delivery system by modifying sterically stable liposome (Lip) with cRGDyK, a pentapeptide that binds to integrin αvβ3 on the surface of a-HSC (Li et al., 2019). cRGDyK-guided Lip showed high selectivity toward activated but not quiescent HSC, and preferentially accumulated in the fibrotic liver (Li et al., 2019; Zhang et al., 2020). We loaded with zileuton, an

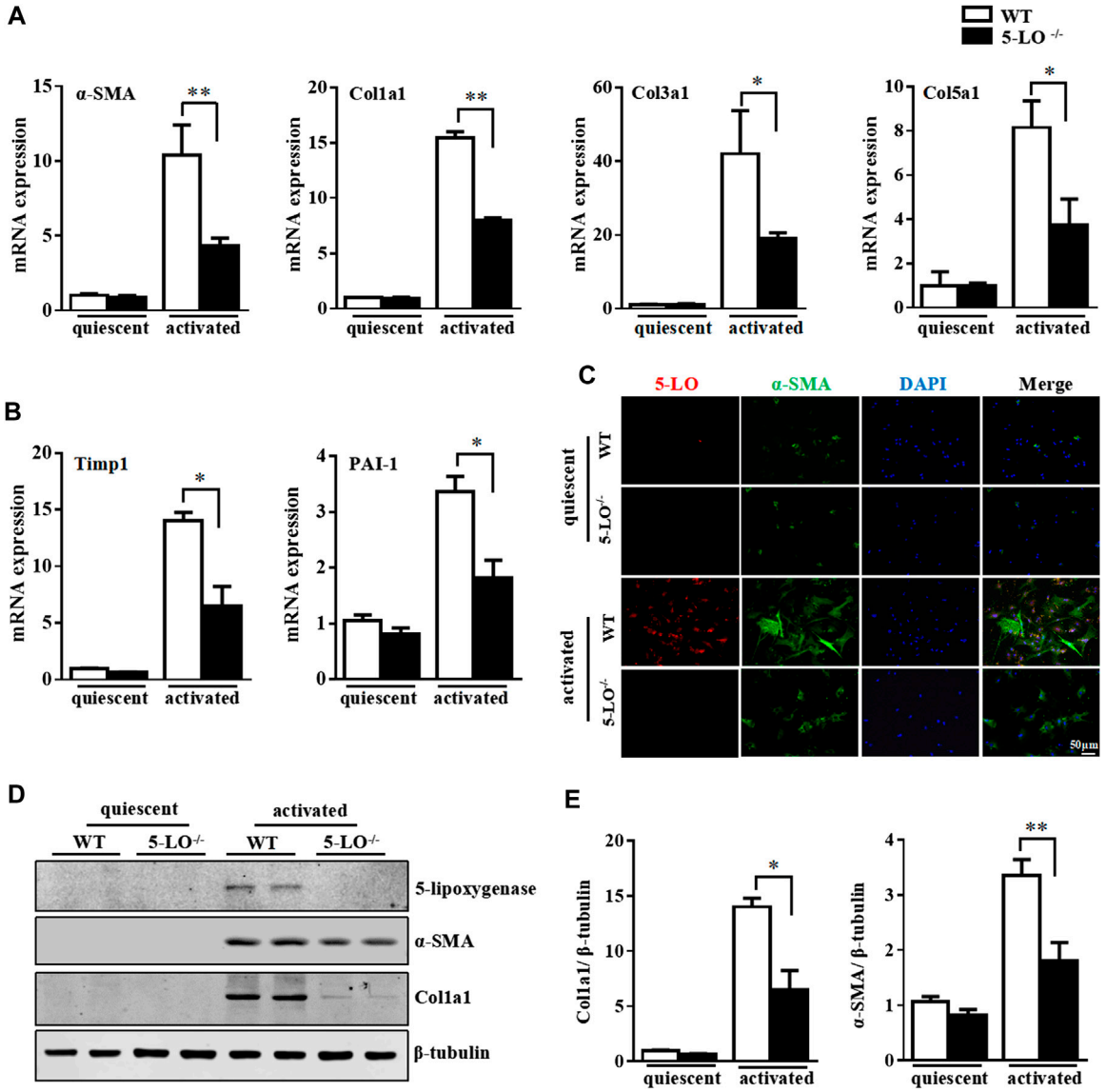


FIGURE 4 | Genetic ablation of 5-LO restrained activation of primary HSC. Primary HSC were isolated from WT and 5-LO $^{-/-}$ mice. **(A,B)** qRT-PCR of mRNA levels of fibrosis genes. **(C)** Immunofluorescence analysis of effect of 5-LO ablation on α-SMA expression. **(D,E)** Western blot analysis of α-SMA and Col1a1 protein levels in q-HSC and a-HSC. Data are mean ± SEM, n = 5, $^{*}p < 0.05$, $^{**}p < 0.01$.

inhibitor of 5-LO, into this delivery system (RGD-Lip/zileuton). The schematic illustration, particle size, morphology and entrapment efficiency were comparable to regular liposome (**Supplementary Figures S8A,B**, **Supplementary Table S3**). As expected, RGD-Lip/zileuton significantly suppressed the secretion of LTB_4 by a-HSC (**Supplementary Figure S9**), which indicates the inhibition of 5-LO. In a-HSC, zileuton delivered by RGD-Lip greatly inhibited the expression of fibrotic genes including α-SMA, Col1a1, Col3a1, Col5a1, Timp-1 and PAI-1 (**Figures 6A,B**). These effects were further confirmed by immunofluorescent staining and western blot analysis (**Figures 6C–E**). Therefore, pharmacological inhibition of 5-LO suppressed HSC activation.

Targeted Delivery of Zileuton to HSC Is Efficient Against Liver Fibrosis

We then evaluated the *in vivo* therapeutic effect of RGD-Lip/zileuton in CCl_4-and MCD diet-induced liver fibrosis. In this experiment, mice were injected with CCl_4 for 4 weeks, then treated with RGD-Lip/zileuton (10 mg/kg) every 3 days (**Supplementary Figure S10A**). RGD-Lip could specifically deliver zileuton to HSC because the concentration of zileuton

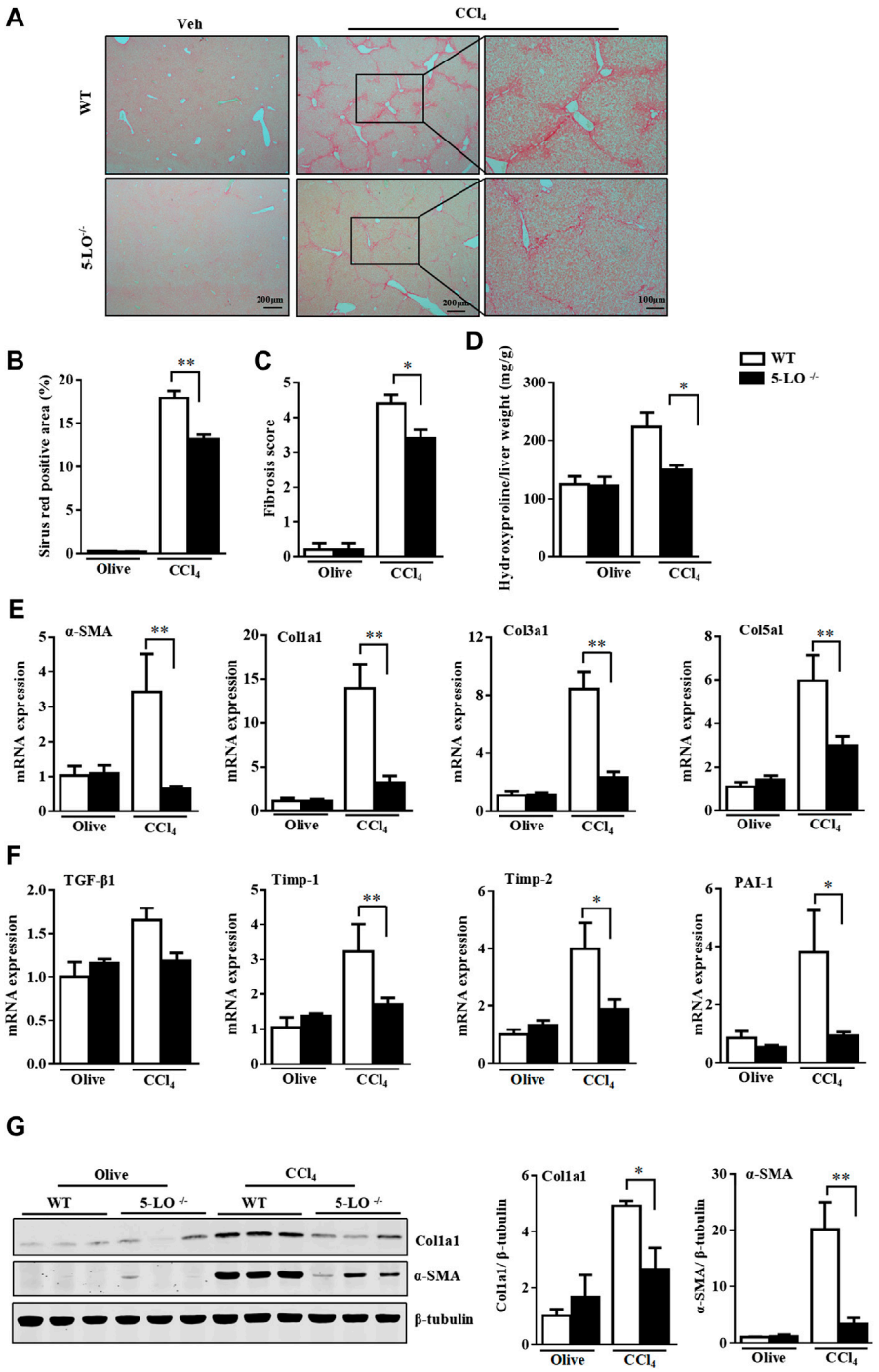


FIGURE 5 | Genetic ablation of 5-LO ameliorated liver fibrosis after CCl_4 injection. WT and 5-LO $^{-/-}$ mice were treated with olive oil or CCl_4 for 8 weeks. Fibrosis stage was assessed by picrosirius red staining **(A,B)** for collagen according to the Ishak criteria **(C)**. **(D)** Detection of hepatic hydroxyproline level. **(E,F)** qRT-PCR analysis of mRNA levels of fibrosis genes in livers of 4 groups. **(G)** Western blot analysis of the protein levels of α-SMA and Col1a1. Data are mean ± SEM, n = 7, $^{*}p < 0.05$, $^{**}p < 0.01$.

in HSC was about 28.99-, 4.71-, 4.67- and 34.01-times higher than that in hepatocytes, Kupffer cells, endothelial cells and biliary epithelial cells, respectively (**Supplementary Figure S10B**). Specific inactivation of 5-LO by RGD-Lip/zileuton in HSC greatly decreased liver fibrosis as shown by picrosirius red staining and liver hydroxyproline quantification (**Figures 7A–D**). The expression of fibrotic genes such as α-SMA, Col1a1, Col3a1, Col5a1, Timp1 and PAI-1 was also mitigated

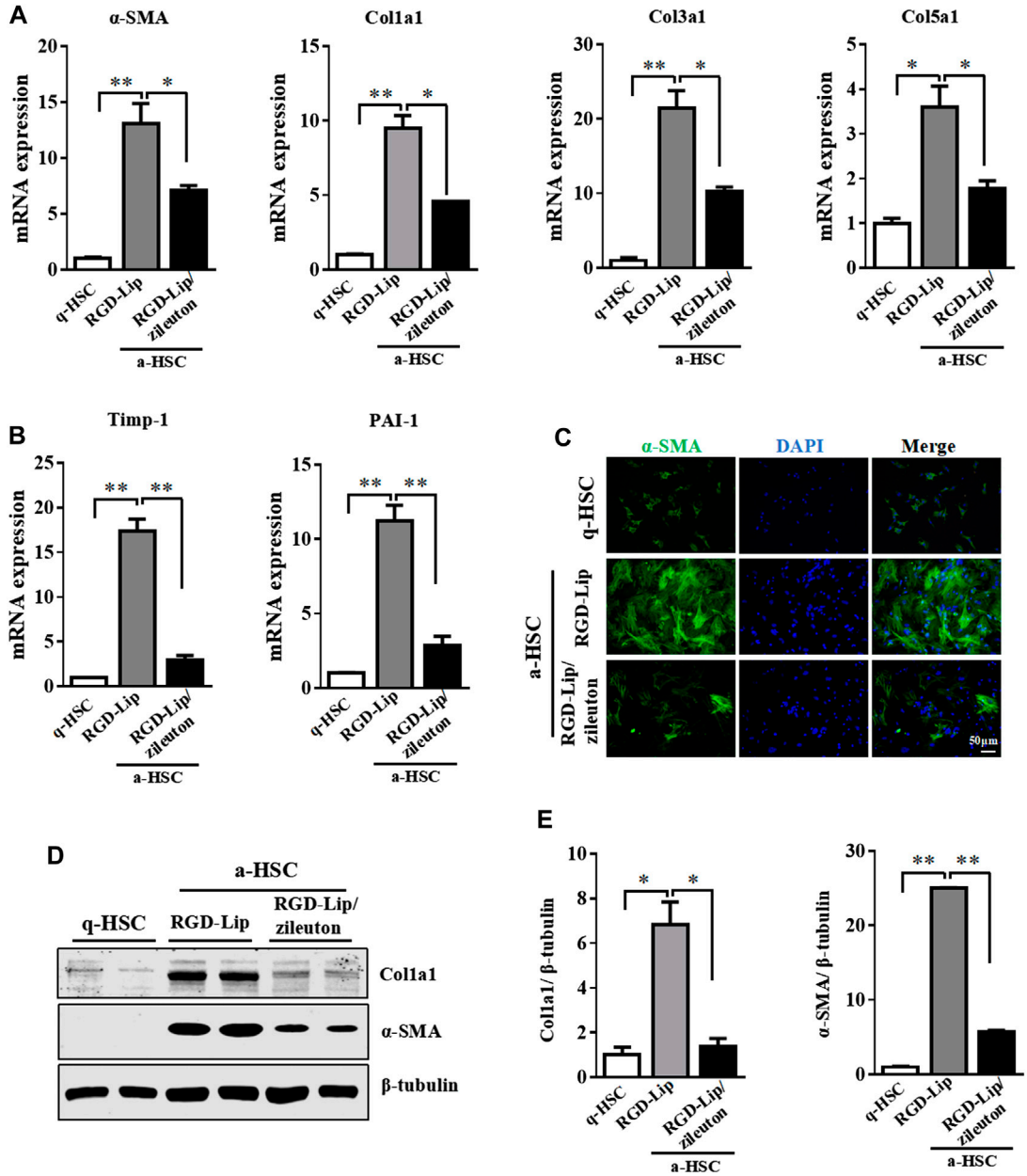


FIGURE 6 | Pharmacological inhibition of 5-LO suppressed activation of HSC. Primary HSC were isolated from WT mice and cultured in DMEM with high glucose and 10% heat-inactivated fetal bovine serum for 2 days (q-HSC) or 7 days (a-HSC). Primary HSC were treated with RGD-Lip or RGD-Lip/zileuton for 48 h **(A,B)** qRT-PCR analysis of effect of RGD-Lip/zileuton treatment on the mRNA expression of fibrotic genes. **(C)** Immunofluorescence analysis of effect of RGD-Lip/zileuton treatment on α-SMA expression. **(D,E)** Western blot analysis of α-SMA and Col1a1 protein levels in q-HSC and a-HSC. Data are mean ± SEM, n = 5, $^{*}p < 0.05$, $^{**}p < 0.01$.

(**Figures 6E,F**). Western blot analysis confirmed the reduced protein levels of Col1a1 and α-SMA (**Figures 6G,H**). Targeted inhibition of 5-LO in HSC also alleviated CCl_4-induced liver injury and hepatic inflammation (**Supplementary Figures S11A–C**), but did not reduce the accumulation of F4/80 positive cells (**Supplementary Figure S11D**).

The therapeutic effects of RGD-Lip/zileuton were further demonstrated in an MCD diet-induced NASH model (**Supplementary Figure S12**). Specific inactivation of 5-LO in HSC explicitly alleviated MCD diet-induced liver fibrosis (**Supplementary Figures S13A–D**). Expression of fibrotic genes was suppressed in RGD-Lip/zileuton-treated mice (**Supplementary Figures S13E,F**) and α-SMA and collagen accumulation was reduced (**Supplementary Figures S13G,H**). Targeted delivery of zileuton also relieved liver injury in MCD-induced NASH (**Supplementary Figure S14A**). H&E staining and the expression of proinflammatory genes such as TNF-α and Mcp-1 indicated decreased inflammation in livers of

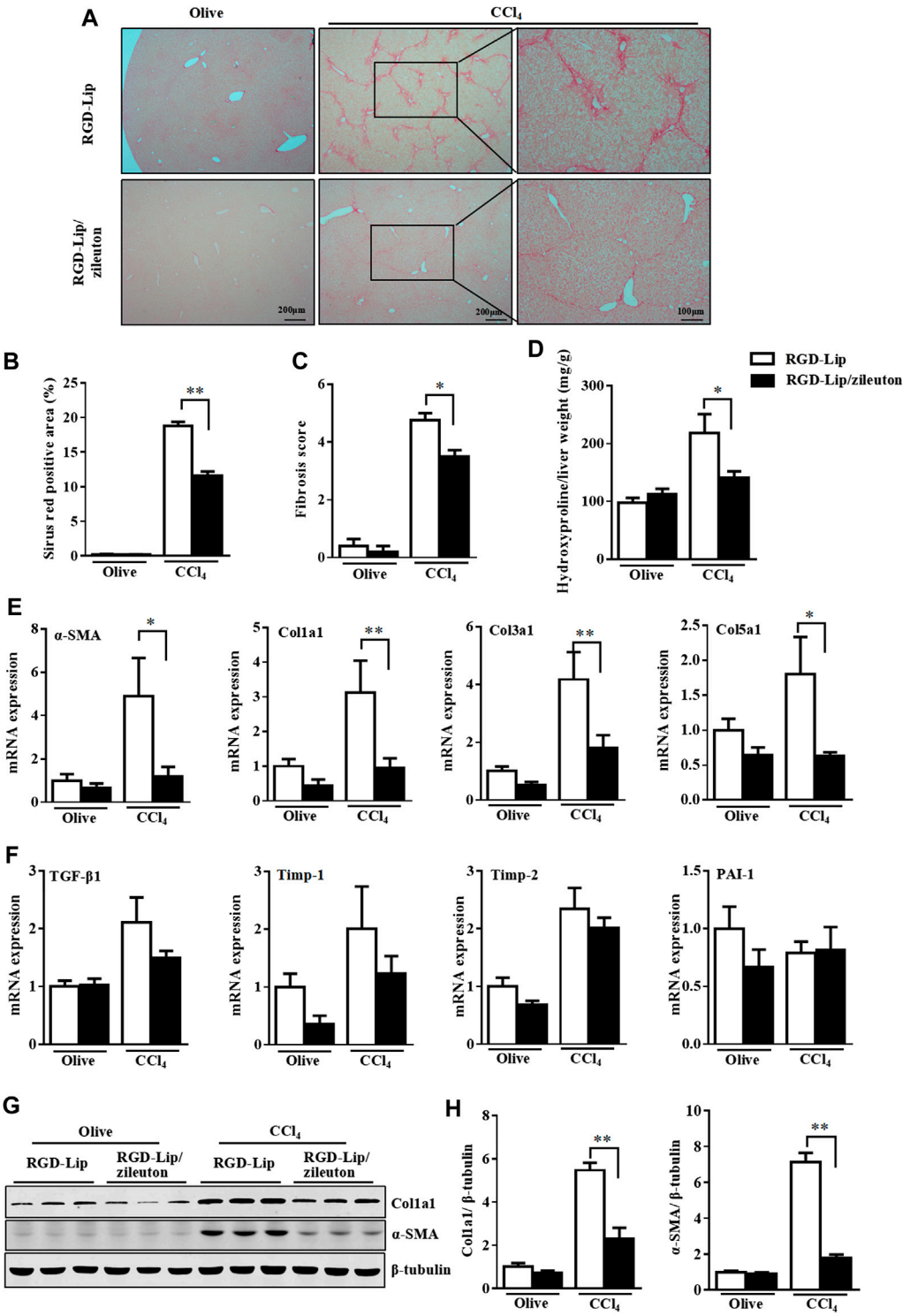


FIGURE 7 | Targeted delivery of zileuton to HSC is efficient against CCl_4-induced liver fibrosis. WT mice were treated with olive oil or CCl_4 for 8 weeks. During the last 4 weeks, mice given RGD-Lip or RGD-Lip/zileuton (10 mg/kg) every 3 days by tail vein injection. **(A,B)** Liver sections were collected for picrosirius red staining. **(C)** Fibrosis score was assessed for collagen according to the Ishak criteria. **(D)** Detection of hepatic hydroxyproline level. **(E,F)** qRT-PCR analysis of mRNA levels of fibrotic genes in livers of 4 groups. **(G)** Western blot analysis of the protein levels of α-SMA and Col1a1. Data are mean ± SEM, n = 7, $^{*}p < 0.05$, $^{**}p < 0.01$.

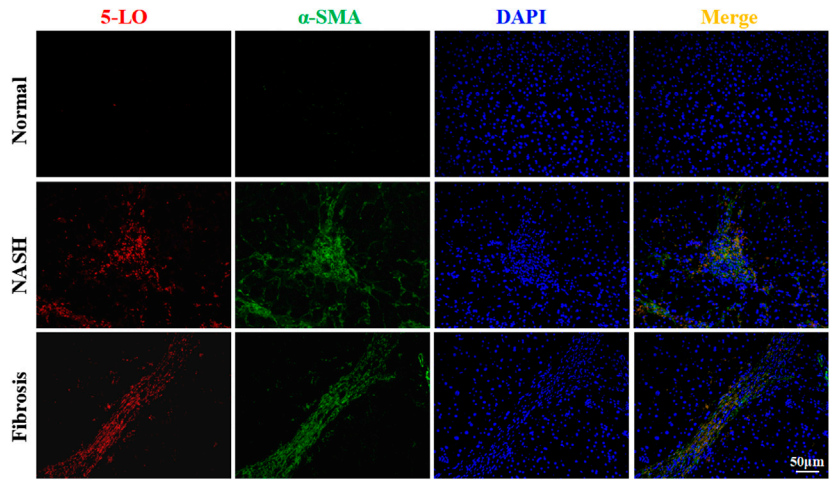


FIGURE 8 | The expression of 5-LO was increased in liver sections of patients with fibrosis. Liver sections were collected from normal individuals or patients with non-alcoholic steatohepatitis or liver fibrosis and were stained with 5-LO and α-SMA. Data are mean ± SEM, n = 3.

RGD-Lip/zileuton-treated mice (**Supplementary Figures S14B–D**).

Increased Expression of 5-LO in Patients with Hepatic Fibrosis

We next determined whether 5-LO expression was changed in patients with NASH or liver fibrosis. The diagnosis of NASH and fibrosis was confirmed by H&E and picrosirius red staining (**Supplementary Figures S15A–C**). As compared with healthy individuals, the expression of 5-LO was increased in liver sections from patients with NASH and fibrosis (**Figure 8**). The expression of 5-LO was largely co-localized in α-SMA-positive cells, which were HSC (**Figure 8**). These results were consistent with 5-LO possibly having a positive role in activation of HSC in rodents.

DISCUSSION

In this study, we found increased secretion of LTB_4 and LTC_4 in a-HSC. LTB_4 and LTC_4 contributed to HSC activation via ERK signaling. Elevated LTB_4 and LTC_4 was likely a result of increased expression of 5-LO during HSC activation. Genetic ablation of 5-LO protected mice against CCl_4- and MCD diet-induced fibrosis and liver injury. Pharmacological inhibition of 5-LO in HSC by targeted delivery of zileuton prevented CCl_4- and MCD diet-induced liver fibrosis. Finally, we found 5-LO level increased in liver sections of patients with liver fibrosis.

Several reports have suggested that 5-LO may play a role in fibrosis (Titos et al., 2004). 5-LO is expressed in various fibroblast cells, such as pulmonary fibroblasts, human myofibroblasts and skin fibroblasts (Nagy et al., 2011; Xiao et al., 2011) (Su et al., 2016). Titos et al. found 5-LO expressed in Kupffer cells (Titos et al., 2004). Pharmacological inhibition of 5-LO protected mice from CCl_4-induced liver fibrosis (Horrillo et al., 2007). However, the following study could not confirm the expression of 5-LO in Kupffer cells (Takeda et al., 2017). Also, 5-LO expression was detected in HSC isolated from mice and rats (Paiva et al., 2010; Shajari et al., 2015). However, the function of 5-LO in HSC was not known. In our study, we found 5-LO expressed in HSC, and its expression was increased during their activation. With increased expression of 5-LO, the secretion of LTB_4 and LTC_4 was significantly elevated in a-HSC (**Figures 1A,B**; **Supplementary Figure S1**). LTB_4 and LTC_4 promoted HSC activation via ERK1 signaling pathway. This finding was consistent with a previous report of LTB_4 and LTC_4 leading to pulmonary fibrosis because of stimulating the activation and differentiation of fibroblasts (Hirata et al., 2013). Other lipoxygenases, such as 12-lipoxygenase, was also upregulated in a-HSC compared with q-HSC (Mori et al., 2020). However, we did not found the difference of 12-HETE, a metabolic of arachidonic acid through 12-lipoxygease, in q-HSC and a-HSC supernatant (**Supplementary Figure S1**). The role of 12-lipoxygenase in HSC deserves further study.

Liver fibrosis homeostasis is maintained by the balance of extracellular matrix synthetic machinery, contributing to increased rate of collagen synthesis and activities of the cellular fibrinolytic system. Timp-1 belongs to the Timp family and participates in degrading the extracellular matrix (Iredale, 2007). PAI-1 is a member of the serine protease inhibitor family, the main physiological inhibitor of serine protease, and contributes to the fibrinolytic system (Wang et al., 2007). Several studies have shown that Timp-1 and PAI-1 are key factors modulating fibrolysis and extracellular matrix deposition (Iredale, 2007; Wang et al., 2007). Knockout or pharmacological inhibition of Timp1 and PAI-1 inhibited fibrosis in liver (Parsons et al., 2004). Our *in vitro* results showed significantly increased expression of Timp-1 and PAI-1 in culture-activated HSC as compared with q-HSC. However, genetic ablation of 5-LO in HSC decreased levels of Timp1 and PAI-1, which may contribute to suppressed extracellular matrix deposition. *In vivo*, 5-LO ablation or pharmacological inhibition

reduced the Timp-1 and PAI-1 expression, which helped reduce hydroxyproline level in mouse liver.

Oral treatment or injection of the 5-LO inhibitor zileuton causes systemic pharmacological side effects. Zileuton could increase oxidative stress in hepatocytes and may cause hepatocyte damage (Altumina, 1995). In addition, zileuton treatment was found to increase serum ALT and AST levels (Watkins et al., 2007). These results suggest that systemic zileuton administration may cause drug-induced side effects. cRGD is pentapeptide that binds with high affinity to integrin αV and β3 which are highly expressed in a-HSC (Li et al., 2019). It was also confirmed that cRGD-guided Lips specifically target activated HSC *in vitro* and *vivo* (Li et al., 2019; Zhang et al., 2020). In agreement with a previous report, we found that RGD-Lip-delivered zileuton was highly enriched in HSC but not hepatocytes, Kupffer cells, endothelial cells or biliary cells (**Supplementary Figure S9B**). RGD-Lip/zileuton administration significantly protected mice against CCl_4-and MCD diet-induced liver fibrosis (**Figure 7**; **Supplementary Figure S12**). Therefore, targeted delivery of zileuton to inhibit 5-LO by RGD-Lip may be a promising way to manage liver fibrosis.

Obviously, both CCl_4 and MCD-diet treatments induce inflammation, which were reduced by 5-LO ablation or RGD/Lip-zileuton administration. Horrillo et al. also found that 5-LO inhibitor protected mice from CCl_4-induced liver inflammation (Horrillo et al., 2007). In our study, knockout of 5-LO did reduce the accumulation of F4/80 positive cells in fibrotic liver (**Supplementary Figure S5C**). However, treatment of RGD/Lip-zileuton did not reduce the accumulation of F4/80 positive cells (**Supplementary Figure S11D**). It was reported that activation of HSC mediated immune response (Chou et al., 2011; Chang et al., 2013; Bigorgne et al., 2016). We speculate that the beneficial effect of RGD/Lip-zileuton is more due to reduce in the HSC fibrosis compartment than reduced inflammation in the Kupffer cell compartment. The changes of these inflammatory indicators are related to the decrease of HSC activation.

LTB_4 and LTC_4 were reported as lipid mediators for attracting neutrophils and for lipid accumulation (Lund et al., 2017). Induction of LTB_4 and LTC_4 biosynthesis might cause hepatotoxicity via neutrophil activation (Shiratori et al., 1989; Takeda et al., 2017). 5-LO is the key enzyme that catalyzes arachidonic acid to form LTB_4 and LTC_4 (Alexander et al., 2011). In our study, both deletion of 5-LO and targeted inhibition of 5-LO in HSC protected mice against CCl_4-and MCD diet-induced liver injury, at least in part by reducing LTB_4 and LTC_4 production in the liver.

In summary, we demonstrate that 5-LO inhibition confers resistance to CCl_4- and MCD diet-induced hepatic fibrosis. The protective effect of 5-LO deletion was partially due to decreased level of LTB_4 as well as LTC_4 and reduced activation of HSC. Our data show that 5-LO is critical for liver fibrosis in the setting of supporting HSC activation. 5-LO expression was also increased in HSC in liver sections of patients with fibrosis. Strategies to target inhibition of 5-LO in HSC may be useful for treating liver fibrosis.

DATA AVAILABILITY STATEMENT

The original contributions presented in the study are included in the article/**Supplementary Material**. Further inquiries can be directed to the corresponding author.

ETHICS STATEMENT

Ethical review and approval was not required for the study on human participants in accordance with the local legislation and institutional requirements. Written informed consent for participation was not required for this study in accordance with the national legislation and institutional requirements. The animal study was reviewed and approved by the Animal Care and Utilization Committee of West China Hospital.

AUTHOR CONTRIBUTIONS

Participated in research design: SP, YL and JH. Conducted experiments: SP, YL, QL, XZ, LC, RL, JZ, TW, QT, XY, ZZ, YH, JK, and HL. Performed data analysis: MZ and WJ. Wrote or contributed to the writing of the manuscript: SP, YL, and JH.

FUNDING

This work was supported by the National Natural Science Foundation of China (81471068, 81603035 and 81870599), China Postdoctoral Fellowship (2018T110986), Young Scientist Fellowship of Sichuan University (2017SCU11026), Postdoctoral Fellowship of Sichuan University (2017SCU12036), and the 1.3.5 project for disciplines of excellence, West China Hospital, Sichuan University (ZYJC18008).

ACKNOWLEDGMENTS

The authors thank Miss Huifang Li and Miss Ge Liang from Core Facility of West China Hospital for technical assistance.

SUPPLEMENTARY MATERIAL

The Supplementary Material for this article can be found online at: https://www.frontiersin.org/articles/10.3389/fphar.2021.628583/full#supplementary-material.

REFERENCES

Alexander, S. P., Mathie, A., and Peters, J. A. (2011). Guide to receptors and channels (GRAC), 5th edition. *Br. J. Pharmacol.* 164 (1), S1–S3. doi:10.1111/j.1476-5381.2011.01649_1.x

Altumina, M. M. (1995). Several characteristics of the pulmonary *tuberculosis* course in patients with different degree of diabetes mellitus compensation. *Probl. Tuberk.* 6,15–17.

Anstee, Q. M., and Goldin, R. D. (2006). Mouse models in non-alcoholic fatty liver disease and steatohepatitis research. *Int. J. Exp. Pathol.* 87, 1–16. doi:10.1111/j.0959-9673.2006.00465.x

Bigorgne, A. E., John, B., Ebrahimkhani, M. R., Shimizu-Albergine, M., Campbell, J. S., and Crispe, I. N. (2016). TLR4-Dependent secretion by hepatic stellate cells of the neutrophil-chemoattractant CXCL1 mediates liver response to gut microbiota. *PLoS One* 11, e0151063. doi:10.1371/journal.pone.0151063

Chang, J., Hisamatsu, T., Shimamura, K., Yoneno, K., Adachi, M., Naruse, H., et al. (2013). Activated hepatic stellate cells mediate the differentiation of macrophages. *Hepatol. Res.* 43, 658–669. doi:10.1111/j.1872-034X.2012.01111.x

Chen, L., Liu, Q., Tang, Q., Kuang, J., Li, H., Pu, S., et al. (2019). Hepatocyte-specific Sirt6 deficiency impairs ketogenesis. *J. Biol. Chem.* 294, 1579–1589. doi:10.1074/jbc.RA118.005309

Chen, Q., Chen, L., Kong, D., Shao, J., Wu, L., and Zheng, S. (2016). Dihydroartemisinin alleviates bile duct ligation-induced liver fibrosis and hepatic stellate cell activation by interfering with the PDGF-βR/ERK signaling pathway. *Int. Immunopharm.* 34, 250–258. doi:10.1016/j.intimp.2016.03.011

Chou, H. S., Hsieh, C. C., Yang, H. R., Wang, L., Arakawa, Y., Brown, K., et al. (2011). Hepatic stellate cells regulate immune response by way of induction of myeloid suppressor cells in mice. *Hepatology* 53, 1007–1019. doi:10.1002/hep.24162

De Corso, E., Anzivino, R., Galli, J., Baroni, S., Di Nardo, W., De Vita, C., et al. (2019). Antileukotrienes improve naso-ocular symptoms and biomarkers in patients with NARES and asthma. *Laryngoscope* 129, 551–557. doi:10.1002/lary.27576

De Minicis, S., Candelaresi, C., Marzioni, M., Saccomano, S., Roskams, T., Casini, A., et al. (2008). Role of endogenous opioids in modulating HSC activity *in vitro* and liver fibrosis *in vivo*. *Gut* 57, 352–364. doi:10.1136/gut.2007.120303

Feng, X. H., and Derynck, R. (2005). Specificity and versatility in tgf-beta signaling through Smads. *Annu. Rev. Cell Dev. Biol.* 21, 659–693. doi:10.1146/annurev.cellbio.21.022404.142018

Harizi, H., Corcuff, J. B., and Gualde, N. (2008). Arachidonic-acid-derived eicosanoids: roles in biology and immunopathology. *Trends Mol. Med.* 14, 461–469. doi:10.1016/j.molmed.2008.08.005

Higashi, T., Friedman, S. L., and Hoshida, Y. (2017). Hepatic stellate cells as key target in liver fibrosis. *Adv. Drug Deliv. Rev.* 121, 27–42. doi:10.1016/j.addr.2017.05.007

Hirata, H., Arima, M., Fukushima, Y., Sugiyama, K., Tokuhisa, T., and Fukuda, T. (2013). Leukotriene C4 aggravates bleomycin-induced pulmonary fibrosis in mice. *Respirology* 18, 674–681. doi:10.1111/resp.12072

Hofmann, B., and Steinhilber, D. (2013). 5-Lipoxygenase inhibitors: a review of recent patents (2010-2012). *Expert Opin. Ther. Pat.* 23, 895–909. doi:10.1517/13543776.2013.791678

Horrillo, R., Planagumà, A., González-Périz, A., Ferré, N., Titos, E., Miquel, R., et al. (2007). Comparative protection against liver inflammation and fibrosis by a selective cyclooxygenase-2 inhibitor and a nonredox-type 5-lipoxygenase inhibitor. *J. Pharmacol. Exp. Therapeut.* 323, 778–786. doi:10.1124/jpet.107.128264

Iredale, J. P. (2007). Models of liver fibrosis: exploring the dynamic nature of inflammation and repair in a solid organ. *J. Clin. Invest.* 117, 539–548. doi:10.1172/JCI30542

Ishak, K., Baptista, A., Bianchi, L., Callea, F., De Groote, J., Gudat, F., et al. (1995). Histological grading and staging of chronic hepatitis. *J. Hepatol.* 22, 696–699. doi:10.1016/0168-8278(95)80226-6

Kowal, K., Gielicz, A., and Sanak, M. (2017). The effect of allergen-induced bronchoconstriction on concentration of 5-oxo-ETE in exhaled breath condensate of house dust mite-allergic patients. *Clin. Exp. Allergy* 47, 1253–1262. doi:10.1111/cea.12990

Kwon, H. J., Won, Y. S., Park, O., Chang, B., Duryee, M. J., Thiele, G. E., et al. (2014). Aldehyde dehydrogenase 2 deficiency ameliorates alcoholic fatty liver but worsens liver inflammation and fibrosis in mice. *Hepatology* 60, 146–157. doi:10.1002/hep.27036

Li, Y., Pu, S., Liu, Q., Li, R., Zhang, J., Wu, T., et al. (2019). An integrin-based nanoparticle that targets activated hepatic stellate cells and alleviates liver fibrosis. *J. Contr. Release* 303, 77–90. doi:10.1016/j.jconrel.2019.04.022

Lin, H. C., Lin, T. H., Wu, M. Y., Chiu, Y. C., Tang, C. H., Hour, M. J., et al. (2014). 5-Lipoxygenase inhibitors attenuate TNF-α-induced inflammation in human synovial fibroblasts. *PLoS One* 9, e107890. doi:10.1371/journal.pone.0107890

Locatelli, I., Sutti, S., Jindal, A., Vacchiano, M., Bozzola, C., Reutelingsperger, C., et al. (2014). Endogenous annexin A1 is a novel protective determinant in nonalcoholic steatohepatitis in mice. *Hepatology* 60, 531–544. doi:10.1002/hep.27141

Lund, S. J., Portillo, A., Cavagnero, K., Baum, R. E., Naji, L. H., Badrani, J. H., et al. (2017). Leukotriene C4 potentiates IL-33-induced group 2 innate lymphoid cell activation and lung inflammation. *J. Immunol.* 199, 1096–1104. doi:10.4049/jimmunol.1601569

Mori, Y., Kawakami, Y., Kanzaki, K., Otsuki, A., Kimura, Y., Kanji, H., et al. (2020). Arachidonate 12S-lipoxygenase of platelet-type in hepatic stellate cells of methionine and choline-deficient diet-fed mice. *J. Biochem.* 168, 455–463. doi:10.1093/jb/mvaa062

Nagy, E., Andersson, D. C., Caidahl, K., Eriksson, M. J., Eriksson, P., Franco-Cereceda, A., et al. (2011). Upregulation of the 5-lipoxygenase pathway in human aortic valves correlates with severity of stenosis and leads to leukotriene-induced effects on valvular myofibroblasts. *Circulation* 123, 1316–1325. doi:10.1161/CIRCULATIONAHA.110.966846

Nasr, P., Ignatova, S., Kechagias, S., and Ekstedt, M. (2018). Natural history of nonalcoholic fatty liver disease: a prospective follow-up study with serial biopsies. *Hepatol. Commun.* 2, 199–210. doi:10.1002/hep4.1134

Ogawa, T., Tateno, C., Asahina, K., Fujii, H., Kawada, N., Obara, M., et al. (2007). Identification of vitamin A-free cells in a stellate cell-enriched fraction of normal rat liver as myofibroblasts. *Histochem. Cell Biol.* 127, 161–174. doi:10.1007/s00418-006-0237-7

Paiva, L. A., Maya-Monteiro, C. M., Bandeira-Melo, C., Silva, P. M., El-Cheikh, M. C., Teodoro, A. J., et al. (2010). Interplay of cysteinyl leukotrienes and TGF-β in the activation of hepatic stellate cells from Schistosoma mansoni granulomas. *Biochim. Biophys. Acta.* 1801, 1341–1348. doi:10.1016/j.bbalip.2010.08.014

Parsons, C. J., Bradford, B. U., Pan, C. Q., Cheung, E., Schauer, M., Knorr, A., et al. (2004). Antifibrotic effects of a tissue inhibitor of metalloproteinase-1 antibody on established liver fibrosis in rats. *Hepatology* 40, 1106–1115. doi:10.1002/hep.20425

Puche, J. E., Saiman, Y., and Friedman, S. L. (2013). Hepatic stellate cells and liver fibrosis. *Comp. Physiol.* 3, 1473–1492. doi:10.1002/cphy.c120035

Qian, J., Tian, W., Jiang, X., Tamosiuniene, R., Sung, Y. K., Shuffle, E. M., et al. (2015). Leukotriene B4 activates pulmonary artery adventitial fibroblasts in pulmonary hypertension. *Hypertension* 66, 1227–1239. doi:10.1161/HYPERTENSIONAHA.115.06370

Shajari, S., Laliena, A., Heegsma, J., Tuñón, M. J., Moshage, H., and Faber, K. N. (2015). Melatonin suppresses activation of hepatic stellate cells through RORα-mediated inhibition of 5-lipoxygenase. *J. Pineal Res.* 59, 391–401. doi:10.1111/jpi.12271

Shiratori, Y., Moriwaki, H., Muto, Y., Onishi, H., Kato, M., and Asano, F. (1989). Production of leukotriene B4 in parenchymal and sinusoidal cells of the liver in rats treated simultaneously with D-galactosamine and endotoxin. *Gastroenterol. Jpn.* 24, 640–645. doi:10.1007/BF02774162

Silverman, E. S., and Drazen, J. M. (1999). The biology of 5-lipoxygenase: function, structure, and regulatory mechanisms. *Proc. Assoc. Am. Phys.* 111, 525–536. doi:10.1046/j.1525-1381.1999.t01-1-99231.x

Su, H. H., Lin, H. T., Suen, J. L., Sheu, C. C., Yokoyama, K. K., Huang, S. K., et al. (2016). Aryl hydrocarbon receptor-ligand axis mediates pulmonary fibroblast migration and differentiation through increased arachidonic acid metabolism. *Toxicology* 370, 116–126. doi:10.1016/j.tox.2016.09.019

Takeda, T., Komiya, Y., Koga, T., Ishida, T., Ishii, Y., Kikuta, Y., et al. (2017). Dioxin-induced increase in leukotriene B4 biosynthesis through the aryl hydrocarbon receptor and its relevance to hepatotoxicity owing to

neutrophil infiltration. *J. Biol. Chem.* 292, 10586–10599. doi:10.1074/jbc.M116.764332

Thi Thanh Hai, N., Thuy, L. T. T., Shiota, A., Kadono, C., Daikoku, A., Hoang, D. V., et al. (2018). Selective overexpression of cytoglobin in stellate cells attenuates thioacetamide-induced liver fibrosis in mice. *Sci. Rep.* 8, 17860. doi:10.1038/s41598-018-36215-4

Titos, E., Planagumà, A., López-Parra, M., Villamor, N., Miquel, R., Jiménez, W., et al. (2004). 5-Lipoxygenase (5-LO) is involved in kupffer cell survival. Possible role of 5-LO products in the pathogenesis of liver fibrosis. *Comp. Hepatol.* 3 (1), S19. doi:10.1186/1476-5926-2-S1-S19

Wang, H., Zhang, Y., and Heuckeroth, R. O. (2007). PAI-1 deficiency reduces liver fibrosis after bile duct ligation in mice through activation of tPA. *FEBS Lett.* 581, 3098–3104. doi:10.1016/j.febslet.2007.05.049

Watkins, P. B., Dube, L. M., Walton-Bowen, K., Cameron, C. M., and Kasten, L. E. (2007). Clinical pattern of zileuton-associated liver injury: results of a 12-month study in patients with chronic asthma. *Drug Saf.* 30, 805–815. doi:10.2165/00002018-200730090-00006

Woodhoo, A., Iruarrizaga-Lejarreta, M., Beraza, N., García-Rodríguez, J. L., Embade, N., Fernández-Ramos, D., et al. (2012). Human antigen R contributes to hepatic stellate cell activation and liver fibrosis. *Hepatology* 56, 1870–1882. doi:10.1002/hep.25828

Wu, X., Zhi, F., Lun, W., Deng, Q., and Zhang, W. (2018). Baicalin inhibits PDGF-BB-induced hepatic stellate cell proliferation, apoptosis, invasion, migration and activation via the miR-3595/ACSL4 axis. *Int. J. Mol. Med.* 41, 1992–2002. doi:10.3892/ijmm.2018.3427

Xiao, R., Yoshida, N., Higashi, Y., Lu, Q. J., Fukushige, T., Kanzaki, T., et al. (2011). Retinoic acids exhibit anti-fibrotic activity through the inhibition of 5-lipoxygenase expression in scleroderma fibroblasts. *J. Dermatol.* 38, 345–353. doi:10.1111/j.1346-8138.2010.00993.x

Xie, Y. X., Liao, R., Pan, L., and Du, C. Y. (2017). ERK pathway activation contributes to the tumor-promoting effects of hepatic stellate cells in hepatocellular carcinoma. *Immunol. Lett.* 188, 116–123. doi:10.1016/j.imlet.2017.06.009

Yu, J., Hu, Y., Gao, Y., Li, Q., Zeng, Z., Li, Y., et al. (2018). Kindlin-2 regulates hepatic stellate cells activation and liver fibrogenesis. *Cell Death Dis.* 4, 34. doi:10.1038/s41420-018-0095-9

Zhang, J., Li, Y., Liu, Q., Huang, Y., Li, R., Wu, T., et al. (2020). Sirt6 alleviated liver fibrosis by deacetylating conserved lysine 54 on Smad2 in hepatic stellate cells. *Hepatology*. doi:10.1002/hep.31418

Zhang, X., Tan, Z., Wang, Y., Tang, J., Jiang, R., Hou, J., et al. (2015). PTPRO-associated hepatic stellate cell activation plays a critical role in liver fibrosis. *Cell. Physiol. Biochem.* 35, 885–898. doi:10.1159/000369746

Conflict of Interest: The authors declare that the research was conducted in the absence of any commercial or financial relationships that could be construed as a potential conflict of interest.

Copyright © 2021 Pu, Li, Liu, Zhang, Chen, Li, Zhang, Wu, Tang, Yang, Zhang, Huang, Kuang, Li, Zou, Jiang and He. This is an open-access article distributed under the terms of the Creative Commons Attribution License (CC BY). The use, distribution or reproduction in other forums is permitted, provided the original author(s) and the copyright owner(s) are credited and that the original publication in this journal is cited, in accordance with accepted academic practice. No use, distribution or reproduction is permitted which does not comply with these terms.

frontiers in Pharmacology

REVIEW
published: 24 March 2021
doi: 10.3389/fphar.2021.645703

Targeting Certain Interleukins as Novel Treatment Options for Liver Fibrosis

Su Yeon An[1], *Anca D. Petrescu*[1] *and Sharon DeMorrow*[1,2,3]*

[1]Division of Pharmacology and Toxicology, College of Pharmacy, The University of Texas at Austin, Austin, TX, United States, [2]Department of Internal Medicine, Dell Medical School, The University of Texas at Austin, Austin, TX, United States, [3]Research Division, Central Texas Veterans Healthcare System, Temple, TX, United States

The liver is a major metabolic organ and an immunologically complex organ. It produces and uses many substances such as acute phase proteins, cytokines, chemokines, and complementary components to maintain the balance between immunity and tolerance. Interleukins are important immune control cytokines, that are produced by many body cells. In liver injury, interleukins are produced in large amount by various cell types, and act as pro-inflammatory (e.g. interleukin (IL)-6, IL-13, IL-17, and IL-33) as well as anti-inflammatory (e.g. IL-10) functions in hepatic cells. Recently, interleukins are regarded as interesting therapeutic targets for the treatment of liver fibrosis patients. Hepatic cells such as hepatocytes, hepatic stellate cells, and hepatic macrophages are involved to the initiation, perpetuation, and resolution of fibrosis. The understanding of the role of interleukins in such cells provides opportunity for the development of therapeutic target drugs. This paper aims to understand the functional roles of interleukins in hepatic and immune cells when the liver is damaged, and suggests the possibility of interleukins as a new treatment target in liver fibrosis.

Keywords: interleukins, hepatocytes, macrophages, hepatic stellate cells, CD4$^+$ T helper cells, liver fibrosis

OPEN ACCESS

Edited by:
Ralf Weiskirchen,
RWTH Aachen University, Germany

Reviewed by:
Steven O'Reilly,
Durham University, United Kingdom
Wei Chen,
Stanford University, United States

***Correspondence:**
Sharon DeMorrow
sharon.demorrow@austin.utexas.edu

Specialty section:
This article was submitted to Gastrointestinal and Hepatic Pharmacology, a section of the journal Frontiers in Pharmacology

Received: *23 December 2020*
Accepted: *16 February 2021*
Published: *24 March 2021*

Citation:
An SY, Petrescu AD and DeMorrow S (2021) Targeting Certain Interleukins as Novel Treatment Options for Liver Fibrosis. Front. Pharmacol. 12:645703. doi: 10.3389/fphar.2021.645703

INTRODUCTION

Fibrosis is the pathological feature and the end result of chronic inflammatory reaction induced by various types of injuries in several organs including skin, kidney, lung, heart, intestine, and liver. Therefore chronic fibroproliferative diseases is a major public health problem (Nanchahal and Hinz, 2016). In the liver, progressive fibrosis caused by injury, inflammation, and extracellular matrix (ECM) accumulation ultimately results in cirrhosis or hepatocellular carcinoma. The only effective treatment for these terminal liver disorders is liver transplantation (Bataller and Brenner, 2005; Bansal et al., 2016). For this reason, treatment at the liver fibrosis stage that prevents the progression of the disease, and that leads to resolution is very important.

Abbreviations: α-SMA, α-smooth muscle actin; CCl4, Carbon tetrachloride; CD4 T cells; CD4+ T helper cells; DAMP, Danger associated molecular patterns; ECM, Extracellular matrix; ERK, Extracellular signal regulated kinase; HSCs, Hepatic stellate cells; IL, Interleukin; IL-10R, IL-10 receptor; ILC2, Innate lymphoid cells; JAK, Janus kinase; MAPK; Mitogen-activated protein kinase; MCs, Mast cells; MoMFs, Monocytes-derived macrophages; MyD88, Myeloid differentiation primary response gene 88; NF-κB; Nuclear factor-κB, PDGF, Platelet-derived growth factor; STAT, Signal transducer and activator of transcription; TGF-β, Transforming growth factor-β; Th, T helper; TRAF6, Tumor necrosis factor receptor-associated factor 6; Tregs, Regulatory T cells; TYK, Tyrosine kinase.

The initiation, perpetuation and resolution of liver fibrosis is a complex process of communication between cells receiving a multitude of signals consisting of various growth factors, chemokines and cytokines (Kubes and Jenne, 2018). Interleukins, a cytokine family that include chemokines, interferons, lymphokines, and tumor necrosis factors, were first thought to be expressed in leukocytes alone, but it was later found that about 40 types of interleukins were produced by many other body cells. Interleukins play an essential role in the activation and differentiation of immune cells as well as proliferation, maturity, migration, and adhesion. They can also have pro-inflammatory or anti-inflammatory or both properties (Hammerich and Tacke, 2014).

IL-6 and IL-1 are representative keystone cytokines in liver disease and have both pro and anti-inflammatory properties. IL-6 is a main regulatory factor in processes of wound healing and tissue regeneration related to various liver injures. It was concluded that IL-6/STAT3 signaling prevents cholestasis and liver fibrosis and has role in regulation of hepatocyte and cholangiocyte functions in the model of sclerosing cholangitis (Mair et al., 2010). However, more recent publications reveal negative effects of IL-6 which can directly induce transition of HSCs to myofibroblast-like cells, in hepatic fibrosis (Kagan et al., 2017). Very recent studies on the role of JAK-STAT signaling in hepatocellular carcinoma (HCC) emphasized that members of IL-6 family of cytokines have emerged as important regulatory factors and are considered to be targets for therapeutic intervention (Lokau et al., 2019). IL-1 family consists of 11 cytokines of the innate immune system. These cytokines trigger various immune responses to liver injuries, i.e. IL-1α, β and IL-33 are proinflammatory cytokines; in contrast, IL-1Ra, IL-36Ra, IL-37, and IL-38 have anti-inflammatory responses, while IL-18 was found to be pro- and anti-inflammatory under different circumstances (Barbier et al., 2019; Chan and Schroder, 2020). Additionally, IL-1 cytokines activate mast cells (MCs) to secrete inflammatory mediators (chemokines and cytokines including IL-1, IL-33 and TNF), and this effect can be counteracted by IL-37 (Gallenga et al., 2019). Thus, it has been determined that IL-37 is an anti-inflammatory cytokine that interacts with IL-18Ra chain and decreases the inflammatory effects of IL-1 cytokines (Toniato et al., 2017; Caraffa et al., 2019; Gugliandolo et al., 2019). Cytokines from IL-36 subfamily of IL-1 are produced by activated MCs and have strong pro-inflammatory effects which can be balanced by IL-38 which binds to IL-36R inducing anti-inflammatory activity (Varvara et al., 2018; Gallenga et al., 2019). Numerous studies have investigated the role of each cytokine and receptor from this family in various types of liver injuries, and have been reviewed in detail recently (He et al., 2021).

This review presents and emphasizes certain interleukins as potential therapeutic targets for liver fibrosis. We specifically focused on the pro-inflammatory interleukins: interleukin (IL)-13, IL-17, and IL-33, anti-inflammatory interleukin: IL-10 based on the numerous studies published in recent years that clearly showed their functions and effects. Furthermore, this review summarizes the origin, function, and signal pathway of these selected interleukins and, also shows the functions of these specific interleukins in hepatocytes, hepatic stellate cells (HSCs), and hepatic macrophages which are main players in liver fibrosis.

$CD4^+$ T HELPER CELLS

The innate and adaptive immune responses occurring simultaneously or sequentially in time, are initiated by Kupffer cells that recognize liver damage. Following liver injury, inflammatory lymphocytes infiltrate the damaged hepatic parenchyma (Dong et al., 2019; Li et al., 2019). T lymphocytes, which are activated through antigen-specific manner of dendritic cells, help the B lymphocytes to create antigen-specific antibodies, or to remove infected cells. Specially, $CD4^+$ T helper cells (CD4 T cells) serve as the total commander of immunity. CD4 T cells can be classified into at least four subsets, referred to as T helper (Th) cells type 1, Th2, Th17, and induced regulatory T cells (Tregs). These cells play a major role in mediating immune response through the secretion of specific cytokines (Luckheeram et al., 2012).

Th1 cells play a particularly important role in mediating immune responses against intracellular pathogens, resistance to mycobacterial infections, and induction of some autoimmune diseases. Their principal cytokine products are interferon gamma, lymphotoxin α, and IL-2 (Paul and Seder, 1994). Th2 cells mediate immune response to extracellular parasites, including helminths, and play an important role in induction and persistence of asthma and other allergic diseases. Th2 cells produce IL-4, IL-5, IL-9, IL-13, IL-10, IL-25, and amphiregulin (Luckheeram et al., 2012). Th17 cells are responsible for mediating immune responses against extracellular fungi and bacteria, and for inducing the many organ-specific autoimmune diseases. Th17 cells produce IL-17, IL-17f, IL-21, and IL-22 (Zhu and Paul, 2008). IL-17 leads to the induction of pro-inflammatory cytokines, including IL-6, IL-1, tumor necrosis factor-α (TNF-α), and thus has an important role in inducing inflammatory responses (Luckheeram et al., 2012). Tregs play a critical role in the maintenance of self-tolerance to self and foreign antigen. Increasing Tregs numbers and/or enhancing their suppressive function may be beneficial for preventing allograft rejection and treating autoimmune diseases. The main effector cytokines of Tregs include IL-10, transforming growth factor-β (TGF-β), and IL-35 (Zhu and Paul, 2008; Luckheeram et al., 2012).

CD4 T cells release a wide range of inflammatory intermediates, particularly interleukins, which can act as the pro-inflammatory, anti-inflammatory, or two functions in liver fibrosis (Hammerich and Tacke, 2014; Sziksz et al., 2020). However, selecting interleukins with conflicting functions depending on the stage of liver disease as a therapeutic target requires more attention in the treatment process. In the case of IL-6 or IL-22, it prevents fibrogenesis but promotes hepatocellular carcinoma, so the risk of tumor occurrence should be considered in the treatment of patients with hepatic fibrosis (Schmidt-Arras and Rose-John, 2016; Wu et al., 2020). Therefore, it is very important to select and study targets capable

of blocking pro-inflammatory (IL-13, IL-17, and IL-33) or inducing anti-inflammatory interleukin (IL-10) in the complex process of liver fibrosis.

TARGET INTERLEUKINS

Interleukin-10

IL-10, one of the major anti-inflammatory cytokines, controls neutrophil infiltration and suppresses various pro-inflammatory mediators (Louis et al., 1998; Sziksz et al., 2020). IL-10 can be produced by Th2 cells but also by Th1, Th17, Tregs, $CD8^+$ T, and B lymphocytes. In the liver, IL-10 is expressed in various cell types, including hepatocytes, Kupffer cells, sinusoidal endothelial cells, HSCs, and lymphocytes (Hammerich and Tacke, 2014; Sziksz et al., 2020). Functional IL-10 receptor (IL-10R) complexes are tetramers consisting of two IL-10R1 and two IL-10R2 chains. IL-10 homodimer binding to its receptor activate Janus kinase (JAK) 1 and Tyrosine kinase (TYK) 2. Signal transducer and activator of transcription (STAT) 3 binds to IL-10R1 and phosphorylates, and then phosphorylated STAT3 translocate to the nucleus (**Figure 1**) (Verma et al., 2016).

Interleukin-13

IL-13 is an immunoregulatory cytokine secreted by predominantly Th2 cells. IL-13 has multiple effects on the differentiation and function of monocytes and macrophages. Although IL-13 plays an important role in the induction of allergic responses and inflammation as anti-inflammatory cytokine, it is a critical pro-fibrotic factor in liver fibrosis associated with Schistosoma and non-Schistosoma infection (De Vries, 1998; Liu et al., 2012). Additionally, IL-13 has been implicated in inflammatory bowel disease, asthma, and parasitic nematode expulsion (Grunig et al., 1998; Hershey, 2003). IL-13 induces many of the same responses and functional properties as IL-4 and shares a receptor subunit, the α subunit of the IL-4 receptor. IL-13 binds to the complex receptor system comprised of IL-4 receptor and two IL-13 binding proteins, IL-13Rα1 and IL-13Rα2. Signaling through the type II receptor (IL-4 receptor and IL13Rα1) leads to activation of JAK1 or JAK2/TYK2, STAT6, STAT3, and STAT1. Then, STAT dimerization and nuclear translocation occurs, followed by activation of gene transcription (**Figure 1**) (McCormick and Heller, 2015). IL-13 receptor is expressed on human B cells, basophils, eosinophils, mast cells, endothelial cells, fibroblasts, monocytes, macrophages, respiratory epithelial cells, and smooth muscle cells (Hershey, 2003).

Interleukin-17

IL-17 (now IL-17A) is an ancient pro-inflammatory cytokine with important roles in defense against bacteria and fungi. IL-17 are produced primarily by a T-cell subset termed Th17 cells, but can also be produced by neutrophils and other lymphocytes (Onishi and Gaffen, 2010). IL-17 signals through the IL-17RA-RC complex, and the IL-17 receptor recruits Act1 for downstream signaling. The Act1 with the IL-17 receptor complex contributes to the recruitment of Tumor necrosis factor receptor associated factor 6 (TRAF6). Then, these kinases promote the production of pro-inflammatory cytokines, chemokines, and-microbial peptides, through the pathway such as nuclear factor-κB (NF-κB), activator protein, and CCAAT/enhancer binding protein pathways (**Figure 1**) (Onishi and Gaffen, 2010; Meng et al., 2012).

Interleukin-33

IL-33 is the most recently identified member of IL-1 family of cytokines and is mainly expressed by stromal cells. IL-33 has been shown to induce the Th2 phenotype in Th cell, and therefore promotes progression of Th2-related diseases like several acute and chronic inflammatory diseases, including asthma, atopic dermatitis, rheumatoid arthritis, and ulcerative colitis among others (Schmitz et al., 2005; Sanada et al., 2007). The activity of IL-33 is mediated by binding to the heterodimeric ST2/IL-1 receptor associated protein receptor. Afterward, the complex recruits intracellular signaling molecules, including myeloid differentiation primary response 88 (MyD88)/IL-1 receptor-associated kinase/TRAF6, activating NF-κB, as well as extracellular signal regulated kinase (ERK) 1/2, c-Jun N-terminal kinase, p38 and phosphatidylinositol 3-kinase/protein kinase B (**Figure 1**) (Pinto et al., 2018; Barbier et al., 2019). Recently, IL-33 has gained attention as a new target or as an early alarm of liver fibrogenesis, as Th2 cells are strongly associated with fibrosis progression (Hammerich and Tacke, 2014; Weiskirchen and Tacke, 2016).

CONTRIBUTION OF THESE TARGET INTERLEUKINS IN THE HEPATIC CELLS

Interleukins in Hepatocytes

Hepatocytes are the major parenchymal cells that are important for liver function in metabolism, detoxification, and alcohol processing, and protein synthesis. Hepatocytes also activate innate and adaptive immunity when they are damaged by hepatotropic virus, an intracellular bacterium, or repeated or continuous injury (Crispe, 2016; Zhou et al., 2016). The initial reaction of hepatocytes injury by multiple factors is cell stress and cell death. The stressed and dying hepatocytes release damage-associated molecular patterns (DAMPs), reactive oxygen species, pro-inflammatory signals, and proliferation-associated cytokines through cross-talk with surrounding cells such as HSCs, endothelial cells, and immune cells (Tu et al., 2015; Yan et al., 2018). The reaction of hepatocytes indicate that hepatocytes contribute to the progress and resolution of liver fibrosis as active participants, not victims or bystanders (Tu et al., 2015).

McHedlidze et al. showed that damaged hepatocytes secreted IL-33 and that extracellular IL-33 leads to accumulation and activation of innate lymphoid cells (ILC2) (McHedlidze et al., 2013). Activated ILC2 by IL-33 produce IL-13, which induced the activation and trans-differentiation of HSCs through type-II IL-4 receptor-dependent signaling and STAT6. Further studies have identified IL-33 as key mediator of hepatic fibrosis by demonstrating that IL-33 deficiency ameliorates liver fibrosis

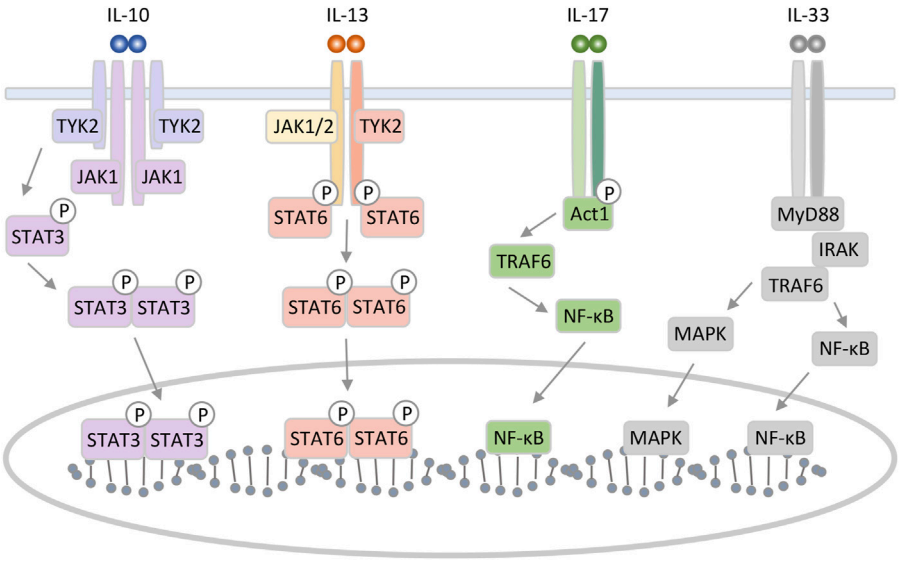


FIGURE 1 | Schematic representation of IL-10, 13, 17, and 33 interaction mechanism with their specific receptors. IL-10 can form a homodimer that binds to the tetrameric heterodimer IL-10 receptor and initiates an intracellular signaling pathway involving STAT3 as key translocation nuclear factor. IL-13 binding to type II receptor complex leads to activation of JAK and phosphorylation of members of the STAT family. The IL-17 receptor complex, which consists of IL-17RA and IL-17RC, activates downstream signaling pathways by recruiting an adaptor molecule named Act1. IL-33 triggers MAPK and NF-κB leading to inflammatory response.

induced by bile duct ligation and carbon tetrachloride (CCl_4) (McHedlidze et al., 2013).

Hepatocytes produce IL-10 which downregulates pro-inflammatory responses and has a potential modulatory effect on liver fibrosis (Sziksz et al., 2020). IL-10 gene therapy attenuated hepatic fibrosis and prevented cell apoptosis in a thioacetamide-treated liver. IL-10 gene transfer reduced not only mRNA level of liver TGF-β1, TNF-α, collagen α1, and cell adhesion molecule, but also decreased the activation of α-smooth muscle actin (α-SMA) and cyclooxygenase-2 (Hung et al., 2005). Other studies have shown that the modification with the IL-10 gene on the buffalo rat liver cells, a rat hepatocytes line, decreased a marked ability to stimulate the primary HSCs proliferation and their expression of α-SMA and procollagen type I, and an accelerated apoptosis of the HSCs was induced (Chen et al., 2012). These results suggest that IL-10 gene therapy might be an effective therapeutic reagent for liver fibrosis.

Interleukins in HSCs

HSCs play a pivotal role in the initiation, perpetuation, and resolution of liver fibrosis. In response to liver injury, quiescent HSCs trans-differentiate into myofibroblasts, and activated HSCs secrete pro-fibrogenic cytokines, growth factors, and ECM molecules (Higashi et al., 2017). Action of HSCs is also regulated by several soluble factors such as TGFβ, platelet-derived growth factor (PDGF), IL-1β, and interleukins. These soluble factors are derived from hepatocytes, macrophages, and other immune cells. In the case of interleukins, IL-17, IL-13, and IL-33 promote hepatic fibrogenesis through activation of hepatic stellate cells. In contrast, IL-10 and IL-22 protect from development of fibrosis by suppressing pro-fibrogenic function of HSCs (Hammerich and Tacke, 2014).

Many studies demonstrated that IL-13 is the pre-dominant profibrotic Th2 cytokine in Schistosomiasis infection which leads to granuloma formation and subsequent fibrosis development in the liver. Also, they show that blockade of IL-13 prevented liver fibrogenesis (Chiaramonte et al., 1999; Fallon et al., 2000; Chiaramonte et al., 2001). In the liver, IL-13 directly induces expression of collagen I and other critical fibrosis-associated genes such as α-SMA and connective tissue growth factor (CTGF) in HSCs (Liu et al., 2012). In HSCs, IL-13 induced CTGF by activating TGF-β-independent activin receptor-like kinase/Smad signaling via the Erk-mitogen-activated protein kinase (MAPK) pathway (Liu et al., 2011). A different study by Sui et al. showed that IL-13 stimulated proliferation of HSCs and secretion of TGF-β and PDGF by activation protein kinase C in LX-2, a cell line of human HSCs (Sui et al., 2018).

Numerous studies show that levels of IL-17 and its receptor increased in response to liver injury. Specially, the pro-inflammatory signaling of IL-17 has been widely studied in HSCs and Kupffer cells (Meng et al., 2012; Tan et al., 2013). Meng et al. demonstrated that IL-17 induced production of collagen type 1 in HSCs through activation of STAT3 signaling pathway. In addition, the author has demonstrated that the activation of fibrin in IL-17-induced HSCs required STAT3 by showing failure to induce collagen-a1 expression in STAT3-deficient HSCs (Meng et al., 2012). A different study showed that pharmacologic inhibition of IL-17-induced ERK1/2 or p38 significantly attenuated HSCs activation and collagen expression (Tan et al., 2013). *In vivo* experiments demonstrated that blocking IL-17 with anti-IL-17A mAb significantly improved liver function and decreased hepatocellular necrosis, pro-inflammatory cytokines,

neutrophils and macrophages influx in bile duct ligation-induced liver fibrosis mice (Zhang et al., 2016).

Previous studies have shown that soluble IL-33 increases the secretion of Th2 cytokines such as IL-6, IL-4 and IL-13, which promote HSCs proliferation, TGF-β synthesis and fibrogenesis (Wynn, 2004; Schmitz et al., 2005). Meanwhile, another study showed that activated HSCs with recombinant IL-33 released IL-6, TGF-β, α-SMA, and collagen via MAPK pathways mediated by ERK, c-Jun N-terminal kinase, and p38 protein kinases. Furthermore, the activation of HSCs, liver injury, and inflammatory cell infiltration were reduced in ST2 (IL-33 receptor)-deficient mice (Tan et al., 2017). Marvie et al. identified that IL-33 is upregulated in human and murine fibrosis, and is expressed by HSCs. Activated HSCs was a source of IL-33 that is strongly associated with fibrosis in chronic liver injury (Marvie et al., 2009). These results suggest that IL-33 can play an important role in the cross-talk between HSCs and Th2 cells in liver fibrosis.

The profibrogenic function of HSCs is suppresses by IL-10 which is one of the major anti-inflammatory cytokines. The increase of α-SMA and NF-κB in HSCs was attenuated by ectogenic IL-10 in CCl4-induced liver fibrosis (Zhang et al., 2006). Recently, studies demonstrated that IL-10 induced senescence of activated HSCs via STAT3-p53 pathway to attenuate liver fibrosis (Huang et al., 2020). The therapeutic effects of IL-10 were shown in experiments *in vivo* in which IL-10 gene therapy reduced the expression of fibrosis-related genes including TGF-β, TNF-α, and collagen α1, and also decreased the activation of α-SMA in thioacetamide-induced liver fibrosis (Hung et al., 2005).

Interleukins in Hepatic Macrophages

Hepatic macrophages consist of Kupffer cells, the largest population of liver resident macrophages, and inflammatory monocytes-derived macrophages (MoMFs) recruited from blood circulation and originated from bone marrow, spleen, and peritoneum. Recruited MoMFs undergo a process of differentiation into M1 (classically activated) or M2 (alternatively activated) species depending on the micro-environment (Van der Heide et al., 2019). Generally, following liver injury by many different factors, the resident Kupffer cells are activated and produce cytokines and chemokines to recruit monocytes and neutrophils. The recruited Ly6C+ MoMFs release pro-fibrotic molecules like TGF-β, TNF-α, IL-1β, PDGF and CC chemokine ligand 2, and these cytokines activate HSCs and promote liver fibrosis (Dong et al., 2019; Van der Heide et al., 2019). Recently, novel methods on targeting liver macrophages in fibrosis focus on regulating the activation of Kupffer cells, MoMFs recruitment, and macrophage polarization and differentiation (Tacke, 2017).

Kupffer cells not only express the receptor of IL-17, but also produce IL-17 which is mainly produced by Th17 cells (Ge and You, 2008). Meng et al. demonstrated that Kupffer cells, stimulated by IL-17, expressed inflammatory cytokines IL-6, IL-1β, TNF-α, and TGF-β1, which in turn, induced trans-differentiation of HSCs into fibrogenic myofibroblasts, and further facilitated differentiation of IL-17 producing cells (Meng et al., 2012). A very recent study showed that IL-17 is a cytokine that promotes tumors, critically controlling the inflammatory response in macrophages and the cholesterol synthesis in steatotic hepatocytes in the experimental model of alcohol-induced hepatocellular carcinoma. Therefore, the authors suggested the possibility of IL-17 as a potential treatment target for patients with alcohol-induced hepatocellular carcinoma as well as fibrosis (Ma et al., 2020).

Kupffer cells provide an anti-inflammatory microenvironment by secreting the anti-inflammatory cytokines IL-10 (Heymann et al., 2015; Van der Heide et al., 2019). Antigen presentation to Kupffer cells induces the arrest of CD4 T cells and the secretion of IL-10, an immunosuppressive cytokine, which results in promoting the immune tolerance (Van der Heide et al., 2019). Alternatively, activated M2 macrophages inhibit inflammatory reactions and secrete IL-10, IL-4/IL-13, TGF-β, and vascular endothelial growth factor-α to facilitate tissue repair. In contrast to the M2, M1 is pro-inflammatory, microbicidal, and tumoricidal. M1 also releases numerous inflammatory cytokines e.g., TNF-α, IL-1, IL-6, IL-12, IL-15, and IL-18 (Roszer, 2015; Wang et al., 2018). IL-10 mRNA was upregulated from both Kupffer cells *in vitro* and in whole liver after treatment with lipopolysaccharide or CCl4. Also, IL-10 inhibited production of superoxide and TNF-α in rat Kupffer cells following lipopolysaccharide treatment. Furthermore, IL-10−/− mice showed significantly more severe fibrosis than wild type controls after 70 days of injection with CCl4. The authors concluded that synthesized IL-10 may modulate Kupffer cells action during the liver inflammation and fibrosis, and influence subsequent progression of fibrosis (Thompson et al., 1998).

DISCUSSION

In this review, we have shown the main roles of interleukins in a complex and active cross-talk between hepatic cells responses during liver injury, and their potential as therapeutic targets. Fibrosis is characterized by abnormal ECM derived from HSCs, but it is a dynamic process driven by cytokine-mediated signaling pathways, starting with hepatocytes which are directly involved in the initiation and progression of fibrosis, continuing with macrophages that promote inflammation and present antigens to CD4 T cells which then adjust the immune responses. Interleukins are an immunomodulatory cytokine that is deeply involved from the initiation to the resolution of fibrosis. Recently, the development of a targeted therapy related to liver fibrosis using monoclonal antibodies against interleukins has received considerable interest (**Table 1**). This antibody treatment targeting interleukins has shown potential as a therapeutic agent in various liver diseases through animal experiments. Treatment with monoclonal antibody neutralizing IL-1β and IL-1 receptor antagonist have been tested in clinical trials. While the anti-cytokine therapies can prevent the progression of hepatic fibrogenesis in the early stages of liver injury, they are not a cure for advanced liver fibrosis. Therefore, treatment at the liver fibrosis stage that prevents the progression of the disease, and that leads to resolution is very important. In addition, hepatic fibrosis

TABLE 1 | Strategies targeting interleukins for liver disease.

Agent	Condition or disease	Objective or effector function	Trial number	References
		Antibodies		
Monoclonal antibody neutralizing IL-1β (Canakinumab)	Alcoholic hepatitis	Explore the potential benefits of the IL-1β antibody (Canakinumab) in the treatment of alcoholic hepatitis	NCT03775109	Dinarello et al. (2012)
IL-1 receptor antagonist (Anakinra)	Alcoholic hepatitis	Determine the clinical efficacy and safety of IL-1 receptor antagonist (Anakinra, plus zinc) in participants with clinically severe alcoholic hepatitis	NCT04072822	Meier et al. (2019), Dasarathy et al. (2020)
Polymorphism of IL-1β and TNF-α	Hepatitis B, HCC, Chronic liver disease	Find the effects of polymorphism of IL-1β and TNF-α and their interaction on susceptibility and severity of HBV-related HCC	NCT00629486	Dondeti et al. (2016)
Anti-IL-20 or IL-20R1 monoclonal antibody	Short-term and long-term CCl4 -induced liver injury	Attenuated hepatocyte damage, inhibited TGF-β1 production, liver fibrosis, HSC activation, and ECM accumulation	—	Chiu et al. (2014)
Monoclonal antibody neutralizing IL-11 and anti-IL11RA	Non-alcoholic steatohepatitis	Prevents liver inflammation and steatosis, reverses severe hepatocyte damage, reduces hepatic immune cells and TGFβ1 levels	—	Widjaja et al. (2019)
		Fusion protein		
Nanocomplexes with IL-22 gene	Acetaminophen-induced liver injury, Concanavalin A-induced hepatitis. NAFLD	Activated STAT3/Erk signaling, inhibition of reactive oxygen species generation, ameliorate acetaminophen-induced liver injury	—	Chen et al. (2017), Chen et al. (2018), Zai et al. (2019)
Fusion protein of IL-6 and the soluble IL-6 receptor	D-galactosamine induced acute liver injury	Reversed the state of hepatotoxicity, stimulated liver regeneration	—	Galun et al. (2000)
Fusion protein of IL-28B and human serum albumin	Cell culture-derived hepatitis C virus	Inhibited hepatitis C virus infection	—	Fayad et al. (2013)
Fusion protein of IL-13 cytotoxin	Nonalcoholic steatohepatitis	Decline in fibrosis and liver enzymes without organ toxicity, ameliorates pathological features of NASH	—	Shimamura et al. (2008)

CCl4, carbon tetrachloride; ECM, extracellular matrix; HBV, hepatitis B virus; HCC, hepatocellular carcinoma; HSC, hepatic stellate cells; IL, interleukin; NAFLD, nonalcoholic fatty liver disease; STAT3/Erk, signal transducer and activator of transcription 3/extracellular signal regulated kinase; TGF, tumor growth factor; TNF, tumor necrosis factor.

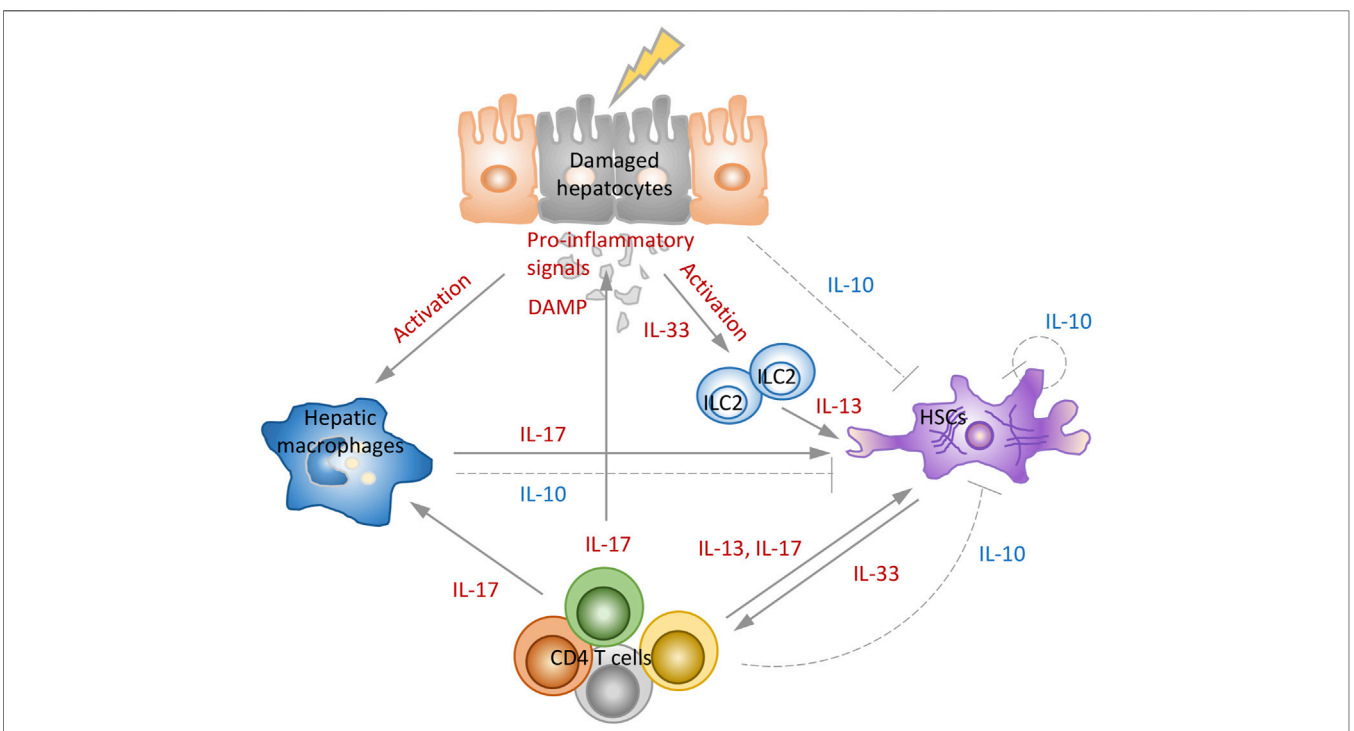


FIGURE 2 | Role of interleukins in development and resolution of liver fibrosis. The combination of signals from inflammatory environment, hepatocytes death, activated macrophages and CD4 T cells stimulates HSCs to proliferate and synthesize collagen and induce fibrosis. IL-33 induces the production of IL-13, and IL-13 and IL-17 directly mediate the activation of HSCs. In the model of fibrosis resolution, hepatocytes, macrophages, HSCs, and CD4 T cells activate the negative feedback loops that reduce immune-mediated fibrosis by secreting IL-10 that prevent activation of HSCs and production of collagen.

TABLE 2 | Roles of IL-10, 13, 17, and 33 in fibrotic disease.

Interleukin	Producing cell	Receptor	Liver	Lung	Heart	Intestine
IL-10	Basophils, B cells, dendritic cells, eosinophils, neutrophils, macrophages Mast cells, Th2 cells	IL-10R1(a), IL-10R2 (b)	IL-10 inhibited HSCs activation Louis et al. (1998) IL-gene therapy reduced the expression of profibrotic genes Hung et al. (2005) IL-10 KO mice showed more severe liver fibrosis Thompson et al. (1998)	IL-10 KO mice increased inflammation after intratracheal instillation of silica Huaux et al. (1998) genetic delivery of IL-10 attenuated the TGF-β production Nakagome et al. (2006)	The lack of IL-10 resulted more severe myocardial fibrosis Verma et al. (2012) the administration of rIL-10 improved cardiac remodeling Krishnamurthy et al. (2009) IL-10 treatment decreased the myocardial inflammation in mice with autoimmune myocarditis Zimmermann et al. (2012)	Loss of function mutations in the gene of IL-10 caused early onset of IBD Kotlarz et al. (2012) IL-10 supplementation did not result clinical improvements in CD patients Marlow et al. (2013)
IL-13	Basophils, B cells, endothelial cells, eosinophils, epithelial cells, fibroblasts, mast cells, macrophages, monocytes, smooth muscle cells, Th2 cells	IL-4Rα, IL13Rα1	Blockade of IL-13 prevented liver fibrogenesis Chiaramonte et al. (2001) IL-13 induced production of collagen, α-SMA Chiaramonte et al. (1999)	IL-13–/– and IL-4/13–/– mice were protected from lung fibrosis development in response to FITC inoculation Kolodsick et al. (2004) IL-13 and IL-4 are elevated in the bronchial alveolar lavage fluid of IPF patients Park et al. (2009)	Il13Rα1-deficient mice develop severe myocardial dysfunction Amit et al. (2017) deficiency of IL-13 leads to increased leukocyte infiltration and reduced M2-like differentiation of the monocytes in the myocardium Hofmann et al. (2014)	IL-13 production by type 2 NKT cells demonstrated to be critical for colitis development Heller et al. (2002) IL-13 is not increased in fibrotic CD muscle layer Vainer et al. (2000)
IL-17	B cells, dendritic cells, macrophages, Th17 cells	IL-17RA, IL-17RC	The increased level of IL-17 activated HSCs and induced collagen production Meng et al. (2012) elevated levels of IL-17 were also found in the fibrotic livers of patients with hepatitis B virus and cirrhosis related liver damage Du et al. (2013)	Anti-IL-17A neutralizing antibody attenuated pulmonary fibrosis and ECM deposition Chen et al. (2014) in humans, elevated levels of IL-17 and IL-1β were seen in the BAL fluid of patients with IPE Wilson et al. (2010)	IL-17 directly induced VA *in vivo* and *in vitro* in a dose-dependent manner Chang et al. (2018) IL-17 induced cardiac fibrosis both *in vitro* and *in vivo* via PKCβ/Erk1/2/NF-κB signaling pathway Liu et al. (2012)	IL-17 induced HSP47 as well as type I collagen in human intestinal myofibroblasts Honzawa et al. (2014) IL-17 contributed significantly for stricture development in CD Yagi et al. (2007) level of fecal IL-17 was elevated in patients with active CD Biancheri et al. (2013)
IL-33	Basophils, B cells, CD8+T cells, dendritic cells, eosinophils, ILC2s, macrophages, mast cells, natural killer cells, Th2 cells, Tregs cells	ST2, IL1RAcP	IL-33–/– mice showed decrease in collagen deposition and ECM-related gene expression McHedlidze et al. (2013) production of IL-13 in Th2 cells Marvie et al. (2009) IL-33 exacerbated liver fibrosis in mice Gao et al. (2016)	Level of IL-33 was elevated in the bronchoalveolar lavage fluids of patients with IPF Lee et al. (2017) treatment with anti-IL-33 antibody markedly reduced airway inflammation and lung fibrosis Luzina et al. (2013)	Recombinant IL-33 reduced aortic atherosclerotic plaque development Miller et al. (2008) ST2–/– mice showed more cardiac fibrosis and impaired survival Sanada et al. (2007) expression levels of IL-33/ST2 in human myocardial tissue were associated with cardiac fibrosis Tseng et al. (2017)	Inhibition of endogenous ST2-mediated signaling by treatment with neutralizing antibody improved DSS-induced colitis Sedhom et al. (2013) IL-33 has extenuating effects in chronic DSS-induced colitis Grobeta et al. (2012)

BAL, bronchoalveolar lavage; CD, crohn's disease; DSS, dextran sulfate sodium; ECM, extracellular matrix; Erk, extracellular signal regulated kinase; HSCs, hepatic stellate cells; HSP, heat shock protein; IBD, inflammatory bowel diseases; IL, interleukin; IPF, idiopathic pulmonary fibrosis; KO, knock-out; NF-κb, nuclear factor-κb; NKT, natural killer T cells; PCK, protein kinase C; r, recombinant; SMA, smooth muscle actin; TGF, tumor growth factor; VA, ventricular arrhythmia.

treatment strategies using various fusion proteins are detailed in **Table 1**. Targeting IL-22 is particularly promising as an alternative strategy to directly break the cycle of inflammatory cytokine and chemokine signaling, and the fusion protein using the IL-22 gene and nanocomplex is considered a new strategy to improve liver disease (Chen et al., 2017; Chen et al., 2018; Chen et al., 2020).

Damaged hepatocytes activate hepatic macrophages, and release DAMPs and IL-33. ILC2, which is activated by IL-33 released by hepatocytes, secretes IL-13, that can induce the activity of HSCs. Stimulated macrophages modulate antigen-presentation of CD4 T cells and produce IL-17 together with CD4 T cells, directly affecting the activity of HSCs and collagen production. Additionally, CD4 cells can promote fibrosis by stimulating macrophages and HSCs with IL-17 or IL-13. The quiescent HSCs receiving various pro-inflammatory signals not only transdifferentiate into myofibroblasts to produce collagen, but secrete pro-fibrogenic cytokines such as IL-33 to play pivotal role in fibrosis. On the other hand, during fibrosis resolution, these cells reverse myofibroblast activation with IL-10 and

regulate the restoration of homeostasis (**Figure 2**). This suggests that strategies using prevention of pro-inflammatory interleukins or induction of anti-inflammatory interleukins for the treatment of liver fibrosis may be effective.

IL-3, IL-17 and IL-33 induce liver fibrosis through various mechanisms, therefore an approach targeting them as a major participant in the "fibrosis pathway" is expected to be worthwhile. The blockade of IL-13 can be reversed to reduce liver pathology even when fibrosis is already established. IL-17 signals contribute to the pathogenesis of liver damage and IL-17 inhibition can potentially be an effective treatment for liver disease. Furthermore, IL-17 may be a treatment target for alcohol-induced liver damage and hepatocellular carcinoma. An approach aimed at the IL-33/ST2 path could be a potential therapeutic target for human patients suffering from chronic hepatitis and liver fibrosis (Hammerich and Tacke, 2014; Weiskirchen and Tacke, 2016; Zhang et al., 2016; Ma et al., 2020). IL-10 is a typical anti-inflammatory cytokine that shows signals of conservation mechanism in multiple organs. Specially in the fibrous liver, IL-10 has been proven to induce resolution of fibrosis, therefore it is suggested as a potential therapeutic target (Steen et al., 2020). However, the half-life of recombinant IL-10 *in vivo* is relatively short, and non-targeted administration can cause systemic side effects (Chen et al., 2012). Therefore, increasing numbers of studies have aimed to use IL-10 gene transfer and IL-10 gene therapy might be an effective treatment for liver fibrosis.

Fibrosis can occur in almost any organ or tissue, including lung, heart, and intestine, and is associated with a variety of diseases. Although liver fibrosis has been addressed in this review, treatment with specific interleukins can be applied to several tissue fibrosis. **Table 2** shows studies using interleukin 10, 13, 17, and 33 in various fibrotic tissues (Ng et al., 2018; Wijsenbeek et al., 2018; Sziksz et al., 2020). However, there are some practical problems such as the relevant doses of recombinant interleukins, the route of administration, and the costs of production of the cytokine itself, that need to be addressed to move from the experimental stage to the clinical stage. If these hurdles are overcome, a new treatment strategy targeting specific interleukins will be able to deliver expected therapeutic effects not only in the liver, but also in other tissues as well.

AUTHOR CONTRIBUTIONS

SA and SD developed the outline for this review, SA wrote the first draft with the assistance of AP, SD edited and approved the final version.

FUNDING

This study was funded by NIH R01 awards (DK082435 and DK112803) and a VA Merit award (BX002638) from the United States Department of Veterans Affairs Biomedical Laboratory Research and Development Service to DeMorrow.

ACKNOWLEDGMENTS

This work was completed with support from the Veterans Health Administration and with resources and the use of facilities at the Central Texas Veterans Health Care System, Temple, Texas. The contents do not represent the views of the U.S. Department of Veterans Affairs or the United States Government.

REFERENCES

Amit, U., Kain, D., Wagner, A., Sahu, A., Nevo-Caspi, Y., Gonen, N., et al. (2017). New role for interleukin-13 receptor α1 in myocardial homeostasis and heart failure. *J. Am. Heart Assoc.* 6 (5), e005108. doi:10.1161/JAHA.116.005108

Bansal, R., Nagórniewicz, B., and Prakash, J. (2016). Clinical advancements in the targeted therapies against liver fibrosis. *Mediators Inflamm.* 2016, 7629724. doi:10.1155/2016/7629724

Barbier, L., Ferhat, M., Salamé, E., Robin, A., Herbelin, A., Gombert, J. M., et al. (2019). Interleukin-1 family cytokines: keystones in liver inflammatory diseases. *Front. Immunol.* 10, 2014. doi:10.3389/fimmu.2019.02014

Bataller, R., and Brenner, D. A. (2005). Liver fibrosis. *J. Clin. Invest.* 115, 209–218. doi:10.1172/JCI24282

Biancheri, P., Pender, S. L., Ammoscato, F., Giuffrida, P., Sampietro, G., Ardizzone, S., et al. (2013). The role of interleukin 17 in Crohn's disease-associated intestinal fibrosis. *Fibrogenesis Tissue Repair* 6, 13. doi:10.1186/1755-1536-6-13

Caraffa, A., Gallenga, C. E., Kritas, S. K., Ronconi, G., Di Emidio, P., and Conti, P. (2019). CAR-T cell therapy causes inflammation by IL-1 which activates inflammatory cytokine mast cells: anti-inflammatory role of IL-37. *J. Biol. Regul. Homeost Agents* 33, 1981–1985. doi:10.23812/EditorialCaraffa

Chan, A. H., and Schroder, K. (2020). Inflammasome signaling and regulation of interleukin-1 family cytokines. *J. Exp. Med.* 217, e20190314. doi:10.1084/jem.20190314

Chang, S. L., Hsiao, Y. W., Tsai, Y. N., Lin, S. F., Liu, S. H., Lin, Y. J., et al. (2018). Interleukin-17 enhances cardiac ventricular remodeling via activating MAPK pathway in ischemic heart failure. *J. Mol. Cell. Cardiol.* 122, 69–79. doi:10.1016/j.yjmcc.2018.08.005

Chen, W., Zai, W., Fan, J., Zhang, X., Zeng, X., Luan, J., et al. (2020). Interleukin-22 drives a metabolic adaptive reprogramming to maintain mitochondrial fitness and treat liver injury. *Theranostics* 10, 5879–5894. doi:10.7150/thno.43894

Chen, W., Zhang, X., Fan, J., Zai, W., Luan, J., Li, Y., et al. (2017). Tethering interleukin-22 to apolipoprotein A-I ameliorates mice from acetaminophen-induced liver injury. *Theranostics* 7, 4135–4148. doi:10.7150/thno.20955

Chen, W., Luan, J., Wei, G., Zhang, X., Fan, J., Zai, W., et al. (2018). Vivo hepatocellular expression of interleukin-22 using penetratin-based hybrid nanoparticles as potential anti-hepatitis therapeutics. *Biomaterials*, 187, 66–80. doi:10.1016/j.biomaterials.2018.09.046

Chen, Y., Li, C., Weng, D., Song, L., Tang, W., Dai, W., et al. (2014). Neutralization of interleukin-17A delays progression of silica-induced lung inflammation and fibrosis in C57BL/6 mice. *Toxicol. Appl. Pharmacol.* 275, 62–72. doi:10.1016/j.taap.2013.11.012

Chen, Y. X., Huang, Y. H., Zheng, W. D., Chen, Z. X., Zhang, L. J., and Wang, X. Z. (2012). Interleukin-10 gene modification attenuates hepatocyte activation of rat hepatic stellate cells *in vitro*. *Mol. Med. Rep.* 7, 371–378. doi:10.3892/mmr.2012.1228

Chiaramonte, M. G., Cheever, A. W., Malley, J. D., Donaldson, D. D., and Wynn, T. A. (2001). Studies of murine schistosomiasis reveal interleukin-13 blockade as a treatment for established and progressive liver fibrosis. *Hepatology* 34, 273–282. doi:10.1053/jhep.2001.26376

Chiaramonte, M. G., Donaldson, D. D., Cheever, A. W., and Wynn, T. A. (1999). An IL-13 inhibitor blocks the development of hepatic fibrosis during a T-helper type 2-dominated inflammatory response. *J. Clin. Invest.* 104, 777–785. doi:10.1172/JCI7325

Chiu, Y. S., Wei, C. C., Lin, Y. J., Hsu, Y. H., and Chang, M. S. (2014). IL-20 and IL-20R1 antibodies protect against liver fibrosis. *Hepatology* 60, 1003–1014. doi:10.1002/hep.27189

Crispe, I. N. (2016). Hepatocytes as immunological agents. *J. Immunol.* 196, 17–21. doi:10.4049/jimmunol.1501668

Dasarathy, S., Mitchell, M. C., Barton, B., Mcclain, C. J., Szabo, G., Nagy, L. E., et al. (2020). Design and rationale of a multicenter defeat alcoholic steatohepatitis trial: (DASH) randomized clinical trial to treat alcohol-associated hepatitis. *Contemp. Clin. Trials* 96, 106094. doi:10.1016/j.cct.2020.106094

De Vries, J. E. (1998). The role of IL-13 and its receptor in allergy and inflammatory responses. *J. Allergy Clin. Immunol.* 102, 165–169. doi:10.1016/s0091-6749(98)70080-6

Dinarello, C. A., Simon, A., and Van Der Meer, J. W. (2012). Treating inflammation by blocking interleukin-1 in a broad spectrum of diseases. *Nat. Rev. Drug Discov.* 11, 633–652. doi:10.1038/nrd3800

Dondeti, M. F., El-Maadawy, E. A., and Talaat, R. M. (2016). Hepatitis-related hepatocellular carcinoma: insights into cytokine gene polymorphisms. *World J. Gastroenterol.* 22, 6800–6816. doi:10.3748/wjg.v22.i30.6800

Dong, X., Liu, J., Xu, Y., and Cao, H. (2019). Role of macrophages in experimental liver injury and repair in mice. *Exp. Ther. Med.* 17, 3835–3847. doi:10.3892/etm.2019.7450

Du, W. J., Zhen, J. H., Zeng, Z. Q., Zheng, Z. M., Xu, Y., Qin, L. Y., et al. (2013). Expression of interleukin-17 associated with disease progression and liver fibrosis with hepatitis B virus infection: IL-17 in HBV infection. *Diagn. Pathol.* 8, 40. doi:10.1186/1746-1596-8-40

Fallon, P. G., Richardson, E. J., Mckenzie, G. J., and Mckenzie, A. N. (2000). Schistosome infection of transgenic mice defines distinct and contrasting pathogenic roles for IL-4 and IL-13: IL-13 is a profibrotic agent. *J. Immunol.* 164, 2585–2591. doi:10.4049/jimmunol.164.5.2585

Fayad, H. J., Lamare, F., Le Rest, C. C., Bettinardi, V., and Visvikis, D. (2013). Generation of 4-dimensional CT images based on 4-dimensional PET-derived motion fields. *J. Nucl. Med.* 54, 631–638. doi:10.2967/jnumed.112.110809

Gallenga, C. E., Pandolfi, F., Caraffa, A., Kritas, S. K., Ronconi, G., Toniato, E., et al. (2019). Interleukin-1 family cytokines and mast cells: activation and inhibition. *J. Biol. Regul. Homeost Agents* 33, 1–6.

Galun, E., Zeira, E., Pappo, O., Peters, M., and Rose-John, S. (2000). Liver regeneration induced by a designer human IL-6/sIL-6R fusion protein reverses severe hepatocellular injury. *FASEB J.* 14, 1979–1987. doi:10.1096/fj.99-0913com

Gao, Y., Liu, Y., Yang, M., Guo, X., Zhang, M., Li, H., et al. (2016). IL-33 treatment attenuated diet-induced hepatic steatosis but aggravated hepatic fibrosis. *Oncotarget* 7, 33649–33661. doi:10.18632/oncotarget.9259

Ge, D., and You, Z. (2008). Expression of interleukin-17RC protein in normal human tissues. *Int. Arch. Med.* 1, 19. doi:10.1186/1755-7682-1-19

Groβ, P., Doser, K., Falk, W., Obermeier, F., and Hofmann, C. (2012). IL-33 attenuates development and perpetuation of chronic intestinal inflammation. *Inflamm. Bowel Dis.* 18, 1900–1909. doi:10.1002/ibd.22900

Grünig, G., Warnock, M., Wakil, A. E., Venkayya, R., Brombacher, F., Rennick, D. M., et al. (1998). Requirement for IL-13 independently of IL-4 in experimental asthma. *Science* 282, 2261–2263. doi:10.1126/science.282.5397.2261

Gugliandolo, A., Caraffa, A. L., Gallenga, C. E., Kritas, S. K., Ronconi, G., Trubiani, O., et al. (2019). Mesenchymal stem cells and IL-37: a powerful combination. *J. Biol. Regul. Homeost Agents* 33, 1019–1022.

Hammerich, L., and Tacke, F. (2014). Interleukins in chronic liver disease: lessons learned from experimental mouse models. *Clin. Exp. Gastroenterol.* 7, 297–306. doi:10.2147/CEG.S43737

He, Y., Hwang, S., Ahmed, Y. A., Feng, D., Li, N., Ribeiro, M., et al. (2021). Immunopathobiology and therapeutic targets related to cytokines in liver diseases. *Cell. Mol. Immunol.* 18, 18–37. doi:10.1038/s41423-020-00580-w

Heller, F., Fuss, I. J., Nieuwenhuis, E. E., Blumberg, R. S., and Strober, W. (2002). Oxazolone colitis, a Th2 colitis model resembling ulcerative colitis, is mediated by IL-13-producing NK-T cells. *Immunity* 17, 629–638. doi:10.1016/s1074-7613(02)00453-3

Hershey, G. K. (2003). IL-13 receptors and signaling pathways: an evolving web. *J. Allergy Clin. Immunol.* 111, 677–691. doi:10.1067/mai.2003.1333

Heymann, F., Peusquens, J., Ludwig-Portugall, I., Kohlhepp, M., Ergen, C., Niemietz, P., et al. (2015). Liver inflammation abrogates immunological tolerance induced by Kupffer cells. *Hepatology* 62, 279–291. doi:10.1002/hep.27793

Higashi, T., Friedman, S. L., and Hoshida, Y. (2017). Hepatic stellate cells as key target in liver fibrosis. *Adv. Drug Deliv. Rev.* 121, 27–42. doi:10.1016/j.addr.2017.05.007

Hofmann, U., Knorr, S., Vogel, B., Weirather, J., Frey, A., Ertl, G., et al. (2014). Interleukin-13 deficiency aggravates healing and remodeling in male mice after experimental myocardial infarction. *Circ. Heart Fail.* 7, 822–830. doi:10.1161/CIRCHEARTFAILURE.113.001020

Honzawa, Y., Nakase, H., Shiokawa, M., Yoshino, T., Imaeda, H., Matsuura, M., et al. (2014). Involvement of interleukin-17A-induced expression of heat shock protein 47 in intestinal fibrosis in Crohn's disease. *Gut* 63, 1902–1912. doi:10.1136/gutjnl-2013-305632

Huang, Y. H., Chen, M. H., Guo, Q. L., Chen, Z. X., Chen, Q. D., and Wang, X. Z. (2020). Interleukin-10 induces senescence of activated hepatic stellate cells via STAT3-p53 pathway to attenuate liver fibrosis. *Cell. Signal.* 66, 109445. doi:10.1016/j.cellsig.2019.109445

Huaux, F., Louahed, J., Hudspith, B., Meredith, C., Delos, M., Renauld, J. C., et al. (1998). Role of interleukin-10 in the lung response to silica in mice. *Am. J. Respir. Cell Mol. Biol.* 18, 51–59. doi:10.1165/ajrcmb.18.1.2911

Hung, K. S., Lee, T. H., Chou, W. Y., Wu, C. L., Cho, C. L., Lu, C. N., et al. (2005). Interleukin-10 gene therapy reverses thioacetamide-induced liver fibrosis in mice. *Biochem. Biophys. Res. Commun.* 336, 324–331. doi:10.1016/j.bbrc.2005.08.085

Kagan, P., Sultan, M., Tachlytski, I., Safran, M., and Ben-Ari, Z. (2017). Both MAPK and STAT3 signal transduction pathways are necessary for IL-6-dependent hepatic stellate cells activation. *PLoS One* 12, e0176173. doi:10.1371/journal.pone.0176173

Kolodsick, J. E., Toews, G. B., Jakubzick, C., Hogaboam, C., Moore, T. A., Mckenzie, A., et al. (2004). Protection from fluorescein isothiocyanate-induced fibrosis in IL-13-deficient, but not IL-4-deficient, mice results from impaired collagen synthesis by fibroblasts. *J. Immunol.* 172, 4068–4076. doi:10.4049/jimmunol.172.7.4068

Kotlarz, D., Beier, R., Murugan, D., Diestelhorst, J., Jensen, O., Boztug, K., et al. (2012). Loss of interleukin-10 signaling and infantile inflammatory bowel disease: implications for diagnosis and therapy. *Gastroenterology* 143, 347–355. doi:10.1053/j.gastro.2012.04.045

Krishnamurthy, P., Rajasingh, J., Lambers, E., Qin, G., Losordo, D. W., and Kishore, R. (2009). IL-10 inhibits inflammation and attenuates left ventricular remodeling after myocardial infarction via activation of STAT3 and suppression of HuR. *Circ. Res.* 104, e9–18. doi:10.1161/CIRCRESAHA.108.188243

Kubes, P., and Jenne, C. (2018). Immune responses in the liver. *Annu. Rev. Immunol.* 36, 247–277. doi:10.1146/annurev-immunol-051116-052415

Lee, J. U., Chang, H. S., Lee, H. J., Jung, C. A., Bae, D. J., Song, H. J., et al. (2017). Upregulation of interleukin-33 and thymic stromal lymphopoietin levels in the lungs of idiopathic pulmonary fibrosis. *BMC Pulm. Med.* 17, 39. doi:10.1186/s12890-017-0380-z

Li, S., Tan, H. Y., Wang, N., Feng, Y., Wang, X., and Feng, Y. (2019). Recent insights into the role of immune cells in alcoholic liver disease. *Front. Immunol.* 10, 1328. doi:10.3389/fimmu.2019.01328

Liu, Y., Meyer, C., Müller, A., Herweck, F., Li, Q., Müllenbach, R., et al. (2011). IL-13 induces connective tissue growth factor in rat hepatic stellate cells via TGF-β-independent Smad signaling. *J. Immunol.* 187, 2814–2823. doi:10.4049/jimmunol.1003260

Liu, Y., Munker, S., Müllenbach, R., and Weng, H. L. (2012). IL-13 signaling in liver fibrogenesis. *Front. Immunol.* 3, 116. doi:10.3389/fimmu.2012.00116

Lokau, J., Schoeder, V., Haybaeck, J., and Garbers, C. (2019). Jak-stat signaling induced by interleukin-6 family cytokines in hepatocellular carcinoma. *Cancers (Basel)* 11, 1704. doi:10.3390/cancers11111704

Louis, H., Van Laethem, J. L., Wu, W., Quertinmont, E., Degraef, C., Van Den Berg, K., et al. (1998). Interleukin-10 controls neutrophilic infiltration, hepatocyte proliferation, and liver fibrosis induced by carbon tetrachloride in mice. *Hepatology* 28, 1607–1615. doi:10.1002/hep.510280621

Luckheeram, R. V., Zhou, R., Verma, A. D., and Xia, B. (2012). $CD4^+$T cells: differentiation and functions. *Clin. Dev. Immunol.* 2012, 925135. doi:10.1155/2012/925135

Luzina, I. G., Kopach, P., Lockatell, V., Kang, P. H., Nagarsekar, A., Burke, A. P., et al. (2013). Interleukin-33 potentiates bleomycin-induced lung injury. *Am. J. Respir. Cell Mol. Biol.* 49, 999–1008. doi:10.1165/rcmb.2013-0093OC

Ma, H. Y., Yamamoto, G., Xu, J., Liu, X., Karin, D., Kim, J. Y., et al. (2020). IL-17 signaling in steatotic hepatocytes and macrophages promotes hepatocellular

carcinoma in alcohol-related liver disease. *J. Hepatol.* 72, 946–959. doi:10.1016/j.jhep.2019.12.016

Mair, M., Zollner, G., Schneller, D., Musteanu, M., Fickert, P., Gumhold, J., et al. (2010). Signal transducer and activator of transcription 3 protects from liver injury and fibrosis in a mouse model of sclerosing cholangitis. *Gastroenterology* 138, 2499–2508. doi:10.1053/j.gastro.2010.02.049

Marlow, G. J., Van Gent, D., and Ferguson, L. R. (2013). Why interleukin-10 supplementation does not work in Crohn's disease patients. *World J. Gastroenterol.* 19, 3931–3941. doi:10.3748/wjg.v19.i25.3931

Marvie, P., Lisbonne, M., L'helgoualc'h, A., Rauch, M., Turlin, B., Preisser, L., et al. (2009). Interleukin-33 overexpression is associated with liver fibrosis in mice and humans. *J. Cell Mol. Med.* 14, 1726–1739. doi:10.1111/j.1582-4934.2009.00801.x

McCormick, S. M., and Heller, N. M. (2015). Commentary: IL-4 and IL-13 receptors and signaling. *Cytokine* 75, 38–50. doi:10.1016/j.cyto.2015.05.023

McHedlidze, T., Waldner, M., Zopf, S., Walker, J., Rankin, A. L., Schuchmann, M., et al. (2013). Interleukin-33-dependent innate lymphoid cells mediate hepatic fibrosis. *Immunity* 39, 357–371. doi:10.1016/j.immuni.2013.07.018

Meier, R. P. H., Meyer, J., Montanari, E., Lacotte, S., Balaphas, A., Muller, Y. D., et al. (2019). Interleukin-1 receptor antagonist modulates liver inflammation and fibrosis in mice in a model-dependent manner. *Int. J. Mol. Sci.* 20 (6), 1295. doi:10.3390/ijms20061295

Meng, F., Wang, K., Aoyama, T., Grivennikov, S. I., Paik, Y., Scholten, D., et al. (2012). Interleukin-17 signaling in inflammatory, Kupffer cells, and hepatic stellate cells exacerbates liver fibrosis in mice. *Gastroenterology* 143, 765–776.e3. doi:10.1053/j.gastro.2012.05.049

Miller, A. M., Xu, D., Asquith, D. L., Denby, L., Li, Y., Sattar, N., et al. (2008). IL-33 reduces the development of atherosclerosis. *J. Exp. Med.* 205, 339–346. doi:10.1084/jem.20071868

Nakagome, K., Dohi, M., Okunishi, K., Tanaka, R., Miyazaki, J., and Yamamoto, K. (2006). *In vivo* IL-10 gene delivery attenuates bleomycin induced pulmonary fibrosis by inhibiting the production and activation of TGF-beta in the lung. *Thorax* 61, 886–894. doi:10.1136/thx.2005.056317

Nanchahal, J., and Hinz, B. (2016). Strategies to overcome the hurdles to treat fibrosis, a major unmet clinical need. *Proc. Natl. Acad. Sci. U.S.A.* 113, 7291–7293. doi:10.1073/pnas.1607896113

Ng, B., Dong, J., D'agostino, G., Viswanathan, S., Widjaja, A. A., Lim, W. W., et al. (2018). Interleukin-11 is a therapeutic target in idiopathic pulmonary fibrosis. *Sci. Transl Med.* 11, eaaw1237. doi:10.1126/scitranslmed.aaw1237

Onishi, R. M., and Gaffen, S. L. (2010). Interleukin-17 and its target genes: mechanisms of interleukin-17 function in disease. *Immunology* 129, 311–321. doi:10.1111/j.1365-2567.2009.03240.x

Park, S. W., Ahn, M. H., Jang, H. K., Jang, A. S., Kim, D. J., Koh, E. S., et al. (2009). Interleukin-13 and its receptors in idiopathic interstitial pneumonia: clinical implications for lung function. *J. Korean Med. Sci.* 24, 614–620. doi:10.3346/jkms.2009.24.4.614

Paul, W. E., and Seder, R. A. (1994). Lymphocyte responses and cytokines. *Cell* 76, 241–251. doi:10.1016/0092-8674(94)90332-8

Pinto, S. M., Subbannayya, Y., Rex, D. A. B., Raju, R., Chatterjee, O., Advani, J., et al. (2018). A network map of IL-33 signaling pathway. *J. Cell Commun. Signal.* 12, 615–624. doi:10.1007/s12079-018-0464-4

Roszer, T. (2015). Understanding the mysterious M2 macrophage through activation markers and effector mechanisms. *Mediators Inflamm.* 2015, 816460. doi:10.1155/2015/816460

Sanada, S., Hakuno, D., Higgins, L. J., Schreiter, E. R., Mckenzie, A. N., and Lee, R. T. (2007). IL-33 and ST2 comprise a critical biomechanically induced and cardioprotective signaling system. *J. Clin. Invest.* 117, 1538–1549. doi:10.1172/JCI30634

Schmidt-Arras, D., and Rose-John, S. (2016). IL-6 pathway in the liver: from physiopathology to therapy. *J. Hepatol.* 64, 1403–1415. doi:10.1016/j.jhep.2016.02.004

Schmitz, J., Owyang, A., Oldham, E., Song, Y., Murphy, E., Mcclanahan, T. K., et al. (2005). IL-33, an interleukin-1-like cytokine that signals via the IL-1 receptor-related protein ST2 and induces T helper type 2-associated cytokines. *Immunity* 23, 479–490. doi:10.1016/j.immuni.2005.09.015

Sedhom, M. A., Pichery, M., Murdoch, J. R., Foligné, B., Ortega, N., Normand, S., et al. (2013). Neutralisation of the interleukin-33/ST2 pathway ameliorates experimental colitis through enhancement of mucosal healing in mice. *Gut* 62, 1714–1723. doi:10.1136/gutjnl-2011-301785

Shimamura, T., Fujisawa, T., Husain, S. R., Kioi, M., Nakajima, A., and Puri, R. K. (2008). Novel role of IL-13 in fibrosis induced by nonalcoholic steatohepatitis and its amelioration by IL-13R-directed cytotoxin in a rat model. *J. Immunol.* 181, 4656–4665. doi:10.4049/jimmunol.181.7.4656

Steen, E. H., Wang, X., Balaji, S., Butte, M. J., Bollyky, P. L., and Keswani, S. G. (2020). The role of the anti-inflammatory cytokine interleukin-10 in tissue fibrosis. *Adv. Wound Care (New Rochelle)* 9, 184–198. doi:10.1089/wound.2019.1032

Sui, G., Cheng, G., Yuan, J., Hou, X., Kong, X., and Niu, H. (2018). Interleukin (IL)-13, prostaglandin E2 (PGE2), and prostacyclin 2 (PGI2) activate hepatic stellate cells via protein kinase C (PKC) pathway in hepatic fibrosis. *Med. Sci. Monit.* 24, 2134–2141. doi:10.12659/msm.906442

Sziksz, E., Pap, D., Lippai, R., Béres, N. J., Fekete, A., Szabó, A. J., et al. (2020). Fibrosis related inflammatory mediators: role of the IL-10 cytokine family. *Mediators Inflamm.* 2015, 764641. doi:10.1155/2015/764641

Tacke, F. (2017). Targeting hepatic macrophages to treat liver diseases. *J. Hepatol.* 66, 1300–1312. doi:10.1016/j.jhep.2017.02.026

Tan, Z., Liu, Q., Jiang, R., Lv, L., Shoto, S. S., Maillet, I., et al. (2017). Interleukin-33 drives hepatic fibrosis through activation of hepatic stellate cells. *Cell. Mol. Immunol.* 15, 388–398. doi:10.1038/cmi.2016.63

Tan, Z., Qian, X., Jiang, R., Liu, Q., Wang, Y., Chen, C., et al. (2013). IL-17A plays a critical role in the pathogenesis of liver fibrosis through hepatic stellate cell activation. *J. Immunol.* 191, 1835–1844. doi:10.4049/jimmunol.1203013

Thompson, K., Maltby, J., Fallowfield, J., Mcaulay, M., Millward-Sadler, H., and Sheron, N. (1998). Interleukin-10 expression and function in experimental murine liver inflammation and fibrosis. *Hepatology* 28, 1597–1606. doi:10.1002/hep.510280620

Toniato, E., Frydas, I., Robuffo, I., Ronconi, G., Caraffa, A., Kritas, S. K., et al. (2017). Activation and inhibition of adaptive immune response mediated by mast cells. *J. Biol. Regul. Homeost Agents* 31, 543–548.

Tseng, C. C. S., Huibers, M. M. H., Van Kuik, J., De Weger, R. A., Vink, A., and De Jonge, N. (2018). The interleukin-33/ST2 pathway is expressed in the failing human heart and associated with pro-fibrotic remodeling of the myocardium. *J. Cardiovasc. Transl Res.* 11, 15–21. doi:10.1007/s12265-017-9775-8

Tu, T., Calabro, S. R., Lee, A., Maczurek, A. E., Budzinska, M. A., Warner, F. J., et al. (2015). Hepatocytes in liver injury: victim, bystander, or accomplice in progressive fibrosis? *J. Gastroenterol. Hepatol.* 30, 1696–1704. doi:10.1111/jgh.13065

Vainer, B., Nielsen, O. H., Hendel, J., Horn, T., and Kirman, I. (2000). Colonic expression and synthesis of interleukin 13 and interleukin 15 in inflammatory bowel disease. *Cytokine* 12, 1531–1536. doi:10.1006/cyto.2000.0744

Van der Heide, D., Weiskirchen, R., and Bansal, R. (2019). Therapeutic targeting of hepatic macrophages for the treatment of liver diseases. *Front. Immunol.* 10, 2852. doi:10.3389/fimmu.2019.02852

Varvara, G., Tettamanti, L., Gallenga, C. E., Caraffa, A., D'ovidio, C., Mastrangelo, F., et al. (2018). Stimulated mast cells release inflammatory cytokines: potential suppression and therapeutical aspects. *J. Biol. Regul. Homeost Agents* 32, 1355–1360.

Verma, R., Balakrishnan, L., Sharma, K., Khan, A. A., Advani, J., Gowda, H., et al. (2016). A network map of Interleukin-10 signaling pathway. *J. Cell Commun. Signal.* 10, 61–67. doi:10.1007/s12079-015-0302-x

Verma, S. K., Krishnamurthy, P., Barefield, D., Singh, N., Gupta, R., Lambers, E., et al. (2012). Interleukin-10 treatment attenuates pressure overload-induced hypertrophic remodeling and improves heart function via signal transducers and activators of transcription 3-dependent inhibition of nuclear factor-κB. *Circulation* 126, 418–429. doi:10.1161/CIRCULATIONAHA.112.112185

Wang, L. X., Zhang, S. X., Wu, H. J., Rong, X. L., and Guo, J. (2019). M2b macrophage polarization and its roles in diseases. *J. Leukoc. Biol.* 106, 345–358. doi:10.1002/JLB.3RU1018-378RR

Weiskirchen, R., and Tacke, F. (2016). Interleukin-33 in the pathogenesis of liver fibrosis: alarming ILC2 and hepatic stellate cells. *Cell Mol. Immunol.* 14, 143–145. doi:10.1038/cmi.2016.62

Widjaja, A. A., Singh, B. K., Adami, E., Viswanathan, S., Dong, J., D'agostino, G. A., et al. (2019). Inhibiting interleukin 11 signaling reduces hepatocyte death and liver fibrosis, inflammation, and steatosis in mouse models of nonalcoholic steatohepatitis. *Gastroenterology* 157, 777–792. doi:10.1053/j.gastro.2019.05.002

Wijsenbeek, M. S., Kool, M., and Cottin, V. (2018). Targeting interleukin-13 in idiopathic pulmonary fibrosis: from promising path to dead end. *Eur. Respir. J.* 52, 1802111. doi:10.1183/13993003.02111-2018

Wilson, M. S., Madala, S. K., Ramalingam, T. R., Gochuico, B. R., Rosas, I. O., Cheever, A. W., et al. (2010). Bleomycin and IL-1beta-mediated pulmonary fibrosis is IL-17A dependent. *J. Exp. Med.* 207, 535–552. doi:10.1084/jem.20092121

Wu, Y., Min, J., Ge, C., Shu, J., Tian, D., Yuan, Y., et al. (2020). Interleukin 22 in liver injury, inflammation and cancer. *Int. J. Biol. Sci.* 16, 2405–2413. doi:10.7150/ijbs.38925

Wynn, T. A. (2004). Fibrotic disease and the T(H)1/T(H)2 paradigm. *Nat. Rev. Immunol.* 4, 583–594. doi:10.1038/nri1412

Yagi, Y., Andoh, A., Inatomi, O., Tsujikawa, T., and Fujiyama, Y. (2007). Inflammatory responses induced by interleukin-17 family members in human colonic subepithelial myofibroblasts. *J. Gastroenterol.* 42, 746–753. doi:10.1007/s00535-007-2091-3

Yan, Y. Y., Lin, S., and Zhu, Y. Y. (2018). Damage-associated molecular patterns and liver failure. *Zhonghua Gan Zang Bing Za Zhi* 24, 636–640. doi:10.3760/cma.j.issn.1007-3418.2016.08.017

Zai, W., Chen, W., Wu, Z., Jin, X., Fan, J., Zhang, X., et al. (2019). Targeted interleukin-22 gene delivery in the liver by polymetformin and penetratin-based hybrid nanoparticles to treat nonalcoholic fatty liver disease. *ACS Appl. Mater. Inter.* 11, 4842–4857. doi:10.1021/acsami.8b19717

Zhang, L. J., Zheng, W. D., Shi, M. N., and Wang, X. Z. (2006). Effects of interleukin-10 on activation and apoptosis of hepatic stellate cells in fibrotic rat liver. *World J. Gastroenterol.* 12, 1918–1923. doi:10.3748/wjg.v12.i12.1918

Zhang, S., Huang, D., Weng, J., Huang, Y., Liu, S., Zhang, Q., et al. (2016). Neutralization of interleukin-17 attenuates cholestatic liver fibrosis in mice. *Scand. J. Immunol.* 83, 102–108. doi:10.1111/sji.12395

Zhou, Z., Xu, M. J., and Gao, B. (2016). Hepatocytes: a key cell type for innate immunity. *Cell Mol. Immunol.* 13, 301–315. doi:10.1038/cmi.2015.97

Zhu, J., and Paul, W. E. (2008). CD4 T cells: fates, functions, and faults. *Blood* 112, 1557–1569. doi:10.1182/blood-2008-05-078154

Zimmermann, O., Homann, J. M., Bangert, A., Müller, A. M., Hristov, G., Goeser, S., et al. (2012). Successful use of mRNA-nucleofection for overexpression of interleukin-10 in murine monocytes/macrophages for anti-inflammatory therapy in a murine model of autoimmune myocarditis. *J. Am. Heart Assoc.* 1, e003293. doi:10.1161/JAHA.112.003293

Conflict of Interest: The authors declare that the research was conducted in the absence of any commercial or financial relationships that could be construed as a potential conflict of interest.

Copyright © 2021 An, Petrescu and DeMorrow. This is an open-access article distributed under the terms of the Creative Commons Attribution License (CC BY). The use, distribution or reproduction in other forums is permitted, provided the original author(s) and the copyright owner(s) are credited and that the original publication in this journal is cited, in accordance with accepted academic practice. No use, distribution or reproduction is permitted which does not comply with these terms.

frontiers in Pharmacology

REVIEW
published: 31 March 2021
doi: 10.3389/fphar.2021.641436

The Placebo and Nocebo Responses in Clinical Trials in Inflammatory Bowel Diseases

Paul Enck and Sibylle Klosterhalfen*

Department of Internal Medicine VI: Psychosomatic Medicine and Psychotherapy, University Hospital Tübingen, Tübingen, Germany

Placebo and nocebo responses are mostly discussed in clinical trials with functional bowel disorders. Much less has been investigated and is known in gastrointestinal diseases beyond irritable bowel syndrome (IBS), especially in inflammatory bowel diseases (IBD). For the purpose of this review, we screened the Journal of Interdisciplinary Placebo Studies (JIPS) database with approximately 4,500 genuine placebo research articles and identified nine meta-analyses covering more than 135 randomized and placebo-controlled trials (RCTs) with more than 10,000 patients with Crohn´s disease (CD) and another five meta-analyses with 150 RCTs and more than 10,000 patients with ulcerative colitis (UC). Only three discussed nocebo effects, especially in the context of clinical use of biosimilars to treat inflammation. The articles were critically analyzed with respect to the size of the placebo response in CD and UC, its effects on clinical improvement versus maintenance of remission, and mediators and moderators of the response identified. Finally, we discussed and compared the differences and similarities of the placebo responses in IBD and IBS and the nocebo effect in switching from biologics to biosimilars in IBD management.

Keywords: placebo and nocebo effects, clinical trial, systematic (literature) review, inflammatory bowel disease, Crohn´s disease, ulcerative colitis

OPEN ACCESS

Edited by:
Wolfgang Richard Stremmel, Germany

Reviewed by:
Mohammad Bashashati, Texas Tech University Health Sciences Center, El Paso, TX, United States
Lorenzo Bertani, University of Pisa, Italy

****Correspondence:***
Paul Enck
paul.enck@uni-tuebingen.de

Specialty section:
This article was submitted to Gastrointestinal and Hepatic Pharmacology, a section of the journal Frontiers in Pharmacology

Received: *14 December 2020*
Accepted: *28 January 2021*
Published: *31 March 2021*

Citation:
Enck P and Klosterhalfen S (2021) The Placebo and Nocebo Responses in Clinical Trials in Inflammatory Bowel Diseases. Front. Pharmacol. 12:641436. doi: 10.3389/fphar.2021.641436

INTRODUCTION

According to consented definitions, "placebo and nocebo response includes all health changes that result after administration of an inactive treatment (i.e., differences in symptoms before and after treatment), thus including natural history and regression to the mean. The placebo and nocebo effect refers to the changes specifically attributable to placebo and nocebo mechanisms, including the neurobiological and psychological mechanisms of expectancies" (Evers et al., 2018). In this respect, this article will exclusively deal with the placebo and nocebo response in randomized controlled trials (RCTs), as little to nothing has been investigated related to the underlying mechanisms of the response in inflammatory bowel diseases (IBD), in sharp contrast to functional bowel disorders such as the irritable bowel syndrome (IBS) (Enck and Klosterhalfen, 2020), but also to other and specifically pain-associated disorders (Elsenbruch and Enck, 2015). However, as we have argued before (Enck and Klosterhalfen, 2019), meta-analyses and systematic reviews of RCTs in specific areas can generate substantial contributions to the understanding of the responses (Weimer et al., 2015a; Weimer et al., 2015b), even though they would need empirical, experimental validation. An excellent example for this is the old question of whether or not there are sex differences in the placebo response: As we (Enck and Klosterhalfen, 2019) have shown, experimental work underlines that men and women differ with respect to the utilized mechanisms (learning and expectation) for the placebo

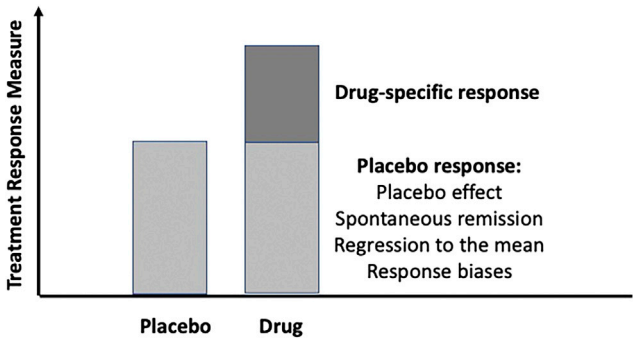


FIGURE 1 | The conventional model of the placebo response in randomized, placebo-controlled trials (RCT): It is assumed that in the drug arm of the RCT, the placebo response is equal to its size in the placebo arm. In both, the effects of the spontaneous course of symptoms, methodological effects such as the "regression to the mean," and responses biases contribute to its size, in addition to the placebo effect, which is the individual response of a patient towards placebo provision.

effects, while in clinical trials, these differences are equalized, resulting in similar placebo responses. A similar challenging task is evaluating whether or not age affects the placebo response and whether children exhibit more or less placebo/nocebo responses in RCT (Weimer et al., 2013; Weimer et al., 2015b)—this question still awaits its answer.

While we are aware that the placebo and nocebo responses have substantial effects on the design of clinical trials (Enck and Klosterhalfen, 2019), we will abstain from discussing this in more detail and rely on the traditional concept (**Figure 1**); that is, in placebo-controlled RCT, the placebo response includes not only the placebo effect (as defined above) but also other factors such as the spontaneous course of the disease if untreated and response biases and regression-to-the-mean effects. This is of specific relevance in chronic diseases where remission rather than healing is the primary goal of treatment. To uncover the contribution of spontaneous recovery, "no-treatment" control conditions would be needed that are deemed unethical in the care of IBD, at least in the acute disease condition.

Instead of questioning this principle concept, we imply that the global concept will remain valid, even if—for political, ethical, or other reasons—placebo-controlled trials are questioned or dismissed in the future. Comparator trials, where the placebo is replaced with an already drug available, have been shown to produce higher placebo response rates compared to placebos in a placebo-controlled trial; however, the true drug effect might be not identified and its efficacy tends to be overrated (Rutherford et al., 2009), and these trials require more patients to be included for statistical reasons (Weimer and Enck, 2014).

We will also abstain from discussing the option of "harnessing the placebo response" in clinical routine, beyond RCT (Enck et al., 2013), or implementing "open-label placebo" treatment (Ballou et al., 2017)—neither has yet been discussed for IBD patients. As mentioned above, IBD patients have rarely been exposed to placebo experiments, except in one brain imaging study (Schmid et al., 2015), discussed later.

In placebo research, nocebo responses and nocebo effects have only lately come into focus, which is evident from the small number of articles related to the topic in the specialized JIPS database (below): only about 650 of 4,500 genuine articles mention the term and a few have investigated such effects experimentally. Initially, the term was reserved for adverse events (AE) developed in RCT in the placebo arm of the trial, but the word "nocebo" has found a wider meaning, e.g., with the increased AE reports on patients switching from biologics to biosimilars in inflammatory diseases—we will get back to this later.

Definitions, Mechanisms, and Measures

By definition (Evers et al., 2018), placebo responses refer to the (averaged) symptom response of a group of patients receiving a placebo during a randomized, placebo-controlled trial, e.g., of drugs. In contrast, the placebo effects refer to the individual change in symptoms that can be attributed to a known mechanism eliciting this change. Therefore, the placebo response in RCT includes factors that may not be driven by placebo effects but by the natural course of the disease or by methodological biases, e.g., repeated measures eliciting the "regression-to-the-mean" effect. The placebo effect in individual patients (as well as in many patients) is thought to be due to two major mechanisms: expectations that treatment will result in improved or disappearing symptoms because this is the reason for the treatment; learning, based on previous experience with the same or different symptoms, treatments, or medical settings. In experimental medicine, both factors can be separated to investigate their contribution, whereas in clinical medicine, they are usually may be compounded but their relative contribution may vary between individual patients. In theory, however, learning and expectations are not completely independent drivers of the placebo response. And finally, the nocebo responses or nocebo effects are thought to be governed by similar mechanisms (Elsenbruch and Enck, 2015; Enck and Klosterhalfen, 2019; Enck and Klosterhalfen, 2020)

METHODS

The origin of the Journal of Interdisciplinary Placebo Studies (JIPS) database has been described previously (Colloca et al., 2016; Enck, 2018). Instead of a complex search algorithm, the search term "placebo" is applied to the PubMed metadatabase, resulting in between 150 and 250 new citations per week that are screened for relevance for placebo research. Searches were and still are supplemented by hand-searched articles from other publications and meanwhile members of the scientific community that submit their newly published placebo articles. JIPS is also distributed to members of the Society of Interdisciplinary Placebo Studies (SIPS, www.placebosociety.com) for both service and supplementation. This database currently contains around 4,500 genuine placebo articles of all kinds, experimental data, reviews, and meta-analyses.

This database was started in 2004, and it has been searched retrospectively for all papers published until 2004 (approximately 100,000) and prospectively ever since. All identified articles are

added to an EndNote-type database, including all metadata available in PubMed. This database (but not the PDFs collected) is accessible for the scientific community (upon registration on the JIPS website, www.JIPS.online). Since 2016, a monthly newsletter is distributed to subscribers that contains new citations for the IPS community and interested scientists.

The most recent use of the database was to conduct systematic reviews of specific areas (Colloca et al., 2016). We have employed it to identify knowledge gaps in placebo research, e.g., related to food and nutrition trials, sport interventions, and physical therapies and ethical, legal, and cultural aspects of the placebo phenomenon; similarly, we have determined that eHealth and mHealth applications of the placebo response/effects are clearly underrepresented, as compared to their current and future relevance (Enck et al., 2017). JIPS was screened for the terms "inflammatory bowel diseases" or "Crohns disease" or "colitis", as of December 2020, for the purpose of this article.

RESULTS

The database contained (as of Dec 2020) nine meta-analyses of placebo-controlled RCT of Crohn's disease (CD); however, there was substantial overlap between the meta-analyses. The largest of these (Jairath et al., 2017) reported data from 100 studies (depending on the read-out, see below), including 7,638 patients that received placebo, but excluded studies on CD patients postsurgery, which were exclusively covered by another meta-analysis (Renna et al., 2008) (15 studies). A more recent meta-analysis of five trials (Duijvestein et al., 2020) analyzed these trials after access to individual patient data rather than relying on published reports. Ford (Ford et al., 2014) finally added ten more studies specifically related to CD patients with fistulas, assessing partial or complete fistula closure. In the oldest meta-analysis, ten studies conducted before 1990 were covered (Salomon et al., 1992). In summary, therefore, there are data from 135 RCTs with approximately 10,000 CD patients.

The situation is similar in ulcerative colitis (UC). There are five rather large meta-analyses, with the latest and largest, with respect to the number of patients (Ma et al., 2018), including 51 RCTs with 5,182 individuals. Earlier RCT from an early meta-analysis (Ilnyckyj et al., 1997; Garud et al., 2008) and additional studies from more recent analyses (Jairath et al., 2016; Macaluso et al., 2019) included more than 150 RCTs with more than 10.000 UC patients. An early meta-analysis (but according to today's standards, a systematic review) of 11 RCTs on treatment active colitis and five on patients in remission (Kornbluth et al., 1993) does not add much to the outcome, as it was not focusing on the placebo response but rather on the drug-placebo difference. To the best of our knowledge, only one meta-analysis has investigated placebo response rates in RCTs in patients with pouchitis (Athayde et al., 2018).

Depending on the clinical status of patients included in RCTs, different read-outs from studies need to be distinguished. In acutely diseased CD and UC patients, clinical improvement can either be partial, based on clinical, histologic, or endoscopic findings, or complete (achieving remission), based on similar criteria. In CD, improvement and remission were mostly based on the Crohn's Disease Activity Index (CDAI). In patients in remission, in contrast, the efficacy of interventions is assessed either via maintenance of remission or via recurrence of symptoms, in both cases measured as the duration of being symptom-free.

One of the pitfalls of merging data from different meta-analyses is the fact that studies reporting more than just one drug arm, e.g., with different dosing or with different compounds, compared to one placebo arm, often are counted as two (or more) studies—but this is a questionable practice, since increasing the drug: placebo ratio also may affect the placebo (and drug) response rates (Papakostas and Fava, 2009). It is at least confusing when meta-analyses are performed with multiple endpoints, of which some are identified in all studies, whereas others are only found in some; hence, the numbers of studies and patients are inconsistently reported.

Finally, while most but not all studies attempted to identify single predictors of high or low placebo response but regression analysis, a few have gone beyond to construct multifactorial prediction models and one (Duijvestein et al., 2020) has done the latter based on individualized patient data rather than summary data from published articles, usually not available for drug studies.

Size of the Placebo Response

Table 1 summarizes the pooled placebo response rates in CD and UC according to the meta-analyses performed and based on the clinical conditions and the respective endpoints of the studies.

As can be seen both across the meta-analyses and within some of them [e.g., (Gallahan et al., 2010)], the placebo response rates vary between 5 and 50% in CD and between 10 and 35% in UC, with respect to clinical improvement and remission. As expected, remission rates are lower than improvement rates, and the higher the standard of criteria (clinical vs. endoscopic), the lower the placebo response. Remission maintenance rates can also vary between 15 and 50%, following similar rules. Postsurgery placebo remission and recurrence rates are as high as 50%, while placebo response rates for fistula closures are lower, below 20%. Only one study has focused on pouchitis, but the reported 24% placebo clinical improvement response is well within the range of the effects in CD and UC.

Some of the variances between studies may be due to different sensitivities and specificities of the various IBD activity scores used or differences in the cut-off or response criteria, e.g., CDAI-based definition of remission. How much of these placebo responses can be attributed to a true placebo effect or to the natural course of the disease cannot be judged from these meta-analyses. We will discuss this further below.

Predictors of the Placebo Response

While there is no consistent factor that has been reported in all or most meta-analyses, a few factors are listed more than once. They can be separated into disease, design, and other factors.

Disease factors: As with many other and noninflammatory diseases, lower disease activity at the beginning of the study was associated with higher placebo responses (Su et al., 2004; Jairath et al., 2016; Jairath et al., 2017); the same mechanism may be seen when "prior surgery, concomitant small bowel and colonic disease,

TABLE 1 | Pooled placebo responses (%) in randomized placebo-controlled trials according to different meta-analyses in Crohn´s Disease (CD), Ulcerative Colitis (UC) and pouchitis in patients with active disease or in remission (CDAI: Crohn´s Disease Activity Index).

Author	Year	No. of studies	No. of patients*	Active Disease		Patients in Remission		Not all studies have recorded the same outputs, hence the statistical basis for the pooled PE estimate may vary substantially
				Clinically Improved (%)	Achieving Remission (%)	Maintaining Remission (%)	Recurring of Symptoms (%)	
Crohn's Disease (CD)								
Salomon	1992	10	339	19.6	28.4	37.5	–	different endpoints
Su	2004	21	707	19.0	18.0	–	–	CDAI defined
Gallahan	2010	20	1795	7–56	0–46	–	–	70/100 points CDAI decrease
Jairath	2017	100	7638	28.0	18.0	32	26	CDAI defined
Duijvesten	2019	5	580	16.2	5.2	–	–	>50% reduction in CD activity
CD Subgroups								
Pascua	2008	12	687	–	–	56	58	endoscopic evaluation
Renna	2008	16	799	–	–	–	23.7/50	relapse/severe relapse
Ford	2014	13	579	18.3	15.6	–	–	complete or partial closure
Ulcerative Colitis (UC)								
Kornbluth	1993	16	403	39.7	7.7/10.0	40.1	–	partial/complete/endoscopic
Ilnyckyj	1997	35	NR	26.7/30.3/25.2	9.1/13.5./8.6	–	–	clinical/endoscopic/histologic
Garud	2008	110	3982	32.1/40/36.6	23/28/–	53.1		clinical/endoscopic/histologic
Jairath	2016	51	4062	33	10/14	19	22	more interaction, duration
Ma	2018	64	5182	35	23/14	30	–	endoscopic/histologic
Macaluso	2018	31	2702	34/26	9	14	23/19	Mayo Score: clinical/histologic
UC-Pouchitis								
Athayde	2018	12	229	24	–	–	47	various pouchitis scores

fistulizing phenotype, or prior immunomodulator therapy" (Pascua et al., 2008), "prior exposure to TNF antagonists and increased concentrations of CRP at baseline" (Duijvestein et al., 2020), disease duration, and " being non-naïve to anti-TNF's"" (Macaluso et al., 2019) were found to be associated with lower placebo responses, while—not surprising—higher "placebo remission was associated with concomitant corticosteroids" (Ma et al., 2018; Macaluso et al., 2019).

Design factors: The study duration in CD (Su et al., 2004; Gallahan et al., 2010; Ford et al., 2014; Jairath et al., 2017) and UC (Garud et al., 2008; Jairath et al., 2016) is among the factors found to affect the placebo response, but data are less consistent in UC. Another factor associated with higher placebo responses is the number of study visits during the trials (Ilnyckyj et al., 1997; Su et al., 2004; Jairath et al., 2016) (**Figure 2**).

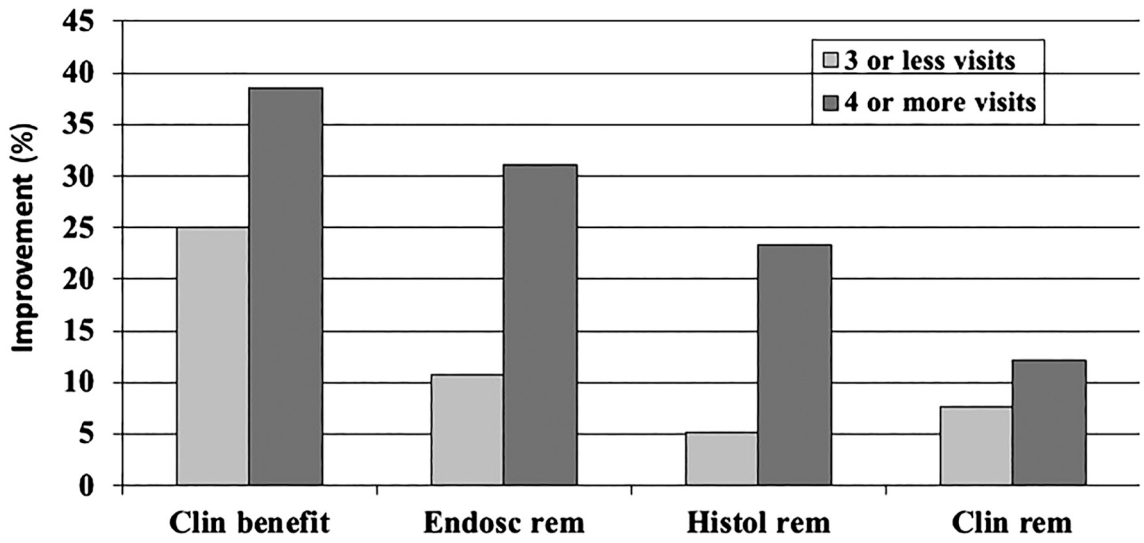


FIGURE 2 | Dose-dependent function of the (pooled,%) placebo response in a meta-analysis of randomized and placebo-controlled trials (RCT) in ulcerative colitis (22): the number of doctor visits during the trial has an effect on all clinical outcome parameters, clinical benefit (improvement), endoscopically assessed remission, histologically assessed remission, and clinical remission measures.

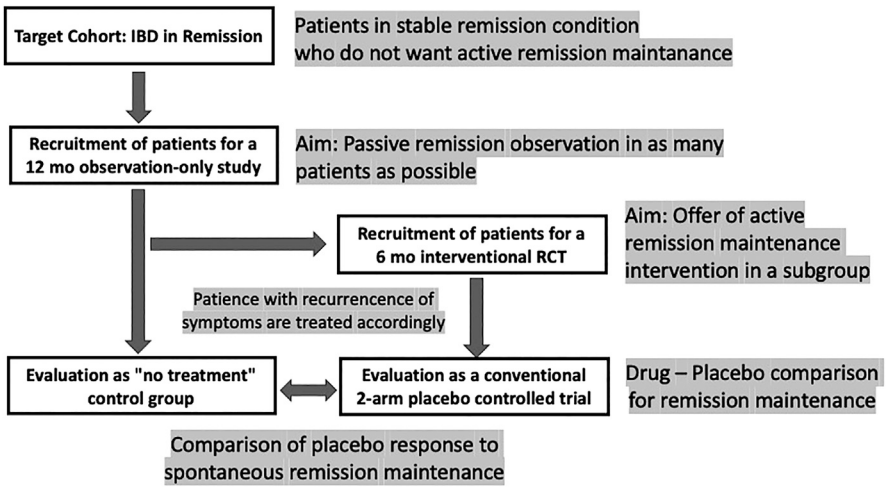


FIGURE 3 | Design scheme for a remission maintenance study in IBD that would allow including a "no-treatment" arm to assess the spontaneous course of the disease. The concept has been called "cohort multiple randomized and placebo-controlled trials (cmRCT)" (Relton et al., 2010); for a discussion see (Weimer and Enck 2014).

A factor that has frequently been discussed in areas outside IBD, e.g., in depression and other neurological and psychiatric diseases [e.g., (Enck, 2016)], was explicitly found not to be of relevance in IBD, i.e., the increase of placebo response rates in RCTs over time, with more recent studies exhibiting higher rates (Gallahan et al., 2010; Ma et al., 2018). The number of study centers was found to be effective as well, with more centers being associated with lower placebo responses (Jairath et al., 2017). One meta-analysis of UC trials found the country to determine the placebo response, with higher values in European countries (pooled improvement rate 36.4%) than those in the United States (24.9%) (Garud et al., 2008).

Other factors: It is not surprising that studies providing a new and expensive class of drugs such as biologics produce higher placebo response rates (Jairath et al., 2017). They also found the route of administration to be predictive of the placebo response—this is in line with data from the general literature: the more invasive procedures produce higher responses and injections are more effective than pills.

Increased placebo response can also be expected when instead of biomarkers and clinical disease signs, subjective, patient-reported outcomes (PRO) are used to assess the clinical efficacy of an intervention—this was shown in a meta-analysis of 16 RCTs in IBD (11 UC and 15 CD) in which IBS-specific (IBDQL) and generic (SF36) health-related quality of life was measured as the primary outcome (Estevinho et al., 2018): while overall drug-over-placebo benefit was maintained, the placebo response rates were high with 41% for clinical improvement and 31% for remission. This effect is as well established in the literature, but for many diseases, appropriate biomarkers are unfortunately missing. However, as has been shown recently that for IBD, fecal calprotectin may serve as such an appropriate biomarker (Bertani et al., 2020), possibly able to reduce (or limit) placebo responses, specifically if coupled with PRO. The important role of disease biomarkers is also evident in **Figure 2** (above), where histological and endoscopic findings produce overall lower placebo response rates than clinical assessments, irrespective of the number of study visits.

Placebo Effect Versus Spontaneous Remission (Natural Course)

To distinguish and parcel out true placebo effects from the placebo response as a summary of different mechanisms in RCT (**Figure 1**), it would be necessary to conduct a three-arm trial in which an equal fraction of patients would receive the active drug, the placebo, and no treatment, and this should be fully randomized and blinded—which of course is impossible for the "no-treatment" control, and ethically questionable as well. One way around this problem has been to install "waiting list controls" where patients are kept on a waiting list for a specific period of time before receiving treatment or being randomized into the RCT. In this case, the trial would be applied in clinical conditions of minor severity such as depression, nausea, and functional bowel disorders or with therapies other than drugs, e.g., with psychotherapy. Meta-analyses have shown that about 50% of the placebo response in RCT may be attributed to the spontaneous course of the disease—whether this holds true for IBD is an open question. When placebo arms of RCTs were used to estimate the natural course of IBD patients in remission (Meyers and Janowitz, 1989), about 50% of patients remained in remission for at least 1 year. Whether this allows concluding that a "true" placebo effect in IBS should be beyond 50% in remission trials remains to be known.

However, there should be better ways to test this hypothesis, at least in maintenance trials, e.g., with the cohort multiple randomized controlled trial (cmRCT) (Relton et al., 2010) or the so-called Zelen design (Zelen, 1979). Such a trial would follow a stacked approach with double recruitment: first for an observation-only study, a large cohort of IBD patients in remission are recruited who are not taking any remission

drug; subsequently, a subset of them is recruited for an interventional, placebo-controlled trial of a maintenance trial. This, to the best of our knowledge, has never been tried in IBD (**Figure 3**).

The ethical limitations of such a trial are at hand: leaving a group of patients with UC in remission untreated for some time can only be accomplished when narrow monitoring is warranted (Colombel et al., 2017), with patients who have minor symptoms during remission, and who, without the interference of the treating physician, would abstain from medication as long as possible anyway. Once remission is terminated, all patients need to receive appropriate standard treatment as soon as possible.

IBD Versus IBS

During the discussion of the placebo responses in IBD, as above, it occurred to us that while the placebo response may be somewhat higher in IBS (across around 100 RCTs approximately 40% (Ford and Moayyedi, 2010)) than in IBD, the moderators and mediators were remarkably similar. As we have shown in recent systematic reviews (Enck and Klosterhalfen, 2020), these factors may be grouped in both conditions into disease factors (severity, duration, and pre- and concomitant treatments), design factors (duration of treatment, number of visits, number of centers, and number of study arms), individual conditions (age, sex, race, and proxies), and environmental factors (setting, therapists, healthcare plans, nationality, etc.). Clearly, many have been found to be in effect also in IBD, but whether they can be ruled out as relevant or irrelevant also depends on the focus these factors given in RCT and whether such determinants are part of the study reporting and publishing routine. These arguments have also been summarized by other studies (Sands, 2009). Probably the most neglected area in IBD research is the influence of the treating physician and his/her empathy and management skills in the therapy procedure—but that has probably surfaced in the IBS world only because of the lack of effective drug therapies.

To the best of our knowledge, only one study (Schmid et al., 2015) has compared central processing of placebo analgesia using an established experimental model in both patients with IBS and IBD (UC), compared to healthy control volunteers, and found that while IBS patients lacked downregulation of brain activity in relevant areas of the pain matrix during placebo application, no difference was observed in UC patients and healthy controls in terms of their ability of proper pain control, indicating normal placebo responses in UC.

Nocebo Effects in IBD

To the best of our knowledge, there is only one meta-analysis (Ma et al., 2019) that has focused on AE reporting in the placebo arm of RCT, much in contrast to many such analyses in other areas of medicine, especially in the pain literature. This meta-analysis included 124 CD and 71 UC RCTs, so most of the trials that have also been included are the above placebo regression studies. The authors reported a pooled AE reporting of 70.6% in CD and 54.4% in UC and noted no differences in comparison to the respective active arms of the trials for AE reporting, severe AE reporting, and withdrawal due to AE, but a lower risk of symptom worsening in the active arms for both diseases. This is to some degree surprising given that overall AE reports are high compared to other reports on anti-inflammatory drug classes. This may support the notion that the high global symptom burden and the chronic nature of the IBD let the patients expect and tolerate substantially more AE anyway before leaving RCT.

TABLE 2 | Mediators and moderators of the placebo response in RCT in inflammatory bowel diseases (IBD) and the irritable bowel syndrome (IBS) and other functional gastrointestinal disorders, as evidenced (yes) in this and in previous reviews (e.g. Enck and Klosterhalfen 2020); question marks indicate a lack of knowledge.

IBD	Mediators/Moderators	IBS
Patient Factors		
?	age	yes
?	sex/gender	yes
?	personality	yes
?	race/culture	?
?	proxies	?
Disease Factors		
yes	severity of disease	yes
yes	duration of disease	yes
yes	previous treatments	yes
yes	concomintant therapies	?
yes	route of administration	?
Design Factors		
yes	No of study visits	yes
yes	No of study centers	yes
?	No of patients	yes
yes	Duration of RCT	yes
Therapist Factors		
?	Therapist (age, sex)	?
?	Clinical setting	yes
?	Health care system	?
yes	Nationality	yes
?	Culture	yes

Nocebo responses, the second aspect in IBD trials, are of a different nature, i.e., the report of increased AE when patients are switched from an established though expensive therapy with biologics to the more reasonably priced therapy with "biosimilars." PubMed counts (as of Dec 2020) more than 50 publications in which biosimilar usage is linked to the term nocebo, despite the fact that direct (blinded) comparison of biologics with biosimilars usually does not result in higher AE and SAE reporting with biosimilars [e.g., (Boone et al., 2018)]. The nocebo reports in daily clinical routine, however, appears to be driven by media reports, self-aid groups, and Internet-based "fake" news. One may even wonder whether solely the selection of the term "biosimilar"—suggesting similarity but not equality—may have forced or supported this discussion.

However, since this phenomenon dominates medical practice but not medical research, e.g., in RCT, little is known about its mediators and moderators. It is, furthermore, not unique to biologics/biosimilars in IBD, but became visible also in other conditions, e.g., for statin use in blood pressure regulation (Pedro-Botet et al., 2019), lactose usage in individuals claiming lactose intolerance (Vernia et al., 2010), and wheat product consumption in nonceliac gluten hypersensitivity (Biesiekierski et al., 2013) and, in general, when patients are switched from a branded to a generic drug (MacKrill et al., 2019).

However, the pitfalls of this discussion are evident: with any drug taken, separating between an AE and a nocebo response is impossible in the individual patient, even if RCT provides some evidence for an AE being a nocebo response. Furthermore, nocebo responses are not personal characteristics of patients—anxiety may be a sign, but it is not proof of it. And as with the placebo response, the healthcare provider probably contributes as much or even more to a nocebo response as does the patient. In the early days of the biosimilar development, a survey among 1,200 physicians, nearly half of the physicians (and 43.8 in gastroenterology) questioned the equivalence and efficacy of biosimilars across many medical subspecialties (Cohen et al., 2017)—and this may reflect patients concerns and AE reports.

SUMMARY

While there are distinct differences between IBD and other conditions, especially IBS, the placebo response in RCT bears some similarities at different levels: the individual patient, the disease, the study design, and the healthcare system in general. Factors driving the placebo response have been identified in both conditions (IBD and IBS), but to a different degree. The size of the placebo response appears to be somewhat higher in IBS than in IBD, but in both cases, the contribution of the spontaneous course of the disease (e.g., spontaneous symptom recovery and remission) may contribute 50% or more to the placebo response. While nocebo responses in RCT are easy to identify—as AE in placebo arms, applying the label "nocebo effect" is difficult if at all possible in the individual patient in case of AE reports, e.g., following drug application or medication switch.

AUTHOR CONTRIBUTIONS

PE drafted the concept and wrote the paper; SK wrote and corrected the manuscript.

REFERENCES

Athayde, J., Davies, S. C., Parker, C. E., Guizzetti, L., Ma, C., Khanna, R., et al. (2018). Placebo rates in randomized controlled trials of pouchitis therapy. *Dig. Dis. Sci.* 63 (10), 2519–2528. doi:10.1007/s10620-018-5199-9

Ballou, S., Kaptchuk, T. J., Hirsch, W., Nee, J., Iturrino, J., Hall, K. T., et al. (2017). Open-label versus double-blind placebo treatment in irritable bowel syndrome: study protocol for a randomized controlled trial. *Trials* 18 (1), 234. doi:10.1186/s13063-017-1964-x

Bertani, L., Mumolo, M. G., Tapete, G., Albano, E., Baiano Svizzero, G., Zanzi, F., et al. (2020). Fecal calprotectin: current and future perspectives for inflammatory bowel disease treatment. *Eur. J. Gastroenterol. Hepatol.* 32 (9), 1091–1098. doi:10.1097/MEG.0000000000001731

Biesiekierski, J. R., Peters, S. L., Newnham, E. D., Rosella, O., Muir, J. G., and Gibson, P. R. (2013). No effects of gluten in patients with self-reported non-celiac gluten sensitivity after dietary reduction of fermentable, poorly absorbed, short-chain carbohydrates. *Gastroenterology* 145 (2), 320. doi:10.1053/j.gastro.2013.04.051

Boone, N. W., Liu, L., Romberg-Camps, M. J., Duijsens, L., Houwen, C., van der Kuy, P. H. M., et al. (2018). The nocebo effect challenges the non-medical infliximab switch in practice. *Eur. J. Clin. Pharmacol.* 74.(5), 655–661. doi:10.1007/s00228-018-2418-4

Cohen, H., Beydoun, D., Chien, D., Lessor, T., McCabe, D., Muenzberg, M., et al. (2017). Awareness, knowledge, and perceptions of biosimilars among specialty physicians. *Adv. Ther.* 33 (12), 2160–2172. doi:10.1007/s12325-016-0431-5

Colloca, L., Enck, P., and DeGrazia, D. (2016). Relieving pain using dose-extending placebos: a scoping review. *Pain* 157 (8), 1590–1598. doi:10.1097/j.pain.0000000000000566

Colombel, J. F., Panaccione, R., Bossuyt, P., Lukas, M., Baert, F., Vaňásek, T., et al. (2017). Effect of tight control management on Crohn's disease (CALM): a multicentre, randomised, controlled phase 3 trial. *Lancet* 390.(10114), 2779–2789. doi:10.1016/S0140-6736(17)32641-7

Duijvestein, M., Jeyarajah, J., Guizzetti, L., Zou, G., Parker, C. E., van Viegen, T., et al. (2020). Response to placebo, measured by endoscopic evaluation of crohn's disease activity, in a pooled analysis of data from 5 randomized controlled induction trials. *Clin. Gastroenterol. Hepatol.* 18 (5), 1121–1132.

Elsenbruch, S., and Enck, P. (2015). Placebo effects and their determinants in gastrointestinal disorders. *Nat. Rev. Gastroenterol. Hepatol.* 12 (8), 472–485. doi:10.1038/nrgastro.2015.117

Enck, P., Bingel, U., Schedlowski, M., and Rief, W. (2013). The placebo response in medicine: minimize, maximize or personalize? *Nat. Rev. Drug Discov.* 12 (3), 191–204. doi:10.1038/nrd3923

Enck, P., and Klosterhalfen, S. (2020). Placebo responses and placebo effects in functional gastrointestinal disorders. *Front. Psychiatry* 11, 797. doi:10.3389/fpsyt.2020.00797

Enck, P., and Klosterhalfen, S. (2019). Placebos and the placebo effect in drug trials. *Handb. Exp. Pharmacol.* 260, 399–431. doi:10.1007/164_2019_269

Enck, P., Klosterhalfen, S., and Weimer, K. (2017). Unsolved, forgotten, and ignored features of the placebo response in medicine. *Clin. Ther.* 39 (3), 458–468. doi:10.1016/j.clinthera.2016.11.016

Enck, P. (2016). Placebo response in depression: is it rising? *Lancet Psychiatry* 3 (11), 1005–1006. doi:10.1016/s2215-0366(16)30308-x

Enck, P. (2018). Living systematic reviews, not only for clinical (placebo) research. *J. Clin. Epidemiol.* 98, 152–153. doi:10.1016/j.jclinepi.2018.01.001

Estevinho, M. M., Afonso, J., Rosa, I., Lago, P., Trindade, E., Correia, L., et al. (2018). Placebo effect on the health-related quality of life of inflammatory bowel disease patients: a systematic review with meta-analysis. *J. Crohns Colitis* 12 (10), 1232–1244. doi:10.1093/ecco-jcc/jjy100

Evers, A. W. M., Colloca, L., Blease, C., Annoni, M., Atlas, L. Y., Benedetti, F., et al. (2018). Implications of placebo and nocebo effects for clinical practice: expert consensus. *Psychother. Psychosom.* 87 (4), 204–210. doi:10.1159/000490354

Ford, A. C., Luthra, P., Hanauer, S. B., Travis, S. P., Harris, M. S., and Reinisch, W. (2014). Placebo response rate in clinical trials of fistulizing Crohn's disease: systematic review and meta-analysis. *Clin. Gastroenterol. Hepatol.* 12 (12), 1981–1990. doi:10.1016/j.cgh.2014.08.038

Ford, A. C., and Moayyedi, P. (2010). Meta-analysis: factors affecting placebo response rate in the irritable bowel syndrome. *Aliment. Pharmacol. Ther.* 32 (2), 144–158. doi:10.1111/j.1365-2036.2010.04328.x

Gallahan, W. C., Case, D., and Bloomfeld, R. S. (2010). An analysis of the placebo effect in Crohn's disease over time. *Aliment. Pharmacol. Ther.* 31 (1), 102–107. doi:10.1111/j.1365-2036.2009.04125.x

Garud, S., Brown, A., Cheifetz, A., Levitan, E. B., and Kelly, C. P. (2008). Meta-analysis of the placebo response in ulcerative colitis. *Dig. Dis. Sci.* 53 (4), 875–891. doi:10.1007/s10620-007-9954-6

Ilnyckyj, A., Shanahan, F., Anton, P. A., Cheang, M., and Bernstein, C. N. (1997). Quantification of the placebo response in ulcerative colitis. *Gastroenterology* 112 (6), 1854–1858. doi:10.1053/gast.1997.v112.pm9178676

Jairath, V., Zou, G., Parker, C. E., Macdonald, J. K., Mosli, M. H., Khanna, R., et al. (2016). Systematic review and meta-analysis: placebo rates in induction and maintenance trials of ulcerative colitis. *J. Crohns Colitis* 10 (5), 607–618. doi:10.1093/ecco-jcc/jjw004

Jairath, V., Zou, G., Parker, C. E., MacDonald, J. K., Mosli, M. H., AlAmeel, T., et al. (2017). Systematic review with meta-analysis: placebo rates in induction and maintenance trials of Crohn's disease. *Aliment. Pharmacol. Ther.* 45 (8), 1021–1042. doi:10.1111/apt.13973

Kornbluth, A. A., Salomon, P., Sacks, H. S., Mitty, R., and Janowitz, H. D. (1993). Meta-analysis of the effectiveness of current drug therapy of ulcerative colitis. *J. Clin. Gastroenterol.* 16 (3), 215–218. doi:10.1097/00004836-199304000-00010

Ma, C., Guizzetti, L., Panaccione, R., Fedorak, R. N., Pai, R. K., Parker, C. E., et al. (2018). Systematic review with meta-analysis: endoscopic and histologic placebo rates in induction and maintenance trials of ulcerative colitis. *Aliment. Pharmacol. Ther.* 47 (12), 1578–1596. doi:10.1111/apt.14672

Ma, C., Panaccione, N. R., Nguyen, T. M., Guizzetti, L., Parker, C. E., Hussein, I. M., et al. (2019). Adverse events and nocebo effects in inflammatory bowel disease: a systematic review and meta-analysis of randomized controlled trials. *J. Crohns Colitis* 13.(9), 1201–1216. doi:10.1093/ecco-jcc/jjz087

Macaluso, F. S., Maida, M., Ventimiglia, M., Renna, S., Cottone, M., and Orlando, A. (2019). Factors affecting clinical and endoscopic outcomes of placebo arm in trials of biologics and small molecule drugs in ulcerative colitis: a meta-analysis. *Inflamm. Bowel Dis.* 25 (6), 987–997. doi:10.1093/ibd/izy365

MacKrill, K., Kleinstäuber, M., and Petrie, K. J. (2019). The effect of rebranding generic medicines on drug efficacy and side effects. *Psychol. Health* 34.(12), 1470–1485. doi:10.1080/08870446.2019.1616088

Meyers, S., and Janowitz, H. D. (1989). The "natural history" of ulcerative colitis: an analysis of the placebo response. *J. Clin. Gastroenterol.* 11 (1), 33–37. doi:10.1097/00004836-198902000-00008

Papakostas, G. I., and Fava, M. (2009). Does the probability of receiving placebo influence clinical trial outcome? A meta-regression of double-blind, randomized clinical trials in mdd. *Eur. Neuropsychopharmacol.* 19 (1), 34–40. doi:10.1016/j.euroneuro.2008.08.009

Pascua, M., Su, C., Lewis, J. D., Brensinger, C., and Lichtenstein, G. R. (2008). Meta-analysis: factors predicting post-operative recurrence with placebo therapy in patients with Crohn's disease. *Aliment. Pharmacol. Ther.* 28 (5), 545–556. doi:10.1111/j.1365-2036.2008.03774.x

Pedro-Botet, J., Climent, E., and Benaiges, D. (2019). Muscle and statins: from toxicity to the nocebo effect. *Expert Opin. Drug Saf.* 18.(7), 573–579. doi:10.1080/14740338.2019.1615053

Relton, C., Torgerson, D., O'Cathain, A., and Nicholl, J. (2010). Rethinking pragmatic randomised controlled trials: introducing the "cohort multiple randomised controlled trial" design. *BMJ* 340, 1066. doi:10.1136/bmj.c1066

Renna, S., Cammà, C., Modesto, I., Cabibbo, G., Scimeca, D., Civitavecchia, G., et al. (2008). Meta-analysis of the placebo rates of clinical relapse and severe endoscopic recurrence in postoperative Crohn's disease. *Gastroenterology* 135 (5), 1500–1509. doi:10.1053/j.gastro.2008.07.066

Rutherford, B. R., Sneed, J. R., and Roose, S. P. (2009). Does study design influence outcome? The effects of placebo control and treatment duration in antidepressant trials. *Psychother. Psychosom.* 78 (3), 172–181. doi:10.1159/000209348

Salomon, P., Kornbluth, A., Aisenberg, J., and Janowitz, H. D. (1992). How effective are current drugs for Crohn's disease? A meta-analysis. *J. Clin. Gastroenterol.* 14 (3), 211–215. doi:10.1097/00004836-199204000-00006

Sands, B. E. (2009). The placebo response rate in irritable bowel syndrome and inflammatory bowel disease. *Dig. Dis.* 27 (1), 68–75. doi:10.1159/000268123

Schmid, J., Langhorst, J., Gab, F., Theysohn, N., Benson, S., Engler, H., et al. (2015). Placebo analgesia in patients with functional and organic abdominal pain: a fMRI study in IBS, UC and healthy volunteers. *Gut.* 64 (3), 418–427. doi:10.1136/gutjnl-2013-306648

Su, C., Lichtenstein, G. R., Krok, K., Brensinger, C. M., and Lewis, J. D. (2004). A meta-analysis of the placebo rates of remission and response in clinical trials of active Crohn's disease. *Gastroenterology* 126 (5), 1257–1269. doi:10.1053/j.gastro.2004.01.024

Vernia, P., Di Camillo, M., Foglietta, T., Avallone, V. E., and De Carolis, A. (2010). Diagnosis of lactose intolerance and the "nocebo" effect: the role of negative expectations. *Dig. Liver Dis.* 42 (9), 616–619. doi:10.1016/j.dld.2010.02.005

Weimer, K., Colloca, L., and Enck, P. (2015a). Age and sex as moderators of the placebo response – an evaluation of systematic reviews and meta-analyses across medicine. *Gerontology* 61 (2), 97–108. doi:10.1159/000365248

Weimer, K., Colloca, L., and Enck, P. (2015b). Placebo effects in psychiatry: mediators and moderators. *Lancet Psychiatry* 2 (3), 246–257. doi:10.1016/s2215-0366(14)00092-3

Weimer, K., and Enck, P. (2014). Traditional and innovative experimental and clinical trial designs and their advantages and pitfalls. *Handb. Exp. Pharmacol.* 225, 237–272. doi:10.1007/978-3-662-44519-8_14

Weimer, K., Gulewitsch, M. D., Schlarb, A. A., Schwille-Kiuntke, J., Klosterhalfen, S., and Enck, P. (2013). Placebo effects in children: a review. *Pediatr. Res.* 74 (1), 96–102. doi:10.1038/pr.2013.66

Zelen, M. (1979). A new design for randomized clinical trials. *N. Engl. J. Med.* 300 (22), 1242–1245. doi:10.1056/nejm197905313002203

Conflict of Interest: The authors declare that the research was conducted in the absence of any commercial or financial relationships that could be construed as a potential conflict of interest.

Copyright © 2021 Enck and Klosterhalfen. This is an open-access article distributed under the terms of the Creative Commons Attribution License (CC BY). The use, distribution or reproduction in other forums is permitted, provided the original author(s) and the copyright owner(s) are credited and that the original publication in this journal is cited, in accordance with accepted academic practice. No use, distribution or reproduction is permitted which does not comply with these terms.

frontiers in Pharmacology

REVIEW
published: 12 April 2021
doi: 10.3389/fphar.2021.655054

An Update for Pharmacologists on New Treatment Options for Inflammatory Bowel Disease: The Clinicians' Perspective

Carsten Schmidt[1], *Philip C. Grunert*[2] *and Andreas Stallmach*[2]*

[1]Medizinische Klinik II, Klinikum Fulda AG, Universitätsmedizin Marburg - Campus Fulda, Fulda, Germany, [2]Klinik für Innere Medizin IV, Universitätsklinikum Jena, Friedrich-Schiller Universität Jena, Jena, Germany

The introduction of anti-tumor necrosis factor antibodies resulted in a considerable expansion of the options available for the treatment of inflammatory bowel disease. Unfortunately, approximately one third of treated patients do not respond to these modalities, and drug efficacy may be lost over time. These drugs are also associated with contraindications, adverse events, and intolerance. As such, there is an ongoing need for new therapeutic strategies. Despite several recent advances, including antibodies against pro-inflammatory cytokines and cell adhesion molecules, Janus kinase inhibitors, and modulators of sphingosine-1-phosphate receptors, not all problems associated with IBD have been solved. In this manuscript, we review the current state of development of several new treatment options. Ongoing evaluation will require specific proof of efficacy as well as direct comparisons with established treatments. Results from head-to-head comparisons are needed to provide clinicians with critical information on how to formulate effective therapeutic approaches for each patient.

Keywords: interleukin-23, anti-integrin drugs, sphingosine-1-phosphate receptor modulator, JAK inhibitor, fecal microbiota transplantation, biologics, small molecule

OPEN ACCESS

Edited by:
Wolfgang Richard Stremmel, Medical Center Baden-Baden, Germany

Reviewed by:
Lorenzo Bertani, University of Pisa, Italy
Jonas Zeitz, University Hospital Zürich, Switzerland

***Correspondence:**
Andreas Stallmach, andreas.stallmach@med.uni-jena.de

Specialty section:
This article was submitted to Gastrointestinal and Hepatic Pharmacology, a section of the journal Frontiers in Pharmacology

Received: *18 January 2021*
Accepted: *22 February 2021*
Published: *12 April 2021*

Citation:
Schmidt C, Grunert PC and Stallmach A (2021) An Update for Pharmacologists on New Treatment Options for Inflammatory Bowel Disease: The Clinicians' Perspective. Front. Pharmacol. 12:655054. doi: 10.3389/fphar.2021.655054

INTRODUCTION

Patients diagnosed with inflammatory bowel disease (IBD), including those with Crohn´s disease (CD) and ulcerative colitis (UC), can be difficult to manage clinically given the broad spectrum of disease, including both intestinal and extraintestinal manifestations. IBD is an immunologically-mediated disease with increasing prevalence across Western Europe, North America, and Australia, as well as in newly-industrialized areas of Asia and South America. The prevalence of IBD has been estimated at 0.3–0.5% in Western Europe, including at least 420,000 patients in Germany alone. Similarly, population-based data from Canada predict that the prevalence of IBD, estimated at 725 patients per 100,000 (0.73%) in 2018 will increase to as many as 981 patients per 100,000 (0.98%) in 2030 (Coward et al., 2019). If we apply this calculation to the current patient population in Germany, we might anticipate an increase to 0.67% in 2030, representing >560,000 patients.

While the physiologic mechanisms contributing to the development of IBD have not been fully clarified, current research suggests that genetically-susceptible individuals respond to routine environmental factors with alterations at the gastrointestinal barrier and exaggerated (or poorly-suppressed) innate and adaptive immune responses. These findings have provided a theoretical and practical basis for the development of new therapies. Indeed, the introduction of the anti-tumor

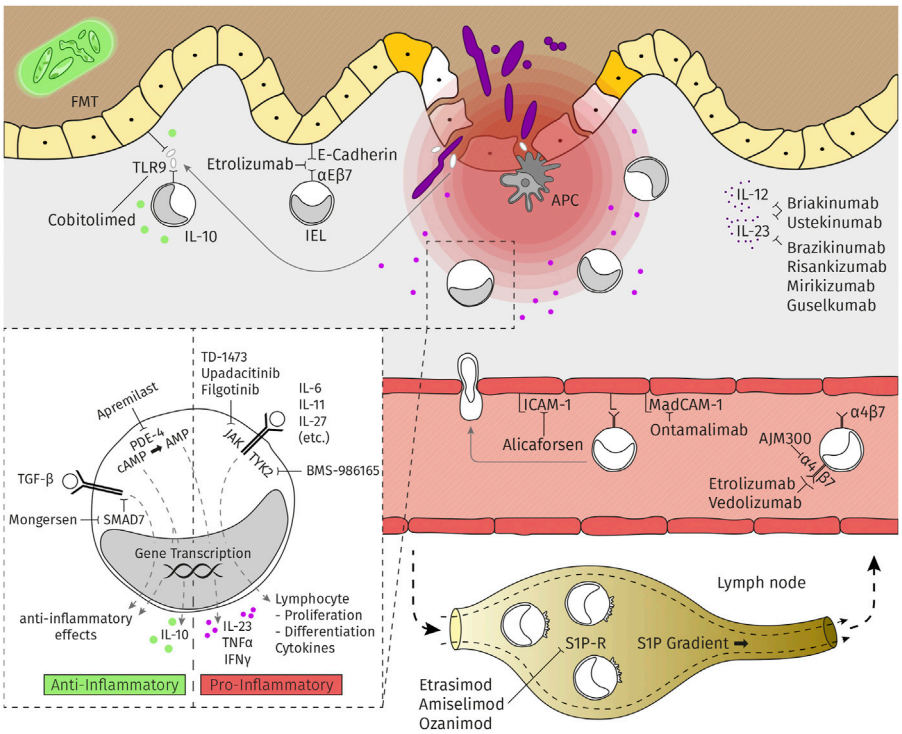


FIGURE 1 | Mechanisms of action of several of the new therapeutic agents used to treat IBD.

necrosis factor (TNF) antibody, infliximab, first for CD (in 1999) and later for UC (in 2006), revolutionized the treatment of these conditions. Other anti-TNF antibodies (all under the broad category known as "biologics"), including adalimumab, golimumab, or certolizumab pegol [certolizumab pegol is not approved by the European Medicines Agency (EMA)] were developed shortly thereafter. With the availability of biosimilars for infliximab and adalimumab and the approval of both ustekinumab, a monoclonal antibody (mAb) that antagonizes the actions of proinflammatory cytokines IL-12 and IL-23, and vedolizumab, a mAb that specifically targets $\alpha_4\beta_7$-integrin, physicians now have access to a broad range of unique biologics that can be used to manage intestinal inflammation. This armamentarium also includes tofacitinib, which is a small-molecule inhibitor of Janus kinases (JAKs) that can be used to treat patients diagnosed with UC. Unfortunately, not all patients respond to these new therapies (known as "primary non-responders"). Depending on the respective phase III study, the proportion of primary non-responders may be as high as 30–50%. Other patients may experience secondary loss of response due to the development of neutralizing antibodies or *via* other, as yet not well-understood mechanisms (e.g., as observed in patients treated with tofacitinib). The comparatively high incidence of adverse events also limits the use of these new therapeutic options. As such, additional research is needed that focuses on approaches that can be used to achieve long-lasting, steroid-free remission without adverse effects in all patients diagnosed with IBD.

The mechanisms of action of the new therapeutic agents used to treat IBD are summarized in **Figure 1**. It is critical to understand that the published studies focused on each of these agents feature different patient populations and have different inclusion and exclusion criteria; among these are differences in disease duration and activity, previous experience with anti-IBD therapies, duration of induction therapy, primary endpoints, and design of maintenance protocols (i.e., "treat-through" vs. "randomized responder"). As such, significant caution must be exercised when comparing the results of different studies.

Due to the multitude of new as well as already established modes of action and specific substances for the treatment of IBD a targeted selection of a medication for an individual patient is of utmost importance. Therefore, several biomarkers (e.g., fecal calprotectin, CRP, serological and genetic parameters, histological findings and microbiota) have been and are currently being evaluated with regard to the prediction of treatment response. At present, however, biomarkers of this type are not yet established for daily clinical practice. Further, from a clinical point of view improvement of disease activity and patient related outcome parameters are more important than changes in biomarkers. For these reasons, we aimed not to discuss such parameters in this overview on the effectiveness and safety of new therapeutics.

An electronic database search using PubMed, spanning up to November 2020, was conducted. Abstracts were also reviewed from Digestive Diseases Week, European Crohn's and Colitis Organization congress, and United European Gastroenterology Week 2019 and 2020, respectively.

ANTI-INTEGRIN ANTIBODIES

Integrins are cell adhesion molecules that form transmembrane dimers consisting of α- and β-chains. The goal of an anti-integrin strategy is to block the actions of adhesion molecules on circulating immune cells and/or those of their receptors on endothelial cells. For example, $\alpha_4\beta_7$-integrin on the surface of $CD4^+$ T lymphocytes binds specifically to MadCAM-1 (mucosal addressin cell adhesion molecule-1) on endothelial cells in the gastrointestinal tract and thereby mediates "gut-selective" lymphocyte migration into the gastrointestinal mucosa. **Vedolizumab** is a humanized mAb that targets $\alpha_4\beta_7$-integrin and was first approved for the treatment of CD and UC in 2014 with a favorable safety profile in clinical trials. This assessment was reinforced with the first direct, head-to-head comparison of biologic therapies for IBD carried out in 2019 as the VARSITY study. The results of this study revealed that vedolizumab had a more favorable therapeutic impact on inducing clinical remission compared to results obtained using adalimumab (Sands et al., 2019a).

Given the overall efficacy and "gut-selective" effects of vedolizumab, it is not surprising that cell adhesion molecules are among the most prominent targets of new therapeutics under development. Various inhibitors of the integrin β_7-subunit and its endothelial ligand, MadCAM-1, are currently undergoing evaluation in numerous studies. For example, in one phase II study, Vermeire and colleagues (Vermeire et al., 2014) found that the anti-β_7 antibody, **etrolizumab**, was more effective than placebo at inducing remission in patients with symptomatic UC. One important aspect of etrolizumab is the fact that it targets not only $\alpha_4\beta_7$-integrin (similar to vedolizumab) but also can inhibit $\alpha_E\beta_7$-integrin-mediated interactions between intraepithelial lymphocytes and E-cadherin expressed by enterocytes, thereby reducing the extent of lymphocyte accumulation at this site. This is a critical finding, as the probability of remission correlated strongly with mucosal expression of the α_E-subunit, which was also identified as the first established predictor of the response to mAb therapy. These results were followed by eight randomized-controlled and open-label studies of this modality for the treatment of CD and UC. More than 3,000 UC and CD patients were enrolled in two open-label and safety studies as well as in six phase III trials, including comparative studies against both adalimumab and infliximab (Sandborn et al., 2020e). However, in August 2020, Roche investigators reported mixed results from their studies and announced that the study program for patients diagnosed with UC was to be halted, while studies focused on CD were to be continued. The favorable safety profile for etrolizumab was consistent with the results of previous studies, although the results of the various treatment studies for UC were not as convincing. In the "Hibiscus-I" induction study, the primary endpoint of clinical remission at week 10 was achieved in response to etrolizumab among patients who had not undergone prior treatment with anti-TNF mAbs (19.4 vs. 6.9%; $p = 0.0173$). By contrast, in the "*Hibiscus* II" induction study (which also included anti-TNF-naïve patients) the same primary endpoint was not met (18.2 vs. 11.1%; $p = 0.1729$) (Dotan et al., 2020). In the "Hickory" study, the primary endpoint of induction (clinical remission at week 14: 18.5 vs. 6.3%; $p = 0.0033$), but not maintenance of remission (among clinical responders at week 14) was achieved in response to etrolizumab among patients with a history of previous anti-TNF treatment (24.1 vs. 20.2% at week 66; $p = 0.4956$) (Peyrin-Biroulet et al., 2020a). Finally, in the "Laurel" maintenance study, the primary endpoint of clinical remission at week 62 among responders at week 10 was not achieved in patients with no history of anti-TNF treatment (29.6 vs. 20.6%; $p = 0.1942$) (Vermeire et al., 2020). The consequences of these results and their impact on the further development of etrolizumab remain to be determined.

AJM300 is a small molecule administered orally that blocks the α_4-integrin subunit that has been investigated in patients with moderately-active UC. In one phase II study, 102 patients were treated with 960 mg AJM300 or placebo three times a day for 8 weeks. 62.7% of the patients in the treatment (AJM300) group exhibited a clinical response (a decrease in the Mayo Score by >3 points or at least 30% with a reduction in the rectal bleeding subscore by >1 point) compared to only 25.5% of the patients in the placebo group ($p = 0.002$). Furthermore, clinical remission was observed in 23.5% vs. 3.9% of patients ($p = 0.01$) (Yoshimura et al., 2015); This drug is currently undergoing evaluation in a phase III study involving patients with UC.

Ontamalimab (PF-00547659) is a mAb that targets MadCAM-1. A phase II study in patients with UC documented the superiority of this drug in inducing clinical remission compared to placebo (16.7% vs. 2.7% at week 12; $p = 0.01$). Patients who responded to therapy were treated for up to 72 weeks in an open-label extension study; in this study, positive effects on the maintenance of remission were more pronounced in patients that received higher drug doses. By contrast, no differences were observed in a comparison between PF-00547659 and placebo in patients with moderate-to-severe CD, despite the observed decreases in the concentration of circulating MAdCAM-1 and a dose-dependent increase in $\beta7^+$ memory T-cells, which are both findings that document the pharmacologic efficacy of the drug (Sandborn et al., 2018). Takeda (who acquired ontamalimab through the acquisition of Shire in 2018) announced the end of the study program in May 2020.

The results of six studies focused on achieving clinical remission in both CD and UC using anti-integrin strategies are summarized in **Table 1**.

COMMENT

Given the well-characterized positive responses to treatment with vedolizumab, the largely negative results of studies focused on etrolizumab for the treatment of UC are somewhat surprising. The full publications may ultimately provide more information to explain the underlying issues. Given the well-established favorable safety profile for vedolizumab, therapeutic agents directed against integrin-mediated interactions might be suitable for use as combination therapy with drugs that have

TABLE 1 | Frequency of achieving clinical remission in anti-integrin directed studies of patients with CD (a) and UC (b).

Drug	Study phase	Induction treatment				Study type	Maintenance treatment				References
		Week	Study drug	Placebo	*p*		Week	Study drug	Placebo	*p*	
a) CD											
Vedolizumab[a]	III	6	14.5	6.8%	0.02	rr	85	39.0	21.6%	<0.001	Sandborn et al. (2013)
Ontamalimab	II	8	29.1	16.7%	n.s						Sandborn et al. (2018)

Drug	Study phase	Induction treatment				Study type	Maintenance treatment				References
		Week	Study drug	Placebo	*p*		Week	Study drug	Placebo	*p*	
b) UC											
Vedolizumab[a]	III	6	16.9	5.4%	<0.001	rr	52	44.8	15.9%	<0.001	Feagan et al. (2013)
Etrolizumab	III	10	19.4	6.9%	0.0173	rr	62	29.6	20.6%	0,194	Dotan et al. (2020)
	III	10	18.2	11.1%	0.1729						Vermeire et al. (2020)
Etrolizumab	III	14	18.5	6.3%	0.0033	rr	66	24.1	20.2%	0,4956	Peyrin-Biroulet et al. (2020a)
Ontamalimab	II	12	16.7	2.7%	0.01	OLE	40–72	22.8	nd	Na	Vermeire et al. (2017a), Danese et al. (2019)
AJM300	II	8	23.5	3.9%	0.01						Yoshimura et al. (2015)

NB: In studies that feature different dosages or intervals, the most effective treatment has been presented.

[a]currently licensed for use as therapy in CD and UC; OLE, open-label extension; tt, treat-through; r, continuation of assigned treatment in responders; r 26, remission at week 26; rr, randomized responder; nd, not done; na, not applicable.

different mechanisms of action. Results of phase III studies of etrolizumab combined with other therapies may provide further insight into this possibility.

BLOCKADE OF INTERLEUKIN-23

Interleukin-12 (IL-12) and interleukin-23 (IL-23) are heterodimeric cytokines that share a common p40 subunit; this subunit has been identified as an effective target for mAbs designed to inhibit the actions of both pro-inflammatory mediators. By contrast, mAbs that target the second subunit of IL-23 (p19) alone promote selective inhibition of this cytokine. The anti-p40 mAb, **ustekinumab,** was approved for use in 2016, has proven effectiveness and a good safety profile when used to treat patients with CD and UC (Feagan et al., 2016; Sands et al., 2019b).

Briakinumab is another anti-p40 mAb that is currently under study for the treatment of psoriasis. Although higher response and remission rates were observed at weeks 6, 12, and 24 in a phase IIb study of patients with CD, the primary endpoint of the study, clinical remission at week 6, was not achieved (13,7 vs. 8.7%; $p = 0.157$) (Panaccione et al., 2015).

The potential use of **brazikumab (MEDI2070)**, a selective anti-p19mAb, was evaluated in a phase IIa study. In this trial, 119 patients with CD who had failed previous treatment with anti-TNF antibodies achieved a clinical response to brazikumab after 8 weeks, at a significantly higher rate than was observed for patients in the placebo-control group (49.2 vs. 26.7%; $p = 0.01$). Interestingly, higher serum concentrations of interleukin 22 (a "downstream" mediator in the IL-23 signaling pathway) were positively associated with treatment response; as such, IL-22 levels may be a predictor of treatment response (Sands et al., 2017).

Similarly, results of a phase II trial involving **risankizumab**, another anti-p19 mAb, revealed clinical remission at 12 weeks in 121 patients with CD significantly more frequently than in those receiving placebo (36.6 vs. 15.4%; $p = 0.0252$) (Feagan et al., 2017). When therapy was continued in the subset of patients who had achieved remission at week 26, clinical and endoscopic remission was achieved in 71 and 55% of the patients examined at week 52, respectively (Feagan et al., 2018).

In a phase II study of the anti-p19 mAb, **mirikizumab**, in 168 patients with UC, clinical remission was observed significantly more frequently in patients who received the study drug than in those receiving placebo (22.6 vs. 4.8%; $p = 0.004$), In this study, clinical responses were observed after intravenous induction therapy at a dose of 200 mg at weeks 0, 4 and 8; however, as insufficient responses were observed to doses of 50 or 600 mg, the primary endpoint of the study was not met. Nonetheless, it is important to note that clinical responses to therapy were observed more frequently among those who received one of the two higher doses (60 and 49% to 200 and 600 mg, respectively) than those in the placebo group (21%). Upon continuation of therapy, clinical remission was maintained up to week 52 in 37–47% of patients, depending on the dosage interval. As such, any future studies must first address the issue of the optimal dosage for induction therapy (Sandborn et al., 2020b).

In another phase II study featuring mirikizumab carried out in 191 CD patients, an endoscopic response (primary endpoint) was achieved significantly more frequently with induction doses of 600 mg (37.5%; $p = 0.03$) or 1,000 mg (43.8%; $p < 0.001$) than with placebo (10.9%). The rate of clinical response and clinical remission [600 mg: 40.6% ($p < 0.001$), 1,000 mg: 26.6% ($p = 0.013$) vs. placebo (9.4%), respectively] was also achieved significantly more frequently with mirikizumab (Sands et al., 2019). Findings in a recently published abstract reported that maintenance therapy after successful induction of an endoscopic response was successful in 59% of patients up to week 52, while

TABLE 2 | Frequency of achieving clinical remission in anti-IL-23 (±anti-IL-12) directed studies of patients with CD (a) or UC (b).

Drug	Study phase	Induction treatment				Study type	Maintenance treatment				References
		Week	Study drug	Placebo	*p*		Week	Study drug	Placebo	*p*	
a) CD											
Ustekinumab[a]	III	8	29.8	13.0%	<0.001	rr	52	53.1	35.9%	0.005	Feagan et al. (2016)
Briakinumab	II	6	17.3	8.7%	0.157						Panaccione et al. (2015)
Risankizumab	II	12	36.6	15.4%	0.0252	r 26	52	71.0	nd	Na	Feagan et al. (2017), Feagan et al. (2018)
Mirikizumab	II	12	40.6	9.4%	<0.001	rr	52	56.5	nd	Na	Sands et al. (2019), Sands et al. (2020b)
Brazikumab	II	8	27.1	15.0%	0.1						Sands et al. (2017)
Guselkumab	II	12	56.0	15.7%	0.001						(Sandborn et al., 2020)

Drug	Study phase	Induction treatment				Study type	Maintenance treatment				References
		Week	Study drug	Placebo	*p*		Week	Study drug	Placebo	*p*	
b) UC											
Ustekinumab[a]	III	8	15.5	5.3%	<0.001	rr	52	43.8	24.0%	<0.001	Sands et al. (2019b)
Mirikizumab	II	12	22.6	4.8%	0.004						Sandborn et al. (2020b)

NB: In studies that feature different dosages or intervals, the most effective treatment has been presented.

[a]currently licensed for use as therapy in CD and UC; OLE, open-label extension; tt, treat-through; r, continuation of assigned treatment in responders; r 26, remission at week 26; rr, randomized responder; nd, not done; na, not applicable.

clinical remission was achieved in 46% of patients (Sands et al., 2020a). A phase III study program (VIVID) aimed at evaluating the clinical efficacy of mirikizumab for the treatment of patients with CD is currently underway.

At United European Gastroenterology (UEG) Week 2020, data from the GALAXI 1 study that featured the treatment of CD patients with the anti-p19 mAb, **guselkumab,** were presented. Similar to risankizumab, this drug has already been approved for the treatment of plaque psoriasis. In this phase II study, the effectiveness of intravenous induction therapy with guselkumab was compared to placebo and induction with ustekinumab in 250 patients. Clinical remission was observed in 50–56% of patients at week 12 (and in 16 and 45% to placebo and ustekinumab, respectively). Other endpoints, including clinical, biochemical, and endoscopic responses were also achieved significantly more frequently with guselkumab than with placebo, although no dose-dependency was observed (Sandborn et al., 2020).

The results of eight studies focused on achieving clinical remission in both CD and UC using anti-IL-23 strategies are summarized in **Table 2**.

COMMENT

Taken together, results from the aforementioned studies suggest that combined inhibition of both IL-12 and IL-23 (as achieved with ustekinumab and possibly briakinumab) as well as selective inhibition of IL-23 alone (with brazikumab, risankizumab, mirikizumab, and guselkumab) are all effective therapies for patients with CD, and probably also for those with UC. It is not yet clear whether inhibition of one vs. two of the target cytokines offers advantages with regard to effectiveness and/or safety. In particular, ustekinumab, which has been approved for use as a treatment for both CD and UC, has a documented favorable safety profile based on the results of individual studies of patients who received this therapy for more than 5 years. We can assume that this good safety profile will most likely apply to the other, related drugs considered here, although their individual adverse event profiles require specific evaluation in future studies.

JAK INHIBITORS

The therapeutic modalities considered above were designed to interact with extracellular targets, including pro-inflammatory cytokines or cell-adhesion molecules. Another concept under development involves the blockade of intracellular signaling using inhibitors of tyrosine kinases. While more than 80 tyrosine kinases have been characterized, the Janus kinases (JAKs) have been identified as critical targets. Tofacitinib is a small-molecule inhibitor of JAK1 and JAK3 that has already been approved for the treatment of UC. A clinically relevant advantage of this class of medications is that unlike biologics, they are largely non-immunogenic. This is an important attribute, given that neutralizing immune responses are often the cause of secondary loss of response to biologics [see Overview (Vulliemoz et al., 2020)].

However, one notable disadvantage of tofacitinib is the increased risk for primary infection or reactivation of herpes zoster, as well as deep vein thrombosis and pulmonary embolism, especially in elder patients. **Upadacitinib**, a selective JAK1 inhibitor, has already been approved for the treatment of refractory rheumatoid arthritis and is currently under evaluation as induction and maintenance therapy for moderate to severe CD and UC. Clinical and endoscopic remissions after 16 weeks were defined as primary clinical end-points in these studies. The current results reveal endoscopic improvement and

TABLE 3 | Frequency of achieving clinical remission in studies featuring JAK inhibitors in patients with CD (a) or UC (b).

Drug	Study phase	Induction treatment				Study type	Maintenance treatment				Ref
		Week	Study drug	Placebo	*p*		Week	Study drug	Placebo	*p*	
a) CD											
Tofacitinib[a]	II	8	43.5	36.7%	0.325	rr	26	55.8	38.1%	0.13	Panés et al. (2017)
Upadacitinib	II	16	27.0	11.0%	<0.1	rr	52	41.0	32.0%	n.s	Sandborn et al. (2020c)
Filgotinib	II	10	47.0	23.0%	0.008						Vermeire et al. (2017b)

Drug	Study phase	Induction treatment				Study type	Maintenance treatment				Ref
		Week	Study drug	Placebo	*p*		Week	Study drug	Placebo	*p*	
b) UC											
Tofacitinib[a]	III	8	17.6	6.0%	<0.001	rr	52	40.6	11.0%	<0.001	Sandborn et al. (2017)
Upadacitinib	II	8	19.6	0.0%	0.002						Sandborn et al. (2020c)
Filgotinib	II/III	10	18.2	9.7%	0.001	rr	58	37.2	11.2%	<0.001	Feagan et al. (2020b), pooled data, Peyrin-Biroulet et al. (2020b)

NB: In studies that feature different dosages or intervals, the most effective treatment has been presented.
[a]currently licensed for use as therapy in CD and UC; OLE, open-label extension; tt, treat-through, r, continuation of assigned treatment in responders; r 26, remission at week 26; rr, randomized responder; nd, not done, na, not applicable.

clinical responses to induction therapy at daily doses of 6 and 7.5 mg, respectively. Of significant clinical relevance, the results of this study revealed that extraintestinal manifestations improved more frequently in response to upadacitinib compared to placebo in patients with CD (Peyrin-Biroulet et al., 2019).

Interestingly, more infections and more serious infections occurred in patients with CD in the upadacitinib treatment group than were reported in the group receiving placebo. While this was largely expected, this was not observed in studies involving the treatment of patients with UC (Sandborn et al., 2020a; Sandborn et al., 2020c).

Filgotinib is a selective JAK1 inhibitor that has recently been approved in Europe for the treatment of rheumatoid arthritis (September 2020); it has also been evaluated in patients with CD in the FITZROY phase II trial. Clinical remission was observed after 10 weeks in 47% of the patients receiving the study drug, compared to 23% in the placebo group ($p = 0.008$) (Vermeire et al., 2017b). A phase III trial in patients with CD is currently ongoing, together with additional phase II trials that feature subgroups of CD patients, including those with perianal fistulas or primarily small bowel disease. The recently closed phase IIb/III SELECTION study examined 1,348 patients with moderate to severe UC. Although the full publication remains pending, preliminary data reveal a significantly higher rate of clinical remission after 10 and 58 weeks among patients treated with 200 mg of filgotinib compared to placebo.

The results of six studies focused on achieving clinical remission in both CD and UC using JAK inhibitors are summarized in **Table 3**.

In addition to the previously characterized JAK inhibitors, other innovative approaches are currently under evaluation in clinical trials. For example, another potential therapeutic target is tyrosine kinase 2 (TYK2); this kinase is involved in the signal transduction mediated by the IBD-associated cytokines IL-12, IL-13, and the interferons. The TYK2 inhibitor, BMS-986165, is currently under evaluation for induction and maintenance of remission in a phase II trial in patients with CD.

Local/topical administration of JAK inhibitors is an important approach that is currently under consideration in an effort to reduce the frequency of treatment-associated infections. Toward this end, TD 1473 is a high-affinity JAK1-, JAK2-, JAK3- and TYK2-inhibitor that cannot be resorbed; this property results in high levels of drug within the inflamed gut mucosa with only minimal systemic exposure. Results of phase I trials indicated low plasma levels of this drug despite high concentrations in the colon. Data obtained in trials that included healthy subjects and also patients with UC revealed that a single dose of up to 1,000 mg or 14 days of a 300 mg daily dose appear to be safe and well-tolerated. As such, this might prove to be a promising approach for the treatment of UC.

COMMENT

In the coming years, additional tyrosine kinase inhibitors will be available for the treatment of IBD. Before treatment, the risk of herpes zoster reactivation and postherpetic neuralgia should be assessed and susceptible patients should be vaccinated. Likewise, there is an urgent need for direct head-to-head studies that compare the therapeutic potential of JAK inhibitors with previously-approved biological therapies. Due to the complexity of the JAK-mediated intracellular signaling pathways, it will be necessary to establish intensive long-term monitoring of patients who participated in registry studies to identify any long-term sequelae, including the potential for malignancies.

MODULATION OF SPHINGOSINE-1-PHOSPHATE RECEPTORS

Naïve lymphocytes reach the lymph nodes via afferent lymphatic vessels and ultimately enter the systemic circulation in response

to an S1P gradient. Ligand-mediated activation leads to S1P-receptor (S1PR) internalization and therefore to a functional blockade of lymphocyte migration.

Fingolimod is an S1PR1 modulator that has already been approved for the treatment of multiple sclerosis. However, the use of this medication is associated with severe adverse effects, including cardiac sequelae, varicella zoster-encephalitis, hepatopathies, macular edema, and progressive multifocal leukoencephalopathy. A recent "Direct Health Care Professional Communication" issued by the EMA focused on fingolimod-induced liver injury, which can progress to acute liver failure requiring a liver transplant.

The TOUCHSTONE study featured responses of patients with UC to 32 weeks of therapy with the S1PR1/R5-modulator, **ozanimod**. The results of this study revealed a higher rate of clinical remission among those treated with the higher dose (1 mg/day) but not the lower dose (0.5 mg/day) of drug vs. those receiving placebo; this response was accompanied by a higher rate of mucosal healing (Sandborn et al., 2016). Data from the prolonged follow-up study (currently available as an abstract only) suggest that long-term control of inflammation can be achieved for up to 200 weeks.

An abstract of the results of the phase III study (TRUE NORTH) was presented at UEG Week 2020. In this study, 645 patients with UC were randomized 2:1 to receive treatment with 1 mg ozanimod (1 mg/day vs. placebo). After 10 weeks of therapy, clinical remission was achieved in 18.4 vs. 6.0% (p = 0.001) of the study participants, respectively; clinical remission was associated with a higher rate of mucosal healing. In the maintenance study that followed, 37% of the patients, that initially responded to the induction therapy reached a clinical remission after 52 weeks, compared to only 18.5% of those receiving placebo (p < 0.001) (Danese et al., 2020b; Sandborn et al., 2020f).

Preliminary data indicate that ozanimod is also effective in patients with CD. Sixty-nine patients were treated with ozanimod in the open STEPSTONE trial; after 12 weeks, 56.5% had a clinical response, 39.1% experienced clinical remission, and 23.2% had an endoscopic response (Feagan et al., 2020a). A placebo-controlled, phase III trial has been initiated.

A phase II study of the efficacy of **etrasimod**, an S1PR1/R4/R5 receptor modulator, in patients with UC indicated that treatment with this drug resulted in a marked improvement in the modified Mayo Scores when compared to placebo; this was especially notable in response to the higher dose (2 mg/day). Furthermore, a larger proportion of patients who achieved in clinical remission (33.0 vs. 8.1%; p < 0.001) and endoscopic improvement (41.8 vs. 17.8%; p = 0.003) could be identified after 12 weeks (Sandborn et al., 2020d).

Moreover, data from CD patients are available from a proof-of-concept-study that featured the S1PR1-modulator, **amiselimod**, although no clinical responses or biochemical improvement of disease activity was observed in comparison to placebo.

The results of four studies focused on achieving clinical remission in both CD and UC using S1PR modulators are summarized in **Table 4**.

COMMENT

As the modulation of the S1PRs is a novel therapeutic approach, its overall efficacy specifically for the treatment of patients with IBD requires further examination. Initial findings suggest no essential advantages when compared to previously established therapeutic regimens. Furthermore, it is unclear as to what might happen when the drug is discontinued. Of concern is the possibility of excessive rebound inflammation due to sudden removal of the blockade to lymphocyte migration.

PHOSPHODIESTERASE INHIBITORS

Apremilast is an inhibitor of the intracellular enzyme, phosphodiesterase 4. Blockade of this signaling pathway results in increased concentrations of intracellular cyclic AMP (cAMP); this leads to the inhibition of TNF-α−release and an increase in the level of the anti-inflammatory cytokine, IL-10. Apremilast has already been approved for the treatment of psoriasis. Although higher rates of clinical remission were observed at week 12 in comparison to placebo (30 mg: 31.6% and 40 mg 21.8 vs. Placebo: 12.1%; p = 0.269 and p = 0.01, resp.) in a current phase II study with 170 UC patients, these results did not achieve statistical significance (hierarchical, stepdown testing procedure), and as such, the primary endpoint of the study was not reached. However, remission was maintained in up to 40% of the patients that remained on the medication at week 52 (Danese et al., 2020b).

COMMENT

Inhibition of TNF-α *via* a mechanism that is unlikely to be vulnerable to immune-mediated loss of response is an interesting new therapeutic approach. However, the efficacy of this modality remains to be verified in future studies.

OLIGONUCLEOTIDE-BASED THERAPEUTICS

Specific inactivation of genes known to be involved in disease pathogenesis might constitute an effective therapeutic modality with fewer adverse effects. Clinical experience with this type of therapy is currently very limited. The phase III study featuring administration of **mongersen**, an antisense oligonucleotide inhibitor of Smad7, which is a critical regulator of TGF-ß mediated down-regulation of pro-inflammatory cytokines, did not fulfill the high expectations from the phase II study for patients with CD. The study was terminated early due to insufficient efficacy (Sands et al., 2020a).

The anti-sense oligonucleotide therapeutic, **alicaforsen,** leads to down-regulation of intercellular adhesion molecule-1 (ICAM-1). Although this agent had some impact on disease activity, no convincing efficacy was demonstrated in a phase II trial with patients diagnosed with IBD. There is an ongoing phase III trial in which this agent is administered *via* an enema preparation

TABLE 4 | Frequency of achieving clinical remission in studies featuring S1P-receptor modulators to treat patients with CD (a) or UC (b).

Drug	Study phase	Induction treatment				Study type	Maintenance treatment				Ref
		Week	Study drug (%)	Placebo	*p*		Week	Study drug	Placebo	*p*	
a) CD											
Ozanimod	II	12	39.1	nd	Na						Feagan et al. (2020a)
Amiselimod	II	12	28.2	40.5%	ns						D'Haens et al. (2019)

Drug	Study phase	Induction treatment				Study type	Maintenance treatment				Ref
		Week	Study drug	Placebo	*p*		Week	Study drug (%)	Placebo	*p*	
b) UC											
Ozanimod	III	10	18.4	6.0%	<0.001	rr	52	37.0	18.5%	<0.001	Danese et al. (2020a), Sandborn et al. (2020)
Etrasimod	II	12	33.0	8.1%	<0.001	tt	46	39.3	nd	Na	Vermeire et al. (2019), Sandborn et al. (2020d)

OLE, open-label extension; tt, treat-through; r, continuation of assigned treatment in responders; r 26, remission at week 26; rr, randomized responder; nd, not done; na, not applicable; ns not significant. NB: In studies that feature different dosages or intervals, the most effective treatment has been presented.

specifically in patients with pouchitis. At UEG Week 2020, the first findings released from a phase IIb study with **cobitolimod** used to treat patients with left-sided ulcerative colitis were presented. This oligonucleotide TLR 9-agonist induces the expression of both IL-10 and type I-interferon. Two topical administrations of 250 mg were well tolerated by 42 of the total 213 patients participating in the study. The initial findings also suggest superiority regarding clinical remission after 6 weeks. No long-term data are currently available, but a phase III study is planned.

COMMENT

The Mongersen study is an impressive example of the fact that positive results from phase II trials, notably those that mainly rely on subjective criteria such as the Clinical disease Activity Index (CDAI) as endpoints, may ultimately fail to be reproduced in larger phase III studies that apply objective criteria (e.g., luminal inflammation markers, such as fecal calprotectin, and/or endoscopic changes.) Likewise, although the study examining the rectal administration of cobitolimod provided useful proof of efficacy, this route is not suitable for long-term therapy of chronic diseases. Other modes of application will need to be developed.

FECAL MICROBIOTA TRANSPLANTATION: READY FOR PRIME TIME?

An inappropriate immunologic response to the gastrointestinal microbiota is thought to be of great importance in the pathogenesis of IBD. Numerous clinical observations suggest a close connection between pathologic gastrointestinal microbiota and the manifestation of disease in patients with IBD. However, considering that genetic factors and inflammatory reactions can change the composition of the gastrointestinal microbiota, it is not clear whether changes in the gut microbiome are the causes or consequences of the disease process. While FMT may be among the more drastic of the interventions used to influence the gastrointestinal microbiome, this modality is now an accepted regimen for the treatment of recurrent *Clostridium difficile* infection (Khoruts et al., 2020).

Multiple case studies and several randomized trials have explored this concept in patients with IBD. While most randomized studies involving patients with UC revealed that FMT had a significant impact on induction of remission (Stallmach et al., 2019; Tan et al., 2020), its efficacy has not been verified for patients with CD. Placebo-controlled trials involving patients with UC revealed that, although one out of every 3 to 4 patients achieved remission after FMT, one-time or short-term FMT leads to clinical failure over time. To address this problem, repeat colonoscopic FMT was performed once every 8 weeks in patients with UC; this led to the maintenance of both endoscopic and histologic remission. The role of FMT for the treatment of CD has been explored in case series and a single randomized study (Tan et al., 2020). Despite the very heterogeneous approaches, including different applications, target criteria, and patient groups (children, teenagers, or adults with CD), the data suggest an ~30% probability (76/255 patients) of remission in response to FMT. However, in the first and thus far only published controlled study, Sokol et al. (Sokol et al., 2020) reported no difference in the remission rates maintained at 24 weeks between the FMT and sham-control group (4/8 vs. 3/9). As such, proof of the efficacy of FMT in patients with CD remains pending.

COMMENT

To induce long-term and sustainable changes in microbiota, repetitive FMT applications are required. Our data in patients with UC have revealed that the diversity of gastrointestinal microbiota increases significantly and remains stable in response to the daily application of FMT-capsules over a 3 month period. Before the therapeutic concept of FMT can be established as a routine treatment for UC, several critical questions remain to be answered:

- Are certain donors more likely to be effective than others? Are there patient-specific factors that might be used to inform donor selection?
- When should FMT be performed in patients diagnosed with IBD? At an early stage of the disease or after exhaustion of all other established treatments?
- What is the influence of emerging infectious disease challenges (e.g., the COVID-19 pandemic) on the long-term success of an FMT protocol?

Of course, identification of the therapeutically active substance or substances in fecal microbiota presents the possibility that they might be produced exogenously and provided by more routine therapeutic routes. Nevertheless, FMT is an extremely interesting therapeutic concept that merits further consideration. However, due to multiple limitations and many as-yet unanswered, this procedure should not be performed outside of clinical trials.

CONCLUSION

This review covers the current status of seven different new therapeutic approaches that may be on the horizon for the treatment of IBD. The modalities shown to be effective in phase II studies of course require confirmation in larger phase III studies; in most cases, these trials are already underway. The approval of several new therapeutic agents is anticipated in the near future, including many with unique pharmacological mechanisms of action. By their nature, these novel therapeutics will enhance and broaden the scope of our currently available drug treatments for IBD. This of course leads to further questions as clinicians attempt to determine which therapeutic approach is the best option for each patient. Given the broad scope of disease manifestations, it is unlikely that all patients will benefit equally from each new drug or drug class. One important focus of future studies will be the identification of biomarkers that can be used to predict individual responses to therapy. Until such predictors are available, the responsible clinician focusing on personalized therapy will have the option to select a given therapy based on individual disease characteristics, treatment targets, and published literature.

AUTHOR CONTRIBUTIONS

CS and AS wrote the first draft of the article, PCG prepared figure and tables. All authors reviewed and edited the article. All authors read and approved the final article. AS had the final responsibility for the decision to submit for publication.

REFERENCES

Coward, S., Clement, F., Benchimol, E. I., Bernstein, C. N., Avina-Zubieta, J. A., Bitton, A., et al. (2019). Past and future burden of inflammatory bowel diseases based on modeling of population-based data. *Gastroenterology* 156 (5), 1345–1353. doi:10.1053/j.gastro.2019.01.002e1344

Danese, S., Feagan, B. G., Wolf, D. C., Hanauer, S. B., Jovanovic, I., Ghosh, S., et al. (2020a). "Ozanimod as maintenance therapy in patients with moderate-to-severe ulcerative colitis: results from the phase 3, randomized, double-blind," in *Placebo-controlled true north study* (Vienna, Austria: United European Gastroenterology Week), LB10.

Danese, S., Neurath, M. F., Kopoń, A., Zakko, S. F., Simmons, T. C., Fogel, R., et al. (2020b). Effects of apremilast, an oral inhibitor of phosphodiesterase 4, in a randomized trial of patients with active ulcerative colitis. *Clin. Gastroenterol. Hepatol.* 18 (11), 2526–2534. doi:10.1016/j.cgh.2019.12.032

Danese, S., Sandborn, W. J., Reinisch, W., Hébuterne, X., Kłopocka, M., Tarabar, D., et al. (2019). Long-term mucosal healing, clinical response and clinical remission in patients with ulcerative colitis treated with the anti-mucosal addressin cell adhesion molecule-1 (MAdCAM-1) antibody ontamalimab (SHP647): results from the open-label extension study TURANDOT II. *United European Gastroenterol. J.* 7 (8 Suppl. l), 84. doi:10.14309/01.ajg.0000592624.44779.ee

Dotan, I. P. J., Duvall, A., Bouhnik, Y., Radford-Smith, G., Higgins, P. D. R., Mishkin, D. S., et al. (2020). *Etrolizumab compared with adalimumab or placebo as induction therapy for ulcerative colitis: results from the randomized, phase 3* Hibiscus *I & ii trials*, LB09. Vienna, Austria: United European Gastroenterology Week.

D'Haens, G., D. S., Davies, M., Watanabe, M., and Hibi, T. (2019). Amiselimod, a selective S1P receptor modulator in Crohn's disease patients: a proof-of-concept study. *J. Crohns Colitis* 13 (S1), S055–S056. doi:10.1093/ecco-jcc/jjy222.082

Feagan, B. G., Loftus, E. V., Jr., Danese, S., Vermeire, S., Sandborn, W. J., Ritter, T., et al. (2020a). *Efficacy and safety of filgotinib as induction therapy for patients with moderately to severely active ulcerative colitis: results from the phase 2b/3 selection study*. Vienna, Austria: United European Gastroenterology Week, LB19

Feagan, B. G., Panés, J., Ferrante, M., Kaser, A., D'Haens, G. R., Sandborn, W. J., et al. (2018). Risankizumab in patients with moderate to severe Crohn's disease: an open-label extension study. *Lancet Gastroenterol. Hepatol.* 3 (10), 671–680. doi:10.1016/s2468-1253(18)30233-4

Feagan, B. G., Rutgeerts, P., Sands, B. E., Hanauer, S., Colombel, J.-F., Sandborn, W. J., et al. (2013). Vedolizumab as induction and maintenance therapy for ulcerative colitis. *N. Engl. J. Med.* 369 (8), 699–710. doi:10.1056/NEJMoa1215734

Feagan, B. G., Sandborn, W. J., D'Haens, G., Panés, J., Kaser, A., Ferrante, M., et al. (2017). Induction therapy with the selective interleukin-23 inhibitor risankizumab in patients with moderate-to-severe Crohn's disease: a randomised, double-blind, placebo-controlled phase 2 study. *The Lancet* 389 (10080), 1699–1709. doi:10.1016/s0140-6736(17)30570-6

Feagan, B. G., Sandborn, W. J., Danese, S., Wolf, D. C., Liu, W. J., Hua, S. Y., et al. (2020b). Ozanimod induction therapy for patients with moderate to severe Crohn's disease: a single-arm, phase 2, prospective observer-blinded endpoint study. *Lancet Gastroenterol. Hepatol.* 5 (9), 819–828. doi:10.1016/s2468-1253(20)30188-6

Feagan, B. G., Sandborn, W. J., Gasink, C., Jacobstein, D., Lang, Y., Friedman, J. R., et al. (2016). Ustekinumab as induction and maintenance therapy for crohn's disease. *N. Engl. J. Med.* 375 (20), 1946–1960. doi:10.1056/NEJMoa1602773

Khoruts, A., Staley, C., and Sadowsky, M. J. (2020). Faecal microbiota transplantation for Clostridioides *difficile*: mechanisms and pharmacology. *Nat. Rev. Gastroenterol. Hepatol.* 18, 67. doi:10.1038/s41575-020-0350-4

Panaccione, R., Sandborn, W. J., Gordon, G. L., Lee, S. D., Safdi, A., Sedghi, S., et al. (2015). Briakinumab for treatment of Crohn's disease. *Inflamm. Bowel Dis.* 21 (6), 1–1340. doi:10.1097/MIB.0000000000000366

Panés, J., Sandborn, W. J., Schreiber, S., Sands, B. E., Vermeire, S., D'Haens, G., et al. (2017). Tofacitinib for induction and maintenance therapy of Crohn's disease: results of two phase IIb randomised placebo-controlled trials. *Gut* 66 (6), 1049–1059. doi:10.1136/gutjnl-2016-312735

Peyrin-Biroulet, L., Danese, S., Louis, E., Higgins, P. D. R., Dubinsky, M., Cataldi, F., et al. (2019). DOP50 Effect of upadacitinib on extra-intestinal manifestations in patients with moderate to severe Crohn's disease: data from the CELEST study. *J. Crohns Colitis* 13 (S1), S057. doi:10.1093/ecco-jcc/jjy222.084

Peyrin-Biroulet, L., Hassan, A. L., Bossuyt, P., Long, M., Allez, M., Juillerat, P., et al. (2020a). "Etrolizumab as induction and maintenance therapy in patients with ulcerative colitis previously exposed to anti-tumor necrosis factor Agent: the randomized," in *Phase 3 hickory trial*, LB08.

Peyrin-Biroulet, L., Loftus, E. V., Jr, Danese, S., Vermeire, S., Sandborn, W. J., Fogel, R., et al. (2020b). *Efficacy and safety of filgotinib as maintenance therapy for patients with moderately to severely active ulcerative colitis: results from the phase 2b/3 selection study*. Vienna, Austria: United European Gastroenterology Week, LB20.

Sandborn, W. J., D'Haens, G. R., Wolf, D. C., Hanauer, S. B., Jovanovic, I., Ghosh, S., et al. (2020). "Ozanimod as induction therapy," in *Moderate-to severe ulcerative colitis: results from the phase 3, randomized, double-blind, placebo-controlled true North study* (Vienna, Austria: United European Gastroenterology Week), LB02. doi:10.1177/2050640620968709

Sandborn, W. J., Feagan, B. G., Loftus, E. V., Jr., Peyrin-Biroulet, L., Van Assche, G., D'Haens, G., et al. (2020b). Efficacy and safety of upadacitinib in a randomized trial of patients with crohn's disease. *Gastroenterology* 158 (8), 2123–2138. doi:10.1053/j.gastro.2020.01.047

Sandborn, W. J., Feagan, B. G., Rutgeerts, P., Hanauer, S., Colombel, J.-F., Sands, B. E., et al. (2013). Vedolizumab as induction and maintenance therapy for Crohn's disease. *N. Engl. J. Med.* 369 (8), 711–721. doi:10.1056/NEJMoa1215739

Sandborn, W. J., Feagan, B. G., Wolf, D. C., D'Haens, G., Vermeire, S., Hanauer, S. B., et al. (2016). Ozanimod induction and maintenance treatment for ulcerative colitis. *N. Engl. J. Med.* 374 (18), 1754–1762. doi:10.1056/NEJMoa1513248

Sandborn, W. J., Ferrante, M., Bhandari, B. R., Berliba, E., Feagan, B. G., Hibi, T., et al. (2020c). Efficacy and safety of mirikizumab in a randomized phase 2 study of patients with ulcerative colitis. *Gastroenterology* 158 (3), 537–549. doi:10.1053/j.gastro.2019.08.043e510

Sandborn, W. J., Ghosh, S., Panes, J., Schreiber, S., D'Haens, G., Tanida, S., et al. (2020d). Efficacy of upadacitinib in a randomized trial of patients with active ulcerative colitis. *Gastroenterology* 158 (8), 2139–2149. doi:10.1053/j.gastro.2020.02.030e2114

Sandborn, W. J., Lee, S. D., Tarabar, D., Louis, E., Klopocka, M., Klaus, J., et al. (2018). Phase II evaluation of anti-MAdCAM antibody PF-00547659 in the treatment of Crohn's disease: report of the OPERA study. *Gut* 67 (10), 1824–1835. doi:10.1136/gutjnl-2016-313457

Sandborn, W. J., Peyrin-Biroulet, L., Zhang, J., Chiorean, M., Vermeire, S., Lee, S. D., et al. (2020e). Efficacy and safety of etrasimod in a phase 2 randomized trial of patients with ulcerative colitis. *Gastroenterology* 158 (3), 550–561. doi:10.1053/j.gastro.2019.10.035

Sandborn, W. J., Su, C., Sands, B. E., D'Haens, G. R., Vermeire, S., Schreiber, S., et al. (2017). Tofacitinib as induction and maintenance therapy for ulcerative colitis. *N. Engl. J. Med.* 376 (18), 1723–1736. doi:10.1056/NEJMoa1606910

Sandborn, W. J., Vermeire, S., Vermeire, S., Tyrrell, H., Hassanali, A., Lacey, S., et al. (2020f). Etrolizumab for the treatment of ulcerative colitis and crohn's disease: an overview of the phase 3 clinical program. *Adv. Ther.* 37 (7), 3417–3431. doi:10.1007/s12325-020-01366-2

Sandborn, W. J., Wolf, C. D., Johanns, J., Lang, G., Adedokun, O. J., Afzali, A., et al. (2020a). The efficacy and safety of guselkumab induction therapy in patients with moderately to severely active Crohn's disease: week 12 interim analyses from the phase 2 galaxi 1 study. *United Eur. Gastroenterol J* 8 (8 Suppl. l), 64.

Sands, B., S. W., Peyrin-Biroulet, L., Higgins, P., Hirai, F., Belin, R., Gomez Valderas, E., et al. (2019). Efficacy and safety of mirikizumab (LY3074828) in a phase 2 study of patients with Crohn's disease. *United Eur. Gastroenterol J* 7 (8 Suppl. l), 92. doi:10.1177/2050640619854670

Sands, B. E., Chen, J., Feagan, B. G., Penney, M., Rees, W. A., Danese, S., et al. (2017). Efficacy and safety of MEDI2070, an antibody against interleukin 23, in patients with moderate to severe crohn's disease: a phase 2a study. *Gastroenterology* 153 (1), 77–86. doi:10.1053/j.gastro.2017.03.049

Sands, B. E., Feagan, B. G., Sandborn, W. J., Schreiber, S., Peyrin-Biroulet, L., Frédéric Colombel, J., et al. (2020b). Mongersen (GED-0301) for active crohn's disease: results of a phase 3 study. *Am. J. Gastroenterol.* 115 (5), 738–745. doi:10.14309/ajg.0000000000000493

Sands, B. E., Peyrin-Biroulet, L., Loftus, E. V., Jr., Danese, S., Colombel, J.-F., Törüner, M., et al. (2019a). Vedolizumab versus adalimumab for moderate-to-severe ulcerative colitis. *N. Engl. J. Med.* 381 (13), 1215–1226. doi:10.1056/NEJMoa1905725

Sands, B. E., Sandborn, W. J., Panaccione, R., O'Brien, C. D., Zhang, H., Johanns, J., et al. (2019b). Ustekinumab as induction and maintenance therapy for ulcerative colitis. *N. Engl. J. Med.* 381 (13), 1201–1214. doi:10.1056/NEJMoa1900750

Sands, B. E., Scully, S. W. J., Peyrin-Biroulet, L., Higgins, P., Hirai, F., Jairath, V., et al. (2020a). Efficacy and safety of mirikizumab after 52-weeks maintenance treatment in patients with moderate-to-severe Crohn's disease. *United Eur. Gastroenterol J* 8 (8 Suppl. l), 75–76. doi:10.1177/2050640620927344

Sokol, H., Landman, C., Landman, C., Seksik, P., Berard, L., Montil, M., et al. (2020). Fecal microbiota transplantation to maintain remission in Crohn's disease: a pilot randomized controlled study. *Microbiome* 8 (1), 12. doi:10.1186/s40168-020-0792-5

Stallmach, A., Grunert, P., Pieper, D., and Steube, A. (2019). Colitis ulcerosa: kann eine Modulation der intestinalen Mikrobiota eine langfristige Remission bedingen? *Z. Gastroenterol.* 57 (7), 834–842. doi:10.1055/a-0874-6603

Tan, P., Li, X., Shen, J., and Feng, Q. (2020). Fecal microbiota transplantation for the treatment of inflammatory bowel disease: an update. *Front. Pharmacol.* 11, 574533. doi:10.3389/fphar.2020.574533

Vermeire, S., L, P. L., Ritter, T., Hanauer, S., Bressler, B., Khanna, R., et al. (2020). *Etrolizumab versus placebo in tumor necrosis factor Antagonist naive patients with ulcerative colitis: results from the randomized phase 3 laurel trial*. Vienna, Austria: United European Gastroenterology Week, LB18.

Vermeire, S., O'Byrne, S., Keir, M., Williams, M., Lu, T. T., Mansfield, J. C., et al. (2014). Etrolizumab as induction therapy for ulcerative colitis: a randomised, controlled, phase 2 trial. *The Lancet* 384 (9940), 309–318. doi:10.1016/S0140-6736(14)60661-9

Vermeire, S., Pulley, J., Chiorean, M., Peyrin-Biroulet, L., Zhang, J., Sands, B. E., et al. (2019). Long-term efficacy and safety of etrasimod for ulcerative colitis: results from the open-label extension of the OASIS study. *United Eur. Gastroenterol. J.* 7 (8 Suppl. l), 352. doi:10.1177/2050640619854670

Vermeire, S., Sandborn, W. J., Danese, S., Hébuterne, X., Salzberg, B. A., Klopocka, M., et al. (2017a). Anti-MAdCAM antibody (PF-00547659) for ulcerative colitis (TURANDOT): a phase 2, randomised, double-blind, placebo-controlled trial. *The Lancet* 390 (10090), 135–144. doi:10.1016/s0140-6736(17)30930-3

Vermeire, S., Schreiber, S., Petryka, R., Kuehbacher, T., Hebuterne, X., Roblin, X., et al. (2017b). Clinical remission in patients with moderate-to-severe Crohn's disease treated with filgotinib (the FITZROY study): results from a phase 2, double-blind, randomised, placebo-controlled trial. *The Lancet* 389 (10066), 266–275. doi:10.1016/S0140-6736(16)32537-5

Vulliemoz, M., Brand, S., Juillerat, P., Mottet, C., Ben-Horin, S., and Michetti, P. (2020). TNF-alpha blockers in inflammatory bowel diseases: practical recommendations and a user's guide: an update. *Digestion* 101 (Suppl. 1), 16–26. doi:10.1159/000506898

Yoshimura, N., Watanabe, M., Motoya, S., Tominaga, K., Matsuoka, K., Iwakiri, R., et al. (2015). Safety and efficacy of AJM300, an oral antagonist of α4 integrin, in induction therapy for patients with active ulcerative colitis. *Gastroenterology* 149 (7), 1775–1783. doi:10.1053/j.gastro.2015.08.044

Conflict of Interest: CS obtained consulting fees from Abbvie, Biogen, Ewopharma, Janssen, MSD, Pfizer, and Takeda, lecture fees and travel support from Abbvie, Berlin Chemie, Biogen, Ewopharma, Falk, Janssen, Merckle, MSD, Norgine, Novartis, Pfizer, Shire, Shield Therapeutics, and Takeda, and research support from Abbvie. PCG obtained consulting fees from Janssen and Takeda and lecture fees and travel support from AbbVie, Janssen, Pfizer, and Takeda. AS obtained consulting fees from Abbvie, Amgen, Astellas, Biogen, Celltrion, Consal, CSL Behring, Galapagos, Gilead, Institut Allergosan, Janssen, MSD, Norgine, Pfizer Pharma, Roche, Shire, Summit Therapeutics, and Takeda, lecture fees and travel support from Abbvie, Astellas, Celltrion, Falk Foundation, Ferring, Janssen, MSD, Recordati Pharma, and Takeda, and research support from Abbvie.

The reviewer JZ declared a past co-authorship with one of the authors AS to the handling editor.

Copyright © 2021 Schmidt, Grunert and Stallmach. This is an open-access article distributed under the terms of the Creative Commons Attribution License (CC BY). The use, distribution or reproduction in other forums is permitted, provided the original author(s) and the copyright owner(s) are credited and that the original publication in this journal is cited, in accordance with accepted academic practice. No use, distribution or reproduction is permitted which does not comply with these terms.

frontiers in Pharmacology

ORIGINAL RESEARCH
published: 14 April 2021
doi: 10.3389/fphar.2021.654985

Development and Validation of an Interleukin-6 Nomogram to Predict Primary Non-response to Infliximab in Crohn's Disease Patients

Yueying Chen[1], *Hanyang Li*[1], *Qi Feng*[2] *and Jun Shen*[1]*

[1]Division of Gastroenterology and Hepatology, Key Laboratory of Gastroenterology and Hepatology, Ministry of Health, Inflammatory Bowel Disease Research Center, Renji Hospital, School of Medicine, Shanghai Jiao Tong University, Shanghai Institute of Digestive Disease, Shanghai, China, [2]Department of Radiology, Renji Hospital, School of Medicine, Shanghai Jiao Tong University, Shanghai, China

Background: The primary non-response (PNR) rate of infliximab (IFX) varies from 20 to 46% for the treatment of Crohn's disease (CD). Detected PNR reduces the improper use of specific treatments. To date, there is hardly any knowledge regarding early markers of PNR. The aim of this study was to evaluate the role of Interleukin-6 (IL-6) as an early predictor of PNR of IFX for the treatment of CD.

Methods: We enrolled 322 bio-naïve patients diagnosed with CD from January 2016 to May 2020. Primary response was determined at week 14. Multivariable logistic regression was used to construct prediction models. Area under the curve (AUC), calibration and decision curve analyses (DCA) were assessed in the validation cohort. GEO data were analyzed to identify potential mechanisms of *IL-6* in IFX therapy for CD.

Results: PNR occurred in 31.06% (100 of 322) patients who were assessable at week 14. IL-6 levels significantly decreased after IFX therapy ($p < 0.001$). The validation model containing IL-6 presented enhanced discrimination with an AUC of 0.908 and high calibration. Decision curve analysis (DCA) indicated that the model added extra predictive value. GEO data confirmed the IL-6 levels were increased in the PNR group and IL-6-related differentially expressed genes (DEGs) were enriched in the inflammatory response.

Conclusions: We concluded that IL-6 may be used as a predictive factor to assess the risk of PNR to IFX therapy.

Keywords: interleukin-6, primary non-response, crohn's disease, infliximab, bioinfomatics

OPEN ACCESS

Edited by:
Ralf Weiskirchen,
RWTH Aachen University, Germany

Reviewed by:
Chuan Hu,
Qingdao University Medical College, China
Christoph Roderburg,
Charité – Universitätsmedizin Berlin, Germany

***Correspondence:**
Jun Shen
shenjun_renji@163.com

Specialty section:
This article was submitted to Gastrointestinal and Hepatic Pharmacology, a section of the journal Frontiers in Pharmacology

Received: *18 January 2021*
Accepted: *16 March 2021*
Published: *14 April 2021*

Citation:
Chen Y, Li H, Feng Q and Shen J (2021) Development and Validation of an Interleukin-6 Nomogram to Predict Primary Non-response to Infliximab in Crohn's Disease Patients. Front. Pharmacol. 12:654985. doi: 10.3389/fphar.2021.654985

INTRODUCTION

Crohn's disease (CD) is a chronic inflammatory disease with a relapsing history. The incidence and prevalence of CD have both increased worldwide and this disease has gradually become a more severe socioeconomic burden (Ng et al., 2013). Recently, the treatment of CD entered a new era. Anti-tumor necrosis factor (anti-TNF) therapy has been the first-line therapy for treating CD according to ECCO guidelines (Torres et al., 2020). Infliximab (IFX) is the most widely used anti-TNF agent that promotes mucosal healing and changes the natural history of the disease (Singh et al.,

2018). However, there are still 20–46% of CD patients that show primary non-response (PNR) to IFX (Roda et al., 2016; Yokoyama et al., 2016). Leapfrogging IFX in PNR patients to other medications such as anti-IL-12/23 monoclonal antibodies or anti-leucocyte adhesion molecules avoid ineffective processes of IFX and saves medical resources. Therefore, developing a model to predict PNR to IFX in CD patients will help doctors make better decisions for CD patients.

Previous studies have proposed several factors to predict the efficacy of IFX in CD, including age, BMI, previous surgery history (Billiet et al., 2015), disease behavior (Sprakes et al., 2012), disease duration (Matsuoka et al., 2018), and pro-inflammatory biomarkers (Billiet et al., 2017). Despite evidence, a clinical prediction model is still lacking to assess the possibility of PNR prior to IFX administration based on clinical and biochemical markers. As a chronic inflammatory disease, the regulation of cytokines is associated with the pathogenesis and progression of CD (Chen and Sundrud, 2016). IL-6 is a proinflammatory factor that can exacerbate inflammation by promoting the survival of T cells and the secretion of other cytokines (Hunter and Jones, 2015). *IL-6* levels were shown to be elevated in CD patients compared to healthy individuals (Engel et al., 2015). A randomized trial showed that an anti-IL-6 antibody promoted a clinical response and clinical remission in CD patients (Danese et al., 2019). Furthermore, IL-6 served as a predictor of PNR to anti-TNF treatment in CD and patients failing anti-TNF therapy showed increased expression of IL-6 and persistent IL-6 pathway activity (Leal et al., 2015; Soendergaard et al., 2018). A prospective, multicenter study confirmed the predictive roles of IL-6 in patients treated with anti-TNF therapy (Bertani et al., 2020a). Additionally, the single nucleotide polymorphisms of IL-6 may be a promising tool for identifying CD patient response to IFX therapy (Salvador-Martín et al., 2019).

To promote individualized treatment in CD patients, it is crucial to identify predictors to estimate PNR to IFX. Different IL-6 levels present before treatment may contribute to the contrasting response to IFX therapy. Detecting PNR reduces inaccurate treatments while a predictive model determining PNR to IFX in bio-naive CD is lacking. Therefore, we aimed to identify the predictive value of IL-6 in IFX therapy and to construct a model predicting PNR in bio-naive CD patients based on clinical information and IL-6 levels.

METHODS

Patients and Samples

A retrospective and single-center study was performed for CD cases in the Division of Gastroenterology and Hepatology, Renji hospital. Patients enrolled in this study from January 2016 to June 2019 and from July 2019 to May 2020 were assigned to the training and the validation cohorts, respectively. CD was diagnosed based on the ECCO consensus (Maaser et al., 2019). Bio-naïve patients were included and induced with 5 mg/kg of IFX (Janssen Pharmaceutical Ltd, United States). Baseline characteristics were collected prior to treatment.

Levels of biochemical indicators, including IL-6, albumin, hemoglobin, platelets, erythrocyte sedimentation rate (ESR) and CRP were obtained from previous blood analysis, and blood samples were collected for each participant before and after IFX therapy. The Westergren method and nephelometry were used to measure CRP and ESR levels. Enzyme Linked Immunosorbent Assay (ELISA) was used to detect IL-6 levels using a DPC IMMULITE 1000 system of Siemens, and the average CV value about 8.33%. The Clinical Laboratory Department (Renji Hospital, School of Medicine, Shanghai Jiao Tong University, China) performed an analysis of each sample in duplicate. This study was approved by the IRB of Shanghai Jiaotong University School of Medicine, Renji Hospital Ethics Committee (KY2020–115).

Outcomes and Definitions

Our study defined the primary outcome as the proportion of response to IFX, which was determined when achieving clinical response or remission at week 14 (after three IFX injections and before the fourth) using an MDT (multi-disciplinary team) of experienced experts combined with endoscopic and radiological examinations (Hanauer et al., 2002; Wong and Cross, 2017). PNR was defined as: 1) failure to achieve clinical response or clinical remission, clinical response and clinical remission have been defined as a decrease in Harvey Bradshaw indices (HBI) $\geq$ 2, and total HBI $\leq$ 4, respectively (Sprakes et al., 2012). 2) need for treatment modification (discontinuation, escalation or surgery) (Roda et al., 2016; Bar-Yoseph et al., 2018; Beltrán et al., 2019).

Statistical Analysis

Results for continuous variables were represented as mean (SDs) or median (interquartile ranges [IQRs]). Categorical variables were shown as proportions. Univariate logistic regression was applied to analyze the relationships between different factors and PNR to IFX therapy. A Chi-square test was used to compare categorical variables. The *t* test or Mann-Whitney *U* test were used to compare continuous variables.

Multivariable regression models with forward stepwise likelihood ratio algorithms were used to develop models predicting the response to infliximab 5 mg/kg through 14 weeks. Akaike information criterion (AIC) was performed to assessed the goodness of fit of two models. Discrimination of the prediction models was evaluated by receiver operating characteristics (ROC) analysis and presented as area under the curve (AUC). Odds ratios (OR) having 95% confidence intervals (CI) of final predictors were calculated. Calibration curves were used to assess the calibration of nomograms by comparing the predicted and observed probabilities. The clinical effectiveness of the models was assessed using decision curve analysis (DCA). Integrated Discrimination Improvement (IDI) was a reclassification measures showed the difference in discrimination slopes of two models, and was used to assess the improvement of risk differences between cases and non-cases (Pencina et al., 2008;

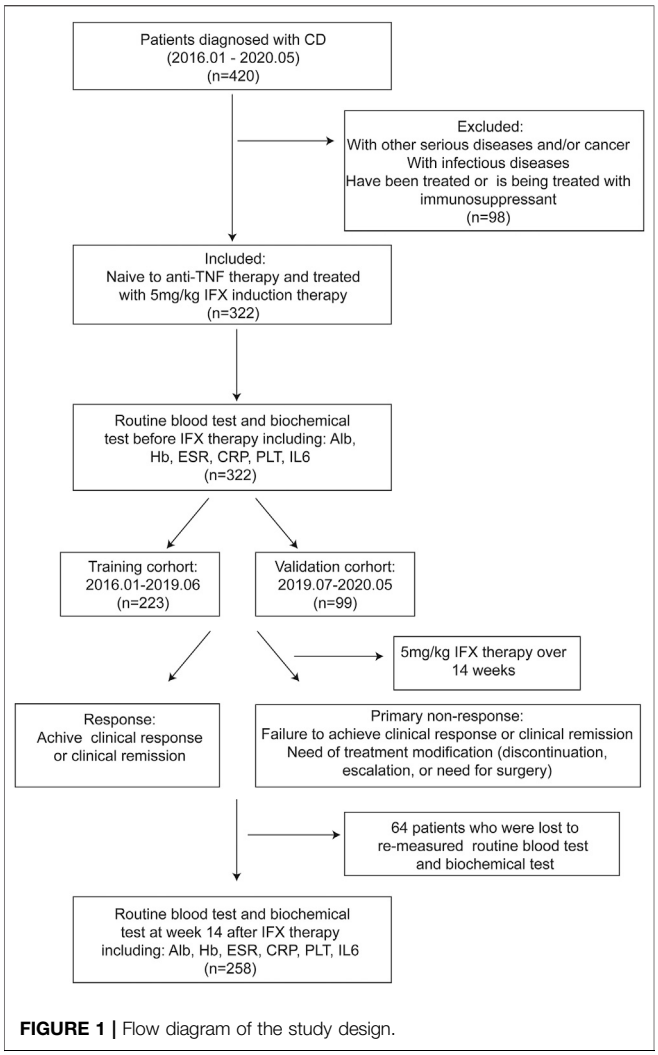


FIGURE 1 | Flow diagram of the study design.

Steyerberg et al., 2010; Kerr et al., 2011). All statistical analyses were performed using SPSS 25.0 and R 3.6.3 with a statistical significance of $p < 0.05$.

Bioinformatic Analysis

Data Source

A gene expression microarray dataset (GSE111761) of Schmitt's study from the GEO database was selected (Schmitt et al., 2019). GSE111761 contained three samples from anti-TNF non-responders and three from responders. The patients were diagnosed as CD and defined as responders or non-responders when they had ongoing anti-TNF therapy for over 3 months. The GSE111761 dataset was available on the GPL13497 platform (Agilent-026652 Whole Human Genome Microarray 4 × 44K v2).

Identification of Differentially Expressed Genes (DEGs)

R software (version 3.6.3) and the limma package in Bioconductor were used to detect DEGs in GSE111761 (Ritchie et al., 2015). DEGs were identified using selection criteria of an adjusted p value < 0.05 and |logFC|>1.0.

TABLE 1 | Multivariate regression analyses of the model 1 and model 2.

Variables	B	Or (95% CI)	P	s.e
(a) Multivariate regression analysis including BMI, behavior, and CRP				
BMI	−0.217	0.805 (0.731–0.908)	0.000	0.061
Behavior	1.281	3.602 (1.881–6.895)	0.000	0.331
CRP	0.025	1.025 (1.009–1.041)	0.002	0.008
(b) Multivariate regression analysis including BMI, behavior, CRP, and IL-6				
BMI	−0.212	0.809 (0.716–0.914)	0.001	0.062
Behavior	1.252	3.499 (1.809–6.766)	0.000	0.336
CRP	0.024	1.024 (1.008–1.041)	0.003	0.008
IL-6	0.237	1.267 (1.041–1.541)	0.018	0.100

BMI, Body Mass Index; CRP, C-reactive protein; IL6, interleukin-6; CI, confidence interval; OR, odds ratio; s.e., standard error

Enrichment Analysis

Gene Set Enrichment Analysis (GSEA) was performed using the ClusterProfile package in Bioconductor with a statistical significance of $p < 0.05$ (Yu et al., 2012).

Protein-Protein Interaction (PPI) Network Construction

PPI network reveals the specific and unspecific interactions of proteins, and promotes to identify therapeutic target (Petta et al.,

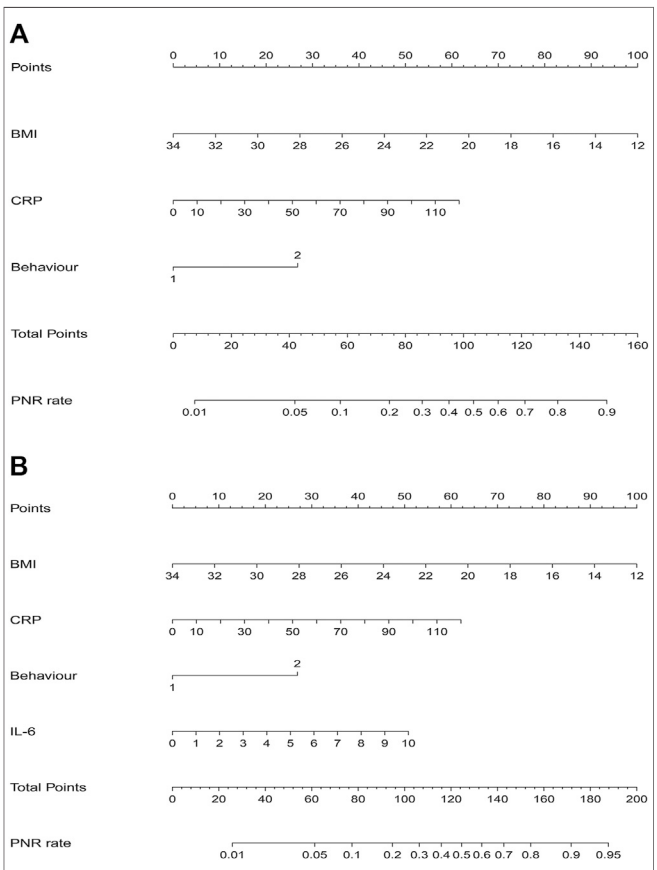


FIGURE 2 | Nomograms for model 1 and model 2 were developed in the training cohort **(A)** Nomogram one for model 1, with BMI, behavior, and CRP. BMI, Body Mass Index; CRP, C-reactive protein **(B)** Nomogram two for model 2, with BMI, behavior, CRP, and IL6. IL6, interleukin-6.

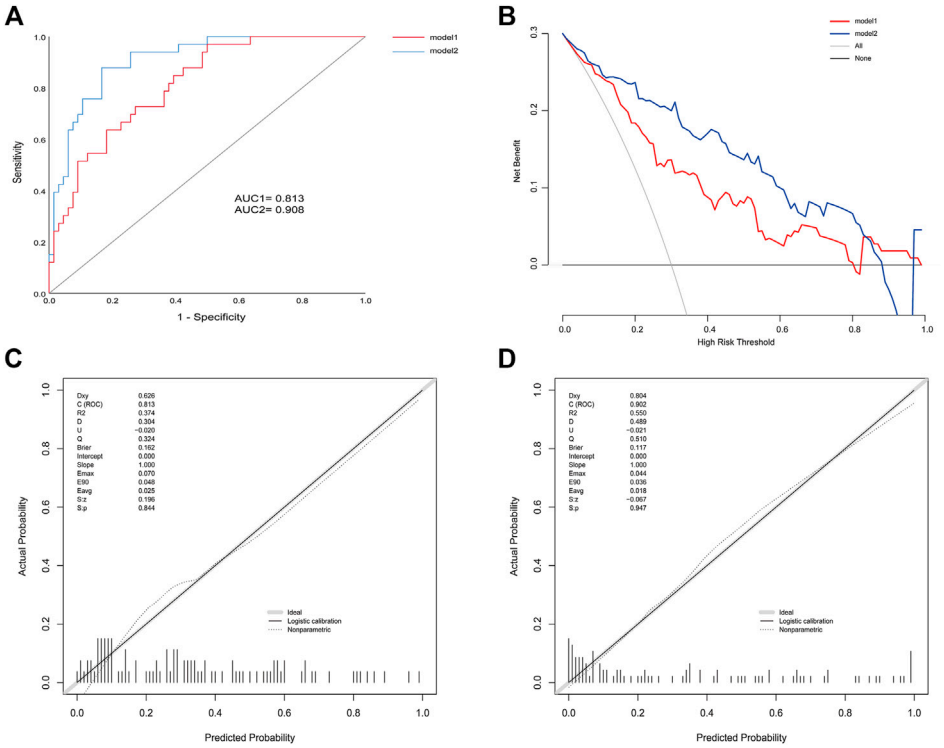


FIGURE 3 | (A) ROC for model 1 and model 2 in the validation cohort **(B)** Calibration plots for model 1 **(C)** Calibration plots for model 2 **(D)** DCA for model 1 and model 2 in the validation cohort.

2016; Maurel et al., 2019). STRING (version 11.0), a freely accessible database that collects, scores and integrates data, was used to predict functional relationships between proteins (Szklarczyk et al., 2019). A PPI network of genes with a score > 0.4 in STRING was constructed using Cytoscape software (version 3.7.2) (Smoot et al., 2011). The degree of protein nodes was calculated using the Cytoscape plugin CytoHubba to identify hub genes (Chin et al., 2014). Hub genes were selected with a score ≥ 4.5 based on the EPC algorithm.

Construction of Regulatory Network

The network of genes and their corresponding miRNAs and lncRNAs was constructed using starbase, a publicly available database mainly focusing on miRNA-target interactions (Li et al., 2014). Transcription factors (TFs) were downloaded from TRRUST (http://www.grnpedia.org/trrust/), a public database for predicting TFs of various genes through DNA sequences (Farre et al., 2003). These tools were combined to construct a multi-factor regulation network.

RESULTS

Baseline Characteristics and Univariate Analyses

From a total of 322 active CD patients receiving 5 mg/kg IFX induction therapy, 223 and 99 were assigned to training and validation groups, respectively (**Figure 1**). Disease behavior was merged into two categories, including nonstricturing and nonpenetrating (B1) into one category, and stricturing and/or penetrating (B2/B3) subtypes into another category. The baseline characteristics are shown in **Supplementary Table S1**. The incidence of PNR in the training cohort was 30.0% (n = 67), while the incidence in the validation cohort was 33.3% (n = 33). Baseline characteristics of patients were similar between the two cohorts. Univariate regressions showed that BMI ($p < 0.001$), disease behavior ($p < 0.001$), CRP levels ($p = 0.001$), and IL-6 levels before IFX therapy ($p = 0.002$) were strongly associated with PNR to IFX treatment (**Supplementary Table S2**).

IL-6 levels were measured in 258 of the studied 322 patients before initiation and at week 14 before the fourth IFX injection. IL-6 levels were found to significantly decrease after IFX therapy ($p < 0.001$) and were obviously different between PNR and response groups ($p = 0.001$) (**Supplementary Figure S1**).

Development of Prediction Models and Nomogram Construction

Results of multiple logistic regression suggested BMI, disease behavior, CRP levels and IL-6 levels before IFX therapy were determined as predicting factors. To identify the true predictive effects of IL-6, we built a model contained IL-6 and the other one did

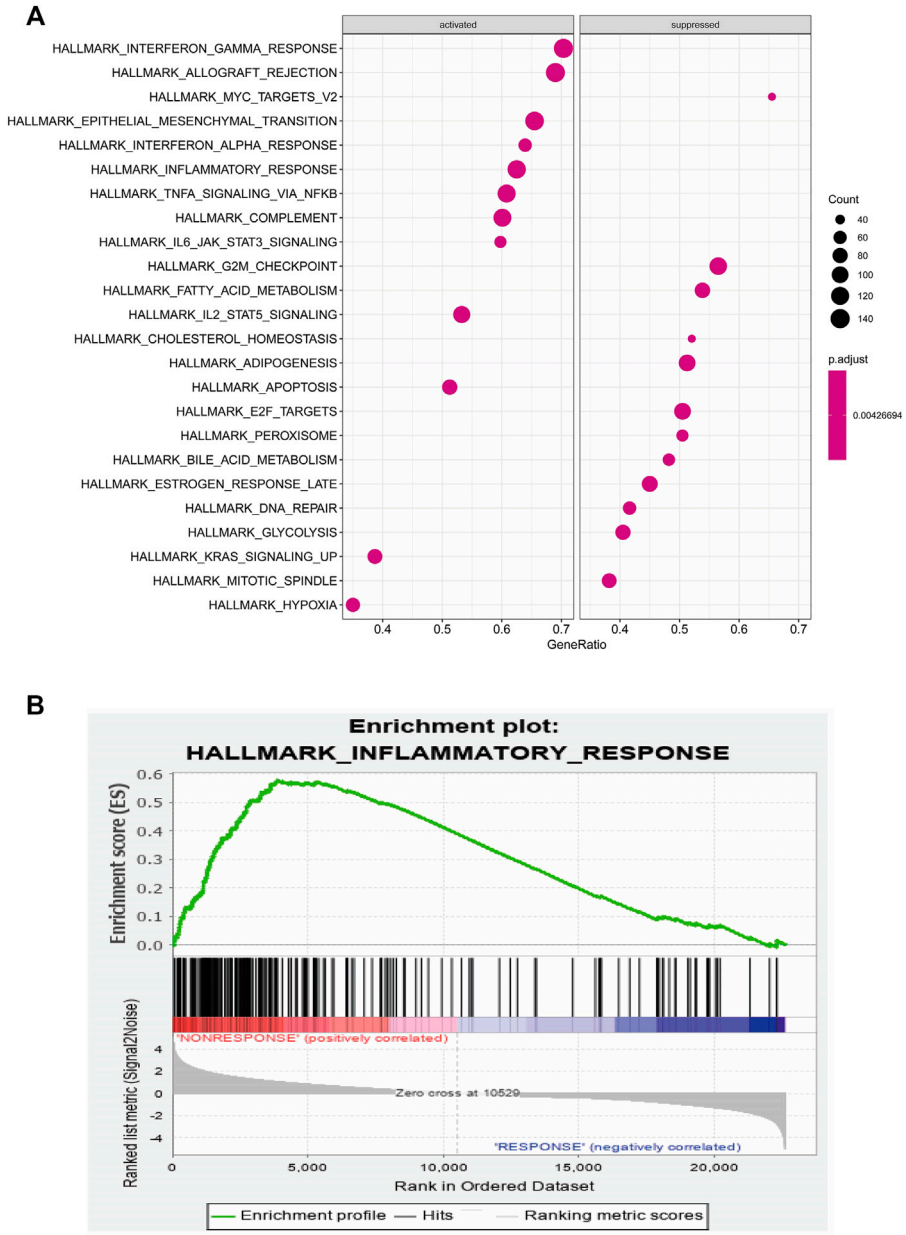


FIGURE 4 | (A) GSEA analysis of *IL-6* and *IL-6* related genes **(B)** Inflammatory response of GSEA analysis.

not. The diagnostic equations of models were: logitP = 1.162–0.217* BMI +1.281 * behavior +0.025 * CRP, and logitP = 0.144–0.212* BMI +1.252 * behavior +0.024 * CRP +0.237* IL-6, respectively. The results of multivariate regression analyses are shown in **Table 1**. These two models are presented as nomograms, which containing these independent predictors to calculate the risk of PNR based on the total points (**Figure 2**).

Validation of Prediction Models

Efficacies of the two models were compared to the validation cohort. AIC was 111.3 and 99.1 of model1 and model2, respectively. ROC analysis indicated and the AUC of BMI, behavior, CRP, and IL-6 were 0.652 (95% CI: 0.540–0.764), 0.674 (95% CI: 0.563–0.785), 0.744 (95% CI: 0.646–0.842), and 0.787 (95% CI: 0.698–0.877) respectively. An AUC of 0.813 (95% CI: 0.729–0.897) in model 1 and 0.908 (95% CI: 0.851–0.966) in model 2 **(Figure 3)**. The p value = 0.005 of DeLong's test showed that an AUC of model 2 was significantly better than model 1. Calibration plots showed that the average differences (E aver) were 2.5 and 1.8% in model 1 and 2, and no significant differences ($P_1 = 0.844$, $P_2 = 0.947$) between the predicted and the calibrated probabilities. DCA showed that if the risk thresholds were between 12 and 85%, model 2 added more clinical net benefit compared to model 1. To explore additional benefits conferred by

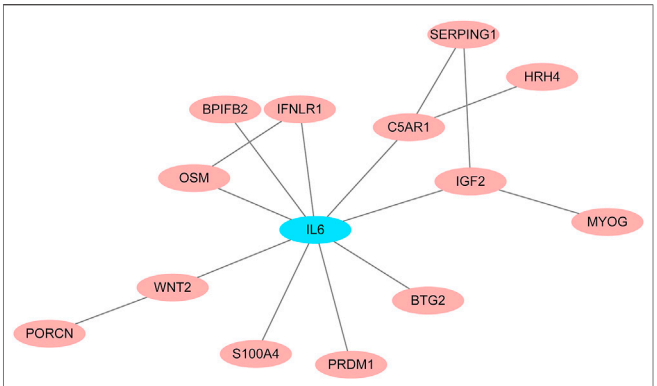


FIGURE 5 | PPI networks for *IL-6* and *IL-6* related genes with the top 50 highest correlation coefficients.

IL-6 levels, we compared IDI between models and found this improvement index was improved upon addition of IL-6 (IDI = 19%; 95% CI, 0.10–0.28; $p < 0.000$).

Identification of Pathway and Regulatory Network of IL-6

To identify potential pathways and regulatory network of IL-6 in IFX therapy of CD, the GSE111761 dataset contained lamina propria mononuclear cells from three anti-TNF non-responders and three responders were included to identify DEGs. The samples were obtained from the patients with anti-TNF therapy for over 3 months and the Simple Endoscopic Score for Crohn's disease (SES-CD) <5. There were 2,228 DEGs including 1,384 upregulated genes and 844 downregulated genes and IL-6 expression levels were significantly elevated in PNR patients (**Supplementary Figure S2**). Spearman correlation was performed to investigate the connections between *IL-6* and other DEGs. Genes with a $p < 0.05$ were selected for GSEA. Results indicated that *IL-6* and relative genes were mainly involved in inflammatory response (**Figure 4**; **Supplementary Table S3**). We selected *IL-6* related genes with the top 50 highest correlation coefficients to create PPIs, and identified five hub genes, including *IL-6, IGF2, C5AR1, IFNLR1* and *OSM* with score ≥ 4.5 based on the EPC algorithm (**Figure 5**). We found that the expression of Oncostatin M (*OSM*) coordinated with *IL-6* and also belonged to the inflammatory response in GSEA. To identify potential biological mechanisms between *IL-6* and *OSM*, we found a total of 10 miRNAs, 25 lncRNAs, and 1 TF shared in common with both *IL-6* and *OSM*. Data of these two genes and their miRNAs, lncRNAs and TF were integrated into a regulatory network (**Figure 6**). It was suggested that *IL-6* and *OSM* may be involved in the inflammatory response through a regulation network based on common lncRNAs, miRNAs and TF.

DISCUSSION

Even though anti-TNF agents have shown to be effective in inducing clinical response and mucosal healing, there are still a considerable proportion of patients who do not respond (Ding et al., 2016). Previous studies have identified several predictors of PNR to IFX in CD, such as BMI, fecal calprotectin (Pavlidis et al., 2016), proinflammatory biomarkers (Billiet et al., 2017), and genetic markers (Barber et al., 2016). These studies have also established prediction models based on these factors. IL-6 is a proinflammatory cytokine and expression levels alter after IFX therapy. It is considered a good predictor of IFX response (Suzuki et al., 2015; Salvador-Martín et al., 2019). However, there are few prediction models for PNR to IFX treatment in CD. In this study, we showed that IL-6 levels before IFX therapy predicted the response to IFX treatment and alter after IFX therapy.

This retrospective study included 322 CD patients who were naive to anti-TNF therapy and both their clinical and serological data were collected. Logarithmic transformation was performed for IL-6 levels to decrease the undulation of data. Consistent with previous reports, IL-6 levels were significantly reduced after 14 weeks of IFX therapy. Univariate and multivariate regression analyses found that BMI, disease behavior, CRP and

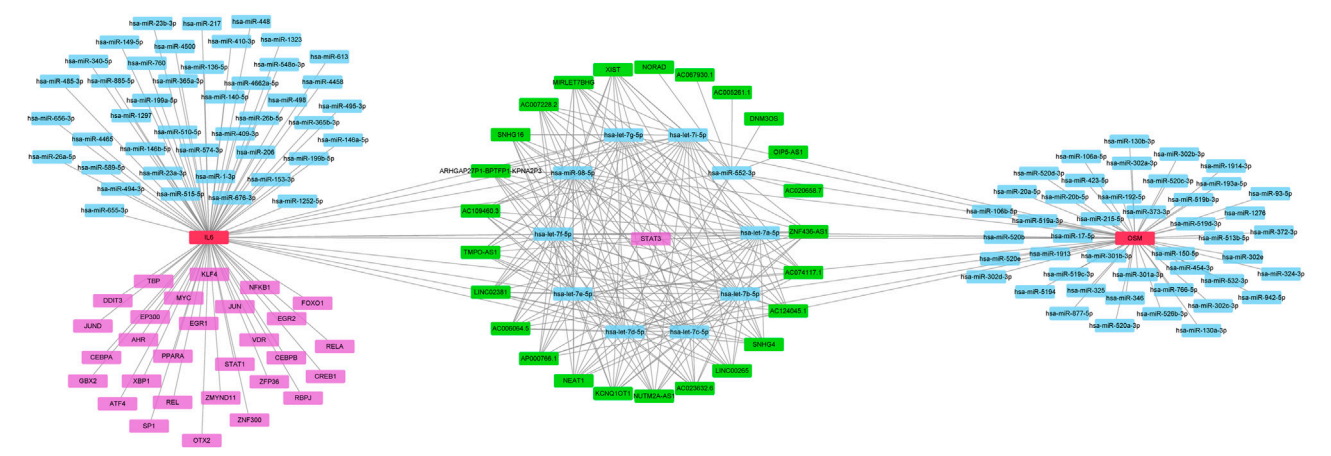


FIGURE 6 | Multi-factor regulation network for *IL-6* and *OSM*.

IL-6 levels before IFX therapy independently predicted the response to IFX treatment. To explore the predictive ability of IL-6, we established two prediction models, one containing BMI, disease behavior and CRP levels, and the other including BMI, disease behavior, CRP levels, and IL-6 levels. Results of AIC and ROC in the validation cohort, indicated that the goodness of fit and discrimination of model containing IL-6 was better than the model not including IL-6. And the AUC of the model incorporating IL-6 was higher than that in single factors, including BMI, disease behavior and CRP levels. The calibration curve and DCA curve demonstrated a greater consistency and clinical validity in the model containing IL-6. IDI analysis showed that incorporation of IL-6 with BMI, behavior, and CRP significantly improved the discriminatory accuracy for PNR with IDI of 19% ($p < 0.000$). Furthermore, the improvement of IDI for discriminating PNR to IFX therapy is consistent with previous studies, such as Leal et al. (Leal et al., 2015), which revealed the predictive effect of IL-6 on risk of PNR to anti-TNF therapy in CD patients. Therefore, we suggested that IL-6 played a central role in assessing the possibility of PNR to IFX therapy.

Furthermore, we analyzed GEO data to verify the predictive power of IL-6. It was found that expression of *IL-6* significantly increased in non-responders compared with responders to IFX therapy. GSEA of *IL-6* and its relative genes with high correlation coefficients showed that these genes mainly were enriched in the inflammatory response. Through the construction of PPI networks, we found that *OSM* directly connected to *IL-6* and its expression was consistent with *IL-6* in the inflammatory response. *OSM* regulates the production of proinflammatory cytokines such as IL-6 through the JAK-STAT pathway (Hermanns, 2015). Studies demonstrated that *OSM* induced intestinal inflammation, while mechanisms remained unclear (Thomas, 2017). Furthermore, *OSM* has been considered a novel biomarker to predict the efficacy of anti-TNF therapy. One study showed that *OSM* was enriched in CD mucosa and complete mucosal healing was more likely to occur in patients with low *OSM* expression levels. Notably, the expression of *OSM* was strongly correlated with PNR to IFX (West et al., 2017). Another clinical study suggested that *OSM* was an appreciable biomarker in predicting the possibility of mucosal healing compared with fecal calprotectin, which indicated *OSM* may be a predictive indicator for IFX therapy (Bertani et al., 2020b). To explore the common mechanisms of *IL-6* and *OSM* in IFX treatment, we found that they both shared 10 miRNAs, 25 lncRNAs and 1 TF, which provides potential targets and pathways research diving into deeper mechanistic studies.

Although this study developed a new prediction model based on clinical and serological data, it faced several limitations. First, as a retrospective study, we defined PNR through chart review rather than prospectively collected disease activity indices. To ensure homogeneousness of the study, all CD patients were evaluated by the same physician group over the duration of IFX treatment. Second, IL-6 levels were detected in peripheral blood rather than mucosal tissue. As a result, findings represented the state of the peripheral immune system instead of the inflamed mucosa. Furthermore, external validation is required to confirm the validity of these results in clinical practice.

CONCLUSION

This study found IL-6 levels altered after IFX therapy and added IL-6 to enhance the predictive value of PNR to IFX therapy in CD bio-naïve patients. A novel prediction model was developed, including IL-6 levels combined with BMI, disease behavior and CRP levels. With this model, clinicians can estimate the risk of PNR to IFX therapy and select the optimal treatment for individual patients. Furthermore, this study also constructed a multi-factor regulation network of *IL-6* and its relative gene *OSM*, providing stronger direction for exploring the predictive and therapeutic targets of IFX treatment in CD. Further investigation is needed to determine the association between IL-6 from either peripheral or inflamed mucosal and anti-TNF treatment responses.

DATA AVAILABILITY STATEMENT

The raw data supporting the conclusions of this article will be made available by the authors, without undue reservation.

ETHICS STATEMENT

This study was approved by the IRB of Shanghai Jiaotong University School of Medicine, Renji Hospital Ethics Committee (KY2020-115).

AUTHOR CONTRIBUTIONS

YC and HL, collected the papers and analyzed data, analyzed the conclusions, drafted the manuscript; QF reviewed the data and conclusions; JS presented the idea of this paper, supported the funding, analyzed the conclusions, drafted and revised the manuscript.

FUNDING

Supported by grants from National Natural Science Foundation of China (Grant No. 81770545, and 81701746) and MDT Project of Clinical Research Innovation Foundation, Renji Hospital, School of Medicine, Shanghai Jiaotong University (Grant No. PYI-17-003).

SUPPLEMENTARY MATERIAL

The Supplementary Material for this article can be found online at: https://www.frontiersin.org/articles/10.3389/fphar.2021.654985/full#supplementary-material.

REFERENCES

Bar-Yoseph, H., Levhar, N., Selinger, L., Manor, U., Yavzori, M., Picard, O., et al. (2018). Early drug and anti-infliximab antibody levels for prediction of primary nonresponse to infliximab therapy. *Aliment. Pharmacol. Ther.* 47 (2), 212–218. doi:10.1111/apt.14410

Barber, G. E., Yajnik, V., Khalili, H., Giallourakis, C., Garber, J., Xavier, R., et al. (2016). Genetic markers predict primary non-response and durable response to anti-TNF biologic therapies in crohn's disease. *Am. J. Gastroenterol.* 111 (12), 1816–1822. doi:10.1038/ajg.2016.408

Beltrán, B., Iborra, M., Sáez-González, E., Marqués-Miñana, M. R., Moret, I., Cerrillo, E., et al. (2019). Fecal calprotectin pretreatment and induction infliximab levels for prediction of primary nonresponse to infliximab therapy in crohn's disease. *Dig. Dis.* 37 (2), 108–115. doi:10.1159/000492626

Bertani, L., Caviglia, G. P., Antonioli, L., Pellicano, R., Fagoonee, S., Astegiano, M., et al. (2020a). Serum interleukin-6 and -8 as predictors of response to vedolizumab in inflammatory bowel diseases. *J. Clin. Med.* 9 (5). doi:10.3390/jcm9051323

Bertani, L., Fornai, M., Fornili, M., Antonioli, L., Benvenuti, L., Tapete, G., et al. (2020b). Serum oncostatin M at baseline predicts mucosal healing in Crohn's disease patients treated with infliximab. *Aliment. Pharmacol. Ther.* 52 (2), 284–291. doi:10.1111/apt.15870

Billiet, T., Cleynen, I., Ballet, V., Claes, K., Princen, F., Singh, S., et al. (2017). Evolution of cytokines and inflammatory biomarkers during infliximab induction therapy and the impact of inflammatory burden on primary response in patients with Crohn's disease. *Scand. J. Gastroenterol.* 52 (10), 1086–1092. doi:10.1080/00365521.2017.1339825

Billiet, T., Papamichael, K., de Bruyn, M., Verstockt, B., Cleynen, I., Princen, F., et al. (2015). A matrix-based model predicts primary response to infliximab in crohn's disease. *Eccojc* 9 (12), 1120–1126. doi:10.1093/ecco-jcc/jjv156

Chen, M. L., and Sundrud, M. S. (2016). Cytokine networks and T-cell subsets in inflammatory bowel diseases. *Inflamm. Bowel Dis.* 22 (5), 1157–1167. doi:10.1097/mib.0000000000000714

Chin, C.-H., Chen, S.-H., Wu, H.-H., Ho, C.-W., Ko, M.-T., and Lin, C.-Y. (2014). cytoHubba: identifying hub objects and sub-networks from complex interactome. *BMC Syst. Biol.* 8 (Suppl. 4), S11. doi:10.1186/1752-0509-8-s4-s11

Danese, S., Vermeire, S., Hellstern, P., Panaccione, R., Rogler, G., Fraser, G., et al. (2019). Randomised trial and open-label extension study of an anti-interleukin-6 antibody in Crohn's disease (ANDANTE I and II). *Gut* 68 (1), 40–48. doi:10.1136/gutjnl-2017-314562

Ding, N. S., Hart, A., and De Cruz, P. (2016). Systematic review: predicting and optimising response to anti-TNF therapy in Crohn's disease - algorithm for practical management. *Aliment. Pharmacol. Ther.* 43 (1), 30–51. doi:10.1111/apt.13445

Engel, T., Ben-Horin, S., and Beer-Gabel, M. (2015). Autonomic dysfunction correlates with clinical and inflammatory activity in patients with crohn's disease. *Inflamm. Bowel Dis.* 21 (10), 2320–2326. doi:10.1097/MIB.0000000000000508

Farre, D., Roset, R., Huerta, M., Adsuara, J. E., Rosello, L., Alba, M. M., et al. (2003). Identification of patterns in biological sequences at the ALGGEN server: PROMO and MALGEN. *Nucleic Acids Res.* 31 (13), 3651–3653. doi:10.1093/nar/gkg605

Hanauer, S. B., Feagan, B. G., Lichtenstein, G. R., Mayer, L. F., Schreiber, S., Colombel, J. F., et al. (2002). Maintenance infliximab for Crohn's disease: the ACCENT I randomised trial. *The Lancet* 359 (9317), 1541–1549. doi:10.1016/s0140-6736(02)08512-4

Hermanns, H. M. (2015). Oncostatin M and interleukin-31: cytokines, receptors, signal transduction and physiology. *Cytokine Growth Factor. Rev.* 26 (5), 545–558. doi:10.1016/j.cytogfr.2015.07.006

Hunter, C. A., and Jones, S. A. (2015). IL-6 as a keystone cytokine in health and disease. *Nat. Immunol.* 16 (5), 448–457. doi:10.1038/ni.3153

Kerr, K. F., McClelland, R. L., Brown, E. R., and Lumley, T. (2011). Evaluating the incremental value of new biomarkers with integrated discrimination improvement. *Am. J. Epidemiol.* 174 (3), 364–374. doi:10.1093/aje/kwr086

Leal, R. F., Planell, N., Kajekar, R., Lozano, J. J., Ordás, I., Dotti, I., et al. (2015). Identification of inflammatory mediators in patients with Crohn's disease unresponsive to anti-TNFα therapy. *Gut* 64 (2), 233–242. doi:10.1136/gutjnl-2013-306518

Li, J.-H., Liu, S., Zhou, H., Qu, L.-H., and Yang, J.-H. (2014). starBase v2.0: decoding miRNA-ceRNA, miRNA-ncRNA and protein-RNA interaction networks from large-scale CLIP-Seq data. *Nucl. Acids Res.* 42, D92–D97. doi:10.1093/nar/gkt1248

Maaser, C., Sturm, A., Vavricka, S. R., Kucharzik, T., Fiorino, G., Annese, V., et al. (2019). ECCO-ESGAR Guideline for Diagnostic Assessment in IBD Part 1: initial diagnosis, monitoring of known IBD, detection of complications. *J. Crohn's colitis* 13 (2), 144–164K. doi:10.1093/ecco-jcc/jjy113

Matsuoka, K., Hamada, S., Shimizu, M., Nanki, K., Mizuno, S., Kiyohara, H., et al. (2018). Factors predicting the therapeutic response to infliximab during maintenance therapy in Japanese patients with Crohn's disease. *PloS one* 13 (10), e0204632. doi:10.1371/journal.pone.0204632

Maurel, M., Obacz, J., Avril, T., Ding, Y. P., Papadodima, O., Treton, X., et al. (2019). Control of anterior GRadient 2 (AGR2) dimerization links endoplasmic reticulum proteostasis to inflammation. *EMBO Mol. Med.* 11 (6). doi:10.15252/emmm.201810120

Ng, S. C., Tang, W., Ching, J. Y., Wong, M., Chow, C. M., Hui, A. J., et al. (2013). Incidence and phenotype of inflammatory bowel disease based on results from the Asia-pacific Crohn's and colitis epidemiology study. *Gastroenterology* 145 (1), 158–165. doi:10.1053/j.gastro.2013.04.007

Pavlidis, P., Gulati, S., Dubois, P., Chung-Faye, G., Sherwood, R., Bjarnason, I., et al. (2016). Early change in faecal calprotectin predicts primary non-response to anti-TNFα therapy in Crohn's disease. *Scand. J. Gastroenterol.* 51 (12), 1447–1452. doi:10.1080/00365521.2016.1205128

Pencina, M. J., D' Agostino, R. B., D' Agostino., Vasan, R. S., Jr., and Vasan, R. S. (2008). Evaluating the added predictive ability of a new marker: from area under the ROC curve to reclassification and beyond. *Statist. Med.* 27 (2), 157–172. discussion 207-12. doi:10.1002/sim.2929

Petta, I., Lievens, S., Libert, C., Tavernier, J., and De Bosscher, K. (2016). Modulation of protein-protein interactions for the development of novel therapeutics. *Mol. Ther.* 24 (4), 707–718. doi:10.1038/mt.2015.214

Ritchie, M. E., Phipson, B., Wu, D., Hu, Y., Law, C. W., Shi, W., et al. (2015). Limma powers differential expression analyses for RNA-sequencing and microarray studies. *Nucleic Acids Res.* 43 (7), e47. doi:10.1093/nar/gkv007

Roda, G., Jharap, B., Neeraj, N., and Colombel, J.-F. (2016). Loss of response to anti-TNFs: definition, epidemiology, and management. *Clin. translational Gastroenterol.* 7, e135. doi:10.1038/ctg.2015.63

Salvador-Martín, S., López-Cauce, B., Nuñez, O., Laserna-Mendieta, E. J., García, M. I., Lobato, E., et al. (2019). Genetic predictors of long-term response and trough levels of infliximab in crohn's disease. *Pharmacol. Res.* 149, 104478. doi:10.1016/j.phrs.2019.104478

Schmitt, H., Billmeier, U., Dieterich, W., Rath, T., Sonnewald, S., Reid, S., et al. (2019). Expansion of IL-23 receptor bearing TNFR2+ T cells is associated with molecular resistance to anti-TNF therapy in Crohn's disease. *Gut* 68 (5), 814–828. doi:10.1136/gutjnl-2017-315671

Singh, S., Fumery, M., Sandborn, W. J., and Murad, M. H. (2018). Systematic review and network meta-analysis: first- and second-line biologic therapies for moderate-severe Crohn's disease. *Aliment. Pharmacol. Ther.* 48 (4), 394–409. doi:10.1111/apt.14852

Smoot, M. E., Ono, K., Ruscheinski, J., Wang, P.-L., and Ideker, T. (2011). Cytoscape 2.8: new features for data integration and network visualization. *Bioinformatics* 27 (3), 431–432. doi:10.1093/bioinformatics/btq675

Soendergaard, C., Seidelin, J. B., Steenholdt, C., and Nielsen, O. H. (2018). Putative biomarkers of vedolizumab resistance and underlying inflammatory pathways involved in IBD. *BMJ open Gastroenterol.* 5 (1), e000208. doi:10.1136/bmjgast-2018-000208

Sprakes, M. B., Ford, A. C., Warren, L., Greer, D., and Hamlin, J. (2012). Efficacy, tolerability, and predictors of response to infliximab therapy for Crohn's disease: a large single centre experience. *J. Crohn's Colitis* 6 (2), 143–153. doi:10.1016/j.crohns.2011.07.011

Steyerberg, E. W., Vickers, A. J., Cook, N. R., Gerds, T., Gonen, M., Obuchowski, N., et al. (2010). Assessing the performance of prediction models. *Epidemiology (Cambridge, Mass)* 21 (1), 128–138. doi:10.1097/ede.0b013e3181c30fb2

Suzuki, Y., Matsui, T., Ito, H., Ashida, T., Nakamura, S., Motoya, S., et al. (2015). Circulating interleukin 6 and albumin, and infliximab levels are good predictors of recovering efficacy after dose escalation infliximab therapy in patients with loss of response to treatment for Crohn's disease. *Inflamm. Bowel Dis.* 21 (9), 2114–2122. doi:10.1097/mib.0000000000000475

Szklarczyk, D., Gable, A. L., Lyon, D., Junge, A., Wyder, S., Huerta-Cepas, J., et al. (2019). STRING v11: protein-protein association networks with increased coverage, supporting functional discovery in genome-wide experimental datasets. *Nucleic Acids Res.* 47 (D1), D607–D613. doi:10.1093/nar/gky1131

Thomas, H. (2017). Oncostatin M promotes inflammation in IBD. *Nat. Rev. Gastroenterol. Hepatol.* 14 (5), 261. doi:10.1038/nrgastro.2017.47

Torres, J., Bonovas, S., Doherty, G., Kucharzik, T., Gisbert, J. P., Raine, T., et al. (2020). ECCO guidelines on therapeutics in crohn's disease: medical treatment. *J. Crohn's colitis* 14 (1), 4–22. doi:10.1093/ecco-jcc/jjz180

West, N. R., Hegazy, A. N., Hegazy, A. N., Owens, B. M. J., Bullers, S. J., Linggi, B., et al. (2017). Oncostatin M drives intestinal inflammation and predicts response to tumor necrosis factor-neutralizing therapy in patients with inflammatory bowel disease. *Nat. Med.* 23 (5), 579–589. doi:10.1038/nm.4307

Wong, U., and Cross, R. K. (2017). Primary and secondary nonresponse to infliximab: mechanisms and countermeasures. *Expert Opin. Drug Metab. Toxicol.* 13 (10), 1039–1046. doi:10.1080/17425255.2017.1377180

Yokoyama, K., Yamazaki, K., Katafuchi, M., and Ferchichi, S. (2016). A retrospective claims database study on drug utilization in Japanese patients with crohn's disease treated with adalimumab or infliximab. *Adv. Ther.* 33 (11), 1947–1963. doi:10.1007/s12325-016-0406-6

Yu, G., Wang, L.-G., Han, Y., and He, Q.-Y. (2012). clusterProfiler: an R package for comparing biological themes among gene clusters. *OMICS: A J. Integr. Biol.* 16 (5), 284–287. doi:10.1089/omi.2011.0118

Conflict of Interest: The authors declare that the research was conducted in the absence of any commercial or financial relationships that could be construed as a potential conflict of interest.

Copyright © 2021 Chen, Li, Feng and Shen. This is an open-access article distributed under the terms of the Creative Commons Attribution License (CC BY). The use, distribution or reproduction in other forums is permitted, provided the original author(s) and the copyright owner(s) are credited and that the original publication in this journal is cited, in accordance with accepted academic practice. No use, distribution or reproduction is permitted which does not comply with these terms.

frontiers in Pharmacology

REVIEW
published: 14 April 2021
doi: 10.3389/fphar.2021.651415

Novel and Emerging Therapies for Inflammatory Bowel Disease

Badr Al-Bawardy[1]*, *Raina Shivashankar*[2] and *Deborah D. Proctor*[1]

[1]Section of Digestive Diseases, Yale School of Medicine, New Haven, CT, United States, [2]Division of Gastroenterology and Hepatology, Thomas Jefferson University, Philadelphia, PA, United States

Inflammatory bowel diseases (IBD) such as ulcerative colitis and Crohn's disease are chronic, relapsing and remitting disorders of intestinal inflammation with potential systemic manifestations. Despite the availability of current biologics, such as anti-tumor necrosis factor (anti-TNF), anti-integrins, anti-interleukins and small molecules such as tofacitinib, the rates of primary and secondary treatment failure remain high in IBD. This highlights the importance of continued development of new therapeutic targets and modifications of existing ones to improve the treatment response rates and to also improve the safety profile and tolerability of these medications. In this review we will discuss novel treatment target agents including selective janus kinase (JAK) inhibitors, anti-interleukin (IL) (IL-12/IL-23), leukocyte trafficking/migrating inhibitors (such as sphingosine-1-phosphate receptor modulator) and other small molecules currently in development.

Keywords: inflammatory bowel disease, small molecule, biologic, novel therapy, emerging therapy

OPEN ACCESS

Edited by:
Dario Sorrentino,
Virginia Tech Carilion, United States

Reviewed by:
Marco Marino,
Azienda Sanitaria Universitaria Friuli Centrale (ASU FC), Italy
Vu Nguyen,
Virginia Tech Carilion, United States

***Correspondence:**
Badr Al-Bawardy
badr.albawardy@yale.edu

Specialty section:
This article was submitted to Gastrointestinal and Hepatic Pharmacology, a section of the journal Frontiers in Pharmacology

Received: *09 January 2021*
Accepted: *01 March 2021*
Published: *14 April 2021*

Citation:
Al-Bawardy B, Shivashankar R and Proctor DD (2021) Novel and Emerging Therapies for Inflammatory Bowel Disease. Front. Pharmacol. 12:651415. doi: 10.3389/fphar.2021.651415

INTRODUCTION

Inflammatory bowel disease (IBD) is a chronic, progressive disease that can lead to complications including bowel damage, need for hospitalizations and surgery, decreased quality of life, and disability. The incidence rates of IBD have been increasing world-wide. While the highest rates have been noted in North America and Europe, increasing incidence rates have been observed in previously low-incidence regions such as Asia as these countries become more developed (Loftus Jr, 2004; Molodecky et al., 2012; Shivashankar and Lewis, 2017a). The cause for this phenomenon is largely unknown, however it may be related to the complex interplay between genetics and the environment (Shivashankar and Lewis, 2017a). The latter has been implicated in the development of IBD because of the observation that higher incidence rates are seen in industrialized nations; therefore diet, pollution, microbial exposure, and sanitation may be involved (Molodecky and Kaplan, 2010; Shivashankar and Lewis, 2017a).

Since IBD can be a chronic and progressive disease, optimal treatment early in the disease course to prevent complications is paramount. The current treatment paradigm for moderate-severe Crohn's disease (CD) and ulcerative colitis (UC) is to use biologic therapy early to achieve clinical remission and mucosal healing, which will ultimately decrease the risk of corticosteroid use, surgeries, hospitalizations and increase quality of life (Klenske et al., 2019).

The currently available biologic agents include anti-tumor necrosis factor-alpha (TNF-α) agents (infliximab, adalimumab, certolizumab, and golimumab); anti-integrin agents (vedolizumab,

Abbreviations: AE, adverse event; CD, crohn's disease; CRP, C-reactive protein; FDA, food and drug administration; IBD, inflammatory bowel disease; IL, interleukin; IFN, interferon; IV, intravenous; JAK, janus kinase; NF-κB, nuclear transcription factor kappaB; PRO, patient reported outcome; S1P, sphingosine 1-phosphate; SC, subcutaneous; TNF-α, tumor necrosis factor alpha; TYK, tyrosine kinase; UC, ulcerative colitis.

TABLE 1 | Target, mode of delivery and development phase of emerging therapeutic agents in IBD.

Drug class	Agent	Target	Mode of delivery	Crohn's disease	Ulcerative colitis
JAK inhibitors	Tofacitinib	JAK1/JAK3	Oral	N/A	FDA approved
	Filgotinib	JAK1	Oral	Phase III recruiting	Phase IIb/III completed
	Upadacitinib	JAK1	Oral	Phase III recruiting	Phase III recruiting
	TD-1473	Pan-JAK (gut selective)	Oral	Phase II recruiting	Phase IIb/III recruiting
	Brepocitinib (PF-06700841)	TYK2/JAK1	Oral	Phase IIa recruiting	Phase IIb recruiting
	PF-06651600	JAK3	Oral		
	BMS-986165	TYK2	Oral	Phase II recruiting	Phase II recruiting
Anti-trafficking therapies	Vedolizumab SC	α4β7 integrin	SC	N/A	Phase III completed
	Etrolizumab	α4β7 and αEβ7 integrins	SC	Phase III recruiting	Phase III completed
	AJM300	α4 integrin	Oral	N/A	Phase III recruiting
	PF-00547659	MAdCAM	SC	Phase II completed	Phase II completed
IL-23 inhibitors	Risankizumab	IL23/p19 subunit	IV, SC	Phase III active, not recruiting	Phase III enrolling by invitation
	Brazikumab	IL23/p19 subunit	IV, SC	Phase IIb/III recruiting	Phase 2/OLE enrolling by invitation
	Mirikizumab	IL23/p19 subunit	IV, SC	Phase III recruiting	Phase III recruiting
	Guselkumab	IL23/p19 subunit	IV, SC	Phase II/III recruiting	Phase II/III recruiting
S1P receptor modulators	Ozanimod	S1PR1 and S1PR5	Oral	Phase III recruiting	Phase III completed
	Etrasimod	S1PR1, S1PR4 and S1PR5	Oral	Phase II/III recruiting	Phase III recruiting
	Amiselimod (MT-1303)	S1PR1	Oral	Phase II completed	N/A
PDE4 inhibitors	Apremilast	PDE4	Oral	N/A	Phase II completed
TLR9 agonist	Cobitolimod	TLR9	Topical (enema)	N/A	Phase IIb completed, Phase III planned

JAK, janus kinase; TYK 2, tyrosine kinase 2; S1P, sphingosine 1 phosphate; S1PR sphingosine 1 phosphate receptor; PDE4, phosphodiesterase 4; TLR9, toll-like receptor 9; α4β7, alpha4-beta7; αEβ7, alphaE-beta7; α4, alpha4; MAdCAM, mucosal addressin cell adhesion molecule-1; IL-23, interleukin 23; IV, intravenous; SC, subcutaneous; OLE, open label extension.

natalizumab); and an anti-interleukin (IL) 12-23 agent (ustekinumab). Finally, tofacitinib, a non-biologic small molecule is approved for the treatment of moderate-severe UC. The choice between these agents depends on IBD phenotype and behavior, previous biologic exposure and response, potential adverse effects of therapy, patient co-morbidities, and shared-decision making with patients.

Despite the number of available medications, there are appreciable rates of primary non-response, loss of response, or adverse reactions thereby necessitating additional treatment options. Therefore, the purpose of this review article is to describe novel and emerging therapies for IBD. In this review we will discuss novel treatment target agents including selective janus kinase (JAK) inhibitors, anti-interleukin (IL) (IL-12/IL-23), leukocyte trafficking/migrating inhibitors (such as sphingosine-1-phosphate receptor modulator) and other small molecules currently in development (**Table 1**). This review will focus on the pipeline of these new therapeutic agents and will not include other novel and emerging therapeutic modalities such as stem cell therapy or microbiome targeted therapies.

JAK Inhibitors

Cytokine mediators of inflammation in IBD such as IL-9, IL-12, IL-23 and interferon-gamma (IFN-γ) are reliant on the Janus Kinase Signal Transducer and Activator of Transcription (JAK-STAT) pathway signaling (Salas et al., 2020). In addition, genome wide association studies have demonstrated risk loci in the JAK region in IBD (Barrett et al., 2008; Anderson et al., 2011). Therefore, targeting the JAK-STAT is an appealing therapeutic modality in IBD. JAK1, JAK2, JAK3 and tyrosine kinase 2 (TYK2) are all part of the JAK family of tyrosine kinase proteins.

Tofacitinib

Tofacitinib, a non-selective JAK inhibitor, was approved by the US food and drug administration (FDA) in May 2018 for the treatment of UC. The pivotal induction and maintenance clinical trials, OCTAVE 1-3, have demonstrated efficacy of tofacitinib in inducing and maintaining clinical and endoscopic remission in UC (Sandborn et al., 2017b). Notably, tofacitinib was also shown to be effective in the more refractory anti-TNF-α exposed UC patients compared to placebo. On the other hand, a phase IIb randomized clinical trial of tofacitinib in CD failed to meet the primary endpoints (Panés et al., 2017). Multiple factors might have contributed to the negative results of the study including: study design and high placebo response rate. Subsequently, a systematic review and meta-analysis of clinical trials of different JAK inhibitors (tofacitnib, filgotinib, pefecitinib, upadacitinib, TD-1473) in CD demonstrated the effectiveness of JAK inhibitors in inducing clinical remission (Ma et al., 2019).

Tofacitinib provided the advantage being an oral agent compared to current intravenous (IV) or subcutaneous (SC) biologic agent formulations. The rapid onset of action of tofacitinib is a positive feature as improvement in symptoms of rectal bleeding and stool frequency can occur within 3 days of starting treatment in UC patients according to post-hoc analysis of the pivotal trials (Hanauer et al., 2019). Conversely, tofacitinib

has been associated with increased risk of herpes zoster infection and hyperlipidemia (Winthrop et al., 2018). In addition, tofacitinib has a black box warning for venous thromboembolism and mortality after risk was noted in a subset of patients with rheumatoid arthritis taking the 10 mg p.o. BID dose (FDA Drug Safety Communication, 2019). Therefore, there has been an increased interest in the development of more selective JAK inhibitors to enhance the effectiveness and the safety profile in IBD.

Filgotinib

Filgotinib is a once daily oral small molecule with higher selectivity for JAK 1 inhibition. JAK 1 (in addition to JAK 3) have been shown to be expressed on both B cells and T cells within the healthy colon mucosa (Salas et al., 2020). The efficacy of filgotinib in CD was evaluated in a phase II, double-blinded, placebo controlled randomized clinical trial, FITZROY. In this trial, patients were randomized to filgotinib 200 mg once a day or placebo and after 10 weeks based on response, patients received either once daily filgotinib 200 mg, filgotinib 100 mg or placebo for another 10 weeks (Vermeire et al., 2017b). A significantly higher proportion of patients in the filgotinib groups achieved the primary endpoint of clinical remission [defined as Crohn's disease activity index (CDAI) < 150] at week 10 compared to placebo (47 vs. 23%; $p = 0.0077$) (Vermeire et al., 2017b). In anti-TNF-α naïve patients, the rate of clinical remission at week 10 was 60% (n = 34) compared to 37% (n = 26) in anti-TNF-α experienced patients. The rate of endoscopic response and mucosal healing in the overall filgotinib group was numerically higher but did not reach statistical significance. However, endoscopic assessment in this trial was limited by short follow up time. In terms of safety, up to 20 weeks follow up, serious infections were noted in 3% in the filgotinib group with none reported in the placebo group.

A phase IIB/III study (SELECTION) evaluating filgotinib for induction and maintenance therapy for moderate to severe UC was recently completed (Feagan et al., 2020b). The induction study included a cohort of biologic exposed and another cohort of biologic naïve patients (Feagan et al., 2020b; Peyrin-Biroulet et al., 2020). In each cohort patients were randomized to either filgotinib 100 mg, filgotinib 200 mg or placebo daily. The composite primary endpoint of endoscopic, rectal bleeding and stool frequency (EBS) remission (defined as Mayo endoscopic subscore ≤1, rectal bleeding subscore of 0, stool frequency subscore decrease of 1 or more points from baseline and ≤1) rates were significantly higher in the 200 mg filgotinib groups (26.1% in the biologic naïve cohort and 11.5% in the biologic experienced cohort) compared to the placebo groups. One case of pulmonary embolism in the filgotinib 200 mg group was noted and four total cases of herpes zoster in filgotinib groups were noted (1 in the 100 mg group and three in the 200 mg group) (Feagan et al., 2020b).

Patients who achieved clinical remission or response after 10 weeks of induction therapy with either filgotinib or placebo were included in the maintenance study (Peyrin-Biroulet et al., 2020). In this study 664 patients with moderate to severe UC who received placebo induction remained in the placebo maintenance arm, while patients randomized to the filgotinib induction were re-randomized to filgotinib induction dose maintenance arm or placebo arm (Peyrin-Biroulet et al., 2020). The composite primary endpoint of EBS remission at week 58 was achieved in 37.2% in the filgotinib 200 mg group vs. 11.2% in the placebo arm ($p < 0.025$) and 23.8% in the filgotinib 100 mg group vs. 13.5% in the placebo arm ($p < 0.05$) (Peyrin-Biroulet et al., 2020). Overall, filgotinib was well tolerated. Two cases of venous thromboembolism were reported in the placebo arm but none in the filgotinib group. Herpes zoster was reported in two patients in the filgotinib arms (one in each of the filgotinib groups) but none in the placebo groups (Peyrin-Biroulet et al., 2020).

A phase III clinical trial of filgotinib in CD is currently in progress (NCT02914561; NCT02914600). In addition, a phase II study evaluating filgotinib in perianal fistulizing CD is ongoing (NCT03077412).

Upadacitinib

Upadacitinib is an oral JAK inhibitor that has high selectivity for JAK 1 inhibition. It is currently approved for the treatment of rheumatoid arthritis with moderate to severe activity who have either failed or are intolerant to methotrexate. In a phase II clinical trial (CELEST), patients with moderate to severe CD (n = 220) who failed immunosuppressants or biologics were assigned to either placebo or upadacitinib at the following doses: 3 mg twice a day (BID), 6 mg BID, 12 mg BID, 24 mg BID for 16-weeks induction (Sandborn et al., 2020c). Post-induction, patients were re-randomized to upadacitinib at the following doses: 3 mg BID, 12 mg BID, 24 mg once daily (QD) for 36 weeks (maintenance). Although clinical remission at week 16 was not significantly different between the treatment groups and placebo, endoscopic remission at week 12/16 was significantly higher in the upadacitinib groups compared to placebo (Sandborn et al., 2020c). Higher doses of upadacitinib were associated with higher rates of endoscopic remission in this trial.

In the phase II UC-ACHIEVE trial, moderate to severe UC patients (n = 250) who failed or were intolerant to immunosuppressive or biologic therapy were assigned to placebo or upadacitinib at the following once daily doses: 7.5, 15, 30, 45 mg (Sandborn et al., 2020e). Clinical remission was significantly higher in the 15 mg (14.3%; $p = 0.013$), 30 mg (13.5%; $p = 0.011$), and the 45 mg groups (19.6%; $p = 0.002$) compared to 0% in the placebo group. Similarly, endoscopic improvement at week 8 (Mayo endoscopic subscore ≤1) was significantly higher in a dose dependent manner in the upadacitinib groups compared to placebo (Sandborn et al., 2020e).

In terms of safety, there were a total of three cases of herpes zoster in the upadacitinib group compared to none in the placebo group in the CELEST trial and 1 case in the upadacitinib group compared to none in the placebo group in the UC-ACHIEVE trial (Sandborn et al., 2020c; Sandborn et al., 2020e). Once case of thromboembolism occurred in a patient on the 45 mg upadacitinib dose in the UC-ACHIEVE trial.

Currently, upadacitinib is in phase III clinical trials for CD (NCT03345836, NCT03345823) and UC (NCT03653026, NCT03006068, NCT02819635).

TD-1473

TD-1473 is an oral pan-JAK inhibitor that is designed to be gut specific to limit systemic toxicity of pan-JAK inhibition. In a phase 1b trial, patients with moderate to severe UC (n = 40) were assigned to placebo or one of the following once daily TD-1473 doses: 20 mg, 80 mg or 270 mg) for 28 days (Sandborn et al., 2020f). Only five of the 40 patients were exposed to anti-TNF therapies in the past. Clinical response rate was 20% in the 20 and 80 mg groups compared to 55% in the 270 mg group while the clinical response rate was 11% in the placebo group (no statistical analyses performed as study not powered for outcomes) (Sandborn et al., 2020f). There were also trends in endoscopic improvement along with reduction in fecal calprotectin and c-reactive protein (CRP) levels with TD-1473. Overall adverse event rates were similar in the placebo group at 44.4 and 38.7% in the TD-1473 groups. Phase IIb/III studies of TD-1473 for moderate to severe UC are currently recruiting (NCT03758443, NCT03920254). In addition, a phase II study of TD-1473 in moderate to severe CD in underway (NCT03635112).

TYK2 Inhibitors

TYK2 is one of the JAK-STAT family proteins. It is involved in intracellular cytokine signaling. Brepocitinib (PF-06700841) is an oral TYK2/JAK1 inhibitor that has been shown to be well tolerated and effective in phase I and phase IIa studies of patients with plaque psoriasis (Banfield et al., 2018; Forman et al., 2020). PF-06651600 is an oral selective JAK3 inhibitor. Phase IIa/IIb trials of combination brepocitinib (PF-06700841) and PF-06651600 are currently recruiting for moderate to severe CD (NCT03395184) and UC (NCT02958865).

BMS-986165 is an oral selective TYK2 inhibitor. Phase II trials of BMS-986165 in CD (NCT03599622) and UC (NCT03934216) are currently recruiting.

IL-12/IL-23 Inhibitors

IL-23 is a regulator of T-helper (Th)-17 cell and type 3 innate lymphoid cell (ILC3) pathways that lead to inflammatory cytokine production and inflammation and polymorphisms of the IL-23 receptor gene may be associated with increased susceptibility to CD (Feagan et al., 2017). IL-23 prevents regulatory T-cell response in the intestine, and therefore increases inflammation in this gut (Feagan et al., 2017; Sands et al., 2017). Ustekinumab, which inhibits both IL-12 and the IL-23 p40 subunit, has been shown to be effective for induction and maintenance of remission in patients with moderate-severe CD and UC (Feagan et al., 2016; Sands et al., 2019a).

However, it is unclear if the effect of ustekinumab is mainly driven by its inhibition of IL-12, IL-23 or both (Deepak and Sandborn, 2017). Selective inhibition of the IL-23 pathway, which leaves the IL-12 pathway intact, carries the potential advantage of less severe infection and decreased malignancy risk (Deepak and Sandborn, 2017; Baker and Isaacs, 2018). A potential benefit of only blocking the p19 subunit of IL-23 is possible increased safety since the IL-12 mediated Th1 response, which is required in the immune response to intracellular pathogens, is left intact (Deepak and Sandborn, 2017).

Risankizumab

Risankizumab is a humanized monoclonal antibody against the p19 subunit of IL-23. The induction dosing is provided intravenously (IV) while the maintenance dosing is a subcutaneous (SC) injection. A phase II trial of induction therapy with risankizumab was conducted in patients with moderate-severe CD; 93% of patients were previously exposed to at least one anti-TNF agent (Deepak and Sandborn, 2017; Feagan et al., 2017). Risankizumab (200 mg or 600 mg IV) was compared to placebo at weeks 0, 4, and 8. The primary outcome was clinical remission (defined as a CDAI <150) at week 12 (Feagan et al., 2017).

At week 12, those treated with risankizumab had significantly higher rates of clinical remission vs. placebo (30.5 vs. 15.4%, p = 0.0489), clinical response (39 vs. 20.5%, 0 = 0.0273), endoscopic remission (17 vs. 3%, p = 0.0015), and deep remission (7 vs. 0, p = 0.0107) (Feagan et al., 2017). There was no difference in the proportion of mucosal healing between those treated with risankizumab (200 mg: 2%, 600 mg 7%) vs. placebo (3%) (200 mg v. placebo, p = 0.97 and 600 mg v. placebo, p = 0.31) (Feagan et al., 2017). Rates of adverse events (AEs) were similar between those treated with placebo and risankizumab. The most common AE was worsening of underlying CD (Feagan et al., 2017). Other AEs included nausea, abdominal pain, arthralgia, and headache (Feagan et al., 2017). There were no dose-related increases in AE in those treated with risankizumab (Feagan et al., 2017).

An open-label extension (OLE) study was completed to study the efficacy and safety of extended IV induction and SC maintenance therapy (Feagan et al., 2018). Those who did not achieve deep remission in the 12-weeks induction phase of the previously described phase II induction study received open-label IV risankizumab 600 mg every 4 weeks for 12 weeks; patients who were in clinical remission at week 26 were included in the maintenance phase and received open-label SC risankizumab 180 mg every 8 weeks for 26 weeks (Feagan et al., 2018). The following definitions were used: clinical remission (CDAI <150), endoscopic response (>50% Crohn's disease Endoscopic Index of Severity [CDEIS] reduction from baseline), endoscopic remission (CDEIS ≤4, or ≤2 for patients with isolated ileitis) (Feagan et al., 2018). One-hundred and one patients received the extended induction dose, and 53% (54/101 patients) were in clinical remission at week 26 (Feagan et al., 2018). Sixty-two patients received risankizumab maintenance therapy, and at week 52 clinical remission was maintained in 71% (44/62 patients), 81% (50/62) had clinical response, 35% (22/62) were in endoscopic remission, 24% (15/62) had mucosal healing, and 29% (18/62) achieved deep remission (Feagan et al., 2018). There were no new safety signals noted and the most frequent AEs included arthralgia, headache, abdominal pain, nasopharyngitis, nausea, and pyrexia (Feagan et al., 2018).

The long-term safety of risankizumab was studied in the phase 2 OLE study and no new safety signals were noted; 92% of patients reported AEs and 35% of patients experienced serious adverse events (Ferrante et al., 2020). The most common AEs included nasopharygnitis (31%), gastroenteritis (23%), and

fatigue (20%) (Ferrante et al., 2020). Nine percent of patients had serious infections while 5% of patients reported opportunistic infections. There were no malignancies or deaths (Ferrante et al., 2020).

Overall, risankizumab was well-tolerated and found to be effective compared to placebo in inducing clinical remission, response, and endoscopic remission at week 12. Currently, we are awaiting results from phase III clinical trials (NCT03105128; estimated study completion date February 2021). In addition, a phase II/III clinical trial of risankizumab in ulcerative colitis is currently recruiting (NCT03398148).

Brazikumab (MEDI 2070)

Brazikumab, a human immunoglobulin G2 monoclonal antibody, selectively binds the p19 subunit of IL-23 (Sands et al., 2017). Like risankizumab, the induction dose is an IV infusion while the maintenance dose is a SC injection. A phase IIa trial included 119 patients with moderate-severe CD who either failed or were intolerant to anti-TNF agents; 31% of patients were exposed to at least one anti-TNF. Patients were given either brazikumab 700 mg IV or placebo at weeks 0 and 4, and then received open label brazikumab 210 mg subcutaneously every 4 weeks from weeks 12 to 112 (Sands et al., 2017). The primary outcome was clinical response (CDAI decrease of 100 points from baseline or clinical remission [CDAI <150]) at week 8 (Sands et al., 2017). Compared to placebo, a higher proportion of patients treated with brazikumab achieved clinical response at week 8 (49.2% v. 26.7%, $p = 0.01$) as well as a composite outcome of clinical response and 50% reduction from baseline in either fecal calprotectin or CRP concentration (42.4% v. 10%, $p < 0.001$) (Sands et al., 2017). There was no difference in clinical remission at week eight between those treated with brazikumab vs. placebo (27.1 vs. 15%, $p = 0.10$) (Sands et al., 2017). A similar proportion of patients who received placebo and active treatment during the initial double-blind period achieved clinical response, clinical remission, the composite outcome of clinical response and at least 50% reduction from baseline in either fecal calprotectin or CRP concentration at week 24 (57.7 vs. 53.8%, 40.4 vs. 42.3%, and 48.1 vs. 46.2%, respectively) (Sands et al., 2017). Patients with higher baseline serum concentration of IL-22 were found to be more likely to responds to brazikumab than to placebo (Sands et al., 2017; Sabino et al., 2019).

There was no difference in proportions of patients with treatment-emergent AEs or serious AEs between placebo and brazikumab treated groups (Sands et al., 2017). Equal numbers of clinically significant infections occurred in patients receiving brazikumab in both study periods and in patients receiving placebo in the double-blind period (Sands et al., 2017). The most common AEs included headache, nasopharyngitis, and abdominal pain (Sands et al., 2017).

In summary, two infusions of brazikumab at weeks 0 and 4 achieved a higher rate of clinical response at week 8 compared to placebo and continued SC dosing every 4 weeks led to ongoing clinical response and remission at week 24 (Sands et al., 2017). Brazikumab was generally well-tolerated in this study with follow-up to 24 weeks (Sands et al., 2017). Of note, there was no endoscopic evaluation or imaging as part of this phase 2a study (Sands et al., 2017). Currently, brazikumab is in a phase IIb/III trial in patients with CD (NCT03759288; anticipated completion date Dec 2022) and is in a phase II/open label extension in UC patients (NCT03616821; anticipated completion date april 2023).

Mirikizumab

Mirikizumab is an IV and SC immunoglobulin G4-variant monoclonal antibody, and it binds to the p19 subunit of IL23 (Sandborn et al., 2020d). A phase II study of 249 patients with moderate-severe UC was conducted to assess the efficacy and safety of mirikizumab; 63% of patients were previously exposed to a biologic (Sandborn et al., 2020d). Patients were randomized to either IV placebo, mirikizumab 50 mg, or 200 mg, or mirikizumab 600 mg at weeks 0, 4, and 8 (Sandborn et al., 2020d). Those with clinical response to mirikizumab at week 12 were then randomized to maintenance mirikizumab 200 mg every 4 weeks or every 12 weeks (Sandborn et al., 2020d). The primary endpoint was clinical remission (Mayo rectal bleeding subscore 0, with 1-point decrease from baseline for stool frequency, and 0 or one for endoscopy) (Sandborn et al., 2020d). Clinical remission at week 12 is as follows: 15.9% (95% CI, 6.8–24.9; $p = 0.66$) in the mirikizumab 50 mg group; 22.6% (12.2–33.0; $p = 0.004$) in the mirikizumab 200 mg group; and 11.5% (3.5–19.5, $p = 0.142$) in the 600 mg group vs. 4.8% (0–10) in the placebo groups (Sandborn et al., 2020d). Endoscopic improvement at week 12 was seen in 23.8% (13.3–34.3, $p = 0.12$) of the mirikizumab 50 mg group; 30.6% (23.3–34.3; $p = 0.0007$) in the 200 mg group, and 13.1% (4.6–21.6; $p = 0.215$) in the 600 mg group vs. 6.3% (0.3–12.4) in the placebo treated groups (Sandborn et al., 2020d).

Following the 12 weeks induction period, 93 mirikizumab treated patients achieved clinical response and were randomized to SC mirikizumab at 200 mg every 4 weeks or every 12 weeks (Sandborn et al., 2020d). At week 52, 53.7 and 39.7% of patients treated every 4 weeks and every 12 weeks, achieved clinical remission, respectively (Sandborn et al., 2020d). These rates were similar in those who were both biologic-exposed and biologic-naïve (Sandborn et al., 2020d). Endoscopic remission (Mayo endoscopic subscore = 0) at week 52 were 14.8% (every 4 weeks) and 28.3% (every 12 weeks) (Sandborn et al., 2020d). Durable clinical remission (clinical remission at both weeks 12 and 52) was 61.1% in the every 4 weeks maintenance dose and 38.5% in the every 12 weeks group (Sandborn et al., 2020d).

The most frequent AEs included nasopharyngitis, worsening of UC, headache, anemia, cough, nausea; no dose related increases in AEs were reported (Sandborn et al., 2020d).

An open label extension of this phase II study looked at the outcome of patients treated with mirikizumab who did not respond clinically in the initial induction period (Sandborn et al., 2020a). These patients were randomized to either 600 mg IV mirikizumab or 1,000 mg IV mirikizumab every 4 weeks (Sandborn et al., 2020a). At week 24, those who had a clinical response continued the maintenance period of 200 mg SC mirikizumab (Sandborn et al., 2020a). Endpoints included clinical remission (Mayo rectal bleeding = 0, 0 or 1 with a 1 point decrease from baseline), clinical response, endoscopic remission (Mayo endoscopic subscore = 0), or endoscopic

improvement (endoscopic subscore of 0 or 1) at weeks 24 or 52 (Sandborn et al., 2020a). In the 12 weeks extension of the mirikizumab 600 mg dose and 1,000 mg mirikizumab dose, 50 and 43.8%, respectively, achieved clinical response and 15 and 9.4%, respectively, achieved clinical remission (Sandborn et al., 2020a). Endoscopic improvement was seen in 20% of patients in the 600 mg group and 15.6% of patients in the 1,000 mg group (Sandborn et al., 2020a). In those who had clinical response at week 24 and continued to maintenance therapy, 65.8% remained in clinical response, 26.3% had clinical remission, and 34.2% had endoscopic improvement at week 52 (Sandborn et al., 2020a). No new AEs identified.

In summary, the phase II dose ranging study of mirikizumab showed a trend toward inducing clinical remission and response around week 12 in patients with moderate-severe UC (Sandborn et al., 2020d). In those who did not initially respond to induction dosing, extended IV dosing of mirikizumab for 12 additional weeks showed a clinical response in about 50% of patients (Sandborn et al., 2020a).

Given its efficacy in patients with UC, mirikizumab was studied for its safety and efficacy in patients with CD in a phase II study (Sands et al., 2019b). Patients were randomized to mirkizumab 200 mg, 600 mg, 1,000 mg and placebo and this was administered at weeks 0, 4, and 8 (Sands et al., 2019b). The primary endpoint was endoscopic response (50% reduction from baseline in SES-CD) at week 12 (Sands et al., 2019b). Endoscopic response rates were higher in the mirkizumab groups compared to placebo at week 12 [200 mg: 25.8% (95% CI: 10.4–41.2), p = 0.079; 600 mg: 37.5% (20.7–54.3), p = 0.003; 1,000 mg: 43.8 (31.6–55.9), p < 0.001; placebo: 10.9 (3.3–18.6)] (Sands et al., 2019b). Additionally, patient reported outcome remission rates and CDAI response rates were greater in the 600 and 1000 mg mirikizumab group compared to placebo (Sands et al., 2019b). The frequencies of serious AEs and treatment-emergent AEs were similar between placebo and treatment groups (Sands et al., 2019b).

Mirikizumab was also evaluated for long-term efficacy and safety over 52 weeks in the phase II maintenance SERENITY study (Sands et al., 2020). Patients who achieved ≥1 point improvement in SES-CD at week 12 on mirikizumab were then re-randomized to maintenance mirikizumab IV or SC every 4 weeks (Sands et al., 2020). The primary endpoints were CDAI remission (<150 points), patient reported outcome (PRO) remission (stool frequency ≤2.5 and abdominal pain ≤1 and not worse than baseline), endoscopic response (50% reduction from baseline in SES-CD), and endoscopic remission (SES-CD score <4 for ileal-colonic disease or <2 for isolated ileal disease, and no subscore >1) (Sands et al., 2020). Endoscopic response rates were 58.5 and 58.7%; PRO remission rates were 46.3 and 45.7% in the IV and SC groups, respectively (Sands et al., 2020). In those who achieved endoscopic response at week 12, 69.6 and 66.7% had an endoscopic response at week 52 in the IV and SC groups, respectively (Sands et al., 2020). Also, in those who had endoscopic remission at week 12, 50 and 64.3% maintained endoscopic remission at week 52, respectively, in the IV and SC groups (Sands et al., 2020). There were similar treatment-emergent AEs and serious AEs in both the IV and SC groups (Sands et al., 2020).

Treatment with mirikizumab did have a dose-dependent improvement in endoscopic response and remission as well as patient-reported response and remission at week 12 in patients with CD (Authors, 2019) (A SPECIAL MEETING REVIEW EDITION: Highlights in Inflammatory Bowel Disease From the 14th Congress of ECCO: A Review of Selected Presentations From the 14th Congress of the European Crohn's and Colitis Organization (ECCO) * March 6–9, 2019 * Copenhagen, DenmarkSpecial Reporting on:* VARSITY: A Double-Blind, Double-Dummy, Randomized Controlled Trial of Vedolizumab vs. Adalimumab in Patients With Active Ulcerative Colitis* Analyses of Data From the VISIBLE 1 and 2 Trials: Vedolizumab in Patients With Ulcerative Colitis or Crohn's Disease* Improved Endoscopic Outcomes and Mucosal Healing of Upadacitinib as an Induction Therapy in Adults With Moderately to Severely Active Ulcerative Colitis: Data From the U-ACHIEVE Study* Long-Term Safety of Vedolizumab in Ulcerative Colitis and Crohn's Disease: Final Results From the GEMINI LTS Study* Pediatric Crohn's Disease Adalimumab Level-Based Optimization Treatment (PAILOT) Randomized Controlled Trial* Maintenance Treatment With Mirikizumab, a P19-Directed IL-23 Antibody: 52-Week Results in Patients With Moderately to Severely Active Ulcerative Colitis* Real-World Effectiveness and Safety of Vedolizumab and Anti-TNF Therapy in Biologic-Naive Patients With Ulcerative Colitis or Crohn's disease: Results From the EVOLVE Study* A Randomized, Multicenter, Double-Blind, Placebo-Controlled Study of a Targeted-Release Oral Cyclosporine Formulation in the Treatment of Mild to Moderate Ulcerative Colitis: Efficacy Results* Real-World Analyses of Patients With IBD Treated With VedolizumabPLUS Meeting Abstract Summaries With Expert Commentary by: Edward V. Loftus Jr, MD Professor of Medicine Division of Gastroenterology and Hepatology Mayo Clinic Rochester, Minnesota, 2019). Mirikizumab also had been shown to have sustained efficacy to week 52 (Sands et al., 2020). Mirkizumab for CD is currently being studied in a phase III trial (NCT03926130). Phase III Induction, maintenance and open label extension studies are currently recruiting for UC (NCT03518086, NCT03524092, NCT03519945).

Guselkumab

Guselkumab is an IV and SC anti-IL23 that is currently approved for the treatment of moderate-severe plaque psoriasis (Sandborn et al., 2020i). GALAXI 1 is a phase II study that evaluated the efficacy and safety of guselkumab in patients with moderate-severe CD who either had intolerance or inadequate response to corticosteroids, immunosuppressive agents and/or biologics (Sandborn et al., 2020i). Patients were randomized to guselkumab 200 mg, 600 mg, or 1,200 mg at weeks 0, 4, and 8; ustekinumab (the reference arm) ~6 mg/kg IV at week 0 and 90 mg SC at week 8; or placebo IV (Sandborn et al., 2020i). Outcomes of interest included change in CDAI scores compared to baseline, clinical remission (CDAI < 150) and response, clinical biomarker response (clinical response and ≥50% reduction from baseline in CRP or fecal calprotectin), endoscopic response, and

safety (Sandborn et al., 2020i). Two-hundred and fifty CD patients were included in this study and about 50% had failed biologics (Sandborn et al., 2020i). There were significant decreases of CDAI from baseline in all guselkumab groups compared to placebo at week 12 (Sandborn et al., 2020i). Compared to placebo, there was a higher proportion patients in all guselkumab groups who achieved clinical remission (200 mg: 54%, 600 mg: 56%, 1,200 mg: 50%, placebo: 15.7%), clinical biomarker response (200 mg: 54%, 600 mg: 48%, 1,200 mg: 42%, placebo: 11.8%), and endoscopic response (200 mg: 36%, 600 mg: 40%, 1,200 mg: 36%, placebo: 11.8%) (Sandborn et al., 2020i). In those who failed biologics, 45.5% (35/77) in the guselkumab group and 12.5% (3/24) in the placebo group achieved clinical remission at week 12 (Sandborn et al., 2020i). The rates of AE, infections, and serious AE were similar across all guselkumab treatment arms compared to placebo (Sandborn et al., 2020i).

In summary, in patients with moderate-severe CD, guselkumab was more efficacious in terms of clinical response, remission, endoscopic response, and clinical-biomarker response compared to placebo. There was no clear dose-response in this phase II study (Sandborn et al., 2020i). Guselkumab Is currently in phase II/III trials with an estimated study completion date in October 2024 (NCT03466411).

Additionally, a phase IIb/III study of the safety and efficacy of guselkumab in patients with moderate-severe UC was started in September 2019 (NCT04033445; anticipated completion by July 2025). In addition, a phase IIa study is evaluating combination treatment of guselkumab and golimumab in moderate-severe UC (NCT03662542) (Hanzel and D'Haens, 2020).

IL-6 Inhibitors

PF-04236921

PF-04236921 is a fully human immunoglobulin G2 monoclonal antibody that binds IL-6, which has many pro-inflammatory effects. A phase II study (ANDANTE I) aimed to evaluate the efficacy and safety of PF-04236921 in patients with moderate-to-severe CD who had inadequately responded to anti-TNF therapy (Danese et al., 2019). This study was then followed by an open-label extension study (ANDANTE II) with the primary aim of studying long-term safety, tolerability, and immunogenicity. For the phase II study, patients were randomized 1:1:1:1 to receive placebo or PF-04236921 10, 50, or 200 mg SC on days 1 and 28. The primary endpoint for the induction study was CDAI-70 response at weeks 8 or 12. Secondary endpoints included CDAI-70 and CDAI-100 response rates, CDAI remission (CDAI score <150). The primary aim of the OLE study was safety (Danese et al., 2019).

In the induction study PF-04236921 50 mg was found to have significantly higher CDAI-70 rates compared to placebo at weeks 8 (49.3 vs. 30.6%, $p < 0.05$) and 12 (47.4 vs. 28.6%, $p < 0.05$) (Danese et al., 2019). CDAI remission rates with PF-04236921 50 mg daily were significantly higher at week 12 compared to placebo 27.4 vs. 10.9%, $p < 0.05$) (Danese et al., 2019). The PF-04236921 10 mg dose did not meet the primary end point.

One-hundred and nine one patients entered the OLE study, and 89 (46%) were CDAI responders at OLE baseline. A majority of patients (77.8%) had their PF-04236921 dose escalated to 100 mg between weeks 8 and 48. In those who had been on drug in the induction period (n = 65), the HBI response and remission rates were 40 and 32%, respectively, at week 48 (Danese et al., 2019). It was rare to find antidrug antibodies. One out of 680 serum samples (0.1%) were found to be positive for anti-drug antibody (at week 4 with dose of 50 mg). CRP levels were noted to be suppressed during the OLE treatment period.

The most common serious adverse effects with CD-related, such as worsening of CD and abdominal pain, and nasopharyngitis. In the OLE study, most AEs were mild-moderate in severity. One death occurred in the induction study, and this was in the 50 mg group; the patient died of respiratory failure secondary to pneumonia and was thought to be unrelated to the treatment. Cases of GI perforation and GI abscesses were seen in the induction and OLE studies of patients on PF-04236921; most cases were identified in areas of previous disease involvement or surgery.

In summary, in patients with moderate-severe CD, PF-04236921 50 mg was more efficacious than placebo in inducing response and remission at week 12. In those in the OLE, who were initially on active drug during the induction period, about 40% had an HBI response rate at week 48. There are signals of GI perforation and abscess in the PF-04236921 treatment groups, and therefore this signal will need to be carefully monitored in any future clinical trials. At this time there are no phase three trials of PF-04236921.

Human IL-22Fc Fusion Protein

UTTR1147A

The activation of the IL-22 pathway may help to increase epithelial tight junctions, promote mucus production, and lead to secretion of antimicrobial peptides (Rothenberg et al., 2019). Ultimately this pathway may promote tissue regeneration, and therefore it is a valuable treatment target. UTTR1147A (IL-22Fc) is a fusion protein consisting of a linked human IL-22 and crystallizable fragment (Fc) of the human IgG4 (Rothenberg et al., 2019). A recent phase 1a trial studied single, ascending intravenous (1–120 μg/kg) and subcutaneous (3–120 μg/kg) doses of UTTR1147A on safety and tolerability in healthy volunteers (Rothenberg et al., 2019). The maximum tolerated IV dose was 90 μg/kg and most common AEs were dose-dependent but reversible skin effects. UTTR1147A increased proportionally to the doses given, and this caused elevations of IL-22 signaling biomarkers without causing systemic inflammation. Thus, preliminary data shows that UTTR1147A promotes the IL-22 signaling pathway and may lead to tissue regeneration without immunosuppression. This would be a novel mechanism of action in those with epithelial injury, such as what occurs in patients with IBD.

A phase Ib study analyzed UTTR1147A in healthy volunteers and UC patients. 38 healthy volunteers and 24 UC patients were given UTTR1147A or placebo at doses ranging between 30–90 μg/kg either weekly or monthly (6:2 UTTR1147A: placebo per cohort) (Wagner et al., 2020). The Mayo Clinic score was evaluated at baseline, day 30, and day 85. The study found that UTTR1147A was safe and well tolerated in both

groups of patients and most common side effects were dermatologic effects of dry skin, erythema, and pruritis. Interestingly, at the same dose level, UC patients had relatively lower drug exposures than healthy volunteers and this was thought to be due to faster drug clearance (Wagner et al., 2020). Additionally, UC patients had attenuated pharmacodynamics response (production of biomarkers such as CRP) compared to healthy volunteers (Wagner et al., 2020). However, this study showed that there was an adequate safety and PK profile in both cohorts, and UTTR1147A did produce pharmacodynamics biomarkers in both cohorts. Further data would be important to study this novel mechanism of action in the treatment of patients with IBD.

Anti-Adhesion Molecules

Migration of pro-inflammatory T cells into the gut facilitates inflammation which is characteristic of CD and UC (Targan et al., 2007; Lin et al., 2015; Shivashankar and Pardi, 2017b). Interaction between surface-expressed α4β1 and α4β7 integrins on lymphocytes and adhesion molecules [vascular cell adhesion molecule-1 (VCAM-1) or mucosal addressin cell adhesion molecule-1 (MAdCAM-1)], which are present on endothelial cells, allow for activated effector T cells to target the gut (Shivashankar and Pardi, 2017b). This interaction allows for movement of T cells out of the blood stream and into the gastrointestinal tract (Sugiura et al., 2013; Shivashankar and Pardi, 2017b; Sandborn et al., 2020b). Natalizumab (NAT), a humanized IgG4 monoclonal antibody that targets the α4-integrin subunit of α4β1 and α4β7 on the surface of lymphocytes, has been approved for CD and multiple sclerosis since it blocks lymphocyte trafficking to the gut and brain. NAT has been associated with progressive multifocal leukoencephalopathy (PML) (Feagan et al., 2013; Park and Jeen, 2018). On the other hand, vedolizumab (VDZ) is a humanized IgG1 monoclonal antibody that specifically targets the α4β7 integrin, and it has been approved for UC and CD and therefore selectively prevents leukocyte migration to the gut (Feagan et al., 2013; Park and Jeen, 2018). In this section, we will focus on novel anti-adhesion molecules and a novel method of administration of VDZ.

SC Vedolizumab

VDZ, an infusion medication, was approved in 2014 for moderate-severe UC and CD. From clinical trial data, CD patients who responded to induction dosing at week 6 were more likely to achieve clinical remission, clinical response, and corticosteroid-free remission at week 52 compared to placebo (Sandborn et al., 2013). In addition, UC patients treated with VDZ in clinical trials had a significantly higher rate of clinical remission, clinical response, mucosal healing, and corticosteroid-free remission at week 52 compared to placebo (Feagan et al., 2013).

A new SC formulation of VDZ has been studied in those with UC; the benefit of this formulation is its convenient route of administration for patients who would like to avoid maintenance IV infusion therapy. A phase III open-label study (VISIBLE 1) of patients with moderate-severely active UC was conducted to assess the efficacy of SC VDZ as maintenance therapy (Sandborn et al., 2020b). The primary endpoint was clinical remission (total Mayo score ≤2 and no subscore >1) at week 52. VDZ 300 mg IV was administered at weeks 0 and 2 (Sandborn et al., 2020b). Those with clinical response at week 6 were then randomized to maintenance treatment with SC VDZ 108 mg every 2 weeks, IV VDZ 300 mg every 8 weeks, or placebo (Sandborn et al., 2020b). SC VDZ had a higher rate of clinical remission at week 52 compared to placebo in both anti-TNF naïve and anti-TNF exposed patients (53.7 vs. 18.9%, $p < 0.01$ and 33.3 vs. 5.3%, $p = 0.023$, respectively) (Sandborn et al., 2020b). There were also significantly higher rates of endoscopic improvement (56.6 vs. 21.4%, $p < 0.001$) and durable clinical response (64.2 and 28.6%, $p < 0.001$) when SC VDZ was compared to placebo (Sandborn et al., 2020b). There was no significant difference between SC VDZ and placebo in terms of durable clinical remission (15.1 vs. 5.4%, $p = 0.076$) or corticosteroid-free remission (28.9 vs. 8.3%, $p = 0.067$) (Sandborn et al., 2020b). Endpoints were generally similar between SC VDZ and IV VDZ.

There were no new safety signals when SC VDZ was compared to IV VDZ. The most common AE was worsening of UC disease activity, nasopharyngitis, upper respiratory infections, and anemia (Sandborn et al., 2020b). Eleven patients (10.4%) receiving SC VDZ had injection-site reactions characterized by rash, swelling, erythema, and pruritis (Sandborn et al., 2020b). There were no cases of PML or deaths. The VDZ pharmacokinetics achieved with SC VDZ was similar to that of the IV formulation (Sandborn et al., 2020b).

Overall, this study showed that SC vedolizumab was effective and well-tolerated as maintenance therapy for UC following an induction with IV VDZ. Efficacy outcomes were generally similar between maintenance SC VDZ and IV VDZ. Also, the safety profile was encouraging, and no new safety signals were identified. SC VDZ will give patients an option for an alternate mode of administration if they prefer to avoid long-term infusions. SC VDZ for moderate-severe UC will potentially be available in 2022.

Etrolizumab

While VDZ targets only the α4β7 integrin, etrolizumab is a SC humanized monoclonal anti-integrin antibody that selectively binds the β7 subunit of both α4β7 and αEβ7 integrins (Vermeire et al., 2014; Sandborn et al., 2020h). Therefore, etrolizumab controls movement of inflammatory cells into the gastrointestinal tract and also mediates inflammatory effects on the gut mucosa (Vermeire et al., 2014; Sandborn et al., 2020h). The phase II EUCALYPTUS study showed that etrolizumab was beneficial over placebo in patients with moderate-severe UC (Vermeire et al., 2014). In this study, 124 patients were randomized to two doses of SC etrolizumab—either 100 mg at weeks 0, 4, and 8 with placebo at week 2; or 420 mg loading lose (LD) at week 0, followed by 300 mg at weeks 2, 4, and 8—or placebo (Vermeire et al., 2014). The primary endpoint was clinical remission at week 10 (Mayo clinic score ≤2 with no individual subscore >1). Compared to placebo (0 patients in clinical remission), etrolizumab (100 mg: 21%, $p = 0.004$; LD+

300 mg: 10%, $p = 0.048$) treatment was found to lead to a higher proportion of patients in clinical remission at week 10 (Vermeire et al., 2014). Adverse events occurred at a similar frequency across all groups—61% of 100 mg etrolizumab group, 49% in the LD+ 300 mg group, and 72% in the placebo group. No patients developed PML.

Etrolizumab has an extremely active phase III clinical trial program and includes direct comparisons to infliximab and adalimumab. There are currently six randomized controlled trials and two open label extension studies. The aim of HIBISCUS I and II (identical induction trials of etrolizumab 105 mg vs. adalimumab and placebo), GARDENIA (maintenance study studying etrolizumab 105 mg vs. infliximab), and LAUREL (maintenance trial evaluating etrolizumab 105 mg against placebo) is to study UC patients who are anti-TNF naïve. HICKORY is a maintenance trial studying etrolizumab 105 mg vs. placebo in anti-TNF exposed UC patients (Sandborn et al., 2020h). The primary endpoints are based on clinical response (≥3 point decrease and 30% reduction in Mayo clinic score and ≥1 point decrease in rectal bleeding or an absolute rectal bleeding score of 0 or 1), remission (MCS ≤2, with individual subscore ≤1 and rectal bleeding score of 0) at each trial's specified time points (Sandborn et al., 2020h). COTTONWOOD is the open-label extension and safety monitoring study of UC patients treated with etrolizumab who were followed until week 108 (Sandborn et al., 2020h).

Early results from the HICKORY study included 130 UC patients and 45% had previously been exposed to ≥2 anti-TNFs (Peyrin-Biroulet et al., 2017). Stool frequency rates improved from baseline to week 4 in 30% and at week 14 in 50% of patients (Peyrin-Biroulet et al., 2017). Rectal bleeding remission rates were observed from baseline to week 4 in about 30% of patients and at week 14 in about 50% of patients (Peyrin-Biroulet et al., 2017). Biomarkers decreased at week 14 (fecal calprotectin: mean 57% decrease; CRP: 33% decrease) (Peyrin-Biroulet et al., 2017). Therefore, in patients previously exposed to anti-TNFs, etrolizumab led to symptom improvement as early as week 4 (Peyrin-Biroulet et al., 2017).

For patients with CD, the BERGAMOT study is an induction and maintenance trial evaluating anti-TNF naïve and experienced patients (etrolizumab 105 and 210 mg vs. placebo) (Sandborn et al., 2020h). Eligible patients may enter JUNIPER study, which will be the open label extension of etrolizumab 105 mg (Sandborn et al., 2020h). The co-primary endpoint for BERGAMOT is clinical remission (unweighted abdominal pain score ≤1 and stool frequency ≤3) and endoscopic improvement (>50% reduction in SES-CD from baseline) at weeks 14 and 62 (Sandborn et al., 2020h). The primary outcome for JUNIPER is long term efficacy (clinical remission assessed at 12 weeks intervals), endoscopic remission (SES-CD ≤4 [≤2 for pts with ileal disease] with no segment >1) at week 108 and incidence and severity of AEs (Sandborn et al., 2020h).

The BERGAMOT induction cohort included 300 CD patients who were randomized to etrolizumab 105 mg SC every 4 weeks, 210 mg at weeks 0, 2, 4, 8, and 12, or placebo for a 14 weeks induction period (Selinger et al., 2018). Previous anti-TNF exposure was noted in 73% of patients (Selinger et al., 2018). Symptomatic remission was seen in a greater number of patients treated with etrolizumab [105 mg: 20.8% (90% confidence interval 15.4–27.5); 210 mg: 24.8 (18.9–31.8)] compared to placebo (11.9 [6.6–20.5]) at week 14 (Selinger et al., 2018). Similarly, more patients treated with etrolizumab (105 mg: 21 [15.6–27.8] and 210 mg: 17.4 [12.4–23.7] achieved endoscopic improvement compared to placebo (3.4 [1.1–9.7]) at week 14 (Selinger et al., 2018). AEs were comparable between etrolizumab and placebo; there were no cases of PML or death (Selinger et al., 2018).

In addition to providing further data on clinical response, remission, and endoscopic remission data for etrolizumab, these data may help clinicians decide which biologic is an ideal first-line agent for their patient (Sandborn et al., 2020h). The HIBISCUS I and II and GARDENIA studies will be the first phase III trials in UC to study the efficacy of a novel agent directly compared to another agent, i.e., infliximab and adalimumab (Sandborn et al., 2020h).

AJM300

α4 or α4β7 targets have been shown to be possible therapeutic targets in the treatment of IBD since suppression of these integrins have controlled development of colitis in an animal model (Sugiura et al., 2013). A variety of small molecule α4 integrin antagonists have been studied in clinical trials for conditions such as asthma and multiple sclerosis. AJM300 is an oral small molecule that targets α4 integrin, and it is classified as a phenylalanine derivative (Yoshimura et al., 2015). This small molecule's duration of action is very short, within one day of last dose as described in a phase IIa study (Yoshimura et al., 2015). AJM300 has been shown to be effective in experimental colitis model in mice; this study showed that the active metabolite of AJM300 inhibited the binding of α4β1/α4β7 integrin-expressing cells to VCAM-1/MAdCAM-1 *in vitro* (Sugiura et al., 2013). Given the α4 blockade, there may be a potential risk for PML in AJM-300 therapy (Yoshimura et al., 2015).

A phase IIa study including 102 patients with moderate active UC was conducted to assess the primary outcome measure of clinical response (decrease in Mayo score of at least 3 points and decrease of at least 30% from baseline, with decrease in rectal bleeding subscore of at least 1 point or an absolute rectal bleeding score of 0 or 1) at week 8 (Yoshimura et al., 2015). Patients who had inadequate response or intolerance to mesalamine or corticosteroids were given AJM300 960 mg orally or placebo three times daily for 8 weeks (Yoshimura et al., 2015). Compared to placebo, those treated with AJM300 had higher rates of clinical response (62.7 vs. 25.5%, $p = 0.0002$), clinical remission (23.5 vs. 3.9%, $p = 0.0099$), and mucosal healing (58.8 vs. 29.4%, $p = 0.0014$) (Yoshimura et al., 2015).

There was a significant increase in peripheral leukocyte count as would be expected from an anti-α4 integrin; this increase was seen as early as week 2 (Yoshimura et al., 2015). However, this finding normalized the day after the last dose given at week 8 thereby suggesting a short duration of action (Yoshimura et al., 2015). The most common adverse events were nasopharyngitis and UC, with higher AEs seen with UC in the placebo group (Yoshimura et al., 2015). Overall, however, there were similar

rates of AEs observed between the treatment and placebo arms (Sabino et al., 2019). There were no serious AEs observed, and infection, and PML were not seen in this study (Yoshimura et al., 2015).

In summary, AJM-300 was more effective than placebo in inducing clinical response, clinical remission, and mucosal healing in moderately active UC patients who had only been exposed to mesalamine or steroids in the past. However, the study was limited by a small sample size and a short study duration (8 weeks) (Yoshimura et al., 2015). Unfortunately, there were extremely low number of patients who were intolerant or inadequately responding to steroids in this study, and there was no information on exposure to immunomodulators and anti-TNFs (Yoshimura et al., 2015). AJM300 is currently in phase III trials for UC patients, and the estimated study completion date is February 2021 (NCT03531892).

Abrilumab (AMG 181or MEDI 7183)

Abrilumab is an injectable fully human monoclonal immunoglobulin G2 antibody that targets the α4β7 integrin and prevents interaction with MADCAM-1 (Sandborn et al., 2017a). Abrilumab has a high bioavailability after SC dosing and a long half-life (about 31 days) (Sandborn et al., 2019).

A phase IIb study in patients with CD who had inadequate or loss of response or intolerance to immunosuppressives, anti-TNFs, or corticosteroids were randomized to receive placebo or abrilumab (21 mg or 70 mg) SC on day 1, weeks 2 and 4, and then every 4 for 24 weeks, or one dose of abrilumab 210 mg SC on day 1 (Sandborn et al., 2017a). The primary endpoint was clinical remission (CDAI < 150) at week 8 (Sandborn et al., 2017a). There was no significant difference in clinical remission at week 8 between abrilumab at any dose when compared to placebo (Sandborn et al., 2017a). Of note, there were higher rates of clinical remission at week 12 in those treated with a single dose of abrilumab 210 mg when compared to placebo in those who previously failed anti-TNF therapy (Sandborn et al., 2017a). AE rates were similar among all groups through week 24, and there were no cases of PML or death (Sandborn et al., 2017a).

A phase II induction and sustained remission study of abrilumab was conducted in patients with active moderate-severe UC who did not respond or lost response to usual medical therapy (Sandborn et al., 2019). Patients were randomized to SC placebo or abrilumab (7, 21, 70 mg) on day 1, week 2, week 4, and then every 4 weeks thereafter until week 24 or a single dose of 210 mg abrilumab on day 1 followed by placebo at the same dosing scheduled noted previously until week 24 (Sandborn et al., 2019). An open-label phase of the study involved administration of abrilumab 210 mg once every 3 months (Sandborn et al., 2019). The primary endpoint was remission (total Mayo score ≤2 points with no individual sub-score >1 point) at week 8 (Sandborn et al., 2019). There were significantly higher odds of achieving clinical remission, clinical response, and mucosal healing at week 8 in those treated with abrilumab 70 and 210 mg compared to placebo (Sandborn et al., 2019). In those with prior anti-TNF failure, there were greater clinical remission rates at week 8 in the abrilumab 70 and 210 mg dose (Sandborn et al., 2019).

However, there were no clear benefits of abrilumab treatment at week 24—in this study, patients continued their initial treatment regardless of whether they responded after the induction period (Sandborn et al., 2019). The odds of sustained remission did increase in patients who continued to take multiple doses of abrilumab 70 mg every 4 weeks compared to placebo (Sandborn et al., 2019).

There were no differences in AEs across treatment groups through week 24. The most common AE were non-serious infections, gastrointestinal effects, headache, and arthralgia (Sandborn et al., 2019). The only serious AE noted in more than one patient in the abrilumab treated group was worsening of UC (Sandborn et al., 2019). There were no cases of PML or death. Ten patients (8.6%) in the placebo group and 9 (3.8%) in the abrilumab group reported neoplasms (Sandborn et al., 2019). A limitation of this phase II study of abrilumab in UC include its short duration; phase III studies are needed to assess the long-term response of the 70 mg dose after 24 weeks (Sandborn et al., 2019).

In conclusion, while the phase II study of abrilumab in CD failed to meet its primary endpoint, the study in UC patients showed efficacy at week 8 with higher rates of clinical remission, clinical response, and mucosal healing. Since there was no clear benefit of abrilumab at week 24 in UC patients, longer term phase III studies are required to better assess this finding. Phase 3 studies have not yet started.

PF-00547659 (SHP647)

PF-00547659 is a SC fully human monoclonal antibody that binds to MAdCAM, thereby decreasing lymphocyte trafficking to the gut and leading to decreased gastrointestinal inflammation (Sandborn et al., 2018). A phase II dose ranging study of PF-00547659 was conducted in patients with moderate-severe CD who have a history of failure or intolerance to immunosuppressives and/or anti-TNF therapy (Sandborn et al., 2018). This study included 265 patients who were randomized to PF-00547659 22.5, 75 mg, or 225 mg or placebo (Sandborn et al., 2018). The primary endpoint was a CDAI 70-point decrease from baseline at week eight or 12 (Sandborn et al., 2018). There was no significant difference in CDAI response between the treatment group and placebo at week 8 (22.5 mg: 52.7%, 75 mg: 60.1%, 225 mg: 62.7%) or 12 (22.5 mg: 62%, 75 mg: 64.7%, 225 mg: 57.5%); this was likely due to a high clinical response in the placebo group (47.7% at week 8 and 58.6% at week 12) (Sandborn et al., 2018).

In a post-hoc analysis, the proportions of patients who achieved clinical remission were higher in all PF-00547659 dose groups than in placebo at weeks 8 and 12 in those with higher inflammatory burden as evidenced by higher median high sensitivity CRP values (>5 mg/L or >18.8 mg/L) or higher baseline SES-CD scores (>17) at baseline (Sandborn et al., 2018). The incidence of AEs, serious AEs, and discontinuation was similar across all treatment groups.

The long-term safety and efficacy portion of the study followed patients for a further 6 months (D'Haens et al., 2018a). The most common AEs with treatment included nasopharyngitis (5.6%), arthralgia (6.0%), and headache (5.2%) (D'Haens et al., 2018a).

There were two deaths (multiorgan failure after postoperative aspiration following resection of the terminal ileum and metastatic adenocarcinoma of unknown primary) however neither were thought to be drug related (D'Haens et al., 2018a). Harvey Bradshaw Index response rates were sustained over 6 months of treatment (D'Haens et al., 2018a).

A post-hoc analysis also looked at endoscopic outcomes following induction therapy with PF-00547659 (D′Haens et al., 2018b). Mean total SES-CD scores across four colon and one ileal segments were found to trend toward a decrease across all treatment arms (except for the 75 mg dose) (D′Haens et al., 2018b). The 22.5 mg dose showed the largest trend toward improvement in endoscopic disease severity (mean change from baseline to week 10 at 22.5 mg dose: 4.0; 75 mg: 0; 225 mg: −1; placebo: 1.5) (D′Haens et al., 2018b). However, no consistent association between clinical and endoscopic improvement was observed (D′Haens et al., 2018b).

In patients with moderate-severe UC, a phase II study that evaluated the efficacy and safety of PF-00547659 in 357 patients who had failed or were intolerant to at least one usual therapy found the drug to be superior to placebo (Vermeire et al., 2017a; Sabino et al., 2019). The primary endpoint was clinical remission (Mayo score ≤2 with no individual subscore >1 and rectal bleeding subscore ≤1) at week 12 (Vermeire et al., 2017a). The remission rates in those treated with PF-00547659 (7.5 mg: 11.3%; 22.5 mg: 16.7%; 75 mg: 15.5%; 225 mg: 5.7%) were higher than placebo (2.7%) at week 12; the 225 mg dosing did not achieve statistical significance compared to placebo (Vermeire et al., 2017a). Similar to the findings from the CD trial, PF-00547659 was overall well-tolerated (Vermeire et al., 2017a).

In conclusion, in patients with CD, PF00547659 was not significantly different compared to placebo in achieving clinical response at weeks 8 or 12 likely due to high placebo response rates (Sabino et al., 2019). On the other hand, three out of four doses of PF00547659 did achieve significantly higher rates of clinical remission than placebo in patents with UC. Phase III studies in patients with IBD have not yet been announced.

Oral Anti-tumor Necrosis Factor Agents

Anti-TNF agents were the first class of biologics approved for the treatment of moderate to severe UC and CD. They have revolutionized the treatment paradigm of IBD and have proven to be effective (Sands et al., 2004; Rutgeerts et al., 2005; Hanauer et al., 2006; Sandborn et al., 2007; Schreiber et al., 2007). One of the limitations of current anti-TNF agents is that they are currently administered by IV or as SC injectables only. This is associated with risk of infusion/injection reactions, systemic side effects and increased cost of repeated infusions/injections. An oral and intestinally restricted anti-TNF agent would help overcome some of these challenges of current anti-TNF agents.

AVX-470

AVX-470 is an oral polyclonal immunoglobulin that is derived from the colostrum of cows that have been immunized with human recombinant anti-TNF. In the first human study, 36 patients with UC received either AVX-470 (pH dependent delayed release capsules) at doses of 0.2, 1.6, and 3.5 g/day or placebo (Harris et al., 2016). In terms of safety, AVX-470 was well tolerated and the total rate of AEs was 52% compared to 78% in the placebo group. At 4 weeks, the overall clinical response and remission rates were 25.9 and 3.7% in the AVX-470 group compared to 11.1 and 0% in the placebo group, respectively. Endoscopic remission was achieved in 7.4% in the AVX-470 group compared to none in the placebo group. In term of immunogenicity, no human anti-bovine antibodies were detected.

OPRX-106

OPRX-106 is an oral anti-TNF agent. It is a combination of plant cell-expressed human anti-TNF receptor II fused to IgG1 Fc domain. The plant cells function as a delivery mechanism. A phase II randomized, 2-arm, open label clinical trial of 25 patients with UC treated with OPRX-106 at 2 or 8 mg daily for 8 weeks was performed (Almon et al., 2020). A total of 18 patients completed the study. Clinical response defined as a decrease in the Mayo score by at least 3 points was achieved in 67% and clinical remission (Mayo score ≤2 without sub-score being greater than 1) was achieved in 28%. Mucosal healing (Mayo endoscopic score ≤1) was achieved in 33% (Almon et al., 2020). In terms of immunogenicity, no anti-drug antibodies were detected.

Oral anti-TNF agents have the potential of enhanced safety, decreased immunogenicity and higher patient acceptance. Although promising, the current available data on efficacy and safety of oral anti-TNF agents is limited and future larger trials are needed to evaluate efficacy, safety, feasibility and cost effectiveness.

Sphingosine-1-Phosphate Receptor Modulators

Sphigosine-1-phosphate is a sphingolipid ligand of G protein coupled receptors (S1P1-S1P5) which are responsible for controlling the egress of lymphocytes from lymphoid organs. The S1P/S1PR interaction can also result in internalization of the S1PR which leads to decrease lymphocyte release from the lymphoid tissue into the circulation. Fingolimod was the first S1P receptor modulator approved for the treatment of multiple sclerosis in 2010 (Cohen et al., 2010; Kappos et al., 2010). Fingolimod is a non-selective S1P receptor modulator and has high affinity for S1PR 1 and S1PR3-5. Although overall well tolerated, fingolimod has been associated with adverse events such as bradycardia, hypertension, infection and elevated liver tests (Danese et al., 2018).

Ozanimod

Ozanimod is a S1P receptor modulator with selective affinity for S1PR1 and S1PR5. It was approved by the US FDA in 2020 for the treatment of relapsing MS (Cohen et al., 2016; Cohen et al., 2019; Comi et al., 2019).

TOUCHSTONE is a phase II double blind, randomized clinical trial of ozanimod 0.5 or 1 mg vs. placebo daily in moderate to severe UC (n = 197). The primary outcome was

clinical remission at 8 weeks (Mayo clinic score ≤2; No sub-score > 1). The primary outcome was achieved in 16% in the ozanimod 1 mg group vs. 14% in the ozanimod 0.5 mg group vs. 6% in the placebo group ($p = 0.048$ and $p = 0.14$, respectively) (Sandborn et al., 2016). Mucosal healing at week 8 (defined as Mayo endoscopy sub-score ≤1) was achieved in 34% in the 1 mg group vs. 28% in the 0.5 mg group compared to 12% in the placebo group ($p = 0.002$ and $p = 0.03$, respectively). At week 32, clinical remission was 21% in the 1 mg group and 26% in the 0.5 mg group compared to 6% in the placebo group ($p = 0.01$ and $p = 0.002$, respectively). Mucosal and histologic healing rates were similarly significantly higher in the ozanimod groups compared to placebo at 32 weeks (Sandborn et al., 2016). In the ozanimod groups, one patient developed bradycardia (patient had previous history of bradycardia) and four patients developed elevated liver enzymes.

TRUE-NORTH is a phase III randomized, double-blind, placebo-controlled trial of induction and maintenance ozanimod in UC completed in 2020 (Danese et al., 2020a; Sandborn W. et al., 2020). In the induction phase of 10 weeks, moderately to severely active UC patients received either ozanimod 1 mg or placebo daily. The primary endpoint of clinical remission (based on 3-component Mayo score) was met in 18.4% in the ozanimod group vs. 6% in the placebo group ($p < 0.0001$) (Sandborn W. et al., 2020). Clinical remission was numerically higher then placebo but did not achieve statistical significance in the anti-TNF exposed patients who received ozanimod (10 vs. 4.6%; $p = 0.195$). Secondary outcomes of clinical response, endoscopic improvement and mucosal healing (both endoscopy and histology) rates were significantly in the total ozanimod group compared to placebo. The reported rate of bradycardia was 0.5% in the ozanimod group.

In the maintenance trial, 457 moderate to severe UC patients who achieved clinical response after 10 weeks of ozanimod induction therapy were then re-randomized at 1:1 to either ozanimod 1 mg or placebo and outcomes assessed at week 52 (Sandborn W. et al., 2020). Clinical remission (based on 3-component Mayo score) rates were significantly higher in the ozanimod group at 37% compared to 18.5% in the placebo group ($p < 0.0001$) (Danese et al., 2020a). Anti-TNF exposed patients who received ozanimod also had a significantly higher rate of clinical remission compared to placebo (28.9% vs. 10.1; $p = 0.0053$). All secondary endpoints of the trial were also met in the ozanimod group including: clinical response, endoscopic improvement, corticosteroid-free remission, maintenance of clinical remission, durable clinical remission and mucosal healing (both endoscopic and histologic) (Danese et al., 2020a). In this trial, ozanimod was also well tolerated with the most common reported AEs being abnormal liver tests and headaches. Elevation of alanine aminotransferase (ALT) was noted in 4.8% in the ozanimod group compared to 0.4% in the placebo group (Danese et al., 2020a).

For CD, ozanimod was evaluated in a phase II multicenter, uncontrolled, prospective observer-blinded endpoint trial, STEPSTONE (Feagan et al., 2020a). The trial had a 12-weeks induction period followed by a 100-weeks extension study. Patients with moderately to severely active CD (n = 69) received a 7-days dose escalation of ozanimod followed by 11 weeks of ozanimod 1 mg oral capsule daily. The primary endpoint was reduction in the Simple Endoscopic Score for Crohn's disease (SES-CD) at 12 weeks from baseline. The mean change of SES-CD at week 12 was – 2.2 ± 6 and 23.2% of patients achieved endoscopic response (defined as SES-CD decrease by ≥ 50%) (Feagan et al., 2020a). Clinical remission (defined as CDAI <150) was noted in 39.1% of patients. The most common AE was CD flare and there were no cases of bradycardia or arrhythmias reported (Feagan et al., 2020a).

Phase III, placebo-controlled induction and maintenance studies of ozanimod in moderate to severe CD are currently recruiting (NCT03440372, NCT03440385, NCT03464097, NCT03467958).

Etrasimod

Etrasimod is an oral S1P receptor modulator with selectivity for S1PR1, S1PR4 and S1PR5. A phase II (OASIS; proof of concept), double-blinded trial randomized moderate to severe UC patients (n = 156) to either etrasimod 1 mg, etrasimod 2 mg or placebo in a 1:1:1 fashion for 12 weeks (Sandborn et al., 2020g). The primary endpoint was improvement in the modified Mayo Clinic score at 12 weeks from baseline and secondary endpoints included: the improvement in the total Mayo Clinic score, improvement in the two component Mayo Clinic score (rectal bleeding and endoscopy) and endoscopic improvement (endoscopy sub-score ≤ 1). The primary endpoint was achieved in the etrasimod 2 mg group compared to placebo (least square mean difference, 0.99; 90% CI, 0.30–1.68; $p = 0.009$) but not in the etrasimod 1 mg group. Compared to placebo, the etrasimod 2 mg group had higher rates of: endoscopic improvement (41.8 vs. 17.8%; $p = 0.003$), improvement in the total Mayo score ($p = 0.010$) and improvement in the 2 component Mayo score ($p = 0.002$) (Sandborn et al., 2020g). Histologic remission (defined as Geboes score <2) was an exploratory endpoint of the trial and was significantly higher in the etrasimod 2 mg group compared to placebo (19.5 vs. 6.1%; $p = 0.03$) (Sandborn et al., 2020g).

In this trial there was significantly higher rates of discontinuation of drug due to AEs in the etrasimod groups (n = 7) compared to placebo (n = 0) (Sandborn et al., 2020g). The most common AEs other than disease worsening are upper respiratory tract infections, nasopharyngitis and anemia. In etrasimod 2 mg group, transient first-degree heart block occurred in two patients and type 1 s degree heart block was noted in one patient. The authors report that all three patients had evidence of atrioventricular block noted on electrocardiography prior to receiving the study drug (Sandborn et al., 2020g).

Phase III induction and maintenance trials of etrasimod for moderate to severe UC are currently recruiting (NCT03996369, NCT03945188, NCT03950232, NCT04176588). A phase II/III study of etrasimod induction and maintenance in CD has recently opened and is currently recruiting (NCT04173273).

Amiselimod (MT-1303)

Amiselimod is an oral S1P receptor modulator with higher selectivity for S1PR1 than other S1P receptors. Phase II study of amiselimod demonstrated that is well tolerated and potentially effective for multiple sclerosis (Kappos et al., 2016). A phase II randomized, placebo-controlled trial of amiselimod in CD (NCT02378688) was completed and at this time results are not published. A proof of concept study randomized 78 patients to either amiselimod 0.4 mg (n = 40) or placebo (n = 38) (D'Haens et al., 2019). The primary outcomes of clinical response (decrease in CDAI by 100 points) at week 12 was achieved in 48.7 vs. 54.1% in the placebo group. No significant differences were noted in the fecal calprotectin and CRP in the two groups (D'Haens et al., 2019).

Phosphodiesterase 4 Inhibitors

Phosphodiesterases (PDE1-PDE11) are a group of intracellular enzymes that catalyze the breakdown of cyclic adenosine monophosphate (cAMP) and cyclic guanosine monophosphate (cGMP). PDE4 catalyzes the breakdown of 3, 5′ cAMP in multiple cell types including T-cells, macrophages and monocytes. This leads to activation of nuclear transcription factor kappaB (NF-κB) which eventually promotes downstream proinflammatory effects. Therefore, inhibition of PDE4 can lead to suppression of NF-κB and subsequently reduce TNF-α mRNA expression and production of nitric oxide and also increase synthesis of anti-inflammatory cytokines such as IL-10 and IL-6 (Ollivier et al., 1996; Gobejishvili et al., 2008; Kwak et al., 2005; Platzer et al., 1999). Therefore, there has been interest in developing PDE4 inhibitors as therapeutic agents in IBD.

Apremilast

Apremilast is an oral PDE4 inhibitor that is currently approved by the US FDA for the treatment of psoriasis and psoriatic arthritis. A double-blind, phase II trial randomized UC patients to apremilast 30 mg (n = 57), apremilast 40 mg (n = 55) or placebo (n = 58) twice daily (Danese et al., 2020b). The primary endpoint of clinical remission (defined as total Mayo UC score ≤2; no individual score >1) was achieved in 31.6% in the 30 mg group ($p = 0.01$ compared to placebo), 21.8% in the 40 mg group compared to 12.1% in the placebo group ($p = 0.27$) (Danese et al., 2020b). Endoscopic response (defined as a decrease in the Mayo endoscopic subscore by ≥ 1) was achieved in 41.4% of patients in the placebo group compared to 73.7% in the 30 mg group ($p < 0.0001$) and 47.3% in the 40 mg group ($p = 0.69$). Both the 30 and 40 mg apremilast groups showed greater reduction in CPR and fecal calprotectin compared to placebo. Although the primary endpoint was not reached in this trial, post hoc analysis demonstrated that a significantly higher proportion of patient in both apremilast groups had a Mayo endoscopic subscore of ≤1 compared to placebo (Danese et al., 2020b).

In terms of safety, the most common side effect reported in the apremilast groups were headaches at 25.5% in the 40 mg group and 21.1% in the 30 mg group compared to 6.9% in the placebo group. Serious AE rate was 2.4% in the placebo group and 1.8% in the 40 mg apremilast group (1 patient who experienced pancreatitis but thought not to be related to study drug) (Danese et al., 2020b). Currently, a phase III UC trial of apremilast has not been registered.

Cobitolimod

Cobitolimod is an oligodeoxynucleotide that is DNA-based and binds to Toll-like receptor 9 (TLR9) on lymphocytes and antigen presenting cells. It activates TLR 9 which lead to induction of regulatory T-cells that produce anti-inflammatory IL-10 in addition to suppressing proinflammatory TH-17 cells. Cobitolimod is a topical agent and is supposed to have low systemic absorption.

A double-blind study (COLLECT) randomized 131 patients with moderate to severe UC to two topically administered doses (during colonoscopy) of cobitolimod 30 mg (n = 87) or placebo (n = 44) (Atreya et al., 2016). The primary endpoint of induction of clinical remission at week 12 (defined as Clinical Activity Index (CAI) ≤4) was 44.4% in the cobitolimod group vs. 46.5% in the placebo group ($p = 0.91$) (Atreya et al., 2016). However, the study did meet multiple secondary endpoints including symptomatic remission, clinical remission with mucosal healing and histologic improvement.

A dose ranging, double-blinded phase IIb study (CONDUCT) randomized 213 patients with moderate to severe left-sided UC into five different treatment arms that received drug or placebo via rectal enemas: cobitolimod 31 mg, 125 mg, or 250 mg at weeks 0 and 3; cobitolimod 125 mg at weeks 0, 1,2 and 3 or placebo (Atreya et al., 2020). The primary endpoint of clinical remission at 6 weeks (defined as Mayo subscore of 0 for rectal bleeding, 0 or 1 for stool frequency + ≥ 1-point decrease from baseline, endoscopy subscore of 0 or 1-excluding friability) was achieved in the cobitolimod 250 mg group at 21% (n = 9) vs. 7% (n = 3) in the placebo group ($p = 0.025$) (Atreya et al., 2020). The rest of the dosing groups did not achieve the primary endpoint compared to placebo. Cobitolimod was well tolerated with an adverse event rate across the dosing groups from 25 to 43% compared to 48% in the placebo group (Atreya et al., 2020). Phase 3 studies are planned for UC (not yet registered at this time).

CONCLUSION

In conclusion, the armamentarium of IBD therapeutic agents is ever expanding. This review highlights some of these novel and emerging therapies. For example, there has been significant development in the small molecules class of agents such as JAK inhibitors and S1P receptor modulators. These agents offer the advantages of ease of administration as they are oral agents and do not have the downside of immunogenicity and antibody formation seen with some of the IV/SC biologics. Some of these agents such might also have the possibility of more rapid onset of action as seen with tofacitinib. In addition, some of these agents will likely have the potential of having a more favorable safety profile compared to anti-TNF agents. This includes for example the development of the intestinally restricted pan-JAK inhibitor (TD-1473), anti-integrins/anti-MAdCAM therapies and IL-23 therapies. In the era of increasing therapeutic agents to treat IBD, the challenge will the

ability to select the best agent for the individual patient. This calls for the development of precision/personalized medicine approach to the treatment of IBD.

DISCLOSURES

BA-B is on the Speaker Bureau of Takeda and AbbVie. RS is on the Speaker Bureau of and received clinical research grant support from AbbVie, and is on the advisory board of Pfizer. DP has no conflicts to disclose.

AUTHOR CONTRIBUTIONS

BA-B, Literature search, manuscript draft, final review and editing. RS, Literature search, manuscript draft, manuscript review. DP, Manuscript draft, critical review and final editing.

REFERENCES

Almon, E., Shaaltiel, Y., Sbeit, W., Fich, A., Schwartz, D., Waterman, M., et al. (2020). Novel orally administered recombinant anti-TNF alpha fusion protein for the treatment of ulcerative colitis: results from a phase 2a clinical trial. *J. Clin. Gastroenterol.* 55(2). 134–140. doi:10.1097/MCG.0000000000001314

Anderson, C. A., Boucher, G., Lees, C. W., Franke, A., D'Amato, M., Taylor, K. D., et al. (2011). Meta-analysis identifies 29 additional ulcerative colitis risk loci, increasing the number of confirmed associations to 47. *Nat. Genet.* 43, 246–252. doi:10.1038/ng.764

Atreya, R., Bloom, S., Scaldaferri, F., Gerardi, V., Admyre, C., Karlsson, Å., et al. (2016). Clinical effects of a topically applied toll-like receptor 9 agonist in active moderate-to-severe ulcerative colitis. *Eccojc* 10, 1294–1302. doi:10.1093/ecco-jcc/jjw103

Atreya, R., Peyrin-Biroulet, L., Klymenko, A., Augustyn, M., Bakulin, I., Slankamenac, D., et al. (2020). Cobitolimod for moderate-to-severe, left-sided ulcerative colitis (CONDUCT): a phase 2b randomised, double-blind, placebo-controlled, dose-ranging induction trial. *Lancet Gastroenterol. Hepatol.* 5, 1063–1075. doi:10.1016/s2468-1253(20)30301-0

Authors (2019). A SPECIAL MEETING review EDITION: highlights in inflammatory bowel disease from the 14th congress of ECCO: a review of selected Presentations from the 14th congress of the European Crohn's and colitis organisation (ECCO) * March 6-9, 2019 * copenhagen, DenmarkSpecial reporting on:* VARSITY: a double-blind, double-dummy, randomized controlled trial of vedolizumab versus adalimumab in patients with active ulcerative colitis* analyses of data from the VISIBLE 1 and 2 trials: vedolizumab in patients with ulcerative colitis or Crohn's disease* improved endoscopic outcomes and mucosal healing of upadacitinib as an induction therapy in Adults with moderately to severely active ulcerative colitis: data from the U-achieve study* long-term safety of vedolizumab in ulcerative colitis and Crohn's disease: final results from the GEMINI LTS study* pediatric Crohn's disease adalimumab level-based optimization treatment (PAILOT) randomized controlled trial* maintenance treatment with mirikizumab, a P19-directed IL-23 antibody: 52-week results in patients with moderately to severely active ulcerative colitis* real-world effectiveness and safety of vedolizumab and anti-TNF therapy in biologic-naive patients with ulcerative colitis or Crohn's disease: results from the EVOLVE study* A randomized, multicenter, double-blind, placebo-controlled study of a targeted-release oral cyclosporine formulation in the treatment of mild to moderate ulcerative colitis: efficacy results* real-world analyses of patients with IBD treated with VedolizumabPLUS meeting Abstract Summaries with Expert commentary by: edward V. Loftus Jr, MDProfessor of MedicineDivision of Gastroenterology and HepatologyMayo ClinicRochester, Minnesota. *Gastroenterol. Hepatol. (N Y)* 15, 1–24.

Baker, K. F., and Isaacs, J. D. (2018). Novel therapies for immune-mediated inflammatory diseases: what can we learn from their use in rheumatoid arthritis, spondyloarthritis, systemic lupus erythematosus, psoriasis, Crohn's disease and ulcerative colitis? *Ann. Rheum. Dis.* 77, 175–187. doi:10.1136/annrheumdis-2017-211555

Banfield, C., Scaramozza, M., Zhang, W., Kieras, E., Page, K. M., Fensome, A., et al. (2018). The safety, tolerability, pharmacokinetics, and pharmacodynamics of a TYK2/JAK1 inhibitor (PF-06700841) in healthy subjects and patients with plaque psoriasis. *J. Clin. Pharmacol.* 58, 434–447. doi:10.1002/jcph.1046

Barrett, J. C., Hansoul, S., Nicolae, D. L., Cho, J. H., Duerr, R. H., Rioux, J. D., et al. (2008). Genome-wide association defines more than 30 distinct susceptibility loci for Crohn's disease. *Nat. Genet.* 40, 955–962. doi:10.1038/ng.175

Cohen, J. A., Arnold, D. L., Comi, G., Bar-Or, A., Gujrathi, S., Hartung, J. P., et al. (2016). Safety and efficacy of the selective sphingosine 1-phosphate receptor modulator ozanimod in relapsing multiple sclerosis (RADIANCE): a randomised, placebo-controlled, phase 2 trial. *Lancet Neurol.* 15, 373–381. doi:10.1016/s1474-4422(16)00018-1

Cohen, J. A., Barkhof, F., Comi, G., Hartung, H.-P., Khatri, B. O., Montalban, X., et al. (2010). Oral fingolimod or intramuscular interferon for relapsing multiple sclerosis. *N. Engl. J. Med.* 362, 402–415. doi:10.1056/nejmoa0907839

Cohen, J. A., Comi, G., Selmaj, K. W., Bar-Or, A., Arnold, D. L., Steinman, L., et al. (2019). Safety and efficacy of ozanimod versus interferon beta-1a in relapsing multiple sclerosis (RADIANCE): a multicentre, randomised, 24-month, phase 3 trial. *Lancet Neurol.* 18, 1021–1033. doi:10.1016/s1474-4422(19)30238-8

Comi, G., Kappos, L., Selmaj, K. W., Bar-Or, A., Arnold, D. L., Steinman, L., et al. (2019). Safety and efficacy of ozanimod versus interferon beta-1a in relapsing multiple sclerosis (SUNBEAM): a multicentre, randomised, minimum 12-month, phase 3 trial. *Lancet Neurol.* 18, 1009–1020. doi:10.1016/s1474-4422(19)30239-x

Danese, S., Feagan, B. G., Wolf, D. C., et al. (2020a), Ozanimod as maintenance therapy in patients with moderate-to-severe ulcerative colitis: results from the phase 3, randomized, double-blind, placebo-controlled true north study. UEG week, virtual conference

Danese, S., Furfaro, F., and Vetrano, S. (2018). Targeting S1P in inflammatory bowel disease: new avenues for modulating intestinal leukocyte migration. *J. Crohns Colitis* 12, S678–S686. doi:10.1093/ecco-jcc/jjx107

Danese, S., Neurath, M. F., Kopoń, A., Zakko, S. F., Simmons, T. C., Fogel, R., et al. (2020b). Effects of apremilast, an oral inhibitor of phosphodiesterase 4, in a randomized trial of patients with active ulcerative colitis. *Clin. Gastroenterol. Hepatol.* 18, 2526–2534. doi:10.1016/j.cgh.2019.12.032

Danese, S., Vermeire, S., Hellstern, P., Panaccione, R., Rogler, G., Fraser, G., et al. (2019). Randomised trial and open-label extension study of an anti-interleukin-6 antibody in Crohn's disease (ANDANTE I and II). *Gut* 68, 40–48. doi:10.1136/gutjnl-2017-314562

Deepak, P., and Sandborn, W. J. (2017). Ustekinumab and anti-interleukin-23 agents in Crohn's disease. *Gastroenterol. Clin. North America* 46, 603–626. doi:10.1016/j.gtc.2017.05.013

D'Haens, G., Danese, S., Davies, M., and Hibi, T (2019). DOP48 Amiselimod, a selective S1P receptor modulator in Crohn's disease patients: a proof-of-concept study. *J. Crohn's Colitis* 13, S055–S056. doi:10.1093/ecco-jcc/jjy222.082

D'Haens, G. R., Reinisch, W., Lee, S. D., Tarabar, D, Louis, E, Kłopocka, M., et al. (2018a). OP024 Long-term safety and efficacy of the anti-MAdCAM monoclonal antibody SHP647 for the treatment of Crohn's disease: the OPERA II study. *J. Crohn's Colitis* 12, S017–S018. doi:10.1093/ecco-jcc/jjx180.023

D'Haens, G. R., Gorelick, K., Wang, Y., Cataldi, F., and Sandborn, W J. (2018b). DOP062 the anti-MAdCAM antibody SHP647 in Crohn's disease: endoscopic effects of induction therapy. *J. Crohn's Colitis* 12, S073. doi:10.1093/ecco-jcc/jjx180.099

FDA Drug Safety Communication (2019). *FDA approves boxed warning about increased risk of blood clots and death with higher dose of arthritis and ulcerative colitis medicine tofacitinib.* XeljanzXeljanz XR).

Feagan, B. G., Panés, J., Ferrante, M., Kaser, A., D'Haens, G. R., Sandborn, W. J., et al. (2018). Risankizumab in patients with moderate to severe Crohn's disease:

an open-label extension study. *Lancet Gastroenterol. Hepatol.* 3, 671–680. doi:10.1016/s2468-1253(18)30233-4

Feagan, B. G., Rutgeerts, P., Sands, B. E., Hanauer, S., Colombel, J.-F., Sandborn, W. J., et al. (2013). Vedolizumab as induction and maintenance therapy for ulcerative colitis. *N. Engl. J. Med.* 369, 699–710. doi:10.1056/nejmoa1215734

Feagan, B. G., Sandborn, W. J., D'Haens, G., Panés, J., Kaser, A., Ferrante, M., et al. (2017). Induction therapy with the selective interleukin-23 inhibitor risankizumab in patients with moderate-to-severe Crohn's disease: a randomised, double-blind, placebo-controlled phase 2 study. *Lancet* 389, 1699–1709. doi:10.1016/s0140-6736(17)30570-6

Feagan, B. G., Sandborn, W. J., Danese, S., Wolf, D. C., Liu, W. J., Hua, S. Y., et al. (2020a). Ozanimod induction therapy for patients with moderate to severe Crohn's disease: a single-arm, phase 2, prospective observer-blinded endpoint study. *Lancet Gastroenterol. Hepatol.* 5, 819–828. doi:10.1016/s2468-1253(20)30188-6

Feagan, B. G., Sandborn, W. J., Gasink, C., Jacobstein, D., Lang, Y., Friedman, J. R., et al. (2016). Ustekinumab as induction and maintenance therapy for Crohn's disease. *N. Engl. J. Med.* 375, 1946–1960. doi:10.1056/nejmoa1602773

Feagan, B. G., Loftus, E. V., Jr, Danese, S., Vermeire, S., Sandborn, W J., Ritter, T., Mehta, R., et al. (2020b), Efficacy and safety OF filgotinib as induction therapy for patients with moderately to severely active ulcerative colitis: results from the phase 2B/3 SELECTION study. UEG, virtual conference *Journal of the Canadian Association of Gastroenterology*. 4(Supplement_1):18-20. doi:10.1093/jcag/gwab002.014

Ferrante, M., Feagan, B. G., Panés, J., Baert, F., Louis, E., Dewit, O., et al. (2020). OP27 Long-term safety and efficacy of risankizumab treatment in patients with Crohn's disease: final results from the Phase 2 open-label extension study. *J. Crohn's Colitis* 14, S024–S025. doi:10.1093/ecco-jcc/jjz203.026

Forman, S. B., Pariser, D. M., Poulin, Y., Vincent, M. S., Gilbert, S. A., Kieras, E. M., et al. (2020). TYK2/JAK1 inhibitor PF-06700841 in patients with plaque psoriasis: phase IIa, randomized, double-blind, placebo-controlled trial. *J. Invest. Dermatol.* 140(12):2359–2370.e5 .doi:10.1016/j.jid.2020.03.962

Gobejishvili, L., Barve, S., Joshi-Barve, S., and McClain, C. (2008). Enhanced PDE4B expression augments LPS-inducible TNF expression in ethanol-primed monocytes: relevance to alcoholic liver disease. *Am. J. Physiology-Gastrointestinal Liver Physiol.* 295, G718–G724. doi:10.1152/ajpgi.90232.2008

Hanauer, S. B., Sandborn, W. J., Rutgeerts, P., Fedorak, R. N., Lukas, M., MacIntosh, D., et al. (2006). Human anti-tumor necrosis factor monoclonal antibody (adalimumab) in Crohn's disease: the CLASSIC-I trial. *Gastroenterology* 130, 323–333. quiz 591. doi:10.1053/j.gastro.2005.11.030

Hanauer, S., Panaccione, R., Danese, S., Cheifetz, A., Reinisch, W., Higgins, P. D. R., et al. (2019). Tofacitinib induction therapy reduces symptoms within 3 Days for patients with ulcerative colitis. *Clin. Gastroenterol. Hepatol.* 17, 139–147. doi:10.1016/j.cgh.2018.07.009

Hanzel, J., and D'Haens, G. R. (2020). Anti-interleukin-23 agents for the treatment of ulcerative colitis. *Expert Opin. Biol. Ther.* 20, 399–406.

Harris, M. S., Hartman, D., Lemos, B. R., Erlich, E. C., Spence, S., Kennedy, S., et al. (2016). AVX-470, an orally delivered anti-tumour necrosis factor Antibody for treatment of active ulcerative colitis: results of a first-in-human trial. *Eccojc* 10, 631–640. doi:10.1093/ecco-jcc/jjw036

Kappos, L., Arnold, D. L., Bar-Or, A., Camm, J., Derfuss, T., Kieseier, B. C., et al. (2016). Safety and efficacy of amiselimod in relapsing multiple sclerosis (MOMENTUM): a randomised, double-blind, placebo-controlled phase 2 trial. *Lancet Neurol.* 15, 1148–1159. doi:10.1016/s1474-4422(16)30192-2

Kappos, L., Radue, E.-W., O'Connor, P., Polman, C., Hohlfeld, R., Calabresi, P., et al. (2010). A placebo-controlled trial of oral fingolimod in relapsing multiple sclerosis. *N. Engl. J. Med.* 362, 387–401. doi:10.1056/nejmoa0909494

Klenske, E., Bojarski, C., Waldner, M., Rath, T., Neurath, M. F., Atreya, R., et al. (2019). Targeting mucosal healing in Crohn's disease: what the clinician needs to know. *Therap Adv. Gastroenterol.* 12, 1756284819856865. doi:10.1177/1756284819856865

Kwak, H. J., Song, J. S., No, Z. S., Song, J. H., Yang, S. D., and Cheon, H. G. (2005). The inhibitory effects of roflumilast on lipopolysaccharide-induced nitric oxide production in RAW264.7 cells are mediated by heme oxygenase-1 and its product carbon monoxide. *Inflamm. Res.* 54, 508–513. doi:10.1007/s00011-005-1386-1

Lin, L., Liu, X., Wang, D., and Zheng, C. (2015). Efficacy and safety of antiintegrin antibody for inflammatory bowel disease. *Medicine (Baltimore)* 94, e556. doi:10.1097/md.0000000000000556

Loftus, E. V., Jr. (2004). Clinical epidemiology of inflammatory bowel disease: incidence, prevalence, and environmental influences. *Gastroenterology* 126, 1504–1517. doi:10.1053/j.gastro.2004.01.063

Ma, C., Lee, J. K., Mitra, A. R., Teriaky, A., Choudhary, D., Nguyen, T. M., et al. (2019). Systematic review with meta-analysis: efficacy and safety of oral Janus kinase inhibitors for inflammatory bowel disease. *Aliment. Pharmacol. Ther.* 50, 5–23. doi:10.1111/apt.15297

Molodecky, N. A., and Kaplan, G. G. (2010). Environmental risk factors for inflammatory bowel disease. *Gastroenterol. Hepatol. (N Y)* 6, 339–346.

Molodecky, N. A., Soon, I. S., Rabi, D. M., Ghali, W. A., Ferris, M., Chernoff, G., et al. (2012). Increasing incidence and prevalence of the inflammatory bowel diseases with time, based on systematic review. *Gastroenterology* 142, 46–54. e42; quiz e30. doi:10.1053/j.gastro.2011.10.001

Ollivier, V., Parry, G. C. N., Cobb, R. R., de Prost, D., and Mackman, N. (1996). Elevated cyclic AMP inhibits NF-κB-mediated transcription in human monocytic cells and endothelial cells. *J. Biol. Chem.* 271, 20828–20835. doi:10.1074/jbc.271.34.20828

Panés, J., Sandborn, W. J., Schreiber, S., Sands, B. E., Vermeire, S., D'Haens, G., et al. (2017). Tofacitinib for induction and maintenance therapy of Crohn's disease: results of two phase IIb randomised placebo-controlled trials. *Gut* 66, 1049–1059. doi:10.1136/gutjnl-2016-312735

Park, S. C., and Jeen, Y. T. (2018). Anti-integrin therapy for inflammatory bowel disease. *Wjg* 24, 1868–1880. doi:10.3748/wjg.v24.i17.1868

Peyrin-Biroulet, L., Feagan, B. G., Mansfield, J., Rubin, D. T., Arulmani, U., Maciuca, R., et al. (2017). OP011 Etrolizumab treatment leads to early improvement in symptoms and inflammatory biomarkers in anti-TNF-refractory patients in the open-label induction cohort of the phase 3 HICKORY study. *J. Crohn's Colitis* 11, S6–S7. doi:10.1093/ecco-jcc/jjx002.010

Peyrin-Biroulet, L., Loftus, E. V., Jr, Danese, S., Vermeire, S., Sandborn, W. J., Fogel, R., Nijhawan, S., et al. (2020), Efficacy and safety OF filgotinib as maintenance therapy for patients with moderately to severely active ulcerative colitis: results from the phase 2B/3 SELECTION study. UEG, virtual conference *Journal of the Canadian Association of Gastroenterology*. 4(Supplement_1):21-23. doi:10.1093/jcag/gwab002.016

Platzer, C., Fritsch, E., Elsner, T., Lehmann, M. H., Volk, H.-D., and Prösch, S. (1999). Cyclic adenosine monophosphate-responsive elements are involved in the transcriptional activation of the human IL-10 gene in monocytic cells. *Eur. J. Immunol.* 29, 3098–3104. doi:10.1002/(sici)1521-4141(199910)29:10<3098::aid-immu3098>3.0.co;2-h

Rothenberg, M. E., Wang, Y., Lekkerkerker, A., Danilenko, D. M., Maciuca, R., Erickson, R., et al. (2019). Randomized phase I healthy volunteer study of UTTR 1147A (IL -22Fc): a potential therapy for epithelial injury. *Clin. Pharmacol. Ther.* 105, 177–189. doi:10.1002/cpt.1164

Rutgeerts, P., Sandborn, W. J., Feagan, B. G., Reinisch, W., Olson, A., Johanns, J., et al. (2005). Infliximab for induction and maintenance therapy for ulcerative colitis. *N. Engl. J. Med.* 353, 2462–2476. doi:10.1056/nejmoa050516

Sabino, J., Verstockt, B., and Vermeire, S., (2019). New biologics and small molecules in inflammatory bowel disease: an update. *Therap Adv. Gastroenterol.* 12, 1756284819853208. doi:10.1177/1756284819853208

Salas, A., Hernandez-Rocha, C., Duijvestein, M., Faubion, W., McGovern, D., Vermeire, S., et al. (2020). JAK-STAT pathway targeting for the treatment of inflammatory bowel disease. *Nat. Rev. Gastroenterol. Hepatol.* 17, 323–337. doi:10.1038/s41575-020-0273-0

Sandborn, W. J., Ferrante, M., Bhandari, B. R., Berliba, E., Hibi, T., D'Haens, G. R., et al. (2020a). Efficacy and safety of continued treatment with mirikizumab in a phase 2 trial of patients with ulcerative colitis. *Clin. Gastroenterol. Hepatol.* doi:10.1016/j.cgh.2020.09.028

Sandborn, W. J., Baert, F., Danese, S., Krznarić, Ž., Kobayashi, T., Yao, X., et al. (2020b). Efficacy and safety of vedolizumab subcutaneous formulation in a randomized trial of patients with ulcerative colitis. *Gastroenterology* 158, 562–572. doi:10.1053/j.gastro.2019.08.027

Sandborn, W. J., Cyrille, M., Berner Hansen, M., Feagan, B. G., Loftus, E. V., Vermeire, S., et al. (2017a). OP035 Efficacy and safety of abrilumab (AMG 181/MEDI 7183) therapy for moderate to severe Crohn's disease. *J. Crohn's Colitis* 11, S22–S23. doi:10.1093/ecco-jcc/jjx002.034

Sandborn, W. J., Cyrille, M., Hansen, M. B., Feagan, B. G., Loftus, E. V., Rogler, G., et al. (2019). Efficacy and safety of abrilumab in a randomized, placebo-

controlled trial for moderate-to-severe ulcerative colitis. *Gastroenterology* 156, 946–957. doi:10.1053/j.gastro.2018.11.035

Sandborn, W. J., Feagan, B. G., Loftus, E. V., Jr., Peyrin-Biroulet, L., Van Assche, G., D'Haens, G., et al. (2020c). Efficacy and safety of upadacitinib in a randomized trial of patients with Crohn's disease. *Gastroenterology* 158, 2123–2138. doi:10.1053/j.gastro.2020.01.047

Sandborn, W. J., Feagan, B. G., Rutgeerts, P., Hanauer, S., Colombel, J.-F., Sands, B. E., et al. (2013). Vedolizumab as induction and maintenance therapy for Crohn's disease. *N. Engl. J. Med.* 369, 711–721. doi:10.1056/nejmoa1215739

Sandborn, W. J., Feagan, B. G., Wolf, D. C., D'Haens, G., Vermeire, S., Hanauer, S. B., et al. (2016). Ozanimod induction and maintenance treatment for ulcerative colitis. *N. Engl. J. Med.* 374, 1754–1762. doi:10.1056/nejmoa1513248

Sandborn, W. J., Ferrante, M., Bhandari, B. R., Berliba, E., Feagan, B. G., Hibi, T., et al. (2020d). Efficacy and safety of mirikizumab in a randomized phase 2 study of patients with ulcerative colitis. *Gastroenterology* 158, 537–549. doi:10.1053/j.gastro.2019.08.043

Sandborn, W. J., Ghosh, S., Panes, J., Schreiber, S., D'Haens, G., Tanida, S., et al. (2020e). Efficacy of upadacitinib in a randomized trial of patients with active ulcerative colitis. *Gastroenterology* 158, 2139–2149. doi:10.1053/j.gastro.2020.02.030

Sandborn, W. J., Hanauer, S. B., Rutgeerts, P., Fedorak, R. N., Lukas, M., MacIntosh, D. G., et al. (2007). Adalimumab for maintenance treatment of Crohn's disease: results of the CLASSIC II trial. *Gut* 56, 1232–1239. doi:10.1136/gut.2006.106781

Sandborn, W. J., Lee, S. D., Tarabar, D., Louis, E., Klopocka, M., Klaus, J., et al. (2018). Phase II evaluation of anti-MAdCAM antibody PF-00547659 in the treatment of Crohn's disease: report of the OPERA study. *Gut* 67, 1824–1835. doi:10.1136/gutjnl-2016-313457

Sandborn, W. J., Nguyen, D. D., Beattie, D. T., Brassil, P., Krey, W., Woo, J., et al. (2020f). Development of gut-selective pan-janus kinase inhibitor TD-1473 for ulcerative colitis: a translational medicine programme. *J. Crohns Colitis* 14, 1202–1213. doi:10.1093/ecco-jcc/jjaa049

Sandborn, W. J., Peyrin-Biroulet, L., Zhang, J., Chiorean, M., Vermeire, S., Lee, S. D., et al. (2020g). Efficacy and safety of etrasimod in a phase 2 randomized trial of patients with ulcerative colitis. *Gastroenterology* 158, 550–561. doi:10.1053/j.gastro.2019.10.035

Sandborn, W. J., Su, C., Sands, B. E., D'Haens, G. R., Vermeire, S., Schreiber, S., et al. (2017b). Tofacitinib as induction and maintenance therapy for ulcerative colitis. *N. Engl. J. Med.* 376, 1723–1736. doi:10.1056/nejmoa1606910

Sandborn, W. J., Vermeire, S., Vermeire, S., Tyrrell, H., Hassanali, A., Lacey, S., et al. (2020h). Etrolizumab for the treatment of ulcerative colitis and Crohn's disease: an overview of the phase 3 clinical program. *Adv. Ther.* 37, 3417–3431. doi:10.1007/s12325-020-01366-2

Sandborn, W. J., Chan, D., and Johanns, J., (2020i). The efficacy and safety OF guselkumab induction therapy IN patients with moderately to severely active CROHN'S disease: week 12 interim analyses from the phase 2 GALAXI 1 study. UEG, virtual conference

Sandborn, W., D'Haens, G. R., and Wolf, D. C., (2020), Ozanimod as induction therapy IN moderate-to-severe ulcerative colitis: results from the phase 3, randomized, double-blind, placebo-controlled true north study. UEG, virtual conference

Sands, B. E., Anderson, F. H., Bernstein, C. N., Chey, W. Y., Feagan, B. G., Fedorak, R. N., et al. (2004). Infliximab maintenance therapy for fistulizing Crohn's disease. *N. Engl. J. Med.* 350, 876–885. doi:10.1056/nejmoa030815

Sands, B. E., Chen, J., Feagan, B. G., Penney, M., Rees, W. A., Danese, S., et al. (2017). Efficacy and safety of MEDI2070, an antibody against interleukin 23, in patients with moderate to severe Crohn's disease: a phase 2a study. *Gastroenterology* 153, 77–86. doi:10.1053/j.gastro.2017.03.049

Sands, B. E., Sandborn, W. J., Panaccione, R., O'Brien, C. D., Zhang, H., Johanns, J., et al. (2019a). Ustekinumab as induction and maintenance therapy for ulcerative colitis. *N. Engl. J. Med.* 381, 1201–1214. doi:10.1056/nejmoa1900750

Sands, B. E., Sandborn, W. J., Peyrin-Biroulet, L., Higgins, P. D., Hirai, F., Belin, R., et al. (2019b). 1003 - efficacy and safety of mirikizumab (LY3074828) in a phase 2 study of patients with Crohn's disease. *Gastroenterology* 156, S. doi:10.1016/s0016-5085(19)37335-4

Sands, B. E., Sandborn, W. J., and Peyrin-Biroulet, L., (2020), Efficacy and safety OF mirikizumab after 52-WEEKS maintenance treatment IN patients with moderate-to-severe CROHN'S disease. UEG virtual conference 2020.

Schreiber, S., Khaliq-Kareemi, M., Lawrance, I. C., Thomsen, O. Ø., Hanauer, S. B., McColm, J., et al. (2007). Maintenance therapy with certolizumab pegol for Crohn's disease. *N. Engl. J. Med.* 357, 239–250. doi:10.1056/nejmoa062897

Selinger, C., Sandborn, W., Panes, J., Jones, J., Hassanali, A., Jacob, R., et al. (2018). OTU-003 Etrolizumab as induction therapy in moderate to severe crohn's disease: results from bergamot cohort 1. *Gut* 67, A53. doi:10.1136/gutjnl-2018-bsgabstracts.106

Shivashankar, R., and Lewis, J. D. (2017a). The role of diet in inflammatory bowel disease. *Curr. Gastroenterol. Rep.* 19, 22. doi:10.1007/s11894-017-0563-z

Shivashankar, R., and Pardi, D. S. (2017b). Use of anti-tumor necrosis factors and anti-integrins in the treatment of Crohn's disease. *Gastroenterol. Clin. North America* 46, 589–601. doi:10.1016/j.gtc.2017.05.012

Sugiura, T., Kageyama, S., Andou, A., Miyazawa, T., Ejima, C., Nakayama, A., et al. (2013). Oral treatment with a novel small molecule alpha 4 integrin antagonist, AJM300, prevents the development of experimental colitis in mice. *J. Crohn's Colitis* 7, e533–e542. doi:10.1016/j.crohns.2013.03.014

Targan, S. R., Feagan, B. G., Fedorak, R. N., Lashner, B. A., Panaccione, R., Present, D. H., et al. (2007). Natalizumab for the treatment of active Crohn's disease: results of the ENCORE Trial. *Gastroenterology* 132, 1672–1683. doi:10.1053/j.gastro.2007.03.024

Vermeire, S., O'Byrne, S., Keir, M., Williams, M., Lu, T. T., Mansfield, J. C., et al. (2014). Etrolizumab as induction therapy for ulcerative colitis: a randomised, controlled, phase 2 trial. *Lancet* 384, 309–318. doi:10.1016/s0140-6736(14)60661-9

Vermeire, S., Sandborn, W. J., Danese, S., Hébuterne, X., Salzberg, B. A., Klopocka, M., et al. (2017a). Anti-MAdCAM antibody (PF-00547659) for ulcerative colitis (TURANDOT): a phase 2, randomised, double-blind, placebo-controlled trial. *The Lancet* 390, 135–144. doi:10.1016/s0140-6736(17)30930-3

Vermeire, S., Schreiber, S., Petryka, R., Kuehbacher, T., Hebuterne, X., Roblin, X., et al. (2017b). Clinical remission in patients with moderate-to-severe Crohn's disease treated with filgotinib (the FITZROY study): results from a phase 2, double-blind, randomised, placebo-controlled trial. *Lancet* 389, 266–275. doi:10.1016/s0140-6736(16)32537-5

Wagner, F., Mansfield, J., Geier, C., Dash, A., Wang, Y., Li, C., et al. (2020). P420 A randomised, observer-blinded phase Ib multiple, ascending dose study of UTTR1147A, an IL-22Fc fusion protein, in healthy volunteers and ulcerative colitis patients. *J. Crohn's Colitis* 14, S382–S383. doi:10.1093/ecco-jcc/jjz203.549

Winthrop, K. L., Melmed, G. Y., Vermeire, S., Long, M. D., Chan, G., Pedersen, R. D., et al. (2018). Herpes zoster infection in patients with ulcerative colitis receiving tofacitinib. *Inflamm. Bowel Dis.* 24, 2258–2265. doi:10.1093/ibd/izy131

Yoshimura, N., Watanabe, M., Motoya, S., Tominaga, K., Matsuoka, K., Iwakiri, R., et al. (2015). Safety and efficacy of AJM300, an oral antagonist of α4 integrin, in induction therapy for patients with active ulcerative colitis. *Gastroenterology* 149, 1775–1783. doi:10.1053/j.gastro.2015.08.044

Conflict of Interest: The authors declare that the research was conducted in the absence of any commercial or financial relationships that could be construed as a potential conflict of interest.

Copyright © 2021 Al-Bawardy, Shivashankar and Proctor. This is an open-access article distributed under the terms of the Creative Commons Attribution License (CC BY). The use, distribution or reproduction in other forums is permitted, provided the original author(s) and the copyright owner(s) are credited and that the original publication in this journal is cited, in accordance with accepted academic practice. No use, distribution or reproduction is permitted which does not comply with these terms.

frontiers in Pharmacology

ORIGINAL RESEARCH
published: 22 April 2021
doi: 10.3389/fphar.2021.663774

Targeting Gremlin 1 Prevents Intestinal Fibrosis Progression by Inhibiting the Fatty Acid Oxidation of Fibroblast Cells

Yang Yang[1,2,3], *Qi-Shan Zeng*[1,2], *Min Zou*[1,2], *Jian Zeng*[4], *Jiao Nie*[2,5], *DongFeng Chen*[3] *and Hua-Tian Gan*[1,2,5]*

[1]Department of Gastroenterology and the Center of Inflammatory Bowel Disease, West China Hospital, Sichuan University, Chengdu, China, [2]Lab of Inflammatory Bowel Disease, Clinical Institute of Inflammation and Immunology, Frontiers Science Center for Disease-related Molecular Network, West China Hospital, Sichuan University, Chengdu, China, [3]Department of Gastroenterology, Daping Hospital, Army Medical University, Chongqing, China, [4]Department of Gastroenterology, Chongqing Traditional Chinese Medicine Hospital, Chongqing, China, [5]Department of Geriatrics and National Clinical Research Center for Geriatric, West China Hospital, Sichuan University, Chengdu, China

Intestinal fibrosis is a consequence of continuous inflammatory responses that negatively affect the quality of life of patients. By screening altered proteomic profiles of mouse fibrotic colon tissues, we identified that GREM1 was dramatically upregulated in comparison to that in normal tissues. Functional experiments revealed that GREM1 promoted the proliferation and activation of intestinal fibroblast cells by enhancing fatty acid oxidation. Blocking GREM1 prevented the progression of intestinal fibrosis *in vivo*. Mechanistic research revealed that GREM1 acted as a ligand for VEGFR2 and triggered downstream MAPK signaling. This facilitated the expression of FAO-related genes, consequently enhancing fatty acid oxidation. Taken together, our data indicated that targeting GREM1 could represent a promising therapeutic approach for the treatment of intestinal fibrosis.

Keywords: intestinal fibrosis, gremlin 1, fibroblast cell, fatty acid oxidation, VEGFR2

OPEN ACCESS

Edited by:
Barbara Romano,
University of Naples Federico II, Italy

Reviewed by:
David Michael Dolivo,
Northwestern University,
United States
Yun Zhang,
University Hospital Erlangen, Germany

***Correspondence:**
Hua-Tian Gan
ght_2021@163.com

Specialty section:
This article was submitted to Gastrointestinal and Hepatic Pharmacology, a section of the journal Frontiers in Pharmacology

Received: *03 February 2021*
Accepted: *08 April 2021*
Published: *22 April 2021*

Citation:
Yang Y, Zeng Q-S, Zou M, Zeng J, Nie J, Chen D and Gan H-T (2021) Targeting Gremlin 1 Prevents Intestinal Fibrosis Progression by Inhibiting the Fatty Acid Oxidation of Fibroblast Cells. Front. Pharmacol. 12:663774. doi: 10.3389/fphar.2021.663774

INTRODUCTION

Intestinal fibrosis, a common complication of inflammatory bowel disease (IBD) (Leake, 2015), is characterized by exaggerated scar tissue formation in the colon mucosa (Rieder and Fiocchi, 2009) resulting from intestinal damage induced by chronic inflammation (Lawrance et al., 2017). Despite great progress in the treatment of IBD, the incidence of intestinal fibrosis has not markedly reduced (Su et al., 2016; Vítek and Tiribelli, 2020), indicating that the development of new targeted therapies or effective interventions for intestinal fibrosis are urgently needed.

Intestinal fibroblasts, the major effector cells of gastrointestinal fibrosis (Weder et al., 2018), mainly account for the synthesis of several extracellular matrix proteins. This includes collagens, vimentin, and fibronectin (Hagenlocher et al., 2017). During chronic inflammation processes, local gut mesenchymal cells are activated and proliferated. This leads to enhanced deposition of extracellular-matrix proteins. Previous studies reported that resident fibroblasts can be activated by inflammation-related proteins (Lawrance et al., 2001), including the growth factors IGF-I, FGF, and PDGF, and the pro-inflammatory cytokines IL-1β and TNF-α (Simmons et al., 2002). This results in expansion of fibroblast cell numbers and fibroblast differentiation. In addition, colonic

transforming growth factor (TGF)-β1 overexpression results in fibroblast accumulation and bowel wall thickening (Vallance et al., 2005). Apart from cytokines, growth factors, and chemokines, local fibroblasts resident in the colon can also respond to other biological mediators (Fichtner-Feigl et al., 2007; Burke et al., 2008). Thus, screening new biological mediators may provide potential therapeutic targets.

GREM1, encoded by the *GREM1* gene (Mezzano et al., 2018), is an important protein secreted in development, including organ formation, physique development, and tissue differentiation. GREM1 is considered to be an antagonist of the bone morphogenetic protein (BMP) family members and binds to BMP2 to regulate the BMP signaling pathway (Hsu et al., 1998). Later studies revealed that GREM1 can act as a vascular endothelial growth factor receptor 2 (VEGFR2) ligand in vascular endothelial cells to regulate angiogenesis (Mitola et al., 2010). Additionally, GREM1 has been reported to be both tumor promotive and suppressive in cancer. Elevated GREM1 expression is associated with favorable outcomes in several malignancies, including colon adenocarcinoma (Nyqvist et al., 2017) and gastric cancer (Honma et al., 2018). On the other hand, increased GREM1 expression facilitates the proliferation of cancer cells in lung adenocarcinoma and glioma. However, the role of GREM1 in intestinal fibrosis remains unknown.

In this study, we found that protein levels of GREM1 were dramatically increased in fibrotic colon. The loss and gain of function experiments revealed that GREM1 promoted intestinal fibroblast cell proliferation by enhancing fatty acid oxidation. Further mechanistic studies revealed that GREM1 could activate VEGFR2 and trigger downstream MAPK signaling. This facilitates FAO-related gene expression, consequently enhancing fatty acid oxidation and results in fibroblast cell proliferation and activation. Taken together, these results provide evidence that GREM1 could be a potential target for intestinal fibrosis therapy.

MATERIALS AND METHODS

Animal Experiments

All animal experiments were approved by the Institutional Animal Care and Use Committee (IACUC) of the Army Medical University, and were authorized by the Institutional Animal Care and Use Committee of the Laboratory Animal Center of Daping Hospital, Army Medical University. Mouse intestinal fibrosis was induced by the administration of 2.5% dextran sulfate sodium (DSS) in tap water for 5 days followed by 1°week of normal drinking water for three cycles (Speca et al., 2016). The mice were sacrificed at nine weeks after DSS treatment. Intestinal tissues were formalin-fixed and embedded in paraffin for further analysis.

Cell Lines

Human intestinal fibroblast cell lines CCD-18Co and CCD-112Co were maintained at the Daping Hospital, Army Medical University. Cells were cultured in Dulbecco's modified Eagle's medium (DMEM) supplemented with 10% fetal bovine serum (FBS, Gibco), 100°U/ml penicillin and 100 μg/ml streptomycin at 37°C in a 5% CO_2 atmosphere. Exogenous GREM1, used for cell treatment, purchased from R&D system (cat#:5190-GR-050). STR identification was conducted to exclude exogenic cell contamination.

Cell Proliferation Assays

Enumeration of fibroblasts was performed using Cell Counting Kit-8 (CCK8, NCM), according to the manufacturer's instructions. Cells were cultured in 96-well plates at 3,000 cells/well. Serum conditions included no serum added to the culture medium, and other components were consistent with full medium. At the indicated time points, the cell culture medium was changed to a CCK8 buffer, and after 90 min incubation at 37°C, under 5% CO_2, OD_{450} values were measured to determine cell viability.

Transfection and RNA Interference

siRNA transfection was conducted using Lipofectamine® 2000 (Invitrogen) according to the manufacturer's instructions. siRNA was purchased from GenePharma and Shanghai BioTend Biotech Co. Total cellular RNA was extracted after 48 h of transfection. SiRNA sequences are presented in **Supplementary Material**.

RNA Isolation and Q-PCR

Total RNA was isolated using Trizol reagent (Takara, 9109) and reverse transcription was performed using PrimeScript kits (Takara, RR037A). To detect gene expression, RT-qPCR assays were performed using SYBR Premix Ex Taq (Roche) using the recommended thermal settings. Relative mRNA expression was analyzed using the 2 (-ΔΔCt) method and normalized to that of 18S ribosomal RNA. PCR primer sequences are presented in Supplementary materials.

Immunoblotting

Whole cell lysates were prepared with RIPA lysis buffer (share-bio Tech) and membrane proteins were extracted using a Membrane and Cytosol Protein Extraction Kit (Beyotime). Quantification of protein concentrations was performed using a BCA protein assay kit (Thermo Fisher Scientific Proteins were resolved by 4–20% SDS-PAGE and transferred to NC membranes (Whatman), then antibody and ECL methods were employed to measure protein expression levels. Primary antibodies used were as follows: anti-GREM1 (R&D Systems, AF956, 1:1,000), anti-phospho-VEGF Receptor 2 (Tyr1175) (CST, #3770, 1:1,000), anti-VEGF receptor 2 (CST, #2479, 1:1,000), anti-phospho-MEK1/2 (Ser217/221) (CST, #3958, 1:1,000), anti-MEK1/2 (CST, #4694, 1:1,000), anti-phospho-p44/42 MAPK (Erk1/2) (Thr202/Tyr204) (CST, #9101,1:1,000), and anti-p44/42 MAPK (Erk1/2) (CST, #4695, 1:1,000). The secondary antibodies were anti-rabbit (share-bio, SB-AB0101, Abways Technology, AB0151), anti-mouse (share-bio, SB-AB0102, Yeasen Biotech Co., 33206ES60), and anti-goat (Immunoway Biotech Co., RS2123; Abcam, ab175776).

Sample Preparation and Proteomic Analyses

The fibrosis colon and control group samples were grinded by liquid nitrogen into cell powder and then transferred to a 5-ml

centrifuge tube. After that, four volumes of lysis buffer (8 M urea, 1% protease Inhibitor Cocktail) was added to the cell powder, followed by sonication three times on ice using a high intensity ultrasonic processor (Scientz). The remaining debris was removed by centrifugation at 12,000 g at 4°C for 10 min. As for proteomic analyses, trypsin was added into the protein solution at 1:50 trypsin-to-protein mass ratio for the first digestion overnight and 1:100 trypsin-to-protein mass ratio for a second 4 h-digestion. Then, the tryptic peptides were dissolved in 0.1% formic acid (solvent A), directly loaded onto a home-made reversed-phase analytical column (15-cm length, 75 μm i.d.). The gradient was comprised of an increase from 6 to 23% solvent B (0.1% formic acid in 98% acetonitrile) over 26 min, 23–35% in 8 min and climbing to 80% in 3 min then holding at 80% for the last 3 min, all at a constant flow rate of 400 nL/min on an EASY-nLC 1000 UPLC system.

The peptides were subjected to NSI source followed by tandem mass spectrometry (MS/MS) in Q ExactiveTM Plus (Thermo) coupled online to the UPLC. The electrospray voltage applied was 2.0 kV. The m/z scan range was 350–1800 for full scan, and intact peptides were detected in the Orbitrap at a resolution of 70,000. Peptides were then selected for MS/MS using NCE setting as 28 and the fragments were detected in the Orbitrap at a resolution of 17,500. A data-dependent procedure that alternated between one MS scan followed by 20 MS/MS scans with 15.0 s dynamic exclusion. Automatic gain control (AGC) was set at 5E4. Fixed first mass was set as 100 m/z. The resulting MS/MS data were processed using Maxquant search engine (v.1.5.2.8). Tandem mass spectra were searched against human uniprot database concatenated with reverse decoy database. Trypsin/*P* was specified as cleavage enzyme allowing up to four missing cleavages. The mass tolerance for precursor ions was set as 20 ppm in First search and 5 ppm in Main search, and the mass tolerance for fragment ions was set as 0.02 Da. Carbamidomethyl on Cys was specified as fixed modification and acetylation modification and oxidation on Met were specified as variable modifications. FDR was adjusted to <1% and minimum score for modified peptides was set >40.

Histology Score

We scored all histological sections of the colonic samples in double-blind, according to the presence of ulcerations (0 = absent, 1 = small ulcers, 2 = big ulcers), degree of inflammation (0 = absent, 1 = mild, 2 = moderate, and 3 = severe), depth of the lesions (0 = absent, 1 = lesions extending in the submucosa, 2 = lesions in the muscularis propria, and 3 = lesions in the serosa), and degree of fibrosis (0 = absent; 1 = mild, 2 = moderate, and 3 = severe). The sum of these scores was expressed as total microscopic score.

Immunofluorescence and Immunohistochemistry

Cells cultured on Millicell® EZ SLIDE (MILLIPORE) were fixed with 4% paraformaldehyde for 15 min and permeabilized with 0.1% Triton X-100 for 1 min at room temperature. After blocking with BSA (Sangon Biotech), samples were incubated with the primary antibody (1:200) overnight at 4°C, and the secondary antibody–labeled with fluorescein (1:200)–for 1 h at room temperature. Finally, DAPI was used to counterstain nuclei and the sample images were captured using a confocal microscope. For immunofluorescent staining of living cells to locate membrane proteins, cells were rinsed with cold PBS, followed by incubation with primary and secondary antibodies (1:500) for 1 h at 4°C. Next, the cells were fixed with 4% paraformaldehyde and stained with DAPI. For immunohistochemistry, slides were deparaffinized in xylene, and then antigen retrieval was performed using a citrate antigen retrieval solution. Endogenous peroxidase activity was blocked through the addition of hydrogen peroxide. After blocking with 10% BSA at room temperature, slides were incubated with primary antibodies at 4°C overnight. Following 1 h incubation with HPR-conjugated secondary antibody (anti-mouse, 1:500, Jackson ImmunoResearch, 115–035–003 or rabbit secondary antibodies 1:500 Jackson ImmunoResearch, 111–035–003), slides were developed in DAB (CST, 8059) and counterstained with hematoxylin.

BODIPY Staining

BODIPY staining was conducted according to standard procedures. Briefly, control and GREM1 treated fibroblasts were incubated with the BODIPY dye solution (Servicebio, GP1104) at room temperature in the dark for 1 h, followed by nuclear staining with DAPI and examination by confocal microscopy. Cells in five images of each sample were counted using ImageJ software.

Lipid Lysis Product Analysis

The amounts of acylcarnitine and acetyl-CoA were measured according to a previously reported method (Cheng et al., 2020). Briefly, serum-free cultured fibroblasts were treated with GREM1 and were collected and homogenized. They were then suspended in chloroform/methanol (1:1), and analyzed by mass spectrometry. The amounts of acylcarnitine and acetyl-CoA were normalized to the total protein content of fibroblast cells.

Public Dataset Bioinformatic Analysis

SRA datasets (SRP077046 and SRP100787) containing data for tissues from both healthy controls and CD and UC patients. The mRNA expression level of *GREM1* was compared in both healthy controls and CD and UC patients.

Seahorse Assays

The extracellular acidification rate (ECAR) and oxygen consumption rate (OCR) were determined using standard methods. Briefly, cells were seeded in XF96-well plates at a density of 2×10^4/well. For glycolytic stress testing (Seahorse Bioscience, catalog no. 103020–100), 10 mmol/L glucose, 1 mmol/L oligomycin, and 50 mmol/L 2-deoxyglucose (2-DG) were used. For mitochondrial stress tests (Seahorse Bioscience, catalog no. 103015–100), 1 mmol/L oligomycin, 1 mmol/L FCCP, 0.5 mmol/L rotenone, and 0.5 mmol/L actinomycin A were used. Total cellular protein was used to normalize the measurements.

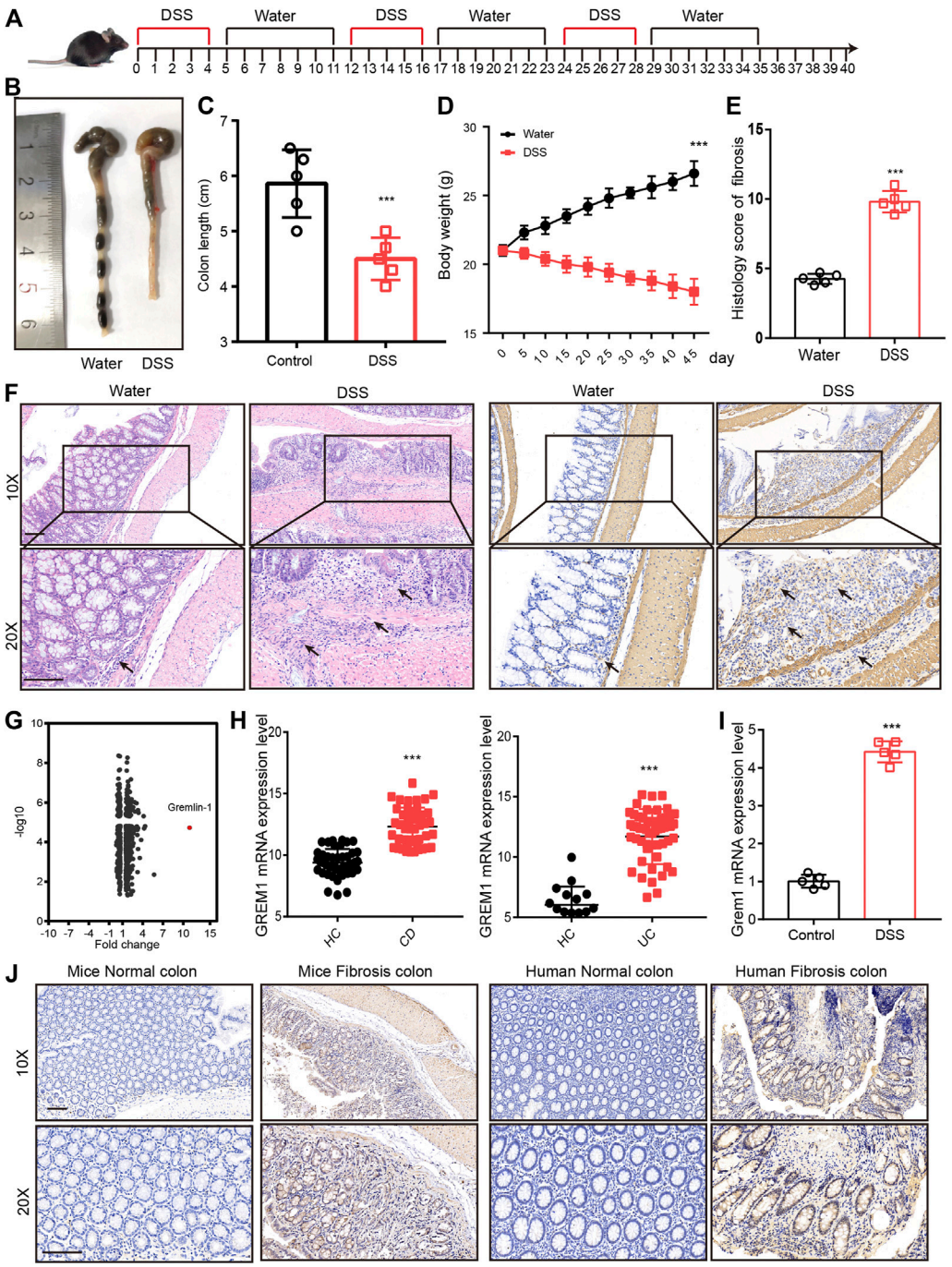


FIGURE 1 | GREM1 expression increased in intestinal fibrosis. **(A)**. C57BL/6J mice were subjected to three cycles of 2.5% DSS for 5°days followed by 1 week of recuperation to establish mice intestinal fibrosis model. **(B)**. The appearance of the colons from the mice in control or DSS treated groups. **(C)**. The colon length statical results of mice from control or DSS treated group ($n = 5$). **(D)**. The body weight curve of mice received control or DSS treatment ($n = 5$), p values are derived from one-way ANOVA analysis. **(E)**. The histology score of intestinal fibrosis mice with different treatment. Fibrosis was quantified using a combined score of fibrosis severity, circularity and the extent of fibrosis ($n = 5$). **(F)**. The hematoxylin and eosin staining **(left panel)** and α-SMA IHC staining **(right panel)** of distal colon sections from control and DSS treated mice. scale bar 200 μm. **(G)**. The different expressed protein in DSS treatment mice and control mice that derived from proteomics analysis. **(H)**. The mRNA expression of GREM1 (human) in healthy control (HC) and IBD patient's data from SRP077046 and SRP100787. **(I)**. The mRNA expression of *Grem1* in control and intestinal fibrosis mice ($n = 5$). **(J)**. IHC staining of GREM1 in both mice and human in intestinal fibrosis tissues. scale bar 200 μm. p values are derived from two-sided Student's t test. $^{**}p \leq 0.01$; $^{***}p \leq 0.001$.

Statistical Analysis

All statistical analyses were carried out using GraphPad Prism v.7.0. D'Agostino and Pearson omnibus normality test to determine whether the data are normally distributed. For two-group comparisons, two-tailed Student's *t*-test was used for statistical analysis. After testing for normal distribution, statistical analysis was performed using ANOVA when more than two groups were compared. All data are presented as means ± SD (n.s., $p > 0.05$; *$p \leq 0.05$; **$p \leq 0.01$; ***,$p \leq 0.001$).

RESULTS

Increased GREM1 Expression in Intestinal Fibrosis

To screen for potential therapeutic targets for intestinal fibrosis, we established an intestinal fibrosis mouse model by oral administration of three 2.5% DSS cycles to C57BL/6J mice (**Figure 1A**). The results showed that all DSS-treated mice developed serious colitis, and colon length and body weight were significantly lower in DSS-treated mice (**Figures 1B–E**). Further, intestinal tissue sections were subjected to hematoxylin-eosin (H&E) and anti-α-SMA immunohistochemical (IHC) staining. Pathological examination revealed that mice that received DSS treatment developed intestinal fibrosis, with fibroblast proliferation and ECM deposition (**Figure 1F**). Proteomic analysis of intestinal tissues indicated that GREM1 protein levels were dramatically elevated in fibrosed colon compared to that in normal colon tissue (**Figure 1G**). To confirm this in humans, we first compared *GREM1* mRNA expression using SRA datasets (SRP077046 and SRP100787) containing data for tissues from both healthy controls and CD and UC patients. The results showed that *GREM1* mRNA levels were significantly increased in human intestinal colitis samples (**Figure 1H**). Furthermore, we detected *GREM1* mRNA expression in intestinal fibrosis tissue and found that *GREM1* mRNA expression was also upregulated in fibrosed colon (**Figure 1I**). In line with this, IHC staining results revealed that GREM1 protein levels were greatly elevated in both murine and human intestinal fibrosis sections (**Figure 1J**). Collectively, these results suggested that GREM1 abundance was significantly increased in fibrosed colon tissues.

GREM1 Promotes Intestinal Fibroblast Proliferation and Activation

Next, we aimed to investigate the functional roles of GREM1 in the process of intestinal fibrosis development. Given that fibroblasts are the dominant effector cells in the development of intestinal fibrosis, we postulated whether GREM1 could promote proliferation and activation of intestinal fibroblasts. Two human intestinal fibroblast cell lines, CCD-18Co and CCD-112Co, were treated with different doses of the GREM1 protein in a serum-free culture medium. The results showed that GREM1 promoted fibroblast cell growth in a dose-dependent manner (**Figure 2A**). Further, to reveal whether GREM1 could facilitate the activation of fibroblasts, RT-qPCR was performed to detect altered expression of several typical fibroblast activation related genes, including *ACTA2*, *COL1A1, COL4A1*, and *VIM* in fibroblast cells upon administration of GREM1. Consistently, GREM1 treatment significantly increased the expression of these genes (**Figures 2B–E**). Given that activated fibroblasts could facilitate the progression of intestinal fibrosis by secreting cytokines, ELISA was performed to detect protein levels of IL-6, IL-1β, MCP1, and TNF. Levels of these cytokines were greatly increased after GREM1 treatment (**Figure 2F**). To further confirm this, intestinal fibroblast cell lines derived from patients with colon fibrosis were established following GREM1 ectopic expression or knockdown (**Supplementary Figure S1**). The results showed that additional GREM1 treatment significantly promoted the proliferation and activation of fibroblasts (**Figure 2G**). Conversely, the silencing of *GREM1* in fibroblasts delayed the fibrotic process (**Figure 2H**). Taken together, these data indicated that GREM1 could promote intestinal fibroblast proliferation and activation.

GREM1 Promotes Intestinal Fibroblast Proliferation by Enhancing Fatty Acid Oxidation

After stimulation with inflammatory effectors, fibroblasts start to proliferate and undergo trans-differentiation into contractile myofibroblasts, accompanied by energy status switching from quiescent to activated. In the kidney fibroblasts, Dario reported that Interleukin-1β activates a MYC-dependent metabolic switch in kidney stromal cells necessary for progressive tubulointerstitial fibrosis (Lemos et al., 2018). In addition, proceeding study reported that lipid metabolism in activated hepatic stellate cells is enhanced during liver fibrosis (Khomich et al., 2019); thus, we measured the lipid droplet content in GREM1-treated fibroblasts. BODIPY staining results showed that the abundance of lipid droplets was significantly decreased in GREM1 treated fibroblasts (**Figure 3A**). Next, the two major fatty acid oxidation products were measured in fibroblast cells treated with GREM1 or not. The results showed that acylcarnitine, derived from fatty acid oxidation by carnitine palmitoyl-transferase 1, (Schreurs et al., 2010; Qu et al., 2016), was significantly increased (**Figure 3B**). In line with this, the amounts of acetyl-CoA and fatty acid β-oxidation breakdown products were greatly elevated (**Figure 3C**). Furthermore, the OCR of GREM1-treated fibroblast cells was detected using a Seahorse. The data showed that GREM1 treatment markedly enhanced OCRs in fibroblast cells (**Figure 3D**, **Supplementary Figure S2A**). Moreover, GREM1 treatment did not affect the ECAR (**Supplementary Figure S2B**). Given that fatty acid oxidation produced much amount of energy, which could support the activation and proliferation of fibroblast. Furthermore, we aim to identify whether the promoting effects of GREM1 depended on enhanced FAO

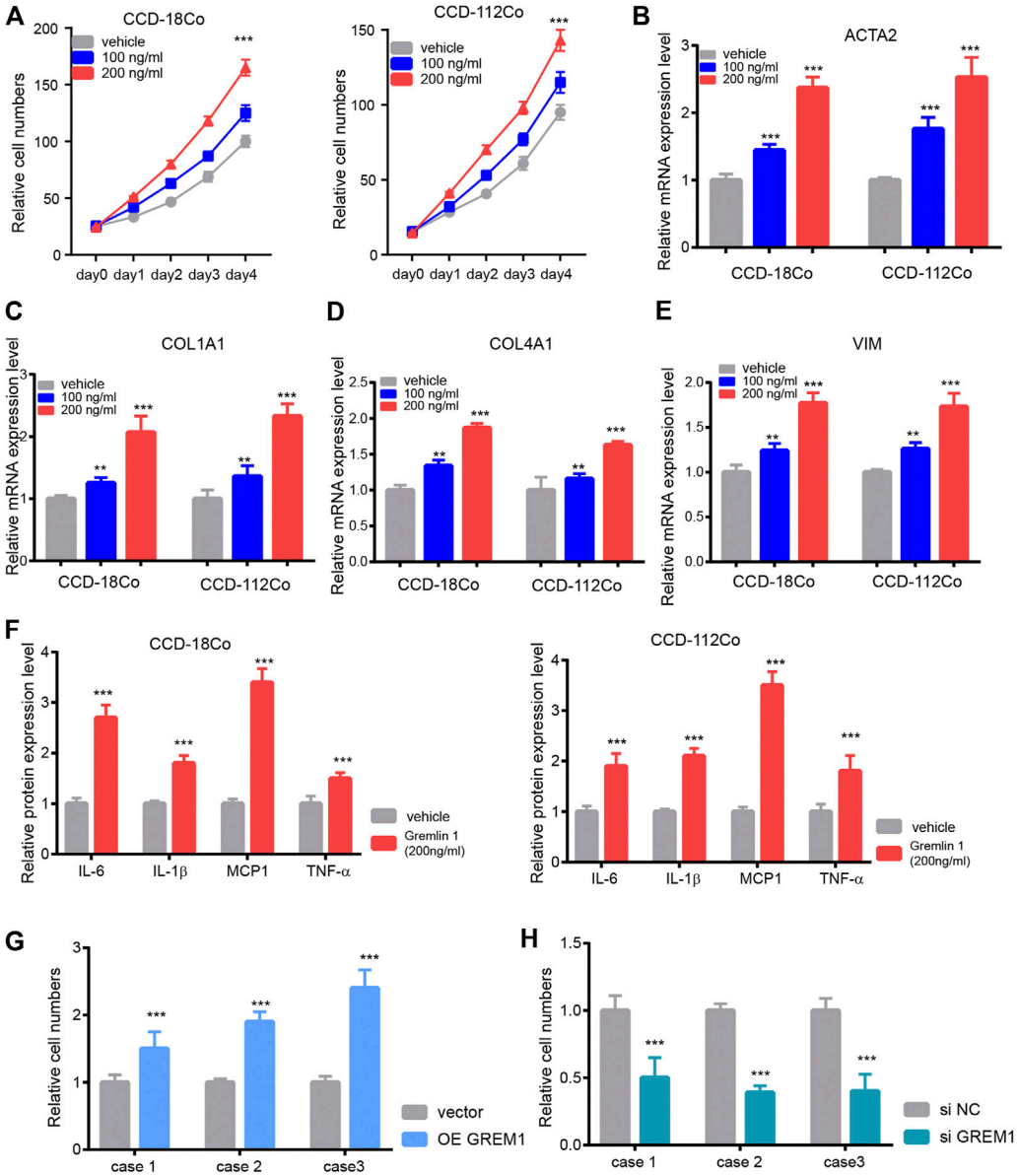


FIGURE 2 | Gremlin 1 promotes the proliferation and activation of intestinal fibroblast. **(A)**. Cell viability assay of human intestinal fibroblast cells CCD-18Co and CCD-112Co upon different dose of Gremlin 1 (100 and 200 ng/ml) treatment. **(B–E)**. The Q-PCR results of ACTA2 **(B)**, COL1A1 **(C)**, COL4A1 **(D)** and VIM **(E)**, intestinal fibroblast cells CCD-18Co and CCD-112Co upon 100 and 200 ng/ml of Gremlin 1 treatment for 24 h. **(F)**. The foldchanges of inflammation cytokines in human fibroblast cells CCD-18Co and CCD-112Co upon 200 ng/ml Gremlin 1 treatment for 24 h. **(G)**. The system of fibroblast and intestinal organoid culture system. **(H–I)**. The relative IL-1β level in the culture medium of the human intestinal organoid upon co-cultured with GREM1 gene overexpressed fibroblast cell **(H)** or GREM1 gene knockdown fibroblast cell **(I)** for 48 h. These experiments were repeated twice. *p* values are derived from one-way ANOVA analysis. Dunnett's test was used to analysis the difference between control group to the other groups. $^{**}p \leq 0.01$; $^{***}p \leq 0.001$.

in fibroblasts. We firstly detected the expression of FAO related genes in fibroblast cells upon GREM1 treatment. The results showed that *CPT1A, ACADM, ACADS ECI2 ACAT2,* and *ACAA2* expression significantly increased upon GREM1 treatment (**Figure 3E**). Further, we blocked the FAO in mitochondria using Etomoxir, an inhibitor of FAO. As expected, the indicated that Etomoxir usage impeded the proliferation and activation of fibroblasts otherwise mediated by GREM1 treatment (**Supplementary Figure S3**). Collectively, GREM1 promoted intestinal fibroblast proliferation by enhancing fatty acid oxidation.

GREM1 Activated VEGFR-2 Receptor in Fibroblasts

Next, we aimed to identify the receptor that senses GREM1 stimulation. Given that GREM1 is reported to be a BMP2 antagonist and ligand of VEGFR-2, we detected fibroblast cell

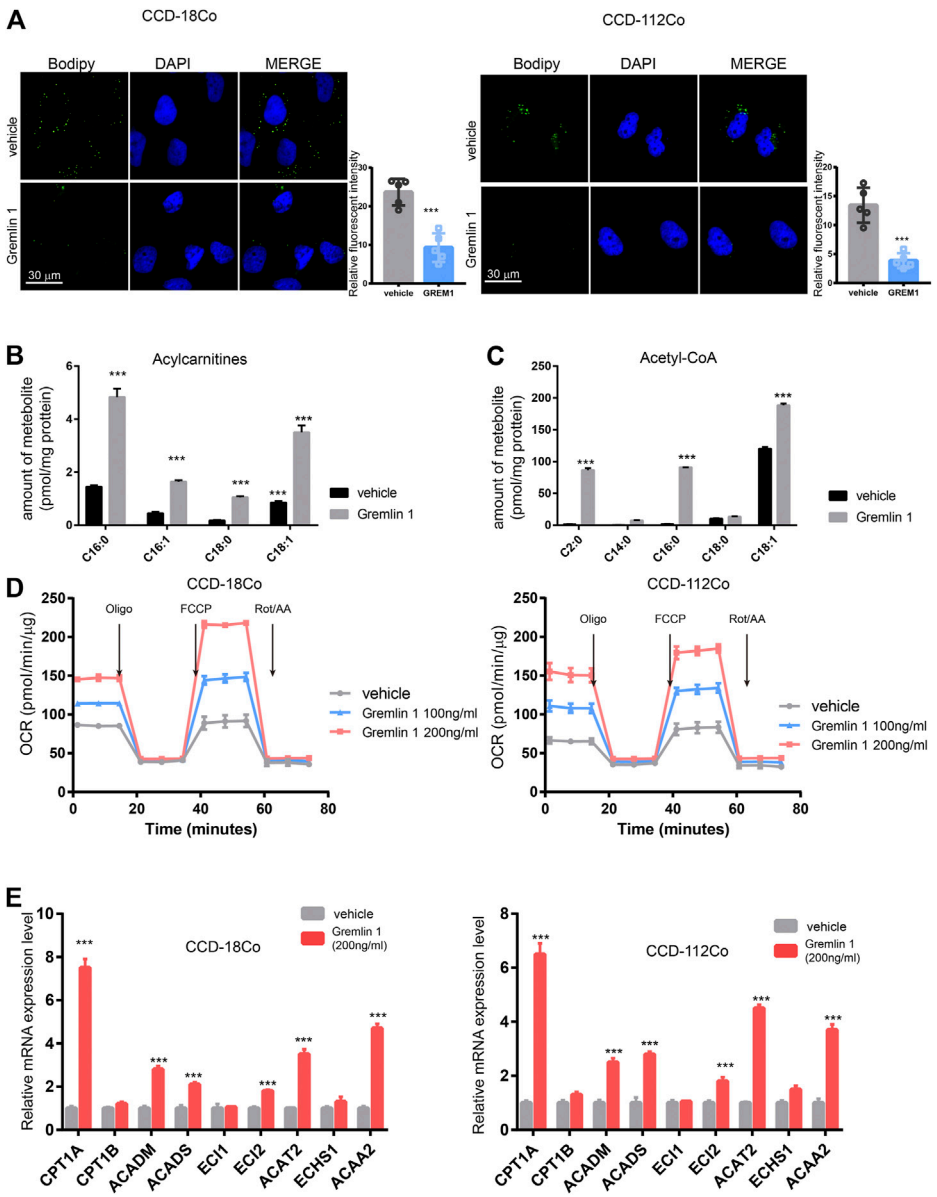


FIGURE 3 | Gremlin 1 facility the FAO of intestinal fibroblast cell. **(A)**. Bodipy assay of human intestinal fibroblast cells CCD-18Co and CCD-112Co cells that treated with 200 ng/ml Gremlin 1 for 24 h or not. Relative fluorescent intensity was calculated of five random fields of slides **(B, C)**. The amount of representative individual lipid species, lipid droplets degraded production, Acylcarnitines **(B)** and Acetyl-CoA **(C)** in human intestinal fibroblast cells CCD-18Co and CCD-112Co cells treated with 200 ng/ml Gremlin 1 for 24 h or not. The amounts of acylcarnitine and acetyl-CoA (were normalized to the total protein of fibroblast cells. **(D)**. The measurement of OCR in human intestinal fibroblast cells CCD-18Co and CCD-112Co cells treated with 200 ng/ml Gremlin 1 for 24 h or not. **(E)**. Q-PCR results of the FAO related genes expression in human intestinal fibroblast cells CCD-18Co and CCD-112Co cells treated with 200 ng/ml Gremlin 1 for 24 h or not. These experiments were repeated twice p values are derived from two-sided Student's t test. $^{**}p \leq 0.01$; $^{***}p \leq 0.001$.

proliferation upon knockdown of BMP2 or VEGFR-2 using siRNA (**Figures 4A,B**). The data showed that silencing VEGFR-2 expression dramatically diminished the growth-promoting effects of GREM1 in fibroblast cells, which was not observed in BMP2-silenced fibroblast cells, indicating that VEGFR-2 may act as a GREM1 receptor in intestinal fibroblasts. To further confirm this, VEGFR-2 was inhibited using the specific inhibitor SU5408. As anticipated, SU5408 also blocked the growth-promoting effects of GREM1 in fibroblasts (**Supplementary Figure S4**). Next, we measured OCRs to determine whether VEGFR-2 inhibition could block the enhanced FAO in fibroblasts. The data showed that both genetic and pharmacological VEGFR-2 inhibition could decrease the enhanced FAO mediated by GREM1 treatment (**Figures 4C,D**). Additionally, FAO-related mRNAs were also measured, and the results showed that expression of such genes decreased with VEGFR-2 inhibition (**Figure 4E**).

Taken together, GREM1 promoted intestinal fibroblast proliferation by activating VEGFR-2 receptor.

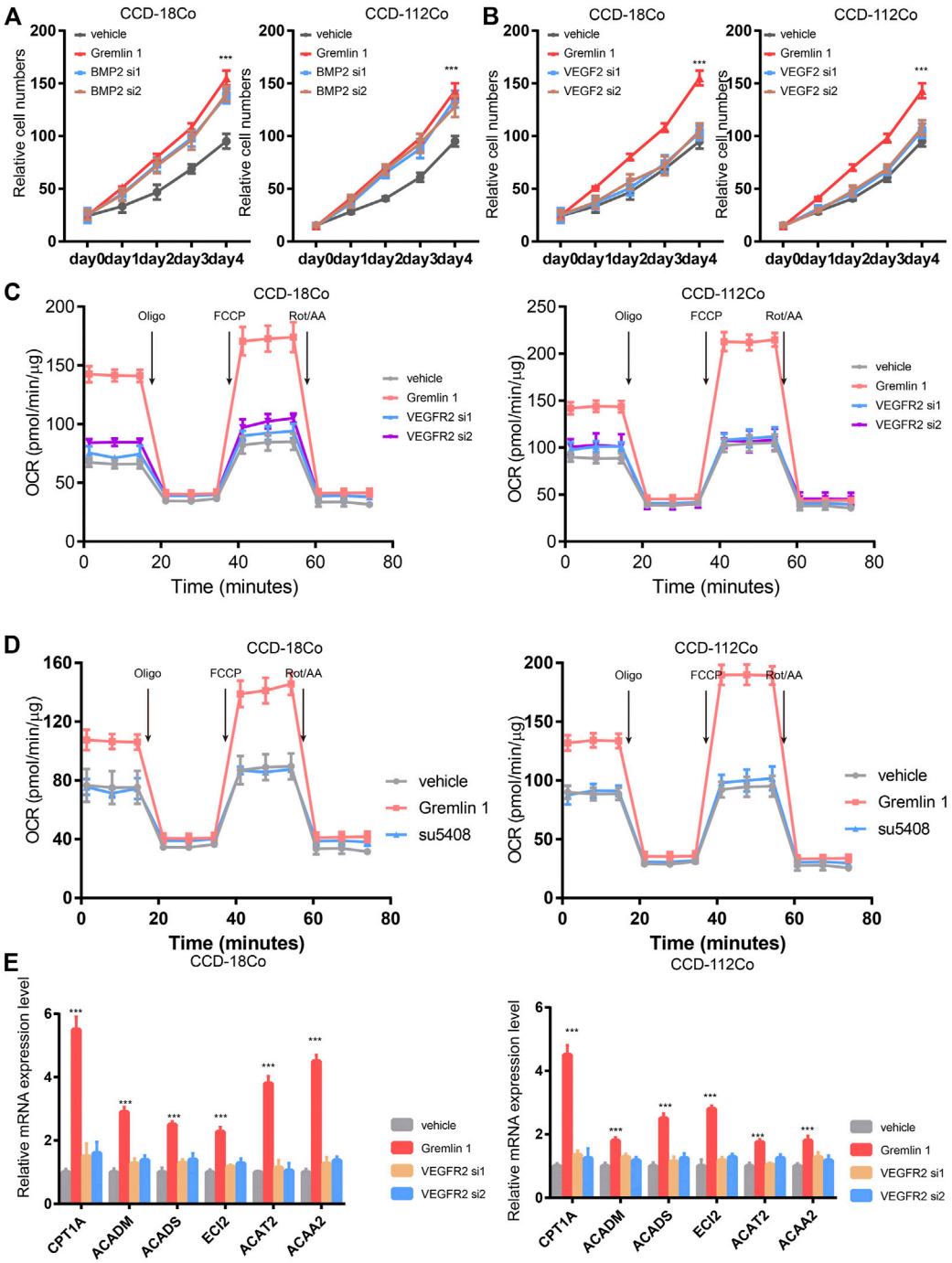


FIGURE 4 | Gremlin 1 activated VEGFR-2 to enhance the FAO of fibroblast. **(A)**. Cell viability assay of human intestinal fibroblast cells CCD-18Co and CCD-112Co treated with 200 ng/ml Gremlin 1 with or with not silencing BMP2 with siRNA. **(B)**. Cell viability assay of human intestinal fibroblast cells CCD-18Co and CCD-112Co treated with 200 ng/ml Gremlin 1 with or with not silencing VEGFR-2 with siRNA. **(C)**. The OCR results of CCD-18Co and CCD-112Co cells treated with 200 ng/ml Gremlin 1 for 24 h, following silencing VEGFR-2 with siRNA or not. **(D)**. The OCR results of human intestinal fibroblast cells CCD-18Co and CCD-112Co cells treated with 200 ng/ml Gremlin 1, following VEGFR-2 inhibitor SU5408 (100 nM) treatment for 24 h. **(E)**. Q-PCR results of genes related with FAO metabolism in the human intestinal fibroblast cells CCD-18Co and CCD-112Co cells. *p* values are derived from two-sided Student's *t* test. $^{**}p \leq 0.01$; $^{***}p \leq 0.001$.

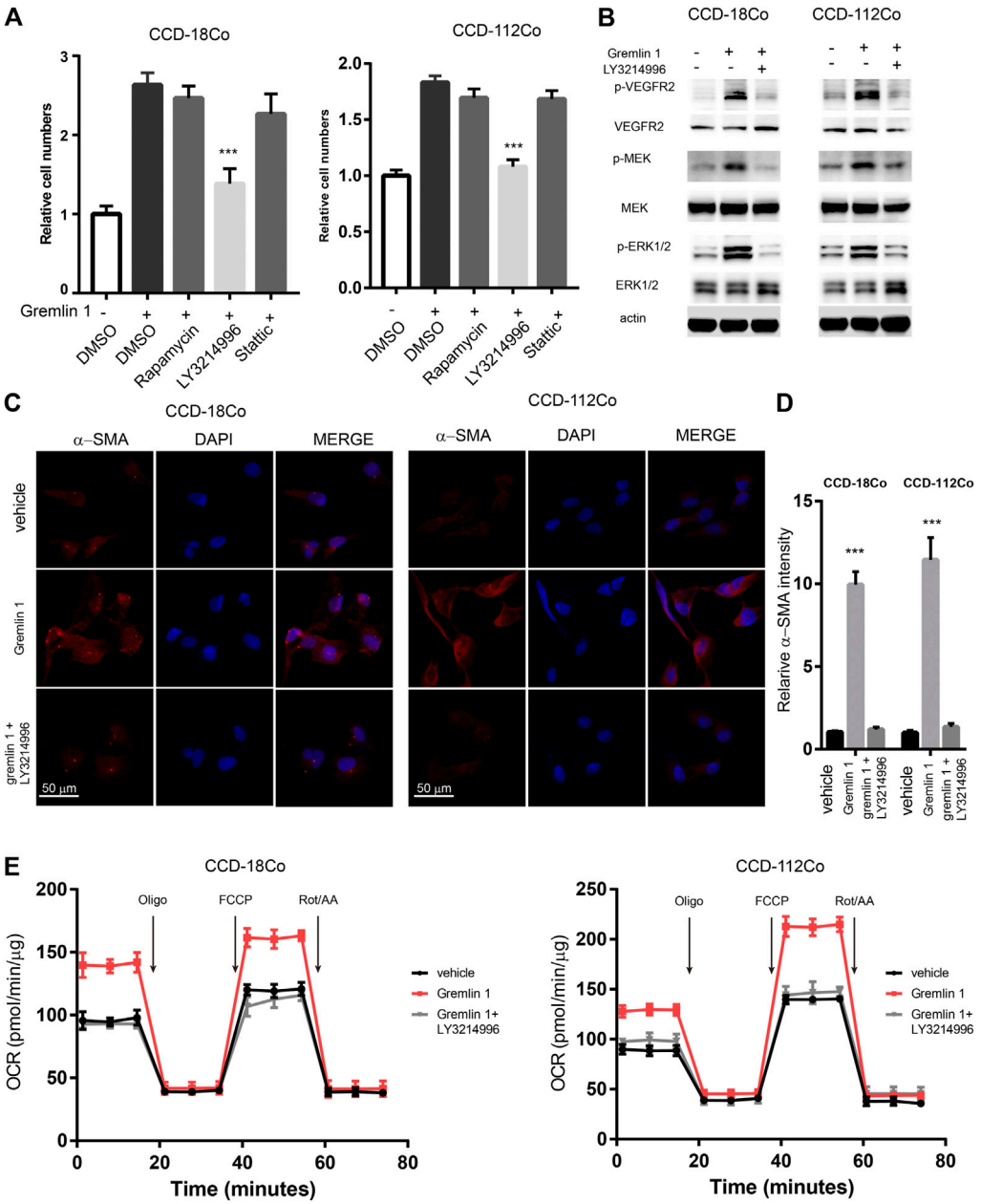


FIGURE 5 | VEGFR2-MEK-ERK axis mediated the enhancement of FAO from Gremlin 1. **(A)**. Cell viability assay of human intestinal fibroblast cells CCD-18Co and CCD-112Co cells treated with 200 ng/ml Gremlin 1 and Rapamycin (10 nM), LY3214996 (10 nM) or stattic (10 μM) for 24 h. **(B)**. Immunoblotting analysis of VEGFR2-MEK-ERK signaling in human intestinal fibroblast cells CCD-18Co and CCD-112Co cells treated with 200 ng/ml Gremlin 1 and LY3214996 (10 nM) for 24 h. Actin acted as loading control and re-used for illustrative purposes. **(C)**. Immunofluorescence staining of a-SMA in human intestinal fibroblast cells CCD-18Co and CCD-112Co cells treated with 200 ng/ml Gremlin 1 and LY3214996 (10 nM). **(D)**. The intensity statistical results of a-SMA immunofluorescence staining from five random fields of slides. E. OCR measurement of CCD-18Co and CCD-112Co cells treated with 200 ng/ml Gremlin 1 and LY3214996 (10 nM) for 24 h. *p* values are derived from one-way ANOVA analysis. Dunnett's test was used to analysis the difference between control group to the other groups. $^{**}p \leq 0.01$; $^{***}p \leq 0.001$.

GREM1 Activates MAPK Pathway to Enhance Fatty Acid Oxidation

In order to uncover the underlying signaling mechanisms leading to FAO enhancement, the reported VEGFR-2 downstream signaling pathways (including the PI3K-mTOR, MAPK, and STAT3 pathways) were inhibited with the specific inhibitors Rapamycin, LY3214996, and Stattic, respectively, (**Figure 5A**). Cell viability assays showed that only the MAPK signaling inhibitor LY3214996 could diminish the otherwise increased proliferation mediated by GREM1. Western blot analysis showed that treatment with GREM1 strongly increased the phosphorylation levels of p-VEGFR-2, its downstream signaling p-MEK, and p-ERK1/2,

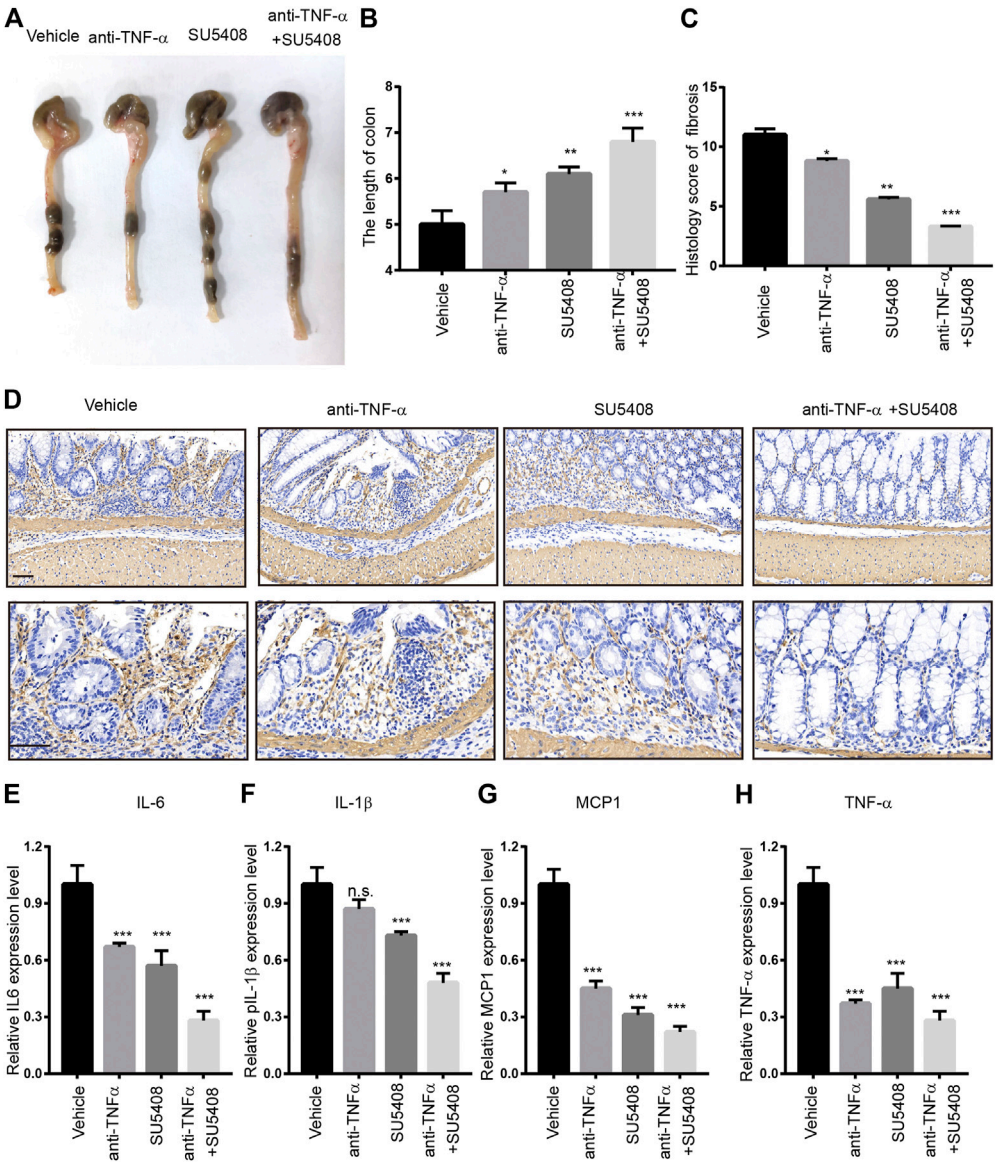


FIGURE 6 | Gremlin 1-VEGFR2 axis disruption impeded the progression of intestinal fibrosis. **(A)**. The appearance of the colons from the mice with intestinal fibrosis treated with vehicle, anti-TNF-α monotherapy (100 μg), SU5408 (5 mg/kg), or anti-TNF-α therapy combined with SU5408 treatment. **(B)**. The statistical results of colon length in mice with vehicle, anti-TNF-α monotherapy (100 μg), SU5408 (5 mg/kg), or anti-TNF-α therapy combined with SU5408 treatment (n = 5). **(C)**. The histology score of intestinal fibrosis mice with different treatment. Fibrosis was quantified using a combined score of fibrosis severity, circularity and the extent of fibrosis (n = 5). **(D)**. α-SMA IHC staining of intestinal sections from intestinal fibrosis mice with different treatment. scale bar 100 μm **(E–H)**. The protein expression level of IL-6, IL-1β, MCP1, and TNF-α in the colon of different group mice treated with vehicle, anti-TNF-α monotherapy (100 μg), SU5408 (5 mg/kg), or anti-TNF-α therapy combined with SU5408 treatment (n = 5). p values are derived from one-way ANOVA analysis. Dunnett's test was used to analysis the difference between control group to the other groups. n. s., $p > 0.05$; *$p \leq 0.05$; **$p \leq 0.01$; ***$p \leq 0.001$.

which were inhibited by LY3214996 treatment (**Figure 5B**). Immunofluorescent imaging also revealed that MAPK signaling inhibition blocked increased α-SMA expression in intestinal fibroblasts (**Figures 5C,D**). Furthermore, we measured OCR levels in intestinal fibroblasts. Accordingly, the elevated OCRs were abolished by LY3214996 treatment (**Figure 5E**). In line with this, the increased acylcarnitine and acetyl-CoA levels decreased upon LY3214996 treatment (**Supplementary Figure S5**). Together, these data sets suggested that GREM1 activated the MAPK pathway to enhance fatty acid oxidation in intestinal fibroblasts.

Blocking GREM1-VEGFR2 Axis Impedes Intestinal Fibrosis Progression *in vivo*

Next, we evaluated whether GREM1-VEGFR2 axis downstream signaling blockage by a VEGFR2-specific inhibitor could prevent

intestinal fibrosis progression upon DSS challenge. Anti-TNFα therapy is one of standard treatment strategies for intestinal fibrosis. We aim to determine whether combine SU5408 with Anti-TNF therapy could provide more benefits for intestinal fibrosis patients. For this purpose, either VEGFR2-specific inhibitor SU5408 or SU5408 plus anti-TNF-α therapy was applied to the intestinal fibrosis mouse model (**Figure 6A**). The results showed that SU5408 usage could restore the duration of colon reduction mediated by DSS challenge, while anti-TNF-α monotherapy was associated with a slight improvement in colonic length. Of note, combining anti-TNF-α antibody with SU5408 significantly restored colonic length (**Figures 6B,C**). Furthermore, the deposition of ECM was found to be dramatically reduced in both groups of mice treated with SU5408 alone or in combination with anti-TNF-α therapy. In addition, α-SMA IHC staining intensity was much weaker in colon sections derived from SU5048-treated mice than in mice in the control group, suggesting a reduction in the proportion of fibroblasts (**Figure 6D**). Additionally, we measured *Col1a1* and *Vim* mRNA expression levels in colon. GREM1-VEGFR2 axis blockage treatment greatly inhibited the expression of *Col1a1* and *Vim* (**Supplementary Figure 6**). Moreover, VEGFR2 inhibition significantly attenuated the levels of the inflammation-related cytokines TNF-α, MCP1, IL-6, and IL-1β (**Figures 6E–H**). Together, these data sets indicated that GREM1-VEGFR2 axis disruption could diminish the proliferation and function of fibroblasts in the colon of mice with intestinal fibrosis.

DISCUSSION

In this study, we found that GREM1 levels were greatly increased in both human and murine fibrosed colon. Functional experiments revealed that GREM1 promoted intestinal fibroblast cell proliferation by enhancing fatty acid oxidation. Further mechanistic studies revealed that GREM1 could activate VEGFR2 and trigger downstream MAPK signaling, which facilitated the expression of FAO-related genes, consequently enhancing fatty acid oxidation.

Intestinal fibrosis is a common finding in patients with IBD (Latella et al., 2014). Current studies indicate that only anti-inflammatory therapy does not impede the development of fibrosis (Latella and Papi, 2012). Fibroblast expansion and activation are major factors that facilitate the progression of intestinal fibrosis. Rapid growth and ECM deposition require a huge amount of energy. Previous studies reported that fibroblasts could reprogram their metabolism by enhancing glycolysis and FAO to sustain cell proliferation and activation (Schreurs et al., 2010; Latella and Papi, 2012; Latella et al., 2014; Qu et al., 2016; Khomich et al., 2019; Chen et al., 2020). In kidney stromal cells, Interleukin-1β induced glycolysis enhancement is necessary for progressive tubulointerstitial fibrosis (Lemos et al., 2018). Additionally, hepatic stellate cell activation results in decrease of lipid droplet abundance and increased levels of polyunsaturated fatty acids (Tuohetahuntila et al., 2015). We consistently observed significant numbers of lipid droplets and enhanced FAO in intestinal fibroblast cells upon GREM1 treatment. On the other hand, Chung et al. (Chen et al., 2020) reported that the expression of FAO-associated enzymes in renal tubule epithelium is reduced in aged rat kidneys. This facilitates the progression of renal fibrosis indicating that FAO alterations in fibroblast and epithelial cells affect the progression of fibrosis differently.

Recent studies have shown that GREM1 is mainly secreted by fibroblast cells, including cancer-associated fibroblasts (Worthley et al., 2015) which can promote the proliferation of cancer cells (Sneddon et al., 2006). High GREM1 expression is related to poorer outcomes in CRC and breast cancer patients (Dutton et al., 2019; Neckmann et al., 2019; Ren et al., 2019). GREM1 also regulates differentiation of glioma cells (Yan et al., 2014). In the current study, we found that GREM1 could activate VEGFR 2, but is not involved in BMP signaling, which further activated downstream MAPK signaling, resulting in FAO enhancement. Recently, GREM1 was reported to activate STAT3 signaling in breast cancer cells (Sung et al., 2020). However, our data suggested that STAT3 was not involved in GREM1-mediated fibroblast cell proliferation and activation, indicating that the signaling regulated by GREM1 is largely context-dependent.

Our *in vivo* experimental results showed that disruption to the GREM1-VEGFR2 axis downstream signaling using SU5408 could delay the progression of intestinal fibrosis. Recently, Kobayashi and colleagues reported that a GREM1-neutralizing antibody could prevent colorectal carcinogenesis (Kobayashi et al., 2020). We realized that a GREM1-neutralizing antibody might be a superior option for our animal studies. However, such a neutralizing antibody is commercially inaccessible. In addition, after carefully checking the patent, such a GREM1-neutralizing antibody was designed to block interactions involving GREM1 and BMP proteins, indicating that this antibody is not the best choice for blocking the GREM1 and VEGFR2 axis. Thus, further efforts are needed to develop neutralizing antibodies or peptides that block interactions between GREM1 and VEGFR2. In addition, our current data showed that blocking the GREM1–VEGFR2 axis combined with anti-TNF-α therapy could provide benefits in mice suffering from intestinal fibrosis, indicating that the combine therapy of anti-TNF-α and GREM1–VEGFR2 blockage could be a potential strategy for intestinal fibrosis patients.

In conclusion, our data revealed that GREM1 promoted the proliferation and activation of fibroblasts by activating VEGFR-2, leading to FAO enhancement. Inhibition of the GREM1-VEGFR2 axis impeded progression in the murine intestinal fibrosis model, indicating that GREM1 could represent a potential target for anti-fibrotic therapy.

DATA AVAILABILITY STATEMENT

The raw data supporting the conclusions of this article will be made available by the authors, without undue reservation, to any qualified researcher.

ETHICS STATEMENT

The studies involving human participants were reviewed and approved by Institutional Animal Care and Use Committee of

Laboratory Animal Center of Daping Hospital, Army Medical University. The patients/participants provided their written informed consent to participate in this study. The animal study was reviewed and approved by Institutional Animal Care and Use Committee of Laboratory Animal Center of Daping Hospital, Army Medical University.

AUTHOR CONTRIBUTIONS

H-TG and YY were responsible for the study concept and design. YY and QSZ performed all the experiments with help from JZ and MZ. JN, and DC provided human samples. H-TG, YY, and DC analyzed and all authors helped to interpret the data. All authors revised the manuscript.

FUNDING

This study was supported in part by the National Natural Science Foundation of China (No.81500408 to YY, No. 82070560 and 81470826 to H-TG), Foundation and Frontier Projects of Chongqing Science and Technology Commission (No. cstc2016jcyjA0079 to YY), the Science Foundation from Science and Technology Department of Sichuan Province (No. 2019YFS0262 to H-TG) and 1.3.5 Project for Disciplines of Excellence, West China Hospital, Sichuan University (No. ZYGD18023 to H-TG).

ACKNOWLEDGMENTS

We would like to thank editage (www.editage.cn) for English language editing.

SUPPLEMENTARY MATERIAL

The Supplementary Material for this article can be found online at: https://www.frontiersin.org/articles/10.3389/fphar.2021.663774/full#supplementary-material.

REFERENCES

Burke, J. P., Ferrante, M., Dejaegher, K., Watson, R. W. G., Docherty, N. G., De Hertogh, G., et al. (2008). Transcriptomic Analysis of Intestinal Fibrosis-Associated Gene Expression in Response to Medical Therapy in Crohn's Disease. *Inflamm. Bowel Dis.* 14 (9), 1197–1204. doi:10.1002/ibd.20482

Chen, Y., Yan, Q., Lv, M., Song, K., Dai, Y., Huang, Y., et al. (2020). Involvement of FATP2-Mediated Tubular Lipid Metabolic Reprogramming in Renal Fibrogenesis. *Cell Death Dis.* 11 (11), 994. doi:10.1038/s41419-020-03199-x

Cheng, X., Geng, F., Pan, M., Wu, X., Zhong, Y., Wang, C., et al. (2020). Targeting DGAT1 Ameliorates Glioblastoma by Increasing Fat Catabolism and Oxidative Stress. *Cel Metab.* 32 (2), 229–242. doi:10.1016/j.cmet.2020.06.002

Dutton, L. R., Hoare, O. P., McCorry, A. M. B., Redmond, K. L., Adam, N. E., Canamara, S., et al. (2019). Fibroblast-derived Gremlin1 Localises to Epithelial Cells at the Base of the Intestinal Crypt. *Oncotarget* 10 (45), 4630–4639. doi:10.18632/oncotarget.27050

Fichtner-Feigl, S., Fuss, I. J., Young, C. A., Watanabe, T., Geissler, E. K., Schlitt, H.-J., et al. (2007). Induction of IL-13 Triggers TGF-β1-dependent Tissue Fibrosis in Chronic 2,4,6-Trinitrobenzene Sulfonic Acid Colitis. *J. Immunol.* 178, 5859–5870. doi:10.4049/jimmunol.178.9.5859

Hagenlocher, Y., Satzinger, S., Civelek, M., Feilhauer, K., Köninger, J., Bischoff, S. C., et al. (2017). Cinnamon Reduces Inflammatory Response in Intestinal Fibroblasts In Vitro and in Colitis In Vivo Leading to Decreased Fibrosis. *Mol. Nutr. Food Res.* 61 (9), 1601085. doi:10.1002/mnfr.201601085

Honma, R., Sakamoto, N., Ishikawa, A., Taniyama, D., Fukada, K., Hattori, T., et al. (2018). Clinicopathological and Prognostic Significance of Epithelial Gremlin1 Expression in Gastric *Cancer*. *Anticancer Res.* 38 (3), 1419–1425. doi:10.21873/anticanres.12366

Hsu, D. R., Economides, A. N., Wang, X., Eimon, P. M., and Harland, R. M. (1998). The *Xenopus* Dorsalizing Factor Gremlin Identifies a Novel Family of Secreted Proteins that Antagonize BMP Activities. *Mol. Cel.* 1 (5), 673–683. doi:10.1016/s1097-2765(00)80067-2

Khomich, O., Ivanov, A. V., and Bartosch, B. (2019). Metabolic Hallmarks of Hepatic Stellate Cells in Liver Fibrosis. *Cells* 9 (1), 24. doi:10.3390/cells9010024

Kobayashi, H., Gieniec, K., Wright, J., Wang, T., Asai, N., Mizutani, Y., et al. (2020). The Balance of Stromal BMP Signaling Mediated by GREM1 and ISLR Drives Colorectal Carcinogenesis. *Gastroenterology* 160, 1224-1239. doi:10.1053/j.gastro.2020.11.011

Latella, G., and Papi, C. (2012). Crucial Steps in the Natural History of Inflammatory Bowel Disease. *Wjg* 18 (29), 3790–3799. doi:10.3748/wjg.v18.i29.3790

Latella, G., Rogler, G., Bamias, G., Breynaert, C., Florholmen, J., Pellino, G., et al. (2014). Results of the 4th Scientific Workshop of the ECCO (I): Pathophysiology of Intestinal Fibrosis in IBD. *J. Crohn's Colitis* 8 (10), 1147–1165. doi:10.1016/j.crohns.2014.03.008

Lawrance, I. C., Maxwell, L., and Doe, W. (2001). Altered Response of Intestinal Mucosal Fibroblasts to Profibrogenic Cytokines in Inflammatory Bowel Disease. *Inflamm. Bowel Dis.* 7 (3), 226–236. doi:10.1097/00054725-200108000-00008

Lawrance, I. C., Rogler, G., Bamias, G., Breynaert, C., Florholmen, J., Pellino, G., et al. (2017). Cellular and Molecular Mediators of Intestinal Fibrosis. *Eccojc* 11 (12), j.crohns.2014.09.008–503. doi:10.1016/j.crohns.2014.09.008

Leake, I. (2015). Cathelicidin Can Reverse Intestinal Fibrosis in Models of Colitis. *Nat. Rev. Gastroenterol. Hepatol.* 12 (1), 3. doi:10.1038/nrgastro.2014.214

Lemos, D. R., McMurdo, M., Karaca, G., Wilflingseder, J., Leaf, I. A., Gupta, N., et al. (2018). Interleukin-1β Activates a MYC-dependent Metabolic Switch in Kidney Stromal Cells Necessary for Progressive Tubulointerstitial Fibrosis. *Jasn* 29 (6), 1690–1705. doi:10.1681/asn.2017121283

Mezzano, S., Droguett, A., Lavoz, C., Krall, P., Egido, J., and Ruiz-Ortega, M. (2018). Gremlin and Renal Diseases: Ready to Jump the Fence to Clinical Utility?. *Nephrol. Dial. Transplant.*, 33, 735–741. doi:10.1093/ndt/gfx194

Mitola, S., Ravelli, C., Moroni, E., Salvi, V., Leali, D., Ballmer-Hofer, K., et al. (2010). Gremlin Is a Novel Agonist of the Major Proangiogenic Receptor VEGFR2. *Blood* 116 (18), 3677–3680. doi:10.1182/blood-2010-06-291930

Neckmann, U., Wolowczyk, C., Hall, M., Almaas, E., Ren, J., Zhao, S., et al. (2019). GREM1 Is Associated with Metastasis and Predicts Poor Prognosis in ER-Negative Breast Cancer Patients. *Cell Commun Signal* 17 (1), 140. doi:10.1186/s12964-019-0467-7

Nyqvist, J., Persson, F., Parris, T. Z., Helou, K., Kenne Sarenmalm, E., Einbeigi, Z., et al. (2017). Metachronous and Synchronous Occurrence of 5 Primary Malignancies in a Female Patient between 1997 and 2013: A Case Report with Germline and Somatic Genetic Analysis. *Case Rep. Oncol.* 10 (3), 1006–1012. doi:10.1159/000484403

Qu, Q., Zeng, F., Liu, X., Wang, Q. J., and Deng, F. (2016). Fatty Acid Oxidation and Carnitine Palmitoyltransferase I: Emerging Therapeutic Targets in Cancer. *Cel Death Dis.* 7 (5), e2226. doi:10.1038/cddis.2016.132

Ren, J., Smid, M., Iaria, J., Salvatori, D. C. F., van Dam, H., Zhu, H. J., et al. (2019). Cancer-associated Fibroblast-Derived Gremlin 1 Promotes Breast Cancer Progression. *Breast Cancer Res.* 21 (1), 109. doi:10.1186/s13058-019-1194-0

Rieder, F., and Fiocchi, C. (2009). Intestinal Fibrosis in IBD-A Dynamic, Multifactorial Process. *Nat. Rev. Gastroenterol. Hepatol.* 6 (4), 228–235. doi:10.1038/nrgastro.2009.31

Schreurs, M., Kuipers, F., and van der Leij, F. R. (2010). Regulatory Enzymes of Mitochondrial β-oxidation as Targets for Treatment of the Metabolic Syndrome. *Obes. Rev. : official J. Int. Assoc. Study Obes.* 11 (5), 380–388. doi:10.1111/j.1467-789X.2009.00642.x

Simmons, J. G., Pucilowska, J. B., Keku, T. O., and Lund, P. K. (2002). IGF-I and TGF-B1 Have Distinct Effects on Phenotype and Proliferation of Intestinal Fibroblasts. *Am. J. Physiology-Gastrointestinal Liver Physiol.* 283 (3), G809–G818. doi:10.1152/ajpgi.00057.2002

Sneddon, J. B., Zhen, H. H., Montgomery, K., van de Rijn, M., Tward, A. D., West, R., et al. (2006). Bone Morphogenetic Protein Antagonist Gremlin 1 Is Widely Expressed by Cancer-Associated Stromal Cells and Can Promote Tumor Cell Proliferation. *Proc. Natl. Acad. Sci.* 103 (40), 14842–14847. doi:10.1073/pnas.0606857103

Speca, S., Rousseaux, C., Dubuquoy, C., Rieder, F., Vetuschi, A., Sferra, R., et al. (2016). Novel PPARγ Modulator GED-0507-34 Levo Ameliorates Inflammation-Driven Intestinal Fibrosis. *Inflamm. Bowel Dis.* 22 (2), 279–292. doi:10.1097/mib.0000000000000618

Su, H. Y., Gupta, V., Day, A. S., and Gearry, R. B. (2016). Rising Incidence of Inflammatory Bowel Disease in Canterbury, New Zealand. *Inflamm. Bowel Dis.* 22 (9), 2238–2244. doi:10.1097/mib.0000000000000829

Sung, N. J., Kim, N. H., Surh, Y.-J., and Park, S.-A. (2020). Gremlin-1 Promotes Metastasis of Breast *Cancer* Cells by Activating STAT3-MMP13 Signaling Pathway. *Ijms* 21 (23), 9227. doi:10.3390/ijms21239227

Tuohetahuntila, M., Spee, B., Kruitwagen, H. S., Wubbolts, R., Brouwers, J. F., van de Lest, C. H., et al. (2015). Role of Long-Chain Acyl-CoA Synthetase 4 in Formation of Polyunsaturated Lipid Species in Hepatic Stellate Cells. *Biochim. Biophys. Acta (Bba) - Mol. Cel Biol. Lipids* 1851 (2), 220–230. doi:10.1016/j.bbalip.2014.12.003

Vallance, B. A., Gunawan, M. I., Hewlett, B., Bercik, P., Van Kampen, C., Galeazzi, F., et al. (2005). TGF-β1 Gene Transfer to the Mouse Colon Leads to Intestinal Fibrosis. *Am. J. Physiology-Gastrointestinal Liver Physiol.* 289 (1), G116–G128. doi:10.1152/ajpgi.00051.2005

Vítek, L., and Tiribelli, C. (2020). Bilirubin, Intestinal Integrity, the Microbiome, and Inflammation. *N. Engl. J. Med.* 383 (7), 684–686. doi:10.1056/NEJMcibr2013250

Weder, B., Mamie, C., Rogler, G., Clarke, S., McRae, B., Ruiz, P. A., et al. (2018). BCL2 Regulates Differentiation of Intestinal Fibroblasts. *Inflamm. Bowel Dis.* 24 (9), 1953–1966. doi:10.1093/ibd/izy147

Worthley, D. L., Churchill, M., Compton, J. T., Tailor, Y., Rao, M., Si, Y., et al. (2015). Gremlin 1 Identifies a Skeletal Stem Cell with Bone, Cartilage, and Reticular Stromal Potential. *Cell* 160, 269–284. doi:10.1016/j.cell.2014.11.042

Yan, K., Wu, Q., Yan, D. H., Lee, C. H., Rahim, N., Tritschler, I., et al. (2014). Glioma Cancer Stem Cells Secrete Gremlin1 to Promote Their Maintenance within the Tumor Hierarchy. *Genes Development* 28 (10), 1085–1100. doi:10.1101/gad.235515.113

Conflict of Interest: The authors declare that the research was conducted in the absence of any commercial or financial relationships that could be construed as a potential conflict of interest.

Copyright © 2021 Yang, Zeng, Zou, Zeng, Nie, Chen and Gan. This is an open-access article distributed under the terms of the Creative Commons Attribution License (CC BY). The use, distribution or reproduction in other forums is permitted, provided the original author(s) and the copyright owner(s) are credited and that the original publication in this journal is cited, in accordance with accepted academic practice. No use, distribution or reproduction is permitted which does not comply with these terms.

frontiers in Pharmacology

REVIEW
published: 26 April 2021
doi: 10.3389/fphar.2021.679924

Ultrasonographic Evaluation of Intestinal Fibrosis and Inflammation in Crohn's Disease. The State of the Art

Francesca Ferretti[1†], *Rosanna Cannatelli*[1†], *Sandro Ardizzone*[1], *Jeanette A. Maier*[2] *and Giovanni Maconi*[1*]

[1]Gastroenterology Unit—ASST Fatebenefratelli-Sacco, Department of Biomedical and Clinical Sciences (DIBIC) L. Sacco, Università degli Studi di Milano, Milan, Italy, [2]General Pathology—Department of Biomedical and Clinical Sciences (DIBIC) L. Sacco, Università degli Studi di Milano, Milan, Italy

The evaluation of the degree of inflammation and fibrosis, intrinsic elements in intestinal wall damage of Crohn's disease, is essential to individuate the extent of the lesions and the presence of strictures. This information will contribute to the choice of the appropriate therapeutic approach, the prediction of the response to therapy and the course of the disease. The accurate evaluation of the extent and severity of inflammation and/or fibrosis in Crohn's disease currently requires histopathological analysis of the intestinal wall. However, in clinical practice and research, transmural assessment of the intestinal wall with cross sectional imaging is increasingly used for this purpose. The B-mode ultrasonograhic characteristics of the intestinal wall, the assessment of its vascularization by color Doppler and I.V. contrast agents, and the evaluation of the mechanical and elastic properties by sonoelastography, may provide useful and accurate information on the severity and extent of inflammation and intestinal fibrosis in Crohn's disease. The purpose of this review is to provide an update on current sonographic methods to discriminate inflammation and fibrosis in Crohn's disease.

Keywords: Crohn's disease, fibrosis, inflammation, strictures, ultrasound, sonoelastography

OPEN ACCESS

Edited by:
Dario Sorrentino,
Virginia Tech Carilion, United States

Reviewed by:
Marco Marino,
Azienda Sanitaria Universitaria Friuli Centrale (ASU FC), Italy
Vu Nguyen,
Virginia Tech Carilion, United States

****Correspondence:***
Giovanni Maconi
giovanni.maconi@unimi.it

[†]These authors have contributed equally to this work

Specialty section:
This article was submitted to Gastrointestinal and Hepatic Pharmacology, a section of the journal Frontiers in Pharmacology

Received: *12 March 2021*
Accepted: *09 April 2021*
Published: *26 April 2021*

Citation:
Ferretti F, Cannatelli R, Ardizzone S, Maier JA and Maconi G (2021) Ultrasonographic Evaluation of Intestinal Fibrosis and Inflammation in Crohn's Disease. The State of the Art. Front. Pharmacol. 12:679924. doi: 10.3389/fphar.2021.679924

INTRODUCTION

Crohn's disease (CD) is characterized by chronic inflammation and progressive fibrosis. In general, the inflammatory pattern is the most frequent at the onset of the disease, while a stricturing or penetrating evolution can be observed later on (Cosnes et al., 2002).

The complicated course of disease occurs in up to 50% of patients within 20 years of diagnosis, requiring a surgical intervention in half of these cases within 10 years (Peyrin-Biroulet et al., 2010).

The evaluation and characterization of inflammation is pivotal in the detection of the disease, in the characterization of newly diagnosed of CD, and in its monitoring, along with the evaluation of complications (Maaser et al., 2019). The definition of disease activity and onset of fibrosis will shape therapeutic decisions, with prognostic impact on the response to therapy and the risk of recurrence.

Histopathology is still the gold standard for the identification of inflammation and fibrosis. However, despite several scoring systems have been proposed, in particular for strictures, a wide heterogeneity in scoring methods exists and none can be considered as a suitable benchmark (Bettenworth et al., 2019; De Voogd et al., 2020; Gordon et al., 2020). In clinical practice and research, cross-sectional imaging techniques have been proposed as reliable non-invasive alternative

approaches for transmural assessment of the intestinal wall to detect inflammatory or fibrotic patterns.

Among different imaging techniques, intestinal ultrasound (IUS) is a radiation-free and cost-effective technique which is increasingly adopted both for the diagnosis and the monitoring of CD. The introduction of small intestine contrast ultrasonography (SICUS) and the contrast-enhanced ultrasound (CEUS) as well as elastography expanded the potential applications of this technique.

However, reliability of IUS in detecting inflammation and fibrosis is still under investigation, as well as its applicability and usefulness in clinical practice to drive the most appropriate treatment. Most of these gaps rely on the absence of reproducible gold standards for evaluating inflammation and fibrosis to be used for complicated and not complicated patients. In fact, if the assessment of pathological features is still awaiting valid and reproducible parameters, the discrimination of fibrosis and inflammation in non-operated patients is mainly indirect and relies essentially on clinical parameters such as biochemical tests and the response to steroid or biologic treatment.

In this review we evaluated the reliability of IUS in assessing inflammation and fibrosis, mainly focusing on the available studies that have used pathological features or the response to treatment as direct and indirect reference parameters.

INTESTINAL ULTRASOUND AND INFLAMMATION

Applications

The identification and characterization of inflammatory features in the small bowel and/or colon are pivotal both for the diagnosis and the monitoring of IBD. The gold standard in the assessment of bowel inflammatory involvement is histology, but non-invasive approaches are demanded to limit the risks and the costs of repeated endoscopic procedures, considering also the limitation of histology in case of inadequate or superficial biopsy sampling. Thus, different non-invasive approaches have been introduced with different degrees of reliability.

Biomarkers such as C reactive protein (CRP) and fecal calprotectin (FC) are useful for monitoring IBD (Vos et al., 2013) although with some risk of false positive results (Maaser et al., 2019). Thus, the available imaging techniques including IUS, computed tomography (CT) and magnetic resonance imaging (MRI) have been increasingly applied to IBD. In a systematic review, Panes et al. compared the diagnostic accuracy of different cross sectional imaging techniques showing a high accuracy both for the CD diagnosis and CD monitoring, with good reliability for assessing disease severity and complications (Panés et al., 2011). If multiple options are available with comparable local expertize, IUS can be considered the first choice due to its non-invasiveness, low costs and repeatability (Calabrese et al., 2016).

Identification and Characterization of Disease Activity in Suspect Crohn's Disease

In case of suspect CD, IUS has shown a 80% sensitivity and 97% specificity for the CD diagnosis when compared with reference standards including clinical evaluation, endoscopy, histology and/or radiology (Calabrese et al., 2016).

The accuracy of US depends on the location and severity of CD (Hollerbach et al., 1998; Astegiano et al., 2001; Parente et al., 2003). In comparison with endoscopy, cross-sectional techniques are less accurate to detect mild inflammatory luminal lesions (Panés et al., 2011).

In suspected involvement of small bowel (SB), IUS and SB capsule endoscopy (SBCE) yield similar findings. Indeed, IUS shows 72% of sensitivity and 84% of specificity (Carter et al., 2018), which can be slightly increased using oral contrast agents (e.g., SICUS) (Kopylov et al., 2017), in particular for the assessment of proximal SB lesions (Petruzziello et al., 2010).

Finally, a comparison of the diagnostic accuracy between MRI and IUS in detecting active CD—defined as the presence of ulcerations at endoscopy, CRP >8 mg/L, Calprotectin >250 μg/g, histological evidence of activity—demonstrated a lower sensitivity of IUS vs. MRI in active SB disease (90 vs. 96%, p 0.01) and a comparable sensitivity in case of active colonic disease (66 vs 63%, p 0.7) (Taylor et al., 2018).

Monitoring of Disease Activity in Known Crohn's Disease

The role of IUS in the evaluation of disease activity is still controversial (Calabrese et al., 2016). In a systematic review Rimola et al. investigated the accuracy of different cross-sectional imaging techniques in assessing disease activity, and found that four US-based parameters (wall thickening, Doppler signal, loss of stratification and reduced peristalsis/compressibility) showed good correlation with endoscopic reference standard (Rimola et al., 2012). MRI showed a good or very good agreement with endoscopic or histologic reference standard when limited small bowel tracts were analyzed, while the results about colonic CD assessment were more conflicting, mainly because of the inconstant use of colonic intraluminal contrast (Rimola et al., 2012). All the MRI-based indexes included wall thickness (in mm) and the degree of wall enhancement after intravenous contrast injection. To date, magnetic resonance index of activity (MaRIA) (Rimola et al., 2011) and Clermont score (Buisson et al., 2015; Buisson et al., 2017) are the two main indexes in the assessment and grading of CD severity and mucosal lesions, evaluating the presence of ulcerations, edema, bowel thickness and relative contrast enhancement (MaRIA) or apparent diffusion coefficient (Clermont). Both have been validated compared with endoscopy, both in ileal and colonic CD. Even if data are conflicting about the concordance and degree of accuracy of these scores, a recent study demonstrated a high and equal efficacy in the detection of mucosal healing (Buisson et al., 2017), showing a substantial accuracy in the detection of endoscopic ulcerations with high specificity (81–82%) and high negative predictive value (82% NPV), while sensitivity and positive predictive values were moderate. Likewise, in a recent study by Yuksel et al., IUS showed a comparable accuracy to MRE in detecting endoscopic activity (Yuksel et al., 2019) where in endoscopically active disease, the most frequent IUS signs

were increased BWT (>3 mm) and fibrofatty proliferation (not defined in the study). These findings are in keeping with another study by Livne et al., where IUS parameters, and in particular terminal ileum thickness and mesenteric fat hypertrophy, showed a significant correlation with the MaRIA score (Livne et al., 2020).

However, the main limitation and difficulties in obtaining a conclusion regarding IUS assessment of disease activity are the choice of the IUS parameters and/or their combination (e.g., IUS scores) and the choice of the reference standard adopted to assess activity, whether clinical (i.e. elevated CDAI), biochemical (CRP, fecal calprotectin), radiological and/or histological.

Techniques and Parameters

B-Mode Ultrasound and Color Doppler Imaging

The data in the literature agree on the fact that main parameters suggesting inflammation and disease activity in CD are bowel wall thickening (BWT), color Doppler imaging (CDI), and bowel wall stratification (BWS), along with mesenteric fat hypertrophy and regional lymphadenopathy (Livne et al., 2020). However, these evidences come mostly from the changes of these parameters in response to the therapy.

The definition of the main parameters linked to inflammation has been indirectly obtained by assessing the behavior of the same bowel wall parameters, which result mostly affected, after biologic or corticosteroid treatment and by correlating each feature of bowel wall with the clinical (i.e. elevated CDAI, HBI) and biochemical (CRP, calprotectin) parameters (Goodsall et al., 2020). A large German multi-center study showed the improvement of different IUS parameters (BWT, parietal vascularization assessed by color-Doppler grade, lack of bowel stratification and creeping fat and mesenteric lymph nodes) after pharmacological treatment (Kucharzik et al., 2017).

The fact that BWT is one of the main parameters correlated with inflammation has also been suggested by studies showing that transmural healing, namely the normalization of the BWT (e.g., <3 mm), is strongly correlated with mucosa healing, and recent studies have shown a normalization of the thickened wall in up to 25% of patients treated with anti-TNFα drugs (Castiglione et al., 2013). A good concordance of BWT with other diagnostic studies was demonstrated both with ileocolonoscopy and MRI (Castiglione et al., 2013; Castiglione et al., 2017), thus showing the potential role of IUS in monitoring CD patients, even in pediatric age (Civitelli et al., 2016).

The available studies correlating US and histologic features define a hypoechoic echo pattern, namely the absence or disruption of the regular bowel wall stratification, in case of prevalent inflammatory stenosis (Maconi et al., 2003) and color Doppler US abnormalities of bowel wall (Sasaki et al., 2014a; Sasaki et al., 2014b).

A recent study of Bhatnagar et al. evaluates different mural and extramural US features as potential imaging predictors of histologic inflammation by comparing IUS findings with resection specimens and confirms a significant association of bowel wall and mucosal layer thickness with acute inflammation, while mesenteric fat echogenicity correlates with chronic inflammation (Bhatnagar et al., 2021). A retrospective study measured vascularity by means of color Doppler, using the Limberg score to grade the presence of blood flow within and around the bowel wall as an index of activity and inflammation, and compared the findings with the histologic results obtained on ileum biopsies of 32 CD patients. However, the association between the Limberg score and histologic grades of disease activity was poor ($\kappa = 0.4375$) (Drews et al., 2009).

More recently, an ultrasensitive ultrasound microvessel imaging (UMI) technique, able to provide a significant higher sensitivity in depicting smaller vessels compared with conventional Doppler, has been developed and compared to CT/MRI, in a pilot study of Gong et al.(Gong et al., 2020). Altered vascularization was demonstrated in case of severe inflammation, while no significant difference was found between quiescent and mild CD.

Taken into account the data of the literature, an expert consensus on inflammatory activity parameters, combined with a blinded agreement study, showed that BWT is the most important predictor of disease activity for ultrasound with a very high inter-rater agreement and correlation with overall assessment of disease activity. CDI, inflammatory mesenteric fat and BWS, which are important parameters, show moderate or nearly moderate agreement (Novak et al., 2020).

Different US activity scoring systems have been developed so far. A recent systematic review identified different available scoring systems created on the basis of endoscopic, radiologic or histologic reference standards. However, a suboptimal methodology was observed in these studies, suggesting the need for further evaluations to identify a more reliable and standardized index (Bots et al., 2018).

Small Intestine Contrast Ultrasonography (SICUS)

SICUS is a sonographic technique where the evaluation of the small bowel is performed before and after the ingestion of an oral contrast solution (approximately 500 ml of polyethylene glycol solution, PEG). It has been used for the detection and characterization of SB lesions and complications (Pallotta et al., 2012), in particular with a better accuracy than transabdominal US and comparable to radiologic examination (Calabrese et al., 2005; Pallotta et al., 2005). However, an adequate validation for activity monitoring compared with endoscopic score is not available. The actual scores (i.e., SLIC: sonographic lesion index for CD) have been compared to clinical activity (CDAI and CRP levels) and used in the evaluation of the response after induction or maintenance with anti-TNFα therapy (Calabrese et al., 2012; Zorzi et al., 2014). According to this small prospective study, a significant improvement of SLIC was observed after the induction period. Moreover, SICUS-responders to anti-TNFα agents have shown a better long-term outcome in terms of need for surgery, hospitalization rate and use for steroids (Zorzi et al., 2020).

Contrast-Enhanced Ultrasound

Unlike Doppler ultrasound, CEUS is able to detect slow-moving blood flow in small vessels, also in deep-lying bowel wall segments, and can provide qualitative and quantitative evaluations of vascularity and perfusion of the bowel walls. CEUS is performed after the injection of microbubbles

(average diameter of 2.5 μm) in the blood stream. The US signals reflected by microbubbles can be easily separated from tissue signals by the softwares of the sonographic machines, and be used to discriminate vascular from avascuar tissues (e.g., to separate phlegmon from abscesses) and to quantify vascularity within the specific tissues. The latter can be assessed in a dynamic qualitative or semiqualitiative way, according to pattern of enhacement (e.g. absence/presence of enhancement of different wall layers), contrast quantification of peak intensity, or using parameters of dynamic CEUS intensity changes over time (e.g. time-intensity curves). In this setting, the application of CEUS in the evaluation of inflammation and disease activity is raising great interest. Migaleddu et al. reported a 93.5% sensitivity and 93.7% specificity of CEUS enhancement patterns in detecting inflammatory activity with a strong correlation with CDAI in 47 CD patients. CEUS accuracy was higher than US or Color Doppler US (Migaleddu et al., 2009).

Besides the pattern of enhancement of the bowel wall, defined as the description of the arrangement of the enhanced layer, Serra et al. quantified the perfusion by using a quantitative ratio between the major thickness of the enhanced layer (E) and the thickness of the entire wall section (W) (Serra et al., 2007). According to this study, an altered pattern of enhancement and a E/W ratio ranging between 0.43 and 0.47 identified active patients with a sensitivity 81% and specificity of 55–63% (Serra et al., 2007).

The perfusion analysis with CEUS has demonstrated a prognostic value in pharmacologically treated patients. Quaia et al. identified different CEUS parameters, including the overall vascularization assessed by the area under the time-intensity curve, to discriminate responders from non-responders in newly diagnosed and treated CD patients after 3 months of therapy (Quaia et al., 2013). Moreover, Saevik et al. showed that, in case of acute exacerbation requiring anti-TNFα drugs or steroids, an high relative perfusion and thickened proper muscle layer at 1 month was predictive of treatment failure (Saevik et al., 2014). Ripolles et al.(Ripollés et al., 2009) demonstrated that an increase of 46% as the threshold brightness value has a 96% sensitivity and 73% specificity in predicting a moderate-to-severe inflammation by endoscopy in 53 CD patients. Moreover, the association was confirmed even when compared with histopathology. Indeed, Ripolles et al. showed a significant association between increased contrast enhancement (CE) and histologic inflammatory score in 28 analyzed segments (Ripollés et al., 2013).

However, comparisons among CEUS and histopathology findings are limited. In a small prospective study, Wilkens et al. compared US, CEUS and MRE parameters with histopathology of 25 patients with small bowel CD undergoing elective surgery, confirming the role of bowel wall thickness as a marker of inflammation, but reporting the failure of CEUS in discriminating between inflammatory and fibrotic lesions (Wilkens et al., 2018).

CEUS has been applied also for the post-surgery recurrence. Paredes et al. developed and applied an activity index to identify postoperative recurrence in 60 CD patients. They found that the combination of a 34.5% cut-off of maximum CE with the other US parameters predicted endoscopic recurrence with a 94.4% of accuracy and a good correlation ($\kappa = 0.82$; $p < 0.001$). A cut-off >46% CE predicted a moderate–severe endoscopic recurrence (Paredes et al., 2013). Recently, a score combining the US wall thickness, the color Doppler grade and contrast parameters showed an high degree of accuracy in the prediction of endoscopic CD activity. A similar accuracy was maintained even without considering CE results in a simpler version of the score (Ripollés et al., 2021).

However, CEUS has some intrinsic limitations if compared to traditional IUS. The perfusion quantification cannot be compared among different scanners, and both time and costs are higher. Moreover, reproducibility is affected by multiple confounding factors depending on the imaging settings of the available instrumentations, on the operator technique such as the injection method and the pressure exerted by the probe on inflamed bowel wall, and also on patients' characteristics such as the body habitus, the depth of the region of interest and the gas in gut cavity (Cheng et al., 2016). However, the recent introduction of specific software integrated into US devices such as Qontrast (Bracco, Milan, Italy) and QLAB (Philips, Koninklijke, Belgium) allows a quantitative and semiquantitative analysis of contrast enhancement, limiting the subjective component of the evaluation.

Sonoelastography

Sonoelastography is a relatively new sonographic technique that assesses the stiffness of tissues. It is already used in clinical practice for several applications, in particular for breast and thyroid evaluation, and it has been more recently also proposed for assessing gastrointestinal tract. Sonoelastography is able to estimate tissue elasticity by means of US force that propagates a wave into the tissue. Since the wave velocity depends on tissue mechanical properties and mainly on its elasticity, it has been assumed that it is able to provide information on histological features and more precisely on the presence of fibrosis of the bowel wall.

There are two types of elastography: strain and shear wave elastography. With strain elastography compressive force is applied to tissues with repeated pulses to measure lesion stiffness. This can be expressed on a color scale (e.g., from red, soft to blue, hard) for qualitative assessment and/or expressed as wall-to-mesenteric fat strain ratio (i.e., "strain ratio"), for semi-quantitative assessment. In contrast to strain elastography, shear-wave elastography uses an acoustic radiation force impulse, which allows measurement of the propagation speed of shear waves within the tissue. Shear waves propagate faster in hard than in soft tissue and this allows to locally quantify its stiffness. This can be qualitatively assessed by analyzing a colour-scaled image and/or quantitively by determining the maximum elasticity value in either kilopascals (kPa) or meters per second. To date, a limited role is reserved for sonoelastography in the identification of disease activity and inflammation. Only one study assessed inflammation on UC patients, showing a significant correlation between qualitative images of real-time strain-elastography and the severity of lesions at colonoscopy (Ishikawa et al., 2011). However, in more recent studies, Serra et al. and Dillman et al. did not find any significant relationship between elastography parameters and inflammation

TABLE 1 | Imaging techniques and assessment of inflammation in CD compared with histology (i.e., reference standard: histopathology resection). Adapted from Bettenworth et al. (2019) and Gordon et al. (2020).

Study Year Type	Pts (n)	Imaging technique	Features	Results
Maconi et al. (2003) 2003 Prospective	43	US	Evaluation of echo pattern (hypoechoic, stratified or mixed)	Successful differentiation between inflammatory, mixed and fibrotic strictures. Inflammatory stenoses showed a hypoechoic echo pattern
Ripollés et al. (2013) 2013 Prospective	25	CDUS CEUS	Assessment of: -Wall thickness -Inflammatory markers: Loss of stratification, transmural complications, lymphadenopathy -US Doppler signal -Quantitative CE -Presence of stenosis or prestenotic dilation	Successful differentiation in inflammatory and fibrotic strictures Transmural complications, color Doppler grade and percentage of increase in contrast enhancement were significantly associated with the pathology inflammatory score (p = 0.018, p = 0.036 and p = 0.005, respectively) Sonographic and pathology scores showed a good correlation in inflammation (Spearman's, r = 0.53)
Wilkens et al. (2018) 2018 Prospective	25	CEUS (+CE MR enterography)	Peak signal intensity, time to peak, area under the time-intensity curve, wash-in rate, wash-out rate, wash-in perfusion index, area under the curve during wash-in and wash-out, fall time, mean transit time	Unsuccessful differentiation in none, mild/moderate to severe fibrosis and inflammation using CE imaging Successful determination of the degree of inflammation and fibrosis (none, mild/moderate to severe) using US without CE effects Correlation between US wall thickness and histological inflammation (p = 0.001) No correlation was found between the severity of inflammation or fibrosis on histopathology and on CEUS
Girlich et al. (2011) 2011 Prospective	20	CEUS	Description of the perfusion pattern of the inflamed bowel wall Specific quantification software employ for perfusion assessment	Significant correlation with the parameters of the quantitative CEUS analysis Strong negative correlation ($r = -0.677$, $p < 0.01$) between the histopathological score and the time-to-peak (TTP) Strong correlation between TTP and single parameters of the histopathological scoring system (erosion, crypt architecture, crypt, density of eosinophils, excess of intraepithelial neutrophils)
Serra et al. (2017) 2017 Prospective	26	Strain elastography	Strain ratio measurement	Unsuccessful differentiation in fibrosis and inflammation No correlation was found between strain ratio and inflammation (p = 0.53)
Dillman et al. (2014) 2014 Prospective	12	Shear wave elastography	Shear wave speed	No significant difference in mean shear wave speed between high–score and low–inflammation score bowel segments The relationship between bowel wall shear wave speed and inflammation was less correlative and nonsignificant

(**Table 1**) (Dillman et al., 2014; Serra et al., 2017). Thus, this technique is mainly reserved to the assessment of fibrosis and the differentiation between fibrotic and non-fibrotic stenoses.

INTESTINAL ULTRASOUND AND FIBROSIS

Applications

Due to the transmural inflammation in CD patients, endoscopic assessment should be always combined with cross sectional imaging diagnostic techniques, which provide a panoramic evaluation of gut, beyond the evaluation of the mucosal surface. ECCO-ESGAR guidelines suggest using an imaging technique, such as IUS, MRE or CT enterography for the assessment of the small bowel activity, for the response to treatment or in case of relapse, persistent disease activity, new unexplained symptoms, before changing in therapies and in postoperative recurrence. The guidelines underlined the role of both IUS and MRE for the detection of small bowel strictures, but also pointed out their inability in the evaluation of the fibrosis. Moreover, they suggest that the choice of the technique should be taken accordingly to the center experience (Maaser et al., 2019).

In fact, according to an observational study involving 71 CD patients, the overall accuracy of US was similar to MRE for the detection of the mural lesions. However, the specificity of US was superior to MRE for bowel wall thickness, loss of wall stratification and stenosis, while the MRE had higher sensitivity in the detection of loss of wall stratification and

stenosis. US had higher sensitivity in the detection of ascites, while other mesenteric parameters were similar for both techniques (Yuksel et al., 2019).

Identification and Characterization of Strictures

CD is a chronic relapsing inflammatory disease, which evolves in a progressive and irreversible damage of the bowel. According to the Montreal Classification (Sturm et al., 2019), the course of the disease could be penetrating, stricturing or non stricturing/non penetrating. However, this classification is not fixed over time, and the clinical history can change or show mixed types, such as fistula and abscess combined with strictures leading to a high risk of surgery (Gionchetti et al., 2017). This is particularly true for ileal CD, which is usually an inflammatory disease at the time of diagnosis but may become stricturing and penetrating, as well as complicated by strictures and then fistulas and abscesses during the following 10–15 years in almost all patients (Cosnes, 2008).

The stricture, with or without penetrating complication, is still the main indication for surgery, and up to 70% of patients during their life undergo a surgical operation for this complication (Bernell et al., 2000). However, strictures in CD are not always an irreversible condition. The CD strictures show different degrees of inflammation and fibrosis. Rarely, a stricture in CD patients is purely either fibrotic or inflammatory (Rieder et al., 2017).

Since the management and treatment of inflammatory strictures is different from fibrotic strictures, it is useful to differentiate which form is predominant. In particular, inflammation can be successfully treated with medical therapy, such as corticosteroids or targeting TNFα, but fibrosis is an irreversible condition that can be treated only mechanically with balloon dilatation or bowel resection (Gomollón et al., 2017).

Therefore, the differentiation between inflammatory and fibrotic stricture is crucial for the management of CD patients. Unfortunately, no biomarkers, endoscopy or histology could identify the proportion of fibrosis within the stenosis. Likewise, no imaging technique is validated for the identification of the proportion of fibrosis. However, new imaging techniques are emerging and could help in the assessment of the fibrosis within the strictures. In particular, CEUS and Doppler US may evaluate hypervascularity correlated with proportion of inflammation, and sonoelastography, which is a technique that measures the stiffness of tissues, could be used for the identification of fibrosis (Maaser et al., 2019).

The sensitivity and specificity of IUS for the diagnosis of strictures in CD patients range between 80–100% and 63–75%, respectively (Bettenworth et al., 2019), but the differentiation of fibrotic strictures from the inflammatory ones is still a challenge.

The gold standard of the diagnosis of fibrosis remains histology through the analysis of surgical specimens. As reported by Chen et al., smooth muscle hypertrophy and hyperplasia is the most prominent histological change in fibrostenosic bowel strictures. In Crohn's strictures we can find also neuronal and adipose hyperplasia along with active and chronic inflammation and fibrosis. In particular, in Crohn's strictures the normal submucosal collagen and adipose tissue are replaced by fibrosis and accompanied by hyperplasia of the muscularis mucosa, the so called muscularization of the submucosa. The muscularis propria is also thickened and expanded by collagen (Chen et al., 2017). All these factors concur to produce the bowel wall thickening detectable by IUS, and in determining the narrowing of the lumen of the bowel. These are inversely correlated, because even only a bit improvement in the thickening suffice to produce a large increase of the luminal area (Yaffe and Korelitz, 1983).

Several studies have been published about the accuracy of imaging techniques to differentiate between fibrotic and inflammatory components of the stricture. However, only few studies compared these techniques with histology (**Table 2**).

Prognostic Value (Treatment Response)

The assessment of fibrosis on treatment response have been investigated only in one study from Orlando et al. (Orlando et al., 2018). 31 patients without strictures were assessed by strain elastography before a biologic treatment and 3 and 12 months later. Bowel wall thickening and strain ratio have been assessed. The study showed that baseline BWT was not different in patients who responded to the pharmacological treatment and those who underwent operation, while the baseline strain ratio (and so the stiffness of the bowel wall) was significantly greater in patients who underwent operation in the following 2 years and in those who did not reach transmural healing. In particular a SR > 2 was able to discriminate the risk of poor outcome after biologics in the following 2 years (Orlando et al., 2018).

Post Operative Recurrence

A large proportion of CD patients, particularly patients with ileal CD, require surgery due to strictures, penetrating disease, or refractoriness to medical treatment. Noteworthy, more than half of them need further surgeries for the same complication (Buisson et al., 2012). To date, the evaluation of the risk of clinical and surgical recurrence for these patients, relies on assessment of presence and severity of endoscopic recurrence by means of Rutgeert's score, performed within one year after surgery (Gionchetti et al., 2017).

ECCO guidelines have recognized that IUS is a useful emerging tool, alternative to ileocolonoscopy, to identify postoperative recurrence (Maaser et al., 2019). A meta-analysis has shown that the detection by IUS of a pre-anastomic BWT ≥3 mm may detect a postoperative recurrence with an overall sensitivity and specificity of 0.94 (95% CI, 0.86–0.97) and 0.84 (95% CI, 0.62–0.94) and that a post-operative BWT ≥5.5 mm may predict a severe postoperative recurrence (Rutgeert's ≥ 3) with a sensitivity of 83.8% (95% CI, 73.6–90.6%) and specificity of 97.7% (95% CI, 93–99%) (Rispo et al., 2018).

However, it should be acknowledged this meta-analysis included some studies with a small number of patients and with a very high pretest probability of recurrence, thus making the sensitivity of IUS likely oversized. In addition the studies that assessed the accuracy of IUS before 6 months (e.g. at 3 or 6 months) provided disappointing results.

Overall, IUS is now considered a promising tool for assessing postoperative recurrence and to predict the long term outcome of patients. However, prospective studies using IUS coupled with new technologies (e.g., CEUS or elastography) and combined

TABLE 2 | Imaging techniques and characterization of the fibrotic stricture compared with histology.

Study	Year	N pts	Imaging technique	Features	Histopathologic index	Results
Maconi et al. (2003)	2003	43	TUS	Stratified echo pattern or hypoechoic pattern	Fazio et al	Sensitivity 100% specificity 63.3%, PPV 72%, NPV 100% of stratified or mixed echo pattern associated with moderate-severe or intermediate degree of fibrosis in muscolaris mucosae and submucosa
Wilkens et al. (2018)	2018	25	TUS	-Wall thickness	Chiorean et al	-Wall thickness was correlated to fibrosis (r = 0.399, p = 0.048)
			CEUS	-Peak enhancement, total area under curve, wash-in and wash-out area under curve, wash-in perfusion index, wash-in rate, rise and fall time, mean transit time local		-No correlation was found between CEUS and fibrosis (r = -0.28, p = 0.19)
Ripollés et al. (2013)	2013	25	CDUS	-Stenosis, prestenotic dilatation, color Doppler grade 0 or 1, contrast enhancement <46%	Chiorean et al	-Good correlation between US and histopathological score (Spearman's, r = 0.50)
			CEUS	-A formula to calculate the percentage of increase in wall brightness and the "time-to-peak"		-Using a cut-off of 65% of enhancement increase, CEUS had sensitivity 93%, specificity 69%, PPV 78%, NPV 90%, accuracy 82%
Baumgart et al. (2015)	2015	10	US-based real-time elastography	RTE strain mean values	Collagen deposits	RTE strain values were significantly higher in unaffected segments compared with affected (p < 0.001)
Serra et al. (2017)	2017	26	TUS CDUS CEUS RTE	-Thickness and stratification score -Color-Doppler score -CEUS score -Mean strain ratio (MSR)	Chiorean et al.	No correlation was found between thickness score (p = 0.198), stratification score (p = 0.632), Color-Doppler score (p = 0.288), CEUS score (p = 0.205) and MSR (p = 0.877)
Chen et al. (2018)	2018	35	SWE	Shear-wave elastography (SWE)	Semiquantitativscoring system	Cut-off of SWE 22.5 kPa had sensitivity 69.6%, specificity 91.7% and AUROC 0.822 to differentiate between mild/moderate and severe fibrosis
Lu et al. (2017)	2017	15	-CEUS	-Peak enhancement	Active and chronic inflammation, fibrosis, and muscular hypertrophy	-Peak enhancement was negatively correlated with fibrosis (r 1⁄4 20.59, p 1⁄4 0.02)
			-SWE	-SWE measures		-No significant correlation between SWE and fibrosis (p = 0.05)

with fecal calprotectin are awaited to estimate the postoperative risk of stenosis and new surgeries in CD patients. On this regard, it has been demonstrated that in post-operative patients, independently of the time from the previous surgery, a BWT >3 mm may double the risk of surgical recurrence compare to patients with BWT <3 mm, and that the incidence of new surgical interventions is positively correlated with the degree of BWT (Cammarota et al., 2013). Likewise, also in patients who undergo conservative surgery (e.g. stricturoplasties or minimal bowel resections) (Maconi et al., 2001), the behavior of BWT may be a relevant prognostic factor. In fact, the improvement of BWT >2 mm compared to baseline or the normalization of BWT at 6–12 months after surgery has significant favorable prognostic impact on clinical and surgical recurrence, while the IUS detection of unchanged or worsened BWT after surgery predicts a high risk of clinical and surgical recurrence (Maconi et al., 2001). However, the real long term prognostic value of postoperative IUS findings needs further confirmations, as well as the usefulness of therapy escalation, if any, in these patients.

Techniques and Parameters

IUS can detect strictures as intestinal segments characterized by thickened bowel walls, narrowing of the lumen with proximal bowel dilatation greater than 25 mm (Maconi et al., 1996; Panés et al., 2011; Maconi et al., 2018). In particular, in a recent systematic review, the features used to identify the stricture were at least one among luminal narrowing, wall thickness and prestenotic dilatation. Using only one feature, the sensitivity was 80% and specificity 75%. The SICUS which uses 500–750 ml of PEG oral solution before IUS had sensitivity 88–98% and specificity 88–100% for the diagnosis of the stricture using all three parameters (Bettenworth et al., 2019).

B-Mode Ultrasound and Color-Doppler Ultrasound

Regarding the accuracy of IUS in suggesting fibrosis of CD, it has been shown that the thickening of the muscularis propria (clearly visible with IUS), but not the entire bowel wall thickening, was predictive of treatment response and,

in particular, of poor response to anti-TNFα therapy (Saevik et al., 2014).

A prospective study including 43 CD patients operated for a single ileal stricture shows that the stratified or mixed echopattern of the wall of the stricture was associated with a moderate-severe or intermediate degree of fibrosis showing a 100% sensitivity, 63.3% specificity, 72% PPV and 100% NPV. The hypoechoic echopattern was more related to the presence of neutrophil infiltrate (Maconi et al., 2003).

Wall thickness measured by IUS was reported associated to fibrosis in a small cohort of CD patients but without a significant correlation between CEUS and fibrosis (Wilkens et al., 2018).

A recent study assessed the utility of mural and extramural sonographic features of CD as markers of inflammation and fibrosis in comparison to histological sections of the bowel of 12 operated CD patients. It shows that mucosal thickness was mainly associated with fibrosis (Bhatnagar et al., 2021).

Another study evaluated the accuracy of US, by using several parameters - such as wall thickness, transmural complications, color Doppler grade, quantitative analysis of the contrast enhancement at CEUS and the presence and severity of strictures - to characterize intestinal inflammation and fibrosis in CD strictures. When compared to the histopathology findings, a negative association was found between the color Doppler grade and the pathologic fibrostenotic score (Ripollés et al., 2013).

Contrast-Enhanced Ultrasound

International guidelines recommend the use of CEUS to detect hypervascularity and inflammatory activity of CD strictures (Sidhu et al., 2018). Indeed, the intravenous contrast agent enhances the highly vascularized Crohn's stenotic segments, which are more likely inflammatory stenosis, and it does not enhance the non-vascularized ones, which are likely fibrotic (Wilson and Burns, 2010).

However, the quantitative assessment of the blood flow within the wall of strictures, inflammatory or fibrotic, may be difficult and not always reliable. Several parameters have been identified to describe and give an estimation of the flow such as the wash in rate, the time to peak, the peak enhancement and the area under the curve (Quaia et al., 2018). Using some of these parameters, the first studies evaluated the blood flow within the wall of the strictures compared to histologic findings, showing positive and very promising results. A small study, including 8 CD patients who underwent CEUS and surgery in the following year, has shown that three patients with fibrotic strictures had no or low signal echo intensity after contrast administration (Kratzer et al., 2002). These preliminary results have been confirmed by another study showing that a 65% of contrast enhancement within the stricture wall had sensitivity, specificity, PPV, NPV and accuracy of 93, 69, 78, 90, and 82% for discriminating predominant inflammatory from predominant fibrotic stenoses (Ripollés et al., 2013). These promising results have been confirmed by Lu et al. who showed an inverse correlation between the peak enhancement at CEUS and the histological degree of fibrosis (Lu et al., 2017), but not by other studies (Serra et al., 2017; Wilkens et al., 2018). In particular, Wilkens et al. used several CEUS parameters to characterize the stricture but did not find any positive or negative correlation between CEUS parameters and the histological features of the strictures. Interestingly, also MRE parameters did not show any positive or negative correlation with histological fibrosis and inflammation (Wilkens et al., 2018).

Sonoelastography

An interesting sonographic tool that may be used to characterize the strictures and assess fibrosis is elastography, both strain elastography and shear-wave elastography (SWE). The strain elastography investigates the stiffness of the bowel wall by means of repeated pressures with the probe on the abdominal wall. The system informs the operator when the signal is stable and reliable or reproducible and the image is captured and analyzed. Conventionally, the blue or red color means hard or soft tissue, respectively. The system gives either a qualitative and subjective assessment of the stiffness by examining the colors, and a quantitative estimation of the stiffness, by comparing the value within a region of interest in the wall with a similar one outside of the wall, usually taken from the softer tissue around (Stidham et al., 2011; Lu et al., 2019; Vestito et al., 2019). On the contrary, the SWE is a system that directly calculates the elasticity in kPascal thanks to the diffusion of the beam within the tissue in specific regions of interest, without the necessity to pressurize repeatedly the abdomen (Vestito et al., 2019).

A meta-analysis, whose conclusion has some limitations due to high heterogeneity and patient selection between the six studies included, shows that sonoelastography could be useful to detect fibrosis in CD strictures. Three studies used strain elastography and showed that the strain ratio was higher in strictures with fibrosis compared to strictures without fibrosis ($p = 0.05$). Similar results were found by the other three studies that used SWE, where the strain value was statistically higher in fibrotic stenosis ($p = 0.08$) (Vestito et al., 2019).

A few studies have also compared the sonoelastography results with histological evaluation. Fraquelli et al. assessed the ileal strictures in Crohn's patients by strain elastography, comparing the results with the rate of fibrosis assessed by histology. The ileal wall fibrosis percentages in histological sections showed a significant and positive correlation with ileal wall strain ratios obtained by elastography ($p = 0.005$) (Fraquelli et al., 2015).

A small study, including 16 CD patients with either ileocolonic localization or postoperative recurrence, showed that fibrotic strictures had a significantly higher axial-strain sonoelastography scores than inflammatory strictures (Sconfienza et al., 2016). Chen et al. performed SWE in 35 CD patients who underwent surgery within one week and demonstrated that SWE was significantly higher in patients with fibrosis in the stricture than in patients with inflammation. Setting 22.55 kPa as the cut-off value, the sensitivity was 69.6%, the specificity reached 91.7% with the area under the ROC curve (AUROC) of 0.822, thus allowing to differentiate between mild/moderate and severe fibrosis (Chen et al., 2018).

However, not all the studies showed positive and promising results. Lu et al. did not find a significant correlation between SWE and fibrosis ($p = 0.05$) (Lu et al., 2017), but reported a

moderate correlation between SWE and muscular hypertrophy (r 1/4 0.59, p 1/4 0.02) in 15 CD patients. Serra et al. reported data from 26 CD patients who underwent IUS, color-Doppler, CEUS and real time elastography, without finding any correlation between any of the previous techniques and fibrosis score at the histological examination (Serra et al., 2017).

CONCLUSION

Despite the high accuracy of US in detecting strictures, and the promising results obtained with the novel sonographic techniques such as CEUS and sonoelastography, several limitations are still present and more studies are needed before using these technique in routine clinical practice and trials.

Ultrasound is a well-known operator and patient dependent technique and, apart from operator experience, there are bowel segments that are difficult to scan by IUS, such as proximal ileum, jejunum and deep pelvic loops due to intestinal gaseous content, which is rather frequent in patients with chronic strictures. In addition, the fine evaluation of long strictures and multiple strictures may be difficult, particularly in case of quantitative assessment with CEUS and elastography because of need of repeated measurements, and the uncertainty on the exact part of the stenotic segment that should be evaluated. On this regard, MRE, which offers a multiparametric more panoramic view, may be more accurate.

Like MRE, the bowel evaluation with IUS currently allows a multiparametric approach where B-mode, Doppler, CEUS and elastography can be applied to simultaneously assess inflammation and fibrosis in the same segment. A preliminary experience on this multiparametric approach has been performed using in combination IUS, CEUS, and sonoelastography by two readers providing an accuracy of 70 and 75% with the area under the ROC curve (AUROC) of 0.953 and 0.921 and both were significantly higher than the single technique in the detection of fibrosis ($p = 0.001$ and $p < 0.05$, respectively) (Quaia et al., 2018).

In the last years, important steps have been done in this direction. First, a valid gold standard for fibrosis and inflammation, which is mandatory to have reliable studies, has been defined. Important systematic reviews and research groups have appropriately addressed this point (Bettenworth et al., 2019; De Voogd et al., 2020). Then, the concept has emerged that the IUS parameters and scores obtained by each technique need a validation and should be reproducible. This has been done in few studies including this review, but the big challenge remains to assess CD activity (Novak et al., 2020), an issue that will be faced for strictures in the near future.

If these criteria will be fulfilled by IUS and MRI, we will have powerful tools to study strictures and fibrosis of CD, we will able to select the most appropriate diagnostic techniques for our patients, reliable to decide if a stricture should be surgically or medically treated and to monitor its outcome after the therapy.

AUTHOR CONTRIBUTIONS

FF and RC contributed equally. FF and RC: made the literature search, wrote the draft of the manuscript and approved the final manuscript as submitted. SA and JM: edited and critically reviewed the manuscript and approved the final manuscript as submitted. GM: conceptualized and designed the study, made the literature search, critically reviewed the manuscript and approved the final manuscript as submitted.

REFERENCES

Astegiano, M., Bresso, F., Cammarota, T., Sarno, A., Robotti, D., Demarchi, B., et al. (2001). Abdominal Pain and Bowel Dysfunction: Diagnostic Role of Intestinal Ultrasound. *Eur. J. Gastroenterol. Hepatol.* 13 (8), 927–931. doi:10.1097/00042737-200108000-00009

Baumgart, D. C., Müller, H. P., Grittner, U., Metzke, D., Fischer, A., Guckelberger, O., et al. (2015). US-based Real-Time Elastography for the Detection of Fibrotic Gut Tissue in Patients with Stricturing Crohn Disease. *Radiology* 275 (3), 889–899. doi:10.1148/radiol.14141929

Bernell, O., Lapidus, A., and Hellers, G. (2000). Risk Factors for Surgery and Postoperative Recurrence in Crohn's Disease. *Ann. Surg.* 231 (1), 38–45. doi:10.1097/00000658-200001000-00006

Bettenworth, D., Bokemeyer, A., Baker, M., Mao, R., Parker, C. E., Nguyen, T., et al. (2019). Assessment of Crohn's Disease-Associated Small Bowel Strictures and Fibrosis on Cross-Sectional Imaging: a Systematic Review. *Gut* 68 (6), 1115–1126. doi:10.1136/gutjnl-2018-318081

Bhatnagar, G., Rodriguez-Justo, M., Higginson, A., Bassett, P., Windsor, A., Cohen, R., et al. (2021). Inflammation and Fibrosis in Crohn's Disease: Location-Matched Histological Correlation of Small Bowel Ultrasound Features. *Abdom. Radiol.* 46 (1), 144–155. doi:10.1007/s00261-020-02603-6

Bots, S., Nylund, K., Löwenberg, M., Gecse, K., Gilja, O. H., and D'Haens, G. (2018). Ultrasound for Assessing Disease Activity in IBD Patients: A Systematic Review of Activity Scores. *J. Crohn's colitis.* 12 (8), 920–929. doi:10.1093/ecco-jcc/jjy048

Buisson, A., Chevaux, J. B., Allen, P. B., Bommelaer, G., and Peyrin-Biroulet, L. (2012). Review Article: the Natural History of Postoperative Crohn's Disease Recurrence. *Lett. Editors* 35, 625–633. doi:10.1111/j.1365-2036.2012.05002.x

Buisson, A., Hordonneau, C., Goutte, M., Boyer, L., Pereira, B., and Bommelaer, G. (2015). Diffusion-weighted Magnetic Resonance Imaging Is Effective to Detect Ileocolonic Ulcerations in Crohn's Disease. *Aliment. Pharmacol. Ther.* 42 (4), 452–460. doi:10.1111/apt.13287

Buisson, A., Pereira, B., Goutte, M., Reymond, M., Allimant, C., Obritin-Guilhen, H., et al. (2017). Magnetic Resonance Index of Activity (MaRIA) and Clermont Score Are Highly and Equally Effective MRI Indices in Detecting Mucosal Healing in Crohn's Disease. *Dig. Liver Dis.* 49 (11), 1211–1217. doi:10.1016/j.dld.2017.08.033

Calabrese, E., La Seta, F., Buccellato, A., Virdone, R., Pallotta, N., Corazziari, E., et al. (2005). Crohn's Disease: A Comparative Prospective Study of Transabdominal Ultrasonography, Small Intestine Contrast Ultrasonography, and Small Bowel Enema. *Inflamm. Bowel Dis.* 11 (2), 139–145. doi:10.1097/00054725-200502000-00007

Calabrese, E., Zorzi, F., Zuzzi, S., Ooka, S., Onali, S., Petruzziello, C., et al. (2012). Development of a Numerical Index Quantitating Small Bowel Damage as Detected by Ultrasonography in Crohn's Disease. *J. Crohn's Colitis* 6 (8), 852–860. doi:10.1016/j.crohns.2012.01.015

Calabrese, E., Maaser, C., Zorzi, F., Kannengiesser, K., Hanauer, S. B., Bruining, D. H., et al. (2016). Bowel Ultrasonography in the Management of Crohn's Disease. A Review with Recommendations of an International Panel of Experts. *Inflamm. Bowel Dis.* 22 (5), 1168–1183. doi:10.1097/mib.0000000000000706

Cammarota, T., Ribaldone, D. G., Resegotti, A., Repici, A., Danese, S., Fiorino, G., et al. (2013). Role of Bowel Ultrasound as a Predictor of Surgical Recurrence of Crohn's Disease. *Scand. J. Gastroenterol.* 48, 552–555. doi:10.3109/00365521.2013.777774

Carter, D., Katz, L. H., Bardan, E., Salomon, E., Goldstein, S., Ben Horin, S., et al. (2018). The Accuracy of Intestinal Ultrasound Compared with Small Bowel

Capsule Endoscopy in Assessment of Suspected Crohn's Disease in Patients with Negative Ileocolonoscopy. *Therap Adv. Gastroenterol.* 11, 1756284818765908. doi:10.1177/1756284818765908

Castiglione, F., Testa, A., Rea, M., De Palma, G. D., Diaferia, M., Musto, D., et al. (2013). Transmural Healing Evaluated by Bowel Sonography in Patients with Crohn's Disease on Maintenance Treatment with Biologics. *Inflamm. Bowel Dis.* 19 (9), 1928–1934. doi:10.1097/mib.0b013e3182802b87

Castiglione, F., Mainenti, P., Testa, A., Imperatore, N., De Palma, G. D., Maurea, S., et al. (2017). Cross-sectional Evaluation of Transmural Healing in Patients with Crohn's Disease on Maintenance Treatment with Anti-TNF Alpha Agents. *Dig. Liver Dis.* 49 (5), 484–489. doi:10.1016/j.dld.2017.02.014

Chen, W., Lu, C., Hirota, C., Iacucci, M., Ghosh, S., and Gui, X. (2017). Smooth Muscle Hyperplasia/Hypertrophy Is the Most Prominent Histological Change in Crohn's Fibrostenosing Bowel Strictures: A Semiquantitative Analysis by Using a Novel Histological Grading Scheme. *J. Crohns. Colitis.* 11 (1), 92–104. doi:10.1093/ecco-jcc/jjw126

Chen, Y. J., Mao, R., Md, X. H. L., Cao, Q. H., Chen, Z. H., Liu, B. X., et al. (2018). Real-Time Shear Wave Ultrasound Elastography Differentiates Fibrotic from Inflammatory Strictures in Patients with Crohn's Disease. *Inflamm. Bowel Dis.* 24 (10), 2183–2190. doi:10.1093/ibd/izy115

Cheng, W., Gao, X., Wang, W., Zhi, M., Tang, J., Wen, Y.-l., et al. (2016). Preliminary Analysis of Clinical Situations Involved in Quantification of Contrast-Enhanced Ultrasound in Crohn's Disease. *Ultrasound Med. Biol.* 42 (8), 1784–1791. doi:10.1016/j.ultrasmedbio.2016.03.001

Civitelli, F., Nuti, F., Oliva, S., Messina, L., La Torre, G., Viola, F., et al. (2016). Looking beyond Mucosal Healing. *Inflamm. Bowel Dis.* 22 (10), 2418–2424. doi:10.1097/mib.0000000000000897

Cosnes, J., Cattan, S., Blain, A., Beaugerie, L., Carbonnel, F., Parc, R., et al. (2002). Long-term Evolution of Disease Behavior of Crohn's Disease. *Inflamm. Bowel Dis.* 8 (4), 244–250. doi:10.1097/00054725-200207000-00002

Cosnes, J. (2008). Crohn's Disease Phenotype, Prognosis, and Long-Term Complications: what to Expect? *Acta Gastroenterol. Belg.* 71 (3), 303–307.

De Voogd, F. A., Mookhoek, A., Gecse, K. B., De Hertogh, G., Bemelman, W. A., Buskens, C. J., et al. (2020). Systematic Review: Histological Scoring of Strictures in Crohn's Disease. *J. Crohns Colitis* 14 (6), 734–742. doi:10.1093/ecco-jcc/jjz177

Dillman, J. R., Stidham, R. W., Higgins, P. D. R., Moons, D. S., Johnson, L. A., Keshavarzi, N. R., et al. (2014). Ultrasound Shear Wave Elastography Helps Discriminate Low-Grade from High-Grade Bowel Wall Fibrosis in Ex Vivo Human Intestinal Specimens. *J. Ultrasound Med.* 33 (12), 2115–2123. doi:10.7863/ultra.33.12.2115

Drews, B. H., Barth, T. F. E., Hänle, M. M., Akinli, A. S., Mason, R. A., Muche, R., et al. (2009). Comparison of Sonographically Measured Bowel Wall Vascularity, Histology, and Disease Activity in Crohn's Disease. *Eur. Radiol.* 19 (6), 1379–1386. doi:10.1007/s00330-008-1290-5

Fraquelli, M., Branchi, F., Cribiù, F. M., Orlando, S., Casazza, G., Magarotto, A., et al. (2015). The Role of Ultrasound Elasticity Imaging in Predicting Ileal Fibrosis in Crohn's Disease Patients. *Inflamm. Bowel Dis.* 21 (11), 2605–2612. doi:10.1097/mib.0000000000000536

Gionchetti, P., Dignass, A., Danese, S., Magro Dias, F. J., Rogler, G., Lakatos, P. L., et al. (2017). 3rd European Evidence-Based Consensus on the Diagnosis and Management of Crohn's Disease 2016: Part 2: Surgical Management and Special Situations. *J. Crohns Colitis* 11 (2), 135–149. doi:10.1093/ecco-jcc/jjw169

Girlich, C., Jung, E. M., Huber, E., Ott, C., Iesalnieks, I., Schreyer, A., et al. (2011). Comparison between Preoperative Quantitative Assessment of Bowel Wall Vascularization by Contrast-Enhanced Ultrasound and Operative Macroscopic Findings and Results of Histopathological Scoring in Crohn's Disease. *Ultraschall Med.* 32 (2), 154–159. doi:10.1055/s-0029-1245398

Gomollón, F., Dignass, A., Annese, V., Tilg, H., Van Assche, G., Lindsay, J. O., et al. (2017). 3rd European Evidence-Based Consensus on the Diagnosis and Management of Crohn's Disease 2016: Part 1: Diagnosis and Medical Management. *J. Crohns Colitis* 11 (1), 3–25. doi:10.1093/ecco-jcc/jjw168

Gong, P., Song, P., Kolbe, A. B., Sheedy, S. P., Huang, C., Ling, W., et al. (2020). Quantitative Inflammation Assessment for Crohn Disease Using Ultrasensitive Ultrasound Microvessel Imaging. *J. Ultrasound Med.* 39 (9), 1819–1827. doi:10.1002/jum.15290

Goodsall, T. M., Nguyen, T. M., Parker, C. E., Ma, C., Andrews, J. M., Jairath, V., et al. (2020). Systematic Review: Gastrointestinal Ultrasound Scoring Indices for Inflammatory Bowel Disease. *J. Crohns Colitis* 15 (1), 125–142. doi:10.1093/ecco-jcc/jjaa129

Gordon, I. O., Bettenworth, D., Bokemeyer, A., Srivastava, A., Rosty, C., de Hertogh, G., et al. (2020). Histopathology Scoring Systems of Stenosis Associated with Small Bowel Crohn's Disease: A Systematic Review. *Gastroenterology* 158 (1), 137–150. doi:10.1053/j.gastro.2019.08.033

Hollerbach, S., Geissler, A., Schiegl, H., Kullmann, F., Lock, G., Schmidt, J., et al. (1998). The Accuracy of Abdominal Ultrasound in the Assessment of Bowel Disorders. *Scand. J. Gastroenterol.* 33 (11), 1201–1208. doi:10.1080/00365529850172575

Ishikawa, D., Ando, T., Watanabe, O., Ishiguro, K., Maeda, O., Miyake, N., et al. (2011). Images of Colonic Real-Time Tissue Sonoelastography Correlate with Those of Colonoscopy and May Predict Response to Therapy in Patients with Ulcerative Colitis. *BMC Gastroenterol.* 11, 29. doi:10.1186/1471-230x-11-29

Kopylov, U., Yung, D. E., Engel, T., Vijayan, S., Har-Noy, O., Katz, L., et al. (2017). Diagnostic Yield of Capsule Endoscopy versus Magnetic Resonance Enterography and Small Bowel Contrast Ultrasound in the Evaluation of Small Bowel Crohn's Disease: Systematic Review and Meta-Analysis. *Dig. Liver Dis.* 49 (8), 854–863. doi:10.1016/j.dld.2017.04.013

Kratzer, W., von Tirpitz, C., Mason, R., Reinshagen, M., Adler, G., Möller, P., et al. (2002). Contrast-enhanced Power Doppler Sonography of the Intestinal Wall in the Differentiation of Hypervascularized and Hypovascularized Intestinal Obstructions in Patients with Crohn's Disease. *J. Ultrasound Med.* 21 (2), 149. doi:10.7863/jum.2002.21.2.149

Kucharzik, T., Wittig, B. M., Helwig, U., Börner, N., Rössler, A., Rath, S., et al. (2017). Use of Intestinal Ultrasound to Monitor Crohn's Disease Activity. *Clin. Gastroenterol. Hepatol.* 15 (4), 535–542. doi:10.1016/j.cgh.2016.10.040

Livne, M., Amitai, M. M., Klang, E., Ben Horin, S., Ungar, B., Levartovsky, A., et al. (2020). Qualitative Sonographic Assessment of Transmural Ileal Inflammation in Crohn's Disease. *Eur. J. Gastroenterol. Hepatol.* [Epub ahead of print]. doi:10.1097/MEG.0000000000002016

Lu, C., Gui, X., Chen, W., Fung, T., Novak, K., and Wilson, S. R. (2017). Ultrasound Shear Wave Elastography and Contrast Enhancement: Effective Biomarkers in Crohn's Disease Strictures. *Inflamm. Bowel Dis.* 23 (3), 421–430. doi:10.1097/mib.0000000000001020

Lu, C., Merrill, C., Medellin, A., Novak, K., and Wilson, S. R. (2019). Bowel Ultrasound State of the Art: Grayscale and Doppler Ultrasound, Contrast Enhancement, and Elastography in Crohn Disease. *J. Ultrasound Med.* 38 (2), 271–288. doi:10.1002/jum.14920

Maaser, C., Sturm, A., Vavricka, S. R., Kucharzik, T., Fiorino, G., Annese, V., et al. (2019). ECCO-ESGAR Guideline for Diagnostic Assessment in IBD Part 1: Initial Diagnosis, Monitoring of Known IBD, Detection of Complications. *J. Crohn's colitis* 13 (2), 144K–164K. doi:10.1093/ecco-jcc/jjy113

Maconi, G., Bollani, S., and Bianchi Porro, G. (1996). Ultrasonographic Detection of Intestinal Complications in Crohn's Disease. *Dig. Dis Sci.* 41 (8), 1643–1648. doi:10.1007/bf02087914

Maconi, G., Sampietro, G. M., Cristaldi, M., Danelli, P., Russo, A., Porro, G. B., et al. (2001). Preoperative Characteristics and Postoperative Behavior of Bowel Wall on Risk of Recurrence after Conservative Surgery in Crohn's Disease: a Prospective Study. *Ann. Surg.* 233, 345–352. doi:10.1097/00000658-200103000-00007

Maconi, G., Carsana, L., Fociani, P., Sampietro, G. M., Ardizzone, S., Cristaldi, M., et al. (2003). Small Bowel Stenosis in Crohn's Disease: Clinical, Biochemical and Ultrasonographic Evaluation of Histological Features. *Aliment. Pharmacol. Ther.* 18 (7), 749–756. doi:10.1046/j.1365-2036.2003.01673.x

Maconi, G., Nylund, K., Ripolles, T., Calabrese, E., Dirks, K., Dietrich, C., et al. (2018). EFSUMB Recommendations and Clinical Guidelines for Intestinal Ultrasound (GIUS) in Inflammatory Bowel Diseases. *Ultraschall Med.* 39 (3), 304–317. doi:10.1055/s-0043-125329

Migaleddu, V., Scanu, A. M., Quaia, E., Rocca, P. C., Dore, M. P., Scanu, D., et al. (2009). Contrast-enhanced Ultrasonographic Evaluation of Inflammatory Activity in Crohn's Disease. *Gastroenterology* 137 (1), 43–52. doi:10.1053/j.gastro.2009.03.062

Novak, K. L., Nylund, K., Maaser, C., Petersen, F., Kucharzik, T., Lu, C., et al. (2020). Expert Consensus on Optimal Acquisition and Development of the International Bowel Ultrasound Segmental Activity Score (IBUS-SAS): a Reliability and Inter-rater Variability Study on Intestinal Ultrasonography in Crohn's Disease. *J. Crohns Colitis* 15 (4), 609–616. doi:10.1093/ecco-jcc/jjaa216

Orlando, S., Fraquelli, M., Coletta, M., Branchi, F., Magarotto, A., Conti, C. B., et al. (2018). Ultrasound Elasticity Imaging Predicts Therapeutic Outcomes of Patients with Crohn's Disease Treated with Anti-tumour Necrosis Factor Antibodies. *J. Crohns Colitis* 12 (1), 63–70. doi:10.1093/ecco-jcc/jjx116

Pallotta, N., Tomei, E., Viscido, A., Calabrese, E., Marcheggiano, A., Caprilli, R., et al. (2005). Small Intestine Contrast Ultrasonography: an Alternative to Radiology in the Assessment of Small Bowel Disease. *Inflamm. Bowel Dis.* 11 (2), 146–153. doi:10.1097/00054725-200502000-00008

Pallotta, N., Vincoli, G., Montesani, C., Chirletti, P., Pronio, A., Caronna, R., et al. (2012). Small Intestine Contrast Ultrasonography (SICUS) for the Detection of Small Bowel Complications in Crohn's Disease: A Prospective Comparative Study versus Intraoperative Findings. *Inflamm. Bowel Dis.* 18 (1), 74–84. doi:10.1002/ibd.21678

Panés, J., Bouzas, R., Chaparro, M., García-Sánchez, V., Gisbert, J. P., Martínez de Guereñu, B., et al. (2011). Systematic Review: the Use of Ultrasonography, Computed Tomography and Magnetic Resonance Imaging for the Diagnosis, Assessment of Activity and Abdominal Complications of Crohn's Disease. *Aliment. Pharmacol. Ther.* 34 (2), 125–145. doi:10.1111/j.1365-2036.2011.04710.x

Paredes, J. M., Ripollés, T., Cortés, X., Moreno, N., Martínez, M. J., Bustamante-Balén, M., et al. (2013). Contrast-enhanced Ultrasonography: Usefulness in the Assessment of Postoperative Recurrence of Crohn's Disease. *J. Crohn's Colitis* 7 (3), 192–201. doi:10.1016/j.crohns.2012.03.017

Parente, F., Greco, S., Molteni, M., Cucino, C., Maconi, G., Sampietro, G. M., et al. (2003). Role of Early Ultrasound in Detecting Inflammatory Intestinal Disorders and Identifying Their Anatomical Location within the Bowel. *Aliment. Pharmacol. Ther.* 18 (10), 1009–1016. doi:10.1046/j.1365-2036.2003.01796.x

Petruzziello, C., Onali, S., Calabrese, E., Zorzi, F., Ascolani, M., Condino, G., et al. (2010). Wireless Capsule Endoscopy and Proximal Small Bowel Lesions in Crohn's Disease. *World. J. Gastroenterol.* 16 (26), 3299–3304. doi:10.3748/wjg.v16.i26.3299

Peyrin-Biroulet, L., Loftus, E. V., Jr., Colombel, J.-F., and Sandborn, W. J. (2010). The Natural History of Adult Crohn's Disease in Population-Based Cohorts. *Am. J. Gastroenterol.* 105 (2), 289–297. doi:10.1038/ajg.2009.579

Quaia, E., Cabibbo, B., De Paoli, L., Toscano, W., Poillucci, G., and Cova, M. A. (2013). The Value of Time-Intensity Curves Obtained after Microbubble Contrast Agent Injection to Discriminate Responders from Non-responders to Anti-inflammatory Medication Among Patients with Crohn's Disease. *Eur. Radiol.* 23 (6), 1650–1659. doi:10.1007/s00330-012-2754-1

Quaia, E., Gennari, A. G., Cova, M. A., and van Beek, E. J. R. (2018). Differentiation of Inflammatory from Fibrotic Ileal Strictures Among Patients with Crohn's Disease Based on Visual Analysis: Feasibility Study Combining Conventional B-Mode Ultrasound, Contrast-Enhanced Ultrasound and Strain Elastography. *Ultrasound Med. Biol.* 44 (4), 762–770. doi:10.1016/j.ultrasmedbio.2017.11.015

Rieder, F., Fiocchi, C., and Rogler, G. (2017). Mechanisms, Management, and Treatment of Fibrosis in Patients with Inflammatory Bowel Diseases. *Gastroenterology* 152 (2), 340–350. doi:10.1053/j.gastro.2016.09.047

Rimola, J., Ordás, I., Rodriguez, S., García-Bosch, O., Aceituno, M., Llach, J., et al. (2011). Magnetic Resonance Imaging for Evaluation of Crohn's Disease: Validation of Parameters of Severity and Quantitative Index of Activity. Inflammatory Bowel Diseases. *Inflamm. Bowel Dis.* 17 (8), 1759–1768. doi:10.1002/ibd.21551

Rimola, J., Ordás, I., Rodríguez, S., Ricart, E., and Panés, J. (2012). Imaging Indexes of Activity and Severity for Crohn's Disease: Current Status and Future Trends. *Abdom. Imaging* 37 (6), 958–966. doi:10.1007/s00261-011-9820-z

Ripollés, T., Martínez, M. J., Paredes, J. M., Blanc, E., Flors, L., and Delgado, F. (2009). Crohn Disease: Correlation of Findings at Contrast-Enhanced US with Severity at Endoscopy. *Radiology* 253 (1), 241–248. doi:10.1148/radiol.2531082269

Ripollés, T., Rausell, N., Paredes, J. M., Grau, E., Martínez, M. J., and Vizuete, J. (2013). Effectiveness of Contrast-Enhanced Ultrasound for Characterisation of Intestinal Inflammation in Crohn's Disease: a Comparison with Surgical Histopathology Analysis. *J. Crohn's Colitis* 7 (2), 120–128. doi:10.1016/j.crohns.2012.03.002

Ripollés, T., Poza, J., Suarez Ferrer, C., Martínez-Pérez, M. J., Martín-Algíbez, A., and de Las Heras Paez, B. (2021). Evaluation of Crohn's Disease Activity: Development of an Ultrasound Score in a Multicenter Study. *Inflamm. Bowel Dis.* 27 (1), 145–154. doi:10.1093/ibd/izaa134

Rispo, A., Imperatore, N., Testa, A., Nardone, O. M., Luglio, G., Caporaso, N., et al. (2018). Diagnostic Accuracy of Ultrasonography in the Detection of Postsurgical Recurrence in Crohn's Disease: A Systematic Review with Meta-Analysis. *Inflamm. Bowel Dis.* 24, 977–988. doi:10.1093/ibd/izy012

Saevik, F., Nylund, K., Hausken, T., Ødegaard, S., and Gilja, O. H. (2014). Bowel Perfusion Measured with Dynamic Contrast-Enhanced Ultrasound Predicts Treatment Outcome in Patients with Crohn's Disease. *Inflamm. Bowel Dis.* 20 (11), 2029–2037. doi:10.1097/mib.0000000000000159

Sasaki, T., Kunisaki, R., Kinoshita, H., Kimura, H., Kodera, T., Nozawa, A., et al. (2014a). Doppler Ultrasound Findings Correlate with Tissue Vascularity and Inflammation in Surgical Pathology Specimens from Patients with Small Intestinal Crohn's Disease. *BMC Res. Notes* 7, 363. doi:10.1186/1756-0500-7-363

Sasaki, T., Kunisaki, R., Kinoshita, H., Yamamoto, H., Kimura, H., Hanzawa, A., et al. (2014b). Use of Color Doppler Ultrasonography for Evaluating Vascularity of Small Intestinal Lesions in Crohn's Disease: Correlation with Endoscopic and Surgical Macroscopic Findings. *Scand. J. Gastroenterol.* 49 (3), 295–301. doi:10.3109/00365521.2013.871744

Sconfienza, L. M., Cavallaro, F., Colombi, V., Pastorelli, L., Tontini, G., Pescatori, L., et al. (2016). *In-vivo* Axial-Strain Sonoelastography Helps Distinguish Acutely-Inflamed from Fibrotic Terminal Ileum Strictures in Patients with Crohn's Disease: Preliminary Results. *Ultrasound Med. Biol.* 42 (4), 855–863. doi:10.1016/j.ultrasmedbio.2015.11.023

Serra, C., Menozzi, G., Labate, A. M. M., Giangregorio, F., Gionchetti, P., Beltrami, M., et al. (2007). Ultrasound Assessment of Vascularization of the Thickened Terminal Ileum Wall in Crohn's Disease Patients Using a Low-Mechanical Index Real-Time Scanning Technique with a Second Generation Ultrasound Contrast Agent. *Eur. J. Radiol.* 62 (1), 114–121. doi:10.1016/j.ejrad.2006.11.027

Serra, C., Rizzello, F., Pratico', C., Felicani, C., Fiorini, E., Brugnera, R., et al. (2017). Real-time Elastography for the Detection of Fibrotic and Inflammatory Tissue in Patients with Stricturing Crohn's Disease. *J. Ultrasound* 20 (4), 273–284. doi:10.1007/s40477-017-0265-2

Sidhu, P., Cantisani, V., Dietrich, C., Gilja, O., Saftoiu, A., Bartels, E., et al. (2018). The EFSUMB Guidelines and Recommendations for the Clinical Practice of Contrast-Enhanced Ultrasound (CEUS) in Non-hepatic Applications: Update 2017 (Long Version). *Ultraschall Med.* 39 (2), e2–e44. doi:10.1055/a-0586-1107

Stidham, R. W., Xu, J., Johnson, L. A., Kim, K., Moons, D. S., McKenna, B. J., et al. (2011). Ultrasound Elasticity Imaging for Detecting Intestinal Fibrosis and Inflammation in Rats and Humans with Crohn's Disease. *Gastroenterology* 141 (3), 819–826. doi:10.1053/j.gastro.2011.07.027

Sturm, A., Maaser, C., Calabrese, E., Annese, V., Fiorino, G., Kucharzik, T., et al. (2019). ECCO-ESGAR Guideline for Diagnostic Assessment in IBD Part 2: IBD Scores and General Principles and Technical Aspects. *J. Crohns Colitis* 13 (3), 273–284. doi:10.1093/ecco-jcc/jjy114

Taylor, S. A., Mallett, S., Bhatnagar, G., Baldwin-Cleland, R., Bloom, S., Gupta, A., et al. (2018). Diagnostic Accuracy of Magnetic Resonance Enterography and Small Bowel Ultrasound for the Extent and Activity of Newly Diagnosed and Relapsed Crohn's Disease (METRIC): a Multicentre Trial. *Lancet Gastroenterol. Hepatol.* 3 (8), 548–558. doi:10.1016/s2468-1253(18)30161-4

Vestito, A., Marasco, G., Maconi, G., Festi, D., Bazzoli, F., and Zagari, R. M. (2019). Role of Ultrasound Elastography in the Detection of Fibrotic Bowel Strictures in Patients with Crohn's Disease: Systematic Review and Meta-Analysis. *Ultraschall Med.* 40 (5), 646–654. doi:10.1055/a-0865-1842

Vos, M. D., Louis, E. J., Jahnsen, J., Vandervoort, J. G. P., Noman, M., Dewit, O., et al. (2013). Consecutive Fecal Calprotectin Measurements to Predict Relapse in Patients with Ulcerative Colitis Receiving Infliximab Maintenance Therapy. *Inflamm. Bowel Dis.* 19 (10), 2111–2117. doi:10.1097/mib.0b013e31829b2a37

Wilkens, R., Hagemann-Madsen, R. H., Peters, D. A., Nielsen, A. H., Nørager, C. B., Glerup, H., et al. (2018). Validity of Contrast-Enhanced Ultrasonography and Dynamic Contrast-Enhanced MR Enterography in the Assessment of Transmural Activity and Fibrosis in Crohn′s Disease. *J. Crohns Colitis* 12 (1), 48–56. doi:10.1093/ecco-jcc/jjx111

Wilson, S. R., and Burns, P. N. (2010). Microbubble-enhanced US in Body Imaging: what Role? *Radiology* 257 (1), 24–39. doi:10.1148/radiol.10091210

Yaffe, B. H., and Korelitz, B. I. (1983). Prognosis for Nonoperative Management of Small-Bowel Obstruction in Crohn's Disease. *J. Clin. Gastroenterol.* 5 (3), 211–216. doi:10.1097/00004836-198306000-00003

Yuksel, I., Kilincalp, S., Coskun, Y., Akinci, H., Hamamci, M., and Alkan, A. (2019). Diagnostic Accuracy of Intestinal Ultrasound and Magnetic Resonance Enterography for the Detection of Endoscopy-Based Disease Activity in Ileocolonic Crohn's Disease. *Eur. J. Gastroenterol. Hepatol.* 31 (7), 809–816. doi:10.1097/meg.0000000000001438

Zorzi, F., Stasi, E., Bevivino, G., Scarozza, P., Biancone, L., Zuzzi, S., et al. (2014). A Sonographic Lesion Index for Crohn's Disease Helps Monitor Changes in Transmural Bowel Damage during Therapy. *Clin. Gastroenterol. Hepatol.* 12 (12), 2071–2077. doi:10.1016/j.cgh.2014.04.036

Zorzi, F., Ghosh, S., Chiaramonte, C., Lolli, E., Ventura, M., Onali, S., et al. (2020). Response Assessed by Ultrasonography as Target of Biological Treatment for Crohn's Disease. *Clin. Gastroenterol. Hepatol.* 18 (9), 2030–2037. doi:10.1016/j.cgh.2019.10.042

Conflict of Interest: The authors declare that the research was conducted in the absence of any commercial or financial relationships that could be construed as a potential conflict of interest.

Copyright © 2021 Ferretti, Cannatelli, Ardizzone, Maier and Maconi. This is an open-access article distributed under the terms of the Creative Commons Attribution License (CC BY). The use, distribution or reproduction in other forums is permitted, provided the original author(s) and the copyright owner(s) are credited and that the original publication in this journal is cited, in accordance with accepted academic practice. No use, distribution or reproduction is permitted which does not comply with these terms.

frontiers in Pharmacology

ORIGINAL RESEARCH
published: 29 April 2021
doi: 10.3389/fphar.2021.683613

Cichorium pumilum Jacq Extract Inhibits LPS-Induced Inflammation via MAPK Signaling Pathway and Protects Rats From Hepatic Fibrosis Caused by Abnormalities in the Gut-Liver Axis

*Chang Han[1†], Xi Wu[2†], Nan Zou[3], Yunsheng Zhang[4], Jinqi Yuan[3], Yuefeng Gao[5], Wen Chen[1], Jia Yao[1], Cong Li[1], Jinqiu Hou[1] and Dongmei Qin[1]**

[1]Key Laboratory of Xinjiang Phytomedicine Resource and Utilization, Ministry of Education, School of Pharmacy, Shihezi University, Shihezi, China, [2]Dongfang Hospital, Beijing University of Chinese Medicine, Beijing, China, [3]First Affiliated Hospital, School of Medicine, Shihezi University, Shihezi, China, [4]Husbandry Research Institute, Xinjiang Academy of Animal Science, Urumqi, China, [5]State Key Laboratory of Animal Nutrition, College of Animal Science and Technology, China Agricultural University, Beijing, China

OPEN ACCESS

Edited by:
Ralf Weiskirchen, RWTH Aachen University, Germany

Reviewed by:
Wei Liu, University of Science and Technology of China, China
Tarek El-desouky, National Research Center (Egypt), Egypt

***Correspondence:**
Dongmei Qin
qdm_pha@shzu.edu.cn

†These authors share first authorship

Specialty section:
This article was submitted to Gastrointestinal and Hepatic Pharmacology, a section of the journal Frontiers in Pharmacology

Received: *21 March 2021*
Accepted: *19 April 2021*
Published: *29 April 2021*

Citation:
Han C, Wu X, Zou N, Zhang Y, Yuan J, Gao Y, Chen W, Yao J, Li C, Hou J and Qin D (2021) Cichorium pumilum *Jacq Extract Inhibits LPS-Induced Inflammation via MAPK Signaling Pathway and Protects Rats From Hepatic Fibrosis Caused by Abnormalities in the Gut-Liver Axis. Front. Pharmacol. 12:683613. doi: 10.3389/fphar.2021.683613*

The development of liver fibrosis is closely related to the gut microbiota, and the "gut-liver axis" is the most important connection between the two. ethyl acetate extract of *Cichorium pumilum* Jacq (CGEA) is an herbal extract consisting mainly of sesquiterpenoids. The anti-inflammatory and hepatoprotective effects of CGEA have been reported, but the anti-fibrotic effects of CGEA via intestinal microbes and the "gut-liver axis" cycle have rarely been reported. In this study, we observed that CGEA not only directly attenuated inflammatory factor levels in inflamed mice, but also attenuated liver inflammation as well as liver fibrosis degeneration in rats with liver fibrosis caused by colitis. We observed *in vitro* that CGEA significantly promoted the growth of Bifidobacterium adolescentis. Similarly, fecal 16S rDNA sequencing of liver fibrosis rats showed that CGEA intervention significantly altered the composition of the intestinal microbiota of liver fibrosis rats. CGEA increased the abundance of intestinal microbiota, specifically, CGEA increased the ratio of Firmicutes to Bacteroidetes, CGEA could significantly increase the levels of Ruminococcus. In addition, CGEA intervention significantly protected intestinal mucosal tissues and improved intestinal barrier function in rats. Lactucin is the main sesquiterpenoid in CGEA, and HPLC results showed its content in CGEA was up to 6%. Lactucin has been reported to have significant anti-inflammatory activity, and in this study, we found that Lactucin decreased p38 kinases (p38), phosphorylation of the extracellular signal-regulated kinase (ERK) and protein kinase B (AKT) protein phosphorylation in lipopolysaccharide (LPS)-activated RAW264.7 cells, thereby reducing mRNA expression and protein expression of pro-inflammatory factors inducible nitric oxide synthase (iNOS) and cyclooxygenase-2 (COX-2), and inhibiting the release of inflammatory factors interleukin (IL)-6 and nitric oxide (NO), exerting anti-inflammatory effects. In summary, the prevention of liver fibrosis caused by intestinal inflammation by CGEA may be achieved by regulating the intestinal microbiota and restoring the intestinal barrier thereby improving the "gut-liver axis" circulation, reducing liver inflammation, and

ultimately alleviating liver fibrosis. Notably, the direct anti-inflammatory effect of CGEA may be due to its content of Lactucin, which can exert anti-inflammatory effects by inhibiting the phosphorylation of Mitogen-activated protein kinase (MAPK) and Akt signaling pathways.

Keywords: liver fibrosis, *Cichorium pumilum* Jacq, gut microbiota, inflammation, lactucin

INTRODUCTION

Hepatic fibrosis is a chronic liver disease that can lead to end-stage liver disease or cirrhosis and eventually to liver cancer. This causes a serious threat to human health. Extensive researches have been devoted to analyze the mechanisms underlying the pathogenesis of liver fibrosis in recent years, but there are fewer studies on the resistance to liver fibrosis from the perspective of intestinal microbiota and the "gut-liver axis" circulation.

In recent years, the relationship between gut microbes and the liver is receiving increasing attention (Bajaj et al., 2012; Ling et al., 2015). Marshall's (Marshall, 1998) concept of the "gut-liver axis" points out that when the intestinal mucosa is damaged, the permeability of the intestine increases and harmful bacteria and their metabolites [lipopolysaccharide (LPS) and endotoxins] enter the portal vein and move to the liver with blood circulation ("leaky gut") (Marshall, 1998; Kamada et al., 2013; Nakamoto et al., 2017), activate the liver's immune response, and release inflammatory cytokines such as IL-6, IL-1β, TNF-α, etc., thereby accelerate the progression of liver fibrosis (Lau et al., 2015).

In addition, LPS is a key factor in triggering intestinal inflammation (Hu et al., 2016a), which can further affect liver function through the "gut-liver axis" (Li et al., 2018). Also, LPS can directly activate intrahepatic and extrahepatic mononuclear-macrophages, releasing large amounts of inflammatory factors such as nitric oxide (NO), tumor necrosis factor (TNF)-α, interleukin (IL)-1β, interleukin (IL)-6 (Ribeiro et al., 2015; Liu et al., 2017), etc., occurrence of these inflammatory events is regulated by non-receptor-type tyrosine kinases, such as Janus kinase (JAK) 2, phosphoinositide 3-kinase (PI3K), protein kinase B (Akt), and mitogen-activated protein kinases (MAPKs) (Van Dort et al., 2015; Hu et al., 2016b). Especially up-regulating activated MAPK protein expression, including extracellular signal-regulated kinases (ERK), c-Jun N-terminal kinase (JNK), and p38 are closely related to intestinal inflammation (Xie et al., 2019). As reported earlier (Zanello et al., 2011), the inflammatory response of swine intestine caused by E.*coli* infection is closely related to the MAPK signaling pathway, and the Astilbin improves inflammatory bowel disease through PI3K, STAT3, and MAPK signaling pathways (Han et al., 2020). Published work suggests that regulation of gut microbial composition, reduces the phosphorylation of MAPK and AKT proteins (Serreli et al., 2020; Zhang et al., 2020). In summary, by modulating the gut microbial composition and reducing intestinal inflammation, pathogenic bacteria and their metabolites in the liver can be inhibited, thereby reducing liver fibrosis.

Cichorium pumilum Jacq (CG) is a traditional herb in Uighur medicine and is often used in folklore as a remedy for liver disease (Tong et al., 2017). Substantial studies on CG were carried out by our group and it was found that *Cichorium pumilum* Jacq ethyl acetate extract (CGEA) reduces CCl_4 and thioacetamide-induced liver fibrosis in rats via the TGF β/Smad signaling pathway (Qin et al., 2013; Qin et al., 2014). CGEA was also found to have significant growth inhibitory effects on both *Staphylococcus aureus* and *Enterococcus faecalis* (Han et al., 2019). According to Lee CG can significantly promote the growth of probiotic bacteria and reduce the growth of harmful bacteria in the intestine, indicating that CG has a significant "probiotic-like effect" (Lee et al., 2015). Therefore, we predict that CGEA may reduce inflammation by modulating intestinal microbes to combat liver fibrosis.

Studies have shown that the main components of CGEA are sesquiterpene lactones, and the main components are Lactucin and Lactucopicrin (Pyrek, 1985). Our group isolated a total of 25 compounds from CGEA, 14 of which were sesquiterpene lactones (**Supplementary Table S3**), and preliminary experimental results showed that Lactucin has extremely strong anti-inflammatory activity (Dang et al., 2019). Lactucin is the most abundant terpenoid in CGEA with significant antibacterial, adipogenesis-inhibiting effects (Wang et al., 2020). Although Lactucin exhibits excellent anti-inflammatory activity, however, its anti-inflammatory mechanism of action has not been much reported, so we investigated the anti-inflammatory effects of Lactucin in MAPK and AKT signaling pathways at the cellular and molecular biological levels to elucidate the mechanism of Lactucin's anti-inflammatory effects.

On these indications, we predicted that CGEA could improve liver fibrosis through the "gut-liver axis" by reducing intestinal inflammation and promoting probiotic growth, with Lactucin playing a major anti-inflammatory role. Altogether, in the present study, we demonstrated that CGEA can promote probiotic growth and prevent liver fibrosis caused by 2,4,6-trinitrobenzen sulfonic acid (TNBS)-induced intestinal inflammation. We then validated the anti-inflammatory effect of Lactucin *in vitro* using RAW264.7 cells.

MATERIALS AND METHODS

Preparation of CGEA and Lactucin

CGEA and Lactucin were prepared by our research team as follows: 1 kg of dried roots of CG (Xinjiang Medicines Co., Ltd., Xinjiang, China. identified by Prof. Mehmet Nur Ayhoi at Xinjiang Uygur Medical College) was soaked in 95% ethanol for 5 times at room temperature (2 L each time for 3 days), the extract was suspended in water, extracted 1:1 with ethyl acetate and water, and the solvent was volatilized at room temperature to obtain CGEA (7.644 g). The CGEA fraction was fractionated by a

silica gel column chromatograph (CC) eluting with a gradient of CH_2Cl_2-MeOH (from 30:1 to 3:1) to give subfractions B. Fraction B was subjected to a MCI CC to remove pigment eluted excessively with 70, 80, 90 and 100% methyl alcohol to give subfractions B1. Fraction B1 was separated by an RP C18 silica gel CC to give compound 10 (38 mg), and the compound 10 was identified by ^{1}H NMR and ^{13}C NMR spectroscopy as Lactucin (Dang et al., 2019) (**Supplementary Figure S1**).

High Performance Liquid Chromatography Analysis

The composition of CGEA was analyzed using Agilent 1,290 Infinity II HPLC (Agilent, Germany), and the retention time of the detected peaks was compared to that of the Lactucin standard (The standard was prepared by the research group with a purity of ≥95%) for comparison and determination of the Lactucin composition and content in CGEA. HPLC was equipped with a (4.6 × 150 mm, 5 μm) Agilent TC-C18 liquid chromatography column (Agilent, Germany). Mobile phase: Methanol (A)-0.1% formic acid (B), Elution gradient: 0–10 min, 25% A-30% A; 10–20 min, 30% A-70% A; 20–30 min, 70% A-70% A, flow rate 1.0 ml/min, column temperature 30°C, detection wavelength 275 nm, injection volume 5 μL.

Protocol of Animal Experiments *in vivo*

Thirty adult male Sprague Dawley (SD) rats, weighing 180 ± 10 g, were provided by the Xinjiang medical university Experimental Animal center (Xinjiang China) [No. SCXK (Xin) 2016-0004]. The rats reared in alternate light and dark environments at approximately 22°C. All experimental procedures were approved by the Ethics Committee of First Affiliated Hospital, Shihezi University School of Medicine (Approval No. 2020-035-01).

After 7 days of adaptive feeding, the rats were randomly divided into five baskets. The rats fasting the night before modeling, drinking water normally, the rats were given intraperitoneal injection of 10% chloral hydrate (ShangHai Macklin Biochemical Co., Ltd., ShangHai, China) the next day, and the rats except blank control group were inverted after anesthesia to insert a 2 mm-diameter silicone hose with solution (The blank control group was fed with normal saline and the remaining 5% 2,4,6-trinitrobenzensulphonic acid (TNBS, BeiJing OuHe Technology Co., Ltd., BeiJing, China) were mixed with 50% ethanol, 60 mg kg^{-1} TNBS) into the intestinal depth of about 8 cm from the anus. Twice a week for 12 weeks, starting at week 13, except for the blank control group, the rats were randomly divided into model group, positive group (Sulfasalazine, Shanghai Xinyi Tianping Pharmaceutical Co., Ltd., ShangHai, China), high dose group of CGEA-Ⅰ (CGEA-Ⅰ, 150 mg kg^{-1}), low dose group of CGEA-Ⅱ (CGEA-Ⅱ, 100 mg kg^{-1}), the dosage is set based on the previous research basis of our research team (Qin et al., 2019a). Dose groups were fed with the respective medicine. The blank control group and the model group were given normal saline of equal volume once a day for 14 days.

At the end of the experimental period, after fasting for 12 h, all rats were weighed, collected blood by abdominal aorta after anesthetization by injection with 10% chloral hydrate solution and sacrificed. Subsequently, serum was separately prepared by centrifuge at the temperature of 4°C for 15 min for biochemical detection. Rat livers and colon were collected and then a small portion of liver and intestinal tissue samples immediately dissected and fixed in 4% paraformaldehyde (Biosharp Life Sciences Technology Co., Ltd., BeiJing, China). The remaining tissues and the freshly collected feces were rapidly frozen in liquid nitrogen and preserved at −80°C for Tissue homogenate kit analysis and 16S rDNA Gene Sequencing Analysis.

Determination of Serum Biomarkers

According to the manufacturer's commercially available kit instructions (Nanjing Jiancheng Bioengineering Institute, Nanjing, China), the activities of alanine aminotransferase (ALT), aspartate aminotransferase (AST), lactate dehydrogenase (LDH), Albumin (Alb) and gamma-glutamyl transferase (γ-GT) in serum were determined by an enzymatic colorimetric method (Wu et al., 2019).

Assay of IL-6 and TNF-α in Liver

Weigh about 1 g of liver tissue, and add 9 times ice of normal saline, cut the tissue as much as possible with small ophthalmic scissors, use tissue homogenizer to grind into 10% tissue homogenate. The prepared homogenate was prepared with centrifuge at 4°C, 3,000 r/min, 15min centrifugation for supernatant. The levels of IL-6 and TNF-α in liver tissues were determined according to the enzyme-linked immunosorbent assay (ELISA) kit instructions (Shanghai Yaji Biological Co., Ltd., Shanghai, China).

Pathological Assessment of Liver and Colon Tissue

The liver tissues and colon tissues were fixed in 4% paraformaldehyde. The tissues were subsequently dehydrated in a graded ethanol series (75–100%) and embedded in paraffin wax. The tissues were sectioned at 4 μm thickness, liver tissue was stained with hematoxylin and eosin (HE) and Masson, and colon tissue was stained with HE, digitally photographed by light microscopic at total magnifications of ×100.

Determination of Fecal Microbial Composition by16S rDNA Gene Sequencing Analysis

Total Bacterial DNA was isolated from rat fecal samples by TIANamp Stool DNA Kit (TianGen Biotech Co., Ltd., BeiJing, China) and the quality of DNA extraction was detected by 1.2% agarose gel electrophoresis. Design primers based on conserved regions in sequences and add sample specific Barcode sequence. Then the 16S V3-V4 regions were PCR amplified. PCR amplified recovery products were quantified by fluorescence, and each sample was mixed according to the corresponding proportion according to the requirement of sequencing quantity of each sample according to the fluorescence quantitative results. The

sequencing library was prepared using the TruSeq Nano DNA LT Library Prep Kit of Illumina company. Finally, high-throughput sequencing. All procedures, analysis of sequencing and the extracted DNA was subjected to Illumina Miseq PE250 platform. The content of the sequencing was commissioned to Shaanxi Irun Biotechnology Co., China.

In vivo Anti-Inflammatory Effect Study of CGEA

Twenty-four healthy Kunming mice, weighing 25 ± 2 g, were provided by the Xinjiang medical university Experimental Animal center (Xinjiang China) [No. SCXK (Xin) 2016-0004], and all experimental procedures were approved by the Ethics Committee of First Affiliated Hospital, Shihezi University School of Medicine (Approval No. 2020-035-01).

After one week of adaptive feeding, the mice were randomly divided into four groups, namely Normal group, Model group, Treatment group, and Positive group, with six mice in each group. The mice were numbered and weighed, and the Treatment group was given 100 mg kg^{-1} CGEA by oral gavage, the Normal group and the Model group were given saline by oral gavage in equal amounts, and the Positive group was treated with 10 mg kg^{-1} dexamethasone sodium phosphate injection (Hubei Qianjiang Pharmaceutical Co., Ltd., Qianjiang, China) by intraperitoneal injection. All mice were treated twice daily for 7 days, and all mice were fasted but not water after the last dose on the seventh day. Except for the normal group, a single intraperitoneal injection of LPS at a dose of 15 mg kg^{-1} was administered to all groups on day 8 for the establishment of an acute inflammatory model in mice, and blood was obtained immediately after 3 h by removing the eyeballs.

Biochemical Indexes Detection

After the blood was removed from the eyeball, it was left for 30 min, then centrifuged at 4°C, 3,000 r·min^{-1} for 20 min, and the serum was removed, and the content of IL-1β and IL-6 in the serum was measured in strict accordance with the instructions of ELISA kit (Shanghai Yaji Biological Co., Ltd., Shanghai, China).

Determination of Liver and Spleen Index

After blood collection, cervical dislocation and execution of each group of mice, the spleen and thymus were removed intact, washed with saline, swabbed dry, weighed the mass, and calculated the spleen and thymus index.

Organ index (mg·g^{-1}) = Organ mass (mg)/Body mass (g).

Evaluation of CGEA in Promoting Probiotic Growth *in vitro*

Bifidobacterium (BBL) adolescentis [ATCC15703] and *Lactobacillus* acidophilus [ATCC4356] suspensions (10^7 CFU mL^{-1}) were transferred to BBL and DeMan-Rogosa-Sharpe (MRS) liquid medium containing 50, 25, 12.5, 6.25, 3.125, 1.56, 0.78, 0.39, 0.195, and 0.0975 mg mL^{-1} CGEA extracts, respectively, and the initial bacterial volume was adjusted to 10^6 CFU mL^{-1}. The same volume of bacterial suspension without CGEA was used as a normal control, and the wells containing only liquid medium were used as a reference control, and incubated for 12 h at 37°C under anaerobic conditions, and then the optical density value (OD value) of bacterial suspensions at 600 nm were measured with a microplate reader (Thermo Scientific, United States) to determine the optimal growth-promoting concentrations.

The Growth Curve Method was Utilized to Observe the Bacterial Growth Status

The bacteria were treated with the same operation as above, and the optimal concentration of CGEA was added respectively. Under anaerobic conditions, the bacteria were incubated at 37°C for 24 h, and the OD value of the bacteria suspended at 600 nm wavelength was measured every 2 h with a microplate reader, and the bacterial growth curve was plotted with the measurement time and its corresponding OD value to evaluate the effect of CGEA on the growth process of the strain.

Cell Culture and Processing

RAW 264.7 cells were donated by Xinjiang Uygur Autonomous Region Institute of Medicine, Maintain the cells in DMEM/High Glucose medium (HyClone, Logan, Utah, United States) supplemented with 10% v/v fetal bovine serum (FBS, Gibco, United States) and 1% penicillin-streptomycin solution (HyClone, Logan, Utah, United States), and put them into 25 cm^2 culture flasks, and then place them in a constant temperature incubator (Thermo Fisher Scientific, United States) at 37°C and 5% CO_2, Subculture every 2–3 days to maintain logarithmic growth. DMSO (Beijing Solarbio Technology Co., BeiJing, China) was used to prepare Lactucin solutions of different concentrations and added to the cell culture fluid. The proportion of DMSO in the cell culture fluid was 0.1% (v/v).

Cell Viability

MTT (Beijing Solarbio Technology Co., BeiJing, China) was used to determine the effect of Lactucin on cell viability. Cells were propagated in a 96-well flat-bottom plate at a cell density of 1×10^5 and combined for 16 h, the cells were counted using a hemocytometer. Then, the medium in the wells was discarded, and medium containing different concentrations of Lactucin was used to treat the cells for 24 h. At the end of incubation, each well was added with 10% MTT solution and the cells were cultured for another 4 h. Then carefully aspirate the culture solution, add 110 μL of formazan solution to each well, shake on a shaker at low speed for 10 min, and measure each wavelength at 490 nm by a microplate reader the absorbance (OD) value of the well.

Determination of NO, IL-6 and TNF-α Production

Cells were implanted in 96-well flat-bottom plates at a cell density of 1×10^5 for 16 h, and then the culture solution was discarded. The cells in the normal group and the model group were added with DMEM/High Glucose medium, and the drug intervention group was added with low (12.5 μmol L^{-1}), medium

(25 μmol L^{-1}) and high (50 μmol L^{-1}) doses of Lactucin medium to pre-protect the cells for 30 min. Except for the normal group, LPS (Solarbio Technology Co., BeiJing, China) (1 μg mL^{-1}) was added to each well, and the culture was continued for 24 h. To measure NO, mix 100 μL of cell supernatant with an equal volume of Griess reagent (Hu et al., 2016a), measure the absorbance of each well at a wavelength of 550 nm using a microplate reader within 5 min, and calculate the content of NO in the cell culture solution. The levels of IL-6 and TNF-α (Shanghai Yaji Biological Co., Ltd., Shanghai, China) in the culture medium were measured using Elisa kit.

RNA Extraction and Quantitative Real Time-PCR Analysis

Cells were implanted in 6-well plate at a density of 1×10^6 and incubated for 16 h. Then, the drug intervention group was added with low (12.5 μmol L^{-1}), medium (25 μmol L^{-1}) and high doses (50 μmol L^{-1}) of Lactucin medium to pre-protect the cells for 30 min. Except for the normal group, LPS (1 μg mL^{-1}) was added to each well, and the culture was continued for 6 h, and then, according to the manufacturer's instructions, total cell RNA was extracted using Trizol reagent (Invitrogen, Carlsbad, CA, United States). First-strand cDNA was synthesized from the total RNA (1 μg) was used the PrimeScript™ RT reagent Kit with gDNA Eraser (TaKaRa Corporation, Japan). Then use the LightCycler 480 PCR fluorescence quantifier (Roche, Germany) to amplify the target gene according to the method reported previously. The conditions for qPCR were 95°C for 10 min followed by 45 cycles at 95°C for 15 s, 57°C for 15 s, and 72°C for 15 s, with a final extension at 72°C for 10 min. GAPDH was used as the house-keeping genes, and the relative expression change factor of each target gene was calculated by $2^{-\triangle\triangle CT}$ method (Hu et al., 2016b). **Table 1** lists the oligonucleotide primers of the target gene.

Western Blot Analysis

A total of 1×10^6 cells plated in a 6-well plate for 16 h and then exposed to Lactucin for 30 min before stimulation with LPS for indicated time. After washing the cells twice with cold PBS, the cells were scraped to collect the cells, 100 μL of radio immunoprecipitation assay (RIPA) lysis buffer (CoWin Biosciences Co., BeiJing, China) was added, shaken thoroughly and placed in a refrigerator at 4°C, lyzed for 30 min, and then centrifuged at 4°C and 12,000 r/min for 10 min, extracted the total protein of the cell, and used the bicinchoninic acid (BCA) protein concentration determination kit (Solarbio Life Sciences, BeiJing, China) for concentration determination. Sodium dodecyl sulfate-polyacrylamide gel electrophoresis (SDS-PAGE) was used to separate the proteins (50 μg) in each sample and transferred onto polyvinylidene fluoride (PVDF, Millipore, Billerica, MA, United States) membranes. The PVDF membranes were then incubated overnight at 4 °C with primary antibodies including iNOS antibody (1:1,000, Cell Signaling Technology, United States), COX-2 antibody (1:1,000, Bioworld, NanJing China), P-Akt antibody (1:1,000), Akt antibody (1:2000) all from (Boster Biological technology, WuHan, China), p38 antibody (1:2000), P-p38 antibody (1:2000), ERK1/2 antibody (1: 2000), P-ERK1/2 antibody (1:2000), JNK antibody (1:2000), P-JNK antibody (1: 2000), GAPDH antibody (1:2000), Actin antibody (1:2000), all from (Beyotime Biotechnology, ShangHai, China). The membranes were then incubated for 1 h with horseradish peroxidase (HRP)-conjugated goat anti-rabbit/mouse IgG antibody (1:5,000, Zhongshan Jinqiao Biotechnology Co., Beijing, China), and the immunoreactive proteins were visualized using the enhanced chemiluminescence reagent (ECL, Solarbio Technology Co., Beijing, China). The images were obtained using ChemiDoc™ Omnimaging System (Bio-Rad, Hercules, CA, United States) and developed using ImageJ (NIH, United States) Software for quantification.

Statistical Analysis

Each group of experiments was independently repeated 3 times, and the data were expressed as mean ± standard deviation (SD). All date were analyzed with Graph Pad Prism 6.0 software (California, United States). One-way analysis of variance (ANOVA) was used to compare differences among multiple groups, and unpaired Student's t-test was used to analyze the significance between two groups. Values of $p < 0.05$ was considered statistically significant.

RESULTS

HPLC Analysis

By comparing the retention times of CGEA and Lactucin in the chromatograms, we found that the major component and the observed peak at 275 nm were identified as Lactucin (**Figure 1**) at a concentration of 6%.

CGEA Attenuates Liver Fibrosis in Rats

In the process of establishing the animal model, the rats showed thin feces, blood feces, which showed obvious characteristics of colitis. From the fourth week, we used orbital blood collection to determine AST and ALT indicators in some of the rats, and at 6 weeks, AST and ALT in the rats' serum began to appear abnormal compared with the normal group, indicating that the rats began to show liver damage. Our previous experimental results have shown that liver damage lasting more than 6 weeks can cause liver fibrosis (Qin et al., 2019a; Qin et al., 2019b). Therefore, we continued to give rats enemas with TNBS for up to 12 weeks to promote the formation of liver fibrosis in rats. The results showed that no distinct edema lesions or abnormal color was observed in liver tissue of the control group. In contrast, the model group significantly resulted in ischemia and abnormal color of rat liver tissue, however, both CGEA and Sulfasalazine significantly improved the liver congestion function and normalized the color of the liver (**Figure 2A**). The AST, ALB and γ-GT in serum were significantly increased in the model group compared with those of normal group ($p < 0.05$) and ALT, LDH was significantly increased ($p < 0.01$) (**Figures 2B–F**). CGEA-Ⅰ can significantly reduce the levels of AST (**Figure 2B**) and γ-GT (**Figure 2F**) ($p < 0.05$), CGEA-Ⅱ also significantly reduced the level of γ-GT ($p < 0.01$) (**Figure 2F**). In conclusion, we successfully created a new liver injury-hepatic fibrosis model

TABLE 1 | Primer sequences.

Gene	Forward primer 5′-3′	Reverse primer 5′-3′	Amplified fragment
GAPDH	AGGAGAGTGTTTCCTCGTCC	TGAGGTCAATGAAGGGGTCG	145 bp
IL-6	CCGGAGAGGAGACTTCACAG	TCCACGATTTCCCAGAGAAC	121 bp
IL-1β	TGCAGAGTTCCCCAACTGGTACA	GTGCTGCCTAATGTCCCCTTG	102 bp
TNF-α	TCAGCCTCTTCTCATTCCTG	TGAAGAGAACCTGGGAGTAG	136 bp
iNOS	CCCTTCCGAAGTTTCTGGCAGCAG	GGCTGTCAGAGCCTCGTGGCTTTGG	108 bp
COX-2	CACTACATCCTGACCCACTT	ATGCTCCTGCTTGAGTATGT	258 bp

using TNBS-ethanol enemas, and CGEA mitigated liver fibrosis in this model.

CGEA Significantly Improves Histopathological Changes in Liver Fibrosis in Rats

The results of HE staining showed that, compared with those of the normal group, the liver lobules of the model group were blurred in outline, the structure was obviously damaged, the central veins were dilated, the arrangement of the hepatic cord was disordered, and there was a large number of inflammatory cells infiltrating the hepatic lobules and confluent area (**Figure 2A**). Masson's staining results showed that collagen fibrous tissue proliferation and collagen deposition increased around the central vein and in the confluent area of the liver of the model group rats, forming obvious fibrous intervals with typical histological features of liver fibrosis. Compared with those of the normal group, collagen fibers were mainly distributed in the liver interstitium in the CGEA group and were significantly reduced, especially in the CGEA-I group (**Figure 2A**). In conclusion, the rats in this experiment have typical liver fibrosis characteristics, and CGEA can significantly reduce the collagen fibrillar content in the liver, with significant anti-fibrotic activity.

CGEA Reduces Inflammatory Factor Levels in Rat Liver

In order to verify that the effect of CGEA on liver fibrosis in experimental rats is achieved by reducing liver inflammation, we determined the levels of IL-6 and TNF-α in rat liver tissue using the ELISA method. TNF-α and IL-6, are important inflammatory response factors in the organism that promotes fibrosis formation by inducing inflammatory responses in the liver. The results of this study showed that CGEA-II group could significantly reduce the level of IL-6 ($p < 0.001$) (**Figure 2G**), the effect of CGEA on the level of TNF-α was not significant ($p > 0.05$) (**Figure 2H**).

CGEA Improves Colonic Tissue Changes in Rats With Colitis

The results showed that the colon in the control group had no obvious edema and no ulceration, while the colonic tissue in the model group showed obvious ulceration and tissue necrosis, and the CGEA intervention could significantly improve the lesions in the colonic tissue (**Figure 3**). Similarly, the results of HE staining showed that there was no damage to the colon tissue of the normal group of rats, and the glandular structure in the colon was intact. In the model group, the mucosal layer of the colonic tissue was severely damaged, with loss of microvilli and glandular fragmentation. The colon of the treated group had a large amount of granulation tissue proliferation and epithelial regeneration, especially the CGEA-I group had the best repair effect (**Figure 3**). It means that CGEA treatment can significantly improve the damage of colon tissue and reduce the inflammation of colon.

CGEA Alters the Composition of the Microbiota in the Gut of Rats With Hepatic Fibrosis

The Chao1 index and Simpson index represent the richness and diversity of microbes in the gut. Compared with those of the normal group, the enrichment of gut microorganisms in the TNBS group increased slightly and the diversity decreased, while the CGEA and positive drug groups corrected this change, but there was no significant difference among all groups ($p > 0.05$) (**Figures 4A,B**). In order to observe specific changes in microorganisms in the gut, we genetically sequenced microorganisms in intestinal feces by 16S rDNA, and it is noteworthy that the TNBS group and the administration intervention group caused changes in bacterial communities at the level of phylum and genus, and at the taxonomic level of phylum, Proteobacteria, Firmicutes and Bacteroidetes represent the majority of the total sequence of bacteria. Compared with those of the normal group, the abundance of Firmicutes in the intestines of rats in the TNBS group was significantly reduced and the abundance of Bacteroidetes was significantly increased, while the CGEA group and the positive drug group improved this situation by increasing the abundance of Firmicutes, Proteobacteria and Acidobacteria and reducing the abundance of Abundance of Bacteroidetes. (**Figure 4D**); at the level of genus, compared with those of the normal group, after TNBS modeling, the abundance of Prevotella in the intestines of rats was reduced, and the abundance of *Pseudomonas* and Ochrobactrum was increased, and the CGEA intervention could reduce the abundance of Ochrobactrum and increase the abundance of Ruminococcus and *Acinetobacter*, making the intestinal flora more to the normal level (**Figure 4C**).

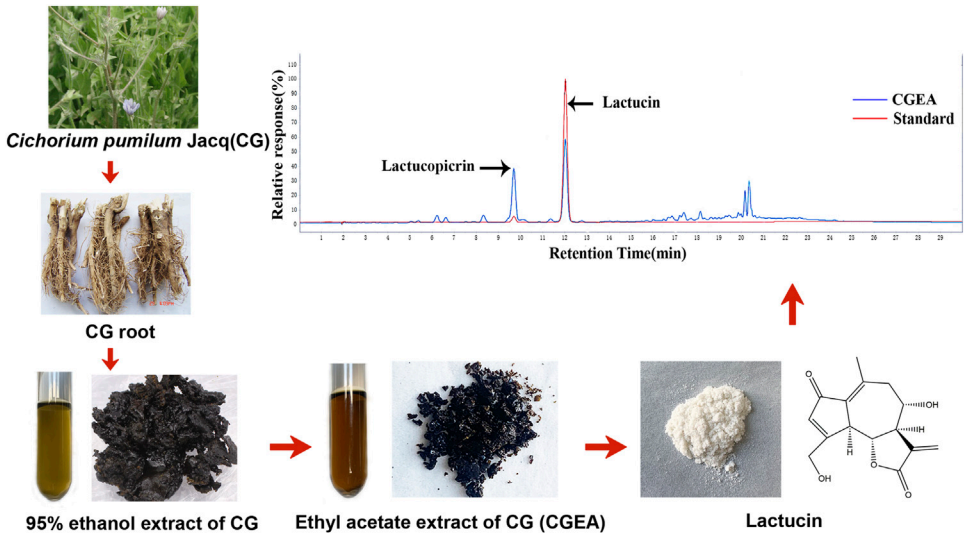


FIGURE 1 | Preparation of CGEA and Lactucin and their analysis by HPLC, HPLC chromatogram of CGEA at 275 nm, peaks is Lactucin.

CGEA Reduces the Level of Inflammation and Improves the Organ Index in Mice

Compared with the normal group, IL-1β and IL-6 in the serum of mice in the model group were highly significantly elevated ($p < 0.001$). Compared with the model group, CGEA significantly reduced the level of IL-6 in the serum of mice ($p < 0.01$). Although CGEA could not significantly reduce the level of IL-1β, the results could indicate that CGEA had a decreasing effect on IL-1β (**Figure 5**). Similarly, CGEA also reduced the spleen index and thymus index in mice (**Table 2**).

CGEA Promotes the Growth of Bifidobacterium Adolescentis

Compared with the Normal group, high concentrations of CGEA significantly inhibited the growth of Bifidobacterium adolescentis and *Lactobacillus acidophilus*, and as the concentration decreased, CGEA showed some microbial growth promoting effects, especially at a concentration of 0.78 mg mL^{-1}, the growth promoting effect of CGEA on Bifidobacterium adolescentis was the most obvious (**Figure 6A**). Further, the growth curve results showed that with the decrease of CGEA concentration, CGEA at 0.78 mg mL^{-1} concentration could significantly promote the growth of Bifidobacterium adolescentis after 16 h of co-interaction ($p < 0.01$), and when the concentration continued to decrease, this promotion effect started to weaken again (**Figure 6C**); the effect of CGEA on the growth promoting effect of CGEA on *Lactobacillus acidophilus* was not significant, but the toxic effect of low concentration of CGEA on *Lactobacillus acidophilus* was also very weak and basically did not affect the normal growth of *Lactobacillus acidophilus* (**Figure 6D**).

Lactucin Significantly Reduces LPS-Induced Levels of Inflammatory Mediator Production in RAW264.7 Cells

To further clarify the potent anti-inflammatory activity of CGEA, we investigated the mechanism of anti-inflammatory action of its main compound, Lactucin, *in vitro*. First, the toxic effect of Lactucin on RAW264.7 cells was determined by MTT, and the results showed that when Lactucin was 50 μmol L^{-1}, the cell viability was recovered 88.08%, which can be considered as no significant cytotoxicity. Similarly, DMSO at a final concentration of 0.1% was not cytotoxic, whereas 100, 200, and 400 μmol L^{-1} all showed significant cytotoxicity with cell survival rates of 55.64, 23.40, and 7.66%, respectively (**Figure 7A**); therefore, subsequent experiments were performed using Lactucin at non-cytotoxic concentrations of 12.5, 25, and 50 μmol L^{-1}, providing a basis for the variation in the experimental data not due to cytotoxicity. The results showed that 50 μmol L^{-1}, 25 μmol L^{-1} Lactucin could significantly inhibit the level of NO production in RAW264.7 cells ($p < 0.01$), and 12.5 μmol L^{-1} Lactucin could also significantly inhibit NO production ($p < 0.05$) (**Figure 7B**); 50 μmol L^{-1}, 25 μmol L^{-1} Lactucin could significantly inhibit IL-6 production ($p < 0.001$), 12.5 μmol L^{-1} Lactucin could also significantly inhibit IL-6 production ($p < 0.01$) (**Figure 7C**); and the inhibitory effect of Lactucin on TNF-α was not significant ($p > 0.05$) (**Figure 7D**).

Lactucin Significantly Inhibits LPS-Induced Inflammatory mRNA Expression Levels in RAW264.7 Cells

It is well known that iNOS is a key enzyme for cellular production of large amounts of NO (Cassini-Vieira et al., 2015), and in addition, COX-2 is an inflammatory gene that catalyzes the production of PGE_2 and is involved in promoting the

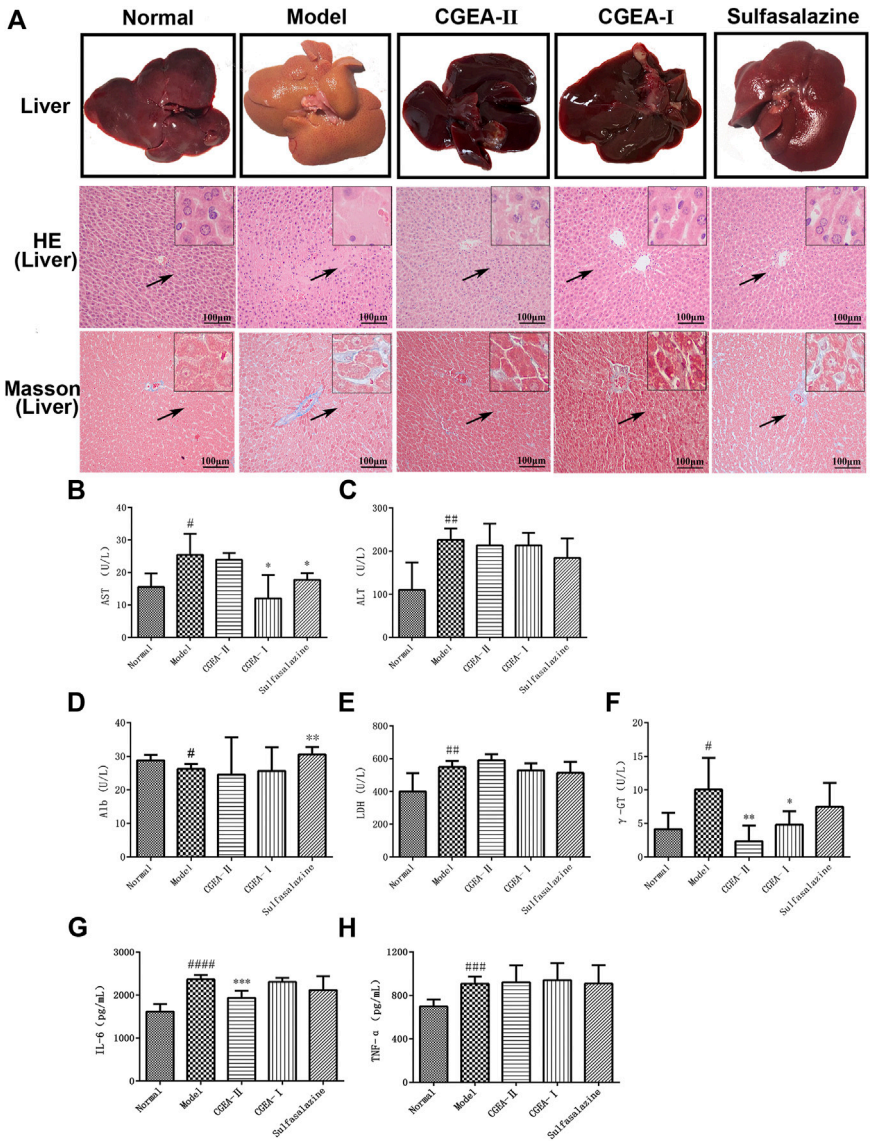


FIGURE 2 | CGEA reduces liver index and inflammation index of liver fibrosis rats. **(A)** Typical images of representative liver pathology for HE staining and Masson staining. **(B–F)** Effects of CGEA on serum AST, ALT, Alb, LDH, and γ-GT activities. **(G–H)** Statistic analysis of liver inflammation scoring (IL-6, TNF-α). Data are shown as mean ± SD in each group (*$p < 0.05$, **$p < 0.01$, ***$p < 0.001$ with the Model Group; #$p < 0.05$, ##$p < 0.01$, ###$p < 0.001$, ####$p < 0.0001$ with the Normal Group; $n = 6$). Abbreviations: Normal, Healthy rats; Model, Rats with enteritis and liver fibrosis; CGEA-II, CGEA low-dose treatment group; CGEA-I, CGEA high-dose treatment group; AST, aspartate transaminase; ALT, alanine transaminase; Alb, albumin; LDH, lactate dehydrogenase; γ-GT, γ-glutamyl transpeptidase.

inflammatory response process (He et al., 2020). To further investigate whether the inhibitory effects of lactucin on NO, PGE_2, IL-6, TNF-α, and IL-1β are related to the genes responsible for regulation, we determined the effects of lactucin on the expression of mRNA with relevant targets. The results showed that the mRNA levels of the target genes were undetectable in the unstimulated RAW264.7 cells. After LPS stimulation, the mRNA expression of iNOS, COX-2, IL-6, IL-1β and TNF-α was significantly increased. Lactucin significantly inhibited the mRNA expression of these genes in a concentration-dependent manner, in which 50 μmol L^{-1} of Lactucin significantly inhibited the mRNA expression of IL-6, IL-1β and COX-2 ($p < 0.05$) (**Figure 8A,B,E**) and extremely significantly inhibited the mRNA expression of iNOS ($p < 0.01$), and 25 μmol L^{-1} of Lactucin had a significant inhibitory effect on the mRNA expression of iNOS ($p < 0.05$) (**Figure 8D**), Lactucin had an inhibitory effect on TNF-α mRNA expression, but there was no significant difference ($p > 0.05$) (**Figure 8C**). These results suggest that the inhibition of inflammatory mediators in LPS-stimulated macrophages by Lactucin can be explained by the inhibition of the mRNA expression achieved in the production of inflammatory mediators.

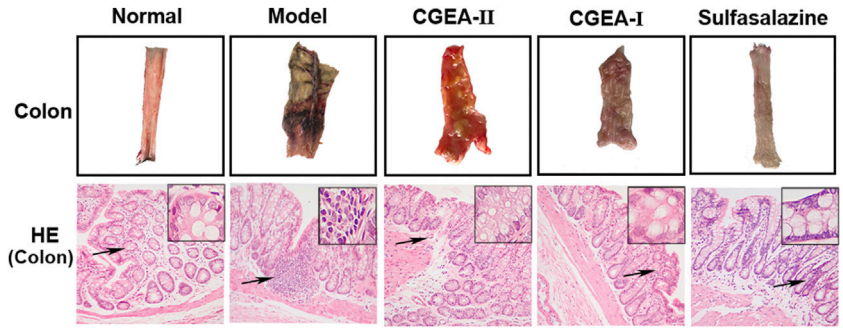


FIGURE 3 | CGEA restores the colonic barrier function of rats with liver fibrosis. Representative colon tissue images and HE-stained images(Normal: Healthy rats, Model: Rats with enteritis and liver fibrosis, CGEA-II: CGEA low-dose treatment group, CGEA-I: CGEA high-dose treatment group.)

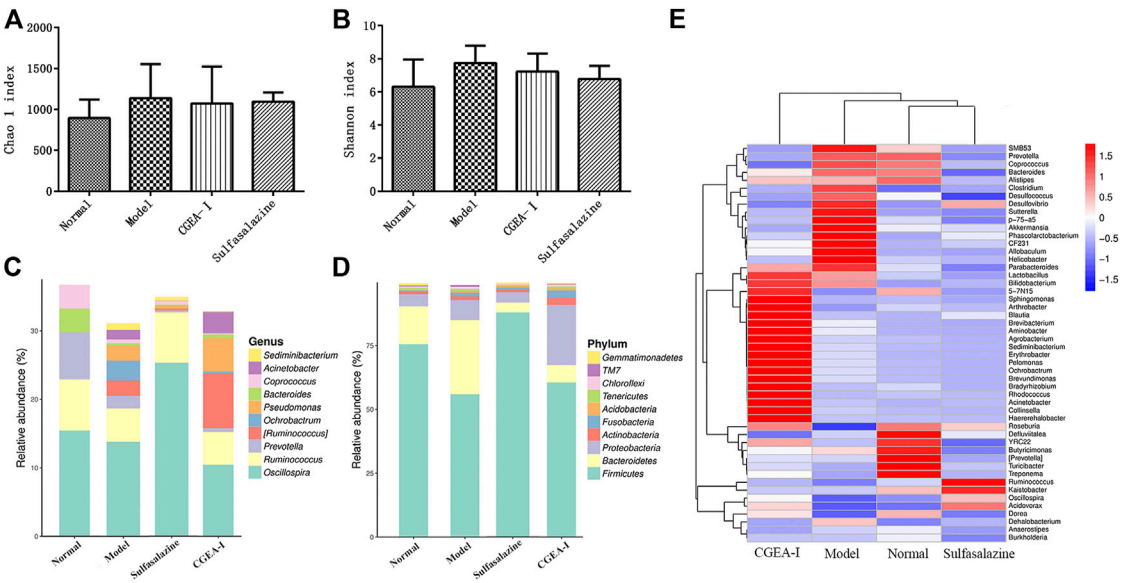


FIGURE 4 | CGEA reverses the changes of intestinal microbes. **(A–B)** Effects of CGEA on the observed species Chao one index and Shannon index in fecal microbiota after long-term TNBS exposure, respectively. **(C)** CGEA significantly ameliorated the relative abundance changes of fecal microbial composition at the genus level due to TNBS intake. **(D)** CGEA dramatically modified TNBS-induced relative abundance alterations of fecal microbial composition at the phylum level. **(F)** Heat map analysis of the gut microbiota. Data are shown as mean ± SD from three independent experiments (Normal: Healthy rats, Model: Rats with enteritis and liver fibrosis, CGEA-I: CGEA high-dose treatment group).

Lactucin Significantly Inhibits iNOS, COX-2 Protein Expression

To further investigate whether the inhibitory effect of Lactucin on inflammatory mediators is related to its associated proteins, Western Blot was used to determine protein expression of iNOS and COX-2. The results showed that after 12 h of LPS stimulation, iNOS and COX-2 proteins were highly expressed in the cells, whereas iNOS and COX-2 proteins were hardly expressed in normal cells, 50 μmol L^{-1} of lactucin could extremely significantly inhibit iNOS and COX-2 protein expression ($p < 0.01$), and 25 μmol L^{-1} of lactucin could also extremely significantly inhibit iNOS protein expression ($p < 0.01$), in addition, it is evident that 0.1% of DMSO had no effect on protein expression (**Figure 9A**).

Lactucin Significantly Inhibits AKT, MAPKs Protein Phosphorylation

Dysregulation of MAPK signaling pathway is one of the key factors that induce inflammation. Inhibition of MAPK signaling pathway can ameliorate many inflammatory diseases (Gong et al., 2014). At the same time, inhibition of Akt protein phosphorylation also prevents NF-κB p50 subunit movement toward the cell nucleus, which in turn inhibits inflammatory factor production (Lai et al., 2015). The results showed that the phosphorylation of MAPKs and AKT proteins could be induced by LPS stimulation for 30 min 50 μmol L^{-1} of Lactucin significantly reduced the phosphorylation of p38, ERK1/2 (**Figure 9B**) and AKT proteins ($p < 0.05$) (**Figure 9C**), had no significant effect on the phosphorylation of JNK proteins, and

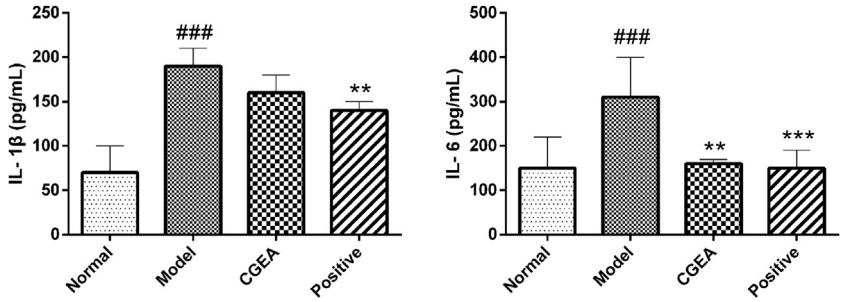


FIGURE 5 | CGEA reduces the serum levels of IL-1β and IL-6 in inflamed mice. Data are shown as mean ± SD in each group (**$p < 0.01$, ***$p < 0.001$ with the Model Group; ###$p < 0.001$ with the Normal Group; $n = 6$). Abbreviations: Normal, Healthy mice; Model, LPS-induced inflammation model mice; CGEA, 100 mg ml^{-1} dose treatment group; Positive, dexamethasone sodium phosphate injection treatment group.

TABLE 2 | Effect of CGEA on spleen index and thymus index in mice with LPS-induced acute inflammation ($x \pm s$, $n = 6$).

Group	Dosage (mg·kg^{-1})	Spleen index (mg·g^{-1})	Thymus index (mg·g^{-1})
Normal	—	3.08 ± 0.49	1.37 ± 0.39
Model	—	4.00 ± 0.85	1.66 ± 0.96
CGEA	100	3.00 ± 0.46	1.57 ± 0.51
Positive	10	2.62 ± 0.87*	1.39 ± 0.16

*$P < 0.05$ with the Model Group.

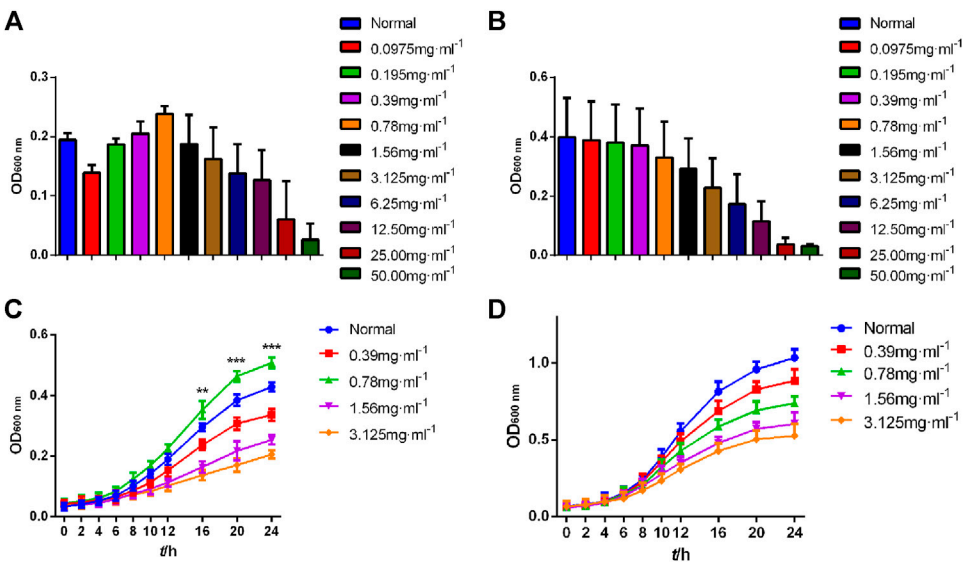


FIGURE 6 | Growth curve of Bifidobacterium adolescentis and *Lactobacillus* acidophilus. Data are shown as mean ± SD in each group (**$p < 0.01$, ***$p < 0.001$ with the Normal Group; $n = 3$). **(A, C)** Bifidobacterium adolescentis. **(B, D)** *Lactobacillus* acidophilus. Abbreviations: Normal, The bacterial suspension without CGEA.

almost no effect on the non-phosphorylated AKT, p38, ERK1/2, and JNK protein content.

DISCUSSION

In this study, we demonstrated that CGEA significantly ameliorated liver fibrosis induced by chronic colitis in rats. Promoting the growth of bifidobacteria. Interestingly, we found that CGEA could alter the composition of microorganisms in the rat intestine, and the gut-liver axis has been reported to be closely associated with liver fibrosis, however, intestinal microbes and intestinal barrier are two key factors associated with liver fibrosis (Tripathi et al., 2018). Our results found that persistent colitis disturbed microbial populations in the rat gut, as evidenced by up-regulating of

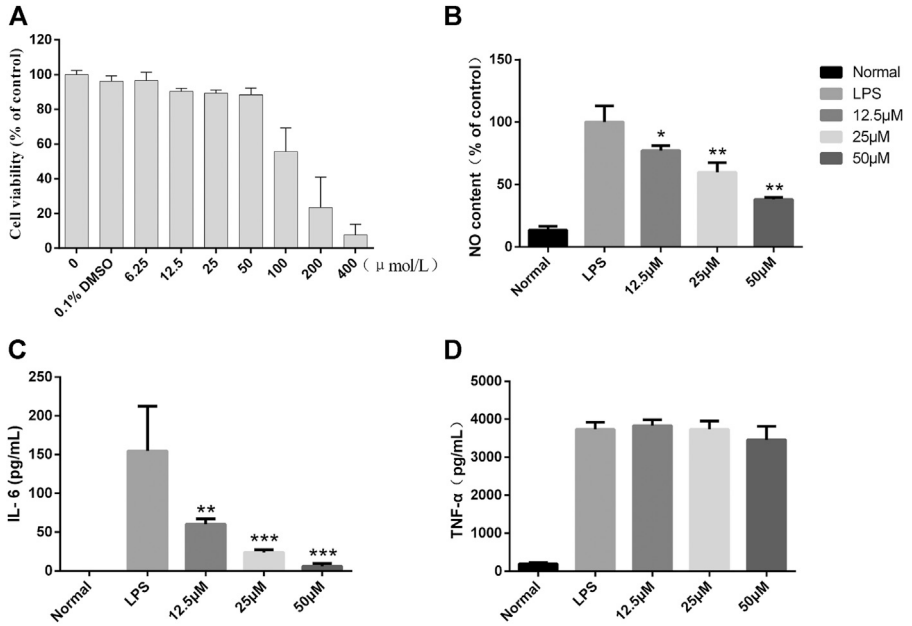


FIGURE 7 | *In vitro* anti-inflammatory effect of Lactucin in LPS-activated RAW 264.7 cells. **(A)** The cell viability of RAW264.7 cells were assessed by MTS assay. **(B)** The concentrations of NO were measured using the Griess reaction, and Lactucin significantly inhibited NO production. **(C, D)** The levels of IL-6 and TNF-α in the culture supernatants were determined by ELISAs, and Lactucin significantly inhibited IL-6 production. Data are shown as mean ± SD in each group (*$p < 0.05$, **$p < 0.01$, ***$p < 0.001$ with the LPS Group, $n = 3$. Normal Group: RAW264.7 cells without LPS activation).

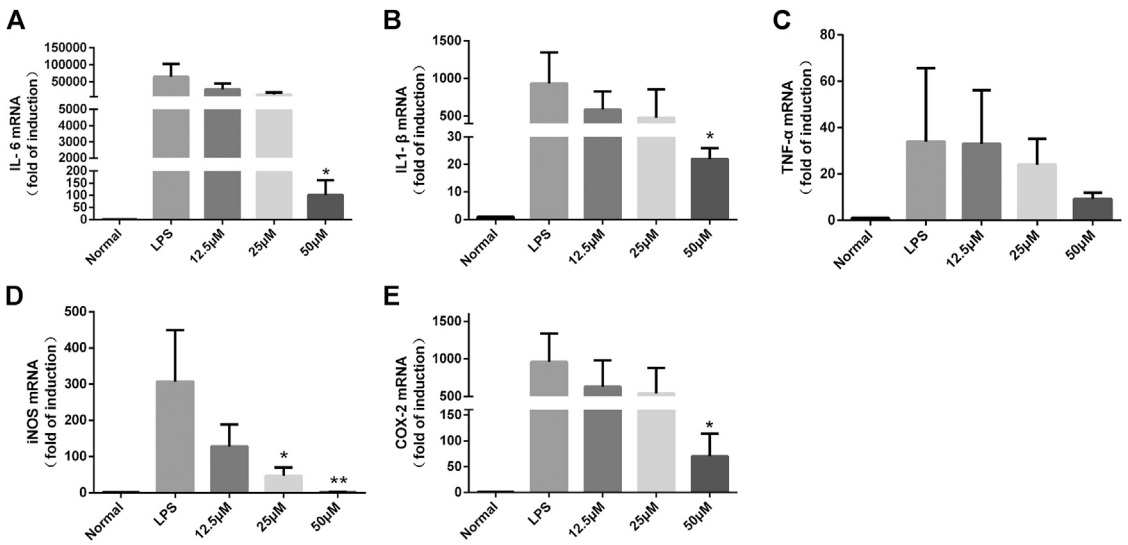


FIGURE 8 | The effect of Lactucin on mRNA expression of a set of inflammatory genes. and Lactucin significantly inhibited IL-6, IL1-β, iNOS, and COX-2 mRNA expression. Data are shown as mean ± SD for each group (*$p < 0.05$, **$p < 0.01$ with the LPS Group, $n = 3$. Normal Group: RAW264.7 cells without LPS activation).

the abundance of Bacteroidetes and down-regulating the abundance of Firmicutes in the intestine, which is consistent with a report by Frank (Frank et al., 2011), and the Bacteroidetes and Firmicutes, as the two main dominant groups in the intestine, participated in the metabolism and absorption of nutrients in the body. Firmicutes can help the body absorb more energy from food (Ley et al., 2006), thus increasing the body's resistance, while patients with liver fibrosis have abnormal liver function and generally weak immunity. CGEA may improve the body's immunity against liver fibrosis by reconfiguring microbial populations in the intestine.

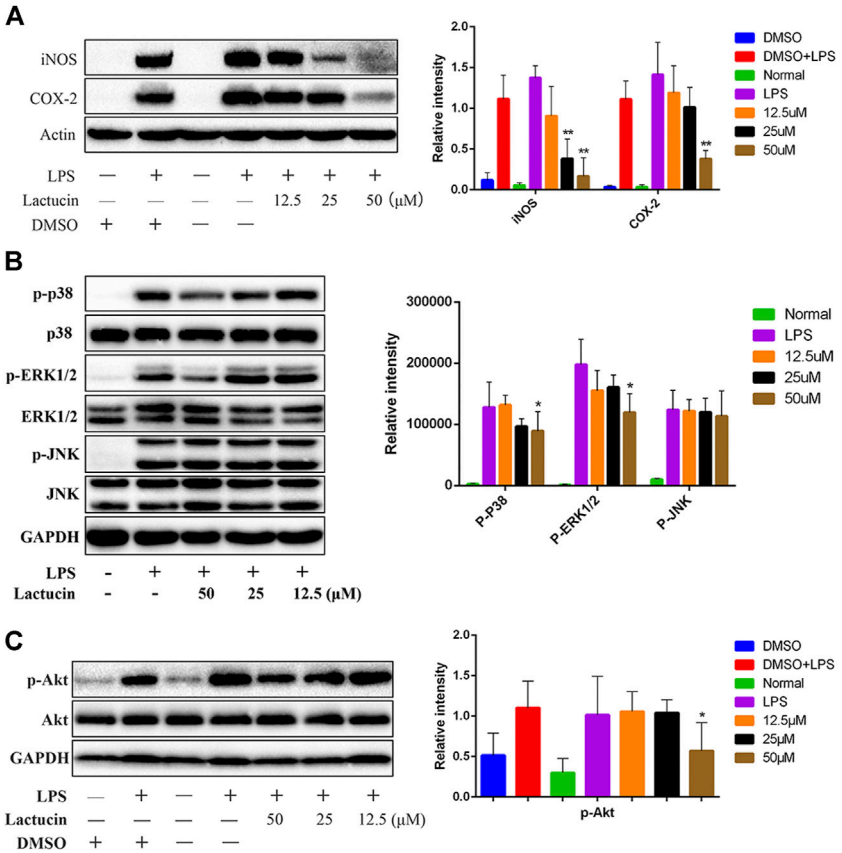


FIGURE 9 | Effect of Lactucin on the activation of signaling pathways. **(A)** The whole-cell lysates were extracted for immunoblotting to determine the level of iNOS, COX-2. **(B, C)** The whole-cell lysates were extracted for immunoblotting to determine the levels of phospho- or total MAPKs (ERK, p38, and JNK) and AKT identified based on their antibodies. Data are shown as mean ± SD for each group (*$p < 0.05$ with the LPS Group, $n = 3$. Normal Group: RAW264.7 cells without LPS activation).

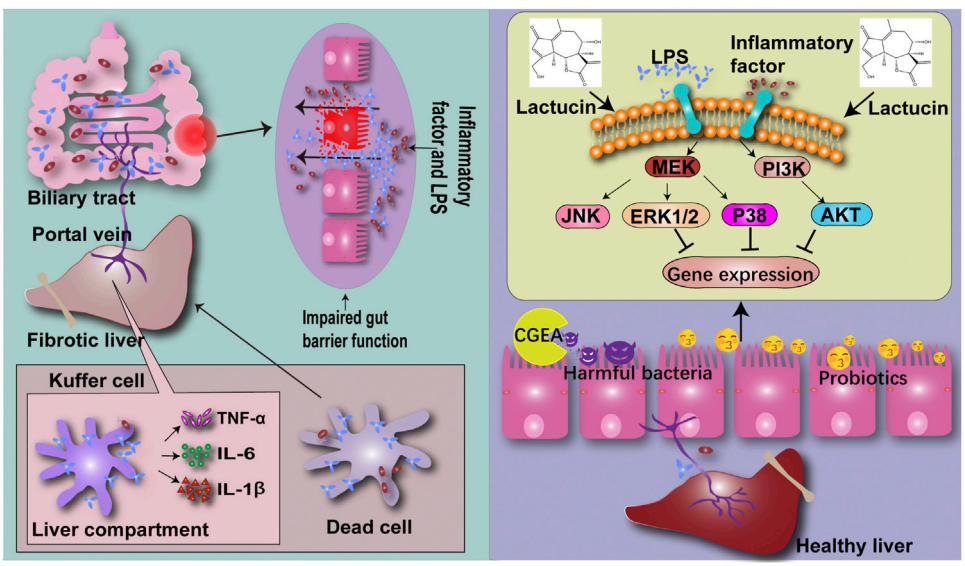


FIGURE 10 | CG confers anti-inflammatory effects by inhibiting the phosphorylation pathway of MAPK signaling pathway, thereby improving the intestinal microenvironment and reducing the production of liver fibrosis through the "gut-liver axis".

On the other hand, when intestinal inflammation persists, the intestinal villi become sparse and damaged, the intestinal barrier function is disrupted, and the metabolites of microorganisms in the gut with harmful flora enter the liver with the enterohepatic axis, stimulating inflammation in the liver. Our results show that increased expression of inflammatory factors in the liver of rats with colitis reveals that functionally impaired intestinal microbes can stimulate intrahepatic inflammation and enter the enterohepatic circulation through the damaged intestinal barrier, exacerbating the development of liver fibrosis. The metabolism of short-chain fatty acids (SCFAs) produced by the Ruminococcus is one of the richest families of Fusobacteria under the Firmicutes (Sagheddu et al., 2016), which enhances the protective effect of the intestinal barrier (Kang et al., 2017; Porras et al., 2017). Therefore, we speculate that the protective effect of CGEA on the rat intestinal barrier may be related to its promotion of the growth of Ruminococcus, however, its specific mechanism of action needs to be further investigated.

Almost all liver diseases are accompanied by inflammation (Bai et al., 2017), and sustained inflammatory stimuli lead to substantial loss of hepatocytes and loss of liver function (Wu et al., 2019), thus reducing the production of inflammatory factors is important to reduce liver injury and fibrosis (O'Reilly et al., 2014; Seki and Schwable, 2015). IL-6 is a proinflammatory cytokine produced after immune activation that can exacerbate chronic inflammation (Cha et al., 2015). And our results table that CGEA significantly reduced serum levels of IL-6 both in acutely inflamed mice and in rats with liver fibrosis. In conclusion, our results suggest that CGEA can reduce the expression of inflammatory factors not only directly, but also indirectly by regulating microorganisms and improving the circulation of the enterohepatic axis.

Earlier experiments demonstrated the most significant anti-inflammatory activity of Lactucin in CGEA (Dang et al., 2019). In the present experiments we further determined the content of Lactucin and the HPLC results showed that the content of Lactucin in CGEA was 6%.Lactucin being the major compound in CGEA, we predict that the anti-inflammatory activity exhibited by CGEA is mainly due to the anti-inflammatory effect exerted by Lactucin. It is well known that dysregulation of MAPK signaling pathway is a key factor in triggering inflammation (Jeong et al., 2014; Duan et al., 2017). Moreover, MAPKs and PI3K/Akt signaling pathways can directly promote DNA binding activity, leading to the up-regulation of iNOS and TNF-α mRNA expression in RAW 264.7 cells (Hu et al., 2016a). The results showed that Lactucin could significantly inhibit LPS-induced iNOS and COX-2 mRNA expression and protein expression in RAW264.7 cells, which is consistent with the findings of Lee et al. (Lee et al., 2010). This suggests to us that Lactucin exert anti-inflammatory effects by suppressing the phosphorylation of ERK1/2 and p38 signaling pathways, which lead to the inhibition of NO production in RAW 264.7 cells.

PI3K/Akt is a serine/threonine-specific protein kinase that plays a key role in many cell growth processes and is closely related to the MAPK signaling pathway, which can both activate and inhibit each other (Meng et al., 2009; Aksamitiene et al., 2012). Our results indicate that Lactucin can significantly inhibit the mRNA expression of IL-6 and IL-1β in RAW264.7 cells and significantly inhibit the phosphorylation of AKT protein. In conclusion, the results here indicate that Lactucin is anti-inflammatory by inhibiting the activation of the MAPK-AKT signaling pathway in RAW264.7 cells, thereby inhibiting the production of inflammatory factors such as NO and IL-6.

CONCLUSION

Taken together, our results indicated that CGEA can ameliorate liver fibrosis induced by 5% TNBS-50% ethanol solution. The mechanism of action may combine the modulation of ERK1/2, p38 and AKT signaling pathways with improvement of the "gut-liver axis" circulation to inhibit inflammation and thus exert an anti-fibrotic effect (**Figure 10**).

DATA AVAILABILITY STATEMENT

The datasets presented in this study can be found in online repositories. The names of the repository/repositories and accession number(s) can be found in the article/ **Supplementary Material**.

ETHICS STATEMENT

The animal study was reviewed and approved by the Animal Experimental Ethical Inspection of First Affiliated Hospital, Shihezi University School of Medicine.

AUTHOR CONTRIBUTIONS

All the authors devoted much effort to the paper. DQ, CH was responsible for experimental design. DQ, CH, XW and NZ were in charge of completing the experiments and writing the paper. DQ, JY, YZ, CL and JH assisted with the acquisition of the samples. DQ, CH, NZ and YG were involved in critical evaluation of the data and preparation of the manuscript.

FUNDING

The National Natural Science Foundation of China (NO.81560680). The Science and Technology Research and Development Project of Shihezi University (RCZK 2018C12). The Major science and technology project of Xinjiang Production and Construction Corps (2020AA005).

ACKNOWLEDGMENTS

We thank the National Natural Science Foundation of China (NO.81560680) for financial support. The authors thank the Science and Technology Research and Development Project of Shihezi University (RCZK 2018C12) for financial support. The

authors thank the Major science and technology project of Xinjiang Production and Construction Corps (2020AA005) for financial support. We thank Dr B Thyagarajan of School of Pharmacy, University of Wyoming for his analysis and guidance of the experiment.

SUPPLEMENTARY MATERIAL

The Supplementary Material for this article can be found online at: https://www.frontiersin.org/articles/10.3389/fphar.2021.683613/full#supplementary-material

REFERENCES

Aksamitiene, E., Kiyatkin, A., and Kholodenko, B. N. (2012). Cross-talk between Mitogenic Ras/MAPK and Survival PI3K/Akt Pathways: a Fine Balance. *Biochem. Soc. Trans.* 40 (1), 139–146. doi:10.1042/BST20110609

Bai, X., Yang, P., Zhou, Q., Cai, B., Buist-Homan, M., Cheng, H., et al. (2017). The Protective Effect of the Natural Compound Hesperetin against Fulminant Hepatitisin Vivoandin Vitro. *Br. J. Pharmacol.* 174 (1), 41–56. doi:10.1111/bph.13645

Bajaj, J. S., Hylemon, P. B., Ridlon, J. M., Heuman, D. M., Daita, K., White, M. B., et al. (2012). Colonic Mucosal Microbiome Differs from Stool Microbiome in Cirrhosis and Hepatic Encephalopathy and Is Linked to Cognition and Inflammation. *Am. J. Physiology-Gastrointestinal Liver Physiol.* 303 (6), G675–G685. doi:10.1152/ajpgi.00152.2012

Cassini-Vieira, P., Araújo, F. A., da Costa Dias, F. L., Russo, R. C., Andrade, S. P., Teixeira, M. M., et al. (2015). iNOS Activity Modulates Inflammation, Angiogenesis, and Tissue Fibrosis in Polyether-Polyurethane Synthetic Implants. *Mediators Inflamm.* 2015, 1–9. doi:10.1155/2015/138461

Cha, B.-J., Park, J.-H., Shrestha, S., Baek, N.-I., Lee, S. M., Lee, T. H., et al. (2015). Glycosyl Glycerides from Hydroponic Panax Ginseng Inhibited No Production in Lipopolysaccharide-Stimulated raw264.7 Cells. *J. Ginseng Res.* 39 (2), 162–168. doi:10.1016/j.jgr.2014.10.005

Dang, T., Zheng, G., Zhang, Q., Jin, P., Zhang, H., Su, L., et al. (2019). Sesquiterpenoids with Diverse Carbon Skeletons from the Roots of Cichorium Glandulosum and Their Anti-inflammatory Activities. *Fitoterapia* 136, 104170. doi:10.1016/j.fitote.2019.104170

Duan, X., Gao, S., Li, J., Wu, L., Zhang, Y., Li, W., et al. (2017). Acute Arsenic Exposure Induces Inflammatory Responses and CD4+ T Cell Subpopulations Differentiation in Spleen and Thymus with the Involvement of MAPK, NF-kB, and Nrf2. *Mol. Immunol.* 81, 160–172. doi:10.1016/j.molimm.2016.12.005

Frank, D. N., Robertson, C. E., Hamm, C. M., Kpadeh, Z., Zhang, T., Chen, H., et al. (2011). Disease Phenotype and Genotype Are Associated with Shifts in Intestinal-Associated Microbiota in Inflammatory Bowel Diseases. *Inflamm. Bowel Dis.* 17 (1), 179–184. doi:10.1002/ibd.21339

Gong, X. W., Yang, Q. H., Yan, H. Z., Zhang, Y. P., Liang, Y. J., Liu, Y. Z., et al. (2014). [Effects of Soothing Liver and Invigorating Spleen Recipes on LPS-Induced Hepatocytes Injury of Rats and TLR4/p38MAPK Signal Pathway]. *Zhongguo Zhong Yao Za Zhi* 39 (20), 4027–4033. doi:10.4268/cjcmm20142024

Han, C., Dang, T., Wang, R., Yao, J., Qin, D. M., and Zhang, Y. S. (2019). Study on Differences in Antibacterial Activity of Ethanol Extracts from Chicory Roots and Stems against *staphylococcus Aureus* and *enterococcus Faecalis*. *Chin. Pharmacol. Bull.* 35 (04), 540–545. doi:10.3969/j.issn.1001-1978.2019.04.019

Han, S., Lin, Z., Wen, J., Wu, K., Xu, Y., Zhang, Y., et al. (2020). Astilbin Promotes the Induction of Regulatory NK1.1− CD4+ NKG2D+ T Cells through the PI3K, STAT3, and MAPK Signaling Pathways. *Int. Immunopharmacol.* 81, 106143. doi:10.1016/j.intimp.2019.106143

He, R., Hua, K., Zhang, S., Wan, Y., Gong, H., Ma, B., et al. (2020). COX-2 Mediated Crosstalk between Wnt/β-Catenin and the NF-Kb Signaling Pathway during Inflammatory Responses Induced by *Haemophilus* Parasuis in PK-15 and NPTr Cells. *Developmental Comp. Immunol.* 105, 103588. doi:10.1016/j.dci.2019.103588

Hu, W., Wang, X., Wu, L., Shen, T., Ji, L., Zhao, X., et al. (2016b). Apigenin-7-O-β-d-glucuronide Inhibits LPS-Induced Inflammation through the Inactivation of AP-1 and MAPK Signaling Pathways in RAW 264.7 Macrophages and Protects Mice against Endotoxin Shock. *Food Funct.* 7 (2), 1002–1013. doi:10.1039/c5fo01212k

Hu, W., Wu, L., Qiang, Q., Ji, L., Wang, X., Luo, H., et al. (2016a). The Dichloromethane Fraction from Mahonia Bealei (fort.) Carr. Leaves Exerts an Anti-inflammatory Effect Both In Vitro and In Vivo. *J. Ethnopharmacol.* 188, 134–143. doi:10.1016/j.jep.2016.05.013

Jeong, J.-J., Jang, S.-E., Hyam, S. R., Han, M. J., and Kim, D.-H. (2014). Mangiferin Ameliorates Colitis by Inhibiting IRAK1 Phosphorylation in NF-Kb and MAPK Pathways. *Eur. J. Pharmacol.* 740, 652–661. doi:10.1016/j.ejphar.2014.06.013

Kamada, N., Seo, S.-U., Chen, G. Y., and Núñez, G. (2013). Role of the Gut Microbiota in Immunity and Inflammatory Disease. *Nat. Rev. Immunol.* 13 (5), 321–335. doi:10.1038/nri3430

Kang, C., Wang, B., Kaliannan, K., Wang, X., Lang, H., Hui, S., et al. (2017). Gut Microbiota Mediates the Protective Effects of Dietary Capsaicin against Chronic Low-Grade Inflammation and Associated Obesity Induced by High-Fat Diet. *MBio* 8 (3). doi:10.1128/mBio.00470-17

Lai, W., Tian, X., Xiang, Q., Chu, K., Wei, Y., Deng, J., et al. (2015). 11β-HSD1 Modulates LPS-Induced Innate Immune Responses in Adipocytes by Altering Expression of PTEN. *Mol. Endocrinol.* 29 (4), 558–570. doi:10.1210/me.2014-1287

Lau, E., Carvalho, D., and Freitas, P. (2015). Gut Microbiota: Association with Nafld and Metabolic Disturbances. *Biomed. Res. Int.* 2015, 1–9. doi:10.1155/2015/979515

Lee, H. J., Lim, H. J., Lee, D. Y., Jung, H., Kim, M.-R., Moon, D.-C., et al. (2010). Carabrol Suppresses LPS-Induced Nitric Oxide Synthase Expression by Inactivation of P38 and JNK via Inhibition of I-Kbα Degradation in RAW 264.7 Cells. *Biochem. Biophysical Res. Commun.* 391 (3), 1400–1404. doi:10.1016/j.bbrc.2009.12.073

Lee, S.-M., Han, H. W., and Yim, S. Y. (2015). Beneficial Effects of Soy Milk and Fiber on High Cholesterol Diet-Induced Alteration of Gut Microbiota and Inflammatory Gene Expression in Rats. *Food Funct.* 6 (2), 492–500. doi:10.1039/c4fo00731j

Ley, R. E., Turnbaugh, P. J., Klein, S., and Gordon, J. I. (2006). Human Gut Microbes Associated with Obesity. *Nature* 444 (7122), 1022–1023. doi:10.1038/4441022a

Li, Y., Liu, T., Yan, C., Xie, R., Guo, Z., Wang, S., et al. (2018). Diammonium Glycyrrhizinate Protects against Nonalcoholic Fatty Liver Disease in Mice through Modulation of Gut Microbiota and Restoration of Intestinal Barrier. *Mol. Pharmaceutics* 15 (9), 3860–3870. doi:10.1021/acs.molpharmaceut.8b00347

Ling, Z., Liu, X., Cheng, Y., Jiang, X., Jiang, H., Wang, Y., et al. (2015). Decreased Diversity of the Oral Microbiota of Patients with Hepatitis B Virus-Induced Chronic Liver Disease: A Pilot Project. *Sci. Rep.* 5, 17098. doi:10.1038/srep17098

Liu, X., Xie, J., Jia, S., Huang, L., Wang, Z., Li, C., et al. (2017). Immunomodulatory Effects of an Acetylated Cyclocarya Paliurus Polysaccharide on Murine Macrophages raw264.7. *Int. J. Biol. Macromolecules* 98, 576–581. doi:10.1016/j.ijbiomac.2017.02.028

Marshall, J. C. (1998). The Gut as a Potential Trigger of Exercise-Induced Inflammatory Responses. *Can. J. Physiol. Pharmacol.* 76 (5), 479–484. doi:10.1139/cjpp-76-5-47910.1139/y98-049

Meng, J., Peng, H., Dai, B., Guo, W., Wang, L., Ji, L., et al. (2009). High Level of Akt Activity Is Associated with Resistance to Mek Inhibitor Azd6244 (Arry-142886). *cbt* 8 (21), 2073–2080. doi:10.4161/cbt.8.21.9844

Nakamoto, N., Amiya, T., Aoki, R., Taniki, N., Koda, Y., Miyamoto, K., et al. (2017). Commensal Lactobacillus Controls Immune Tolerance during Acute Liver Injury in Mice. *Cel Rep.* 21 (5), 1215–1226. doi:10.1016/j.celrep.2017.10.022

O'Reilly, S., Ciechomska, M., Cant, R., and van Laar, J. M. (2014). Interleukin-6 (IL-6) Trans Signaling Drives a STAT3-dependent Pathway that Leads to Hyperactive Transforming Growth Factor-β (TGF-β) Signaling Promoting SMAD3 Activation and Fibrosis via Gremlin Protein. *J. Biol. Chem.* 289 (14), 9952–9960. doi:10.1074/jbc.M113.545822

Porras, D., Nistal, E., Martínez-Flórez, S., Pisonero-Vaquero, S., Olcoz, J. L., Jover, R., et al. (2017). Protective Effect of Quercetin on High-Fat Diet-Induced Non-

alcoholic Fatty Liver Disease in Mice Is Mediated by Modulating Intestinal Microbiota Imbalance and Related Gut-Liver axis Activation. *Free Radic. Biol. Med.* 102, 188–202. doi:10.1016/j.freeradbiomed.2016.11.037

Pyrek, J. S. (1985). Sesquiterpene Lactones of Cichorium Intybus and Leontodon Autumnalis. *Phytochemistry* 24 (1), 186–188. doi:10.1016/S0031-9422(00)80838-9

Qin, D.-M., Hu, L.-P., Zhang, Y., Kang, Y., Han, C., Dang, T., et al. (2019a). Studies on the Protective Effect of Total Flavonoids from Cichorium Glandulosum Roots against Carbon Tetrachloride-Induced Liver Fibrosis in Rats. *Trop. J. Pharm. Res.* 18 (2), 311–319. Available at: https://www.ajol.info/index.php/tjpr/article/view/184523. doi:10.4314/tjpr.v18i2.13

Qin, D.-M., Wang, X.-B., Zou, N., Han, C., and Xu, J. (2019b). Gas chromatography-mass spectrometry (gc-ms) analysis of the volatile oil of cichorium glandulosum boiss et huet and its effects on carbon tetrachloride-induced liver fibrosis in rats. *Med. Sci. Monit.* 25, 3591–3604. doi:10.12659/MSM.913445

Qin, D. M., Nie, Y. R., and Wen, Z. P. (2014). Protection of Rats from Thioacetamide-Induced Hepatic Fibrosis by the Extracts of a Traditional Uighur Medicine Cichorium Glandulosum. *Iran J. Basic Med. Sci.* 17 (11), 879–885. doi:10.3739/ijbms.18739

Qin, D., Wen, Z., Nie, Y., and Yao, G. (2013). Effect of Cichorium Glandulosum Extracts on Ccl4-Induced Hepatic Fibrosis. *Iran Red Crescent Med. J.* 15 (12), e10908. doi:10.5812/ircmj.10908

Ribeiro, D., Freitas, M., Lima, J. L. F. C., and Fernandes, E. (2015). Proinflammatory Pathways: The Modulation by Flavonoids. *Med. Res. Rev.* 35 (5), 877–936. doi:10.1002/med.21347

Sagheddu, V., Patrone, V., Miragoli, F., Puglisi, E., and Morelli, L. (2016). Infant Early Gut Colonization by Lachnospiraceae: High Frequency of Ruminococcus Gnavus. *Front. Pediatr.* 4, 57. doi:10.3389/fped.2016.00057

Seki, E., and Schwabe, R. F. (2015). Hepatic Inflammation and Fibrosis: Functional Links and Key Pathways. *Hepatology* 61 (3), 1066–1079. doi:10.1002/hep.27332

Serreli, G., Melis, M. P., Zodio, S., Naitza, M. R., Casula, E., Peñalver, P., et al. (2020). Altered Paracellular Permeability in Intestinal Cell Monolayer Challenged with Lipopolysaccharide: Modulatory Effects of Pterostilbene Metabolites. *Food Chem. Toxicol.* 145, 111729. doi:10.1016/j.fct.2020.111729

Tong, J., Mo, Q.-G., Ma, B.-X., Ge, L.-L., Zhou, G., and Wang, Y.-W. (2017). The Protective Effects of Cichorium Glandulosum Seed and Cynarin against Cyclophosphamide and its Metabolite Acrolein-Induced Hepatotoxicity In Vivo and In Vitro. *Food Funct.* 8 (1), 209–219. doi:10.1039/c6fo01531j

Tripathi, A., Debelius, J., Brenner, D. A., Karin, M., Loomba, R., Schnabl, B., et al. (2018). Publisher Correction: The Gut-Liver axis and the Intersection with the Microbiome. *Nat. Rev. Gastroenterol. Hepatol.* 15 (12), 785. doi:10.1038/s41575-018-0031-8

Van Dort, M. E., Galbán, S., Wang, H., Sebolt-Leopold, J., Whitehead, C., Hong, H., et al. (2015). Dual Inhibition of Allosteric Mitogen-Activated Protein Kinase (MEK) and Phosphatidylinositol 3-kinase (PI3K) Oncogenic Targets with a Bifunctional Inhibitor. *Bioorg. Med. Chem.* 23 (7), 1386–1394. doi:10.1016/j.bmc.2015.02.053

Wang, X., Liu, M., Cai, G. H., Chen, Y., Shi, X. C., Zhang, C. C., et al. (2020). A Potential Nutraceutical Candidate Lactucin Inhibits Adipogenesis through Downregulation of Jak2/stat3 Signaling Pathway-Mediated Mitotic Clonal Expansion. *Cells* 9 (2), 331. doi:10.3390/cells9020331

Wu, M., Wang, C., Mai, C., Chen, J., Lai, X., He, L., et al. (2019). Flavonoids from livistona Chinensis Fruit Ameliorates Lps/d-Galn-Induced Acute Liver Injury by Inhibiting Oxidative Stress and Inflammation. *J. Funct. Foods* 61, 103460. doi:10.1016/j.jff.2019.103460

Xie, C., Li, X., Zhu, J., Wu, J., Geng, S., and Zhong, C. (2019). Magnesium Isoglycyrrhizinate Suppresses LPS-Induced Inflammation and Oxidative Stress through Inhibiting NF-Kb and MAPK Pathways in RAW264.7 Cells. *Bioorg. Med. Chem.* 27 (3), 516–524. doi:10.1016/j.bmc.2018.12.033

Zanello, G., Berri, M., Dupont, J., Sizaret, P.-Y., d'Inca, R., Salmon, H., et al. (2011). *Saccharomyces cerevisiae* Modulates Immune Gene Expressions and Inhibits Etec-Mediated Erk1/2 and P38 Signaling Pathways in Intestinal Epithelial Cells. *PloS One* 6 (4), e18573, doi:10.1371/journal.pone.0018573

Zhang, J., Hoedt, E. C., Liu, Q., Berendsen, E., Teh, J. J., Hamilton, A., et al. (2021). Elucidation of proteus Mirabilis as a Key Bacterium in Crohns Disease Inflammation. *Gastroenterology* 160 (1), 317–330. doi:10.1053/j.gastro.2020.09.036

Conflict of Interest: The authors declare that the research was conducted in the absence of any commercial or financial relationships that could be construed as a potential conflict of interest.

Copyright © 2021 Han, Wu, Zou, Zhang, Yuan, Gao, Chen, Yao, Li, Hou and Qin. This is an open-access article distributed under the terms of the Creative Commons Attribution License (CC BY). The use, distribution or reproduction in other forums is permitted, provided the original author(s) and the copyright owner(s) are credited and that the original publication in this journal is cited, in accordance with accepted academic practice. No use, distribution or reproduction is permitted which does not comply with these terms.

GLOSSARY

AKT (protein kinase B)
ALT (Alanine aminotransferase)
Alb (Albumin)
AST (Aspartate aminotransferase)
CG (Cichorium pumilum Jacq)
CGEA (Ethyl Acetate Extract of Cichorium pumilum Jacq)
COX-2 (Cyclooxygenase-2)
DMSO (dimethyl sulfoxide)
Elisa (enzyme-linked immunosorbent assay)
ERK1/2 (Extracellular signal-regulated kinase)
IL (Interleukin)
iNOS (Inducible nitric oxide synthase)
JNK (Jun-N-terminal kinase)
LDH (Lactate dehydrogenase)
LPS (Lipopolysaccharide)
MAPKs (Mitogen activated protine kinase)
MTT [3-(4,5-dimethylthiazol-2-yl)-2,5-diphenyltetrazolium bromide]
NO (Nitic oxide)
p38 (p38 kinases)
qPCR (Real-time Quantitative polymerase chain reaction)
γ-GT (gamma-glutamyl transferase)
TNBS (2,4,6-trinitrobenzene sulfonic acid)
TNF-α (Tumor necrosis factor-α)
(BBL) Bifidobacterium
(MRS) DeMan-Rogosa-Sharpe
(RIPA) Radio Immunoprecipitation Assay
(BCA) Bicinchoninic Acid

frontiers in Pharmacology

REVIEW
published: 06 May 2021
doi: 10.3389/fphar.2021.671640

Cellular Mechanisms of Liver Fibrosis

Pragyan Acharya[1]*, *Komal Chouhan*[1], *Sabine Weiskirchen*[2] and *Ralf Weiskirchen*[2]*

[1]Department of Biochemistry, All India Institute of Medical Sciences, New Delhi, India, [2]Institute of Molecular Pathobiochemistry, Experimental Gene Therapy and Clinical Chemistry, RWTH University Hospital Aachen, Aachen, Germany

The liver is a central organ in the human body, coordinating several key metabolic roles. The structure of the liver which consists of the distinctive arrangement of hepatocytes, hepatic sinusoids, the hepatic artery, portal vein and the central vein, is critical for its function. Due to its unique position in the human body, the liver interacts with components of circulation targeted for the rest of the body and in the process, it is exposed to a vast array of external agents such as dietary metabolites and compounds absorbed through the intestine, including alcohol and drugs, as well as pathogens. Some of these agents may result in injury to the cellular components of liver leading to the activation of the natural wound healing response of the body or fibrogenesis. Long-term injury to liver cells and consistent activation of the fibrogenic response can lead to liver fibrosis such as that seen in chronic alcoholics or clinically obese individuals. Unidentified fibrosis can evolve into more severe consequences over a period of time such as cirrhosis and hepatocellular carcinoma. It is well recognized now that in addition to external agents, genetic predisposition also plays a role in the development of liver fibrosis. An improved understanding of the cellular pathways of fibrosis can illuminate our understanding of this process, and uncover potential therapeutic targets. Here we summarized recent aspects in the understanding of relevant pathways, cellular and molecular drivers of hepatic fibrosis and discuss how this knowledge impact the therapy of respective disease.

Keywords: liver fibrosis, cytokines, chemokines, NASH, therapy, alcohol, cholestasis, drugs

OPEN ACCESS

Edited by:
Leo A. van Grunsven,
Vrije University Brussel, Belgium

Reviewed by:
Sonia Michael Najjar,
Ohio University, United States
Stefaan Verhulst,
Vrije University Brussel, Belgium

***Correspondence:**
Pragyan Acharya
pragyan.acharya@aiims.edu
Ralf Weiskirchen
rweiskirchen@ukaachen.de

Specialty section:
This article was submitted to Gastrointestinal and Hepatic Pharmacology, a section of the journal Frontiers in Pharmacology

Received: *24 February 2021*
Accepted: *21 April 2021*
Published: *06 May 2021*

Citation:
Acharya P, Chouhan K, Weiskirchen S and Weiskirchen R (2021) Cellular Mechanisms of Liver Fibrosis. Front. Pharmacol. 12:671640. doi: 10.3389/fphar.2021.671640

INTRODUCTION

The liver is the largest solid organ in the human body, weighing about 1,200–1,500 g, and comprising about 1/50th of the total body weight in an adult (Dooley et al., 2018). Understanding the complex architecture of the liver is key to understanding liver fibrosis and its consequences.

The liver has two major sources of blood supply, namely (i) the portal vein and (ii) the hepatic artery. The portal vein brings venous blood from the intestines and spleen to the liver. The hepatic artery brings arterial blood to the liver from the celiac axis. The liver is encapsulated by the Glisson's capsule which is mainly composed of connective tissue (Junqueira and Carneiro, 2002). Within the Glisson's capsule, the liver is divided into polygonal sections called lobules which are also separated by connective tissue. Each lobule has a characteristic arrangement which is disturbed during liver fibrosis and is completely damaged during cirrhosis (**Figure 1A**) (Sasse et al., 1992). Since liver function is so intricately linked to this arrangement, hepatic function is completely disrupted during cirrhosis leading to complications. The liver lobule, which is roughly hexagonal, harbors the hepatic central vein at its center (Sasse et al., 1992; Junquiera and Carneiro 2002). Hepatocytes are the most abundant cell type in the liver, constituting about 60% of the total cell number and 80% of liver cell volume. Hepatocytes perform the major roles of the liver such as detoxification of xenobiotics, urea cycle and the synthesis of plasma proteins (Zhou et al., 2016). Hepatocytes are arranged in straight

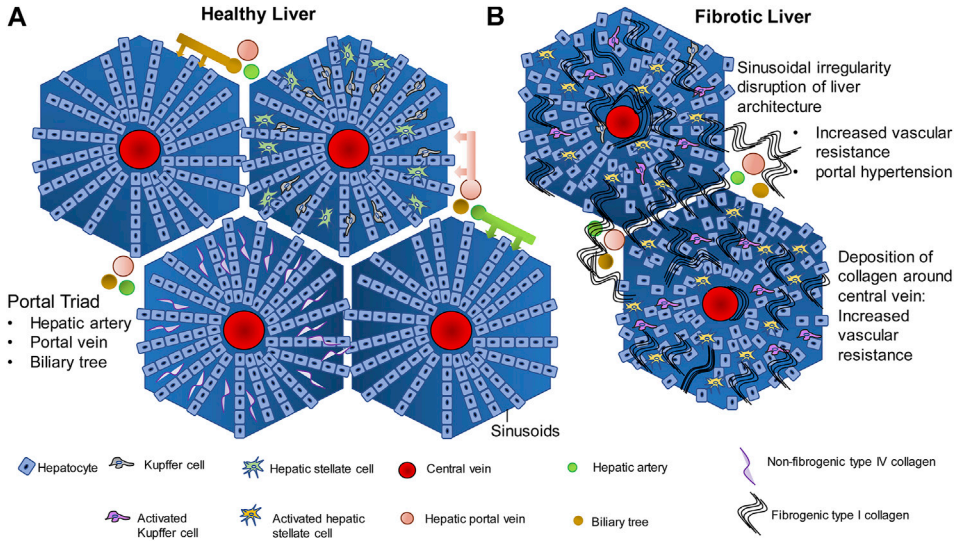


FIGURE 1 | Liver architecture in healthy liver and fibrosis. **(A)** In normal liver, hepatocytes are arranged in rows radiating outwards from the central vein, toward the edge of the lobule. The gaps between the hepatocyte rows are known as sinusoids which are lined with endothelial cells, and contain Kupffer cells, hepatic stellate cells, and contain extracellular material such as the non fibrogenic type IV collagen. Hepatic portal vein, hepatic artery and biliary tree are the three major vessels feeding into the sinusoids and the exchange of blood gases, nutrients and other signaling molecules occurs in the sinusoids. **(B)** Injury to hepatocytes due to any of several causes such as alcohol, drug, genetic predisposition, etc., activates the wound healing fibrogenic response. Chronic injury to the hepatocytes and chronic activation of the fibrogenic pathway in the liver leads to synthesis of fibrogenic type I collagen by the Hepatic stellate cells and its deposition within the sinusoids. Deposition around the central vein and around the portal vein leads to increase in vascular resistance and portal hypertension. Compensatory mechanisms such as esophageal varices and ascites follow.

lines radiating out from the central vein toward the edge of the lobule. The space between the radially arranged files of hepatocytes is commonly termed the sinusoids. Bile duct, lymphatics, neurons, as well as the branches of hepatic artery and portal vein line the periphery of the lobules and feed into the liver sinusoids. The portal vein and hepatic artery branch into the liver sinusoids, toward the central vein. Sinusoids are lined with fenestrated endothelial cells, and harbor immune cells such as Kupffer cells, hepatic stellate cells (HSCs) and hepatic natural killer cells (NK cells). These are known as the non-parenchymal cells of the liver. The space between the periphery of the hepatocyte lining and the endothelial cells is known as the space of Disse. The space of Disse is where the exchange of nutrients and other molecules occurs between the hepatocytes and blood flowing through the blood capillaries from the portal vein and the hepatic artery (Sasse et al., 1992). Interactions between the parenchymal and non-parenchymal cells in this carefully preserved architecture are central to efficient functioning of the liver.

Fibrogenesis is a normal wound healing response to tissue injury. All hepatocellular injuries activate the fibrogenic pathways. Once these pathways are activated, fibrogenic components of the extracellular matrix (ECM) are secreted into the space of Disse in order to encapsulate and isolate the damaged portion of the tissue for repair (Bataller and Brenner, 2005). During the encapsulation, there is an infiltration of immune cells that clear cellular debris and initiate tissue repair. The transition from a normal liver to fibrotic liver involves activation and modulation of complex signaling pathways, cell-cell communication between the hepatocytes and non-parenchymal cells, immune system, tissue repair pathways and the extracellular space. In the normal liver, the ECM present in the space of Disse is made up of glycoproteins like fibronectin and laminin, type IV collagen (non-fibrogenic) and proteoglycans such as heparan sulfate (**Figure 1A**). These components form a lattice-like matrix, which are essential for providing both mechanical support as well as molecular signals for the proper arrangement and functioning of liver cells. When there is hepatic injury, the composition and density of the ECM changes. There is almost a 6–8 fold increase in the production of ECM components. Non-fibrogenic type IV collagen is replaced by fibrogenic type I and II collagen (**Figure 1B**). There is additional secretion of fibronectin, hyaluronic acid and α-smooth muscle actin into the ECM. In addition, endothelial cell fenestrations as well as microvilli on the hepatocyte basal membrane are lost thereby compromising exchange of nutrients and metabolites as well as other signaling molecules between the circulation and hepatocytes. While the response to tissue injury is a rapid process and fibrogenesis is intended at promoting wound healing, repeated injury and activation of the fibrogenic pathways result in a chronic activation of fibrogenesis (Iredale et al., 2013). This leads to an increased synthesis and decreased degradation of type I collagen over a period of time. This results in deposition of type I collagen in the ECM

TABLE 1 | Genetic causes predisposing the liver to fibrosis.

Disease	Gene	Gene function	Cause of tissue injury	Clinical presentation with liver involvement
Wilson's Disease	*ATP7B*	Copper transport	Intra-hepatic Cu^{2+} accumulation	Variable presentation. Can be asymptomatic or accompanied by fibrosis, acute hepatitis, end stage liver disease
Progressive familial intrahepatic cholestasis type 3	*ABCB4*	Biliary phospholipid secretion	Accumulation of phospholipids and other xenobiotics; impairment of bile formation	Manifests in early childhood, jaundice, splenomegaly, portal hypertension and physical and mental retardation
Hereditary fructose intolerance	*ALDOB*	Converts fructose into trioses for entry into glycolysis and gluconeogenesis	Accumulation of fructose 1 phosphate and depletion of inorganic phosphate levels, inhibition of glycogenolysis, accumulation of high levels of fructose can be hepatotoxic	Hereditary fructose intolerance, hepatotoxicity, liver dysfunction progressing to cirrhosis
Glycogen storage disease type IV	*GBE1*	Glycogen branching enzyme	Accumulation of unbranched glycogen causing hepatotoxicity	Variable presentation. Hepatic classical presentation includes liver dysfunction progressing to cirrhosis, failure to thrive by 5 years of age. The non-progressive hepatic subtype present with hepatomegaly, liver dysfunction, myopathy, and hypotonia; but likely to survive without further progression to cirrhosis
Tyrosinemia type I	*FAH*	Last step in tyrosine catabolism	Accumulation of fumarylacetoacetate and tyrosine in the hepatocytes and oxidative damage to cells	Presentation as liver or renal failure; in early infancy; liver related symptoms are hypoalbunimea, lowering of synthetic functions of the liver, leading to steatosis, cirrhosis and HCC
Hemochromatosis	*HFE*	Interactions with the transferrin receptor and iron uptake	Intra-hepatic iron overload	Presentation as liver cirrhosis
Argininosuccinate lyase deficiency	*ASL*	Urea cycle enzyme that cleaves argininosuccinate into arginine and succinate	Accumulation of urea cycle intermediates, especially ammonia	Two forms:-Early onset in infancy associated with hyperammonimea and vomiting, failure to thrive, or late onset associated with hyperammonimea episodes, cirrhosis and neurological symptoms
Citrin deficiency	*SLC25A13*	Calcium binding mitochondrial carrier protein Aralar2 (exchange of cytoplasmic glutamate with mitochondrial aspartate across the inner mitochondrial membrane)	Citrullinemia and ammonia accumulation	Neonatal intrahepatic cholestasis: impaired bile flow, fibrosis, cirrhosis; late onset citrullinemia 2: neuropsychiatric symptoms
Cholesteryl ester storage disease	*LIPA*	Lysosomal acid lipase (LAL) catalyses the intracellular hydrolysis of triacylglycerols and cholesteryl ester	Intracellular accumulation of cholesteryl esters, triglycerides in the lysosomal compartment of hepatocytes	Early onset: hepatomegaly, splenomegaly and altered serum transaminases
α1 antitrypsin deficiency	*SERPINA1*	Inhibitor of various proteases including trypsin and therefore, protects cells from inflammatory proteases such as from neutrophils	Accumulation of mutant poly-AAT fibers leading to hepatotoxicity	Variable clinical severity ranging from chronic hepatitis and cirrhosis to fulminant liver failure
Cystic fibrosis	*CFTR*	Membrane chloride channel; expressed on the cholangiocytes	Pathogenesis unknown	Age of onset is late: elevation of serum liver enzymes, hepatic steatosis, focal biliary cirrhosis, multilobular biliary cirrhosis, neonatal cholestasis, cholelithiasis, cholecystitis and micro-gallbladder
Alström syndrome	*ALMS1*	Centrosome and basal body associated protein: microtubule organization	Pathogenesis unknown: likely to be involved in cellular Ca^{2+} signaling	Multiple organ dysfunction: liver involvement can range from steatohepatitis to portal hypertension and cirrhosis and can cause hepatic encephalopathy and life-threatening esophageal varices

(Continued on following page)

TABLE 1 | (*Continued*) Genetic causes predisposing the liver to fibrosis.

Disease	Gene	Gene function	Cause of tissue injury	Clinical presentation with liver involvement
Congenital hepatic fibrosis	Cryptogenic causes	NA	NA	Multiple organ fibrosis and dysfunction: Can present as the following in case of liver involvement: (i) portal hypertension (most common and more severe in the presence of portal vein abnormality), (ii) cholangitis with cholestasis and recurrent cholangitis, (iii) both portal hypertension and cholangitic symptoms; and (iv) latency that appears at a late age with hard hepatomegaly
Non-alcoholic fatty liver disease (NAFLD)	*PNPLA3*	Pleiotropic role with triglyceride lipase and retinyl esterase activity	Accumulation of triglycerides, impaired retinoic acid receptor signaling and activation of HSC fibrogenic pathway	Hepatic steatosis, fibrosis, cirrhosis, hepatocellular carcinoma

surrounding the lobules which is the hallmark of fibrosis. Large amounts of type I collagen deposition around the lobules and within the sinusoidal space disrupts the radial arrangement of the hepatocytes, interfering in the flow of nutrients and signaling molecules from the blood through the sinusoids to the hepatocytes, disrupting hepatocyte function. The deposition of collagen around the lobules causes major structural changes in the liver thereby disrupting liver function as well (Iwakiri, 2014). Accumulation of type I collagen fibers leads to mechanical rigidity in the ECM which puts pressure on the blood vessels flowing through the liver. This leads to intrahepatic vasoconstriction and vascular resistance (Pinzani and Vizzuti, 2005). Therefore, in a major vein like the hepatic portal vein, this leads to portal hypertension, which is a major clinical concern in liver fibrosis. The unchecked development of portal hypertension has two major consequences: (i) development of collateral blood vessels from the systemic and splanchnic circulation and, (ii) vasodilation of the hepatic artery (Bosch, 2007). This further increases blood flow into the hepatic portal vein leading to further portal hypertension. As a compensatory mechanism to relieve pressure, submucosal veins present at the lower portion of the esophagus dilate leading to esophageal varices that have the potential to rupture and can be fatal. Fluid begins accumulating within the peritoneal cavity, leading to ascites-the hallmark of advanced decompensated cirrhosis (Bolognesi, et al., 2014; Perri, 2013). These physiological processes are summarized in **Figure 1B**.

DRIVERS OF LIVER FIBROSIS

Genetic Disorders

Several genetic diseases predispose the liver to fibrosis (Scorza et al., 2014). In all of these diseases, the initiation of fibrosis begins with tissue injury due to a consequence of the genetic defect followed by a fibrogenic wound healing response, as discussed above. Genetic causes for liver fibrosis have come into light due to the advancements in molecular genetic and imaging techniques. Several genetic polymorphisms summarized in **Table 1**, have been implicated in the occurrence of liver fibrosis, leading to cirrhosis (Pinzani and Vizzutti, 2005). Most of these mutations affect many different cell types but predispose the individual to liver fibrosis and in some cases, liver cirrhosis (Scorza et al., 2014). Many of the genes listed in **Table 1**, such as, *ABCB4*, *ALDOB*, *GBE1*, *FAH*, *ASL*, *SLC25A13*, and *SERPINA1* are highly expressed in the liver and therefore, mutations in these genes, the liver is the organ which is most affected. Most genetic disorders that lead to cirrhosis manifest in childhood and are a leading cause of pediatric liver cirrhosis, apart from childhood obesity (Pinto et al., 2015). In addition to the genetic mutations that predispose individuals to hepatic fibrosis that appear in childhood, mutations of the *PNPLA3* gene have been described as a major predisposing factor in non-alcoholic fatty liver disease (NAFLD) (Anstee et al., 2020). *PNPLA3* encodes for Patatin-like phospholipase domain-containing protein 3 or adiponutrin and is abundantly expressed in hepatocytes, adipocytes as well as HSCs (Dong, 2019). The *PNPLA3* I148M variant has been shown to have a positive association with hepatic fat content (steatosis), NAFLD, non-alcoholic steatohepatitis (NASH) as well as hepatocellular carcinoma (Dong, 2019). The global prevalence of NAFLD is about 25% and in obese individuals or in the presence of type 2 diabetes mellitus, it increases to about 60% (Younossi et al., 2016). Therefore, *PNPLA3* gene is a strong predisposing genetic factor for hepatic fibrosis. Although the PNPLA3 protein has been shown to have triacylglycerol lipase and acylglycerol transacylase enzymatic activities, its exact role in hepatocytes have been controversial (Jenkins et al., 2004; Dong, 2019). Other studies have demonstrated a retinyl esterase activity for PNPLA3 (Pirazzi et al., 2014). HSCs are reservoirs for retinoic acid, which activate the retinoic acid receptor (RAR) mediated transcription which keeps fibrogenesis under control (Hellemans, et al., 1999; Hellemans et al., 2004; Wang et al., 2002). Mutations in the *PNPLA3* gene that alter the retinyl esterase activity therefore, decrease the level of retinoic acid in the HSCs and therefore reduce the RAR mediated control of fibrogenesis in HSCs (Bruschi et al., 2017). However, it is now recognized that PNPLA3 has pleiotropic roles in the hepatocyte that are still

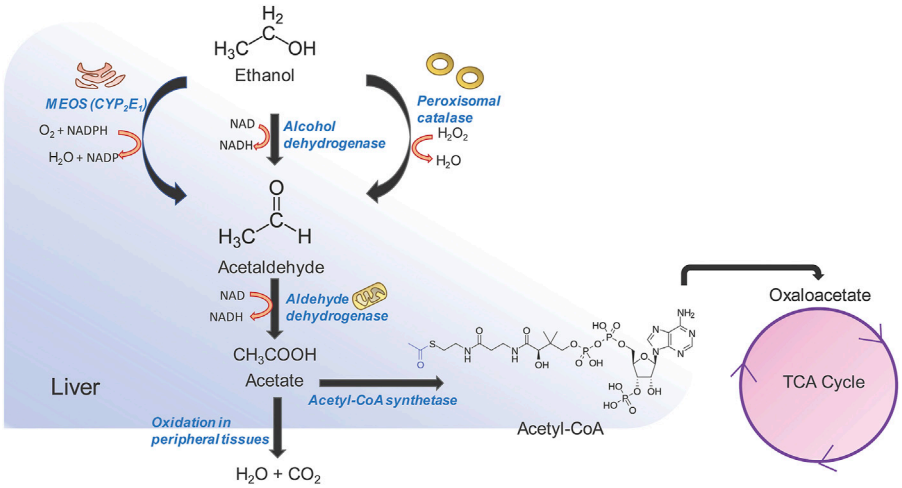


FIGURE 2 | Alcohol metabolism in the liver. Three pathways are involved in alcohol metabolism and all of them converge on the oxidation of ethanol to acetaldehyde. Acetaldehyde is further converted to acetate by aldehyde dehydrogenase in the mitochondria. Acetate can be rapidly oxidized into CO_2 and H_2O by peripheral tissues, or can be diverted to the tri-carboxylic acid (TCA) pathway. The oxidation of ethanol to acetaldehyde by microsomal ethanol oxidation system (MEOS) occurs in the smooth endoplasmic reticulum and changes the NADPH/NADP ratio which in turn influences the regeneration of glutathione thereby increasing cellular oxidative stress. The alcohol dehydrogenase pathway is the major pathway and occurs in the cytosol, generating large amounts of NADH. NADH in turn inhibits TCA cycle enzymes and leads to accumulation of acetyl CoA and increase in ketone body generation and acidosis. NADH also inhibits fatty acid oxidation leading to accumulation of fats and causing "fatty liver." A combination of the above factors leads to tissue injury and activation of the fibrogenic pathway.

under investigation such as in hepatocyte lipid droplet homeostasis, HSC quiescence and proliferation regulation (Dong, 2019). As several roles for PNPLA3 are suggested, PNPLA3 might be a good therapeutic target to control NAFLD related fibrosis and disease progression.

Alcohol

Excessive and continued alcohol intake over large periods of time, i.e., alcohol abuse, can lead to liver fibrosis followed by cirrhosis and liver cancer (Stickel et al., 2017). Alcoholic liver disease (ALD) comprises a spectrum of liver disorders ranging from fatty liver, steatosis, fibrosis with varying degrees of inflammation, cirrhosis. Alcohol abuse contributes to almost 50% of chronic liver disease related deaths globally (Rehm and Shield 2019). While the pathophysiology of alcohol induced cirrhosis is not completely understood, alcohol and its metabolic intermediates such as acetaldehyde are thought to play an important role in it. Alcohol is absorbed from the duodenum and upper jejunum by simple diffusion, reaching peak blood concentration by 20 min post ingestion after which it is quickly redistributed in vascular organs (Koob et al., 2014). Alcohol cannot be stored and needs to undergo obligatory oxidation which occurs predominantly in the liver (**Figure 2**) (Yang et al., 2019). The first step in alcohol oxidation converts alcohol into acetaldehyde. There are three enzymes in the liver that can carry out this reaction (i) alcohol dehydrogenase (ADH) which catalyzes the bulk of ethanol to acetaldehyde conversion, (ii) the alcohol inducible liver cytochrome P450 CYP2E1 (microsomal ethanol oxidizing system or MEOS) and, (iii) peroxisomal catalase. The ethanol to acetaldehyde conversion by ADH generates NADH (Berg et al., 2002). Oxidation of large amounts of alcohol therefore, leads to the accumulation of NADH, which inhibits lactate to pyruvate conversion and promotes the reverse reaction. Lactate to pyruvate conversion is an important means of entry of lactate into gluconeogenesis. As a result, lactic acidosis and hypoglycemia may occur during excessive alcohol consumption. $NADH/NAD^+$ ratio also allosterically regulates fatty acid β-oxidation which breaks down long chain acyl CoA to acetyl CoA for entry into TCA cycle (Berg et al., 2002). Since NADH is a product of fatty acid oxidation, an increase in $NADH/NAD^+$ ratio provides an allosteric feedback to the fatty acid β-oxidation pathway thereby decreasing the catabolism of fatty acids and leading to their intracellular accumulation. This leads to "fatty liver." NADH also inhibits two enzymes of the TCA cycle-isocitrate dehydrogenase and α-ketoglutarate dehydrogenase thereby decreasing the consumption of acetyl CoA by the TCA cycle and leading to increase in intra-hepatic acetyl CoA levels. The accumulation of acetyl CoA, in turn, leads to the increased production and release of ketone bodies exacerbating the acidosis already present in the blood due to increased levels of lactate (McGuire et al., 2006). This is known as alcoholic ketoacidosis, which creates a medical emergency. At very high levels of ethanol consumption, the metabolism of acetate becomes compromised leading to the accumulation of acetaldehyde within the hepatocytes. Acetaldehyde can modify the functional groups of many proteins and enzymes irreversibly forming acetaldehyde adducts which leads to a global dysfunction of hepatocytes and eventually, to cell death (Setshedi et al., 2010). The second major pathway for ethanol metabolism is via the inducible cytochrome P450 CYP1E2, also known as the microsomal ethanol oxidizing system (MEOS) (Lieber, 2004). This is located in the smooth

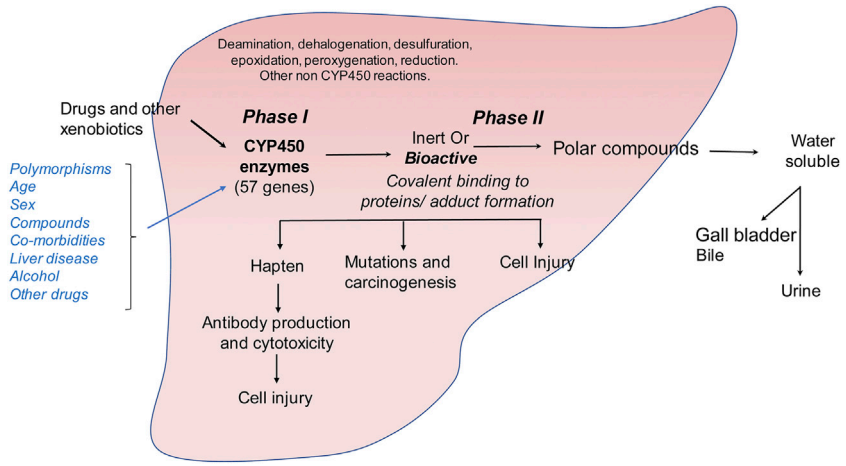


FIGURE 3 | Metabolism of drugs and other xenobiotics in the liver. Drug and xenobiotic metabolism occurs in two phases: (*i*) phase I is catalyzed by the cytochrome P450 family of monooxygenases which metabolize ingested small molecules to form inert or bioactive metabolic intermediates. (*ii*) These intermediates are further catalyzed in phase II reactions to form soluble polar compounds that can be further excreted through urine or bile. Accumulation of bioactive drug or xenobiotic intermediates can lead to the formation of protein or nucleic acid adducts causing autoimmune reaction, carcinogenesis or direct cellular injury.

endoplasmic reticulum of hepatocytes. In normal people with average to below average alcohol consumption, MEOS forms a minor pathway for intracellular alcohol metabolism (Lieber, 2004). However, it increases manifold upon chronic alcohol consumption. MEOS catalyzes a redox reaction converting molecular oxygen to water and NADPH to NADP (**Figure 2**). In the liver, glutathione plays an important role in maintaining the cellular redox status and participates in xenobiotic metabolism (Yuan and Kaplowitz, 2009). NADPH is essential in the regeneration of glutathione. The consumption of cellular NADPH leads to a decrease in regeneration of glutathione thereby leading to oxidative stress. This results in cell death and inflammation leading to alcoholic hepatitis which, in itself can be fatal (Morgan, 2007). Often, these processes occur hand in hand. Cellular depletion of glutathione has an additional consequence. Glutathione is required for the detoxification of several drugs including acetaminophen (van de Straat et al., 1987). In the hepatocytes, acetaminophen is modified to form a cytotoxic metabolite known as N-acetyl-p-benzoquinone imine (NAPQI) via CYP2E1 (van de Straat et al., 1987). Conjugation of NAPQI to glutathione results in an S-glutathione product that detoxifies the molecule and allows safe excretion in the urine. However, depletion of glutathione reserves allows unconjugated NAPQI to prevail in the cells which reacts with DNA and proteins to form adducts, thereby causing cytotoxicity and hepatocyte death (Macherey and Dansette, 2015). Long term alcohol use induces CYP2E1 and therefore facilitates rapid NAPQI formation when the liver encounters acetaminophen. At the same time, chronic alcohol abuse leads to low glutathione reserves. A combination of both these changes makes the liver highly susceptible to acetaminophen induced liver injury as well as injury due to other drugs or metabolites that go through the glutathione detoxification pathway. While drug overuse is, in itself a cause for liver injury, in a background of alcoholic liver disease, it can lead to massive liver damage. Damage to hepatocytes, either due to chronic alcohol abuse, exacerbated by drug use, activates the fibrogenic pathway leading to hepatic fibrosis, cirrhosis and hepatocellular carcinoma.

Drugs

Drugs induce hepatic fibrosis by causing drug-induced liver injury (DILI) that causes the initiation of fibrogenic tissue repair mechanisms. While the prevalence of DILI is lower as compared to other causes of liver injury, such as alcohol, hepatisis or steatosis, it can lead to life-threatening complications. DILI can be of two types: (i) intrinsic (due to injury caused by a known on-target drug) or (ii) idosyncratic (due to injury caused by an unknown factor and cannot be explained by known pharmacological elements e.g., herbal preparations of unknown compositions) (DiPaola and Fontana, 2018). Among intrinsic causes, acetaminophen induced DILI is the most common. As described above, acetaminophen overload combined with alcohol abuse can exacerbate the liver injury that can occur due to either alcohol or acetaminophen alone. A major function of the liver is detoxification of xenobiotic compounds that enter our circulation either through diet or through intravenous drug usage. Detoxification mechanisms in the liver mainly involve the cytochrome P450 family (*CYP* gene families *CYP1*, *CYP2*, *CYP3*) (McDonnell and Dang, 2013) (**Figure 3**). Cytochrome P450s are a group of heme proteins that are involved in the initial detoxification reactions of small molecules such as dietary and physiological metabolites, as well as drugs (Zanger and Schwab, 2013; Todorovic Vukotic et al., 2021). The expression of the *CYP* genes is influenced by several factors such as age, sex, promoter polymorphisms, cytokines, xenobiotic compounds and hormones, to name a few (Zanger and Schwab, 2013). Cytochrome P450 mainly carry out a monooxygenation reaction and carry oxidation of drugs/xenobiotic compounds.

This can either convert the molecule into an inert or bioactive molecule.

Bioactive compounds can covalently modify intracellular proteins, leading to direct cellular injury, carcinogenesis or production of hapten-protein conjugates that can lead to antibody mediated cytotoxicity (**Figure 3**). Although the classical view of DILI is that drugs become hepatotoxic as a consequence of or defects in their metabolism, several factors may influence the final outcome of drug intake such as age, gender, comorbidities, intake of alcohol, other drugs or herbal preparations and polymorphisms of the *CYP* genes (Tarantino et al., 2009). The exact mechanism of DILI in specific cases depends on the nature of the molecule and its CYP-transformed metabolites. Drug metabolism can generate free radicals or electrophiles that can be chemically reactive. This can lead to the depletion of reduced glutathione, formation of protein, lipid or nucleic acid adducts and lipid peroxidation. Unless these metabolic intermediates are rapidly neutralized through phase II reactions, they can contribute to cellular stress and injury (**Figure 3**). They can also lead to modulation of signaling pathways, induce transcription factors, and alter gene expression profiles. In the liver, accumulation of large quantities of reactive drug metabolites can lead to hepatocellular injury, formation of protein adducts that can act as haptens and stimulate production of auto-antibodies or promote cellular transformation. Cellular injury then leads to induction of fibrogenic responses as described above.

Cholestasis

Cholestasis is emerging as a leading cause for liver injury and fibrosis. Cholestatic liver diseases can occur due to primary biliary cirrhosis and primary sclerosing cholangitis and involve injury to the intra- and extra-hepatic biliary tree (Penz-Österreicher et al., 2011). The pathogenesis of cholestasis is unclear but is believed to have an autoimmune component to it (Karlsen et al., 2017). I primary sclerosing cholangitis (PSC) several strictures appear around the bile ducts and cause bile duct injury. This activates the portal fibroblasts around the bile duct, which then differentiate into collagen secreting myofibroblasts (MFBs) similar to those derived from HSC activation. Recent studies have shown that fibrogenic MFBs have inherent heterogeneity and can be derived from both HSCs and portal fibroblasts (Karlsen et al., 2017). PSC has been shown to be associated with a varied manifestation of other diseases such as inflammatory bowel disease, cholangiocarcinoma, high IgG4 levels, autoimmune hepatitis and colonic neoplasia (Wee et al., 1985; Broomé et al., 1992; Perdigoto et al., 1992; Siqueira et al., 2002; Mendes et al., 2006; Berntsen et al., 2015). Due to its association with autoimmune responses, PSC is thought to involve a genetic predisposition which is activated by an as yet unidentified environmental trigger such as gut dysbiosis (Rossen et al., 2015). Although PSC is traditionally recognized as a rare disease, its incidence is on the rise due to an increase in unknown environmental triggers (Karlsen et al., 2017). Therefore, the pathogenesis of PSC is varied and injury to the bile ducts can occur through multiple pathways. However, the resultant bile duct injury leads to activation of the portal fibroblasts and consequent fibrogenesis.

Metabolic Disorders: Non-alcoholic Fatty Liver Disease and Non-alcoholic Steatohepatitis

The metabolic syndrome is a group of associated diseases that increase cardiovascular risk factors and are linked with obesity and type 2 diabetes mellitus (Rosselli et al., 2014). Liver manifestations of the metabolic syndrome result in NAFLD (Rosselli et al., 2014). NAFLD is attaining epidemic proportions all over the world. The global prevalence of NAFLD is about 25% and in obese individuals or in the presence of type 2 diabetes mellitus, it increases to about 60% (Younossi et al., 2016). NAFLD is linked to increased risk of hepatic fibrosis, hepatocellular carcinoma and mortality due to cardiovascular disease. The more severe subtype of NAFLD is NASH, which has a global prevalence of about 2–6% and which is associated with severe hepatic inflammation, fibrosis leading to cirrhosis and HCC as well as end stage liver disease (Younossi et al., 2016; Younossi et al., 2019). Recently reported trends in the incidence of NAFLD over time suggest that NAFLD will become the leading cause of end stage liver disease in the decades to come. Emerging data from India, suggests that the national prevalence of NAFLD is about 9–32% in the general population and about 53% in obese individuals (Kalra et al., 2013; Duseja, 2010). Therefore, NAFLD is a global clinical concern. The molecular pathogenesis of NAFLD is complex. However, all pathways in NAFLD converge at the conversion of HSCs into profibrogenic MFBs, through the activation of the TGF-β pathway (Buzzetti et al., 2016) (**Figure 4**). TGF-β is a pleiotropic cytokine and is involved in various cellular processes like cell proliferation, survival, angiogenesis, differentiation, and the wound healing response (Mantel and Schmidt-Weber, 2011). TGF-β binds to the TGF-β receptor type II, which in turn phosphorylates TGF-β receptor type I thereby recruiting and phosphorylating the intracellular signal transducer proteins belonging to the SMAD superfamily. The SMAD superfamily is composed of intracellular signal transducers that specifically respond to the TGF-β receptor modulation. Phosphorylated SMADs subsequently translocate into the nucleus and control the expression of the TGF-β regulated target genes (Mantel and Schmidt-Weber, 2011) (**Figure 4**). The activation of HSCs via TGF-β plays a major role in the advanced NAFLD in both experimental animal models, as well as in human liver injury (Yang et al., 2014). In addition to HSC activation, TGF-β signaling followed by SMAD phosphorylation is known to cause hepatocyte death driving progression to NASH (Yang et al., 2017). Hepatocyte death via TGF-β signaling is accompanied by generation of reactive oxygen species as well as lipid accumulation in hepatocytes (Yang et al., 2017). Activation of the TGF-β pathway also leads to HSC differentiation into MFBs leading to formation of fibrillar collagen and exacerbating the combined effects of hepatocyte injury, fibrosis and inflammation, leading to NASH (Yang et al., 2014). While the TGF-β pathway is central to liver fibrogenesis, emerging proteome and transcriptome studies have suggested

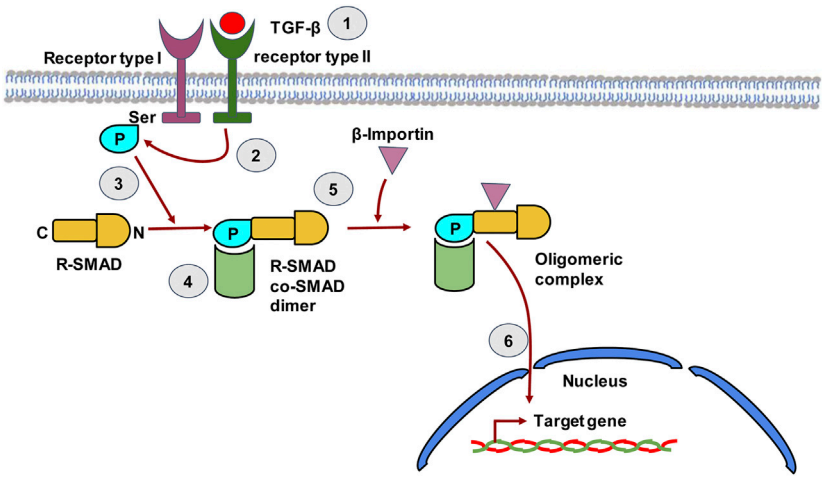


FIGURE 4 | The TGF-β signaling pathway in hepatic stellate cells. TGF-β binds to type II TGF-β receptor leading to receptor dimerization i.e. recruitment of the type I TGF-β receptor. The kinase domain of Type II TGF-β receptor then phosphorylates the Ser residue of type I TGF-β receptor. The phosphorylated receptor now recruits R-SMAD, which binds to receptor through its N-terminal region and gets phosphorylated by the Type II receptor. The C-terminal of R-SMAD has a DNA binding domain (DBD) that can act as a transcription factor. The co-SMAD now binds to R-SMAD and β-Importin binds to the dimer forming an oligomeric complex that guides the R-SMAD and Co-SMAD into the nucleus. The dimer enters the nucleus and the DBD of SMAD now acts as transcription factor that can transcribe target genes.

additional regulatory genes and pathways. These studies have been carried out in animal models of NAFLD or NASH and human liver biopsies obtained from patients. Comparative transcriptomic studies between mouse models of NAFLD and human liver biopsies obtained from NASH patients reveal major differences between human NASH liver transcriptome and mouse NAFLD transcriptomes even at severe stages (Teufel et al., 2016). This suggests major pathophysiological differences between human disease and animal models of the disease and the need to design studies in humanized models of disease or in liver organoid systems (Suppli et al., 2019). A meta-analysis of transcriptomic studies carried out with human liver biopsies suggests the upregulation of several genes within the lipogenesis pathway (**Table 2**). Interestingly, genes such as *ACACA* (Acetyl carboxylase 1) which catalyzes the synthesis of malonyl CoA from acetyl CoA, the rate limiting step in fatty acid biosynthesis and *ACACB* (Acetyl carboxylase 2) which regulates fatty acid oxidation, are associated with NAFLD liver tissue demonstrating the association of lipogenic functions within the tissue with active disease (**Table 2**) (Widmer et al., 1996; Locke et al., 2008). In several cases, NAFLD has been shown to be linked to progression toward hepatocellular carcinoma. Recent studies have led to the understanding that the evolution of NAFLD to NASH and HCC is multifactorial and involves the innate immune system to a great extent (Chen et al., 2019). Lipid accumulation and mitochondrial dysfunction have been identified as critical components of the pathways leading to NAFLD (Margini and Dufour, 2016). Many new genes and pathways have been implicated at every stage of NAFLD to NASH to HCC progression (**Figure 5**). Regulation in PPAR-γ, Insulin and p53-mediated signaling have been implicated in NAFLD development, whereas signatures of inflammatory signaling such as Toll-like receptor (TLR) and Nucleotide-binding, oligomerization domain (NOD) protein signaling pathways, in addition to pathways reflecting mitochondrial dysfunction characterize NASH (**Figure 5**) (Ryaboshapkina and Hammar, 2017).

There are only a limited number of proteomics studies in human NAFLD. A comparative quantitative proteomics study between NAFLD and Metabolic Healthy Obese (MHO) individuals was carried out using liver tissue obtained during surgery (Yuan et al., 2020). This study demonstrated the relevance of PPAR signaling, ECM-receptor interaction and oxidative phosphorylation in resisting NAFLD. Proteins upregulated in NAFLD were involved in organization of the ECM, and proteins downregulated in NAFLD were involved in redox processes. A schematic of pathways relevant in NAFLD progression, as gleaned from various "omics" approaches is summarized in **Figure 5**.

Viral Hepatitis

In older children, autoimmune hepatitis and viral hepatitis are the leading causes of liver fibrosis followed by cirrhosis. Viral hepatitis can be caused by any one of the five viruses: Hepatitis A, B, C, D, and E of which A and E are usually acute, while B, C, and D are chronic (Zuckerman 1996). All hepatitis viruses are infectious, while alcohol, other toxins and autoimmune mediated hepatitis are usually non-infectious. HBV and HCV lead to hepatic inflammation (Gutierrez-Reyes et al., 2007). Several viral components are known to induce cellular damage in hepatocytes and liver constituents. For instance, the HCV core protein in chronic infections is known to interact with the TNF-α receptors (TNFRSF1A) which subsequently induces a pro-apoptotic signal in hepatocytes (Zhu et al., 1998). Polymorphisms in *TNFRSF1A* have been shown to be associated with HCV outcomes (Yue et al., 2021). The HCV core protein is also known to interact with ApoA1and ApoA2, thereby interfering with the assembly and secretion of

TABLE 2 | Summary of pathways from transcriptomics analyses implicated in NAFLD

Gene		Function/remarks	References
LEP	Leptin	Anti-steatotic, but also a proinflammatory and profibrogenic action	Polyzos et al. (2015)
PEMT	Phosphatidylethanolamine *N*-methyltransferase	Governs the secretion of hepatic triglycerides in the form of very low-density lipoprotein	Tan et al. (2016)
PPAR-γ2	Peroxisome proliferator activated receptor gamma	Pparγ2 is expressed in the liver, specifically in hepatocytes, and its expression level positively correlates with fat accumulation induced by pathological conditions such as obesity and diabetes	Lee et al. (2018)
TNF-α	Tumor necrosis factor	Tumor necrosis factor (TNF)-α is associated with insulin resistance and systemic inflammatory responses	Seo et al. (2013)
PNPLA3	Patatin like phospholipase domain containing 3	Polymorphisms in *PNPLA3* have been linked to obesity and insulin sensitivity	Chen et al. (2010)
CD14	CD14 molecule	Upregulation of *CD14* in liver cells show increased sensitivity to LPS, changes in *CD14* expression could represent a mechanism regulating liver sensitivity to LPS toxicity	Satoh et al. (2013)
ACACA	Acetyl-coa carboxylase α	Low level is correlated with long time survival	Liu et al, (2020)
ACACB	Acetyl-coa carboxylase β	Involved in insulin signaling pathway and adipokine metabolic pathway	Li et al. (2019)
ASPG	Asparaginase	The bacterial enzyme L-Asparaginase is a common cause of anti-neoplastic-induced liver injury with occurrence of jaundice and marked steatosis	Kamal et al. (2019)
CCS	Copper chaperone for superoxide dismutase	*CCS* expression is regulated by copper by modulating its degradation by the 26S proteosome	Bertinato and L'Abbé (2003)
CHEK1	Checkpoint kinase 1	This kinase is necessary to preserve genome integrity	Zhang and Hunter (2014)
HDAC9	Histone deacetylase 9	Downregulation of *HDAC9* decrease TGF-β1-induced fibrogenic gene expression in hepatic stellate cells	Yang et al. (2017)
NADSYN1	NAD synthetase 1	Reduced NAD concentrations contribute to the dysmetabolic imbalance and consequently to the pathogenesis of NAFLD	Guarino and Dufour (2019)
NHP2L1	Small nuclear ribonucleoprotein 13	This genes encodes a protein of the spliceosome complex	Liu et al. (2020)
OAS3	2′-5′-oligoadenylate synthetase 3	OAS3 is an interferon-induced aniviral enzyme	Zhang and Yu (2020)
PCNA	Proliferating cell nuclear antigen	*PCNA* encodes the protein which is found in the nucleus and is a cofactor of DNA polymerase delta and involved in the RAD6-dependent DNA repair pathway in response to DNA damage	Xing et al. (2018)
RPL10L	Ribosomal protein L10 like	The encoded protein shares sequence similarity with ribosomal protein L10	Liu et al. (2020)
RSL24D1	Ribosomal L24 domain containing 1	The encoded protein is involved in involved in the biogenesis of the early pre-60S ribonucleoparticle	Xie et al. (2020)
SRC	*SRC* proto-oncogene, non-receptor tyrosine kinase	*SRC* is a proto-oncogene encoding a non-receptor tyrosine kinase	Amanatidou and Dedoussis (2021)
TOP2A	DNA topoisomerase II alpha	Regulates the topologic states of DNA and controls tumor cell response	Wong et al. (2009)
TP53	Tumor protein p53	Induces apoptosis but the association between p53 and NAFLD remains controversial, P53 plays an essential role in the pathogenesis of NAFLD, whereas others have indicated that suppression of p53 activation aggravates liver steatosis	Yan et al. (2018)
TWISTNB	RNA polymerase I subunit F	This gene (i.e. TWIST Neighbor) is ubiquitous expressed in all tissues	Liu et al. (2020)
UMPS	Uridine monophosphate synthetase	Lack of this gene results in reduced cell membrane stability	Wortmann and Mayr (2019)
HORMAD2	HORMA domain containing 2	Decreases with advancing fibrosis	Liu et al. (2020)
LINC01554	Long intergenic non-protein coding RNA 1554	*LINC01554*, one kind of lncRNA, has been found specifically enriched in liver tissue and have strong association with pathogenesis and clinical evaluation of HCC	Ding et al. (2020)

very low density lipoprotein (VLDL), thus cause the accumulation of triglycerides in the liver through the interaction of both viral and metabolic factors and subsequent cell death (Gutierrez-Reyes et al., 2007). Furthermore, the viral core protein as well as the HCV non-structural protein 5A (NS5A) are known to cause mitochondrial ROS production and cellular stress leading to cell death (Bataller et al., 2004). Interestingly, HCV and NAFLD can co-exist and have been shown to have a more rapid disease progression than either disease alone (Patel and Harrison, 2012; Dyson et al., 2014). About 50% of HCV patients have steatosis with significant fibrosis and the HCV genotype 3 is mainly associated with the steatosis, however the exact mechanism leading to steatosis in HCV patients is not fully elucidated.

The association of hepatitis B virus (HBV) infection with NAFLD however, appears to be controversial. Some studies suggest that HBV infection is protective against steatosis, insulin resistance and metabolic syndrome (Morales et al., 2017; Xiong et al., 2017) while others suggest that chronic HBV infections can co-exist with NAFLD and can actively worsen the disease (Zhang et al., 2020). The presence of Hepatitis B protein X (HBx) in the cells has been shown to increase the production of reactive oxygen species (ROS) increasing the formation of lipids in the cells and therefore HBx could be a risk factor for the development of NAFLD (Wang et al., 2019). Therefore, an alternative mechanism by which viral hepatitis can induce fibrosis is through their ability to cause NAFLD.

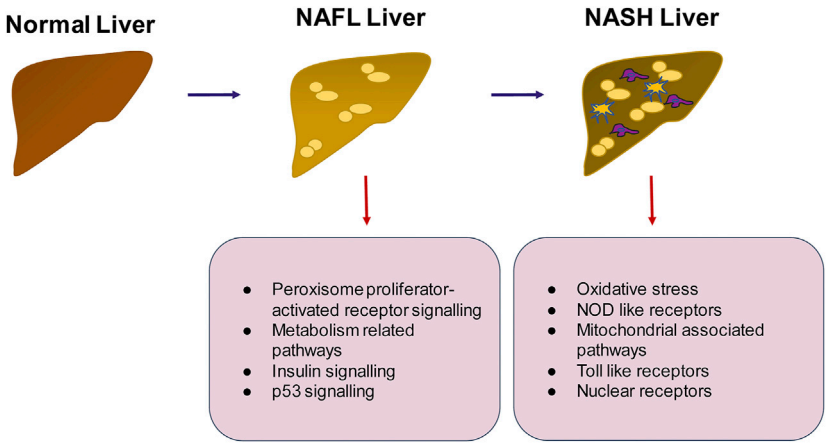


FIGURE 5 | Summary of pathways that may be important in the progression of NAFLD to NASH. The transition from healthy to NAFLD involves the activation of peroxisome proliferator activated receptor signaling, insulin signaling and p53 signaling whereas the switch to NASH involves activation of inflammatory pathways such as TLR and NOD like receptor mediated signaling, generation of intracellular oxidative stress and mitochondrial signaling.

Parasitic Infections

The liver is capable of hosting a wide range of parasites which vary in host cell requirement (extra or intracellular), sizes (unicellular to multicellular) and potential harm to the host cells or organs (Dunn, 2011). Parasites which have co-evolved with humans through centuries, such as the malaria parasites cause minimal injury to the host liver and move on to the blood with ease (Acharya et al., 2017). However, some parasites can cause injury to the cells of the liver and trigger the activation of the fibrogenic pathway. Some of these parasites are discussed below:

Leishmania is an intracellular protozoan parasite that infects the reticuloendothelial system (RES) in the body, i.e., circulating monocytes as well as tissue-resident macrophages (Magill et al., 1993). Leishmaniasis is transmitted by the bite of infected sandflies (Dunn, 2011). Visceral leishmaniasis (kala-azar) involves the RES infection of the visceral organs like the liver, spleen, bone marrow and other lymph nodes. Kupffer cells, the tissue resident macrophages of the liver, take up the amastigote stage of Leishmania from circulating infected reticuloendothelial cells. The parasite then replicates within the macrophages and activates the host inflammatory and Th1 and Th17 mediated adaptive immune responses in immunocompetent individuals (Pitta et al., 2009). Leishmaniasis is typically associated with increased liver fibrosis (Melo et al., 2009). Leishmania parasites have been shown to use host ECM components such as fibronectin and laminin to access Kupffer cells for infection (Wyler et al., 1985; Wyler, 1987; Vannier-Santos et al., 1992; Figueira et al., 2015). Visceral leishmaniasis has been frequently studied in dogs as a model system. These studies suggest that dogs infected with Leishmania have a significantly higher level of collagen and fibronectin deposition (Melo et al., 2009). Intra-lobular collagen deposition, appearance of MFBs and effacement of the space of Disse are characteristic of overt Leishmania infection in slightly or severely immunocompromized individuals (Dunn, 2011). Leishmania associated fibrosis is completely reversible once the parasitic infection has been treated. However, since overt disease and severe fibrosis usually occurs in immunocompromized individuals such as those infected with HIV, relapses typically occur once treatment ceases (Dunn, 2011).

Schistosomiasis is caused by Schistosoma species which are a group of blood flukes belonging to the trematode or flatworm family (Andrade, 2009). It is prevalent mainly in the tropical and sub-tropical regions of the world. Schistosoma use freshwater snails as intermediate hosts, which release eggs into water bodies which then come into contact with humans and infect them (WHO. World Health Organization, 2021). Schistosomiasis can be intestinal (wherein the liver is involved) or urogenital. Intestinal schistosomiasis can be caused by many different species such as *Schistosoma mansoni* (found in Africa, Middle East, Caribbean, Brazil, Venezuela and Suriname), *S. japonicum* (found in China, Indonesia and the Philippines), *S. mekongi* (Cambodia, and the Lao People's Democratic Republic), *S. guineensis* and *S. intercalatum* (found in the rain forests of central Africa). Urogenital infection is caused by *S. hematobium* (found in Africa, the Middle East and Corsica in France) (WHO. World Health Organization, 2021).

Schistosoma mansoni are associated with liver fibrosis (Andrade, 2009). Schistosome eggs are carried to the liver by the portal vein and stop in the pre-sinusoidal vessels (Andrade, 2004). The development of severe schistosomiasis is thought to have two components- (a) a major determinant is the high worm load and, (b) a secondary determinant is thought to be genetic predisposition. At low to moderate worm loads, many patients are asymptomatic and the lesions heal automatically due to the appropriate activation of T-cell mediated host immune responses (Andrade, 2004). A high worm load is also associated with damage to the portal vein and appearance of MFBs and collagen deposition around the portal stem leading to portal fibrosis called pipestem fibrosis (Andrade et al., 1999). Since all infected individuals do not develop severe liver disease, or liver

fibrosis, schistosomiasis linked liver fibrosis development is also thought to have a genetic component. A metaanalysis of genetic polymorphisms associated with severe liver disease and fibrosis in schistosomiasis reveals several genetic polymorphisms (Dessein et al., 2020). Several polymorphisms in genes related to the TGF-β pathway were found to be associated with severe fibrosis in schistosomiasis e.g., *TGFBR1*, *TGFBR2*, *ACVRL1*, *SMAD3* and *SMAD9* (Dassein et al., 2020). Polymorphisms in the connective tissue growth factor (CTGF) as well as the IL-22 pathway were also observed. In addition, several associations have been reported between severe hepatic fibrosis during Schistosomiasis and genes encoding for IL-13, TNF-α, MAPKAP1, ST2, IL-10, M1CA, HLADRB1, IL-4, ECP, and IFN-γ, have been reported from various studies (Hirayama et al., 1998; Chevillard et al., 2003; Eriksson et al., 2007; Gong et al., 2012; Silva et al., 2014; Zhu et al., 2014; Long et al., 2015; Oliveira et al., 2015; Long et al., 2017; Silva et al., 2017). These observations suggest that while infectious agents such as schistosoma can drive hepatic fibrosis by mediating tissue damage, genetic predispositions to TGF-β pathway activation or a specific inflammatory response may make the hepatic environment conducive to fibrosis in the presence of an infectious agent.

Fasciola hepatica, also known as the liver fluke is also a trematode parasite that infects humans (Machicado et al., 2016). Fascioliasis is a neglected tropical disease. A recent meta-analysis has found an association of Fasciola infections with liver fibrosis, cirrhosis and hepatocellular carcinoma (Machicado et al., 2016). The mechanism of fibrosis development is thought to be due to the activation of HSCs by parasite encoded cathepsins (Marcos et al., 2011). As with schistosoma, worm-load seems to be an important determinant of fibrosis. However, there are a very limited number of studies available on the pathogenesis, molecular epidemiology and prevalence of fascioliasis with liver fibrosis and this area needs further investigation.

Cryptogenic Causes

Cryptogenic causes of liver fibrosis are cases with unknown causes but it is believed that a high proportion of the cryptogenic liver fibrosis cases could be linked to NAFLD or NASH (Caldwell, 2010; Patel et al., 2020). Other causes could include occult alcohol intake, viral hepatitis, autoimmune hepatitis, biliary disease, vascular disease, celiac disease, mitochondriopathies, systemic lupus erythematosus, Alstrom syndrome, Apolipoprotein B with LDL cholesterol, and genetic disorders such as short telomere syndrome, keratin 18 mutations and glutathione-S-transferase mutations (Caldwell, 2010; Patel et al., 2020).

SOLUBLE MEDIATORS IN LIVER FIBROSIS

The development of liver fibrosis occurs as a result of interaction between several different cell types including hepatocytes, HSCs, Kupffer cells, as well as infiltrating immune cells. These intercellular interactions involve several soluble and secreted mediators which regulate inflammatory pathways, chemotaxis and HSC activation. Some of the known soluble mediators are briefly discussed below.

Cytokines and Chemokines

Cytokines are regulatory soluble small molecular weight proteins or glycoproteins released by several cells and mediate interaction, communication between different cell types. Cytokines play an important role in the progress of liver fibrosis (Xu et al., 2012). In liver they mediate the interactions of the various cell types and contribute to either the production of proinflammatory or hepatoprotective responses (Kong et al., 2012). Cells of the immune system such as Kupffer cells and neutrophils produce many cytokines and chemokines that can affect the gene expression, proliferation, contractility and activation of HSCs. The interaction between HSCs and immune cells are bidirectional, i.e., while immune cells produce cytokines to activate HSCs. HSCs also regulate immune cell chemotaxis and response by secreting soluble mediators themselves (Weiskirchen, 2016). For instance, the pro-inflammatory cytokines TGF-α increases HSC proliferation, TGF-β inhibits HSC apoptosis and promotes ECM remodeling leading to a pro-fibrogenic phenotype, TNF-α inhibits HSC apoptosis and induces chemokines and ICAM-1 in HSCs (Maher, 2001). IL-4 in concert with MMP-2 and ROS increase ECM synthesis and fibrosis. At the same time, anti-fibrogenic cytokines are also released from immune cells that can control the pro-fibrogenic HSC activation, such as IL-10, IFN-α, IFN-γ. A balance of these factors results in a net pro-or anti-fibrogenic effects on HSCs. The HSCs also secretes several molecules which are instrumental in recruiting immune cells at the site of activation such as M-CSF that causes macrophage proliferation and maintenance, PAF, MIP-2 and CINC/IL-8 which cause neutrophil chemotaxis and MCP-1 which recruits monocytes (Maher, 2001).

While activation of the TGF-β pathway is a central event in the induction of hepatic fibrosis, HSC activation is regulated by other pathways and molecular mechanisms as well, such as the Hippo pathway and autophagy (Tsuchida and Friedman, 2017). The Hippo signaling pathway is an evolutionarily conserved pathway that derives its name from its key player, the protein kinase "Hippo", which is involved in the regulation of cell and organ size (Saucedo and Edgar, 2007). However, Hippo pathway components such as the transcriptional co-activator Yes-associated protein 1 (YAP1) and the protein kinases macrophage stimulating 1 (MST1) and MST 2 have been shown to be important in initial HSC activation (Manmadhan and Ehmer, 2019). Inhibition or silencing of YAP1, and inactivation of MST1 and MST2 have been shown to have therapeutic effects in mouse models of fibrosis but the human clinical impact of such approaches is presently not known (Manmadhan and Ehmer, 2019).

Chemokines are a subgroup of cytokines that have chemotactic properties. They are synthesized by most liver cells as well as by infiltrating immune cells and their effects depend on their local concentrations at the site of injury (Sahin et al., 2010). Typically, chemokines bind G-protein coupled receptors (GPCRs) and induce signaling in target cells (Bonecchi et al., 2009). Stellate cells express several

chemokines as well as chemokine receptors. HSCs have been shown to secrete CCL2, CCL3, CCL5, CXCL1, CXCL8, CXCL9 and CXCL10 (Holt et al., 2009; Wasmuth et al., 2009; Zaldivar et al., 2010; Marra and Tacke, 2014). Portal fibroblasts which are involved in cholestastis-associated fibrosis are also capable of secreting chemokines (Dranoff and Wells, 2010]. Targeting of chemokines and chemokine receptors in experimental models of fibrosis has been shown to control fibrosis and therefore warrants further investigation as a potential therapeutic anti-fibrosis strategy (Sahin et al., 2010).

In addition to these cytokines and chemokines, several miRNA have been recently identified to be involved in the HSC-immune cell cross-talk (Zhangdi et al., 2019).

Lipid Mediators

Lipid mediators in hepatic fibrosis are mainly studied in the context of NAFLD and NASH (Liangpunsakul and Chalasani, 2019). Several different types of lipid species have been shown to be associated with NAFLD such as saturated free fatty acids (FFA), diacylglycerols, ceramides, lysophosphatidylcholine, eicosanoids and free cholesterol (Feldstein et al., 2003; Caballero et al., 2009; Gorden et al., 2011; Luukkonen et al., 2016). Increased triglyceride accumulation is a hallmark of NAFLD and is associated mainly with hepatic steatosis (Yamaguchi et al., 2007). While triacylglycerol (TAG) accumulation has not been found sufficient for causing insulin resistance, excessive TAG accumulation can increase mechanical pressure on hepatic sinusoids leading to the impairment of hepatic blood flow, and generation of compensatory collateral flow (Wanless and Shiota, 2004). Excessive amounts of free fatty acids can act directly as TLR agonists in the liver or are taken up by the liver, converted into lipotoxic intermediates that activate the JNK, IKK pathway leading to cell injury, inflammation and apoptosis (Yu et al., 2002).

Extracellular Vesicles

Cellular injury to hepatocytes can lead to many outcomes. In addition to hepatocyte cell death, injured and stressed hepatocytes have been shown to release extracellular vesicles (EV) (Ibrahim et al., 2016; Schattenberg and Lee, 2016). EV are nanovesicles released by almost all cell types (Dooyle et al., 2018). They constitute two major size categories, namely plasma membrane derived microvesicles (50–1,000 nm) and endosome-derived exosomes (30–150 nm in diameter) as defined by the International Society for Extracellular Vesicles" (ISEV) and according to the Minimal Information for Studies of Extracellular Vesicles (MISEV) guidelines of 2014 (Lötvall et al., 2014). In fact, lipid overload has been shown to activate hepatocyte signaling through the death receptor 5 (DR5) followed by release of hepatocyte-derived pro-inflammatory EV containing TNF-α (Cazanave et al., 2011). These EV activated macrophage induced inflammation leading to further cellular injury and the development of NASH in experimental mouse models (Cazanave et al., 2011). Administration of EV isolated from high fat diet (HFD) mice into normal fed mice have been shown to result in exacerbation of hepatic steatosis and accumulation of activated myeloid cells in the liver through the release of chemotactic EV (Ibrahim et al., 2016). In addition to hepatocyte-derived EV, extra-hepatic EV have also been implicated in the progression of NAFLD, NASH and associated fibrosis (Srinivas et al., 2021). Due to their ability to carry signal from one cell type to another, they can activate or modulate target cell responses and are therefore an emerging therapeutic targets in NAFLD and NASH.

Autophagy and Unfolded Protein Response

Autophagy in response to endoplasmic reticulum (ER) stress has also been recognized as an activator of HSCs. Under normal circumstances, autophagy is an important regulator of hepatic homeostasis (Mallat et al., 2014). While normally, autophagy is believed to have a protective effect on injured hepatocytes, recent studies demonstrate that ER stress signals activate autophagy and a profibrogenic phenotype in HSCs (Mallat et al., 2014). HSC activation is linked to increased flux in autophagy-related metabolic pathways and inhibition of this process can prevent HSC activation (Thoen et al., 2012). Similarly, there is evidence that the accumulation of misfolded or unfolded proteins in the ER triggering a process called unfolded protein response is a critical feature during early activation of profibrogenic cells such as HSCs (Mannaerts et al., 2019), suggesting that the development of interventions targeting the processes of autophagy or unfolded proteins response might be effective in therapy of hepatic fibrosis.

CELLULAR MEDIATORS OF HEPATIC FIBROSIS

The hallmark of hepatic fibrosis is the increased expression and deposition of ECM compounds. There are different resident and infiltrating cells that can either be activated or produced by progenitors that transform into a phenotype capable to synthesize ECM. Each of these cell types have specific pro-fibrogenic features and expression potential. Other cells invade the inflamed tissue and acquire a matrix-synthesizing phenotype by reprogramming their cell fate (**Figure 6**). In most cases, TGF-β regulated pathways contribute to the acquirement of fibrogenic features. However, this might be due to the fact that several cell types were only recently added to the list of profibrogenic progenitors and relevant signaling pathways still need to be defined. In the following we will discuss how the different cells contribute to hepatic fibrosis.

Hepatic Stellate Cells and Myofibroblasts

HSCs reside in the perisinusoidal space between hepatocytes and the sinusoids (i.e., the space of Disse). In the normal liver, these cells exhibit a quiescent phenotype with the main known function of storing vitamin A. During chronic hepatic disease, these cells progressively lose their vitamin A, become activated and transdifferentiate into fibrogenic MFBs that are supposed to be the central cellular drivers of hepatic fibrosis in experimental and human liver injury (Tsuchida and Friedman, 2017). In this process, the induction of α-SMA is the most reliable marker indicating cellular activation HSC. Fundamental fate tracing experiments in mice have demonstrated that HSCs are the

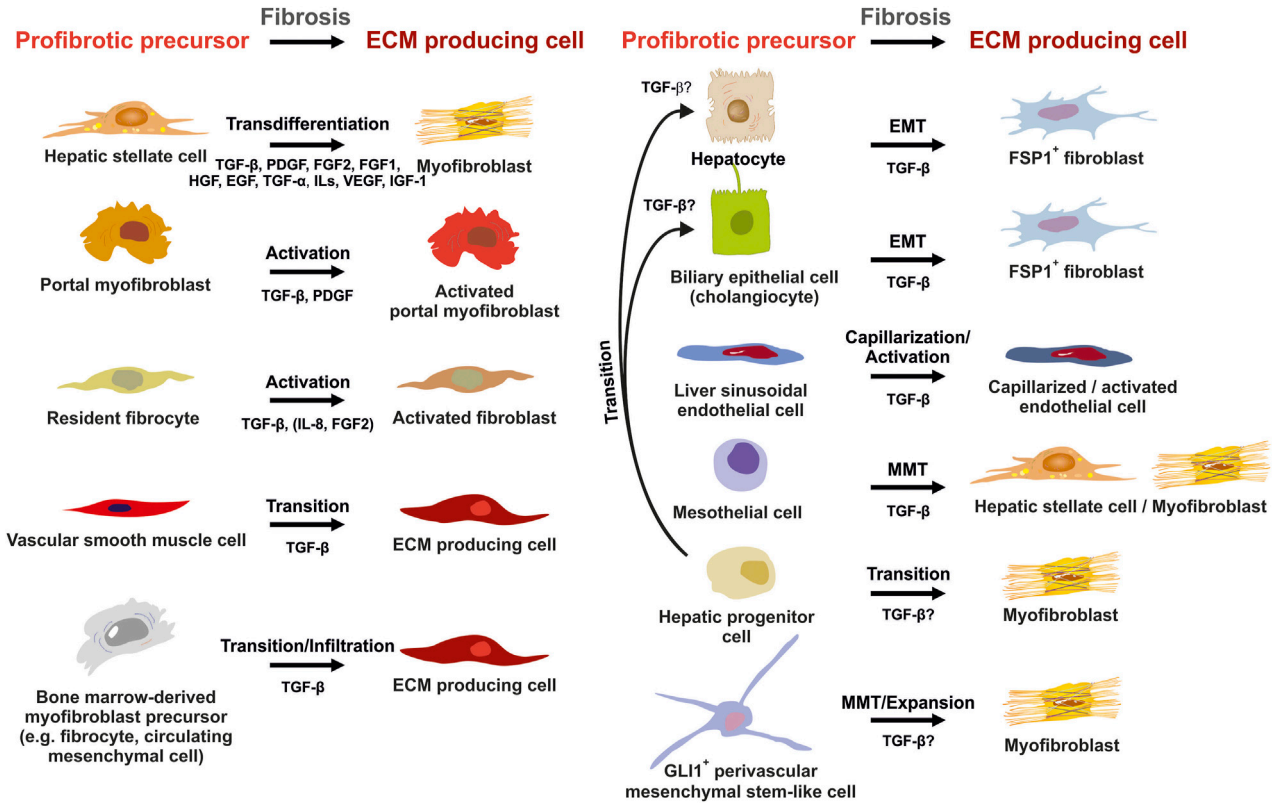


FIGURE 6 | Potential sources of extracellular matrix (ECM) producing cells in liver fibrosis. ECM producing cells during hepatic fibrosis can originate from many sources. Hepatic stellate cells (HSCs) that transdifferenatiate into myofibroblasts (MFBs), activated portal myofibroblasts and activated resident fibroblasts are rich sources of ECM. In addition, several other cell types that become activated, infiltrate the liver, or originate by diverse transition processes are suitable to express large quantities of ECM. Major pathways driving establishment of myofibrogenic features are indicated for each progenitor. Abbreviations used are: ECM, extracellular matrix; EGF, epithelial growth factor; EMT, epithelial-to-mesenchymal transition; FGF1/2, fibroblast growth factor 1/2; GLI1, glioma-associated oncogene homolog 1; HGF, hepatocyte growth factor; IGF-1, insulin growth factor-1; IL, interleukin; MMT, mesothelial-to-mesenchymal transition; PDGF, platelet-derived growth factor; TGF-α/β, transforming growth factor-α/β; VEGF, vascular endothelial growth factor. For details see text.

most important profibrogenic cell type in the liver giving rise to 82–96% of all MFBs in models of toxic, cholestatic and fatty liver disease (Mederacke et al., 2013). HSCs typically express desmin and vimentin, but other markers such as glial fibrillary acidic protein (GFAP), lecithin retinol acyltransferase (LRAT), synemin, platelet-derived growth factor receptor-β (PDGFRβ), p75 neurotrophin receptor peptide (p75NTR), heart- and neural crest derivatives-expressed 2 (HAND2), cytoglobin, and cysteine and glycine-rich protein 2 (CRP2) have been discussed as HSC specific markers within the liver (Weiskirchen et al., 2001; Suzuki et al., 2008; Iwaisako et al., 2014; Kisseleva 2017; Tsuchida and Friedman, 2017). However, the definition of general markers for HSCs is rather complex because reporter microarray analysis, gene mouse models and single cell RNA sequencing have demonstrated the existence of distinct and functionally relevant subsets of resting HSCs and activated MFBs, both *in vivo* and *in vitro* (Magness et al., 2004; D'Ambrosio et al., 2011; 9,; Krenkel et al., 2019). Nevertheless, the expression of α-SMA and collagen type I is significantly increased during progression of hepatic fibrosis confirming the view that MFBs are still most likely the most relevant cell population contributing to hepatic

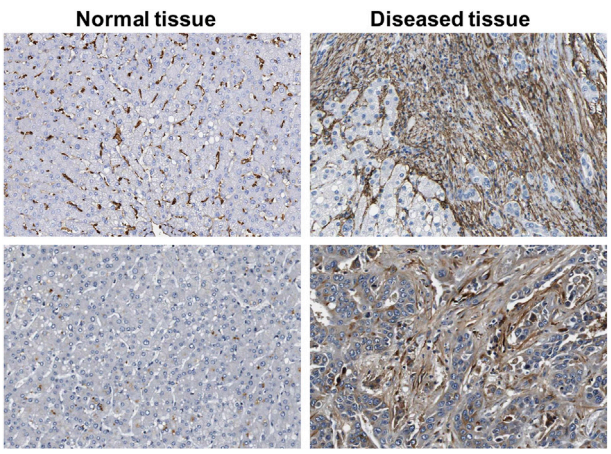


FIGURE 7 | Expression of fibrogenic markers in liver. The figure was compiled using immunohistochemical data from the Human Protein Atlas (www.proteinatlas.org/) (Uhlén et al., 2015). α-smooth muscle actin (α-SMA) and collagen type 1α1 (COL1A1) proteins were stained in normal and diseased livers.

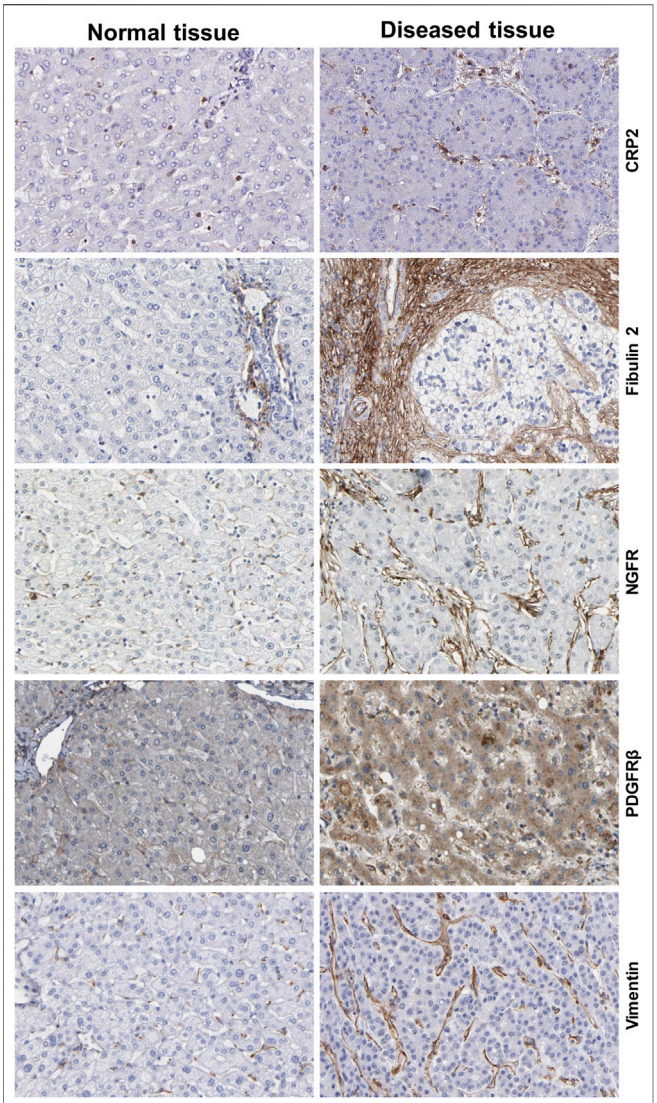


FIGURE 8 | Additional markers of hepatic stellate cells and portal myofibroblasts. The figure was compiled from data deposited from Human Protein Atlas (www.proteinatlas.org/) (Uhlén et al., 2015). Immunohistochemistry of the cysteine and glycine rich protein 2 (CRP2), Fibulin 2, nerve growth factor receptor (NGFR), platelet-derived growth factor-β (PDGFRβ) and Vimentin in normal and diseased liver tissue. Liver damage is associated with increased expression of these profibrogenic markers. Image credit: Human Protein Atlas.

fibrosis (**Figure 7**). In addition, the expression of CRP2, Fibulin 2, NGFR, PDGFRβ, Vimentin and many other genes is often used as markers that become increased expressed during hepatic fibrosis (**Figure 8**).

Recent studies have shown that there exists complex cellular heterogeneity even within activated HSCs that convert into collagen-secreting MFBs. Recent single-cell RNA sequencing (scRNA-seq) studies in a CCl_4-induced hepatic fibrosis model in mice, clearly showed the presence of four sub-populations of MFBs in the fibrotic liver that all express collagen but differentially express chemokines (Krenkel et al., 2019). Similarly, a very recent human liver scRNA-seq study has revealed HSC heterogeneity along the porto-central axis of the healthy liver lobule (Valery et al., 2021). Two major HSC sub-populations were obtained from the healthy human liver lobules. One sub-population (HSC1) expressed high levels of the cell surface proteoglycan glypican 3 (*GPC3*) and the neurotrophic tyrosine kinase receptor type 2 (*NTRK2*) along with other commonly expressed HSC markers, whereas the second sub-population (HSC2) expressed high levels of the genes encoding for dopamine-norepinephrine converting enzyme (*DBH*), hedgehog-interacting protein (*HHIP*), and the G-protein coupled receptors (GPCRs) vasoactive intestinal peptide receptor 1 (*VIPR1*), parathyroid hormone 1 receptor (*PTH1R*), receptor activity-modifying protein 1 (*RAMP1*), endothelin receptor type B (*EDNRB*), and angiotensin receptor 1A (*AGTR1A*) (Valery et al., 2021). In addition, beside the identification of novel quiescent markers such as Quiescin Q6 sulfhydryl oxidase 1 (*QSOX1*) and six-transmembrane epithelial antigen of prostate 4 (*STEAP4*), these scRNA-seq studies have also confirmed well-established HSC marker including the regulator of G protein signaling (*RGS5*), pleiotrophin (*PTN*), nerve growth factor receptor (*NGFR*), lecithin retinol acyltransferase (*LRAT*), fibulin 5 (*FBLN5*), dihydrolipoamide branched-chain transacylase (*DPT*), decorin (*DCN*), cytoglobin (*CYGB*), collectin 11 (*COLEC11*), olfactomedin-like 3 (*OLFML3*), and tropomysosin 2 (*TPM2*), respectively (Valery et al., 2021). All these findings established by scRNA-seq suggests this methodology as an emerging area and promising experimental tool to reveal deeper insights into HSC biology.

Portal Fibroblasts

In the normal liver, they encompass a quiescent phenotype with a spindle-shaped fibroblastic phenotype that surrounds the portal vein to maintain integrity of portal tract. In cholestatic liver injury, portal MFBs are supposed to be a more important source of activated MFBs than HSCs around proliferating bile ducts (Tsuchida and Friedman, 2017). However, in contrast to the well-characterized HSCs/MFBs the biology of these cells is only partially known. Studies on rat portal MFB cell lines and fibrotic mouse livers have shown that typical markers of this profibrogenic cells are elastin, type XV collagen α1, ectonucleoside triphosphate diphosphohydrolase-2 (ENTPD2/CD39L1) and cofilin 1, while these cells are negative for the HSC markers desmin, cytoglobin, and LRAT (Iwaisako et al., 2014; Fausther et al., 2015). However, likewise HSCs, these cells are positive for typical myofibroblastic markers including α-SMA, type I collagen α1, and tissue inhibitor of metalloproteinase-1 (Fausther et al., 2015). Other markers for portal MFBs were identified by immunohistochemistry of fibrotic liver and FACS sorting of liver cell preparations. These include Gremlin 1, Thy1/CD90, Fibulin 2, mesothelin, asporin, and Mucin-16 (Iwaisako et al., 2014; Kisseleva, 2017). Some of them are drastically induced during progression of hepatic fibrosis, while their expression signature might dependent on the hepatic insult analyzed (Iwaisako et al., 2014).

Fibrocytes

Each organ has multiple populations of resident mesenchymal cells capable of producing ECM. In the liver, HSCs and portal fibroblasts are supposed to be the major cell types implicated in the pathogenesis of liver fibrosis. Nevertheless, dependent of the nature of hepatic insult, ECM producing cells may also originate from many other sources. Fibrocytes are defined monocyte-derived spindle-shaped cells having features of both macrophages and fibroblasts (Reilkoff et al., 2011). Animal experimentation using chimeric mice transplanted with donor bone marrow from collagen α1(I)-GFP$^+$ reporter mice has shown that collagen-producing fibrocytes are recruited from the bone marrow to the damage liver tissue when recipient mice were subjected to bile duct ligation (Kisseleva et al., 2006). Moreover, when treated in culture with TGF-β1, these cells differentiated into α-SMA and desmin positive collagen-producing MFBs.

Vascular Smooth Muscle Cells

Vascular smooth muscle cells (VSMCs) are integral components of the blood vessel wall contributing to structural stability and regulating vessel diameter. As such these contractile cells are highly responsive toward vasoactive stimuli and contain a large repertoire of specific contractile proteins facilitating their dynamic phenotype (Metz et al., 2012). In response to injury, VSMCs can shift from a contractile to a synthetic phenotype characterized by increased expression of ECM compounds such as collagen I and III and elevated expression of various non-muscle myosin heavy chain isoforms (Metz et al., 2012). In normal human liver, these cells are positive for α-SMA and smoothelin representing a 59-kD cytoskeletal protein that is found exclusively in contractile smooth muscle cells (Lepreux et al., 2013). During the pathogenesis of advanced human liver fibrosis, the cellular fraction of MFBs positive for both α-SMA and smoothelin expanses to 5–10% suggesting a progressive involvement of these resident cells in MFB recruitment (Lepreux et al., 2013). Comparative transcriptome profiling of endothelial cells and VSMCs from canine vessels revealed an enrichment of expression in genes associated with cytoskeleton composition and actin filament organization including transforming growth factor-β1 (*TGFB1*), collagen type I α1 (*COL1A1*), nephroblastoma overexpressed gene (*NOV*), Tenascin c (TNC), tissue factor pathway inhibitor 2 (*TFPI2*), Tubulin α-4A (*TUBA4A*), Retinol–binding protein (*RBP4*), insulin-like growth factor-binding protein 5 (*IGFBP5*), and Cingulin-like 1 (*CGNL1*) (Oosterhoff et al., 2019). Single cell transcriptomic further showed that VSMC in mouse and human livers can be differentiated from other pro-fibrogenic cells of mesenchymal origin (fibroblasts, HSCs) by their expression of Calponin 1 (*CNN1*) or Myosin heavy chain 11 (*MYH11*) (Dobie et al., 2019).

Bone Marrow-Derived Fibrocytes

The first hints for a unique population of collagen-producing fibrocytes derived from the bone marrow that could participate in the pathogenesis of hepatic fibrosis were established in chimeric mice transplanted with donor bone marrow from collagen α1(I)-GFP$^+$ reporter mice (Kisseleva et al., 2006). In livers of respective mice, a significant increase in GFP$^+$/CD45$^+$ positive myofibroblastic cells was observed when animals were subjected to bile duct ligation, that however, were not positive for the typical HSC markers α-SMA or vimentin underpinning their lymphoid origin (Kisseleva et al., 2006). However, these cells differentiated into α-SMA and desmin positive cells when cultured in the presence of TGF-β1. A relevant functional contribution of fibrocytes to the pathogenesis of hepatic fibrosis was demonstrated in a mouse model in which fibrocytes were specifically depleted utilizing a herpes simplex thymidine kinase/ganciclovir suicide approach in the thioacetamide-induced liver fibrosis model (Hempel et al., 2019). Although the depletion of fibrocytes resulted in reduced deposition of fibrillar collagen, the antifibrotic effect was not accompanied by a reduction of MFBs. In the multidrug resistance gene 2 knockout (*Mdr2*$^{-/-}$) mice spontaneously developing cholestatic fibrosis, fibrocytes only minimally contributed to the deposition of ECM in the injured livers (Nishio et al., 2019). It will now be of fundamental interest, to better define the autocrine and paracrine functions of fibrocytes during initiation and progression of hepatic fibrosis in these and other models.

Hepatocytes

Hepatocytes are specialized epithelial cells making up 80% of the total mass of the liver. They perform numerous vital functions, including protein synthesis, metabolism of lipids and carbohydrates, biotransformation and detoxification of xenobiotics that enter the body. In addition, hepatocytes synthesize and secrete bile and must therefore establish a unique polarity in which apical (canalicular) and basolateral (sinusoidal) plasma membranes are equipped with highly specialized surface proteins, channels, and receptors (Schulze et al., 2019). During liver injury these cells can contribute to fibrogenesis by acquiring myofibroblastic phenotypes/features by undergoing a process termed epithelial-to-mesenchymal transition (EMT) (Zeisberg et al., 2007). During this process the cells downregulate epithelial features, lose their apical-basal polarity, cell-cell adhesion properties and obtain migratory/invasive properties, and acquire mesenchymal characteristics allowing synthesizing ECM compounds (Yang et al., 2020). Lineage-tracing experiments performed in transgenic mice in which liver fibrosis were induced by repeated injections of carbon tetrachloride demonstrated that up to 45% of fibroblast-specific protein 1 (FSP1) positive fibroblasts originated from hepatocytes via EMT (Zeisberg et al., 2007). In line with the concept of EMT, primary mouse hepatocytes transit in culture to FSP1 positive fibroblasts when cultured in the presence of TGF-β1 (Zeisberg et al., 2007). However, the concept that fibrogenic cells capable to express type I collagen can originate *in vivo* from hepatocytes was challenged by other studies (Taura et al., 2010; Xie and Diehl, 2013). It was argued that potential interpretational pitfalls may arise from the fact that FSP1 is not only expressed in subsets of fibroblasts but is also expressed by cells of the myeloid-monocytic lineage (Scholten and Weiskirchen, 2011). However, the evidence for and against EMT for the generation of myofibroblastic cells

from intrahepatic cells is still controversially discussed (Taura et al., 2016; Munker et al., 2017; Chen et al., 2020).

Biliary Epithelial Cells

Similar to hepatocyte it was proposed that biliary epithelial cells (i.e., cholangiocytes) can change their fate and transit to invasive fibroblasts by EMT. In particular, in primary cirrhosis it was demonstrated that bile duct epithelial cells express FSP1 and vimentin as early markers of fibroblasts in the ductular reaction (Robertson et al., 2007). In line, the stimulation of cultured human cholangiocytes with TGF-β induced expression of FSP1 and vimentin suggesting that these cells can contribute significantly to portal tract fibrosis (Rygiel et al., 2008). The resulting cells formed in this localized EMT showed coexpression of both cytokeratin-7 (CK-7) and FSP1 indicating that these cells have the capacity to migrate out of the ductular structure (Rygiel et al., 2008). Several reports suggested that sonic hedgehog signaling promotes EMT by inducing myofibroblast specific genes and repressing epithelial genes during the pathogenesis of chronic biliary injury and NAFLD (Omenetti et al., 2008; Syn et al., 2009). However, bile duct ligation experiments performed in adult mice tagged with a YFP reporter directed under regulatory control of the cholangiocyte marker keratin 19 (K19) showed that cholangiocytes that were positive for YFP revealed no expression of EMT markers α-SMA, desmin, or FSP1 (Scholten et al., 2010).

Hepatic Progenitor Cells

The liver is the only visceral organ that can replace lost or damaged tissue from the remaining tissue in a well-orchestrated program, in which progenitor cells derived from the biliary epithelium transdifferentiate to restore the hepatocyte compartment (Michalopoulos 2013). Therefore, the occurrence of resident hepatic progenitor cells (HPCs) was proposed that should contain a defined cell fraction located in the canal of Hering. The proposed cells should be characterized by a high cellular plasticity and proliferation potential, the ability to differentiate into hepatocytes and cholangiocytes, and to mediate liver repopulation after injury (Li W et al., 2020). However, also the conversion of hepatocytes to progenitor-like cells has been documented *in vitro* (Li W et al., 2020). HPCs isolated from chronically injured liver were shown to have trilineage differentiation potential serving as progenitors for hepatocytes, cholangiocytes and MFBs Sekiya et al., 2016). Although the frequency of MFBs from HPCs was very low, it can be speculated that HPCs can contribute to the MFB pool during hepatic fibrogenesis (Sekiya et al., 2016).

Sinusoidal Endothelial Cells

Liver sinusoidal endothelial cells (LSEC) are a fenestrated cell type without an organized basement membrane that forms the predominant population in the hepatic sinusoid. In normal liver, these cells form a selective barrier between the hepatocytes and blood, possess a high endocytotic capacity allowing them to act as an initial line of defense against invading pathogens, and are critically involved in regulating vascular tone and permeability (Hutchins et al., 2013). Under certain conditions these cells can acquire an active phenotype characterized by swelling and bulging of the cell body combined with enlargement of the Golgi complex, increase of rough endoplasmic reticulum, and formation of hemidesmosome-like structures that are hallmarks of fibroblastic reticulum cells (Bardadin and Desmet, 1985). During liver injury LSEC lose their fenestration, form a continuous basal membrane, and develop inflammatory and fibrotic features, a process referred to as capillarization (Baiocchini et al., 2019). Noteworthy, capillarized LSECs can be an active contributor to the production of a fibrotic environment during fibrogenesis by synthesis of collagen and fibronectin (Natarajan et al., 2017).

Mesothelial Cells

Mesothelial cells are specialized pavement-like cells forming a protective layer of epithelial cells (i.e., the mesothelium) around serous cavities and internal organs. These cells facilitate transport of fluid across these compartments and produce a lubricating fluid that is helpful in protecting the body against infections (Mutsaers 2004). Observations from different animal models and organ systems have shown that the adult mesothelium of mice and humans contains a sub-population of quiescent cells with stem-like properties (Koopmans and Rinkevich, 2018). Upon peritoneal damage and appropriate stimulus, these cells can be triggered to undergo a transition process, termed "mesothelial-to-mesenchymal transition" (MMT). The molecular reprogramming is associated with morphological and functional changes and lead to cells producing ECM compounds and pro-fibrogenic mediators (Koopmans and Rinkevich, 2018). In line, TGF-β1 *in vitro* induced morphologic and functional reformation of differentiated human mesothelial cells to MFBs that become positive for α-SMA (Yang et al., 2003). In regard to liver fibrogenesis, conditional cell lineage tracing in mice confirmed that liver mesothelial cells can be driven by TGF-β to generate both HSCs and MFBs depending on injury signals in the liver (Li et al., 2013). While mesothelial cells preferentially transit into HSCs in biliary fibrosis induced by bile duct ligation, the cells majorly convert into MFBs in carbon tetrachloride-induced fibrosis (Li Y et al., 2016). On the basis of lineage tracing studies, it was supposed that mesothelial cells are triggered by TGF-β to undergo MMT and contribute to the MFB fraction in peritoneal fibrosis, in which up to 16.8% of all MFBs were derived from peritoneal mesothelial cells (Lua et al., 2015).

GLI1 Positive Perivascular Mesenchymal Stem-like Cells

The glioma-associated oncogene homolog 1 (GLI1) belongs to the family of three GLI C_2H_2-Kruppel type transcription factors that contain five zinc finger domains and either activate or repress gene expression by binding to specific consensus DNA sequences (**Figure 9**). Traditionally, GLI proteins are viewed as downstream effectors of the Hedgehog (HH) signaling pathways, but are now also known to be regulated transcriptionally and

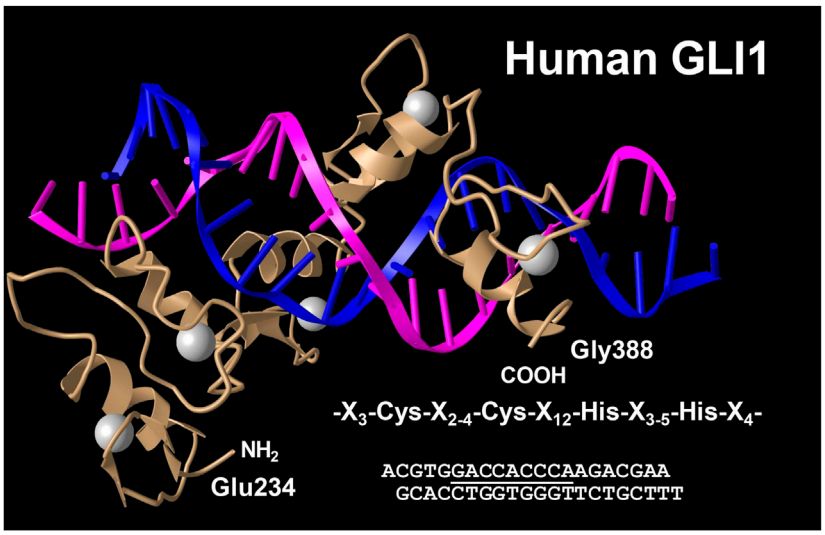


FIGURE 9 | Crystal structure of the five Zn fingers from human GLI1 in complex with a high-affinity DNA binding site. Shown is a complex of a peptide derived from the human GLI1 oncoprotein spanning region Glu 234 to Gly388 with a DNA fragment containing the specific binding site 5′-GACCACCCA-3′ (underlined). Each of the five zinc fingers has a conserved sequence motif that is characterized by the consensus sequence X_3-Cys-X_{2-4}-Cys-X_{12}-His-X_{3-5}-His-X_4 (where X is any acid residue). The structure has been determined at 2.6 Å resolution. Structure coordinates were taken from the PDB Protein Data Bank (access. no. 2GLI). For details see (Pavletich and Pabo 1993).

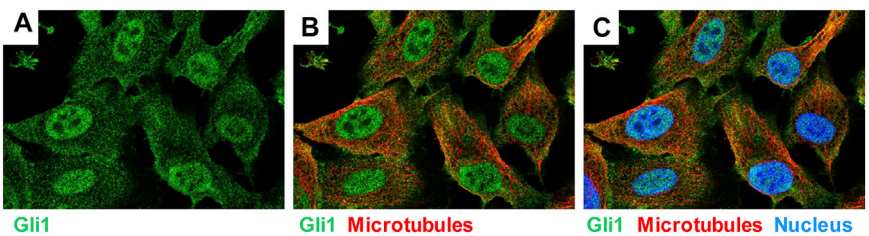


FIGURE 10 | Expression of GLI1 in human bone osteocarcoma cell line U-2 OS. The cell line U-2 OS originating from human mesenchymal tumors express large quantities of GLI1 (*green*), which is localized in the nucleus and the cytoplasm. Microtubuli (*red*) and nucleus (*blue*) are stained by a specific antibody or DAPI. The figure was compiled using immunocytochemical data taken from the Human Protein Atlas v.20 (www.proteinatlas.org/) (Uhlén et al., 2015). They can be found at: https://www.proteinatlas.org/ENSG00000111087-GLI1/cell#img.

post-transcriptionally through non-canonical mechanisms involving RAS-RAF-MEK-ERK and PI3K-AKT-mTOR (Dusek and Hadden, 2021). This zinc finger protein was originally identified as an oncogene that was amplified more than 50-fold and highly expressed in some cases of malignant glioma (Kinzler et al., 1987). GLI1 localize predominantly to the nucleus (**Figure 10**) and bind the 9-base-pair consensus DNA 5′-GACCACCCA-3′ with high affinity (Kinzler and Vogelstein, 1990). It has turned out that the individual GLI proteins play fundamental and distinct roles both in chronic inflammation and cancer. In some organs the lack of HH expression promotes chronic inflammation and tumor formation, while aberrantly activated HH/GLI signaling is also capable to foster tumor growth and simultaneously dampening inflammation and favoring immunosuppression (Grund-Gröschke et al., 2019). Genetic lineage tracing analysis in mice demonstrated that tissue-resident, but not circulating, GLI1 positive mesenchymal-stem-cell-like cells can generate MFBs in kidney, lung, liver, or heart after injury (Kramann et al., 2015). Genetic ablation of GLI1 positive cells abolished bone marrow fibrosis and rescued bone marrow failure (Schneider et al., 2017). More recently it was demonstrated that the pro-fibrogenic activity of osteopontin in promoting HSC activation and ECM deposition during liver fibrogenesis is strongly dependent on GLI1 function (Rao et al., 2019). In the human HSC line LX-2, PAX6 binds to the promoter of the *GLI1* gene, thereby promoting fibrogenic activities and proliferation (Li C. et al., 2020). In the same cell line, GLI1 was further shown to be integrated in a complex network of Wnt/β-catenin, which regulates cellular contraction (Zhang F. et al., 2020). However, the significance of GLI1 positive perivascular mesenchymal stem-like cells for liver fibrogenesis is still unknown. Publicly available

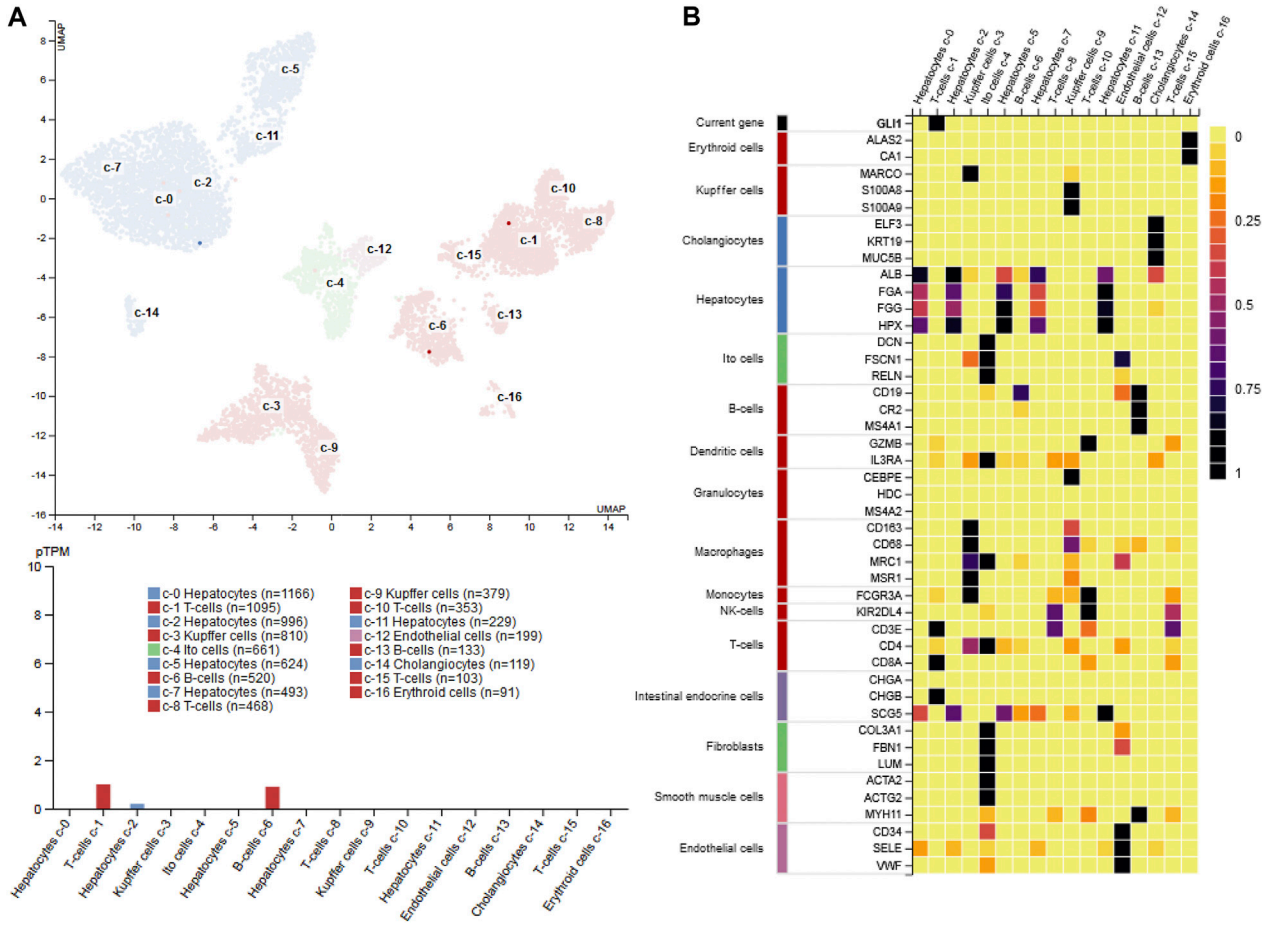


FIGURE 11 | GLI1 expression in liver **(A)** single cell PCR data shows that *GLI1* mRNA expression in normal human liver is rather low (<1 protein-coding transcript per million) and majorly restricted to a subpopulation of T-cells, B-cells and hepatocytes **(B)** Heatmap of marker gene expression in different hepatic cell types. The figure was compiled using expression data from the Human Protein Atlas (www.proteinatlas.org/) (Uhlén et al., 2015). Abbreviations used are: pTPM, protein-coding transcript per million; UMAP, uniform manifold approximation and projection.

data obtained by single cell PCR shows that *GLI1* mRNA expression in normal human liver is rather low (<1 protein-coding transcript per million) and restricted to some immune cells and hepatocytes (**Figure 11**), while not found in smooth muscle cells or endothelial cells. It will be now of particular interest to document the existence of respective cells and to clarify how these cells are triggered during hepatic fibrogenesis to generate the proposed large fraction of MFBs.

MECHANISMS OF FIBROSIS REGRESSION AND RESOLUTION

Liver fibrosis is potentially reversible (Ramachandran and Iredale, 2012). Patients undergoing treatment for HCV infection clearly demonstrate reversal of fibrosis upon complete HCV negativity (Brenner, 2013). However, liver fibrosis is reversible only in the early stages (Fibrosis grades 1 and 2). Once fibrosis crosses a threshold (Fibrosis grades 3 and 4), the fibrogenic type I collagen forms crosslinks and is typically associated with cell damage and inflammation, making it harder to recover (Brenner, 2013). Two events are critical in directing the liver pro-fibrogenic phenotype to recovery - (i) Apoptosis of MFBs in the liver and, (ii) switching of macrophages from a pro-inflammatory to a tissue resolution phenotype (Pellicoro et al., 2014). During liver fibrogenesis, the ECM is extensively remodeled leading to accumulation of proteases such as matrix metalloproteinases (MMP) as well as collagenases (Iredale, 2008). However, at the same time, fibrotic liver also accumulates myofibroblast-derived tissue inhibitor of metalloproteinase 1 (TIMP1) which prevents the action of MMPs and ECM turnover (Iredale et al., 1996). As a result, there is an accumulation of collagen and pro-fibrotic ECM. Over a period of time, accumulation of a large number of crosslinked collagen and elastin fibers lead to sequestering of crosslinked fibers within the tissue beds, making them inaccessible for proteolytic digestion (Issa et al., 2004). As the cross links increase, the exposed fibers also become less susceptible to digestion themselves (Issa et al., 2004). The hallmark of a recovering

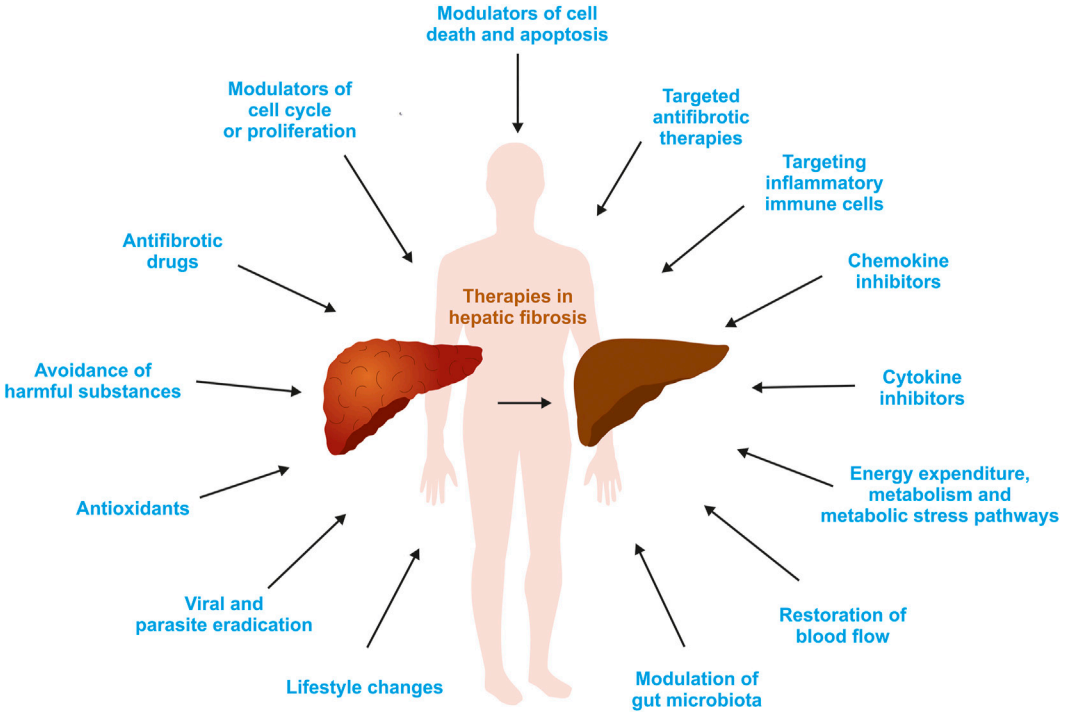


FIGURE 12 | Potential therapeutic options for liver fibrosis. Based on the fact that hepatic fibrosis is driven by different mediators and pathways, there is a plenitude of possibilities to interfere with this process. For more details see text or refer to (Schon et al., 2016; Weiskirchen 2016; Tacke and Weiskirchen, 2018; Weiskirchen et al., 2018; Levada et al., 2019).

fibrotic liver is the termination of cellular injury followed by the absence or disappearance of hepatic MFBs (Kisseleva et al., 2012). Studies show that at least 50% of the activated MFBs revert to less fibrogenic or quiescent HSCs (Kisseleva et al., 2012; Troeger et al., 2012). The role of macrophages and the trigger of switching from pro-inflammatory to pro-resolution macrophages during fibrosis is incompletely understood. However, macrophages in the resolving fibrotic liver have been shown to secrete increased levels of MMPs thereby contributing to ECM reorganization (Li H et al., 2016). Therefore, polarization of macrophages provides a therapeutic opportunity for the resolution of liver fibrosis.

THERAPY OF HEPATIC FIBROSIS

Although numerous drugs have beneficial anti-fibrotic effects *in vitro* and in animal models, none of these drugs has been ultimately shown to be efficacious in the clinic. Moreover, general anti-fibrotic therapies are not available. Instead, clinicians and professional associations have developed some clinical practice guidelines and recommendations for etiology-specific interventions. Most noticed are the guidelines published by the American Association for the Study of Liver Diseases (AASLD) and the European Association for the Study of Liver Diseases (EASL) that both develop evidence-based clinical practice guidelines on a regularly basis. These 'state-of-the-art' recommendations are intended to assist physicians and other healthcare providers in the diagnosis and management of a specific etiology of liver injury. As such they typically contain information about disease definition, epidemiology, etiology, risk factors, incidence, recommended tests and examinations for disease detection, screening tools, preferred staging and grading systems, therapy strategies, surveillance tests/intervals, therapy outcome measures, prevention strategies, ongoing trials, and much other supporting information. From the view of basic scientists some generally applicable concepts should be effective in the therapy of hepatic fibrosis. These include the withdrawal of injurious stimuli, inhibition of ongoing hepatic damage, deactivation and elimination of ECM-producing cells, removal of superfluous scar tissue, counteracting biological mediators driving hepatic inflammation and fibrogenesis, and restoring the normal liver architecture (**Figure 12**). scRNA-seq and genetic cell tracing experiments have shown that the termination of hepatic fibrosis is associated with a reversal of HSC activation and expression of different inactivation markers (Troeger et al., 2012). However, reverted HSCs remain in a primed state maintaining a higher responsiveness toward fibrogenic stimuli.

Arrest of Chronic Liver Damage by Avoiding or Eradication of Harmful Substances and Replacement Therapies

As outlined, there are many genetic and environmental factors that can cause hepatic fibrosis. Most frequent inherited disorders

associated with acute and chronic liver disease include hemochromatosis, Wilson disease, α1-antitrypsin deficiency, and cystic fibrosis. In the case of hemochromatosis, excessive iron can be removed from the body by regularly phlebotomy, or alternatively iron chelating therapy (Murphree et al., 2020). Wilson disease occurring as a consequence of impaired biliary copper excretion can be effectively treated with the chelators D-Penicillamine and trientine or by application of zinc preparations interfering with the gastrointestinal uptake of copper (Stremmel and Weiskirchen, 2021). Shortage of α1-antitrypsin in the lung can be partially overcome by intravenous replacement therapy, while this therapy is not appropriate to people with liver disease. In respective patients, there is emphasis on efforts to prevent progression of related liver injury by reducing of modifiable risk factors (overweight, tobacco, alcohol, non-steroidal anti-inflammatory drugs) or finally liver transplantation that still remains the sole curative option (Narayanan and Mistry, 2020). In cystic fibrosis resulting of mutations in the gene encoding the cystic fibrosis transmembrane conductance regulator (CFTR) the application of Ursodeoxycholic acid (UDCA) is the mainstay of therapy. This secondary bile acid is supposed to stimulate bile acid secretion, but its efficacy is therapy of cystic fibrosis-related liver disease is controversially discussed (Staufer, 2020). In addition, a large number of compounds restoring CFTR protein function (i.e., CFTR modulators) are actually under close investigation (Staufer, 2020).

In regard to alcoholic liver disease, the abstinence from drinking alcoholic beverages is quite the cornerstone of therapy. However, several studies have shown that glucocorticoids given alone or in combinations with antioxidants are beneficial to lower hepatic inflammation (Mitchell et al., 2020). In addition, drugs able to prevent the development of steatosis, modulate innate immune responses, targeting the microbiome, or stimulating liver regeneration are investigated in many clinical studies (Mitchell et al., 2020).

Antiviral treatment strategies are suitable to reduce the burden of chronic hepatitis B (HBV), hepatitis C virus (HCV), or hepatitis D (HDV) infections. In particular, the introduction of direct antiviral drugs offers nowadays a very competent way to obtain viral clearance with sustained virologic response rates greater than 95% (Do and Reau, 2020). Rigorous infant prophylaxis, early childhood and adult immunization programs as well as vaccination of high-risk individuals significantly contribute to prevalence of HBV transmission worldwide (Polaris Observatory Collaborators, 2018). Established interferon-based therapies are established and new encouraging drugs are currently under clinical evaluation for the treatment of HDV (Koh et al., 2019).

Autoimmune diseases of the liver typically affect either the liver parenchyma, which is termed autoimmune hepatitis, or alternatively the bile ducts provoking primary biliary cholangitis (PBC) or primary sclerosing cholangitis (PSC) (Weiskirchen, 2016). Immunosuppressive treatment consisting of either corticosteroids alone or in combination with the purine analog azathioprine is the recommended first-line medical treatment in autoimmune hepatitis (Tanaka, 2020).

There are some pharmacological approaches available for the management of NAFLD and NASH, but an ultimate therapy is still missing and actual guidelines presently only recommend significant changes in lifestyle and nutrition, in particular weight loss and physical exercise (Drescher et al., 2019). Nevertheless, there are several drugs currently at various stages of development for the therapy of NASH, possessing anti-inflammatory activity, improve insulin resistance, reduce *de novo* lipogenesis, modulate lipid transport or oxidation, or evolve anti-apoptotic effects (Tacke and Weiskirchen, 2018).

Liver fibrosis resulting from Schistosomiasis (*S. mansoni* and *S. japonicum*) are presently treated with the pyrazinoisoquinoline derivative praziquantel, while several vaccines that are urgently needed are currently at differing phases of clinical development and not yet been accepted for public use (McManus et al., 2020).

Antioxidants

As discussed, elevated quantities of reactive oxygen species (ROS) are key drivers of hepatic inflammation and fibrosis. Under normal condition, ROS are required for many important signaling processes, impact cell proliferation, contribute to apoptotic pathways, and help phagocytic active cells to destroy and eliminate pathogens (Luangmonkong et al., 2018). They induce apoptosis and necrosis of parenchymal cells (i.e., hepatocytes) resulting in the release of harmful mediators (e.g., TGF-β, TNF-α), stimulate Kupffer cells to produce profibrogenic mediators, prompt recruitment of circulating inflammatory cells into the liver, and contribute to the activation of HSCs (Weiskirchen, 2016). Therefore, an imbalance between ROS production and degradation play an important role in the pathogenesis of liver fibrosis. Consequently, therapeutic interventions targeting elevated cellular oxidative stress should be beneficial for the treatment of liver fibrosis (Luangmonkong et al., 2018). In regard to therapy of liver fibrosis, many ROS inhibitors have been tested successfully in pre-clinical animal models (Weiskirchen, 2016). Most of these antioxidants are scavengers that unspecific alleviate ROS accumulation, while others are more selective by targeting defined molecular pathways involved in ROS generation. In particular, inhibitors of mitochondrial dysfunction (Coenenzyme !0, Mitoquinone mesylate, NIM811), endoplasmic stress (Glycerol phylbutyrate), NADPH oxidases (GKT137831, Docosahexaenoic acid, losartan), and Toll-like receptors (Curcumin, Quercetin, various probiotics, Bicyclol) have attracted widespread attention in recent years (Luangmonkong et al., 2018). Most promising are drugs that interfere with the activity of different NADPH oxidase (NOX) subtypes. In experimental models, both the deficiency of NOX1 or NOX4 as well as the application of the dual NOX1/4 inhibitor GKT137831 was effective in attenuation of carbon tetrachloride-induced liver fibrosis (Lan et al., 2015). Likewise, the NOX inhibitor apocynin was therapeutically

effective in preventing lipopolysaccharide/D-galactosamine-induced acute liver injury (Peng et al., 2020).

Inhibitors of Cytokine Signaling

Several cytokines play a crucial role in the pathogenesis of hepatic fibrosis. Commonly, they bind to specific cell-surface exposed receptors, thereby initiating intracellular signaling cascades ending in modified gene expression. Research performed during the last decades has identified a number of different cytokines relevant during the pathogenesis of hepatic fibrosis. Representative cytokines most prominent involved in disease initiation or progression are members belonging to the family of TGF-β, platelet-derived growth factors (PDGF), vascular endothelial growth factors (VEGF), interleukins (IL), fibroblast growth factors (FGF), interferons (IFN), insulin-like growth factors (IGF), TNF-α, epidermal growth factor (EGF), nerve growth factor (NGF), and hepatocyte growth factor (HGF) (Weiskirchen 2016). Their specific activities were comprehensively explored in many *in vitro* and *in vivo* models of hepatic fibrosis. However, proposed therapies by interfering with cytokine activities using small interfering RNAs, antisense oligonucleotides, aptamers, soluble receptors, scavenger molecules, therapeutic antibodies, or other biological agents have not been translated to the clinics yet (Borkham-Kamphorst and Weiskirchen, 2016; Weiskirchen, 2016; Schuppan et al., 2018).

Inhibitions of Chemokine Signaling

Chemokines are critical immunomodulatory mediators acting in humans through 20 different G-protein-coupled transmembrane receptors. They typically consists of 75–125 amino acids, share a similar tertiary structure, and based on the number and position of cysteine residues can be systematically categorized into four distinct subfamilies, namely CC, CXC, CX_3C, and XC followed by the letter L (standing for 'ligand') and a consecutive number indicating their temporal isolation (Hughes and Nibbs, 2018). The individual ligands and their cognate receptors (i.e., CCR, CXCR, CX_3CR, XCR) form an enormously complex network playing pivotal roles. By far the most studied functions are the control of cell recruitment, inflammation, wound healing, lymphoid trafficking, angiogenesis, and metastasis. For the formation of liver disease, there is now ample evidence that chemokines and their receptors have fundamental importance in both progression and regression of hepatic fibrosis (Marra and Tacke, 2014). Therefore, strategies for inhibiting common or individual chemokine activities are presently intensively investigated. Prototypically, the dual specific CC motif chemokine receptor 2/5 (CCR2/CCR5) antagonist cenicriviroc has been experimentally and clinically shown to block fat accumulation, Kupffer cell activation, monocyte recruitment, HSC activation, and fibrosis (Friedman et al., 2018; Krenkel et al., 2018; Ambade et al., 2019).

Other Anti-fibrotic Therapy Strategies

Besides the elimination of pathogenic causes, usage of replacement therapies, usage of antioxidants, or therapies targeting cytokine or chemokine activities, there are numerous other possibilities to interfere with hepatic fibrosis. In the past, many other drugs or herbal supplements or vitamins were experimentally tested in pre-clinical models of hepatic fibrosis (Weiskirchen, 2016). They act by inducing apoptosis, autophagy or senescence in ECM-producing cells, interfere with pro-fibrogenic target molecules, modulate cell cycle or proliferation synthesis, act hepatoprotective, or generally interfere with gene expression, replication, mitosis or meiosis. However, their efficacy was only successfully proven yet in experimental disease models. Clinical application is hindered in most cases because effective strategies that allow targeting these drugs to fibrogenic effector cells are not available (Schuppan et al., 2018). Other experimental approaches have identified the lysyl oxidase-like 2 (LOXL2) encoding an extracellular copper-dependent amine oxidase catalyzing the covalent cross-linking of collagen and elastin as a promising drug target (Khurana et al., 2021). In two experimental models of hepatic fibrogenesis, the selective LOXL2/3 inhibitor PXS-5153A was shown to dose-dependently diminish collagen content, thereby reducing disease severity and improve liver function (Schilter et al., 2019). In line, the preventive treatment with and anti-LOXL2 antibody was able to prevent ongoing experimental hepatic fibrosis (Ikenaga et al., 2017). Similarly, targeting Galectin-3 representing a 30 kDa protein with important functions in cell-cell adhesion, cell-matrix interaction, angiogenesis, macrophage activation, inflammation, and collagen synthesis has been identified as a suitable drug candidate.

Presently, there is much hope that engineered nanoparticles, magnetic-assisted drug delivery techniques, or therapeutic effective transgenes expressed under fibrosis-related promoters can be optimized in the near future to better target individual fibrogenic cell subpopulations (Herrmann et al., 2004; Schon et al., 2016; Levada et al., 2019).

CONCLUSION

Genetic disorders, alcohol abuse, drugs, cholestasis, metabolic disorders, chronic viral hepatitis, parasitic infections and several cryptogenic causes are major causes that provoke liver fibrosis. During this progressive process accumulation of ECM, disruption of the lobular structure, and progressive deterioration of hepatocellular function lead to fatal complications. In particular, the exuberant collagen deposition is one hallmark of fibrogenesis. Work from the last decades have identified a number of different resident and infiltrating cells that can either be activated or transform into a phenotype capable to synthesize ECM. In addition, cell- and animal-based experiments, clinical studies and complex integrated bioinformatics analysis have unraveled soluble mediators, molecular pathways, and pro-fibrogenic genes that are key drivers in the pathogenesis of hepatic disease. However, despite the important progress, there are currently no approved anti-fibrotic drugs that have been ultimately shown to be efficacious in the clinic. Presently, clinical

practice guidelines are only etiology-specific. They intend to optimize patient care by withdrawal of injurious stimuli, consumption of antioxidant acting compounds, and lifestyle interventions including healthy food, exercised and controlled weight loss. Nevertheless, many experimental studies and clinical trials are currently being conducted to test drugs targeting more specifically inflammation, the cellular activation process, or the activity of inflammatory or fibrotic-acting cytokines or chemokines. There is hope that these compounds will be of fundamental importance in future treatments aiming at impeding or reversing the fibrogenic process.

AUTHOR CONTRIBUTIONS

All authors listed have made a substantial, direct, and intellectual contribution to the work and approved it for publication.

FUNDING

RW is supported by Grants from the German Research Foundation (WE2554/13–1, WE2554/15–1). The funder had no role in the design of the study, interpretation of data or in the decision to publish the results.

REFERENCES

Acharya, P., Garg, M., Kumar, P., Munjal, A., and Raja, K. D. (2017). Host-Parasite Interactions in Human Malaria: Clinical Implications of Basic Research. *Front. Microbiol.* 8, 889. doi:10.3389/fmicb.2017.00889

Amanatidou, A. I., and Dedoussis, G. V. (2021). Bioinformatics Analysis of the NAFLD Interactome: Revealing Candidate Biomarkers of Non-alcoholic Fatty Liver Disease. *Comput. Biol. Med.* 131. 104243. doi:10.1101/2020.12.01.406215

Ambade, A., Lowe, P., Kodys, K., Catalano, D., Gyongyosi, B., Cho, Y., et al. (2019). Pharmacological Inhibition of CCR2/5 Signaling Prevents and Reverses Alcohol-Induced Liver Damage, Steatosis, and Inflammation in Mice. *Hepatology* 69 (3), 1105–1121. doi:10.1002/hep.30249

Andrade, Z. A., Guerret, S., and Fernandes, A. L. (1999). Myofibroblasts in Schistosomal Portal Fibrosis of Man. *Mem. Inst. Oswaldo Cruz* 94 (1), 87–93. doi:10.1590/s0074-02761999000100018

Andrade, Z. A. (2004). Schistosomal Hepatopathy. *Mem. Inst. Oswaldo Cruz* 99 (5 Suppl. 1), 51–57. doi:10.1590/s0074-02762004000900009

Andrade, Z. A. (2009). Schistosomiasis and Liver Fibrosis. *Parasite Immunol.* 31 (11), 656–663. doi:10.1111/j.1365-3024.2009.01157.x

Anstee, Q. M., Darlay, R., Cockell, S., Meroni, M., Govaere, O., Tiniakos, D., et al. (2020). Genome-wide Association Study of Non-alcoholic Fatty Liver and Steatohepatitis in a Histologically Characterised Cohort☆. *J. Hepatol.* 73 (3), 505–515. doi:10.1016/j.jhep.2020.04.003

Baiocchini, A., Del Nonno, F., Taibi, C., Visco-Comandini, U., D'Offizi, G., Piacentini, M., et al. Liver Sinusoidal Endothelial Cells (LSECs) Modifications in Patients with Chronic Hepatitis C. *Sci. Rep.* 2019;9(1):8760. doi:10.1038/s41598-019-45114-1

Bardadin, K. A., and Desmet, V. J. (1985). Ultrastructural Observations on Sinusoidal Endothelial Cells in Chronic Active Hepatitis. *Histopathology* 9 (2), 171–181. doi:10.1111/j.1365-2559.1985.tb02433.x

Bataller, R., and Brenner, D. A. (2005). Liver Fibrosis. *J. Clin. Invest.* 115 (2), 209–218. doi:10.1172/JCI24282

Bataller, R., Paik, Y.-h., Lindquist, J. N., Lemasters, J. J., and Brenner, D. A. (2004). Hepatitis C Virus Core and Nonstructural Proteins Induce Fibrogenic Effects in Hepatic Stellate Cells. *Gastroenterology* 126 (2), 529–540. doi:10.1053/j.gastro.2003.11.018

Berg, J. M., Tymoczko, J. L., and Stryer, L. (2002). Section 30.5, Ethanol Alters Energy Metabolism in the Liver. *Biochemistry*. 5th edition. New York: W. H. Freeman. Available at: https://www.ncbi.nlm.nih.gov/books/NBK22524/ (Accessed February 23, 2021).

Berntsen, N. L., Klingenberg, O., Juran, B. D., Benito de Valle, M., Lindkvist, B., Lazaridis, K. N., et al. (2015). Association between HLA Haplotypes and Increased Serum Levels of IgG4 in Patients with Primary Sclerosing Cholangitis. *Gastroenterology* 148 (5), 924–927. doi:10.1053/j.gastro.2015.01.041

Bertinato, J., and L'Abbé, M. R. (2003). Copper Modulates the Degradation of Copper Chaperone for Cu,Zn Superoxide Dismutase by the 26 S Proteosome. *J. Biol. Chem.* 278 (37), 35071–35078. doi:10.1074/jbc.m302242200

Bolognesi, M., Di Pascoli, M., Verardo, A., and Gatta, A. (2014). Splanchnic Vasodilation and Hyperdynamic Circulatory Syndrome in Cirrhosis. *Wjg* 20 (10), 2555–2563. doi:10.3748/wjg.v20.i10.2555

Bonecchi, R., Galliera, E., Borroni, E. M., Corsi, M. M., Locati, M., and Mantovani, A. (2009). Chemokines and Chemokine Receptors: an Overview. *Front. Biosci.* 14, 540–551. doi:10.2741/3261

Borkham-Kamphorst, E., and Weiskirchen, R. (2016). The PDGF System and its Antagonists in Liver Fibrosis. *Cytokine Growth Factor. Rev.* 28, 53–61. doi:10.1016/j.cytogfr.2015.10.002

Bosch, J. (2007). Vascular Deterioration in Cirrhosis. *J. Clin. Gastroenterol.* 41 (Suppl. 3), S247–S253. doi:10.1097/MCG.0b013e3181572357

Brenner, D. A. (2013). Reversibility of Liver Fibrosis. *Gastroenterol. Hepatol. (N Y)* 9 (11), 737–739. doi:10.1007/0-387-26476-0_12

Broomé, U., Lindberg, G., and Löfberg, R. (1992). Primary Sclerosing Cholangitis in Ulcerative Colitis-A Risk Factor for the Development of Dysplasia and DNA Aneuploidy?. *Gastroenterology* 102 (6), 1877–1880. doi:10.1016/0016-5085(92)90308-l

Bruschi, F. V., Claudel, T., Tardelli, M., Caligiuri, A., Stulnig, T. M., Marra, F., et al. (2017). The PNPLA3 I148M Variant Modulates the Fibrogenic Phenotype of Human Hepatic Stellate Cells. *Hepatology* 65 (6), 1875–1890. doi:10.1002/hep.29041

Buzzetti, E., Pinzani, M., and Tsochatzis, E. A. (2016). The Multiple-Hit Pathogenesis of Non-alcoholic Fatty Liver Disease (NAFLD). *Metabolism* 65 (8), 1038–1048. doi:10.1016/j.metabol.2015.12.012

Caballero, F., Fernández, A., De Lacy, A. M., Fernández-Checa, J. C., Caballería, J., and García-Ruiz, C. (2009). Enhanced Free Cholesterol, SREBP-2 and StAR Expression in Human NASH. *J. Hepatol.* 50 (4), 789–796. doi:10.1016/j.jhep.2008.12.016

Caldwell, S. (2010). Cryptogenic Cirrhosis: what Are We Missing?. *Curr. Gastroenterol. Rep.* 12 (1), 40–48. doi:10.1007/s11894-009-0082-7

Cazanave, S. C., Mott, J. L., Bronk, S. F., Werneburg, N. W., Fingas, C. D., Meng, X. W., et al. (2011). Death Receptor 5 Signaling Promotes Hepatocyte Lipoapoptosis. *J. Biol. Chem.* 286 (45), 39336–39348. doi:10.1074/jbc.M111.280420

Chen, K., Ma, J., Jia, X., Ai, W., Ma, Z., and Pan, Q. (2019). Advancing the Understanding of NAFLD to Hepatocellular Carcinoma Development: From Experimental Models to Humans. *Biochim. Biophys. Acta (Bba) - Rev. Cancer* 1871 (1), 117–125. doi:10.1016/j.bbcan.2018.11.005C

Chen, W., Chang, B., Li, L., and Chan, L. (2010). Patatin-like Phospholipase Domain-Containing 3/adiponutrin Deficiency in Mice Is Not Associated with Fatty Liver Disease. *Hepatology* 52 (3), 1134–1142. doi:10.1002/hep.23812

Chen, Y., Fan, Y., Guo, D.-y., Xu, B., Shi, X.-y., Li, J.-t., et al. (2020). Study on the Relationship between Hepatic Fibrosis and Epithelial-Mesenchymal Transition in Intrahepatic Cells. *Biomed. Pharmacother.* 129, 110413. doi:10.1016/j.biopha.2020.110413

Chevillard, C., Moukoko, C. E., Elwali, N.-E. M. A., Bream, J. H., Kouriba, B., Argiro, L., et al. (2003). IFN-γ Polymorphisms (IFN-γ +2109 and IFN-γ +3810) Are Associated with Severe Hepatic Fibrosis in Human Hepatic Schistosomiasis (*Schistosoma Mansoni*). *J. Immunol.* 171 (10), 5596–5601. doi:10.4049/jimmunol.171.10.5596

D'Ambrosio, D. N., Walewski, J. L., Clugston, R. D., Berk, P. D., Rippe, R. A., and Blaner, W. S. (2011). Distinct Populations of Hepatic Stellate Cells in the Mouse Liver Have Different Capacities for Retinoid and Lipid Storage. *PLoS One* 6 (9), e24993. doi:10.1371/journal.pone.0024993

Dessein, H., Duflot, N., Romano, A., Opio, C., Pereira, V., Mola, C., et al. (2020). Genetic Algorithms Identify Individuals with High Risk of Severe Liver Disease Caused by Schistosomes. *Hum. Genet.* 139 (6-7), 821–831. doi:10.1007/s00439-020-02160-4

Ding, Y., Sun, Z., Zhang, S., Chen, Y., Zhou, B., Li, G., et al. (2020). Down-regulation of Long Non-coding RNA LINC01554 in Hepatocellular Cancer and its Clinical Significance. *J. Cancer* 11 (11), 3369–3374. doi:10.7150/jca.40512

DiPaola, F. W., and Fontana, R. J. (2018). "Drug-induced Liver Injury," in *Sherlock's Diseases of the Liver and Biliary System*. Editors J. S. Dooley, A. S. F. Lok, G. Garcia-Tsao, et al. (Hoboken, NJ: John Wiley & Sons), 468–493. doi:10.1002/9781119237662.ch24

Do, A., and Reau, N. S. (2020). Chronic Viral Hepatitis: Current Management and Future Directions. *Hepatol. Commun.* 4 (3), 329–341. doi:10.1002/hep4.1480

Dobie, R., Wilson-Kanamori, J. R., Henderson, B. E. P., Smith, J. R., Matchett, K. P., Portman, J. R., et al. (2019). Single-cell Transcriptomics Uncovers Zonation of Function in the Mesenchyme during Liver Fibrosis. *Cel Rep.* 29 (7), 1832–1847. doi:10.1016/j.celrep.2019.10.024

Dong, X. C. (2019). PNPLA3-A Potential Therapeutic Target for Personalized Treatment of Chronic Liver Disease. *Front. Med.* 6, 304. doi:10.3389/fmed.2019.00304

Dooley, J. S., Lok, A. S. F., and Garcia-Tsaqo, B. (2018). in *Sherlock's Diseases of the Liver and Biliary System*. Editors J. S. Dooley, A. S. F. Lok, B. Garcia-Tsaqo, and M. Pinzani. Thirteenth edition (Berlin: Springer).

Dranoff, J. A., and Wells, R. G. (2010). Portal Fibroblasts: Underappreciated Mediators of Biliary Fibrosis. *Hepatology* 51 (4), 1438–1444. doi:10.1002/hep.23405

Drescher, H., Weiskirchen, S., and Weiskirchen, R. (2019). Current Status in Testing for Nonalcoholic Fatty Liver Disease (NAFLD) and Nonalcoholic Steatohepatitis (NASH). *Cells* 8 (8), 845. doi:10.3390/cells8080845

Dunn, M. A. Parasitic Diseases. In: *Schiff's Diseases of the Liver* 11th Edition (2011). Chapter 39. pp. 1017–1033. ISBN: 9780470654682. doi:10.1002/9781119950509.ch39

Duseja, A. (2010). Nonalcoholic Fatty Liver Disease in India - a Lot Done, yet More Required!. *Indian J. Gastroenterol.* 29 (6), 217–225. doi:10.1007/s12664-010-0069-1

Dusek, C. O., and Hadden, M. K. (2021). Targeting the GLI Family of Transcription Factors for the Development of Anti-cancer Drugs. *Expert Opin. Drug Discov.* 16 (3), 289–302. doi:10.1080/17460441.2021.1832078

Dyson, J. K., Anstee, Q. M., and McPherson, S. (2014). Non-alcoholic Fatty Liver Disease: a Practical Approach to Diagnosis and Staging. *Frontline Gastroenterol.* 5 (3), 211–218. doi:10.1136/flgastro-2013-100403

Eriksson, J., Reimert, C. M., Kabatereine, N. B., Kazibwe, F., Ireri, E., Kadzo, H., et al. (2007). The 434(G>C) Polymorphism within the Coding Sequence of Eosinophil Cationic Protein (ECP) Correlates with the Natural Course of *Schistosoma Mansoni* Infection. *Int. J. Parasitol.* 37 (12), 1359–1366. doi:10.1016/j.ijpara.2007.04.001

Fausther, M., Goree, J. R., Lavoie, É. G., Graham, A. L., Sévigny, J., and Dranoff, J. A. (2015). Establishment and Characterization of Rat Portal Myofibroblast Cell Lines. *PLoS One* 10 (3), e0121161. doi:10.1371/journal.pone.0121161

Feldstein, A. E., Canbay, A., Guicciardi, M. E., Higuchi, H., Bronk, S. F., and Gores, G. J. (2003). Diet Associated Hepatic Steatosis Sensitizes to Fas Mediated Liver Injury in Mice. *J. Hepatol.* 39 (6), 978–983. doi:10.1016/s0168-8278(03)00460-4

Figueira, C. P., Carvalhal, D. G. F., Almeida, R. A., Hermida, M. d. E.-R., Touchard, D., Robert, P., et al. (2015). Leishmania Infection Modulates Beta-1 Integrin Activation and Alters the Kinetics of Monocyte Spreading over Fibronectin. *Sci. Rep.* 5, 12862. doi:10.1038/srep12862

Friedman, S. L., Ratziu, V., Harrison, S. A., Abdelmalek, M. F., Aithal, G. P., Caballeria, J., et al. (2018). A Randomized, Placebo-Controlled Trial of Cenicriviroc for Treatment of Nonalcoholic Steatohepatitis with Fibrosis. *Hepatology* 67 (5), 1754–1767. doi:10.1002/hep.29477

Gong, Z., Luo, Q.-Z., Lin, L., Su, Y.-P., Peng, H.-B., Du, K., et al. (2012). Association of MICA Gene Polymorphisms with Liver Fibrosis in Schistosomiasis Patients in the Dongting Lake Region. *Braz. J. Med. Biol. Res.* 45 (3), 222–229. doi:10.1590/s0100-879x2012007500024

Gorden, D. L., Ivanova, P. T., Myers, D. S., McIntyre, J. O., VanSaun, M. N., Wright, J. K., et al. (2011). Increased Diacylglycerols Characterize Hepatic Lipid Changes in Progression of Human Nonalcoholic Fatty Liver Disease; Comparison to a Murine Model. *PLoS One* 6 (8), e22775. doi:10.1371/journal.pone.0022775

Grund-Gröschke, S., Stockmaier, G., and Aberger, F. (2019). Hedgehog/GLI Signaling in Tumor Immunity—New Therapeutic Opportunities and Clinical Implications. *Cell Commun. Signal* 17 (1), 172. doi:10.1186/s12964-019-0459-7

Guarino, M., and Dufour, J.-F. (2019). Nicotinamide and NAFLD: Is There Nothing New under the Sun?. *Metabolites* 9 (9), 180. doi:10.3390/metabo9090180

Gutierrez-Reyes, G., Gutierrez-Ruiz, M. C., and Kershenobich, D. (2007). Liver Fibrosis and Chronic Viral Hepatitis. *Arch. Med. Res.* 38 (6), 644–651. doi:10.1016/j.arcmed.2006.10.001

Hellemans, K., Grinko, I., Rombouts, K., Schuppan, D., and Geerts, A. (1999). All-trans and 9-cis Retinoic Acid Alter Rat Hepatic Stellate Cell Phenotype Differentially. *Gut* 45 (1), 134–142. doi:10.1136/gut.45.1.134

Hellemans, K., Verbuyst, P., Quartier, E., Schuit, F., Rombouts, K., Chandraratna, R. A. S., et al. (2004). Differential Modulation of Rat Hepatic Stellate Phenotype by Natural and Synthetic Retinoids. *Hepatology* 39 (1), 97–108. doi:10.1002/hep.20015

Hempel, F., Roderfeld, M., Savai, R., Sydykov, A., Irungbam, K., Schermuly, R., et al. (2019). Depletion of Bone Marrow-Derived Fibrocytes Attenuates TAA-Induced Liver Fibrosis in Mice. *Cells* 8 (10), 1210. doi:10.3390/cells8101210

Herrmann, J., Arias, M., Van De Leur, E., Gressner, A. M., and Weiskirchen, R. (2004). CSRP2, TIMP-1, and SM22alpha Promoter Fragments Direct Hepatic Stellate Cell-specific Transgene Expression In Vitro, but Not In Vivo. *Liver Int.* 24 (1), 69–79. doi:10.1111/j.1478-3231.2004.00891.x

Hirayama, K., Chen, H., Kikuchi, M., Yin, T., Itoh, M., Gu, X., et al. (1998). Glycine-Valine Dimorphism at the 86th Amino Acid ofHLA-DRB1Influenced the Prognosis of Postschistosomal Hepatic Fibrosis. *J. Infect. Dis.* 177 (6), 1682–1686. doi:10.1086/515299

Holt, A. P., Haughton, E. L., Lalor, P. F., Filer, A., Buckley, C. D., and Adams, D. H. (2009). Liver Myofibroblasts Regulate Infiltration and Positioning of Lymphocytes in Human Liver. *Gastroenterology* 136 (2), 705–714. doi:10.1053/j.gastro.2008.10.020

Hughes, C. E., and Nibbs, R. J. B. (2018). A Guide to Chemokines and Their Receptors. *FEBS J.* 285 (16), 2944–2971. doi:10.1111/febs.14466

Hutchins, N. A., Chung, C.-S., Borgerding, J. N., Ayala, C. A., and Ayala, A. (2013). Kupffer Cells Protect Liver Sinusoidal Endothelial Cells from Fas-dependent Apoptosis in Sepsis by Down-Regulating Gp130. *Am. J. Pathol.* 182 (3), 742–754. doi:10.1016/j.ajpath.2012.11.023

Ibrahim, S. H., Hirsova, P., Tomita, K., Bronk, S. F., Werneburg, N. W., Harrison, S. A., et al. (2016). Mixed Lineage Kinase 3 Mediates Release of C-X-C Motif Ligand 10-bearing Chemotactic Extracellular Vesicles from Lipotoxic Hepatocytes. *Hepatology* 63 (3), 731–744. doi:10.1002/hep.28252

Ikenaga, N., Peng, Z.-W., Vaid, K. A., Liu, S. B., Yoshida, S., Sverdlov, D. Y., et al. (2017). Selective Targeting of Lysyl Oxidase-like 2 (LOXL2) Suppresses Hepatic Fibrosis Progression and Accelerates its Reversal. *Gut* 66 (9), 1697–1708. doi:10.1136/gutjnl-2016-312473

Iredale, J. (2008). Defining Therapeutic Targets for Liver Fibrosis: Exploiting the Biology of Inflammation and Repair. *Pharmacol. Res.* 58 (2), 129–136. doi:10.1016/j.phrs.2008.06.011

Iredale, J. P., Benyon, R. C., Arthur, M. J., Ferris, W. F., Alcolado, R., Winwood, P. J., et al. (1996). Tissue Inhibitor of Metalloproteinase-1 Messenger RNA Expression Is Enhanced Relative to Interstitial Collagenase Messenger RNA in Experimental Liver Injury and Fibrosis. *Hepatology* 24 (1), 176–184. doi:10.1002/hep.510240129

Iredale, J. P., Thompson, A., and Henderson, N. C. (2013). Extracellular Matrix Degradation in Liver Fibrosis: Biochemistry and Regulation. *Biochim. Biophys. Acta (Bba) - Mol. Basis Dis.* 1832 (7), 876–883. doi:10.1016/j.bbadis.2012.11.002

Issa, R., Zhou, X., Constandinou, C. M., Fallowfield, J., Millward-Sadler, H., Gaca, M. D. A., et al. (2004). Spontaneous Recovery from Micronodular Cirrhosis: Evidence for Incomplete Resolution Associated with Matrix Cross-Linking☆. *Gastroenterology* 126 (7), 1795–1808. doi:10.1053/j.gastro.2004.03.009

Iwaisako, K., Jiang, C., Zhang, M., Cong, M., Moore-Morris, T. J., Park, T. J., et al. (2014). Origin of Myofibroblasts in the Fibrotic Liver in Mice. *Proc. Natl. Acad. Sci.* 111 (32), E3297–E3305. doi:10.1073/pnas.1400062111

Iwakiri, Y. (2014). Pathophysiology of Portal Hypertension. *Clin. Liver Dis.* 18 (2), 281–291. doi:10.1016/j.cld.2013.12.001

Jenkins, C. M., Mancuso, D. J., Yan, W., Sims, H. F., Gibson, B., and Gross, R. W. (2004). Identification, Cloning, Expression, and Purification of Three Novel Human Calcium-independent Phospholipase A2 Family Members Possessing Triacylglycerol Lipase and Acylglycerol Transacylase Activities. *J. Biol. Chem.* 279 (47), 48968–48975. doi:10.1074/jbc.M407841200

Junqueira, L. C., and Carneiro, J. (2002). *Basic Histology*. 10th edition Lange International Edition. London: McGraw-Hill/Appleton Lange, 332–343. 9780071378291.

Kalra, S., Vithalani, M., Gulati, G., Kulkarni, C. M., Kadam, Y., Pallivathukkal, J., et al. (2013). Study of Prevalence of Nonalcoholic Fatty Liver Disease (NAFLD) in Type 2 Diabetes Patients in India (SPRINT). *J. Assoc. Physicians India* 61 (7), 448–453. doi:10.21276/iabcr.2016.2.4.11

Kamal, N., Koh, C., Koh, C., Samala, N., Fontana, R. J., Stolz, A., et al. (2019). Asparaginase-induced Hepatotoxicity: Rapid Development of Cholestasis and Hepatic Steatosis. *Hepatol. Int.* 13 (5), 641–648. doi:10.1007/s12072-019-09971-2

Karlsen, T. H., Folseraas, T., Thorburn, D., and Vesterhus, M. (2017). Primary Sclerosing Cholangitis-a Comprehensive Review. *J. Hepatol.* 67 (6), 1298–1323. doi:10.1016/j.jhep.2017.07.022

Khurana, A., Sayed, N., Allawadhi, P., and Weiskirchen, R. (2021). It's All about the Spaces between Cells: Role of Extracellular Matrix in Liver Fibrosis. *Ann. Transl Med.* 11, 39. doi:10.21037/atm-20-2948

Kinzler, K., Bigner, S., Bigner, D., Trent, J., Law, M., O'Brien, S., et al. (1987). Identification of an Amplified, Highly Expressed Gene in a Human Glioma. *Science* 236 (4797), 70–73. doi:10.1126/science.3563490

Kinzler, K. W., and Vogelstein, B. (1990). The GLI Gene Encodes a Nuclear Protein Which Binds Specific Sequences in the Human Genome. *Mol. Cel. Biol.* 10 (2), 634–642. doi:10.1128/mcb.10.2.634

Kisseleva, T., Cong, M., Paik, Y., Scholten, D., Jiang, C., Benner, C., et al. (2012). Myofibroblasts Revert to an Inactive Phenotype during Regression of Liver Fibrosis. *Proc. Natl. Acad. Sci.* 109 (24), 9448–9453. doi:10.1073/pnas.1201840109

Kisseleva, T. (2017). The Origin of Fibrogenic Myofibroblasts in Fibrotic Liver. *Hepatology* 65 (3), 1039–1043. doi:10.1002/hep.28948

Kisseleva, T., Uchinami, H., Feirt, N., Quintana-Bustamante, O., Segovia, J. C., Schwabe, R. F., et al. (2006). Bone Marrow-Derived Fibrocytes Participate in Pathogenesis of Liver Fibrosis. *J. Hepatol.* 45 (3), 429–438. doi:10.1016/j.jhep.2006.04.014

Koh, C., Heller, T., and Glenn, J. S. (2019). Pathogenesis of and New Therapies for Hepatitis D. *Gastroenterology* 156 (2), 461–476. doi:10.1053/j.gastro.2018.09.058

Kong, X., Horiguchi, N., Mori, M., and Gao, B. (2012). Cytokines and STATs in Liver Fibrosis. *Front. Physio.* 3, 69. doi:10.3389/fphys.2012.00069

Koob, G. F., Arends, M. A., and Le Moal, M. (2014), Chapter 6—Alcohol, Editors: G. F. Koob, M. A. Arends, and M. Le. Moal, *Drugs, Addiction, and the Brain*, London: Academic Press, pp. 173–219. ISBN 9780123869371. doi:10.1016/B978-0-12-386937-1.00006-4

Koopmans, T., and Rinkevich, Y. (2018). Mesothelial to Mesenchyme Transition as a Major Developmental and Pathological Player in Trunk Organs and Their Cavities. *Commun. Biol.* 1, 170. doi:10.1038/s42003-018-0180-x

Kramann, R., Schneider, R. K., DiRocco, D. P., Machado, F., Fleig, S., Bondzie, P. A., et al. (2015). Perivascular Gli1+ Progenitors Are Key Contributors to Injury-Induced Organ Fibrosis. *Cell Stem Cell* 16 (1), 51–66. doi:10.1016/j.stem.2014.11.004

Krenkel, O., Hundertmark, J., Ritz, T., Weiskirchen, R., and Tacke, F. (2019). Single Cell RNA Sequencing Identifies Subsets of Hepatic Stellate Cells and Myofibroblasts in Liver Fibrosis. *Cells* 8 (5), 503. doi:10.3390/cells8050503

Krenkel, O., Puengel, T., Govaere, O., Abdallah, A. T., Mossanen, J. C., Kohlhepp, M., et al. (2018). Therapeutic Inhibition of Inflammatory Monocyte Recruitment Reduces Steatohepatitis and Liver Fibrosis. *Hepatology* 67 (4), 1270–1283. doi:10.1002/hep.29544

Lan, T., Kisseleva, T., and Brenner, D. A. (2015). Deficiency of NOX1 or NOX4 Prevents Liver Inflammation and Fibrosis in Mice through Inhibition of Hepatic Stellate Cell Activation. *PLoS One* 10 (7), e0129743. doi:10.1371/journal.pone.0129743

Lee, Y. K., Park, J. E., Lee, M., and Hardwick, J. P. (2018). Hepatic Lipid Homeostasis by Peroxisome Proliferator-Activated Receptor Gamma 2. *Liver Res.* 2 (4), 209–215. doi:10.1016/j.livres.2018.12.001

Lepreux, S., Guyot, C., Billet, F., Combe, C., Balabaud, C., Bioulac-Sage, P., et al. (2013). Smoothelin, a New Marker to Determine the Origin of Liver Fibrogenic Cells. *Wjg* 19 (48), 9343–9350. doi:10.3748/wjg.v19.i48.9343

Levada, K., Omelyanchik, A., Rodionova, V., Weiskirchen, R., and Bartneck, M. (2019). Magnetic-assisted Treatment of Liver Fibrosis. *Cells* 8 (10), 1279. doi:10.3390/cells8101279

Li, C., Tan, Y. H., Sun, J., Deng, F. M., and Liu, Y. L. (2020). PAX6 Contributes to the Activation and Proliferation of Hepatic Stellate Cells via Activating Hedgehog/GLI1 Pathway. *Biochem. Biophysical Res. Commun.* 526 (2), 314–320. doi:10.1016/j.bbrc.2020.03.086

Li, H., You, H., Fan, X., and Jia, J. (2016). Hepatic Macrophages in Liver Fibrosis: Pathogenesis and Potential Therapeutic Targets. *BMJ Open Gastroenterol.* 3 (1), e000079. doi:10.1136/bmjgast-2016-000079

Li, T., Yan, H., Geng, Y., Shi, H., Li, H., Wang, S., et al. (2019). Target Genes Associated with Lipid and Glucose Metabolism in Non-alcoholic Fatty Liver Disease. *Lipids Health Dis.* 18 (1), 211. doi:10.1186/s12944-019-1154-9

Li, W., Li, L., and Hui, L. (2020). Cell Plasticity in Liver Regeneration. *Trends Cel Biol.* 30 (4), 329–338. doi:10.1016/j.tcb.2020.01.007

Li, Y., Lua, I., French, S. W., and Asahina, K. (2016). Role of TGF-β Signaling in Differentiation of Mesothelial Cells to Vitamin A-Poor Hepatic Stellate Cells in Liver Fibrosis. *Am. J. Physiol.-Gastrointestinal Liver Physiol.* 310 (4), G262–G272. doi:10.1152/ajpgi.00257.2015

Li, Y., Wang, J., and Asahina, K. (2013). Mesothelial Cells Give Rise to Hepatic Stellate Cells and Myofibroblasts via Mesothelial-Mesenchymal Transition in Liver Injury. *Proc. Natl. Acad. Sci.* 110 (6), 2324–2329. doi:10.1073/pnas.1214136110

Liangpunsakul, S., and Chalasani, N. (2019). Lipid Mediators of Liver Injury in Nonalcoholic Fatty Liver Disease. *Am. J. Physiol.-Gastrointestinal Liver Physiol.* 316 (1), G75–G81. doi:10.1152/ajpgi.00170.2018

Lieber, C. S. (2004). The Discovery of the Microsomal Ethanol Oxidizing System and its Physiologic and Pathologic Role. *Drug Metab. Rev.* 36 (3-4), 511–529. doi:10.1081/dmr-200033441

Liu, J., Lin, B., Chen, Z., Deng, M., Wang, Y., Wang, J., et al. (2020). Identification of Key Pathways and Genes in Nonalcoholic Fatty Liver Disease Using Bioinformatics Analysis. *Aoms* 16 (2), 374–385. doi:10.5114/aoms.2020.93343

Locke, G. A., Cheng, D., Witmer, M. R., Tamura, J. K., Haque, T., Carney, R. F., et al. (2008). Differential Activation of Recombinant Human Acetyl-CoA Carboxylases 1 and 2 by Citrate. *Arch. Biochem. Biophys.* 475 (1), 72–79. doi:10.1016/j.abb.2008.04.011

Long, X., Chen, Q., Zhao, J., Rafaels, N., Mathias, P., Liang, H., et al. (2015). An IL-13 Promoter Polymorphism Associated with Liver Fibrosis in Patients with Schistosoma Japonicum. *PLoS One* 10 (8), e0135360. doi:10.1371/journal.pone.0135360

Long, X., Daya, M., Zhao, J., Rafaels, N., Liang, H., Potee, J., et al. (2017). The Role of ST2 and ST2 Genetic Variants in Schistosomiasis. *J. Allergy Clin. Immunol.* 140 (5), 1416–1422. doi:10.1016/j.jaci.2016.12.969

Lötvall, J., Hill, A. F., Hochberg, F., Buzás, E. I., Di Vizio, D., Gardiner, C., et al. (2014). Minimal Experimental Requirements for Definition of Extracellular Vesicles and Their Functions: a Position Statement from the International Society for Extracellular Vesicles. *J. Extracellular Vesicles* 3, 26913. doi:10.3402/jev.v3.26913

Lua, I., Li, Y., Pappoe, L. S., and Asahina, K. (2015). Myofibroblastic Conversion and Regeneration of Mesothelial Cells in Peritoneal and Liver Fibrosis. *Am. J. Pathol.* 185 (12), 3258–3273. doi:10.1016/j.ajpath.2015.08.009

Luangmonkong, T., Suriguga, S., Mutsaers, H. A. M., Groothuis, G. M. M., Olinga, P., and Boersema, M. (2018). Targeting Oxidative Stress for the Treatment of Liver Fibrosis. *Rev. Physiol. Biochem. Pharmacol.* 175, 71–102. doi:10.1007/112_2018_10

Luukkonen, P. K., Zhou, Y., Sädevirta, S., Leivonen, M., Arola, J., Orešič, M., et al. (2016). Hepatic Ceramides Dissociate Steatosis and Insulin Resistance in Patients with Non-alcoholic Fatty Liver Disease. *J. Hepatol.* 64 (5), 1167–1175. doi:10.1016/j.jhep.2016.01.002

Macherey, A.-C., and Dansette, P. M. (2015). "Biotransformations Leading to Toxic Metabolites," in *Rognan D. The Practice of Medicinal Chemistry*. Editors C. G. Wermuth, D. Aldous, and P. Raboisson. Fourth Edition (London: Academic Press), 585–614. doi:10.1016/B978-0-12-417205-0.00025-0

Machicado, C., Machicado, J. D., Maco, V., Terashima, A., and Marcos, L. A. (2016). Association of *Fasciola Hepatica* Infection with Liver Fibrosis,

Cirrhosis, and *Cancer*: A Systematic Review. *Plos Negl. Trop. Dis.* 10 (9), e0004962. doi:10.1371/journal.pntd.0004962

Magill, A. J., Grögl, M., Gasser, R. A., Jr, Sun, W., and Oster, C. N. (1993). Visceral Infection Caused by Leishmania Tropica in Veterans of Operation Desert Storm. *N. Engl. J. Med.* 328 (19), 1383–1387. doi:10.1056/NEJM199305133281904

Magness, S. T., Bataller, R. n., Yang, L., and Brenner, D. A. (2004). A Dual Reporter Gene Transgenic Mouse Demonstrates Heterogeneity in Hepatic Fibrogenic Cell Populations. *Hepatology* 40 (5), 1151–1159. doi:10.1002/hep.20427

Maher, J. J. (2001). Interactions between Hepatic Stellate Cells and the Immune System. *Semin. Liver Dis.* 21 (3), 417–426. doi:10.1055/s-2001-17555

Mallat, A., Lodder, J., Teixeira-Clerc, F., Moreau, R., Codogno, P., and Lotersztajn, S. (2014). Autophagy: a Multifaceted Partner in Liver Fibrosis. *Biomed. Res. Int.* 2014, 1–7. doi:10.1155/2014/869390

Manmadhan, S., and Ehmer, U. (2019). Hippo Signaling in the Liver - A Long and Ever-Expanding Story. *Front. Cel Dev. Biol.* 7, 33. doi:10.3389/fcell.2019.00033

Mannaerts, I., Thoen, L. F. R., Eysackers, N., Cubero, F. J., Batista Leite, S., Coldham, I., et al. (2019). Unfolded Protein Response Is an Early, Non-critical Event during Hepatic Stellate Cell Activation. *Cell Death Dis* 10 (2), 98. doi:10.1038/s41419-019-1327-5

Mantel, P.-Y., and Schmidt-Weber, C. B. (2011). Transforming Growth Factor-Beta: Recent Advances on its Role in Immune Tolerance. *Methods Mol. Biol.* 677, 303–338. doi:10.1007/978-1-60761-869-0_21

Marcos, L. A., Terashima, A., Yi, P., Andrade, R., Cubero, F. J., Albanis, E., et al. (2011). Mechanisms of Liver Fibrosis Associated with Experimental *Fasciola Hepatica* Infection: Roles of Fas2 Proteinase and Hepatic Stellate Cell Activation. *J. Parasitol.* 97 (1), 82–87. doi:10.1645/GE-2420.1

Margini, C., and Dufour, J. F. (2016). The Story of HCC in NAFLD: from Epidemiology, across Pathogenesis, to Prevention and Treatment. *Liver Int.* 36 (3), 317–324. doi:10.1111/liv.13031

Marra, F., and Tacke, F. (2014). Roles for Chemokines in Liver Disease. *Gastroenterology* 147 (3), 577–594. doi:10.1053/j.gastro.2014.06.043

McDonnell, A. M., and Dang, C. H. (2013). Basic Review of the Cytochrome P450 System. *J. Adv. Pract. Oncol.* 4 (4), 263–268. doi:10.6004/jadpro.2013.4.4.7

McGuire, L. C., Cruickshank, A. M., and Munro, P. T. (2006). Alcoholic Ketoacidosis. *Emerg. Med. J.* 23 (6), 417–420. doi:10.1136/emj.2004.017590

McManus, D. P., Bergquist, R., Cai, P., Ranasinghe, S., Tebeje, B. M., and You, H. (2020). Schistosomiasis-from Immunopathology to Vaccines. *Semin. Immunopathol.* 42 (3), 355–371. doi:10.1007/s00281-020-00789-x

Mederacke, I., Hsu, C. C., Troeger, J. S., Huebener, P., Mu, X., Dapito, D. H., et al. (2013). Fate Tracing Reveals Hepatic Stellate Cells as Dominant Contributors to Liver Fibrosis Independent of its Aetiology. *Nat. Commun.* 4, 2823. doi:10.1038/ncomms3823

Melo, F. A., Moura, E. P., Ribeiro, R. R., Alves, C. F., Caliari, M. V., Tafuri, W. L., et al. (2009). Hepatic Extracellular Matrix Alterations in Dogs Naturally Infected withLeishmania (Leishmania) Chagasi. *Int. J. Exp. Pathol.* 90 (5), 538–548. doi:10.1111/j.1365-2613.2009.00681.x

Mendes, F. D., Jorgensen, R., Keach, J., Katzmann, J. A., Smyrk, T., Donlinger, J., et al. (2006). Elevated Serum IgG4 Concentration in Patients with Primary Sclerosing Cholangitis. *Am. J. Gastroenterol.* 101 (9), 2070–2075. doi:10.1111/j.1572-0241.2006.00772.x

Metz, R. P., Patterson, J. L., and Wilson, E. (2012). Vascular Smooth Muscle Cells: Isolation, Culture, and Characterization. *Methods Mol. Biol.* 843, 169–176. doi:10.1007/978-1-61779-523-7_16

Michalopoulos, G. K. (2013). Principles of Liver Regeneration and Growth Homeostasis. *Compr. Physiol.* 3 (1), 485–513. doi:10.1002/cphy.c120014

Mitchell, M. C., Kerr, T., and Herlong, H. F. (2020). Current Management and Future Treatment of Alcoholic Hepatitis. *Gastroenterol. Hepatol.* 16, 178–189. doi:10.14218/jcth.2016.00006

Morales, M. R., Sendra, C., and Romero-Gomez, M. (2017). Hepatitis B and NAFLD: Lives Crossed. *Ann. Hepatol.* 16 (2), 185–187. doi:10.5604/16652681.1231556

Morgan, T. R. (2007). Management of Alcoholic Hepatitis. *Gastroenterol. Hepatol. (N Y)* 3 (2), 97–99. doi:10.3109/9780203301388-10

Munker, S., Wu, Y.-L., Ding, H.-G., Liebe, R., and Weng, H.-L. (2017). Can a Fibrotic Liver Afford Epithelial-Mesenchymal Transition? *Wjg* 23 (26), 4661–4668. doi:10.3748/wjg.v23.i26.4661

Murphree, C. R., Nguyen, N. N., Raghunathan, V., Olson, S. R., DeLoughery, T., and Shatzel, J. J. (2020). Diagnosis and Management of Hereditary Haemochromatosis. *Vox Sang* 115 (4), 255–262. doi:10.1111/vox.12896

Mutsaers, S. E. (2004). The Mesothelial Cell. *Int. J. Biochem. Cel Biol.* 36 (1), 9–16. doi:10.1016/s1357-2725(03)00242-5

Narayanan, P., and Mistry, P. K. (2020). Update on Alpha-1 Antitrypsin Deficiency in Liver Disease. *Clin. Liver Dis.* 15 (6), 228–235. doi:10.1002/cld.896

Natarajan, V., Harris, E. N., and Kidambi, S. (2017). SECs (Sinusoidal Endothelial Cells), Liver Microenvironment, and Fibrosis. *Biomed. Res. Int.* 2017, 1–9. doi:10.1155/2017/4097205

Nishio, T., Hu, R., Koyama, Y., Liang, S., Rosenthal, S. B., Yamamoto, G., et al. (2019). Activated Hepatic Stellate Cells and Portal Fibroblasts Contribute to Cholestatic Liver Fibrosis in MDR2 Knockout Mice. *J. Hepatol.* 71 (3), 573–585. doi:10.1016/j.jhep.2019.04.012

Oliveira, J. B., Silva, P. C. V., Vasconcelos, L. M., Gomes, A. V., Coêlho, M. R. C. D., Cahu, G. G. O. M., et al. (2015). Influence of Polymorphism (-G308A) TNF-α on the Periportal Fibrosis Regression of Schistosomiasis after Specific Treatment. *Genet. Test. Mol. Biomarkers* 19 (11), 598–603. doi:10.1089/gtmb.2015.0091

Omenetti, A., Porrello, A., Jung, Y., Yang, L., Popov, Y., Choi, S. S., et al. (2008). Hedgehog Signaling Regulates Epithelial–Mesenchymal Transition during Biliary Fibrosis in Rodents and Humans. *J. Clin. Invest.* 118 (10), 3331–3342. doi:10.1172/JCI35875

Oosterhoff, L. A., Kruitwagen, H. S., van Wolferen, M. E., van Balkom, B. W. M., Mokry, M., Lansu, N., et al. (2019). Characterization of Endothelial and Smooth Muscle Cells from Different Canine Vessels. *Front. Physiol.* 10, 101. doi:10.3389/fphys.2019.00101

Patel, A., and Harrison, S. A. (2012). Hepatitis C Virus Infection and Nonalcoholic Steatohepatitis. *Gastroenterol. Hepatol. (N Y)* 8 (5), 305–312.

Patel, N., Sharma, B., and Samant, H. (2020). Cryptogenic Cirrhosis. Available from: https://www.ncbi.nlm.nih.gov/books/NBK534228/ (Accessed February 23, 2021).

Pavletich, N., and Pabo, C. (1993). Crystal Structure of a Five-Finger GLI-DNA Complex: New Perspectives on Zinc Fingers. *Science* 261 (5129), 1701–1707. doi:10.1126/science.8378770

Pellicoro, A., Ramachandran, P., Iredale, J. P., and Fallowfield, J. A. (2014). Liver Fibrosis and Repair: Immune Regulation of Wound Healing in a Solid Organ. *Nat. Rev. Immunol.* 14 (3), 181–194. doi:10.1038/nri3623

Peng, X., Yang, Y., Tang, L., Wan, J., Dai, J., Li, L., et al. (2020). Therapeutic Benefits of Apocynin in Mice with lipopolysaccharide/D-Galactosamine-Induced Acute Liver Injury via Suppression of the Late Stage Pro-apoptotic AMPK/JNK Pathway. *Biomed. Pharmacother.* 125, 110020. doi:10.1016/j.biopha.2020.110020

Penz-Österreicher, M., Österreicher, C. H., and Trauner, M. (2011). Fibrosis in Autoimmune and Cholestatic Liver Disease. *Best Pract. Res. Clin. Gastroenterol.* 25 (2), 245–258. doi:10.1016/j.bpg.2011.02.001

Perdigoto, R., Carpenter, H. A., and Czaja, A. J. (1992). Frequency and Significance of Chronic Ulcerative Colitis in Severe Corticosteroid-Treated Autoimmune Hepatitis. *J. Hepatol.* 14 (2–3), 325–331. doi:10.1016/0168-8278(92)90178-r

Perri, G. A. (2013). Ascites in Patients with Cirrhosis. *Can. Fam. Physician* 59 (12), 1297–1299.

Pinto, R. B., Schneider, A. C., and da Silveira, T. R. (2015). Cirrhosis in Children and Adolescents: An Overview. *Wjh* 7 (3), 392–405. doi:10.4254/wjh.v7.i3.392

Pinzani, M., and Vizzutti, F. (2005). "Anatomy and Vascular Biology of the Cells in the Portal Circulation," in *Portal Hypertension Clinical Gastroenterology*. Editors A. J. Sanyal and V. H. Shah (London: Humana Press). doi:10.1007/978-1-59259-885-4

Pirazzi, C., Valenti, L., Motta, B. M., Pingitore, P., Hedfalk, K., Mancina, R. M., et al. (2014). PNPLA3 Has Retinyl-Palmitate Lipase Activity in Human Hepatic Stellate Cells. *Hum. Mol. Genet.* 23 (15), 4077–4085. doi:10.1093/hmg/ddu121

Pitta, M. G. R., Romano, A., Cabantous, S., Henri, S., Hammad, A., Kouriba, B., et al. (2009). IL-17 and IL-22 Are Associated with Protection against Human Kala Azar Caused by Leishmania Donovani. *J. Clin. Invest.* 119 (8), 2379–2387. doi:10.1172/JCI38813

Polaris Observatory Collaborators (2018). Global Prevalence, Treatment, and Prevention of Hepatitis B Virus Infection in 2016: a Modelling Study. *Lancet Gastroenterol. Hepatol.* 3 (6), 383–403. doi:10.1016/S2468-1253(18)30056-6

Polyzos, S. A., Kountouras, J., and Mantzoros, C. S. (2015). Leptin in Nonalcoholic Fatty Liver Disease: a Narrative Review. *Metabolism* 64 (1), 60–78. doi:10.1016/j.metabol.2014.10.012

Ramachandran, P., and Iredale, J. P. (2012). Liver Fibrosis: a Bidirectional Model of Fibrogenesis and Resolution. *QJM* 105 (9), 813–817. doi:10.1093/qjmed/hcs069

Rao, S., Xiang, J., Huang, J., Zhang, S., Zhang, M., Sun, H., et al. (2019). PRC1 Promotes GLI1-dependent Osteopontin Expression in Association with the Wnt/β-Catenin Signaling Pathway and Aggravates Liver Fibrosis. *Cell Biosci* 9, 100. doi:10.1186/s13578-019-0363-2

Rehm, J., and Shield, K. D. (2019). Global Burden of Alcohol Use Disorders and Alcohol Liver Disease. *Biomedicines* 7 (4), 99. doi:10.3390/biomedicines7040099

Reilkoff, R. A., Bucala, R., and Herzog, E. L. (2011). Fibrocytes: Emerging Effector Cells in Chronic Inflammation. *Nat. Rev. Immunol.* 11 (6), 427–435. doi:10.1038/nri2990

Robertson, H., Kirby, J. A., Yip, W. W., Jones, D. E. J., and Burt, A. D. (2007). Biliary Epithelial-Mesenchymal Transition in Posttransplantation Recurrence of Primary Biliary Cirrhosis. *Hepatology* 45 (4), 977–981. doi:10.1002/hep.21624

Rosselli, M., Lotersztajn, S., Vizzutti, F., Arena, U., Pinzani, M., and Marra, F. (2014). The Metabolic Syndrome and Chronic Liver Disease. *Cpd* 20 (31), 5010–5024. doi:10.2174/1381612819666131206111352

Rossen, N. G., Fuentes, S., Boonstra, K., D'Haens, G. R., Heilig, H. G., Zoetendal, E. G., et al. (2015). The Mucosa-Associated Microbiota of PSC Patients Is Characterized by Low Diversity and Low Abundance of Uncultured Clostridiales II. *J. Crohns Colitis* 9 (4), 342–348. doi:10.1093/ecco-jcc/jju023

Ryaboshapkina, M., and Hammar, M. (2017). Human Hepatic Gene Expression Signature of Non-alcoholic Fatty Liver Disease Progression, a Meta-Analysis. *Sci. Rep.* 7 (1), 12361. doi:10.1038/s41598-017-10930-w

Rygiel, K. A., Robertson, H., Marshall, H. L., Pekalski, M., Zhao, L., Booth, T. A., et al. (2008). Epithelial-mesenchymal Transition Contributes to Portal Tract Fibrogenesis during Human Chronic Liver Disease. *Lab. Invest.* 88 (2), 112–123. doi:10.1038/labinvest.3700704

Sahin, H., Trautwein, C., and Wasmuth, H. E. (2010). Functional Role of Chemokines in Liver Disease Models. *Nat. Rev. Gastroenterol. Hepatol.* 7 (12), 682–690. doi:10.1038/nrgastro.2010.168

Sasse, D., Spornitz, U. M., and Piotr Maly, I. (1992). Liver Architecture. *Enzyme* 46 (1–3), 8–32. doi:10.1159/000468776

Satoh, D., Yagi, T., Nagasaka, T., Shinoura, S., Umeda, Y., Yoshida, R., et al. (2013). CD14 Upregulation as a Distinct Feature of Non-alcoholic Fatty Liver Disease after Pancreatoduodenectomy. *Wjh* 5 (4), 189–195. doi:10.4254/wjh.v5.i4.189

Saucedo, L. J., and Edgar, B. A. (2007). Filling Out the Hippo Pathway. *Nat. Rev. Mol. Cel Biol.* 8 (8), 613–621. doi:10.1038/nrm2221

Schattenberg, J. M., and Lee, M.-S. (2016). Extracellular Vesicles as Messengers between Hepatocytes and Macrophages in Nonalcoholic Steatohepatitis. *Gastroenterology* 150 (4), 815–818. doi:10.1053/j.gastro.2016.02.064

Schilter, H., Findlay, A. D., Perryman, L., Yow, T. T., Moses, J., Zahoor, A., et al. (2019). The Lysyl Oxidase like 2/3 Enzymatic Inhibitor, PXS-5153A, Reduces Crosslinks and Ameliorates Fibrosis. *J. Cel Mol. Med.* 23 (3), 1759–1770. doi:10.1111/jcmm.14074

Schneider, R. K., Mullally, A., Dugourd, A., Peisker, F., Hoogenboezem, R., Van Strien, P. M. H., et al. (2017). Gli1 + Mesenchymal Stromal Cells Are a Key Driver of Bone Marrow Fibrosis and an Important Cellular Therapeutic Target. *Cell Stem Cell* 20 (6), 785–800. doi:10.1016/j.stem.2017.03.008

Scholten, D., Österreicher, C. H., Scholten, A., Iwaisako, K., Gu, G., Brenner, D. A., et al. (2010). Genetic Labeling Does Not Detect Epithelial-To-Mesenchymal Transition of Cholangiocytes in Liver Fibrosis in Mice. *Gastroenterology* 139 (3), 987–998. doi:10.1053/j.gastro.2010.05.005

Scholten, D., and Weiskirchen, R. (2011). Questioning the Challenging Role of Epithelial-To-Mesenchymal Transition in Liver Injury. *Hepatology* 53 (3), 1049–1051. doi:10.1002/hep.24191

Schon, H.-T., Bartneck, M., Borkham-Kamphorst, E., Nattermann, J., Lammers, T., Tacke, F., et al. (2016). Pharmacological Intervention in Hepatic Stellate Cell Activation and Hepatic Fibrosis. *Front. Pharmacol.* 7, 33. doi:10.3389/fphar.2016.00033

Schulze, R. J., Schott, M. B., Casey, C. A., Tuma, P. L., and McNiven, M. A. (2019). The Cell Biology of the Hepatocyte: A Membrane Trafficking Machine. *J. Cel Biol.* 218 (7), 2096–2112. doi:10.1083/jcb.201903090

Schuppan, D., Ashfaq-Khan, M., Yang, A. T., and Kim, Y. O. (2018). Liver Fibrosis: Direct Antifibrotic Agents and Targeted Therapies. *Matrix Biol.* 68–69, 435–451. doi:10.1016/j.matbio.2018.04.006

Scorza, M., Elce, A., Zarrilli, F., Liguori, R., Amato, F., and Castaldo, G. (2014). Genetic Diseases that Predispose to Early Liver Cirrhosis. *Int. J. Hepatol.* 2014, 1–11. doi:10.1155/2014/713754

Sekiya, S., Miura, S., Matsuda-Ito, K., and Suzuki, A. (2016). Myofibroblasts Derived from Hepatic Progenitor Cells Create the Tumor Microenvironment. *Stem Cel Rep.* 7 (6), 1130–1139. doi:10.1016/j.stemcr.2016.11.002

Seo, Y. Y., Cho, Y. K., Bae, J.-C., Seo, M. H., Park, S. E., Rhee, E.-J., et al. (2013). Tumor Necrosis Factor-α as a Predictor for the Development of Nonalcoholic Fatty Liver Disease: A 4-Year Follow-Up Study. *Endocrinol. Metab.* 28 (1), 41–45. doi:10.3803/enm.2013.28.1.41

Setshedi, M., Wands, J. R., and de la Monte, S. M. (2010). Acetaldehyde Adducts in Alcoholic Liver Disease. *Oxidative Med. Cell Longevity* 3 (3), 178–185. doi:10.4161/oxim.3.3.12288

Silva, P. C. V., Gomes, A. V., de Britto, L. R. P. B., de Lima, E. L. S., da Silva, J. L., Montenegro, S. M. L., et al. (2017). Influence of a TNF-α Polymorphism on the Severity of Schistosomiasis Periportal Fibrosis in the Northeast of Brazil. *Genet. Test. Mol. Biomarkers* 21 (11), 658–662. doi:10.1089/gtmb.2017.0133

Silva, P. C. V., Gomes, A. V., de Souza, T. K. G., Coêlho, M. R. C. D., Cahu, G. G. d. O. M., Muniz, M. T. C., et al. (2014). Association of SNP (-G1082A)IL-10with Increase in Severity of Periportal Fibrosis in Schistosomiasis, in the Northeast of Brazil. *Genet. Test. Mol. Biomarkers* 18 (9), 646–652. doi:10.1089/gtmb.2014.0098

Siqueira, E., Schoen, R. E., Silverman, W., Martini, J., Rabinovitz, M., Weissfeld, J. L., et al. (2002). Detecting Cholangiocarcinoma in Patients with Primary Sclerosing Cholangitis. *Gastrointest. Endosc.* 56 (1), 40–47. doi:10.1067/mge.2002.125105

Srinivas, A. N., Suresh, D., Santhekadur, P. K., Suvarna, D., and Kumar, D. P. (2021). Extracellular Vesicles as Inflammatory Drivers in NAFLD. *Front. Immunol.* 11, 627424. doi:10.3389/fimmu.2020.627424

Staufer, K. (2020). Current Treatment Options for Cystic Fibrosis-Related Liver Disease. *Ijms* 21 (22), 8586. doi:10.3390/ijms21228586

Stickel, F., Datz, C., Hampe, J., and Bataller, R. (2017). Pathophysiology and Management of Alcoholic Liver Disease: Update 2016. *Gut Liver* 11 (2), 173–188. doi:10.5009/gnl16477

Stremmel, W., and Weiskirchen, R. (2021). Therapeutic Strategies in Wilson Disease: Pathophysiology and Mode of Action. *Ann. Transl Med.* 13, 271. doi:10.21037/atm-20-3090

Suppli, M. P., Rigbolt, K. T. G., Veidal, S. S., Heebøll, S., Eriksen, P. L., Demant, M., et al. (2019). Hepatic Transcriptome Signatures in Patients with Varying Degrees of Nonalcoholic Fatty Liver Disease Compared with Healthy Normal-Weight Individuals. *Am. J. Physiology-Gastrointestinal Liver Physiol.* 316 (4), G462–G472. doi:10.1152/ajpgi.00358.2018

Suzuki, K., Tanaka, M., Watanabe, N., Saito, S., Nonaka, H., and Miyajima, A. (2008). p75 Neurotrophin Receptor Is a Marker for Precursors of Stellate Cells and Portal Fibroblasts in Mouse Fetal Liver. *Gastroenterology* 135 (1), 270–281. doi:10.1053/j.gastro.2008.03.075

Syn, W. K., Jung, Y., Omenetti, A., Abdelmalek, M., Guy, C. D., Yang, L., et al. (2009). Hedgehog-mediated Epithelial-To-Mesenchymal Transition and Fibrogenic Repair in Nonalcoholic Fatty Liver Disease. *Gastroenterology* 137 (4), 1478–1488. doi:10.1053/j.gastro.2009.06.051

Tacke, F., and Weiskirchen, R. (2018). An Update on the Recent Advances in Antifibrotic Therapy. *Expert Rev. Gastroenterol. Hepatol.* 12 (11), 1143–1152. doi:10.1080/17474124.2018.1530110

Tan, H.-L., Mohamed, R., Mohamed, Z., and Zain, S. M. (2016). Phosphatidylethanolamine N-Methyltransferase Gene Rs7946 Polymorphism Plays a Role in Risk of Nonalcoholic Fatty Liver Disease. *Pharmacogenet Genomics* 26 (2), 88–95. doi:10.1097/FPC.0000000000000193

Tanaka, A. (2020). Autoimmune Hepatitis: 2019 Update. *Gut and Liver* 14 (4), 430–438. doi:10.5009/gnl19261

Tarantino, G., Minno, M. N. D. D., and Capone, D. (2009). Drug-induced Liver Injury: Is it Somehow Foreseeable?. *Wjg* 15 (23), 2817–2833. doi:10.3748/wjg.15.2817

Taura, K., Iwaisako, K., Hatano, E., and Uemoto, S. (2016). Controversies over the Epithelial-To-Mesenchymal Transition in Liver Fibrosis. *Jcm* 5 (1), 9. doi:10.3390/jcm5010009

Taura, K., Miura, K., Iwaisako, K., Österreicher, C. H., Kodama, Y., Penz-Österreicher, M., et al. (2010). Hepatocytes Do Not Undergo Epithelial-Mesenchymal Transition in Liver Fibrosis in Mice. *Hepatology* 51 (3), 1027–1036. doi:10.1002/hep.23368

Teufel, A., Itzel, T., Erhart, W., Brosch, M., Wang, X. Y., Kim, Y. O., et al. (2016). Comparison of Gene Expression Patterns between Mouse Models of Nonalcoholic Fatty Liver Disease and Liver Tissues from Patients. *Gastroenterology* 151 (3), 513–525. doi:10.1053/j.gastro.2016.05.051

Thoen, L. F. R., Guimarães, E. L., and van Grunsven, L. A. (2012). Autophagy: a New Player in Hepatic Stellate Cell Activation. *Autophagy* 8 (1), 126–128. doi:10.4161/auto.8.1.18105

Todorović Vukotić, N., Đorđević, J., Pejić, S., Đorđević, N., and Pajović, S. B. (2021). Antidepressants- and Antipsychotics-Induced Hepatotoxicity. *Arch. Toxicol.* 95, 1–23. doi:10.1007/s00204-020-02963-4

Troeger, J. S., Mederacke, I., Gwak, G. Y., Dapito, D. H., Mu, X., Hsu, C. C., et al. (2012). Deactivation of Hepatic Stellate Cells during Liver Fibrosis Resolution in Mice. *Gastroenterology* 143 (4), 1073–1083. doi:10.1053/j.gastro.2012.06.036

Tsuchida, T., and Friedman, S. L. (2017). Mechanisms of Hepatic Stellate Cell Activation. *Nat. Rev. Gastroenterol. Hepatol.* 14 (7), 397–411. doi:10.1038/nrgastro.2017.38

Uhlén, M., Fagerberg, L., Hallström, B. M., Lindskog, C., Oksvold, P., Mardinoglu, A., et al. (2015). Tissue-based Map of the Human Proteome. *Science* 347 (6220), 1260419. doi:10.1126/science.1260419

Valéry, L. P., Arnaud, L., Niki, A. S., Megan, C., Latifa, K., Manon, D., et al. (2021). Single-cell RNA Sequencing of Human Liver Reveals Hepatic Stellate Cell Heterogeneity. *JHEP Rep.* 7, 184. doi:10.1016/j.jhepr.2021.100278

van de Straat, R., de Vries, J., Debets, A. J. J., and Vermeulen, N. P. E. (1987). The Mechanism of Prevention of Paracetamol-Induced Hepatotoxicity by 3,5-dialkyl Substitution. *Biochem. Pharmacol.* 36 (13), 2065–2070. doi:10.1016/0006-2952(87)90132-8

Vannier-Santos, M. A., Saraiva, E. M., Martiny, A., Neves, A., and de Souza, W. (1992). Fibronectin Shedding by Leishmania May Influence the Parasite-Macrophage Interaction. *Eur. J. Cel Biol* 59 (2), 389–397.

Wang, B., Li, W., Fang, H., and Zhou, H. (2019). Hepatitis B Virus Infection Is Not Associated with Fatty Liver Disease: Evidence from a Cohort Study and Functional Analysis. *Mol. Med. Rep.* 19 (1), 320–326. doi:10.3892/mmr.2018.9619

Wang, L., Rennie Tankersley, L., Tang, M., Potter, J. J., and Mezey, E. (2002). Regulation of the Murine α2(I) Collagen Promoter by Retinoic Acid and Retinoid X Receptors. *Arch. Biochem. Biophys.* 401 (2), 262–270. doi:10.1016/S0003-9861(02)00058-9

Wanless, I. R., and Shiota, K. (2004). The Pathogenesis of Nonalcoholic Steatohepatitis and Other Fatty Liver Diseases: a Four-step Model Including the Role of Lipid Release and Hepatic Venular Obstruction in the Progression to Cirrhosis. *Semin. Liver Dis.* 24 (1), 99–106. doi:10.1055/s-2004-823104

Wasmuth, H. E., Lammert, F., Zaldivar, M. M., Weiskirchen, R., Hellerbrand, C., Scholten, D., et al. (2009). Antifibrotic Effects of CXCL9 and its Receptor CXCR3 in Livers of Mice and Humans. *Gastroenterology* 137 (1), 309–319. doi:10.1053/j.gastro.2009.03.053

Wee, A., Ludwig, J., Coffey, R. J., Jr, LaRusso, N. F., and Wiesner, R. H. (1985). Hepatobiliary Carcinoma Associated with Primary Sclerosing Cholangitis and Chronic Ulcerative Colitis. *Hum. Pathol.* 16 (7), 719–726. doi:10.1016/s0046-8177(85)80158-1

Weiskirchen, R. (2016). Hepatoprotective and Anti-fibrotic Agents: It's Time to Take the Next Step. *Front. Pharmacol.* 6, 303. doi:10.3389/fphar.2015.00303

Weiskirchen, R., Moser, M., Weiskirchen, S., Erdel, M., Dahmen, S., Buettner, R., et al. (2001). LIM-domain Protein Cysteine- and Glycine-Rich Protein 2 (CRP2) Is a Novel Marker of Hepatic Stellate Cells and Binding Partner of the Protein Inhibitor of Activated STAT1. *Biochem. J.* 359 (Pt 3), 485–496. doi:10.1042/0264-6021:3590485

Weiskirchen, R., Weiskirchen, S., and Tacke, F. (2018). Recent Advances in Understanding Liver Fibrosis: Bridging Basic Science and Individualized Treatment Concepts. *F1000Res* 7, F1000. doi:10.12688/f1000research.14841.1

WHO. World Health Organization (2020). Schistosomiasis Fact Sheet. Available at: https://www.who.int/news-room/fact-sheets/detail/schistosomiasis (Accessed February 23, 2021).

Widmer, J., Fassihi, K. S., Schlichter, S. C., Wheeler, K. S., Crute, B. E., King, N., et al. (1996). Identification of a Second Human Acetyl-CoA Carboxylase Gene. *Biochem. J.* 316 (Pt 3), 915–922. doi:10.1042/bj3160915

Wong, N., Yeo, W., Wong, W.-L., Wong, N. L.-Y., Chan, K. Y.-Y., Mo, F. K.-F., et al. (2009). TOP2A Overexpression in Hepatocellular Carcinoma Correlates with Early Age Onset, Shorter Patients Survival and Chemoresistance. *Int. J. Cancer* 124 (3), 644–652. doi:10.1002/ijc.23968

Wortmann, S. B., and Mayr, J. A. (2019). Choline-related-inherited Metabolic Diseases-A Mini Review. *J. Inherit. Metab. Dis.* 42 (2), 237–242. doi:10.1002/jimd.12011

Wyler, D. J. (1987). Fibronectin in Parasitic Diseases. *Rev. Infect. Dis.* 9 (Suppl. 4), S391–S399. doi:10.1093/clinids/9.supplement_4.s391

Wyler, D. J., Sypek, J. P., and McDonald, J. A. (1985). *In vitro* parasite-monocyte Interactions in Human Leishmaniasis: Possible Role of Fibronectin in Parasite Attachment. *Infect. Immun.* 49 (2), 305–311. doi:10.1128/IAI.49.2.305-311.1985

Xie, G., and Diehl, A. M. (2013). Evidence for and against Epithelial-To-Mesenchymal Transition in the Liver. *Am. J. Physiology-Gastrointestinal Liver Physiol.* 305 (12), G881–G890. doi:10.1152/ajpgi.00289.2013

Xie, J.-Q., Lu, Y.-P., Sun, H.-L., Gao, L.-N., Song, P.-P., Feng, Z.-J., et al. (2020). Sex Difference of Ribosome in Stroke-Induced Peripheral Immunosuppression by Integrated Bioinformatics Analysis. *Biomed. Res. Int.* 2020, 1–15. doi:10.1155/2020/3650935

Xing, T., Yan, T., and Zhou, Q. (2018). Identification of Key Candidate Genes and Pathways in Hepatocellular Carcinoma by Integrated Bioinformatical Analysis. *Exp. Ther. Med.* 15 (6), 4932–4942. doi:10.3892/etm.2018.6075

Xiong, J., Zhang, H., Wang, Y., Wang, A., Bian, J., Huang, H., et al. (2017). Hepatitis B Virus Infection and the Risk of Nonalcoholic Fatty Liver Disease: a Meta-Analysis. *Oncotarget* 8 (63), 107295–107302. doi:10.18632/oncotarget.22364

Xu, R., Zhang, Z., and Wang, F.-S. (2012). Liver Fibrosis: Mechanisms of Immune-Mediated Liver Injury. *Cell Mol Immunol* 9 (4), 296–301. doi:10.1038/cmi.2011.53

Yamaguchi, K., Yang, L., McCall, S., Huang, J., Yu, X. X., au, S. K., et al. (2007). Inhibiting Triglyceride Synthesis Improves Hepatic Steatosis but Exacerbates Liver Damage and Fibrosis in Obese Mice with Nonalcoholic Steatohepatitis. *Hepatology* 45 (6), 1366–1374. doi:10.1002/hep.21655

Yan, Z., Miao, X., Zhang, B., and Xie, J. (2018). p53 as a Double-Edged Sword in the Progression of Non-alcoholic Fatty Liver Disease. *Life Sci.* 215, 64–72. doi:10.1016/j.lfs.2018.10.051

Yang, A. H., Chen, J. Y., and Lin, J. K. (2003). Myofibroblastic Conversion of Mesothelial Cells. *Kidney Int.* 63 (4), 1530–1539. doi:10.1046/j.1523-1755.2003.00861.x

Yang, J., Antin, P., Antin, P., Berx, G., Blanpain, C., Brabletz, T., et al. (2020). Guidelines and Definitions for Research on Epithelial-Mesenchymal Transition. *Nat. Rev. Mol. Cel Biol.* 21 (6), 341–352. doi:10.1038/s41580-020-0237-9

Yang, L., Roh, Y. S., Song, J., Zhang, B., Liu, C., Loomba, R., et al. (2014). Transforming Growth Factor Beta Signaling in Hepatocytes Participates in Steatohepatitis through Regulation of Cell Death and Lipid Metabolism in Mice. *Hepatology* 59 (2), 483–495. doi:10.1002/hep.26698

Yang, L., Yang, C., Thomes, P. G., Kharbanda, K. K., Casey, C. A., McNiven, M. A., et al. (2019). Lipophagy and Alcohol-Induced Fatty Liver. *Front. Pharmacol.* 10, 495. doi:10.3389/fphar.2019.00495

Yang, Y., Bae, M., Park, Y.-K., Lee, Y., Pham, T. X., Rudraiah, S., et al. (2017). Histone Deacetylase 9 Plays a Role in the Antifibrogenic Effect of Astaxanthin in Hepatic Stellate Cells. *J. Nutr. Biochem.* 40, 172–177. doi:10.1016/j.jnutbio.2016.11.003

Younossi, Z. M., Golabi, P., de Avila, L., Paik, J. M., Srishord, M., Fukui, N., et al. (2019). The Global Epidemiology of NAFLD and NASH in Patients with Type 2 Diabetes: A Systematic Review and Meta-Analysis. *J. Hepatol.* 71 (4), 793–801. doi:10.1016/j.jhep.2019.06.021

Younossi, Z. M., Koenig, A. B., Abdelatif, D., Fazel, Y., Henry, L., and Wymer, M. (2016). Global Epidemiology of Nonalcoholic Fatty Liver Disease-Meta-Analytic Assessment of Prevalence, Incidence, and Outcomes. *Hepatology* 64 (1), 73–84. doi:10.1002/hep.28431

Yu, C., Chen, Y., Cline, G. W., Zhang, D., Zong, H., Wang, Y., et al. (2002). Mechanism by Which Fatty Acids Inhibit Insulin Activation of Insulin Receptor Substrate-1 (IRS-1)-Associated Phosphatidylinositol 3-kinase Activity in Muscle. *J. Biol. Chem.* 277 (52), 50230–50236. doi:10.1074/jbc.M200958200

Yuan, L., and Kaplowitz, N. (2009). Glutathione in Liver Diseases and Hepatotoxicity. *Mol. Aspects Med.* 30 (1-2), 29–41. doi:10.1016/j.mam.2008.08.003

Yuan, X., Sun, Y., Cheng, Q., Hu, K., Ye, J., Zhao, Y., et al. (2020). Proteomic Analysis to Identify Differentially Expressed Proteins between Subjects with Metabolic Healthy Obesity and Non-alcoholic Fatty Liver Disease. *J. Proteomics* 221, 103683. doi:10.1016/j.jprot.2020.103683

Yue, M., Huang, P., Wang, C., Fan, H., Tian, T., Wu, J., et al. (2021). Genetic Variation on TNF/LTA and TNFRSF1A Genes Is Associated with Outcomes of Hepatitis C Virus Infection. *Immunological Invest.* 50 (1), 1–11. doi:10.1080/08820139.2019.1708384

Zaldivar, M. M., Pauels, K., von Hundelshausen, P., Berres, M.-L., Schmitz, P., Bornemann, J., et al. (2010). CXC Chemokine Ligand 4 (Cxcl4) Is a Platelet-Derived Mediator of Experimental Liver Fibrosis. *Hepatology* 51 (4), 1345–1353. doi:10.1002/hep.23435

Zanger, U. M., and Schwab, M. (2013). Cytochrome P450 Enzymes in Drug Metabolism: Regulation of Gene Expression, Enzyme Activities, and Impact of Genetic Variation. *Pharmacol. Ther.* 138 (1), 103–141. doi:10.1016/j.pharmthera.2012.12.007

Zeisberg, M., Yang, C., Martino, M., Duncan, M. B., Rieder, F., Tanjore, H., et al. (2007). Fibroblasts Derive from Hepatocytes in Liver Fibrosis via Epithelial to Mesenchymal Transition. *J. Biol. Chem.* 282 (32), 23337–23347. doi:10.1074/jbc.M700194200

Zhang, F., Wang, F., He, J., Lian, N., Wang, Z., Shao, J., et al. (2020). Regulation of Hepatic Stellate Cell Contraction and Cirrhotic Portal Hypertension by Wnt/β-catenin Signalling via Interaction with Gli1. *Br. J. Pharmacol.* 16, 59. doi:10.1111/bph.15289

Zhang, J., Lin, S., Jiang, D., Li, M., Chen, Y., Li, J., et al. (2020). Chronic Hepatitis B and Non-alcoholic Fatty Liver Disease: Conspirators or Competitors? *Liver Int.* 40 (3), 496–508. doi:10.1111/liv.14369

Zhang, Y., and Hunter, T. (2014). Roles of Chk1 in Cell Biology and Cancer Therapy. *Int. J. Cancer* 134 (5), 1013–1023. doi:10.1002/ijc.28226

Zhang, Y., and Yu, C. (2020). Prognostic Characterization of OAS1/OAS2/OAS3/OASL in Breast Cancer. *BMC Cancer* 20 (1), 575. doi:10.1186/s12885-020-07034-6

Zhangdi, H.-J., Su, S.-B., Wang, F., Liang, Z.-Y., Yan, Y.-D., Qin, S.-Y., et al. (2019). Crosstalk Network Among Multiple Inflammatory Mediators in Liver Fibrosis. *Wjg* 25 (33), 4835–4849. doi:10.3748/wjg.v25.i33.4835

Zhou, Z., Xu, M.-J., and Gao, B. (2016). Hepatocytes: a Key Cell Type for Innate Immunity. *Cel Mol Immunol* 13 (3), 301–315. doi:10.1038/cmi.2015.97

Zhu, N., Khoshnan, A., Schneider, R., Matsumoto, M., Dennert, G., Ware, C., et al. (1998). Hepatitis C Virus Core Protein Binds to the Cytoplasmic Domain of Tumor Necrosis Factor (TNF) Receptor 1 and Enhances TNF-Induced Apoptosis. *J. Virol.* 72 (5), 3691–3697. doi:10.1128/JVI.72.5.3691-3697.1998

Zhu, X., Zhang, J., Fan, W., Gong, Y., Yan, J., Yuan, Z., et al. (2014). MAPKAP1 Rs10118570 Polymorphism Is Associated with Anti-infection and Anti-hepatic Fibrogenesis in Schistosomiasis Japonica. *PLoS One* 9 (8), e105995. doi:10.1371/journal.pone.0105995

Zuckerman, A. J. Hepatitis Viruses. In: S. Baron, editor. *Medical Microbiology*. 4th edition. Galveston, TXUniversity of Texas Medical Branch at Galveston; 1996. Chapter 70. Available at: https://www.ncbi.nlm.nih.gov/books/NBK7864/ (Accessed February 23, 2021).

Conflict of Interest: The authors declare that the research was conducted in the absence of any commercial or financial relationships that could be construed as a potential conflict of interest.

Copyright © 2021 Acharya, Chouhan, Weiskirchen and Weiskirchen. This is an open-access article distributed under the terms of the Creative Commons Attribution License (CC BY). The use, distribution or reproduction in other forums is permitted, provided the original author(s) and the copyright owner(s) are credited and that the original publication in this journal is cited, in accordance with accepted academic practice. No use, distribution or reproduction is permitted which does not comply with these terms.

frontiers in Pharmacology

ORIGINAL RESEARCH
published: 11 May 2021
doi: 10.3389/fphar.2021.676608

Antisense Tissue Factor Oligodeoxynucleotides Protected Diethyl Nitrosamine/Carbon Tetrachloride-Induced Liver Fibrosis Through Toll Like Receptor4-Tissue Factor-Protease Activated Receptor1 Pathway

Maha M. Shouman[1], Rania M. Abdelsalam[2,3], Mahmoud M. Tawfick[4], Sanaa A. Kenawy[2] and Mona M. El-Naa[5]*

[1]Department of Pharmacology and Toxicology, Faculty of Pharmacy, Modern Sciences and Arts University (MSA), Giza, Egypt, [2]Department of Pharmacology and Toxicology, Faculty of Pharmacy, Cairo University, Cairo, Egypt, [3]Department of Biology, Faculty of Pharmacy, New Giza University, Giza, Egypt, [4]Department of Microbiology and Immunology, Faculty of Pharmacy (Boys), Al-Azhar University, Cairo, Egypt, [5]Department of Pharmacology and Toxicology, Faculty of Pharmacy, University of Sadat City, Sadat City, Egypt

OPEN ACCESS

Edited by:
Ralf Weiskirchen, RWTH Aachen University, Germany

Reviewed by:
Mohamed Sadek Abdel-Bakky, Nahda University, Egypt
Olfat Ali Hammam, Theodor Bilharz Research Institute, Egypt
Bruno Cogliati, University of São Paulo, Brazil

***Correspondence:**
Maha M. Shouman
mamoussa@msa.edu.eg

Specialty section:
This article was submitted to Gastrointestinal and Hepatic Pharmacology, a section of the journal Frontiers in Pharmacology

Received: *05 March 2021*
Accepted: *27 April 2021*
Published: *11 May 2021*

Citation:
Shouman MM, Abdelsalam RM, Tawfick MM, Kenawy SA and El-Naa MM (2021) Antisense Tissue Factor Oligodeoxynucleotides Protected Diethyl Nitrosamine/Carbon Tetrachloride-Induced Liver Fibrosis Through Toll Like Receptor4-Tissue Factor-Protease Activated Receptor1 Pathway. Front. Pharmacol. 12:676608. doi: 10.3389/fphar.2021.676608

Tissue factor (TF) is a blood coagulation factor that has several roles in many non-coagulant pathways involved in different pathological conditions such as angiogenesis, inflammation and fibrogenesis. Coagulation and inflammation are crosslinked with liver fibrosis where protease-activated receptor1 (PAR1) and toll-like receptor4 (TLR4) play a key role. Antisense oligodeoxynucleotides are strong modulators of gene expression. In the present study, antisense TF oligodeoxynucleotides (TFAS) was evaluated in treating liver fibrosis via suppression of TF gene expression. Liver fibrosis was induced in rats by a single administration of N-diethyl nitrosamine (DEN, 200 mg/kg; i. p.) followed by carbon tetrachloride (CCl4, 3 ml/kg; s. c.) once weekly for 6 weeks. Following fibrosis induction, liver TF expression was significantly upregulated along with liver enzymes activities and liver histopathological deterioration. Alpha smooth muscle actin (α-SMA) and transforming growth factor-1beta (TGF-1β) expression, tumor necrosis factor-alpha (TNF-α) and hydroxyproline content and collagen deposition were significantly elevated in the liver. Blocking of TF expression by TFAS injection (2.8 mg/kg; s. c.) once weekly for 6 weeks significantly restored liver enzymes activities and improved histopathological features along with decreasing the elevated α-SMA, TGF-1β, TNF-α, hydroxyproline and collagen. Moreover, TFAS decreased the expression of both PAR1 and TLR4 that were induced by liver fibrosis. In conclusion, we reported that blockage of TF expression by TFAS improved inflammatory and fibrotic changes associated with CCl4+DEN intoxication. In addition, we explored the potential crosslink between the TF, PAR1 and TLR4 in liver fibrogenesis. These findings offer a platform on which recovery from liver fibrosis could be mediated through targeting TF expression.

Keywords: TF, PAR1, TLR4, liver fibrosis, inflammation, antisense oligodeoxynucleotides

INTRODUCTION

Liver fibrosis is a response to chronic liver injury induced by diverse causes such as infection, drugs, metabolic disorders, autoimmune diseases and cholestatic liver diseases (Borensztajn et al., 2010). Fibrogenesis is commonly associated with the generation of a chronic inflammation that results in an abnormal wound healing response. Hepatic stellate cells (HSCs) activation is the key pathogenic mechanism for the initiation and progression of liver fibrosis. A complex and tightly regulated cross-talks between HSCs, hepatocytes, Kupffer cells and sinusoidal endothelial cells (SECs) at the level of liver microcirculation are reported during fibrogenesis (Moreira, 2007).

Accumulation of collagen as well as other extracellular matrix (ECM) components in the liver leads to fibrous scar formation, which results in disruption of the liver architecture, hepatocyte loss, deterioration of the normal liver functions and ultimately liver failure (Karsdal et al., 2020). Liver fibrosis is a reversible process, as long as the liver is not at the stage of advanced cirrhosis (Benyon and Iredale, 2000). Given the highly dynamic process of liver fibrosis and the complex and multiple pathways involved in its progress, targeting one pathway that underlies the fibrotic process may not be sufficient to induce its reversal. However, through advances in the understanding of the key events and cellular pathways involved in the pathogenesis of fibrogenesis, the key targets for antifibrotic therapies are likely to be identified (Trautwein et al., 2015).

Recently, the association between chronic liver disease and coagulopathy is well established (Tripodi et al., 2011). Coagulation activity was recorded as a contributor to the pathogenesis of liver toxicity. Furthermore, it was reported that inflammation and coagulation are interrelated for fibrogenesis (Calvaruso et al., 2008).

Tissue factor (TF) is a 47-kDa transmembrane glycoprotein that is normally expressed throughout the body including the liver (Witkowski et al., 2016). TF is the main initiator of the protease coagulation cascade *in vivo*, leading to thrombin generation (Rauch and Nemerson, 2000). It has been reported that under pathological conditions TF expression can be upregulated by many inducers such as cytokines, hypoxia and mechanical injury, thus concentrating TF to the sites of injury (Giesen et al., 1999). TF mediates different pathological signal cascades via a family of G-protein coupled receptors called protease-activated receptors (PARs) (Rao and Pendurthi, 2005).

Four types of PARs have been identified PAR1, PAR2, PAR3 and PAR4. PAR1 receptor was found in the normal liver as well as diseased liver (Rullier et al., 2008; Nault et al., 2016) and has been shown to perform a key role in the pathogenesis of liver fibrosis (Sullivan et al., 2010). PAR1 is expressed by various cells including endothelial cells, fibroblasts, smooth muscle cells and T lymphocytes (Coughlin, 2000). In the liver of patients with cirrhosis and chronic hepatitis, PAR1 was positively stained in fibroblasts in the fibrotic septa in addition to the inflammatory cells infiltrated around newly formed blood vessels and bile ducts (Rullier et al., 2008). PAR1 is primarily activated by thrombin and can be also activated by activated protein C (Riewald et al., 2003), coagulation factor Xa (FXa; Riewald et al., 2001), coagulation factor VIIa (FVIIa; Camerer et al., 2000) and plasmin (Pendurthi et al., 2002). Thrombin-mediated activation of PAR1 has been reported to contribute to several inflammatory and fibrotic diseases including liver fibrosis (Sullivan et al., 2010).

In the liver, toll-like receptor 4 (TLR4) is found on both Kupffer cells and HSCs (Bai et al., 2013). TLR4 is the main target for lipopolysaccharide (LPS) and is largely involved in the inflammatory reaction associated with liver fibrosis (Beutler, 2004). TLR4 signaling through Kupffer cells leads to the release of proinflammatory cytokines such as TNF-α, IL-1 and IL-6 (Beutler, 2004). Moreover, TLR4 expressed on Kupffer cells is involved in the fibrogenic signaling of HSCs and enhancing their response to transforming growth factor-1β (TGF-1β) thus promoting liver fibrosis (Seki et al., 2007). Interestingly, it has been reported that in patients with hepatitis C infection, specific single-nucleotide polymorphisms of TLR4 affected the rate of fibrosis progression (Huang et al., 2007).

Blocking of specific gene expression has recently gained a growing considerable interest as a tool to decrease the expression of a target protein. DNA encodes RNA, which is then translated into proteins (Chery, 2016). Antisense oligodeoxynucleotides (AS-ODNs) are single-stranded oligodeoxynucleotides that bind to compatible mRNA with a high degree of accuracy, leading to a decline in the target protein level (Bennett and Swayze, 2010). Different types of oligonucleotides antisense sequences, including reverse sequences, antisense sequences containing one or more mismatches and scrambled oligonucleotides have been used as a control of AS-ODNs (Gagnon and Corey, 2019). Over the last years, therapeutic strategies including AS-ODNs that suppress translation of mRNA and other oligonucleotides that interfere with RNA pathway have been substantially improved as a therapy platform at both preclinical and clinical levels (Chi et al., 2005; Kastelein et al., 2006). In 1998, fomivirsen was approved as the first agent that inhibits the translation of mRNA encoding for cytomegalovirus at its early immediate region proteins and permitted for treating cytomegalovirus retinitis (Jabs and Griffiths, 2002). Importantly, by January 2020, 10 oligonucleotide drugs have gained regulatory approval from the FDA (Roberts et al., 2020).

The objective of this work is to study the theory that chemically induced liver fibrosis is TF-dependent and consequently inhibition of TF expression by antisense tissue factor oligodeoxynucleotides (TFAS) could be associated with reduced severity of liver fibrosis. In addition, the study aimed at exploring the TLR4-TF-PAR1 signaling loop as a novel pathway that may be involved in liver fibrosis and the possible role of suppressing TF expression in blocking this loop as a form of cross-talk between coagulation, inflammation and fibrogenesis.

MATERIAL AND METHODS

Experimental Animals

Male Sprague Dawley rats with an average weight of 120–150 gm (5–6 weeks old) were purchased from the Egyptian Organization for Biological Products and Vaccines (Cairo, Egypt). Animals

were placed in cages and kept under conventional laboratory conditions throughout the study (room temperature 24–27°C and 55 ± 10% humidity) with alternating 12 h light and dark cycles. Animals were fed normal chow and were permitted water *ad libitum*. They were left in the animal house at Faculty of Pharmacy, Cairo University for acclimatization for one week before the start of the study where rats whose weight exceeded 150 gm were excluded. Male rats are strictly used while female rats are avoided in the experiment to prevent unintended risks. The experimental protocol was approved by the Research Ethics Committee (REC) of Faculty of Pharmacy, Cairo University (PT 1902).

Drugs and Chemicals

N-diethyl nitrosamine (DEN) was purchased from Sigma Chemicals (MO, United States) and dissolved in saline. Carbon tetrachloride (CCl4) was obtained from El Gomhorya Co. (Cairo, Egypt). Tissue factor oligodeoxynucleotides (TF-ODNs) were purchased from Integrated DNA Technologies (San Diego, CA, United States) and dissolved in saline. The sequence of the rat antisense tissue factor oligodeoxynucleotides (TFAS) is 5'-CATGGGGATAGCCAT-3' while the sequence of scrambled control of tissue factor oligodeoxynucleotides (TFSC) is 5'-TGACGCAGAGTCGTA-3'. All chemicals were of the highest purity and analytical grade.

Sample Size Calculation

A total of 40 rats were divided into five groups ($n = 8$) where each group was placed in a cage. The sample size was calculated using G*Power software (GPower 3.1. Ink) where the effect size is 0.77, α level is 0.05 and power (1-β) is 0.95.

Experimental Design

Rats were allocated to cages by simple randomization using a web-based research randomizer and within the same cage, rats received the treatment randomly. The technician was blinded to the group status and the treatment administered to the rats. All the treatments and animals were handled and monitored in the same way. The authors were responsible for treatment preparation, anesthesia and sample collection. The groups were divided as follows:

Control group: healthy rats received saline throughout the experiment, TFAS group: rats treated with TFAS (2.8 mg/kg; s. c.) once a week for six weeks according to Nakamura et al. (2002) and Shimizu et al., (2014).

DEN+CCl4 group: liver fibrosis was induced by injection of a single dose of DEN (200 mg/kg; i. p.) and after one week CCl4 was administered (3 ml/kg; s. c.) once a week for six weeks according to Mansour et al. (2010) with some modification.

TFSC+DEN+CCl4 group: rats intoxicated with DEN and received TFSC (2.8 mg/kg; s. c.) concomitantly with CCl4 for 6 weeks.

TFAS+DEN+CCl4 group: rats intoxicated with DEN and received TFAS (2.8 mg/kg; s. c.) concomitantly with CCl4 for 6 weeks.

Animals were sacrificed following the time frame from starting the experiment till the end of the 7th week.

Sample Collection

Blood samples were collected from the jugular vein and sera were separated. Rats were euthanized using thiopental (85 mg/kg; i. p.; Gonca, 2015). The liver was divided into 2 parts; one part was kept in 10% neutral formalin, whereas the second part was stored in −80°C. The measurements were performed by personnel that were blinded completely to the group status.

Assessment of Liver Functions

Serum liver enzymes activities; alanine aminotransferase (ALT), aspartate aminotransferase (AST) and alkaline phosphatase (ALP) were assessed using colorimetric commercially available assay kits (Biodiagnostic, Giza, Egypt) according to the manufacturer's instructions.

Determination of Liver Content of Tumor Necrosis Factor-alpha

Part of the frozen liver tissue was homogenized in phosphate buffer saline (PBS, pH 7.4) for the assessment of liver TNF-α content using ELISA specific kit (Ray Biotech, United States; ELR-TNFα). The parameter was assessed according to the manufacturer's protocol.

Determination of Liver Hydroxyproline Content

Liver hydroxyproline content was assessed using frozen liver tissue as previously described by Edwards and O'Brien (1980) with slight modifications. Briefly, liver samples were weighed and hydrolyzed in 2.5 ml of 6N HCl at 110°C for 18 h in Teflon coated tubes. The hydrolysate was centrifuged at 3000 rpm for 10 min; the pH of the supernatant was allocated to 7.4 and the absorbance was measured at 558 nm. Total hydroxyproline content was measured against a standard curve established with trans-4-hydroxy-L-proline (Sigma- Aldrich, St Louis, MO, United States).

Analysis of Tissue Factor, Transforming Growth Factor-1beta and Protease-Activated Receptors1 Gene Expression *via* qRT-PCR

Relative quantification of gene expression was performed by extraction of RNA from liver cells using TRIzol plus RNA purification kit (life technologies, Carlsbad, United States) according to the manufacturer's protocol. RNA was reverse transcribed using High Capacity cDNA Reverse Transcription Kit (Applied Biosystems, Foster, CA, United States). Quantification of TGF-1β and PAR1 PCR was carried out using Rotor-Gene Q 5 plex real-time Rotary analyzer (Corbett Life Science, United States). Quantification of TF RNA, TGF-1β RNA and PAR1 RNA was carried out using PCR fluorescence quantitative diagnostic kit, with SYBR Green PCR Master Mix (Applied Biosystems, United States). For quantification of TGF-1 β, the primers 5'-TACCATGCCAACTTCTGTCTGGGA-3' (forward primer) and 5'-ATGTTGACAACTGCTCCACCTTG-

3' (reverse primer) were normalized against β-actin 5'-ATCTGG CACCACACCTTC-3' (forward primer) and 5'-AGCCAGGTC CAGACGCA-3' (reverse primer). For quantification of PAR1, primers 5'-CTTGCTGATCGTCGCCC-3' (forward primer) and 5'-TTCACCGTAGCATCTGTCCT-3' (reverse primer) and for quantification of TF, primers 5'-ATGGCTATCCCCATG-3' (forward primer) and 5'-CATGGGGATAGCCAT-3' (reverse primer) were normalized against GADPH 5'-CTGCACCAC CAACTGCTTAC-3' (forward primer) and reverse 5'-CAG AGGTGCCATCCAGAGTT-3' (reverse primer).

Flow Cytometric Analysis of Toll-Like Receptor4

For detection of TLR4 cell surface expression, frozen liver tissue was homogenized then single-cell suspension was washed with staining buffer (PBS containing 1% FBS). Cells were then incubated with biotin-conjugated rat anti-human TLR4 antibody at a concentration of 20 ml/10^6 cells for 30 min on ice. After washing with staining buffer, the cells were mixed with Streptavidin-phycoerythrin and immediately analyzed with a flow cytometer FACScan and CellQuest Software.

Histopathological Examination of Liver With Collagen and Fibrosis Scoring

Liver samples preserved in 10% neutral formalin were washed under tap water; then serial dilutions of alcohol were used for dehydration. Specimens were cleared in xylene and embedded in paraffin. Sections at 4 μm thicknesses were prepared by slide microtome and stained with hematoxylin and eosin (H and E) and Masson's Trichome staining to examine liver histopathological and fibrotic changes. All histopathological examinations were performed by an experienced pathologist who was blinded to the study groups. All methods of tissue sample preparation and staining were carried out as outlined by Drury and Wallington (1983). Qualitative and quantitative scoring of collagen was performed using a full HD microscopic imaging system (Leica Microsystems GmbH, Germany) operated by Leica Application software. The total

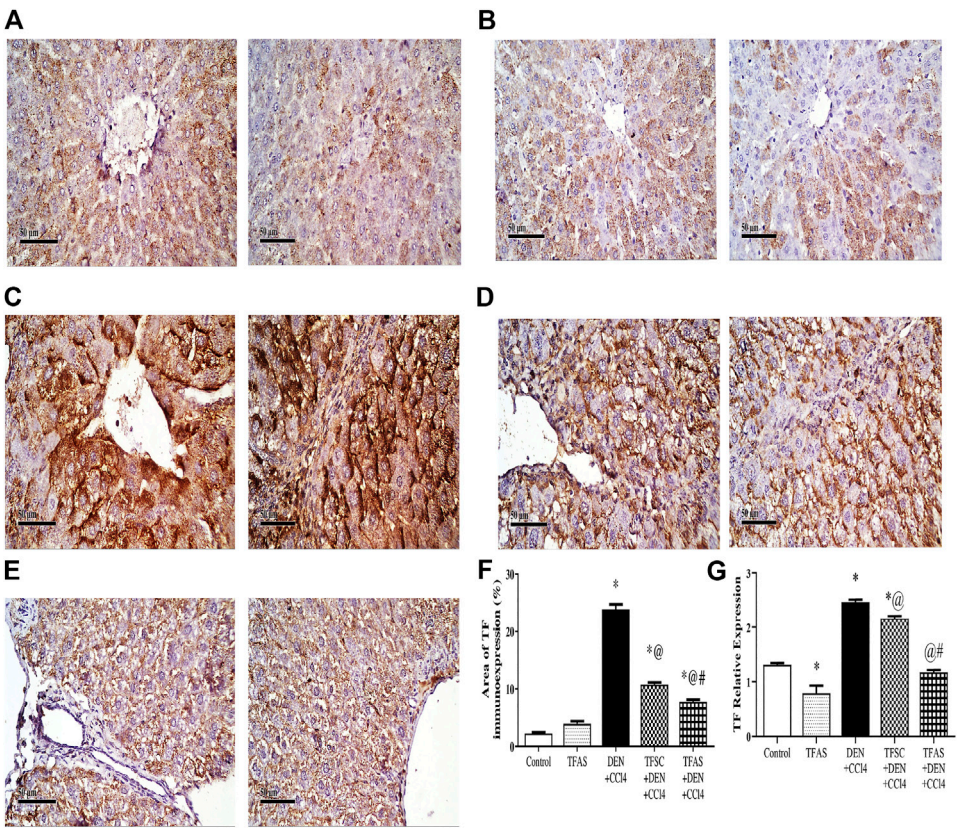


FIGURE 1 | Effect of TF-ODNs on the liver TF expression in DEN+CCl4 intoxicated rats. Immune-stained liver section of TF expression with positive stained grades of cytoplasmic and sub membranous positivity in numerous hepatocytes, **(A)** control group, **(B)** TFAS group, **(C)** DEN+CCl4 group, **(D)** TFSC+DEN+CCl4 group, **(E)** TFAS+DEN+CCl4 group and **(F)** The percentage area of TF immune-expression and **(G)** qPCR determined TF expression in all study groups. Data are expressed as mean ± SEM (n = 8). (*), (@) and (#) indicate significant difference from Control, DEN+CCl4 and TFSC+DEN+CCl4, respectively at $P < 0.05$ using one-way ANOVA followed by Tukey-Kramer post-Hoc test. TF: tissue factor; DEN: N-diethyl nitrosamine; CCl4: carbon tetrachloride; TFSC: scrambled tissue factor oligodeoxynucleotides; TFAS: antisense tissue factor oligodeoxynucleotides.

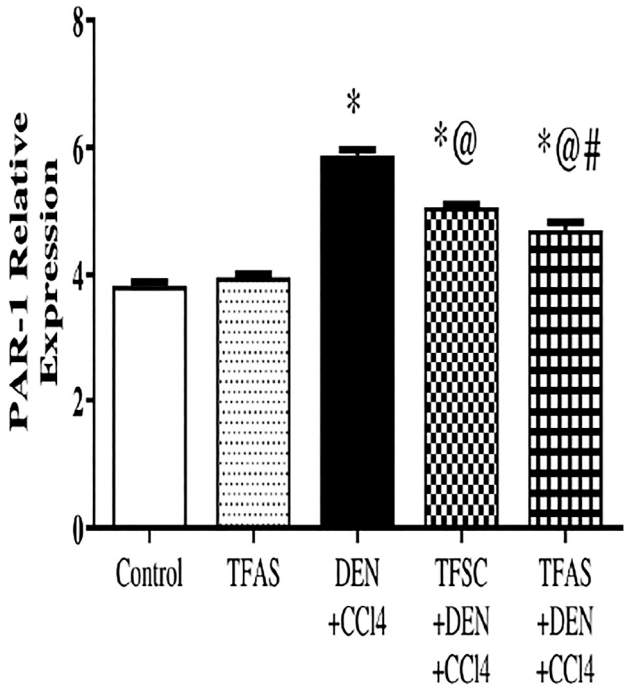


FIGURE 2 | Effect of TF-ODNs on relative expression of PAR1 in liver. Data are expressed as mean ± SEM (n = 8). (*), (@) and (#) indicate significant difference from Control, DEN+CCl4 and TFSC+DEN+CCl4, respectively at $P < 0.05$ using one-way ANOVA followed by Tukey-Kramer post-Hoc test. PAR1: protease activated receptor 1; DEN: N-diethyl nitrosamine; CCl4: carbon tetrachloride; TFSC: scrambled tissue factor oligodeoxynucleotides; TFAS: antisense tissue factor oligodeoxynucleotides.

specimen area and the blue-stained pixels (representing collagen) were segmented. Percent (%) collagen was calculated as the ratio of blue-stained to total specimen pixels. The criteria used for microscopic lesions and fibrosis scoring was listed as follows (Al-Sayed et al., 2019): (−), no lesions were demonstrated; (+), few lesions were demonstrated in one examines section; (++), mild lesions were focally demonstrated in some examined sections; (+++), moderate lesions were diffusely demonstrated in some examined sections; and (++++), severe lesions were diffused in all examined sections.

Immunohistochemical Staining of Alpha Smooth Muscle Actin and Tissue Factor in the Liver

According to the manufacturer's protocol, deparaffinized 4 µm thick tissue sections were treated with 3% H_2O_2 for 20 min, washed, then incubated with anti-alpha smooth muscle actin antibody and anti-tissue factor antibody overnight. Tissue sections were washed with PBS followed by incubation with secondary antibody HRP Envision kit (DAKO) for 20 min and incubated after washing with diaminobenzidine (DAB) for 10 min and then washed finally with PBS and hematoxylin was added for counter staining. Finally, tissue sections were dehydrated and cleared in xylene. Area percentage of immune-expression levels of α-SMA and TF sections were determined using Leica application module for tissue sections analysis attached to full HD microscopic imaging system (Leica Microsystems GmbH, Germany).

Statistical Analysis

Data analysis was carried out with complete blindness to the study group status. Results were expressed as mean ± SEM. Statistical significance was determined by one-way ANOVA followed by Tukey-Kramer post-Hoc test. P value < 0.05 was considered significant. In addition, correlation and linear regression between TF and the assessed parameters as well as between PAR1 and TLR4 were carried out where slope differences were compared, tested and checked for significance at P< 0.0001. Correlation Coefficient "r" was calculated where the difference in "r" value states that variation of one of the variables will affect the variation in the other one through R^2 calculation. GraphPad Prism 8 for Windows (GraphPad Software, Inc, La Jolla, United States) was used in all analyses.

RESULTS

Effect of Tissue Factor-Oligodeoxynucleotides on the Liver Tissue Factor Expression

Immunohistochemical detection of TF expression in liver sections of control and TFAS groups showed weak basal expression of TF (**Figures 1A,B**). However, liver sections of DEN+CCl4 intoxicated rats showed sharply stained positive grades of cytoplasmic and sub membranous positivity in numerous hepatocytes (**Figure 1C**). The liver sections from DEN+CCl4 intoxicated rats received TFSC showed decreased hepatocellular staining compared to the DEN+CCl4 intoxicated group (**Figure 1D**). Rats that received TFAS showed a profound decrease in TF expression (**Figure 1E**). Area of TF expression showed a significant increase in the DEN+CCl4 intoxicated rats by 943.48% comparing to the basal expression of the control group. Treatment of rats with TFSC and TFAS resulted in a significant decrease in the elevated TF expression by 54.16 and 67.92%, respectively in comparison to untreated intoxicated rats. TFAS treatment significantly decreased TF expression by 30% compared to TFSC treatment (**Figure 1F**).

TF expression was determined by qPCR that showed a significant decrease by 39.78% upon treatment with TFAS alone when compared to the control group. TF expression increased significantly in the DEN+CCl4 intoxicated group by 88.03% compared with control group. Treatment of rats with TFSC and TFAS decreased the elevated TF expression by 12.17 and 52.37%, respectively compared with intoxicated group. Intoxicated rats that were treated with TFAS treatment showed a significant decrease by 45.78% when compared to TFSC treatment (**Figure 1G**).

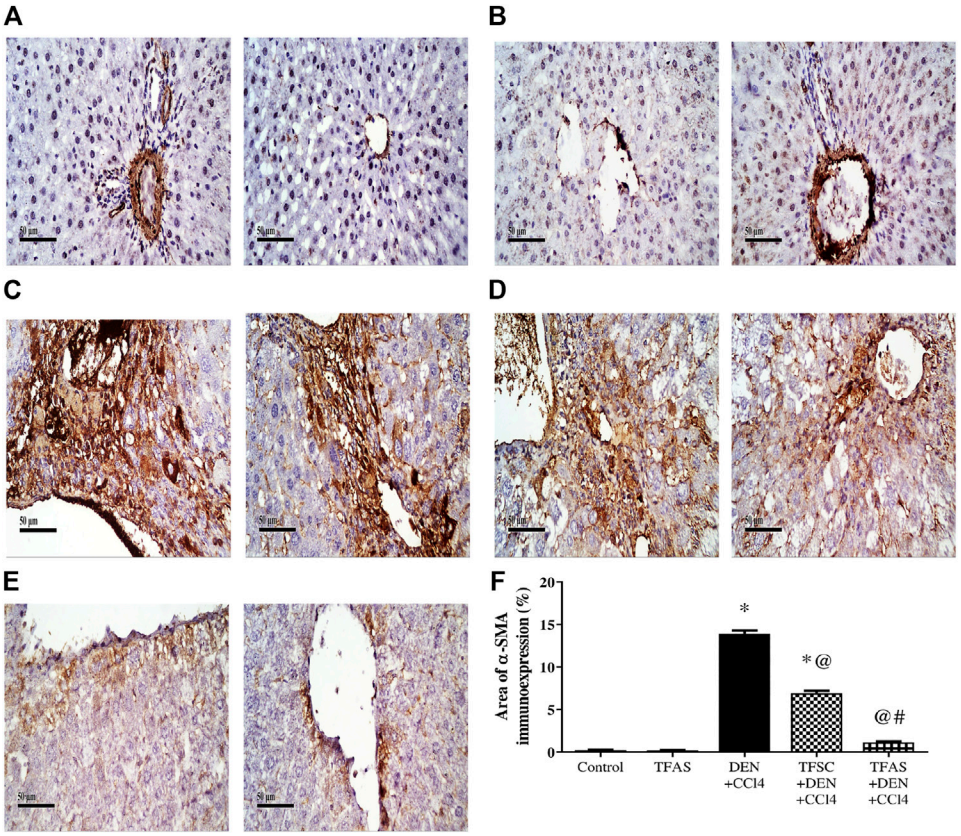


FIGURE 3 | Effect of TF-ODNs on liver α-SMA expression. Immune-stained liver section of α-SMA expression is detected in hepatic stellate cells, fibroblasts and vascular wall, **(A)** control group, **(B)** TFAS group, **(C)** DEN+CCl4 group, **(D)** TFSC+DEN+CCl4 group, **(E)** TFAS+DEN+CCl4 group and **(F)** The percentage of α-SMA expression. Data are expressed as mean ± SEM (n = 8). (*), (@) and (#) indicate significant difference from Control, DEN+CCl4 and TFSC+DEN+CCl4, respectively at $P < 0.05$ using one-way ANOVA followed by Tukey-Kramer post-Hoc test. α-SMA: alpha smooth muscle actin; DEN: N-diethyl nitrosamine; CCl4: carbon tetrachloride; TFSC: scrambled tissue factor oligodeoxynucleotides; TFAS: antisense tissue factor oligodeoxynucleotides.

Effect of Tissue Factor-Oligodeoxynucleotides on Protease-Activated Receptors1 Expression in Liver

PAR1 expression in the livers excised from DEN+CCl4 intoxicated rats was significantly increased by 55.26% compared to the control group. The treatment of intoxicated rats with TFSC and TFAS significantly decreased the elevated level of PAR1 by 13.56 and 20.34%, respectively compared to the DEN+CCl4 group and TFAS treatment manifested a significant decrease in PAR1 expression by 7.84% compared to TFSC (**Figure 2**).

Effect of Tissue Factor-Oligodeoxynucleotides on Liver Alpha-Smooth Muscle Actin Expression

Control and TFAS treated animals showed weak basal expression of α-SMA (**Figures 3A,B**). Rats intoxicated with DEN+CCl4 showed increased α-SMA expression with strongly stained hepatic cells, fibroblasts and vascular wall (**Figure 3C**). DEN+CCl4 intoxicated group treated with TFSC revealed a decreased area of α-SMA positive cells (**Figure 3D**). In the DEN+CCl4 intoxicated group treated with TFAS, the area of α-SMA expression was nearly similar to that of control animals (**Figure 3E**). Area of α-SMA stained liver cells showed a significant decrease with both TFSC and TFAS treatment when compared to DEN+CCl4 intoxicated animals by 50.71 and 91.43%, respectively. In addition, TFAS treatment showed a significant decrease in α-SMA expression by 82.61% compared to TFSC treatment of intoxicated rats (**Figure 3F**).

Effect of Tissue Factor-Oligodeoxynucleotides on Serum Activities of Alanine aminotransferase, Aspartate aminotransferase and Alkaline Phosphatase

As shown in **Figure 4**, serum activities of ALT (**A**), AST (**B**) and ALP (**C**) are elevated significantly upon DEN+CCl4 intoxication by 18.75, 48.28 and 29.17%, respectively compared to the control group. These elevations were significantly decreased in rats intoxicated with the DEN+CCl4 and treated with TFAS by 7.89, 19.77 and 8.06%, respectively, compared to the untreated

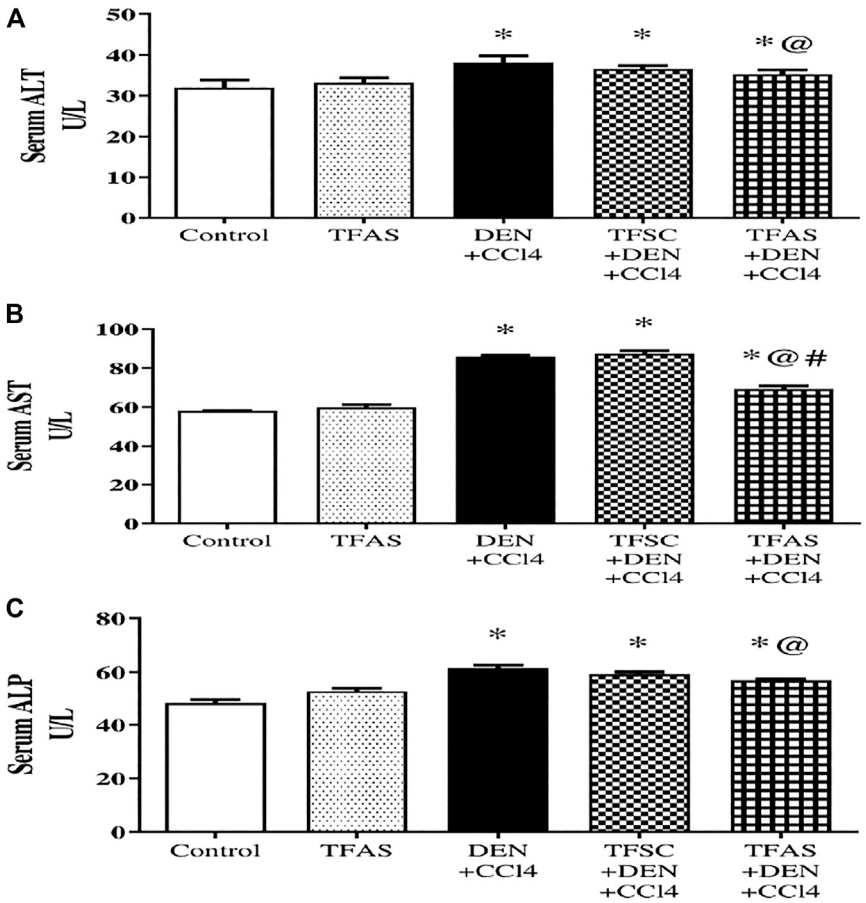


FIGURE 4 | Effect of TF-ODNs on serum activities of ALT, AST and ALP enzymes. Liver enzymes activities of ALT, AST and ALP are presented in figure **(A)**, **(B)** and **(C)**, respectively. Data are expressed as mean ± SEM (n = 8). (*), (@) and (#) indicate significant difference from Control, DEN+CCl4 and TFSC+DEN+CCl4, respectively at $P < 0.05$ using one-way ANOVA followed by Tukey-Kramer post-Hoc test. ALT: alanine aminotransferase; AST: aspartate aminotransferase; ALP: alkaline phosphatase; DEN: N-diethyl nitrosamine; CCl4: carbon tetrachloride; TFSC: scrambled tissue factor oligodeoxynucleotides; TFAS: antisense tissue factor oligodeoxynucleotides.

intoxicated rats. There was a non-significant difference in serum enzymes activities between the DEN+CCl4 group and that treated with TFSC. On the other hand, serum activity of AST was significantly improved in the intoxicated animals treated TFAS compared to those treated with TFSC.

Effect of Tissue Factor-Oligodeoxynucleotides on Histopathological Features

The control group of rats showed normal histology of the liver (**Figure 5A**) as well as apparent normal features in TFAS-treated rats (**Figure 5B**). However, rats intoxicated with DEN+CCl4 showed a severe loss in hepatic architecture (**Figure 5C**) where degeneration of hepatocytes, area of coagulative hepatocellular necrosis, sinusoidal dilatation, the proliferation of biliary epithelium with periportal infiltration of inflammatory cells in portal areas as well as fibroblastic proliferation and bridging were demonstrated in this group (**Table 1**). These histopathological alterations were moderately reduced in the group intoxicated and treated with TFAS (**Figure 5E**). In contrast, treatment with TFSC didn't significantly improve the histopathological features (**Figure 5D**).

Effect of Tissue Factor-Oligodeoxynucleotides on Collagen Deposition and Liver Hydroxyproline Content

Control and TFAS-treated normal rats showed uniform collagen distribution (**Figures 6A,B**). Animals intoxicated with DEN+CCl4 showed central vein, portal tract and septal fibrosis that were stained positively for collagen fiber bundles in Masson's Trichome stained liver sections (**Figure 6C**). Treatment with TFSC showed relatively decreased area of collagen accumulation in liver sections (**Figure 6D**) but animals treated with TFAS after intoxication restored collagen distribution nearly to the control rats (**Figure 6E**). The elevated area of collagen deposition in rats intoxicated with DEN+CCl4 was significantly declined with treatment with TFSC and TFAS by 61 and 80%, respectively. In

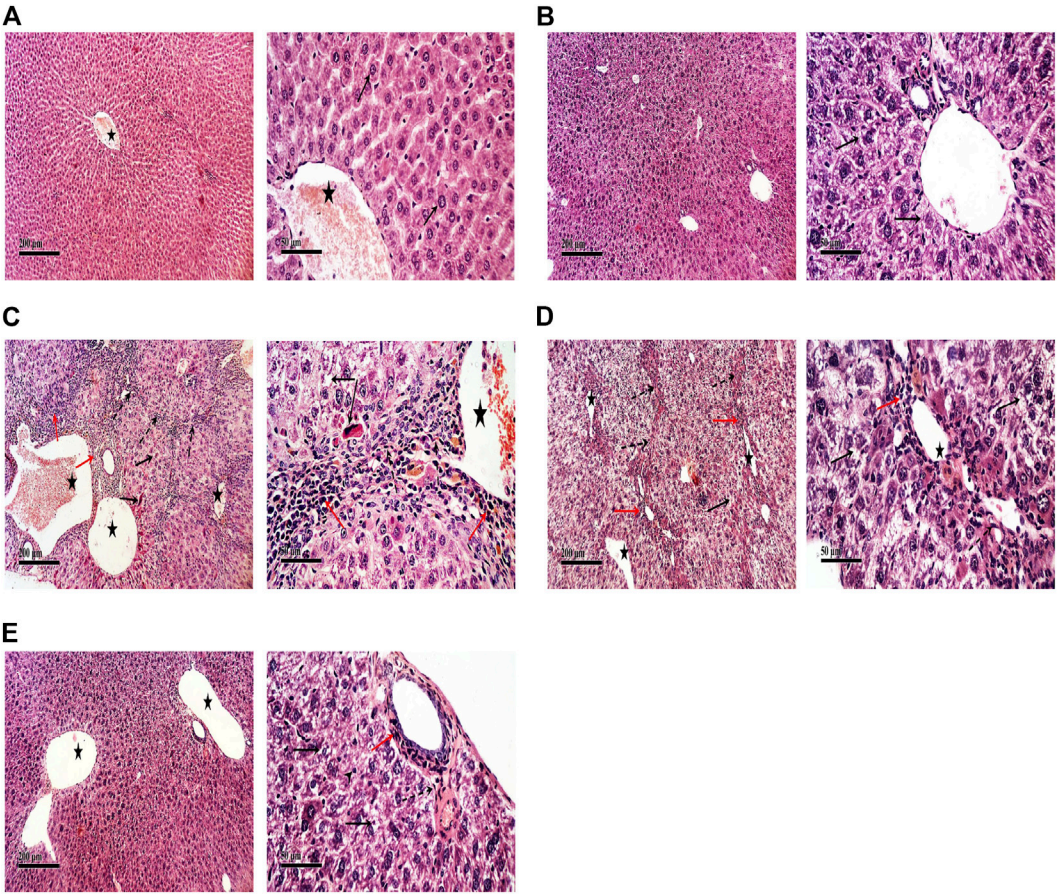


FIGURE 5 | Effect of DEN+CCl4 and TF-ODNs on histopathological features. **(A)** normal histologic structure showing central vein (star) from control group, **(B)** TFAS treated rats showing apparently normal histological features with minimal degenerative changes, **(C)** DEN+CCl4 intoxicated rats showing sever vacuolar degenerative and necrotic hepatocellular changes (black arrow) accompanied with many dilated liver blood vessels (star) and sever periportal inflammatory cells infiltrates (red arrow), **(D)** TFSC treated intoxicated rats showing slight amelioration of abnormal morphological changes with persistence of sever vacuolar degenerative of hepatocytes (arrow), **(E)** TFAS treated intoxicated rats showing moderate amelioration of morphological changes with dilated blood vessels and mild periportal inflammatory cells infiltrates (arrow head); DEN: N-diethyl nitrosamine; CCl4: carbon tetrachloride; TFSC: scrambled tissue factor oligodeoxynucleotides; TFAS: antisense tissue factor oligodeoxynucleotides.

TABLE 1 | Effect of TF-ODNs on liver histopathological and fibrotic changes.

Groups	Degenerative/necrotic changes	Inflammatory cells infiltrates	Fibroblastic proliferation and bridging	Dilated blood vessels
Control	–	–	–	–
TFAS	+	–	–	–
DEN+CCl4	++++	++++	++++	+++
TFSC+DEN+CCl4	++++	+++	+++	+++
TFAS+DEN+CCl4	+++	++	+	+++

– nil: no lesions were demonstrated; +: few lesions were demonstrated in one examined section; ++: mild lesions were focally demonstrated in some examined section; +++: moderate lesions were diffusely demonstrated in some examined section; ++++: severe lesions were diffused in all examined sections.

addition, TFAS showed a more significant decrease by 48.72% compared to rats treated with TFSC (**Figure 6F**). Animals intoxicated with DEN+CCl4 showed a significant increase in liver hydroxyproline content by 42.7% compared to the control group. In contrast to collagen deposition, treatment with TFSC didn't show significant difference in hydroxyproline content, while TFAS showed a significant decrease by 10.68% compared to DEN+CCl4 intoxicated group (**Figure 6G**).

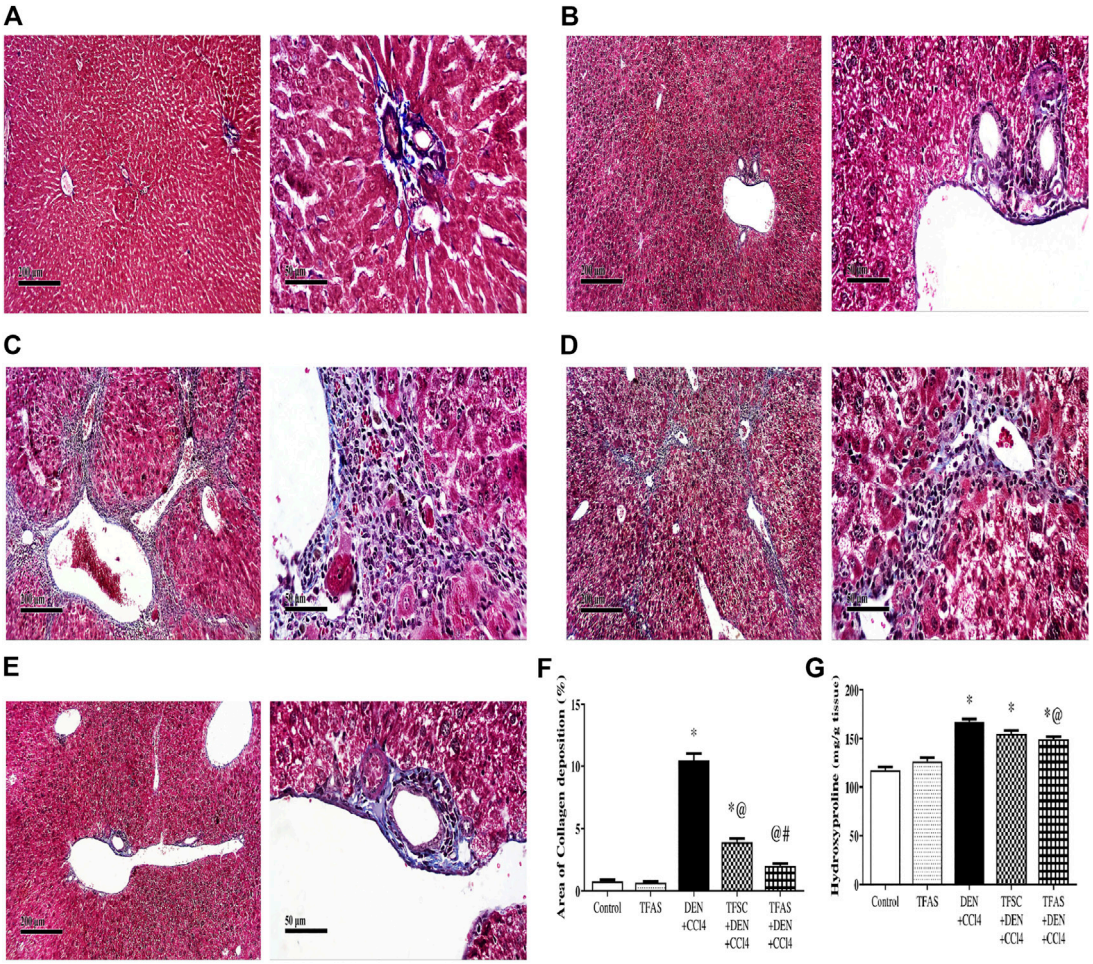


FIGURE 6 | Effect of TF-ODNs on collagen deposition and hydroxyproline content in the liver. **(A)** Masson's Trichome-stained liver section of control group, **(B)** TFAS group, **(C)** DEN+CCl4 group where obvious periportal proliferation of fibroblasts are detected as well as bridging of fibroblasts with abundant formation of collagen fibers, **(D)** TFSC+DEN+CCl4 group and **(E)** TFAS+DEN+CCl4 group showed significant reduction of activated fibroblasts and collagen fibers, **(F)** Percentage area of collagen deposition and **(G)** liver hydroxyproline content in different study groups. Data are expressed as mean ± SEM (n = 8). (*), (@) and (#) indicate significant difference from Control, DEN+CCl4 and TFSC+DEN+CCl4, respectively at $P < 0.05$ using one-way ANOVA followed by Tukey-Kramer post-Hoc test. DEN: N-diethyl nitrosamine; CCl4: carbon tetrachloride; TFSC: scrambled tissue factor oligodeoxynucleotides; TFAS: antisense tissue factor oligodeoxynucleotides.

Effect of Tissue Factor-Oligodeoxynucleotides Effect on Toll-Like Receptor4 Expression in the Liver

Flow cytometric analysis revealed low TLR4 expression on liver cells in the control group as well as TFAS treated normal rats (**Figures 7A,B,F**). Rats intoxicated with DEN+CCl4 showed significant increase in TLR4 expression by 386.67% (**Figures 7C,F**). The intoxicated group treated with TFAS showed a significant reduction in the expression of TLR4 by 47.95% (**Figures 7E,F**). Also, TLR4 expression was significantly decreased in intoxicated group with TFAS treatment by 39.68% compared to TFSC treated one.

Effect of Tissue Factor-Oligodeoxynucleotides on Transforming Growth Factor-1beta Expression and Tumor Necrosis Factor-alpha Content

Induction of liver fibrosis by DEN+CCl4 significantly raised liver TGF-1β expression and TNF-α content by 39.44 and 66.64%, respectively compared to the control group. Treatment with TFAS significantly decreased the elevated levels of liver TGF-1β expression and TNF-α content by 18.18 and 25.43%, respectively. Also, TGF-1β expression and TNF-α content significantly decreased by 12.91 and 18.34%, respectively in TFAS treated intoxicated group compared to the TFSC treatment (**Figure 8A** and **Figure 8B**).

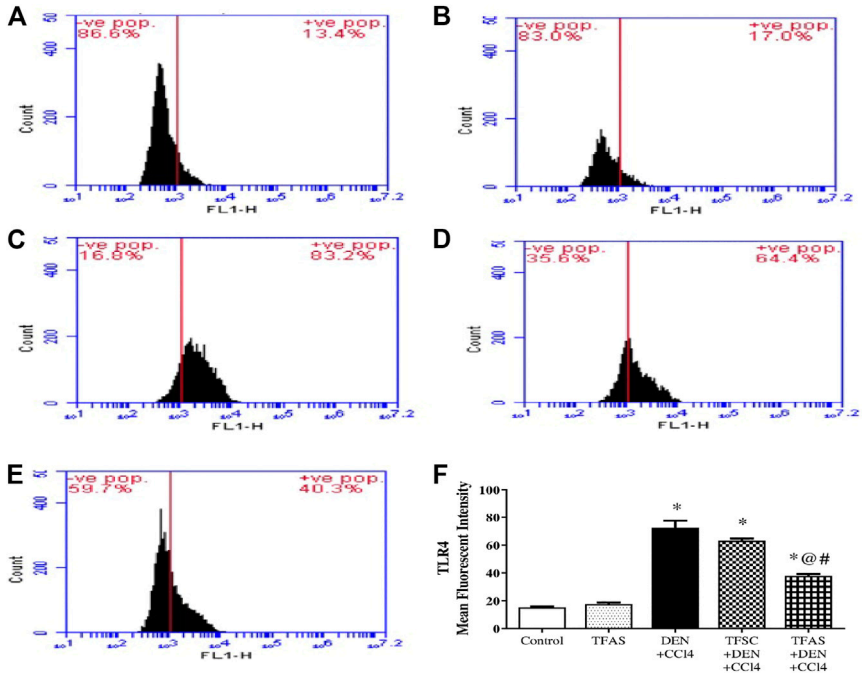


FIGURE 7 | Flow cytometric analysis of the effect of TF-ODNs on TLR4 expression in the liver. Histogram plots of **(A)** Control group, **(B)** TFAS group, **(C)** DEN+CCl4 group, **(D)** TFSC+DEN+CCl4, **(E)** TFAS+DEN+CCl4 and **(F)** Mean fluorescence intensity of TRL4. Data are expressed as mean ± SEM (n = 8). (*), (@) and (#) indicate significant difference from Control, DEN+CCl4 and TFSC+DEN+CCl4, respectively at $P < 0.05$ using one-way ANOVA followed by Tukey-Kramer post-Hoc test. TLR4: toll like receptor 4; DEN: N-diethyl nitrosamine; CCl4: carbon tetrachloride; TFSC: scrambled tissue factor oligodeoxynucleotides; TFAS: antisense tissue factor oligodeoxynucleotides.

Correlation Between Tissue Factor and the Assessed Liver Enzymes Activities, Inflammatory and Fibrotic Markers as Well as Between Protease-Activated Receptors1 and Toll-Like Receptor4 Expression

Figure 9 shows the scatter plot of the positive correlation between TF expression and the assessed parameters; ALT, AST and ALP enzyme activities (**Figure 9A**). There is also a positive correlation between TF expression and the fibrotic markers; α-SMA and PAR1 (**Figure 9B**) as well as collagen and hydroxyproline (**Figure 9C**). A positive correlation was displayed also between TF expression and remodeling and inflammatory markers; TLR4 (**Figure 9D**), TGF-1β (**Figure 9E**) and TNF-α (**Figure 9F**). Also, there is a positive correlation between TLR4 and PAR1 expression (**Figure 9G**) in all study groups.

DISCUSSION

TF is the transmembrane receptor for FVII/VIIa and the TF-FVIIa complex functions as the primary initiator of coagulation *in vivo*. TF is also recognized as a signaling receptor in different pathological conditions such as angiogenesis, tumor, inflammation and fibrogenesis (Lento et al., 2015). In normal liver, TF has been reported to be expressed primarily by hepatocytes (Sullivan et al., 2013) as well as HSCs, SECs and Kupffer cells (Arai et al., 1995).

In accordance with previous studies, liver fibrosis is induced in rats by co-administration of DEN and CCl4 (Uehara et al., 2013; Uehara et al., 2014; Marrone et al., 2016; Sung et al., 2018). Liver sections excised from animals intoxicated with DEN+CCl4 had intense TF staining in hepatocellular cytoplasm. In accordance with these results, overexpression and a profound role of TF have been reported in different models of chemically induced liver injury (Hammad et al., 2011; Abdel-Bakky et al., 2020), including CCl4-induced fibrosis (Duplantier et al., 2004). Furthermore, Knight et al. (2017) reported that mice with deletion of the cytoplasmic TF domain had amelioration of liver fibrosis compared to wild type mice following 8 weeks of CCl4 exposure. Thus, the overexpression of TF observed in this study and the previously reported implementation of TF in the pathogenesis of different models of liver injuries rose the assumption that targeting TF could be of benefit in managing liver fibrosis.

TF-ODNs were reported to inhibit TF production at both transcriptional and translational levels (Yin et al., 2010; Hammad et al., 2013). In addition, TF-ODNs have been reported to be accumulated predominantly in the rat liver following systemic administration (Nakamura et al., 2002; Shimizu et al., 2014). Indeed, in this study, subcutaneous injection of TFAS significantly inhibited the elevated expression of TF in different liver cells. Similarly, Abdel-Bakky et al. (2011);

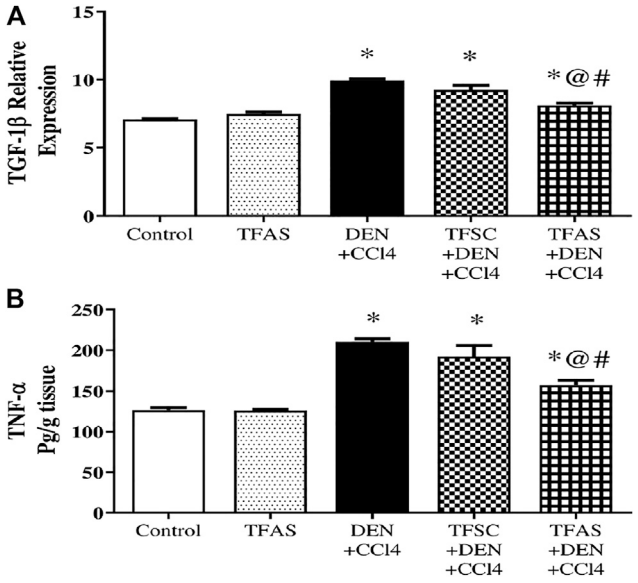


FIGURE 8 | Effect of TF-ODNs on TGF-1β expression and TNF-α content. Data are expressed as mean ± SEM (n = 8). (*), (@) and (#) indicate significant difference from Control, DEN+CCl4 and TFSC+DEN+CCl4, respectively at $P < 0.05$ using one-way ANOVA followed by Tukey-Kramer post-Hoc test. TGF-1β: transforming growth factor beta; TNF-α: tumor necrosis factor alpha; DEN: N-diethyl nitrosamine; CCl4: carbon tetrachloride; TFSC: scrambled tissue factor oligodeoxynucleotides; TFAS: antisense tissue factor oligodeoxynucleotides.

Abdel-Bakky et al. (2015) and Abdel-Bakky et al. (2020) reported significant changes in TF expression pattern in the liver sections excised from mice intoxicated with thioacetamide and CCl4 upon treatment with TFAS.

In this study animals intoxicated with DEN+CCl4 showed significant elevation in the activities of liver enzymes; ALT, AST and ALP along with severe histopathological deterioration of the liver. These observations are consistent with previous findings that animals treated with CCl4 or DEN+CCl4 showed pronounced biochemical and histopathological fibrotic alterations (Poojari et al., 2010; Uehara et al., 2013; Serag et al., 2019; Tripathy et al., 2020). However, treatment with TFAS significantly improved the abnormal activities of liver enzymes and the histopathological inflammatory and fibrotic changes associated with DEN+CCl4 intoxication. The improvement in enzyme activities is positively correlated with TF expression. In agreement with our findings, blockage of TF expression using TFAS improved histopathological and biochemical deteriorations in chemically intoxicated mice (Hammad et al., 2013; Abdel-Bakky et al., 2015 and Abdel-Bakky et al., 2020). Moreover, Luyendyk et al. (2010) demonstrated that liver macrophage and neutrophil aggregation were significantly reduced in mice with low TF expression compared to heterozygous control mice fed diet deficient in methionine and choline.

The distinguished role of HSCs in liver fibrosis was previously documented (Kisseleva and Brenner, 2021). The extent of HSCs activation and proliferation rates is indicated by the expression of characteristic specific receptors such as α-SMA (Jiang and Torok, 2013; Lin et al., 2018) and excessive production of collagen, where the deposition of collagen fibrils in liver connective tissues provides a hallmark of liver fibrosis development (Hernandez-Gea and Friedman, 2011; Bai et al., 2013). The stability of collagen fibrils is maintained by deposition of hydroxyproline amino acid, which is commonly applied as a marker for fibrogenesis and directly correlated with the total collagen and the stage of liver fibrosis (Ding et al., 2017). In the current study, DEN+CCl4-intoxicated rats showed increased α-SMA expression, collagen production and elevation of liver hydroxyproline content. These results indicated a profound activation of HSCs in response to DEN+CCl4 intoxication. Similarly, previous studies showed that α-SMA expression as well as collagen and hydroxyproline content were significantly elevated in response to injection with CCl4 alone or in combination with DEN (Mansour et al., 2010; Abdel-Moneim et al., 2015; Ahmed and Tag, 2017).

In addition to HSCs, activated Kupffer cells and infiltrated macrophages play a pivotal role in liver fibrogenesis. Activated macrophages release TGF-1β which, among growth factors, is the "master" modulator in fibrogenesis and involved in HSCs activation (Nakazato et al., 2010; Meng et al., 2016). Furthermore, they release, among other proinflammatory cytokines, TNF-α which is one of the early events in many types of liver damage and can activate HSCs and modulate innate immune and inflammatory responses (Gupta et al., 2019). In the present study, liver content of both TGF-1β and TNF-α were significantly increased upon administration of DEN+CCl4, the results that are in accordance with that reported by Tork et al. (2016), Elguindy et al. (2016) and Knight et al. (2017).

The role of coagulation proteases in liver fibrosis was recently explored. One of the primary mechanisms whereby coagulation proteases could contribute to liver fibrosis is through direct activation of HSCs. In support of this hypothesis, we found that the expression of TF is positively correlated with HSCs activation markers; α-SMA, collagen and hydroxyproline. Furthermore, these markers were significantly decreased upon TFAS treatment; these findings are consistent with Knight et al., (2017), as the authors suggested that activation of the cytoplasmic domain of TF promoted liver fibrosis by inducing HSCs activation.

Another mechanism that could underlie the pathological role of TF in liver fibrosis is via stimulation of local inflammatory cell activity. Macrophages were reported to express TF which is upregulated during macrophage maturation and fibrogenesis (Knight et al., 2017). In the present study, TFAS significantly reduced the elevated content of TGF-1β and TNF-α; the main products of inflammatory cells accompanied with fibrosis. Furthermore, our study showed a positive correlation between TF and each of TGF-1β and TNF-α. Consequently, we could assume that in addition to inhibition of HSCs, TFAS decrease TGF-1β and TNF-α production with subsequent inhibition of fibrogenesis and inflammation. In the line with our findings, Knight et al. (2017) reported that deletion of the TF cytoplasmic domain significantly lower gene and protein expression of TGF-1β by activated Kupffer cells.

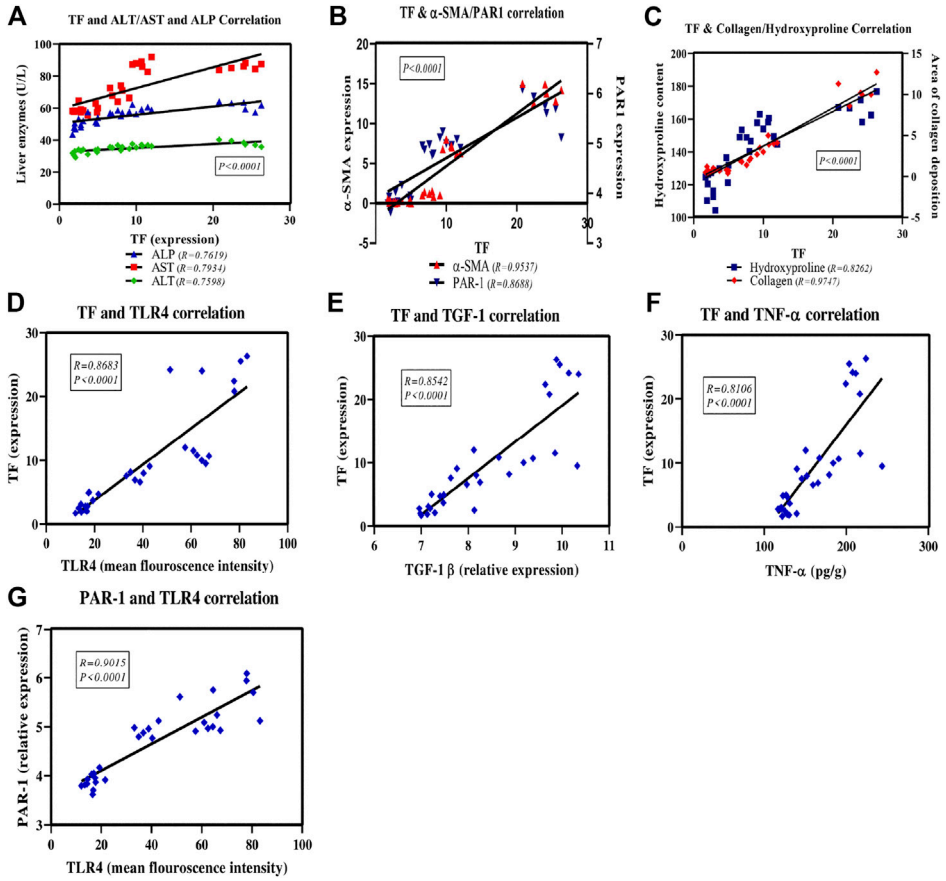


FIGURE 9 | Scatter plots of the correlation between TF and the assessed liver enzymes activities, inflammatory and fibrotic markers as well as between PAR1 and TLR4 expression. The solid lines represent the linear regression and correlation coefficient (r), P is the correlation significance level.

Since inflammation and coagulation are crosslinked with liver fibrosis and given the principal roles of TLR4 and PAR1 in inflammation and coagulation, respectively, we hypothesized that TLR4-TF-PAR1 axis would be a novel pathway involved in the pathogenesis of liver fibrosis and targeting that pathway could underlie the therapeutic benefits of TFAS.

Several studies have explored the role of PARs in liver fibrogenesis (Borensztajn et al., 2010). In chronic liver disease, HSCs express upregulated PAR1 (Fiorucci et al., 2004). Furthermore, it was found that removal of stellate cell-specific PAR1 produced a 35% reduction in the accumulation of liver collagen (Poole et al., 2020) and PAR1 deficient mice appeared to be protected from CCl4-induced liver fibrosis (Rullier et al., 2008; Kallis et al., 2014). In the line with these findings, the current study showed that PAR1 expression was significantly increased in the DEN+CCl4 intoxicated rats.

TLR4 is a main receptor involved in different inflammatory processes (Lucas and Maes, 2013). A crucial role of TLR4 in fibrogenesis was highlighted in experiment where TLR4 mutant mice showed decreased liver fibrosis in response to toxic agents (Seki et al., 2007; El-Kashef and Serrya, 2019). Furthermore, Liang et al. (2016) demonstrated that HSCs activation and proliferation were prohibited through suppression of TLR4 signaling pathway in DEN-induced liver fibrosis. In accordance with these studies, we reported that liver fibrosis induced by DEN+CCl4 injection was associated with significantly increased expression of TLR4 in the liver tissue.

The contribution of both PAR1 and TLR4 in the beneficial effects of TF blockage was clarified in this study, as rats received TFAS showed a significant reduction in the expression of both PAR1 and TLR4 in liver cells. These findings shed the light on the possibility of crosslinking among the three receptors in controlling liver fibrosis.

Thrombin is produced mainly through cleavage of prothrombin by TF (Mann et al., 2003) and blockage of TF expression resulted in decreased thrombin production (Carraway et al., 2003). Thrombin was reported to produce a dual effect on liver fibrosis via action on PAR1 and through TLR4. Firstly, it was proclaimed that thrombin activates PAR1 on both HSCs and Kupffer cells with subsequent progression of fibrosis (Fiorucci et al., 2004; Rullier et al., 2008). Secondly, thrombin was reported as a critical mediator in LPS-induced liver damage (Rondina et al., 2011) and gut-derived-LPS through TLR4 activation was significantly involved in CCl4-induced liver fibrosis (Seki et al., 2007; Rondina et al., 2011; Wang et al., 2020). Accordingly, blockage of thrombin formation through inhibition of TF

could diminish the roles of both PAR1 and TLR4 in the fibrogenic process.

Consequently, based on our findings and the previous studies, we can assume that inhibition of TF expression could censor the downstream production of thrombin with subsequent inhibition of PAR1 and TLR4 mediated fibrogenic and inflammatory process. On the other hand, we can assume that the improvement in the fibrosis observed with TFAS treatment could be reflected in the reduced expression of receptors upregulated under the pathological condition of fibrosis including PAR1 and TLR4.

Notably, the results of this study showed that control oligonucleotides; TFSC resulted in a significant reduction in the expression of TF, PAR1, α-SMA and collagen, although it was significantly less when compared with the effect observed with TFAS. On the other hand, TFSC didn't affect the level of the other assessed parameters compared to DEN+CCl4 group. These results indicate that TFSC may have some specificity towards the TF mRNA binding site and the decreased expression of PAR1, α-SMA and collagen could be the consequences of TFSC-induced inhibition of TF expression. In support of our explanation, it has been reported that various degrees of downregulation of gene expression have been observed with different types of control oligonucleotides that depend on the nature of the used control oligonucleotides, i.e., its base composition, sequence and/or nature of the backbone (Agrawal, 1996).

CONCLUSION

The current study established, for the first time to our knowledge, the potential crosstalk between TF, PAR1 and TLR4 in liver fibrosis. The positive correlation between blockage of TF expression and the downregulation of both PAR1 and TLR4 provides support for the solid crosslink between the receptors. Furthermore, this study reported that blockage of TF expression and gene silencing, using TFAS, reduced liver damage and improved fibrotic changes associated with CCl4+DEN intoxication. These findings offer a platform on which recovery from liver fibrosis could be mediated through targeting TF expression as a key factor in fibrogenesis. Future mechanistic and preclinic studies are recommended to support our findings.

DATA AVAILABILITY STATEMENT

The original contributions presented in the study are included in the article/**Supplementary Material**, further inquiries can be directed to the corresponding author.

ETHICS STATEMENT

The animal study was reviewed and approved by Research Ethics Committee (REC) of Faculty of Pharmacy, Cairo University, Egypt.

AUTHOR CONTRIBUTIONS

MS, ME-N, MT, RA, and SK contributed to conception and design of the study. MS and ME-N organized the database. ME-N and MS performed the statistical analysis. ME-N and MS wrote the first draft of the manuscript. MS, ME-N, MT, and RA wrote sections of the manuscript. All authors contributed to manuscript revision, read, and approved the submitted version.

SUPPLEMENTARY MATERIAL

The Supplementary Material for this article can be found online at: https://www.frontiersin.org/articles/10.3389/fphar.2021.676608/full#supplementary-material

REFERENCES

Abdel-Bakky, M. S., Hammad, M. A., Walker, L. A., and Ashfaq, M. K. (2011). Tissue Factor Dependent Liver Injury Causes Release of Retinoid Receptors (RXR-α and RAR-α) as Lipid Droplets. *Biochem. Biophysical Res. Commun.* 410 (1), 146–151. doi:10.1016/j.bbrc.2011.05.127

Abdel-Bakky, M. S., Helal, G. K., El-Sayed, E. M., Alhowail, A. H., Mansour, A. M., Alharbi, K. S., et al. (2020). Silencing of Tissue Factor by Antisense Deoxyoligonucleotide Mitigates Thioacetamide-Induced Liver Injury. *Naunyn-schmiedeberg's Arch. Pharmacol.* 393, 1887–1898. doi:10.1007/s00210-020-01896-0

Abdel-Bakky, M. S., Helal, G. K., El-Sayed, E. M., and Saad, A. S. (2015). Carbon Tetrachloride-Induced Liver Injury in Mice is Tissue Factor Dependent. *Environ. Toxicol. Pharmacol.* 39 (3), 1199–1205. doi:10.1016/j.etap.2015.02.012

Abdel-Moneim, A. M., Al-Kahtani, M. A., El-Kersh, M. A., and Al-Omair, M. A. (2015). Free Radical-Scavenging, Anti-inflammatory/anti-fibrotic and Hepatoprotective Actions of Taurine and Silymarin against CCl4 Induced Rat Liver Damage. *PLoS ONE* 10 (12), e0144509. doi:10.1371/journal.pone.0144509

Agrawal, S. (1996). Antisense Oligonucleotides: Towards Clinical Trials. *Trends Biotechnology* 14 (10), 376–387. doi:10.1016/0167-7799(96)10053-6

Ahmed, A., Hassanin, A., Hassan, A., Ali, S., and El-Anwar, A. (2017). Therapeutic Effects of Milk Thistle Extract against Renal Toxicity Induced by Diethylnitrosamine and Carbon Tetrachloride in Adult Rats. *J. Vet. Anat.* 10 (1), 107–124. doi:10.21608/jva.2017.37166

Al-Sayed, E., Abdel-Daim, M. M., and Khattab, M. A. (2019). Hepatoprotective Activity of Praecoxin a Isolated from Melaleuca Ericifolia against Carbon Tetrachloride-induced Hepatotoxicity in Mice. Impact on Oxidative Stress, Inflammation, and Apoptosis. *Phytotherapy Res.* 33 (2), 461–470. doi:10.1002/ptr.6242

Arai, M., Mochida, S., Ohno, A., Ogata, I., Obama, H., Maruyama, I., et al. (1995). Blood Coagulation Equilibrium in Rat Liver Microcirculation as Evaluated by Endothelial Cell Thrombomodulin and Macrophage Tissue Factor. *Thromb. Res.* 80 (2), 113–123. doi:10.1016/0049-3848(95)00157-M

Bai, T., Lian, L.-H., Wu, Y.-L., Wan, Y., and Nan, J.-X. (2013). Thymoquinone Attenuates Liver Fibrosis via PI3K and TLR4 Signaling Pathways in Activated Hepatic Stellate Cells. *Int. Immunopharmacol.* 15 (2), 275–281. doi:10.1016/j.intimp.2012.12.020

Bennett, C. F., and Swayze, E. E. (2010). RNA Targeting Therapeutics: Molecular Mechanisms of Antisense Oligonucleotides as a Therapeutic Platform. *Annu. Rev. Pharmacol. Toxicol.* 50, 259–293. doi:10.1146/annurev.pharmtox.010909.105654

Benyon, R. C., and Iredale, J. P. (2000). Is Liver Fibrosis Reversible?. *Gut* 46 (4), 443–446. doi:10.1136/gut.46.4.443

Beutler, B. (2004). Inferences, Questions and Possibilities in Toll-like Receptor Signalling. *Nature* 430 (6996), 257–263. doi:10.1038/nature02761

Borensztajn, K., Von Der Thüsen, J. H., Peppelenbosch, M. P., and Spek, C. A. (2010). The Coagulation Factor Xa/protease Activated Receptor-2 axis in the Progression of Liver Fibrosis: A Multifaceted Paradigm. *J. Cell. Mol. Med.* 14 (1–2), 143–153. doi:10.1111/j.1582-4934.2009.00980.x

Calvaruso, V., Maimone, S., Gatt, A., Tuddenham, E., Thursz, M., Pinzani, M., et al. (2008). Coagulation and Fibrosis in Chronic Liver Disease. *Gut* 57 (12), 1722–1727. doi:10.1136/gut.2008.150748

Camerer, E., Huang, W., Coughlin, S. R., and Majerus, P. W. (2000). Tissue Factor- and Factor X-dependent Activation of Protease-Activated Receptor 2 by Factor VIIa. *Proc. Natl. Acad. Sci.* 97 (10), 5255–5260. doi:10.1073/pnas.97.10.5255

Carraway, M. S., Welty-Wolf, K. E., Miller, D. L., Ortel, T. L., Idell, S., Ghio, A. J., et al. (2003). Blockade of Tissue Factor. *Am. J. Respir. Crit. Care Med.* 167 (9), 1200–1209. doi:10.1164/rccm.200204-287OC

Chery, J. (2016). RNA Therapeutics: RNAi and Antisense Mechanisms and Clinical Applications. *Postdoc J.* 4 (7), 35. doi:10.14304/surya.jpr.v4n7.5

Chi, K. N., Eisenhauer, E., Fazli, L., Jones, E. C., Goldenberg, S. L., Powers, J., et al. (2005). A Phase I Pharmacokinetic and Pharmacodynamic Study of OGX-011, a 2′-Methoxyethyl Antisense Oligonucleotide to Clusterin, in Patients with Localized Prostate Cancer. *J. Natl. Cancer Inst.* 97 (17), 1287–1296. doi:10.1093/jnci/dji252

Coughlin, S. R. (2000). Thrombin Signalling and Protease-Activated Receptors. *Nature* 407 (6801), 258–264. doi:10.1038/35025229

Ding, Y.-F., Wu, Z.-H., Wei, Y.-J., Shu, L., and Peng, Y.-R. (2017). Hepatic Inflammation-Fibrosis-Cancer axis in the Rat Hepatocellular Carcinoma Induced by Diethylnitrosamine. *J. Cancer Res. Clin. Oncol.* 143 (5), 821–834. doi:10.1007/s00432-017-2364-z

Drury, R. A. B., and Wallington, E. A. (1983). *Carleton's Histological Technique*. 5th edn. New York: Churchill Livingstone. doi:10.4095/315163

Duplantier, J. G., Dubuisson, L., Senant, N., Freyburger, G., Laurendeau, I., Herbert, J. M., et al. (2004). A Role for Thrombin in Liver Fibrosis. *Gut* 53 (11), 1682–1687. doi:10.1136/gut.2003.032136

Edwards, C. A., and O'Brien, W. D. (1980). Modified Assay for Determination of Hydroxyproline in a Tissue Hydrolyzate. *Clinica Chim. Acta* 104 (2), 161–167. doi:10.1016/0009-8981(80)90192-8

El-Kashef, D. H., and Serrya, M. S. (2019). Sitagliptin Ameliorates Thioacetamide-Induced Acute Liver Injury via Modulating TLR4/NF-KB Signaling Pathway in Mice. *Life Sci.* 228, 266–273. doi:10.1016/j.lfs.2019.05.019

Elguindy, N. M., Yacout, G. A., El Azab, E. F., and Maghraby, H. K. (2016). Chemoprotective Effect of Elettaria Cardamomum against Chemically Induced Hepatocellular Carcinoma in Rats by Inhibiting NF-Kb, Oxidative Stress, and Activity of Ornithine Decarboxylase. *South Afr. J. Bot.* 105, 251–258. doi:10.1016/j.sajb.2016.04.001

Fiorucci, S., Antonelli, E., Distrutti, E., Severino, B., Fiorentina, R., Baldoni, M., et al. (2004). PAR1 Antagonism Protects Against Experimental Liver Fibrosis. Role of Proteinase Receptors in Stellate Cell Activation. *Hepatology* 39 (2), 365–375. doi:10.1002/hep.20054

Gagnon, K. T., and Corey, D. R. (2019). Guidelines for Experiments Using Antisense Oligonucleotides and Double-Stranded RNAs. *Nucleic Acid Ther.* 29 (3), 116–122. doi:10.1089/nat.2018.0772

Giesen, P. L. A., Rauch, U., Bohrmann, B., Kling, D., Roqué, M., Fallon, J. T., et al. (1999). Blood-borne Tissue Factor: Another View of Thrombosis. *Proc. Natl. Acad. Sci.* 96 (5), 2311–2315. doi:10.1073/pnas.96.5.2311

Gonca, E. (2015). Comparison of Thiopental and Ketamine+xylazine Anesthesia Inischemia/reperfusion-Induced Arrhythmias in Rats. *Turk J. Med. Sci.* 45 (6), 1413–1420. doi:10.3906/sag-1403-25

Gupta, G., Khadem, F., and Uzonna, J. E. (2019). Role of Hepatic Stellate Cell (HSC)-derived Cytokines in Hepatic Inflammation and Immunity. *Cytokine* 124, 154542. doi:10.1016/j.cyto.2018.09.004

Hammad, M. A., Abdel-Bakky, M. S., Walker, L. A., and Ashfaq, M. K. (2011). Oxidized Low-Density Lipoprotein and Tissue Factor Are Involved in Monocrotaline/lipopolysaccharide-Induced Hepatotoxicity. *Arch. Toxicol.* 85 (9), 1079–1089. doi:10.1007/s00204-011-0649-6

Hammad, M. A., Abdel-Bakky, M. S., Walker, L. A., and Ashfaq, M. K. (2013). Tissue Factor Antisense Deoxyoligonucleotide Prevents Monocrotaline/LPS Hepatotoxicity in Mice. *J. Appl. Toxicol.* 33 (8), 774–783. doi:10.1002/jat.2728

Hernandez-Gea, V., and Friedman, S. L. (2011). Pathogenesis of Liver Fibrosis. *Annu. Rev. Pathol. Mech. Dis.* 6, 425–456. doi:10.1146/annurev-pathol-011110-130246

Huang, H., Shiffman, M. L., Friedman, S., Venkatesh, R., Bzowej, N., Abar, O. T., et al. (2007). A 7 Gene Signature Identifies the Risk of Developing Cirrhosis in Patients with Chronic Hepatitis C. *Hepatology* 46 (2), 297–306. doi:10.1002/hep.21695

Jabs, D. A., and Griffiths, P. D. (2002). Fomivirsen for the Treatment of Cytomegalovirus retinitis. *Am. J. Ophthalmol.* 133 (4), 552–556. doi:10.1016/s0002-9394(02)01325-9

Jiang, J. X., and Török, N. J. (2013). Liver Injury and the Activation of the Hepatic Myofibroblasts. *Curr. Pathobiol Rep.* 1 (3), 215–223. doi:10.1007/s40139-013-0019-6

Kallis, Y. N., Scotton, C. J., MacKinnon, A. C., Goldin, R. D., Wright, N. A., Iredale, J. P., et al. (2014). Proteinase Activated Receptor 1 Mediated Fibrosis in a Mouse Model of Liver Injury: A Role for Bone Marrow Derived Macrophages. *PLoS ONE* 9 (1), e86241. doi:10.1371/journal.pone.0086241

Karsdal, M. A., Daniels, S. J., Holm Nielsen, S., Bager, C., Rasmussen, D. G. K., Loomba, R., et al. (2020). Collagen Biology and Non-invasive Biomarkers of Liver Fibrosis. *Liver Int.* 40 (4), 736–750. doi:10.1111/liv.14390

Kastelein, J. J. P., Wedel, M. K., Baker, B. F., Su, J., Bradley, J. D., Yu, R. Z., et al. (2006). Potent Reduction of Apolipoprotein B and Low-Density Lipoprotein Cholesterol by Short-Term Administration of an Antisense Inhibitor of Apolipoprotein B. *Circulation* 114 (16), 1729–1735. doi:10.1161/CIRCULATIONAHA.105.606442

Kisseleva, T., and Brenner, D. (2021). Molecular and Cellular Mechanisms of Liver Fibrosis and its Regression. *Nat. Rev. Gastroenterol. Hepatol.* 18 (3), 1–16. doi:10.1038/s41575-020-00372-7

Knight, V., Lourensz, D., Tchongue, J., Correia, J., Tipping, P., and Sievert, W. (2017). Cytoplasmic Domain of Tissue Factor Promotes Liver Fibrosis in Mice. *World J. Gastroenterol.* 23 (31), 5692–5699. doi:10.3748/wjg.v23.i31.5692

Lento, S., Brioschi, M., Barcella, S., Nasim, M. T., Ghilardi, S., Barbieri, S. S., et al. (2015). Proteomics of Tissue Factor Silencing in Cardiomyocytic Cells Reveals a New Role for This Coagulation Factor in Splicing Machinery Control. *J. Proteomics* 119, 75–89. doi:10.1016/j.jprot.2015.01.021

Liang, L., Yang, X., Yu, Y., Li, X., Wu, Y., Shi, R., et al. (2016). Babao Dan Attenuates Hepatic Fibrosis by Inhibiting Hepatic Stellate Cells Activation and Proliferation via TLR4 Signaling Pathway. *Oncotarget* 7 (50), 82554–82566. doi:10.18632/oncotarget.12783

Lin, L., Li, R., Cai, M., Huang, J., Huang, W., Guo, Y., et al. (2018). Andrographolide Ameliorates Liver Fibrosis in Mice: Involvement of TLR4/NF-Kb and TGF-β1/Smad2 Signaling Pathways. *Oxidative Med. Cell. longevity* 2018, 7808656. doi:10.1155/2018/7808656

Lucas, K., and Maes, M. (2013). Role of the Toll like Receptor (TLR) Radical Cycle in Chronic Inflammation: Possible Treatments Targeting the TLR4 Pathway. *Mol. Neurobiol.* 48 (1), 190–204. doi:10.1007/s12035-013-8425-7

Luyendyk, J. P., Sullivan, B. P., Guo, G. L., and Wang, R. (2010). Tissue Factor-Deficiency and Protease Activated Receptor-1-Deficiency Reduce Inflammation Elicited by Diet-Induced Steatohepatitis in Mice. *Am. J. Pathol.* 176 (1), 177–186. doi:10.2353/ajpath.2010.090672

Mann, K. G., Butenas, S., and Brummel, K. (2003). The Dynamics of Thrombin Formation. *Arterioscler. Thromb. Vasc. Biol.* 23 (1), 17–25. doi:10.1161/01.ATV.0000046238.23903.FC

Mansour, M. A., Bekheet, S. A., Al-Rejaie, S. S., Al-Shabanah, O. A., Al-Howiriny, T. A., Al-Rikabi, A. C., et al. (2010). Ginger Ingredients Inhibit the Development of Diethylnitrosoamine Induced Premalignant Phenotype in Rat Chemical Hepatocarcinogenesis Model. *BioFactors* 36 (6), 483–490. doi:10.1002/biof.122

Marrone, A. K., Shpyleva, S., Chappell, G., Tryndyak, V., Uehara, T., Tsuchiya, M., et al. (2016). Differentially Expressed MicroRNAs Provide Mechanistic Insight into Fibrosis-Associated Liver Carcinogenesis in Mice. *Mol. Carcinog.* 55 (5), 808–817. doi:10.1002/mc.22323

Meng, X.-m., Nikolic-Paterson, D. J., and Lan, H. Y. (2016). TGF-β: The Master Regulator of Fibrosis. *Nat. Rev. Nephrol.* 12 (6), 325–338. doi:10.1038/nrneph.2016.48

Moreira, R. K. (2007). Hepatic Stellate Cells and Liver Fibrosis. *Arch. Pathol. Lab. Med.* 131 (11), 1728–1734. doi:10.5858/2007-131-1728-hscalf

Nakamura, K., Kadotani, Y., Ushigome, H., Akioka, K., Okamoto, M., Ohmori, Y., et al. (2002). Antisense Oligonucleotide for Tissue Factor Inhibits Hepatic Ischemic Reperfusion Injury. *Biochem. Biophysical Res. Commun.* 297 (3), 433–441. doi:10.1016/S0006-291X(02)02024-7

Nakazato, K., Takada, H., Iha, M., and Nagamine, T. (2010). Attenuation of N-Nitrosodiethylamine-Induced Liver Fibrosis by High-Molecular-Weight Fucoidan Derived fromCladosiphon Okamuranus. *J. Gastroenterol. Hepatol. (Australia)* 25 (10), 1692–1701. doi:10.1111/j.1440-1746.2009.06187.x

Nault, R., Fader, K. A., Kopec, A. K., Harkema, J. R., Zacharewski, T. R., and Luyendyk, J. P. (2016). From the Cover: Coagulation-Driven Hepatic Fibrosis Requires Protease Activated Receptor-1 (PAR-1) in a Mouse Model of TCDD-Elicited Steatohepatitis. *Toxicol. Sci.* 154 (2), 381–391. doi:10.1093/toxsci/kfw175

Pendurthi, U. R., Ngyuen, M., Andrade-Gordon, P., Petersen, L. C., and Rao, L. V. M. (2002). Plasmin InducesCyr61Gene Expression in Fibroblasts via Protease-Activated Receptor-1 and P44/42 Mitogen-Activated Protein Kinase-dependent Signaling Pathway. *Arterioscler. Thromb. Vasc. Biol.* 22 (9), 1421–1426. doi:10.1161/01.ATV.0000030200.59331.3F

Poojari, R., Gupta, S., Maru, G., Khade, B., and Bhagwat, S. (2010). Chemopreventive and Hepatoprotective Effects of Embelin on N-Nitrosodiethylamine and Carbon Tetrachloride Induced Preneoplasia and Toxicity in Rat Liver. *Asian Pac. J. Cancer Prev.* 11 (4), 1015–1020. doi:10.1016/j.fitote.2005.04.014

Poole, L. G., Pant, A., Cline-Fedewa, H. M., Williams, K. J., Copple, B. L., Palumbo, J. S., et al. (2020). Liver Fibrosis Is Driven by Protease-activated Receptor-1 Expressed by Hepatic Stellate Cells in Experimental Chronic Liver Injury. *Res. Pract. Thromb. Haemost.* 4 (5), 906–917. doi:10.1002/rth2.12403

Rao, L. V. M., and Pendurthi, U. R. (2005). Tissue Factor-Factor VIIa Signaling. *Arterioscler. Thromb. Vasc. Biol.* 25 (1), 47–56. doi:10.1161/01.ATV.0000151624.45775.13

Rauch, U., and Nemerson, Y. (2000). Tissue Factor, the Blood, and the Arterial Wall. *Trends Cardiovascular Medicine* 10 (4), 139–143. doi:10.1016/s1050-1738(00)00049-9

Riewald, M., Kravchenko, V. V., Petrovan, R. J., O'Brien, P. J., Brass, L. F., Ulevitch, R. J., et al. (2001). Gene Induction by Coagulation Factor Xa Is Mediated by Activation of Protease-Activated Receptor 1. *J. Am. Soc. Hematol.* 97 (10), 3109–3116. doi:10.1182/blood.v97.10.3109

Riewald, M., Petrovan, R. J., Donner, A., and Ruf, W. (2003). Activated Protein C Signals through the Thrombin Receptor PAR1 in Endothelial Cells. *J. Endotoxin Res.* 9 (5), 317–321. doi:10.1179/096805103225002584

Roberts, T. C., Langer, R., and Wood, M. J. A. (2020). Advances in Oligonucleotide Drug Delivery. *Nat. Rev. Drug Discov.* 19 (10), 673–694. doi:10.1038/s41573-020-0075-7

Rondina, M. T., Schwertz, H., Harris, E. S., Kraemer, B. F., Campbell, R. A., Mackman, N., et al. (2011). The Septic Milieu Triggers Expression of Spliced Tissue Factor mRNA in Human Platelets. *J. Thromb. Haemost.* 9 (4), 748–758. doi:10.1111/j.1538-7836.2011.04208.x

Rullier, A., Gillibert-Duplantier, J., Costet, P., Cubel, G., Haurie, V., Petibois, C., et al. (2008). Protease-activated Receptor 1 Knockout Reduces Experimentally Induced Liver Fibrosis. *Am. J. Physiol. Gas-Trointest Liver Physiol.* 294 (1), 226–235. doi:10.1152/ajpgi.00444.2007.-Thrombin

Seki, E., De Minicis, S., Österreicher, C. H., Kluwe, J., Osawa, Y., Brenner, D. A., et al. (2007). TLR4 Enhances TGF-β Signaling and Hepatic Fibrosis. *Nat. Med.* 13 (11), 1324–1332. doi:10.1038/nm1663

Serag, H. M., Komy, M. M. El., and Ahmed, H. S. (2019). Assessment the Role of Bisphenol A on Chemotherapeutic Efficacy of Cisplatin against Hepatocellular Carcinoma in Male Rats. *Egypt. J. Hosp. Med.* 74 (2), 352–363. doi:10.12816/EJHM.2019.23057

Shimizu, R., Kitade, M., Kobayashi, T., Hori, S.-I., and Watanabe, A. (2014). Pharmacokinetic-pharmacodynamic Modeling for Reduction of Hepatic Apolipoprotein B mRNA and Plasma Total Cholesterol after Administration of Antisense Oligonucleotide in Mice. *J. Pharmacokinet. Pharmacodyn* 42 (1), 67–77. doi:10.1007/s10928-014-9398-5

Sullivan, B. P., Kopec, A. K., Joshi, N., Cline, H., Brown, J. A., Bishop, S. C., et al. (2013). Hepatocyte Tissue Factor Activates the Coagulation Cascade in Mice. *Blood* 121 (10), 1868–1874. doi:10.1182/blood10.1182/blood-2012-09-455436

Sullivan, B. P., Weinreb, P. H., Violette, S. M., and Luyendyk, J. P. (2010). The Coagulation System Contributes to αVβ6 Integrin Expression and Liver Fibrosis Induced by Cholestasis. *Am. J. Pathol.* 177 (6), 2837–2849. doi:10.2353/ajpath.2010.100425

Sung, Y.-C., Liu, Y.-C., Chao, P.-H., Chang, C.-C., Jin, P.-R., Lin, T.-T., et al. (2018). Combined Delivery of Sorafenib and a MEK Inhibitor Using CXCR4-Targeted Nanoparticles Reduces Hepatic Fibrosis and Prevents Tumor Development. *Theranostics* 8 (4), 894–905. doi:10.7150/thno.21168

Tork, O. M., Khaleel, E. F., and Abdelmaqsoud, O. M. (2016). Altered Cell to Cell Communication, Autophagy and Mitochondrial Dysfunction in a Model of Hepatocellular Carcinoma: Potential Protective Effects of Curcumin and Stem Cell Therapy. *Asian Pac. J. Cancer Prev.* 16 (18), 8271–8279. doi:10.7314/APJCP.2015.16.18.8271

Trautwein, C., Friedman, S. L., Schuppan, D., and Pinzani, M. (2015). Hepatic Fibrosis: Concept to Treatment. *J. Hepatol.* 62 (1), S15–S24. doi:10.1016/j.jhep.2015.02.039

Tripathy, A., Thakurela, S., Sahu, M. K., Uthansingh, K., Singh, A., Narayan, J., et al. (2020). Fatty Changes Associated with N-Nitrosodiethylamine (DEN) Induced Hepatocellular Carcinoma: a Role of Sonic Hedgehog Signaling Pathway. *Genes Cancer* 11 (1-2), 66. doi:10.18632/genesandcancer.203

Tripodi, A., Mannucci, P. M., and Bonomi Hemophilia, B. (2011). The Coagulopathy of Chronic Liver Disease. *N. Engl. J. Med.* 365 (2), 147–156. doi:10.1056/nejmra1011170

Uehara, T., Ainslie, G. R., Kutanzi, K., Pogribny, I. P., Muskhelishvili, L., Izawa, T., et al. (2013). Molecular Mechanisms of Fibrosis-Associated Promotion of Liver Carcinogenesis. *Toxicol. Sci.* 132 (1), 53–63. doi:10.1093/toxsci/kfs342

Uehara, T., Pogribny, I. P., and Rusyn, I. (2014). The DEN and CCl 4 -Induced Mouse Model of Fibrosis and Inflammation-Associated Hepatocellular Carcinoma. *Curr. Protoc. Pharmacol.* 66 (1), 14–30. doi:10.1002/0471141755.ph1430s66

Wang, K., Yang, X., Wu, Z., Wang, H., Li, Q., Mei, H., et al. (2020). Dendrobium Officinale Polysaccharide Protected CCl4-Induced Liver Fibrosis through Intestinal Homeostasis and the LPS-TLR4-NF-Kb Signaling Pathway. *Front. Pharmacol.* 11, 240. doi:10.3389/fphar.2020.00240

Witkowski, M., Landmesser, U., and Rauch, U. (2016). Tissue Factor as a Link between Inflammation and Coagulation. *Trends Cardiovasc. Med.* 26 (4), 297–303. doi:10.1016/j.tcm.2015.12.001

Yin, J., Luo, X., Yu, W., Liao, J., Shen, Y., and Zhang, Z. (2010). Antisense Oligodeoxynucleotide against Tissue Factor Inhibits Human Umbilical Vein Endothelial Cells Injury Induced by Anoxia-Reoxygenation. *Cell Physiol. Biochem.* 25 (4–5), 477–490. doi:10.1159/000303053

Conflict of Interest: The authors declare that the research was conducted in the absence of any commercial or financial relationships that could be construed as a potential conflict of interest.

Copyright © 2021 Shouman, Abdelsalam, Tawfick, Kenawy and El-Naa. This is an open-access article distributed under the terms of the Creative Commons Attribution License (CC BY). The use, distribution or reproduction in other forums is permitted, provided the original author(s) and the copyright owner(s) are credited and that the original publication in this journal is cited, in accordance with accepted academic practice. No use, distribution or reproduction is permitted which does not comply with these terms.

frontiers in Pharmacology

ORIGINAL RESEARCH
published: 13 May 2021
doi: 10.3389/fphar.2021.677810

Salidroside Inhibits CCl_4-Induced Liver Fibrosis in Mice by Reducing Activation and Migration of HSC Induced by Liver Sinusoidal Endothelial Cell-Derived Exosomal SphK1

Qiannan Ye[1,2], *Yang Zhou*[3], *Changqing Zhao*[1,2], *Lieming Xu*[1,2,4,5]* *and Jian Ping*[1,5]*

[1]*Shuguang Hospital Affiliated to Shanghai University of Traditional Chinese Medicine, Shanghai, China,* [2]*Institute of Liver Diseases, Shanghai University of Traditional Chinese Medicine, Shanghai, China,* [3]*Yueyang Hospital Affiliated to Shanghai University of Traditional Chinese Medicine, Shanghai, China,* [4]*Shanghai Key Laboratory of Traditional Chinese Medicine, Shanghai, China,* [5]*Key Laboratory of Liver and Kidney Diseases, Ministry of Education, Shanghai, China*

OPEN ACCESS

Edited by:
Wolfgang Richard Stremmel, Baden-Baden, Germany

Reviewed by:
Na Chang, Capital Medical University, China
Francisco Javier Cubero, Complutense University of Madrid, Spain
Tao Xu, Anhui Medical University, China

***Correspondence:**
Lieming Xu
xulieming@shutcm.edu.cn
Jian Ping
pingjian@aliyun.com

Specialty section:
This article was submitted to Gastrointestinal and Hepatic Pharmacology, a section of the journal Frontiers in Pharmacology

Received: *08 March 2021*
Accepted: *30 April 2021*
Published: *13 May 2021*

Citation:
Ye Q, Zhou Y, Zhao C, Xu L and Ping J (2021) Salidroside Inhibits CCl_4-Induced Liver Fibrosis in Mice by Reducing Activation and Migration of HSC Induced by Liver Sinusoidal Endothelial Cell-Derived Exosomal SphK1. Front. Pharmacol. 12:677810. doi: 10.3389/fphar.2021.677810

Sphingosine kinase 1 (SphK1)/Sphingosine-1-phosphate (S1P)/S1PRs signaling pathway is known to involve the advancement of liver fibrosis. Exosomal SphK1 promotes hepatic stellate cells (HSC) migration. Salidroside (Sal) inhibits liver fibrosis, but its mechanism is yet to be elucidated. This study was to explore the influences of Sal on the SphK/S1P/S1PRs signaling pathway in liver fibrosis induced by carbon tetrachloride (CCl_4) *in vivo*, and investigated the mechanism of Sal affecting the migration and activation of HSC triggered by exosomal SphK1 *in vitro*. Our data showed that Sal reduced the activities of alanine transaminase (ALT), aspartate aminotransferase (AST) in serum, and hydroxyproline (Hyp) content in the liver tissue. Sal subdued the expression of α-smooth muscle actin (α-SMA), fibronectin (FN) and type I collagen (Col I) of the liver. Sal also reduced mitochondria-induced hepatocyte apoptosis and to inhibit JNK activation. Furthermore, Sal remarkably eradicated the influence of SphK1, SphK2, S1P, and S1PRs triggered by CCl_4, whether stimulating or hindering. Compared with serum-derived exosomes from model group mice, serum-derived exosomes from Sal group mice expressed lower SphK1 and reduced JS 1 (mouse HSC cell line) migration. In addition, Sal was also observed to subdue Col I expression, AKT activation, and LX-2 migration induced by exosomal SphK1 from SK-HEP-1 (a kind of liver sinusoidal endothelial cells (LSEC) cell line). In conclusion, Sal could effectively alleviate liver injury, hepatocyte apoptosis, and liver fibrosis *in vivo*, providing supports that the protective effects of Sal might be realized by suppressing JNK activation and modulating the SphK/S1P/S1PRs axis. *In vitro*, it was observed that Sal might alleviate LX-2 migration and activation induced by exosomal SphK1 by inhibiting the AKT activation.

Keywords: salidroside, liver fibrosis, SphK/S1P/S1PRs, exosomes, liver sinusoidal endothelial cells, hepatic stellate cell

INTRODUCTION

Liver fibrosis involves excessive accumulation of collagen and extracellular matrix (ECM). It is a reversible over-repair process of liver tissue damage due to various chronic liver injuries (Hernandez-Gea and Friedman, 2011). Hepatic stellate cell (HSC) activation is supposedly the critical event that initiates and develops liver fibrosis (Tsuchida and Friedman, 2017), though the exact pathogenesis is yet to be understood. Current effective treatment for liver fibrosis involves etiological treatment, such as antiviral therapy, the use of immunosuppressive agents, and others. This calls for researching effective therapies for alleviating liver fibrosis.

Exosomes are small vesicles released by various cells and distributed in several body fluids. Exosomes can mediate information exchange among cells and are a part of numerous physiological and pathological activities, including cell growth, proliferation, differentiation, and apoptosis (van Niel et al., 2018). Hepatocytes and liver sinusoidal endothelial cells (LSECs) have been shown in recent investigations to interact with HSCs via exosomes, in turn regulating the biological activity of HSCs (Sung et al., 2018). For instance, the miR-192 content in exosomes from palmitic acid-stimulated hepatocytes was found to be considerably increased, and these exosomes stimulated the activation of HSCs (Lee et al., 2017). LSECs secrete exosomes that express high amounts of Sphingosine kinase 1 (SphK1), which promote HSC migration by triggering AKT phosphorylation (Wang et al., 2015).

SphK/Sphingosine-1-phosphate (S1P)/S1PRs signaling pathway participates in tissue fibrosis progression, including liver fibrosis (Kono et al., 2007; Sato et al., 2016; Wang et al., 2019). The renal tissues of mice with unilateral ureteral ligation-caused renal interstitial fibrosis, the SphK1 levels, and autophagy-related proteins were found to have remarkably amplified as fibrosis advanced. The SphK1 protein expression was also detected to be upregulated in the lung tissue of bleomycin-induced pulmonary fibrosis model mice. In addition, when the SphK1 expression was blocked by SphK inhibitors or siRNA, the high expression of α-smooth muscle actin (α-SMA) and fibronectin (FN) induced by transforming growth factor β1 (TGF-β1) was observed to be lowered (Kono et al., 2007). Likewise, the SphK1 expression and its product S1P were recorded to increase progressively as the liver fibrosis advanced in the bile duct ligation (BDL) and carbon tetrachloride (CCl_4)-induced liver fibrosis, mouse model. Furthermore, S1P promoted liver fibrosis angiogenesis via binding to its ligands. Nevertheless, obstructing the binding of S1P to ligands perhaps inhibits angiogenesis in fibrotic liver tissue, in turn lowering the degree of liver fibrosis (Yang et al., 2013). These findings indicate that SphK/S1P/S1PRs signaling pathway plays an essential role in organ fibrosis.

A phenolic compound, Salidroside (Sal), occurs in plants of *Rhodiola rosea* L. Sal has been reported in recent researches to possess several pharmacological properties, such as anti-inflammatory (Xu et al., 2019), antioxidative (Jiansheng and Ying, 2012), and anticancerous (Ren et al., 2019). Earlier researches evidenced Sal to exhibit curative effects on numerous liver diseases. For instance, Sal reduces drug-induced liver injury (Yuan et al., 2019), guards the liver against ischemia/reperfusion injury (Cai et al., 2017), and eases nonalcoholic fatty liver disease (NAFLD) by AMPK-dependent TXNIP/NLRP3 pathway (Zheng et al., 2018). Another study reported Sal obstructing HSC activation and autophagy by downregulating NF-κB and TGF-β1/Smad3 signaling pathway (Feng et al., 2018), though it is unclear whether the effect of Sal on liver fibrosis is correlated to the SphK/S1P/S1PRs signal pathway. In one of our earlier investigations, Sal was observed to hinder the HSCs migration by obstructing AKT phosphorylation (Zhang et al., 2012). Based on literature reports evidencing exosomes to overexpress SphK1 derived from LSEC promoted LX-2-migration by upregulating the AKT activation, Sal was theorized to subdue HSC migration and activation by regulating exosome-mediated communication between LSEC and HSC.

The effects of Sal on SphK/S1P/S1PRs signal pathway in mouse with liver fibrosis caused by CCl_4 and how it regulates the migration and activation of LX-2 induced by exosomal SphK1 from LSECs were explored in this study *in vivo* and *in vitro*, respectively. The outcomes support the efficacy of Sal as an antifibrotic drug and back the SphK/S1P/S1PRs efficiency as a therapeutic target for liver fibrosis.

MATERIALS AND METHODS

Materials

Sal was procured from Shanghai Tauto Biotechnology (Shanghai, China), the alanine transaminase (ALT), aspartate aminotransferase (AST), and hydroxyproline (Hyp) detection kits were acquired from Nanjing Jiancheng Bioengineering Institute (Nanjing, China). FN, type I collagen (Col I), Bax and Bcl-2 antibodies were obtained from Abcam (Cambridge, United Kingdom). JNK, p-JNK, PARP, and cleaved caspase 3 antibodies were purchased from Cell Signaling Technology (Massachusetts, United States). SphK1, SphK2, S1PR1, S1PR2, S1PR3, CD9, and tumor susceptibility gene 101 (TSG101) antibodies were procured from ImmunoWay Biotechnology Company (Suzhou, China). Antibody against GAPDH was provided by Proteintech (Wuhan, China). TdT-mediated dUTP nick end labeling (TUNEL) Apoptosis Assay Kit, 2-(4-Amidinophenyl)-6-indolecarbamidine dihydrochloride (DPAI), and Cy3-labeled goat anti-rabbit IgG were all bought from Beyotime Institute of Biotechnology (Shanghai, China). The S1P Assay Kit (S1P-ELISA) was delivered by Echelon Biosciences (Salt Lake City, United States).

Animals

Male C57BL/6J, SPF grade mice weighing 20 ± 2 g, were supplied by Shanghai Sippr-BK laboratory animal Co. Ltd. (Shanghai, China). They were placed in the experimental animal center of Shanghai University of Traditional Chinese Medicine, China. The Committee on the Care and Use of Live Animals for Teaching and Research of the Shanghai University of Traditional Chinese Medicine sanctioned the animal experiments.

Animal Treatments

Following a week-long adaptive feeding, 45 male mice were divided into the control group included 15 mice, while the modeling group had 30. The modeling group animals were intraperitoneally injected with 15% CCl_4 (diluted with olive oil) at 2 ml/kg thrice a week, whereas those in the control group were administered an equal dosage of olive oil intraperitoneally. After a week of modeling, the modeling group was segregated into Model and Sal groups. The Model and Sal groups were continued to model with CCl_4 for 5 weeks, while the Control group was injected intraperitoneally with equal dose of olive oil. The Sal group animals were administered Sal (20 mg/kg) through gavage for 5 weeks. Simultaneously, those in the Control and Model groups were both treated with equal doses of ddH_2O. At the end of five weeks, the mice were sacrificed on anesthetizing with pentobarbital sodium, and the serum and liver tissue samples were preserved for subsequent experiments.

Serum Biochemical Test

The instructions provided along with the kit were followed to detect ALT and AST levels in the mice serum.

Pathological Evaluation of Liver

Fixation of the liver tissues was carried out in 10% neutral formalin for 48 h. They were then dehydrated stepwise with ethanol, followed by xylene permeation, and finally paraffin-embedded. Sections of 4 μm thickness were prepared for HE and Sirius red staining.

Determination of Hyp Content

Following the kit directions, the Hyp contents in liver tissues were determined.

Human Samples

Healthy volunteers and cirrhosis patients were selected for collecting human liver tissue and serum samples from the Department of Hepatobiliary Surgery, Renji Hospital, Affiliated to Shanghai Jiao Tong University. The Ethics Committee of Shuguang Hospital, Affiliated to Shanghai University of Traditional Chinese Medicine, sanctioned this study.

Isolation of Primary Liver Sinusoidal Endothelial Cells From Mice

Wild and Model groups of five male mice each were formed. The Model group mice were injected with CCl4 intraperitoneally to create a liver fibrosis model. They were then used to isolate primary LSECs. Using density gradient centrifugation in combination with CD146 magnetic bead (Miltenyi Biotec, Germany) separation, the primary LSEC of mice was isolated as the earlier reports (Liu et al., 2011; Meyer et al., 2016). Mouse liver tissue was perfused *in situ* and digested using an enzyme solution of collagenase D and DNase (Roche, Germany). Density gradient centrifugation was performed using OptiPrep solution (Axis-Shield, Norway) and incubation with CD146 magnetic bead for 30 min at 4°C. Thus isolated LSECs were cultured in Col I-coated dishes along with ECM medium, comprising 5% FBS, 2% endothelial cell growth supplement, and maintained with 5% CO_2 at 37°C in a humidified incubator.

Cell Culture

Propagation of human immortalized HSCs (LX-2) and mouse immortalized HSCs (JS 1) was carried out in DMEM, supplemented with 10% FBS, 100 U/ml penicillin, and 0.1 mg/ml streptomycin. The SK-HEP-1 cells, obtained from the Chinese Academy of Sciences, were grown in MEM, containing 10% FBS, 100 U/ml penicillin, and 0.1 mg/ml streptomycin. All cell lines were maintained with 5% CO_2 in a humidified incubator at 37°C.

Cell Transfection

The lentiviral vectors containing human SphK1 (LV-SphK1) or empty plasmid (LV-Cr) were procured from HANBIO Biotech (Shanghai, China). A 24-well plate was used to culture SK-HEP-1 to a confluence of 30–50%. They were then cultured in a fresh medium containing lentiviral vectors (MOI = 30) and polybrene (5 μg/ml) for 24 h, and then in a fresh medium for further culturing, followed by incubation for 48 h. The transfection efficiency of cells was studied using an inverted microscope and were incubated with a medium containing puromycin (1 μg/ml) to eliminate the untransfected cells. The transfected cells were cultured further, and the culture medium was used to isolate exosomes.

Isolation of Exosomes

SK-HEP-1 cells were cultured in 150 mm dishes to a confluence of 80–90%. They were then cultured in MEM with 10% exosome-free serum for 24 h. The supernatant was ultracentrifuged to obtain the exosomes. The supernatant was first centrifuged at 4°C, 300 ×g, for 10 min to eliminate cells. The supernatant was centrifuged again at 4°C, 2,000 ×g, for 10 min to eradicate dead cells. The supernatant was centrifuged at 4°C, 10,000 ×g, for another 30 min to eliminate cell debris. Eventually, the supernatant was ultracentrifuged at 4°C, 100,000 ×g for 70 min, and the precipitate collected was the exosomes. The thus isolated exosomes were resuspended in PBS or DMEM medium for subsequent *in vitro* studies.

Identification of Exosomes

A transmission electron microscope was utilized to study the morphology of isolated exosomes (van Niel et al., 2018). This was followed by detecting typical exosomal marker proteins, CD9 and TSG101, by Western blot (WB) analysis.

Cell Treatment

LX-2 and JS 1 were cultured in 60 mm dishes to a confluence of 80–90%. LX-2 cells were allocated to Cr-exo and Cirrhosis-exo groups and incubated with serum exosomes (30 μg/ml) from healthy volunteers and cirrhosis patients, respectively, to study the migration of LX-2 cells. Also, JS 1 cells were distributed into Cr-exo, M-exo, and Sal-exo groups and incubated with serum exosomes (30 μg/ml) from corresponding mice to detect JS 1 cells' migration. The LX-2 cells were then divided into Cr-exo, $SphK1^+$-exo, Cr-exo + Sal, and $SphK1^+$-exo + Sal groups and incubated

with 30 μg/ml exosomes of transfected SK-HEP-1 cell culture media and/or Sal (10^{-5} M) to study the LX-2 cells migration and activation.

Transwell Migration Assays

LX-2 or JS 1 cells were cultured in Col I-coated migration cups to a confluence of 80–90%. Then, exosomes and/or Sal were added to the lower chamber, and with the same medium being added to the upper chamber as well. Incubation was carried out for 24 h, and the migration cups were then taken out and air-dried. Fixation of the cells on the lower surface of the migration cup was done using 4% paraformaldehyde and staining with crystal violet. The total number of cells that migrated to the bottom was recorded with an inverted microscope (Olympus, Tokyo, Japan) and evaluated using ImageJ software (NIH, United States).

Di-Acetylated-Low-Density Lipoprotein Assays

The adhered LSECs were incubated in ECM medium comprising DiI-Ac-LDL (Yiyuan Biotech, Guangzhou, China) for 4 h in the dark. The cells were then rinsed thrice with PBS, fixed with 4% paraformaldehyde for 15 min, and rinsed again with PBS. The endocytosis of DiI-Ac-LDL by LSECs was studied using an inverted fluorescence microscope (Olympus, Tokyo, Japan).

TUNEL Assay

According to the manufacturer's instructions, sections of frozen liver tissue of 8 μm thickness were prepared and incubated with TUNEL.

Immunofluorescence Staining

The LSECs were collected following 3 days of culturing, rinsed with PBS, and fixed using 4% paraformaldehyde for 30 min at room temperature. The frozen sections of mice liver tissue were fixed with precooled acetone for 15 min. Once fixed, the cells and frozen sections were rinsed again with PBS and incubated using 0.1% X-Triton-100 for 15 min at room temperature to disrupt the membrane. They were permeabilized and blocked using 5% BSA at room temperature for 1 h and then incubated with respective primary antibodies at 4°C overnight. The following day, they were incubated with anti-rabbit IgG (Cy3-labeled) in the dark at room temperature for 1 h and rinsed again with PBS. The cells were then stained using DAPI and rinsed using PBS. The sample was sealed, and their fluorescence was studied with the help of an inverted fluorescence microscope.

Protein Isolation and Western Blotting Analysis

RIPA lysate comprising complete Mini, PMSF, and phosphatase inhibitors was utilized to isolate liver tissues and cells' total protein. Protein quantification was performed with the BCA protein assay kit (Beyotime Institute of Biotechnology, Shanghai, China). An equivalent amount (30 μg) of proteins was electrophoresed by SDS-PAGE and transferred to PVDF membranes (Millipore, United States). The membranes were then incubated with blocking buffer (Beyotime Institute of Biotechnology, Shanghai, China) at room temperature for 1 h and incubated with respective primary antibodies overnight at 4°C. The membranes were rinsed using PBS-T for 20 min and treated with anti-rabbit IgG or anti-mouse IgG for 1 h. The membranes were rinsed with PBS-T again, and the images were recorded by means of Odyssey imaging system (LI-COR, United Kingdom) and analyzed with the ImageJ software. A part of the membranes was also stained with ponceau after incubating with antibodies.

RNA Isolation and RT-PCR Analysis

TRIzol total RNA preparation kit (Shanghai Sangon Biotech, Shanghai, China) was utilized to isolate the total RNA of cells and synthesized to cDNA with a ReverAid First Strand cDNA Synthesis Kit (Thermo, United States) following the manufacturer's procedures. The cDNA was mixed with primers and SYBR Green Real-time PCR Master Mix (TOYOBO, Japan) in a certain ratio; the relative expressions of mRNA were measured utilizing the ViiA 7 Real-Time PCR System (ABI, Carlsbad, CA, United States). Primer sequences used for detection of Sphk1, SphK2, S1PR1,2,3 were shown in **Table 1**.

Statistical Analysis

The outcomes have been recorded in terms of mean ± standard error of the mean. The differences among groups were evaluated via *t*-test or One-way ANOVA using SPSS 21.0 software. Values of $p < 0.05$ were considered statistically significant.

RESULTS

Sal Alleviated CCl_4-Induced Liver Fibrosis in Mice

Serum ATL and AST were detected to be considerably higher in the Model group than those in the Control group ($p < 0.01$) (**Figure 1A**), indicating obvious liver function damage due to CCl_4. Nevertheless, these changes were observed to be reversed by Sal ($p < 0.05$ or $p < 0.01$) (**Figure 1A**). HE staining revealed that CCl_4 resulted in collagen deposition, structural destruction, and inflammatory cell infiltration in liver lobules and portal areas. Sal treatment was found to remarkably alleviate these histopathological lesions (**Figure 1B**).

Besides, Sirius red staining revealed excessive collagen deposition in the Model group than that in the control group, and Sal was noted to lower the collagen deposition (**Figures 1C,D**) substantially. Then, the effect of Sal on liver fibrosis was further examined by identifying the Hyp content in liver tissue and the characteristic indicators of liver fibrosis, including FN, Col I, and α-SMA. The Hyp content in liver tissues of the Model group was found to be remarkably higher as compared with that of the control group. Sal treatment

TABLE 1 | Primer sequences for PCR.

Gene	Forward (5′-3′)	Reverse (5′-3′)
SphK1[a]	TGACTTGGAAAGAAAGGCTCT	GCAATGGGGAGTGTCTTCTAT
SphK2[a]	GCACGGCGAGTTTGGTTC	GAGACCTCATCCAGAGAGACTAG
S1PR1[a]	TGAGCGAGGCTGCTGTTTC	AGAGGGCGAGGTTGAGTGAG
S1PR2[a]	CCT TGA CTG GCT TGA ACT TTC	ACCCTCAGAACACAGACAGGT
S1PR3[a]	ACCAAGAAAATGTCACCGTGT	ACTCCCCTACACACTGCTCTG
SphK1[b]	CGACGAGGACTTTGTGCTAGT	AAACATCTCACTGCCCAGGT
GAPDH[b]	AGCCACATCGCTCAGACACC	GTACTCAGCGCCAGCATCG

[a]*Mouse*
[b]*human.*

reduced the Hyp level ($p < 0.01$) (**Figure 1E**). Moreover, higher quantities of FN, Col I, and α-SMA proteins were expressed in the Model group, which were considerably subdued by Sal administration ($p < 0.05$ or $p < 0.01$) (**Figure 1F**), signifying Sal reduced CCl_4-induced liver fibrosis.

Sal Alleviated CCl_4-Induced Apoptosis of Hepatocytes in Mice via Regulating JNK Activation

Considering the defensive effect of Sal on liver injury and fibrosis, Sal's influence on hepatocyte apoptosis was further studied by TUNEL staining. As indicated in **Figure 2A**, the apoptotic hepatocytes in the Model group were significantly amplified compared with those in the control group. Apoptotic cells in the Sal group as compared with the Model group were observed to be considerably reduced, indicating Sal's efficacy in alleviating CCl_4-induced hepatocyte apoptosis.

Sal's efficiency in expressing classic proteins in the mitochondrial apoptosis pathway and the role of the JNK signaling pathway in CCl_4-induced liver fibrosis were also investigated. Higher levels of cleaved caspase 3, cleaved PARP and Bax were expressed in the Model group, while Bcl-2 was lowered. Sal therapy was detected to reverse these changes and upregulate the ratio of Bcl-2 to Bax ($p < 0.05$ or $p < 0.01$) (**Figure 2B**). As displayed in **Figure 2B**, CCl_4 supported JNK phosphorylation in liver tissues. Sal therapy was recorded to downregulate the enhanced expression of p-JNK in model mice ($p < 0.05$) (**Figure 2B**). These findings indicate Sal considerably reduced mitochondria-mediated hepatocytes apoptosis by inhibiting JNK phosphorylation.

Sal Regulated the SphK/S1P/S1PR Signaling Pathway in the Liver of Mice

Sal's antifibrosis efficacy in relation to the regulation of SphK/S1P/S1PR signaling pathway was studied by examining the expression levels of SphK, S1P, and S1PRs. The protein and mRNA levels of SphK1 were detected to be upregulated, and SphK2 protein and mRNA expression downregulated in the liver tissues of the Model group as compared with those in the control group ($p < 0.05$ or $p < 0.01$) (**Figures 3A,C**). Sal was found to inhibit these effects ($p < 0.01$) (**Figures 3A,C**). Moreover, a high S1P level was observed in the model group ($p < 0.01$) (**Figure 3B**), and Sal was found to lower its level.

In addition, CCl_4 was also detected to regulate S1PRs, the receptors of S1P. Notably, it also amplified the expression of S1PR1 and S1PR3 but subdued that of S1PR2. Sal substantially eradicated the effects of S1PRs triggered by CCl_4, whether stimulating or hindering (**Figure 3C**).

Sal Inhibited the Expression of SphK1 in Serum Exosomes and the Migration of HSC Induced by Serum Exosomes

Serum exosomes from mice and humans were successfully isolated in this research, and their characteristics were analyzed by electron microscopy (**Figure 4A**), while the expression of markers of exosomes, TSG101 and CD9, was identified by Western blot (**Figure 4B**). SphK1 was noted to be highly expressed in serum exosomes from liver cirrhosis patients, which encouraged the migration of LX-2 ($p < 0.01$) (**Figures 4C,D**). A similar remarkably high expression of SphK1 in the serum exosomes derived from mice with liver fibrosis was recorded ($p < 0.01$) (**Figure 4E**). Moreover, Sal treatment was detected to downregulate the expression of SphK1 in serum exosomes ($p < 0.05$) (**Figure 4E**). As theorized, the serum exosomes in the mice with liver fibrosis were also found to encourage the migration of JS 1, and the serum exosomes of the Sal group to subdue the migration of JS 1 ($p < 0.01$) (**Figure 4F**).

SphK1 was Highly Expressed in Primary LSEC of Mice With Liver Fibrosis Induced by CCl_4

Serum-derived exosomes contain too many contents, not limited to a certain organ or even a certain type of cell. Therefore, it is very difficult to trace whether the components in serum exosomes originate from a certain cell. Considering the special anatomical position of LSEC and HSC and the essential role of the interaction between LSECs and HSC in the process of liver fibrosis (Deleve, 2015), we cultured the primary LSEC and detected its expression of SphK1, trying to prove the source of SphK1. The freshly isolated LSECs were

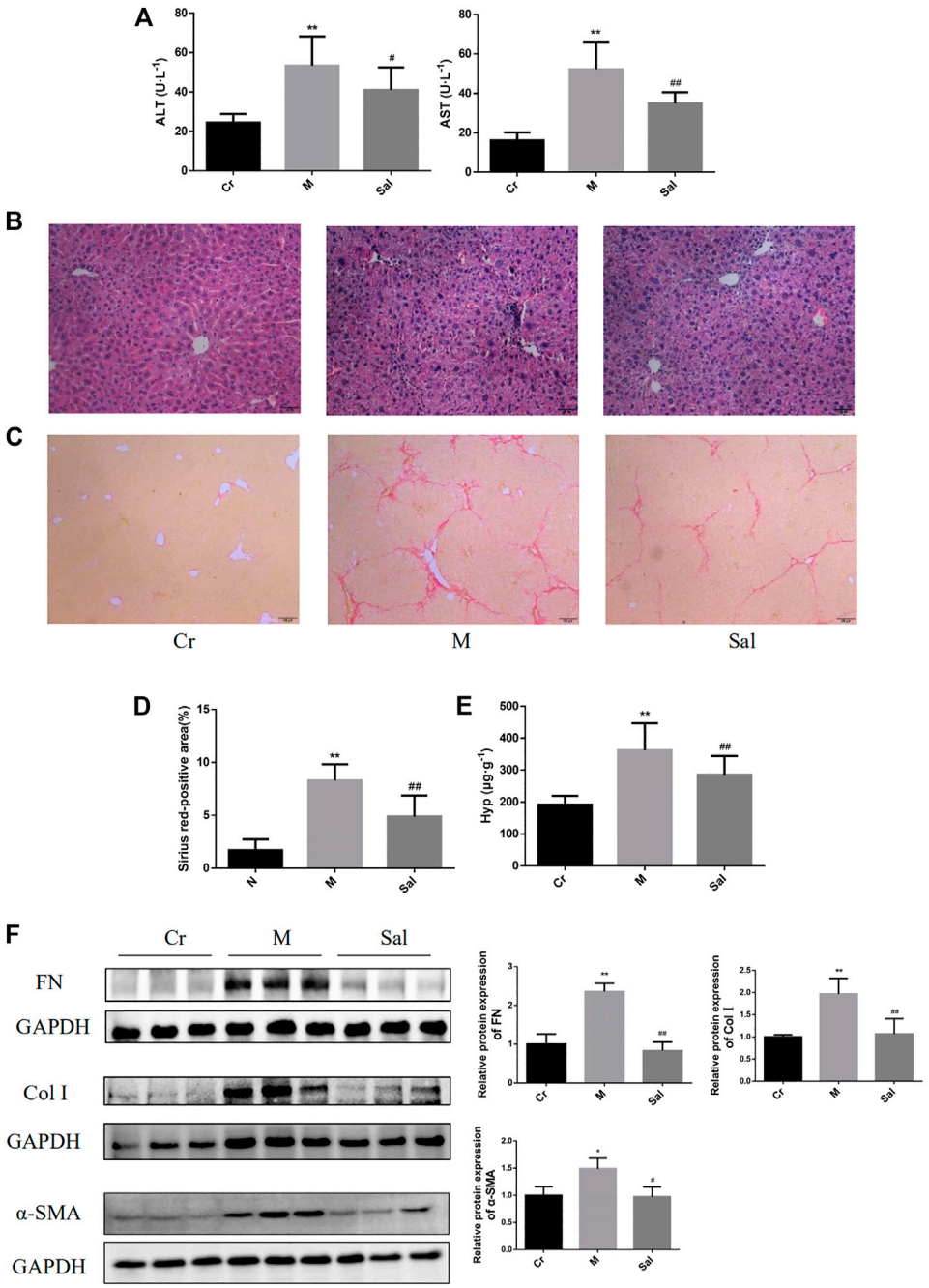


FIGURE 1 | Effects of Sal on liver injury and fibrosis induced by CCl_4. **(A)**: Levels of serum ATL and AST in different groups. **(B)**: HE staining of liver tissues in each group (×100). **(C)**: Sirius red staining of liver tissue sections (×100). **(D)**: Sirius red-positive area. **(E)**: Contents of Hyp in liver tissue. $^{**}p < 0.01$, vs. Cr; $^{\#\#}p < 0.01$, vs. M. **(F)**: Expressions of FN, Col I, and α-SMA in mice liver tissue were detected by WB. ($n = 15$, $^{*}p < 0.05$, $^{**}p < 0.01$, vs Cr; $^{\#}p < 0.05$, $^{\#\#}p < 0.01$, vs M.) ALT: alanine transaminase; AST: aspartate aminotransferase; Hyp: hydroxyproline; Cr: control group; M: model group; Sal: salidroside group. α-SMA: α-smooth muscle actin; FN: fibronectin; Col I: type I collagen; Cr: control group; M: model group; Sal: salidroside group.

small and spherical. During the *in vitro* culture, the LSECs were observed to gradually stretch out and adopt a long spindle shape (**Figure 5A**). **Figures 5B,C** present isolated LSECs phagocytosed Dil-Ac-LDL and expressed CD31, both of which are features of LSECs. Primary LSECs were also isolated from liver fibrosis model mice prompted by CCl_4, which expressed considerably higher SphK1 than that in the Wild mice ($p < 0.01$) (**Figure 5D**).

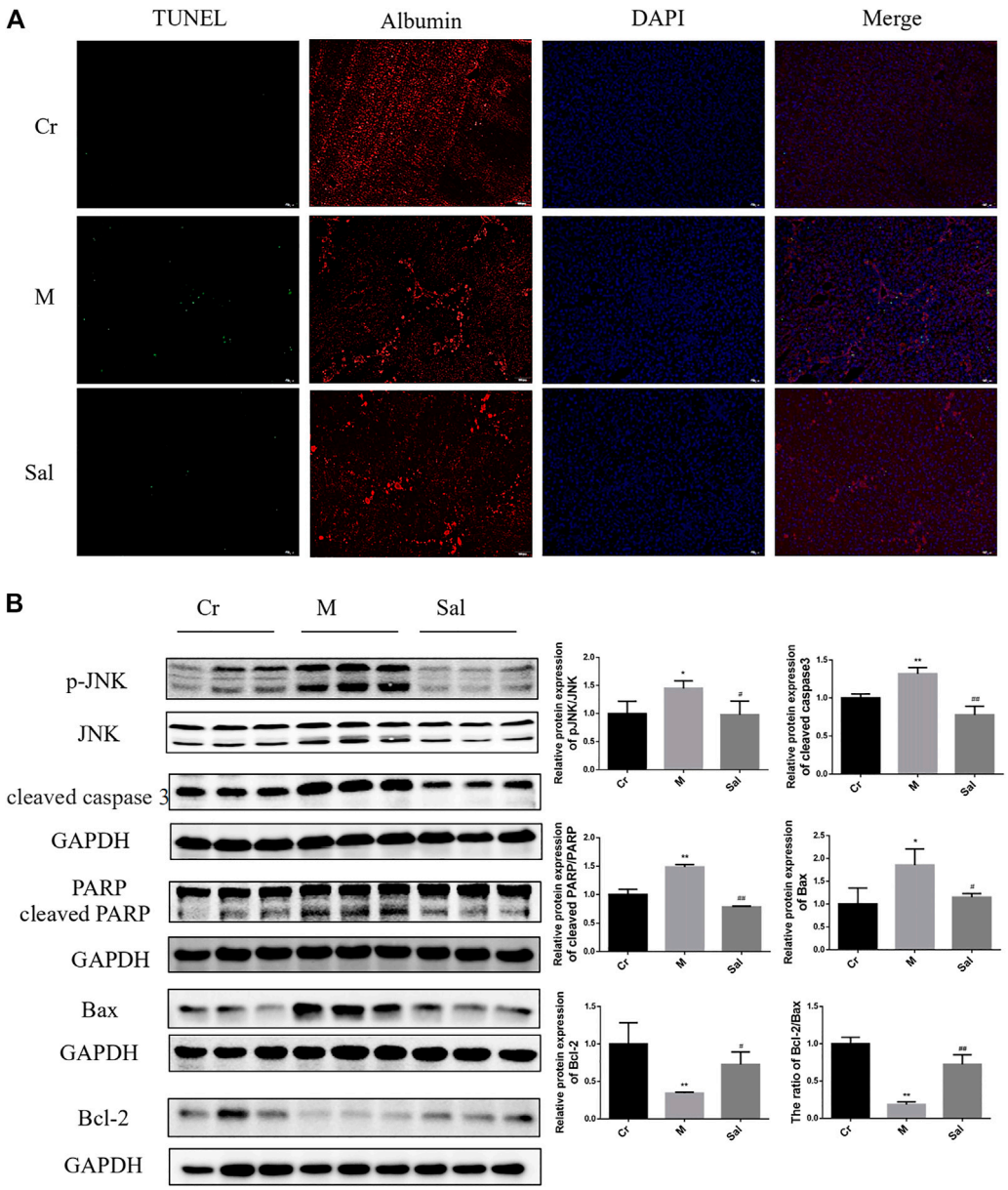


FIGURE 2 | Effect of Sal on apoptosis of hepatocytes in mice with liver fibrosis induced by CCl_4. **(A)**: Immunofluorescence staining of TUNEL and Albumin (×100). **(B)**: Effects of Sal on the expression of p-JNK, cleaved caspase3, cleaved RARP, Bax, and Bcl-2 in mice liver induced by CCl_4. ($n = 15$, $^{*}p < 0.05$, $^{**}p < 0.01$, vs. Cr; $^{\#}p < 0.05$, $^{\#\#}p < 0.01$, vs. M.). DAPI: 4′,6-diamidino-2-phenylindole; TUNEL: TdT-mediated dUTP nick end labeling.

Sal Alleviated Exosomal SphK1-Induced LX-2 Migration and Activation by Inhibiting AKT Activation

High levels of SphK1 were detected in primary mouse LSECs of liver fibrosis mice. Although the effect of exosomal SphK1 was tried to be studied on LSECs and HSC, the exosomes could not be derived owing to the inadequate number of primary LSECs. Thus, SK-HEP-1 cell lines that function similarly to LSECs were used (Cogger et al., 2008). Overexpression SphK1, SK-HEP-1, was established, and exosomes were isolated from the culture medium to study how exosomal SphK1 influenced the function of LX-2. As displayed in **Figures 6A,B**, substantially protein and mRNA expression of SphK1 was detected in SK-HEP-1 cells transfected with the lentivirus carrying SphK1 as compared with empty vector-transfected SK-HEP-1 cells ($p < 0.05$ or $p < 0.01$) (**Figures 6A,B**).

As predicted, the exosomes from the culture medium of $SphK^{+}$-SK-HEP-1 cells released significant quantities of SphK1. Moreover, upregulation of FN was recorded in the exosomes of $SphK^{+}$-SK-HEP-1 cells ($p < 0.05$ or $p < 0.01$) (**Figures 6D,E**). LX-2 cells were incubated with exosomes to

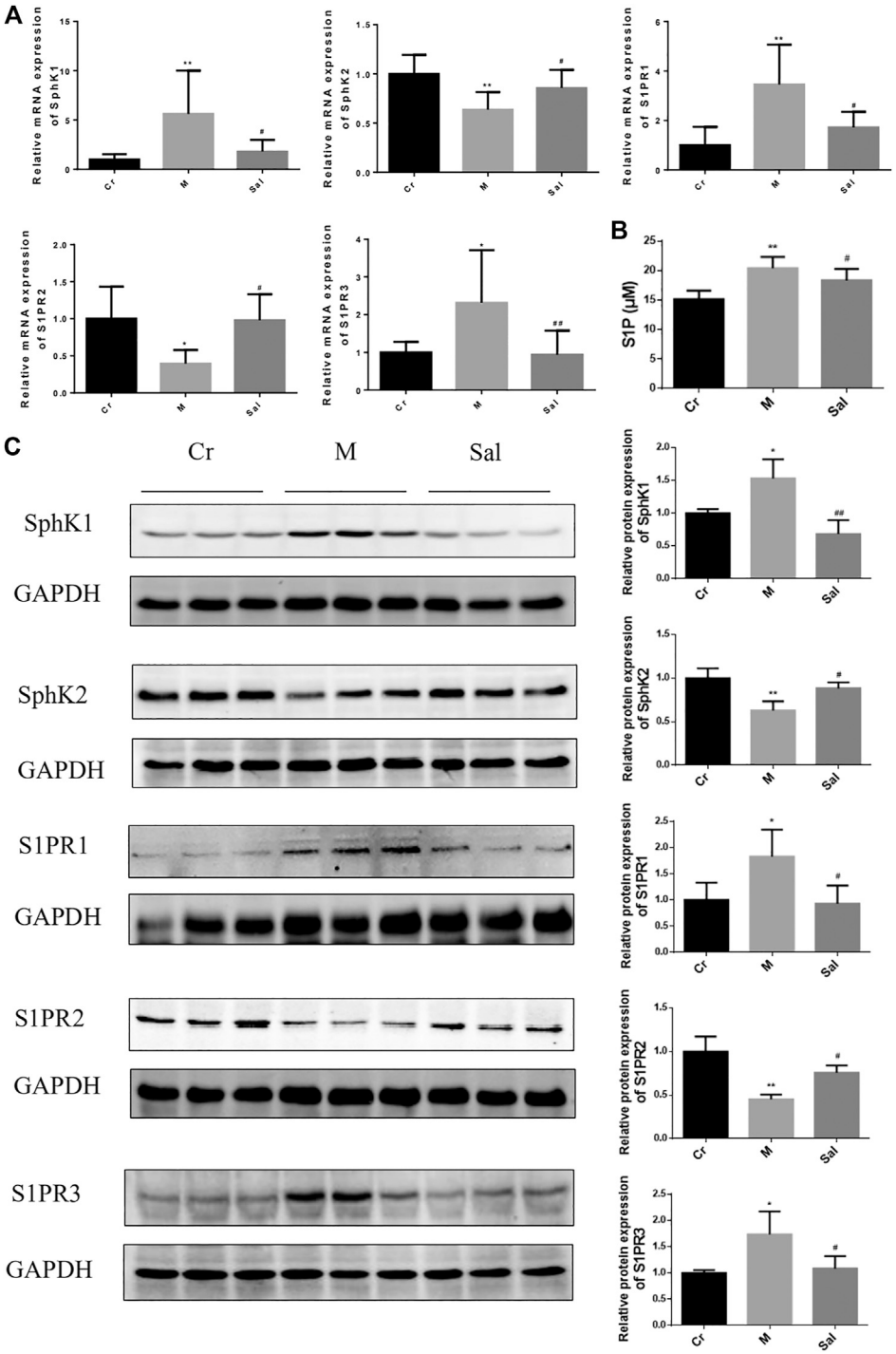


FIGURE 3 | Effects of Sal on the expressions of SphK/S1P/S1PRs signaling pathway in mice liver induced by CCl_4. **(A)**: The mRNA expressions of SphK1, SphK2, SPPR1, S1PR2 and S1PR3 in mice liver tissue. **(B)**: Level of S1P in serum from mice. **(C)**: The protein expressions of SphK1, SphK2, of S1PR1, S1PR2, and S1PR3 in mice liver tissue ($n = 15$, $^{*}p < 0.05$, $^{**}p < 0.01$, vs Cr; $^{\#}p < 0.05$, $^{\#\#}p < 0.01$, vs. M.) SphK1: Sphingosine kinase 1; S1P: Sphingosine-1-phosphate; S1PR1: Sphingosine 1-phosphate receptor 1; S1PR2: Sphingosine 1-phosphate receptor 2; S1PR3: Sphingosine 1-phosphate receptor 3.

explore the influence of exosomal SphK1 on the function of LX-2. As displayed in Figure 8F and G, the exosomal SphK1 caused the migration of LX-2 and the Col I level in LX-2, which could be reversed by Sal ($p < 0.05$ or $p < 0.01$) (**Figures 6F,G**). Earlier studies have evidenced AKT phosphorylation to support HSC activation, while exosomal SphK1 was found to encourage AKT

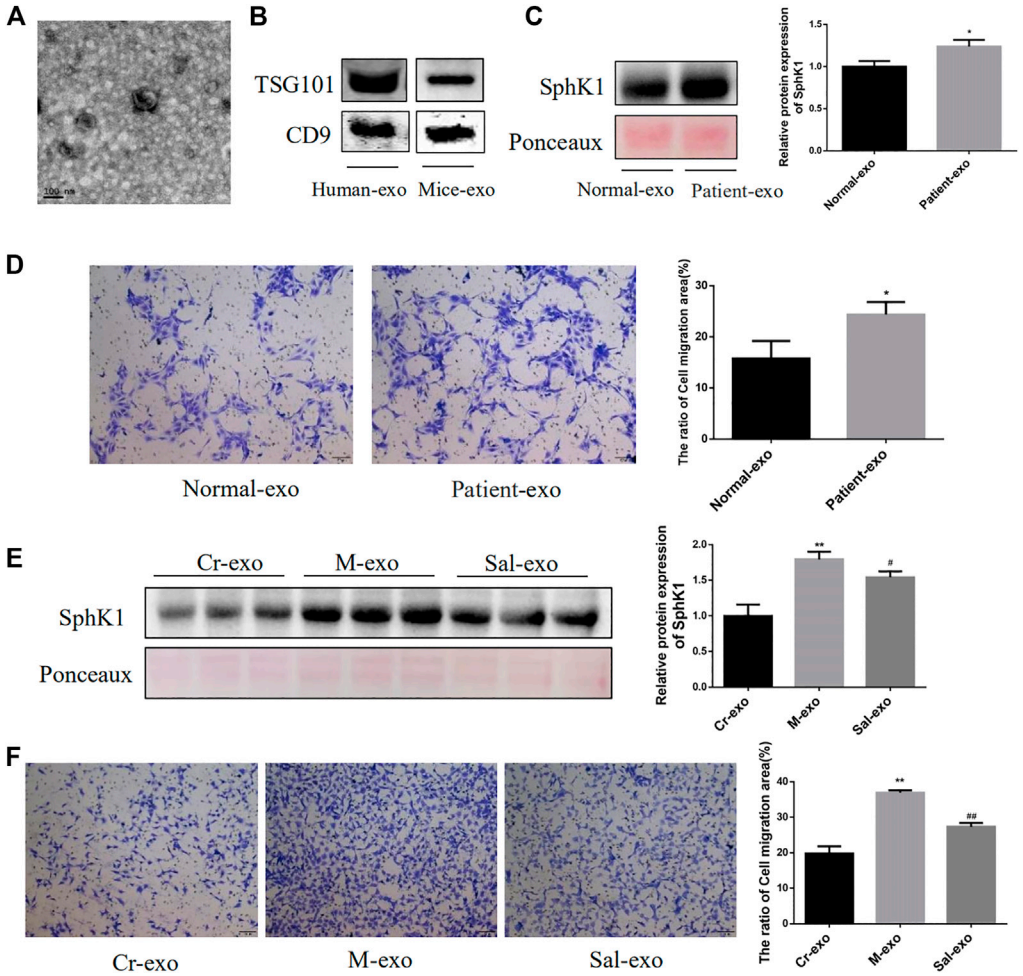


FIGURE 4 | Characteristics of serum exosomes and their effect on migration of HSC. **(A)**: Serum exosomes had a double-layer membrane structure. **(B)**: Expression of TSG101 and CD9 in serum exosomes from human and mice. **(C)**: Expression of SphK1 in serum exosomes from human ($n = 6$, $^{*}p < 0.05$, vs. Normal-exo.) **(D)**: Effects of serum exosomes from different populations on LX-2 migration ($n = 6$, $^{*}p < 0.05$, vs Normal-exo.) **(E)**: Expression of SphK1 in serum exosomes from different groups of mice ($n = 15$, $^{**}p < 0.01$, vs. Cr-exo, $^{\#}p < 0.05$, vs. M-exo,) **(F)**: Effects of serum exosomes from different groups of mice on JS 1 migration ($n = 15$, $^{**}p < 0.01$, vs Cr-exo, $^{\#\#}p < 0.01$, vs. M-exo.) TSG101: tumor susceptibility gene 101.

activation, and Sal reduces this effect in this research ($p < 0.05$ or $p < 0.01$) (**Figure 6G**). Thus, Sal was theorized to lessen LX-2 migration and activation induced by exosomal SphK1 by hindering AKT activation.

DISCUSSION

According to the complex pathological mechanism of fibrosis, multiple targets and pathways are the traits of traditional Chinese medicine. Traditional Chinese herbal medicine has been increasingly substantiated to treat liver fibrosis (Li, 2020), as it has effectively established the protective influence of Sal on liver fibrosis (Wu et al., 2003; Feng et al., 2018). Sal has already been proved to inhibit the migration of HSC in one of our earlier researches (Zhang et al., 2012). Exosomes have been explored extensively in recent years for their vital function as carriers for drug delivery. Earlier studies have revealed curcumin-encapsulated exosomes to possess anti-inflammatory, antioxidant, and anticancerous properties (Oskouie et al., 2018). In this study, a mouse model of liver fibrosis triggered by CCl_4 was replicated further to investigate Sal's potential influence on liver fibrosis. Exosomes carrying SphK1 secreted by SK-HEP-1, a cell line with endothelial cell function, were also isolated, and their effect on HSC function and the effect of Sal treatment *in vitro* was analyzed.

Inflammation is a significant feature of fibrosis; constraining hepatic inflammation is essential in treating liver fibrosis. Previous studies have reported that Sal reduces liver fibrosis through anti-inflammatory (Feng et al., 2018). In this study, Sal was not just found to efficiently reduce the serum concentrations of ALT and AST in CCl_4-induced liver fibrosis mice but also to hinder the infiltration of inflammatory cells into the liver tissue, evidencing that Sal could ease the damage caused by inflammation in the process of liver fibrosis. Unfortunately, in

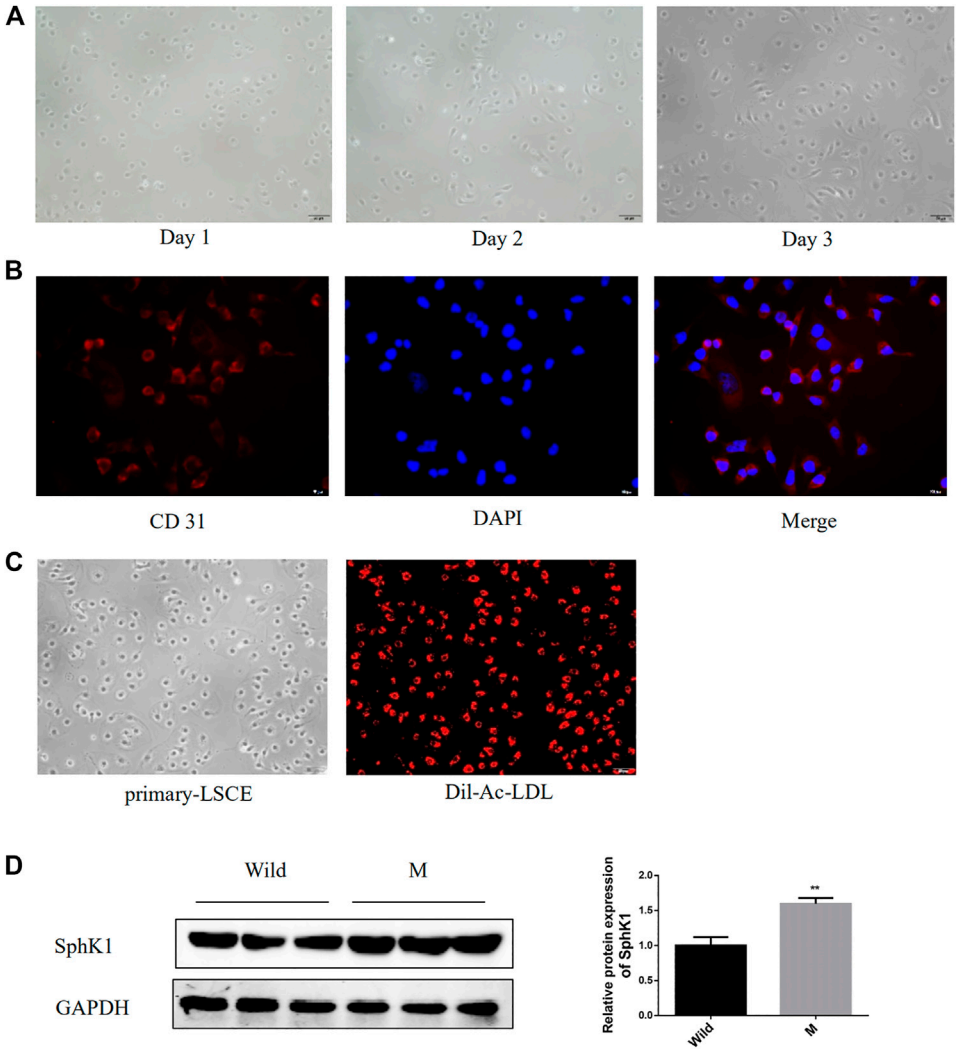


FIGURE 5 | Expression of SphK1 in LSECs isolated from mice with liver fibrosis induced by CCl_4. **(A)**: Morphology of isolated mouse primary LSECs. **(B)**: Isolated mouse primary LSEC could phagocytosis Dil-Ac-LDL. **(C)**: Isolated mouse primary LSECs expressed CD31. **(D)**: LSEC of mice with liver fibrosis upregulated the expression of SphK1 ($n = 5$, $^{**}p < 0.01$, vs. Wild.)

order to reserve as much serum as possible for the extraction of exosomes, this study did not detect IL1, IL6, TNF-α and other inflammatory factors in mouse serum, and failed to explain the anti-inflammatory effect of Sal more intuitively.

Cell apoptosis is known to have an essential role in embryonic development and tissue homeostasis (Tuzlak et al., 2016), but apoptotic cells can activate a series of pathological events under certain circumstances (Schwabe and Luedde, 2018). Apoptosis of damaged hepatocytes amplified inflammation, HSC activation, and liver fibrosis (Kisseleva and Brenner, 2020). Cell apoptosis primarily includes extrinsic and intrinsic pathways. The intrinsic or the mitochondrial-mediated apoptosis pathway is essentially regulated by the Bcl-2 family (Bock and Tait, 2020). Bcl-2 family is divided into 3 categories on the basis of function and structure: BH3, the apoptosis initiator; the antiapoptotic guardians, such as Bcl-2; and the proapoptotic proteins, such as Bax and Bak (Czabotar et al., 2014). Various cytotoxic stimuli activate BH3 pathologically, subduing the expression of antiapoptotic proteins and activating proapoptotic proteins, thus destroying the permeability of the mitochondrial inner membrane. Mitochondrial apoptosis is known to be co-regulated by the Bcl-2 family; the ratio of Bcl-2 to Bax is the key determining factor of apoptosis (Yu et al., 2021). Damaged mitochondria secrete cytochrome C that in turn is known to activate the caspase family, which is a group of cysteine protease that participates in cell apoptosis (Van Opdenbosch and Lamkanfi, 2019). Of these, caspase-3 is the central link and an essential initiator of the apoptosis process (Galluzzi et al., 2016). Caspase-3 physiologically exists as an inactive zymogen. Caspase-3 is rapidly cleaved and activated to trigger cell death signals in case of various injuries (Lim et al., 2021). In the present study, the hepatocyte apoptosis was observed in the Model group, the

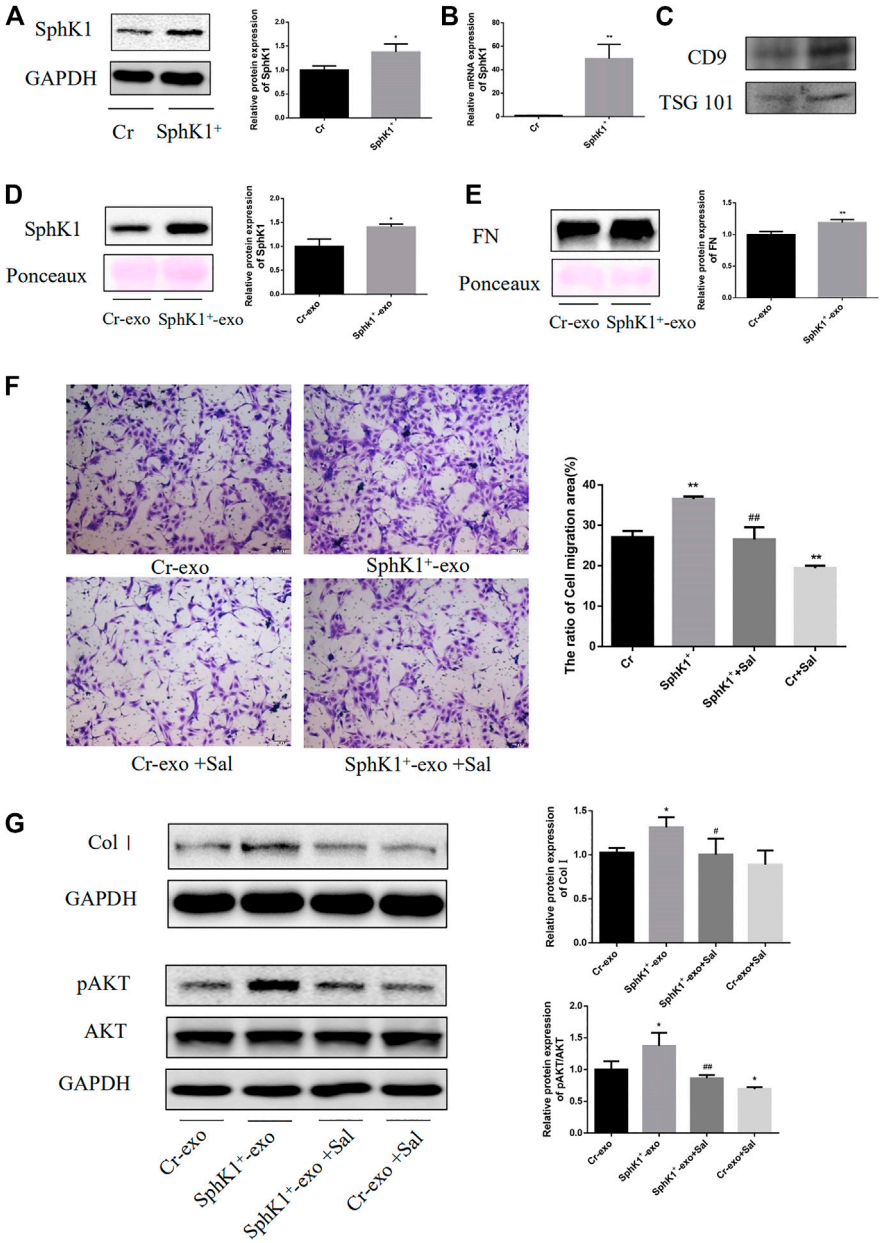


FIGURE 6 | Effects of Sal on exosomal SphK1-induced LX-2 migration and activation. **(A)**: Expression of SphK1 in transfected cells was detected by WB. **(B)**: Expression of SphK1 in transfected cells was detected by PCR. **(C)**: Expression of TSG101 and CD9 in exosomes from culture mediums. **(D,E)**: Expression of SphK1 and FN in exosomes from culture mediums of transfected cells. (n = 3, $^{**}p < 0.01$, vs Cr-exo.) **(F)**: Sal inhibited exosomal SphK1-induced LX-2 migration and activation. **(G)**: Sal inhibited exosomal SphK1-induced AKT phosphorylation in LX-2. (n = 3, $^{*}p < 0.05$, $^{**}p < 0.01$, vs. Cr-exo; $^{\#}p < 0.05$, $^{\#\#}p < 0.01$, vs. SphK1^{+}-exo.).

expression of cleaved caspase 3, cleaved PARP and Bax were upregulated, while Bcl-2 was downregulated. Sal was observed to reverse the high expression of Bax and low expression of Bcl-2 induced by CCl_4 and upregulate the ratio of Bcl-2 to Bax. Sal was also observed to inhibit the activation of caspase-3 and PRAP, the substrate of caspase-3, thereby hindering cell apoptosis.

SphK1 has been shown to be involved in the regulation of mitochondrial permeability transition by several studies. Besides, SphK1 deficiency hinders JNK activation and defends acetaminophen-induced hepatocyte death (Li et al., 2019), whereas SphK1 overexpression was found to aggravate cell apoptosis (Lu et al., 2018). In this study, Sal was detected to alleviate hepatocytes apoptosis as well as JNK activation. The effect of Sal on the SphK/S1P/S1PRs signaling pathway in CCl_4-induced hepatic fibrosis mice was also explored. S1P, bioactive sphingomyelin, is released by Sphingosine kinases (SphKs) catalyzing Sphingosine, which participates in regulating various biological activities such as cell proliferation and migration. Two

subtypes of SphK are SphK1 and SphK2 (Ogretmen, 2018). SphK1 can migrate from the cytoplasm to the plasma membrane and promote S1P formation on the cell membrane under the influence of growth factors, hormones, or cytokines. Furthermore, SphK1 occurs chiefly in the cytoplasm, whereas SphK2 in the nucleus and mitochondrial inner membrane, which can likely upsurge the S1P concentration in the nucleus (Spiegel and Milstien, 2011). High quantities of SphK1 expression have been shown recently to aid in the progression of liver fibrosis (Sato et al., 2016), whereas SphK1 inhibition substantially reduces the degree of liver fibrosis (Yang et al., 2013). Another study found compared with that in healthy volunteers, the level of SphK2 was reduced in the liver of patients with alcoholic cirrhosis and hepatocellular carcinoma, and SphK2 deficiency could aggravate liver injury induced by alcohol (Kwong et al., 2019). Our date suggested that the expression of SphK1 in the fibrotic liver was remarkably upregulated, and the SphK2 level was obviously reduced, in agreement with the findings of earlier researches. While Sal could reverse these changes, whether these changes were stimulating or hindering. Moreover, there are growing researches regarding of the expression level of S1P and its ligands and their roles in liver fibrosis. For instance, Yang et al. (Yang et al., 2013) reported the expression of S1P increased progressively with the aggravation of liver fibrosis in mice induced by CCl_4 or BDL. Besides, their study displayed these changes of S1P are not only manifested in fibrotic animals but also upregulated in liver tissues from hepatitis B, C, and alcoholic cirrhosis patients (Yang et al., 2013). In this study, high concentrations of S1P were also found in the mice serum with liver fibrosis and Sal reversed the change of S1P. Earlier studies have established that S1PR1, S1PR2, and S1PR3 can be expressed in human liver fibroblasts (hepatic myofibroblast, hMFs). Remarkably, S1PR1 and S1PR3 occurred in high concentrations in fibrotic liver tissues, whereas S1PR2 expression was downregulated (Li et al., 2011), the findings being in agreement with those of our experiments. Essentially, Sal reversed the increase in S1PR1 and S1PR3 and the decrease in S1PR2 induced by CCl_4. Based on published research, the differences in the SphK/S1P/S1PRs signaling pathway among humans, rats, and mice samples may be owing to the species differences and diverse fibrogenesis mechanisms. Additional studies are indispensable to investigate the role of the SphK/S1P/S1PRs signaling pathway in regulating liver fibrosis and its therapeutic significance.

After observing the effects of Sal on SphK1 and S1PRs *in vivo*, we tried to clarify whether the influence of Sal on SphK1 and S1PRs in liver tissue could be localized on certain cells. Considering the key role of HSC in liver fibrosis, LX-2 was treated with PMA (an agonist of SphK1) and/or Sal. The results showed that Sal could inhibit HSC migration induced by PMA, but did not affect the expressions of SphK1 and S1PRs in LX-2 (Data not shown). Combined with previous studies reported that exosomal SphK1 derived by LSEC could induce HSC migration (Wang et al., 2015). Therefore, we tried to illustrate effect of Sal on HSC based on regulation of LSEC exosomes on HSC.

Exosomes are extracellular vesicles of diameters ranging from 50 to 150 nm (van Niel et al., 2018). They possess the same characteristics containing "exosome marker" proteins related to exosome biogenesis and secretion, such as the Rab family, GTPase, ALG-2-interacting protein X (ALIX), and TSG101. Exosomes are also rich in heat shock proteins, such as HSP60, HSP70, and HSP90; integrins; and tetraspanins, viz, CD9, CD63, CD81, and CD82. However, the inclusions of exosomes are highly heterogeneous based on the state and type of cells (Sung et al., 2018). For instance, the expression of CD81 in serum exosomes of patients with chronic hepatitis C was significantly higher than that in the healthy volunteers and patients in the virus response phase (Martin-Walter et al., 2012). The exosomes of lipid-induced hepatocyte secreted high amounts of miR-128-3p, which stimulated HSC migration after being taken up by HSC(Povero et al., 2015). In this study, serum exosomes derived from liver cirrhosis patients or mice with liver fibrosis released high concentrations of SphK1 and promoted HSC migration. Simultaneously, compared with serum-derived exosomes from Model group mice, serum-derived exosomes from Sal group mice expressed lower SphK1 and reduced JS 1 migration. In addition, exosome-mediated intercellular communication has been shown to require docking on the plasma membrane in an earlier study (Teng and Fussenegger, 2021). Also, integrins, lipids, heparan sulfate proteoglycans, and ECM components (especially FN and laminin) can function as mediators in the intercellular interaction (van Niel et al., 2018). In this study, the expression of FN was upregulated in exosomes of $SphK^+$-SK-HEP-1 cells, signifying that the FN on the surface of exosomes mediated interactions between exosomes and cells thus influencing the function of the recipient cells. The concentration of SphK1 was amplified in primary LSECs of liver fibrosis mice. Also, exosomal SphK1 derived from SK-HEP-1, a cell line with a similar function to that of LSECs, promoted the migration, activation, and AKT phosphorylation of LX-2. Sal relieved these effects. These outcomes indicated that Sal likely alleviated the migration and activation of LX-2 induced by exosomal SphK1 by inhibiting the activation of AKT.

To conclude, our study evidenced that Sal could effectively reduce liver injury, hepatocyte apoptosis, and liver fibrosis *in vivo*. In addition, the protective efficacy of Sal might be comprehended by regulating JNK activation and controlling the SphK/S1P/S1PRs axis. Moreover, Sal was observed to reduce the migration and activation of LX-2 induced by exosomal SphK1 by subduing the activation of AKT *in vitro*. In summary, the present study explained the anti-fibrosis mechanism of Sal based on the perspective of regulating the biological activity of HSC by LSEC-derived exosomes. More experiments are needed to further explain the role of Sal on liver fibrosis.

DATA AVAILABILITY STATEMENT

The original contributions presented in the study are included in the article/Supplementary Material, further inquiries can be directed to the corresponding authors.

ETHICS STATEMENT

The studies were approved by The Ethics Committee of Shuguang Hospital, Affiliated to Shanghai University of Traditional Chinese Medicine and The Committee on the Care and Use of Live Animals for Teaching and Research of the Shanghai University of Traditional Chinese Medicine. All participants provided written informed consent.

AUTHOR CONTRIBUTIONS

QY carried out the experiment and wrote the manuscript. YZ, CZ, LX, and JP guided the experiments and reviewed the manuscript.

FUNDING

This work was supported by grants from the National Natural Science Foundation of China (No. 81773980).

REFERENCES

Bock, F. J., and Tait, S. W. G. (2020). Mitochondria as Multifaceted Regulators of Cell Death. *Nat. Rev. Mol. Cel Biol* 21 (2), 85–100. doi:10.1038/s41580-019-0173-8

Cai, L., Li, Y., Zhang, Q., Sun, H., Yan, X., Hua, T., et al. (2017). Salidroside Protects Rat Liver against Ischemia/reperfusion Injury by Regulating the GSK-3β/Nrf2-dependent Antioxidant Response and Mitochondrial Permeability Transition. *Eur. J. Pharmacol.* 806, 32–42. doi:10.1016/j.ejphar.2017.04.011

Cogger, V. C., Arias, I. M., Warren, A., Mcmahon, A. C., Kiss, D. L., Avery, V. M., et al. (2008). The Response of Fenestrations, Actin, and Caveolin-1 to Vascular Endothelial Growth Factor in SK Hep1 Cells. *Am. J. Physiology-Gastrointestinal Liver Physiol.* 295 (1), G137–G145. doi:10.1152/ajpgi.00069.2008

Czabotar, P. E., Lessene, G., Strasser, A., and Adams, J. M. (2014). Control of Apoptosis by the BCL-2 Protein Family: Implications for Physiology and Therapy. *Nat. Rev. Mol. Cel Biol* 15 (1), 49–63. doi:10.1038/nrm3722

Deleve, L. D. (2015). Liver Sinusoidal Endothelial Cells in Hepatic Fibrosis. *Hepatology* 61 (5), 1740–1746. doi:10.1002/hep.27376

Feng, J., Chen, K., Xia, Y., Wu, L., Li, J., Li, S., et al. (2018). Salidroside Ameliorates Autophagy and Activation of Hepatic Stellate Cells in Mice via NF-Kb and TGF-β1/Smad3 Pathways. *Dddt* 12, 1837–1853. doi:10.2147/DDDT.S162950

Galluzzi, L., López-Soto, A., Kumar, S., and Kroemer, G. (2016). Caspases Connect Cell-Death Signaling to Organismal Homeostasis. *Immunity* 44 (2), 221–231. doi:10.1016/j.immuni.2016.01.020

Hernandez-Gea, V., and Friedman, S. L. (2011). Pathogenesis of Liver Fibrosis. *Annu. Rev. Pathol. Mech. Dis.* 6 (6), 425–456. doi:10.1146/annurev-pathol-011110-130246

Jiansheng, X., and Ying, L. (2012). Effects of Salidroside on Exhaustive Exercise-Induced Oxidative Stress in Rats. *Mol. Med. Rep.* 6 (5), 1195–1198. doi:10.3892/mmr.2012.1060

Kisseleva, T., and Brenner, D. (2020). Molecular and Cellular Mechanisms of Liver Fibrosis and its Regression. *Nat. Rev. Gastroenterol. Hepatol.* 18 (3), 151–166. doi:10.1038/s41575-020-00372-7

Kono, Y., Nishiuma, T., Nishimura, Y., Kotani, Y., Okada, T., Nakamura, S.-i., et al. (2007). Sphingosine Kinase 1 Regulates Differentiation of Human and Mouse Lung Fibroblasts Mediated by TGF-B1. *Am. J. Respir. Cel Mol Biol* 37 (4), 395–404. doi:10.1165/rcmb.2007-0065OC

Kwong, E. K., Liu, R., Zhao, D., Li, X., Zhu, W., Wang, X., et al. (2019). The Role of Sphingosine Kinase 2 in Alcoholic Liver Disease. *Dig. Liver Dis.* 51 (8), 1154–1163. doi:10.1016/j.dld.2019.03.020

Lee, Y.-S., Kim, S. Y., Ko, E., Lee, J.-H., Yi, H.-S., Yoo, Y. J., et al. (2017). Exosomes Derived from Palmitic Acid-Treated Hepatocytes Induce Fibrotic Activation of Hepatic Stellate Cells. *Sci. Rep.* 7 (1). doi:10.1038/s41598-017-03389-2

Li, C., Zheng, S., You, H., Liu, X., Lin, M., Yang, L., et al. (2011). Sphingosine 1-phosphate (S1P)/S1P Receptors Are Involved in Human Liver Fibrosis by Action on Hepatic Myofibroblasts Motility. *J. Hepatol.* 54 (6), 1205–1213. doi:10.1016/j.jhep.2010.08.028

Li, H. (2020). Advances in Anti Hepatic Fibrotic Therapy with Traditional Chinese Medicine Herbal Formula. *J. Ethnopharmacology* 251, 112442. doi:10.1016/j.jep.2019.112442

Li, L., Wang, H., Zhang, J., Sha, Y., Wu, F., Wen, S., et al. (2019). SPHK1 Deficiency Protects Mice from Acetaminophen-Induced ER Stress and Mitochondrial Permeability Transition. *Cell Death Differ* 27, 1924–1937. doi:10.1038/s41418-019-0471-x

Lim, J.-Y., Lee, J.-H., Yun, D.-H., Lee, Y.-M., and Kim, D.-K. (2021). Inhibitory Effects of Nodakenin on Inflammation and Cell Death in Lipopolysaccharide-Induced Liver Injury Mice. *Phytomedicine* 81, 153411. doi:10.1016/j.phymed.2020.153411

Liu, W., Hou, Y., Chen, H., Wei, H., Lin, W., Li, J., et al. (2011). Sample Preparation Method for Isolation of Single-Cell Types from Mouse Liver for Proteomic Studies. *Proteomics* 11 (17), 3556–3564. doi:10.1002/pmic.201100157

Lu, J., Yi, Y., Pan, R., Zhang, C., Han, H., Chen, J., et al. (2018). Berberine Protects HK-2 Cells from Hypoxia/reoxygenation Induced Apoptosis via Inhibiting SPHK1 Expression. *J. Nat. Med.* 72 (2), 390–398. doi:10.1007/s11418-017-1152-z

Meyer, J., Lacotte, S., Morel, P., Gonelle-Gispert, C., and Bühler, L. (2016). An Optimized Method for Mouse Liver Sinusoidal Endothelial Cell Isolation. *Exp. Cel Res.* 349 (2), 291–301. doi:10.1016/j.yexcr.2016.10.024

Ogretmen, B. (2018). Sphingolipid Metabolism in Cancer Signalling and Therapy. *Nat. Rev. Cancer* 18 (1), 33–50. doi:10.1038/nrc.2017.96

Oskouie, M. N., Aghili Moghaddam, N. S., Butler, A. E., Zamani, P., and Sahebkar, A. (2018). Therapeutic Use of Curcumin-encapsulated and Curcumin-primed Exosomes. *J. Cel. Physiol.* 234 (6), 8182–8191. doi:10.1002/jcp.27615

Povero, D., Panera, N., Eguchi, A., Johnson, C. D., Papouchado, B. G., de Araujo Horcel, L., et al. (2015). Lipid-Induced Hepatocyte-Derived Extracellular Vesicles Regulate Hepatic Stellate Cells via MicroRNA Targeting Peroxisome Proliferator-Activated Receptor-γ. *Cell Mol. Gastroenterol. Hepatol.* 1 (6), 646–663. doi:10.1016/j.jcmgh.2015.07.007

Ren, M., Xu, W., and Xu, T. (2019). Salidroside Represses Proliferation, Migration and Invasion of Human Lung Cancer Cells through AKT and MEK/ERK Signal Pathway. *Artif. Cell Nanomedicine, Biotechnol.* 47 (1), 1014–1021. doi:10.1080/21691401.2019.1584566

Sato, M., Ikeda, H., Uranbileg, B., Kurano, M., Saigusa, D., Aoki, J., et al. (2016). Sphingosine Kinase-1, S1P Transporter Spinster Homolog 2 and S1P2 mRNA Expressions Are Increased in Liver with Advanced Fibrosis in Human. *Sci. Rep.* 6 (1), 32119. doi:10.1038/srep32119

Schwabe, R. F., and Luedde, T. (2018). Apoptosis and Necroptosis in the Liver: a Matter of Life and Death. *Nat. Rev. Gastroenterol. Hepatol.* 15 (12), 738–752. doi:10.1038/s41575-018-0065-y

Spiegel, S., and Milstien, S. (2011). The Outs and the Ins of Sphingosine-1-Phosphate in Immunity. *Nat. Rev. Immunol.* 11 (6), 403–415. doi:10.1038/nri2974

Sung, S., Kim, J., and Jung, Y. (2018). Liver-Derived Exosomes and Their Implications in Liver Pathobiology. *Ijms* 19 (12), 3715. doi:10.3390/ijms19123715

Teng, F., and Fussenegger, M. (2021). Shedding Light on Extracellular Vesicle Biogenesis and Bioengineering. *Adv. Sci.* 8 (1), 2003505. doi:10.1002/advs.202003505

Tsuchida, T., and Friedman, S. L. (2017). Mechanisms of Hepatic Stellate Cell Activation. *Nat. Rev. Gastroenterol. Hepatol.* 14 (7), 397–411. doi:10.1038/nrgastro.2017.38

Tuzlak, S., Kaufmann, T., and Villunger, A. (2016). Interrogating the Relevance of Mitochondrial Apoptosis for Vertebrate Development and Postnatal Tissue Homeostasis. *Genes Dev.* 30 (19), 2133–2151. doi:10.1101/gad.28929810.1101/gad.289298.116

van Niel, G., D'Angelo, G., and Raposo, G. (2018). Shedding Light on the Cell Biology of Extracellular Vesicles. *Nat. Rev. Mol. Cel Biol* 19 (4), 213–228. doi:10.1038/nrm.2017.125

Van Opdenbosch, N., and Lamkanfi, M. (2019). Caspases in Cell Death, Inflammation, and Disease. *Immunity* 50 (6), 1352–1364. doi:10.1016/j.immuni.2019.05.020

Wang, E., He, X., and Zeng, M. (2019). The Role of S1P and the Related Signaling Pathway in the Development of Tissue Fibrosis. *Front. Pharmacol.* 9, 1504. doi:10.3389/fphar.2018.01504

Wang, R., Ding, Q., Yaqoob, U., de Assuncao, T. M., Verma, V. K., Hirsova, P., et al. (2015). Exosome Adherence and Internalization by Hepatic Stellate Cells Triggers Sphingosine 1-phosphate-dependent Migration. *J. Biol. Chem.* 290 (52), 30684–30696. doi:10.1074/jbc.M115.671735

Welker, M. W., Reichert, D., Susser, S., Sarrazin, C., Martinez, Y., Herrmann, E., et al. (2012). Soluble Serum CD81 Is Elevated in Patients with Chronic Hepatitis C and Correlates with Alanine Aminotransferase Serum Activity. *PLoS One* 7 (2), e30796. doi:10.1371/journal.pone.0030796

Wu, X.-L., Zeng, W. Z., Wang, P. L., Lei, C. T., Jiang, M. D., Chen, X. B., et al. (2003). Effect of Compound Rhodiola Sachalinensis A Bor on CCl4-Induced Liver Fibrosis in Rats and its Probable Molecular Mechanisms. *Wjg* 9 (7), 1559–1562. doi:10.3748/wjg.v9.i7.1559

Xu, N., Huang, F., Jian, C., Qin, L., Lu, F., Wang, Y., et al. (2019). Neuroprotective Effect of Salidroside against Central Nervous System Inflammation-induced Cognitive Deficits: A Pivotal Role of Sirtuin 1-dependent N Rf-2/HO -1/NF -κ B Pathway. *Phytotherapy Res.* 33 (5), 1438–1447. doi:10.1002/ptr.6335

Yang, L., Yue, S., Yang, L., Liu, X., Han, Z., Zhang, Y., et al. (2013). Sphingosine Kinase/sphingosine 1-phosphate (S1P)/S1P Receptor axis Is Involved in Liver Fibrosis-Associated Angiogenesis. *J. Hepatol.* 59 (1), 114–123. doi:10.1016/j.jhep.2013.02.021

Yu, H.-h., Qiu, Y.-x., Li, B., Peng, C.-y., Zeng, R., and Wang, W. (2021). Kadsura Heteroclita Stem Ethanol Extract Protects against Carbon Tetrachloride-Induced Liver Injury in Mice via Suppression of Oxidative Stress, Inflammation, and Apoptosis. *J. Ethnopharmacology* 267, 113496. doi:10.1016/j.jep.2020.113496

Yuan, Y., Wu, X., Zhang, X., Hong, Y., and Yan, H. (2019). Ameliorative Effect of Salidroside from Rhodiola Rosea L. On the Gut Microbiota Subject to Furan-Induced Liver Injury in a Mouse Model. *Food Chem. Toxicol.* 125, 333–340. doi:10.1016/j.fct.2019.01.007

Zhang, Z., Ping, J., and Xu, L. (2012). Screening Chinese Medicine Components for Inhibition of Human Hepatic Stellate Cell Migration. *J. Clin. Hepatol.* 28 (3), 183–188. doi:10.3969/j.issn.1001-5256.2012.03.00

Zheng, T., Yang, X., Li, W., Wang, Q., Chen, L., Wu, D., et al. (2018). Salidroside Attenuates High-Fat Diet-Induced Nonalcoholic Fatty Liver Disease via AMPK-dependent TXNIP/NLRP3 Pathway. *Oxidative Med. Cell Longevity* 2018, 1–17. doi:10.1155/2018/8597897

Conflict of Interest: The authors declare that the research was conducted in the absence of any commercial or financial relationships that could be construed as a potential conflict of interest.

Copyright © 2021 Ye, Zhou, Zhao, Xu and Ping. This is an open-access article distributed under the terms of the Creative Commons Attribution License (CC BY). The use, distribution or reproduction in other forums is permitted, provided the original author(s) and the copyright owner(s) are credited and that the original publication in this journal is cited, in accordance with accepted academic practice. No use, distribution or reproduction is permitted which does not comply with these terms.

frontiers in Pharmacology

ORIGINAL RESEARCH
published: 17 May 2021
doi: 10.3389/fphar.2021.589273

Dapagliflozin Alleviates Hepatic Steatosis by Restoring Autophagy via the AMPK-mTOR Pathway

Liuran Li[1†], Qinghua Li[1†], Wenbin Huang[2], Yibing Han[1], Huiting Tan[1], Min An[1], Qianru Xiang[1], Rui Zhou[3], Li Yang[1,4]* and Yanzhen Cheng[1]**

[1]Department of Endocrinology, Zhujiang Hospital, Southern Medical University, Guangzhou, China, [2]Department of Hepatobiliary Surgery II, Zhujiang Hospital, Southern Medical University, Guangzhou, China, [3]Department of Pathology, School of Basic Medical Sciences, Southern Medical University, Guangzhou, China, [4]Department of Nutrition, Zhujiang Hospital, Southern Medical University, Guangzhou, China

OPEN ACCESS

Edited by:
Wolfgang Richard Stremmel, Medical Center Baden-Baden, Germany

Reviewed by:
Wen-Chung Huang, Chang Gung University of Science and Technology, Taiwan
Liwei Xie, Guangdong Institute of Microbiology, China

***Correspondence:**
Yanzhen Cheng
chengyzx@163.com
Li Yang
yangli19762009@163.com
Rui Zhou
yaruisunny@sina.com

[†]These authors have contributed equally to this work

Specialty section:
This article was submitted to Gastrointestinal and Hepatic Pharmacology, a section of the journal Frontiers in Pharmacology

Received: 30 July 2020
Accepted: 30 April 2021
Published: 17 May 2021

Citation:
Li L, Li Q, Huang W, Han Y, Tan H, An M, Xiang Q, Zhou R, Yang L and Cheng Y (2021) Dapagliflozin Alleviates Hepatic Steatosis by Restoring Autophagy via the AMPK-mTOR Pathway. Front. Pharmacol. 12:589273. doi: 10.3389/fphar.2021.589273

As a newly approved oral hypoglycaemic agent, the sodium-glucose cotransporter 2 (SGLT2) inhibitor dapagliflozin, which is derived from the natural product phlorizin can effectively reduce blood glucose. Recent clinical studies have found that dapagliflozin alleviates non-alcoholic fatty liver disease (NAFLD), but the specific mechanism remains to be explored. This study aimed to investigate the underlying mechanism of dapagliflozin in alleviating hepatocyte steatosis *in vitro* and *in vivo*. We fed the spontaneous type 2 diabetes mellitus rats with high-fat diets and cultured human normal liver LO2 cells and human hepatocellular carcinoma HepG2 cells with palmitic acid (PA) to induce hepatocellular steatosis. Dapagliflozin attenuated hepatic lipid accumulation both *in vitro* and *in vivo*. In Zucker diabetic fatty (ZDF) rats, dapagliflozin reduced hepatic lipid accumulation via promoting phosphorylation of acetyl-CoA carboxylase 1 (ACC1), and upregulating lipid β-oxidation enzyme acyl-CoA oxidase 1 (ACOX1). Furthermore, dapagliflozin increased the expression of the autophagy-related markers LC3B and Beclin1, in parallel with a drop in p62 level. Similar effects were observed in PA-stimulated LO2 cells and HepG2 cells. Dapagliflozin treatment could also significantly activated AMPK and reduced the phosphorylation of mTOR in ZDF rats and PA-stimulated LO2 cells and HepG2 cells. We demonstrated that dapagliflozin ameliorates hepatic steatosis by decreasing lipogenic enzyme, while inducing fatty acid oxidation enzyme and autophagy, which could be associated with AMPK activation. Moreover, our results indicate that dapagliflozin induces autophagy via the AMPK-mTOR pathway. These findings reveal a novel clinical application and functional mechanism of dapagliflozin in the treatment of NAFLD.

Keywords: NAFLD, AMPK, mTOR, autophagy, dapagliflozin

INTRODUCTION

Non-alcoholic fatty liver disease (NAFLD), the most common liver disease worldwide, is characterized by the hepatic fat accumulation in patients without alcohol abuse (Angulo, 2002). Metabolic syndromes, such as obesity and hyperglycaemia, predispose patients to developing severe NAFLDs, including nonalcoholic steatohepatitis (NASH), liver cirrhosis, and hepatocellular carcinoma (Lu et al., 2018). In patients with type 2 diabetes mellitus (T2DM), the prevalence rate of NAFLD is approximately 70%, among which 20% develops advanced fibrosis, revealing the high correlation between diabetes and NAFLD (Bril et al., 2016). In fact, NAFLD is only one outcome of multisystem diseases, in which the most frequent causes of high morbidity and mortality are cardiovascular diseases, extrahepatic malignant

tumors and liver-related complications (Adams et al., 2017). At present, the common measures for NAFLD treatment are restricted to diet adjustment, exercise and bariatric surgery, due to lacking of effective and safe medications. Therefore, a pharmacological treatment for NAFLD is urgently required.

Dapagliflozin, a sodium-glucose cotransporter 2 (SGLT2) inhibitor, is a novel antidiabetic agent that is approved for the treatment of T2DM by based on its ability to inhibit SGLT2-mediated renal glucose reabsorption. In addition to providing effective glycaemic control, dapagliflozin help decrease body weight, reduce rate of cardiovascular death, and possibly slow the progression of diabetic kidney diseases (Dhillon, 2019). Dapagliflozin has been reported to alleviate hepatic steatosis in patients with type 2 diabetes and NAFLD; however, whether the improvement in liver steatosis is related to the reduction in body weight by dapagliflozin cannot be ruled out (Kurinami et al., 2018; Shimizu et al., 2019). A recent study suggested that dapagliflozin attenuated SGLT2 expression, which could prevent excessive glucose absorption and increase AMPK phosphorylation in HFD-induced obese mice or OA-stimulated HuS-E/2 cells (Chiang et al., 2020), but the explicit mechanism has not yet been fully clarified. Thus, whether dapagliflozin can moderate hepatic steatosis independent of hypoglycaemic control and body weight loss requires further investigation.

Acetyl-CoA carboxylase 1 (ACC1), a rate-controlling enzyme in *de novo* lipogenesis, plays a crucial role in fatty acid metabolism. Inhibition of ACC1 can significantly reduce hepatic steatosis and hepatic insulin resistance (Brownsey et al., 1997; Goedeke et al., 2018). Acyl-CoA oxidase 1 (ACOX1), a rate-limiting enzyme in the peroxisomal β-oxidation pathway, promotes catabolism of very long–chain fatty acids. ACOX1-deficient mice exhibit spontaneous hepatic steatosis and steatohepatitis (Sheridan et al., 2011; Moreno-Fernandez et al., 2018). Hepatic lipid accumulation is caused by an imbalance between lipid synthesis and lipid degradation, which are mediated through several pathways, such as increased *de novo* lipogenesis and reduced fatty acid oxidation. AMPK is a vital energy sensor that regulates hepatic lipid metabolism (Madiraju et al., 2016). mTOR, a crucial downstream target of AMPK, negatively regulates autophagy (Kim and Guan., 2015). It was reported that the hepatic autophagy was suppressed by inhibiting AMPK, which caused the development of hepatic steatosis (You et al., 2004). Although the pathogenesis of NAFLD is elusive, increasing evidence suggests that impaired autophagy plays a vital role in the development of NAFLD. In the present study, we investigated the protective effect of the SGLT2 inhibitor dapagliflozin in alleviating NAFLD both *in vivo* and *in vitro*, and further clarified the role of AMPK activation in ameliorating hepatic lipid accumulation and the involvement of the AMPK-mTOR signaling pathway in autophagy induction.

MATERIALS AND METHODS

Antibodies and Reagents

Protein expression was assessed by immunoblot analysis of cell lysates (20–60 μg) in RIPA buffer in the presence of the following antibodies: including anti-p-AMPK (Affinity, AF3423), anti-AMPK (Affinity, AF6423), anti-p-ACC1 (Cell Signaling Technology, 11818s), anti-ACC1(Cell Signaling Technology, 4190s), anti-ACOX1 (Santa Cruz Biotechnology, sc-517306), anti-p-mTOR (Affinity, AF3308), anti-mTOR (Affinity, AF6308), anti-SGLT2 (Abcam, ab37296), anti-LC3B (Cell Signaling Technology, 12741S), anti-Beclin1 (Cell Signaling Technology, 4122s), anti-p62/SQSTM1 (Proteintech, 18420-1-AP), and anti-GAPDH (Abcam, ab8245).

Unless otherwise specified, all chemicals were purchased from Sigma-Aldrich (St. Louis, MO, United States). Dulbecco's modified Eagle's medium (DMEM), fetal bovine serum (FBS, Gibco) were obtained from Gibco; palmitate (PA) was obtained from Sigma-Aldrich (P9767); compound C (Comp C) was purchased from AbMole (M2238), chloroquine (CQ, S4157) and dapagliflozin (S1548) were bought from Selleck; and Oil Red O and triglyceride detection kit (G1262; BC0625) were obtained from Solarbio.

Animal Model

Eight-week-old male Zucker Diabetic Fatty (ZDF, fa/fa) rats and Zucker lean (ZL, fa/+) rats were purchased from the Laboratory Animal Center of Vital River [Beijing, China; license number, SYXK (Yue) 2011–0,074]. Five ZL rats and 10 male ZDF rats, at 8 weeks of age, were fed with a high-fat diet Purina #5008 for 4 weeks to induce diabetes. At the age of 12 weeks, the ZDF rats were randomly separated into two groups (n = 5 in each group) including: the diabetic control group (ZDF) and the diabetic group treated with dapagliflozin (ZDF + Dapa). In addition, the rats in ZL group were used as the non-diabetic controls. High-fat diet Purina #5008 was provided from 8 weeks of age to the end of the experiment. The rats in the ZDF + Dapa group were administered with dapagliflozin at a dosage of 1.0 mg/kg/day using intragastric gavage, while the ZL group and the ZDF group were treated with a vehicle via gavage as control. The interventions had been maintained for 9 weeks. Glucose levels of all the rats in different groups were measured every week. At the age of 21 weeks, all rats were anesthetized and sacrificed, blood was collected via the tail vein, and liver tissues were weighed at once after sampling and then stored at −80°C for subsequent measurements. All animal experimental procedures were performed with the approval of the Southern Medical University Animal Care and Use Committee in accordance with established ethical guidelines for animal studies (Resolution No. L2015039).

Oral Glucose Tolerance Tests

Oral glucose tolerance tests (2 g/kg of body weight) were performed on overnight fasted rats using a glucometer, and the blood samples were obtained from the tail vein at 0, 30, 60, and 120 min to measure blood glucose levels. Ultimately, the area under the curve (AUC) of blood glucose was calculated by the trapezoidal method (AUC = 1/4*fasting glucose +1/2*30-min glucose +3/4*60-min glucose +1/2*120-min glucose).

Cell Viability Assay

Cell viability assays of HepG2 cells and LO2 cells were carried out using Cell Counting Kit 8 (CCK8) (Dojindo; Kumamoto, Japan). Cells were plated into 96-well plates at a density of 1 × 10^4 cells

per well and cultured overnight. Then, the culture medium was replaced by DMEM supplemented with PA (0.3 mM) and dapagliflozin (0, 10, 20, 40, 80, and 100 μg/ml). After incubation for 24 h, 10 μL CCK-8 reagent and 90 μL DMEM were added to each well for an additional 2 h of cultivation and the absorbance value was analyzed with a microplate reader at the wavelength of 450 nm.

Cell Culture and Treatments

Immortalized normal human hepatocyte-derived liver cells (LO2) and human hepatocellular carcinoma cells (HepG2) were obtained from Shanghai Institute of Cellular Biology of Chinese Academy of Sciences. When cultured in DMEM supplemented with 10% FBS at 37°C in a humidified incubator containing 5% CO2, the cells were treated with 0.3 mM PA for 24 h to create the hepatocyte steatosis model *in vitro*. Then, hepatocytes were exposed to dapagliflozin at a concentration of 20 μM with or without chloroquine for 24 h. To study the effect of AMPK inhibition on autophagy, cells were treated with 10 μM compound C (Comp C) for 24 h.

Western Blot Analysis

HepG2 cells, LO2 cells and rat liver tissues were extracted in RIPA lysis buffer with protease inhibitor (Beyotime, Biotechnology). Phosphatase inhibitor was added to detect phosphorylated proteins. The protein concentrations of the lysates were quantified using the BCA Protein Assay Kit (Beyotime). Equal amounts of proteins were size-separated on a 10% SDS-polyacrylamide gel and then electroblotted onto PVDF membranes. Membranes were blocked by using a blocking reagent (0.1% Tween 20 and 5% Bovine Serum Albumin in TBS) for 1 h and subsequently incubated with specific primary antibodies (1:1,000) against LC3B, AMPK, p-AMPK, p62, Beclin1, ACC1, p-ACC1, ACOX1, p-mTOR, mTOR, SGLT2, and GAPDH overnight at 4 °C. After incubation with the secondary antibodies (1:10,000) for 1 h at room temperature, the signals were developed with an ECL luminescent kit and detected using enhanced chemiluminescence detection system (Pierce, Rockford, IL). The protein bands were analyzed densitometrically by ImageJ, and GAPDH protein was used as an internal control.

RNA Isolation and Quantitative Real-Time PCR Analysis

Total RNA was extracted from liver tissues and cells using TRIzol reagent and reverse-transcribed into cDNA according to the manufacturer's protocols. A quantitative PCR (qPCR) analysis was performed using SYBR Green PCR master mix (Applied Biosystems; Foster City, CA) on a 7,500 Fast Real-Time PCR system to examine the expression of related genes. The sequences of the primers used in this study are listed in (**Supplementary Table S1**). The expression levels of the target genes were normalized to that of GAPDH, and the ΔΔcycle threshold method was used for the quantitative analysis. All reagents in this study including those for RNA preparation, reverse transcription and quantitative real-time PCR analysis were purchased from Takara (Japan).

Immunofluorescence Staining

Immunofluorescence staining was performed according to standard protocols. Cells were fixed with 4% paraformaldehyde for 10 min, permeabilized in 0.25% Triton X-100 for 15 min and blocked with 5% normal goat serum for 1 h. Samples were incubated with primary antibodies against SGLT2 (1:100) and LC3B (1:100) at 4°C overnight followed by the incubation with secondary antibodies (1:100; Jackson Laboratories) for 1 h at room temperature, and the staining of 4′,6-diamidino-2-phenylindole (DAPI; 1:100; Invitrogen) for 4min. All cells were observed and captured under an Olympus FluoView FV1000 confocal microscope (Olympus, Hamburg, Germany). For the quantitative analysis, the average score of selected areas was calculated using Image Pro Plus 6.0 software (Media Cybernetics, Inc., Rockville, MD, United States).

Intracellular Lipid Droplets Staining

The accumulation of intracellular lipid droplets was detected by BODIPY 493/503 staining. Hepatocytes were treated with the indicated concentrations of PA and dapagliflozin for 24 h. Subsequently, the cells were fixed with 4% paraformaldehyde and stained with 1 μg/ml BODIPY 493/503 for 30 min at 37°C. Cell images and fluorescence intensity were visualized and quantified using an Olympus FluoView FV1000 confocal microscope.

Oil Red O Staining and Cellular Triglyceride Assays

Lipid droplets were visualized and quantified by Oil Red O (ORO) staining. According to the instructions, the cells were fixed with ORO fixative for 20min, and stained with newly prepared ORO staining solution for 20 min. After washing with 60% isopropanol, they were restained by Mayer hematoxylin for 2 min. Then, red-stained lipid droplets were subsequently observed and imaged using a light microscope (Olympus, Japan) at 400 × magnification. To quantify the intracellular lipid accumulation, the TG content in HepG2 cells and LO2 cells was measured using a Triglyceride Content Detection Kit according to the manufacturer's recommended protocols.

Liver Histopathological Examination

For Oil Red O staining, 8-μm-thick frozen sections were prepared and stained with freshly diluted Oil Red O staining solution for 20 min. After washed with 60% isopropanol, the sections were re-stained by Mayer hematoxylin for 2 min. The histological features of the samples were observed and imaged using a light microscopy. For hematoxylin and eosin (H&E) staining, the liver tissue was fixed in 4% formalin for 24 h, and then maintained in 70% alcohol for subsequent processing in paraffin for the histological studies. Paraffin sections were cut at 3 μm before paraffin removal. Then slices were obtained and stained with hematoxylin-eosin reagents.

Immunohistochemistry Staining (IHC)

IHC was used to detect the expression of proteins in 3 μm sections from formalin-fixed and paraffin-embedded tissue specimens as previously described (Tang et al., 2019). The tissues were

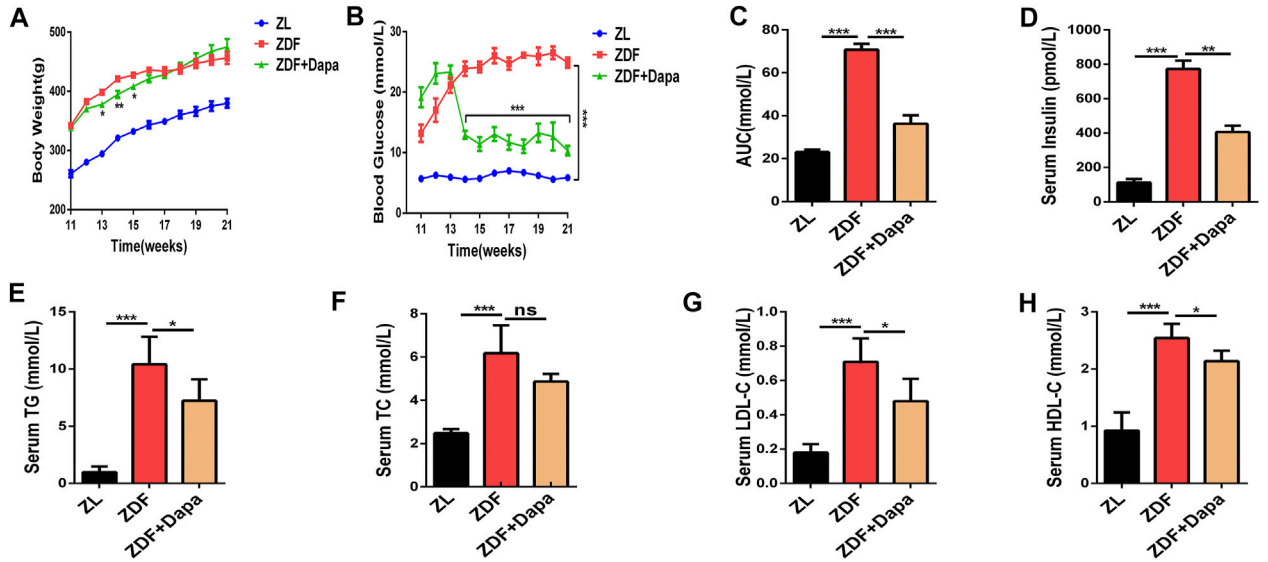


FIGURE 1 | Dapagliflozin improves glucose intolerance and regulates lipid metabolism in ZDF rats. **(A)** Body weight was recorded every week and body weight gain was measured at the end of the 21st week. **(B)** Blood glucose levels were monitored throughout the entire experiment. **(C)** The area under the curve (AUC) of blood glucose was calculated by the trapezoidal method. **(D)** Serum insulin levels were evaluated in groups. **(E–H)** Serum levels of TG, TC, LDL-C, and HDL-C were evaluated in groups. ZL: ZL rats as a normal control, ZDF: ZDF rats fed with a high-fat diet, ZDF + Dapa: dapagliflozin-treated ZDF rats. Data are expressed as the means ± SEM of five animals per group. $^{*}p < 0.05$, $^{**}p < 0.01$, and $^{***}p < 0.001$ compared with the ZDF rat group.

incubated with primary antibodies (1:200) against LC3B, Beclin1, p62, and SGLT-2 at 4°C overnight, followed by incubation with the secondary antibody. Then the sections were stained with a 3,3′-diaminobenzidine solution for 3 min and counterstained with Mayer's hematoxylin. Photomicrographs were captured under an optical microscope at 400 × magnification. Image-Pro Plus 6.0 software was used to select the same brown-yellow color as the unified standard for judging the positiveness of all photos, and analyze each photo to get the cumulative optical density value (IOD) of each photo and the pixel area of to be tested (AREA). The area density value (IOD/AREA) was obtained, and a larger value corresponded to a higher positive expression level.

Statistical Analysis

The results are expressed as the mean ± SEM. Comparisons between two groups were assessed using a *t*-test. Statistical analyses were performed using SPSS 20.0 statistical software and GraphPad Prism 6.02. Statistical significance was defined as a p value of <0.05.

RESULTS

Dapagliflozin Improves Glucose Intolerance and Regulates Lipid Metabolism in ZDF Rats

The ZDF rat is a recognized T2DM animal model characterized with overweight, impaired glucose tolerance and hyperlipidemia due to the leptin receptor mutation (Al-awar et al., 2016). To confirm the influence of dapagliflozin on the metabolic phenotypes of ZDF rats *in vivo*, body weight and blood glucose were weekly assessed in different groups. As shown in **Figure 1A**, the body weight of ZDF rats was significantly higher than that of ZL rats from 11 to 21 weeks. In the first three weeks after the administration of dapagliflozin, the body weight of ZDF rats began to decrease significantly compared to that of the ZDF rats without treatments. At the end of the experiment, the body weights of the ZDF + Dapa and ZDF groups showed no significant difference. In addition, the blood glucose level in the treatment group was dramatically reduced throughout the entire experiment (**Figure 1B**). To investigate the effect of dapagliflozin on glucose tolerance, OGTTs were performed on all animals without anesthesia after an overnight fast. As demonstrated in **Figure 1C**, the AUC revealed that the ZL group was tolerant of glucose, while the rats in ZDF group had an impaired tolerance to glucose. However, the impaired glucose tolerance was significantly improved after dapagliflozin administration. In addition, dapagliflozin treatment also improved whole body insulin sensitivity in this ZDF rat model as reflected by a significant reduction in plasma insulin concentrations (**Figure 1D**).

To evaluate the effect of dapagliflozin on lipid metabolism, serum lipid profiles including total cholesterol (TC), triglyceride (TG), low-density lipoprotein cholesterol (LDL-C) and high-density lipoprotein cholesterol (HDL-C) levels were tested in groups. Compared with the ZL rats, the ZDF rats exhibited markedly increased serum levels of TC, TG and LDL-C, indicating an impaired lipid metabolism. Compared with the ZDF rats, the ZDF rats with the dapagliflozin treatments showed significant decrease in the abnormally elevated serum TG and LDL-C levels, although the TC levels were not statistically impacted by the dapagliflozin intervention (**Figures 1E–H**).

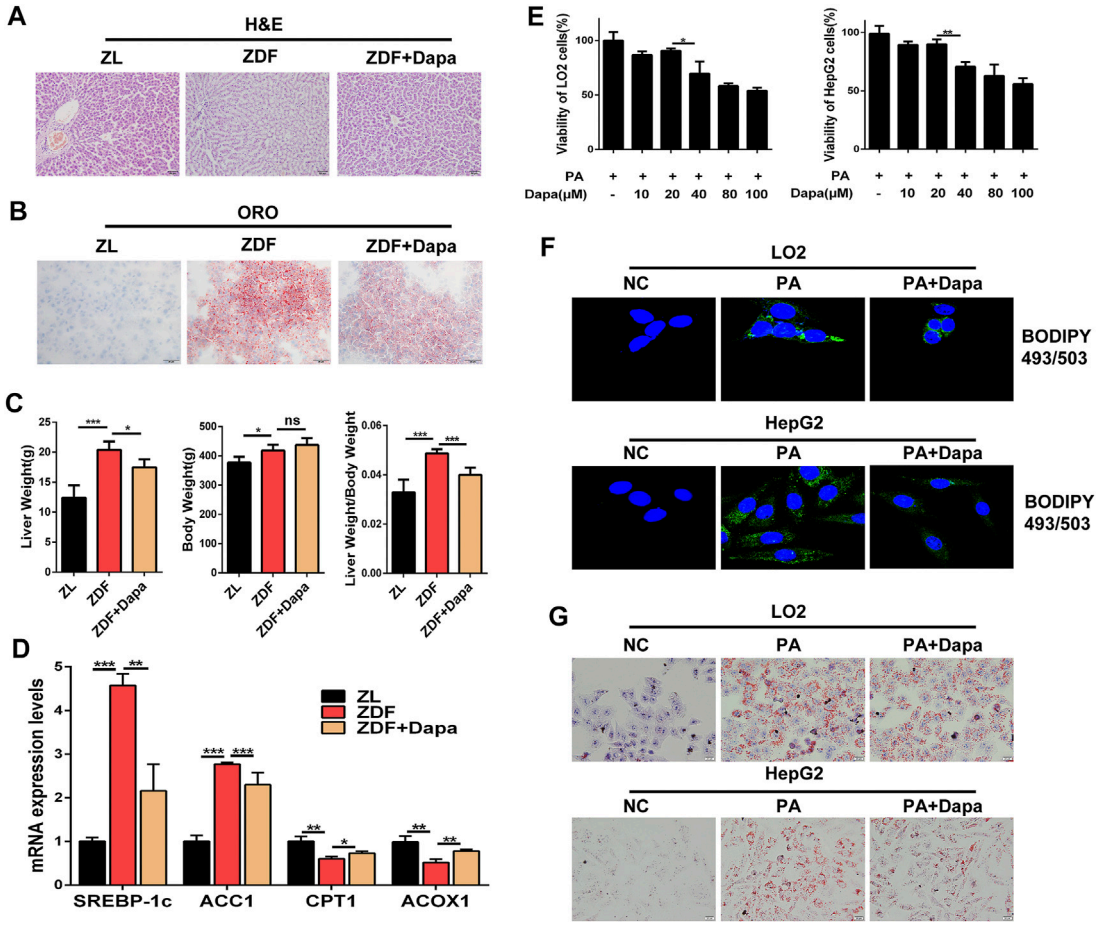


FIGURE 2 | Dapagliflozin alleviates hepatic lipid accumulation in ZDF rats and PA-stimulated LO2 and HepG2 cells. **(A, B)** Liver sections were stained with H&E (Scale bars: 50 μm)and Oil Red O (Scale bars: 20 μm). **(C)** Liver/body weight ratio was calculated by liver weight (g)/body weight (g). **(D)** The mRNA expression levels of hepatic lipogenic genes ACC1, SREBP-1c, and fatty acid oxidation genes CPT1 and ACOX1 were examined by real-time q-PCR **(E)** CCK-8 assays indicate the effect of dapagliflozin (10, 20, 40, 80, and 100 μmol/L) on the viability of HepG2 cells and LO2 cells. **(F)** HepG2 cells and LO2 cells were stained with 1 μg/ml BODIPY 493/503 and fluorescence images were captured by a confocal microscope. **(G)** LO2 and HepG2 cells were stained with Oil Red O. Scale bars: 20 μm. Data are expressed as the means ± SEM from three independent experiments. *$p < 0.05$, **$p < 0.01$, and ***$p < 0.001$.

Dapagliflozin Alleviates Hepatic Lipid Accumulation in ZDF Rats and PA-Stimulated LO2 and HepG2 Cells

To determine whether dapagliflozin alleviated hepatic lipid accumulation *in vivo*, the liver/body weight ratio and hepatic lipid accumulation in hepatic histology were evaluated in groups. The histological observation of H&E and Oil Red O staining indicated that dapagliflozin administration apparently alleviated hepatic steatosis through reducing the fatty degeneration of hepatocytes and intracellular lipid droplet formation (**Figures 2A,B**). As shown in **Figure 2C**, significant differences in body weight were not observed between the ZDF rats with or without dapagliflozin treatment, but the liver weight and the liver/body weight ratio were dramatically reduced in comparison with those of the ZDF group. Moreover, dapagliflozin treatment downregulated the expression of several hepatic lipogenic genes including ACC1 and SREBP-1c, and upregulated genes related to fatty acid oxidation, such as CPT1 and ACOX1 (**Figure 2D**).

Next, we examined the effect of dapagliflozin on lipid accumulation in LO2 and HepG2 cells. Prior to testing the effect of dapagliflozin in cells *in vitro*, a CCK-8 assay was performed to evaluate the cytotoxic effects of dapagliflozin on hepatic cells, and the results showed that dapagliflozin had a limited effect on the viability of LO2 cells and HepG2 cells, even at a concentration up to 20 μmol/L (**Figure 2E**). As shown in **Figure 2F**, the fluorescence intensity of BODIPY 493/503-stained lipid droplets was decreased after dapagliflozin administration in cells. To further confirm the lipid clearance effects of dapagliflozin in hepatic cells, we stained lipid droplets with Oil Red O (ORO). Exposure to 0.3 mM PA for 24 h dramatically increased the intracellular lipid accumulation in LO2 cells and HepG2 cells, whereas cotreatment with dapagliflozin could obviously attenuate the PA-induced lipid accumulation in both of hepatic cell lines (**Figure 2G**). Taken together, these findings indicated that dapagliflozin prevented

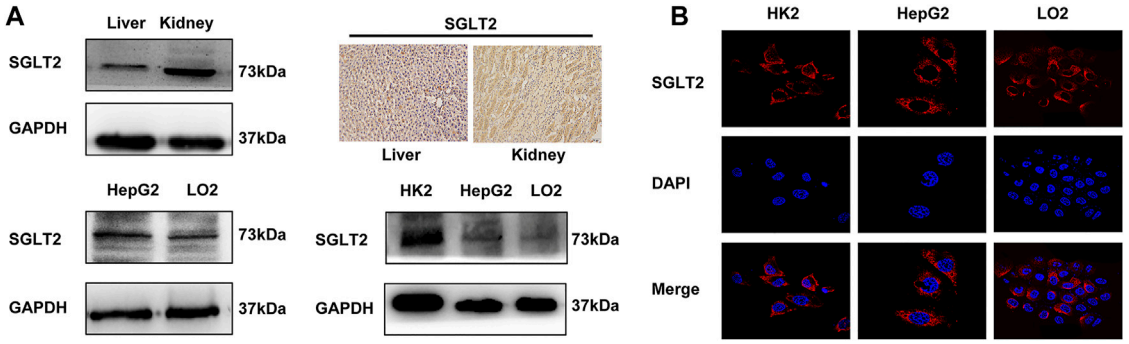


FIGURE 3 | Expression of SGLT2 in rat liver and LO2 and HepG2 cells. **(A)** Western blot analysis and IHC staining demonstrate the protein expression level of SGLT2 in rat liver and kidney tissues. **(B)** Western blot analysis and immunofluorescence staining show the expression of SGLT2 in human hepatic cell lines.

against hepatic lipid deposition in ZDF rats and PA-stimulated hepatic cells.

Expression of SGLT2 in Rat Liver, LO2 Cells and HepG2 Cells

To determine whether dapagliflozin exerted its effects by targeting on SGLT2, we investigated the expression of SGLT2 in LO2, HepG2, HK2 cells, and animal tissues by Western blot, immunofluorescence and immunohistochemistry analyses. As shown in **Figure 3A**, the Western blot analysis showed a band in the liver with the same molecular weight as that in the kidney, which indicates the expression of SGLT2 in rat liver. Immunohistochemical staining also confirmed the expression of SGLT2 predominantly on the cell membrane in both kidney and liver tissues. In addition, immunofluorescence staining and Western blot analysis indicated the expression of SGLT2 in LO2 cells and HepG2 cells (**Figure 3B**).

Dapagliflozin Induces Autophagy and Regulates Fatty Acid Metabolism in ZDF Rats and PA-Stimulated LO2 and HepG2 Cells

We examined the autophagic alterations in the rat liver and compared the effects with PA-stimulated LO2 and HepG2 cells. Detection of autophagy and the expression of autophagy-related genes were evaluated by Western blot analysis and immunohistochemistry (IHC) in the liver tissue of each group. Immunohistochemical staining showed that dapagliflozin administration significantly increased the expression of LC3B and Beclin1, but decreased that of p62 in the liver of ZDF rats (**Figure 4A**). As shown in **Figure 4B**, dapagliflozin significantly upregulated the levels of LC3B-II and Beclin1 and decreased the levels of p62 compared with the ZDF group. In addition, the administration of dapagliflozin increased ACC1 phosphorylation and significantly upregulated fatty acid oxidation gene ACOX1 (**Figure 4C**). These data suggested that dapagliflozin induced autophagy and improved cellular lipid metabolism in ZDF rats.

Moreover, the effects of dapagliflozin on the LC3B expression in PA-induced hepatocytes were detected by immunofluorescence staining and Western blot assays. Administration of dapagliflozin dramatically increased the expression of LC3B, as indicated by the enhanced fluorescence intensity (**Figures 4D,E**). Consistently, the Western blot assays demonstrated that dapagliflozin increased the expression of LC3B-II and Beclin1, and inhibited the expression of p62, which strongly indicated the enhancement of autophagy (**Figures 4F,G**). Similar outcomes on ACC1 phosphorylation and ACOX1 protein expression were also observed after dapagliflozin administration in PA-stimulated LO2 cells and HepG2 cells (**Figures 4H,I**). To assess the influence of dapagliflozin on autophagy, we pharmacologically blocked autophagosome-lysosome fusion using chloroquine diphosphate (CQ, 20 μmol/L), a lysosomal inhibitor. As shown in (**Figures 4J,K**), cotreatment with CQ abolished the effect of dapagliflozin on reducing lipid accumulation, indicating that involvement of autophagy in dapagliflozin alleviated hepatic lipid accumulation.

Dapagliflozin Induces Autophagy via the AMPK-mTOR Pathway *in vitro* and *in vivo*

To test whether autophagy is activated via the AMPK-mTOR pathway, the protein expression of AMPK and mTOR was examined *in vitro* and *in vivo*. As shown in **Figures 5A–C**, the p-AMPK/AMPK ratio was elevated in dapagliflozin-treated ZDF rats or hepatocytes, while the p-mTOR/mTOR ratio was significantly reduced. Then, to determine the association of AMPK activation with dapagliflozin-induced autophagy, AMPK inhibitor compound C (Comp C) was used to block AMPK phosphorylation in hepatic cells. Treatment with Comp C reversed the effect of dapagliflozin on cellular lipid deposition, indicating the involvement of the AMPK pathway in dapagliflozin-mediated protection against hepatic steatosis (**Figures 5D,E**).

DISCUSSION

NAFLD is a burgeoning health problem worldwide and has become a significant risk factor for both hepatic and cardiometabolic mortality (Al-awar et al., 2016). However, effective drugs approved for the treatment of NAFLD are still lacking. SGLT2 inhibitors are listed as a new class of oral anti-hyperglycaemic medications for the pharmacological management of T2DM (Chaudhury et al., 2017).

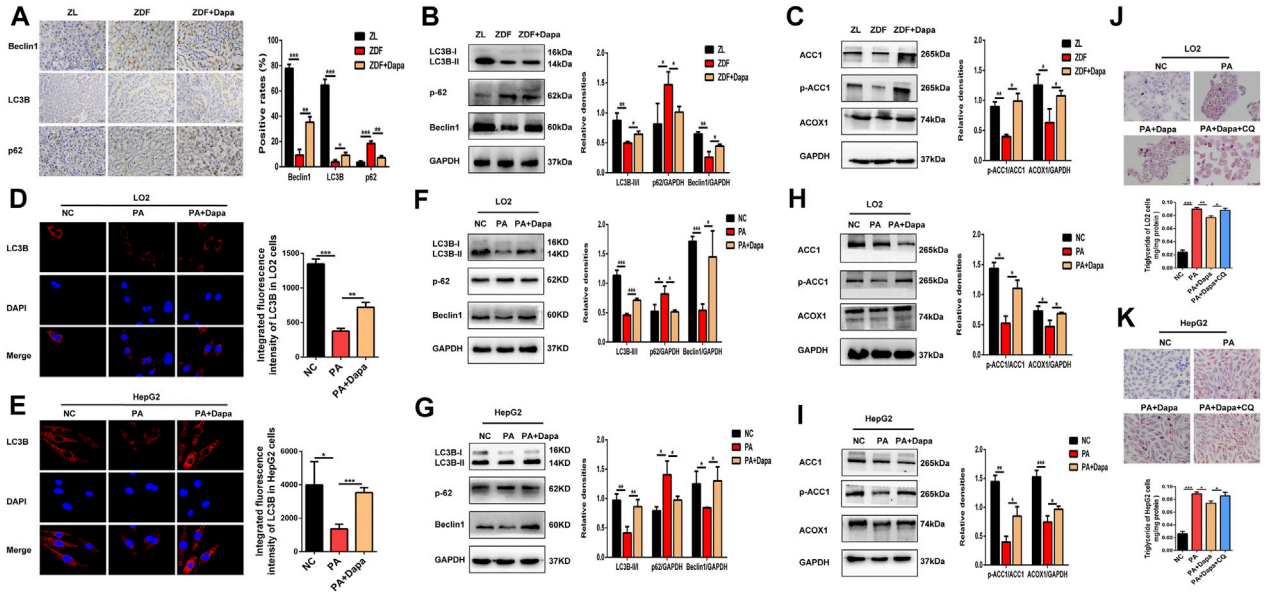


FIGURE 4 | Dapagliflozin induces autophagy and regulates fatty acid metabolism in ZDF rats and PA-stimulated LO2 and HepG2 cells. **(A)** IHC staining detected the expression of LC3B, Beclin-1 and p62 in hepatic tissue. Scale bars: 20 μm. Data are expressed as the means ± SEM of five animals per group. $^{*}p < 0.05$, $^{**}p < 0.01$, and $^{***}p < 0.001$ compared with the ZDF rat group. **(B)** Western blot analysis evaluated the protein expression levels of LC3B, Beclin-1, and p62 in rats. **(C)** Western blot analysis detected the expression of ACC1, p-ACC1, and ACOX1 in the livers of rats. **(D, E)** LC3B immunofluorescence staining showed the endogenous LC3B level of LO2 and HepG2 cells. **(F, G)** Western blot analysis demonstrated the expression of LC3B, Beclin-1, and p62 in LO2 and HepG2 cells. **(H, I)** Western blot analysis detected the protein expression of ACC1, p-ACC1 and ACOX1 in cells. **(J, K)** LO2 and HepG2 cells were treated with 0.3 mM PA, 20 μM dapagliflozin and 20 μM chloroquine (CQ) for 24 h. The cells were stained with Oil Red O and intracellular TG was quantitatively analyzed. Scale bars: 20 μm. Data are expressed as the means ± SEM from three independent experiments. $^{*}p < 0.05$, $^{**}p < 0.01$, and $^{***}p < 0.001$.

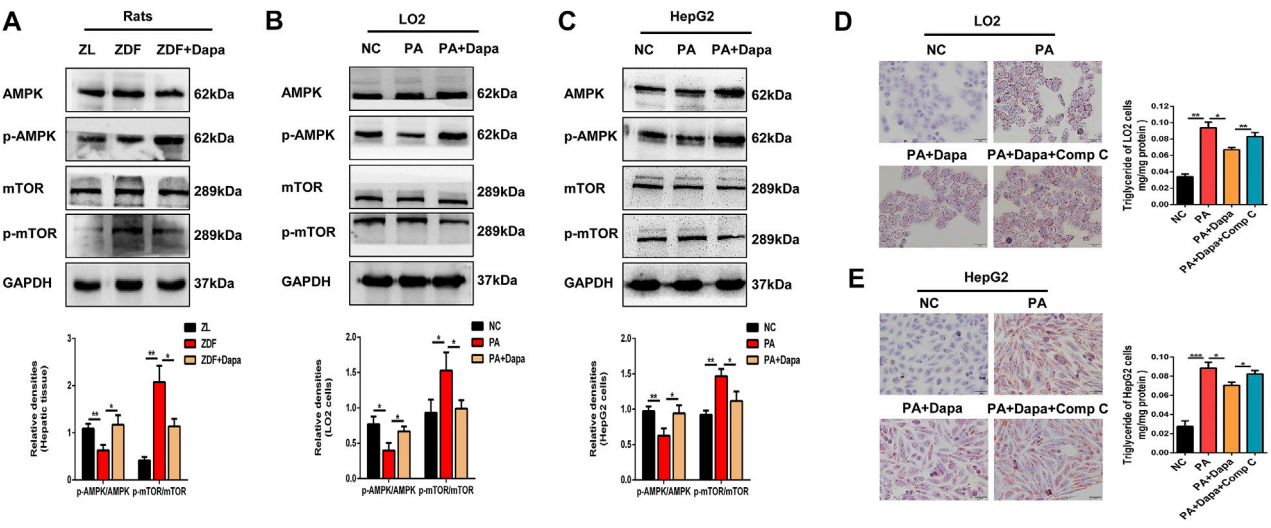


FIGURE 5 | Dapagliflozin induces autophagy via the AMPK-mTOR pathway *in vitro* and *in vivo*. **(A–C)** Western blot analysis evaluated the protein expression levels of p-AMPK, AMPK, p-mTOR, and mTOR in rats and cells. **(D, E)** LO2 and HepG2 cells were treated with 0.3 mM PA, 20 μM dapagliflozin and 10 μM compound C (Comp C) for 24 h. The cells were stained with Oil Red O and intracellular TG was quantitatively analyzed. Scale bars: 20 μm. Data are expressed as the means ± SEM from three independent experiments. $^{*}p < 0.05$, $^{**}p < 0.01$, and $^{***}p < 0.001$.

A single-center retrospective observational study indicated that dapagliflozin and empagliflozin could improve the metabolic and hepatic disorders (Lee et al., 2018). Thus, it is of great significance to explore the underlying specific mechanisms of SGLT2 inhibitors in alleviating the diet-induced metabolic dysfunction and NAFLD. In the present study, we report a beneficial effect of dapagliflozin in

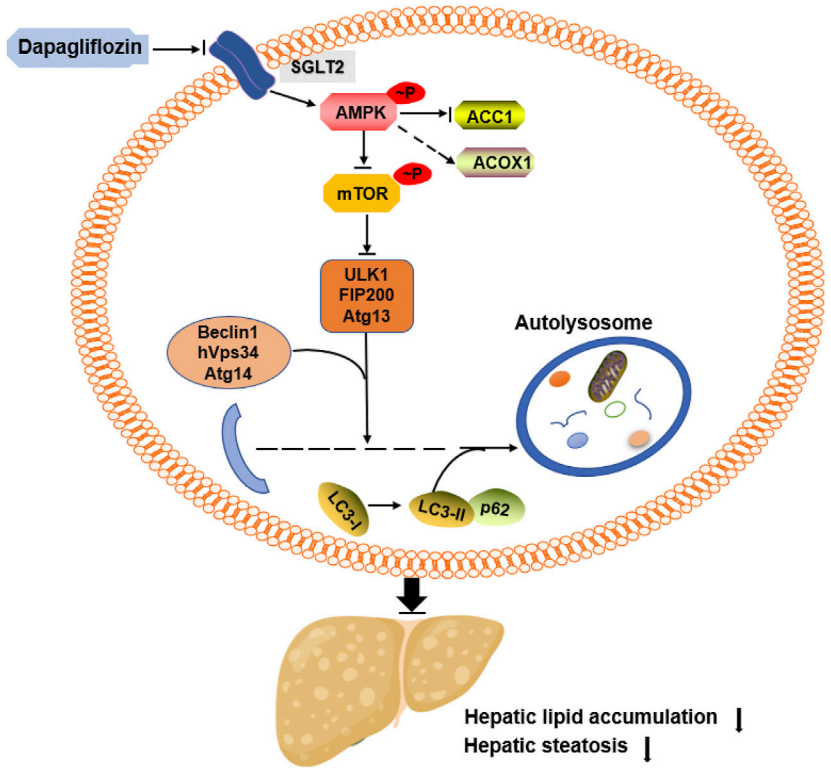


FIGURE 6 | Summary of the underlying mechanism of dapagliflozin on alleviating hepatic steatosis.

ameliorating hepatic steatosis by modulating AMPK-mediated autophagic activation. We observed for the first time that the dapagliflozin alleviated lipid accumulation and lipotoxicity, accompanied by induced autophagy in ZDF rats and PA-induced human hepatic cells, indicating that the antihepatosteatotic effects of dapagliflozin might be independent of its hypoglycaemic activities.

Previous studies have demonstrated that the excessive lipid accumulation can lead to cellular injury and death (Czaja, 2016; Li et al., 2020). In this study, we focused on the effects of dapagliflozin on hepatic steatosis and explored the relevant mechanism using hepatic cells and ZDF rats with obesity, NAFLD and metabolic dysfunction. Both LO2 cells and HepG2 cells were used to study the effects of dapagliflozin with the presence of PA. Our data showed that continuous intervention with dapagliflozin attenuated liver weight, lipotoxicity, dyslipidaemia, impaired glucose tolerance and hepatic lipid deposition in ZDF rats. Meanwhile, BODIPY 493/503 and ORO staining indicated that dapagliflozin prevented against intracellular lipid accumulation in PA-stimulated LO2 cells and HepG2 cells.

SGLT2 is a sodium-glucose transporter that is mainly expressed in the proximal convoluted tubules of the kidney, and its ubiquitous expression has also been detected in other human tissues (Uthman et al., 2018). Some studies have demonstrated that the protein expression of SGLT2 could be detected in the immortalized human primary hepatocytes HuS-E/2 cells, human hepatocellular carcinoma HepG2 cells and mouse hepatic tissue (Hawley et al., 2016; Kaji et al., 2018; Chiang et al., 2020). However, the SGLTs family consists of 12 members, and the expression of these proteins in extrarenal tissues is controversial due to the lack of specific antibodies (Wright et al., 2011). In this study, we demonstrated the expression of SGLT2 in hepatic cell lines and rat liver tissues.

Autophagy is a pathway of lysosome degradation that can ameliorate the state of insulin resistance by regulating cellular lipid metabolism (Amir and Czaja., 2011). Currently, emerging evidence suggests that autophagy may be associated with the pathological and physiological changes of NAFLD (Park and Lee., 2014). Autophagy has been reported to delay the progression of NAFLD and protects against liver injury by decreasing hepatocyte lipid accumulation (Czaja, 2016). However, previous studies have not reported on the role of SGLT2 inhibitors in inducing autophagy and reducing hepatic lipid accumulation by directly targeting hepatocytes. Our data strongly suggest that dapagliflozin administration reduces the intracellular lipid accumulation and activates the autophagy machinery because increased autophagy markers (LC3B and Beclin1 protein levels), and decreased p62 levels were found *in vitro* and *in vivo*. Most importantly, this improvement effect was abolished by incubation with CQ, a lysosomal function inhibitor, suggesting the involvement of autophagy activation in dapagliflozin-mediated hypolipidaemic effects. Hepatic lipid accumulation is caused in part by increased intracellular *de novo* lipogenesis, in which the ACC1 enzyme catalyzes the first rate-controlling step (Goedeke et al., 2018; Ipsen et al., 2018). Specific knockout of ACC1 reduced *de novo* lipogenesis in

hepatocytes and lipid accumulation in the liver of mice (Mao et al., 2006). ACOX1 is the rate-limiting enzyme in peroxisomal fatty acid oxidation (Xiao et al., 2020), and the deficiency of ACOX1 leads to hepatic lipid accumulation, inflammation and fibrosis (Ipsen et al., 2018). Thus, reducing *de novo* lipogenesis or increasing fatty acid oxidation will improve hepatic lipid accumulation. In this study, we demonstrated that dapagliflozin phosphorylated and inactivated ACC1 and increased the expression of ACOX1, which helped to alleviate cellular lipid accumulation *in vitro* and *in vivo*.

AMPK is a crucial metabolic regulator that not only inhibits energy-consuming pathways but also activates the energy-compensating process (Ha et al., 2015). Evidence shows that AMPK plays a critical role in autophagy induction in response to various cellular stresses, such as glucose starvation (Vingtdeux et al., 2010). In the liver, AMPK activation regulates metabolism by increasing catabolic pathways, such as autophagy (Alers et al., 2012) and fatty acid oxidation (Fernandez-Galilea et al., 2014), and decreasing anabolic pathways such as lipid synthesis (Zhou et al., 2001). In addition, mTOR, a downstream target of AMPK, negatively regulates autophagy activity (Kim et al., 2011). Our study demonstrated that dapagliflozin could increase the phosphorylation of AMPK, while suppressing the phosphorylation of mTOR in dapagliflozin-treated ZDF rats and cultured hepatic cells. Meanwhile this phenomenon was reversed by the AMPK specific inhibitor compound C, which strongly suggests that the effects of dapagliflozin on the amelioration in hepatic steatosis are directly mediated through AMPK activation. In addition, these results also illustrate that the AMPK-mTOR pathway plays an important role in the activation of autophagy in steatotic hepatic cells.

In summary, we demonstrated that dapagliflozin ameliorates hepatic steatosis by decreasing the *de novo* lipogenesis enzyme ACC1, increasing the fatty acid oxidation enzyme ACOX1 and inducing autophagy. These beneficial effects seem to be in part mediated through AMPK activation (**Figure 6**). In addition, our data indicate that dapagliflozin induces autophagy via the AMPK-mTOR pathway. Importantly, our findings suggest an important mechanism for the positive effects of dapagliflozin on alleviating hepatic steatosis and provide evidence for the novel clinical usage of dapagliflozin in NAFLD by targeting intracellular autophagy in hepatic cells.

DATA AVAILABILITY STATEMENT

All datasets presented in this study are included in the article/ **Supplementary Material**.

ETHICS STATEMENT

The animal study was reviewed and approved by the Institutional Animal Care and Use Committee of Southern Medical University (Guangzhou, China).

AUTHOR CONTRIBUTIONS

YC, LY, and RZ led the study design and prepared the manuscript. LL and QL carried out the experiments. WH, YH and MA assisted in tissue sample collection. HT and QX performed data analysis and interpretation. All authors read and approved the final manuscript.

FUNDING

This work was supported by the National Natural Science Foundation of China (Grant No. 81500679), Science and Technology Plan of Guangdong Province (Grant No. 2017A020215045), the Science and Technology Plan Project of Guangzhou (Grant No. 202102020165) and Clinical Research Startup Program of Southern Medical University by High-level University Construction Funding of Guangdong Provincial Department of Education (Grant No. LC2016YM007).

SUPPLEMENTARY MATERIAL

The Supplementary Material for this article can be found online at: https://www.frontiersin.org/articles/10.3389/fphar.2021.589273/full#supplementary-material

REFERENCES

Adams, L. A., Anstee, Q. M., Tilg, H., and Targher, G. (2017). Non-alcoholic Fatty Liver Disease and its Relationship with Cardiovascular Disease and Other Extrahepatic Diseases. *Gut* 66, 1138–1153. doi:10.1136/gutjnl-2017-313884

Al-awar, A., Kupai, K., Veszelka, M., Szűcs, G., Attieh, Z., Murlasits, Z., et al. (2016). Experimental Diabetes Mellitus in Different Animal Models. *J. Diabetes Res.* 2016, 1–12. doi:10.1155/2016/9051426

Alers, S., Loffler, A. S., Wesselborg, S., and Stork, B. (2012). Role of AMPK-mTOR-Ulk1/2 in the Regulation of Autophagy: Cross Talk, Shortcuts, and Feedbacks. *Mol. Cell Biol.* 32, 2–11. doi:10.1128/MCB.06159-11

Amir, M., and Czaja, M. J. (2011). Autophagy in Nonalcoholic Steatohepatitis. *Expert Rev. Gastroenterol. Hepatol.* 5, 159–166. doi:10.1586/egh.11.4

Angulo, P. (2002). Nonalcoholic Fatty Liver Disease. *N. Engl. J. Med.* 346, 1221–1231. doi:10.1056/NEJMra011775

Bril, F., and Cusi, K. (2016). Nonalcoholic Fatty Liver Disease. *Endocrinol. Metab. Clin. North America* 45, 765–781. doi:10.1016/j.ecl.2016.06.005

Brownsey, R. W., Zhande, R., and Boone, A. N. (1997). Isoforms of Acetyl-CoA Carboxylase: Structures, Regulatory Properties and Metabolic Functions. *Biochem. Soc. Trans.* 25, 1232–1238. doi:10.1042/bst0251232

Chaudhury, A., Duvoor, C., Reddy Dendi, V. S., Kraleti, S., Chada, A., Ravilla, R., et al. (2017). Clinical Review of Antidiabetic Drugs: Implications for Type 2 Diabetes Mellitus Management. *Front. Endocrinol.* 8, 6. doi:10.3389/fendo.2017.00006

Chiang, H., Lee, J. C., Huang, H. C., Huang, H., Liu, H. K., and Huang, C. (2020). Delayed Intervention with a Novel SGLT2 Inhibitor NGI001 Suppresses Diet-induced Metabolic Dysfunction and Non-alcoholic Fatty Liver Disease in Mice. *Br. J. Pharmacol.* 177, 239–253. doi:10.1111/bph.14859

Czaja, M. J. (2016). Function of Autophagy in Nonalcoholic Fatty Liver Disease. *Dig. Dis. Sci.* 61, 1304–1313. doi:10.1007/s10620-015-4025-x

Dhillon, S. (2019). Dapagliflozin: A Review in Type 2 Diabetes. *Drugs* 79, 1135–1146. doi:10.1007/s40265-019-01148-3

Fernández-Galilea, M., Pérez-Matute, P., Prieto-Hontoria, P. L., Sáinz, N., López-Yoldi, M., Houssier, M., et al. (2014). α-Lipoic Acid Reduces Fatty Acid Esterification and Lipogenesis in Adipocytes from Overweight/obese Subjects. *Obesity* 22, 2210–2215. doi:10.1002/oby.20846

Goedeke, L., Bates, J., Vatner, D. F., Perry, R. J., Wang, T., Ramirez, R., et al. (2018). Acetyl-CoA Carboxylase Inhibition Reverses NAFLD and Hepatic Insulin Resistance but Promotes Hypertriglyceridemia in Rodents. *Hepatology* 68, 2197–2211. doi:10.1002/hep.30097

Ha, J., Guan, K.-L., and Kim, J. (2015). AMPK and Autophagy in Glucose/glycogen Metabolism. *Mol. Aspects Med.* 46, 46–62. doi:10.1016/j.mam.2015.08.002

Hawley, S. A., Ford, R. J., Smith, B. K., Gowans, G. J., Mancini, S. J., Pitt, R. D., et al. (2016). The Na+/Glucose Cotransporter Inhibitor Canagliflozin Activates AMPK by Inhibiting Mitochondrial Function and Increasing Cellular AMP Levels. *Diabetes* 65, 2784–2794. doi:10.2337/db16-0058

Ipsen, D. H., Lykkesfeldt, J., and Tveden-Nyborg, P. (2018). Molecular Mechanisms of Hepatic Lipid Accumulation in Non-alcoholic Fatty Liver Disease. *Cell. Mol. Life Sci.* 75, 3313–3327. doi:10.1007/s00018-018-2860-6

Kaji, K., Nishimura, N., Seki, K., Sato, S., Saikawa, S., Nakanishi, K., et al. (2018). Sodium Glucose Cotransporter 2 Inhibitor Canagliflozin Attenuates Liver Cancer Cell Growth and Angiogenic Activity by Inhibiting Glucose Uptake. *Int. J. Cancer* 142, 1712–1722. doi:10.1002/ijc.31193

Kim, J., Kundu, M., Viollet, B., and Guan, K.-L. (2011). AMPK and mTOR Regulate Autophagy through Direct Phosphorylation of Ulk1. *Nat. Cel Biol.* 13, 132–141. doi:10.1038/ncb2152

Kim, Y. C., and Guan, K.-L. (2015). mTOR: a Pharmacologic Target for Autophagy Regulation. *J. Clin. Invest.* 125, 25–32. doi:10.1172/JCI73939

Kurinami, N., Sugiyama, S., Yoshida, A., Hieshima, K., Miyamoto, F., Kajiwara, K., et al. (2018). Dapagliflozin Significantly Reduced Liver Fat Accumulation Associated with a Decrease in Abdominal Subcutaneous Fat in Patients with Inadequately Controlled Type 2 Diabetes Mellitus. *Diabetes Res. Clin. Pract.* 142, 254–263. doi:10.1016/j.diabres.2018.05.017

Lee, P. C. H., Gu, Y., Yeung, M. Y., Fong, C. H. Y., Woo, Y. C., Chow, W. S., et al. (2018). Dapagliflozin and Empagliflozin Ameliorate Hepatic Dysfunction Among Chinese Subjects with Diabetes in Part through Glycemic Improvement: A Single-Center, Retrospective, Observational Study. *Diabetes Ther.* 9, 285–295. doi:10.1007/s13300-017-0355-3

Li, Y., Zhang, Y., Ji, G., Shen, Y., Zhao, N., Liang, Y., et al. (2020). Autophagy Triggered by Oxidative Stress Appears to Be Mediated by the AKT/mTOR Signaling Pathway in the Liver of Sleep-Deprived Rats. *Oxidative Med. Cell Longevity* 2020, 1–11. doi:10.1155/2020/6181630

Lu, Y., Jiang, Z., Dai, H., Miao, R., Shu, J., Gu, H., et al. (2018). Hepatic Leukocyte Immunoglobulin-like Receptor B4 (LILRB4) Attenuates Nonalcoholic Fatty Liver Disease via SHP1-TRAF6 Pathway. *Hepatology* 67, 1303–1319. doi:10.1002/hep.29633

Madiraju, A. K., Alves, T., Zhao, X., Cline, G. W., Zhang, D., Bhanot, S., et al. (2016). Argininosuccinate Synthetase Regulates Hepatic AMPK Linking Protein Catabolism and Ureagenesis to Hepatic Lipid Metabolism. *Proc. Natl. Acad. Sci. USA* 113, E3423–E3430. doi:10.1073/pnas.1606022113

Mao, J., DeMayo, F. J., Li, H., Abu-Elheiga, L., Gu, Z., Shaikenov, T. E., et al. (2006). Liver-specific Deletion of Acetyl-CoA Carboxylase 1 Reduces Hepatic Triglyceride Accumulation without Affecting Glucose Homeostasis. *Proc. Natl. Acad. Sci.* 103, 8552–8557. doi:10.1073/pnas.0603115103

Moreno-Fernandez, M. E., Giles, D. A., Stankiewicz, T. E., Sheridan, R., Karns, R., Cappelletti, M., et al. (2018). Peroxisomal β-oxidation Regulates Whole Body Metabolism, Inflammatory Vigor, and Pathogenesis of Nonalcoholic Fatty Liver Disease. *JCI Insight* 3. doi:10.1172/jci.insight.93626

Park, H.-W., and Lee, J. H. (2014). Calcium Channel Blockers as Potential Therapeutics for Obesity-Associated Autophagy Defects and Fatty Liver Pathologies. *Autophagy* 10, 2385–2386. doi:10.4161/15548627.2014.984268

Sheridan, R., Lampe, K., Shanmukhappa, S. K., Putnam, P., Keddache, M., Divanovic, S., et al. (2011). Lampe1: an ENU-Germline Mutation Causing Spontaneous Hepatosteatosis Identified through Targeted Exon-Enrichment and Next-Generation Sequencing. *Plos One* 6, e21979. doi:10.1371/journal.pone.0021979

Shimizu, M., Suzuki, K., Kato, K., Jojima, T., Iijima, T., Murohisa, T., et al. (2019). Evaluation of the Effects of Dapagliflozin, a Sodium-Glucose Co-transporter-2 Inhibitor, on Hepatic Steatosis and Fibrosis Using Transient Elastography in Patients with Type 2 Diabetes and Non-alcoholic Fatty Liver Disease. *Diabetes Obes. Metab.* 21, 285–292. doi:10.1111/dom.13520

Tang, Y., Lu, Y., Chen, Y., Luo, L., Cai, L., Peng, B., et al. (2019). Pre-metastatic Niche Triggers SDF-1/CXCR4 axis and Promotes Organ Colonisation by Hepatocellular Circulating Tumour Cells via Downregulation of Prrx1. *J. Exp. Clin. Cancer Res.* 38, 473. doi:10.1186/s13046-019-1475-6

Uthman, L., Baartscheer, A., Schumacher, C. A., Fiolet, J. W. T., Kuschma, M. C., Hollmann, M. W., et al. (2018). Direct Cardiac Actions of Sodium Glucose Cotransporter 2 Inhibitors Target Pathogenic Mechanisms Underlying Heart Failure in Diabetic Patients. *Front. Physiol.* 9. doi:10.3389/fphys.2018.01575

Vingtdeux, V., Giliberto, L., Zhao, H., Chandakkar, P., Wu, Q., Simon, J. E., et al. (2010). AMP-activated Protein Kinase Signaling Activation by Resveratrol Modulates Amyloid-β Peptide Metabolism*. *J. Biol. Chem.* 285, 9100–9113. doi:10.1074/jbc.M109.060061

Wright, E. M., Loo, D. D. F., and Hirayama, B. A. (2011). Biology of Human Sodium Glucose Transporters. *Physiol. Rev.* 91, 733–794. doi:10.1152/physrev.00055.2009

Xiao, Z., Chu, Y., and Qin, W. (2020). IGFBP5 Modulates Lipid Metabolism and Insulin Sensitivity through Activating AMPK Pathway in Non-alcoholic Fatty Liver Disease. *Life Sci.* 256, 117997. doi:10.1016/j.lfs.2020.117997

You, M., Matsumoto, M., Pacold, C. M., Cho, W. K., and Crabb, D. W. (2004). The Role of AMP-Activated Protein Kinase in the Action of Ethanol in the Liver. *Gastroenterology* 127, 1798–1808. doi:10.1053/j.gastro.2004.09.049

Zhou, G., Myers, R., Li, Y., Chen, Y., Shen, X., Fenyk-Melody, J., et al. (2001). Role of AMP-Activated Protein Kinase in Mechanism of Metformin Action. *J. Clin. Invest.* 108, 1167–1174. doi:10.1172/JCI13505

Conflict of Interest: The authors declare that the research was conducted in the absence of any commercial or financial relationships that could be construed as a potential conflict of interest.

Copyright © 2021 Li, Li, Huang, Han, Tan, An, Xiang, Zhou, Yang and Cheng. This is an open-access article distributed under the terms of the Creative Commons Attribution License (CC BY). The use, distribution or reproduction in other forums is permitted, provided the original author(s) and the copyright owner(s) are credited and that the original publication in this journal is cited, in accordance with accepted academic practice. No use, distribution or reproduction is permitted which does not comply with these terms.

frontiers in Pharmacology

REVIEW
published: 09 June 2021
doi: 10.3389/fphar.2021.658505

Exosomes in Intestinal Inflammation

Kanchana K. Ayyar and Alan C. Moss*

Division of Gastroenterology, Department of Medicine, Boston Medical Center, Boston, MA, United States

Exosomes are 30–150 nm sized vesicles released by a variety of cells, and are found in most physiological compartments (feces, blood, urine, saliva, breast milk). They can contain different cargo, including nucleic acids, proteins and lipids. In Inflammatory Bowel Disease (IBD), a distinct exosome profile can be detected in blood and fecal samples. In addition, circulating exosomes can carry targets on their surface for monoclonal antibodies used as IBD therapy. This review aims to understand the exosome profile in humans and other mammals, the cargo contained in them, the effect of exosomes on the gut, and the application of exosomes in IBD therapy.

Keywords: IBD, colitis, extracellular vesicles, exosomes, inflammation

INTRODUCTION

Exosomes are biological nanovesicles (30–150 nm) that are made by most cell types (Gross et al., 2012). They fuse with the plasma membrane of the cell and are released outside, they can be detected in almost all biological fluids (Edgar, 2016). The exosomal membrane is made of lipids and proteins (Mathivanan et al., 2010). The cargo contained within the exosomes can be proteins, nucleic acids and lipids which may or may not be similar to those of the parent cell (Valadi et al., 2007). Neighboring and/or distant cells can benefit from the cargo of circulating exosomes. They function as signaling molecules and can bring about regulation. The knowledge of their autocrine, paracrine, juxtacrine, and endocrine regulation has aroused the curiosity of many researchers. Studies indicate that exosomes play a role in extracellular matrix remodeling and signal transmission (Beshbishy et al., 2020). They also play vital roles in many disease conditions like cancer, neurodegenerative disorders, cardiovascular diseases, diabetes and others like Inflammatory Bowel Disease (IBD) by regulating immunity, inflammation, and tissue homeostasis.

Inflammatory Bowel Disease (IBD) has been widely thought to be a western disease; however, the global prevalence of IBD has been increasing since 2000. One in 200 individuals in Western countries suffers from IBD (Ng et al., 2017). Crohn's disease (CD) and ulcerative colitis (UC) are the two distinct disorders of IBD. CD and UC differ in the symptoms, complications, part of the gastrointestinal (GI) tract they affect, pathophysiology, disease course and management. UC affects the colon and is characterized by continuous lesions and superficial inflammation, which can lead to erosions, ulcers and bloody diarrhea. CD is progressive and destructive—many patients have systemic, extra intestinal manifestations, which strongly affects their quality of life due to risk of hospitalization, complications and surgery (Torres et al., 2017).

The pathogenesis of IBD is still ambiguous, the process is linked to genetic, environmental, gut microbiota and immune response factors (Ocansey et al., 2019). Some individuals with IBD have a genetic predisposition due to which there is a failure in maintaining intestinal homeostasis (Console et al., 2019). Intestinal Epithelial Cells (IECs) are constantly exposed to numerous bacteria and dietary-derived antigens. In order to defend itself, the human body needs to mount a robust immune response against invading pathogens, however if this response is prolonged it can be deleterious to the host leading to acute and chronic inflammatory disorder. Thus, the cells of the body employ intricate signaling network to control inflammation (Ayyar and Reddy, 2018). This system includes

OPEN ACCESS

Edited by:
Dario Sorrentino,
Virginia Tech Carilion, United States

Reviewed by:
Fabio Cominelli,
Case Western Reserve University, United States
Martina Fabris,
University Hospital of Udine, Italy, Italy

****Correspondence:***
Kanchana K. Ayyar
kanchana.ayyar@bmc.org

Specialty section:
This article was submitted to Gastrointestinal and Hepatic Pharmacology, a section of the journal Frontiers in Pharmacology

Received: *25 January 2021*
Accepted: *11 May 2021*
Published: *09 June 2021*

Citation:
Ayyar KK and Moss AC (2021) Exosomes in Intestinal Inflammation. Front. Pharmacol. 12:658505. doi: 10.3389/fphar.2021.658505

many small extra cellular components such as extra-cellular vesicles (EV), non-coding RNAs (ncRNA) like miRNA (microRNA), snRNA (small nucleolar RNA), siRNA (small interfering RNA), lncRNA (long non-coding RNA), and others (Ayyar et al., 2014). The immune system of the intestinal mucosa employs the use of such extra-cellular factors such as exosomes to maintain a balance between exhibiting tolerance toward normal microbiota and food proteins and eliciting an immune response toward enteric pathogens. Exosomes regulate cells of the immune system, gut microbes and factors maintaining the gut barrier within the IBD microenvironment. This helps repair damage and restore intestinal mucosal functions. IBD therapy is directed at improving immune regulation and easing intestinal mucosal inflammation. Exosome based therapy can help achieve these goals. In this article, we review the contents of exosomes and their effects in IBD; focusing on their effect on immune cells and gut microbiota. We also examine the potential applications of exosomes and exosomal cargo as biomarkers of IBD and in IBD therapy.

EXOSOMES

Exosomes, prostasomes, ectosomes, microvesicles, microparticles, tolerosomes, and nanovesicles are collectively referred as EVs. Currently, exosomes cannot be easily separated from other EVs (Beshbishy et al., 2020). Thus, exosomes separated from biological fluids and cell culture supernatants that are used for research are regarded as EVs, as stated in the guidelines developed by the International Society of Extracellular Vesicles (ISEV) (Théry et al., 2018). Existence of EVs was documented for the first time in 1946 (Chargaff and West, 1946). By 1977, the release of membrane fragments was considered a ubiquitous feature of viable cells. Till 1980, they were commonly considered as cellular debris (P. Wolf, 1967). The discovery of exosomes occurred in 1983. Pan and Johnstone reported that during maturation of reticulocytes in sheep, small vesicles were engaged in the release of transferrin receptors into the extracellular milieu (Pan and Johnstone, 1983). These vesicles were termed exosomes in 1989 (Johnstone et al., 1989). Subsequent studies demonstrated that exosomes originate from endosomal vesicles.

Biogenesis of Exosomes

Exosomes have a lipid bilayer membrane and are incapable of replicating. The process by which exosomes are synthesized differs from other EVs. These vesicles are forged from a novel multi-step "exosome biogenesis" pathway. The plasma membrane of the cell buds inwards to form membrane enclosed compartments called early endosomes (Pant et al., 2012). Early endosomes mature into late endosomes, these are also called multivesicular bodies (MVB). MVBs acquire intraluminal vesicles (ILVs) in their lumen. Inward budding of early endosomal membrane results in generation of ILVs. ILVs contain biologically active molecules like lipids (Subra et al., 2010), proteins (André et al., 2004) and nucleic acids (Valadi et al., 2007). These components may be selectively enriched by the endosomal sorting complexes required for transport (ESCRTs) (Tamai et al., 2010). The process may also be orchestrated by ESCRT-independent mechanisms which involve tetraspanins or lipids (Colombo et al., 2013). Depending on the molecules used, the mechanism is considered ESCRT dependent or ESCRT independent (Stuffers et al., 2009). The resultant MVBs can have two fates: survive as exosomes or perish. Fusion of MVBs with plasma membrane leads to their release in extracellular space as exosomes (Gruenberg and Goot, 2006). Alternatively, MVBs may fuse with lysosomes which leads to degradation of their content (Palmulli and Van Niel, 2018). Exosomes are released by exocytosis pathway in the course of cellular crosstalk or during receptor removal mechanisms. Growth factor receptors on the plasma membrane play a pivotal role in the exocytosis pathway (Stoorvogel et al., 2002). It is not yet fully understood as to how exosomes are released. Even though considerable progress has been made in this field, substantial gap exists in our knowledge of cargo sorting mechanisms in exosomes and other vesicular bodies.

Characterization of Exosomes

A few minimal requirements have been made mandatory by ISEV to establish the existence of exosome in a study. Experimental methods like electron microscopy, concentration monitoring techniques, and western blotting are needed to identify the presence of exosomes (Théry et al., 2018). Also, physical properties like particle size are calculated during isolation via ultracentrifugation, density gradient separation, and polymer-based precipitation methods. (Chang et al., 2020). Under TEM (Transmission Electron Microscopy), exosomes resemble cup-shaped lipoidal vesicles (Théry et al., 2009). Most exosomes bear tetraspanin proteins and this superfamily of proteins was considered to be a definitive marker of exosomes. Recent research indicates that micro-vesicles (MVs) also bear CD63, CD9, and CD81 tetraspanin proteins (Simons and Raposo, 2009). Many studies on exosomes have shown Alix and TSG101 (Tumor Susceptibility Gene 101 protein) and heat shock proteins HSC70 and HSP90 to be associated with these vesicles (Maas et al., 2017). The main difference between endosomes and MVs is that MVs are derived from outward blebbing of the plasma membrane (Agrahari et al., 2019).

Trafficking of Exosomes

The cell to cell communication by exosomes can occur via three mechanisms. The first mechanism involves receptor-ligand interaction. Signaling receptors of target cell interact directly with exosomal transmembrane proteins (Munich et al., 2012). In the second mechanism, the plasma membrane of target cell fuses with exosome, the contents of the exosome is directly delivered into the cytosol (Mulcahy et al., 2014). In the third mechanism, the exosomes get internalized by target cells. The internalized exosomes may either merge with endosomes, undergo transcytosis and be released for uptake by neighboring cells or the exosomes mature into lysosome in the target cells and are degraded (Tian et al., 2013). Some of the factors that influence internalization of exosomes have been studied. Exosomal lipid rafts and annexins are essential for exosomal internalization (Koumangoye et al., 2011). This is not to say that all factors responsible for internalization of exosomes are present only on exosomes. The proteins mediating internalization of exosomes are present on both target cells and exosomes (Escrevente et al., 2011). Apart from proteins, alteration of cholesterol content leading to disruption of lipid rafts also impairs exosomal internalization (Gonda et al., 2019). We still lack knowledge of how a

mechanism is preferred over another by the exosome and/or the cell; is it condition, cell type or exosome specific?

Exosomal Cargo

Cell-to-cell communication is essential and exosomes help in facilitating this cellular crosstalk (Carrière et al., 2016). The lumen of the exosome contains the cargo-which could be lipids, proteins, nucleic acid like mRNAs, microRNAs, and other non-coding RNAs (ncRNA) (Sato-Kuwabara et al., 2015). The cargo can be same or different from that of the parent cell. Exosomes contain proteins primarily present in endosomes, plasma membrane and cytosol. They rarely enclose factors originating from the nucleus, mitochondria, endoplasmic reticulum or golgi. Also, formation and secretion of exosomes is a cost intensive process for the cell requiring enzymes and ATP (adenosine triphosphate) (J. Zhang et al., 2015). We believe there is mechanism in the cell for actively selecting exosomes and their cargos.

Proteins

Exosomal research data from different sources reveal that they share common exosomal constituents. As of 2016, 41,860 exosomal proteins, >7,540 exosomal RNA, and 1,116 exosomal lipid molecules have been cataloged from more than 286 exosome-based studies defined as per ISEV guidelines (Keerthikumar et al., 2016). Exosomes have two different kinds of protein content. The first kind depends on the cell and tissue from which it originates, while the other kind of protein constitutively occurs in exosomes and can be used as exosomal markers (Console et al., 2019). TSG101, Charged Multivesicular Body Protein 2a (CHMP2A), Ras-related protein Rab-11B (RAB11B), CD9, CD63, and CD81 are currently used as exosomal protein markers (Gross et al., 2012). Other common proteins documented in exosomes include adhesion molecules, heat shock proteins (such as HSC73, HSC90), annexins I, II, V, and VI, cytoskeletal proteins (synenin, actin, moesin, albumin) and GTPases (Samanta et al., 2018). Interestingly, some cytoskeletal proteins, glycolytic enzymes, and argonaute 1–4 (required for miRNA stability) are not detected in exosomes (Jeppesen et al., 2019).

Lipids

The current knowledge regarding the lipid content of exosomes is limited. Exosomes may contain cholesterol, sphingomyelin, ceramide, and phosphatidylserine. Cholesterol was found in the membrane of internal vesicles of MVB (Möbius et al., 2003). This is relevant as many membrane transporters are sensitive to cholesterol (Dickens et al., 2017). The structure of exosomal membrane is analogus to that of the plasma membrane; it also contains detergent resistant subdomains (Colombo et al., 2014).

Nucleic Acids

The other cargo contained within exosomes is nucleic acids (DNA, mRNA, miRNA, lncRNA, and ncRNA). The delivery of nucleic acids to cells can alter expression of genes and regulate the immune status in neighboring tissue. miRNAs can modulate immune responses by production and release of cytokines and chemokines resulting in a feedback regulation of immune homeostasis (Ayyar and Reddy, 2017). The nucleic acid content within exosomes differ. Identifying them will help us understand the role they may play in many processes. As exosomes are produced by almost all cells, they can be harvested from physiological fluids and their contents may indicate health of the tissues (healthy vs. diseased). They have the potential to be used as biomarkers: a diagnostic tool. A recent study suggests that the DNA found in small EVs are of extracellular origin that are released via an autophagy and multivesicular-endosome-dependent but exosome independent mechanism (Jeppesen et al., 2019). The source of different EV components and their functions is listed in **Table 1**.

Exosomes in Inflammatory Bowel Disease

The role of exosomes in IBD has garnered interest among researchers. Exosomal proteins, RNAs and lipids regulate factors of IBD like immune cells, gut microbiota and the mucosal barrier (Chang et al., 2020). Many studies have used exosomes from a variety of starting materials to study the process of IBD alleviation and related factors of interest. Translational studies are being conducted to tap into the possible use of exosomes as diagnostic markers and drug delivery systems, and also on the utility of modified exosomes in IBD therapy (Ocansey et al., 2020). Many of the studies cited in this review do not differentiate between the different types of EVs like exosomes, endosomes and MVBs, hence for the sake of convenience we have used the general term EVs while describing study findings.

Exosomal Profile in Intestinal Mucosa

Epithelial cells, Paneth cells, macrophages, and lymphocytes are cells in the intestinal tract that are directly exposed to digested food, microbes, and foreign antigens making immune homeostasis a challenging and complex process (Peterson and Artis, 2014). While maintaining immune homeostasis, the intestinal barrier strikes a perfect balance by clearing pathogenic bacteria and maintaining immune tolerance with the commensals. Evidence indicates that dysregulation of intestinal homeostasis leads to IBD pathogenesis. Intestinal homeostasis depends on effective crosstalk between extracellular factors, EVs and the host's intestinal immune defense (comprised of the mucus membrane, intestinal epithelial cells (IECs) and the immune cells) (Avila-Calderón et al., 2015). EVs act not only as communicator between cells but also between cells and organisms (Chang et al., 2020). This is important as the mammalian intestine encounters 10 trillion (10^{13}) microbes (10X the number of total cells in a mammalian body) (Sartor, 2008). EVs from micro-organisms and the host body communicate and help maintain a peaceful coexistence, maintaining intestinal immune homeostasis which is a major determinant of health (Sommer et al., 2017). Physiological fluids also contain EVs which affect the intestinal microbiota.

Exosomes From Intestinal Epithelial Cells

IECs play a major role in immune modulation in the gut that even though they are not professional antigen presenting cells (APC), they bear major histocompatibility complex (MHC) I, II, and HLA-DM (Lin et al., 2005). The knowledge of IEC releasing EVs has been known for a while now (Van Niel et al., 2001). IEC EVs like parent cells, contain immunomodulatory molecules. They also express MHC I and II, expression of which is elevated during inflammation as compared to basal

TABLE 1 | Source and function of different extracellular vesicle components in IBD.

Exosomal component	Source	Role	References
A33 antigen	Intestinal epithelial cells	Cell-cell recognition and signaling	Van Niel et al. (2001)
Annexin A1	Intestinal epithelial cells	Promotes wound healing	Leoni et al. (2015)
CCL20 and prostaglandin E2	Intestinal epithelial cells	Recruit Th17 cells through MyD88 mediated pathway	Deng et al. (2015)
CD63 and EpCAM	Intestinal epithelial cells	Induces DC apoptosis Suppresses DC maturation inhibits antigen presentation by DCs in rats	Kojima et al. (2018)
GELNs lipids	Grapes	Induces Lgr5+ stem cells Enhances *in vivo* targeting of intestinal stem cells Remodels and protects intestinal tissue against DSS-induced colitis	Ju et al. (2013)
Integrin αvβ6	Intestinal epithelial cells	Promotes production of active TGF-β in DCs and Tregs	Chen et al. (2011)
Metallothionein-2	Bone marrow-derived MSCs	Maintenance of intestinal barrier integrity Polarization of M2b macrophages Induction of IL-10 from macrophages	(Liu et al. (2019)
MHC I and II	Intestinal epithelial cells	Initiating immune response	Van Niel et al. (2001)
miR-223	Mice colonic epithelial cells	Modulates communication between IL-23 signal pathway and claudin-8 in IBD development Modulates intestinal barrier integrity	Wang et al. (2016)
miR-23a and miR-155	Neutrophils	Induces replication fork collapse Inhibits homologous recombination Induces accumulation of double strand breaks	Butin-Israeli et al. (2019)
miR-34c and PlncRNA1	Intestinal epithelial cell line Caco-2	Modulates ZO-1, MAZ, and occludin expression Modulates intestinal barrier integrity	Chen et al. (2017)
miR-4334, miR-219 and miR-338	Porcine milk	Prevents LPS-induced intestinal inflammation, apoptosis and damage via inhibiting TLR4/NF-κB and p53 pathways	Xie et al. (2019)
Mdo-miR7267–3p	Ginger	Shapes gut microbiota Improves barrier function Ameliorates colitis via IL-22-dependent mechanisms	Teng et al. (2019)
Myeloperoxidase (MPO)	Intestinal epithelial cells	Contributes to oxidative stress against microbes	Zhang et al. (2018)
Myeloperoxidase (MPO)	Neutrophils	Damages intestinal barrier by production of oxidative radicals, inhibiting wound closure and healing	Slater et al. (2017)
NEAT1	Mouse intestinal mucosa and serum	Down-regulation of NEAT1 Suppresses inflammatory response by modulating intestinal epithelial barrier and via exosome-mediated polarization of macrophages in IBD	Liu et al. (2018)
PSMA7	Oral mucosal cells	Responsible for degradation of proteins Controls autoimmune disorders and immune tolerance	Zheng et al. (2017)
Sphingosine-1-phosphate	Intestinal epithelial cells	Promotes tumorigenesis	(Patmanathan et al. (2017)
Tetraspanin 14–3-3 protein, enolase and heat shock proteins	Hookworm	Protection against colitis by significantly suppressing IFNγ, IL-6,IL-1β, and IL-17a and upregulating anti-inflammatory cytokine IL-10	(Eichenberger et al. (2018)
TGF-β	Intestinal epithelial cells	Inhibit $CD4^+$ T cell proliferation	Jiang et al. (2016)

condition (Van Niel et al., 2001). EVs released from these cells can be released apically or basolaterally. They carry A33 antigen, whose expression is confined to the intestinal epithelium (Van Niel et al., 2001). A33 is now considered a marker for IEC exosomes (Van Niel et al., 2003; Lin et al., 2005; Mallegol et al., 2007).

IEC EVs are known to interact with Dendritic cells (DC) (Mallegol et al., 2007). They stimulate DC, Treg and macrophage maturation with tolerogenic properties through immunoregulatory signals (Jeffrey et al., 2018). Also, tolerogenic DCs are essential for maintaining intestinal homeostasis (Peterson and Artis, 2014). The cytokine, TGF-β is produced in tolerogenic DCs and Tregs in its latent form as LTGF-β. IEC EVs carrying integrin αvβ6 are internalized by intestinal tolerogenic DCs, wherein they help activate TGF-β, induce Treg cells and initiate tolerogenic responses in the gut (Chen et al., 2011). $CD4^+$ T cell proliferation is inhibited by TGF-β containing IEC EVs (Jiang et al., 2016). IEC EVs have a wide spectrum immuno modulatory effect. EVs expressing CD63 and EpCAM (Epithelial cell adhesion molecule) suppress DC maturation and inhibit antigen presentation by DCs and also induce DC apoptosis in post-trauma immune dysfunction in rats (Kojima et al., 2018). EpCAM plays a unique role in immuno-modulation by facilitating a physical interaction between intraepithelial lymphocytes and IECs (Jiang et al., 2016). Annexin 1 (ANXA1) is crucial for maintaining the intestinal barrier during inflammatory response; it is found in exosomes released from IECs (Leoni et al., 2015). These ANXA 1 containing EVs help in resolving inflammation in murine colitis, their number increases during wound healing (Leoni et al., 2013; Perretti and D'Acquisto, 2009). These EVs bind to formyl peptide receptors (FPRs) and may be employed to activate wound repair in epithelial cells (Leoni et al., 2015). In IBD patients, mucosal-luminal interface EVs express MPO (myeloperoxidase). MPO is a defense protein which creates oxidative stress against microbes in the intestines (X. Zhang et al., 2018). At the same time, intestinal fluid EVs from IBD patients have a pro-inflammatory effect on IECs *in-vitro* (Mitsuhashi et al., 2017).

This disparity can be attributed to the source of EVs. EVs secreted by *Bacteroides fragilis* induce secretion of host mucosal EVs containing sphingosine-1-phosphate, CCL20, and prostaglandin E2 (Deng et al., 2015). Th17 cells are sequestered by Prostaglandin E2 and CCL20 via MyD88-mediated pathway (Deng et al., 2015), while sphingosine-1-phosphate plays a role in tumorigenesis (Kunkel et al., 2013; Hait and Maiti, 2017; Patmanathan et al., 2017). Conversely, it is possible that CCL20 and other pro-inflammatory cytokines are inhibited by EVs derived from healthy intestinal mucosa (Deng et al., 2015). **Figure 1** summarizes exosomal effects of IEC derived exosomes on intestinal barrier functions and immunity.

Exosomes From Immune Cells

The mucosal barrier maintains immune homeostasis in the gut by spatially separating the gut microbiota from the host immune system. In IBD, there is dysfunction of the barrier, immune dysregulation and dysbiosis. Both the innate and the adaptive immune system signals lead to IBD pathogenesis. The innate immune response is quicker; it involves phagocytosis, antigen presentation and provides stimulus for initiation of the adaptive immune response. The process involves macrophages, DCs, neutrophils, and monocytes (Ayyar et al., 2014). Many APCs have been reported to secrete exosomes, these exosomes may also bear MHC molecules (Morelli et al., 2004).

DCs are professional APCs of the immune system and can initiate an immune response upon sensing antigens. Based on the stage and maturation of parent DCs, DC derived exosomes may have immune stimulatory/suppressive effects (Lindenbergh and Stoorvogel, 2018; H.; Zhang et al., 2019). EVs from DCs can inhibit T-cell proliferation, this could play a key role in modulating inflammation in IBD (Kim et al., 2007; Tkach et al., 2017). Mature DC-derived exosomes that contain tumor antigens potentially could induce anti-tumor immunity in *in-vitro* trials, while immature exosomes could induce peripheral tolerance by T-cell immunosuppression (Yang et al., 2010). TGF-β1-modified bone marrow derived DCs (BMDC) produce exosomes that induce $CD4^{+}Foxp3^{+}$Tregs and attenuate Th17 population in lymphocytes from mesenteric lymph nodes of inflammatory site in DSS induced mice (Cai et al., 2012). Similarly, IL-10 treated DC exosomes inhibit 2,4,6-trinitrobenzenesulfonic acid (TNBS) induced colitis in rats by stimulating $CD4^{+}CD25^{+}$Tregs (Yang et al., 2010). In a similar study, EVs from *Schistosoma japonicum*-soluble antigen-treated DCs provided protection during acute IBD development (Tkach et al., 2017; L. Wang et al., 2017). Immune tolerance can be achieved through regulation of activated T cells, by harnessing the immunosuppressive activity of exosomes. APC derived exosomes can activate $CD4^{+}$ and/or $CD8^{+}$ T lymphocytes, their antigen presentation capacity relies on DC, indicating that APCs take up DC derived exosomes to promote T cell activation. Exosomes may quickly transfer immune information via APCs (Van Niel et al., 2003).

IBD progression is affected in myriad ways by other immune cell derived EVs. Neutrophil infiltration occurs in IBD and is accompanied by liberating MPO into the extracellular space. MPO results in production of oxidative radicals which damage the gut barrier. It was found that MPO was delivered to IEC via EVs and inflammatory response was enhanced, inhibiting wound closure and healing (Slater et al., 2017). EVs also contain miRNAs as cargo; miRNAs are excellent regulators of immune response (Ayyar et al., 2014). EVs containing proinflammatory miRNAs can promote doublestrand breaks (DSBs) in affected colonic epithelia (Butin-Israeli et al., 2019). Neutrophil derived EVs can contain miR-23a and miR-155. These EVs promote lamin B1- dependent replication fork collapse and also suppress homologous recombination (HR) by repressing RAD51 (Bui and Sumagin, 2019; Butin-Israeli et al., 2019). During transepithelial migration of granulocytes, granulocyte EVs accumulate on IECs. This promotes the recruitment of granulocytes accompanied by a loss of epithelial cadherins (Butin-Israeli et al., 2016). On the other hand, granulocytic myeloid-derived suppressor cells-derived EVs diminish number of Th1 cells and a resultant surge is observed in Treg population in colitis induced mice (Y. Wang et al., 2016). WNT signaling is essential for intestinal epithelium and homeostasis (Kuhnert et al., 2004; Gregorieff et al., 2005). Intestinal stem cells can be rescued by macrophage-derived EVs. They can also improve enterocyte survival post radiation via modulation of WNT signaling pathway (Saha et al., 2016). **Figure 2** shows the general modulatory features of immune-cell-derived exosomes on the immune system.

Exosomal Profile in Animals

Many studies have been conducted in rats and mice to study the effects exosomes in IBD. A radical difference was observed in the proportion of gut-bacteria derived EVs in feces of DSS (dextran sulfate sodium) induced colitis mice in comparison with those from healthy mice (Kang et al., 2013). The fecal EVs can be IEC-derived, microbiome-derived or may come from the diet. When healthy exosomes from mice were transferred to IBD-induced mice, it was observed that the disease severity markedly reduced in recipient mice (Jiang et al., 2016). This shows that exosomes have therapeutic potential. Another study showed that the protein load of exosomes in healthy and acute-colitis induced mice was different. A total of 56 acute phase proteins and immunoglobulins were found to be differentially expressed between the two groups (Wong et al., 2016). *Lactobacillus* and Bifidobacterium are known probiotics which are administered to IBD patients. DCs and EV isolated from TLR2 (toll-like-receptor 2) knockout mice and healthy mice were co-cultured with these bacteria. It was observed that TLR2/6 activity in DCs was reduced significantly (van Bergenhenegouwen et al., 2014). The effect was reversed upon EV depletion suggesting an immunosuppressive role of these EVs. Fecal OMVs (outer membrane vesicles) from colitis induced rats (DSS) reduced the expression of enzyme UDP-glucuronosyltransferase 1A1 (UGT1A1) in human Caco-2 cells while OMVs from healthy rats upregulated the enzyme expression (X. J. Gao et al., 2018). UGT1A1 helps in maintaining the Intestinal epithelial barrier. This study shows that rat OMVs can modulate mucosal immunity. EVs isolated from mesenteric lymph modulated the immune response through DC suppression in post-trauma immune dysfunction in rats (Kojima et al., 2018). When exosomes are introduced in naïve rats from IBD induced rats, antigen specific tolerance is detected; these exosomes were briefly called tolerosomes (Karlsson et al., 2001).

Exosomal Profile in Blood

Diseases like Cancer, inflammatory diseases and infections result in change in exosome composition of patients as compared to

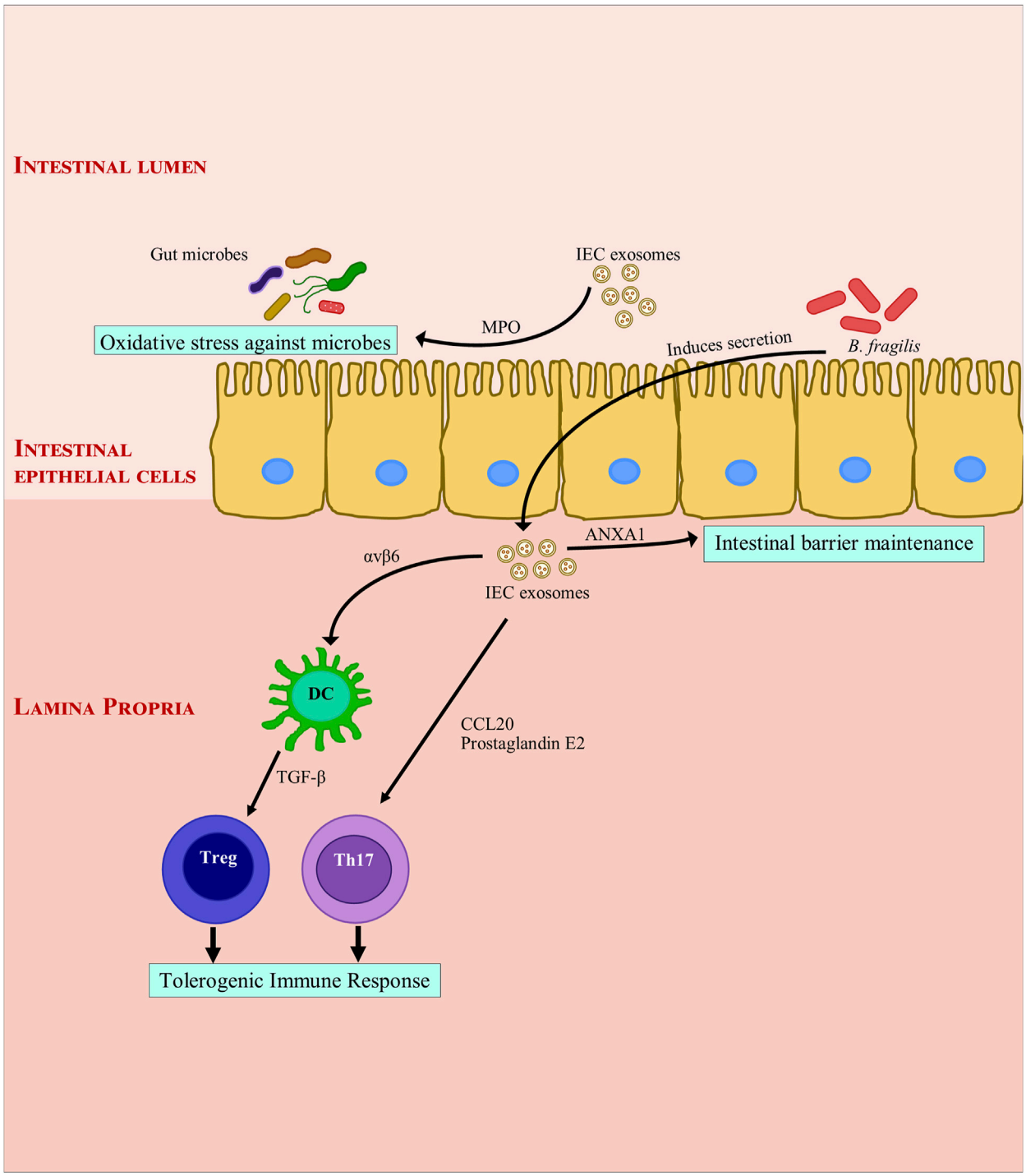


FIGURE 1 | Modulation of intestinal inflammation by intestinal epithelial cell derived exosomes. Intestinal epithelial cell derived exosomes help maintain gut immune homeostasis through secretion of Annexin A1. They induce a tolerogenic immune response by secretion of integrin, cytokines and chemokines. They also protect the gut immune barrier from bacterial invasion by secreting myeloperoxidase which creates oxidative stress against bacteria. ANXA1, Annexin A1; αvβ6, Integrin αvβ6; *B. fragilis*, *Bacteroides fragilis*; CCL20, C-C Motif Chemokine Ligand 20; DC, dendritic cell; IEC, Intestinal epithelial cells; MPO: myeloperoxidase; Th17, TGF-β, transforming growth factor β; T helper 17; Treg, regulatory T cell.

healthy controls. These changes can be observed in biological fluids like blood and blood components, saliva, stool, urine. These fluids represent an excellent tool for identification of biomarkers (Barile and Vassalli, 2017). Unfortunately, there are not many reports of EVs or exosomes in blood/serum. In 2015, Leoni et al. looked at serum exosome levels in IBD patients. They found that

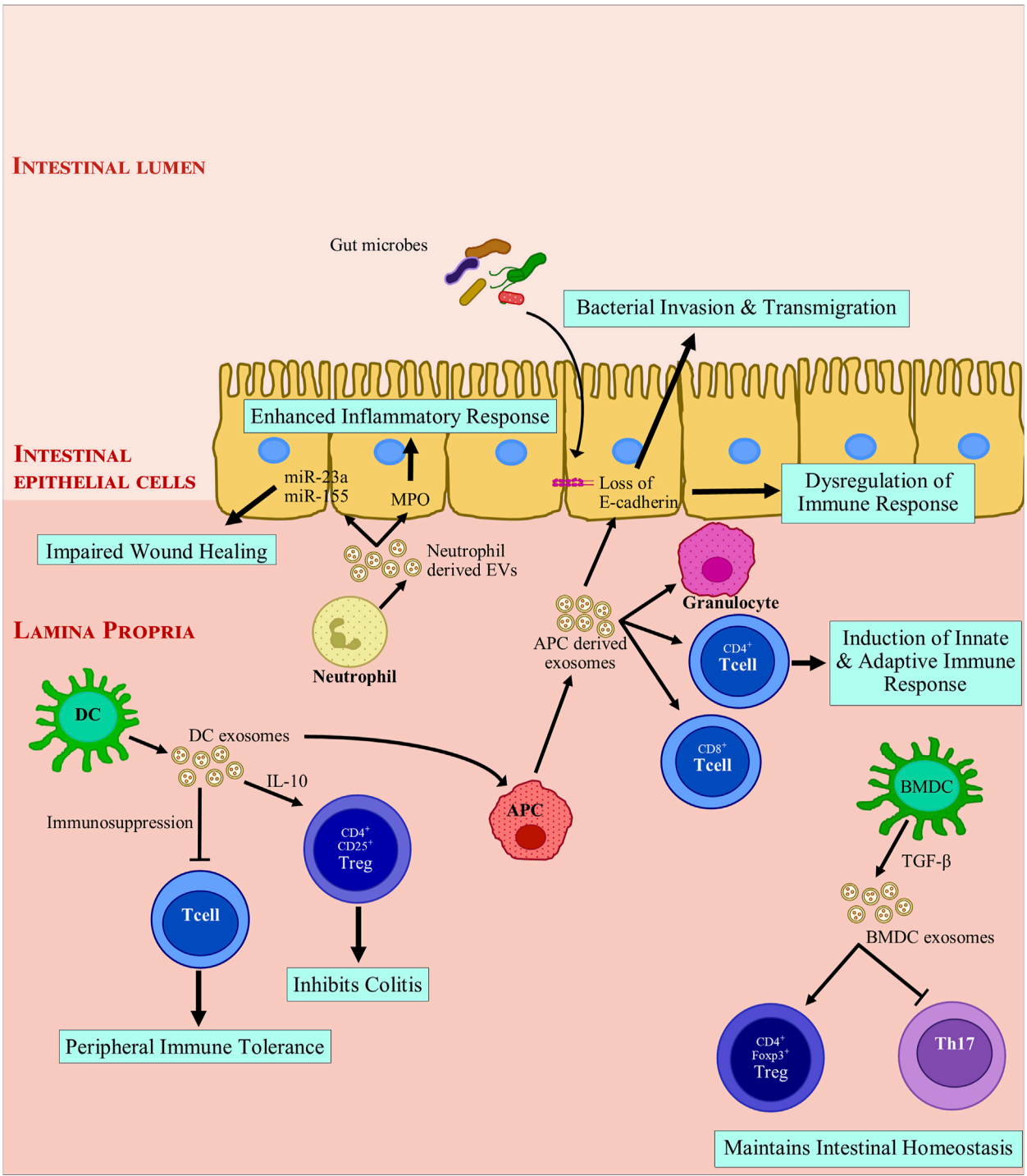


FIGURE 2 | Modulation of intestinal inflammation by immune cell derived extracellular vesicles. Exosomes derived from immune cells promote anti-inflammatory responses by inducing immune tolerance and triggering regulatory T cells (Treg) activation while inhibiting T helper cells. Exosome-treated immune cells further express exosomes that encourage anti-inflammatory responses. Mature APC derived exosomes promote loss of E-cadherin, which leads to breach of barrier integrity and facilitates bacterial invasion and transmigration. These exosomes also recruit immune cells and drive a pro-inflammatory immune response. Neutrophil derived exosomes secrete myeloperoxidase and miRNAs which are taken up by intestinal epithelial cells. miR-23a and miR-155 can introduce double strand breaks and impair wound healing in degenerated colonic epithelium. In summary, depending on the parent cells, exosomes derived from immune cells can drive toward a pro-inflammatory or an anti-inflammatory response. APC, antigen presenting cell; BMDC, Bone marrow derived dendritic cell; CD, cluster of differentiation; DC, dendritic cell; EV, extracellular vesicles; FOXP3, Forkhead box protein 3; IL-10, Interleukin 10; miR, microRNA; MPO: myeloperoxidase; TGF-β, transforming growth factor β; Th17, T helper 17; Treg, regulatory T cell.

exosomes released from IECs, entered circulation and expressed ANXA 1, which is crucial for maintaining the intestinal barrier during inflammatory response. Serum of IBD patients contain good number of such vesicles (Leoni et al., 2015). Additional research on the serum exosomal content in IBD patients will help better our understanding.

Role of Dietary EVs in Inflammatory Bowel Disease

The source of exosome existing in human body could be produced by human cells such as immune cells, IECs, tumor cells or by plant cells which are introduced through dietary food. As almost all biological cells produce exosomes; many of the edible foods that we consume contain exosomes.

Plant Derived Exosomes

Some studies have been conducted on exosomes derived from edible plants. *Curcuma longa* and grapes contain exosomes that helps in alleviating IBD. *Curcuma longa* is a medical herb, the exosomes derived from this plant may inactivate NF-κB to alleviate colitis and improve intestinal wound repair (H. Zhang et al., 2019). Exosome-like nanoparticles (ELN) from grape juice play a protective role in DSS-induced colitis mice when administered via the oral route (Ju et al., 2013). ELNs from ginger rhizome strongly inhibit NLRP3 (nucleotide-binding domain and leucine-rich repeat-containing family, pyrin domain-containing 3) inflammasome activation. Events occurring downstream of inflammasome activation like secretion of cytokines IL-1β and IL-18, auto cleavage of caspase-1 and pyroptotic cell death can also be impeded by these ELNs (Chen et al., 2019). Broccoli derived ELNs inhibit induced colitis in mice. These ELNs help in the activation of AMPK (AMP [adenosine monophosphate]-activated protein kinase) in DCs, which promotes DC tolerance and prevents DC activation, leading to inhibition of DSS induced colitis in mice (Deng et al., 2017).

Milk Derived Exosomes

Breast milk not only provides nutrition but also helps shape the neonate gut immune system (Turfkruyer and Verhasselt, 2015). Breast milk has immunoglobulin which help in responding precisely to encountered antigens (Walker and Iyengar, 2015; Doare et al., 2018). Recent studies have shown EVs contained in milk can affect intestinal homeostasis (Admyre et al., 2007). Bioactive milk exosomes are known to carry miRNAs, mRNAs, lncRNAs, TGF-β and a variety of other proteins and lipids (Reinhardt et al., 2012; Reinhardt et al., 2013; Pieters et al., 2015; Tomé-Carneiro et al., 2018). Exosomes are resistant to the harsh conditions in the gastrointestinal tract (Benmoussa et al., 2016; Liao et al., 2017; Kahn et al., 2018) but are actively captured by intestinal epithelial cells (T. Wolf et al., 2015). It has been observed that a considerable portion of milk exosomes (from consumed milk) enter circulation in rodents and humans (Baier et al., 2014; Manca et al., 2018; Betker et al., 2019). The fate of unabsorbed exosomes is not yet known. There is strong evidence that milk exosomes are crucial for maturation and intestinal function (Gao H. N. et al., 2019; Gao R. et al., 2019; Hock et al., 2017; Li et al., 2019; Miyake et al., 2020; Reif et al., 2019; Xie et al., 2020). Strong evidence indicates that human, porcine and bovine milk exosomes aid intestinal cell growth in mice (Gao H. N. et al., 2019; Hock et al., 2017; Reif et al., 2019). Milk exosomes can also attenuate LPS-induced apoptosis (Xie et al., 2019), and prevent intestinal endothelial cell damage (R. Gao et al., 2019b; Miyake et al., 2020). They also enhance goblet cell numbers and mucin production (Li et al., 2019). They can also modify bacterial growth, and promote intestinal microbiota (Doare et al., 2018; Zhou et al., 2019). Interestingly, pasteurized fresh milk contains more bioactive milk exosomes as compared to fermented milk products like yoghurt (Yu et al., 2017). **Figure 3** describes the role of microbiome derived OMVs and dietary exosomes in modulating intestinal inflammation.

Role of Microbiota Derived Outer Membrane Vesicles in Inflammatory Bowel Disease

All biological life forms are capable of producing EVs. These include micro-organisms encountered in the intestinal tract like protozoa, archaea, bacteria and fungi (Brown et al., 2015). It has been reported that commensal microbes can modulate IECs and immune cells in the intestine by affecting maturation and other related functions. As alterations in intestinal microbiota affect the pathogenesis and development of IBD, the EVs secreted by the commensal microbes may help maintain gut immune homeostasis (Geveres et al., 2014). The involvement of extracellular factors from microbes in modulating immune response has been observed as early as 1967 (S. Chatterjee and Das, 1967). In 1967, Chatterjee and Das showed that the bacteria, *Neisseria meningitides* secreted endotoxins as cell wall blebs *in-vivo* (S. Chatterjee and Das, 1967). However, the mechanism has not yet been understood thoroughly.

Pathogenic bacteria exist in the intestines and their EVs can negatively influence gut homeostasis. They breach the intestinal barrier and facilitate mucosal invasion leading to IBD pathogenesis. *Helicobacter pylori* infection in the gut leads to gastritis, ulceration and malignancy. In 2003, a study found that it was not necessary for the bacterium to associate with the epithelial cell to cause disease, the OMVs released by the bacteria could interact with the host epithelial cell and bring about an adverse reaction (Ismail et al., 2003). Enterohemorrhagic *Escherichia coli* (EHEC) O157 EVs promote IL-8 secretion in IECs through TLR5 and TLR4/MD-2 pathway (Bielaszewska et al., 2018). They also induce apoptosis by delivering hemolysin from EHEC to endothelial cells and mitochondria (Bielaszewska et al., 2013). UGT1A1 is an important part of intestinal epithelial barrier. Fecal OMVs isolated from colitis induced rats (DSS) reduced the expression of UGT1A1 in human Caco-2 cells while, OMVs from healthy rats upregulated UGT1A1 (X. J. Gao et al., 2018). This shows that gut microbiota can regulate intestinal UGT1A1 expression. *Vibrio cholera* secretes two proteases, hemagglutinin protease (HAP) and calcium-dependent trypsin-like serine protease (VesC) in association with OMVs, these are transported to human IECs in an active form. Studies show that HAP induces apoptosis and VesC induces necrosis and increases IL-8 secretion in host cells. Data also suggests that VesC promotes intestinal colonization of *V. cholerae* in mice (Mondal et al., 2016).

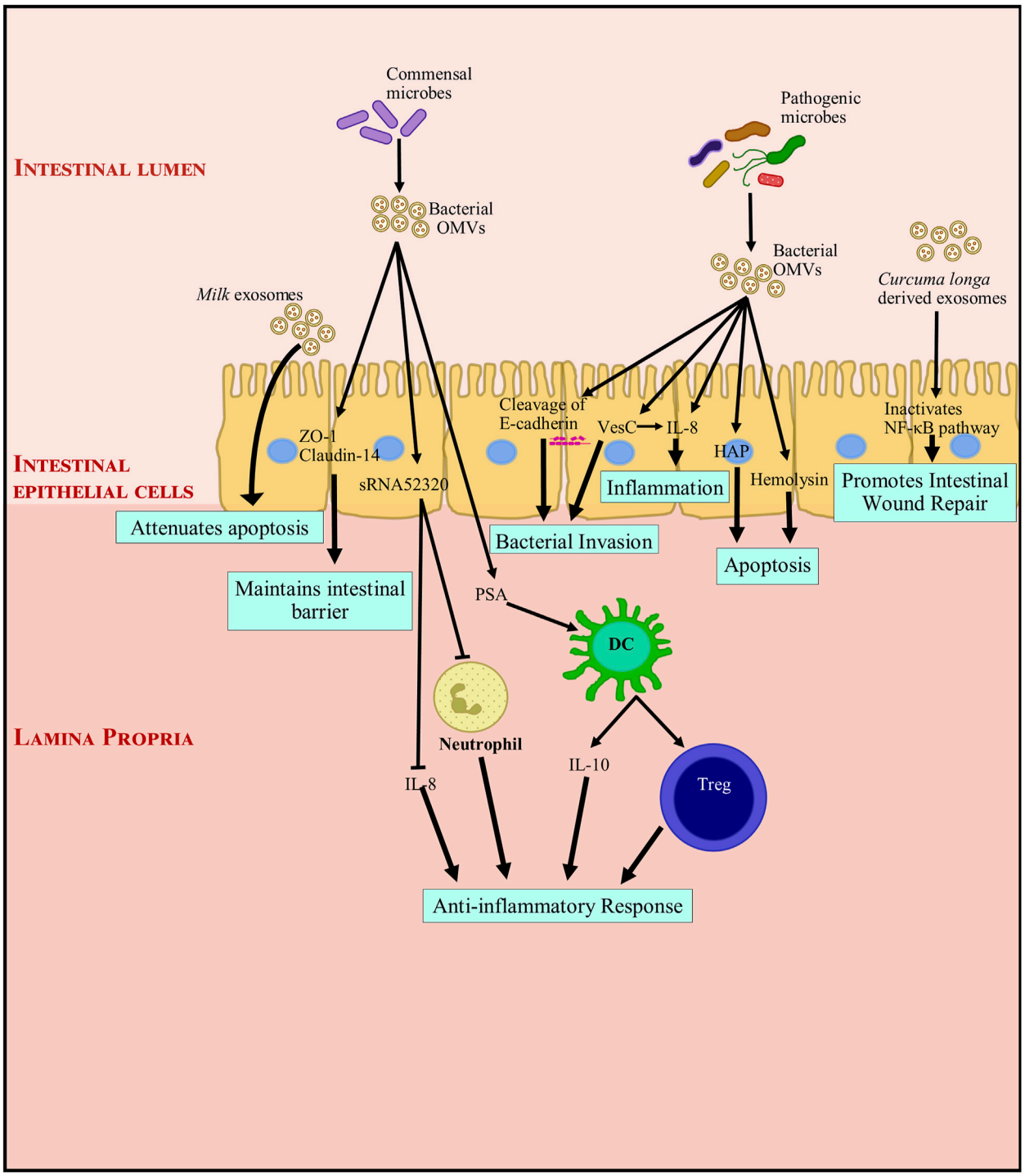


FIGURE 3 | Modulation of intestinal inflammation by microbiome derived outer membrane vesicles and dietary exosomes. Exosomes and OMVs (outer membrane vesicles) through their functional components, directly or indirectly interact with gut intestinal epithelial cells (IECs). Dietary exosomes attenuate apoptosis and promote intestinal wound repair. OMVs from commensal bacteria induce the proliferation of IECs and development of the intestinal tract, and indirectly enhance barrier functions by inhibiting components of the inflammatory environment that negatively impact tight junction molecules and IECs. They also interact with immune cells and promote an anti-inflammatory immune response. On the other hand, pathogenic bacteria, though their OMVs can induce inflammation and apoptosis. They can also cause a breach in the epithelial barrier by cleaving E-cadherin. This facilitates bacterial invasion and transmigration into the intestinal tissue. DC, dendritic cell; HAP, hemagglutinin protease; IL, Interleukin; NF-κB, nuclear factor kappa light chain enhancer of activated B cells; OMV, outer membrane vesicle, PSA: capsular polysaccharide; sRNA52320, shortRNA 52320; Treg, regulatory T cell; VesC, calcium-dependent trypsin-like serine protease; ZO-1, Zonula occludens 1.

Also, IECs take up these EVs and stimulate the MAPK and NF-κB pathways in a nucleotide-binding oligomerization domain-containing 1 (NOD1)-dependent manner. This causes a change in the expression of IL-8, GM-CSF, CCL2, CCL20, and thymic stromal lymphopoietin (D. Chatterjee and Chaudhuri, 2013). Epithelial cadherin is essential for maintaining epithelial integrity, EVs from *Campylobacter jejuni* cleaved epithelial cadherin and facilitated the infiltration of pathogenic bacteria into IECs (Elmi et al., 2016; Boehm et al., 2018). Evidence suggests that immune responses mounted against commensal like *Bacteroides thetaiotaomicron* could trigger colitis in genetically vulnerable hosts (Hickey et al., 2015).

Microbiome derived EVs present in the host can also help maintain gut immune homeostasis. The innate immune defense of the gut relies heavily on the integrity of the epithelial layer which acts as a barrier. Apart from IECs that reinforce this barrier, probiotic bacteria can also influence barrier integrity by regulating the pro-inflammatory signals, reinforcing tight junctions between IECs and by facilitating cross-talk between commensals, gut epithelia and the mucosal immunity. *Escherichia coli* C25, is a commensal organism present in the human gut, the OMVs released by this bacterium elicits a moderate pro-inflammatory response via secretion of IL-8 *in vitro* (Patten et al., 2017). This response is beneficial to the host as healthy human intestine has a low-level inflammatory environment. OMVs from *E. coli* C25 have also shown to regulate the translocation of parent bacteria across the intestinal epithelium. This aids in maintaining a favorable symbiotic relationship with the host (Patten et al., 2017). Another probiotic bacteria, *E. coli* Nissle 1917 (EcN) helps in maintaining tight junctions by secreting OMVs and soluble factors which induce ZO-1 and claudin-14 expression, and inhibit claudin-2 expression (Alvarez et al., 2016). The pro-inflammatory effect of *E. coli* OMVs can be ameliorated by *Akkermansia muciniphila* EVs. Also, *A. muciniphila* EVs are depleted in colitis induced mice as compared to healthy mice, indicating that they play a protective role in IBD. Indeed, IBD indicators like loss of body weight, length of colon, infiltration of colon wall are maintained when *A. muciniphila* EVs are delivered orally (Kang et al., 2013). *B. fragilis* OMVs containing PSA (capsular polysaccharide) can protect against inflammation in TNBS colitis mice model. This is achieved by production of anti-inflammatory cytokines by DCs, enhancing the Treg response (Shen et al., 2012). *Pseudomonas aeruginosa* releases EVs which contains shortRNAs (sRNA), this sRNA was shown to reduce IL-8 secretion from LPS (lipopolysaccharide) induced IECs. This sRNA termed as sRNA52320 can also attenuate cytokine secretion and neutrophil infiltration (Koeppen et al., 2016). *B. thetaiotaomicron* produces a phosphatase, BTMinpp which is packaged inside OMVs, thus protecting its catalytic activity. This enzyme promotes intracellular Ca^{2+} signaling in IECs and thereby the physiological responses of the digestive system are sustained (Stentz et al., 2014). Additionally, *E. coli* OMVs (probiotic and commensal strains) induce more anti-inflammatory cytokines in explanted colonic tissue, although a modest expression of proinflammatory cytokines, such as IL-6 and IL-8 is also observed (Fábrega et al., 2016).

The host can also combat EVs from pathogenic microbes. OMVs secreted from bacteria contain cargo and this cargo is recognized by pattern recognition receptors (PRR) of the host immune system which mount an inflammatory response. The OMV released from *E. coli* contains peptidoglycan which is recognized by NOD1 receptor. This triggers the NOD1 signaling cascade, inducing the expression of pro-inflammatory molecules like NF-κB, IL-6, and IL-8 (Cañas et al., 2018). However, the OMVs may escape immune surveillance and enter IECs via clathrin-dependent endocytosis resulting in host cell DNA damage (Cañas et al., 2016). It's not just the EVs from bacteria that regulate host cells but EVs present in the host's physiological fluid can also interact with bacteria and promote bacterial aggregation (van Bergenhenegouwen et al., 2014). Pathogenic bacteria and commensals derived EVs regulate inter-species communication in the gut which leads to immunoregulation of signaling pathways. The source and functions of different OMV components and their function in IBD is listed in **Table 2**.

EXOSOMAL COMPONENTS AS BIOMARKERS FOR INFLAMMATORY BOWEL DISEASE

Micro-environmental changes take place at the site of intestinal mucosal inflammation: nutrient shortage, dysregulated oxygen supply in tissue and production of reactive nitrogen and oxygen

TABLE 2 | Source and function of different bacterial outer membrane vesicle components in IBD.

Component	Source	Role	References
BTMinpp	*Bacteroides thetaiotaomicron*	Promotes intracellular CA^{++} signaling in IECs	Stentz et al. (2014)
Calcium-dependent trypsin-like serine protease (VesC)	*Vibrio cholera*	Plays a role in intestinal colonization of bacteria Induces necrosis Increase IL-8 secretion in host cells	Mondal et al. (2016)
Capsular polysaccharide (PSA)	*Bacteroides fragilis*	Induces anti-inflammatory cytokine production in DCs Enhances Treg response	Shen et al. (2012)
Hemagglutinin protease (HAP)	*Vibrio cholera*	Induces apoptosis in intestinal epithelial cells	Mondal et al. (2016)
Hemolysin	Enterohemorrhagic *E.coli*	Apoptosis of endothelial cells	Bielaszewska et al. (2013)
Peptidoglycan	*Escherichia coli*	Triggers NOD1 signaling cascade Induces expression of IL-6, IL-8 and NF-κB	Cañas et al. (2018)
sRNA52320	*Pseudomonas aeruginosa*	Reduces IL-8 secretion from LPS induced IECs Attenuates neutrophil infiltration	Koeppen et al. (2016)

species. Mucosal barrier, cell fate, immune regulation, and gut microbiota are affected by the consequent oxidative and hypoxia derived stress (Taylor and Colgan, 2007; Cao, 2018). An inflammatory cascade is triggered within this microenvironment through intricate crosstalk between different cell types (Marafini et al., 2019). Inflammatory cells such as granulocytes, macrophages and monocytes, and also cells of the adaptive immune system like B and T cells are sequestered within the site of active inflammation, by cytokines like IL-8 (Marafini et al., 2019). When the intestinal barrier is intact, it is very difficult for luminal antigens to approach the lamina propria. When immune cells are within the lamina propria, a tolerance system is set in place which limits induction of an immune response. On the other hand, when barrier integrity is compromised, antigens trespass the barrier and the tolerance system is invalidated. This culminates in secretion of chemokines, recruitment and infiltration of immune cells, further aggravating inflammation (Neurath, 2019). The current diagnosis of IBD involves invasive procedures like endoscopy and colonoscopy. They are also expensive, time-consuming and inconvenient for the patients. There is a need to develop a less-invasive, faster, reliable detection method for IBD.

The origin of exosomes present in the intestinal tract can be host cells, diet or microbial organisms (Chang et al., 2020). The EV content in bile samples of individuals suffering from malignant common bile stenosis was significantly higher than those seen in the bile samples of healthy controls, suggesting that the nature of EVs differs with respect to health condition of the body (Severino et al., 2017). ANXA1 is crucial for maintaining the intestinal barrier during inflammatory response; it is found in exosomes released from intestinal epithelial cells (IEC). Serum of IBD patients contain good number of such vesicles, making it a promising biomarker for intestinal inflammation (Leoni et al., 2015). Proteasome Subunit Alpha type 7 (PSMA7) is found in oral exosomes secreted by the oral mucosal cells of IBD patients. The expression of PSMA7 isolated from saliva in IBD patients is remarkably different than those in healthy controls and is a good biomarker candidate (Zheng et al., 2017). More exosomal characterization studies on biological fluids from IBD patients would help in identifying novel biomarkers that could help in early diagnosis of IBD.

EFFECT OF EXOSOMES ON CURRENT INFLAMMATORY BOWEL DISEASE TREATMENT

IBD treatment involves anti-inflammatory drugs, immune system suppressors, and biologics supplemented with antibiotics and dietary supplements. Biologics are the newest category of drugs in IBD treatment. Most of them are monoclonal antibodies which neutralize inflammation causing proteins in the body. The most common form of biologics administered to IBD patients are TNF blocking agents e.g.,: Infliximab, Adalimumab, Golimumab, and Certolizumab. Other biologics used in IBD treatment are Vedolizumab, which is a $\alpha_4\beta_7$ blocker and Ustekinumab, which blocks the IL12-IL23 pathway.

A recent study detected $\alpha_4\beta_7$ integrin expression on the surface of circulating exosomes from serum of IBD patients being treated with Vedolizumab (VDZ) (Domenis et al., 2020). These $\alpha_4\beta_7$ expressing exosomes were able to bind to VDZ competitively *in-vitro*. In IBD treatment, VDZ acts by binding to the $\alpha_4\beta_7$ integrin found on a subset of T cells and prevents their trafficking into the gut. This data suggests that exosomes could be involved in mediating VDZ resistance in IBD patients by sequestration of therapeutic molecules into vesicles. Most IBD patients on treatment with a biologic drug respond poorly to a second biologic drug (Gisbert ad Chaparro, 2020). The study by Domenis et al. (2020) reports that the serum exosomal concentration and vesicle surface expression of $\alpha_4\beta_7$ integrin was greater in the serum of patients on TNF blocking drugs compared to TNF naïve patients. The resultant exosomal sequestration of VDZ also increased in patients on TNF blocking drugs suggesting that previous treatment with a biologic drug alters the expression of α4β7 integrin and binding capacity of circulating exosomes. This potentially explains the reduced efficacy of VDZ in IBD patients who were previously treated with TNF blocking agents.

To date this is the only study correlating the effect of exosomes on IBD treatment modalities. Further studies in this direction would help design better treatment strategies that could increase drug bioavailability.

ROLE OF EXOSOMES IN INFLAMMATORY BOWEL DISEASE THERAPY

Exosomes are natural carriers of functional RNAs, proteins and have the characteristics to be employed for transporting drugs or biologicals. They can also be employed for tissue repair and regeneration. Modification of exosomes either biologically or chemically will boost their therapeutic potential (Ocansey et al., 2020). IBD is characterized by disruption of the immune system and abnormal stimulation of immune cells. As mentioned in this review, DC derived EVs through immune excitation or repression mitigate IBD progression. Hence, it is plausible that immune cells derived EVs may be the new therapeutic intervention for IBD.

The interest in EV research also propels the exploration of artificial nanoparticles as tool for disease treatment. Studies have looked at EV-like nanoparticles as treatment for IBD. Bioadhesive chitosan has been developed, which can be delivered by oral route to accumulate in a safe and specific way to affected areas in the GI tract (Han et al., 2019). Intestinal organoids containing 5-ASA-loaded nanoparticles have been used to relieve IBD (Davoudi et al., 2018). Mannosylated bioreducible cationic polymers have been used to synthesize RNAi (RNA interference) nanoparticles to lower cell-death and improve treatment efficacy in IBD (Xiao et al., 2013). EVs are bio-compatible and stable than artificial nanoparticles as they are innate in nature, being derived from cells and microbes. EVs can also be engineered, enhancing their role in treatment and therapy in IBD (Hood and Wickline, 2012; Hood, 2016). Promising results have been observed with Rifaximin loaded EVs (Kumar and Newton, 2017; García-

Manrique et al., 2018). These studies demonstrate that EVs have a potential use in drug delivery.

Breast milk is known to have immunoglobulins, approximately 15 years ago it was discovered that it contains immune-modulatory EVs (Admyre et al., 2007). Since then milk EVs have received considerable attention and a lot of studies have been conducted to understand the process of drug delivery in the intestinal tract. EVs are resilient to gastric/pancreatic digestion (Hata et al., 2010), indicating that breast milk EVs are delivered to intestines of infants (Kahn et al., 2018). Milk derived EVs were also observed in human intestinal crypt-like cells, indicating a possible role in neonatal mucosal immunity (Liao et al., 2017). Several studies recommend that IEC viability, stem-cell activity and proliferation capacity increase when treated with milk derived EVs (T. Chen et al., 2016; Gao H. N. et al., 2019; Hock et al., 2017). Breast milk EVs can prevent cell death in IECs and decrease necrotizing enterocolitis (NEC) (Lucas and Cole, 1990; Martin et al., 2018). They also offer the possibility of delivering drugs in milk (Schanler et al., 1992; Zamrik et al., 2018). Small molecules such as siRNA are ideal candidate for therapy but they are unstable during delivery. A 2017 study showed that AF488 could be encapsulated in milk whey and EVs would ensure their delivery to Caco-2 cells (Shandilya et al., 2017).

Protein cargo content of EVs have also been researched. Intestinal EVs contain high levels of the cytokine, TGF-β1 which induces Treg cells and immunosuppressive DCs in IBD mice (Jiang et al., 2016). Meanwhile, ANXA1 containing exosomes stimulates epithelial cell repair in a colitis mice-model. Increased amount of ANXA1 is also observed in sera of IBD patients, the increase is directly proportionate to disease severity (Leoni et al., 2015). This provides strong evidence to use EV components as biomarkers for disease severity and IBD progression but may also have a role in therapy. Anti-tumor immunity can be induced by mature DC-derived exosomes carrying tumor antigens in *in-vitro* trials (Yang et al., 2010). Most translational EV studies are still in the pre-clinical stages with data available from animal and cellular models. Additional research would help in exploring the application of EVs in diagnostics and therapeutics in a clinical setting.

DISCUSSION

Evidence from recent studies on exosomes in particular and EVs in general indicate that these extracellular vesicles are capable of modulation of genes and cellular function and can thereby regulate inflammation and immune response. Based on our review of published studies, it is evident that exosomal cargo is strongly associated with the nature of the cells which produces them. Exosomal components are optimal for use as biomarkers as they can be extracted with minimal invasive techniques from most biological fluids like blood, urine, saliva, and feces. Existing data in IBD is limited to initial characterizations of exosomes in blood and fecal samples. Further studies are required to identify sensitive and specific markers of mucosal inflammation, and ideally inflammatory pathways. This could guide treatment decisions when several mechanisms of drug action are available to clinicians. As researchers we need to make efforts to develop robust methodologies for isolation of exosomes from fecal samples to ensure results are reliable and reproducible.

AUTHOR CONTRIBUTIONS

KKA and ACM conceptualized the review. KKA wrote the manuscript. ACM edited the manuscript.

FUNDING

ACM has received grant funding from the Helmsley Trust and Pfizer Inc.

REFERENCES

Admyre, C., Johansson, S. M., Qazi, K. R., Filén, J.-J., Lahesmaa, R., Norman, M., et al. (2007). Exosomes with Immune Modulatory Features Are Present in Human Breast Milk. *J. Immunol.* 179 (3), 1969–1978. doi:10.4049/jimmunol.179.3.1969

Agrahari, V., Agrahari, V., Burnouf, P.-A., Chew, C. H., and Burnouf, T. (2019). Extracellular Microvesicles as New Industrial Therapeutic Frontiers. *Trends Biotechnol.* 37 (7), 707–729. doi:10.1016/j.tibtech.2018.11.012

Alvarez, C.-S., Badia, J., Bosch, M., Giménez, R., and Baldomà, L. (2016). Outer Membrane Vesicles and Soluble Factors Released by Probiotic escherichia Coli Nissle 1917 and Commensal ECOR63 Enhance Barrier Function by Regulating Expression of Tight junction Proteins in Intestinal Epithelial Cells. *Front. Microbiol.* 7 (DEC), 1–14. doi:10.3389/fmicb.2016.01981

André, F., Chaput, N., Schartz, N. E. C., Flament, C., Aubert, N., Bernard, J., et al. (2004). Exosomes as Potent Cell-free Peptide-Based Vaccine. I. Dendritic Cell-Derived Exosomes Transfer Functional MHC Class I/Peptide Complexes to Dendritic Cells. *J. Immunol.* 172 (4), 2126–2136. doi:10.4049/jimmunol.172.4.2126

Avila-Calderón, E. D., Araiza-Villanueva, M. G., Cancino-Diaz, J. C., López-Villegas, E. O., Sriranganathan, N., Boyle, S. M., et al. (2015). Roles of Bacterial Membrane Vesicles. *Arch. Microbiol.* 197 (Issue 1), 1–10. doi:10.1007/s00203-014-1042-7

Ayyar, K. K., and Reddy, K. V. R. (2018). MAPK and NF-κB Signalling Pathways Regulate the Expression of miRNA, Let-7f in Human Endocervical Epithelial Cells. *J. Cel. Biochem.* 119 (January), 4751–4759. doi:10.1002/jcb.26665

Ayyar, K. K., Saha, D., Shroff, A., and Kvr, R. (2014). *MicroRNAs : the Key Regulators of PRR Signaling* 2 (3), 116–121.

Ayyar, K., and Reddy, K. V. R. (2017). Transcription Factor CCAAT/enhancer-binding Protein-β Upregulates microRNA,let-7f-1 in Human Endocervical Cells. *Am. J. Reprod. Immunol.* 78 (6), e12759. doi:10.1111/aji.12759

Baier, S. R., Nguyen, C., Xie, F., Wood, J. R., and Zempleni, J. (2014). MicroRNAs Are Absorbed in Biologically Meaningful Amounts from Nutritionally Relevant Doses of Cow Milk and Affect Gene Expression in Peripheral Blood Mononuclear Cells, HEK-293 Kidney Cell Cultures, and Mouse Livers. *J. Nutr.* 144 (10), 1495–1500. doi:10.3945/jn.114.196436

Barile, L., and Vassalli, G. (2017). Exosomes: Therapy Delivery Tools and Biomarkers of Diseases. *Pharmacol. Ther.* 174, 63–78. doi:10.1016/j.pharmthera.2017.02.020

Benmoussa, A., Lee, C. H. C., Laffont, B., Savard, P., Laugier, J., Boilard, E., et al. (2016). Commercial Dairy Cow Milk Microrna Resist Digestion under Simulated Gastrointestinal Tract Conditions. *J. Nutr.* 146 (11), 2206–2215. doi:10.3945/jn.116.237651

Beshbishy, A. M., Alghamdi, S., Onyiche, T. G. E., Zahoor, M., Rivero-Perez, N., Zaragoza-Bastida, A., et al. (2020). Biogenesis, Biologic Function and Clinical Potential of Exosomes in Different Diseases. *Appl. Sci. (Switzerland)MDPI AG* 10 (13), 4428. doi:10.3390/app10134428

Betker, J. L., Angle, B. M., Graner, M. W., and Anchordoquy, T. J. (2019). The Potential of Exosomes from Cow Milk for Oral Delivery. *J. Pharm. Sci.* 108 (4), 1496–1505. doi:10.1016/j.xphs.2018.11.022

Bielaszewska, M., Marejková, M., Bauwens, A., Kunsmann-Prokscha, L., Mellmann, A., and Karch, H. (2018). Enterohemorrhagic *Escherichia coli* O157 Outer Membrane Vesicles Induce Interleukin 8 Production in Human Intestinal Epithelial Cells by Signaling via Toll-like Receptors TLR4 and TLR5 and Activation of the Nuclear Factor NF-κB. *Int. J. Med. Microbiol.* 308 (7), 882–889. doi:10.1016/j.ijmm.2018.06.004

Bielaszewska, M., Rüter, C., Kunsmann, L., Greune, L., Bauwens, A., Zhang, W., et al. (2013). Enterohemorrhagic *Escherichia coli* Hemolysin Employs Outer Membrane Vesicles to Target Mitochondria and Cause Endothelial and Epithelial Apoptosis. *Plos Pathog.* 9 (12), e1003797–30. doi:10.1371/journal.ppat.1003797

Boehm, M., Simson, D., Escher, U., Schmidt, A.-M., Bereswill, S., Tegtmeyer, N., et al. (2018). Function of Serine Protease HtrA in the Lifecycle of the Foodborne Pathogen Campylobacter Jejuni. *Eur. J. Microbiol. Immunol.* 2 (July), 1–8. doi:10.1556/1886.2018.00011

Brown, L., Wolf, J. M., Prados-Rosales, R., and Casadevall, A. (2015). Through the wall: Extracellular Vesicles in Gram-Positive Bacteria, Mycobacteria and Fungi. *Nat. Rev. Microbiol.* 13 (10), 620–630. doi:10.1038/nrmicro3480

Bui, T. M., and Sumagin, R. (2019). Progressing from Recurring Tissue Injury to Genomic Instability: A New Mechanism of Neutrophil Pathogenesis. *DNA Cel Biol.* 38 (8), 747–753. doi:10.1089/dna.2019.4842

Butin-Israeli, V., Houser, M. C., Feng, M., Thorp, E. B., Nusrat, A., Parkos, C. A., et al. (2016). Deposition of Microparticles by Neutrophils onto Inflamed Epithelium: a New Mechanism to Disrupt Epithelial Intercellular Adhesions and Promote Transepithelial Migration. *FASEB J.* 30 (12), 4007–4020. doi:10.1096/fj.201600734R

Butin-Israeli, V., Bui, T. M., Wiesolek, H. L., Mascarenhas, L., Lee, J. J., Mehl, L. C., et al. (2019). Neutrophil-induced Genomic Instability Impedes Resolution of Inflammation and Wound Healing. *J. Clin. Invest.* 129 (2), 712–726. doi:10.1172/JCI122085

Cai, Z., Zhang, W., Yang, F., Yu, L., Yu, Z., Pan, J., et al. (2012). Immunosuppressive Exosomes from TGF-β1 Gene-Modified Dendritic Cells Attenuate Th17-Mediated Inflammatory Autoimmune Disease by Inducing Regulatory T Cells. *Cell Res* 22 (3), 607–610. doi:10.1038/cr.2011.196

Cañas, M.-A., Fábrega, M.-J., Giménez, R., Badia, J., and Baldomà, L. (2018). Outer Membrane Vesicles from Probiotic and Commensal escherichia Coli Activate NOD1-Mediated Immune Responses in Intestinal Epithelial Cells. *Front. Microbiol.* 9 (MAR), 1–13. doi:10.3389/fmicb.2018.00498

Cañas, M.-A., Giménez, R., Fábrega, M.-J., Toloza, L., Baldomà, L., and Badia, J. (2016). Outer Membrane Vesicles from the Probiotic *Escherichia coli* Nissle 1917 and the Commensal ECOR12 Enter Intestinal Epithelial Cells via Clathrin-dependent Endocytosis and Elicit Differential Effects on DNA Damage. *PLoS ONE* 11 (8), e0160374–22. doi:10.1371/journal.pone.0160374

Cao, S. S. (2018). Cellular Stress Responses and Gut Microbiota in Inflammatory Bowel Disease. *Gastroenterol. Res. Pract.* 2018, 1–13. doi:10.1155/2018/7192646

Carrière, J., Barnich, N., and Nguyen, H. T. T. (2016). Exosomes: From Functions in Host-Pathogen Interactions and Immunity to Diagnostic and Therapeutic Opportunities. *Rev. Physiol. Biochem. Pharmacol.* 172, 39–75. doi:10.1007/112_2016_7

Chang, X., Wang, S.-L., Zhao, S.-B., Shi, Y.-H., Pan, P., Gu, L., et al. (2020). Extracellular Vesicles with Possible Roles in Gut Intestinal Tract Homeostasis and IBD. *Mediators Inflamm.* 2020, 1–14. doi:10.1155/2020/1945832

Chargaff, E., and West, R. (1946). The Biological Significance of the Thromboplastic Protein of Blood. *J. Biol. Chem.* 166, 189–197. doi:10.1016/s0021-9258(17)34997-9

Chatterjee, D., and Chaudhuri, K. (2013). *Vibrio cholerae* O395 Outer Membrane Vesicles Modulate Intestinal Epithelial Cells in a NOD1 Protein-dependent Manner and Induce Dendritic Cell-Mediated Th2/Th17 Cell Responses. *J. Biol. Chem.* 288 (6), 4299–4309. doi:10.1074/jbc.M112.408302

Chatterjee, S. N., and Das, J. (1967). Electron Microscopic Observations on the Excretion of Cell-wall Material by *Vibrio cholerae*. *J. Gen. Microbiol.* 49 (1), 1–11. doi:10.1099/00221287-49-1-1

Chen, T., Xie, M.-Y., Sun, J.-J., Ye, R.-S., Cheng, X., Sun, R.-P., et al. (2016). Porcine Milk-Derived Exosomes Promote Proliferation of Intestinal Epithelial Cells. *Sci. Rep.* 6 (September), 1–12. doi:10.1038/srep33862

Chen, T., Xue, H., Lin, R., Huang, Z., et al. (2017). MiR-34c and PlncRNA1 Mediated the Function of intestinal Epithelial Barrier by regulating Tight Junction Proteins in Inflammatory Bowel Disease. *Biochem. Biophys. Res. Commun.* 486 (1), 6–13. doi:10.1016/j.bbrc.2017.01.115

Chen, X., Song, C.-H., Feng, B.-S., Li, T.-L., Li, P., Zheng, P.-Y., et al. (2011). Intestinal Epithelial Cell-Derived Integrin αβ6 Plays an Important Role in the Induction of Regulatory T Cells and Inhibits an Antigen-specific Th2 Response. *J. Leukoc. Biol.* 90 (4), 751–759. doi:10.1189/jlb.1210696

Chen, X., Zhou, Y., and Yu, J. (2019). Exosome-like Nanoparticles from Ginger Rhizomes Inhibited NLRP3 Inflammasome Activation. *Mol. Pharmaceutics* 16 (6), 2690–2699. doi:10.1021/acs.molpharmaceut.9b00246

Colombo, M., Moita, C., Van Niel, G., Kowal, J., Vigneron, J., Benaroch, P., et al. (2013). Analysis of ESCRT Functions in Exosome Biogenesis, Composition and Secretion Highlights the Heterogeneity of Extracellular Vesicles. *J. Cel Sci.* 126 (24), 5553–5565. doi:10.1242/jcs.128868

Colombo, M., Raposo, G., and Théry, C. (2014). Biogenesis, Secretion, and Intercellular Interactions of Exosomes and Other Extracellular Vesicles. *Annu. Rev. Cel Dev. Biol.* 30 (1), 255–289. doi:10.1146/annurev-cellbio-101512-122326

Console, L., Scalise, M., and Indiveri, C. (2019). Exosomes in Inflammation and Role as Biomarkers. *Clinica Chim. Acta* 488 (July 2018), 165–171. doi:10.1016/j.cca.2018.11.009

Davoudi, Z., Peroutka-Bigus, N., Bellaire, B., Wannemuehler, M., Barrett, T. A., Narasimhan, B., et al. (2018). Intestinal Organoids Containing Poly(lactic-Co-glycolic Acid) Nanoparticles for the Treatment of Inflammatory Bowel Diseases. *J. Biomed. Mater. Res.* 106 (4), 876–886. doi:10.1002/jbm.a.36305

Deng, Z., Mu, J., Tseng, M., Wattenberg, B., Zhuang, X., Egilmez, N. K., et al. (2015). Enterobacteria-secreted Particles Induce Production of Exosome-like S1P-Containing Particles by Intestinal Epithelium to Drive Th17-Mediated Tumorigenesis. *Nat. Commun.* 6 (1), 1–15. doi:10.1038/ncomms7956

Deng, Z., Rong, Y., Teng, Y., Mu, J., Zhuang, X., Tseng, M., et al. (2017). Broccoli-Derived Nanoparticle Inhibits Mouse Colitis by Activating Dendritic Cell AMP-Activated Protein Kinase. *Mol. Ther.* 25 (7), 1641–1654. doi:10.1016/j.ymthe.2017.01.025

Dickens, D., Chiduza, G. N., Wright, G. S. A., Pirmohamed, M., Antonyuk, S. V., and Hasnain, S. S. (2017). Modulation of LAT1 (SLC7A5) Transporter Activity and Stability by Membrane Cholesterol. *Sci. Rep.* 7 (1), 1–13. doi:10.1038/srep43580

Doare, K. Le., Holder, B., Bassett, A., and Pannaraj, P. S. (2018). Mother's Milk: A Purposeful Contribution to the Development of the Infant Microbiota and Immunity. *Front. Immunol.* Vol. 9, 1. doi:10.3389/fimmu.2018.00361

Domenis, R., Marino, M., Cifù, A., Scardino, G., Curcio, F., and Fabris, M. (2020). Circulating Exosomes Express α4β7 Integrin and Compete with CD4+ T Cells for the Binding to Vedolizumab. *PLOS ONE* 15 (11), e0242342. doi:10.1371/journal.pone.0242342

Edgar, J. R. (2016). Q&A: What Are Exosomes, Exactly? *BMC Biol.* 14 (1), 1–7. doi:10.1186/s12915-016-0268-z

Eichenberger, R. M., Ryan, S., Jones, L., Buitrago, G., Polster, R., Montes de Oca, M , et al. (2018). Hookworm Secreted Extracellular Vesicles Interact With Host Cells and Prevent Inducible Colitis in Mice. *Front. Immunol.* 9, 850.

Elmi, A., Nasher, F., Jagatia, H., Gundogdu, O., Bajaj-Elliott, M., Wren, B., et al. (2016). Campylobacter Jejuniouter Membrane Vesicle-Associated Proteolytic Activity Promotes Bacterial Invasion by Mediating Cleavage of Intestinal Epithelial Cell E-Cadherin and Occludin. *Cell Microbiol.* 18 (4), 561–572. doi:10.1111/cmi.12534

Escrevente, C., Keller, S., Altevogt, P., and Costa, J. (2011). Interaction and Uptake of Exosomes by Ovarian Cancer Cells. *BMC Cancer* 11 (1), 108. doi:10.1186/1471-2407-11-108

Fábrega, M. J., Aguilera, L., Giménez, R., Varela, E., Cañas, M. A., Antolín, M., et al. (2016). Activation of Immune and Defense Responses in the Intestinal Mucosa by Outer Membrane Vesicles of Commensal and Probiotic *Escherichia coli* Strains. *Front. Microbiol.* 7 (MAY). doi:10.3389/fmicb.2016.00705

Gao, H. N., Guo, H. Y., Zhang, H., Xie, X. L., Wen, P. C., and Ren, F. Z. (2019a). Yak-milk-derived Exosomes Promote Proliferation of Intestinal Epithelial Cells in an Hypoxic Environment. *J. Dairy Sci.* 102 (2), 985–996. doi:10.3168/jds.2018-14946

Gao, R., Zhang, R., Qian, T., Peng, X., He, W., Zheng, S., et al. (2019b). A Comparison of Exosomes Derived from Different Periods Breast Milk on Protecting against Intestinal Organoid Injury. *Pediatr. Surg. Int.* 35 (12), 1363–1368. doi:10.1007/s00383-019-04562-6

Gao, X.-J., Li, T., Wei, B., Yan, Z.-X., Hu, N., Huang, Y.-J., et al. (2018). Bacterial Outer Membrane Vesicles from Dextran Sulfate Sodium-Induced Colitis Differentially Regulate Intestinal UDP-Glucuronosyltransferase 1A1 Partially through Toll-like Receptor 4/Mitogen-Activated Protein Kinase/ Phosphatidylinositol 3-Kinase Pathway. *Drug Metab. Dispos* 46 (3), 292–302. doi:10.1124/dmd.117.079046

Liu, R., Tang, A., Wang, X., Chen, X., Zhao, L., Xiao, Z., et al.(2018). Inhibition of lncRNA NEAT1 Suppresses the Inflammatory Response in IBD by Modulating the intestinal Epithelial Barrier and by exosome-Mediated Polarization of Macrophages. *Int. J. Mol. Med.* 42, 2903–2913. doi:10.3892/ijmm.2018.3829

García-Manrique, P., Gutiérrez, G., and Blanco-López, M. C. (2018). Fully Artificial Exosomes: Towards New Theranostic Biomaterials. *Trends Biotechnol.* 36 (Issue 1), 10–14. doi:10.1016/j.tibtech.2017.10.005

Geveres, D., Kugathasan, S., Denson, L. A., Vazquez-Baeza, Y., Van Treuren, W., Ren, B., et al. (2014). The Treatment-Naïve Microbiome in New-Onset Crohn ' S Disease. *Cell Host Microbe* 15(3), 382–392. doi:10.1016/j.chom.2014.02.005

Gisbert, J. P., and Chaparro, M. (2020). Predictors of Primary Response to Biologic Treatment [Anti-TNF, Vedolizumab, and Ustekinumab] in Patients with Inflammatory Bowel Disease: From Basic Science to Clinical Practice. *J. Crohn's Colitis* 14 (5), 694–709. doi:10.1093/ecco-jcc/jjz195

Gonda, A., Kabagwira, J., Senthil, G. N., and Wall, N. R. (2019). Internalization of Exosomes through Receptor-Mediated Endocytosis. *Mol. Cancer Res.* 17 (Issue 2), 337–347. doi:10.1158/1541-7786.MCR-18-0891

Gregorieff, A., Pinto, D., Begthel, H., Destrée, O., Kielman, M., and Clevers, H. (2005). Expression Pattern of Wnt Signaling Components in the Adult Intestine. *Gastroenterology* 129 (2), 626–638. doi:10.1016/j.gastro.2005.06.007

Gross, J. C., Chaudhary, V., Bartscherer, K., and Boutros, M. (2012). Active Wnt Proteins Are Secreted on Exosomes. *Nat. Cel Biol* 14 (10), 1036–1045. doi:10.1038/ncb2574

Gruenberg, J., and van der Goot, F. G. (2006). Mechanisms of Pathogen Entry through the Endosomal Compartments. *Nat. Rev. Mol. Cel Biol* 7, 495–504. doi:10.1038/nrm1959

Hait, N. C., and Maiti, A. (2017).The Role of Sphingosine-1-Phosphate and Ceramide-1-Phosphate in Inflammation and Cancer. *Mediators Inflamm.*, 2017. 1–17. doi:10.1155/2017/4806541

Han, W., Xie, B., Li, Y., Shi, L., Wan, J., Chen, X., et al. (2019). Orally Deliverable Nanotherapeutics for the Synergistic Treatment of Colitis-Associated Colorectal Cancer. *Theranostics* 9 (24), 7458–7473. doi:10.7150/thno.38081

Hata, T., Murakami, K., Nakatani, H., Yamamoto, Y., Matsuda, T., and Aoki, N. (2010). Isolation of Bovine Milk-Derived Microvesicles Carrying mRNAs and microRNAs. *Biochem. Biophysical Res. Commun.* 396 (2), 528–533. doi:10.1016/j.bbrc.2010.04.135

Hickey, C. A., Kuhn, K. A., Donermeyer, D. L., Porter, N. T., Jin, C., Cameron, E. A., et al. (2015). Colitogenic Bacteroides Thetaiotaomicron Antigens Access Host Immune Cells in a Sulfatase-dependent Manner via Outer Membrane Vesicles. *Cell Host & Microbe* 17 (5), 672–680. doi:10.1016/j.chom.2015.04.002

Hock, A., Miyake, H., Li, B., Lee, C., Ermini, L., Koike, Y., et al. (2017). Breast Milk-Derived Exosomes Promote Intestinal Epithelial Cell Growth. *J. Pediatr. Surg.* 52 (5), 755–759. doi:10.1016/j.jpedsurg.2017.01.032

Hood, J. L. (2016). Post Isolation Modification of Exosomes for Nanomedicine Applications. *Nanomedicine* 11 (13), 1745–1756. doi:10.2217/nnm-2016-0102

Hood, J. L., and Wickline, S. A. (2012). A Systematic Approach to Exosome-Based Translational Nanomedicine. *WIREs Nanomed Nanobiotechnol* 4 (4), 458–467. doi:10.1002/wnan.1174

Ismail, S., Hampton, M. B., and Keenan, J. I. (2003). *Helicobacter pylori* Outer Membrane Vesicles Modulate Proliferation and Interleukin-8 Production by Gastric Epithelial Cells. *Iai* 71 (10), 5670–5675. doi:10.1128/IAI.71.10.5670-5675.2003

Jeffrey, M. P., Strap, J. L., Jones Taggart, H., and Green-Johnson, J. M. (2018). Suppression of Intestinal Epithelial Cell Chemokine Production by Lactobacillus Rhamnosus R0011 and Lactobacillus Helveticus R0389 Is Mediated by Secreted Bioactive Molecules. *Front. Immunol.* 9 (NOV), 1–13. doi:10.3389/fimmu.2018.02639

Jeppesen, D. K., Fenix, A. M., Franklin, J. L., Higginbotham, J. N., Zhang, Q., Zimmerman, L. J., et al. (2019). Reassessment of Exosome Composition. *Cell* 177 (2), 428–445. doi:10.1016/j.cell.2019.02.029

Jiang, L., Shen, Y., Guo, D., Yang, D., Liu, J., Fei, X., et al. (2016). EpCAM-dependent Extracellular Vesicles from Intestinal Epithelial Cells Maintain Intestinal Tract Immune Balance. *Nat. Commun.* 7, 1–15. doi:10.1038/ncomms13045

Johnstone, R., Bianchini, A., and Teng, K. (1989). Reticulocyte Maturation and Exosome Release: Transferrin Receptor Containing Exosomes Shows Multiple Plasma Membrane Functions. *Blood* 74 (5), 1844–1851. doi:10.1182/blood.v74.5.1844.1844

Ju, S., Mu, J., Dokland, T., Zhuang, X., Wang, Q., Jiang, H., et al. (2013). Grape Exosome-like Nanoparticles Induce Intestinal Stem Cells and Protect Mice from DSS-Induced Colitis. *Mol. Ther.* 21 (7), 1345–1357. doi:10.1038/mt.2013.64

Kahn, S., Liao, Y., Du, X., Xu, W., Li, J., and Lönnerdal, B. (2018). Exosomal MicroRNAs in Milk from Mothers Delivering Preterm Infants Survive *In Vitro* Digestion and Are Taken up by Human Intestinal Cells. *Mol. Nutr. Food Res.* 62 (11), 1701050. doi:10.1002/mnfr.201701050

Kang, C.-S., Ban, M., Choi, E.-J., Moon, H.-G., Jeon, J.-S., Kim, D.-K., et al. (2013). Extracellular Vesicles Derived from Gut Microbiota, Especially Akkermansia Muciniphila, Protect the Progression of Dextran Sulfate Sodium-Induced Colitis. *PLoS ONE* 8 (10), e76520. doi:10.1371/journal.pone.0076520

Karlsson, M., Lundin, S., Dahlgren, U., Kahu, H., Pettersson, I., and Telemo, E. (2001). "Tolerosomes" Are Produced by Intestinal Epithelial Cells. *Eur. J. Immunol.* 31 (10), 2892–2900. doi:10.1002/1521-4141(2001010)31:10<2892::AID-IMMU2892>3.0.CO;2-I

Keerthikumar, S., Chisanga, D., Ariyaratne, D., Al Saffar, H., Anand, S., Zhao, K., et al. (2016). ExoCarta: A Web-Based Compendium of Exosomal Cargo. *J. Mol. Biol.* 428 (4), 688–692. doi:10.1016/j.jmb.2015.09.019

Kim, S. H., Bianco, N. R., Shufesky, W. J., Morelli, A. E., and Robbins, P. D. (2007). Effective Treatment of Inflammatory Disease Models with Exosomes Derived from Dendritic Cells Genetically Modified to Express IL-4. *J. Immunol.* 179 (4), 2242–2249. doi:10.4049/jimmunol.179.4.2242

Koeppen, K., Hampton, T. H., Jarek, M., Scharfe, M., Gerber, S. A., Mielcarz, D. W., et al. (2016). A Novel Mechanism of Host-Pathogen Interaction through sRNA in Bacterial Outer Membrane Vesicles. *Plos Pathog.* 12 (6), e1005672. doi:10.1371/journal.ppat.1005672

Kojima, M., Costantini, T. W., Eliceiri, B. P., Chan, T. W., Baird, A., and Coimbra, R. (2018). Gut Epithelial Cell-Derived Exosomes Trigger Posttrauma Immune Dysfunction. *J. Trauma Acute Care Surg.* 84 (2), 257–264. doi:10.1097/TA.0000000000001748

Koumangoye, R. B., Sakwe, A. M., Goodwin, J. S., Patel, T., and Ochieng, J. (2011). Detachment of Breast Tumor Cells Induces Rapid Secretion of Exosomes Which Subsequently Mediate Cellular Adhesion and Spreading. *PLoS ONE* 6 (9), e24234. doi:10.1371/journal.pone.0024234

Kuhnert, F., Davis, C. R., Wang, H.-T., Chu, P., Lee, M., Yuan, J., et al. (2004). Essential Requirement for Wnt Signaling in Proliferation of Adult Small Intestine and colon Revealed by Adenoviral Expression of Dickkopf-1. *Proc. Natl. Acad. Sci.* 101 (1), 266–271. doi:10.1073/pnas.2536800100

Kumar, J., and Newton, A. M. J. (2017). Rifaximin - Chitosan Nanoparticles for Inflammatory Bowel Disease (IBD). *Iad* 11 (1). doi:10.2174/1872213x10666161230111226

Kunkel, G. T., MacEyka, M., Milstien, S., and Spiegel, S. (2013). Targeting the Sphingosine-1-Phosphate axis in Cancer, Inflammation and beyond. *Nat. Rev. Drug Discov.* 12 (Issue 9), 688–702. doi:10.1038/nrd4099

Leoni, G., Alam, A., Neumann, P.-A., Lambeth, J. D., Cheng, G., McCoy, J., et al. (2013). Annexin A1, Formyl Peptide Receptor, and NOX1 Orchestrate Epithelial Repair. *J. Clin. Invest.* 123 (1), 443–454. doi:10.1172/JCI65831

Leoni, G., Neumann, P.-A., Kamaly, N., Quiros, M., Nishio, H., Jones, H. R., et al. (2015). Annexin A1-Containing Extracellular Vesicles and Polymeric Nanoparticles Promote Epithelial Wound Repair. *J. Clin. Invest.* 125 (3), 1215–1227. doi:10.1172/JCI76693

Li, B., Hock, A., Wu, R. Y., Minich, A., Botts, S. R., Lee, C., et al. (2019). Bovine Milk-Derived Exosomes Enhance Goblet Cell Activity and Prevent the Development of Experimental Necrotizing Enterocolitis. *PLoS ONE* 14 (1), e0211431–12. doi:10.1371/journal.pone.0211431

Liao, Y., Du, X., Li, J., and Lönnerdal, B. (2017). Human Milk Exosomes and Their microRNAs Survive Digestion *In Vitro* and Are Taken up by Human Intestinal Cells. *Mol. Nutr. Food Res.* 61 (11), 1700082. doi:10.1002/mnfr.201700082

Lin, X. P., Almqvist, N., and Telemo, E. (2005). Human Small Intestinal Epithelial Cells Constitutively Express the Key Elements for Antigen Processing and the Production of Exosomes. *Blood Cell Mol. Dis.* 35 (2), 122–128. doi:10.1016/j.bcmd.2005.05.011

Lindenbergh, M. F. S., and Stoorvogel, W. (2018). Antigen Presentation by Extracellular Vesicles from Professional Antigen-Presenting Cells. *Annu. Rev. Immunol.* 36, 435–459. doi:10.1146/annurev-immunol-041015-055700

Liu, H., Liang, Z., Wang, F., et al. (2019). Exosomes From Mesenchymal Stromal Cells Reduce Murine Colonic Inflammation Via A Macrophage-Dependent Mechanism. *JCI Insight* 4(24), e131273. doi:10.1172/jci.insight.131273

Liu, R., Tang, A., Wang, X., Chen, X., Zhao, L., Xiao, Z., and Shen, S. (2018). Inhibition of lncRNA NEAT1 suppresses the inflammatory response in IBD by modulating the intestinal epithelial barrier and by exosome-mediated polarization of macrophages. *International Journal of Molecular Medicine.* 42, 2903–2913. doi:10.3892/ijmm.2018.3829

Lucas, A., and Cole, T. J. (1990). Breast Milk and Neonatal Necrotising Enterocolitis. *The Lancet* 336 (8730–8731), 1519–1523. doi:10.1016/0140-6736(90)93304-8

Maas, S. L. N., Breakefield, X. O., and Weaver, A. M. (2017). Extracellular Vesicles: Unique Intercellular Delivery Vehicles. *Trends Cel Biol.* 27 (3), 172–188. doi:10.1016/j.tcb.2016.11.003

Mallegol, J., Van Niel, G., Lebreton, C., Lepelletier, Y., Candalh, C., Dugave, C., et al. (2007). T84-Intestinal Epithelial Exosomes Bear MHC Class II/Peptide Complexes Potentiating Antigen Presentation by Dendritic Cells. *Gastroenterology* 132 (5), 1866–1876. doi:10.1053/j.gastro.2007.02.043

Manca, S., Upadhyaya, B., Mutai, E., Desaulniers, A. T., Cederberg, R. A., White, B. R., et al. (2018). Milk Exosomes Are Bioavailable and Distinct microRNA Cargos Have Unique Tissue Distribution Patterns. *Sci. Rep.* 8 (1), 1–11. doi:10.1038/s41598-018-29780-1

Marafini, I., Sedda, S., Dinallo, V., and Monteleone, G. (2019). Inflammatory Cytokines: from Discoveries to Therapies in IBD. *Expert Opin. Biol. Ther.* 19 (Issue 11), 1207–1217. doi:10.1080/14712598.2019.1652267

Martin, C., Patel, M., Williams, S., Arora, H., and Sims, B. (2018). Human Breast Milk-Derived Exosomes Attenuate Cell Death in Intestinal Epithelial Cells. *Innate Immun.* 24 (5), 278–284. doi:10.1177/1753425918785715

Mathivanan, S., Ji, H., and Simpson, R. J. (2010). Exosomes: Extracellular Organelles Important in Intercellular Communication. *J. Proteomics* 73 (10), 1907–1920. doi:10.1016/j.jprot.2010.06.006

Mitsuhashi, S., Feldbrügge, L., Csizmadia, E., Mitsuhashi, M., Robson, S. C., Moss, A. C., et al. (2016). Luminal Extracellular Vesicles (EVs) in Inflammatory Bowel Disease (IBD) Exhibit Proinflammatory Effects on Epithelial Cells and Macrophages. *Inflamm. Bowel Dis.* 22 (7), 1587–1595. doi:10.1097/MIB.0000000000000840

Miyake, H., Lee, C., Chusilp, S., Bhalla, M., Li, B., Pitino, M., et al. (2020). Human Breast Milk Exosomes Attenuate Intestinal Damage. *Pediatr. Surg. Int.* 36 (2), 155–163. doi:10.1007/s00383-019-04599-7

Möbius, W., van Donselaar, E., Ohno-Iwashita, Y., Shimada, Y., Heijnen, H. F. G., Slot, J. W., et al. (2003). Recycling Compartments and the Internal Vesicles of Multivesicular Bodies Harbor Most of the Cholesterol Found in the Endocytic Pathway. *Traffic* 4 (4), 222–231. doi:10.1034/j.1600-0854.2003.00072.x

Mondal, A., Tapader, R., Chatterjee, N. S., Ghosh, A., Sinha, R., Koley, H., et al. (2016). Cytotoxic and Inflammatory Responses Induced by Outer Membrane Vesicle-Associated Biologically Active Proteases from *Vibrio cholerae*. *Infect. Immun.* 84 (5), 1478–1490. doi:10.1128/IAI.01365-15

Morelli, A. E., Larregina, A. T., Shufesky, W. J., Sullivan, M. L. G., Stolz, D. B., Papworth, G. D., et al. (2004). Endocytosis, Intracellular Sorting, and Processing of Exosomes by Dendritic Cells. *Blood* 104 (10), 3257–3266. doi:10.1182/blood-2004-03-0824

Mulcahy, L. A., Pink, R. C., and Carter, D. R. F. (2014). Routes and Mechanisms of Extracellular Vesicle Uptake. *J. Extracellular Vesicles* 3 (1), 24641. doi:10.3402/jev.v3.24641

Munich, S., Sobo-Vujanovic, A., Buchser, W. J., Beer-Stolz, D., and Vujanovic, N. L. (2012). Dendritic Cell Exosomes Directly Kill Tumor Cells and Activate Natural Killer Cells via TNF Superfamily Ligands. *OncoImmunology* 1 (7), 1074–1083. doi:10.4161/onci.20897

Neurath, M. F. (2019). Targeting Immune Cell Circuits and Trafficking in Inflammatory Bowel Disease. *Nat. Immunol.* 20 (8), 970–979. doi:10.1038/s41590-019-0415-0

Ng, S. C., Shi, H. Y., Hamidi, N., Underwood, F. E., Tang, W., Benchimol, E. I., et al. (2017). Worldwide Incidence and Prevalence of Inflammatory Bowel Disease in the 21st century: a Systematic Review of Population-Based Studies. *The Lancet* 390 (10114), 2769–2778. doi:10.1016/S0140-6736(17)32448-0

Ocansey, D. K. W., Wang, L., Wang, J., Yan, Y., Qian, H., Zhang, X., et al. (2019). Mesenchymal Stem Cell-Gut Microbiota Interaction in the Repair of Inflammatory Bowel Disease: an Enhanced Therapeutic Effect. *Clin. Translational Med.* 8 (1). doi:10.1186/s40169-019-0251-8

Ocansey, D. K. W., Zhang, L., Wang, Y., Yan, Y., Qian, H., Zhang, X., et al. (2020). Exosome-mediated Effects and Applications in Inflammatory Bowel Disease. *Biol. Rev.* 95 (5), 1287–1307. doi:10.1111/brv.12608

Palmulli, R., and Van Niel, G. (2018). To Be or Not to be... Secreted as Exosomes, a Balance Finely Tuned by the Mechanisms of Biogenesis. *Essays Biochem.* 62 (2), 177–191. doi:10.1042/EBC20170076

Pan, B.-T., and Johnstone, R. M. (1983). Fate of the Transferrin Receptor during Maturation of Sheep Reticulocytes *In Vitro*: Selective Externalization of the Receptor. *Cell* 33 (3), 967–978. doi:10.1016/0092-8674(83)90040-5

Pant, S., Hilton, H., and Burczynski, M. E. (2012). The Multifaceted Exosome: Biogenesis, Role in normal and Aberrant Cellular Function, and Frontiers for Pharmacological and Biomarker Opportunities. *Biochem. Pharmacol.* 83 (11), 1484–1494. doi:10.1016/j.bcp.2011.12.037

Patmanathan, S. N., Wang, W., Yap, L. F., Herr, D. R., and Paterson, I. C. (2017). Mechanisms of Sphingosine 1-phosphate Receptor Signalling in Cancer. *Cell Signal.* 34, 66–75. doi:10.1016/j.cellsig.2017.03.002

Patten, D. A., Hussein, E., Davies, S. P., Humphreys, P. N., and Collett, A. (2017). Commensal-derived OMVs Elicit a Mild Proinflammatory Response in Intestinal Epithelial Cells. *Microbiology (United Kingdom)* 163 (5), 702–711. doi:10.1099/mic.0.000468

Perretti, M., and D'Acquisto, F. (2009). Annexin A1 and Glucocorticoids as Effectors of the Resolution of Inflammation62–70). *Nat. Rev. ImmunologyNat Rev Immunol* 9 (Issue 1), 62–70. doi:10.1038/nri2470

Peterson, L. W., and Artis, D. (2014). Intestinal Epithelial Cells: Regulators of Barrier Function and Immune Homeostasis. *Nat. Rev. Immunol.* 14 (Issue 3), 141–153. doi:10.1038/nri3608

Pieters, B. C. H., Arntz, O. J., Broeren, M. G. A., van Caam, A. P. M., Koenders, M. I., et al. (2015). Commercial Cow Milk Contains Physically Stable Extracellular Vesicles Expressing Immunoregulatory TGF-β. *PLoS ONE* 10 (3), e0121123. doi:10.1371/journal.pone.0121123

Reif, S., Elbaum Shiff, Y., and Golan-Gerstl, R. (2019). Milk-derived Exosomes (MDEs) Have a Different Biological Effect on normal Fetal colon Epithelial Cells Compared to colon Tumor Cells in a miRNA-dependent Manner. *J. Transl Med.* 17 (1), 1–10. doi:10.1186/s12967-019-2072-3

Reinhardt, T. A., Lippolis, J. D., Nonnecke, B. J., and Sacco, R. E. (2012). Bovine Milk Exosome Proteome. *J. Proteomics* 75 (5), 1486–1492. doi:10.1016/j.jprot.2011.11.017

Reinhardt, T. A., Sacco, R. E., Nonnecke, B. J., and Lippolis, J. D. (2013). Bovine Milk Proteome: Quantitative Changes in normal Milk Exosomes, Milk Fat Globule Membranes and Whey Proteomes Resulting from *Staphylococcus aureus* Mastitis. *J. Proteomics* 82, 141–154. doi:10.1016/j.jprot.2013.02.013

Saha, S., Aranda, E., Hayakawa, Y., Bhanja, P., Atay, S., Brodin, N. P., et al. (2016). Macrophage-derived Extracellular Vesicle-Packaged WNTs rescue Intestinal Stem Cells and Enhance Survival after Radiation Injury. *Nat. Commun.* 7. doi:10.1038/ncomms13096

Samanta, S., Rajasingh, S., Drosos, N., Zhou, Z., Dawn, B., and Rajasingh, J. (2018). Exosomes: New Molecular Targets of Diseases. *Acta Pharmacol. Sin* 39 (4), 501–513. doi:10.1038/aps.2017.162

Sartor, R. B. (2008). Microbial Influences in Inflammatory Bowel Diseases. *Gastroenterology* 134 (2), 577–594. doi:10.1053/j.gastro.2007.11.059

Sato-Kuwabara, Y., Melo, S. A., Soares, F. A., and Calin, G. A. (2015). The Fusion of Two Worlds: Non-coding RNAs and Extracellular Vesicles - Diagnostic and Therapeutic Implications (Review). *Int. J. Oncol.* 46 (1), 17–27. doi:10.3892/ijo.2014.2712

Schanler, R. J., Burns, P. A., Abrams, S. A., and Garza, C. (1992). Bone Mineralization Outcomes in Human Milk-Fed Preterm Infants. *Pediatr. Res.* 31 (6), 583–586. doi:10.1203/00006450-199206000-00009

Shandilya, S., Rani, P., Onteru, S. K., and Singh, D. (2017). Small Interfering RNA in Milk Exosomes Is Resistant to Digestion and Crosses the Intestinal Barrier *In Vitro*. *J. Agric. Food Chem.* 65 (43), 9506–9513. doi:10.1021/acs.jafc.7b03123

Shen, Y., Torchia, M. L. G., Lawson, G. W., Karp, C. L., Ashwell, J. D., and Mazmanian, S. K. (2012). Outer Membrane Vesicles of a Human Commensal Mediate Immune Regulation and Disease protection. *Cell Host & Microbe* 12 (4), 509–520. doi:10.1016/j.chom.2012.08.004

Simons, M., and Raposo, G. (2009). Exosomes - Vesicular Carriers for Intercellular Communication. *Curr. Opin. Cel Biol.* 21 (4), 575–581. doi:10.1016/j.ceb.2009.03.007

Slater, T. W., Finkielsztein, A., Mascarenhas, L. A., Mehl, L. C., Butin-Israeli, V., and Sumagin, R. (2017). Neutrophil Microparticles Deliver Active Myeloperoxidase to Injured Mucosa to Inhibit Epithelial Wound Healing. *J.I.* 198 (7), 2886–2897. doi:10.4049/jimmunol.1601810

Sommer, F., Anderson, J. M., Bharti, R., Raes, J., and Rosenstiel, P. (2017). The Resilience of the Intestinal Microbiota Influences Health and Disease. *Nat. Rev. Microbiol.* 15 (Issue 10), 630–638. doi:10.1038/nrmicro.2017.58

Stentz, R., Osborne, S., Horn, N., Li, A. W. H., Hautefort, I., Bongaerts, R., et al. (2014). A Bacterial Homolog of a Eukaryotic Inositol Phosphate Signaling Enzyme Mediates Cross-Kingdom Dialog in the Mammalian Gut. *Cel Rep.* 6 (4), 646–656. doi:10.1016/j.celrep.2014.01.021

Stoorvogel, W., Kleijmeer, M. J., Geuze, H. J., and Raposo, G. (2002). The Biogenesis and Functions of Exosomes. *Traffic* 3 (5), 321–330. doi:10.1034/j.1600-0854.2002.30502.x

Stuffers, S., Sem Wegner, C., Stenmark, H., and Brech, A. (2009). Multivesicular Endosome Biogenesis in the Absence of ESCRTs. *Traffic* 10 (7), 925–937. doi:10.1111/j.1600-0854.2009.00920.x

Subra, C., Grand, D., Laulagnier, K., Stella, A., Lambeau, G., Paillasse, M., et al. (2010). Exosomes Account for Vesicle-Mediated Transcellular Transport of Activatable Phospholipases and Prostaglandins. *J. Lipid Res.* 51 (8), 2105–2120. doi:10.1194/jlr.M003657

Tamai, K., Tanaka, N., Nakano, T., Kakazu, E., Kondo, Y., Inoue, J., et al. (2010). Exosome Secretion of Dendritic Cells Is Regulated by Hrs, an ESCRT-0 Protein. *Biochem. Biophysical Res. Commun.* 399 (3), 384–390. doi:10.1016/j.bbrc.2010.07.083

Taylor, C. T., and Colgan, S. P. (2007). Hypoxia and Gastrointestinal Disease. *J. Mol. Med.* 85 (12), 1295–1300. doi:10.1007/s00109-007-0277-z

Teng, Y., Ren, Y., Sayed, M., Hu, X., Lei, C., Kumar, A., et al. (2018). Plant-Derived Exosomal MicroRNAs Shape the Gut Microbiota. *Cell Host Microbe* 24 (5), 637–652.e8. doi:10.1016/j.chom.2018.10.001

Théry, C., Ostrowski, M., and Segura, E. (2009). Membrane Vesicles as Conveyors of Immune Responses. *Nat. Rev. Immunol.* 9 (8), 581–593. doi:10.1038/nri2567

Théry, C., Witwer, K. W., Aikawa, E., Alcaraz, M. J., Anderson, J. D., Andriantsitohaina, R., et al. (2018). Minimal Information for Studies of Extracellular Vesicles 2018 (MISEV2018): a Position Statement of the International Society for Extracellular Vesicles and Update of the MISEV2014 Guidelines. *J. Extracellular Vesicles* 7 (1). doi:10.1080/20013078.2018.1535750

Tian, T., Zhu, Y.-L., Hu, F.-H., Wang, Y.-Y., Huang, N.-P., and Xiao, Z.-D. (2013). Dynamics of Exosome Internalization and Trafficking. *J. Cel. Physiol.* 228 (7), 1487–1495. doi:10.1002/jcp.24304

Tkach, M., Kowal, J., Zucchetti, A. E., Enserink, L., Jouve, M., Lankar, D., et al. (2017). Qualitative Differences in T-cell Activation by Dendritic Cell-derived Extracellular Vesicle Subtypes. *Embo J.* 36 (20), 3012–3028. doi:10.15252/embj.201696003

Tomé-Carneiro, J., Fernández-Alonso, N., Tomás-Zapico, C., Visioli, F., Iglesias-Gutierrez, E., and Dávalos, A. (2018). Breast Milk microRNAs Harsh Journey towards Potential Effects in Infant Development and Maturation. Lipid Encapsulation Can Help. *Pharmacol. Res.* 132, 21–32. doi:10.1016/j.phrs.2018.04.003

Torres, J., Mehandru, S., Colombel, J.-F., and Peyrin-Biroulet, L. (2017). Crohn's Disease. *The Lancet* 389 (10080), 1741–1755. doi:10.1016/S0140-6736(16)31711-1

Turfkruyer, M., and Verhasselt, V. (2015). Breast Milk and its Impact on Maturation of the Neonatal Immune System. *Curr. Opin. Infect. Dis.* 28 (Issue 3), 199–206. doi:10.1097/QCO.0000000000000165

Valadi, H., Ekström, K., Bossios, A., Sjöstrand, M., Lee, J. J., and Lötvall, J. O. (2007). Exosome-mediated Transfer of mRNAs and microRNAs Is a Novel Mechanism of Genetic Exchange between Cells. *Nat. Cel Biol* 9 (6), 654–659. doi:10.1038/ncb1596

van Bergenhenegouwen, J., Kraneveld, A. D., Rutten, L., Kettelarij, N., Garssen, J., and Vos, A. P. (2014). Extracellular Vesicles Modulate Host-Microbe Responses by Altering TLR2 Activity and Phagocytosis. *PLoS ONE* 9 (2), e89121. doi:10.1371/journal.pone.0089121

Van Niel, G., Mallegol, J., Bevilacqua, C., Candalh, C., Brugière, S., Tomaskovic-Crook, E., et al. (2003). Intestinal Epithelial Exosomes Carry MHC Class II/peptides Able to Inform the Immune System in Mice. *Gut* 52 (12), 1690–1697. doi:10.1136/gut.52.12.1690

Van Niel, G., Raposo, G., Candalh, C., Boussac, M., Hershberg, R., Cerf–Bensussan, N., et al. (2001). Intestinal Epithelial Cells Secrete Exosome-like Vesicles. *Gastroenterology* 121 (2), 337–349. doi:10.1053/gast.2001.26263

Walker, W. A., and Iyengar, R. S. (2015). Breast Milk, Microbiota, and Intestinal Immune Homeostasis. *Pediatr. Res.* 77, 220–228. doi:10.1038/pr.2014.160

Wang, L., Yu, Z., Wan, S., Wu, F., Chen, W., Zhang, B., et al. (2017). Exosomes Derived from Dendritic Cells Treated with Schistosoma Japonicum Soluble Egg Antigen Attenuate DSS-Induced Colitis. *Front. Pharmacol.* 8 (SEP), 651. doi:10.3389/fphar.2017.00651

Wang, Y., Tian, J., Tang, X., Rui, K., Tian, X., Ma, J., et al. (2016). Exosomes Released by Granulocytic Myeloid-Derived Suppressor Cells Attenuate DSS-Induced Colitis in Mice. *Oncotarget* 7 (13), 15356–15368. doi:10.18632/oncotarget.7324

Wolf, P. (1967). The Nature and Significance of Platelet Products in Human Plasma. *Br. J. Haematol.* 13 (3), 269–288. doi:10.1111/j.1365-2141.1967.tb08741.x

Wolf, T., Baier, S. R., and Zempleni, J. (2015). The Intestinal Transport of Bovine Milk Exosomes Is Mediated by Endocytosis in Human Colon Carcinoma Caco-2 Cells and Rat Small Intestinal IEC-6 Cells. *J. Nutr.* 145 (10), 2201–2206. doi:10.3945/jn.115.218586

Wong, W.-Y., Lee, M. M.-L., Chan, B. D., Kam, R. K.-T., Zhang, G., Lu, A.-P., et al. (2016). Proteomic Profiling of Dextran Sulfate Sodium Induced Acute Ulcerative Colitis Mice Serum Exosomes and Their Immunomodulatory Impact on Macrophages. *Proteomics* 16 (7), 1131–1145. doi:10.1002/pmic.201500174

Xiao, B., Laroui, H., Ayyadurai, S., Viennois, E., Charania, M. A., Zhang, Y., et al. (2013). Mannosylated Bioreducible Nanoparticle-Mediated Macrophage-specific TNF-α RNA Interference for IBD Therapy. *Biomaterials* 34 (30), 7471–7482. doi:10.1016/j.biomaterials.2013.06.008

Xie, M.-Y., Chen, T., Xi, Q.-Y., Hou, L.-J., Luo, J.-Y., Zeng, B., et al. (2020). Porcine Milk Exosome miRNAs Protect Intestinal Epithelial Cells against Deoxynivalenol-Induced Damage. *Biochem. Pharmacol.* 175 (November 2019), 113898. doi:10.1016/j.bcp.2020.113898

Xie, M.-Y., Hou, L.-J., Sun, J.-J., Zeng, B., Xi, Q.-Y., Luo, J.-Y., et al. (2019). Porcine Milk Exosome MiRNAs Attenuate LPS-Induced Apoptosis through Inhibiting TLR4/NF-κB and P53 Pathways in Intestinal Epithelial Cells. *J. Agric. Food Chem.* 67 (34), 9477–9491. doi:10.1021/acs.jafc.9b02925

Yang, X., Meng, S., Jiang, H., Chen, T., and Wu, W. (2010). Exosomes Derived from Interleukin-10-Treated Dendritic Cells Can Inhibit Trinitrobenzene Sulfonic Acid-Induced Rat Colitis. *Scand. J. Gastroenterol.* 45 (10), 1168–1177. doi:10.3109/00365521.2010.490596

Yu, S., Zhao, Z., Sun, L., and Li, P. (2017). Fermentation Results in Quantitative Changes in Milk-Derived Exosomes and Different Effects on Cell Growth and Survival. *J. Agric. Food Chem.* 65 (6), 1220–1228. doi:10.1021/acs.jafc.6b05002

Zamrik, S., Giachero, F., Heldmann, M., Hensel, K. O., Wirth, S., and Jenke, A. C. (2018). Impact of an In-House Pediatric Surgery Unit and Human Milk Centered Enteral Nutrition on Necrotizing Enterocolitis. *Biomed. Res. Int.* 2018, 1–6. doi:10.1155/2018/5042707

Zhang, H., Wang, L., Li, C., Yu, Y., Yi, Y., Wang, J., et al. (2019). Exosome-induced Regulation in Inflammatory Bowel Disease. *Front. Immunol.* 10 (JUN), 1–9. doi:10.3389/fimmu.2019.01464

Zhang, J., Li, S., Li, L., Li, M., Guo, C., Yao, J., et al. (2015). Exosome and Exosomal microRNA: Trafficking, Sorting, and Function. *Genomics, Proteomics & Bioinformatics* 13 (1), 17–24. doi:10.1016/j.gpb.2015.02.001

Zhang, X., Deeke, S. A., Ning, Z., Starr, A. E., Butcher, J., Li, J., et al. (2018). Metaproteomics Reveals Associations between Microbiome and Intestinal Extracellular Vesicle Proteins in Pediatric Inflammatory Bowel Disease. *Nat. Commun.* 9 (1), 1–14. doi:10.1038/s41467-018-05357-4

Zheng, X., Chen, F., Zhang, Q., Liu, Y., You, P., Sun, S., et al. (2017). Salivary Exosomal PSMA7: a Promising Biomarker of Inflammatory Bowel Disease. *Protein Cell* 8 (9), 686–695. doi:10.1007/s13238-017-0413-7

Zhou, F., Paz, H. A., Sadri, M., Cui, J., Kachman, S. D., Fernando, S. C., et al. (2019). Dietary Bovine Milk Exosomes Elicit Changes in Bacterial Communities in C57BL/6 Mice. *Am. J. Physiology-Gastrointestinal Liver PhysiologyGastrointestinal Liver Physiol.* 317 (5), G618–G624. doi:10.1152/ajpgi.00160.2019

Conflict of Interest: Author ACM has received grant support from Pfizer inc.

The remaining authors declare that the research was conducted in the absence of any commercial or financial relationships that could be construed as a potential conflict of interest.

Copyright © 2021 Ayyar and Moss. This is an open-access article distributed under the terms of the Creative Commons Attribution License (CC BY). The use, distribution or reproduction in other forums is permitted, provided the original author(s) and the copyright owner(s) are credited and that the original publication in this journal is cited, in accordance with accepted academic practice. No use, distribution or reproduction is permitted which does not comply with these terms.

frontiers in Pharmacology

ORIGINAL RESEARCH
published: 10 June 2021
doi: 10.3389/fphar.2021.655887

Noncanonical NF-κB Signaling Upregulation in Inflammatory Bowel Disease Patients is Associated With Loss of Response to Anti-TNF Agents

Vu Q. Nguyen[1†], Kristin Eden[2,3†], Holly A. Morrison[2†], Megan B. Sammons[2], Kristin K. Knight[1], Siena Sorrentino[2], Rebecca M. Brock[4], Douglas J. Grider[5], Irving C. Allen[2,3,4‡] and Dario Sorrentino[1,6‡]*

[1]IBD Center, Division of Gastroenterology, Virginia Tech Carilion School of Medicine, Roanoke, VA, United States, [2]Department of Biomedical Sciences and Pathobiology, Virginia-Maryland College of Veterinary Medicine, Virginia Tech, Blacksburg, VA, United States, [3]Department of Basic Science Education, Virginia Tech Carilion School of Medicine, Roanoke, VA, United States, [4]Graduate Program in Translational Biology, Medicine, and Health, Virginia Tech, Blacksburg, VA, United States, [5]Department of Pathology, Virginia Tech Carilion School of Medicine, Roanoke, VA, United States, [6]Department of Clinical and Experimental Medical Sciences, University of Udine School of Medicine, Udine, Italy

OPEN ACCESS

Edited by:
Stefano Fiorucci,
University of Perugia, Italy

Reviewed by:
Sambit Nanda,
University of Dundee, United Kingdom
Luisa Guidi,
Catholic University of the Sacred Heart, Italy

***Correspondence:**
Dario Sorrentino
drsorrentino@carilionclinic.org

[†]These authors have contributed equally to this work
[‡]These authors share senior authorship

Specialty section:
This article was submitted to Gastrointestinal and Hepatic Pharmacology, a section of the journal Frontiers in Pharmacology

Received: 19 January 2021
Accepted: 20 May 2021
Published: 10 June 2021

Citation:
Nguyen VQ, Eden K, Morrison HA, Sammons MB, Knight KK, Sorrentino S, Brock RM, Grider DJ, Allen IC and Sorrentino D (2021) Noncanonical NF-κB Signaling Upregulation in Inflammatory Bowel Disease Patients is Associated With Loss of Response to Anti-TNF Agents. Front. Pharmacol. 12:655887. doi: 10.3389/fphar.2021.655887

Objectives: Targeting tumor necrosis factor (TNF) with biologic agents, such as infliximab and adalimumab, is a widely used and effective therapeutic strategy in inflammatory bowel disease (IBD). Unfortunately, a significant number of patients fail to respond or lose response over time to these agents. Previous studies have defined multiple complex roles for canonical NF-κB signaling in the pathogenesis of IBD. However, preliminary evidence suggests that the lesser defined noncanonical NF-κB signaling pathway also contributes to disease pathogenesis and response to anti-TNF agents. The objective of this study was to evaluate this hypothesis in Crohn's disease (CD) and ulcerative colitis (UC) patients.

Design: A total of 27 subjects with IBD (19 with CD and 8 with UC) and 15 control subjects were tested. Clinical criteria, patient history, and endoscopic disease activity were factors used to categorize patients and define therapeutic response. Biopsy specimens were collected during colonoscopy and expression was determined for 88 target genes known to be associated with noncanonical NF-κB signaling and IBD.

Results: Noncanonical NF-κB signaling was significantly upregulated in IBD patients and was associated with increased gastrointestinal inflammation, epithelial cell death, lymphocyte migration, and Nod-like receptor signaling. Furthermore, noncanonical NF-κB signaling was further upregulated in patients unresponsive to anti-TNF agents and was suppressed in responsive patients. *MAP3K14, NFKB2, CCL19, CXCL12*, and *CXCL13* were significantly dysregulated, as were genes that encode pathway regulators, such as *CYLD, NLRP12,* and *BIRC2/3*.

Conclusion: Our study identifies a previously uncharacterized role for the understudied noncanonical NF-κB signaling pathway in the pathogenesis of IBD and anti-TNF therapy

responsiveness. The genes and pathways identified may ultimately prove useful in IBD management and could potentially be used as biomarkers of drug response.

Keywords: noncanonical NF-κB pathway, anti-TNF agents, inflammatory bowel disease, Crohn's disease, ulcerative colitis, alternative pathway, NIK, therapeutic response

INTRODUCTION

Inflammatory bowel diseases (IBD)–Crohn's disease (CD) and ulcerative colitis (UC)-are characterized by chronic inflammation of the gastrointestinal tract, driven by elements of both the innate and adaptive immune systems in genetically susceptible individuals. Together these diseases afflict approximately over 6 million people worldwide, which makes them a significant global health and economic burden (Ng et al., 2018). The nuclear factor kappa B (NF-κB) family of transcription factors are master regulators of inflammation and drive a diverse spectrum of biological processes (Rothschild et al., 2018). This signaling cascade is commonly found dysregulated in IBD patients, leading to dysfunctional cytokine and chemokine production in the gastrointestinal tract. NF-κB signaling occurs through two distinct pathways, defined as the canonical pathway and the noncanonical (or alternative) pathway.

In the context of IBD, the overwhelming majority of studies have focused on the canonical NF-κB signaling cascade. This cascade relies on the proteins RelA (p65) and p50 which form the heterodimer RelA/p50. Upon activation of this pathway, this heterodimer translocates into the nucleus, where it functions as a transcription factor. In this pathway, signaling is rapid and constitutive. Activation of the cascade results in the transcription of a wide range of well characterized inflammatory mediators such as IL-1β, TNF, and IL-6 (McDaniel et al., 2016). TNF in particular plays a central role in the pathogenesis of IBD (Billmeier et al., 2016) as shown by the clinical efficacy of anti-TNF medications such as infliximab (IFX) or adalimumab (ADA)-mainstay therapies for both CD and UC. These therapies have been shown to reduce the risk of hospitalization, surgery, and improve quality of life (Mao et al., 2017). In addition, they have been shown to prevent CD relapse after surgery (Sorrentino 2013). However, up to 40% of IBD patients do not respond to initial treatment with anti-TNF agents [primary nonresponse (PNR)], and a similar proportion of patients lose response over time [secondary loss of response (SLR)] after initially achieving clinical remission (Danese et al., 2011; Ben-Horin et al., 2014). The mechanism of PNR and SLR to anti-TNF agents is not completely understood and likely to be multifactorial. Several explanations have been suggested, including the immune system switch to an alternative inflammatory pathway, immunogenicity with production of drug neutralizing antibodies and medical unresposiveness due to advanced disease (Sorrentino 2008; Yarur et al., 2014; Biancheri et al., 2015; Brandse et al., 2016). While one mechanism does not exclude others and they might all play a role in different circumstances, the possibility of alternative pathways driving inflammation in IBD may provide insight into why medications targeting molecules different from TNF might be effective in SLR and PNR.

Unlike the canonical pathway, there is minimal data on the role of this signaling cascade in IBD. Noncanonical NF-κB signaling is highly regulated at the post-transcriptional and post-translational level, resulting in a slower, more controlled, and chronic signaling response. The noncanonical pathway relies on a heterodimer different from that of the canonical pathway and is comprised of RelB and 100, which is later cleaved into its active form of RelB and p52 (Sun 2011). In the noncanonical signaling cascade, NF-κB initiates the transcription of a limited repertoire of target genes, including those coding for the chemokines CXCL12, CXCL13, CCL19, and CCL21 (**Supplementary Figure S1**). Prior research from our group using a pre-clinical mouse model found that mice lacking negative regulators of noncanonical NF-κB signaling - such as the Nod-like receptor NLRP12-demonstrated increased noncanonical pathway activation and susceptibility to models of IBD and inflammation-driven colon tumorigenesis (Allen et al., 2012). These findings suggest a role of noncanonical NF-κB signaling in IBD pathogenesis. In this study, we examine the hypothesis that this pathway may be involved in anti-TNF agents response in IBD patients.

MATERIALS AND METHODS

Protection of Human Subjects

All studies were conducted following the regulations, policies, and guidelines set forth by the National Institutes of Health for research involving human subjects. All studies were conducted under the approval of the Institutional Review Board of Carilion Clinic and Virginia Tech Carilion School of Medicine.

Patient Selection

A total of 27 established IBD patients (19 with CD and 8 with UC) and 15 control subjects were prospectively recruited from the IBD Center at Carilion Clinic from 2015 to 2018. Patients were ≥ 18 years of age, without other gastrointestinal or systemic disorders, without recent NSAIDs use, and scheduled for colonoscopy for clinical indications. Pregnant patients were excluded.

Sample Collection

Tissue samples from each patient were obtained through biopsies of both visible lesions and non-affected areas in the colon and/or the terminal ileum. Tissue samples were stored in RNAlater at −80°C. Patients were separated into different groups based on diagnosis (CD or UC), type of medication use, and response to therapy. Tissue from controls was obtained from patients

undergoing colonoscopy for reasons other than IBD (e.g., rectal bleeding) and included in the study only after endoscopy and histology proved to be normal.

Data Collection

Clinical data were abstracted from the patient medical charts. Demographics variables collected included age, gender, and smoking status. For IBD patients, disease diagnosis, and phenotype were determined at the time of study enrollment based on the Montreal disease classification (Satsangi et al., 2006). IBD medications and response to anti-TNF agents were recorded. Anti-TNF agents consisted of IFX and ADA in this patient cohort. Loss of response to anti-TNF therapy was classified as PNR or SLR. PNR was defined as complete lack of response to initiation of anti-TNF therapy whereas patients with SLR were those who initially responded to an anti-TNF agent - at least through the induction phase - but subsequently lost response. Clinical symptoms, inflammatory markers, imaging, and/or endoscopy findings were used to determine response.

Tissue Processing and Data Analysis

Biopsy samples were removed from RNAlater, finely minced, and homogenized in RLT buffer (Qiagen) with 2-mercaptoethanol. Tissues were processed using an AllPrep Kit (Qiagen) following the manufacturer's protocol. RNA was analyzed for quality and concentration using a NanoDrop™. Pools were made using equal concentrations of RNA from each patient sample for each experimental group. Patient samples were assigned to pools randomly and at least three pools were generated for each experimental group. The total amount of RNA used for each cDNA reaction was 600 ng and cDNA was generated using a First Strand Kit (Qiagen) following manufacturer's protocols. Following cDNA preparation, gene expression was evaluated using a custom Qiagen RT^2 Superarray following manufacturer's protocol. A list of 88 candidate genes for the custom Superarray platform is provided in **Supplementary Figure S2**. For each array, gene expression was determined utilizing the ΔΔCt method, using a panel of five housekeeping genes and internal controls provided on each array. Gene expression was determined using a 7,500 Fast Block Real-Time PCR System (ABI). Data was analyzed using SA Biosciences Data Analysis Center and Ingenuity Pathway Analysis (IPA). IPA images were then generated using BioRender.

In addition to the analysis of pooled samples, quantitative rtPCR was also performed in select genes of interest for each individual specimen. Complimentary DNA was generated from each specimen using an ABI High Capacity cDNA kit, in accordance with the manufacturer's protocol and 1 μg amplified using the Taqman-based rtPCR platform (ThermoFisher) on the ABI system. Gene expression was determined using the ΔΔCt method. All data were normalized to 18s and the fold change in gene expression was determined.

Statistical Analysis

For gene expression analysis, data was analyzed using GraphPad Prism, version 6 (GraphPad Software, Inc., San Diego, CA). Student's two-tailed t test was used for comparison between experimental groups. Multiple comparisons were conducted using one-way and two-way ANOVA where appropriate followed by Tukey post-test for multiple pairwise examinations. Correlation was computed using GraphPad Prism. Changes were identified as statistically significant if *p*-value was less than 0.05. Mean values were reported together with the SEM. The number of patients were determined based on a power analysis conducted using findings from a retrospective metadata analysis of publicly accessible gene expression data from dataset GSE16879. Gene expression was determined for a single marker of noncanonical NF-κB signaling (CXCL13) and the average and standard deviation of expression for this gene was used to determine the number of patients to target in the clinical study presented here.

TABLE 1 | Patient characteristics.

	IBD	Controls
N	27	15
Age (years)	41 ± 15	55 ± 14
Female	12 (44%)	6 (40%)
Smoker	4 (15%)	2 (13%)
CD	19 (70%)	
CD extent		
L1 (ileal)	5 (26%)	
L2 (colonic)	7 (37%)	
L3 (ileocolonic)	7 (37%)	
UC extent		
E1 (rectum)	2 (25%)	
E2 (left sided)	2 (25%)	
E3 (extensive)	4 (50%)	
IBD medications		
Anti-TNF agents	15 (56%)	
Non-anti-TNF therapies	10 (37%)	
No therapy	2 (7%)	
Anti-TNF responsive	5/15 (33%)	

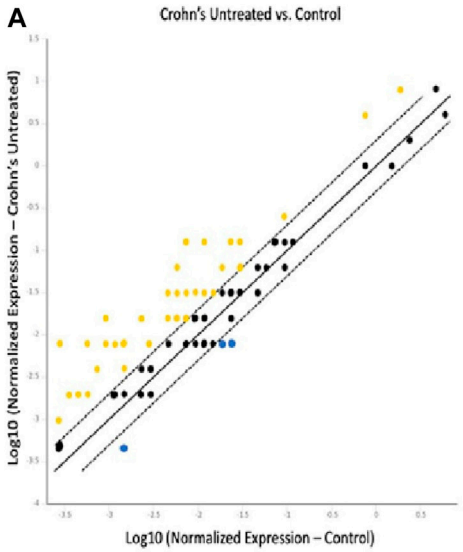
Age is reported as mean ± SD.

RESULTS

Noncanonical NF-κB is Upregulated in IBD

Tissues samples were obtained from 27 IBD patients and 15 controls. In the IBD group, 19 patients had CD and eight patients had UC (**Table 1**). The mean age of IBD patients was 41 years, 44% were females and 15% were active smokers. Of this patient pool, 33% of IBD patients were anti-TNF responders while 44% were not on medications or were taking medications other than anti-TNF agents. All anti-TNF non-responders in this study experienced SLR. The majority of CD and UC patients had ileocolonic and extensive colonic involvement respectively.

First, we examined the association of the noncanonical NF-κB pathway in IBD patients compared to controls. We found a



Upregulated		Downregulated	
Gene Symbol	Fold Regulation	Gene Symbol	Fold Regulation
IL6	28.22	NLRX1	-3.22
PTGS2	17.15	IRAK1	-3.00
CXCL13	17.13	BCL2L1	-2.36
CXCL2	16.98		
TLR2	13.64		
CXCL3	10.75		
CCL19	10.62		
TNF	8.49		
LTB	6.71		
CD40	6.69		
CCR7	6.56		
TNFRSF13C	5.41		
NLRP6	5.41		
CCL21	5.40		
TNFSF13B	5.41		
IRAK3	5.32		
CD40LG	5.29		
TNFAIP2	5.26		
HGDC	5.21		
CXCR5	4.31		
CYLD	4.23		
BIRC3	4.23		
RTC	4.16		
LTA	3.57		
MAP3K1	3.39		
NLRP3	3.38		
CXCR4	3.37		
CCL20	3.34		
NOD1	2.75		
TNFRSF10B	2.73		
TLR4	2.69		
CCL22	2.65		
CASP1	2.67		
FBXW7	2.65		
IKBKB	2.13		
NLRC5	2.12		
CASP4	2.12		
CASP5	2.10		
SUMO1	2.10		

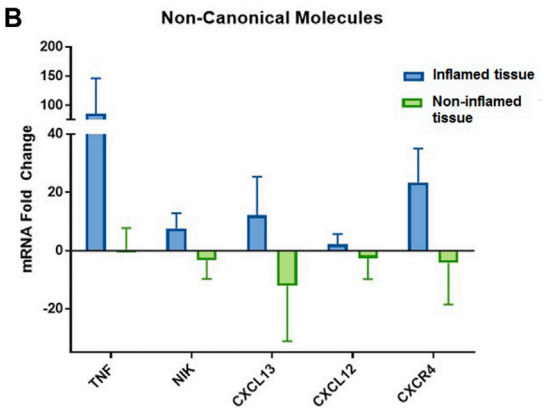
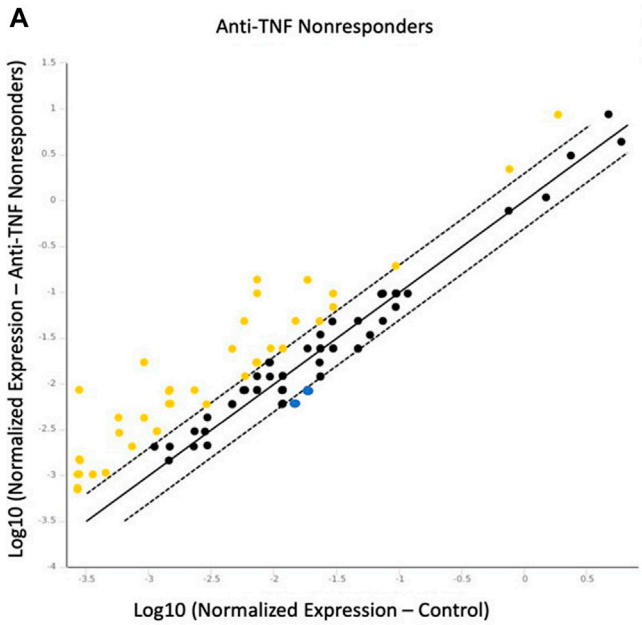


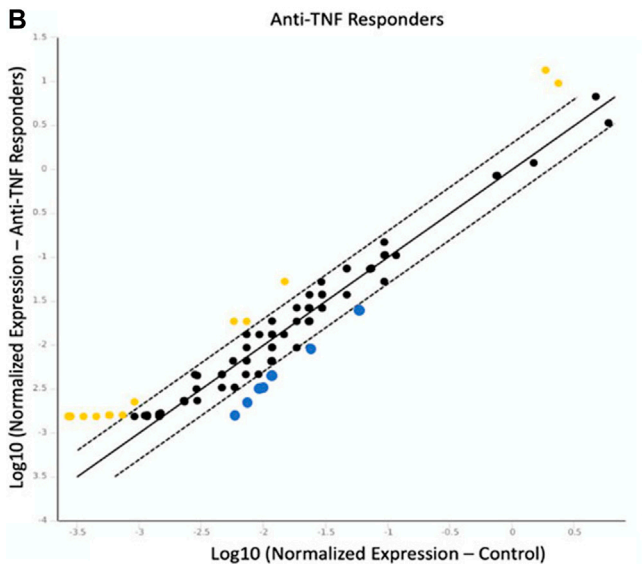
FIGURE 1 | Noncanonical NF-κB Signaling is Upregulated in Inflammatory Bowel Disease Patients **(A)** Left: Compared to gene expression from intestinal tissues of controls (n = 15, 3 pools), 39 genes related to noncanonical NF-κB pathway were upregulated in intestinal tissues obtained from untreated CD patients (n = 2, 1 pool) with yellow indicating upregulation and blue indicating downregulation (lines represent 1, 0, and −1 fold change; genes outside of dashed lines are considered significantly dysregulated). Housekeeping genes used for normalization include *ACTB, B2M,* and *GADPH;* Right: list of 39 upregulated genes and three downregulated genes and fold change values. **(B)**. Using real-time PCR of individual patient samples, the main noncanonical NF-kB pathway components TNF, NIK, CXCL12, CXCL13, and CXCR4 were found to be upregulated in inflamed areas compared to non-inflamed areas obtained from the same individual patients (inflamed lesions n = 4; non-inflamed tissue n = 4).

significant upregulation of 39 genes and downregulation of three genes associated with noncanonical NF-κB signaling in the pooled untreated CD patients (**Figure 1A**). These dysregulated genes encode for proteins with crucial roles in the signaling cascade. We also conducted individual real-time PCR analysis on a selection of these genes to validate the findings of the gene expression arrays. Individual qPCR was conducted on five genes that were significantly dysregulated in the custom gene expression arrays and are critical points in the noncanonical NF-κB signaling pathway (**Supplementary Figure S1**). TNF is one of the activating molecules; NIK is a critical kinase required for perpetuation of this activating signal; and CXCL12, CXCL13, and CXCR4 are products of the signaling pathway. The individual gene expression was consistent with custom arrays: *TNF*, *MAP3K14* (NIK), *CXCL12*, *CXCL13*, and *CXCR4* genes were all significantly upregulated in biopsies collected from inflamed areas compared to biopsies collected from non-inflamed areas in the same individual patients (**Figure 1B**).



Anti-TNF Nonresponders

Upregulated		Downregulated	
Gene Symbol	Fold Regulation	Gene Symbol	Fold Regulation
IL6	30.86	TLR3	-2.43
PTGS2	18.79	BCL2L1	-2.16
CXCL13	18.77		
CXCL2	13.13		
CXCL3	8.29		
TLR2	7.46		
CCL20	7.30		
CCL22	5.81		
NLRP6	5.75		
CD70	5.36		
LTB	5.20		
NLRC3	5.15		
NLRP3	5.02		
TNF	4.64		
RTC	4.59		
TNFSF13B	4.14		
IRAK3	4.06		
NOD2	3.78		
CD27	3.69		
CD40	3.68		
CASP5	3.27		
BIRC3	3.26		
HGDC	2.90		
TNFRSF13C	2.88		
CD40LG	2.81		
NLRP12	2.68		
IRAK2	2.60		
CXCR4	2.59		
PPC	2.59		
LTA	2.59		
TNFRSF8	2.59		
CCR7	2.58		
TNFRSF12A	2.35		
CXCR5	2.35		
CYLD	2.33		
CASP4	2.31		
RELA	2.07		
CASP1	2.07		
TNFAIP2	2.06		
FBXW7	2.06		
CCL19	2.06		
RELB	2.05		



Anti-TNF Responders

Upregulated		Downregulated	
Gene Symbol	Fold Regulation	Gene Symbol	Fold Regulation
RTC	7.14	TNFAIP2	-3.70
NOD2	5.63	CXCL13	-3.25
TNFRSF8	5.63	TNFRSF1B	-2.94
NLRP12	5.63	CXCR4	-2.83
LTA	5.63	IRAK1	-2.54
PPC	5.63	TRAF2	-2.52
IL6	5.51	TNFRSF1A	-2.25
CD27	5.50		
CD70	5.49		
NLRC3	5.43		
TNFRSF13C	4.30		
RPLP0	3.99		
CASP5	3.56		
CXCR5	3.39		
CXCL3	3.18		
TLR2	2.76		
NLRP3	2.73		
CYLD	2.52		
TNF	2.44		
CD40LG	2.16		

FIGURE 2 | Noncanonical NF-κB is Downregulated in IBD Patients Responding To Anti-TNF Therapy. **(A)**: Inflamed tissues from anti-TNF nonresponders (*n* = 10, two pools, CD patients and UC patients) showed 39 upregulated genes related to the noncanonical NF-κB signaling, compared to only 19 genes in anti-TNF responders (*n* = 5, two pools) **(B)**, with yellow indicating upregulation and blue indicating downregulation (lines represent 1, 0, and −1 fold change; genes outside of dashed lines are considered significantly dysregulated). A list of the involved genes is provided next to each graph. Housekeeping genes used for normalization include *ACTB, B2M,* and *GADPH* **(C–F)**: Ingenuity Pathway Analysis revealed that noncanonical NF-κB was a significant signaling hub that was downregulated in patients responding to anti-TNF therapy. Expression levels of the main noncanonical genes *NIK (MAP3K14), CXCL12, CXCL13*, and *CCL21* were upregulated in both untreated patients (*n* = 2, one pool) **(C)** and patients treated with non-anti-TNF medications (*n* = 10, two pools) **(D)**. However, anti-TNF responders (*n* = 5, two pools) **(E)**, showed a distinct attenuation of expression of these genes. Meanwhile, anti-TNF non-responders showed upregulation of *CXCL12* and *CXCL13* and downregulation of *CCL21*. Note: green represents downregulation; red represents upregulation.

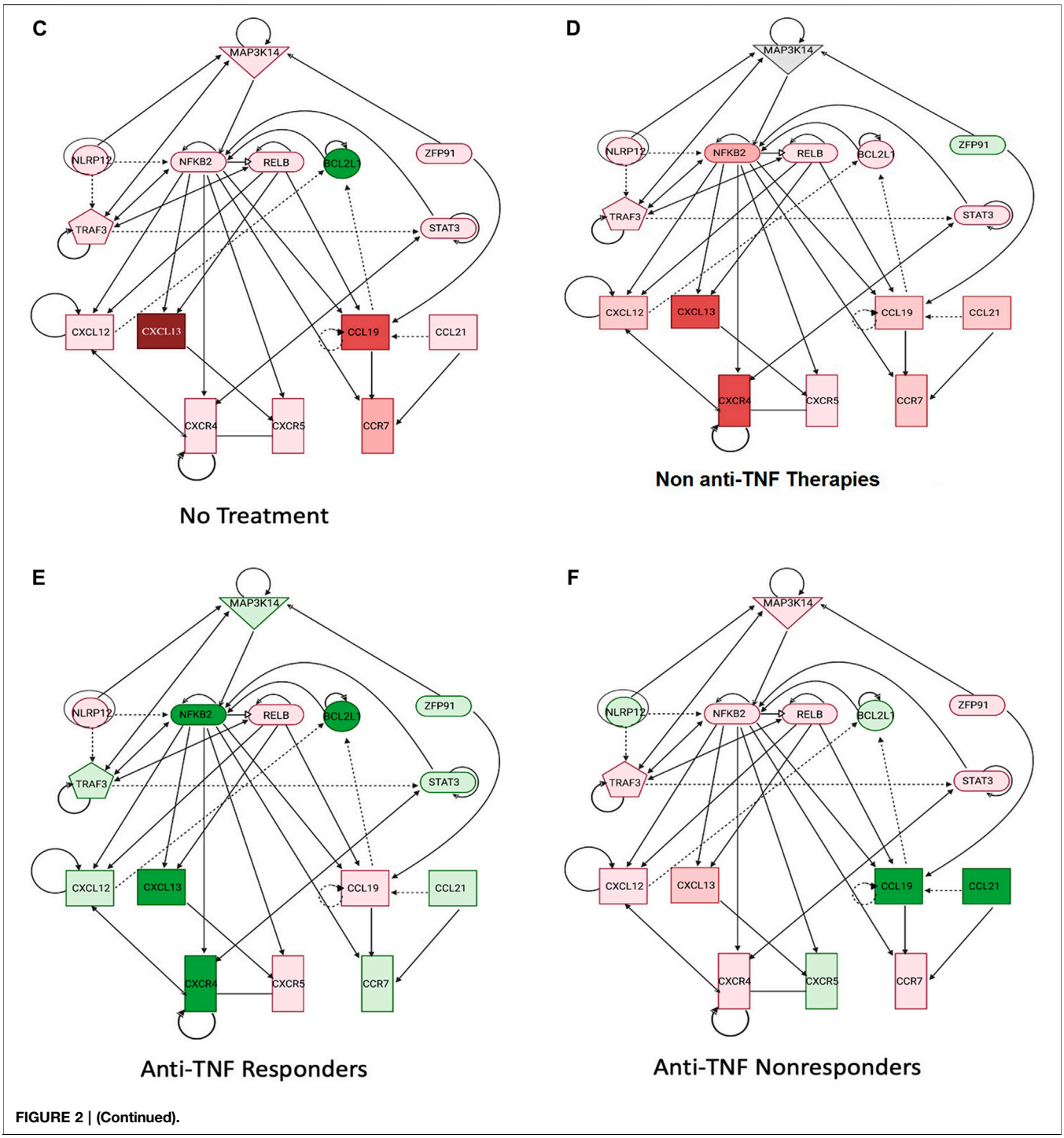


FIGURE 2 | (Continued).

Noncanonical NF-κB Signaling is Downregulated in Anti-TNF Responsive Patients

We then examined the role of the noncanonical NF-κB pathway in IBD patients in relation to their responsiveness to anti-TNF agents. Compared to controls, in IBD patients not responding to anti-TNF therapy, we identified 42 upregulated genes and only two downregulated genes (**Figure 2A**). Notably, CXCL13 was significantly upregulated (+18.77 fold) in nonresponders.

Conversely, in IBD patients responding to anti-TNF agents we identified 20 upregulated genes and seven downregulated genes involved in noncanonical NF-κB signaling (**Figure 2B**). Upregulated genes included *NLRP12*, a negative regulator of noncanonical signaling, while downregulated genes included

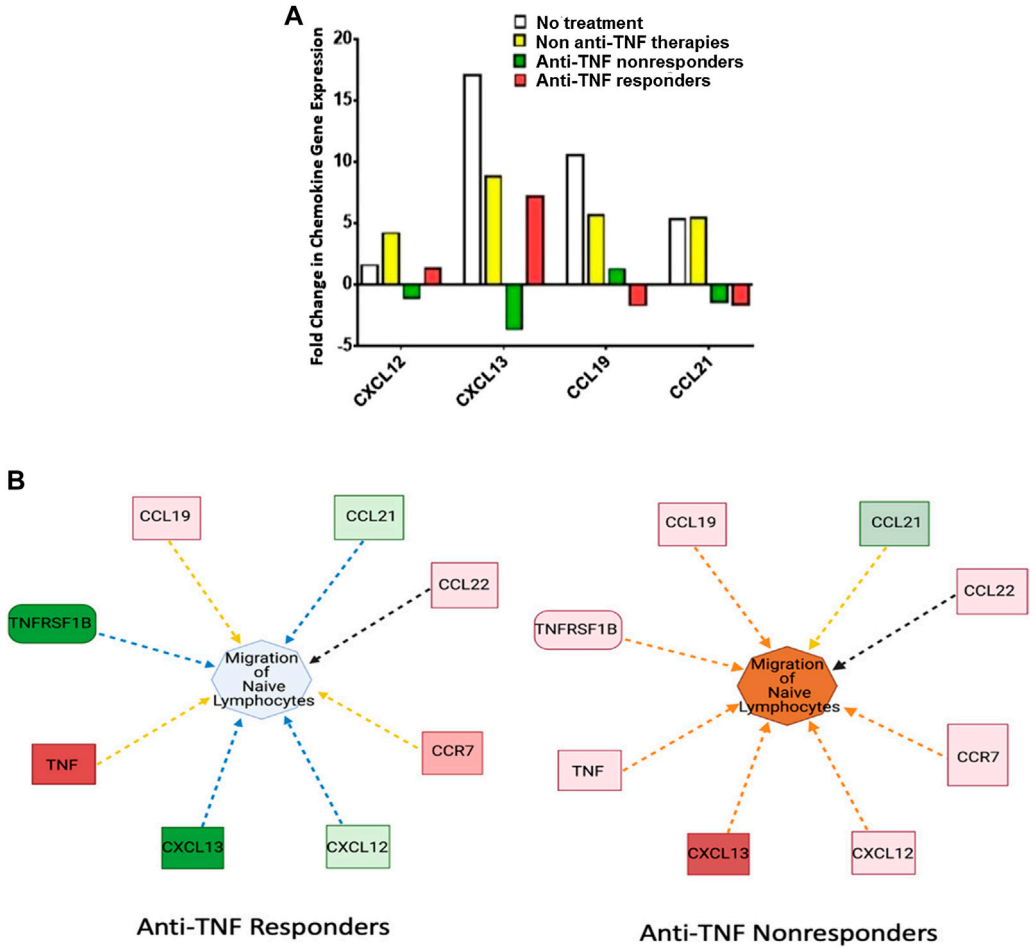


FIGURE 3 | CXCL12 and CXCL13 are Downregulated in IBD Patients Responding to Anti-TNFα Therapy. **(A)** CXCL12, CXCL13, CCL19, and CCL21 were significantly upregulated in both untreated IBD patients (n = 2, one pool) and IBD patients treated with non-anti-TNF medications (n = 10, two pools). CXCL12, CXCL13, and CCL19 displayed opposite expression profiles based on anti-TNF responsiveness, with upregulation in anti-TNF nonresponders (n = 10, two pools) and downregulation in responders (n = 5, two pools) for CXCL12 and CXCL13. CCL21 remained downregulated regardless of response to anti-TNF agents. **(B)** Predicted effect on the migration of naïve lymphocytes to inflamed tissue based on changes of the noncanonical chemokines which are involved in lymphocyte trafficking. In anti-TNF responders, lymphocyte trafficking is reduced. By contrast anti-TNF nonresponders demonstrate increased lymphocyte trafficking. In general, the increase in noncanonical signaling molecules results in a large increase in predicted lymphocyte migration. Note: Blue and orange dashed lines with arrows indicate indirect inhibition and activation, respectively. Yellow and black dashed lines with arrows depict inconsistent effects and no prediction, respectively.

noncanonical chemokine *CXCL13* and noncanonical receptor for *CXCR4*.

Pathway analysis revealed significant downregulation of noncanonical NF-κB signaling in IBD patients responsive to anti-TNFα therapy compared to untreated IBD patients and IBD patients treated with other (non-anti-TNF) medications (**Figures 2C–F**). This decreased expression was observed in several genes throughout the signaling pathway, and specifically included reduced expression of *MAP3K14, NFKB2, TRAF3, STAT3, CXCL12, CXCL13, CXCR4*, and *CCR7* that were not observed in the other IBD patient groups. Interestingly, in IBD patients unresponsive to anti-TNF therapy, noncanonical NF-κB signaling was upregulated compared to untreated IBD patients. In these patients, upregulation of noncanonical NF-κB signaling was strongly associated with the downregulation of *NLRP12* and upregulation of *MAP3K14, CXCL12,* and *CXCL13*. Together, these data demonstrate that noncanonical NF-κB signaling was significantly decreased in anti-TNF responders and increased in anti-TNF nonresponders.

CXCL12 and CXCL13 Expression is Correlated to Anti-TNF Responsiveness

Currently, only four major chemokines have been associated with the noncanonical NF-κB signaling cascade, CCL19, CCL21, CXCL12, and CXCL13. We examined these chemokine expression patterns in relation to anti-TNF responsiveness. In untreated IBD patients and in those treated with other (non-anti-TNF) therapies, *CCL19, CCL21, CXCL12, and CXCL13* expression were upregulated. IBD patients responding to anti-

TNF therapy demonstrated a significant decrease in *CXCL12, CXCL13*, and *CCL21* compared to those in the untreated IBD group (**Figure 3A**). By contrast, *CXCL12* and *CXCL13* were significantly upregulated in IBD patients not responding to anti-TNF therapy while *CCL19* and *CCL21* were downregulated in these patients. Both *CXCL12* and *CXCL13* were strongly correlated with anti-TNF responsiveness, whereas *CCL19* and *CCL21* only demonstrated a weak correlation. Based on the expression profile associated with these chemokines, it appears that migration of naïve lymphocytes was the signaling network most strongly altered in patients not responding to anti-TNF agents (**Figure 3B**). Hence, by contrast with nonresponders, in IBD patients responding to anti-TNF therapy, the downregulation of *CXCL12* and *CXCL13* could result in reduced migration of lymphocytes to inflamed tissues.

DISCUSSION

Anti-TNF therapy acting through the canonical NF-κB signaling pathway has been the cornerstone of IBD treatment for the past several years. Despite its success, a significant proportion of IBD patients may not respond or lose response over time to anti-TNF therapy. This population of anti-TNF nonresponders has an increased risk of disease complications but might respond to newer biologic medications such as ustekinumab or vedolizumab (Feagan et al., 2016 and Feagan et al.2017). The mechanisms of PNR and SLR to anti-TNF agents are poorly understood. One possible explanation is that the driving mechanism of inflammation in these IBD patients may have shifted to an alternative signaling pathway.

The noncanonical NF-κB pathway has been recognized as a key regulator and promoter of the adaptive immune system, particularly in the development of secondary lymphoid organs. Prior studies from our group have demonstrated the role of this signaling pathway in mouse models of colon inflammation and eosinophilic esophagitis (Allen et al., 2012; Eden et al., 2017).

In this study, we found significant upregulation of the genes involved in the noncanonical NF-κB pathway in IBD patients compared to healthy controls. Furthermore, the main chemokines in this pathway, namely CXCL12 and CXCL13, were significantly downregulated in IBD patients who responded to anti-TNF agents and were upregulated in nonresponders. These findings suggest that the activation of the noncanonical NF-κB signaling pathway may contribute to the mechanism underlying the lack/loss of response to anti-TNF therapy. The upregulated genes in the noncanonical NF-κB pathway involved in lack/loss of response to anti-TNF therapy may involve leukocyte migration to the affected tissue as predicted by IPA analysis.

The relatively small sample size and single center nature are limitations of our study. In addition, it is unclear how many of our anti-TNF nonresponders would respond to additional anti-TNF agents (Swaminath et al., 2009; Löfberg et al., 2012). Whether the expression pattern of the noncanonical genes differs in patients who respond to a second anti-TNF agent compared to those who do not respond to any anti-TNF medication remains unknown. Also, our study does not clarify the role of this pathway in PNR–since all of our patients experienced SLR.

In conclusion, this is the first study in humans that has explored the role of the noncanonical NF-κB signaling in the pathogenesis of IBD. More importantly, our findings provide a potential mechanistic insight into the lack/loss of response to anti-TNF agents in IBD. If our observations are confirmed, targeting the noncanonical NF-κB signaling pathway could significantly impact IBD management and therapy outcomes.

DATA AVAILABILITY STATEMENT

The authors acknowledge that the data presented in this study must be deposited and made publicly available in an acceptable repository, prior to publication. Frontiers cannot accept a article that does not adhere to our open data policies.

ETHICS STATEMENT

The studies involving human participants were reviewed and approved by IRB Carilion Clinic. The patients/participants provided their written informed consent to participate in this study.

AUTHOR CONTRIBUTIONS

VN was responsible for investigation and writing (review and editing); HM, KE, KK, SS, RB, and DG were responsible for investigation, DS and IA were responsible for conceptualization, investigation, methodology, formal analysis, supervision, and writing (initial draft, review and editing).

FUNDING

Carilion Research Advancement Program (RAP) Grant 13 Role of the Non-Canonical NFkB Inflammatory Cascade in Therapeutic Response and Pathogenesis of IBD.

SUPPLEMENTARY MATERIAL

The Supplementary Material for this article can be found online at: https://www.frontiersin.org/articles/10.3389/fphar.2021.655887/full#supplementary-material

SUPPLEMENTARY FIGURE 1 | Schematic Illustration of Key Components of Noncanonical NF-κB Signaling Significantly Dysregulated in IBD Patients. Our data revealed a significant increase in chemokines associated with noncanonical NF-κB signaling, including CXCL12, CXCL13, CCL9, and CCL21. Additional pathway analysis revealed that these changes were associated with increased expression of genes encoding a variety of proteins that regulate the non-canonical NF-κB signaling pathway through modulation of NIK, including the up-regulation of cIAP1, cIAP2, CYLD, and NLRP12 and the down-regulation of BCL10, ZPF91, and A20. Created with BioRender.com.

SUPPLEMENTARY TABLE 1 | Custom Gene Array to Evaluate Noncanonical NF-κB Signaling in IBD Patients. The gene list for the custom superarray platform is provided with RefSeq Number and Gene Symbol. These 88 gene candidates serve a role in the noncanonical NF-κB pathway and dysregulated transcription levels may have implications on IBD pathogenesis and drug responsiveness. For each array, gene expression was determined utilizing the delta-deltaCt method, using a panel of five housekeeping genes and internal controls provided on each array.

REFERENCES

Allen, I. C., Wilson, J. E., Schneider, M., Lich, J. D., Roberts, R. A., Arthur, J. C., et al. (2012). NLRP12 Suppresses Colon Inflammation and Tumorigenesis through the Negative Regulation of Noncanonical NF-κB Signaling. *Immunity* 36, 742–754. doi:10.1016/j.immuni.2012.03.012

Ben-Horin, S., Kopylov, U., and Chowers, Y. (2014). Optimizing Anti-TNF Treatments in Inflammatory Bowel Disease. *Autoimmun. Rev.* 13, 24–30. doi:10.1016/j.autrev.2013.06.002

Biancheri, P., Brezski, R. J., Di Sabatino, A., Greenplate, A. R., Soring, K. L., Corazza, G. R., et al. (2015). Proteolytic Cleavage and Loss of Function of Biologic Agents that Neutralize Tumor Necrosis Factor in the Mucosa of Patients with Inflammatory Bowel Disease. *Gastroenterology* 149, 1564–1574. doi:10.1053/j.gastro.2015.07.002

Billmeier, U., Dieterich, W., Neurath, M. F., and Atreya, R. (2016). Molecular Mechanism of Action of Anti-tumor Necrosis Factor Antibodies in Inflammatory Bowel Diseases. *World J. Gastroenterol.* 22, 9300–9313. doi:10.3748/wjg.v22.i42.9300

Brandse, J. F., Mathôt, R. A., van der Kleij, D., Rispens, T., Ashruf, Y., Jansen, J. M., et al. (2016). Pharmacokinetic Features and Presence of Antidrug Antibodies Associate With Response to Infliximab Induction Therapy in Patients With Moderate to Severe Ulcerative Colitis. *Clin. Gastroenterol. Hepatol.* 14, 251–258. doi:10.1016/j.cgh.2015.10.029

Danese, S., Fiorino, G., and Reinisch, W. (2011). Review Article: Causative Factors and the Clinical Management of Patients with Crohn's Disease Who Lose Response to Anti-TNF-α Therapy. *Aliment. Pharmacol. Ther.* 34, 1–10. doi:10.1111/j.1365-2036.2011.04679.x

Eden, K., Rothschild, D. E., McDaniel, D. K., Heid, B., and Allen, I. C. (2017). Noncanonical NF-κB Signaling and the Essential Kinase NIK Modulate Crucial Features Associated with Eosinophilic Esophagitis Pathogenesis. *Dis. Model. Mech.* 10, 1517–1527. doi:10.1242/dmm.030767

Feagan, B. G., Rubin, D. T., Danese, S., Vermeire, S., Abhyankar, B., Sankoh, S., et al. (2017). Efficacy of Vedolizumab Induction and Maintenance Therapy in Patients With Ulcerative Colitis, Regardless of Prior Exposure to Tumor Necrosis Factor Antagonists. *Clin. Gastroenterol. Hepatol.* 15, 229–239. doi:10.1016/j.cgh.2016.08.044

Feagan, B. G., Sandborn, W. J., Gasink, C., Jacobstein, D., Lang, Y., Friedman, J. R., et al. (2016). Ustekinumab as Induction and Maintenance Therapy for Crohn's Disease. *N. Engl. J. Med.* 375, 1946–1960. doi:10.1056/NEJMoa1602773

Löfberg, R., Louis, E. V., Reinisch, W., Robinson, A. M., Kron, M., Camez, A., et al. (2012). Adalimumab Produces Clinical Remission and Reduces Extraintestinal Manifestations in Crohn's Disease: Results from CARE. *Inflamm. Bowel Dis.* 18, 1–9. doi:10.1002/ibd.21663

Mao, E. J., Hazlewood, G. S., Kaplan, G. G., Peyrin-Biroulet, L., and Ananthakrishnan, A. N. (2017). Systematic Review with Meta-Analysis: Comparative Efficacy of Immunosuppressants and Biologics for Reducing Hospitalisation and Surgery in Crohn's Disease and Ulcerative Colitis. *Aliment. Pharmacol. Ther.* 45, 3–13. doi:10.1111/apt.13847

McDaniel, D. K., Eden, K., Ringel, V. M., and Allen, I. C. (2016). Emerging Roles for -κB Signaling in the Modulation of Inflammatory Bowel Disease Pathobiology. *Inflamm. Bowel Dis.* 22, 2265–2279. doi:10.1097/MIB.0000000000000858

Ng, S. C., Shi, H. Y., Hamidi, N., Underwood, F. E., Tang, W., Benchimol, E. I., et al. (2018). Worldwide Incidence and Prevalence of Inflammatory Bowel Disease in the 21st century: a Systematic Review of Population-Based Studies. *Lancet* 390, 2769–2778. doi:10.1016/S0140-6736(17)32448-0

Rothschild, D. E., McDaniel, D. K., Ringel-Scaia, V. M., and Allen, I. C. (2018). Modulating Inflammation through the Negative Regulation of NF-κB Signaling. *J. Leukoc. Biol.* 103, 1131–1150. doi:10.1002/JLB.3MIR0817-346RRR

Satsangi, J., Silverberg, M. S., Vermeire, S., and Colombel, J.-F. (2006). The Montreal Classification of Inflammatory Bowel Disease: Controversies, Consensus, and Implications. *Gut* 55, 749–753. doi:10.1136/gut.2005.082909

Sorrentino, D. (2008). Role of Biologics and Other Therapies in Stricturing Crohn's Disease: what Have We Learnt So Far? *Digestion* 77, 38–47. doi:10.1159/000117306

Sorrentino, D. (2013). State-of-the-art Medical Prevention of Postoperative Recurrence of Crohn's Disease. *Nat. Rev. Gastroenterol. Hepatol.* 10, 413–422. doi:10.1038/nrgastro.2013.69

Sun, S.-C. (2011). Non-canonical NF-κB Signaling Pathway. *Cell Res.* 21, 71–85. doi:10.1038/cr.2010.177

Swaminath, A., Ullman, T., Rosen, M., Mayer, L., Lichtiger, S., and Abreu, M. T. (2009). Early Clinical Experience with Adalimumab in Treatment of Inflammatory Bowel Disease with Infliximab-Treated and Naïve Patients. *Aliment. Pharmacol. Ther.* 29, 273–278. doi:10.1111/j.1365-2036.2008.03878.x

Yarur, A. J., Abreu, M. T., Deshpande, A. R., Kerman, D. H., and Sussman, D. A. (2014). Therapeutic Drug Monitoring in Patients with Inflammatory Bowel Disease. *World J. Gastroenterol.* 20, 3475–3484. doi:10.3748/wjg.v20.i13.3475

Conflict of Interest: The authors declare that the research was conducted in the absence of any commercial or financial relationships that could be construed as a potential conflict of interest.

Copyright © 2021 Nguyen, Eden, Morrison, Sammons, Knight, Sorrentino, Brock, Grider, Allen and Sorrentino. This is an open-access article distributed under the terms of the Creative Commons Attribution License (CC BY). The use, distribution or reproduction in other forums is permitted, provided the original author(s) and the copyright owner(s) are credited and that the original publication in this journal is cited, in accordance with accepted academic practice. No use, distribution or reproduction is permitted which does not comply with these terms.

frontiers in Pharmacology

ORIGINAL RESEARCH
published: 28 June 2021
doi: 10.3389/fphar.2021.690736

Kaempferol Alleviates Steatosis and Inflammation During Early Non-Alcoholic Steatohepatitis Associated With Liver X Receptor α-Lysophosphatidylcholine Acyltransferase 3 Signaling Pathway

Hongjiao Xiang[1,2†], *Mingmei Shao*[1,2†], *Yifei Lu*[1,2], *Junmin Wang*[1,2], *Tao Wu*[1,2*] *and Guang Ji*[2*]

[1]*Institute of Interdisciplinary Integrative Medicine Research, Shanghai University of Traditional Chinese Medicine, Shanghai, China,* [2]*Institute of Digestive Disease, Longhua Hospital, Shanghai University of Traditional Chinese Medicine, Shanghai, China*

OPEN ACCESS

Edited by:
Ralf Weiskirchen, RWTH Aachen University, Germany

Reviewed by:
Brijesh Kumar Singh, Duke-NUS Medical School, Singapore
Wei Liu, University of Science and Technology of China, China

***Correspondence:**
Guang Ji
jiliver@vip.sina.com
Tao Wu
wutao001827@163.com

†These authors have contributed equally to this work

Specialty section:
This article was submitted to Gastrointestinal and Hepatic Pharmacology, a section of the journal Frontiers in Pharmacology

Received: *04 April 2021*
Accepted: *15 June 2021*
Published: *28 June 2021*

Citation:
Xiang H, Shao M, Lu Y, Wang J, Wu T and Ji G (2021) Kaempferol Alleviates Steatosis and Inflammation During Early Non-Alcoholic Steatohepatitis Associated With Liver X Receptor α-Lysophosphatidylcholine Acyltransferase 3 Signaling Pathway. Front. Pharmacol. 12:690736. doi: 10.3389/fphar.2021.690736

Background: Kaempferol (KP) has a variety of biological effects such as anti-inflammatory, anti-oxidant, anti-aging and cardiovascular protection. Whether KP has a therapeutic effect on non-alcoholic steatohepatitis (NASH), and the detailed mechanism is currently unclear. This study aims to explore the mechanism of KP in the treatment of NASH through *in vivo* and *in vitro* experiments.

Methods: 1) *In vivo* experiment: In the C57BL/6 NASH mice model induced by high fat diet (HFD), KP was administered by gavage at a dose of 20 mg/kg/day. 2) *In vitro* experiment: Palmitic acid/Oleic acid (PA/OA, 0.375/0.75 mM) was used to intervene HepG2 and AML12 cells to establish a steatosis cell model. Three concentrations of KP, low (20 μmol/L), medium (40 μmol/L) and high (60 μmol/L) were used *in vitro*. The mRNA and protein expression of related molecules involved in LXRα-LPCAT3-ERS pathway were detected using RT-qPCR and Western blot.

Results: In the NASH mouse model, KP can significantly reduce the expression of LXRα, LPCAT3 and ERS-related factors PERK, eIF2α, ATF6, ATF4, XBP1, CHOP, IRE1α and GRP78. In the PA/OA-induced cell model, KP could decrease the content of triglyceride and lipid droplets, and also decrease the expression of LXR α, LPCAT3 and ERS related factors PERK, eIF2α, ATF6, ATF4, XBP1, CHOP, IRE1α and GRP78.

Abbreviations: ABCA1, ATP binding cassette transporter A1; ALT, Alanine aminotransferase; ATF6, Activating transcription factor 6; BCA, Bicinchoninic acid; CCL5, C-C chemokine ligand 5; CCK8, Cell counting kit-8; CHOP, C/EBP homologous protein; CXCL10, C-X-C motif chemokine 10; eIF-2α, Eukaryotic translation initiation factor 2; ER, Endoplasmic reticulum; ERS, Endoplasmic reticulum stress; GPR78, Glucose-regulated protein 78; HFD, High-fat diet; HDL, High-density lipoprotein; IL6, Interleukin 6; IRE1, Inositol-requiring enzyme 1; KP, Kaempferol; LDL, Low density lipoprotein; LPCAT3, Lysophosphatidylcholine acyltransferase 3; LXRs, Liver X receptors; MAPK, Mitogen-activated protein kinase; MCP-1, Monocyte chemoattractant protein-1; NAFL, Non-alcoholic fatty liver; NAFLD, Non-alcoholic fatty liver disease; NASH, Non-alcoholic steatohepatitis; PA/OA, Palmitic acid/oleic acid; PERK, Protein kinase R-like ER kinase; PLs, Phospholipids; PPAR, Peroxisome proliferator-activated receptor; ROS, Reactive oxygen species; SREBP, Sterol regulatory element bingding proteins; TC, Total cholesterol; TG, Triglyceride; TNFα, Tumor necrosis factor α; UPR, Unfolded protein response; XBP1, X-box-binding protein 1.

Conclusion: KP may decrease the expression level of LXRα and LPCAT3, thus improve ERS and reduce hepatic steatosis and inflammation.

Keywords: kaempferol, NASH, LXR, LPCAT3, ERS

INTRODUCTION

Non-alcoholic fatty liver disease (NAFLD) is a clinical pathological syndrome, which includes simple steatosis, steatohepatitis (NASH), liver fibrosis and cirrhosis and their clinical consequences (Nobili et al., 2019). NASH is usually associated with more severer liver cirrhosis and liver cancer (Friedman et al., 2018). NAFLD is one of the leading cause of liver disease in the world, which is closely linked to the increased prevalence of obesity and metabolic diseases. NAFLD affects more than 20% of the population of the Europe and United States. NAFLD prevalence varies widely from the Asia-pacific region, ranging from about 5 to 32% (Younossi et al., 2018). Approximately one third of NAFLD patients will progress to NASH (Takahashi and Fukusato, 2014).

Phospholipids (PLs) is an important part of biological membranes and the precursors of many signal molecules (Vance, 2015). Liver X receptors (LXRs) are regulators of membrane phospholipid composition, important regulators for regulating cholesterol and fatty acid homeostasis, and effective inflammation inhibitors (Rong et al., 2013). Lysophosphatidylcholine acyltransferase 3 (LPCAT3) is a key enzyme that encodes the remodeling pathway to PLs, and is a direct target gene of mouse and human LXR (Demeure et al., 2011; Wang et al., 2016). LPCAT3 modulates the activation of inflammatory kinases by changing membrane components, and regulates inflammation by affecting the availability of substrates produced by inflammatory mediators (Singh and Liu, 2017b). Rong et al. stated that LXR activation increased the expression of LPCAT3 and reduced the saturation of the ER membrane. Acute knockout of LPCAT3 in the liver could aggravate endoplasmic reticulum stress (ERS). At the same time, the inflammation of the liver would increase because the activity of LPCAT3 was inhibited. It can be concluded that the LXR-LPCAT3 pathway is important to regulating ERS, and is involved in the progress of NASH.

Apoptosis is an active cell death process controlled by gene, which is mainly divided into endogenous pathway (mitochondrial pathway), exogenous pathway (death receptor pathway) and ERS induced apoptosis (Hu et al., 2018). The link between ERS and liver disease has been found in a growing number of studies, including NAFLD, alcoholic fatty liver, viral hepatitis, NASH, liver cancer, etc., (Brenner et al., 2013; Li F. et al., 2017). Endoplasmic reticulum (ER) is the main site for protein synthesis, lipid production and calcium ion storage in eukaryotic cells. When cells are stimulated externally, the ER produces a large number of unfolded or misfolded proteins, which leads to the unfolded protein response (UPR) (Chaudhari et al., 2014; Demirtas et al., 2016). In the early stage, UPR can relieve the pressure on the ER and promote the restoration of normal function of ER. However, sustained ERS induces apoptosis through UPR (Ozcan and Tabas, 2012). Cell signal transduction pathways induced by UPR include three pathways: protein kinase R-like ER kinase/eukaryotic translation initiation factor 2 (PERK/eIF-2α), activating transcription factor 6 (ATF6) pathway and inositol-requiring enzyme 1/X-box-binding protein 1 (IRE1/XBP1) (Wang and Kaufman, 2016). ERS activates sterol regulatory element binding protein (SREBP) through the ATF6, PERK and IRE1 signaling pathways to promote lipid accumulation in the liver (Zhang et al., 2012). It has been proved that ERS can activate the apoptotic pathway and induce apoptosis by activating downstream signal molecules (Iurlaro and Muñoz-Pinedo, 2016). Dasgupta et al. (2020) demonstrated that the destruction of IRE1A or inhibition of Ire1a in liver cells reduces the release of inflammatory extracellular vesicles (EVs), and reduces liver damaged and inflammation in the mice were fed a diet high in fat, fructose, and cholesterol. Bax inhibitor-1 (BI-1) is a negative regulator of the ER stress sensor IRE1α. Lebeaupin et al. (2018) treated BI-$1^{-/-}$ mice on a high-fat diet (HFD) with tunicamycin and developed liver failure of a short period of time. After IRE1α inhibitors were used to treat BI-$1^{-/-}$ mice, liver inflammation was significantly improved. Hernández-Alvarez et al. (2019) found that the lack of Mfn2 would promote ERS, leading to the progression of NASH to liver cancer. Therefore, regulating ERS can be considered as an important approach and new strategy for prevention and treatment of steatosis.

Kaempferol (KP) is a dietary bioflavonoid, which is widely present in various plants. It has a variety of biological effects such as anti-inflammatory, anti-oxidant, anti-aging and cardiovascular protection (Li and Pu, 2011; Lee B. et al., 2015; Suchal et al., 2017; Kouhestani et al., 2018). Lee B. et al. (2015) found that KP may bind to PPARα during adipocyte differentiation to stimulate fatty acid oxidation signals in adipocytes, thereby reducing cellular triglyceride (TG) accumulation. Lee Y.-J. et al. (2015) used zebrafish to verify the inhibitory effect of KP on lipid accumulation. KP inhibited lipid accumulation in zebrafish by inhibiting fat-related genes (Lee B. et al., 2015). Wang et al. (2019) found that KP can improve liver failure induced by lipopolysaccharide-galactosamine by reducing ERS. Other studies have shown that the regulation of KP on ERS was bidirectional, which can promote the apoptosis of tumor cells and inhibit the apoptosis of non-tumor cells (Ashrafizadeh et al., 2020). Our previous review summarized the application of KP in treating diseases and the underlying mechanisms that are currently being studied (Ren et al., 2019). In our previous study, it has been demonstrated that KP not only reduced serum alanine aminotransferase (ALT), low density lipoprotein (LDL), TG and total cholesterol (TC) content, but also reduced the accumulation of lipids in the liver (Lu et al., 2020). However, there are insufficient studies on the detailed mechanism of KP on improving NASH.

In this study, we revealed that the expression of LXR-LPCAT3-ERS pathway-related factors was remarkably increased to the liver of mice fed a HFD, and the similar results were observed in palmitic acid/oleic acid (PA/OA)-induced steatotic cells. After intervention with KP, either *in vitro* or *in vivo*, KP significantly reduced the expression of LXR-LPCAT3 pathway, inhibited the expression of molecules involved in ERS, and then improved HFD-related liver damage. Finally, we conclude that KP is a promising drug for the treatment of NASH.

MATERIALS AND METHODS

Animals and Treatment

Six-week-old male C57BL/6J mice were purchased from Shanghai SLAC Experimental Animal Co., Ltd. China. The experimental animals are kept in the specific pathogen free environment of the Experimental Animal Center of Shanghai University of Traditional Chinese Medicine. The temperature is about 20 ± 4°C, and the humidity is about 15–16%. C57BL/6J mice were randomly divided into normal control group (Control, NC group, N = 7), HFD (Calorie composition: fat 60%, protein 20%, carbohydrate 20%, D12492, Research Diets, United States) fed group (HFD model, HFD group, N = 8) and HFD fed with KP (HFD + KP, HFD + KP group, N = 8). The mice in group NC were fed normal diet, and the mice in group HFD and HFD + KP were fed HFD for 24 weeks. At the beginning of the 21st week, KP (4 mg/ml) was gavaged in the HFD + KP group at a dose of 0.5 ml/100 g on the basis of HFD feeding. At the same time, mice in NC and HFD groups received equal volume of normal saline (**Supplementary Figure S1**). The serum and liver tissue of mice was collected. All the experimental procedures were approved by the Institutional Animal Care and Use Committee at the Shanghai University of Traditional Chinese Medicine (SYXKhu 2014-0008).

Cell Lines

HepG2 and AML12 cells were obtained from the Cell bank of typical culture preservation Committee of Chinese Academy of Sciences. The cells were cultured in high glucose DMEM (containing 10% fetal bovine serum, 100 U/ml penicillin, 100 μg/ml streptomycin and 1‰ Amphotericin B) and was maintained at 37°C, 95% air humidity and 5% CO_2.

Establishment of Steatosis Cell Line

PA (P0500, Sigma, United States) was dissolved in methanol, and OA (0550, Sigma, United States) was dissolved in PBS. PA:OA was then added to the culture solution at a ratio of 1: 2. Final concentrations of PA/OA were as below: ①0 mM, ②0.25/0.5 mM, ③0.375/0.75 mM, ④0.5/1 mM, ⑤0.625/1.25 mM and ⑥0.75/1.5 mM. HepG2 and AML12 cells were cultured for 24 h to observe the morphological changes. Cells were detected with cell counting kit-8 (CCK8), TG kit and Oil-Red O staining.

Real-Time Quantitative PCR

Total RNA was extracted from mouse livers, HepG2 and AML12 cells using Trizol reagents (R0016, Beyotime Biotechnology, Shanghai, China). cDNA were transcribed according to the instructions in the reverse transcription kit (A5001, Promega, United States). The cDNA was using real-time quantitative polymerase chain reaction (RT-qPCR) performed with the SYBR Green PCR Master Mix (11201E03, YEASEN, Shanghai, China) and gene-specific primers. The results were normalized with β-actin as control RT-qPCR was performed using a CFX-96 Real Time System (Bio-Rad, United States). Polymerase chains reaction primers are listed in Supplementary Table S1.

Western Blot

Liver and cell sample were lysed with radio immunoprecipitation assay (RIPA) buffer (WB0102, Weiao, Shanghai, China) containing phenylmethylsulfonyl fluoride (PMSF) (WB0122, Weiao, Shanghai, China). The proteins were extracted after centrifugation, and subsequently a bicinchoninic acid (BCA) (B48110, YEASEN, Shanghai, China) protein quantitation kit was used to determine the concentrations. 30 μg of protein was subjected to 10% sodium dodecyl sulfate-polyacrylamide (SDS-PAGE) gel electrophoresis, then transferred to a polyvinylidene fluoride membrane, and then incubated with the corresponding primary antibody overnight at 4°C. Antibodies and dilution ratio were as below: 1:1,000 for rabbit anti-Actin (R1207, HUABIO, Hangzhou, China), 1:1,000 for rabbit anti-LXRα (ab176323, Abcam, Cambridge, MA), 1:500 for rabbit anti-LPCAT3 (HAPL0516, HUABIO, Hangzhou, China), 1:1,000 for rabbit anti-phospho-PERK (3,179, Cell Signaling Technology, MA), 1: 1,000 for rabbit anti-PERK (20582-1-AP, Proteintech Group, MA), 1:1,000 for rabbit anti-phospho-eIF2α (3398S, Cell Signaling Technology, MA), 1:1,000 for rabbit anti-eIF2α (3398S, Cell Signaling Technology, MA), 1:500 for rabbit anti-ATF4 (10835-1-AP, Proteintech Group, MA), 1:200 for rabbit anti-CHOP (15204-1-AP, Proteintech Group, MA), 1:500 for rabbit anti-ATF6 (ab203119, Abcam, Cambridge, MA), 1:1,000 for rabbit anti-GRP78 (3177S, Cell Signaling Technology, MA), 1:1,000 for rabbit anti-phospho-IRE1α (AF7150, Affbiotech, China), 1:1,000 for rabbit anti-IRE1α (3294S, Cell Signaling Technology, MA), 1: 1,000 for rabbit anti-XBP1 (ab220783, Abcam, Cambridge, MA), 1: 200 for rabbit anti-PPARα (ab215270, Abcam, Cambridge, MA), 1: 200 for rabbit anti-ABCA1 (ab18180, Abcam, Cambridge, MA). The membrane was then incubated with a secondary antibody (1: 5,000, Peroxidase-conjugated affinity goat anti-mice IgG, HA1001, HUABIO, China). ImageJsoftware (National Institutes of Health, Bethesda, MD) was used to scan and analyze the western blot band to obtain protein quantitative data.

Cell Proliferation Assay

The cells were planted in 96-well plates with a density of 1×10^4 cells per well. After the cells were cultured for 24 h, 10 μl of CCK8 solution was added to each well of the 96-well plate and mixed. After in a 37°C incubator for 3 h, the optical density was measured at 450 nm wavelength with a microplate reader (Infinite M200 PRO, TECAN, Switzerland).

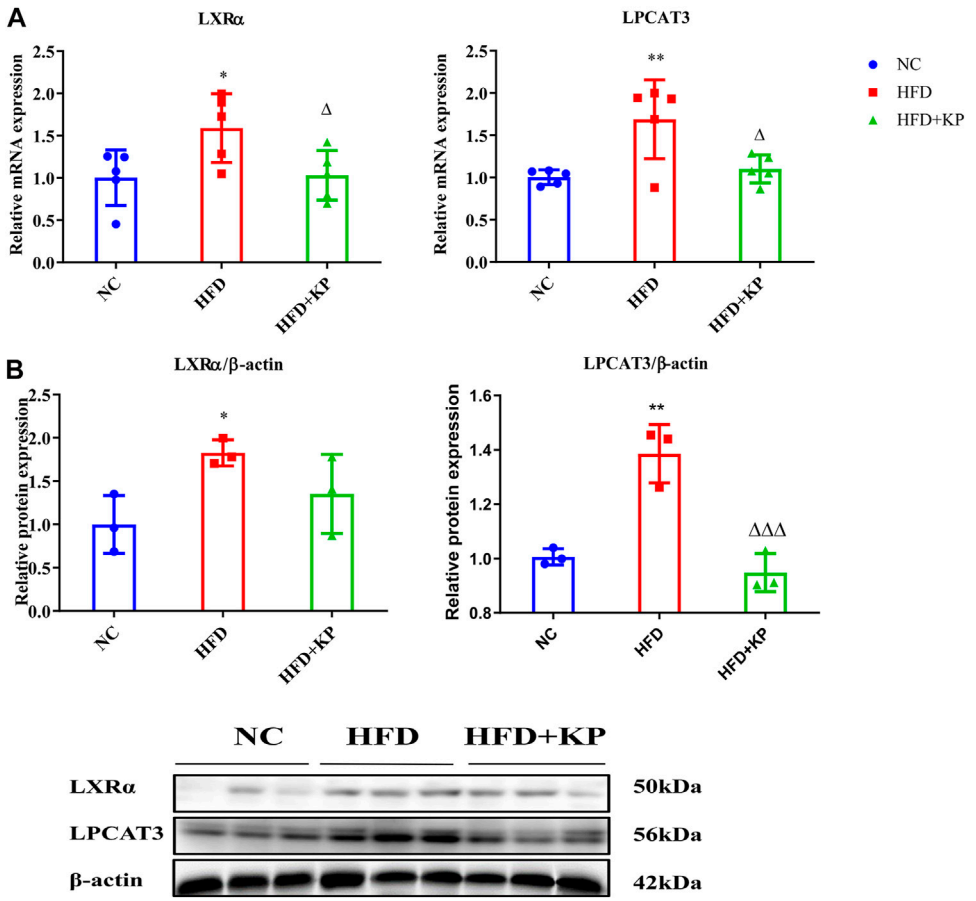


FIGURE 1 | KP regulated the mRNA and protein expression of LXRα and LPCAT3 *in vivo*. **(A)**: mRNA level expression of LXRα and LPCAT3 in liver samples; **(B)**: Protein level expression of LXRα and LPCAT3 in liver samples. NC: Normal control group, HFD: HFD group, HFD + KP: HFD + KP group. Quantification of mRNA and protein level expression was normalized to ß-actin levels. Compared with group NC, *, $p < 0.05$, **, $p < 0.01$; Compared with group HFD, △, $p < 0.05$.

Triglyceride Detection

The cells were planted in 96-well plates with a density of 1×10^4 cells per well. After 24 h of incubation, the cell suspension was extracted, and TG was detected according to the instructions in the intracellular TG kit (A110-1, Jiancheng, Nanjing, China).

Oil Red O Staining

The cells were cultured in a 12-well plate with a cell density of 2×10^5 cells per well. After the cells were cultured for 24 h, the culture medium in the 12-well plate was discarded. The cells were washed twice with PBS and fixed with 4% paraformaldehyde for 30 min. The fixatives were removed in the 12-well plate and cells were washed twice with PBS. Oil Red O staining solution (G1262, Solarbio, Beijing, China) was added to the 12-well plate and incubate for 30 min. The cells were washed with 60% isopropanol and stained with hematoxylin for 30 s. Finally, the cells were rinsed three times with distilled water.

Statistical Analysis

All experimental data were analyzed using GraphPad Prism version 8.0, and all data are presented as the means ± SEM. One-way analysis of variance assessment with Tukey's test and Bonferroni's post hoc test was used to statistically analyze differences among groups. $p < 0.05$ was considered significant.

RESULTS

Kaempferol Significantly Reduced the Expression of Liver X Receptors α and Lysophosphatidylcholine Acyltransferase 3 in High-Fat Diet-Induced Non-Alcoholic Steatohepatitis Mouse Model

In order to study whether KP played a role in the LXRα-LPCAT3-ERS pathway, the mRNA and protein expression of LXRα and LPCAT3 levels in liver in the NASH mice model were first studied. Compared with group NC, the mRNA expression of LXRα and LPCAT3 in the liver in group HFD were significantly higher ($p < 0.05$ and $p < 0.01$, respectively) (**Figure 1A**). Compared with the HFD group, the expression of LXRα and LPCAT3 mRNA in the group HFD + KP was drastically

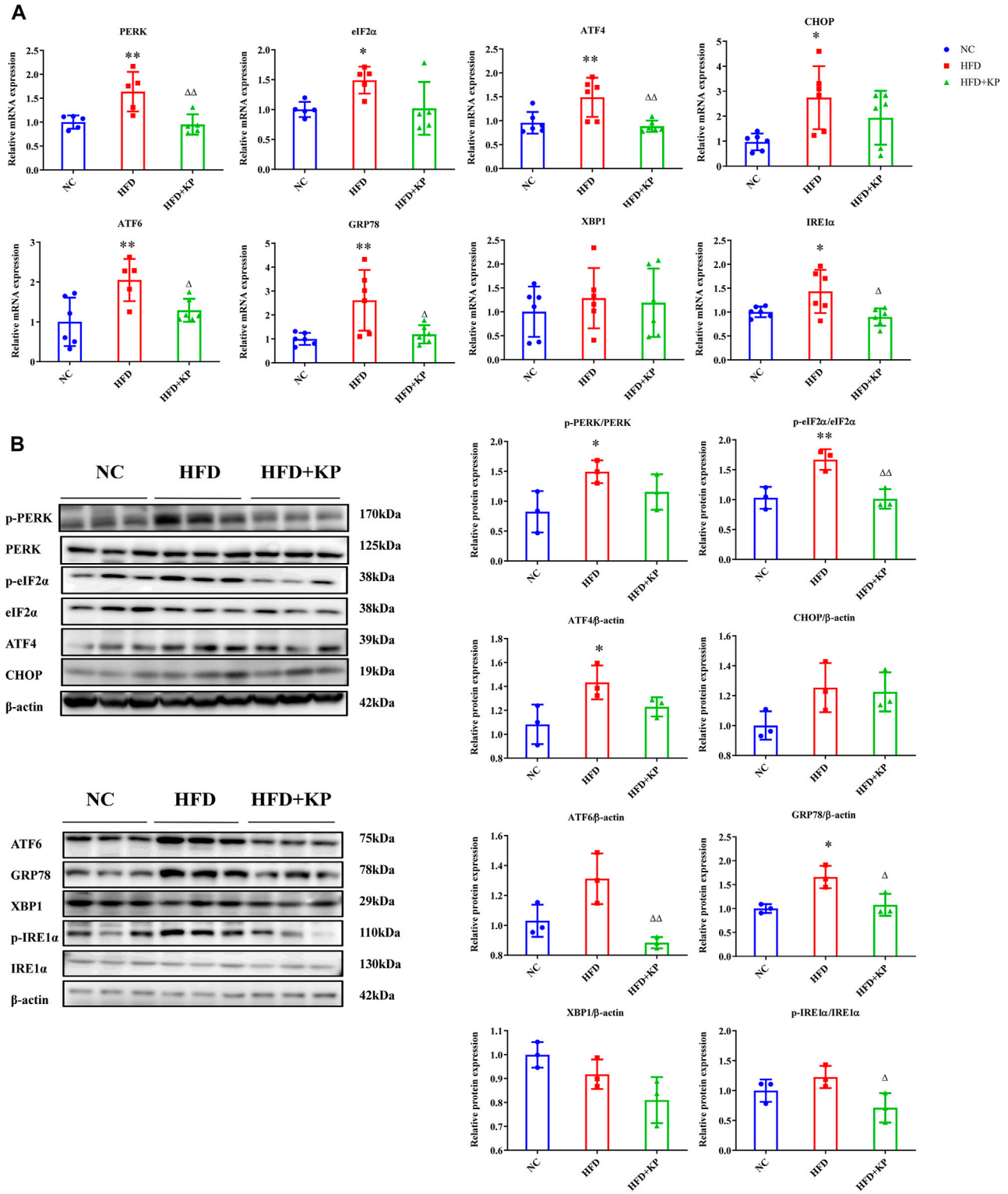


FIGURE 2 | KP regulated the mRNA and protein expression of factors related to ERS *in vivo*. **(A)**: mRNA expression in liver samples; **(B)**: protein expression in liver samples. NC: Normal control group, HFD: HFD group, HFD + KP: HFD + KP group. For **(A,B)**, Quantification of mRNA and protein level expression was normalized to β-actin levels, except protein phosphorylation level expression of PERK, eIF2α, IRE1α expression was normalized to their prototypes. Compared with group NC, *, $p < 0.05$, **, $p < 0.01$; Compared with group HFD, △, $p < 0.05$, △△, $p < 0.01$.

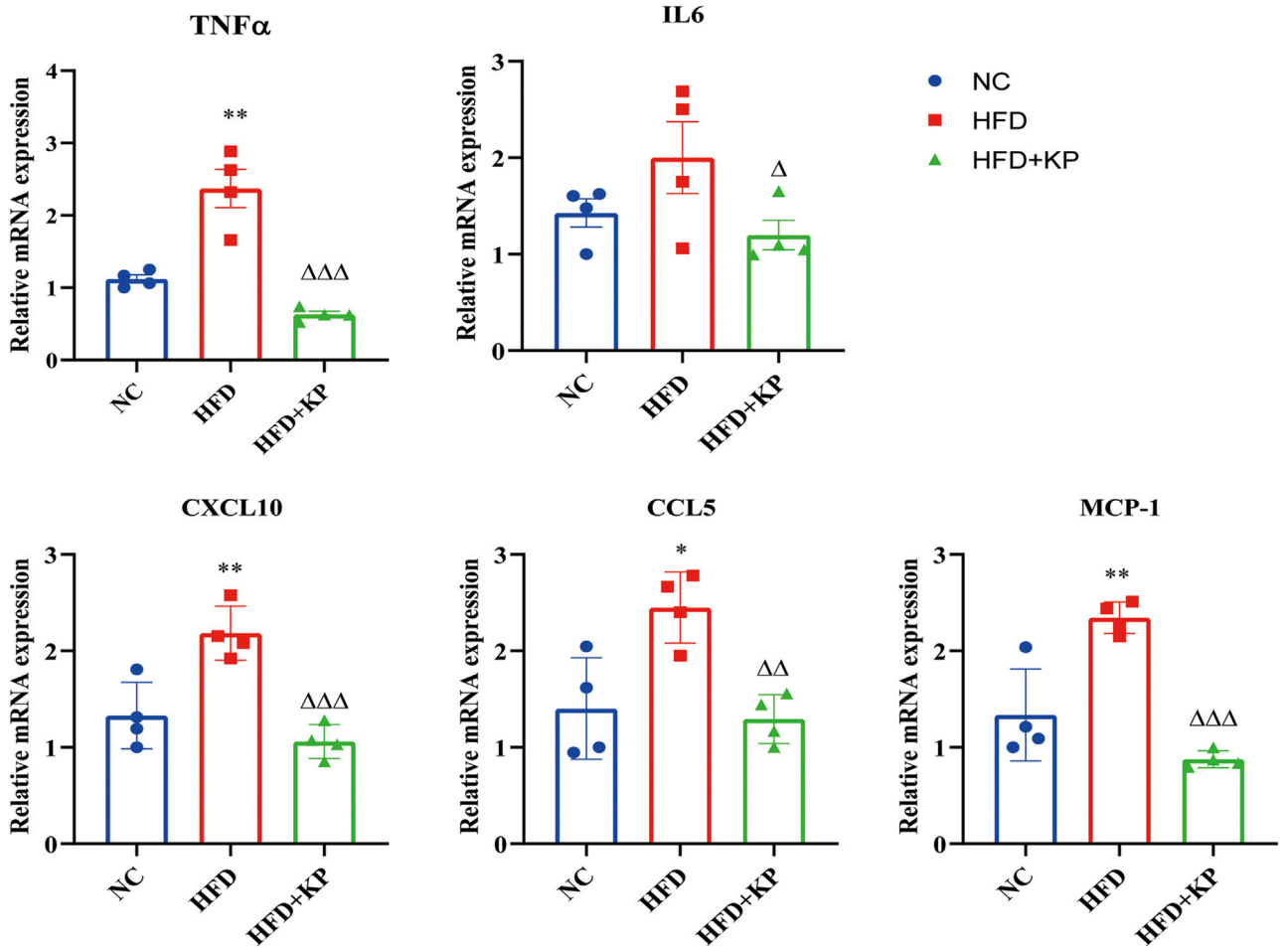


FIGURE 3 | KP reduced the mRNA expression of inflammatory factors *in vivo*. NC: Normal control group, HFD: HFD group, HFD + KP: HFD + KP group. Quantification of mRNA level expression was normalized to β-actin levels. Compared with group NC, *, $p < 0.05$, **, $p < 0.01$; Compared with group HFD, △, $p < 0.05$, △△, $p < 0.01$, △△△, $p < 0.001$.

decreased ($p < 0.05$ and $p < 0.05$, respectively) (**Figure 1A**). The similar result was obtained at the protein level. However, though the protein expression of LXRα in group HFD + KP was lower than that in group M, there was no statistical difference (**Figure 1B**).

Kaempferol Regulated the Expression of Factors Related to the Endoplasmic Reticulum Stress Signaling Pathway in High-Fat Diet-Induced Non-Alcoholic Steatohepatitis Mouse Model

Next, we further analyzed the expression of related molecules in the following step involved in ERS. RT-qPCR results showed that the mRNA levels of PERK, eIF2α, ATF4, CHOP, ATF6, GRP78 and IRE1α in the liver in the HFD group were significantly increased than thoses in NC group. After KP intervention, the mRNA expressions of PERK, ATF4, ATF6, GRP78 and IRE1α were significantly reduced. However, there was no statistically significance of the mRNA levels of eIF2α, CHOP and XBP1 (**Figure 2A**).

At the protein level, compared with the NC group, the phosphorylation levels of PERK and eIF2α in the liver in the HFD group have been extensively multiplied ($p < 0.05$ and $p < 0.01$, respectively), and the protein expression of ATF4 and GRP78 also elevated notably ($p < 0.05$). However, the protein expression of ATF6, XBP1 and IRE1α in group HFD did not change appreciably compared with group NC. After KP intervention, the phosphorylation levels of eIF2α and IRE1α were significantly reduced, and the protein expression levels of eIF2α, ATF6 and GRP78 were also significantly reduced. The differences between PERK, ATF4, CHOP and XBP1 expression among groups were not statistically significant (**Figure 2B**). Collectively, these results indicate that KP can protect liver from ERS damage induced by HFD.

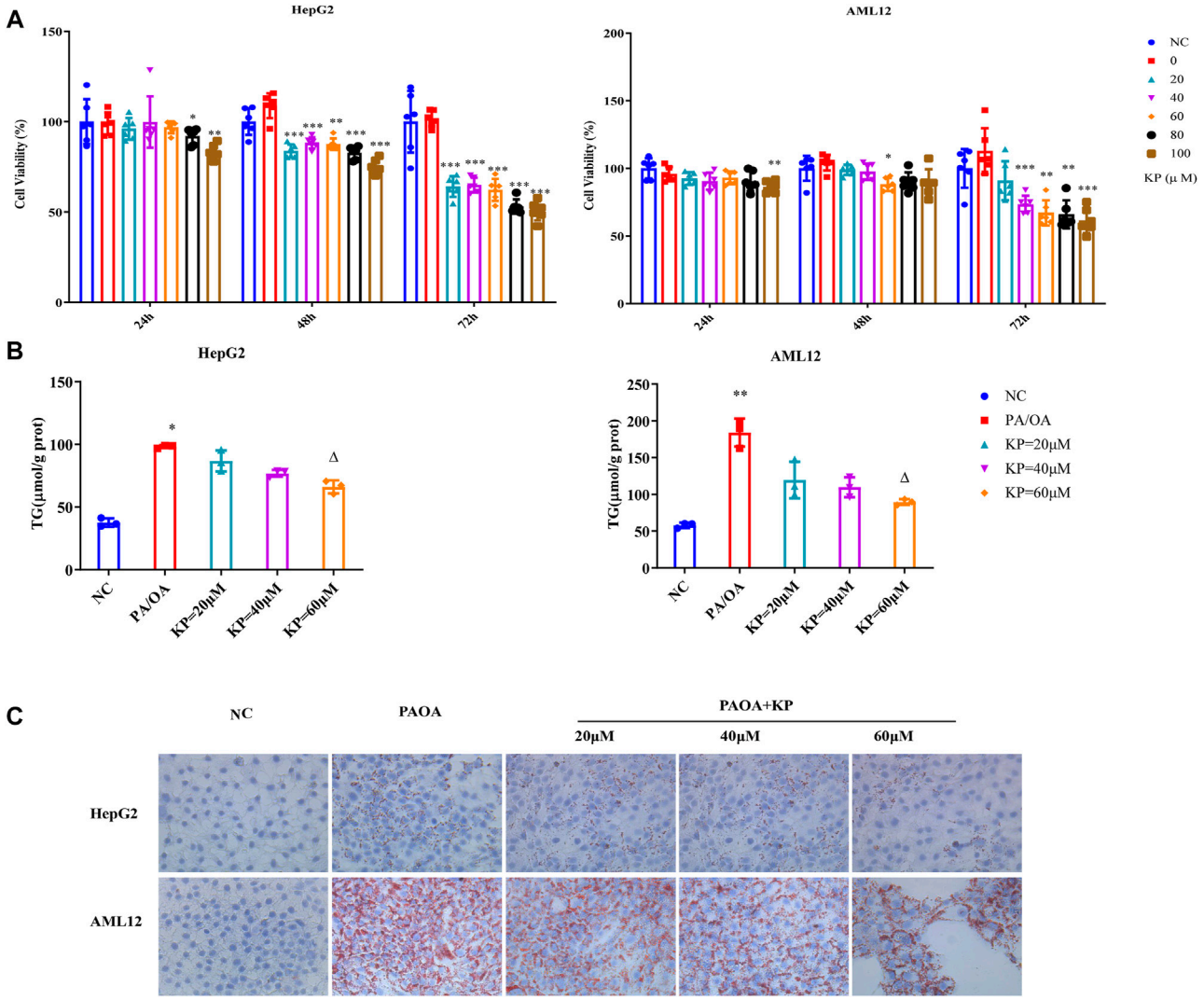


FIGURE 4 | KP reduced the deposition of lipid droplets in cells induced by PA/OA. **(A)**: The survival rate of HepG2 and AML12 cells after the intervention of KP in different concentration and time; **(B)**: The change of TG content after different concentration of KP in HepG2 and AML12 cells interfered with PA/OA (0.375/0.75 mM); **(C)**: The oil red O staining in HepG2 and AML12 cells interfered with PA/OA (0.375/0.75 mM) and/or KP with different concentrations (× 400). NC: Normal control group, PA/OA: PA/OA group, KP = 20 μM: KP low concentration group, KP = 40 μM: KP medium concentration group, KP = 60 μM: KP high concentration group. Compared with group NC, *, $p < 0.05$, **, $p < 0.01$, ***, $p < 0.001$; Compared with group PA/OA, △, $p < 0.05$.

Kaempferol Reduced the mRNA Expression of Inflammatory Factors in the High-Fat Diet-Induced Non-Alcoholic Steatohepatitis Mouse Model

In order to find out whether KP can improve the state of NASH, qRT-PCR was used to detect the mRNA expression of inflammation-related factors in liver tissues. Compared with the NC group, the expressions of tumor necrosis factor α (TNFα), C-X-C motif chemokine 10 (CXCL10), C-C chemokine ligand 5 (CCL5) and monocyte chemoattractant protein-1 (MCP-1) mRNA in the HFD group increased, and interleukin 6 (IL6) had a rising trend, but there was no statistical difference. After KP treatment, the mRNA expression levels of TNF-α, IL6, CXCL10, CCL5 and MCP-1 in the HFD + KP group were significantly reduced (**Figure 3**).

Kaempferol Reduced the Deposition of Lipid Droplets in Cells Induced by Palmitic Acid/Oleic Acid

In order to verify the efficacy of KP on NASH, we further established an *in vitro* steatosis model. First of all, the best simulation condition of PA/OA and the best intervention condition of KP in cells were selected. PA/OA was used to establish the model in HepG2 and AML12 cells. The three test results of CCK8 cell viability detection, oil red O staining method and cell TG content were comprehensively analyzed. We found

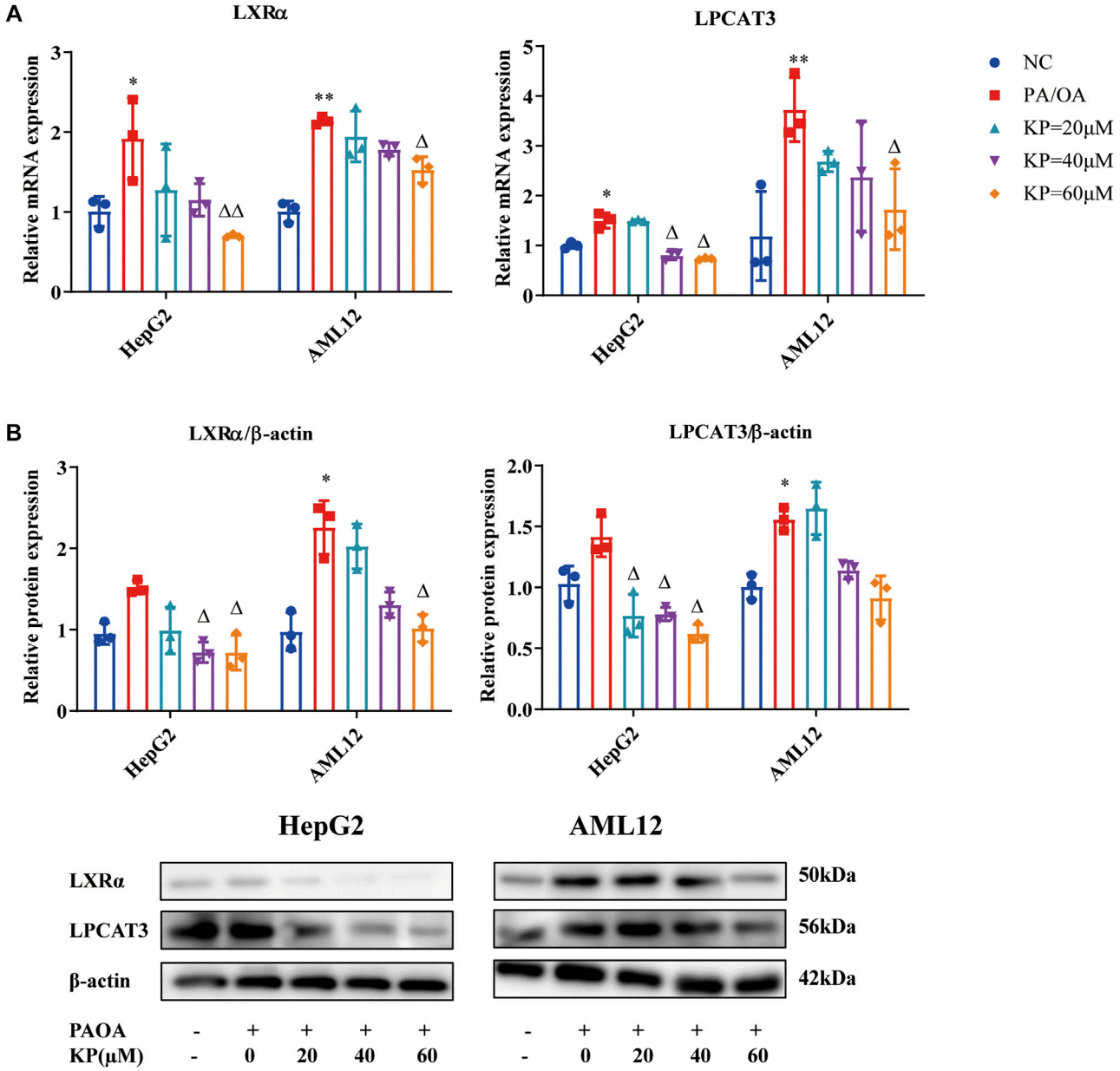


FIGURE 5 | KP regulated the mRNA and protein expression of LXRα and LPCAT3 *in vitro*. **(A)**: mRNA level expression of LXRα and LPCAT3 in HepG2 and AML12 cells; **(B)**: Protein level expression of LXRα and LPCAT3 in HepG2 and AML12 cells. NC: Normal control group, PA/OA: PA/OA group, KP = 20 μM: KP low concentration group, KP = 40 μM: KP medium concentration group, KP = 60 μM: KP high concentration group. Quantification of mRNA and protein level expression was normalized to ß-actin levels. Compared with group NC, *, $p < 0.05$, **, $p < 0.01$; Compared with group PA/OA, △, $p < 0.05$, △△, $p < 0.01$.

that when the PA/OA concentration was 0.375/0.75 mM, the activity of HepG2 and AML12 cells was not significantly affected. At the same time, a large number of intracellular lipid droplets were formed, and the intracellular TG content was significantly higher than that of the normal control group (**Supplementary Figure S2**). Therefore, 0.375/0.75 mM PA/OA was selected as the best concentration for modeling. To evaluate the effect of KP on cell viability, KP at concentrations of 0, 20, 40, 60, 80, and 100 μM were added to HepG2 and AML12 cells, and then were cultured for 24, 48, and 72 h, respectively. It was finally found that when the concentration was not higher than 60 μM and within a 24 h time, KP was safe and non-toxic to HepG2 and AML12 cells. Therefore, this concentration range and time were selected as the intervention conditions for subsequent KP intervention experiments (**Figure 4A**).

Based on the above conditions, it was divided into normal control group (NC), PA/OA group (PA/OA 0.375/0.75 mM), KP low-dose group (PA/OA 0.375/0.75 mM + KP 20 μM), KP medium dose group (PA/OA 0.375/0.75 mM + KP 40 μM), KP high-dose group (PA/OA 0.375/0.75 mM + KP 60 μM) *in vitro*. In

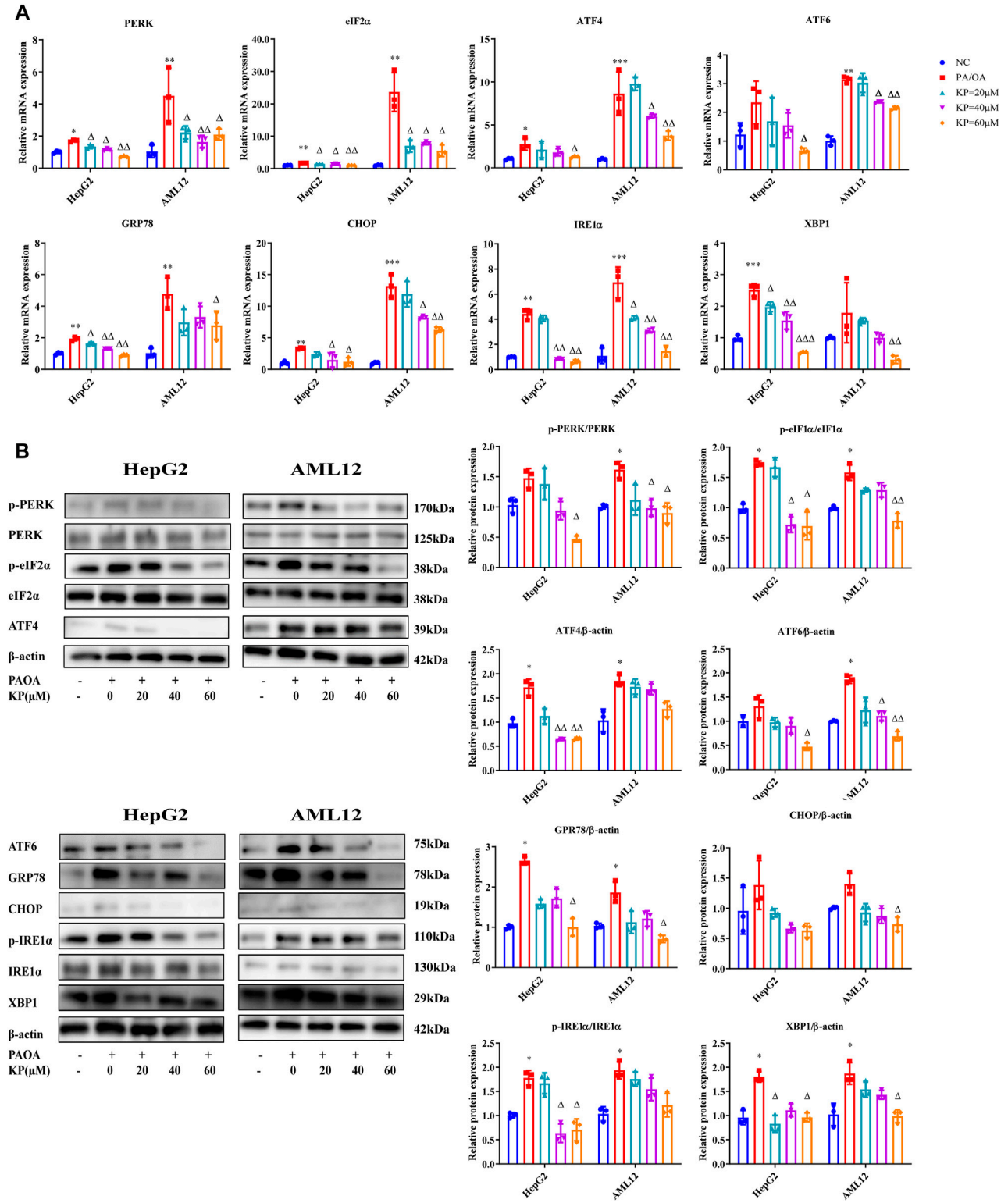


FIGURE 6 | KP regulated the mRNA and protein expression of factors related to ERS *in vitro*. **(A)**: mRNA Expression in HepG2 and AML12 cells; **(B)**: protein Expression in HepG2 and AML12 cells. NC: Normal control group, PA/OA: PA/OA group, KP = 20 μM: KP low concentration group, KP = 40 μM: KP medium concentration group, KP = 60 μM: KP high concentration group. Quantification of mRNA and protein level expression was normalized to β-actin levels, except protein phosphorylation level expression of PERK, eIF2α, IRE1α expression was normalized to their prototypes. Compared with group NC, *, $p < 0.05$, **, $p < 0.01$, ***, $p < 0.001$; Compared with group PA/OA, △, $p < 0.05$, △△, $p < 0.01$.

different dose groups of KP, PA/OA and KP were added to the medium at the same time and cultured for 24 h. The results confirmed that, in contrast with group NC, TG content in HepG2 cells and AML12 cells in group PA/OA were significantly increased ($p < 0.05$ and $p < 0.01$, respectively). After treatment with KP at three concentrations of 20, 40 and 60 μM, the TG content of HepG2 and AML12 cells decreased, and the concentration decreased notably at 60 μM ($p < 0.05$) (**Figure 4B**). Oil red O staining showed that the deposition of lipid droplets in HepG2 and AML12 cells in the PA/OA group increased compared with that in the NC group, and KP significantly reduced lipid deposition in both cells (**Figure 4C**).

Kaempferol Reduced the Expression of Liver X Receptors α and Lysophosphatidylcholine Acyltransferase 3 in Palmitic Acid/Oleic Acid-Induced Steatosis Model Cells

It has been validated that KP can reduce the expression of LXRα and LPCAT3 in liver tissue, and an *in vitro* model has been used to further verify this result.

The mRNA levels of LXRα and LPCAT3 in the PA/OA group were substantially up-regulated in both HepG2 and AML12 cells induced by PA/OA. After KP intervention, the mRNA transcription of LXRα and LPCAT3 were significantly down-regulated (**Figure 5A**).

Western blot results showed that the level of LXRα protein increased in the two cells in the PA/OA group, and it was more obvious in AML12 cells ($p < 0.05$). After the intervention of different concentrations of KP, the LXRα protein levels of the two cells were all down-regulated (**Figure 4B**). Compared with group NC, the protein level of LPCAT3 in each cell of group PA/OA was increased, while it was significantly increased in AML12 cells ($p < 0.05$) (**Figure 5B**). The protein level of LPCAT3 in the two cells decreased in a concentration-dependent manner when the KP concentration was 40 and 60 μM. It can be seen from the above results that KP can significantly reduce the expression of LXRα and LPCAT3 in the steatosis model.

Kaempferol Regulated the Expression of Factors Related to the Endoplasmic Reticulum Stress Signaling Pathway in Palmitic Acid/Oleic Acid-Induced Steatosis Model Cells

Subsequently, the mRNA expression and protein expression levels of the ERS-related factors of HepG2 and AML12 cells were detected.

Compared with group NC, the mRNA levels of PERK, eIF2α, ATF4, CHOP, ATF6, GRP78, XBP1 and IRE1α in group PA/OA were increased. The expression of PERK, eIF2α, ATF4, CHOP, ATF6, GRP78, XBP1 and IRE1α mRNA in the KP group were significantly reduced. After KP intervention, the down-regulation of eIF2α, ATF4, XBP1 and IRE1α mRNA in the two types of cells all showed concentration-dependent tolerance, whilst the down-regulation of PERK and CHOP mRNA was only concentration-dependent in HepG2 cells (**Figure 6A**).

The phosphorylation levels of PERK, eIF2α and IRE1α in the PA/OA group were higher than those in the NC group not only in HepG2 but also in AML12 cells, however the adjustments in the phosphorylation level of PERK in HepG2 cells were not statistically significant. The protein expressions of ATF4, CHOP, ATF6, GRP78 and XBP1 in the PA/OA group of the two cells also increased significantly. After the intervention of different concentrations of KP, the protein expression levels of these factors in the two cells were reduced, and the phosphorylation levels of PERK and eIF2α in the high-concentration group of KP decreased more significantly. In the two kinds of cells, the protein levels of ATF6, ATF4, CHOP, GRP78 and XBP1 were significantly reduced in the high concentration group. The phosphorylation level of IRE1α in the KP medium and high concentration groups of HepG2 cells extensively decreased, and the phosphorylation level of IRE1α in the KP intervention groups in AML12 cells showed a downward trend, but it was not obvious (**Figure 6B**).

Kaempferol Reduced the mRNA Expression of Inflammatory Factors in Palmitic Acid/Oleic Acid-Induced Steatosis Model Cells

We also examined the mRNA expression of inflammation-related factors in cells using qRT-PCR.

Compared with the NC group, the mRNA levels of TNFα, IL6, CXCL10, CCL5 and MCP-1 in the PA/OA group increased significantly in the two types of cells. In hepG2 cells, TNF-α, IL6, CCL5 and MCP-1 all showed a decrease in KP concentration dependent tolerance, and CXCL10 only decreased in the middle and high concentration groups of KP. In AML12 cells, the mRNA levels of IL6, CXCL10 and CCL5 were significantly down-regulated after KP intervention. TNFα did not decrease significantly when KP = 20 μM, but mRNA levels decreased significantly at KP = 40 and 60 μM. The expression of MCP-1 showed no obvious downward trend after KP intervention (**Figure 7**).

Kaempferol Regulated Lipid Metabolism Both *in vivo* and *in vitro*

Peroxisome proliferator-activated receptor-α (PPAR-α) belongs to the PPAR subfamily, which is a type of nuclear receptor highly expressed in the liver. PPARα will be activated to enhance the oxidation of fatty acids when fatty acids in the liver are elevated (Pawlak et al., 2015). It was found that when liver PPARα was specifically knocked out, liver steatosis would increase (Montagner et al., 2016a). ATP binding cassette transporter A1 (ABCA1) is a transport protein involved in high-density lipoprotein (HDL) biosynthesis and cellular cholesterol homeostasis. Phospholipids and free cholesterol can be transferred to apolipoprotein A1 by ABCA1, and then form new HDL particles (Phillips, 2018). Previous studies have shown that overexpression of ABCA1 can reduce liver lipid

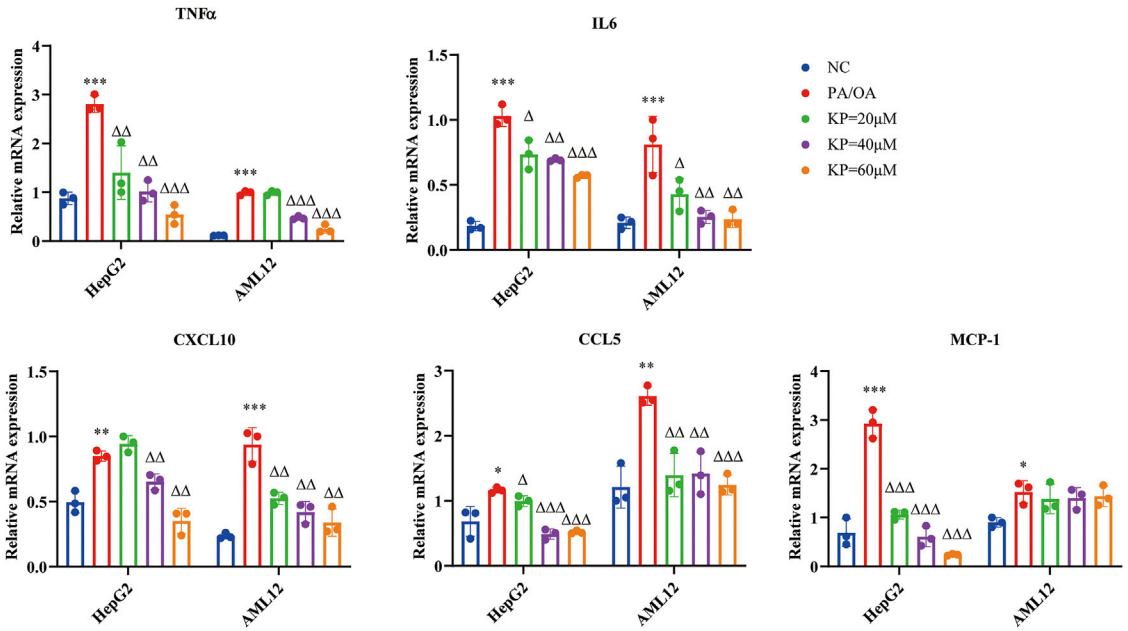


FIGURE 7 | KP reduced the mRNA expression of inflammatory factors *in vitro*. NC: Normal control group, PA/OA: PA/OA group, KP = 20 μM: KP low concentration group, KP = 40 μM: KP medium concentration group, KP = 60 μM: KP high concentration group. Quantification of mRNA expression was normalized to β-actin levels. Compared with group NC, *, $p < 0.05$, **, $p < 0.01$, ***, $p < 0.001$; Compared with group PA/OA, △, $p < 0.05$, △△, $p < 0.01$, △△△, $p < 0.001$.

levels (Yang et al., 2010; Liu et al., 2014). In the present study, we found that the mRNA and protein expression of PPAR-α and ABCA1 decreased in the HFD-induced NASH model than the control group, and also in the PA/OA-induced steatosis cell model, while KP could increase their expression both *in vivo* and *in vitro* (**Supplementary Figure S3**). These results suggest that KP plays a role in regulating lipid metabolism.

DISCUSSION

NAFLD, as one of the common diseases affecting human life and health in the world, has attracted more and more attention to researchers (Fan et al., 2017; Younossi et al., 2018). It is expected that the incidence of NAFLD would increase to 314.58 million by 2030 in China. Compared with the number of cases in 2016 (246.33 million cases), the increase was 29.1% (Estes et al., 2018). NASH is a type of NAFLD, and approximately 20% of NASH patients will develop liver cirrhosis. Now, NASH has become the main cause of liver transplantation in American patients (Sheka et al., 2020).

Our former study has shown that KP was effective against improving liver injury in HFD-induced NASH mice model (Lu et al., 2020). In the present study, we further demonstrated that KP can modulate the mRNA or the protein expression of the molecules involved in LXRα-LPCAT3-ERS pathway in both HFD-induced mice model and PA/OA-induced steatosis cell model. To our best knowledge, it is the first time to illustrate the molecular mechanism of KP on improving NASH.

KP is a type of aglycone flavonoids existing in a variety of plants, which has antibacterial, anti-inflammatory, antioxidant, anti-tumor, heart protection, neuroprotective and anti-diabetes effects (Chen and Chen, 2013; Dabeek and Marra, 2019; Imran et al., 2019). In our previous studies, it has been proved that KP can alleviate liver injury in HFD-induced NASH mice model (Lu et al., 2020). In this study, in order to verify the efficacy of KP on NASH, HepG2 and AML12 cell lines were selected to establish an *in vitro* cell model of steatosis using PA/OA. As similiar as the results *in vivo*, the content of TG in the steatosis model group decreased after the intervention of KP (20, 40, and 60 μM), in particular in the high concentration group, suggesting that KP attenuates the TG storage of PA/OA-induced steatosis cell model. From the results of oil red O staining, KP can also substantially decrease lipid deposition in fatty degeneration cells. These data further verified that KP can improve PA/OA induced liver steatosis.

The LXRα-LPCAT3 pathway is an important regulator of PLs metabolism, metabolic stress response and inflammation. Till now, there are different points on the role of LPCAT3 in the lipogenesis. LXR activation promotes the entry of unsaturated fatty acids into PLs through LPCAT3, thereby reducing liver ERS and inflammation (Rong et al., 2013). Patrick et al. (Ferrara et al., 2021) found that mice with skeletal muscle-specific knockout of LPCAT3 (LPCAT3-MKO) exhibited greater muscle lyso-PC/PC, concomitant with improved skeletal muscle insulin sensitivity. Conversely, skeletal muscle-specific overexpression of LPCAT3 (LPCAT3-MKI) promoted glucose intolerance. Thibaut et al. (Bourgeois et al., 2020) found that deletion of

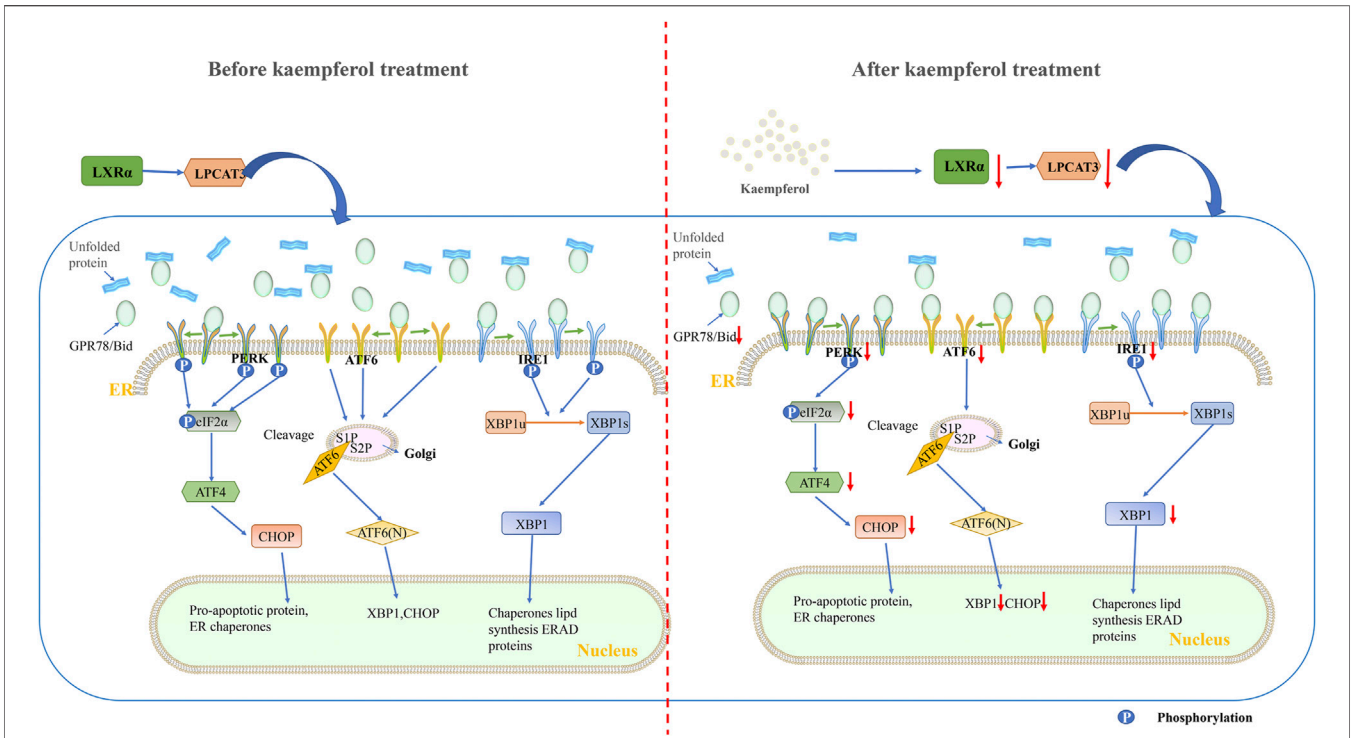


FIGURE 8 | Schematic diagram of the mechanism of KP regulating LXRα-LPCAT3 signaling pathway. KP intervention suppressed endoplasmic reticulum stress. The LXR-LPCAT3-ERS pathway is activated when induced by HFD or PA/OA. This allows unfolded proteins to accumulate in the ER. At the same time, GPR78 dissociates from PERK, IRE1, and ATF6, and then binds to the unfolded protein. The dissociated PERK, IRE1 and ATF6 were activated. CHOP-induced apoptosis occurs when PERK, IRE1, ATF6 and their downstream pathways are continuously activated. The expression of LXR and LPCAT3 decreased significantly when treated with KP, and then the unfolded protein decreased, PERK, IRE1 and ATF6 dissociated from GRP78 decreased. Abbreviations: HFD: high fat diet, PA/OA: Palmitic acid/Oleic acid, LPCAT3: lysophosphatidylcholine acyltransferase 3, LXR α: liver X receptor alpha, PERK: protein kinase R-like ER kinase, Eif-2α: eukaryotic translation initiation factor 2α, ATF6: activating transcription factor 6, IRE1: inositol-requiring enzyme 1, XBP1: X-box-binding protein 1, ATF4: activating transcription factor 4, CHOP: C/EBP homologous protein, ERAD: Endoplasmic reticulum-associated degradation.

LPCAT3 in myeloid cells worsened hepatic steatosis after a high-fat diet. Recent study has shown that LPCAT3 is a direct PPAR-δ target gene and has a novel function of PPAR-δ in regulation of phospholipid metabolism through LPCAT3 (Singh and Liu, 2017a).

In this study, after the intervention of KP, the mRNA levels and protein expression levels of LXR and LPCAT3 were decreased in the liver tissues of the NASH mice model. Our studies supported that LPCAT3 was highly expressed in NASH model by the involvement of lipogenesis. The above studies support that KP can improve lipid accumulation through LXR-LPCAT3.

Wang et al. (2013) showed that LPCAT3 regulated the formation of ERS and inflammation. ERS is considered to be one of the necessary mechanisms that purpose liver steatosis and inflammatory changes (Rong et al., 2013). After ERS stimulation, the PERK/elF2α, ATF6 and IRE1/XBP-1 signal pathways are activated, and the mRNA and protein expression of PERK, eIF2α, ATF4, ATF6, IRE1α and GRP78 are considerably increased, which induces CHOP expression and promotes cell apoptosis (Wang and Kaufman, 2016). ERS will dissociate PERK from GPR78/bid, and then the downstream elF2α will be phosphorylated (Donnelly et al., 2013). Phosphorylated elF2α reduced the general translation rate, but activated the downstream translation of ATF4 and CHOP (Malhi and Kaufman, 2011; Luhr et al., 2019). The expression of the anti-apoptotic gene BCL-2 can be inhibited by CHOP, thereby accelerating cell death (Marciniak et al., 2004). ATF6 will transfer to the Golgi apparatus when it is activated. It becomes ATF6 (n) after being cleaved in the Golgi apparatus and regulates ERS together with XBP1s (Walter et al., 2018). The misfolded protein phosphorylates IRE1α and induces conformational changes in the RNase domain (Ghosh et al., 2014). Next, XBP1 is cut into XBP1s, which initiates the UPR gene expression program in response to ERS (Yoshida et al., 2001; Huang et al., 2019).

In our study, KP was used to interfere with NASH mouse model and PA/OA-induced steatosis model cells. It was found that after KP intervention, the expression of factors related to ERS decreased significantly from both mice and cells. First, the levels of PERK, eIF2α, ATF4 and CHOP in the PERK pathway were significantly decreased. Second, the expression of ATF6 in the ATF6 pathway also decreased. Third, the expression of IRE1α and XBP1 in the IRE1α pathway was also significantly inhibited. In addition, the expression of GPR78 was also suppressed, possibly because the dissociation of GPR78 from PERK, ATF6 and IRE1α became less. We concluded that KP regulates ERS status by

reducing the expression of LXR-LPACT3, thereby improving lipid degeneration (**Figure 8**).

Cytokines are the main mediators required for the comprehensive response to various stimuli in the immune and inflammatory process. It includes interleukin, tumor necrosis factor, chemokine family, etc. These factors are key regulators that initiate and drive inflammatory diseases (Borish and Steinke, 2003). TNFα and IL6 are up-regulated in many inflammatory diseases, such as rheumatoid arthritis (van Schouwenburg et al., 2013; Pandolfi et al., 2020), inflammatory lung diseases (Malaviya et al., 2017) and tumors (Balkwill, 2006; Jones and Jenkins, 2018). Malaviya et al. (2017) showed that TNFα antagonists showed a good effect on inflammatory lung disease. Nakagawa et al. (2014) found that inflammatory macrophages activated by ERS promote the release of inflammatory mediators such as TNFα and IL6. In the liver, CCL5 and CXCL10 can regulate the cytopathic and antiviral immune response of T cells and natural killer cells. MCP-1 can promote the accumulation of macrophages, steatosis and inflammation (Marra and Tacke, 2014). Fan et al. (2020) found that CXCL10 promoted the recruitment of natural killer cells to the liver in the NASH model induced by the methionine-and choline-deficient diet (MCD). CCL5 was significantly up-regulated in HFD-induced liver fibrosis model (Li B.-H. et al., 2017). Baeck et al. (2012) found that blocking MCP-1 can reduced macrophage infiltration and reduced the release of pro-inflammatory factors TNFα, interferon g and IL6. Our results showed that KP can regulate the release of inflammatory factors in the NASH mouse model and cell model by improving ERS, and ultimately reduce liver inflammation.

However, there are still several limitations in the present study. For example, LPCAT3 gene knockout animal models or siRNA interference techniques have not been used to further confirm the role of LPCAT3 in the mechanism of KP on improving NASH. Primary cells have not been used to build cell models. In a bioinformatics analysis study on NAFLD, it is mentioned that the occurrence of NAFLD is also related to insulin signaling pathway, PPAR signaling pathway, p53 signaling pathway and mitogen-activated protein kinase (MAPK) signaling pathway (Liu et al., 2020). The study found that giving p53 knockout mice a high-fat diet reduced the occurrence of NAFLD. Moreover, knocking out P53 in the cell also reduced the accumulation of lipids in the cell (Zhang et al., 2020). Tomita et al. (2012) showed that the expression of p53 and p66Shc was up-regulated in the liver tissue of the NASH mouse model. Montagner et al. (2016a) found that lack of PPARα in hepatocytes leads to susceptibility to steatosis, which may be related to the damage of fatty acid catabolism. Inhibition of MAPK signaling pathway also showed the effect of reducing liver lipid deposition and liver fibrosis in rats (Shen et al., 2019). It has been discovered that KP intervention affects the expression of PPARα and ABCA1, but the specific mechanism is still unclear. The role of the above pathways in the occurrence of NAFLD and NASH, and whether KP also plays a therapeutic role through these pathways will be the direction of our further research.

CONCLUSION

In summary, this study has confirmed that KP can improve liver damage by regulating LXRα-LPCAT3 and inhibiting ERS from both *in vivo* and *in vitro*. At the same time, the expression of inflammatory factors is reduced. The role of KP provides a new direction for the treatment of NASH. LPCAT3 can also be used as a potential target for NASH treatment.

DATA AVAILABILITY STATEMENT

The raw data supporting the conclusions of this article will be made available by the authors, without undue reservation, to any qualified researcher.

ETHICS STATEMENT

The animal study was reviewed and approved by the Shanghai University of Traditional Chinese Medicine. Written informed consent was obtained from the owners for the participation of their animals in this study.

AUTHOR CONTRIBUTIONS

TW and GJ, study design and conceptualization; HX, MS, and YL, Animal feeding and sample collection; HX, YL, and JW, data analysis; HX, MS, and TW, drafting the manuscript; TW and GJ, revising the manuscript and obtaining the funding. All authors have approved the final draft submitted.

FUNDING

This work was supported by the National Natural Science Foundation of China (81620108030, 81873076), the Shanghai Talents development fund Project (2017090) and the Hundred Talents Program from Shanghai University of Traditional Chinese Medicine.

SUPPLEMENTARY MATERIAL

The Supplementary Material for this article can be found online at: https://www.frontiersin.org/articles/10.3389/fphar.2021.690736/full#supplementary-material

REFERENCES

Ashrafizadeh, M., Tavakol, S., Ahmadi, Z., Roomiani, S., Mohammadinejad, R., and Samarghandian, S. (2020). Therapeutic Effects of Kaempferol Affecting Autophagy and Endoplasmic Reticulum Stress. *Phytother Res.* 34, 911–923. doi:10.1002/ptr.6577

Baeck, C., Wehr, A., Karlmark, K. R., Heymann, F., Vucur, M., Gassler, N., et al. (2012). Pharmacological Inhibition of the Chemokine CCL2 (MCP-1) Diminishes Liver Macrophage Infiltration and Steatohepatitis in Chronic Hepatic Injury. *Gut* 61, 416–426. doi:10.1136/gutjnl-2011-300304

Balkwill, F. (2006). TNF-alpha in Promotion and Progression of Cancer. *Cancer Metastasis Rev.* 25, 409–416. doi:10.1007/s10555-006-9005-3

Borish, L. C., and Steinke, J. W. (2003). 2. Cytokines and Chemokines. *J. Allergy Clin. Immunol.* 111, S460–S475. doi:10.1067/mai.2003.108

Bourgeois, T., Jalil, A., Thomas, C., Magnani, C., Le Guern, N., Gautier, T., et al. (2020). Deletion of Lysophosphatidylcholine Acyltransferase 3 in Myeloid Cells Worsens Hepatic Steatosis after a High-Fat Diet. *J. Lipid Res.* 62, 100013. doi:10.1194/jlr.RA120000737

Brenner, C., Galluzzi, L., Kepp, O., and Kroemer, G. (2013). Decoding Cell Death Signals in Liver Inflammation. *J. Hepatol.* 59, 583–594. doi:10.1016/j.jhep.2013.03.033

Chaudhari, N., Talwar, P., Parimisetty, A., Lefebvre D'hellencourt, C., and Ravanan, P. (2014). A Molecular Web: Endoplasmic Reticulum Stress, Inflammation, and Oxidative Stress. *Front Cel Neurosci* 8, 213. doi:10.3389/fncel.2014.00213

Chen, A. Y., and Chen, Y. C. (2013). A Review of the Dietary Flavonoid, Kaempferol on Human Health and Cancer Chemoprevention. *Food Chem.* 138, 2099–2107. doi:10.1016/j.foodchem.2012.11.139

Dabeek, W. M., and Marra, M. V. (2019). Dietary Quercetin and Kaempferol: Bioavailability and Potential Cardiovascular-Related Bioactivity in Humans. *Nutrients* 11. doi:10.3390/nu11102288

Dasgupta, D., Nakao, Y., Mauer, A. S., Thompson, J. M., Sehrawat, T. S., Liao, C. Y., et al. (2020). IRE1A Stimulates Hepatocyte-Derived Extracellular Vesicles that Promote Inflammation in Mice with Steatohepatitis. *Gastroenterology* 159, 1487–e17. doi:10.1053/j.gastro.2020.06.031

Demeure, O., Lecerf, F., Duby, C., Desert, C., Ducheix, S., Guillou, H., et al. (2011). Regulation of LPCAT3 by LXR. *Gene* 470, 7–11. doi:10.1016/j.gene.2010.09.002

Demirtas, L., Guclu, A., Erdur, F. M., Akbas, E. M., Ozcicek, A., Onk, D., et al. (2016). Apoptosis, Autophagy & Endoplasmic Reticulum Stress in Diabetes Mellitus. *Indian J. Med. Res.* 144, 515–524. doi:10.4103/0971-5916.200887

Donnelly, N., Gorman, A. M., Gupta, S., and Samali, A. (2013). The eIF2α Kinases: Their Structures and Functions. *Cell Mol Life Sci* 70, 3493–3511. doi:10.1007/s00018-012-1252-6

Estes, C., Anstee, Q. M., Arias-Loste, M. T., Bantel, H., Bellentani, S., Caballeria, J., et al. (2018). Modeling NAFLD Disease burden in China, France, Germany, Italy, Japan, Spain, United Kingdom, and United States for the Period 2016-2030. *J. Hepatol.* 69, 896–904. doi:10.1016/j.jhep.2018.05.036

Fan, J. G., Kim, S. U., and Wong, V. W. (2017). New Trends on Obesity and NAFLD in Asia. *J. Hepatol.* 67, 862–873. doi:10.1016/j.jhep.2017.06.003

Fan, Y., Zhang, W., Wei, H., Sun, R., Tian, Z., and Chen, Y. (2020). Hepatic NK Cells Attenuate Fibrosis Progression of Non-alcoholic Steatohepatitis in Dependent of CXCL10-mediated Recruitment. *Liver Int.* 40, 598–608. doi:10.1111/liv.14307

Ferrara, P. J., Rong, X., Maschek, J. A., Verkerke, A. R., Siripoksup, P., Song, H., et al. (2021). Lysophospholipid Acylation Modulates Plasma Membrane Lipid Organization and Insulin Sensitivity in Skeletal Muscle. *J. Clin. Invest.* 131, 135963. doi:10.1172/JCI135963

Friedman, S. L., Neuschwander-Tetri, B. A., Rinella, M., and Sanyal, A. J. (2018). Mechanisms of NAFLD Development and Therapeutic Strategies. *Nat. Med.* 24, 908–922. doi:10.1038/s41591-018-0104-9

Ghosh, R., Wang, L., Wang, E. S., Perera, B. G., Igbaria, A., Morita, S., et al. (2014). Allosteric Inhibition of the IRE1α RNase Preserves Cell Viability and Function during Endoplasmic Reticulum Stress. *Cell* 158, 534–548. doi:10.1016/j.cell.2014.07.002

Hernández-Alvarez, M. I., Sebastián, D., Vives, S., Ivanova, S., Bartoccioni, P., Kakimoto, P., et al. (2019). Deficient Endoplasmic Reticulum-Mitochondrial Phosphatidylserine Transfer Causes Liver Disease. *Cell* 177, 881–e17. doi:10.1016/j.cell.2019.04.010

Hu, H., Tian, M., Ding, C., and Yu, S. (2018). The C/EBP Homologous Protein (CHOP) Transcription Factor Functions in Endoplasmic Reticulum Stress-Induced Apoptosis and Microbial Infection. *Front. Immunol.* 9, 3083. doi:10.3389/fimmu.2018.03083

Huang, S., Xing, Y., and Liu, Y. (2019). Emerging Roles for the ER Stress Sensor IRE1α in Metabolic Regulation and Disease. *J. Biol. Chem.* 294, 18726–18741. doi:10.1074/jbc.REV119.007036

Imran, M., Salehi, B., Sharifi-Rad, J., Aslam Gondal, T., Saeed, F., Imran, A., et al. (2019). Kaempferol: A Key Emphasis to its Anticancer Potential. *Molecules* 24. doi:10.3390/molecules24122277

Iurlaro, R., and Muñoz-Pinedo, C. (2016). Cell Death Induced by Endoplasmic Reticulum Stress. *FEBS J.* 283, 2640–2652. doi:10.1111/febs.13598

Jones, S. A., and Jenkins, B. J. (2018). Recent Insights into Targeting the IL-6 Cytokine Family in Inflammatory Diseases and Cancer. *Nat. Rev. Immunol.* 18, 773–789. doi:10.1038/s41577-018-0066-7

Kouhestani, S., Jafari, A., and Babaei, P. (2018). Kaempferol Attenuates Cognitive Deficit via Regulating Oxidative Stress and Neuroinflammation in an Ovariectomized Rat Model of Sporadic Dementia. *Neural Regen. Res.* 13, 1827–1832. doi:10.4103/1673-5374.238714

Lebeaupin, C., Vallée, D., Rousseau, D., Patouraux, S., Bonnafous, S., Adam, G., et al. (2018). Bax Inhibitor-1 Protects from Nonalcoholic Steatohepatitis by Limiting Inositol-Requiring Enzyme 1 Alpha Signaling in Mice. *Hepatology* 68, 515–532. doi:10.1002/hep.29847

Lee, B., Kwon, M., Choi, J. S., Jeong, H. O., Chung, H. Y., and Kim, H. R. (2015a). Kaempferol Isolated from *Nelumbo nucifera* Inhibits Lipid Accumulation and Increases Fatty Acid Oxidation Signaling in Adipocytes. *J. Med. Food* 18, 1363–1370. doi:10.1089/jmf.2015.3457

Lee, Y.-J., Choi, H.-S., Seo, M.-J., Jeon, H.-J., Kim, K.-J., and Lee, B.-Y. (2015b). Kaempferol Suppresses Lipid Accumulation by Inhibiting Early Adipogenesis in 3T3-L1 Cells and Zebrafish. *Food Funct.* 6, 2824–2833. doi:10.1039/c5fo00481k

Li, B.-H., He, F.-P., Yang, X., Chen, Y.-W., and Fan, J.-G. (2017a). Steatosis Induced CCL5 Contributes to Early-Stage Liver Fibrosis in Nonalcoholic Fatty Liver Disease Progress. *Translational Res. : J. Lab. Clin. Med.* 180. doi:10.1016/j.trsl.2016.08.006

Li, F., Yang, Y., Yang, L., Wang, K., Zhang, X., Zong, Y., et al. (2017b). Resveratrol Alleviates FFA and CCl4 Induced Apoptosis in HepG2 Cells via Restoring Endoplasmic Reticulum Stress. *Oncotarget* 8, 43799–43809. doi:10.18632/oncotarget.16460

Li, S., and Pu, X.-P. (2011). Neuroprotective Effect of Kaempferol against a 1-Methyl-4-Phenyl-1,2,3,6-Tetrahydropyridine-Induced Mouse Model of Parkinson's Disease. *Biol. Pharm. Bull.* 34, 1291–1296. doi:10.1248/bpb.34.1291

Liu, J., Lin, B., Chen, Z., Deng, M., Wang, Y., Wang, J., et al. (2020). Identification of Key Pathways and Genes in Nonalcoholic Fatty Liver Disease Using Bioinformatics Analysis. *Arch. Med. Sci.* 16, 374–385. doi:10.5114/aoms.2020.93343

Liu, W., Qin, L., Yu, H., Lv, F., and Wang, Y. (2014). Apolipoprotein A-I and Adenosine Triphosphate-Binding Cassette Transporter A1 Expression Alleviates Lipid Accumulation in Hepatocytes. *J. Gastroenterol. Hepatol.* 29, 614–622. doi:10.1111/jgh.12430

Lu, Y., Shao, M., Xiang, H., Zheng, P., Wu, T., and Ji, G. (2020). Integrative Transcriptomics and Metabolomics Explore the Mechanism of Kaempferol on Improving Nonalcoholic Steatohepatitis. *Food Funct.* 11, 10058–10069. doi:10.1039/d0fo02123g

Luhr, M., Torgersen, M. L., Szalai, P., Hashim, A., Brech, A., Staerk, J., et al. (2019). The Kinase PERK and the Transcription Factor ATF4 Play Distinct and Essential Roles in Autophagy Resulting from Tunicamycin-Induced ER Stress. *J. Biol. Chem.* 294, 8197–8217. doi:10.1074/jbc.RA118.002829

Malaviya, R., Laskin, J. D., and Laskin, D. L. (2017). Anti-Tnfα Therapy in Inflammatory Lung Diseases. *Pharmacol. Ther.* 180, 90–98. doi:10.1016/j.pharmthera.2017.06.008

Malhi, H., and Kaufman, R. J. (2011). Endoplasmic Reticulum Stress in Liver Disease. *J. Hepatol.* 54, 795–809. doi:10.1016/j.jhep.2010.11.005

Marciniak, S. J., Yun, C. Y., Oyadomari, S., Novoa, I., Zhang, Y., Jungreis, R., et al. (2004). CHOP Induces Death by Promoting Protein Synthesis and Oxidation in the Stressed Endoplasmic Reticulum. *Genes Dev.* 18, 3066–3077. doi:10.1101/gad.1250704

Marra, F., and Tacke, F. (2014). Roles for Chemokines in Liver Disease. *Gastroenterology* 147, 577–e1. doi:10.1053/j.gastro.2014.06.043

Montagner, A., Polizzi, A., Fouché, E., Ducheix, S., Lippi, Y., Lasserre, F., et al. (2016a). Liver PPARα Is Crucial for Whole-Body Fatty Acid Homeostasis and Is Protective against NAFLD. *Gut* 65, 1202–1214. doi:10.1136/gutjnl-2015-310798

Nakagawa, H., Umemura, A., Taniguchi, K., Font-Burgada, J., Dhar, D., Ogata, H., et al. (2014). ER Stress Cooperates with Hypernutrition to Trigger TNF-dependent Spontaneous HCC Development. *Cancer cell* 26, 331–343. doi:10.1016/j.ccr.2014.07.001

Nobili, V., Alisi, A., Valenti, L., Miele, L., Feldstein, A. E., and Alkhouri, N. (2019). NAFLD in Children: New Genes, New Diagnostic Modalities and New Drugs. *Nat. Rev. Gastroenterol. Hepatol.* 16, 517–530. doi:10.1038/s41575-019-0169-z

Ozcan, L., and Tabas, I. (2012). Role of Endoplasmic Reticulum Stress in Metabolic Disease and Other Disorders. *Annu. Rev. Med.* 63, 317–328. doi:10.1146/annurev-med-043010-144749

Pandolfi, F., Franza, L., Carusi, V., Altamura, S., Andriollo, G., and Nucera, E. (2020). Interleukin-6 in Rheumatoid Arthritis. *Int. J. Mol. Sci.* 21. doi:10.3390/ijms21155238

Pawlak, M., Lefebvre, P., and Staels, B. (2015). Molecular Mechanism of PPARα Action and its Impact on Lipid Metabolism, Inflammation and Fibrosis in Non-alcoholic Fatty Liver Disease. *J. Hepatol.* 62, 720–733. doi:10.1016/j.jhep.2014.10.039

Phillips, M. C. (2018). Is ABCA1 a Lipid Transfer Protein? *J. Lipid Res.* 59, 749–763. doi:10.1194/jlr.R082313

Ren, J., Lu, Y., Qian, Y., Chen, B., Wu, T., and Ji, G. (2019). Recent Progress Regarding Kaempferol for the Treatment of Various Diseases. *Exp. Ther. Med.* 18, 2759–2776. doi:10.3892/etm.2019.7886

Rong, X., Albert, C. J., Hong, C., Duerr, M. A., Chamberlain, B. T., Tarling, E. J., et al. (2013). LXRs Regulate ER Stress and Inflammation through Dynamic Modulation of Membrane Phospholipid Composition. *Cell Metab* 18, 685–697. doi:10.1016/j.cmet.2013.10.002

Sheka, A. C., Adeyi, O., Thompson, J., Hameed, B., Crawford, P. A., and Ikramuddin, S. (2020). Nonalcoholic Steatohepatitis: A Review. *JAMA* 323, 1175–1183. doi:10.1001/jama.2020.2298

Shen, X., Guo, H., Xu, J., and Wang, J. (2019). Inhibition of lncRNA HULC Improves Hepatic Fibrosis and Hepatocyte Apoptosis by Inhibiting the MAPK Signaling Pathway in Rats with Nonalcoholic Fatty Liver Disease. *J. Cel Physiol* 234, 18169–18179. doi:10.1002/jcp.28450

Singh, A. B., and Liu, J. (2017a). Identification of Hepatic Lysophosphatidylcholine Acyltransferase 3 as a Novel Target Gene Regulated by Peroxisome Proliferator-Activated Receptor δ. *J. Biol. Chem.* 292, 884–897. doi:10.1074/jbc.M116.743575

Suchal, K., Malik, S., Khan, S. I., Malhotra, R. K., Goyal, S. N., Bhatia, J., et al. (2017). Molecular Pathways Involved in the Amelioration of Myocardial Injury in Diabetic Rats by Kaempferol. *Int. J. Mol. Sci.* 18. doi:10.3390/ijms18051001

Takahashi, Y., and Fukusato, T. (2014). Histopathology of Nonalcoholic Fatty Liver Disease/nonalcoholic Steatohepatitis. *World J. Gastroenterol.* 20, 15539–15548. doi:10.3748/wjg.v20.i42.15539

Tomita, K., Teratani, T., Suzuki, T., Oshikawa, T., Yokoyama, H., Shimamura, K., et al. (2012). p53/p66Shc-mediated Signaling Contributes to the Progression of Non-alcoholic Steatohepatitis in Humans and Mice. *J. Hepatol.* 57, 837–843. doi:10.1016/j.jhep.2012.05.013

Van Schouwenburg, P. A., Rispens, T., and Wolbink, G. J. (2013). Immunogenicity of Anti-TNF Biologic Therapies for Rheumatoid Arthritis. *Nat. Rev. Rheumatol.* 9, 164–172. doi:10.1038/nrrheum.2013.4

Vance, J. E. (2015). *Phospholipid Synthesis and Transport in Mammalian Cells*. Copenhagen, Denmark: Traffic, 16.

Walter, F., O'brien, A., Concannon, C. G., Düssmann, H., and Prehn, J. H. M. (2018). ER Stress Signaling Has an Activating Transcription Factor 6α (ATF6)-dependent "Off-Switch". *J. Biol. Chem.* 293, 18270–18284. doi:10.1074/jbc.RA118.002121

Wang, B., Rong, X., Duerr, M. A., Hermanson, D. J., Hedde, P. N., Wong, J. S., et al. (2016). Intestinal Phospholipid Remodeling Is Required for Dietary-Lipid Uptake and Survival on a High-Fat Diet. *Cel Metab* 23, 492–504. doi:10.1016/j.cmet.2016.01.001

Wang, H., Chen, L., Zhang, X., Xu, L., Xie, B., Shi, H., et al. (2019). Kaempferol Protects Mice from D-GalN/LPS-Induced Acute Liver Failure by Regulating the ER Stress-Grp78-CHOP Signaling Pathway. *Biomed. Pharmacother.* 111, 468–475. doi:10.1016/j.biopha.2018.12.105

Wang, M., and Kaufman, R. J. (2016). Protein Misfolding in the Endoplasmic Reticulum as a Conduit to Human Disease. *Nature* 529, 326–335. doi:10.1038/nature17041

Wang, M., Sun, S., Wu, T., Zhang, L., Song, H., Hao, W., et al. (2013). Inhibition of LXRα/SREBP-1c-Mediated Hepatic Steatosis by Jiang-Zhi Granule. *Evid. Based Complement. Alternat Med.* 2013, 584634. doi:10.1155/2013/584634

Yang, Y., Jiang, Y., Wang, Y., and An, W. (2010). Suppression of ABCA1 by Unsaturated Fatty Acids Leads to Lipid Accumulation in HepG2 Cells. *Biochimie* 92, 958–963. doi:10.1016/j.biochi.2010.04.002

Yoshida, H., Matsui, T., Yamamoto, A., Okada, T., and Mori, K. (2001). XBP1 mRNA Is Induced by ATF6 and Spliced by IRE1 in Response to ER Stress to Produce a Highly Active Transcription Factor. *Cell* 107, 881–891. doi:10.1016/s0092-8674(01)00611-0

Younossi, Z., Anstee, Q. M., Marietti, M., Hardy, T., Henry, L., Eslam, M., et al. (2018). Global burden of NAFLD and NASH: Trends, Predictions, Risk Factors and Prevention. *Nat. Rev. Gastroenterol. Hepatol.* 15, 11–20. doi:10.1038/nrgastro.2017.109

Zhang, C., Chen, X., Zhu, R. M., Zhang, Y., Yu, T., Wang, H., et al. (2012). Endoplasmic Reticulum Stress Is Involved in Hepatic SREBP-1c Activation and Lipid Accumulation in Fructose-Fed Mice. *Toxicol. Lett.* 212, 229–240. doi:10.1016/j.toxlet.2012.06.002

Zhang, X., Lin, Y., Lin, S., Li, C., Gao, J., Feng, Z., et al. (2020). Silencing of Functional P53 Attenuates NAFLD by Promoting HMGB1-Related Autophagy Induction. *Hepatol. Int.* 14, 828–841. doi:10.1007/s12072-020-10068-4

Conflict of Interest: The authors declare that the research was conducted in the absence of any commercial or financial relationships that could be construed as a potential conflict of interest.

Copyright © 2021 Xiang, Shao, Lu, Wang, Wu and Ji. This is an open-access article distributed under the terms of the Creative Commons Attribution License (CC BY). The use, distribution or reproduction in other forums is permitted, provided the original author(s) and the copyright owner(s) are credited and that the original publication in this journal is cited, in accordance with accepted academic practice. No use, distribution or reproduction is permitted which does not comply with these terms.

frontiers in Pharmacology

ORIGINAL RESEARCH
published: 21 July 2021
doi: 10.3389/fphar.2021.686502

Bicyclol Alleviates Signs of BDL-Induced Cholestasis by Regulating Bile Acids and Autophagy-Mediated HMGB1/p62/Nrf2 Pathway

Jingwen Zhao[1]†, Maojuan Ran[1,2]†, Ting Yang[1,3]†, Liwei Chen[1], Peixu Ji[1], Xiuxiu Xu[1], Lu Zhang[1], Siyuan Sun[1], Xin Liu[1], Simin Zhou[1], Lu Zhou[1]* and Jie Zhang[1]**

[1]Department of Gastroenterology and Hepatology, Tianjin Medical University General Hospital, Tianjin Institute of Digestive Disease, Tianjin Key Laboratory of Digestive Diseases, Tianjin, China, [2]Department of Gastroenterology and Hepatology, Chengdu Second People's Hospital, Chengdu, China, [3]Department of Gastroenterology, Shanxi Provincial People's Hospital, Taiyuan, China

Cholestasis is a liver disease characterized by the accumulation of toxic bile salts, bilirubin, and cholesterol, resulting in hepatocellular damage. Recent findings have revealed several key steps of cholestasis liver injury including the toxicity of bile acids and accumulation of proinflammatory mediator. In this study, we investigated the protective effect of bicyclol in cholestasis caused by bile duct ligation (BDL), as well as relevant mechanisms. Bicyclol attenuated liver damage in BDL mice by increasing the levels of hydrophilic bile acid such as α-MCA and β-MCA, regulating bile acid-related pathways and improving histopathological indexes. High-mobility group box 1 (HMGB1) is an extracellular damage-associated molecular pattern molecule which can be used as biomarkers of cells and host defense. Bicyclol treatment decreased extracellular release of HMGB1. In addition, HMGB1 is also involved in regulating autophagy in response to oxidative stress. Bicyclol promoted the lipidation of LC3 (microtubule-associated protein 1 light chain 3)-II to activate autophagy. The nuclear factor, E2-related factor 2 (Nrf2) and its antioxidant downstream genes were also activated. Our results indicate that bicyclol is a promising therapeutic strategy for cholestasis by regulating the bile acids and autophagy-mediated HMGB1/p62/Nrf2 pathway.

Keywords: liver injury, cholestasis, BDL, high mobility group box 1, autophagy, Nrf2, bicyclol

OPEN ACCESS

Edited by:
Ralf Weiskirchen,
RWTH Aachen University, Germany

Reviewed by:
Yao Wang,
Renmin Hospital of Wuhan University, China
Shih-Yi Lin,
Taichung Veterans General Hospital, Taiwan
Sun Lixin,
China Pharmaceutical University, China

***Correspondence:**
Jingwen Zhao
jingwenzhao@tmu.edu.cn
Lu Zhou
zhou_lu@126.com
Jie Zhang
zhangjiezhj@163.com

†*These authors have contributed equally to this work and share first authorship*

Specialty section:
This article was submitted to Gastrointestinal and Hepatic Pharmacology, a section of the journal Frontiers in Pharmacology

Received: *27 March 2021*
Accepted: *05 July 2021*
Published: *21 July 2021*

Citation:
Zhao J, Ran M, Yang T, Chen L, Ji P, Xu X, Zhang L, Sun S, Liu X, Zhou S, Zhou L and Zhang J (2021) Bicyclol Alleviates Signs of BDL-Induced Cholestasis by Regulating Bile Acids and Autophagy-Mediated HMGB1/p62/Nrf2 Pathway. Front. Pharmacol. 12:686502. doi: 10.3389/fphar.2021.686502

INTRODUCTION

Cholestasis is a pathological condition caused by obstruction or cessation of bile flow resulting in intrahepatic cholestasis and accompanied by cell injury, inflammatory infiltration, cell apoptosis, liver fibrosis, and even cirrhosis (Yokoda and Carey, 2019). Currently, the main drug treatment for chronic cholestatic liver injury is ursodeoxycholic acid (UDCA). However, some patients do not respond to this treatment (Wagner and Fickert, 2020). Hence, novel treatment approaches, which could be based on a comprehensive understanding of the mechanisms of the different stages of disease progression, are urgently needed.

A previous study found that primary bile acids conjugated with glycine or taurine were significantly increased in serum of patients with cholestasis liver injury (Woolbright et al., 2015). Bile acids (BAs), such as taurocholic acid (TCA), glycocholic acid (GCA), glycochenodeoxycholic acid (GCDCA), and glycodeoxycholic acid (GDCA), can be used as biomarkers of liver injury or as indicators of drug-induced liver injury (DILI) (Yang et al., 2019). The hydrophobicity of bile acids was affected by the number and orientation of the hydrophilic region, where lithocholic acid (LCA) was the most hydrophobic while cholic acid (CA) was less hydrophobic (Ashby et al., 2018). On the other hand, the conjugated groups also affected the hydrophobicity of bile acids, where unconjugated was the most hydrophobic and glycine conjugated was more hydrophobic than taurine or sulphate conjugated (Ashby et al., 2018). The toxicity of bile acids is mostly dependent on its hydrophobicity. According to previous studies, TCA, the major endogenous BAs in rodents, significantly increases the mRNA level of inflammatory cytokines monocyte chemotactic protein 1 (Ccl2) and macrophage inflammatory protein 2α (cxcl2) (Cai et al., 2017). The toxicity of BAs during obstructive cholestatic liver injury likely occurs because of biliary BAs leakage. Previous studies proved that biliary BAs at 0.5x dose resulted in significant hepatocyte necrosis (Woolbright et al., 2015).

High-mobility group box-1 (HMGB1) protein, a member of the high-mobility group 1 (HMG-1) family, modulates cell death in acute liver injury by NF-κB signal pathway activated by advanced glycan end products (RAGE) and toll-like receptor 4 (TLR4) (Eguchi et al., 2014). HMGB1 is involved in many liver diseases. Previous studies have found that the level of liver HMGB1 protein was correlated with alcoholic steatohepatitis (ASH) and primary biliary cirrhosis (PBC) in patients with chronic Hepatitis C virus (HCV), as well as in chronic carbon tetrachloride (CCl4) treated mice (Ge et al., 2018). HMGB1 levels also increased in BDL induced cholestatic mice (Woolbright et al., 2013; Dondorf et al., 2017), while carnosic acid provided protection against BDL induced fibrosis by inhibiting HMGB1 expression (Zhang et al., 2017a). HMGB1 is a proinflammatory cytokine released by injured cells and the innate immune system, which alerts other cells that infection or sterile injury has occurred (Andersson and Tracey, 2011). Neutrophils and Cxcl2, Ccl2 mRNA levels were significantly decreased in mice with hepatocyte-specific Hmgb1 knockout (Huebener et al., 2019).

Autophagy deficiency leads to the rise of HMGB1 levels and promotes ductular reaction and tumorigenesis *via* its receptor RAGE (Khambu et al., 2018). HMGB1 regulates autophagy under the circumstances of oxidative stress (Kang et al., 2011). The oxidation HMGB1 binding to Beclin1 causes the dissociation of Bcl-2 from Beclin1, leading to the induction of autophagy (Tang et al., 2010). So, autophagy and HMGB1 are closely connected. Autophagy includes five processes: initiation, elongation, closure, maturation, and degradation. LC3B and p62 are the most commonly used markers of autophagy. The carboxyl terminus of the LC3 protein is specifically cleaved to form LC3-Ⅰ with the exposed carboxyl-terminal glycine, which is combined with phosphatidylethanolamine to form LC3-Ⅱ (Kuma et al., 2017). LC3-Ⅱ targets the inner and outer membranes of autophagosomes to participate in the elongation step of autophagy (Kuma et al., 2017; Qian et al., 2017). P62 as a receptor for ubiquitinated proteins and organelles is selectively transported into the autophagosomes, after which it is degraded by autophagy (Ichimura and Komatsu, 2010).

The high levels of p62 associated with the suppression of autophagy competitively interacts with Kelch-like ECH-associated protein-1 (Keap1), the nuclear factor Nrf2-binding site, resulting in activation of Nrf2 and its target genes (Komatsu et al., 2010; Jiang et al., 2015). The activation of Nrf2 protects from various liver diseases through different molecular mechanisms (Xu et al., 2018). After activation, Nrf2 is translocated to the nucleus to activate heme oxygenase-1 (HO-1), NADPH quinone oxidoreductase-1 (NQO1), glutamate cysteine ligase (GCLC), and other genes to resist damage caused by oxidative stress (Galicia-Moreno et al., 2020). Nrf2-knockout mice are more susceptible to hepatic injury after BDL, as vitamin A activates Nrf2 to protect liver function in BDL rats, thus proving that Nrf2 activation is beneficial in cholestatic liver injury (Weerachayaphorn et al., 2012; Shin et al., 2013; Wang et al., 2014).

Bicyclol (4,4′-dimethoxy-5,6,5′,6′-bis (methylenedioxy)-2-hydroxymethyl-2′-methoxycarbonyl biphenyl) is a synthetic drug widely used to treat HCV (Li et al., 2018; Huang et al., 2019). Bicyclol has been proven to induce autophagy and inhibit cell proliferation through PI3K/AKT and MEK/ERK pathways (Wang et al., 2016b). Previous studies in our laboratory have shown that bicyclol can activate Nrf2 to act against CCl_4 induced hepatotoxicity (Zhao et al., 2020). What's more, Zhen, Yong-Zhan et al. have found that BDL-induced liver fibrosis can be significantly attenuated by bicyclol through reversing fibrogenic gene expression (Zhen et al., 2015). Nonetheless, there are still few studies on the mechanism of the protective effect of bicyclol in BDL-induced liver damage.

In this study, we aimed to explore the protective effect of bicyclol in BDL induced liver injury. Our research was mainly based on two aspects: the synthesis, excretion, and composition of bile acid, and the pathway associated with autophagy-mediated by HMGB1.

MATERIALS AND METHODS

Animals

Eleven-weeks old male (22–23 g) c57BL/6 mice were purchased from Beijing HFK Bioscience CO., LTD. All mice were housed in the SPF animal room with a constant temperature (22°C), and a 12/12 h light/dark cycles and were given free access to water and food. Before the experiment, mice were allowed to adapt to the environment for 1 week. All animal studies (including the mice euthanasia procedure) were done in compliance with the regulations and guidelines of the Animal Ethical and Welfare Committee (AEWC) at the Institute of Radiation Medicine

Chinese Academy of Medical Sciences and conducted according to the AAALAC and the IACUC guidelines.

The mice were randomly divided into three groups: Sham group (n = 8), BDL group (n = 6), and BDL + Bicyclol group (n = 6); the different numbers in different groups are due to the injury following BDL surgery. BDL was employed to induce cholestatic liver injury as described in a previous study (Fickert et al., 2002). Briefly, after anesthesia with isoflurane, the bile duct was separated from the portal vein and hepatic artery, then ligated using a 6–0 suture. The sham group underwent similar laparotomy without BDL. BDL + Bicyclol group was orally administered with bicyclol at a dose of 100 mg/kg (Hu and Liu, 2006; Zhen et al., 2015) body weight daily for 14 days, while sham and BDL group were treated with volume-matched 0.5% carboxymethylcellulose sodium (CMC-Na). Bicyclol was a kind gift from the Beijing Union Pharmaceutical Company (Beijing, China) with a purity of over 99%. Animals were sacrificed on days 14 after the operation, after which the blood and liver were collected and stored at −80°C for further research.

Serum Biochemical Analysis

The serum levels of aspartate transaminase (AST), alanine transaminase (ALT), alkaline phosphatase (ALP), γ-glutamyl transpeptadase (GGT), serum bile acid (TBA), and total cholesterol (TC) were measured by the automated chemistry analyzer (AU5800, Beckman Coulter, United States) of the clinical laboratory (Tianjin medical university general hospital).

Histology

Liver tissue was fixed in 4% paraformaldehyde at room temperature and blocked with paraffin wax, after which they were sectioned into 4 um thick slices and stained with hematoxylin and eosin (H&E) according to the standard H&E protocol. The inflammatory cell infiltration and necrosis were assessed by two experienced pathologists according to Ishak scoring criteria, including piece-meal necrosis, fusion necrosis, lytic necrosis, and portal inflammation (Ishak et al., 1995). Images were taken by Leica microscope (Leica DM5000B; Germany) at 200X magnification.

Measurement of Gallbladder Bile Acids Composition

Gallbladder bile was collected, and its composition was measured with liquid chromatography-tandem mass spectrometry (LC-MS/MS) (Yang et al., 2017). Briefly, standard samples were added into 50 ul bile samples, the supernatant was extracted after oscillation and centrifuged at 12,000 rpm for 10 min and then further concentrated on the concentrator. The concentrate was reconstituted in 100 uL of methyl/water (50/50) and analyzed by the LC-MS/MS system. The chromatographic separation was performed on the ACQUITY UPLC HSS T3 column (2.1*100 mm, 1.8 um). Data acquisition systems mainly included Ultra Performance Liquid Chromatography (Shim-pack UFLC SHIMADZU CBM30A) and Tandem mass spectrometry (Applied Biosystems 6500 QTRAP).

Immunofluorescence

The slides with liver samples were dewaxed with xylene and various ethanol concentrations and blocked with 5% bovine serum albumin (BSA) for 30 min. After that, the slides were incubated with primary antibodies against p62/SQSTM1 (no. NBP1-48320SS; Novus) at 4°C overnight. After being washed with PBS, the sections were incubated with secondary antibodies at 37°C for 1 h. The nuclei were stained with 4′-6′-diamino-2-phenylindole dihydrochloride (DAPI), and then sealed with resins. The sections were observed under a fluorescence microscope (Leica DM5000B; Germany).

Cell Culture and Treatment

Alpha mouse liver 12 cell line AML12 were purchased from the Chinese Academy of Sciences Cell Bank (Shanghai, China) and cultured in Dulbecco's Modified Eagle Media: Nutrient Mixture F-12 (DMEM—F12) (#119435; Gibco) supplemented with 10% fetal bovine serum (Gibco), 1% Insulin—Transferrin-Selenium (ITS) (#41400045; Gibco),40 ng/ml dexamethasone. Cells were grown in a humidified atmosphere with 5% CO_2 at 37°C. Once the cells reached confluency near 80%, they were digested with 0.125% trypsin-EDTA and seeded into 6-well plates. For analysis of protein and mRNA levels, cells were stimulated for 24 h with 100 uM TCA and/or 500 uM bicyclol. Taurocholic acid (TCA) was purchased from Sigma-Aldrich.

Western Blot

Liver tissues and cells were homogenized in RIPA buffer (Solarbio, China) that contained PMSF (Solarbio, China) and phosphatase inhibitors on ice. The homogenates were centrifuged, and supernatants were extracted, after which 1/3 volume of loading buffer was added and stored at −80°C for further study. The protein was quantified by a BCA protein assay kit (Solarbio, China). Equal amounts of proteins were separated by SDS-PAGE gels and transferred to nitrocellulose membranes. After blocking with 5% non-fat milk, membranes were incubated with primary antibodies overnight at 4°C. The primary anti-CYP7A1 (#sc-518007, Santa Cruz), anti-BSEP (#sc-74500, Santa Cruz), anti-FXR (#ab235094, Abcam), anti- SQSTM1/p62 (#39749, Cell Signaling Technology), anti-LC3A/B (D11) (#3868, Cell Signaling Technology), anti-Beclin-1 (#3495, Cell Signaling Technology), anti-HMGB1 (#6893, Cell Signaling Technology), anti-RAGE (ab216329, Abcam, Cambridge, MA, United States), anti-TLR4 (#A17436, ABclonal Technology), anti-NRF2 (#12721, Cell Signaling Technology), anti-Keap1 (#A17061, ABclonal Technology) and anti-β-actin (#3700, Cell Signaling Technology) were used. The secondary horseradish peroxidase-conjugated goat anti-rabbit or anti-mouse IgG antibodies (Zhongshan Golden Bridge Biotechnology, Beijing, China) were incubated at room temperature for 1 h. After fully washing, the ECL Reagent (Solarbio, China) and Image Lab (Bio-Rad, America) were used to analyze the bands.

TABLE 1 | Specific qPCR primers used in this study.

Gene name	Forward primer (5'-3')	Reverse primer (5'-3')
Gapdh	GGAGAAACCTGCCAAGTATG	TGGGAGTTGCTGTTGAAGTC
Cyp7a1	AACAACCTGCCAGTACTAGATAG	GTGTAGAGTGAAGTCCTCCTTAGC
Fxr	GGCCTCTGGGTACCACTACA	TGTACACGGCGTTCTTGGTA
Bsep	CTGCCAAGGATGCTAATGCA	CGATGGCTACCCTTTGCTTCT
Tnf-α	GGTGCCATGTCTCAGCCTCTT	GCCATAGAACTGATGAGAGGGAG
IL-1β	GCCATAGAACTGATGAGAGGGAG	GCCATAGAACTGATGAGAGGGAG
Nrf2	CTTTAGTCAGCGACAGAAGGAC	AGGCATCTTGTTTGGGAATGTG
Nqo1	AGGATGGGAGGTACTCGAATC	TGCTAGAGATGACTCGGAAGG
Hmox1	GATAGAGCGCAACAAGCAGAA	CAGTGAGGCCCATACCAGAAG

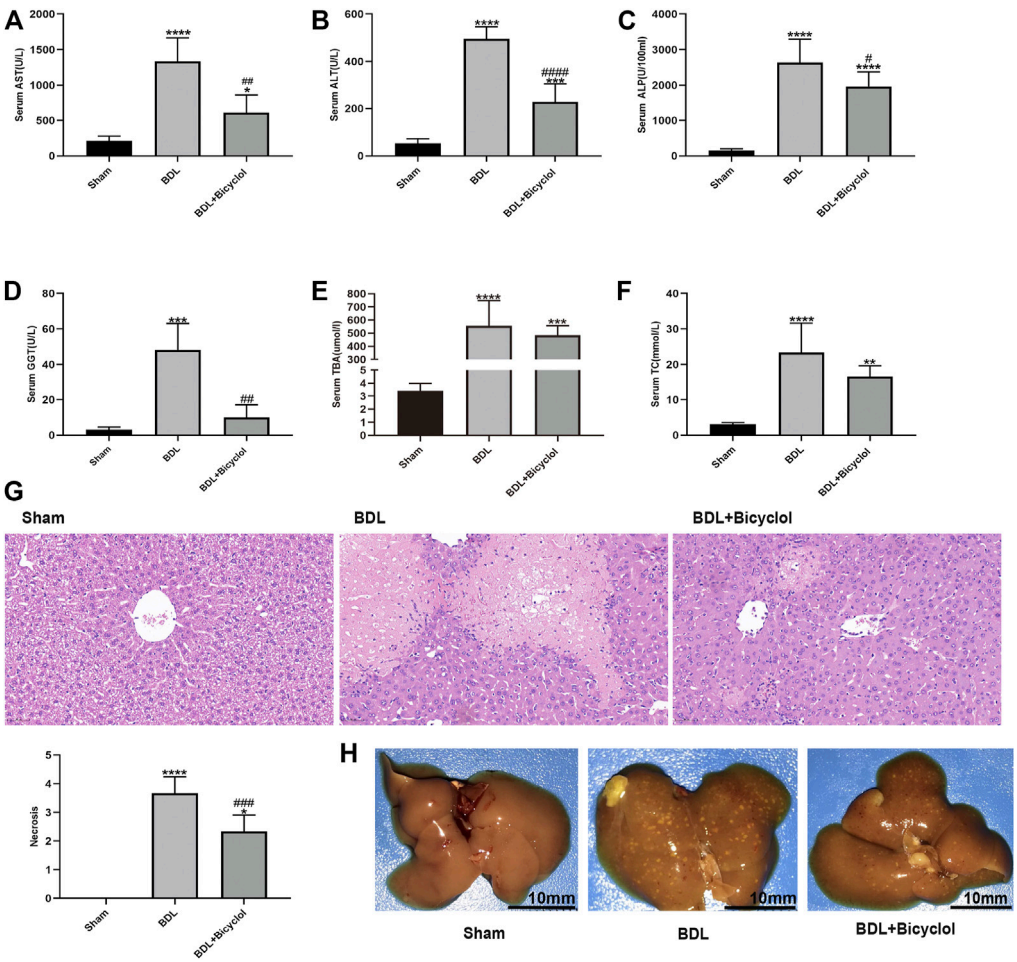


FIGURE 1 | Bicyclol markedly improved the liver enzyme, histology, and liver gross appearance in BDL mice. **(A–F)** Serum biochemistry including AST, ALT, ALP, GGT, TBA, and TC. **(G)** H&E stain liver histology (Scale bar, 100 um). **(H)** Gross liver appearance (Scale bar, 10 mm). AST, aspartate aminotransferase; ALT, alanine aminotransferase; ALP, alkaline phosphatase; GGT, γ-glutamyl transpeptidase; TBA, total bile acid; TC, total cholesterol. $^{*}p < 0.05$, $^{**}p < 0.01$, $^{***}p < 0.001$, $^{****}p < 0.0001$ vs. sham; $^{\#}p < 0.05$, $^{\#\#}p < 0.01$, $^{\#\#\#}p < 0.001$, $^{\#\#\#\#}p < 0.0001$ vs. BDL.

Real-Time RT-PCR

Total RNA was extracted from liver tissues, and AML12 cells using Trizol reagent and the concentration was determined by an enzyme-labeled instrument. The RNA was reverse-transcribed into cDNA using SuperScript III First-Strand Synthesis System (Invitrogen, Carlsbad, CA, United States). The reaction mix was performed as follows: 50°C (2 min); 95°C (5 min); followed by 50 cycles of 95°C (15 s) and 60°C (30 s).

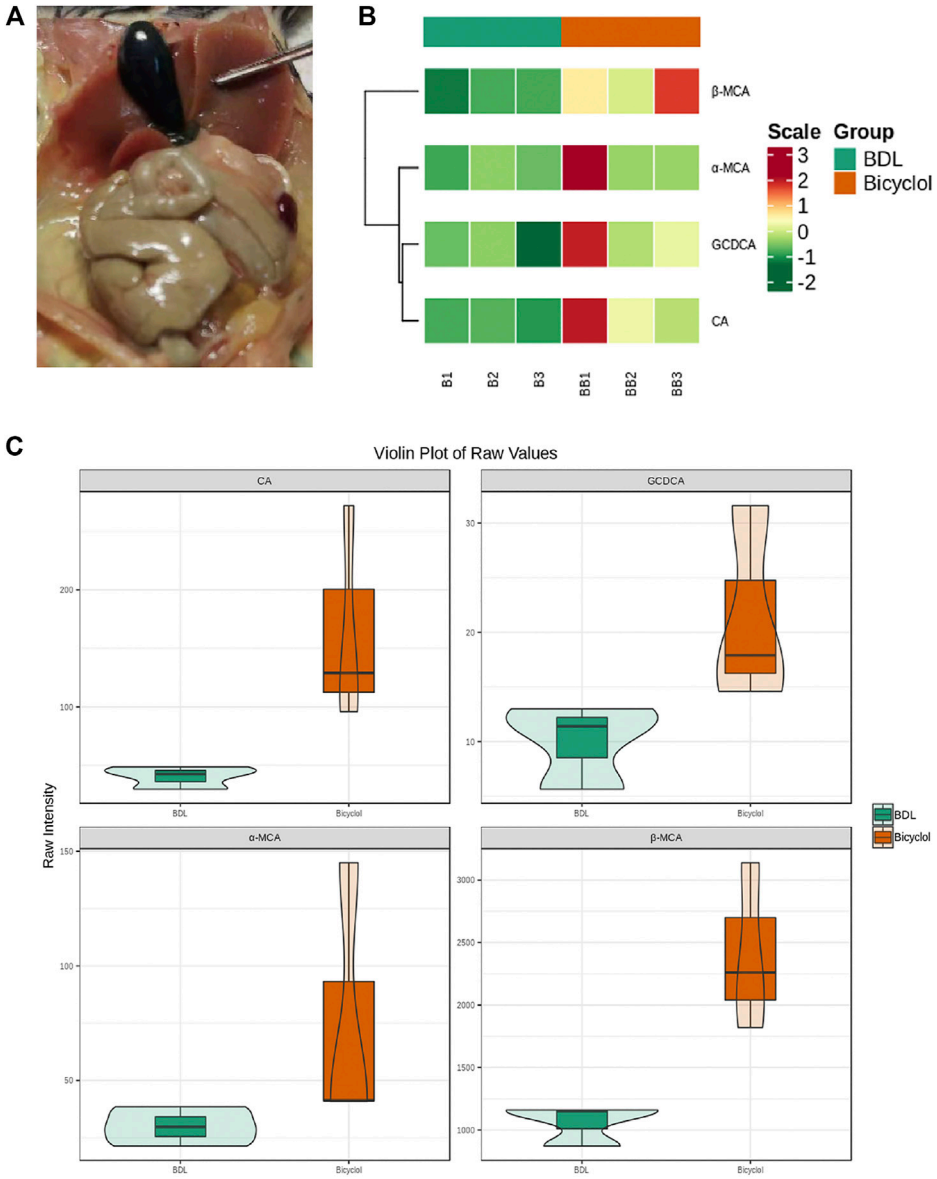


FIGURE 2 | Bile acid composition in the gallbladder. **(A)** The gallbladder of BDL mice. **(B)** Heatmap of differential bile acids of gallbladder bile samples. Rows represent different bile acids, while columns represent different samples. Colors from green to red indicate increasing levels from low to high. **(C)** Violin plot analysis comparing the levels of CA, GCDCA, α-MCA, β-MCA in the BDL and Bicyclol groups. Green represents the BDL group, whereas orange represents the Bicyclol group.

Relative expression of target genes was calculated by the $2^{-\Delta\Delta Ct}$ method and normalized to GAPDH. The primer sequences are shown in **Table 1**.

Statistical Analysis

Data are expressed as mean ± SEM and analyzed with GraphPad Prism 8.0.1 (GraphPad Software, United States). One-way ANOVA followed by Tukey's multiple comparisons test was used to calculate the statistical significance. A p-value of <0.05 was considered statistically significant.

RESULTS

Protective Effects of Bicyclol on Liver Injury in Bile Duct Ligation Mice

To explore the effects of bicyclol on BDL induced mice liver injury, we tested liver enzymes including AST, ALT, ALP, GGT, TBA, and TC, and liver pathology. The serum AST, ALT, ALP, GGT, TBA, and TC levels increased in BDL compared with the sham group (**Figures 1A–F**). Bicyclol significantly decreased the AST, ALT, ALP, and GGT levels. However, the TBA and TC levels were comparable between

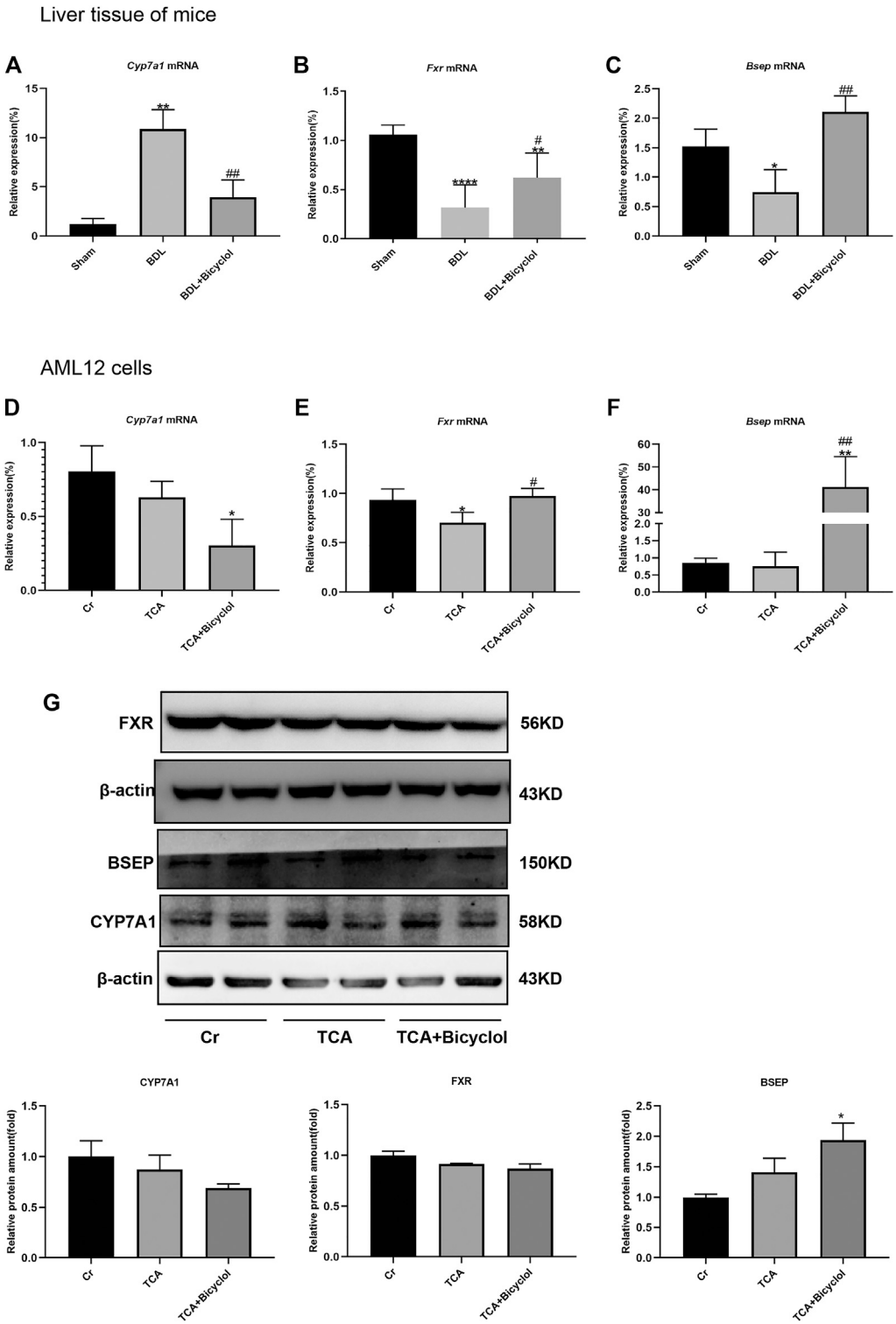


FIGURE 3 | Effects of bicyclol on genes related to bile metabolism. **(A–C)** The mRNA levels of bile metabolism-related genes (Fxr, Cyp7a1, Bsep) in BDL and bicyclol treatment mice. The mRNA levels **(D–F)** and protein levels **(G)** of bile metabolism-related genes (Fxr, Cyp7a1, Bsep) in AML12 cells after TCA and bicyclol exposure. Cr represents control group without special treatment, TCA means cells were stimulated with 100 uM TCA for 24 h, TCA + Bicyclol means cells were pretreated with 500 uM bicyclol for 2 h, then stimulated with 100 uM TCA for 24 h. Data are expressed as mean ± SD. $^{*}p < 0.05$, $^{**}p < 0.01$, $^{***}p < 0.001$, $^{****}p < 0.0001$ vs. sham or Cr; $^{\#}p < 0.05$, $^{\#\#}p < 0.01$ vs. BDL or TCA.

BDL and BDL + Bicyclol groups. As indicated by H&E staining, BDL induced inflammatory cell infiltration and hepatic necrosis in mice liver, the effects of which were then ameliorated by bicyclol (**Figure 1G**). The beneficial effects were also proved by liver appearance, where livers from BDL mice had many yellow-white granules on the surface. In contrast, yellow-white granules of the liver were significantly improved in the bicyclol treatment group (**Figure 1H**). These results revealed that bicyclol could relieve BDL induced liver injury.

Bicyclol Treatment Changed Bile Acid Composition

In those mice with bile duct ligation, the gallbladder volume significantly increased, and the bile was stagnant (**Figure 2A**); thus, we collected the bile in the gallbladder and analyzed the composition. In total, we tested 25 different kinds of bile acids, finding four BAs CA, GCDCA, α-muricholic acid (α-MCA), β-muricholic acid (β-MCA) levels that differed between BDL and bicyclol groups (**Figure 2**). A heatmap was plotted to show the levels of four bile acids (**Figure 2B**). CA, GCDCA, α-MCA, β-MCA in three samples of the bicyclol group were higher than that in the BDL group. In addition, violin plot analysis showed that the levels of bile acids, including CA, GCDCA, α-MCA, and β-MCA were higher in the bicyclol group than in the BDL group (**Figure 2C**). Previous studies have found that cholate and β-muricholate were the main components of mouse bile acid pool (Kerr et al., 2002), with the following order from hydrophobic to hydrophilic: LCA > deoxycholic acid (DCA) > chenodeoxycholic acid (CDCA) > CA > UDCA > MCA (de Aguiar Vallim et al., 2013). Our results showed that bicyclol could increase hydrophilic bile acid, mainly the α-MCA, β-MCA levels.

Bicyclol Prevented Liver Injury by Preventing Hepatic Bile Acid Synthesis and Promoting Bile Acid Excretion

Cyp7a1 is the key enzyme in the classic bile acid synthesis pathway (Chiang and Ferrell, 2019). *Fxr* is a nuclear receptor that suppresses *Cyp7a1* expression (Xu et al., 2016). In our study, liver *Cyp7a1* mRNA expression level was elevated by BDL and significantly reduced post bicyclol treatment (**Figure 3A**). BDL significantly reduced *Fxr* expression at the mRNA level, which was then reversed by bicyclol (**Figure 3B**). *Bsep* expression at the mRNA level was also decreased in the BDL group and increased in BDL + Bicyclol group (**Figure 3C**). TCA resulted in the most abundant BAs in blood, which was significantly increased in cirrhosis and hepatocellular carcinoma (HCC) patients, and induced inflammatory gene expression in liver cells. Consequently, we treated TCA cells to mimic the cell damage caused by bile (Chen et al., 2011; Wang et al., 2016a). TCA caused a down-regulation of *Fxr* [F (2,7) = 7.736], which was reversed by bicyclol. *Fxr* further caused a decrease of *Cyp7a1* and an increase of *Bsep* (**Figures 3D–F**). At the same time, bicyclol significantly up-regulated the protein expression of BSEP and inhibited the protein level of CYP7A1 although there was no significant difference, even if the FXR protein expression was not changed by bicyclol (**Figure 3G**). These results suggested that bicyclol could activate *Fxr* to suppress *Cyp7a1* expression, which led to a reduction of BA synthesis and acceleration of BA excretion.

Bicyclol Ameliorates Bile Duct Ligation-Induced Liver Injury by Down-Regulation of High-Mobility Group Box-1

Inflammatory factors, including tumor necrosis factor-α (TNF-α), interleukin-1 β (IL-1β), interleukin- 6 (IL-6), transforming growth factor-β (TGF-β), are involved in drug-induced liver injury, cholestasis, alcoholic and non-alcoholic fatty liver diseases, and other chronic liver disease processes (Szabo and Csak, 2012). Severe bile duct damage often triggers inflammation. To further verify the liver damage caused by BDL and the effect of bicyclol, we tested the mRNA levels of *TNF-α* and *IL-1β*. The results showed that bicyclol recovered the BDL-induced *IL-1β*, *TNF-α* mRNA higher expression (**Figures 4A,B**). HMGB1, as a member of damage-associated molecular patterns (DAMPs) and its receptor RAGE, promote neutrophil infiltration in necrotic tissue, thus aggravating necrosis (Huebener et al., 2015). So, we also measured the protein expression changes of HMGB1 in the liver and AML12 cells. The HMGB1 expression levels were upregulated in the BDL or TCA groups, and this upregulation was offset by bicyclol (**Figures 4C,E**). Similarly, BDL and TCA also caused the up-regulation of RAGE protein and was also reversed by bicyclol (**Figures 4D,F**). TLR4 can be activated by HMGB1, the expression of TLR4 was upregulated at TCA and TCA + Bicyclol groups compare to Cr group (**Figure 4G**).

Bicyclol Stimulated Autophagy in Mice and Alpha Mouse Liver 12 Cells

To analyze the effect of bicyclol on autophagy, two important markers of autophagy were detected. The conversion from LC3-Ⅰ (soluble form) to LC3-Ⅱ (lapidated form) and p62 protein are autophagy activation indicators. Western blot showed that the expression of LC3-Ⅱ levels was increased, and p62 was decreased in the BDL group. Also, bicyclol treatment further upregulated the LC3-Ⅱ., but the p62 levels were also increased by bicyclol (**Figure 5A**). *In vitro*, bicyclol enhanced the TCA induced accumulation of LC3-Ⅱ and p62 (**Figure 5C**). We also observed the expression of p62 in the liver by immunofluorescence (**Figure 5B**). The results showed that the nucleus of the cholestasis site was broken and dissolved, there was no normal structure, and the fluorescence of p62 was significantly reduced. Bicyclol significantly improved cell necrosis with p62 fluorescence increased dramatically (**Figure 5B**). These results were consistent with the western blot findings. Besides these, the expression levels of pro-autophagy protein Beclin-1 were upregulated by TCA, even though there was no significant difference (**Figure 5D**).

Bicyclol Regulated Nuclear Factor, E2-Related Factor 2 Mediated Antioxidant Response

Cholestasis is related to oxidative stress. Under basal conditions, Nrf2 binds to Keap1 in the cytoplasm; under oxidative stress,

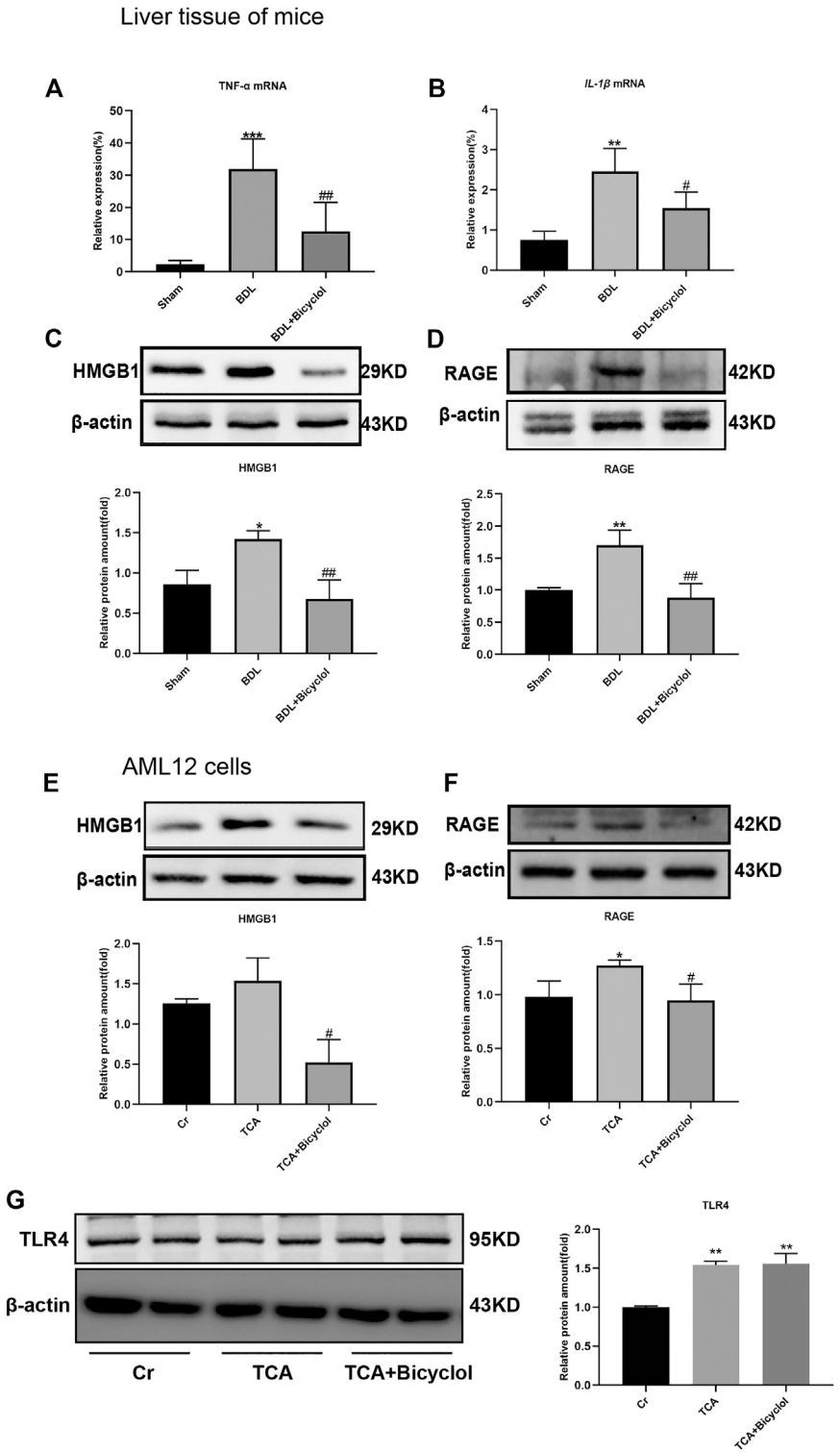


FIGURE 4 | Effect of bicyclol on inflammatory cytokines, HMGB1, and its receptor RAGE and TLR4. The mRNA level of Tnf-α **(A)** and IL-1β **(B)** in mouse liver tissue. **(C,D)** Immunoblots for HMGB1 and RAGE in mouse liver. **(E,F)** Immunoblots for HMGB1 and RAGE in AML12 cells. **(G)** Immunoblots for TLR4 in AML12 cells. $^{*}p < 0.05$, $^{**}p < 0.01$, $^{***}p < 0.001$ vs. sham or Cr; $^{\#}p < 0.05$, $^{\#\#}p < 0.01$ vs. BDL or TCA. Protein levels were normalized to levels of β-actin.

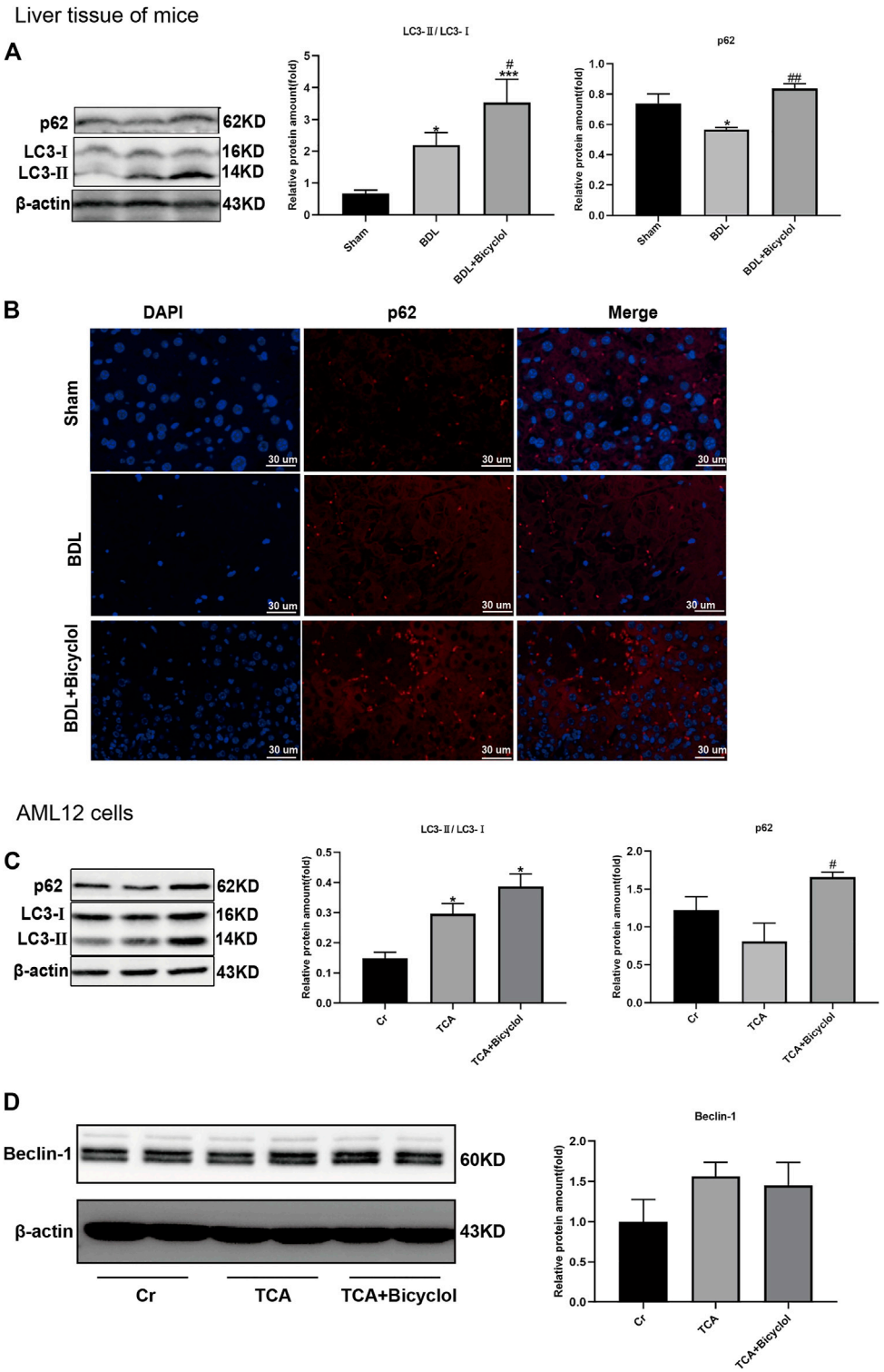


FIGURE 5 | Effect of bicyclol on autophagy. **(A)** P62 and LC3-II protein levels in mice were detected by western blot. **(B)** Paraffin sections of liver tissue were stained with p62 (red) and counterstained with DAPI to visualize nuclei (blue) by immunofluorescence. Scale bar, 30 um. **(C)** Immunoblots for p62 and LC3-II in AML12 cells. **(D)** Immunoblots for Beclin-1 in AML12 cells. $^{*}p < 0.05$ vs. sham or Cr; $^{\#}p < 0.05$, $^{\#\#}p < 0.01$, $^{\#\#\#}p < 0.001$ vs. BDL or TCA. Protein levels were normalized to levels of β-actin.

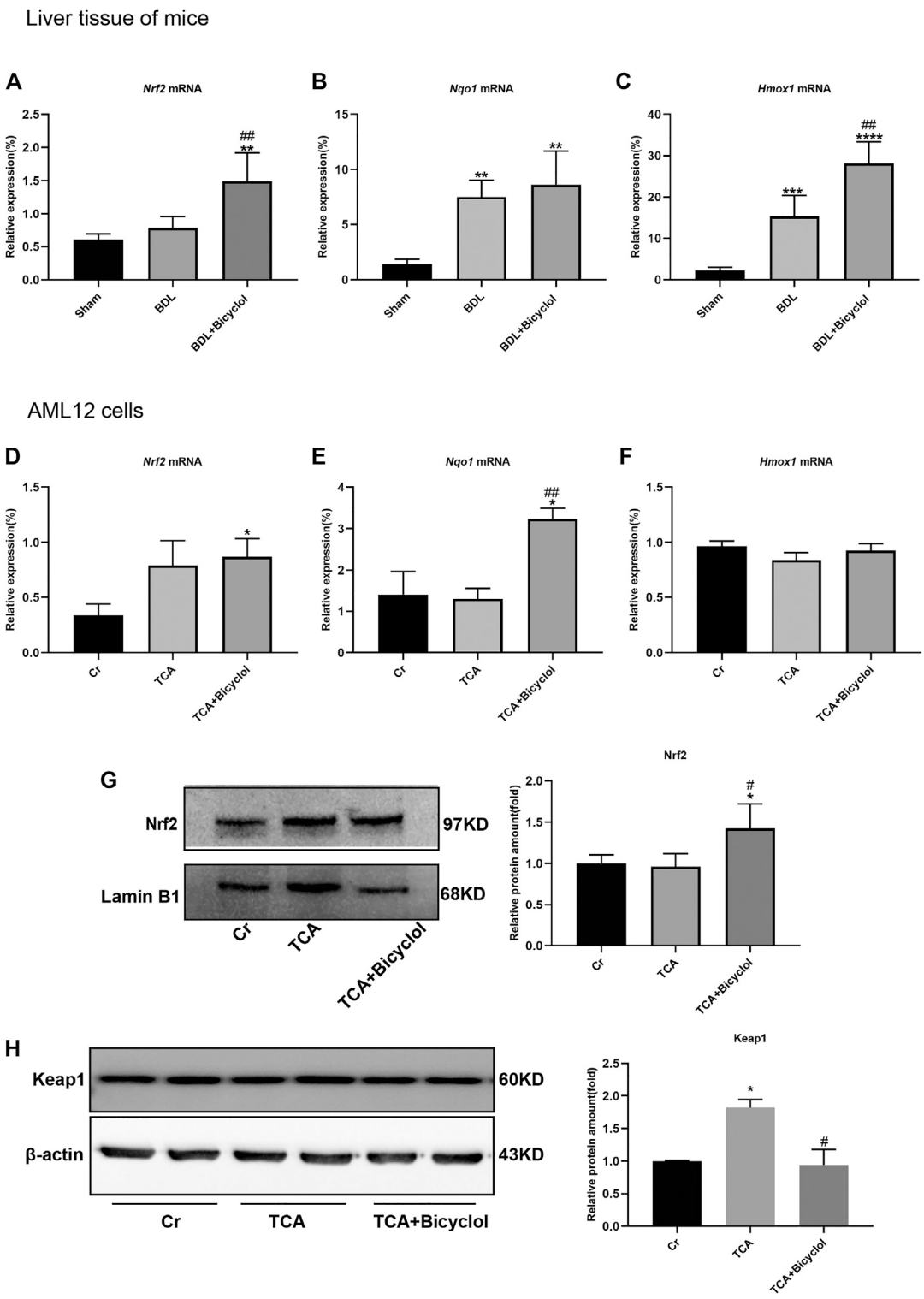


FIGURE 6 | Effects of bicyclol on Nrf2 and its target genes. **(A–C)** The mRNA levels of Nrf2, Nqo1, Hmox1 in BDL and bicyclol treatment mice. **(D–F)** The mRNA levels of Nrf2, Nqo1, Hmox1; The protein levels of Nrf2 **(G)** and Keap1 **(H)** in AML12 cells after TCA and bicyclol exposure. Dates are expressed as mean ± SD. $^{*}p < 0.05$, $^{**}p < 0.01$, $^{***}p < 0.001$, $^{****}p < 0.0001$ vs. sham or Cr; $^{\#}p < 0.05$, $^{\#\#}p < 0.01$ vs. BDL or TCA.

Nrf2 dissociates from the Nrf2/Keap1 complex and translocate to the nucleus, thereby initiating the transcription of anti-oxidative stress genes. As shown in **Figure 6A** *Nrf2* mRNA level was significantly increased in BDL + Bicyclol group compared with the Sham and BDL groups. In addition, the downstream target genes, including NADPH: quinone oxidoreductase 1 (*Nqo1*) and heme oxygenase-1 (*Hmox1*), were also determined. The results showed that *Nqo1* and *Hmox1* were upregulated in BDL and BDL + Bicyclol groups compared with the Sham group (**Figures 6B,C**). The level of *Hmox1* was further upregulated by bicyclol. The *Nrf2* and *Nqo1* mRNA levels were increased in bicyclol-treated AML12 cells; however, there were no significant differences in TCA-treated AML12 cells (**Figures 6D,E**). In addition, the protein level of Nrf2 also increased by bicyclol (**Figure 6G**). The expression level of Keap1 was significant increased after TCA exposure, while pretreatment with bicyclol reversed the upregulation (**Figure 6H**).

DISCUSSION

Cholestasis is a liver disease characterized by the accumulation of toxic bile salts, bilirubin, and cholesterol, resulting in hepatocellular injury, which eventually develop into fibrosis and cirrhosis. UDCA, as an exogenous hydrophilic bile acid that replaces endogenous hydrophobic bile acids and obeticholic acid as FXR agonists, have been used to treat PBC (Gulamhusein and Hirschfield, 2020). Besides UDCA and obeticholic acid, 24-norursodeoxycholic acid (norUDCA) is also used to treat PSC and cholestasis liver diseases with favorable outcomes (Fickert et al., 2013; Fickert et al., 2017). Unfortunately, 40% of patients do not have a satisfactory response to UDCA and are at risk of cirrhosis or non-neoplastic complications (Leung et al., 2020; Wagner and Fickert, 2020). The results of the present study demonstrated that BDL could lead to the accumulation of serum TBA and TC which induce a significant liver injury, as evidenced by the increasing of serum ALT, AST, ALP, GGT and hepatic necrosis. Bicyclol treatment exhibited significant protection against BDL induced liver injury by reducing the elevated serum ALT, AST, ALP, GGT levels and hepatic necrosis. Bicyclol also improved bile stasis in the liver as evidenced by the liver gross appearance that yellow-white granules were significantly decreased by bicyclol. These results are consistent with a previous study that bicyclol treatment ameliorated liver condition in BDL rats (Zhen et al., 2015). In addition, our research supplements the potential mechanisms that may be involved.

The composition of bile acids in different species is different. In the human body, CA and CDCA are the main components, while CA and muricholic acid (MCA) are the main bile acid components in mice (de Aguiar Vallim et al., 2013). Due to the presence or absence of hydroxyl groups in the corresponding position and direction on the molecular skeleton, bile acids' hydrophilicity is different. The order from hydrophilic to hydrophobic reads as follows: MCA > UDCA > CA > CDCA > DCA > LCA (de Aguiar Vallim et al., 2013). The previous study has shown that colesevelam can improve cholestatic liver and biliary tract damage by changing biliary BA composition, mainly by causing hydrophilization of BAs (up-regulating liver and biliary α-MCA, β-MCA and ω-MCA levels) (Fuchs et al., 2018). Another study found that the FXR agonist obeticholic acid increased the levels of α/β MCA from 11.3 to 29.4% and reduced the absorption of cholesterol (Xu et al., 2016). Our experiments revealed that the levels of hydrophilic bile acids such as α-MCA and β-MCA were significantly up-regulated after bicyclol treatment compared to the BDL group. It seems that bicyclol treatment promoted the excretion of the bile acids from the body through the circulation, thus reducing the toxic damage of bile acids. Clinical trials have also found that the bile acid composition in PBC patients treated with UDCA was also changed as the bile was enriched with UDCA, while CA and CDCA were significantly down-regulated, and endogenous bile acids combined with glycine were also increased (Combes et al., 1999). Yet, in our study, we found a different result, i.e., bicyclol treatment increased the levels of CA and GCDCA. Our explanation is that while bicyclol improves the laboratory indicators of BDL accompanied by ongoing liver damage, but GCDCA accumulation can cause liver cell damage because of its hydrophobicity.

BAs are synthesized from cholesterol in the liver through classical and alternative pathways that involve 14 enzymes. Among them, the classical pathway is catalyzed by *Cyp7a1* to synthesize primary bile acids CA and CDCA (Russell, 2003). Cyp7a1 overexpressed mice have increased bile acid pool and a higher level of hepatic cholesterol (Li et al., 2011). Nuclear receptors are also involved in BAs balance. *Fxr* regulates most of the bile acid formation processes, including transport and detoxification, and limits the overload of bile acids in liver cells (Wagner et al., 2011). *Fxr* participates in BAs balance through a variety of ways, including inhibiting liver *Cyp7a1* transcription, inducing intestinal *Fgf-15* to activate liver FGF receptor 4 (FGFR-4), repressing Na/taurocholate cotransporter (NTCP), activating the bile salt export pump *Bsep* and similar (Wagner et al., 2011). The Fxr agonist obeticholic acid (OCA) inhibits the expression of *Cyp7a1* by activating liver *Fxr* and *Shp* expression and changes the bile acid pool size and composition to inhibit intestinal cholesterol absorption (Xu et al., 2016). Our results showed that treatment with bicyclol in BDL mice up-regulated *Fxr* transcription while down-regulating *Cyp7a1* and up-regulating the expression of *Bsep*. Many previous studies have proven that gut microbes are involved in the synthesis and excretion of bile acids and the conversion of components, such as VSL#3 probiotics (including eight different probiotic strains) (Degirolamo et al., 2014) and probiotic *Lactobacillus rhamnosus* GG (LGG) (Liu et al., 2020), while bile acids can also affect bacterial structure *in vitro* and *in vivo* (Tian et al., 2020). Besides affecting the growth of intestinal bacteria, bile also participates in anti-adhesion and neutralizing endotoxins (Wiest et al., 2014). The lack of intestinal bile leads to bacterial translocation and intestinal inflammation, which promotes the progression and development of colorectal cancer (Jia et al., 2018). Therefore, intestinal bacteria and pathological changes after BDL should also be investigated due to the lack of bile in the intestinal.

HMGB1 can have both favorable and unfavorable consequences. On the one hand, hepatocyte-specific HMGB1 knockout mice suffer from increased mitochondrial damage and cell death during liver ischemia/reperfusion (Huang et al., 2014). On the other hand, hepatocyte HMGB1 is involved in the

pathogenesis of ALD (Ge et al., 2014). Zhang *et al* found that NF-KBp65 was significantly up-regulated after treatment with FXR siRNA or inhibitor, accompanied by the up-regulation of IL-1β and TNF-α (Zhang et al., 2017b). In the present study, we found that bicyclol increased the FXR expression while it decreased the mRNA levels of inflammatory factors TNFα and IL-1β and the protein level of HMGB1 in the liver. Autophagy, which maintains liver homeostasis by eliminating toxic substances in the liver, is involved in accumulation disorders, non-alcoholic fatty liver disease, fibrosis, hepatocellular carcinoma, hyperammonaemia, viral infections and other liver diseases (Hazari et al., 2020). HMGB1 can stimulate autophagy in a variety of ways, including BECN1 in the cytoplasm, HSPB1 in the nucleus, and RAGE outside the cell. Previous studies have also shown that HMGB1 deficiency has no adverse impact on liver function, nor does it affect mitochondrial quality and autophagy (Huebener et al., 2014; Sun and Tang, 2014). We detected LC3-II/I and p62, which are two markers of autophagy. The results showed that BDL resulted in the up-regulation of LC3-II/I ratio and the degradation of p62 to activate autophagy and protect the liver from cholestasis damage. Bicyclol further increased the LC3-II/I ratio, but caused the accumulation of p62, which in turn activated autophagy to provide protection. Although our experiment did not find that bicyclol could change the expression of pro-autophagy protein Beclin-1, previous study has reported that Beclin-1 and Atg7 were up-regulated by bicyclol (Zhao et al., 2020). All these demonstrate that bicyclol can resist the progression of cholestasis liver injury through autophagy.

The p62-Keap1-Nrf2 pathway is part of the cellular antioxidant defense mechanism, in which p62 accumulates and competitively combines with Keap1 to activate Nrf2 (Komatsu et al., 2010). A recent study showed that activation of the p62-Keap1-Nrf2 pathway protects the ferroptosis in hepatocellular carcinoma cells (Sun et al., 2016). In our study, we found that the decrease of p62 led to the upregulation of Keap1, and Nrf2 was no significant changes. The accumulation of p62 caused by bicyclol treatment resulted in the degradation of Keap1 and activation of Nrf2. Nrf2 is one of the nuclear transcription factors, which provide protection against oxidative stress by regulating the expression of endogenous antioxidants. Genes regulated by Nrf2 are involved in the synthesis and regeneration of GSH, the expression of GST and GPx, the production of NADPH, and the expression of genes encoding iron chelation (Battino et al., 2018). In this study, we detected the mRNA levels of *Nrf2* and its downstream target genes *Nqo1*, *Hmox1*, and *Gclc*. Our results demonstrate that *Gclc* was not significantly different in animal experiments or cell experiments (data not shown). Heping *et al* reported that the mRNA and protein levels of GCLC, GCLM, and NRF2 all temporarily increased during BDL and then fell to baseline or below. These results suggested that either ursodeoxycholic acid or S-adenosylmethionine therapy alone can prevent the down-regulation of GCLC, GCLM, and NRF2 protein levels, while the combination of the two can increase these levels even higher (Yang et al., 2009). Other studies have shown that BDL leads to increased nuclear migration of NRF2, the expression of downstream target genes *Nqo1*, *Hmox1*, and *Gclm* is also up-regulated, and Vitamin A or baicalin intervention further increases the above performance (Wang et al., 2014; Shen et al., 2017). In our study, the mRNA level of *Nrf2* was not significantly up-regulated in the BDL group, while the levels of *Nqo1* and *Hmox1* were substantially up-regulated. Bicyclol not only up-regulated the mRNA level of *Nqo1* and *Hmox1*, but it also up-regulated the level of *Nrf2*. *In vitro* cell experiments, TCA only up-regulated the level of *Nrf2* mRNA without significant difference, while bicyclol up-regulated the mRNA and protein levels of *Nrf2* and *Nqo1*. So, bicyclol also improved liver damage caused by BDL by activating *Nrf2* and its downstream targets *Nqo1* and *Hmox1*, which is consistent with previous studies (Zhang et al., 2014; Zhao et al., 2020).

CONCLUSION

These results indicate that bicyclol can improve liver damage caused by BDL in obstructive cholestasis. The bicyclol treatment promotes hydrophilization of bile acids, inhibits bile acid synthesis through Fxr/Cyp7a1, and promotes the excretion of bile acids through the Fxr/Bsep pathway. In addition, the fact that bicyclol treatment exerts its therapeutic effect through p62-Nrf2 anti-inflammatory and antioxidant pathways further the research on cholestasis liver injury.

Institutional Review Board Statement: The study was conducted according to the guidelines of the Declaration of Helsinki, and approved by the Institutional Review Board (or Ethics Committee) of Radiation Medicine Chinese Academy of Medical Sciences (IRM-DWLL-2018104, November 20, 2018).

DATA AVAILABILITY STATEMENT

The raw data supporting the conclusions of this article will be made available by the authors, without undue reservation, to any qualified researcher.

ETHICS STATEMENT

The animal study was reviewed and approved by the Institutional Review Board (or Ethics Committee) of Radiation Medicine Chinese Academy of Medical Sciences.

AUTHOR CONTRIBUTIONS

JWZ, JZ, and LZ designed the research; MR, TY, XX, PJ, and LZ performed the experiments; MR, LC, SS, XL, and SZ analyzed data; MR, JWZ, and LC wrote the paper; JWZ, JZ, and LZ read and revised the manuscript.

FUNDING

This research was funded by National Key R&D Program of China (No. 2019YFC0119500), National Natural Science Foundation of China (No. 81960107) and Natural Science Foundation of Tianjin (NO18JCQNJC80700).

REFERENCES

Andersson, U., and Tracey, K. J. (2011). HMGB1 Is a Therapeutic Target for Sterile Inflammation and Infection. *Annu. Rev. Immunol.* 29, 139–162. doi:10.1146/annurev-immunol-030409-101323

Ashby, K., Navarro Almario, E. E., Tong, W., Borlak, J., Mehta, R., and Chen, M. (2018). Review Article: Therapeutic Bile Acids and the Risks for Hepatotoxicity. *Aliment. Pharmacol. Ther.* 47 (12), 1623–1638. doi:10.1111/apt.14678

Battino, M., Giampieri, F., Pistollato, F., Sureda, A., de Oliveira, M. R., Pittalà, V., et al. (2018). Nrf2 as Regulator of Innate Immunity: A Molecular Swiss Army Knife!. *Biotechnol. Adv.* 36 (2), 358–370. doi:10.1016/j.biotechadv.2017.12.012

Cai, S.-Y., Ouyang, X., Chen, Y., Soroka, C. J., Wang, J., Mennone, A., et al. (2017). Bile Acids Initiate Cholestatic Liver Injury by Triggering a Hepatocyte-specific Inflammatory Response. *JCI insight* 2 (5), e90780. doi:10.1172/jci.insight.90780

Chen, T., Xie, G., Wang, X., Fan, J., Qiu, Y., Zheng, X., et al. (2011). Serum and Urine Metabolite Profiling Reveals Potential Biomarkers of Human Hepatocellular Carcinoma. *Mol. Cell Proteomics* 10 (7), M110004945. doi:10.1074/mcp.M110.004945

Chiang, J. Y. L., and Ferrell, J. M. (2019). Bile Acids as Metabolic Regulators and Nutrient Sensors. *Annu. Rev. Nutr.* 39, 175–200. doi:10.1146/annurev-nutr-082018-124344

Combes, B., Carithers, R. L., Maddrey, W. C., Munoz, S., Garcia-Tsao, G., Bonner, G. F., et al. (1999). Biliary Bile Acids in Primary Biliary Cirrhosis: Effect of Ursodeoxycholic Acid. *Hepatology* 29 (6), 1649–1654. doi:10.1002/hep.510290618

de Aguiar Vallim, T. Q., Tarling, E. J., and Edwards, P. A. (2013). Pleiotropic Roles of Bile Acids in Metabolism. *Cell Metab* 17 (5), 657–669. doi:10.1016/j.cmet.2013.03.013

Degirolamo, C., Rainaldi, S., Bovenga, F., Murzilli, S., and Moschetta, A. (2014). Microbiota Modification with Probiotics Induces Hepatic Bile Acid Synthesis via Downregulation of the Fxr-Fgf15 axis in Mice. *Cel Rep.* 7 (1), 12–18. doi:10.1016/j.celrep.2014.02.032

Dondorf, F., Fahrner, R., Ardelt, M., Patsenker, E., Stickel, F., Dahmen, U., et al. (2017). Induction of Chronic Cholestasis without Liver Cirrhosis - Creation of an Animal Model. *Wjg* 23 (23), 4191–4199. doi:10.3748/wjg.v23.i23.4191

Eguchi, A., Wree, A., and Feldstein, A. E. (2014). Biomarkers of Liver Cell Death. *J. Hepatol.* 60 (5), 1063–1074. doi:10.1016/j.jhep.2013.12.026

Fickert, P., Hirschfield, G. M., Denk, G., Marschall, H.-U., Altorjay, I., Färkkilä, M., et al. (2017). norUrsodeoxycholic Acid Improves Cholestasis in Primary Sclerosing Cholangitis. *J. Hepatol.* 67 (3), 549–558. doi:10.1016/j.jhep.2017.05.009

Fickert, P., Pollheimer, M. J., Silbert, D., Moustafa, T., Halilbasic, E., Krones, E., et al. (2013). Differential Effects of norUDCA and UDCA in Obstructive Cholestasis in Mice. *J. Hepatol.* 58 (6), 1201–1208. doi:10.1016/j.jhep.2013.01.026

Fickert, P., Zollner, G., Fuchsbichler, A., Stumptner, C., Weiglein, A. H., Lammert, F., et al. (2002). Ursodeoxycholic Acid Aggravates Bile Infarcts in Bile Duct-Ligated and Mdr2 Knockout Mice via Disruption of Cholangioles. *Gastroenterology* 123 (4), 1238–1251. doi:10.1053/gast.2002.35948

Fuchs, C. D., Paumgartner, G., Mlitz, V., Kunczer, V., Halilbasic, E., Leditznig, N., et al. (2018). Colesevelam Attenuates Cholestatic Liver and Bile Duct Injury in Mdr2−/− Mice by Modulating Composition, Signalling and Excretion of Faecal Bile Acids. *Gut* 67 (9), 1683–1691. doi:10.1136/gutjnl-2017-314553

Galicia-Moreno, M., Lucano-Landeros, S., Monroy-Ramirez, H. C., Silva-Gomez, J., Gutierrez-Cuevas, J., Santos, A., et al. (2020). Roles of Nrf2 in Liver Diseases: Molecular, Pharmacological, and Epigenetic Aspects. *Antioxidants* 9 (10), 980. doi:10.3390/antiox9100980

Ge, X., Antoine, D. J., Lu, Y., Arriazu, E., Leung, T.-M., Klepper, A. L., et al. (2014). High Mobility Group Box-1 (HMGB1) Participates in the Pathogenesis of Alcoholic Liver Disease (ALD). *J. Biol. Chem.* 289 (33), 22672–22691. doi:10.1074/jbc.M114.552141

Ge, X., Arriazu, E., Magdaleno, F., Antoine, D. J., Dela Cruz, R., Theise, N., et al. (2018). High Mobility Group Box-1 Drives Fibrosis Progression Signaling via the Receptor for Advanced Glycation End Products in Mice. *Hepatology* 68 (6), 2380–2404. doi:10.1002/hep.30093

Gulamhusein, A. F., and Hirschfield, G. M. (2020). Primary Biliary Cholangitis: Pathogenesis and Therapeutic Opportunities. *Nat. Rev. Gastroenterol. Hepatolgastroenterology Hepatology* 17 (2), 93–110. doi:10.1038/s41575-019-0226-7

Hazari, Y., Bravo-San Pedro, J. M., Hetz, C., Galluzzi, L., and Kroemer, G. (2020). Autophagy in Hepatic Adaptation to Stress. *J. Hepatol.* 72 (1), 183–196. doi:10.1016/j.jhep.2019.08.026

Hu, Q.-W., and Liu, G.-T. (2006). Effects of Bicyclol on Dimethylnitrosamine-Induced Liver Fibrosis in Mice and its Mechanism of Action. *Life Sci.* 79 (6), 606–612. doi:10.1016/j.lfs.2006.02.025

Huang, H., Nace, G. W., McDonald, K.-A., Tai, S., Klune, J. R., Rosborough, B. R., et al. (2014). Hepatocyte-specific High-Mobility Group Box 1 Deletion Worsens the Injury in Liver Ischemia/reperfusion: a Role for Intracellular High-Mobility Group Box 1 in Cellular protection. *Hepatology* 59 (5), 1984–1997. doi:10.1002/hep.26976

Huang, M.-H., Li, H., Xue, R., Li, J., Wang, L., Cheng, J., et al. (2019). Up-regulation of Glycolipid Transfer Protein by Bicyclol Causes Spontaneous Restriction of Hepatitis C Virus Replication. *Acta Pharmaceutica Sinica. B* 9 (4), 769–781. doi:10.1016/j.apsb.2019.01.013

Huebener, P., Gwak, G.-Y., Pradere, J.-P., Quinzii, C. M., Friedman, R., Lin, C.-S., et al. (2014). High-mobility Group Box 1 Is Dispensable for Autophagy, Mitochondrial Quality Control, and Organ Function *In Vivo*. *Cel Metab.* 19 (3), 539–547. doi:10.1016/j.cmet.2014.01.014

Huebener, P., Pradere, J.-P., Hernandez, C., Gwak, G.-Y., Caviglia, J. M., Mu, X., et al. (2015). The HMGB1/RAGE axis Triggers Neutrophil-Mediated Injury Amplification Following Necrosis. *J. Clin. Invest.* 125 (2), 539–550. doi:10.1172/JCI76887

Huebener, P., Pradere, J.-P., Hernandez, C., Gwak, G.-Y., Caviglia, J. M., Mu, X., et al. (2019). The HMGB1/RAGE axis Triggers Neutrophil-Mediated Injury Amplification Following Necrosis. *J. Clin. Invest.* 129, 1802. doi:10.1172/JCI12697510.1172/jci126976

Ichimura, Y., and Komatsu, M. (2010). Selective Degradation of P62 by Autophagy. *Semin. Immunopathol* 32 (4), 431–436. doi:10.1007/s00281-010-0220-1

Ishak, K., Baptista, A., Bianchi, L., Callea, F., De Groote, J., Gudat, F., et al. (1995). Histological Grading and Staging of Chronic Hepatitis. *J. Hepatol.* 22 (6), 696–699. doi:10.1016/0168-8278(95)80226-6

Jia, W., Xie, G., and Jia, W. (2018). Bile Acid-Microbiota Crosstalk in Gastrointestinal Inflammation and Carcinogenesis. *Nat. Rev. Gastroenterol. Hepatol.* 15 (2), 111–128. doi:10.1038/nrgastro.2017.119

Jiang, T., Harder, B., Rojo de la Vega, M., Wong, P. K., Chapman, E., and Zhang, D. D. (2015). p62 Links Autophagy and Nrf2 Signaling. *Free Radic. Biol. Med.* 88 (Pt B), 199–204. doi:10.1016/j.freeradbiomed.2015.06.014

Kang, R., Livesey, K. M., Zeh, III, H. J., Lotze, M. T., and Tang, D. (2011). HMGB1 as an Autophagy Sensor in Oxidative Stress. *Autophagy* 7 (8), 904–906. doi:10.4161/auto.7.8.15704

Kerr, T. A., Saeki, S., Schneider, M., Schaefer, K., Berdy, S., Redder, T., et al. (2002). Loss of Nuclear Receptor SHP Impairs but Does Not Eliminate Negative Feedback Regulation of Bile Acid Synthesis. *Developmental Cel.* 2 (6), 713–720. doi:10.1016/s1534-5807(02)00154-5

Khambu, B., Huda, N., Chen, X., Antoine, D. J., Li, Y., Dai, G., et al. (2018). HMGB1 Promotes Ductular Reaction and Tumorigenesis in Autophagy-Deficient Livers. *J. Clin. Invest.* 128 (6), 2419–2435. doi:10.1172/JCI91814

Komatsu, M., Kurokawa, H., Waguri, S., Taguchi, K., Kobayashi, A., Ichimura, Y., et al. (2010). The Selective Autophagy Substrate P62 Activates the Stress Responsive Transcription Factor Nrf2 through Inactivation of Keap1. *Nat. Cel Biol.* 12 (3), 213–223. doi:10.1038/ncb2021

Kuma, A., Komatsu, M., and Mizushima, N. (2017). Autophagy-monitoring and Autophagy-Deficient Mice. *Autophagy* 13 (10), 1619–1628. doi:10.1080/15548627.2017.1343770

Leung, K. K., Deeb, M., and Hirschfield, G. M. (2020). Review Article: Pathophysiology and Management of Primary Biliary Cholangitis. *Aliment. Pharmacol. Ther.* 52 (7), 1150–1164. doi:10.1111/apt.16023

Li, H., Li, J.-R., Huang, M.-H., Chen, J.-H., Lv, X.-Q., Zou, L.-L., et al. (2018). Bicyclol Attenuates Liver Inflammation Induced by Infection of Hepatitis C Virus via Repressing ROS-Mediated Activation of MAPK/NF-κB Signaling Pathway. *Front. Pharmacol.* 9, 1438. doi:10.3389/fphar.2018.01438

Li, T., Matozel, M., Boehme, S., Kong, B., Nilsson, L.-M., Guo, G., et al. (2011). Overexpression of Cholesterol 7α-Hydroxylase Promotes Hepatic Bile Acid Synthesis and Secretion and Maintains Cholesterol Homeostasis. *Hepatology* 53 (3), 996–1006. doi:10.1002/hep.24107

Liu, Y., Chen, K., Li, F., Gu, Z., Liu, Q., He, L., et al. (2020). Probiotic Lactobacillus Rhamnosus GG Prevents Liver Fibrosis through Inhibiting Hepatic Bile Acid Synthesis and Enhancing Bile Acid Excretion in Mice. *Hepatology* 71 (6), 2050–2066. doi:10.1002/hep.30975

Qian, M., Fang, X., and Wang, X. (2017). Autophagy and Inflammation. *Clin. translational Med.* 6 (1), 24. doi:10.1186/s40169-017-0154-5

Russell, D. W. (2003). The Enzymes, Regulation, and Genetics of Bile Acid Synthesis. *Annu. Rev. Biochem.* 72, 137–174. doi:10.1146/annurev.biochem.72.121801.161712

Shen, K., Feng, X., Pan, H., Zhang, F., Xie, H., and Zheng, S. (2017). Baicalin Ameliorates Experimental Liver Cholestasis in Mice by Modulation of Oxidative Stress, Inflammation, and NRF2 Transcription Factor. *Oxidative Med. Cell. longevity* 2017, 1–11. doi:10.1155/2017/6169128

Shin, S. M., Yang, J. H., and Ki, S. H. (2013). Role of the Nrf2-ARE Pathway in Liver Diseases. *Oxidative Med. Cell. longevity* 2013, 1–9. doi:10.1155/2013/763257

Sun, X., Ou, Z., Chen, R., Niu, X., Chen, D., Kang, R., et al. (2016). Activation of the P62-Keap1-NRF2 Pathway Protects against Ferroptosis in Hepatocellular Carcinoma Cells. *Hepatology* 63 (1), 173–184. doi:10.1002/hep.28251

Sun, X., and Tang, D. (2014). HMGB1-dependent and -independent Autophagy. *Autophagy* 10 (10), 1873–1876. doi:10.4161/auto.32184

Szabo, G., and Csak, T. (2012). Inflammasomes in Liver Diseases. *J. Hepatol.* 57 (3), 642–654. doi:10.1016/j.jhep.2012.03.035

Tang, D., Kang, R., Livesey, K. M., Cheh, C.-W., Farkas, A., Loughran, P., et al. (2010). Endogenous HMGB1 Regulates Autophagy. *J. Cel. Biol.* 190 (5), 881–892. doi:10.1083/jcb.200911078

Tian, Y., Gui, W., Koo, I., Smith, P. B., Allman, E. L., Nichols, R. G., et al. (2020). The Microbiome Modulating Activity of Bile Acids. *Gut microbes* 11 (4), 979–996. doi:10.1080/19490976.2020.1732268

Wagner, M., and Fickert, P. (2020). Drug Therapies for Chronic Cholestatic Liver Diseases. *Annu. Rev. Pharmacol. Toxicol.* 60, 503–527. doi:10.1146/annurev-pharmtox-010818-021059

Wagner, M., Zollner, G., and Trauner, M. (2011). Nuclear Receptors in Liver Disease. *Hepatology* 53 (3), 1023–1034. doi:10.1002/hep.24148

Wang, G., Xiu, P., Li, F., Xin, C., and Li, K. (2014). Vitamin A Supplementation Alleviates Extrahepatic Cholestasis Liver Injury through Nrf2 Activation. *Oxidative Med. Cell. longevity* 2014, 1–10. doi:10.1155/2014/273692

Wang, X., Xie, G., Zhao, A., Zheng, X., Huang, F., Wang, Y., et al. (2016a). Serum Bile Acids Are Associated with Pathological Progression of Hepatitis B-Induced Cirrhosis. *J. Proteome Res.* 15 (4), 1126–1134. doi:10.1021/acs.jproteome.5b00217

Wang, Y., Nie, H., Zhao, X., Qin, Y., and Gong, X. (2016b). Bicyclol Induces Cell Cycle Arrest and Autophagy in HepG2 Human Hepatocellular Carcinoma Cells through the PI3K/AKT and Ras/Raf/MEK/ERK Pathways. *BMC cancer* 16 (1), 742. doi:10.1186/s12885-016-2767-2

Weerachayaphorn, J., Mennone, A., Soroka, C. J., Harry, K., Hagey, L. R., Kensler, T. W., et al. (2012). Nuclear Factor-E2-Related Factor 2 Is a Major Determinant of Bile Acid Homeostasis in the Liver and Intestine. *Am. J. Physiology-Gastrointestinal Liver Physiol.* 302 (9), G925–G936. doi:10.1152/ajpgi.00263.2011

Wiest, R., Lawson, M., and Geuking, M. (2014). Pathological Bacterial Translocation in Liver Cirrhosis. *J. Hepatol.* 60 (1), 197–209. doi:10.1016/j.jhep.2013.07.044

Woolbright, B. L., Antoine, D. J., Jenkins, R. E., Bajt, M. L., Park, B. K., and Jaeschke, H. (2013). Plasma Biomarkers of Liver Injury and Inflammation Demonstrate a Lack of Apoptosis during Obstructive Cholestasis in Mice. *Toxicol. Appl. Pharmacol.* 273 (3), 524–531. doi:10.1016/j.taap.2013.09.023

Woolbright, B. L., Dorko, K., Antoine, D. J., Clarke, J. I., Gholami, P., Li, F., et al. (2015). Bile Acid-Induced Necrosis in Primary Human Hepatocytes and in Patients with Obstructive Cholestasis. *Toxicol. Appl. Pharmacol.* 283 (3), 168–177. doi:10.1016/j.taap.2015.01.015

Xu, D., Xu, M., Jeong, S., Qian, Y., Wu, H., Xia, Q., et al. (2018). The Role of Nrf2 in Liver Disease: Novel Molecular Mechanisms and Therapeutic Approaches. *Front. Pharmacol.* 9, 1428. doi:10.3389/fphar.2018.01428

Xu, Y., Li, F., Zalzala, M., Xu, J., Gonzalez, F. J., Adorini, L., et al. (2016). Farnesoid X Receptor Activation Increases Reverse Cholesterol Transport by Modulating Bile Acid Composition and Cholesterol Absorption in Mice. *Hepatology* 64 (4), 1072–1085. doi:10.1002/hep.28712

Yang, H., Ramani, K., Xia, M., Ko, K. S., Li, T. W. H., Oh, P., et al. (2009). Dysregulation of Glutathione Synthesis during Cholestasis in Mice: Molecular Mechanisms and Therapeutic Implications. *Hepatology* 49 (6), 1982–1991. doi:10.1002/hep.22908

Yang, T., Khan, G. J., Wu, Z., Wang, X., Zhang, L., and Jiang, Z. (2019). Bile Acid Homeostasis Paradigm and its Connotation with Cholestatic Liver Diseases. *Drug Discov. Today* 24 (1), 112–128. doi:10.1016/j.drudis.2018.09.007

Yang, T., Shu, T., Liu, G., Mei, H., Zhu, X., Huang, X., et al. (2017). Quantitative Profiling of 19 Bile Acids in Rat Plasma, Liver, Bile and Different Intestinal Section Contents to Investigate Bile Acid Homeostasis and the Application of Temporal Variation of Endogenous Bile Acids. *J. Steroid Biochem. Mol. Biol.* 172, 69–78. doi:10.1016/j.jsbmb.2017.05.015

Yokoda, R. T., and Carey, E. J. (2019). Primary Biliary Cholangitis and Primary Sclerosing Cholangitis. *Am. J. Gastroenterol.* 114 (10), 1593–1605. doi:10.14309/ajg.0000000000000268

Zhang, J., Fu, B., Zhang, X., Zhang, L., Bai, X., Zhao, X., et al. (2014). Bicyclol Upregulates Transcription Factor Nrf2, HO-1 Expression and Protects Rat Brains against Focal Ischemia. *Brain Res. Bull.* 100, 38–43. doi:10.1016/j.brainresbull.2013.11.001

Zhang, S., Wang, Z., Zhu, J., Xu, T., Zhao, Y., Zhao, H., et al. (2017a). Carnosic Acid Alleviates BDL-Induced Liver Fibrosis through miR-29b-3p-Mediated Inhibition of the High-Mobility Group Box 1/Toll-like Receptor 4 Signaling Pathway in Rats. *Front. Pharmacol.* 8, 976. doi:10.3389/fphar.2017.00976

Zhang, Y., Xu, Y., Qi, Y., Xu, L., Song, S., Yin, L., et al. (2017b). Protective Effects of Dioscin against Doxorubicin-Induced Nephrotoxicity via Adjusting FXR-Mediated Oxidative Stress and Inflammation. *Toxicology* 378, 53–64. doi:10.1016/j.tox.2017.01.007

Zhao, T.-M., Wang, Y., Deng, Y., Fan, X.-F., Cao, X.-C., Hou, L.-J., et al. (2020). Bicyclol Attenuates Acute Liver Injury by Activating Autophagy, Anti-oxidative and Anti-inflammatory Capabilities in Mice. *Front. Pharmacol.* 11, 463. doi:10.3389/fphar.2020.00463

Zhen, Y.-Z., Li, N.-R., He, H.-W., Zhao, S.-S., Zhang, G.-L., Hao, X.-F., et al. (2015). Protective Effect of Bicyclol against Bile Duct Ligation-Induced Hepatic Fibrosis in Rats. *Wjg* 21 (23), 7155–7164. doi:10.3748/wjg.v21.i23.7155

Conflict of Interest: The authors declare that the research was conducted in the absence of any commercial or financial relationships that could be construed as a potential conflict of interest.

Copyright © 2021 Zhao, Ran, Yang, Chen, Ji, Xu, Zhang, Sun, Liu, Zhou, Zhou and Zhang. This is an open-access article distributed under the terms of the Creative Commons Attribution License (CC BY). The use, distribution or reproduction in other forums is permitted, provided the original author(s) and the copyright owner(s) are credited and that the original publication in this journal is cited, in accordance with accepted academic practice. No use, distribution or reproduction is permitted which does not comply with these terms.

frontiers in Pharmacology

ORIGINAL RESEARCH
published: 12 August 2021
doi: 10.3389/fphar.2021.715752

A Retinoid X Receptor Agonist Directed to the Large Intestine Ameliorates T-Cell-Mediated Colitis in Mice

Ryohtaroh Matsumoto[1], Daisuke Takahashi[1], Masaki Watanabe[2], Shunsuke Nakatani[2], Yuta Takamura[2], Yuji Kurosaki[2], Hiroki Kakuta[2] and Koji Hase[1,3]**

[1]Division of Biochemistry, Graduate School of Pharmaceutical Science and Faculty of Pharmacy, Keio University, Tokyo, Japan, [2]Division of Pharmaceutical Sciences, Graduate School of Medicine Dentistry and Pharmaceutical Sciences, Okayama University, Okayama, Japan, [3]International Research and Development Center for Mucosal Vaccines, The Institute of Medical Science, The University of Tokyo (IMSUT), Tokyo, Japan

OPEN ACCESS

Edited by:
Luca Antonioli, University of Pisa, Italy

Reviewed by:
Guang Chen, Huazhong University of Science and Technology, China
Marta Castro, University of Zaragoza, Spain

***Correspondence:**
Hiroki Kakuta
kakuta-h@okayama-u.ac.jp
Koji Hase
hase-kj@pha.keio.ac.jp

Specialty section:
This article was submitted to Gastrointestinal and Hepatic Pharmacology, a section of the journal Frontiers in Pharmacology

Received: *27 May 2021*
Accepted: *29 July 2021*
Published: *12 August 2021*

Citation:
Matsumoto R, Takahashi D, Watanabe M, Nakatani S, Takamura Y, Kurosaki Y, Kakuta H and Hase K (2021) A Retinoid X Receptor Agonist Directed to the Large Intestine Ameliorates T-Cell-Mediated Colitis in Mice. Front. Pharmacol. 12:715752. doi: 10.3389/fphar.2021.715752

Retinoid X receptor (RXR) is a nuclear receptor that heterodimerizes with several nuclear receptors, integrating ligand-mediated signals across the heterodimers. Synthetic RXR agonists have been developed to cure certain inflammatory diseases, including inflammatory bowel diseases (IBDs). However, pre-existing RXR agonists, which are lipophilic and readily absorbed in the upper intestine, cause considerable adverse effects such as hepatomegaly, hyperlipidemia, and hypothyroidism. To minimize these adverse effects, we have developed an RXR agonist, NEt-3IB, which has lipophilic and thus poorly absorptive properties. In this study, we evaluated the effects of NEt-3IB in an experimental murine colitis model induced through the adoptive transfer of $CD45RB^{high}CD4^{+}$ T cells. Pharmacokinetic studies demonstrated that the major portion of NEt-3IB was successfully delivered to the large intestine after oral administration. Notably, NEt-3IB treatment suppressed the development of T cell-mediated chronic colitis, as indicated by improvement of wasting symptoms, inflammatory infiltration, and mucosal hyperplasia. The protective effect of NEt-3IB was mediated by the suppression of IFN-γ-producing Th1 cell expansion in the colon. In conclusion, NEt-3IB, a large intestine-directed RXR agonist, is a promising drug candidate for IBDs.

Keywords: RXR, NEt-3IB, inflammatory bowel disease, colitis, Th1 cells

INTRODUCTION

Crohn's disease (CD) is an inflammatory bowel disease (IBD) that is characterized by intermittent abdominal pain, diarrhea, bodyweight loss, and hematochezia (bloody stools) (Ho and Khalil, 2015). Although the exact etiology of CD is unknown, genetic variations and immune dysregulation have been implicated in CD development (De Souza and Fiocchi, 2016). In the gastrointestinal mucosal of patients with CD, inflammation is prolonged by excessive activation of immune cells such as effector T cells and inflammatory macrophages (De Souza and Fiocchi, 2016). For decades, steroids have been used to cure CD, although long-term treatment with these agents causes considerable adverse effects such as edema and sleep disturbance (Carter et al., 2004). More recently, biological agents such as anti-TNF-α antibodies were developed to potently suppress the inflammatory response in CD.

However, the cost of biological agents is much higher than that of the classical chemical drugs, and approximately 30% of CD patients fail to respond to therapy using anti-TNF-α antibodies (Adegbola et al., 2018). Moreover, half of the primary responders lose their therapeutic response over time, thereby facing an increased dosage or a revised therapeutic strategy (Adegbola et al., 2018). These facts emphasize the medical need for the development of first-in-class medicines with high efficacy, low cost, and minimal adverse effects.

Retinoid X receptor (RXR) is a nuclear receptor that heterodimerizes with other nuclear receptors such as peroxisome proliferator-activated receptor (PPAR), liver X receptor (LXR), pregnane X receptor (PXR), and NR4A1 (Nur77) (Evans and Mangelsdorf, 2014). Treatment with an RXR agonist can activate these partner nuclear receptors without their own ligand stimulation (Takeuchi et al., 2013; Evans and Mangelsdorf, 2014), a phenomenon termed the "permissive effect." Activation of these nuclear receptors shows an anti-inflammatory effect, at least partly through mitigating the proliferation and differentiation of inflammatory macrophages and effector T cells (Onuki et al., 2018). In particular, activation of PPARγ by agonist treatment inhibits the differentiation of IFN-γ-producing type 1 helper T (Th1) cells by blocking the JAK–STAT signaling pathway (Natarajan and Bright, 2002; Kanakasabai et al., 2010; Solt et al., 2012). Similarly, activation of LXR inhibits the proliferation of T cells by controlling sterol metabolism via induction of ATP-binding cassette transporter G1 (ABCG1), which is involved in the transmembrane transport of sterols (Bensinger et al., 2008). NR4A1 deficiency is reported to expand the Th1 response because activation of NR4A1 also limits the proliferation of $CD4^+$ T cells by controlling oxidative phosphorylation and aerobic glycolysis (Liebmann et al., 2018). Furthermore, treatment with a PXR agonist prevents the expansion of Th1 cells (Dubrac et al., 2010).

RXR agonists can activate these partner receptors simultaneously, and therefore RXR was considered a promising molecular target for inflammatory disorders. Nonetheless, pre-existing RXR agonists have been reported to induce various adverse effects, such as excess bodyweight gain, hepatomegaly, hypothyroidism, and hypertriglyceridemia (Standeven et al., 1997; Liu et al., 2002; de Vries-Van der Weij et al., 2009). To address this issue, we recently developed NEt-3IB, an RXR full agonist with lower lipophilicity compared with pre-existing RXR agonists such as bexarotene (**Figure 1A**) (Kobayashi et al., 2015). We demonstrated that NEt-3IB induces a low blood concentration after oral administration. Furthermore, using PET/CT imaging, we also observed that NEt-3IB exhibited enterohepatic circulation upon intestinal absorption and was delivered to the lower digestive tract (Kobayashi et al., 2015). These pharmacokinetic properties of NEt-3IB may be beneficial in avoiding systemic adverse effects and delivering the drug to the lower intestine (Kakuta et al., 2012). In this study, we evaluated the anti-inflammatory effects of NEt-3IB in an experimental CD model induced by adoptive transfer of $CD45RB^{high}CD4^+$ T cells (Powrie et al., 1993). We report that NEt-3IB was persistent in the intestinal lumen after oral administration and ameliorated the wasting and colitis. This effect was attributed to the reduced accumulation of Th1 cells in the colon.

MATERIALS AND METHODS

Chemical Reagents

Bexarotene and NEt-3IB were synthesized as described previously (Boehm et al., 1994; Takamatsu et al., 2008).

Animals

ICR mice were purchased from Charles River Laboratories Japan (Yokohama, Japan) and maintained under specific pathogen-free (SPF) conditions at Okayama University, Okayama, Japan. C.B-17-*scid*/*scid* and C.B-$17^{+/+}$ mice were purchased from CLEA Japan (Tokyo, Japan) and maintained under SPF conditions at Keio University, Tokyo, Japan. $Rag1^{-/-}$ mice were bred and maintained under SPF conditions at Keio University. C.B-17-scid/scid and $Rag1^{-/-}$ mice were fed with CE-2 diet (CLEA Japan) before T cell transfer and with MF diet (Oriental Yeast, Tokyo, Japan) containing 0.015% NEt-3IB or regular MF after transfer. Foxp3-hCD2 knock-in mice were bred and maintained under SPF conditions at Keio University. C57BL6/J mice were purchased from CLEA Japan. Foxp3-hCD2 knock-in mice and C57BL6/J mice were fed with AIN-93G diet (Research Diet, New Brunswick, NJ, United States) until their use in experiments at 6–12 weeks old. All animal experiments except for pharmacokinetic studies were approved by the Animal Studies Committees of Keio University.

Pharmacokinetic Studies

This experiment was conducted in accordance with the Guidelines for Animal Experiments at Department of Animal Resources, Advanced Science Research Center, Okayama University, and all procedures were approved by the Animal Care and Use Committee, Okayama University. The test compounds were administered to 6-week-old ICR male mice (n = 5 per group). In the oral administration study, the test compounds (10 mg/10 ml/kg) were suspended in 1% ethanol and 0.5% carboxymethyl cellulose (CMC) in distilled water and administered by oral gavage. In the intravenous administration study, the test compounds (1 mg/5 ml/kg) were dissolved in saline containing 20% WellSolve (Celeste Corporation, Tokyo, Japan) and administered via the tail vein. Blood samples (approximately 0.6–1.0 ml each) were taken from the inferior vena cava under isoflurane anesthesia at 0.5, 1, 3, 6, and 24 h after administration. Then the animals were killed by cervical dislocation. Brain, liver, kidney, bile, and large-intestinal contents were immediately extirpated. Blood treated with heparin in a centrifuge tube was centrifuged at 1,900 × g at room temperature for 5 min. To 100 µl of the resulting plasma, 100 µl ice-cold 5.0 mM ammonium acetate solution (adjusted with acetic acid to pH 5.0) and 1.0 ml ice-cold EtOAc were added. The resulting mixture was vortexed for 30 s, kept at room temperature for 10 min, and centrifuged at 1,900 ×g at room temperature for 30 s. An 800 µl aliquot of the EtOAc phase was removed and concentrated to dryness in a centrifugal evaporator.

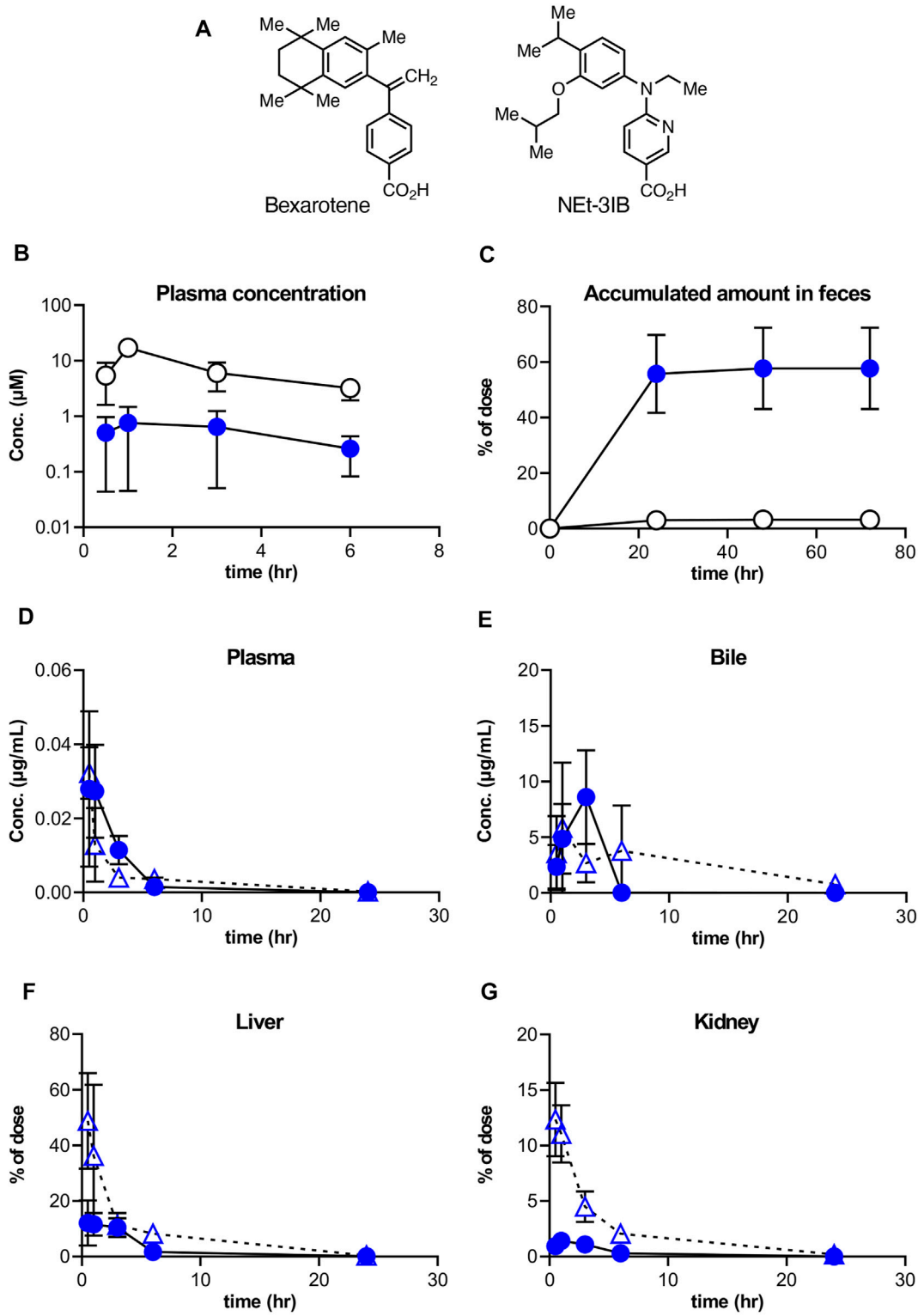


FIGURE 1 | Distribution of NEt-3IB after a single dosage to male mice. **(A, B)** Concentration of bexarotene or NEt-3IB in plasma and feces, respectively. Each compound was orally administered at **(A)** 30 mg/kg and **(B)** 10 mg/kg. **(C–F)** Plasma, bile, liver, and kidney distribution of NEt-3IB after single administration at 1 mg/kg (*i.v.*) and 10 mg/kg (p.o.). Circles and triangles show p.o. and i,v. data, respectively. Data shown are mean [n = 5 **(A, C–F)** or 3 **(B)**] ± SD.

The resulting residue was added to 100 µl acetonitrile. Brain, liver, and kidney samples were homogenized in ice-cold EtOAc (500 µL/100 mg tissue) using a Cell Destroyer PS1000 (BMS, Tokyo, Japan) and steel beads (for 5 mm) at 4,260 rpm for 60 s. Bile was collected by washing out the gallbladder with 500 µl EtOAc. The extract was vortexed for 30 s, kept under ultrasonic irradiation at room temperature for 5 min, and centrifuged at 12,000 ×*g* at 4°C for 10 min. A 200 µl aliquot of the EtOAc phase was collected and concentrated to dryness in a centrifugal evaporator. The resulting residue was dissolved by adding 100 µl acetonitrile. Each solution was directly subjected to LC-MS/MS analysis, and the concentration of each compound was determined from the peak area of the sample with reference to a calibration plot obtained with the authentic compound. All contents in the large intestine were collected, and MeOH (1 ml) was added under ultrasonic irradiation at room temperature for 20 min. The resultant suspension was centrifuged at 1,500 ×*g* at 4°C for 20 min. An 800 µl aliquot of the MeOH phase was diluted 10-fold with methanol. Each solution was directly subjected to High Performance Liquid Chromatography (HPLC) analysis, and the concentration of NEt-3IB was determined from the peak area of the sample with reference to a calibration plot obtained with the authentic compound.

Liquid Chromatography With Tandem Mass Spectrometry

The API4000 LC-MS/MS system (Applied Biosystems, Toronto, Canada) was used, consisting of an LC-20AD pump, an SPD-20AV UV-Vis spectrophotometric detector, and a CTO-20AC column oven (SHIMADZU, Kyoto, Japan) operating at 40°C. A TSKgel ODS-100V column (2.0 i.d. × 50 mm, 3 µm; TOSOH, Tokyo, Japan) was used. The mobile phase was acetonitrile/H_2O = 65/35 containing 0.1% formic acid, v/v, and the flow rate was set at 0.2 ml/min.

High-Performance Liquid Chromatography

A Shimadzu liquid chromatographic system (Kyoto, Japan) consisting of an LC-10AD pump, an SPD-10AV UV–vis spectrophotometric detector, a CTO-10AS column oven, and a C-R5A Chromatopac was used. An Inertsil ODS-3 column (4.6 mm i.d. × 100 mm, 5 µm, GL Sciences, Tokyo, Japan) with a guard column of Inertsil ODS-3 (4.6 mm i.d. × 10 mm, 5 µm, GL Sciences) was operated at 40°C. The mobile phase was methanol/H_2O = 85/15 containing 0.1% formic acid, v/v. The flow rate was set at 0.7 ml/min and the absorbance at 260 nm was monitored.

Induction of Colitis by Adoptive Transfer of $CD4^+$ $CD45RB^{high}$ T Cells

Colitis was induced in C.B-17-scid/scid mice by adoptive transfer of $CD45RB^{high}$ T cells. Mojosort Mouse CD 4 T Cell Isolation Kit (BioLegend, San Diego, CA, United States) and biotin-conjugated anti-mouse TER-119 (TER-119; BioLegend) were used to negatively select $CD4^+$ T cells of splenocytes from C.B-$17^{+/+}$ mice. Negatively selected $CD4^+$ T cells were labeled with Alexa Fluor 647-conjugated anti-mouse CD4 (RM-4-5; BioLegend), BV510-conjugated anti-mouse CD45 (30-F11; BioLegend), and BV421-conjugated anti-mouse CD45RB (16A; BD Horizon, San Jose, CA, United States). Dead cells were labeled with 7-aminoactinomycin D (7-AAD) (BioLegend). $CD45^+CD4^+CD45RB^{high}$ live T cells were isolated by FACS Aria III (BD Biosciences San Jose, CA, United States). The C.B-17-scid/scid recipients were each injected with 2×10^5 cells via the tail vein and transferred to conventional conditions in the animal facilities at Keio University. Mice were fed with 0.015% NEt-3IB-containing MF diet or control MF diet for 7 weeks. The body weights of the mice were measured every week, and the fecal diarrhea score was also measured from week 4. The diarrhea score were assessed as follows: normal stool (0), slightly soft (1), soft but formed (2), not formed (3), and liquid stool (4) (Kjellev et al., 2006). The mice were humanely killed at week 7.

Cell Preparation

Colonic lamina propria (LP) lymphocytes were obtained as follows. Colon tissues were treated with 1 mM dithiothreitol and 20 mM EDTA containing Hank's Balanced Salt Solutions (all from Nacalai-Tesque, Kyoto, Japan) for 20 min in a shaking incubator (37°C, 200 rpm) to remove epithelial cells. After the tissues were treated once more with 20 mM EDTA containing Hank's Balanced Salt Solution for 20 min, the tissues were then minced and dissociated with Liberase solution containing 26 units/ml Liberase TM (Roche, Basel, Switzerland), 5 mg/ml DNase I (Sigma Aldrich, St Louis, MO), 2% newborn calf serum (Thermo Fisher Scientific, Waltham, MA, United States), 100 µg/ml penicillin and streptomycin, and 20 mM HEPES in RPMI 1640 medium (all from Nacalai Tesque) at 37°C for 30 min. The cell suspensions were then filtered to obtain single-cell suspensions. Single-cell suspensions from mesenteric lymph nodes (MLNs) was prepared by mechanically crushing MLNs through 100 µm cell strainers (Greiner Bio-One) in RPMI 1640 medium containing 2% newborn calf serum (Thermo Fisher Scientific).

For cell counts, cells were mixed with Precision Count Beads (BioLegend), anti-mouse CD16/32 (93; BioLegend), eFluor 450-conjugated anti-mouse CD45 (30-F11; Thermo Fisher Scientific), and 7-aminoactinomycin D (7-AAD) (BioLegend) and were analyzed by FACS Celesta and FlowJo software version 10 (BD Biosciences).

Histology

Colonic tissue samples were fixed in Mildform (10% formalin; Wako Pure Chemical Industries, Osaka, Japan) overnight. After fixation, the samples were embedded in paraffin using a Leica EG1160. Samples were cut into 5 µm sections, deparaffinized and rehydrated, and then stained with hematoxylin (Agilent Technologies, Inc., Santa Clara, CA, United States) and eosin (Wako Pure Chemical Industries, Osaka, Japan). Histological colitis scores were reviewed by DT, who was blinded to each experiment. The sections were scored for the presence of crypt abscesses (0–1), the degree of thickness (0–3), and the degree of inflammatory

infiltrate (0–3). The maximum score of the histological index was 7.

Flow Cytometry

For inflammatory T cell analysis of the colitis model, the following monoclonal antibodies were used: BV510-conjugated anti-mouse CD45 (30-F11; BioLegend), redFluor 710-conjugated anti-mouse CD4 (RM4-5; Tonbo Bioscience), BV605-conjugated anti-mouse TCRβ (H57-597; BD Biosciences), BV650-conjugated anti-mouse IFN-γ (XMG1.2; BD Horizon), and BV786-conjugated anti-mouse IL-17A (TC11-18H10.1; BD Horizon). For Treg cell analysis of the colitis model, the following monoclonal antibodies were used: BV510-conjugated anti-mouse CD45 (30-F11; BioLegend), redFluor-710-conjugated anti-mouse CD4 (RM4-5; Tonbo Biosciences, San Diego, CA, United States), FITC-conjugated anti-mouse TCRβ (H57-597; BD Biosciences), and eFluor 660-conjugated anti-mouse Foxp3 (FJK-16s; ThermoFisher Scientific). For macrophage analysis of the colitis model, the following monoclonal antibodies were used: BV510-conjugated anti-mouse CD45 (30-F11; BioLegend), Alexa Fluor 594-conjugated anti-mouse CD3 (17A2; BioLegend), redFluor 710-conjugated anti-mouse B220 (RA3-6B2; Tonbo Biosciences), APC-conjugated anti-mouse Ly-6C (AL-21; BD Pharmagen, San Jose, CA, United States), Alexa Fluor 488-conjugated anti-mouse Ly-6G/Ly-6C (Gr-1; BioLegend), BUV737-conjugated anti-mouse CD11b (M1/70; BD Horizon), BUV 395-conjugated anti-mouse CD11c (HL3; BD Horizon), and PerCP-Cy5.5-conjugated anti-mouse I-A/I-E (M5/114.15.2; BioLegend). For *in vitro* T cell analysis, the following monoclonal antibodies were used: BV510-conjugated anti-mouse CD45 (30-F11; BioLegend), redFluor 710-conjugated anti-mouse CD4 (RM4-5; Tonbo Biosciences), BUV737-conjugated anti-mouse TCRβ (H57-597; BD Horizon), PerCP-Cy5.5-conjugated anti-mouse IFN-γ (XMG1.2; BioLegend), PE-conjugated anti-mouse/human T-bet (O4-46; BD Pharmagen), and eFluor 660-conjugated anti-mouse Foxp3 (FJK-16s; Thermo Fisher Scientific). Dead cells were labeled with Fixable Viability Stain 780 (BD Biosciences). For intracellular cytokine and transcription factor staining, LP lymphocytes and MLN lymphocytes were cultured for 4 h in complete medium (RPMI containing 10% MP Biomedicals, Santa Ana, CA, United States: fetal bovine serum (FBS), Nacalai-Tesque 100 μg/ml penicillin and streptomycin, Thermo Fisher Scientific 55 μM mercaptoethanol, and Nacalai-Tesque 20 mM HEPES), and cultured T cells were cultured for 4 h in half-complete medium (RPMI containing 5% FBS, 100 μg/ml penicillin and streptomycin, 55 μM mercaptoethanol, and 20 mM HEPES), each supplemented with Cell Activation Cocktail (BioLegend) and Protein Transport Inhibitor Cocktail (Thermo Fisher Scientific). Lymphocytes and T cells were first blocked with anti-CD16/32 and then stained with the monoclonal antibodies described above. IC fixation buffer and permeabilization buffer (Thermo Fisher Scientific) were used for intracellular cytokine staining, and the Transcription Factor Buffer Set (BD Pharmagen) was used for transcription factor staining. For absolute cell counts, cells were mixed with Precision Count Beads (BioLegend) and anti-mouse CD16/32 (93; BioLegend) and stained with eFluor 450-conjugated anti-mouse CD45 (30-F11; Thermo Fisher Scientific) and 7-AAD. The stained samples were analyzed using an LSRII or a FACS Celesta (BD Biosciences), and FlowJo software version 10.

In vitro Cultures

$CD4^+$ T cells were enriched from splenocytes from C57BL6/J mice or *Foxp3-hCD2* knock-in mice by a negative selection method with the BD iMag cell separation system, using biotin-conjugated antibodies against mouse CD8α (53-6.7; Tonbo Biosciences), CD11b (M1/70; BioLegend), CD11c (N418; Thermo Fisher Scientific), B220 (RA3-6B2; BioLegend), Ly-6C/Ly6-G (Gr-1; BioLegend), TER-119 (TER-119; BioLegend), and Streptavidin Particle Plus (BD IMag). Negatively selected $CD4^+$ T cells were labeled with BV605-conjugated anti-mouse CD4 (RM4-5; BioLegend), BV510-conjugated anti-mouse CD44 (IM4; BD Horizon), redFluor 710-conjugated anti-mouse CD45 (30-F11; Tonbo Biosciences), PE-Cy7-conjugated anti-CD25 (PC61.5; Thermo Fisher Scientific), APC-eFluor 780-conjugated anti-mouse NK 1.1 (PK136; Thermo Fisher Scientific), eFluor450-conjugated anti-CD62L (MEL-14; Thermo Fisher Scientific), and APC-conjugated anti-human CD2 (RPA-2.10; BioLegend). Dead cells were labeled with 7-AAD (BioLegend). $CD45^+CD4^+CD62L^+CD44^-$NK $1.1^-Foxp3^-(hCD2^-)$ live naive T cells were isolated by FACSAria III (BD Biosciences). In the experiments described in **Figure 4**, 1×10^5 of $CD4^+$ naive T cells were cultured in advanced RPMI containing 5% FBS in the presence or absence of NEt-3IB for 3–5 days. For the experiment using CellTrace Violet (Thermo Fisher Scientific), T cells were incubated at 37°C for 20 min with CellTrace Violet before culture. T cells were polarized to the Th1 subtype by the addition of 10 μg/ml anti-mouse IL-4 (Bio X Cell, Lebanon, NH, United States) and 20 ng/ml recombinant mouse IL-2 and IL-12 (BioLegend). The stained samples were analyzed using FACS LSR II (BD Biosciences) and Flowjo software version 10.

Statistical Analysis

Statistical significance between two groups was calculated by Student's t-test or Welch's t-test. In the *in vitro* study, statistical significance between the control group and other groups was calculated by Dunnet's multiple comparison test or Dunn's multiple comparison test. $p < 0.05$ indicated statistical significance. Data were output by Prism version 9 (GraphPad, San Diego, CA, United States).

RESULTS

NEt-3IB has Low Systemic Transferability and Reaches the Colon

To better understand the pharmacokinetics of NEt-3IB and bexarotene (**Figure 1A**), another RXR agonist clinically used for the treatment of cutaneous T cell lymphoma (Budgin et al., 2005), we initially measured their concentrations in plasma and feces after a single oral administration. The plasma concentrations of NEt-3IB were much lower than those of bexarotene at any timepoint (0.5–6 h post-administration) (**Figure 1B**). Correspondingly, the delivery of

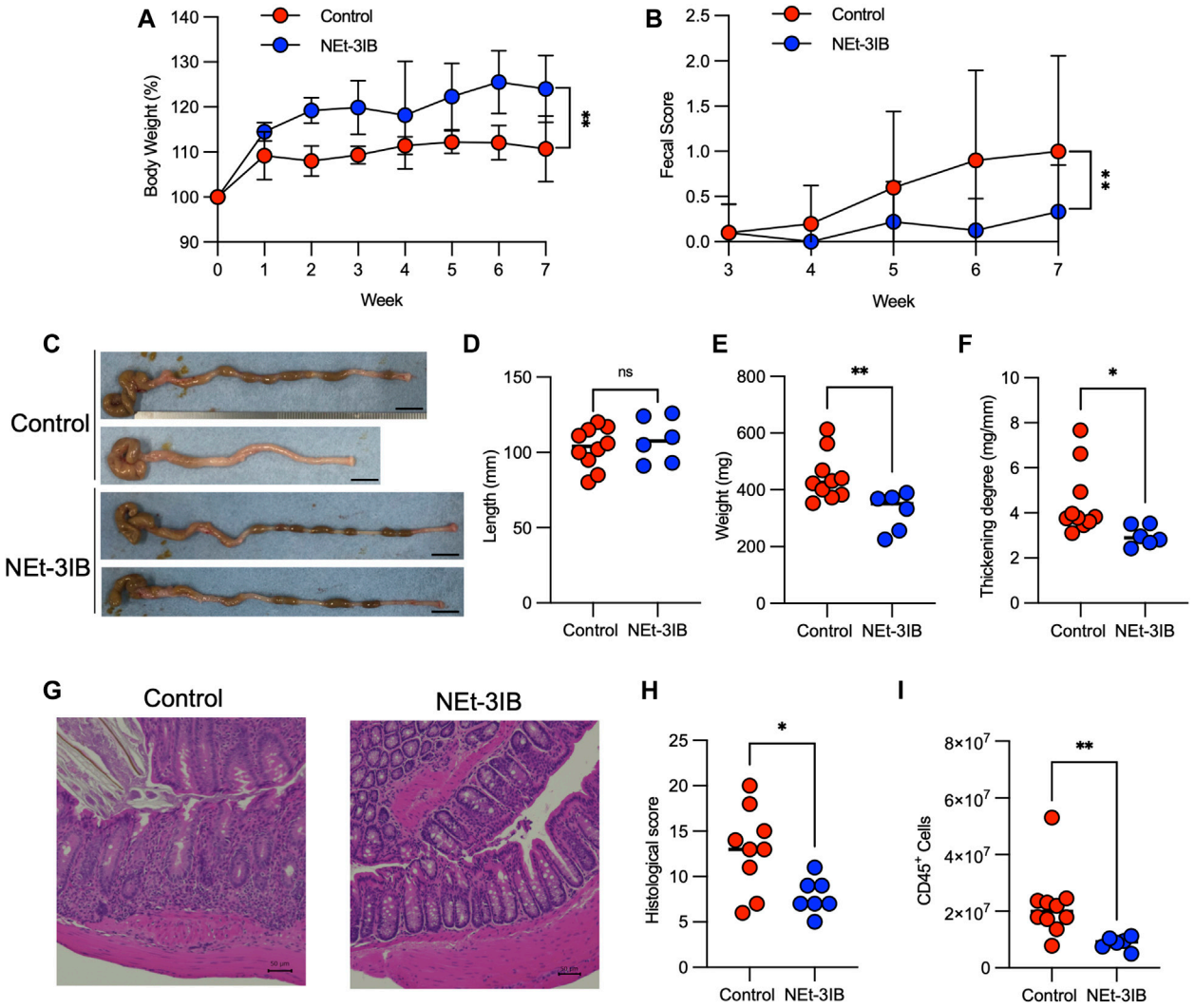


FIGURE 2 | NEt-3IB ameliorates T-cell-dependent experimental colitis. **(A–H)** Experimental colitis was induced by adoptive transfer of $CD4^+CD45RB^{high}$ T cells into C.B-17 scid/scid mice fed with control or NEt-3IB-containing diet for 7 weeks, and bodyweight loss **(A)** and diarrhea score **(B)** were observed. Data shown are the average. Area under the curve of bodyweight change and fecal score. **(C–F)** Colon length, colon weight, and colon thickening were observed and measured in week 7. Scale bar: 1 cm. **(G)** Colonic specimens were stained with hematoxylin and eosin (HE). **(H)** Histological scores of colonic specimens. **(I)** Total $CD45^+$ cells in the colon lamina propria of the $CD4^+$ $CD45RB^{high}$ T cell transfer model. $^*p < 0.05$, $^{**}p < 0.01$.

NEt-3IB to the feces accumulated to approximately 60% of the dosage, whereas that of bexarotene was less than 10% at 24 h post-administration (**Figure 1C**). These data confirm that orally administered NEt-3IB reaches the colon more efficiently compared with bexarotene due to its low systemic transferability.

To further examine the systemic pharmacokinetics of NEt-3IB, mice received intravenous (i.v.) injection (1 mg/kg) and oral administration (p.o.) (10 mg/kg) of NEt-3IB. The concentrations of NEt-3IB in plasma began to decline by 1 h after i.v. or 6 h after p.o. administration, and reciprocally, the concentrations in the bile increased at these time points (**Figures 1D,E**). On the basis of these observations, we assumed that the liver may excrete NEt-3IB to the intestinal tract via the bile duct. To test this assumption, we measured the concentration of NEt-3IB in the liver and the kidney. Although the concentration of NEt-3IB in the liver promptly decreased, that in the bile gradually increased after i.v. injection (**Figure 1F**). The hepatic concentration of NEt-3IB peaked immediately after p.o. administration and then gradually declined (**Figure 1F**). Conversely, NEt-3IB concentration in the kidney rapidly decreased after i.v. administration and remained consistently low after p.o. administration. Thus, NEt-3IB was excreted to the bile in the liver rather than the kidney (**Figure 1G**).

NEt-3IB Treatment Alleviates T Cell-dependent Colitis

We subsequently examined the anti-inflammatory effects of NEt-3IB in an experimental colitis model induced by transferring $CD4^+CD45RB^{high}$ T cells into C.B-17-scid/scid mice and treating with chow containing 0.015% NEt-3IB (approximately 30 mg/kg/

day) or with regular chow as a control. In the control group, bodyweight gain was suppressed from 1-week post-transfer onwards (**Figure 2A**). Meanwhile, the NEt-3IB-treated group gained weight gradually over the course of the experiment, suggesting that NEt-3IB alleviated wasting disease. Similarly, NEt-3IB administration ameliorated diarrhea associated with colitis, even though both groups exhibited only mild symptoms (**Figure 2B**). Likewise, the colon weight and degree of thickening (colon weight/length) were significantly lower in the NEt-3IB group than that in the control group at 7 weeks after cell transfer (**Figures 2C–F**). Histopathological examination also showed massive infiltration of mononuclear cells in the colon of the control group but not in the NEt-3IB group (**Figure 2G**). Furthermore, the control group exhibited more severe crypt loss and edema (**Figures 2G,H**). Flow cytometry confirmed the massive infiltration of leukocytes in the colon lamina propria (cLP) in the control group, whereas fewer inflammatory infiltrates were observed in the NEt-3IB group (**Figure 2I**).

To further confirm the pharmacological effects of NEt-3IB, we also evaluated the progressive bodyweight loss and diarrhea in a similar colitis model using *Rag1*$^{-/-}$ mice as a recipient. The control *Rag1*$^{-/-}$ recipients exhibited progressive body weight loss in association with severe diarrhea. However, the administration of NEt-3IB significantly mitigated the wasting disease (**Supplementary Figure S1A**). Furthermore, NEt-3IB improved colitis symptoms, namely, diarrhea, colon weight, colonic wall thickening, crypt loss, and edema (**Supplementary Figures S1B–G**). Collectively, these data revealed an anti-inflammatory effect of NEt-3IB in the T cell-dependent mouse colitis model.

NEt-3IB Suppressed the Accumulation of Th1 Cells in the cLP

In the CD4^{+}CD45RB^{high} T-cell-transferred colitis model, IFN-γ-producing effector T (T_{eff}) cells including conventional T helper 1 (Th1) cells and IFN-γ/IL-17-co-expressing T helper 17 (IFN-γ-producing Th17) cells are responsible for the pathogenesis (Powrie et al., 1993; Sujino et al., 2011). To determine whether NEt-3IB administration affects the development of these T_{eff} cell subsets, we analyzed T cell profiles in the cLP and MLN of the colitis model at 7 weeks post-transfer by flow cytometry after intracellular cytokine staining. In the cLP, the numbers of Th1 cells, Th17 cells, and IFN-γ-producing Th17 cells in the NEt-3IB group were less than half that in the control group, although the frequencies of these cells were comparable between the two groups (**Supplementary Figure S2A** and **Figure 3A**). Moreover, Th1 and Th17 cells in the MLN were significantly decreased in the NEt-3IB group compared with the control group, and IFN-γ-producing Th17 cells also tended to be reduced. Of note, we also observed that the number of Foxp3^{+} Treg cells was slightly but significantly decreased in both the cLP and MLN of the NEt-3IB group (**Supplementary Figure S2B** and **Figure 3C**). Colonic T_{eff} cell-derived IFN-γ activates macrophages to produce pro-inflammatory cytokines that cause inflammation in the colon (Stout and Bottomly, 1989). Considering that NEt-3IB treatment reduced Th1 cells in the cLP in the colitis model, we analyzed the colonic macrophages at 7 weeks post-transfer. We observed that the total number of macrophages (CD11b^{+} Ly6G^{-}Ly6C^{-}CD11c^{-} MHC class II^{+}) was decreased significantly in the NEt-3IB-treated group compared with the control group (**Supplementary Figure S2C** and **Figure 3D**). These data illustrated that NEt-3IB diminishes colitis by inhibiting the accumulation of IFN-γ-producing T_{eff} cells and inflammatory macrophages in the cLP and MLN.

NEt-3IB Inhibits the Differentiation and Proliferation of Th1 Cells

We further investigated whether NEt-3IB has a direct impact on the differentiation of Th cells using an *in vitro* culture system. Sorted naïve CD4^{+} T cells were cultured under Th1-skewed conditions for 5 days with or without NEt-3IB treatment before flow cytometric analysis for the expression of Th1 markers (T-bet, IFN-γ), and a Treg marker (Foxp3). We found that the frequencies of the T-bet^{+} and IFN-γ^{+} cells decreased in the NEt-3IB-treated group in a dose-dependent manner (**Supplementary Figure S2D** and **Figure 4A**). Surprisingly, NEt-3IB treatment increased the proportion of Foxp3^{+} T cells in a dose-dependent manner despite culture in Th1 conditions (**Supplementary Figure S2E** and **Figure 4B**).

We subsequently examined whether NEt-3IB affected the proliferation of Th1 cells *in vitro*. Fluorescent dye-labeled naïve CD4^{+} T cells were cultured under Th1-differentiating conditions for 5 days with or without Net-3IB treatment, and then the dilution of CellTrace Violet was analyzed to detect proliferating cells. NEt-3IB treatment significantly reduced the frequency of proliferating cells in the T-bet^{+}IFN-γ^{+} Th1 population when compared with the vehicle control (**Supplementary Figure S2F** and **Figure 4C**). Together, these data suggest that NEt-3IB directly inhibits both the differentiation and proliferation of Th1 cells.

DISCUSSION

In this study, we demonstrated that NEt-3IB attenuated the development of wasting disease and colitis in T cell-dependent experimental colitis models by inhibiting the accumulation of Th1 cells, which is the most dominant cell type contributing to the pathogenesis of CD. Furthermore, our *in vitro* data revealed that NEt-3IB directly inhibited the differentiation and expansion of Th1 cells. NEt-3IB was designed to have lower lipophilicity compared with conventional RXR agonists such as bexarotene (Takamatsu et al., 2008; Kobayashi et al., 2015). We confirmed that NEt-3IB exhibits a lower plasma concentration compared with bexarotene after oral administration. In the detailed pharmacokinetics analysis after i.v. administration, the distribution to the liver represented approximately 49% of the total dosage of NEt-3IB, while in the kidney there was only 12% of the total dosage. Considering that the concentration of NEt-3IB in bile rises after its peak in the liver, NEt-3IB is mostly likely to be excreted efficiently to the bile. Notably, we observed that 60% of

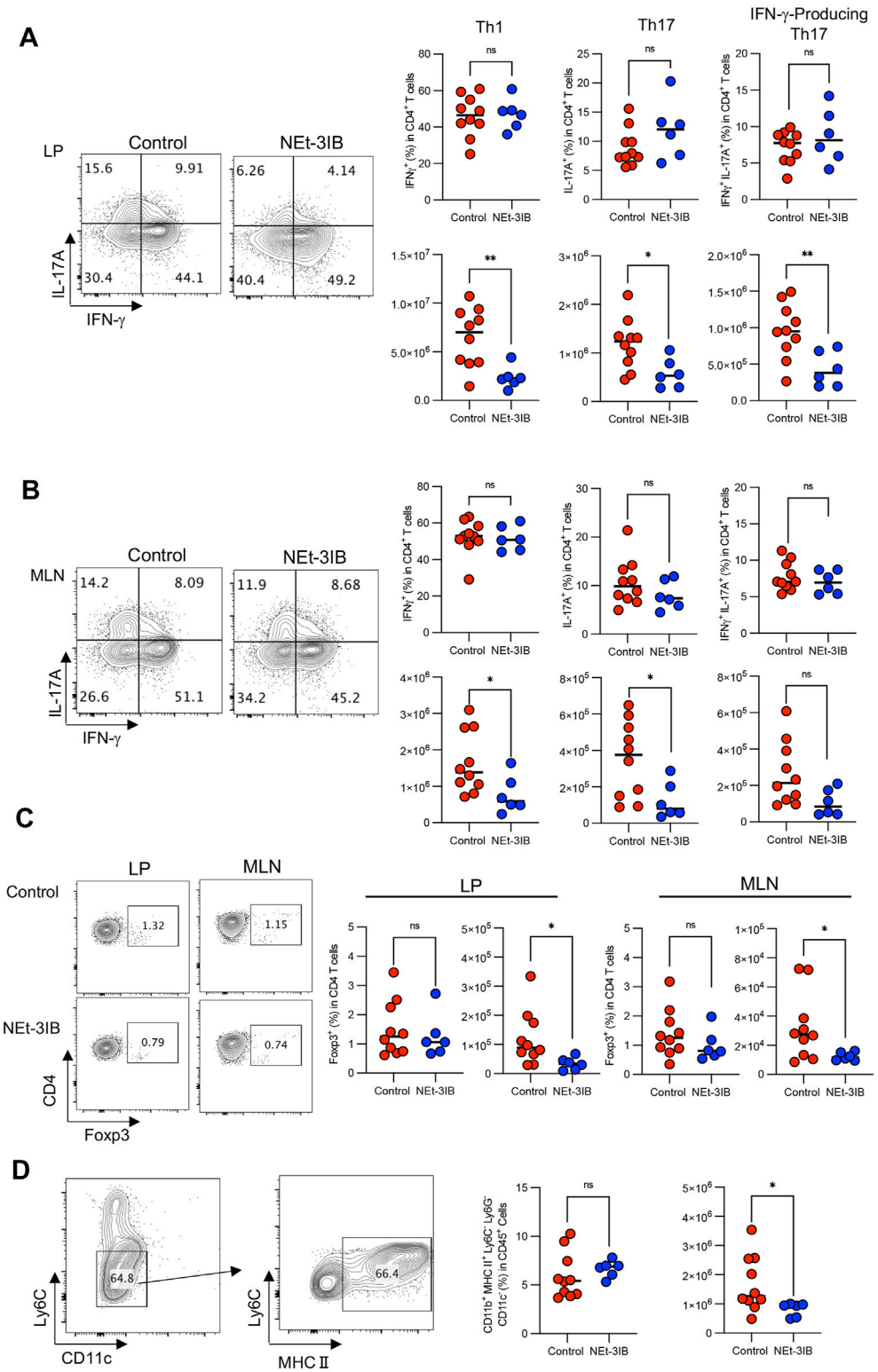


FIGURE 3 | NEt-3IB inhibits inflammatory T cells. **(A)** Frequency and cell number of IFN-γ-producing cells and IL-17A-producing cells in the colon lamina propria. **(B)** Frequency and cell number of Th1 transcription factor T-bet and Th17 transcription factor RORγt-presenting cells of the colon lamina propria and mesenteric lymph nodes. **(C)** Frequency and cell number of Foxp3$^+$ regulatory T cells in the colon lamina propria and mesenteric lymph node of T cell-transferred SCID mice. **(D)** Macrophages were gated as CD11b$^+$Ly6G$^-$Ly6C$^-$CD11c$^-$MHC2$^+$. The right-hand graphs show the frequency of macrophages in CD45$^+$ cells and the number of macrophages. **(A–D)** are from CD45RB^{high} T cell transfer model mice at 7 weeks post-transfer.

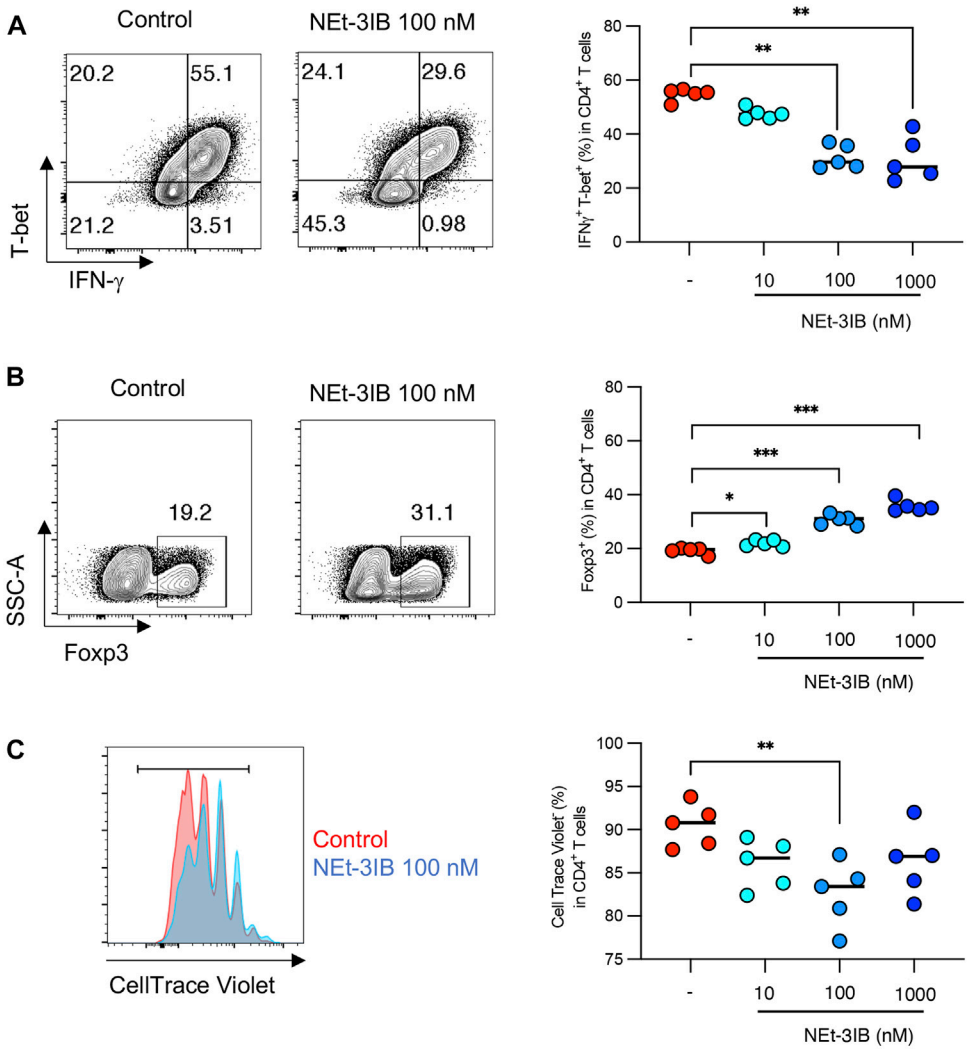


FIGURE 4 | NEt-3IB inhibits differentiation of inflammatory T cells and induces Foxp3$^+$ cells in Th1 and Th17 conditions. **(A, B)** Naïve T cells were cultured in Th1 conditions, with or without NEt-3IB treatment for 5 days and analyzed for T-bet and IFN-γ expression **(A)**, and for Foxp3 expression in the CD4$^+$ T cell population **(B)**. **(C)** Naïve T cells were labeled with CellTrace Violet and cultured in Th1 conditions with or without NEt-3IB treatment for 5 days. Cultured cells were analyzed for their degree of proliferation in the CD4$^+$ T-bet$^+$ IFN-γ^+ population. $^*p < 0.05$, $^{**}p < 0.01$, $^{***}p < 0.005$.

the total dosage reached the colon within 24 h post-oral administration, after the bile concentration peaked at 4 h. These data support the enterohepatic circulation of NEt-3IB, consistent with our previous report (Kobayashi et al., 2015). In contrast, such enterohepatic circulation was not observed in bexarotene, which was readily absorbed in the upper intestine after oral administration with only a small portion delivered to the colon. Thus, NEt-3IB is efficiently delivered to the colonic lumen and should be translocated to the cLP under inflammatory conditions, which are often associated with mucosal barrier disruption.

Early studies showed that the activation and overexpression of certain nuclear receptors exert anti-inflammatory effects. For instance, PPAR agonists suppress the differentiation of Th1 cells *in vitro* by inhibiting the JAK–STAT signaling pathway (Natarajan and Bright, 2002). LXR agonists also display similar effects on the differentiation of Th1 cells (Solt et al., 2012). Moreover, PPARγ and LXR agonists both suppress the proliferation of T cells (Yang et al., 2000; Cunard et al., 2002; Diab et al., 2004; Bensinger et al., 2008; Solt et al., 2012). Given that these nuclear receptors heterodimerize with RXR, and RXR agonists can activate these partner nuclear receptors, the inhibitory effect of NEt-3IB on Th1 response may depend on the activation of LXR and PPAR signaling. Additionally, PPARγ agonists inhibit IL-12 production by macrophages, which is important for the differentiation and survival of Th1 cells (Natarajan and Bright, 2002). Thus, NEt-3IB may directly and indirectly suppress the Th1 response through the inhibition of IL-12 production by macrophages.

Our *in vitro* experiments demonstrated that Foxp3$^+$ cells arose in the NEt-3IB-treated group despite the Th1-differentiation conditions. Given that RXR agonists modulate Foxp3$^+$ Treg cell differentiation (Takeuchi et al., 2013), NEt-3IB may drive naïve CD4$^+$ T cells to upregulate Foxp3 regardless of the culture conditions. Because ectopic Foxp3 expression represses IFN-γ expression, it is possible that NEt-3IB reduced the number of Th1 cells *in vitro* by downregulating T-bet expression. Nevertheless, in the CD4$^+$CD45RB^{high} T-cell-transfer colitis model, no significant difference in the frequency of Treg cells was identified between the control and NEt-3B-treated groups. This observation implies that NEt-3IB may repress IFN-γ expression via an unknown mechanism other than upregulation of Foxp3. For instance, NEt-3IB may indirectly dampen Th1 cell expansion by diminishing Th17 cell differentiation. We observed a reduction in IFN-γ-producing Th17 cells in the cLP of the NEt-3IB-treated group. This transient cell population is generated from conventional Th17 cells and further differentiates into Th1 cells (Sujino et al., 2011; Basdeo et al., 2017). Therefore, the reduction in IFN-γ-producing Th17 cells in the cLP of the NEt-3IB group cells may lead to a decrease in Th1 cells. Notably, RXR and LXR agonists negatively regulate the differentiation of Th17 cells *in vitro* (Solt et al., 2012; Takeuchi et al., 2013). Thus, NEt-3IB possibly restricted the development of Th17 cells in the colitis model mice, resulting in the reduction of IFN-γ-producing Th17, and in turn, Th17 cell-derived Th1 cells.

NEt-3IB treatment also reduced the number of macrophages. NEt-3IB is likely to indirectly suppress the infiltration of macrophages by inhibiting the expansion of IFN-γ-producing Th17 and Th1 cells. Furthermore, NEt-3IB may directly diminish macrophage activation. In support of this, we previously found that a partial RXR agonist, CBT-PMN, downregulates the production of pro-inflammatory cytokines by bone marrow-derived macrophages (Onuki et al., 2018). Furthermore, other groups showed that FXR agonist treatment significantly downregulated IFN-γ-related gene expression (Renga et al., 2009), and that PPAR and LXR agonists also suppress the production of inflammatory cytokines from macrophages (Birrell et al., 2007; Paukkeri et al., 2013) Additionally, overexpression of NR4A1 and NR4A2 in human macrophages inhibits pro-inflammatory cytokines (Bonta et al., 2006). All these nuclear receptors form heterodimers with RXR and are activated by RXR agonists. These facts support the possibility that NEt-3IB directly inhibits the activation and cytokine production of macrophages by activating RXR partner nuclear receptors.

In conclusion, the present study demonstrated that NEt-3IB ameliorated colitis by inhibiting both the expansion of Th1 cells and the activation of inflammatory macrophages locally in the colon. Our results indicate that NEt-3IB is a promising candidate for IBD treatment as a small molecule inhibitor.

DATA AVAILABILITY STATEMENT

The original contributions presented in the study are included in the article **Supplementary Material**, further inquiries can be directed to the corresponding authors.

ETHICS STATEMENT

The animal studies were reviewed and approved by Animal Studies Committees of Keio University, and the Animal Care and Use Committee of Okayama University.

AUTHOR CONTRIBUTIONS

MW, SN, and YT synthesized NEt-3IB and bexarotene. MW, SN, and YK performed the pharmacokinetic experiments and analysis. RM and DT performed the colitis experiments, and RM performed the *in vitro* experiments. HK and KH designed the study. RM, MW, and DT wrote the manuscript. HK and KH revised the manuscript.

FUNDING

This study was supported by grants from the Japan Society for the Promotion of Science (20H00509, and 20H05876 to KH), JST Moonshot (21-201033024 to KH), AMED-Crest (18gm1010004h0103, 19gm1010004s0104, 20gm1010004h0105, and 20gm1310009h0001 to KH), The Science Research Promotion Fund, and The Promotion and Mutual Aid Corporation for Private Schools of Japan (KH). Furthermore, this study received funding from AIBIOS Co., Ltd. (HK and KH). The funder was not involved in the study design, collection, analysis, interpretation of data, the writing of this article or the decision to submit it for publication.

ACKNOWLEDGMENTS

We thank Yumiko Fujimura for assistance with the animal experiments. The authors are grateful to the Division of Instrumental Analysis, Okayama University for the NMR and MS measurements. We also thank H. Nikki March, from Edanz (https://jp.edanz.com/ac) for editing a draft of this manuscript.

SUPPLEMENTARY MATERIAL

The Supplementary Material for this article can be found online at: https://www.frontiersin.org/articles/10.3389/fphar.2021.715752/full#supplementary-material

REFERENCES

Adegbola, S. O., Sahnan, K., Warusavitarne, J., Hart, A., and Tozer, P. (2018). Anti-TNF Therapy in Crohn's Disease. *Ijms* 19, 2244–2321. doi:10.3390/ijms19082244

Basdeo, S. A., Cluxton, D., Sulaimani, J., Moran, B., Canavan, M., Orr, C., et al. (2017). Ex-Th17 (Nonclassical Th1) Cells Are Functionally Distinct from Classical Th1 and Th17 Cells and Are Not Constrained by Regulatory T Cells. *J.I.* 198, 2249–2259. doi:10.4049/jimmunol.1600737

Bensinger, S. J., Bradley, M. N., Joseph, S. B., Zelcer, N., Janssen, E. M., Hausner, M. A., et al. (2008). LXR Signaling Couples Sterol Metabolism to Proliferation in the Acquired Immune Response. *Cell* 134, 97–111. doi:10.1016/j.cell.2008.04.052

Birrell, M. A., Catley, M. C., Hardaker, E., Wong, S., Willson, T. M., McCluskie, K., et al. (2007). Novel Role for the Liver X Nuclear Receptor in the Suppression of Lung Inflammatory Responses. *J. Biol. Chem.* 282, 31882–31890. doi:10.1074/jbc.M703278200

Boehm, M. F., Zhang, L., Badea, B. A., White, S. K., Mais, D. E., Berger, E., et al. (1994). Synthesis and Structure-Activity Relationships of Novel Retinoid X Receptor-Selective Retinoids. *J. Med. Chem.* 37, 2930–2941. doi:10.1021/jm00044a014

Bonta, P. I., Van Tiel, C. M., Vos, M., Pols, T. W. H., Van Thienen, J. V., Ferreira, V., et al. (2006). Nuclear Receptors Nur77, Nurr1, and NOR-1 Expressed in Atherosclerotic Lesion Macrophages Reduce Lipid Loading and Inflammatory Responses. *Atvb* 26, 2288. doi:10.1161/01.ATV.0000238346.84458.5d

Budgin, J. B., Richardson, S. K., Newton, S. B., Wysocka, M., Zaki, M. H., Benoit, B., et al. (2005). Biological Effects of Bexarotene in Cutaneous T-Cell Lymphoma. *Arch. Dermatol.* 141, 315–320. doi:10.1001/archderm.141.3.315

Carter, M. J., Lobo, A. J., and Travis, S. P. L. (2004). Guidelines for the Management of Inflammatory Bowel Disease in Adults. *Gut* 53, v1–v16. doi:10.1136/gut.2004.043372

Cunard, R., Ricote, M., DiCampli, D., Archer, D. C., Kahn, D. A., Glass, C. K., et al. (2002). Regulation of Cytokine Expression by Ligands of Peroxisome Proliferator Activated Receptors. *J. Immunol.* 168, 2795–2802. doi:10.4049/jimmunol.168.6.2795

De Souza, H. S. P., and Fiocchi, C. (2016). Immunopathogenesis of IBD: Current State of the Art. *Nat. Rev. Gastroenterol. Hepatol.* 13, 13–27. doi:10.1038/nrgastro.2015.186

de Vries-van der Weij, J., De Haan, W., Hu, L., Kuif, M., Oei, H. L., Van Der Hoorn, J. W., et al. (2009). Bexarotene Induces Dyslipidemia by Increased Very Low-Density Lipoprotein Production and Cholesteryl Ester Transfer Protein-Mediated Reduction of High-Density Lipoprotein. *Endocrinology* 150, 2368–2375. doi:10.1210/en.2008-1540

Diab, A., Drew, P. D., Racke Judy Choy, M. K., Rocchini, A., Matthes, L., Amy E Lovett-Racke, J. A., et al. (2004). Peroxisome Proliferator-Activated Receptor Agonists as Therapy for Autoimmune Disease. *J. Immunol.* doi:10.4049/jimmunol.172.9.5790

Dubrac, S., Elentner, A., Ebner, S., Horejs-Hoeck, J., and Schmuth, M. (2010). Modulation of T Lymphocyte Function by the Pregnane X Receptor. *J.I.* 184, 2949–2957. doi:10.4049/jimmunol.0902151

Evans, R. M., and Mangelsdorf, D. J. (2014). Nuclear Receptors, RXR, and the Big Bang. *Cell* 157, 255–266. doi:10.1016/j.cell.2014.03.012

Ha, F., and Khalil, H. (2015). Crohn's Disease: a Clinical Update. *Therap. Adv. Gastroenterol.* 8, 352–359. doi:10.1177/1756283X15592585

Kakuta, H., Ohsawa, F., Yamada, S., Makishima, M., Tai, A., Yasui, H., et al. (2012). Feasibility of Structural Modification of Retinoid X Receptor Agonists to Separate Blood Glucose-Lowering Action from Adverse Effects: Studies in KKAy Type 2 Diabetes Model Mice. *Biol. Pharm. Bull.* 35, 629–633. doi:10.1248/bpb.35.629

Kanakasabai, S., Chearwae, W., Walline, C. C., Iams, W., Adams, S. M., and Bright, J. J. (2010). Peroxisome Proliferator-Activated Receptor δ Agonists Inhibit T Helper Type 1 (Th1) and Th17 Responses in Experimental Allergic Encephalomyelitis. *Immunology* 130, 572–588. doi:10.1111/j.1365-2567.2010.03261.x

Kjellev, S., Lundsgaard, D., Poulsen, S. S., and Markholst, H. (2006). Reconstitution of Scid Mice with CD4+CD25− T Cells Leads to Rapid Colitis: An Improved Model for Pharmacologic Testing. *Int. Immunopharmacology* 6, 1341–1354. doi:10.1016/j.intimp.2006.04.017

Kobayashi, T., Furusawa, Y., Yamada, S., Akehi, M., Takenaka, F., Sasaki, T., et al. (2015). Positron Emission Tomography to Elucidate Pharmacokinetic Differences of Regioisomeric Retinoid X Receptor Agonists. *ACS Med. Chem. Lett.* 6, 334–338. doi:10.1021/ml500511m

Liebmann, M., Hucke, S., Koch, K., Eschborn, M., Ghelman, J., Chasan, A. I., et al. (2018). Nur77 Serves as a Molecular Brake of the Metabolic Switch during T Cell Activation to Restrict Autoimmunity. *Proc. Natl. Acad. Sci. USA* 115, E8017–E8026. doi:10.1073/pnas.1721049115

Liu, S., Ogilvie, K. M., Klausing, K., Lawson, M. A., Jolley, D., Li, D., et al. (2002). Mechanism of Selective Retinoid X Receptor Agonist-Induced Hypothyroidism in the Rat. *Endocrinology* 143, 2880–2885. doi:10.1210/endo.143.8.8930

Natarajan, C., and Bright, J. J. (2002). Peroxisome Proliferator-Activated Receptor-Gamma Agonists Inhibit Experimental Allergic Encephalomyelitis by Blocking IL-12 Production, IL-12 Signaling and Th1 Differentiation. *Genes Immun.* 3, 59–70. doi:10.1038/sj.gene.6363832

Onuki, M., Watanabe, M., Ishihara, N., Suzuki, K., Takizawa, K., Hirota, M., et al. 2018). A Partial Agonist for Retinoid X Receptor Mitigates Experimental Colitis. *Int Immunol.* 31, 251–262. doi:10.1093/intimm/dxy089

Paukkeri, E.-L., Leppänen, T., Lindholm, M., Yam, M. F., Asmawi, M., Kolmonen, A., et al. (2013). Anti-inflammatory Properties of a Dual PPARgamma/alpha Agonist Muraglitazar in *In Vitro* and *In Vivo* Models. *Arthritis Res. Ther.* 15, R51. doi:10.1186/ar4211

Powrie, F., Leach, M. W., Mauze, S., Caddie, L. B., and Coffman, R. L. (1993). Phenotypically Distinct Subsets of CD4+ T Cells Induce or Protect from Chronic Intestinal Inflammation in C. B-17 Scid Mice. *Int. Immunol.* 5, 1461–1471. doi:10.1093/intimm/5.11.1461

Renga, B., Migliorati, M., Mencarelli, A., and Fiorucci, S. (2009). Reciprocal Regulation of the Bile Acid-Activated Receptor FXR and the Interferon-γ-STAT-1 Pathway in Macrophages. *Biochim. Biophys. Acta (Bba) - Mol. Basis Dis.* 1792, 564–573. doi:10.1016/j.bbadis.2009.04.004

Solt, L. A., Kamenecka, T. M., and Burris, T. P. (2012). LXR-mediated Inhibition of CD4+ T Helper Cells. *PLoS One* 7, e46615. doi:10.1371/journal.pone.0046615

Standeven, A. M., Escobar, M., Beard, R. L., Yuan, Y. D., and Chandraratna, R. A. S. (1997). Mitogenic Effect of Retinoid X Receptor Agonists in Rat Liver. *Biochem. Pharmacol.* doi:10.1016/S0006-2952(97)00209-8

Stout, R. D., and Bottomly, K. (1989). Antigen-specific Activation of Effector Macrophages by IFN-Gamma Producing (TH1) T Cell Clones. Failure of IL-4-producing (TH2) T Cell Clones to Activate Effector Function in Macrophages. *J. Immunol.* 142, 760–765. Available at: http://www.jimmunol.org/content/142/3/760.abstract.

Sujino, T., Kanai, T., Ono, Y., Mikami, Y., Hayashi, A., Doi, T., et al. (2011). Regulatory T Cells Suppress Development of Colitis, Blocking Differentiation of T-Helper 17 into Alternative T-Helper 1 Cells. *Gastroenterology* 141, 1014–1023. doi:10.1053/j.gastro.2011.05.052

Takamatsu, K., Takano, A., Yakushiji, N., Morohashi, K., Morishita, K.-i., Matsuura, N., et al. (2008). The First Potent Subtype-Selective Retinoid X Receptor (RXR) Agonist Possessing a 3-Isopropoxy-4-Isopropylphenylamino Moiety, NEt-3IP (RXRα/β-Dual Agonist). *ChemMedChem* 3, 780–787. doi:10.1002/cmdc.200700313

Takeuchi, H., Yokota-Nakatsuma, A., Ohoka, Y., Kagechika, H., Kato, C., Song, S.-Y., et al. (2013). Retinoid X Receptor Agonists Modulate Foxp3+ Regulatory T Cell and Th17 Cell Differentiation with Differential Dependence on Retinoic Acid Receptor Activation. *J.I.* 191, 3725–3733. doi:10.4049/jimmunol.1300032

Yang, X. Y., Wang, L. H., Chen, T., Hodge, D. R., Resau, J. H., DaSilva, L., et al. (2000). Activation of Human T Lymphocytes Is Inhibited by Peroxisome Proliferator-Activated Receptor γ (PPARγ) Agonists. *J. Biol. Chem.* 275, 4541–4544. doi:10.1074/jbc.275.7.4541

Conflict of Interest: The authors declare that the research was conducted in the absence of any commercial or financial relationships that could be construed as a potential conflict of interest.

Publisher's Note: All claims expressed in this article are solely those of the authors and do not necessarily represent those of their affiliated organizations, or those of the publisher, the editors and the reviewers. Any product that may be evaluated in this article, or claim that may be made by its manufacturer, is not guaranteed or endorsed by the publisher.

Copyright © 2021 Matsumoto, Takahashi, Watanabe, Nakatani, Takamura, Kurosaki, Kakuta and Hase. This is an open-access article distributed under the terms of the Creative Commons Attribution License (CC BY). The use, distribution or reproduction in other forums is permitted, provided the original author(s) and the copyright owner(s) are credited and that the original publication in this journal is cited, in accordance with accepted academic practice. No use, distribution or reproduction is permitted which does not comply with these terms.

frontiers in Pharmacology

ORIGINAL RESEARCH
published: 31 August 2021
doi: 10.3389/fphar.2021.724514

AICAR, an AMP-Activated Protein Kinase Activator, Ameliorates Acute Pancreatitis-Associated Liver Injury Partially Through Nrf2-Mediated Antioxidant Effects and Inhibition of NLRP3 Inflammasome Activation

Lijun Kong[1], Hewei Zhang[1], Chaosheng Lu[2], Keqing Shi[3], Hongjian Huang[1], Yushu Zheng[1], Yongqiang Wang[1], Dan Wang[2], Hongwei Wang[1] and Wei Huang[4]**

[1]Key Laboratory of Diagnosis and Treatment of Severe Hepato-Pancreatic Diseases of Zhejiang Province, The First Affiliated Hospital of Wenzhou Medical University, Wenzhou, China, [2]Department of Pediatrics, The First Affiliated Hospital of Wenzhou Medical University, Wenzhou, China, [3]Translational Medicine Laboratory, The First Affiliated Hospital of Wenzhou Medical University, Wenzhou, China, [4]Department of Nutrition, The First Affiliated Hospital of Wenzhou Medical University, Wenzhou, China

Acute pancreatitis (AP) is a highly fatal acute inflammation and is often accompanied by multiple organ dysfunction syndrome (MODS). The liver, one of the most vulnerable extrapancreatic organs in AP, is the major organ involved in the evolution of the disease and correlates strongly with the occurrence of MODS. However, the etiology of pancreatitis-associated liver injury (PALI) has not been clarified and currently lacks an effective treatment. 5-Aminoimidazole-4-carboxamide ribonucleotide (AICAR) is a cell permeable nucleoside with pleiotropic effects on anti-inflammatory and antioxidant stress that binds with adenosine monophosphate protein kinase (AMPK) and induces AMPK activation. However, the role of AICAR in PALI remains elusive. Here, we show that activation of AMPK by AICAR, a direct AMPK agonist, significantly ameliorates sodium taurocholate-induced PALI in rats, whereas treatment of PALI rats with the AMPK antagonist Compound C profoundly exacerbates the degree of liver injury, suggesting that hepatic AMPK activation exerts an essential protective role in PALI. Mechanistically, AICAR induces AMPK activation, which in turn activates nuclear factor erythroid 2-related factor 2(Nrf2) -regulated hepatic antioxidant capacity and inhibits NLRP3 inflammasome-mediated pyrolysis, protecting rats from sodium taurocholate-induced PALI. In addition, Nrf2 deficiency strikingly weakens the beneficial effects of AICAR on alleviation of liver injury, oxidative stress and NLRP3 inflammasome activation in L-arginine-induced PALI mice. Thus, AICAR protects against PALI in rodents by triggering AMPK, which is mediated at least in part by Nrf2-modulated antioxidant effects and NLRP3 inflammasome activation.

Keywords: pancreatitis, liver injury, AMPK, Nrf2, NLRP3 inflammasome

OPEN ACCESS

Edited by:
Ralf Weiskirchen,
RWTH Aachen University, Germany

Reviewed by:
Wei Huang,
Sichuan University, China
Qiao Shi,
Renmin Hospital of Wuhan University, China
Wei Liu,
University of Science and Technology of China, China

****Correspondence:***
Hongwei Wang
15258085168@163.com
Wei Huang
hw120418@163.com

Specialty section:
This article was submitted to Gastrointestinal and Hepatic Pharmacology, a section of the journal Frontiers in Pharmacology

Received: *13 June 2021*
Accepted: *12 August 2021*
Published: *31 August 2021*

Citation:
Kong L, Zhang H, Lu C, Shi K, Huang H, Zheng Y, Wang Y, Wang D, Wang H and Huang W (2021) AICAR, an AMP-Activated Protein Kinase Activator, Ameliorates Acute Pancreatitis-Associated Liver Injury Partially Through Nrf2-Mediated Antioxidant Effects and Inhibition of NLRP3 Inflammasome Activation. Front. Pharmacol. 12:724514. doi: 10.3389/fphar.2021.724514

INTRODUCTION

Acute pancreatitis (AP) is a highly fatal acute inflammation with rapid progression. (Argaiz and de Moraes, 2021). There is an increasing prevalence of AP, with an estimated 33.74 cases per 100,000 people worldwide each year (Garg and Singh, 2019). The high mortality of AP is largely attributed to multiple organ dysfunction syndrome (MODS), such as liver or lung injury (Shi et al., 2020). The liver, a major organ involved in the evolution of AP, is strikingly vulnerable to inflammatory cytokines and correlates strongly with the occurrence of MODS (Li S. et al., 2019; Mei et al., 2019). Pancreatitis-associated liver injury (PALI) is a serious and even fatal complication in the development of AP (Wang et al., 2018). Mechanistically, a series of endogenous vasoactive substances released during AP lead to hepatic microcirculation disturbance, which is the essential cause of liver injury (Wenhong et al., 2012). Liver injury in turn triggers a systemic inflammatory response by affecting toxin metabolism and releasing massive inflammatory mediators (Rios et al., 2010; Ou et al., 2017). The PALI phenomenon has been observed in both clinical and experimental settings (Wang et al., 2006; Wenhong et al., 2012; Lv et al., 2015; Bakır et al., 2016; Ou et al., 2017). Notably, Curbey et al. reported that 80% of AP patients had liver damage and the liver injury aggravates the degree of pancreatitis if it is not intervened in time, which significantly prolongs the course of pancreatitis (Ou et al., 2017; Li X. et al., 2019). To date, the etiology of PALI has not been clarified, and no effective treatment has been developed. Thus, finding a promising therapeutic way to prevent or treat this devastating and fatal disease is urgently needed.

Adenosine monophosphate protein kinase (AMPK) is the main energy receptor regulating cell metabolism (Yang et al., 2021; Zhao et al., 2021). The activation of AMPK depends on the phosphorylation of Thr172 of the α subunit (Garcia and Shaw, 2017). In general, AMPK is activated under energy stress by sensing an increase in the ratios of AMP/ATP and ADP/ATP, thereby stimulating the catabolic process and maintaining energy homeostasis (Lin and Hardie, 2018). In addition to its role in energy dynamic balance, activated AMPK is also associated with reducing redox stress, inhibiting inflammation or limiting cell proliferation (Zimmermann et al., 2015; Liu et al., 2020; Chin et al., 2021). Recent studies indicate that AMPK activation plays an inhibitory role in mediating ethanol-induced oxidative stress in human pancreatic acinar cells, whereas AMPK inhibition can aggravate liver inflammation in mice with hepatic ischemia-reperfusion (Zhou et al., 2018; Srinivasan et al., 2020). Although the anti-inflammatory and antioxidant stress functions of AMPK activation have been well characterized, little is known about the pathophysiological roles in PALI, and the potential mechanism whereby AMPK activation protects against PALI remains poorly defined.

Under physiological conditions, serine 374, 408 and 433 of nuclear factor erythroid related factor 2 (Nrf2) are hyperphosphorylated with the activation of AMPK (Matzinger et al., 2020). Early studies have reported that AMPK activation enhances cellular antioxidant potential by activating the transcriptional activity of Nrf2 (Garcia and Shaw, 2017; Xu et al., 2020). Nrf2 is a member of the Cap'n'Collar (CNC) family of basic leucine zipper (bZIP) transcription factors, which activates the endogenous antioxidant defense system through translocation into the nucleus, thus combating inflammation and oxidative stress (Tonelli et al., 2018; Lyu et al., 2020; Gong et al., 2021; Tan et al., 2021). Inflammation causes oxidative stress; in turn, oxidative stress also boosts the production of inflammatory cytokines through activation of proinflammatory pathways, including the known Nod-like Receptor Protein 3 (NLRP3) inflammasome pathway (Zeng et al., 2017). It consists of NLRP3 scaffold, adaptor protein apoptosis-associated speck-like protein (ASC) and proinflammatory caspase-1 (Zou et al., 2021). When NLRP3 is activated, the p20 subunit and p10 subunit are heterodimerized to form bioactive caspase-1, which processes the release of IL-1β and induces a unique inflammatory type of cell death called pyroptosis (Chen et al., 2017; Unamuno et al., 2021). Growing evidence has established that NLRP3 inflammasome activation leads to hepatocyte pyroptosis and severe liver inflammation (Han et al., 2018; Wree et al., 2018). Recently, the inverse correlation between the activated Nrf2 and NLRP3 inflammasome pathway that inhibits inflammation through augmenting antioxidant capacity in mice have been proved in acute lung injury (Liu et al., 2017). Nonetheless, whether the activation of AMPK plays an antioxidative and anti-inflammatory role through Nrf2-mediated antioxidant effects and inhibition of the NLRP3 inflammasome pathway in PALI remain to be determined.

5-Aminoimidazole-4-formamide ribonucleotide (AICAR) is a kind of cellular permeable nucleoside that activates AMPK to play anti-inflammatory and antioxidant stress effects (Swinnen et al., 2005; Bone et al., 2017; Kaphalia et al., 2019). AICAR is converted into ZMP (an AMP mimic) in cells to bind to the γ subunit of AMPK, causing conformational changes in the enzyme and promoting the phosphorylation of Thr172 of the AMPKα subunit by liver kinase B1 (LKB1) or other upstream AMPK kinases (AMPKK) (Sun et al., 2007; Hill et al., 2016; Lane et al., 2020; Višnjić et al., 2021). Emerging evidence indicates that the activation of AMPK by AICAR attenuates high glucose-induced oxidative stress in rat cardiomyocytes (Shen et al., 2019). Moreover, the direct AMPK agonist AICAR negatively regulates the IL-6-stimulated inflammatory response in human liver cells by suppressing the phosphorylation of STAT3 (Nerstedt et al., 2010). However, it is not clear whether pharmacological activation of AMPK by the direct AMPK small molecule agonist AICAR is a therapeutic strategy for PALI.

In the present study, we investigated whether activation of AMPK by AICAR limits the inflammatory response and oxidative stress in the progression of PALI in two rodent models of severe acute pancreatitis (SAP) *via* Nrf2-mediated antioxidant effects and NLRP3 inflammasome activation. Our results provide the first direct evidence of the beneficial effects of pharmacological activation of AMPK by AICAR against the progression of PALI, including reduced redox stress and decreased NLRP3 inflammasome activation. Moreover, Nrf2 deficiency dramatically weakened these beneficial effects of AICAR in L-arginine-induced PALI mice. Thus, AICAR protects against PALI at least in part through Nrf2-mediated

antioxidant effects and inhibition of NLRP3 inflammasome activation.

MATERIALS AND METHODS

Animal Experiments

Male SD rats (220–250 g, age 7–8 weeks) were obtained from the Experimental Animal Center of Wenzhou Medical University. Nrf2-knockout ($Nrf2^{-/-}$) mice on C57BL/6 background were procured from Jackson Laboratory (Bar Harbor, Maine, United States). These homozygous $Nrf2^{-/-}$ mice were backcrossed with C57BL/6 wild type mice. Heterozygous offspring were then further bred to gain wild type and $Nrf2^{-/-}$ littermates. Genotypes of $Nrf2^{-/-}$ mice were identified by PCR. All rats and mice were fed randomly at 24 ± 2°C and 40–60% humidity with a 12 h dark cycle before the experiment. All animal procedures were reviewed and approved by the Animal Ethics Committee of Wenzhou Medical University.

Wild-type rats were randomly divided into four groups: the control group (n = 10), severe acute pancreatitis (SAP) group (n = 10), AMPK agonist (AICAR) group (n = 8) and AMPK inhibitor (Compound C, CC) group (n = 8). Sham operation was performed in the control group. Pancreatitis was induced in the SAP, AICAR and CC groups by retrograde injection of 3% sodium taurocholate (STC, 0.1 ml/100 g of body weight, YZ-110815, Solarbio, Beijing, China) *via* the pancreatic duct using a syringe pump as previously described (Fang et al., 2020). The AICAR group received intraperitoneal injection of AICAR (400 mg/kg) 1 h before the operation. In the CC group, CC (13.8 mg/kg) was also injected intraperitoneally 1 h before the operation. AMPK agonist (AICAR) and AMPK inhibitor (CC) were purchased from MedChemExpress (HY-13417, HY-13418A, MedChemExpress, New Jersey, United States). The specific dosages of AICAR and CC used in this study based in the description in previous studies with minor modifications (Saito et al., 2012; Guo et al., 2014; Martin et al., 2019). 24 h after injection of sodium taurocholate, the rats were anesthetized with isoflurane (in 4% for induction and 3% for maintenance; R510, RWD Life Science, Shenzhen, China) on the anesthetic machine. Rats were sacrificed, and pancreatic tissues, liver tissues and blood samples were collected for further study.

Male C57BL/6 mice or $Nrf2^{-/-}$ mice were randomly divided into three groups: the control group (n = 6), SAP group (n = 6) and AMPK agonist (AICAR) group (n = 6). The control group mice were intraperitoneally injected with 0.9% normal saline. In the SAP and AICAR groups, the pancreatitis model was established by intraperitoneal injection of 8% L-arginine (pH = 7.0, 4.0 g/kg, A5006, Sigma, Missouri, United States) twice at an interval of 1 h as previously described (Liu et al., 2016). In the AICAR group, mice were intraperitoneally injected with AICAR (400 mg/kg) twice: 1 h before and 24 h after model establishment. 48 h after the injection of L-arginine, the mice were anesthetized with isoflurane (in 3.5% for induction and 2.5% for maintenance) on the anesthesia machine. Finally, the mice were sacrificed, and pancreatic tissues, liver tissues and blood samples were collected for subsequent experiments.

Histopathological Analysis

Pancreatic and liver tissues were collected, fixed immediately in 4% paraformaldehyde for 24 h, dehydrated in a graded ethanol series, and then embedded in paraffin. The tissue blocks were cut into 4.5 μm-thick sections, dewaxed, and hydrated. Then, pancreatic and liver sections were stained with hematoxylin and eosin (H&E) staining (G1120, Solarbio, Beijing, China) according to the manufacturer's instructions. After observation under an Olympus BX-51 microscope (Olympus Corporation, Tokyo, Japan), histological scores were obtained to evaluate the degree of pancreatic and liver injury with Image-Pro Plus 6.0 software (Media Cybernetics, Bethesda, United States) as described elsewhere (Rongione et al., 1997; Elshal et al., 2019).

Immunohistochemistry Analysis

Immunohistochemistry was used to qualitatively analyze the expression of phenotypic markers. The liver sections (4.5 μm) were boiled in antigen retrieval buffer containing citrate-hydrochloric acid (C8532, Sigma, Missouri, United States) for 15 min. Then, hydrogen peroxide (3%) was used for 10 min to block the activity of endogenous peroxidase and subsequently blocked with 5% bovine serum albumin (A1933, Sigma, Missouri, United States) for 30 min at 37°C. Primary antibodies for IL-6 (1: 200; MB9296, Bioworld Technology, Minnesota, United States), IL-1β (1:200; BS6067, Bioworld Technology, Minnesota, United States), TNF-α (1:200; BS6000, Bioworld Technology, Minnesota, United States), MCP-1 (1:200; DF7577, Affinity, Ohio, United States), HO-1 (1:200; ab13243, Abcam, Massachusetts, United States) and NQO-1 (1:200; ab28947, Abcam, Massachusetts, United States) were added and incubated at 4°C overnight. After washing, the sections were incubated with secondary antibodies (1:200; A0277, Beyotime Institute of Biotechology; Goat anti-rabbit IgG-HRP) for 1 h at 37 °C. Finally, the slides were stained using diaminobenzidine (DAB, P0202, Beyotime, Shanghai, China) for color visualization. Images of representative tissue spots were captured with an Olympus BX-51 microscope (Olympus Corporation, Tokyo, Japan) and analyzed with Image-Pro Plus 6.0 software (Media Cybernetics, Bethesda, United States).

Biochemical Indexes Assay

Fresh pancreatic and liver tissues and blood samples were collected for biochemical analysis. The levels of serum amylase and lipase were measured by assay kit (C016-1-1, A054-1-1, Nanjing Jiancheng Bioengineering Institute, Nanjing, China) to evaluate the degree of pancreatitis. The serum levels of alanine aminotransferase (ALT) and aspartate aminotransferase (AST) were measured with commercial kit (C009-2-1, C010-2-1, Nanjing Jiancheng Bioengineering Institute, Nanjing, China) to evaluate the degree of liver injury and function. The contents of malondialdehyde (MDA) and superoxide dismutase (SOD) in pancreas and liver homogenate were determined with commercial kit (A003-1-2, A001-3-2, Nanjing Jiancheng Bioengineering Institute, Nanjing, China). The contents of myeloperoxidase (MPO) were measured with commercial kit (A044-1-1, Nanjing Jiancheng Bioengineering Institute, Nanjing, China). All measurements were conducted according to the manufacturer's instructions of the assay kit.

Western Blot Analysis

The liver tissues were homogenized in RIPA lysis buffer (P0013C, Beyotime, Shanghai, China), and then the extract was transferred to a centrifuge tube and centrifuged at 12,000 rpm for 20 min. After testing the total protein concentration with a BCA protein analysis kit (P0012S, Beyotime, Shanghai, China), 40 μg of protein sample was separated on a 10% sodium dodecyl sulfate-polyacrylamide gel and transferred to a PVDF membrane. The membrane was blocked with 5% skim milk for 1 h and then incubated with specific primary antibodies against *p*-AMPK (Thr172; 1:1,000; 8208S, Cell Singling Technology, Boston, United States), AMPK (1:1,000; 5832S, Cell Singling Technology, Boston, United States), CD68 (1:1,000; ab125212, Abcam, Massachusetts, United States), NLRP3 (1:1,000; ab263899, Abcam, Massachusetts, United States), Caspase-1 (1:1,000; 22915-1-AP, Proteintech, Wuhan, China), cleaved IL-1β (1:1,000; AF4006, Proteintech, Wuhan, China), Nrf2 (1:1,000; 20733S, Cell Singling Technology, Boston, United States), HO-1 (1:1,000; ab13243, Abcam, Massachusetts, United States), NQO-1 (1:1,000; ab28947, Abcam, Massachusetts, United States), Lamin B (1:1,000; 12987-1-AP, Proteintech, Wuhan, China) and GAPDH (1:5,000; A00227-1, Boster, Wuhan, China) at 4°C overnight. All membranes were washed with TBST 3 times and incubated with horseradish peroxidase-conjugated secondary antibody (1: 5,000; A25012, Abbkine Scientific Co., Ltd, Wuhan, China) for 1 h. Finally, the bands were visualized using enhanced chemiluminescence (WP20005, Thermo Fisher Scientific, California, United States), and densitometry analysis was performed using VisionWorks imaging software (Eastman Kodak Company, New York, United States).

Nuclear Protein Extraction

Nuclear components were extracted from fresh liver tissues using a nuclear protein extraction kit (P0027, Beyotime, Shanghai, China) according to the manufacturer's instructions.

RNA Extraction and qRT-PCR

Total RNA was extracted from liver tissues with TRIzol Reagent (15596026, Thermo Fisher Scientific, California, United States) according to the manufacturer's specifications. Reverse transcription was completed by a Prime-Script RT Master Mix transcription kit (RR036A, TaKaRa, Tokyo, Japan). mRNA-specific primers (Sangon Biotech, China) were used to detect the RNA expression of IL-6, IL-1β and TNF-α. A 7500 Fast system (Applied Biosystems, United States) was used for qRT-PCR analysis. The results were analyzed using the $2^{-\Delta\Delta Ct}$ method, and GAPDH was amplified as an internal standard. The primer sequences are listed in **Supplementary Table S1**.

Statistical Analysis

All experiments were independently repeated three times. Values are presented as the mean ± SD (standard deviation). Statistical analysis was performed using GraphPad Prism 7.0 software (GraphPad Software, Inc., La Jolla, CA United States). Statistical significance was assessed by Student's t-test and one-way analysis of variance. Multiple comparisons between groups were analyzed using Tukey's post hoc test. $p < 0.05$ was considered statistically significant.

RESULTS

Direct AMPK Agonist AICAR Attenuates Pancreatitis-Associated Liver Injury and Restores Liver Function in Sodium Taurocholate-Induced SAP Rats

We investigated whether the direct AMPK activator AICAR (400 mg/kg) alleviates pancreatitis-associated liver injury by AMPK activation in a rat model of sodium taurocholate-induced SAP. We first validated the AMPK activator activity of AICAR in liver tissues of sodium taurocholate-induced SAP rats. Interestingly, the ratio of *p*-AMPK/AMPK in liver tissues significantly decreased after sodium taurocholate treatment. However, administration of AICAR by intraperitoneal injection into sodium taurocholate-treated rats resulted in a dramatic elevation of this ratio, suggesting that the reduced AMPK phosphorylation levels in the liver tissues of SAP rats were effectively activated by AICAR (**Figure 1A**). Hematoxylin and eosin staining demonstrated that the pancreas in SAP rats presented with notable interstitial edema, inflammatory cell infiltration and hemorrhagic necrosis, with the pancreatitis score analysis indicating a >5-fold increase over the control (**Figures 1B,D**). Likewise, the liver tissues of SAP rats were accompanied by obvious hepatocyte edema, necrosis, liver sinusoid congestion and dramatically damaged hepatic lobular structure, with the liver score analysis indicating a >4-fold increase compared with the control groups (**Figures 1C,D**). However, these negative changes were markedly reduced in the AICAR treatment groups (**Figures 1B–D**). Consistent with our histologic findings, the plasma levels of amylase and lipase, two common clinical indicators for assessing pancreatic injury (Steinberg et al., 2017), were elevated in SAP rats compared with control rats, whereas AICAR treatment prevented these increases (**Figure 1E**). Meanwhile, the increased levels of MDA and decreased concentrations of SOD in the pancreas of SAP rats indicated oxidative stress injury and downregulated antioxidant ability of the pancreas; however, administration of AICAR in rats significantly decreased the levels of MDA and increased the concentrations of SOD in pancreatic tissues of SAP rats, suggesting that AICAR supplementation restores the antioxidant ability of the pancreas in sodium taurocholate-induced SAP rats (**Figure 1F**). Correspondingly, evaluation of liver function in the SAP rats indicated that both the serum values of ALT and AST were significantly increased. In the presence of the AMPK activator AICAR, liver function was improved (**Figure 1G**). Taken together, the above results suggest that sodium taurocholate infusion established a successful rat model of PALI and that supplementation with AICAR not only reduces the severity of pancreatitis but also attenuates PALI and restores liver function in sodium taurocholate-induced SAP rats.

AICAR Prevents SAP-Induced Hepatic Inflammation in a Sodium Taurocholate-Induced SAP Rat Model

We explored the hypothesis that the molecular basis of AICAR in improving PALI is attributed to its anti-inflammatory

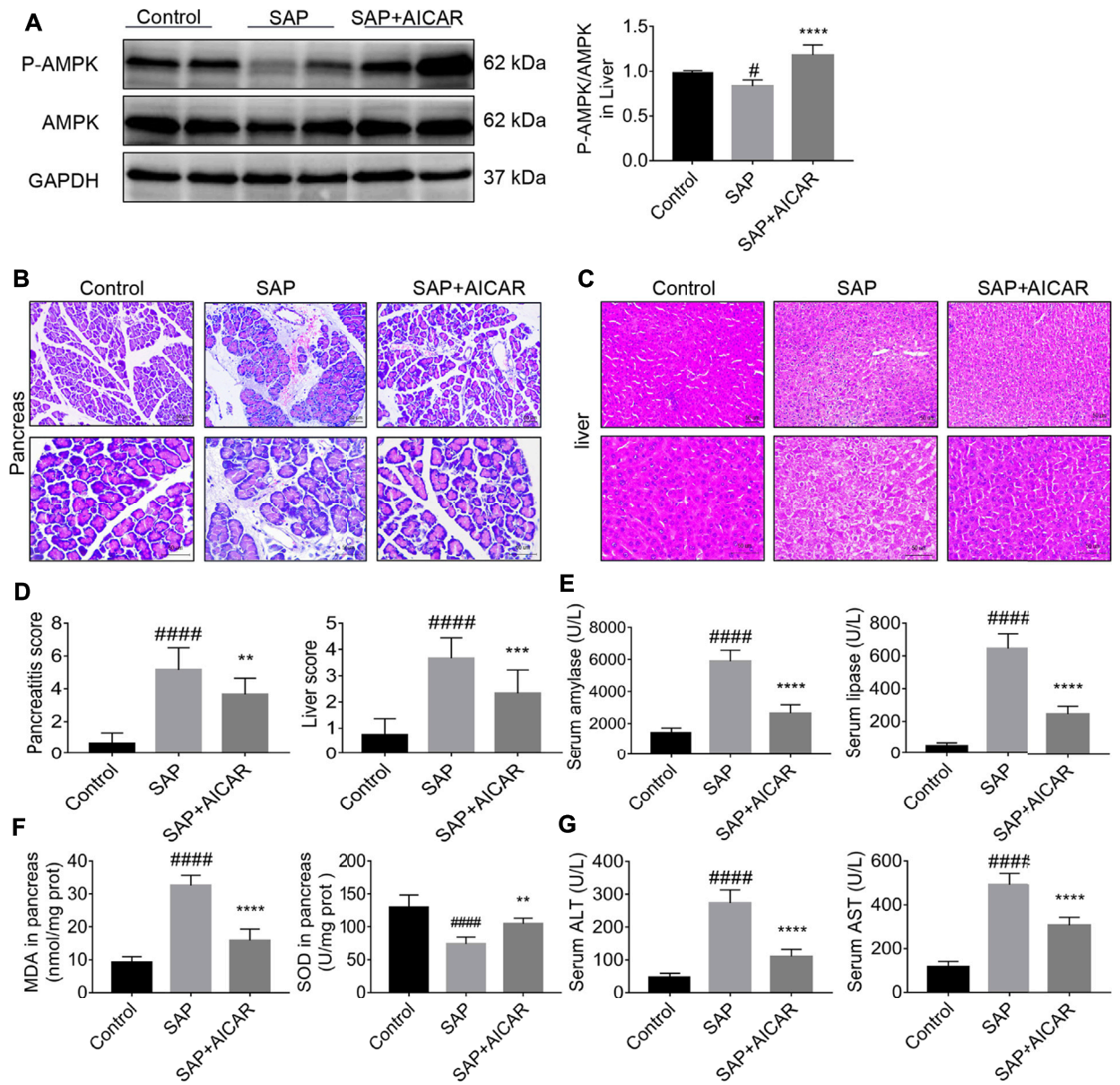


FIGURE 1 | The therapeutic effects of AICAR on pancreatitis-associated liver injury (PALI) in sodium taurocholate-induced SAP rats. 7–8 week-old wild-type male SD rats were randomly divided into three groups: the control group (control, n = 10) was treated with sham operation and injected with 0.9% normal saline; the severe acute pancreatitis (SAP) group (n = 10) was infused with 3% sodium taurocholate (0.1 ml/100 g); and the AMPK agonist (AICAR) group (n = 8) received intraperitoneal injection of AICAR (400 mg/kg) 1 h before the operation. **(A)** The protein expression levels of phosphorylated AMPK (*p*-AMPK) and AMPK were detected by Western blot, and the relative ratios of *p*-AMPK/AMPK were quantified by VisionWorks imaging software. The normalized values are indicated in the histogram. GAPDH expression was used as loading control. **(B,C)** Representative pathological images of the pancreas and liver (200x and 400x) under a light microscope (H&E staining, Bar = 50 μm). **(D)** Histological scores were obtained to evaluate the degree of pancreas and liver injury from H&E staining. **(E)** Serum amylase and lipase levels in rats. **(F)** The MDA and SOD contents in pancreatic tissues of rats in each group. **(G)** Detection of serum ALT and AST activity. Data are presented as the mean ± SD of three independent experiments. $^{\#}p < 0.05$, $^{\#\#}p < 0.01$, $^{\#\#\#}p < 0.001$, $^{\#\#\#\#}p < 0.0001$ vs. control group; $^{*}p < 0.05$, $^{**}p < 0.01$, $^{***}p < 0.001$, $^{****}p < 0.0001$ vs. SAP group.

capability. Our results indicated that the SAP rats exhibited higher hepatic expression of monocyte chemotactic protein 1 (MCP-1, a protein that specifically affects chemotaxis and activates macrophages) and CD68 (a rat macrophage marker) as well as increased concentrations of MPO (a functional and activation marker of neutrophils) in liver tissues compared with the control groups, whereas AICAR treatment profoundly downregulated the expression levels of these inflammatory mediators (**Figures 2A,B,D,E**). In addition, immunohistochemical staining and qRT-PCR indicated that

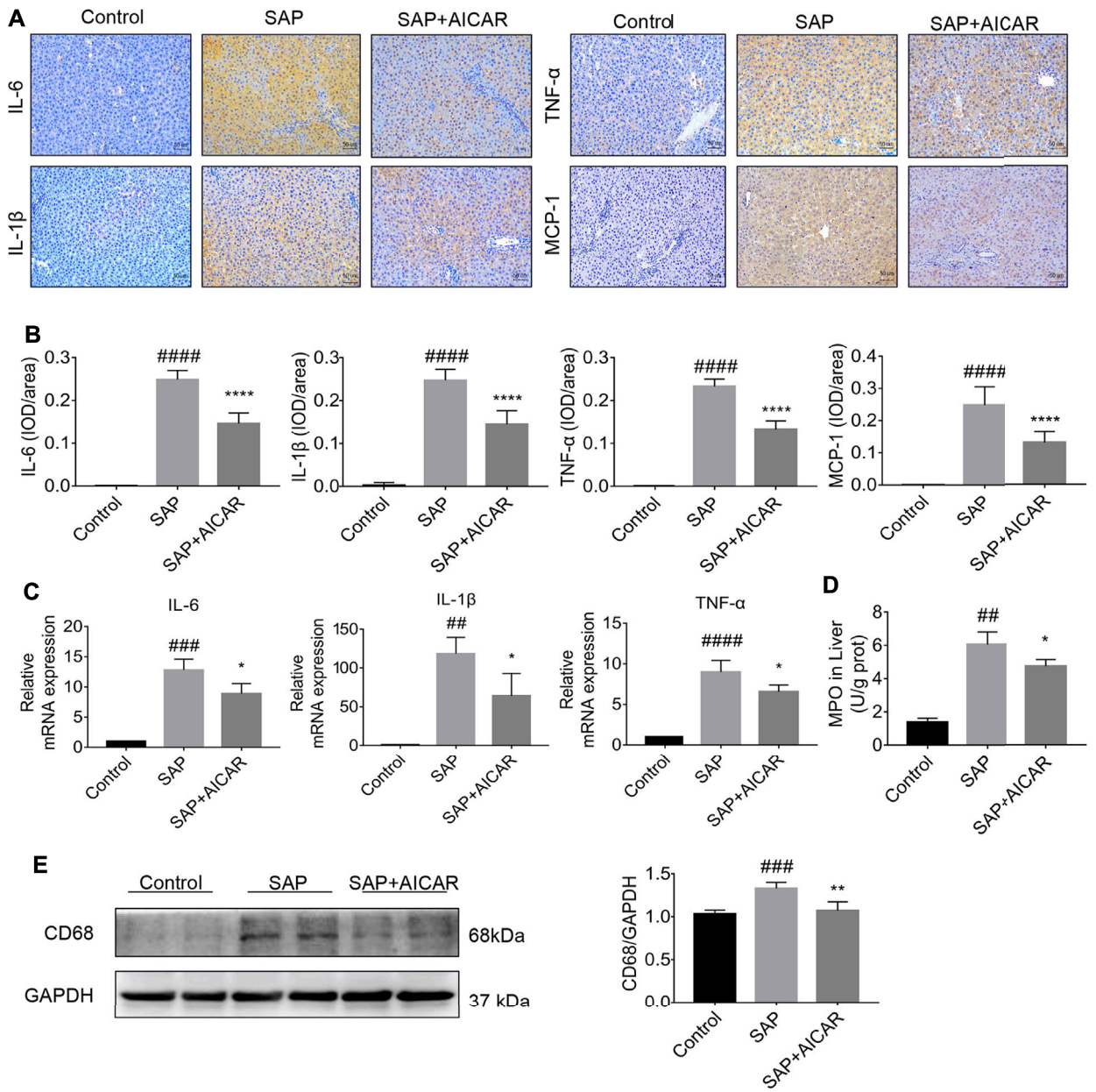


FIGURE 2 | AICAR protects against SAP-induced hepatic inflammation in a sodium taurocholate-induced PALI rat model. 7–8 week-old wild-type male SD rats were randomly divided into three groups: the control group (control, n = 10) was treated with sham operation and injected with 0.9% normal saline; the severe acute pancreatitis (SAP) group (n = 10) was infused with 3% sodium taurocholate (0.1 ml/100 g); and the AMPK agonist (AICAR) group (n = 8) received intraperitoneal injection of AICAR (400 mg/kg) 1 h before the operation. **(A,B)** The protein expression of IL-6, IL-1β, TNF-α and MCP-1 in liver sections was detected by immunohistochemistry (original magnification ×200, Bar = 50 μm). Image-Pro Plus 6.0 software was used for statistical analysis. **(C)** The mRNA levels of IL-6, IL-1β, and TNF-α in liver tissues were measured by RT-qPCR. **(D)** MPO contents in liver tissues. **(E)** The protein expression of CD68 was assessed by Western blot and quantified by densitometry using VisionWorks imaging software. GAPDH expression was used as a loading control. Each value represents the mean ± SD. $^{\#}p < 0.05$, $^{\#\#}p < 0.01$, $^{\#\#\#}p < 0.001$, $^{\#\#\#\#}p < 0.0001$ vs control group; $^{*}p < 0.05$, $^{**}p < 0.01$, $^{***}p < 0.001$, $^{****}p < 0.0001$ vs. SAP group.

the protein and messenger RNA (mRNA) expression levels of IL-6, IL-1β and TNF-α were significantly elevated in the liver tissues of SAP rats compared with the control group; however, replenishment of AICAR inhibited the increased expression of these inflammatory cytokines (**Figures 2A–C**). These observations confirm that AICAR treatment protects against PALI in sodium taurocholate-induced SAP rats, likely by inhibiting the inflammatory response in the liver.

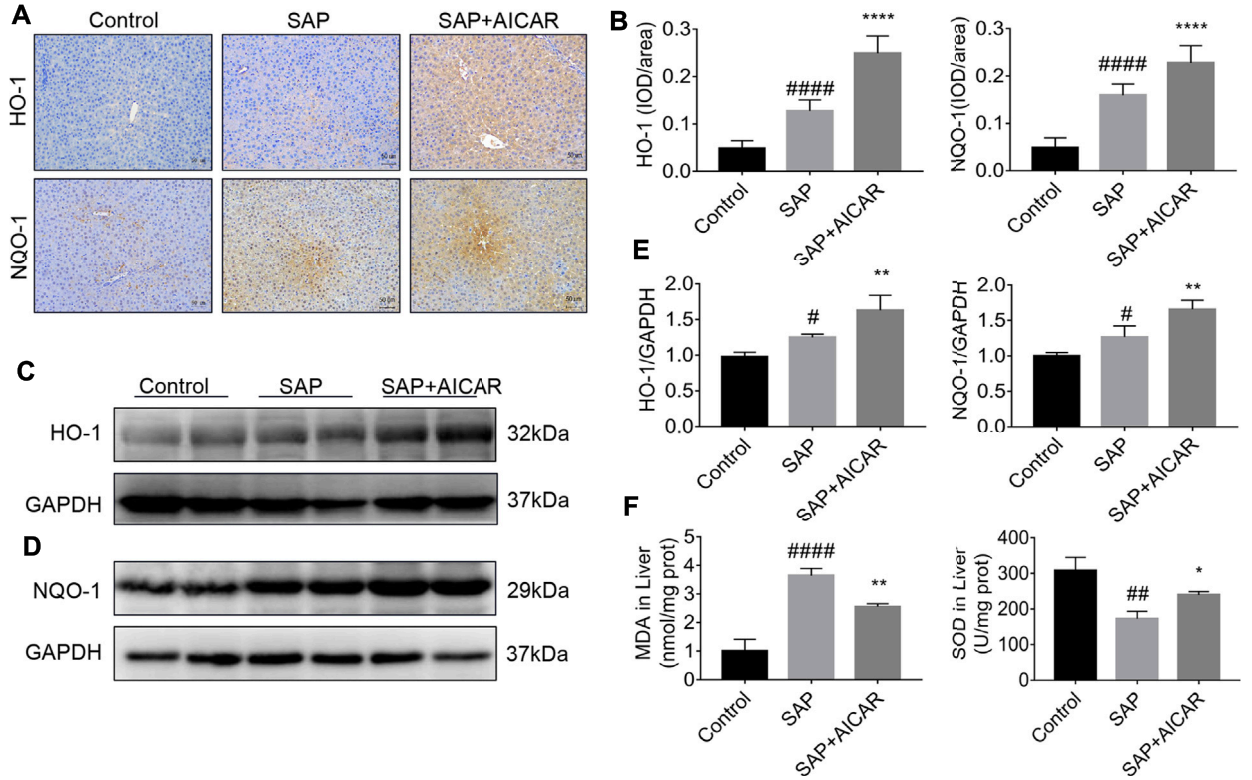


FIGURE 3 | AICAR prevents hepatic oxidative stress in a sodium taurocholate-induced PALI rat model. 7–8 week-old wild-type male SD rats were randomly divided into three groups: the control group (control, n = 10) was treated with sham operation and injected with 0.9% normal saline; the severe acute pancreatitis (SAP) group (n = 10) was infused with 3% sodium taurocholate (0.1 ml/100 g); and the AMPK agonist (AICAR) group (n = 8) received intraperitoneal injection of AICAR (400 mg/kg) 1 h before the operation. **(A,B)** Liver sections were collected and stained with antibodies against HO-1 and NQO-1, and the average integrated optical density (IOD)/area of HO-1 and NQO-1 was quantified using Image-Pro Plus 6.0 software (original magnification ×200, Bar = 50 μm). **(C–E)** The protein expression levels of HO-1 and NQO-1 in liver tissues were assessed by Western blot and quantified by densitometry using VisionWorks imaging software. The level of GAPDH was used as a loading control. **(F)** MDA and SOD contents were measured in liver tissues. Data are presented as the mean ± SD obtained from three independent experiments. $^{\#}p < 0.05$, $^{\#\#}p < 0.01$, $^{\#\#\#}p < 0.001$, $^{\#\#\#\#}p < 0.0001$ vs control group; $^{*}p < 0.05$, $^{**}p < 0.01$, $^{***}p < 0.001$, $^{****}p < 0.0001$ vs. SAP group.

AICAR Treatment Markedly Increases the Antioxidant Abilities of the Liver in Sodium Taurocholate-Induced SAP Rats

To further determine the roles of AICAR in PALI, we next investigated whether replenishment of AICAR can rescue the damaged antioxidant system in sodium taurocholate-induced SAP rats. Not surprisingly, immunohistochemical staining and Western blot results indicated that the hepatic expression levels of antioxidant proteins heme oxygenase-1 (HO-1) and NADPH quinone oxidoreductase 1 (NQO-1) were slightly upregulated in sodium taurocholate-induced SAP rats, which may represent a stress protection for the liver to defend against pancreatitis-induced liver injury. Notably, AICAR supplementation further augmented the hepatic expression levels of HO-1 and NQO-1 after sodium taurocholate treatment in rats (**Figures 3A–E**). Furthermore, the detection results of hepatic tissues in sodium taurocholate-induced SAP rats showed that the levels of MDA were significantly elevated, whereas the concentrations of SOD were strikingly decreased, suggesting that the antioxidant capacity of the liver in sodium taurocholate-induced SAP rats was disrupted. However, treatment with AICAR significantly restored the antioxidant abilities of the liver, as evidenced by an obvious elevation in hepatic concentrations of SOD and a marked decline in the hepatic levels of MDA (**Figure 3F**). These data suggest that AICAR supplementation prevents sodium taurocholate-induced PALI in rats by increasing antioxidant activities in the liver.

AICAR Treatment Activates the AMPK/Nrf2 Signaling Pathway and Inhibits NLRP3 Inflammasome Activation in the Liver Tissues of Sodium Taurocholate-Induced SAP Rats

Next, we focused on dissecting the deeper molecular mechanism by which AICAR inhibits oxidative stress and inflammation in the liver tissues of sodium taurocholate-induced SAP rats by activating AMPK phosphorylation. We performed Western blot to test the nuclear translocation of Nrf2 and the protein expression of NLRP3 as well as its downstream proteins caspase-1 and cleaved IL-1β in hepatic tissues of sodium

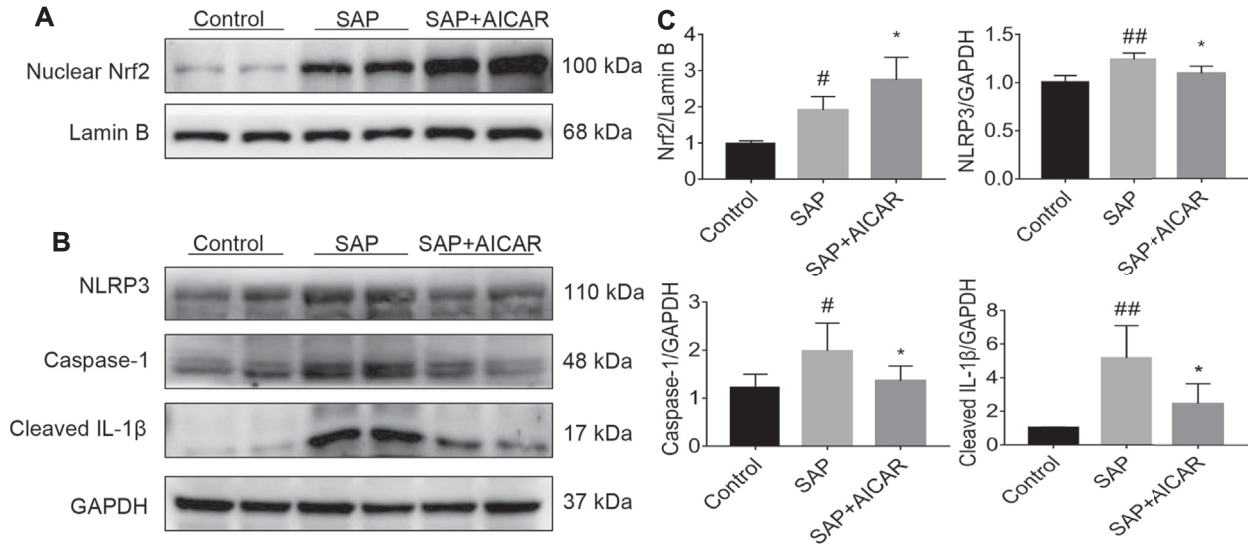


FIGURE 4 | The effects of AICAR on the activation of the AMPK/Nrf2 signaling pathway and inhibition of NLRP3 inflammasome activation in the liver tissues of sodium taurocholate-induced SAP rats. 7–8 week-old wild-type male SD rats were randomly divided into three groups: the control group (control, n = 10) was treated with sham operation and injected with 0.9% normal saline; the severe acute pancreatitis (SAP) group (n = 10) was infused with 3% sodium taurocholate (0.1 ml/100 g); and the AMPK agonist (AICAR) group (n = 8) received intraperitoneal injection of AICAR (400 mg/kg) 1 h before the operation. **(A)** The levels of nuclear accumulation of Nrf2 in liver tissues of each group were detected by Western blot analysis. For the internal control, Lamin B was used. **(B)** The protein expression levels of NLRP3, caspase-1, and cleaved IL-1β in liver tissues were measured by Western blot using anti-NLRP3, anti-caspase-1 and anti-cleaved IL-1β antibodies. GAPDH was used as an internal control. **(C)** Relative band densities were quantified using VisionWorks imaging software, and the results are expressed in the histogram. Data are presented as the mean ± SD obtained from three independent experiments. $^{\#}p < 0.05$, $^{\#\#}p < 0.01$, $^{\#\#\#}p < 0.001$, $^{\#\#\#\#}p < 0.0001$ vs control group; $^{*}p < 0.05$, $^{**}p < 0.01$, $^{***}p < 0.001$, $^{****}p < 0.0001$ vs. SAP group.

taurocholate-induced SAP rats after treatment with AICAR. The nuclear translocation of Nrf2 was increased following sodium taurocholate treatment, whereas AICAR supplementation further promoted the nuclear accumulation of Nrf2 (**Figures 4A,C**). Moreover, sodium taurocholate treatment significantly increased the hepatic expression of NLRP3, caspase-1 and cleaved-IL-1β, while AICAR supplementation reversed this phenomenon (**Figures 4B,C**). These findings suggest that AICAR markedly alters the nuclear accumulation of Nrf2 and inhibits NLRP3 inflammasome activation in sodium taurocholate-induced PALI rats by activating AMPK phosphorylation. Thus, we speculate that Nrf2 and NLRP3 inflammasome pathway may mediate essential parts in the protective roles of AICAR against oxidative stress and inflammation in sodium taurocholate-induced PALI rats.

Inhibition of AMPK Activation by Compound C Markedly Aggravates PALI in Sodium Taurocholate-Induced SAP Rats

To further elucidate the role of AMPK in PALI, we treated rats with the AMPK inhibitor Compound C (CC, 13.8 mg/kg) by intraperitoneal injection to block the phosphorylation of AMPK in liver tissues, followed by sodium taurocholate infusion. Unsurprisingly, Western blot results showed that sodium taurocholate infusion significantly reduced the ratio of *p*-AMPK/AMPK in liver tissues. As expected, this ratio was further reduced by CC treatment, suggesting that CC treatment successfully inhibited AMPK phosphorylation levels in the liver tissues of SAP rats (**Figure 5A**). Interestingly, treatment with CC significantly exacerbated sodium taurocholate-induced pancreatic injury in rats, as evidenced by further increased acinar necrosis and inflammatory cell infiltration (**Figure 5B**). Evaluation of the pancreatitis score in pancreatic sections also revealed that CC treatment was accompanied by more severe pancreatic injury than SAP (**Figure 5D**). We also observed that administration of CC in rats augmented SAP-induced edema, necrosis and structural disorder in hepatic lobules with further increased liver injury scores compared with SAP rats (**Figures 5C,D**). In addition, the amplitude of SAP-induced elevation of serum levels of both ALT and AST, two markers of liver injury, in CC-treated rats was higher than that in the SAP groups (**Figure 5E**). The above results indicate that inhibition of AMPK phosphorylation by CC enhances sodium taurocholate-induced PALI in rats.

AMPK Inhibition by Compound C Enhances Hepatic Oxidative Stress and NLRP3 Inflammasome Activation in Sodium Taurocholate-Induced PALI Rats

We next explored whether inhibition of AMPK activation by CC could promote hepatic oxidative stress and inflammation levels in sodium taurocholate-induced SAP rats. We found that the increase in the nuclear translocation of Nrf2 in the hepatic tissues of SAP rats was markedly reduced after CC treatment

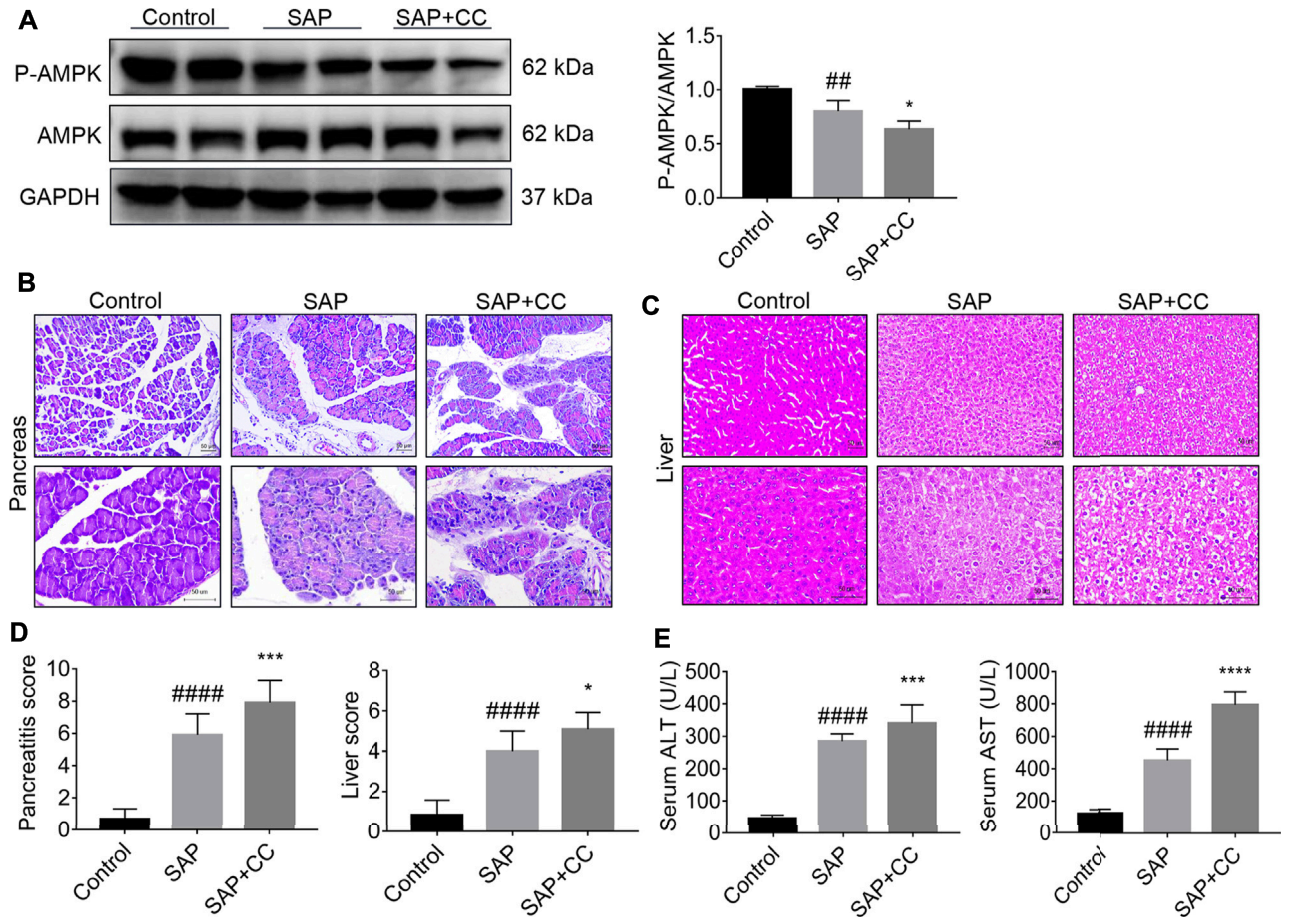


FIGURE 5 | Inhibition of AMPK phosphorylation by Compound C markedly aggravates PALI in sodium taurocholate-induced SAP rats. Seven-to eight-week-old wild-type male SD rats were randomly divided into three groups: the control group (control, n = 10) was treated with a sham operation and injected with 0.9% normal saline; the severe acute pancreatitis (SAP) group (n = 10) was infused with 3% sodium taurocholate (0.1 ml/100 g); and the AMPK inhibitor (CC) group (n = 8) received intraperitoneal injection of CC (Compound C, 13.8 mg/kg) 1 h before the operation. **(A)** The protein expression levels of AMPK and phosphorylated AMPK (*p*-AMPK) in liver tissues were detected by Western blot using anti-AMPK and anti-*p*-AMPK antibodies. GAPDH was used as the internal reference control. Data are presented as mean ± SD of three independent experiments. **(B,C)** Histological images of H&E staining in pancreas and liver tissues (200x and 400x) under a light microscope (Bar = 50 μm). **(D)** Histological scores were obtained to evaluate the degree of pancreas and liver injury from H&E staining. **(E)** Serum ALT and AST concentrations were detected. Data are presented as the mean ± SD of three independent experiments. $^{\#}p < 0.05$, $^{\#\#}p < 0.01$, $^{\#\#\#}p < 0.001$, $^{\#\#\#\#}p < 0.0001$ vs control group; $^{*}p < 0.05$, $^{**}p < 0.01$, $^{***}p < 0.001$, $^{****}p < 0.0001$ vs. SAP group.

(**Figures 6A,B**). We further measured MDA and SOD levels, which are indicators of oxidative damage, in the liver tissues of each group. The levels of hepatic MDA in rats treated with CC were significantly augmented compared to those in the SAP groups (**Figure 6C**). Alternatively, treatment with CC had a reduced effect on the magnitude of sodium taurocholate-induced decline in hepatic SOD levels (**Figure 6D**). Moreover, these changes in CC-treated SAP rats were accompanied by significantly increased hepatic expression of NLRP3, caspase-1 and cleaved IL-1β compared with SAP rats (**Figures 6E,F**), which results in a certain type of inflammatory response-related cell death called pyroptosis (Guo et al., 2021). Thus, we next compared the levels of IL-6, IL-1β and TNF-α in the liver tissues of SAP rats by q-PCR analysis with or without CC treatment. Consistent with our previous findings, the expression of these inflammatory cytokines was upregulated in the SAP groups, whereas CC treatment led to a further increase in the mRNA abundance of the aforementioned inflammatory genes (**Figure 6G**). Ultimately, our data suggest that inhibition of AMPK phosphorylation by CC aggravates PALI in sodium taurocholate-induced SAP rats, likely by repressing Nrf2-mediated antioxidant stress and anti-inflammatory roles.

Nrf2 Knockout Weakens the Protective Effects of AICAR on PALI in L-Arginine-Induced SAP Mice

Since the aforementioned data indicate that the anti-inflammatory and antioxidant stress effects of AICAR may be related to the induction of Nrf2 nuclear translocation, we further investigated whether Nrf2 deficiency would affect the protective effects of AICAR against PALI in L-arginine-

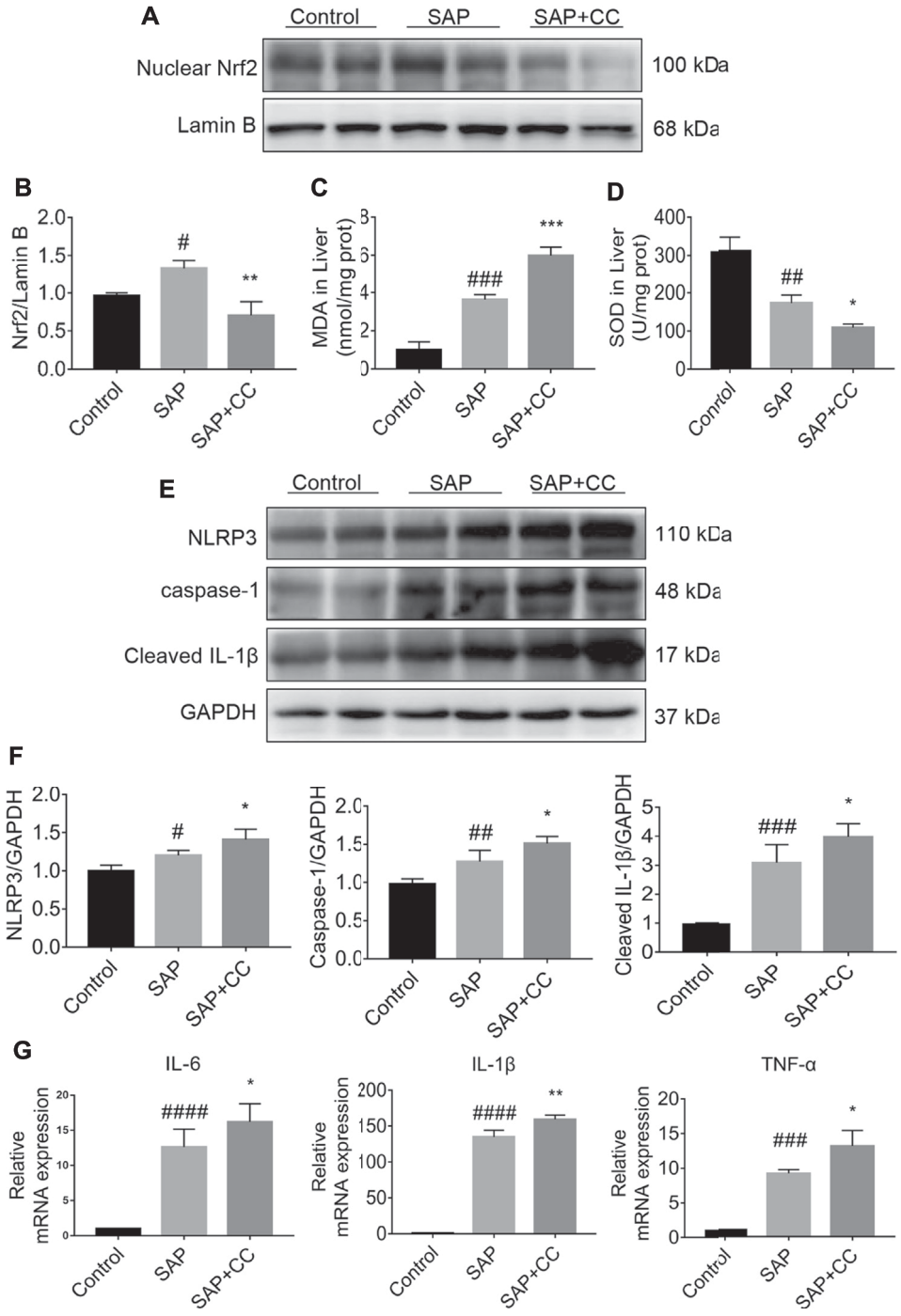


FIGURE 6 | Inhibition of AMPK phosphorylation by Compound C enhances hepatic oxidative stress and inflammation levels in sodium taurocholate-induced SAP rats. Seven-to eight-week-old wild type male SD rats were randomly divided into three groups: the control group (control, n = 10) was treated with a sham operation and injected with 0.9% normal saline; the severe acute pancreatitis (SAP) group (n = 10) was infused with 3% sodium taurocholate (0.1 ml/100 g); and the AMPK inhibitor (CC) group (n = 8) received intraperitoneal injection of CC (Compound C, 13.8 mg/kg) 1 h before the operation. **(A)** The nuclear translocation levels of Nrf2 in liver tissues were determined by Western blot. For the internal control, Lamin B was used. **(C,D)** The contents of MDA and SOD in liver tissues were determined. **(E)** The protein expression of NLRP3, caspase-1, and cleaved IL-1β was detected by Western blot. GAPDH was used as the internal reference control. **(B,F)** The relative ratios of Nrf2, NLRP3, caspase-1, and cleaved IL-1β were quantified using VisionWorks imaging software. **(G)** The mRNA levels of IL-6, IL-1β, and TNF-α in liver tissues were measured by RT-qPCR. Data are presented as the mean ± SD of three independent experiments. $^{\#}p < 0.05$, $^{\#\#}p < 0.01$, $^{\#\#\#}p < 0.001$, $^{\#\#\#\#}p < 0.0001$ vs control group; $^{*}p < 0.05$, $^{**}p < 0.01$, $^{***}p < 0.001$, $^{****}p < 0.0001$ vs. SAP group.

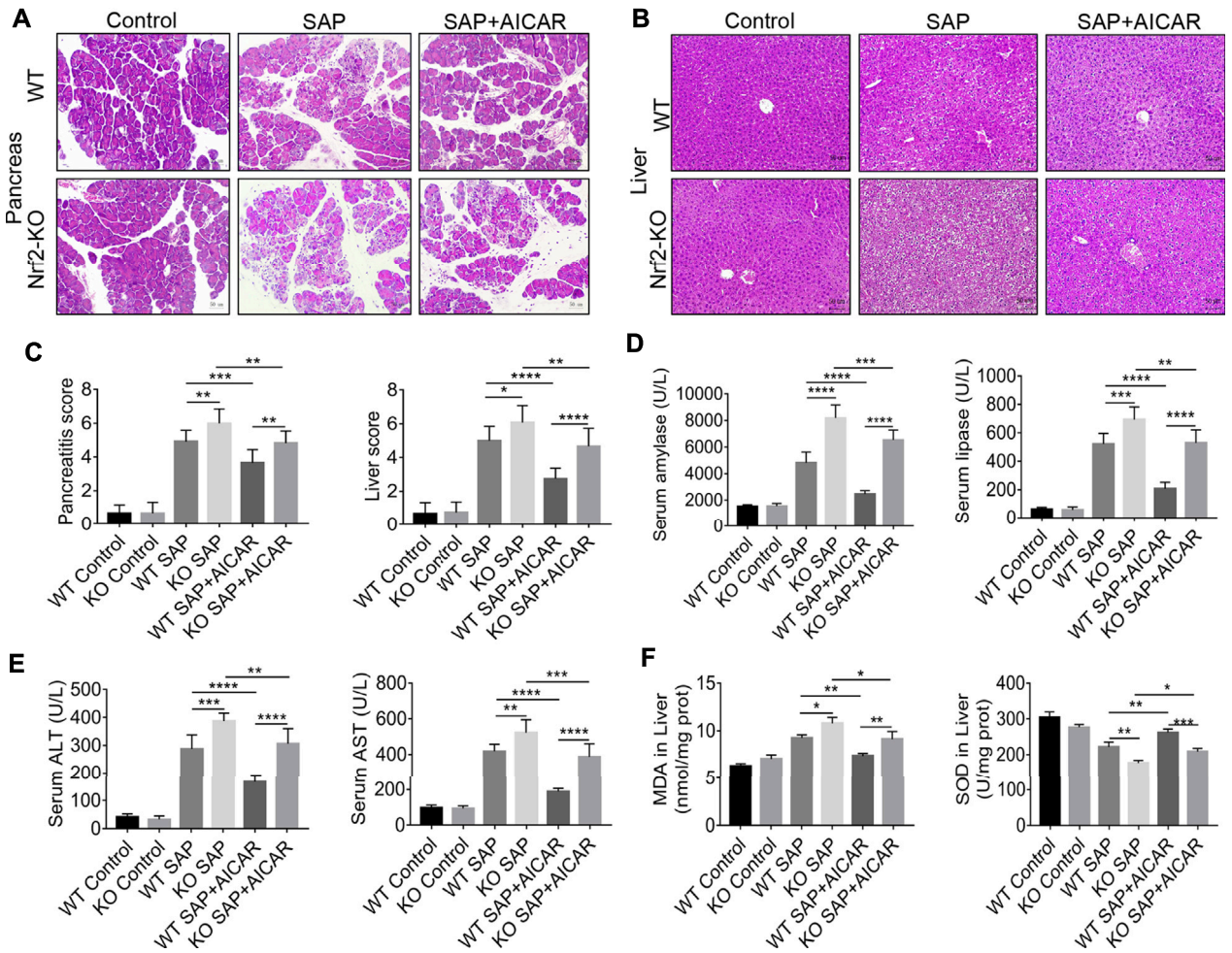


FIGURE 7 | Nrf2 knockout attenuates the protective effects of AICAR on PALI and the inhibitory effects of hepatic oxidative stress in L-arginine-induced SAP mice. Male wild-type mice or Nrf2$^{-/-}$ mice were divided into three groups: the control group (control, n = 6) was intraperitoneally injected with 0.9% normal saline; the SAP group (n = 6) was intraperitoneally injected with 8% L-arginine hydrochloride (pH = 7.0, 4 g/kg) twice at an interval of 1 h; and the AMPK agonist (AICAR, n = 6) group was intraperitoneally injected with AICAR (400 mg/kg) twice: 1 h before and 24 h after L-arginine hydrochloride administration. **(A,B)** Representative pathological images of the pancreas and liver (200x) under a light microscope (H&E staining, Bar = 50 μm). **(C)** Histological scores were obtained to evaluate the degree of pancreas and liver injury from H&E staining. **(D)** The concentrations of serum amylase and lipase were detected. **(E)** The levels of serum ALT and AST were measured to evaluate liver function. **(F)** Concentrations of MDA and SOD in liver tissues from different groups. Data are presented as the mean ± SD of three independent experiments. Data are presented as mean ± SD of three independent experiments. *p < 0.05, **p < 0.01, ***p < 0.001, ****p < 0.0001.

induced SAP mice. L-arginine-induced elevations in serum levels of pancreas injury enzymes (amylase and lipase) and the pathological changes as well as pancreatitis scores analyzed in H&E-stained pancreas sections in Nrf2 knockout (KO) mice were higher than those in WT SAP mice (**Figures 7A–D**). Meanwhile, the beneficial effects of AICAR against L-arginine-induced pancreatic injury reflected by the above indicators were significantly attenuated in Nrf2 KO mice compared with WT littermates (**Figures 7A,C**). Likewise, the pathological changes in liver sections of the Nrf2 KO SAP mice were more severe than those in the WT SAP groups by H&E staining (**Figure 7B**). Additionally, treatment of WT SAP mice with AICAR markedly reduced these negative pathological changes (**Figure 7B**); however, these protective effects mediated by AICAR were weakened in Nrf2 KO mice (**Figure 7B**). The liver injury scores, consistent with the pathological appearance in each group, further confirmed our findings (**Figure 7C**). Moreover, the serum levels of ALT and AST in both WT and Nrf2 KO mice were augmented after L-arginine administration. Notably, the levels of these two markers indicated that liver injury in Nrf2 KO mice was higher than that in WT mice (**Figure 7E**). Alternatively, AICAR treatment markedly attenuated the L-arginine-induced elevation in the serum levels of ALT and AST in WT SAP mice, while these phenomena were significantly inhibited in Nrf2 KO mice (**Figure 7E**). Therefore, these results indicate that Nrf2 plays an important role in the protective effects of AICAR against L-arginine-induced PALI in mice.

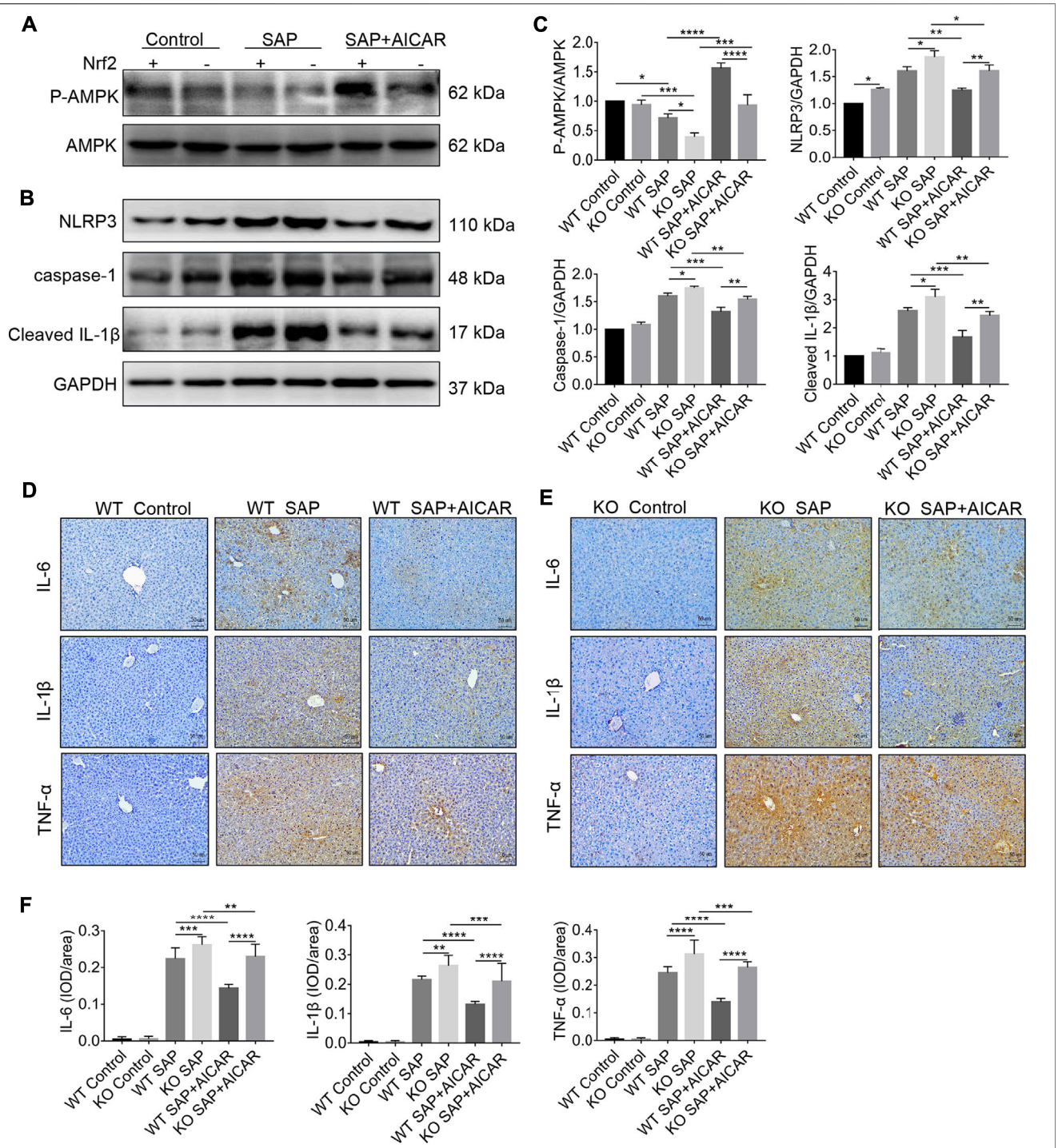


FIGURE 8 | Nrf2 deficiency impairs the inhibitory effects of AICAR against hepatic NLRP3 inflammasome activation in L-arginine-induced SAP mice. Male wild type mice or Nrf2$^{-/-}$ mice were divided into three groups: the control group (control, n = 6) was intraperitoneally injected with 0.9% normal saline; the SAP group (n = 6) was intraperitoneally injected with 8% L-arginine hydrochloride (pH = 7.0, 4 g/kg) twice at an interval of 1 h; and the AMPK agonist (AICAR, n = 6) group wasintraperitoneally injected with AICAR (400 mg/kg) twice: 1 h before and 24 h after L-arginine hydrochloride administration. **(A–C)** The protein expression levels of phosphorylated AMPK, total AMPK, NLRP3, caspase-1, and cleaved IL-1β were measured by Western blot, and the relative ratios of *p*-AMPK/AMPK and band densities of Nrf2, NLRP3, caspase-1, and cleaved IL-1β were quantified using VisionWorks imaging software. GAPDH was used as an internal reference. **(D–F)** The protein expression of IL-6, IL-1β and TNF-α in liver sections was detected by immunohistochemistry (original magnification ×200, Bar = 50 μm). Image-Pro Plus 6.0 software was used for statistical analysis. Data are presented as the mean ± SD of three independent experiments. $^{*}p < 0.05$, $^{**}p < 0.01$, $^{***}p < 0.001$, $^{****}p < 0.0001$.

Nrf2 Deficiency Impairs the Inhibitory Effects of AICAR Against PALI-Related Hepatic Oxidative Stress and NLRP3 Inflammasome Activation in L-Arginine-Induced SAP Mice

To further clarify whether the beneficial effect of AICAR on antioxidant stress was Nrf2 dependent, we measured MDA and SOD levels in the liver tissues of L-arginine-treated Nrf2 KO mice and WT littermates with or without AICAR supplementation. After L-arginine treatment, the production of MDA in liver tissues was conspicuously increased, and the levels of SOD were significantly decreased in Nrf2 KO mice compared to WT mice. Additionally, administration of AICAR was associated with markedly reduced MDA levels, and the concentrations of SOD were significantly augmented compared to those in the WT SAP group. However, these beneficial antioxidant effects of AICAR were largely blocked in Nrf2 KO mice compared to WT littermates (**Figure 7F**). These observations indicate that the antioxidant ability of AICAR in the liver tissues of L-arginine-induced PALI mice was partially dependent on Nrf2.

We next determined whether induction of Nrf2 is required for the inhibition of the NLRP3 inflammasome-associated inflammatory response in the liver tissues of L-arginine-induced PALI mice. Thus, we performed Western blot to compare the hepatic expression levels of NLRP3, caspase-1 and cleaved-IL-1β between L-arginine-treated Nrf2 KO mice and WT littermates with or without AICAR administration. The results showed that the hepatic expression of NLRP3, caspase-1 and cleaved-IL-1β in Nrf2 KO mice was higher than that in WT littermates after L-arginine treatment (**Figures 8A–C**). Furthermore, replenishment of AICAR profoundly decreased the expression of these indicators in the liver tissues of WT littermates compared with the WT SAP group; however, these observed trends were significantly reversed in Nrf2 KO mice (**Figures 8B,C**). Thus, our findings suggest that Nrf2 deficiency impairs the inhibitory effect of AICAR against NLRP3 inflammasome activation in L-arginine-induced PALI mice. To further elucidate the role of Nrf2 in the anti-inflammatory effects of AICAR, we detected the expression levels of several inflammatory factors, including IL-6, IL-1β and TNF-α, in each group of Nrf2 KO mice and WT littermates. Immunohistochemistry analysis showed that L-arginine induced the expression of these inflammatory factors in the liver tissues of both Nrf2 KO mice and WT littermates, resulting in a further increase in their expression (**Figures 8D–F**). Moreover, replenishment of AICAR decreased L-arginine-induced hepatic inflammatory factor accumulation in WT littermates, while these anti-inflammatory effects of AICAR were markedly reversed in Nrf2 KO mice compared with WT controls (**Figures 8D–F**). Taken together, our results suggest that Nrf2 deficiency largely eliminates the negative regulation of AICAR on the NLRP3 inflammasome activation associated inflammatory response in the liver tissues of L-arginine-induced PALI mice.

DISCUSSION

The central goal of this study was to investigate the pharmacological activation of AMPK by AICAR as a therapeutic strategy for the treatment of PALI. Our findings demonstrated that AICAR activates AMPK, which leads to Nrf2-mediated antioxidant stress and inhibition of NLRP3-related inflammation, and thus improving PALI. This study indicated that AMPK exerted an essential role in the pathological processes of PALI and presented the first evidence that pharmacological activation of AMPK by AICAR ameliorates PALI, suggesting that AICAR may be a promising therapeutic agent for the treatment of PALI.

In the current study, we demonstrated that both 1 day after sodium taurocholate infusion in rats and 2 days after intraperitoneal injection of L-arginine in mice successfully induced rodent models of PALI, as evidenced by marked elevation in the plasma levels of amylase, lipase, ALT and AST as well as severe pathological injury of the pancreas and liver in the two experimental SAP models (**Figures 1B–G**, **Figures 7A–F**). This study provided novel evidence that SAP caused a drastic reduction in hepatic expression levels of phosphorylated AMPK in sodium taurocholate- and L-arginine-induced rodent SAP models, suggesting that AMPK may be involved in the pathogenesis of PALI (**Figure 1A**, **Figures 8A,C**). Herein, we obtained two lines of evidence to demonstrate our hypothesis. On the one hand, administration of the direct AMPK activator AICAR led to a dramatic elevation in hepatic expression levels of phosphorylated AMPK and prevented PALI in sodium taurocholate- and L-arginine-induced rodent SAP models (**Figures 1A–G**, **Figures 7A–E**, **Figures 8A,C**). On the other hand, inhibiting the activity of AMPK in liver tissues by using the AMPK inhibitor Compound C profoundly exacerbated PALI in sodium taurocholate-induced SAP rats (**Figures 5A–E**). Although previous studies have shown that compound C may play roles independent of AMPK inhibition, such as anti-glioma and inhibition of Bone morphogenetic protein (BMP) pathway, it is still the only available cell permeability AMPK antagonist (Yu et al., 2008; Liu et al., 2014). Similar to our findings, AMPK activation by AICAR has been shown to protect the kidney from overt damage in a rat model of kidney ischemia-reperfusion injury (Lempiäinen et al., 2012). In addition, a Compound C-induced reduction in myocardial AMPK activity impaired cardiac function and aggravated oxidative stress in cardiomyocytes in DOX-induced acute cardiotoxicity mice (Liu et al., 2018).

In the pathogenesis of PALI, the uncontrollable hepatic inflammatory response and elevated oxidative stress triggered by SAP will continue to damage hepatocytes, which are central mediators for accelerating the development of PALI (Yang et al., 2003; Moniaux et al., 2011). According to previous reports, AMPK activation is involved in the inhibition of the

IL-6-stimulated inflammatory response in human liver cells and mediates the antioxidant stress ability of fibroblast growth factor (FGF) one in a mouse model of nonalcoholic fatty liver disease (Nerstedt et al., 2013; Liu et al., 2020). Therefore, we explored the hypothesis that the molecular basis of AICAR in improving PALI is attributed to its anti-inflammatory capability and reduction of hepatic oxidative stress by AMPK activation. Our findings demonstrated that AMPK was required for the regulation of hepatic inflammation and oxidative stress in sodium taurocholate-induced PALI rats and that AICAR ameliorated PALI by AMPK activation in this rat model, which was associated with its anti-inflammatory and antioxidative actions.

Next, we focused on dissecting the molecular mechanism to explain how AMPK activation by AICAR reduced hepatic inflammation and oxidative stress in PALI. In response to inflammatory reaction, Nrf2 is released from Keap1 and translocates to the nucleus, thus activating the endogenous antioxidant defense system by enhancing the transcription of a variety of antioxidant enzymes, such as HO-1 and NQO-1, presenting a superior effect in oxygen reduction balance. In particular, oxidative stress and inflammation are closely connected, and increased levels of proinflammatory cytokines induce oxidative stress. In turn, oxidative stress overactivation further exacerbates the inflammatory response (Dandekar et al., 2015; Antonucci et al., 2017). Furthermore, studies have also shown that the activation of Nrf2 can inhibit inflammation-mediated injury *via* its antioxidant cascade (Joo Choi et al., 2014; Saha et al., 2020). Notably, several recent studies have demonstrated that Nrf2 negatively regulates the activity of the NLRP3 inflammasome, which is a central regulator of inflammation required for PALI (Hou et al., 2018; Chen et al., 2019). Upon stimulation, NLRP3 collects ASC protein and converts procaspase-1 into active caspase-1, which cleaves pro-IL-β or pro-IL-18 into mature forms, ensuing and promoting hepatic inflammatory injury (Mridha et al., 2017). However, the crosstalk between Nrf2 and the NLRP3 inflammasome pathway in PALI remains to be determined. In addition, previous reports found that AMPK also inhibits NLRP3 inflammasome activation in a mouse model of diabetic cardiomyopathy and acute pancreatitis (Chen et al., 2020; Yang et al., 2020). In fact, AMPK phosphorylates Nrf2 at serine 374, 408, and 433, moves Nrf2 from the cytoplasm to the nucleus, and binds to the antioxidant response element (ARE) gene to exert its antioxidant effect (Matzinger et al., 2020). In the current study, rats treated with AMPK agonists (AICAR) and inhibitors (CC) demonstrated that AMPK plays an important role in activating Nrf2 signaling and inhibiting NLRP3 inflammasome pathways in PALI and that hepatic Nrf2 may act as a key mediator of AICAR protection against PALI-associated oxidative stress and NLRP3 inflammasome activation. Therefore, we speculate that the direct activation of AMPK by AICAR exerts its antioxidant and anti-inflammatory roles to prevent PALI through Nrf2-mediated antioxidant effects and inhibition of the NLRP3 inflammasome pathway.

To verify our hypothesis, we used Nrf2 KO mice and WT mice to conduct a comparative study in an L-arginine-induced PALI model with or without AICAR treatment. We found that knockout of Nrf2 limited the ability of AICAR to reduce the severity of PALI in mice (**Figures 7A–E**). Most importantly, Nrf2 gene deletion markedly weakened the protective effects of AICAR to prevent SAP-induced oxidative stress and NLRP3 inflammasome activation in the liver tissues of L-arginine-induced PALI mice (**Figure 7F**, **Figures 8B,C**). However, AICAR still had a slight protective effect on PALI in Nrf2 KO mice. AMPK can regulate a variety of physiological and pathological effects through multiple pathways to affect cell metabolism and survival (Carling, 2017; Ramirez Reyes et al., 2021). This result may be attributed to the activation of AMPK by AICAR leading to other pathway modulations independent of Nrf2 signaling in PALI and resulting in other biological effects, such as AMPK-related mitochondrial homeostasis, ferroptosis and necroptosis, which are worthy of further exploration in our future research (Herzig et al., 2018; Song et al., 2018; Lee et al., 2020). Nonetheless, our findings indicate that activation of Nrf2 by AICAR mediates important roles in ameliorating hepatic oxidative stress and inhibiting NLRP3 inflammasome pathway activation in PALI mice regardless of whether Nrf2 is the master pathway.

Despite our novel findings, the current study has some limitations. First, our observations are only based on two rodent PALI models. AICAR has been used clinically for myocardial protection in coronary artery bypass grafting and myocardial ischemic injury (Rao et al., 2016). We should further determine the role of AICAR in PALI in humanoid large animals and in clinical studies. Second, our results demonstrated that AICAR protects against PALI partially through Nrf2-mediated antioxidant effects and inhibition of NLRP3 inflammasome activation, whether AICAR plays these positive roles mainly depends on reducing the activation of inflammatory cells, such as macrophages and neutrophils, exerting a protective effect on hepatocytes or inducing other hepatoprotective factors requires further investigation. Third, although AICAR is a widely used AMPK agonist, it also plays important AMPK-independent effects including regulating gluconeogenesis and oxidative phosphorylation (OXPHOS). Therefore, in addition to its inhibitory effects on inflammation and oxidative stress by activating ampk, AICAR may play protective roles of PALI through these AMPK-independent pathways which need to be further explored (Višnjić et al., 2021). Fourth, this study predominantly focuses on the AMPK/Nrf2 signaling pathway. However, there are also many other important regulatory pathways involved in the course of PALI such as Toll like receptor 4 (TLR4) signaling pathway, transforming growth factor β1 (TGF-β1) and p38 mitogen-activated protein kinase (MAPK) signaling pathway (TGF-β1-p38 MAPK), which need to be investigated in our future study (Wang et al., 2018). Fifth, given the powerful therapeutic effect of AICAR in PALI, the potential effect of AICAR in other organ dysfunctions including respiratory, renal, and cardiovascular of SAP needs to be further explored.

In summary, our data indicate that AICAR, a direct AMPK activator, exhibits significant therapeutic effects against PALI in sodium taurocholate- and L-arginine-induced rodent models by promoting AMPK phosphorylation by effectively inhibiting hepatic oxidative stress and inflammation. Thus, as a cell permeable nucleoside, AICAR has high therapeutic value for

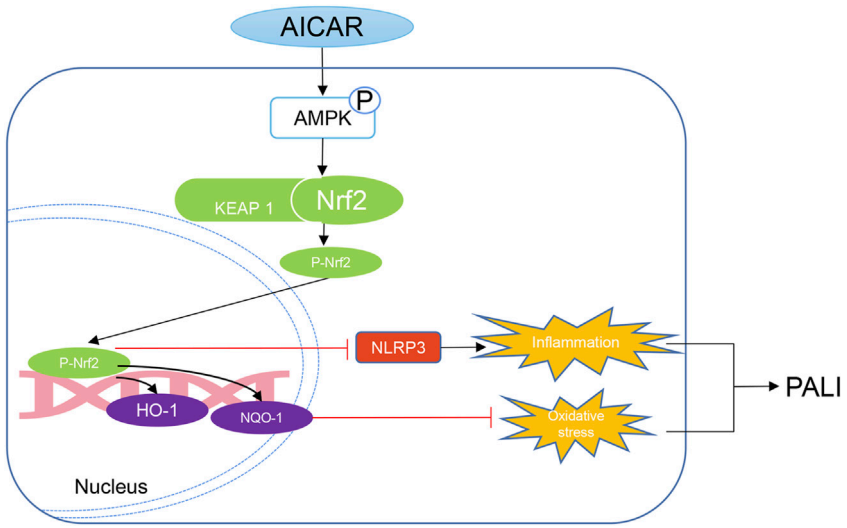


FIGURE 9 | Mechanistic illustration of the basis of AICAR protection against pancreatitis-associated liver injury (PALI). AICAR inhibits hepatic oxidative stress and inflammation by promoting AMPK phosphorylation partially *via* Nrf2-mediated antioxidant effects and inhibition of NLRP3 inflammasome activation, resulting in protection against PALI in sodium taurocholate- and L-arginine-induced SAP models.

the treatment of PALI. Importantly, this study provides new insight into the mechanisms underlying the improvement of hepatic oxidative stress and inflammation in PALI by AICAR. AMPK activation promotes the nuclear accumulation of Nrf2, which partially mediates antioxidant effects and inhibits NLRP3 inflammasome activation and thus is important for AICAR protection against PALI (**Figure 9**). We conclude that because AICAR is already used in the clinic, the development of novel therapies using AICAR to promote AMPK phosphorylation is promising for future medical interventions of PALI.

DATA AVAILABILITY STATEMENT

The original contributions presented in the study are included in the article/**Supplementary Material**, further inquiries can be directed to the corresponding authors.

ETHICS STATEMENT

The animal study was reviewed and approved by the Animal Ethics Committee of Wenzhou Medical University.

AUTHOR CONTRIBUTIONS

WH and HW designed the experiments. LK, HZ, and CL conducted the experiments and co-wrote the manuscript. KS, HH, YZ, YW, and DW analyzed the data. All authors contributed to the article and approved the submitted version.

FUNDING

This work was supported by grants from Wenzhou Science and Technology Bureau (No. Y20180506), the Research incubation Project of the first affiliated Hospital of Wenzhou Medical University (No. FHY2019032 and No. FHY2019058) and National Natural Science Foundation of China (No. 82070834; 81800567).

SUPPLEMENTARY MATERIAL

The Supplementary Material for this article can be found online at: https://www.frontiersin.org/articles/10.3389/fphar.2021.724514/full#supplementary-material

REFERENCES

Antonucci, L., Porcu, C., Iannucci, G., Balsano, C., and Barbaro, B. (2017). Non-Alcoholic Fatty Liver Disease and Nutritional Implications: Special Focus on Copper. *Nutrients* 9, 1137. doi:10.3390/nu9101137

Argaiz, E. R., and de Moraes, A. G. (2021). Acute Pancreatitis. *Lancet* 397, 279. doi:10.1016/s0140-6736(21)00092-1

Bakır, M., Geyikoglu, F., Colak, S., Turkez, H., Bakır, T. O., and Hosseinigouzdagani, M. (2016). The Carvacrol Ameliorates Acute Pancreatitis-Induced Liver Injury via Antioxidant Response. *Cytotechnology* 68, 1131–1146. doi:10.1007/s10616-015-9871-z

Bone, N. B., Liu, Z., Pittet, J. F., and Zmijewski, J. W. (2017). Frontline Science: D1 Dopaminergic Receptor Signaling Activates the AMPK-Bioenergetic Pathway in Macrophages and Alveolar Epithelial Cells and Reduces Endotoxin-Induced ALI. *J. Leukoc. Biol.* 101, 357–365. doi:10.1189/jlb.3HI0216-068RR

Carling, D. (2017). AMPK Signalling in Health and Disease. *Curr. Opin. Cel Biol* 45, 31–37. doi:10.1016/j.ceb.2017.01.005

Chen, H., Ning, X., and Jiang, Z. (2017). Caspases Control Antiviral Innate Immunity. *Cell Mol Immunol* 14, 736–747. doi:10.1038/cmi.2017.44

Chen, H., Tran, D., Yang, H. C., Nylander, S., Birnbaum, Y., and Ye, Y. (2020). Dapagliflozin and Ticagrelor Have Additive Effects on the Attenuation of the Activation of the NLRP3 Inflammasome and the Progression of Diabetic Cardiomyopathy: an AMPK-mTOR Interplay. *Cardiovasc. Drugs Ther.* 34, 443–461. doi:10.1007/s10557-020-06978-y

Chen, Z., Zhong, H., Wei, J., Lin, S., Zong, Z., Gong, F., et al. (2019). Inhibition of Nrf2/HO-1 Signaling Leads to Increased Activation of the NLRP3 Inflammasome in Osteoarthritis. *Arthritis Res. Ther.* 21, 300. doi:10.1186/s13075-019-2085-6

Chin, W. Y., He, C. Y., Chow, T. W., Yu, Q. Y., Lai, L. C., and Miaw, S. C. (2021). Adenylate Kinase 4 Promotes Inflammatory Gene Expression via Hif1α and AMPK in Macrophages. *Front. Immunol.* 12, 630318. doi:10.3389/fimmu.2021.630318

Dandekar, A., Mendez, R., and Zhang, K. (2015). Cross Talk between ER Stress, Oxidative Stress, and Inflammation in Health and Disease. *Methods Mol. Biol.* 1292, 205–214. doi:10.1007/978-1-4939-2522-3_15

Elshal, M., Abu-Elsaad, N., El-Karef, A., and Ibrahim, T. (2019). Retinoic Acid Modulates IL-4, IL-10 and MCP-1 Pathways in Immune Mediated Hepatitis and Interrupts CD4+ T Cells Infiltration. *Int. Immunopharmacol* 75, 105808. doi:10.1016/j.intimp.2019.105808

Fang, D., Lin, Q., Wang, C., Zheng, C., Li, Y., Huang, T., et al. (2020). Effects of Sildenafil on Inflammatory Injury of the Lung in Sodium Taurocholate-Induced Severe Acute Pancreatitis Rats. *Int. Immunopharmacol* 80, 106151. doi:10.1016/j.intimp.2019.106151

Garcia, D., and Shaw, R. J. (2017). AMPK: Mechanisms of Cellular Energy Sensing and Restoration of Metabolic Balance. *Mol. Cel* 66, 789–800. doi:10.1016/j.molcel.2017.05.032

Garg, P. K., and Singh, V. P. (2019). Organ Failure Due to Systemic Injury in Acute Pancreatitis. *Gastroenterology* 156, 2008–2023. doi:10.1053/j.gastro.2018.12.041

Gong, C., Yang, H., Wang, S., Liu, J., Li, Z., Hu, Y., et al. (2021). hTERT Promotes CRC Proliferation and Migration by Recruiting YBX1 to Increase NRF2 Expression. *Front Cel Dev Biol* 9, 658101. doi:10.3389/fcell.2021.658101

Guo, X., Hu, S., Liu, J. J., Huang, L., Zhong, P., Fan, Z. X., et al. (2021). Piperine Protects against Pyroptosis in Myocardial Ischaemia/reperfusion Injury by Regulating the miR-383/RP105/AKT Signalling Pathway. *J. Cel Mol Med* 25, 244–258. doi:10.1111/jcmm.15953

Guo, Y., Zhang, Y., Hong, K., Luo, F., Gu, Q., Lu, N., et al. (2014). AMPK Inhibition Blocks ROS-Nfκb Signaling and Attenuates Endotoxemia-Induced Liver Injury. *PLoS One* 9, e86881. doi:10.1371/journal.pone.0086881

Han, C. Y., Rho, H. S., Kim, A., Kim, T. H., Jang, K., Jun, D. W., et al. (2018). FXR Inhibits Endoplasmic Reticulum Stress-Induced NLRP3 Inflammasome in Hepatocytes and Ameliorates Liver Injury. *Cell Rep* 24, 2985–2999. doi:10.1016/j.celrep.2018.07.068

Hennig, P., Garstkiewicz, M., Grossi, S., Di Filippo, M., French, L. E., and Beer, H. D. (2018). The Crosstalk between Nrf2 and Inflammasomes. *Int. J. Mol. Sci.* 19, 562. doi:10.3390/ijms19020562

Herzig, S., and Shaw, R. J. (2018). AMPK: Guardian of Metabolism and Mitochondrial Homeostasis. *Nat. Rev. Mol. Cel Biol* 19, 121–135. doi:10.1038/nrm.2017.95

Hill, J. L., Kobori, N., Zhao, J., Rozas, N. S., Hylin, M. J., Moore, A. N., et al. (2016). Traumatic Brain Injury Decreases AMP-Activated Protein Kinase Activity and Pharmacological Enhancement of its Activity Improves Cognitive Outcome. *J. Neurochem.* 139, 106–119. doi:10.1111/jnc.13726

Hou, Y., Wang, Y., He, Q., Li, L., Xie, H., Zhao, Y., et al. (2018). Nrf2 Inhibits NLRP3 Inflammasome Activation through Regulating Trx1/TXNIP Complex in Cerebral Ischemia Reperfusion Injury. *Behav. Brain Res.* 336, 32–39. doi:10.1016/j.bbr.2017.06.027

Joo Choi, R., Cheng, M. S., and Shik Kim, Y. (2014). Desoxyrhapontigenin Up-Regulates Nrf2-Mediated Heme Oxygenase-1 Expression in Macrophages and Inflammatory Lung Injury. *Redox Biol.* 2, 504–512. doi:10.1016/j.redox.2014.02.001

Kaphalia, L., Srinivasan, M. P., Kakumanu, R. D., Kaphalia, B. S., and Calhoun, W. J. (2019). Ethanol Exposure Impairs AMPK Signaling and Phagocytosis in Human Alveolar Macrophages: Role of Ethanol Metabolism. *Alcohol. Clin. Exp. Res.* 43, 1682–1694. doi:10.1111/acer.14131

Lane, S. L., Houck, J. A., Doyle, A. S., Bales, E. S., Lorca, R. A., Julian, C. G., et al. (2020). AMP-activated Protein Kinase Activator AICAR Attenuates Hypoxia-Induced Murine Fetal Growth Restriction in Part by Improving Uterine Artery Blood Flow. *J. Physiol.* 598, 4093–4105. doi:10.1113/jp279341

Lee, H., Zandkarimi, F., Zhang, Y., Meena, J. K., Kim, J., Zhuang, L., et al. (2020). Energy-stress-mediated AMPK Activation Inhibits Ferroptosis. *Nat. Cel Biol* 22, 225–234. doi:10.1038/s41556-020-0461-8

Lempiäinen, J., Finckenberg, P., Levijoki, J., and Mervaala, E. (2012). AMPK Activator AICAR Ameliorates Ischaemia Reperfusion Injury in the Rat Kidney. *Br. J. Pharmacol.* 166, 1905–1915. doi:10.1111/j.1476-5381.2012.01895.x

Li, S., Zhou, J., Xu, S., Li, J., Liu, J., Lu, Y., et al. (2019). Induction of Nrf2 Pathway by Dendrobium Nobile Lindl. Alkaloids Protects against Carbon Tetrachloride Induced Acute Liver Injury. *Biomed. Pharmacother.* 117, 109073. doi:10.1016/j.biopha.2019.109073

Li, X., Cao, Y., Liu, Z., Chen, H., and Mao, H. (2019). The Relationship between Liver Injury and Serum Levels of C-Reactive Protein and Procalcitonin in Patients with Acute Pancreatitis. *J. Coll. Physicians Surg. Pak* 29, 287–289. doi:10.29271/jcpsp.2019.03.287

Lin, S. C., and Hardie, D. G. (2018). AMPK: Sensing Glucose as Well as Cellular Energy Status. *Cell Metab* 27, 299–313. doi:10.1016/j.cmet.2017.10.009

Liu, B., Huang, J., and Zhang, B. (2016). Nobiletin Protects against Murine L-Arginine-Induced Acute Pancreatitis in Association with Downregulating p38MAPK and AKT. *Biomed. Pharmacother.* 81, 104–110. doi:10.1016/j.biopha.2016.03.051

Liu, C. Y., Zhou, Y., Chen, T., Lei, J. C., and Jiang, X. J. (2020). AMPK/SIRT1 Pathway Is Involved in Arctigenin-Mediated Protective Effects against Myocardial Ischemia-Reperfusion Injury. *Front. Pharmacol.* 11, 616813. doi:10.3389/fphar.2020.616813

Liu, D., Ma, Z., Di, S., Yang, Y., Yang, J., Xu, L., et al. (2018). AMPK/PGC1α Activation by Melatonin Attenuates Acute Doxorubicin Cardiotoxicity via Alleviating Mitochondrial Oxidative Damage and Apoptosis. *Free Radic. Biol. Med.* 129, 59–72. doi:10.1016/j.freeradbiomed.2018.08.032

Liu, Q., Lv, H., Wen, Z., Ci, X., and Peng, L. (2017). Isoliquiritigenin Activates Nuclear Factor Erythroid-2 Related Factor 2 to Suppress the NOD-like Receptor Protein 3 Inflammasome and Inhibits the NF-Kb Pathway in Macrophages and in Acute Lung Injury. *Front. Immunol.* 8, 1518. doi:10.3389/fimmu.2017.01518

Liu, X., Chhipa, R. R., Nakano, I., and Dasgupta, B. (2014). The AMPK Inhibitor Compound C Is a Potent AMPK-independent Antiglioma Agent. *Mol. Cancer Ther.* 13, 596–605. doi:10.1158/1535-7163.Mct-13-0579

Lv, P., Fan, L. J., Li, H. Y., Meng, Q. S., and Liu, J. (2015). Protective Effect of Thalidomide on Liver Injury in Rats with Acute Pancreatitis via Inhibition of Oxidative Stress. *Ann. Clin. Lab. Sci.* 45, 508–514.

Lyu, H., Wang, H., Li, L., Zhu, J., Chen, F., Chen, Y., et al. (2020). Hepatocyte-specific Deficiency of Nrf2 Exacerbates Carbon Tetrachloride-Induced Liver Fibrosis via Aggravated Hepatocyte Injury and Subsequent Inflammatory and Fibrogenic Responses. *Free Radic. Biol. Med.* 150, 136–147. doi:10.1016/j.freeradbiomed.2020.02.015

Martin, L. M., Möller, M., Weiss, U., Russe, O. Q., Scholich, K., Pierre, S., et al. (2019). 5-Amino-1-β-D-Ribofuranosyl-Imidazole-4-Carboxamide (AICAR) Reduces Peripheral Inflammation by Macrophage Phenotype Shift. *Int. J. Mol. Sci.* 20, 3255. doi:10.3390/ijms20133255

Matzinger, M., Fischhuber, K., Pölöske, D., Mechtler, K., and Heiss, E. H. (2020). AMPK Leads to Phosphorylation of the Transcription Factor Nrf2, Tuning Transactivation of Selected Target Genes. *Redox Biol.* 29, 101393. doi:10.1016/j.redox.2019.101393

Mei, F., Yu, J., Li, M., Xiang, M., Hong, Y., Zhou, Y., et al. (2019). Magnesium Isoglycyrrhizinate Alleviates Liver Injury in Obese Rats with Acute Necrotizing Pancreatitis. *Pathol. Res. Pract.* 215, 106–114. doi:10.1016/j.prp.2018.10.030

Moniaux, N., Song, H., Darnaud, M., Garbin, K., Gigou, M., Mitchell, C., et al. (2011). Human Hepatocarcinoma-Intestine-Pancreas/pancreatitis-Associated Protein Cures Fas-Induced Acute Liver Failure in Mice by Attenuating Free-Radical Damage in Injured Livers. *Hepatology* 53, 618–627. doi:10.1002/hep.24087

Mridha, A. R., Wree, A., Robertson, A. A. B., Yeh, M. M., Johnson, C. D., Van Rooyen, D. M., et al. (2017). NLRP3 Inflammasome Blockade Reduces Liver Inflammation and Fibrosis in Experimental NASH in Mice. *J. Hepatol.* 66, 1037–1046. doi:10.1016/j.jhep.2017.01.022

Nerstedt, A., Cansby, E., Amrutkar, M., Smith, U., and Mahlapuu, M. (2013). Pharmacological Activation of AMPK Suppresses Inflammatory Response

Evoked by IL-6 Signalling in Mouse Liver and in Human Hepatocytes. *Mol. Cel Endocrinol* 375, 68–78. doi:10.1016/j.mce.2013.05.013

Nerstedt, A., Johansson, A., Andersson, C. X., Cansby, E., Smith, U., and Mahlapuu, M. (2010). AMP-activated Protein Kinase Inhibits IL-6-stimulated Inflammatory Response in Human Liver Cells by Suppressing Phosphorylation of Signal Transducer and Activator of Transcription 3 (STAT3). *Diabetologia* 53, 2406–2416. doi:10.1007/s00125-010-1856-z

Ou, Z. B., Miao, C. M., Ye, M. X., Xing, D. P., He, K., Li, P. Z., et al. (2017). Investigation for Role of Tissue Factor and Blood Coagulation System in Severe Acute Pancreatitis and Associated Liver Injury. *Biomed. Pharmacother.* 85, 380–388. doi:10.1016/j.biopha.2016.11.039

Ramirez Reyes, J. M. J., Cuesta, R., and Pause, A. (2021). Folliculin: A Regulator of Transcription through AMPK and mTOR Signaling Pathways. *Front. Cel Dev Biol* 9, 667311. doi:10.3389/fcell.2021.667311

Rao, E., Zhang, Y., Li, Q., Hao, J., Egilmez, N. K., Suttles, J., et al. (2016). AMPK-dependent and Independent Effects of AICAR and Compound C on T-Cell Responses. *Oncotarget* 7, 33783–33795. doi:10.18632/oncotarget.9277

Rios, E. C., Moretti, A. I., de Souza, H. P., Velasco, I. T., and Soriano, F. G. (2010). Hypertonic saline Reduces Metalloproteinase Expression in Liver during Pancreatitis. *Clin. Exp. Pharmacol. Physiol.* 37, 35–39. doi:10.1111/j.1440-1681.2009.05220.x

Rongione, A. J., Kusske, A. M., Kwan, K., Ashley, S. W., Reber, H. A., and McFadden, D. W. (1997). Interleukin 10 Reduces the Severity of Acute Pancreatitis in Rats. *Gastroenterology* 112, 960–967. doi:10.1053/gast.1997.v112.pm9041259

Saha, S., Buttari, B., Panieri, E., Profumo, E., and Saso, L. (2020). An Overview of Nrf2 Signaling Pathway and its Role in Inflammation. *Molecules* 25, 5474. doi:10.3390/molecules25225474

Saito, S., Furuno, A., Sakurai, J., Park, H. R., Shin-ya, K., and Tomida, A. (2012). Compound C Prevents the Unfolded Protein Response during Glucose Deprivation through a Mechanism Independent of AMPK and BMP Signaling. *PLoS One* 7, e45845. doi:10.1371/journal.pone.0045845

Shen, Z., Chen, Q., Jin, T., Wang, M., Ying, H., Lu, J., et al. (2019). Theaflavin 3,3'-digallate Reverses the Downregulation of Connexin 43 and Autophagy Induced by High Glucose via AMPK Activation in Cardiomyocytes. *J. Cel Physiol* 234, 17999–18016. doi:10.1002/jcp.28432

Shi, N., Liu, T., de la Iglesia-Garcia, D., Deng, L., Jin, T., Lan, L., et al. (2020). Duration of Organ Failure Impacts Mortality in Acute Pancreatitis. *Gut* 69, 604–605. doi:10.1136/gutjnl-2019-318241

Song, X., Zhu, S., Chen, P., Hou, W., Wen, Q., Liu, J., et al. (2018). AMPK-mediated BECN1 Phosphorylation Promotes Ferroptosis by Directly Blocking System Xc- Activity. *Curr. Biol.* 28, 2388. doi:10.1016/j.cub.2018.05.094

Srinivasan, M. P., Bhopale, K. K., Caracheo, A. A., Amer, S. M., Khan, S., Kaphalia, L., et al. (2020). Activation of AMP-Activated Protein Kinase Attenuates Ethanol-Induced ER/oxidative Stress and Lipid Phenotype in Human Pancreatic Acinar Cells. *Biochem. Pharmacol.* 180, 114174. doi:10.1016/j.bcp.2020.114174

Steinberg, W. M., Buse, J. B., Ghorbani, M. L. M., Ørsted, D. D., and Nauck, M. A. (2017). Amylase, Lipase, and Acute Pancreatitis in People with Type 2 Diabetes Treated with Liraglutide: Results from the LEADER Randomized Trial. *Diabetes Care* 40, 966–972. doi:10.2337/dc16-2747

Sun, Y., Connors, K. E., and Yang, D. Q. (2007). AICAR Induces Phosphorylation of AMPK in an ATM-dependent, LKB1-independent Manner. *Mol. Cel Biochem* 306, 239–245. doi:10.1007/s11010-007-9575-6

Swinnen, J. V., Beckers, A., Brusselmans, K., Organe, S., Segers, J., Timmermans, L., et al. (2005). Mimicry of a Cellular Low Energy Status Blocks Tumor Cell Anabolism and Suppresses the Malignant Phenotype. *Cancer Res.* 65, 2441–2448. doi:10.1158/0008-5472.Can-04-3025

Tan, X., Jiao, P. L., Sun, J. C., Wang, W., Ye, P., Wang, Y. K., et al. (2021). β-Arrestin1 Reduces Oxidative Stress via Nrf2 Activation in the Rostral Ventrolateral Medulla in Hypertension. *Front. Neurosci.* 15, 657825. doi:10.3389/fnins.2021.657825

Tonelli, C., Chio, I. I. C., and Tuveson, D. A. (2018). Transcriptional Regulation by Nrf2. *Antioxid. Redox Signal.* 29, 1727–1745. doi:10.1089/ars.2017.7342

Unamuno, X., Gómez-Ambrosi, J., Ramírez, B., Rodríguez, A., Becerril, S., Valentí, V., et al. (2021). NLRP3 Inflammasome Blockade Reduces Adipose Tissue Inflammation and Extracellular Matrix Remodeling. *Cel Mol Immunol* 18, 1045–1057. doi:10.1038/s41423-019-0296-z

Višnjić, D., Lalić, H., Dembitz, V., Tomić, B., and Smoljo, T. (2021). AICAr, a Widely Used AMPK Activator with Important AMPK-independent Effects: A Systematic Review. *Cells* 10, 1095. doi:10.3390/cells10051095

Wang, Q., Zhang, X., Lei, S., Wang, Y., Zhuang, Y., Chen, Y., et al. (2018). RNA Sequence Analysis Reveals Pathways and Candidate Genes Associated with Liver Injury in a Rat Pancreatitis Model. *Pancreatology* 18, 753–763. doi:10.1016/j.pan.2018.08.006

Wang, X., Zhao, X., Shi, C., Börjesson, A., Chen, Z., Axelsson, J., et al. (2006). Potential Mechanisms and Significance of Acute Pancreatitis-Associated Liver Injury. *Scand. J. Gastroenterol.* 41, 604–613. doi:10.1080/00365520500347105

Wenhong, D., Jia, Y., Weixing, W., Xiaoyan, C., Chen, C., Sheng, X., et al. (2012). Zerumbone Attenuates the Severity of Acute Necrotizing Pancreatitis and Pancreatitis-Induced Hepatic Injury. *Mediators Inflamm.* 2012, 156507. doi:10.1155/2012/156507

Wree, A., McGeough, M. D., Inzaugarat, M. E., Eguchi, A., Schuster, S., Johnson, C. D., et al. (2018). NLRP3 Inflammasome Driven Liver Injury and Fibrosis: Roles of IL-17 and TNF in Mice. *Hepatology* 67, 736–749. doi:10.1002/hep.29523

Xu, W., Zhao, T., and Xiao, H. (2020). The Implication of Oxidative Stress and AMPK-Nrf2 Antioxidative Signaling in Pneumonia Pathogenesis. *Front. Endocrinol. (Lausanne)* 11, 400. doi:10.3389/fendo.2020.00400

Yang, J., Fier, A., Carter, Y., Liu, G., Epling-Burnette, P. K., Bai, F., et al. (2003). Liver Injury during Acute Pancreatitis: the Role of Pancreatitis-Associated Ascitic Fluid (PAAF), P38-MAPK, and Caspase-3 in Inducing Hepatocyte Apoptosis. *J. Gastrointest. Surg.* 7, 200–208. doi:10.1016/s1091-255x(02)00134-8

Yang, J., Zhou, Y., and Shi, J. (2020). Cordycepin Protects against Acute Pancreatitis by Modulating NF-Kb and NLRP3 Inflammasome Activation via AMPK. *Life Sci.* 251, 117645. doi:10.1016/j.lfs.2020.117645

Yang, M., Luo, S., Jiang, N., Wang, X., Han, Y., Zhao, H., et al. (2021). DsbA-L Ameliorates Renal Injury through the AMPK/NLRP3 Inflammasome Signaling Pathway in Diabetic Nephropathy. *Front. Physiol.* 12, 659751. doi:10.3389/fphys.2021.659751

Yu, P. B., Hong, C. C., Sachidanandan, C., Babitt, J. L., Deng, D. Y., Hoyng, S. A., et al. (2008). Dorsomorphin Inhibits BMP Signals Required for Embryogenesis and Iron Metabolism. *Nat. Chem. Biol.* 4, 33–41. doi:10.1038/nchembio.2007.54

Zeng, J., Chen, Y., Ding, R., Feng, L., Fu, Z., Yang, S., et al. (2017). Isoliquiritigenin Alleviates Early Brain Injury after Experimental Intracerebral Hemorrhage via Suppressing ROS- And/or NF-Kb-Mediated NLRP3 Inflammasome Activation by Promoting Nrf2 Antioxidant Pathway. *J. Neuroinflammation* 14, 119. doi:10.1186/s12974-017-0895-5

Zhao, Y., Ye, S., Lin, J., Liang, F., Chen, J., Hu, J., et al. (2021). NmFGF1-Regulated Glucolipid Metabolism and Angiogenesis Improves Functional Recovery in a Mouse Model of Diabetic Stroke and Acts via the AMPK Signaling Pathway. *Front. Pharmacol.* 12, 680351. doi:10.3389/fphar.2021.680351

Zhou, H., Wang, H., Ni, M., Yue, S., Xia, Y., Busuttil, R. W., et al. (2018). Glycogen Synthase Kinase 3β Promotes Liver Innate Immune Activation by Restraining AMP-Activated Protein Kinase Activation. *J. Hepatol.* 69, 99–109. doi:10.1016/j.jhep.2018.01.036

Zimmermann, K., Baldinger, J., Mayerhofer, B., Atanasov, A. G., Dirsch, V. M., and Heiss, E. H. (2015). Activated AMPK Boosts the Nrf2/HO-1 Signaling axis--A Role for the Unfolded Protein Response. *Free Radic. Biol. Med.* 88, 417–426. doi:10.1016/j.freeradbiomed.2015.03.030

Zou, J., Wang, S. P., Wang, Y. T., and Wan, J. B. (2021). Regulation of the NLRP3 Inflammasome with Natural Products against Chemical-Induced Liver Injury. *Pharmacol. Res.* 164, 105388. doi:10.1016/j.phrs.2020.105388

Conflict of Interest: The authors declare that the research was conducted in the absence of any commercial or financial relationships that could be construed as a potential conflict of interest.

Publisher's Note: All claims expressed in this article are solely those of the authors and do not necessarily represent those of their affiliated organizations, or those of the publisher, the editors and the reviewers. Any product that may be evaluated in this article, or claim that may be made by its manufacturer, is not guaranteed or endorsed by the publisher.

Copyright © 2021 Kong, Zhang, Lu, Shi, Huang, Zheng, Wang, Wang, Wang and Huang. This is an open-access article distributed under the terms of the Creative Commons Attribution License (CC BY). The use, distribution or reproduction in other forums is permitted, provided the original author(s) and the copyright owner(s) are credited and that the original publication in this journal is cited, in accordance with accepted academic practice. No use, distribution or reproduction is permitted which does not comply with these terms.

frontiers in Pharmacology

ORIGINAL RESEARCH
published: 30 September 2021
doi: 10.3389/fphar.2021.726707

Metformin Exerts Anti-inflammatory and Mucus Barrier Protective Effects by Enriching Akkermansia muciniphila in Mice With Ulcerative Colitis

Haoran Ke[1†], *Fang Li*[1,2†], *Wenlin Deng*[1,3†], *Zitong Li*[1†], *Siqi Wang*[1], *Pinjing Lv*[1] *and Ye Chen*[1*]

[1]Department of Gastroenterology, State Key Laboratory of Organ Failure Research, Guangdong Provincial Key Laboratory of Gastroenterology, Nanfang Hospital, Southern Medical University, Guangzhou, China, [2]Hainan General Hospital, Haikou, China, [3]Department of Pediatrics, The Sixth Affiliated Hospital of Sun Yat-sen University, Guangzhou, China

OPEN ACCESS

Edited by:
Ralf Weiskirchen,
RWTH Aachen University, Germany

Reviewed by:
Waranya Chatuphonprasert,
Mahaasarakham University, Thailand
Talha Bin Emran,
Begum Gulchemonara Trust University, Bangladesh

***Correspondence:**
Ye Chen
yechen@smu.edu.cn

[†]These authors have contributed equally to this work and share first authorship

Specialty section:
This article was submitted to Gastrointestinal and Hepatic Pharmacology, a section of the journal Frontiers in Pharmacology

Received: 17 June 2021
Accepted: 13 September 2021
Published: 30 September 2021

Citation:
Ke H, Li F, Deng W, Li Z, Wang S, Lv P and Chen Y (2021) Metformin Exerts Anti-inflammatory and Mucus Barrier Protective Effects by Enriching Akkermansia muciniphila in Mice With Ulcerative Colitis. Front. Pharmacol. 12:726707. doi: 10.3389/fphar.2021.726707

The present study aimed to determine if metformin exerts anti-inflammatory and mucus-protective effects *via* the gut microbiota. Metformin has extensive benefits including anti-inflammatory effects. Previous studies showed that metformin changed the gut microbiota composition and increases the number of goblet cells. Intestinal dysbiosis and goblet cell depletion are important features of ulcerative colitis (UC). The underlying mechanism and whether metformin can improve the mucus barrier in UC remain unclear. Metformin (400 mg/kg/day) was administered to mice with dextran sulfate sodium (DSS)-induced UC for 2 wk to investigate the effects of metformin on the intestinal mucus barrier. The gut microbiota was depleted, using antibiotics, to explore its role in the mucus-protecting effects of metformin. *Akkermansia muciniphila (A. muciniphila)*, which was enriched in metformin-treated mice, was administered to mice to investigate the effects of the bacteria on UC and the mucus barrier. Metformin attenuated DSS-induced UC in mice, as evidenced by the alleviation of diarrhea, hematochezia, and the decrease in body weight. The expression of mucin2, a prominent mucus barrier protein, was increased in the metformin-treated group compared to the DSS-treated group. Furthermore, fecal 16S rRNA analysis showed that metformin treatment changed the gut microbiota composition by increasing the relative abundance of *Lactobacillus* and *Akkermansia* species while decreasing *Erysipelatoclostridium* at the genus level. Antibiotic treatment partly abolished the anti-inflammatory and mucus-protecting effects of metformin. Administration of *A. muciniphila* alleviated the colonic inflammation and mucus barrier disruption. Metformin alleviated DSS-induced UC in mice and protected against cell damage *via* affecting the gut microbiota, thereby providing a new mechanism for the therapeutic effect of metformin in patients with UC. This study also provides evidence that *A. muciniphila* as a probiotic has potential benefits for UC.

Keywords: intestinal barrier, inflammatory bowel diseases, probiotics, gut microbiota, mucin2

INTRODUCTION

Ulcerative colitis (UC), characterized by chronic and relapsing inflammation in the colon, is becoming a global disease (M'Koma, 2013). However, the underlying pathogenesis of UC is incompletely understood. It is thought to involve genetic factors, abnormal immune responses, environmental factors, intestinal barrier dysfunction, and dysbiosis (Zhang and Li, 2014; Testa et al., 2017; Ungaro et al., 2017). Goblet cell depletion and gut dysbiosis are important features of UC (Strugala et al., 2008; Gersemann et al., 2009; Johansson et al., 2014).

Mucus barrier dysfunction plays a significant role in the pathogenesis of UC. The mucus barrier, organized by the Mucin2 (Muc2) mucin, is a gel that covers the intestinal epithelium (Johansson and Hansson, 2011; Kühn and Klar, 2015). Several studies have shown that the thickness of the mucus is decreased in wild-type mice with DSS-induced UC, while Muc2-deficient mice developed spontaneous UC and were more susceptible to DSS-induced colitis (Van der Sluis et al., 2006; Heazlewood et al., 2008; Petersson et al., 2010). The mucus barrier is also impaired in patients with UC (Shen et al., 2018) (Van der Post et al., 2019).

The gut microbiota plays an important role in the pathogenesis of UC. The composition, diversity and richness of the gut microbiota are altered in patients with inflammatory bowel disease (IBD) (Knox et al., 2019) and are related to disease severity as well as treatment efficacy (Zhou et al., 2018). Furthermore, in animal models, the absence of gut microbiota reduces inflammation in the mouse colon (Hernández-Chirlaque et al., 2016). The manipulation of the microbiota by fecal microbiota transplantation (FMT) or administration of probiotics may have potential benefits in the treatment of IBD (Shen et al., 2014; Paramsothy et al., 2017).

Metformin, with a relatively low cost and a superior safety profile, is the first-line treatment for type 2 diabetes (McCreight et al., 2016). Recent studies have demonstrated that metformin has extensive benefits, besides its anti-diabetic effects, including anticancer effects (Leone et al., 2014), cardiovascular benefits (Rena and Lang, 2018; Van der Post et al., 2019), anti-aging effects (Anisimov, 2013), and anti-inflammatory effects (Saisho, 2015; Cameron Amy et al., 2016). In particular, metformin treatment increases the number of goblet cells in the intestine (Shin et al., 2014; Xue et al., 2016), indicating that metformin may have mucus protective effects. Several studies have established that metformin can attenuate colitis in mice by suppressing nuclear factor kappa-light-chain-enhancer of activated B cells (NF-kB) (Koh et al., 2014), Phosphorylated-Signal transducer and activator of transcription 3 (pSTAT3) (Lee et al., 2015), Jun N-terminal kinases (JNK) (Deng et al., 2018) and p38 mitogen-activated protein kinase (MAPK) activation (Di Fusco et al., 2018). However, most of these studies focus on the mechanisms involved in the host factor and the influence of gut microbiota on the therapeutic effects of metformin in colitis the is not fully understood.

Metformin can alter the gut microbiota by increasing the abundance of *Akkermansia muciniphila (A. muciniphila)* and *Lactobacillus* (Hur and Lee, 2015; Bauer et al., 2018; Zhang, 2019), both of which have an anti-inflammatory profile. Emerging evidence shows that *A. muciniphila* is decreased in inflammatory bowel diseases, which is negatively associated with inflammation scores (Png et al., 2010; Rajilić-Stojanović et al., 2013; Earley et al., 2019). *Lactobacillus* also shows potential benefits for IBD, as it has anti-inflammatory and gut barrier-protective effects (Vich Vila et al., 2018). The gut microbiota also has significant impacts on the mucus barrier: gut microbiota and their bacterial products regulate Muc2 secretion by goblet cells, and, hence, the properties of the mucus barrier (Petersson et al., 2010; Jakobsson et al., 2015; Birchenough et al., 2016). These studies suggest that gut microbiota altered by metformin may play a critical role in its anti-inflammatory effects. However, whether metformin exerts its anti-inflammatory and mucus barrier protective effects in UC *via* affecting the gut microbiota has not been determined.

Here, the present study proved that metformin exerted its anti-inflammatory and mucus-protective effects *via* affecting the gut microbiota, particularly, *via* enriching *A. muciniphila*.

METHODS

Animal Model

All animal studies were carried out in specific pathogen-free (SPF) laboratory of the Department of Laboratory Animal, Southern Medical University, in accordance with the guidelines of the Southern Medical University Committee for Experimental Animals. And the protocols were approved by the Animal Experimental Ethics Committee of the Southern Medical University, China (**L2018225**). Wild-type male C57BL/6 mice (6–8-wk-old) ranging from 20 to 25 g in weight were purchased from the Animal Center of the Southern Medical University in China. The animals were housed at 22–24°C with an artificial 12 h/12 h day/night cycle in SPF conditions. Mice (6–8-wk-old) were treated with metformin (400 mg/kg/d), administered *via* oral gavage, 7 days before dextran sulfate sodium salt (DSS) treatment, and then in parallel with DSS treatment. Colitis in mice was induced as previously described (Chassaing et al., 2014). To be brief, DSS (MPbio, Solon, OH, United States) (2% w/v), with a molecular weight of 36,000–50,000 Da, was added to drinking water and administered to the mice for 6 days, followed by 1 day of regular water administration. The disease activity index (DAI) was evaluated after DSS administration as previously described (Wang et al., 2015). Fecal samples were collected on day 6 following DSS treatment. The mice were anesthetized by 100 mg/kg pentobarbital sodium (provide by the Department of Laboratory Animal, Nanfang Hospital) and euthanized by using cervical dislocation on day 7 after DSS treatment and the colons were removed.

Depletion of the Gut Microbiota Using Antibiotics

The gut microbiota of mice was depleted according to a method described previously (Chen et al., 2020) with minor adjustments.

Mice were administered with an antibiotic cocktail consisting of vancomycin 100 mg/kg/day, metronidazole 200 mg/kg/day, gentamicin 40 mg/kg/day, and ampicillin 200 mg/kg/day. The antibiotic cocktail was administered to the mice by oral gavage for 5 days prior to metformin treatment and the induction of experimental colitis described above. The fecal substance was collected on day 5 to evaluate the effect of the antibiotic treatment on the gut microbiota by using gel electrophoresis.

Bacterial Culture and Animal Treatment

Akkermansia muciniphila bacteria (ATTC BAA-835), purchased from ATCC (Manassas, VA, United States), were cultured anaerobically (80% N2, 10% CO2, and 10% H2) at 37°C in brain heart infusion (BHI) medium (Zhai et al., 2019) with an AnoxomatTM MarkII anaerobic system (Mart Microbiology). Bacteria used for oral gavage were washed once using 5 ml of anaerobic phosphate-buffered saline (PBS, pH = 7.4) after centrifugation, and then resuspended in anaerobic PBS. The mice were orally gavaged with 1.50×10^{11} CFU bacterial cells per kilogram of body weight per day for 7 days prior to DSS treatment and 6 days parallel with DSS treatment. All the experiments were performed according to the General Requirements for Biosafety (GB 19489-2008).

Histological Analysis

Tissues were embedded in paraffin and were cut into 4-μm sections and stained with hematoxylin and eosin (HE). The scores were assessed by two blinded investigators from the aspects of inflammation level, inflammation extent, crypt damage and involvement percentage according to the protocols devised by Deng et al. (Deng et al., 2018). Briefly, the level of inflammation was graded as (0) none; (1) slight; (2) moderate; (3) severe. The inflammation extent was graded as: (0) none; (1) mucosa; (2) mucosa and submucosa; (3) transmural. The crypt damage was graded on a scale from 0 to 4: (0) none; (1) basal 1/3 damaged; (2) basal 2/3 damaged; (3) only surface epithelium intact; (4) entire crypt and epithelium lost. These changes were quantified based on the percentage of disease process involvement as follows: (1) 1–25%; (2) 26–50%; (3) 51–75%; (4) 76–100% (**Supplementary Table S1**).

Immunofluorescence

Immunofluorescence staining was performed as previously described with minor modifications (Robertson et al., 2008). Sections were deparaffinized in xylene three times for 10 min, and their endogenous peroxidase was quenched for 15 min using 3% hydrogen peroxide in methanol. Subsequently, the sections were rehydrated using a graded ethanol series and antigen retrieval was performed using a sodium citrate buffer at a sub-boiling temperature for 10 min. The slides were then cooled at the bench-top and washed with PBS three times for 5 min, blocked with 10% BSA for 1 h, and incubated overnight at 4°C with the following primary antibodies: anti-MUC2 (1:200, #MA5-12345; Invitrogen), anti-Kruppel-like factor 4 (KLF4) (1:100, #ab129473; Abcam), anti-mouse atonal homolog 1 (MATH1) (1:300, #PA5-29392; Abcam), anti-hairy and enhancer of split type-1 (Hes1) (1:200, #ab71559; Abcam), anti-SAM pointed domain-containing ETS transcription factor (SPDEF) (1:100, #LS-C749124; LSBIO). After washing three times for 5 min with PBS, the slides were incubated with the appropriate secondary antibodies conjugated with a fluorescent label for 1 h at room temperature in the dark. The sections were washed three times for 5 min in PBS and incubated with 4′,6-diamidino-2-phenylindole (DAPI) for 3 min at room temperature followed by PBS washing for another three times. Finally, the slides were mounted and investigated under a fluorescence microscope (BX53F; Olympus, Tokyo, Japan) using cellSens Dimension software.

Alcian Blue-periodic Acid-Shiff (AB-PAS) Staining and Goblet Cell Counting

AB-PAS staining was performed using commercial kits (DG0007100; Solarbio, Beijing, China) according to the manufacturer's manual. The number of goblet cells was determined by counting the Alcian Blue positive vacuoles (Becker et al., 2013).

RNA Extraction

The total RNA from colon tissue was isolated using the Trizol method (Rio et al., 2010). Briefly, the colon samples were homogenized using 1 ml Trizol reagent per 80 mg of tissue. The homogenized samples were incubated for 10 min at room temperature. A total of 0.2 ml chloroform per 1 ml homogenized sample was used and the mixture was vortexed vigorously for 15 s. Then, the samples were incubated for 10 min at room temperature and centrifuged at 12,000 g for 10 min at 4°C. After centrifugation, the upper layer was transferred into a fresh tube. Then, 0.5 ml isopropyl alcohol was added to each tube and the samples were incubated for 10 min at room temperature. Next, the samples were centrifuged at 12,000 g for 10 min at 4°C and the supernatant was completely removed. A total of 1 ml of 75% ethanol was added per tube and the tube was washed gently. The samples were incubated for 10 min at room temperature and then centrifuged at 12,000 g for 10 min at 4°C. All the remaining ethanol was removed, the samples were air-dried and 20 μl diethylpyrocarbonate (DEPC) water was added per tube to dissolve the RNA.

Real-time Quantitative PCR (RT-qPCR)

First-strand cDNA was synthesized using the PrimeScript RT Master Mix (Takara) according to the manufacturer's manual, and RT-qPCR was performed using the Roche LightCycler 480II with the SYBR Premix Ex Taq. The primer sequences are provided in **Supplementary Table S2**. The $2^{\Delta\Delta CT}$ method was used to calculate the expression of the detected mRNA using β-actin as the reference gene (Deng et al., 2018).

DNA Extraction

DNA was extracted from fecal samples by using the TIANamp Stool DNA Kit (#DP328; TIANGEN Biotech) according to the manufacturer's instructions (Shao et al., 2017). The DNA was diluted to 1 ng/μl.

PCR Amplification

Fecal DNA was amplified using the TIANGEN 2× Taq PCR MasterMix (KT201), according to the manufacturer's manual

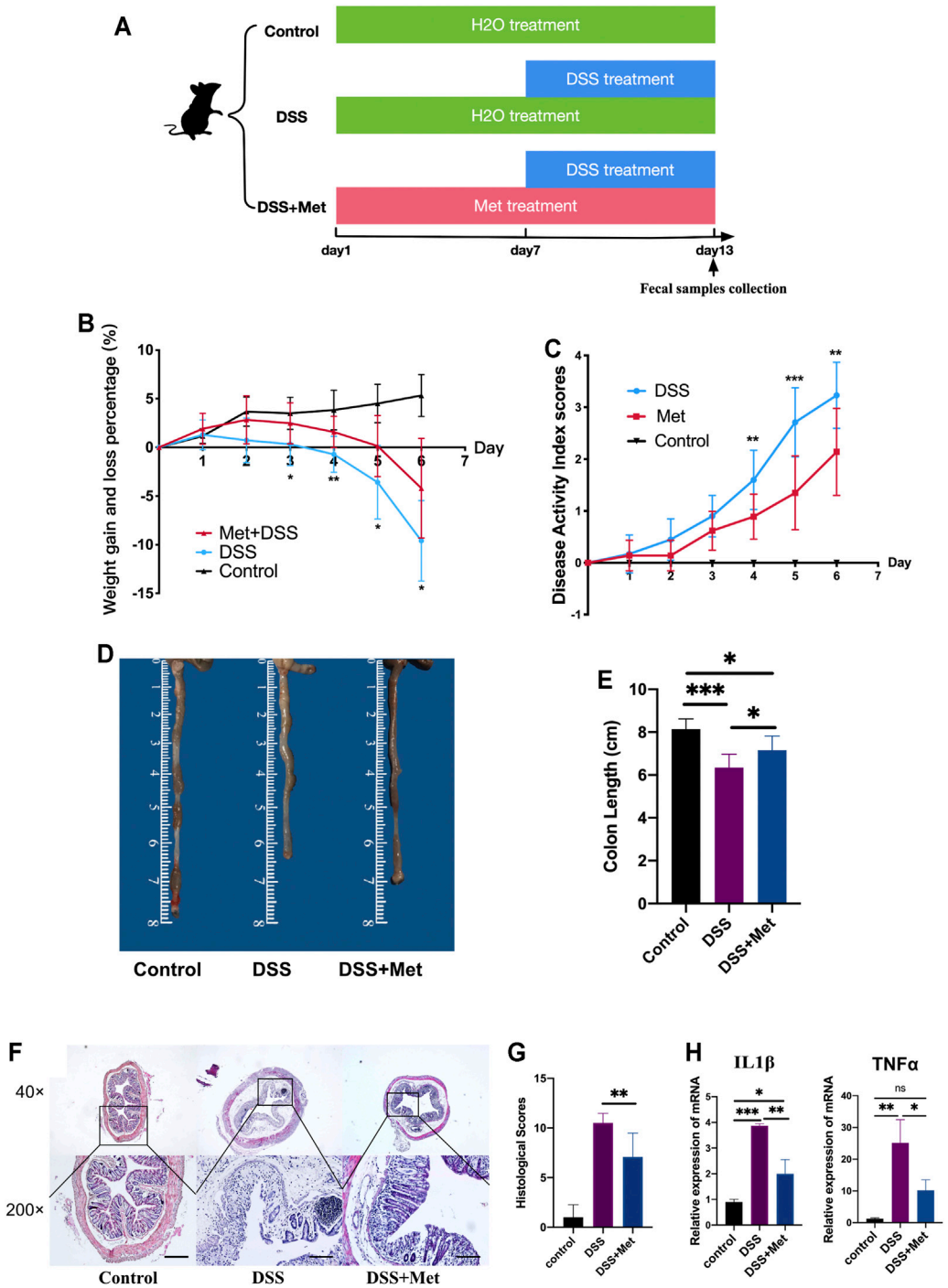


FIGURE 1 | Metformin alleviates dextran sulfate sodium (DSS)-induced ulcerative colitis (UC) in mice. Flow chart of animal treatment (n = 6–10) **(A)**, weight loss and gain (n = 6–10) **(B)**, disease activity index (DAI) scores (n = 6–10) **(C)**, representative pictures of the mouse colon (n = 6–10) **(D)**, colon length (n = 6–10) **(E)**, hematoxylin and eosin (HE) staining (scale bars, 400 μm) (n = 6–10) **(F)**, and histological scores (n = 6–10) **(G)**. RT-qPCR assay of tumor necrosis factor-α (TNF-α) and interleukin 1β (IL1β) in colon tissue (n = 3) **(H)** and statistical comparison was made using an ANOVA test followed by Tukey-Kramer *post-hoc* tests. *p < 0.05, **p < 0.01, ***p < 0.001.

and the V4 primers 514F (5′-GTGCCAGCMGCCGCGGTAA-3′) and 805R (5′-GGACTACHVGGGTWTCTAAT-3′) (Yin et al., 2015).

16S rRNA Sequencing

16S rRNA sequencing was performed as previously described (Janda and Abbott, 2007). Briefly, fecal DNA amplification

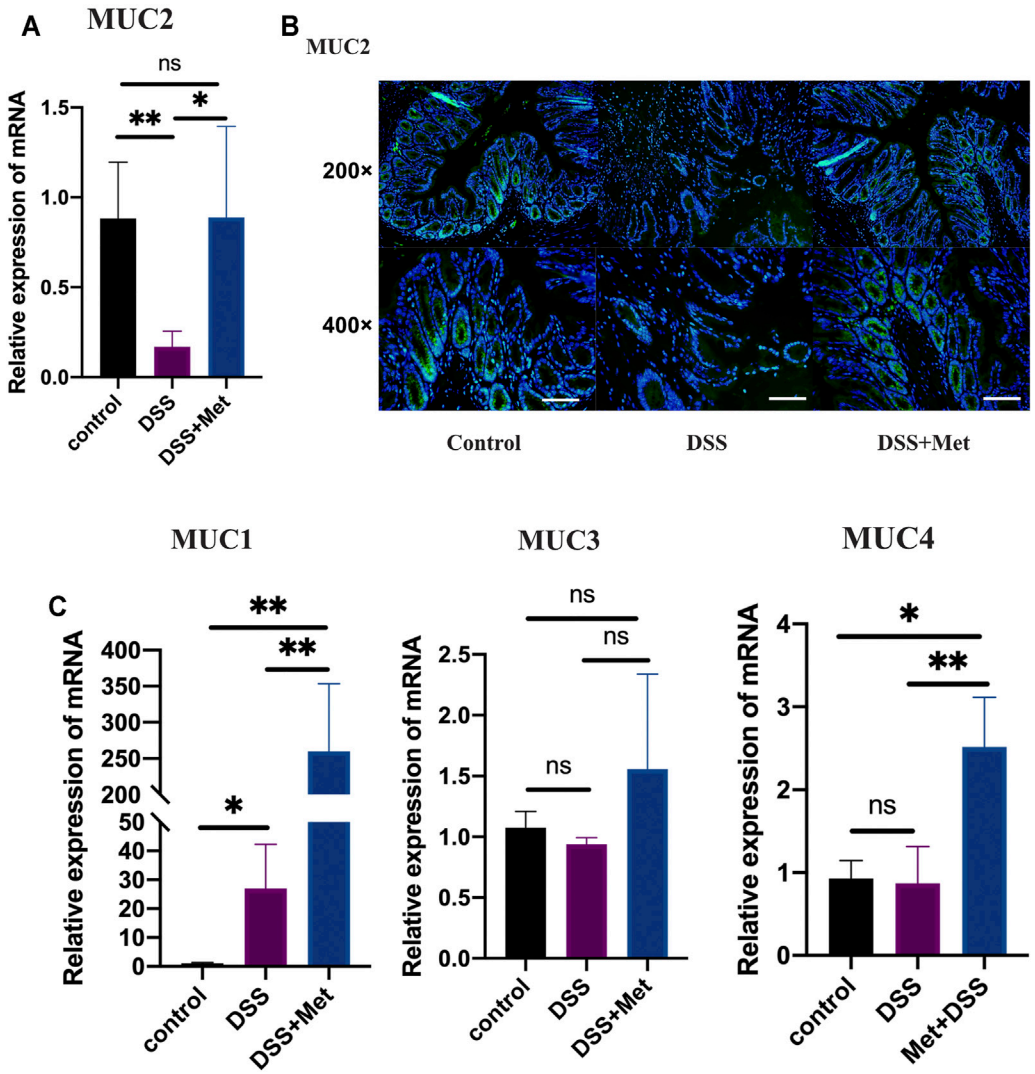


FIGURE 2 | Metformin protects the mucus barrier by increasing the expression of mucins in ulcerative colitis (UC). RT-qPCR assay of mucin 2 (MUC2) expression of colon tissue (n = 3–4) **(A)**, immunofluorescence assay showing the expression of mucin2 protein in colon tissue (scale bars, 200 μm) (n = 4) **(B)**, and RT-qPCR assay (n = 3–6) of the relative expression levels of MUC1, MUC3, and MUC4 in colon tissue at mRNA level **(C)** and statistical comparison was made using an ANOVA test followed by Tukey-Kramer *post-hoc* tests. *p < 0.05, **p < 0.01, ***p < 0.001, ns, no significance.

was performed using the TIANGEN 2× Taq PCR MasterMix (KT201), according to the manufacturer's manual. Amplification of the 16S/18S rRNA genes was performed using the specific primers with the barcodes: 16S V4: 515F-806R; 18S V4: 528F-706R; 18S V9: 1380F-1510R; ITS1: ITS5-1737F, ITS2-2043R; ITS2: ITS3-2024F, ITS4-2409R. Then, the PCR products were sequenced using the Illumina GAII (Illumina, San Diego, CA, United States) at the Beijing Genomic Institute (Shenzhen, China) and the data were clustered using the Illumina paired barcoded-sequencing (end) (BIPES) (PE) process for preliminary analysis. The rest of the sequences were screened by UCHIME and the suspected chimeric sequences were removed. All the reads were sorted into different samples according to their barcodes.

Statistical Analysis

All the data from at least three independent experiments were displayed as the mean ± standard deviation (SD). The student's t-test and/or one-way analysis of variance (ANOVA) with a proper post hoc Tukey-Kramer test comparison was carried out to determine if the differences were statistically significant. A p value of less than 0.05 was considered statistically significant.

RESULTS

Metformin Alleviated DSS-induced UC in Mice

To determine if metformin can attenuate colitis, mice were first treated with 2% DSS to induce colitis and then treated with

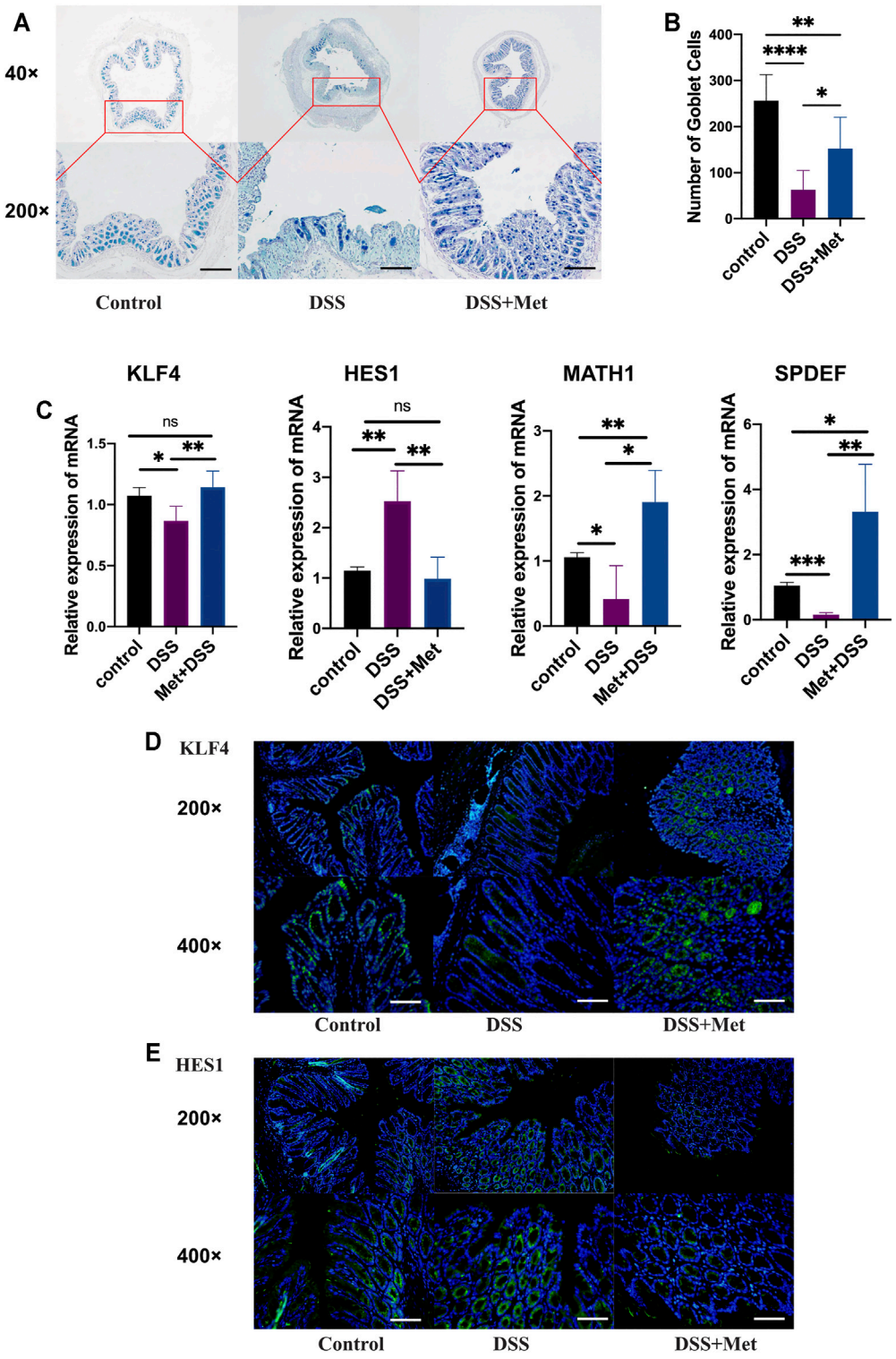


FIGURE 3 | Metformin positively regulates the differentiation of goblet cells. Alcian blue-periodic acid-Shiff (AB-PAS) staining of colon tissue (scale bars, 400 μm) (n = 4–7) **(A)** and count of goblet cells (n = 4–7) **(B)**, RT-qPCR assay (n = 3–6) of Kruppel-like factor 4 (KLF4), hairy and enhancer of split type-1 (HES1), MATH1 and SAM pointed domain containing ETS transcription factor (SPDEF) at the mRNA level **(C)**, immunofluorescence assay of Klf4 (scale bars, 200 m) (n = 4) **(D)** and Hes1 (scale bars, 200 μm) (n = 4) **(E)** protein detection in the mouse colon and statistical comparison was made using an ANOVA test followed by Tukey-Kramer *post-hoc* tests. $^{*}p < 0.05$, $^{**}p < 0.01$, $^{***}p < 0.001$.

400 mg/kg/day metformin or PBS solution (**Figure 1A**). Metformin reduced the severity of UC in mice as manifested by the reduced weight loss and less severe DAI scores (**Figures 1B,C**). Next, the colon length of mice was measured, and less colon length shortening was found in metformin-treated mice compared to mice treated with PBS (**Figures 1D,E**). Colon histology showed that metformin alleviated the damage and inflammation caused by DSS and reduced the histological scores (**Figures 1F,G**). The expression of pro-inflammatory cytokines interleukin 1β (IL1β) and tumor necrosis factor-α (TNF-α) in the colon were assessed. Consistent with previous results, metformin significantly reduced the level of IL1β and TNF-α (**Figure 1H**). These indicated that metformin had an anti-inflammatory effect.

Metformin Protected Against Mucus Barrier Dysfunction in DSS-induced UC

Mucus barrier dysfunction plays an important role in the pathogenesis of UC. The present study has shown that metformin can attenuate UC in mice. We explored the effects of metformin on the mucus barrier of the mouse colon. The expression of MUC2, the major component of the mucus barrier, was increased in DSS-induced colitis at the mRNA level (**Figure 2A**). Additionally, immunofluorescence assays were performed to assess the expression level of mucin2 protein. Metformin treatment also increased mucin2 expression at the protein level (**Figure 2B**). Mucin1 (Muc1), mucin3 (Muc3), and mucin4 (Muc4) are critical components of the colon mucus barrier. Metformin treatment significantly increased the expression of Muc1 and Muc4 (**Figure 2C**). These results suggested that metformin can protect against mucus barrier dysfunction by increasing the expression of mucins, particularly that of mucin2, in the colon and thus contributed to its anti-inflammatory effect.

Metformin Positively Regulated the Differentiation of Goblet Cells

Mucin2 is synthesized and secreted by goblet cells. To explore the effects of metformin on goblet cells, the numbers of goblet cells in the colon were measured. Metformin treatment significantly increased the number of goblet cells (**Figures 3A,B**). KLF4, MATH1, SPDEF and HES1 play an important role in regulating the differentiation of goblet cells: KLF4, MATH1 and SPDEF can promote the differentiation of goblet cells while HES1 has an opposite effect. The expressions of them were assessed by RT-qPCR assays. Mice treated with metformin had a higher expression of KLF4, MATH1 and SPDEF and a lower expression of HES1 (**Figure 3C**). Furthermore, immunofluorescence assays showed that metformin treatment increased the expression of Klf4 and decreased that of Hes1 in colon tissue (**Figures 3D,E**), which suggested that metformin increased the number of goblet cells by promoting its differentiation.

Metformin Changed the Structure of the Gut Microbiota in DSS-induced UC in Mice

Previous studies have shown that metformin altered the structure of the gut microbiota of mice on a high-fat diet (Shin et al., 2014), which may play an important role in the anti-inflammatory and mucus-protective effects of metformin. 16S rRNA sequencing was performed to investigate the influence of metformin on the gut microbiota in DSS-induced UC in mice. At the phylum level, DSS treatment decreased the relative abundance of Bacteroidetes and Proteobacteria while it increased the relative abundance of Firmicutes compared with the normal control (**Figure 4A**). However, metformin treatment partly restored the structure of the gut microbiota in DSS-induced UC. The relative abundance of the phylum Bacteroidetes in the metformin group was increased, while the relative abundance of the phylum Firmicutes was decreased compared with the DSS group (**Figure 4A**). Furthermore, the relative abundance of the phylum Verrucomicrobia was increased after metformin treatment compared with the DSS and control groups (**Figure 4A**). At the genus level, metformin increased the abundance of *Bacteroides* and *Lactobacillus* compared with the DSS group. Metformin also increased the abundance of the genus *Akkermansia* compared with the DSS and control groups (**Figure 4B**). Increased or decreased Firmicutes/Bacteroidetes (F/B) ratio is regard as dysbiosis (Mariat et al., 2009). The F/B ratio increased by DSS treatment was lowered by metformin (**Figure 4C**), indicating that metformin reversed the dysbiosis in colitis mice. Importantly, the relative abundance of the genus *Akkermansia* was enriched in the metformin group (**Figure 4D**). These results showed that metformin can partly restore the structure of gut microbiota impaired by DSS treatment and enrich *Akkermansia* at the same time.

Antibiotic Treatment Abolished the Anti-inflammatory Effects of Metformin

To further investigate the effects of the gut microbiota on the anti-inflammatory beneficence of metformin, mice were treated with an antibiotic cocktail to deplete the gut microbiota (**Figure 5A**). The microbiota was depleted effectively after a 5-day antibiotic cocktail treatment (**Supplementary Figure S1**). There was no significant difference between the DSS and the antibiotics + DSS + metformin (abx + DSS + Met) group in weight loss and DAI (**Figures 5B,C**), which indicated that antibiotic treatment abolished the protective effects of metformin in DSS-induced UC. Mice in the abx + DSS + Met group also experienced more severe colon shortening compared with mice in the DSS + metformin (DSS + Met) group (**Figures 5D,E**). Histological analysis of colon tissue was performed for further verification. Although metformin inhibited the damage of colon tissue in DSS-induced UC, antibiotic treatment abolished these protective effects (**Figures 5F,G**), which suggested that gut microbiota is of great significance in the anti-inflammatory effects of metformin.

Antibiotic Treatment Abolished the Mucus-protective Effects of Metformin

Furthermore, the effects of the depletion of the gut microbiota on the mucus-protective effects of metformin were investigated by

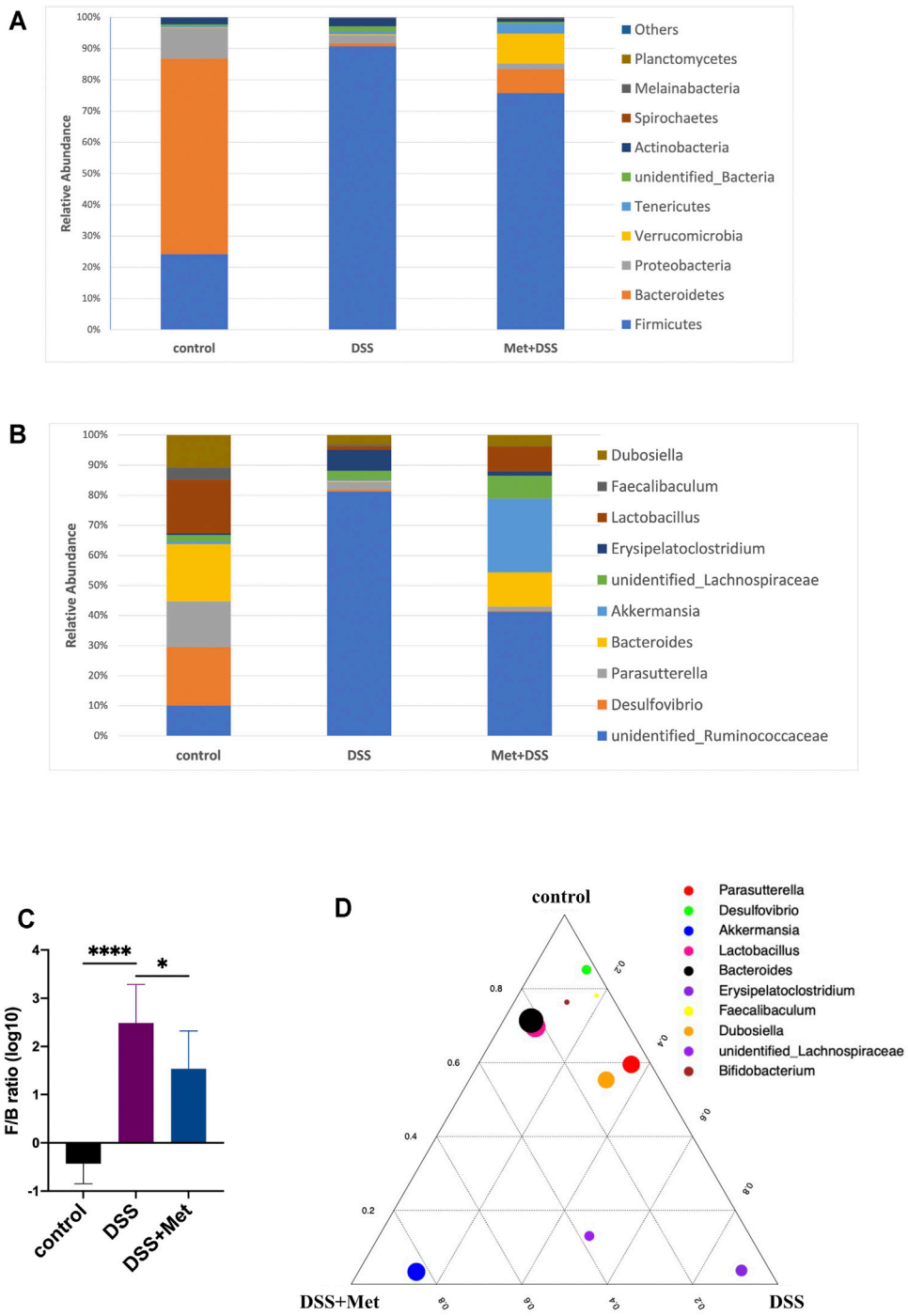


FIGURE 4 | Metformin changes the structure of the gut microbiota (n = 4–10). Fecal 16S rRNA sequencing of gut microbiota of the metformin, dextran sulfate sodium (DSS) and control group. Relative abundance (% of the total community) of 10 most abundant phyla **(A)** and 10 most abundant genera **(B)**, Firmicutes/Bacteroidetes (F/B) ratio (log10 transformation) **(C)** and ternary plot indicating the fraction of 10 most abundant genera in the metformin group (bottom left corner), dextran sulfate sodium (DSS) group (bottom right corner) and control group (top corner) with the size of each dot representing the relative abundance **(D)**.

assessing the number of goblet cells and the expression of mucin2 at the mRNA and protein levels. The number of goblet cells in the DSS + Met group was increased compared with that of the DSS group while antibiotics treatment abolished such effects (**Figures 6A,B**). Antibiotics also inhibited the metformin-induced expression of MUC2 at the mRNA level and of mucin2 at the

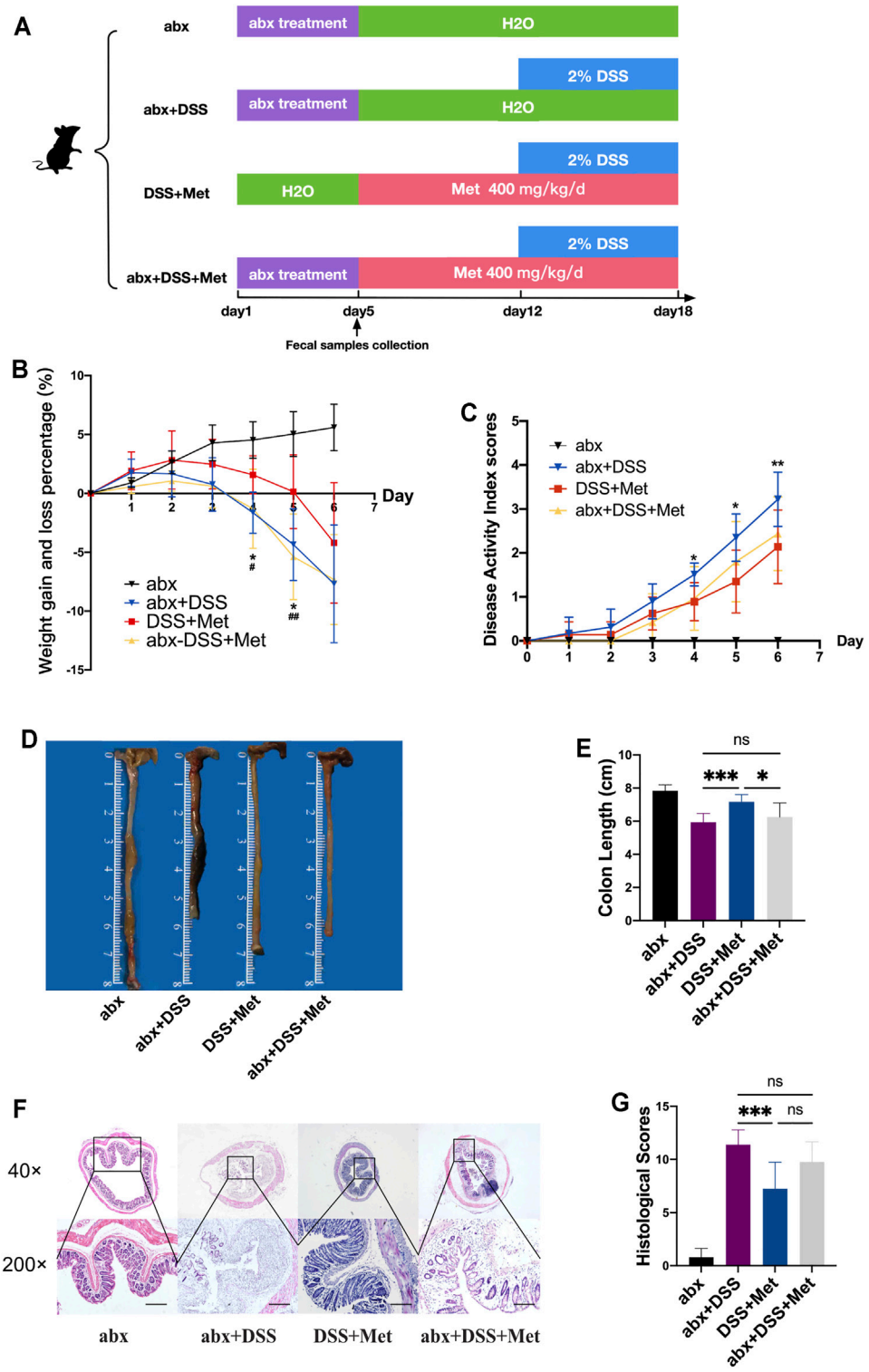


FIGURE 5 | Antibiotics abolish the anti-inflammatory effects of metformin. Flow chart of animal treatment **(A)**, weight loss and gain (n = 6–10) **(B)**, disease activity index (DAI) scores (n = 6–10) **(C)**, representative pictures of the mouse colon (n = 6–10) **(D)**, colon length (n = 6–10) **(E)**, hematoxylin and eosin (HE) staining (scale bars, 400 μm) **(F)**, histological scores (n = 5–8) **(G)** *p < 0.05 (DSS+Met vs abx+DSS) and statistical comparison was made using an ANOVA test followed by Dunnett's *post-hoc* tests. **p < 0.01, ***p < 0.00, $^{\#}p$ < 0.05 (DSS+Met vs abx+DSS+Met), $^{\#\#}p$ < 0.01.

protein level (**Figures 6C,D**). The mucus-protective effect of metformin was also influenced by gut microbiota.

A. muciniphila Exerted Anti-inflammatory and Mucus-protective Effects Similar to Those of Metformin

To explore whether *A. muciniphila* (akk)—which was enriched in the metformin group-exerts anti-inflammatory and mucus-barrier-protective effects like metformin, mice were administered with *A. muciniphila via* oral gavage (**Figure 7A**). *A. muciniphila* reduced weight loss (**Figures 7B,C**) and DAI scores (**Figure 7D**) in mice treated with DSS. Significant differences were found between the akk + DSS and DSS groups in colon length (**Figures 7E,F**) and histological scores (**Figures 7G,H**). Administration of *A. muciniphila* reduced the expression of TNF-α and IL1β, which were induced by DSS treatment (**Figure 7I**). In addition, *A. muciniphila* increased the number of goblet cells (**Figures 8A,B**) and the expression of mucin2 mucins (**Figures 8C,D**) compared with the DSS group, demonstrating that *A. muciniphila* has similar anti-inflammatory and mucus-protective effects.

DISCUSSION

The present study shows that metformin reduced colonic inflammation and protected against mucus barrier disruption along with an alteration of the gut microbiota during UC. Importantly, depletion of the gut microbiota partly abolished the anti-inflammatory and mucus-protective effects of metformin, indicating that metformin exerts its effects *via* the gut microbiota. Furthermore, administration of *A. muciniphila* alone, which was enriched in the metformin-treated group, to mice with DSS-induced UC mimicked the anti-inflammatory and mucus-protective effects of metformin. Based on these results the current study provides a critical understanding of the role of the gut microbiota in the anti-inflammatory and mucus-protective effects of metformin.

The results show that metformin mitigates the severity of mouse UC. Consistently, there is evidence showing that metformin exerts anti-inflammatory effects in mouse colitis: Di Fusco et al. reported that metformin reduced colonic inflammation by activating the AMP-activated protein kinase (AMPK) signaling pathway (Di Fusco et al., 2018); Lee et al. showed that metformin ameliorated colitis by suppressing STAT3 signaling *via* activating the AMPK signaling pathway (Lee et al., 2015). Deng et al. also has proved that metformin protected against intestinal barrier dysfunction *via* AMPKa1-dependent inhibition of JNK signaling activation and, thus, attenuated mouse colitis (Deng et al., 2018).

Accompanied by reduced colonic inflammation, metformin also restored the DSS-induced mucus barrier destruction by increasing the expression of mucin2, mucin1, mucin3, mucin4 and the number of goblet cells. Mucin1, mucin3 and mucin4 are transmembrane mucins. Their highly glycosylated extracellular domains can form a tight mesh structure and exert a barrier function. And their intracellular domains are involved in signaling pathways that regulate inflammation and cell differentiation (Putten and Strijbis, 2017). Mucin1 is upregulated in inflammation (Paone and Cani, 2020) which is consistent with the results of the present study. Mucin1 serves as a negative regulator of inflammation by suppressing the T helper 17-cell response (Nishida et al., 2012), toll-like receptor pathway and NLRP3 inflammasome complex activation (Dhar and McAuley, 2019), which may contribute to the anti-inflammatory effects of metformin in the current research. On the contrary, mucin3 and mucin4 are decreased during inflammation (Lindén et al., 2008). Mucin3 is negatively correlated with inflammation and dysbiosis levels (Algieri et al., 2021) *in vivo*, and can inhibit bacteria adherence *in vitro* (Pan et al., 2013). Kim et al. showed that mucin4 expression was decreased during DSS-induced colitis (Kim et al., 2019). However, contrary to Kim's and results of the present research, Song et al. found that mucin3 was increased in the azoxymethane (AOM)/DSS colon cancer mouse model (Song et al., 2018). These may be due to the different experimental models that were used. Consistently, Xue et al. showed that metformin treatment increased the number of goblet cells by promoting secretory cell lineage differentiation, and reduced colonic inflammation *via* AMPK activation in IL10-knockout mice (Xue et al., 2016). Shin et al. also found that metformin treatment increased the number of goblet cells in mice fed a high-fat diet (Shin et al., 2014). In the clinic, goblet cell depletion and mucus barrier disruption were common in UC patients (Swidsinski et al., 2007; Strugala et al., 2008; Van der Post et al., 2019). Furthermore, the abnormality of the mucus barrier plays an important role in the pathogenesis of UC. Previous studies have shown that the aberrant mucus barrier structure caused by Muc2 deficiency led to a more severe colonic inflammation in a mouse colitis model (Van der Sluis et al., 2006; Heazlewood et al., 2008; Petersson et al., 2010). In this study metformin also promoted the differentiation of goblet cells by increasing the expression of KLF4, MATH1 and SPDEF and decreasing that of HES1. Wnt and Notch signaling play a central role in the regulation of intestinal epithelium differentiation (van der Flier and Clevers, 2009). More specifically, Wnt signaling promotes secretory cells differentiation (i.e., goblet, Paneth and enteroendocrine cells) and Notch signaling is required for enterocyte development. KLF4, MATH1 and SPDEF, which are stimulated by the Wnt pathway and inhibited by the Notch pathway, are critical for goblet cells formation (Gregorieff et al., 2009; van der Flier and Clevers, 2009). HES1, on the contrary, is promoted by Notch signaling and inhibits goblet cells development by decreasing the expression of MATH1 (van der Flier and Clevers, 2009). These findings indicate that the mucus barrier may have a critical protective effect against UC and metformin exerts a mucus-protective effect in DSS-induced colitis. Thus, we conclude that the mucus-barrier-protective effects of metformin may be attributed to its anti-inflammatory effects in the colon.

Metformin is a widely used anti-diabetic treatment. The interaction between metformin and the gut microbiota has been reported in previous studies. The concentrations of

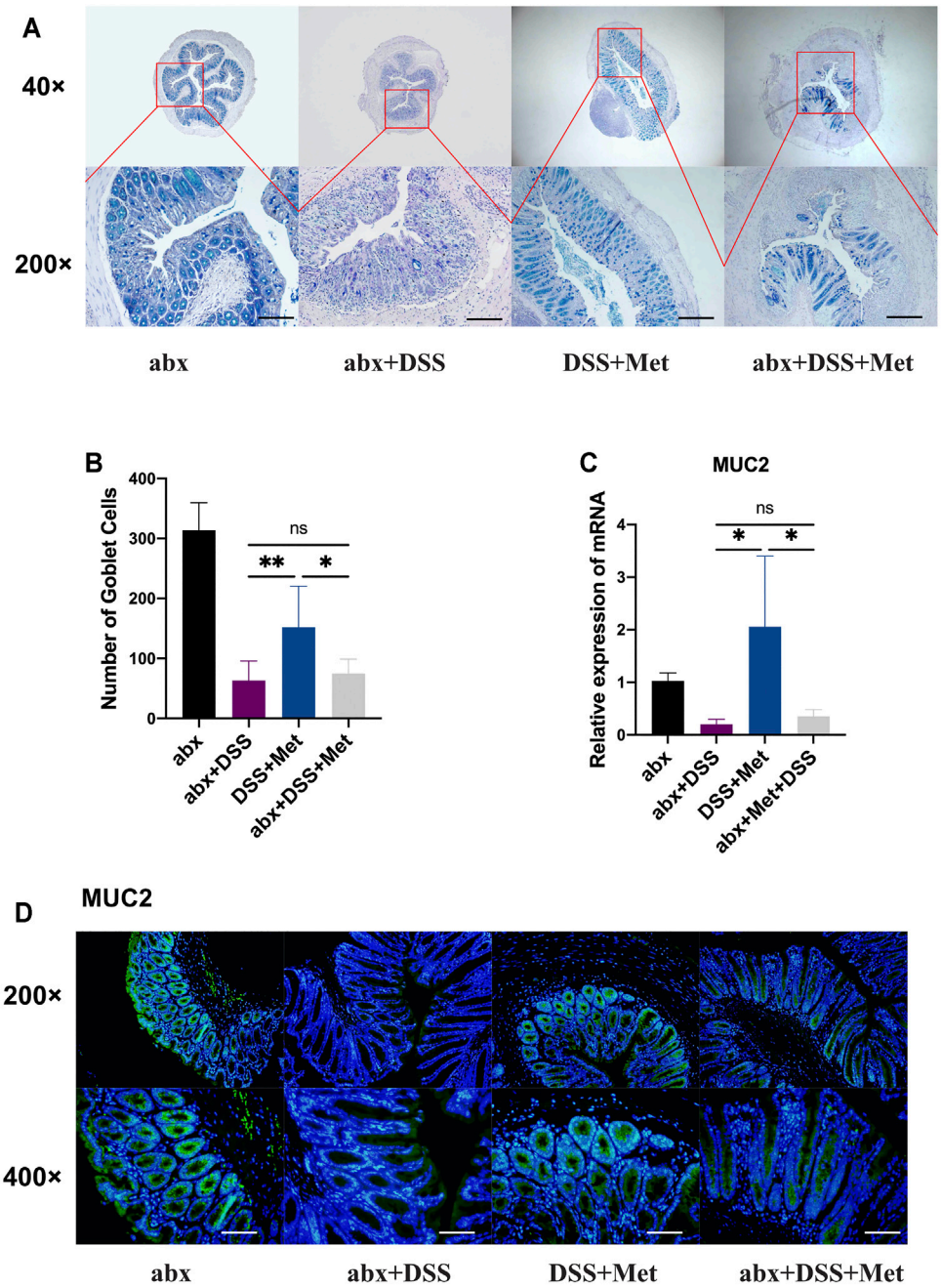


FIGURE 6 | Antibiotics abolish the mucus-protective effects of metformin. Alcian blue-periodic acid-Shiff (AB-PAS) staining (scale bars, 400 μm) (n = 5–7) **(A)** and count of goblet cells (n = 5–7) **(B)**, relative expression levels of mucin 2 (MUC2) (n = 3–4) **(C)**, and immunofluorescence assay of mucin2 protein in the mouse colon (scale bars, 200 μm) (n = 3) **(D)** and statistical comparison was made using an ANOVA test followed by Dunnett's *post-hoc* tests. *p < 0.05, **p < 0.01, ***p < 0.001.

metformin in the intestine are much higher than those in the plasma (Bailey et al., 2008). Shin et al. showed that metformin exerted its pharmacological effects by modulating the gut microbiota in a diet-induced diabetes mouse model (Shin et al., 2014). Similar results have been reported by Bauer et al. (Bauer et al., 2018). However, most of these studies focus on diabetes mellitus. Although the gut microbiota plays a critical role in the pathogenesis of UC (Zhang and Li, 2014; Testa et al., 2017; Ungaro et al., 2017), its role in the pharmacological effects of metformin on UC remains unclear. In the current study, we showed that metformin changed the structure of the gut microbiota. At the phylum level, the alteration of the gut microbiota in IBD remains controversial. Santoru et al. showed that the levels of Firmicutes and Proteobacteria were increased in IBD, whereas those of Bacteroidetes were decreased (Santoru et al., 2017). In contrast, Frank et al. reported that the

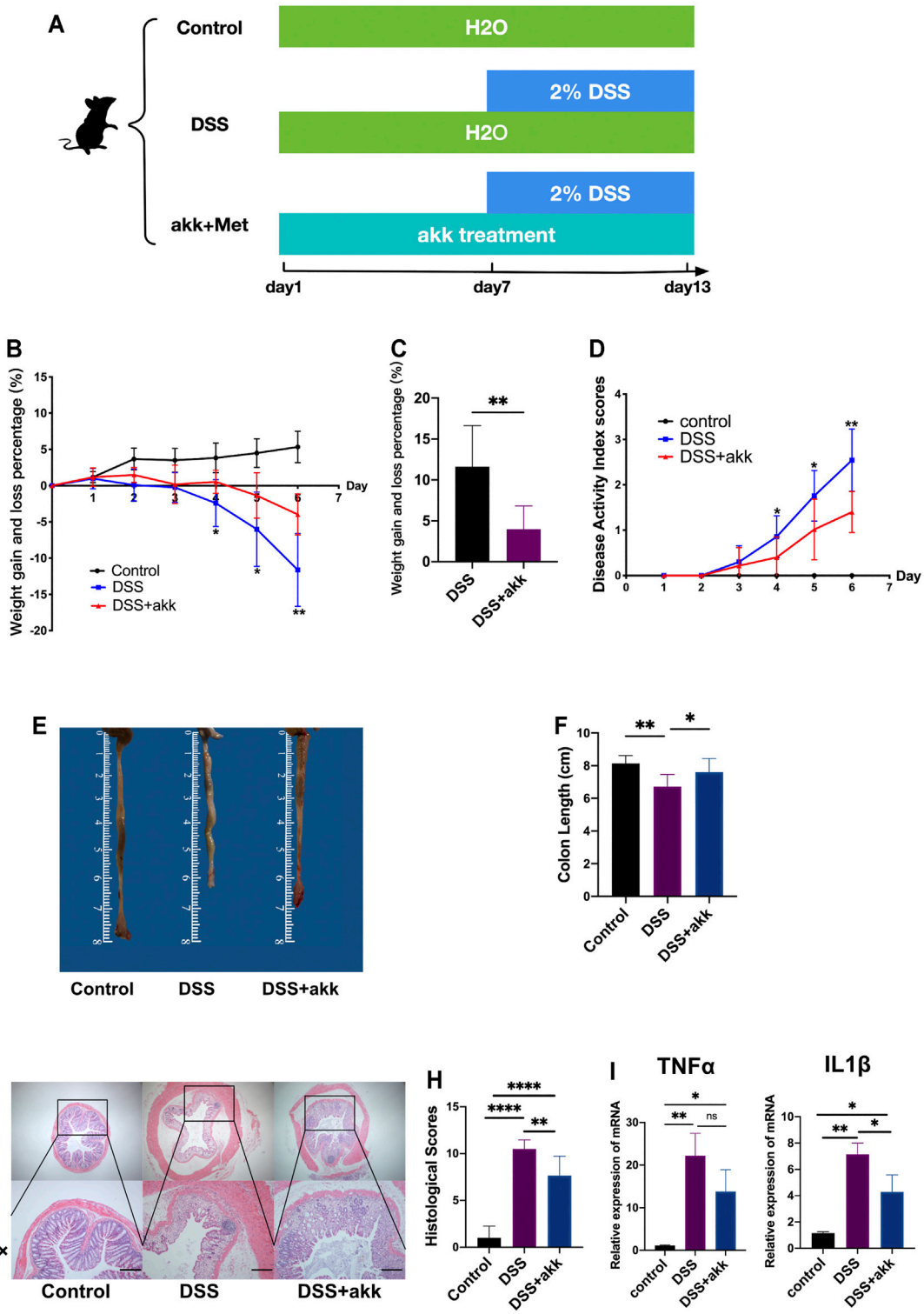


FIGURE 7 | *Akkermansia muciniphila* alleviates dextran sulfate sodium (DSS)-induced ulcerative colitis (UC) in mice. Flow chart of animal treatment **(A)**, weight loss and gain during DSS treatment (n = 6–14) **(B)** and weight loss percentage at day 6 (n = 6–14) **(C)**, disease activity index (DAI) scores (n = 6–14) **(D)**, representative pictures of the mouse colon (n = 6–14) **(E)**, colon length (n = 6–14) **(F)**, hematoxylin and eosin (HE) staining of colon tissue (scale bars, 400 μm) (n = 6–10) **(G)**, colon histological scores (n = 6–10) **(H)**, and RT-qPCR assay of tumor necrosis factor-α (TNF-α) and interleukin 1β (IL1β) in colon tissue (n = 2–6) **(I)** and statistical comparison was made using an ANOVA test followed by Tukey-Kramer *post-hoc* tests. *$p < 0.05$, **$p < 0.01$, ***$p < 0.001$.

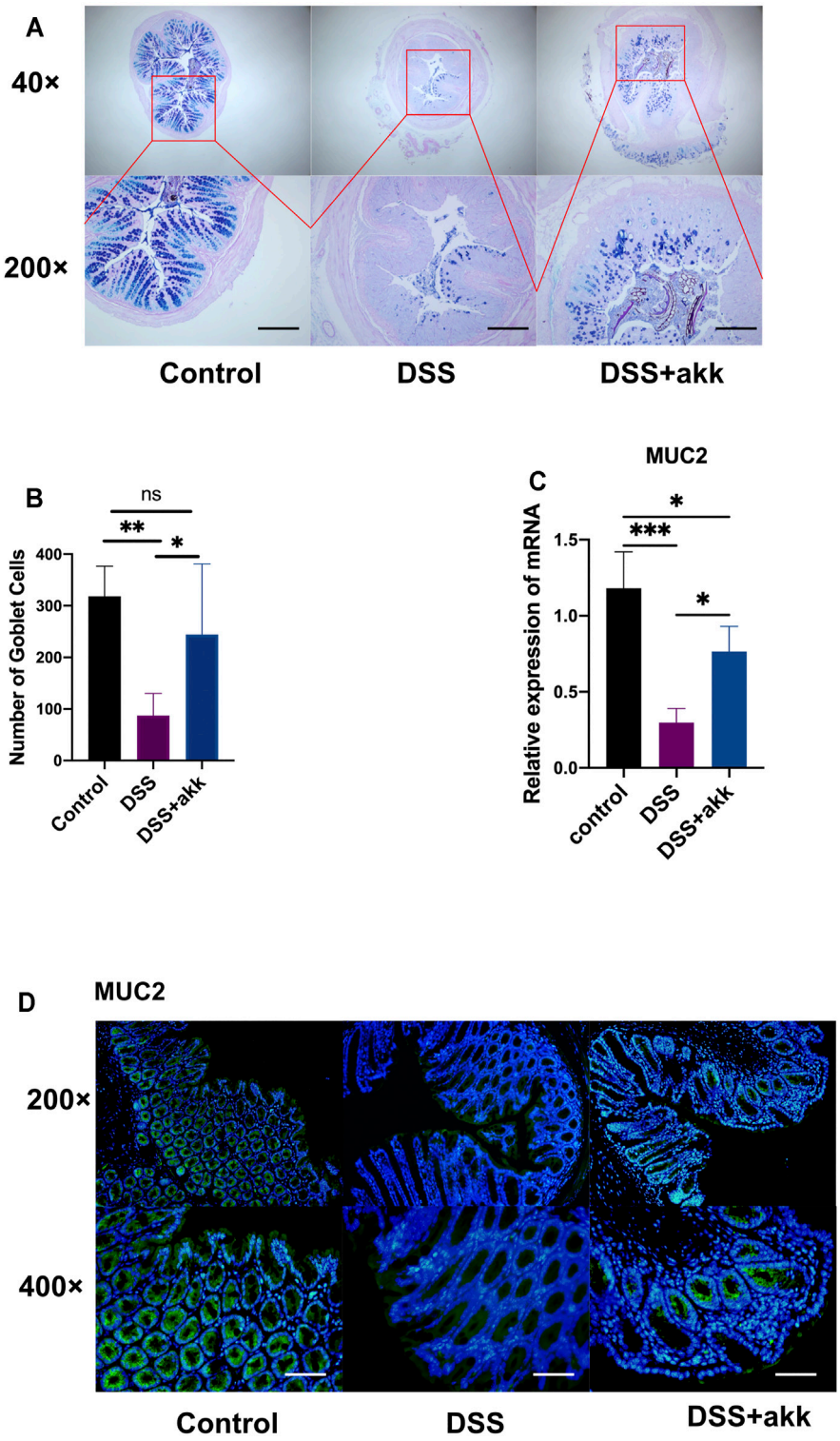


FIGURE 8 | *Akkermansia muciniphila* protects the mucus barrier in ulcerative colitis (UC). Alcian blue-periodic acid-Shiff (AB-PAS) staining of colon tissue (scale bars, 400 μm) (n = 6–7) **(A)** and count of goblet cells (n = 6–7) **(B)**, RT-qPCR assay of mucin 2 (MUC2) (n = 3–4) **(C)**, and immunofluorescence assay of mucin2 protein detection in colon tissue (scale bars, 200 μm) (n = 4) **(D)** and statistical comparison was made using an ANOVA test followed by Tukey-Kramer *post-hoc* tests. $^{*}p < 0.05$, $^{**}p < 0.01$, $^{***}p < 0.001$, ns, no significance.

levels of Firmicutes and Bacteroidetes were decreased in IBD (Frank et al., 2007). Furthermore, Walker et al. showed that Firmicutes levels were decreased while those of Bacteroidetes were increased in IBD (Walker et al., 2011). Although the results of these studies are contradictory, they are to a certain extent consistent with our results. Importantly, metformin treatment partly restored the structure of the gut microbiota which was altered by DSS treatment at the phylum level. Furthermore, similar results were found at the genus level. Moreover, metformin treatment increased the relative abundance of the genera *Bacteroides*, *Lactobacillus* and *Akkermansia*, which are considered to be potential probiotics (Shin et al., 2014; Bauer et al., 2018; Tan et al., 2019). Accordingly, the F/B ratio increased by DSS treatment was restored by metformin. F/B ratio is widely accepted as a significant marker for intestinal homeostasis-increased or decreased F/B ratio is regarded as dysbiosis (Mariat et al., 2009). Previous studies have shown that the F/B ratio was increased in the DSS model and decreased when colitis was alleviated (Rodríguez-Nogales et al., 2018; Yeo et al., 2020). Taken together, these findings suggest that metformin may exert its anti-inflammatory and mucus-protective effects *via* modulating the gut microbiota. To confirm the hypothesis, we administered an antibiotic cocktail to mice *via* oral gavage to deplete the gut microbiota and the anti-inflammatory and mucus-protective effects of metformin were partly abrogated. The gut microbiota also has an important role in shaping the mucus barrier (Jakobsson et al., 2015). In germ-free rats, the structure of mucus in the colon is impaired and the thickness is reduced (Schroeder, 2019). Bergström et al. reported that compared with germ-free mice, the presence of the microbiota increased the expression level of Muc2 (Bergström et al., 2012). Moreover, Troll et al. reported that the microbiota promoted the differentiation of goblet cells by activating the Notch signaling pathway (Troll et al., 2018).

Notably, in the current study, *A. muciniphila* was enriched only in the metformin-treated group. *A. muciniphila* is a gram-negative, anaerobic bacterium (Derrien, 2004) which has been reported to be decreased in patients with UC (Earley et al., 2019). Shin et al. have shown that metformin increased the levels of *A. muciniphila* in mice on a high-fat diet, improved glucose homeostasis, and, interestingly, increased the number of goblet cells (Shin et al., 2014). The present study found that administration of *A. muciniphila* reduced the colonic inflammation and protected the mucus barrier disruption in UC. Bian et al. reported that the severity of DSS-induced colitis in mice was relieved upon administration of A. muciniphila (Bian et al., 2019), whereas Kang et al. reported that extracellular vesicles derived from A. muciniphila protected against DSS-induced colitis (Kang et al., 2013). These results further confirmed that metformin exerted its therapeutic effects on UC *via* modulating the gut microbiota and increasing the levels of potential probiotics (e.g. *A. muciniphila*).

The doses of metformin that used in this study are similar to those in patients receiving metformin treatment. In clinical practice, patients typically receive 500–2000 mg metformin per day (Scarpello and Howlett, 2008). According to a method based on body surface area normalization (Nair and Jacob, 2016), the human equivalent dose of 400 mg/kg/d in mice is 32.43 mg/kg/day or 1946 mg per day for a 60 kg adult, which is within the recommended range. Although lower doses of metformin may have fewer side effects, DSS-treated mice receiving 100 mg/kg/day metformin (equivalent to 486 mg per day for human) or 200 mg/kg/day metformin (equivalent to 972 mg per day for human) had more weight loss and more severe DAI scores compared to those treated with DSS and 400 mg/kg/day metformin (**Supplementary Figure S2**) in the current experimental settings. The current study chose the dose of metformin at 400 mg/kg/day. However, further study may be needed to investigate the effects of lower doses of metformin especially from the aspects of adverse events.

The limitations of the present study should be also mentioned. First, instead of germ-free mice, which are inaccessible to our facility, antibiotic-treated mice were used to explore the role of the gut microbiota in the effects of metformin on UC. Compared with germ-free mice, which is considered to be the golden standard for the study of microbiota, antibiotic-treated models may be more inconsistent. However, an antibiotic-treated mouse model is a less expensive and more accessible alternative that has been widely used by many researchers for the study of microbiota (Kennedy et al., 2018). Second, although significant differences were not observed between conventional mice and antibiotic-treated mice in the DSS-induced colitis model (data not shown), other potential unknown effects of antibiotic treatment on DSS-induced colitis were not taken into account in the present study. DSS-induced colitis model is very popular in IBD research because of its rapidity, reproducibility and similarities to human IBD (Solomon et al., 2010; Chassaing et al., 2014). But the exact mechanism through which DSS initiates colitis is unknown (Solomon et al., 2010). Previous studies have successfully developed DSS-induced colitis in germ-free and antibiotic-treated "pseudo-germ-free" mice (Hudcovic et al., 2001; Hernández-Chirlaque et al., 2016; Gancarcikova et al., 2020), indicating that gut microbiota may not be indispensable for the initiation of DSS-induced colitis. In addition, the manifestations of DSS-induced colitis in antibiotic-treated "pseudo-germ-free" mice are similar to those in conventional mice. Hernández-Chirlaque et al. showed that antibiotic-treated "pseudo-germ-free" mice had similar manifestations of DSS-induced colitis in aspects of weight loss, colonic inflammation and mucosal barrier function (Hernández-Chirlaque et al., 2016). Accordingly, Gancarcikova et al. revealed that antibiotic-treated "pseudo-germ-free" mice did not have changes that could influence the initiation or development of DSS-induced colitis, and the inflammatory process developed during DSS treatment was mostly due to the exposure to DSS and its toxic action on compactness and integrity of mucosal barrier (Gancarcikova et al., 2020). So, it is a feasible solution to use the antibiotic cocktail to explore the role of gut microbiota in the therapeutic effects of metformin in the DSS model. Third, except for *A. muciniphila*, the roles of other bacteria were not investigated, which may influence the pharmacological effects of metformin on colonic inflammation and the mucus barrier. The

current study focused on the effects of *A. muciniphila* as it was enriched only in the metformin-treated group. However, these topics will be further investigated.

In summary, the results suggest that metformin alters the composition of the gut microbiota by increasing the levels of potential probiotics (e.g. *A. muciniphila*) and restoring the dysbiosis in mice with DSS-induced UC, which play a critical role in its anti-inflammatory and mucus-protective effects. The novelty of the current study is offering new insights into the role of the gut microbiota in the mucus-barrier-protective and anti-inflammatory effects of metformin, which indicates that metformin has the potential as a supplement or alternative to existing treatment for UC. It also provides evidence that A. muciniphila as a probiotic has potential benefits for the treatment of UC.

DATA AVAILABILITY STATEMENT

The data presented in the study are deposited in the NCBI Bioproject, accession number PRJNA760645.

ETHICS STATEMENT

All animal studies were carried out in accordance with the guidelines of the Southern Medical University Committee for Experimental Animals. And the protocols were approved by the Animal Experimental Ethics Committee of the Southern Medical University, China (L2018225).

AUTHOR CONTRIBUTIONS

All authors contributed to the study's conception and design. YC, HK, FL, WD, and ZL were involved in the study design. Material preparation, data collection, and analysis were performed by HK, FL, WD, ZL, SW, and PL. The first draft of the manuscript was written by HK and FL. All authors commented on previous versions of the manuscript. All authors read and approved the final manuscript.

FUNDING

This project is supported by the National Natural Science Foundation of China (No. 81770529); National S&T Megaprojects (2020ZX09201017); Guangdong gastrointestinal disease research center (No. 2017B020209003); and Guangdong gastrointestinal disease research center (No. 2017B030314037).

ACKNOWLEDGMENTS

The authors thank Xia Chen, Yuyan Xu, Qin Liu, Zhanjun Chen, Zhigang Hu, Yanfei Gao, and Qingmao Zhang for their general support.

SUPPLEMENTARY MATERIAL

The Supplementary Material for this article can be found online at: https://www.frontiersin.org/articles/10.3389/fphar.2021.726707/full#supplementary-material

REFERENCES

Algieri, F., Garrido-Mesa, J., Vezza, T., Rodríguez-Sojo, M. J., Rodríguez-Cabezas, M. E., Olivares, M., et al. (2021). Intestinal Anti-inflammatory Effects of Probiotics in DNBS-Colitis via Modulation of Gut Microbiota and microRNAs. *Eur. J. Nutr.* 60, 2537–2551. doi:10.1007/s00394-020-02441-8

Anisimov, V. N. (2013). Metformin: Do We Finally Have an Anti-aging Drug. *Cell Cycle* 12, 3483–3489. doi:10.4161/cc.26928

Bailey, C. J., Wilcock, C., and Scarpello, J. H. (2008). Metformin and the Intestine. *Diabetologia* 51, 1552–1553. doi:10.1007/s00125-008-1053-5

Bauer, P. V., Duca, F. A., Waise, T. M. Z., Rasmussen, B. A., Abraham, M. A., Dranse, H. J., et al. (2018). Metformin Alters Upper Small Intestinal Microbiota that Impact a Glucose-SGLT1-Sensing Glucoregulatory Pathway. *Cell Metab* 27, 101–117.e5. doi:10.1016/j.cmet.2017.09.019

Becker, S., Oelschlaeger, T. A., Wullaert, A., Vlantis, K., Pasparakis, M., Wehkamp, J., et al. (2013). Bacteria Regulate Intestinal Epithelial Cell Differentiation Factors Both In Vitro and In Vivo. *PLOS ONE* 8, e55620. doi:10.1371/journal.pone.0055620

Bergström, A., Kristensen, M. B., Bahl, M. I., Metzdorff, S. B., Fink, L. N., Frøkiaer, H., et al. (2012). Nature of Bacterial Colonization Influences Transcription of Mucin Genes in Mice during the First Week of Life. *BMC Res. Notes* 5, 402. doi:10.1186/1756-0500-5-402

Birchenough, G. M., Nyström, E. E., Johansson, M. E., and Hansson, G. C. (2016). A Sentinel Goblet Cell Guards the Colonic Crypt by Triggering Nlrp6-dependent Muc2 Secretion. *Science* 352, 1535–1542. doi:10.1126/science.aaf7419

Cameron, A. R., Morrison, V. L., Levin, D., Mohan, M., Forteath, C., Beall, C., et al. (2016). Anti-Inflammatory Effects of Metformin Irrespective of Diabetes Status. *Circ. Res.* 119, 652–665. doi:10.1161/CIRCRESAHA.116.308445

Chassaing, B., Aitken, J. D., Malleshappa, M., and Vijay-Kumar, M. (2014). Dextran Sulfate Sodium (DSS)-Induced Colitis in Mice. *Curr. Protoc. Immunol.* 104, 15–1415. doi:10.1002/0471142735.im1525s104

Chen, X., Li, P., Liu, M., Zheng, H., He, Y., Chen, M. X., et al. (2020). Gut Dysbiosis Induces the Development of Pre-eclampsia Through Bacterial Translocation. *Gut* 69, 513–522. doi:10.1136/gutjnl-2019-319101

Deng, J., Zeng, L., Lai, X., Li, J., Liu, L., Lin, Q., et al. (2018). Metformin Protects Against Intestinal Barrier Dysfunction via AMPKα1-dependent Inhibition of JNK Signalling Activation. *J. Cel. Mol. Med.* 22, 546–557. doi:10.1111/jcmm.13342

Derrien, M., Vaughan, E. E., Plugge, C. M., and de Vos, W. M. (2004). Akkermansia Muciniphila Gen. nov., Sp. nov., a Human Intestinal Mucin-Degrading Bacterium. *Int. J. Syst. Evol. Microbiol.* 54, 1469–1476. doi:10.1099/ijs.0.02873-0

Dhar, P., and McAuley, J. (2019). The Role of the Cell Surface Mucin MUC1 as a Barrier to Infection and Regulator of Inflammation. *Front. Cel. Infect. Microbiol.* 9, 117. doi:10.3389/fcimb.2019.00117

Di Fusco, D., Dinallo, V., Monteleone, I., Laudisi, F., Marafini, I., Franzè, E., et al. (2018). Metformin Inhibits Inflammatory Signals in the Gut by Controlling AMPK and P38 MAP Kinase Activation. *Clin. Sci. (Lond)* 132, 1155–1168. doi:10.1042/CS20180167

Earley, H., Lennon, G., Balfe, Á., Coffey, J. C., Winter, D. C., and O'Connell, P. R. (2019). The Abundance of Akkermansia Muciniphila and its Relationship with Sulphated Colonic Mucins in Health and Ulcerative Colitis. *Sci. Rep.* 9, 15683–15689. doi:10.1038/s41598-019-51878-3

Frank, D. N., St Amand, A. L., Feldman, R. A., Boedeker, E. C., Harpaz, N., and Pace, N. R. (2007). Molecular-phylogenetic Characterization of Microbial Community Imbalances in Human Inflammatory Bowel Diseases. *Proc. Natl. Acad. Sci. U S A.* 104, 13780–13785. doi:10.1073/pnas.0706625104

Gancarcikova, S., Lauko, S., Hrckova, G., Andrejcakova, Z., Hajduckova, V., Madar, M., et al. (2020). Innovative Animal Model of DSS-Induced Ulcerative Colitis in Pseudo Germ-free Mice. *Cells* 9, 2571. doi:10.3390/cells9122571

Gersemann, M., Becker, S., Kübler, I., Koslowski, M., Wang, G., Herrlinger, K. R., et al. (2009). Differences in Goblet Cell Differentiation Between Crohn's Disease and Ulcerative Colitis. *Differentiation* 77, 84–94. doi:10.1016/j.diff.2008.09.008

Gregorieff, A., Stange, D. E., Kujala, P., Begthel, H., van den Born, M., Korving, J., et al. (2009). The Ets-Domain Transcription Factor Spdef Promotes Maturation of Goblet and Paneth Cells in the Intestinal Epithelium. *Gastroenterology* 137, 1333–1345.e1-e3. doi:10.1053/j.gastro.2009.06.044

Heazlewood, C. K., Cook, M. C., Eri, R., Price, G. R., Tauro, S. B., Taupin, D., et al. (2008). Aberrant Mucin Assembly in Mice Causes Endoplasmic Reticulum Stress and Spontaneous Inflammation Resembling Ulcerative Colitis. *Plos Med.* 5, e54. doi:10.1371/journal.pmed.0050054

Hernández-Chirlaque, C., Aranda, C. J., Ocón, B., Capitán-Cañadas, F., Ortega-González, M., Carrero, J. J., et al. (2016). Germ-free and Antibiotic-Treated Mice Are Highly Susceptible to Epithelial Injury in DSS Colitis. *J. Crohns Colitis* 10, 1324–1335. doi:10.1093/ecco-jcc/jjw096

Hudcovic, T., Stěpánková, R., Cebra, J., and Tlaskalová-Hogenová, H. (2001). The Role of Microflora in the Development of Intestinal Inflammation: Acute and Chronic Colitis Induced by Dextran Sulfate in Germ-free and Conventionally Reared Immunocompetent and Immunodeficient Mice. *Folia Microbiol. (Praha)* 46, 565–572. doi:10.1007/BF02818004

Hur, K. Y., and Lee, M. S. (2015). New Mechanisms of Metformin Action: Focusing on Mitochondria and the Gut. *J. Diabetes Investig.* 6, 600–609. doi:10.1111/jdi.12328

Jakobsson, H. E., Rodríguez-Piñeiro, A. M., Schütte, A., Ermund, A., Boysen, P., Bemark, M., et al. (2015). The Composition of the Gut Microbiota Shapes the Colon Mucus Barrier. *EMBO Rep.* 16, 164–177. doi:10.15252/embr.201439263

Janda, J. M., and Abbott, S. L. (2007). 16S rRNA Gene Sequencing for Bacterial Identification in the Diagnostic Laboratory: Pluses, Perils, and Pitfalls. *J. Clin. Microbiol.* 45, 2761–2764. doi:10.1128/JCM.01228-07

Johansson, M. E., Gustafsson, J. K., Holmén-Larsson, J., Jabbar, K. S., Xia, L., Xu, H., et al. (2014). Bacteria Penetrate the Normally Impenetrable Inner Colon Mucus Layer in Both Murine Colitis Models and Patients with Ulcerative Colitis. *Gut* 63, 281–291. doi:10.1136/gutjnl-2012-303207

Johansson, M. E., and Hansson, G. C. (2011). Microbiology. Keeping Bacteria at a Distance. *Science* 334, 182–183. doi:10.1126/science.1213909

Kennedy, E. A., King, K. Y., and Baldridge, M. T. (2018). Mouse Microbiota Models: Comparing Germ-free Mice and Antibiotics Treatment as Tools for Modifying Gut Bacteria. *Front. Physiol.* 9, 1534. doi:10.3389/fphys.2018.01534

Kim, W.-K., Jang, Y. J., Seo, B., Han, D. H., Park, S., and Ko, G. (2019). Administration of Lactobacillus Paracasei Strains Improves Immunomodulation and Changes the Composition of Gut Microbiota Leading to Improvement of Colitis in Mice. *J. Funct. Foods* 52, 565–575. doi:10.1016/j.jff.2018.11.035

Knox, N. C., Forbes, J. D., Van Domselaar, G., and Bernstein, C. N. (2019). The Gut Microbiome as a Target for IBD Treatment: Are We There yet. *Curr. Treat. Options. Gastroenterol.* 17, 115–126. doi:10.1007/s11938-019-00221-w

Koh, S. J., Kim, J. M., Kim, I. K., Ko, S. H., and Kim, J. S. (2014). Anti-inflammatory Mechanism of Metformin and its Effects in Intestinal Inflammation and Colitis-Associated Colon Cancer. *J. Gastroenterol. Hepatol.* 29, 502–510. doi:10.1111/jgh.12435

Kühn, F., and Klar, E. (2015). Surgical Principles in the Treatment of Ulcerative Colitis. *Viszeralmedizin* 31, 246–250. doi:10.1159/000438894

Lee, S. Y., Lee, S. H., Yang, E. J., Kim, E. K., Kim, J. K., Shin, D. Y., et al. (2015). Metformin Ameliorates Inflammatory Bowel Disease by Suppression of the STAT3 Signaling Pathway and Regulation of the Between Th17/Treg Balance. *PLOS ONE* 10, e0135858. doi:10.1371/journal.pone.0135858

Leone, A., Di Gennaro, E., Bruzzese, F., Avallone, A., and Budillon, A. (2014). "New Perspective for an Old Antidiabetic Drug: Metformin as Anticancer Agent," in *Advances In Nutrition And Cancer Treatment and Research*. Editors V. Zappia, S. Panico, G. L. Russo, A. Budillon, and F. Della Ragione (Berlin, Heidelberg: Springer), 355–376. doi:10.1007/978-3-642-38007-5_21

Lindén, S. K., Florin, T. H. J., and McGuckin, M. A. (2008). Mucin Dynamics in Intestinal Bacterial Infection. *PLOS ONE* 3, e3952. doi:10.1371/journal.pone.0003952

M'koma, A. E. (2013). Inflammatory Bowel Disease: An Expanding Global Health Problem. *Clin. Med. Insights Gastroenterol.* 6, 33–47. doi:10.4137/CGast.S12731

Mariat, D., Firmesse, O., Levenez, F., Guimarães, V., Sokol, H., Doré, J., et al. (2009). The Firmicutes/Bacteroidetes Ratio of the Human Microbiota Changes with Age. *BMC Microbiol.* 9, 123–126. doi:10.1186/1471-2180-9-123

McCreight, L. J., Bailey, C. J., and Pearson, E. R. (2016). Metformin and the Gastrointestinal Tract. *Diabetologia* 59, 426–435. doi:10.1007/s00125-015-3844-9

Nair, A. B., and Jacob, S. (2016). A Simple Practice Guide for Dose Conversion Between Animals and Human. *J. Basic Clin. Pharm.* 7, 27–31. doi:10.4103/0976-0105.177703

Nishida, A., Lau, C. W., Zhang, M., Andoh, A., Shi, H. N., Mizoguchi, E., et al. (2012). The Membrane-Bound Mucin Muc1 Regulates T Helper 17-Cell Responses and Colitis in Mice. *Gastroenterology* 142, 865–874.e2. doi:10.1053/j.gastro.2011.12.036

Pan, Q., Tian, Y., Li, X., Ye, J., Liu, Y., Song, L., et al. (2013). Enhanced Membrane-Tethered Mucin 3 (MUC3) Expression by a Tetrameric Branched Peptide with a Conserved TFLK Motif Inhibits Bacteria Adherence. *J. Biol. Chem.* 288, 5407–5416. doi:10.1074/jbc.M112.408245

Paone, P., and Cani, P. D. (2020). Mucus Barrier, Mucins and Gut Microbiota: The Expected Slimy Partners. *Gut* 69, 2232–2243. doi:10.1136/gutjnl-2020-322260

Paramsothy, S., Kamm, M. A., Kaakoush, N. O., Walsh, A. J., van den Bogaerde, J., Samuel, D., et al. (2017). Multidonor Intensive Faecal Microbiota Transplantation for Active Ulcerative Colitis: A Randomised Placebo-Controlled Trial. *Lancet* 389, 1218–1228. doi:10.1016/S0140-6736(17)30182-4

Petersson, J., Schreiber, O., Hansson, G. C., Gendler, S. J., Velcich, A., Lundberg, J. O., et al. (2010). Importance and Regulation of the Colonic Mucus Barrier in a Mouse Model of Colitis. *Am. J. Physiol. Gastrointest. Liver Physiol.* 300, G327–G333. doi:10.1152/ajpgi.00422.2010

Png, C. W., Lindén, S. K., Gilshenan, K. S., Zoetendal, E. G., McSweeney, C. S., Sly, L. I., et al. (2010). Mucolytic Bacteria with Increased Prevalence in IBD Mucosa Augment In Vitro Utilization of Mucin by Other Bacteria. *Am. J. Gastroenterol.* 105, 2420–2428. doi:10.1038/ajg.2010.281

Rajilić-Stojanović, M., Shanahan, F., Guarner, F., and de Vos, W. M. (2013). Phylogenetic Analysis of Dysbiosis in Ulcerative Colitis During Remission. *Inflamm. Bowel Dis.* 19, 481–488. doi:10.1097/MIB.0b013e31827fec6d

Rena, G., and Lang, C. C. (2018). Repurposing Metformin for Cardiovascular Disease. *Circulation* 137, 422–424. doi:10.1161/CIRCULATIONAHA.117.031735

Rio, D. C., Ares, M., Hannon, G. J., and Nilsen, T. W. (2010). Purification of RNA Using TRIzol (TRI Reagent). *Cold Spring Harb. Protoc.* 2010, 5439. doi:10.1101/pdb.prot5439

Robertson, D., Savage, K., Reis-Filho, J. S., and Isacke, C. M. (2008). Multiple Immunofluorescence Labelling of Formalin-Fixed Paraffin-Embedded (FFPE) Tissue. *BMC Cel Biol* 9, 13. doi:10.1186/1471-2121-9-13

Rodríguez-Nogales, A., Algieri, F., Garrido-Mesa, J., Vezza, T., Utrilla, M. P., Chueca, N., et al. (2018). The Administration of *Escherichia coli* Nissle 1917 Ameliorates Development of DSS-Induced Colitis in Mice. *Front. Pharmacol.* 9, 468. doi:10.3389/fphar.2018.00468

Saisho, Y. (2015). Metformin and Inflammation: Its Potential beyond Glucose-Lowering Effect. *Endocr. Metab. Immune Disord. Drug Targets* 15, 196–205. doi:10.2174/1871530315666150316124019

Santoru, M. L., Piras, C., Murgia, A., Palmas, V., Camboni, T., Liggi, S., et al. (2017). Cross Sectional Evaluation of the Gut-Microbiome Metabolome Axis in an Italian Cohort of IBD Patients. *Sci. Rep.* 7, 9523. doi:10.1038/s41598-017-10034-5

Scarpello, J. H., and Howlett, H. C. (2008). Metformin Therapy and Clinical Uses. *Diab. Vasc. Dis. Res.* 5, 157–167. doi:10.3132/dvdr.2008.027

Schroeder, B. O. (2019). Fight Them or Feed Them: How the Intestinal Mucus Layer Manages the Gut Microbiota. *Gastroenterol. Rep. (Oxf)* 7, 3–12. doi:10.1093/gastro/goy052

Shao, Y., Ding, R., Xu, B., Hua, R., Shen, Q., He, K., et al. (2017). Alterations of Gut Microbiota After Roux-En-Y Gastric Bypass and Sleeve Gastrectomy in Sprague-Dawley Rats. *Obes. Surg.* 27, 295–302. doi:10.1007/s11695-016-2297-7

Shen, J., Zuo, Z. X., and Mao, A. P. (2014). Effect of Probiotics on Inducing Remission and Maintaining Therapy in Ulcerative Colitis, Crohn's Disease, and Pouchitis: Meta-Analysis of Randomized Controlled Trials. *Inflamm. Bowel Dis.* 20, 21–35. doi:10.1097/01.MIB.0000437495.30052.be

Shen, Z. H., Zhu, C. X., Quan, Y. S., Yang, Z. Y., Wu, S., Luo, W. W., et al. (2018). Relationship Between Intestinal Microbiota and Ulcerative Colitis: Mechanisms and Clinical Application of Probiotics and Fecal Microbiota Transplantation. *World J. Gastroenterol.* 24, 5–14. doi:10.3748/wjg.v24.i1.5

Shin, N. R., Lee, J. C., Lee, H. Y., Kim, M. S., Whon, T. W., Lee, M. S., et al. (2014). An Increase in the Akkermansia Spp. Population Induced by Metformin Treatment Improves Glucose Homeostasis in Diet-Induced Obese Mice. *Gut* 63, 727–735. doi:10.1136/gutjnl-2012-303839

Solomon, L., Mansor, S., Mallon, P., Donnelly, E., Hoper, M., Loughrey, M., et al. (2010). The Dextran Sulphate Sodium (DSS) Model of Colitis: An Overview. *Comp. Clin. Pathol.* 19, 235–239. doi:10.1007/s00580-010-0979-4

Song, C. H., Kim, N., Sohn, S. H., Lee, S. M., Nam, R. H., Na, H. Y., et al. (2018). Effects of 17β-Estradiol on Colonic Permeability and Inflammation in an Azoxymethane/Dextran Sulfate Sodium-Induced Colitis Mouse Model. *Gut Liver* 12, 682–693. doi:10.5009/gnl18221

Strugala, V., Dettmar, P. W., and Pearson, J. P. (2008). Thickness and Continuity of the Adherent Colonic Mucus Barrier in Active and Quiescent Ulcerative Colitis and Crohn's Disease. *Int. J. Clin. Pract.* 62, 762–769. doi:10.1111/j.1742-1241.2007.01665.x

Swidsinski, A., Loening-Baucke, V., Theissig, F., Engelhardt, H., Bengmark, S., Koch, S., et al. (2007). Comparative Study of the Intestinal Mucus Barrier in Normal and Inflamed Colon. *Gut* 56, 343–350. doi:10.1136/gut.2006.098160

Tan, H., Zhai, Q., and Chen, W. (2019). Investigations of Bacteroides Spp. Towards Next-Generation Probiotics. *Food Res. Int.* 116, 637–644. doi:10.1016/j.foodres.2018.08.088

Testa, A., Castiglione, F., Nardone, O. M., and Colombo, G. L. (2017). Adherence in Ulcerative Colitis: An Overview. *Patient Prefer Adherence* 11, 297–303. doi:10.2147/PPA.S127039

Troll, J. V., Hamilton, M. K., Abel, M. L., Ganz, J., Bates, J. M., Stephens, W. Z., et al. (2018). Microbiota Promote Secretory Cell Determination in the Intestinal Epithelium by Modulating Host Notch Signaling. *Development* 145, dev155317. doi:10.1242/dev.155317

Ungaro, R., Mehandru, S., Allen, P. B., Peyrin-Biroulet, L., and Colombel, J. F. (2017). Ulcerative Colitis. *Lancet* 389, 1756–1770. doi:10.1016/S0140-6736(16)32126-2

van der Flier, L. G., and Clevers, H. (2009). Stem Cells, Self-Renewal, and Differentiation in the Intestinal Epithelium. *Annu. Rev. Physiol.* 71, 241–260. doi:10.1146/annurev.physiol.010908.163145

van der Post, S., Jabbar, K. S., Birchenough, G., Arike, L., Akhtar, N., Sjovall, H., et al. (2019). Structural Weakening of the Colonic Mucus Barrier Is an Early Event in Ulcerative Colitis Pathogenesis. *Gut* 68, 2142–2151. doi:10.1136/gutjnl-2018-317571

Van der Sluis, M., De Koning, B. A., De Bruijn, A. C., Velcich, A., Meijerink, J. P., Van Goudoever, J. B., et al. (2006). Muc2-Deficient Mice Spontaneously Develop Colitis, Indicating that MUC2 Is Critical for Colonic Protection. *Gastroenterology* 131, 117–129. doi:10.1053/j.gastro.2006.04.020

van Putten, J. P. M., and Strijbis, K. (2017). Transmembrane Mucins: Signaling Receptors at the Intersection of Inflammation and Cancer. *J. Innate Immun.* 9, 281–299. doi:10.1159/000453594

Vich Vila, A., Imhann, F., Collij, V., Jankipersadsing, S. A., Gurry, T., Mujagic, Z., et al. (2018). Gut Microbiota Composition and Functional Changes in Inflammatory Bowel Disease and Irritable Bowel Syndrome. *Sci. Transl. Med.* 10, eaap8914. doi:10.1126/scitranslmed.aap8914

Walker, A. W., Sanderson, J. D., Churcher, C., Parkes, G. C., Hudspith, B. N., Rayment, N., et al. (2011). High-throughput Clone Library Analysis of the Mucosa-Associated Microbiota Reveals Dysbiosis and Differences Between Inflamed and Non-inflamed Regions of the Intestine in Inflammatory Bowel Disease. *BMC Microbiol.* 11, 7. doi:10.1186/1471-2180-11-7

Wang, Z., Li, R., Tan, J., Peng, L., Wang, P., Liu, J., et al. (2015). Syndecan-1 Acts in Synergy with Tight Junction Through Stat3 Signaling to Maintain Intestinal Mucosal Barrier and Prevent Bacterial Translocation. *Inflamm. Bowel Dis.* 21, 1894–1907. doi:10.1097/MIB.0000000000000421

Xue, Y., Zhang, H., Sun, X., and Zhu, M.-J. (2016). Metformin Improves Ileal Epithelial Barrier Function in Interleukin-10 Deficient Mice. *PLoS ONE* 11, e0168670. doi:10.1371/journal.pone.0168670

Yeo, S., Park, H., Seo, E., Kim, J., Kim, B. K., Choi, I. S., et al. (2020). Anti-Inflammatory and Gut Microbiota Modulatory Effect of Lactobacillus Rhamnosus Strain LDTM 7511 in a Dextran Sulfate Sodium-Induced Colitis Murine Model. *Microorganisms* 8, 845. doi:10.3390/microorganisms8060845

Yin, J., Liao, S. X., He, Y., Wang, S., Xia, G. H., Liu, F. T., et al. (2015). Dysbiosis of Gut Microbiota with Reduced Trimethylamine-N-Oxide Level in Patients with Large-Artery Atherosclerotic Stroke or Transient Ischemic Attack. *J. Am. Heart Assoc.* 4, e002699. doi:10.1161/JAHA.115.002699

Zhai, R., Xue, X., Zhang, L., Yang, X., Zhao, L., and Zhang, C. (2019). Strain-Specific Anti-inflammatory Properties of Two Akkermansia Muciniphila Strains on Chronic Colitis in Mice. *Front. Cel. Infect. Microbiol.* 9, 239. doi:10.3389/fcimb.2019.00239

Zhang, M. (2019). Tu1852 – Metformin Ameliorated Inflammatory Bowel Disease by Enhancing Akkermansia Muciniphila. *Gastroenterology* 156, S1148. doi:10.1016/S0016-5085(19)39838-5

Zhang, Y. Z., and Li, Y. Y. (2014). Inflammatory Bowel Disease: Pathogenesis. *World J. Gastroenterol.* 20, 91–99. doi:10.3748/wjg.v20.i1.91

Zhou, Y., Xu, Z. Z., He, Y., Yang, Y., Liu, L., Lin, Q., et al. (2018). Gut Microbiota Offers Universal Biomarkers Across Ethnicity in Inflammatory Bowel Disease Diagnosis and Infliximab Response Prediction. *mSystems* 3, 1–14. doi:10.1128/mSystems.00188-17

Conflict of Interest: The authors declare that the research was conducted in the absence of any commercial or financial relationships that could be construed as a potential conflict of interest.

Publisher's Note: All claims expressed in this article are solely those of the authors and do not necessarily represent those of their affiliated organizations, or those of the publisher, the editors and the reviewers. Any product that may be evaluated in this article, or claim that may be made by its manufacturer, is not guaranteed or endorsed by the publisher.

Copyright © 2021 Ke, Li, Deng, Li, Wang, Lv and Chen. This is an open-access article distributed under the terms of the Creative Commons Attribution License (CC BY). The use, distribution or reproduction in other forums is permitted, provided the original author(s) and the copyright owner(s) are credited and that the original publication in this journal is cited, in accordance with accepted academic practice. No use, distribution or reproduction is permitted which does not comply with these terms.

frontiers in Pharmacology

SYSTEMATIC REVIEW
published: 03 November 2021
doi: 10.3389/fphar.2021.732496

The Effects of Vitamin D Supplementation on Anthropometric and Biochemical Indices in Patients With Non-alcoholic Fatty Liver Disease: A Systematic Review and Meta-analysis

*Shahla Rezaei[1,2], Reza Tabrizi[3], Peyman Nowrouzi-Sohrabi[2,4], Mohammad Jalali[5], Mojtaba Shabani-Borujeni[6], Shayan Modaresi[2], Maryam Gholamalizadeh[7] and Saeid Doaei[8]**

[1]Nutrition Research Center, School of Nutrition and Food Sciences, Shiraz University of Medical Sciences, Shiraz, Iran, [2]Student Research Committee, Shiraz University of Medical Sciences, Shiraz, Iran, [3]Non-Communicable Diseases Research Center, Fasa University of Medical Sciences, Fasa, Iran, [4]Department of Biochemistry, School of Medicine, Shiraz University of Medical Sciences, Shiraz, Iran, [5]Nutrition Research Center, Student Research Committee, Shiraz University of Medical Sciences, Shiraz, Iran, [6]Department of Clinical Pharmacy, Faculty of Pharmacy, Shiraz University of Medical Sciences, Shiraz, Iran, [7]Student Research Committee, Cancer Research Center, Shahid Beheshti University of Medical Sciences, Tehran, Iran, [8]Research Center of Health and Enviroment, School of Health, Guilan University of Medical Sciences, Rasht, Iran

Background: Vitamin D was reported to be associated with non–alcoholic fatty liver disease (NAFLD). This systematic review and meta–analysis aimed to investigate the effects of the vitamin D supplementation on anthropometric and biochemical indices in patient with NAFLD.

Methods: PubMed, Web of science, Scopus, and Embase databases were explored to identify all randomized controlled trial (RCT) investigating the effects of vitamin D supplementation on anthropometric and biochemical indices in patients with NAFLD. A random–effects model was used to pool weighted mean difference (WMD) and corresponding 95% confidence intervals (CIs). The statistical heterogeneity among the studies was assessed using I2 statistic (high ≥ 50%, low < 50%) and Cochran's Q–test.

Results: Sixteen RCTs were included in this meta–analysis. The results identified that high–density lipoprotein–cholesterol (HDL–C) level significantly increased following vitamin D supplementation (P = 0.008). Vitamin D reduced body weight (P = 0.007), body mass index (P = 0.002), waist circumstance (WC) (P = 0.02), serum alanine transaminase (ALT) (P = 0.01), fasting blood sugar (FBS) (P = 0.01), homeostatic model assessment for insulin resistance (HOMA–IR) (P = 0.004), and calcium (P = 0.01). No significant changes were found on body fat, triglyceride (TG), total cholesterol, low–density lipoprotein–cholesterol

Abbreviations: NAFLD, with non-alcoholic fatty liver disease; BMI, body mass index; WC, waist circumstance; ALT, alanine transaminase; FBS, fasting blood sugar; HOMA-IR, homeostatic model assessment for insulin resistance; TG: triglyceride.

OPEN ACCESS

Edited by:
Wolfgang Richard Stremmel, Medical Center Baden-Baden, Germany

Reviewed by:
Yu Zhao, Shanghai University of Traditional Chinese Medicine, China
Guang Chen, Huazhong University of Science and Technology, China

***Correspondence:**
Saeid Doaei
sdoaee@yahoo.com

Specialty section:
This article was submitted to Gastrointestinal and Hepatic Pharmacology, a section of the journal Frontiers in Pharmacology

Received: *29 June 2021*
Accepted: *06 October 2021*
Published: *03 November 2021*

Citation:
Rezaei S, Tabrizi R, Nowrouzi-Sohrabi P, Jalali M, Shabani-Borujeni M, Modaresi S, Gholamalizadeh M and Doaei S (2021) The Effects of Vitamin D Supplementation on Anthropometric and Biochemical Indices in Patients With Non-alcoholic Fatty Liver Disease: A Systematic Review and Meta-analysis. Front. Pharmacol. 12:732496. doi: 10.3389/fphar.2021.732496

(LDL–C), aspartate transaminase, alkaline phosphatase, gamma–glutamyl transferase, and adiponectin following vitamin D supplementation.

Conclusion: Vitamin D had significant effects on anthropometric and biochemical indices including HDL–C, body weight, BMI, WC, serum ALT, serum FBS, HOMA–IR, and calcium. Vitamin D supplementation can be considered as an effective strategy in management of patients with NAFLD.

Systematic Review Registration: [website], identifier [registration number]

Keywords: vitamin D, NAFLD, liver enzyme, anthropometry, biochemical indices

BACKGROUND

Non-alcoholic fatty liver disease (NAFLD) is considered to be the most common cause of chronic liver disorders (Younossi, 2019). NAFLD includes a wide range of liver diseases such as fibrosis, cirrhosis and non–alcoholic hepatitis (Petta et al., 2016; Morvaridzadeh et al., 2021). The prevalence of NAFLD is about 20% in general population and about 70–90% in patients with type 2 diabetes (Tolman et al., 2007; Chalasani et al., 2012). The main causes of NAFLD are obesity, excessive dietary fat intake, insulin resistance, and dyslipidemia (Ludwig et al., 1980). Over the past few decades, various pharmacological and nutritional interventions have been assessed to treat NAFLD, but none indicated significant improvements. Currently, no medically approved drugs are available for NAFLD (Del Ben et al., 2014). Weight loss and nutritional interventions are considered standard treatments for NAFLD. Insulin resistance increases the rate of adipose tissue lipolysis and the flow of free fatty acids to the liver cell. Hyperglycemia also causes lipid–related changes in the liver cells by increasing lipogenesis while blocking fatty acid oxidation (FAO) and lipid transport in the liver (Kleiner et al., 2005; Schwimmer et al., 2005).

Vitamin D plays an important role in reducing insulin resistance, obesity, cardiovascular risk, prediabetes, metabolic syndrome, cancer, and cardiovascular diseases (CVD_s) (Sepidarkish et al., 2019; Gholamalizadeh et al., 2020). Low serum level of 25-hydroxyvitamin D [25 (OH) D] is reported to be a risk factor for NAFLD disease (Forouhi et al., 2008; Sepidarkish et al., 2019). Vitamin D hypovitaminosis is associated with the severity and incidence of NAFLD in patients with normal liver enzymes. Vitamin D can affect the liver function through the vitamin D receptor (VDR). VDR is naturally present in the liver cells and its higher expression can reduce inflammation in chronic liver diseases (Benetti et al., 2018). Vitamin D also has anti–fibrotic, proliferative, and inflammatory effects on the liver. Some studies on the effects of vitamin D on anthropometric and biochemical indices reported that vitamin D was associated with body weight, fasting blood sugar (FBS), homeostatic model assessment for insulin resistance (HOMA–IR), glucose homeostasis, insulin resistance, high–density lipoprotein–cholesterol (HDL-C), low-density lipoprotein-cholesterol (LDL-C), triglycerides (TG), total cholesterol (TC), liver enzyme, and adiponectin (Sarathy et al., 2015; Foroughi et al., 2016; Doaei et al., 2019). A recent systematic review also reported that vitamin D improves the level of inflammatory mediators in patients with nonalcoholic fatty liver disease, but has no effect on anthropometric and glycemic indexes (Hariri and Zohdi, 2019; Mehrdad et al., 2020). However, the findings on the effects of vitamin D on NAFLD were contradictory (Sharifi et al., 2014; Sarathy et al., 2015). Therefore, this study aimed to investigate the effect of Vitamin D supplementation on anthropometric and biochemical indices in patient with NAFLD.

METHODS

Preferred reporting items for systematic reviews and meta–analyses (PRISMA) (Moher et al., 2009) was used to demonstrate the process of study selection (**Figure 1**).

Search Strategy

Two independent researchers performed the process of the systematic search using the online databases such as PubMed, embase, Scopus, Web of Science, and Cochrane Library for publications from 1980 up to 2021 on the effects of vitamin D supplementation on anthropometric and biochemical indices in patients with NAFLD, without considering any restriction on the language to detect the relevant citations. The PubMed search strategy was improved by consulting with an epidemiologist and was designed as a combination of the following search terms: "Vitamin D OR Cholecalciferol OR Calciol OR "Vitamin D 3" OR "Vitamin D3" OR Cholecalciferols OR Hydroxycholecalciferols OR "Hydroxyvitamins D″ OR Hydroxycholecalciferol OR Calcifediol OR "25–Hydroxyvitamin D 3" OR "25 Hydroxyvitamin D 3" OR "25–Hydroxycholecalciferol" OR Calcidiol OR Hydroxycholecalciferol OR Dedrogyl OR Hidroferol OR Calderol OR Dihydroxycholecalciferols OR "Dihydroxyvitamins D" OR "24,25–Dihydroxyvitamin D 3" OR Dihydroxyvitamin OR "24,25-Dihydroxyvitamin" OR "24,25-Dihydroxycholecalciferol" OR Dihydroxyvitamin OR Calcitriol OR "1 alpha,25-Dihydroxyvitamin" OR "1,25-Dihydroxyvitamin" OR "1,25-Dihydroxyvitamin" OR "1 alpha,25-Dihydroxycholecalciferol" OR "1,25–Dihydroxycholecalciferol" OR Dihydroxycholecalciferol OR Bocatriol OR Calcijex OR Decostriol OR MC1288 OR "MC–1288" OR "MC 1288" OR Osteotriol OR Renatriol OR Rocaltrol OR Silkis OR Sitriol OR Soltriol OR Tirocal" AND "Fatty Liver" OR

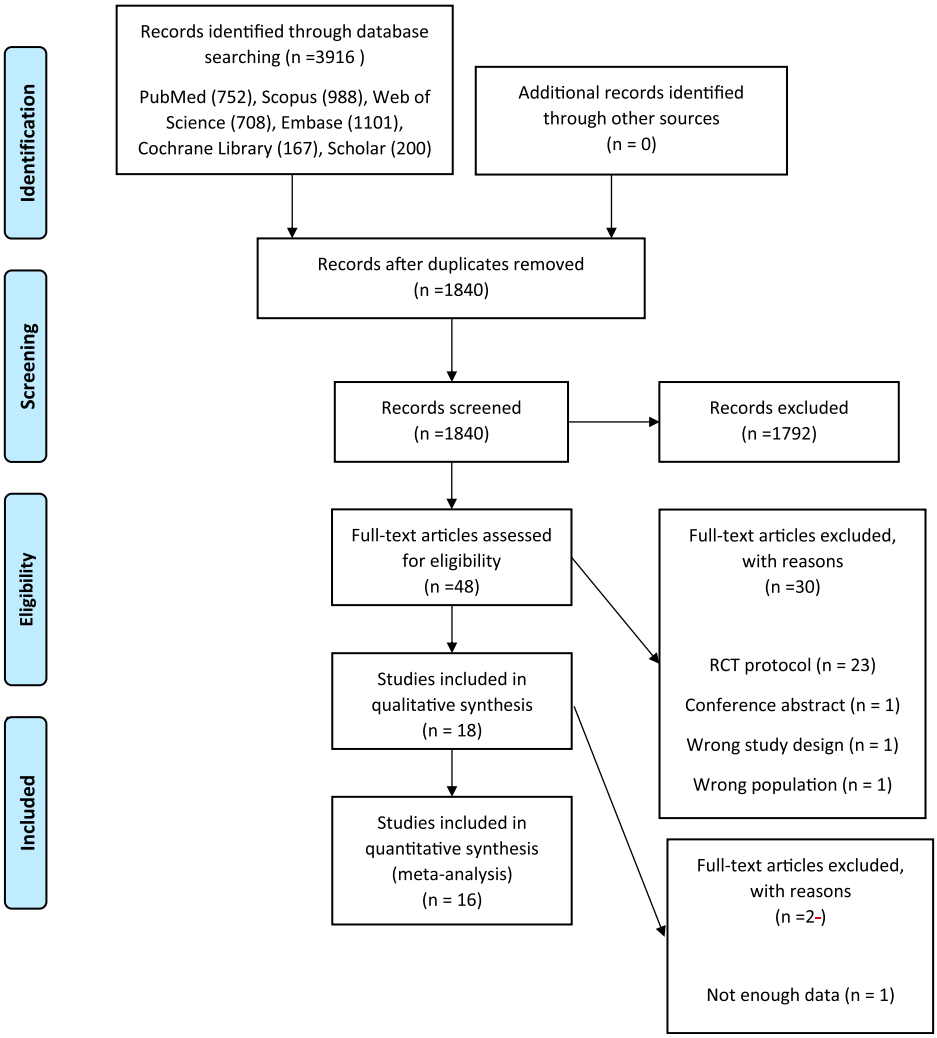


FIGURE 1 | Flow chart of the literature search strategy and study selection.

"Fatty Liver" OR Steatohepatitis OR Steatohepatitides OR "Steatosis of Liver" OR "Visceral Steatosis" OR Steatoses OR Steatosis OR "Visceral Steatoses" OR "Liver Steatosis" OR "Liver Steatoses" OR "Non–alcoholic Fatty Liver Disease" OR "Non–alcoholic Fatty Liver Disease" OR "Nonalcoholic Fatty Liver Disease" OR NAFLD OR "Nonalcoholic Fatty Liver Disease" OR Nonalcoholic OR "Nonalcoholic" OR "Nonalcoholic Fatty" OR "Non–alcoholic Fatty" OR "Nonalcoholic Fatty Liver" OR "Nonalcoholic Fatty Livers" OR NASH OR "Nonalcoholic Steatohepatitis" OR "Nonalcoholic Steatohepatitides" OR Steatohepatitis OR "liver cirrhosis" OR cirrhosis OR cirrhosis. To improve the search strategy, the wild–card term "*" was implicated and the reference lists of relevant articles were hand–scanned. Any doubts were resolved through discussing with the corresponding author.

Inclusion and Exclusion Criteria

Based on PICOS criteria, the aim of the present review study on patients with NAFLD (as population) was to evaluate the effect of vitamin D supplementation (as intervention) compared with placebo (as comparator) on anthropometric and biochemical outcomes (as outcome) in randomized interventional trials (as study design). Two independent reviewers initiated the assessment process of the collected papers and following inclusion criteria were considered (Younossi, 2019): randomized controlled trials (RCTs) with parallel design (Petta et al., 2016), studies that assessed the effects of vitamin D supplementation on patients with NAFLD. The exclusion criteria were (Younossi, 2019) being experimental study (Petta et al., 2016), lacking the essential data, for example, non–extractable or unconvertable data (Morvaridzadeh et al., 2021), studies without a suitable control group (Chalasani et al., 2012), trials with combined supplementation of nutrients or/and medicines besides vitamin D and also (Tolman et al., 2007) unpublished data, grey literature, conference abstracts, book chapters, and brief reports. The corresponding author was involved to solve disagreements.

Data Extraction

Following data were extracted from the included trials by two independent investigators: first authors' last name, publication date, country of study, study design, participants' characteristics, dosage of the supplement, intervention duration, quality of trials, mean changes and standard deviations (SDs) for each outcomes in pre–treatment and post–treatment. The third reviewer solved disagreements.

Risk of Bias Assessment

Two independent reviewers were assigned to qualify the included RCTs and explore the potential risk of bias for the following domains using the Cochrane Risk of Bias Tool: random sequence generation, allocation concealment, blinding of participants and personnel, blinding of outcome assessment, incomplete outcome data, and selective outcome reporting and other biases. "low", "high" or "unclear" terms were used to grade each item (Higgins et al., 2011).

Each question was answered as low risk of bias (score = 1), high risk of bias (score = −1), or unclear (score = 0). Disagreements was resolved by the third author. Scores were summed and studies with scores −6–0, 1–3 and 4–6 considered as low, medium and high quality, respectively (**Table 3**).

Statistical Analysis

A meta–analysis was performed using *STATA* software v13 (StataCorp, Texas) and a random–effects model was used to pool weighted mean difference (WMD) and corresponding 95% confidence intervals (CIs). The statistical heterogeneity among the studies was assessed using I^2 statistic (high ≥50%, low <50%) and Cochran's Q–test (Higgins et al., 2019). In presence of high inter–study heterogeneity, a random–effects meta–regression was performed to find its potential sources. Subgroup analysis was done based on country (Iran vs. other), duration of treatment (>12 weeks, ≤ 12 weeks), and dosage (>25,000 IU/day, ≤ 25,000 IU/day). Mean changes of the interested outcomes and the relevant SDs were obtained executing following formulas, respectively: (mean at post intervention–mean at baseline), SD = $\sqrt{([SD2–baseline + SD^2–post] – [2r \times SD–baseline \times SD–post])}$, assuming correlation coefficient (r) as 0.5 (Higgins et al., 2019). Sensitivity analysis was planned to assess the impact of each study on the pooled results by removing one study in a turn (Higgins et al., 2019). Potential publication bias was evaluated applying Egger regression and Begg's tests. If there was a significant publication bias, "trim and fills" analysis was done to check the possible change of the significance of the result (Duval and Tweedie, 2000). A P–value < 0.05 was considered as statistically significant.

RESULTS

Literature Search

A total of 3,916 potentially relevant articles were collected in the primary search (**Figure 1**). No additional article was detected via the hand searching. Among all of the references, 1840 were removed as duplicates. After title and abstract screening, 48 articles remained and after full-text review, 32 articles were excluded from the current study for different reasons. Thus, the final systematic review and meta-analysis was done on 16 papers (**Table 1**) (Sharifi et al., 2014; Foroughi et al., 2015; Barchetta et al., 2016; Foroughi et al., 2016; Nadjarzadeh et al., 2016; Sharifi et al., 2016; Lorvand Amiri et al., 2017; Sakpal et al., 2017; Dabbaghmanesh et al., 2018; Geier et al., 2018; Mansourian Hosseini et al., 2018; MOUODI et al., 2018; Hajiaghamohammadi et al., 2019; Hussain et al., 2019; Shidfar et al., 2019; Foroughi et al., 2014).

Meta–Analyses

Effect of Vitamin D on Lipid Profile

A significant improvement of serum HDL–C [WMD = 1.60, 95% CI = (0.41, 2.78), p = 0.008, I^2 = 0.0%] was found following vitamin D intake compared to the controls. Serum levels of TG [WMD = 0.65, 95% CI = (−12.60, 13.91), p = 0.92, I^2 = 40.9%], TC [WMD = 5.62, 95% CI = (−4.20, 15.45), p = 0.26, I^2 = 69.0%] and LDL–C [WMD = 3.53, 95% CI = (−0.91, 7.97), p = 0.11, I^2 = 12.8%] were not significantly affected in the group receiving vitamin D (**Figure 2**).

Effect of Vitamin D on Anthropometric Indices

Pooled results of the meta–analysis revealed a significant reduction in body weight [WMD = −0.88, 95% CI = (−1.52, −0.24), p = 0.007, I^2 = 29.7%], BMI [WMD = −0.33, 95% CI = (−0.54, −0.12), p = 0.002, I^2 = 21.5%], and WC [WMD = −1.04, 95% CI = (−1.97, −0.10), p = 0.02, I^2 = 64.0%] in the treatment groups compared with the controls. In contrast, body fat [WMD = 0.46, 95% CI = (−0.47, 1.40), p = 0.33, I^2 = 60.5%] was not changed following vitamin D supplementation (**Figure 3**).

Effect of Vitamin D on Liver Enzymes

Pooled estimate of 16 papers indicated a significant reduction of serum ALT [WMD = −4.03, 95% CI = (−7.41, −0.66), p = 0.01, I^2 = 78.5%] following vitamin D supplementation. However, serum AST [WMD = −1.05, 95% CI = (−3.50, 1.39), p = 0.39, I^2 = 78.2%], ALP [WMD = −5.43, 95% CI = (−18.08, 7.22), p = 0.40, I^2 = 62.4%], and GGT [WMD = −2.24, 95% CI = (−9.66, 5.18), p = 0.54, I^2 = 0.0%] were not affected by vitamin D supplementation (**Figure 4**).

Effect of Vitamin D on Glycemic Indices

As shown in **Figure 5**, receiving vitamin D significantly improved serum FBS [WMD = −5.02, 95% CI = (−8.95, −1.09), p = 0.01, I^2 = 81.6%] and HOMA–IR [WMD = −0.79, 95% CI = (−1.33, −0.25), p = 0.004, I^2 = 89.0%] compared with to the controls.

Effect of Vitamin D on Adiponectin and Calcium

As shown in **Figure 5**, serum calcium was significantly increased after vitamin D supplementation [WMD = 1.97, 95% CI = (0.38, 3.55), p = 0.01, I^2 = 99.3%]. Adiponectin was not significantly affected [WMD = 0.45, 95% CI = (−0.35, 1.24), p = 0.26, I^2 = 88.3%] by vitamin D supplementation.

Subgroup Analyses

As shown in **Table 2,** serum HDL–C was significantly affected by vitamin D supplementation when subgroup analysis conducted

TABLE 1 | Characteristics of the primary studies included in the meta–analysis.

Authors	Publication year	Country	Sample size case/ control	Dosage of vitamin D	Type of intervention in control group	Follow–up duration	Significant out comes
Foroughi et al. (Foroughi et al., 2015)	2015	Iran	30/30	50,000 IU/ week	Placebo	10 weeks	Vitamin D supplementation resulted in increased serum 25–hydroxy vitamin D concentration in the intervention group compared to the control group. Intake of vitamin D supplements led to a marginally significant decrease in fasting blood glucose in the intervention group compared to the control group. HOMA–IR decreased in the intervention group compared to the control group
Mansourian Hosseini et al. (Mansourian Hosseini et al., 2018)	2018	Iran	41/41	600,000 IU	Placebo	4 weeks	serum 25–hydroxyvitamin D significantly increased in the intervention group vs. the control. Total body fat decreased in the intervention group. while visceral fat was significantly different between the groups. Adiponectin, calcium, phosphors, and PTH levels increased, while liver enzymes, insulin, and HOMA–IR decreased in both. There were significant differences in mean changes of serum 25(OH) D, PTH, ALT, AST, ALP, and FBS between the groups after adjusting for baseline, TF and VF. Vitamin D injection did improve NAFLD severity
Hajiaghamoham madi et al. (Hajiaghamohammadi et al., 2019)	2019	Iran	40/40	50,000 IU/ week	Placebo	10 weeks	A significant reduction in the variables including AST, ALT, total cholesterol, and LDL–C in both groups ($p < 0.05$). As for the two indices of FBG and TG, the control group exhibited significantly less variations ($p < 0.05$)
Shidfar et al. (Shidfar et al., 2019)	2019	Iran	Group1: ($n = 37$), group2 ($n = 37$) group3 ($n = 36$)	Group1: ($n = 37$) 1000 IU vitamin D + Group2: ($n = 37$) 1000 IU vitamin D + 500 mg/d as calcium Group3: ($n = 36$), placebo	Placebo	12 weeks	Reduction in serum ALT, AST, LDL–C/ HDL–C, TC/HDL–C, and non–HDL C were significantly higher in the CaD compared with the P group
Geier et al. (Geier et al., 2018)	2018	Switzerland	30/30	2100 IU/daily	Placebo	18 weeks	Significant change was not observed in AST, AP, and GGT levels; significant change was observed in ALT
Dabbaghmanesh et al. (Dabbaghmanesh et al., 2018)	2018	Iran	Group1: 35, group2: 35, group3: 36	Group1:50,000 IU vitamin, Group2: 0.25 mg calcitriol, Group3: placebo	Placebo	12 weeks	serum alkaline phosphatase levels was significantly decreased from baseline levels in vitamin D3 group. Serum and gamma GGT level was also significantly decreased compared to the baseline levels in treatment group. There was no statistically significant difference between placebo and vitamin D3 group in terms of serum aminotransferase, ALP, serum GGT and lipid profile serum ALP levels was significantly decreased from baseline levels in calcitriol treated group. There was no statistically significant difference between placebo and calcitriol groups in terms of serum aminotransferase, ALP, serum GGT and lipid profile

(Continued on following page)

TABLE 1 | (*Continued*) Characteristics of the primary studies included in the meta–analysis.

Authors	Publication year	Country	Sample size case/ control	Dosage of vitamin D	Type of intervention in control group	Follow–up duration	Significant out comes
Hussain et al. (Hussain et al., 2019)	2019	Iran	55/54	50,000 IU vitamin	Placebo	12 weeks	A reduction in HOMA–IR, liver enzymes ALT, AST, serum CRP and increase in serum adiponectin as compared to placebo group. However no significant changes were observed in both groups in terms of body weight, BMI, and serum lipid profiles
Taghvaei et al. (MOUODI et al., 2018)	2018	Iran	20/20	50,000 IU vitamin	Placebo	12 weeks	Mean BMI and serum liver enzymes decreased significantly in two groups. A significant improvement was observed in steatosis in both groups. No significant differences were observed between the two groups in steatosis when measured by CAP parameter
Foroughi et al. (Foroughi et al., 2016)	2020	Iran	30/30	50,000 IU vitamin	Placebo	10 weeks	Vitamin D supplementation resulted in an increase of serum 25(OH) D concentrations in inter group and intra–group in intervention group. At the end of the study, in the intervention group, TG and CRP reduced significantly compare with baseline. A significant increase was seen in calcium serum in the intervention group in comparison with baseline and compared with the placebo group
Nadjarzadeh et al. (Nadjarzadeh et al., 2016)	2010	Iran	36/37	Group1: low calorie diet+ 50,000 IU vitamin D, Group2: low calorie diet + placebo	Placebo	12 weeks	Significant reduction was observed in ALT and AP Significant change was not observed in AST levels
Amiri et al. (Lorvand Amiri et al., 2017)	2016	Iran	37/36	1000 IU/day	Placebo	12 weeks	Significant reduction in FPG, insulin, insulin resistance (by HOMA–IR) and TG concentrations and an increase in HDL.C was seen over the 12 weeks of study in each group. Adjusting to the baseline measurements, there was significant difference in FPG, HOMA–IR, serum insulin, TG and HDL.C among the groups after 12 weeks of the study. The calcium plus calcitriol group showed a significant decrease in ALT and FPG and increase in HDL.C level compared with the calcitriol group, adjusted to the baseline measures
Sharifiet al. (Sharifi et al., 2016)	2016	Iran	27/26	50,000 IU vitamin D	Placebo	every 14 days for 4 months	In both genders, serum 25(OH) D3 increased significantly. This increase was accompanied by significant decrease in serum TC and LDL–C in women. However, in men, vitamin D supplementation increased the levels of serum TC with no significant effects on LDL–C. Moreover, vitamin D significantly reduced serum hs–CRP in women. The median daily calcium intake in both genders was well below the dietary reference intake for adults
Sharifi et al. (Sharifi et al., 2014)	2014	Iran	27/26	50,000 IU/ 2 weeks	Placebo	12 weeks	In vitamin D supplementation compared to the controls, the median of serum 25(OH)D3 significantly increased. This increase accompanied by significant decrease in serum MDA and near significant changes in serum hs–CRP. Other variables showed no significant changes

(Continued on following page)

TABLE 1 | (*Continued*) Characteristics of the primary studies included in the meta–analysis.

Authors	Publication year	Country	Sample size case/ control	Dosage of vitamin D	Type of intervention in control group	Follow–up duration	Significant out comes
Barchetta et al. (Barchetta et al., 2016)	2016	Italia	26/29	2000 IU/daily	Placebo	48 weeks	25(OH) vitamin D significantly increased in the treated group, no group differences were found in HFF, transaminases, CK18–M30, P3NP levels or FLI after 24 weeks. Vitamin D neither changed the metabolic profile nor the cardiovascular parameters
Foroughi et al. (Foroughi et al., 2016)	2014	Iran	30/30	50,000 IU vitamin D	Placebo	10 weeks	Vitamin D supplementation resulted in an increase of serum 25(OH) D concentrations in inter group and intra–group in intervention group. At the end of the study, in the intervention group, TG and CRP reduced significantly compare with baseline. A significant increase was seen in calcium serum in the intervention group in comparison with baseline and compared with the placebo group
Sakpal et al. (Sakpal et al., 2017)	2010	India	51/30	600,000 IU	Placebo	24 weeks	Significant improvement in serum ALT and serum adiponectin levels of intervention group

by country (Iran), duration (≤12 weeks), and dose (≤25,000 IU). BMI was changed in country (Iran), duration (>12 weeks), and dose (≤25,000 IU) subgroups. Body weight was changed in studies conducted in Iran and also when used >25,000 IU doses of when which interventions last >12 weeks, serum FBS was significantly affected when studies performed in Iran, last ≤12 weeks, and used doses more than 25,000 IU vitamin D. HOMA–IR was significantly improved all subgroups, except in trials last more than 12 weeks.

Meta–Regression and Sensitivity Analysis

The results of meta–regression and sensitivity analysis indicated that total sample size was regarded as a source of inter–study heterogeneity for AST [Coefficient: −0.19, 95% CI = (−0.29, −0.08), p = 0.001]. Sensitivity analyses showed that pooled results of interested outcomes are not sensitive to removing any of included trials.

Publication Bias

A significant publication bias was found for HOMA-IR, HDL-C and GGT. Hence, trim and fill analysis was done to detect the potential change of their results. Only the significance of HDL–C was changed and turned into non–significant.

DISCUSSION

To the best of the authors' knowledge, this is the first study to systematically review and meta analyze the findings of intervention studies on the effect of vitamin D on a wide range of anthropometric and biochemical indices in patient with NAFLD. The results of the present study indicated that vitamin D supplementation significantly improved the body weight, BMI, WC, HDL-C, ALT, FBS, and HOMA-IR in the intervention group compared to the control group. However, no significant differences were found on body fat, TG, LDL-C, AST, and GGT. Subgroup analyses also showed that the effect of vitamin D on most indices was affected by study location, duration of study and dose used for vitamin D.

Some studies investigated the association between vitamin D supplementation with lipid profile in NAFLD. In line with this study, Dabaghmanesh et al. indicated that 12 weeks of vitamin D supplementation significantly increased HDL-C (Dabbaghmanesh et al., 2018). Another study found that supplementation with calcium combined with vitamin D improved serum ALT and HDL-C levels (Lorvand Amiri et al., 2017).

However, the results regarding the effect of vitamin D on lipid profile have been contradictory. Sharifi et al. found that vitamin D intake supplementation for 4 months significantly decreed LDL-C and total cholesterol in woman (Sharifi et al., 2016). A meta-analysis indicated that supplementation with vitamin D significantly increased LDL-C and had not significant effect on TG and HDL-C in patients with CVDs (Wang et al., 2012). One study found that vitamin D supplementation reduced LDL-C but no significant change was found on HDL-C (Hajiaghamohammadi et al., 2019). In another study supplementation with vitamin D3 as 50,000 IU per week for 12 weeks in NAFLD had no significant effect on lipid profile and body composition (Hussain et al., 2019). The effect of vitamin D on lipid profile in people with NAFLD may be different from its effect in healthy people or in people with other chronic diseases.

Some effects of vitamin D are exerted through its effect on increasing calcium absorption. Therefore, dietary calcium intake can also affect the role of vitamin D in determining serum lipid profile. Shidfar et al. found that vitamin D combined with calcium

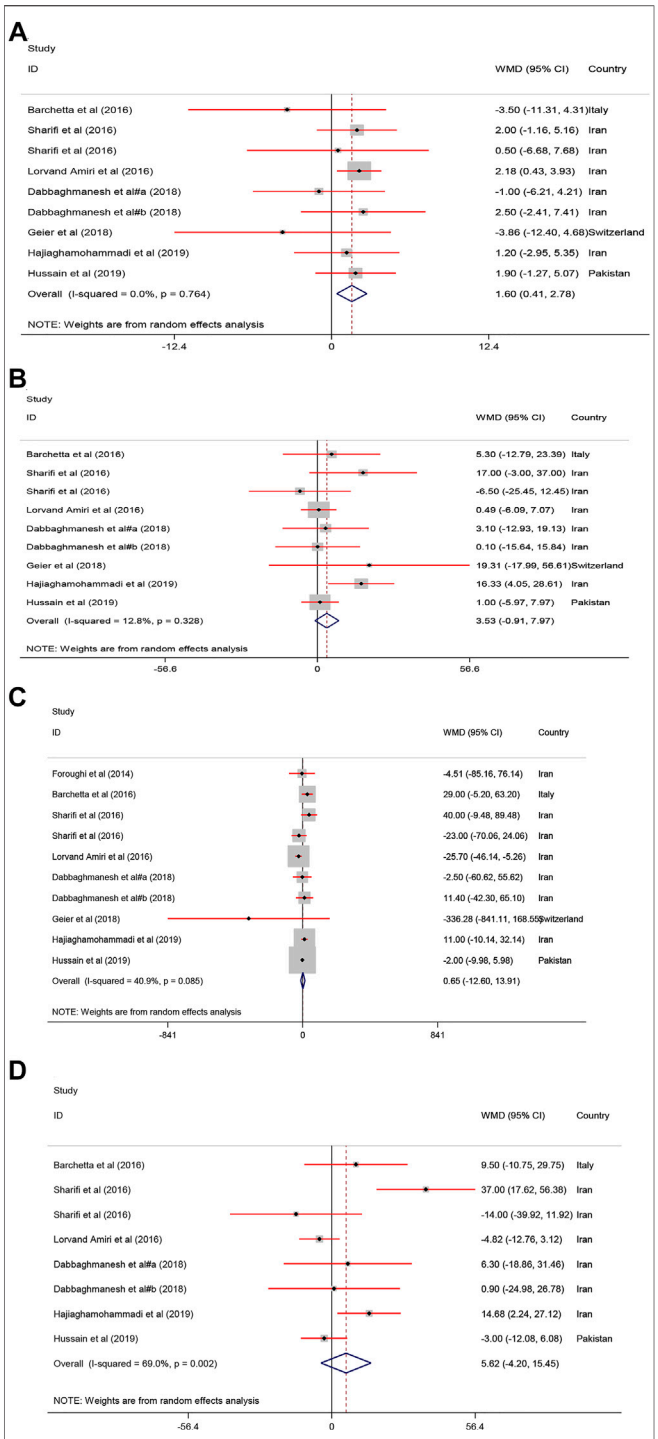


FIGURE 2 | The lipid profile standardized mean differences estimates for **(A)** HDL–C, **(B)** LDL–C, **(C)** TG and **(D)** TC between intervention group (receiving vitamin D supplementation) and placebo groups.

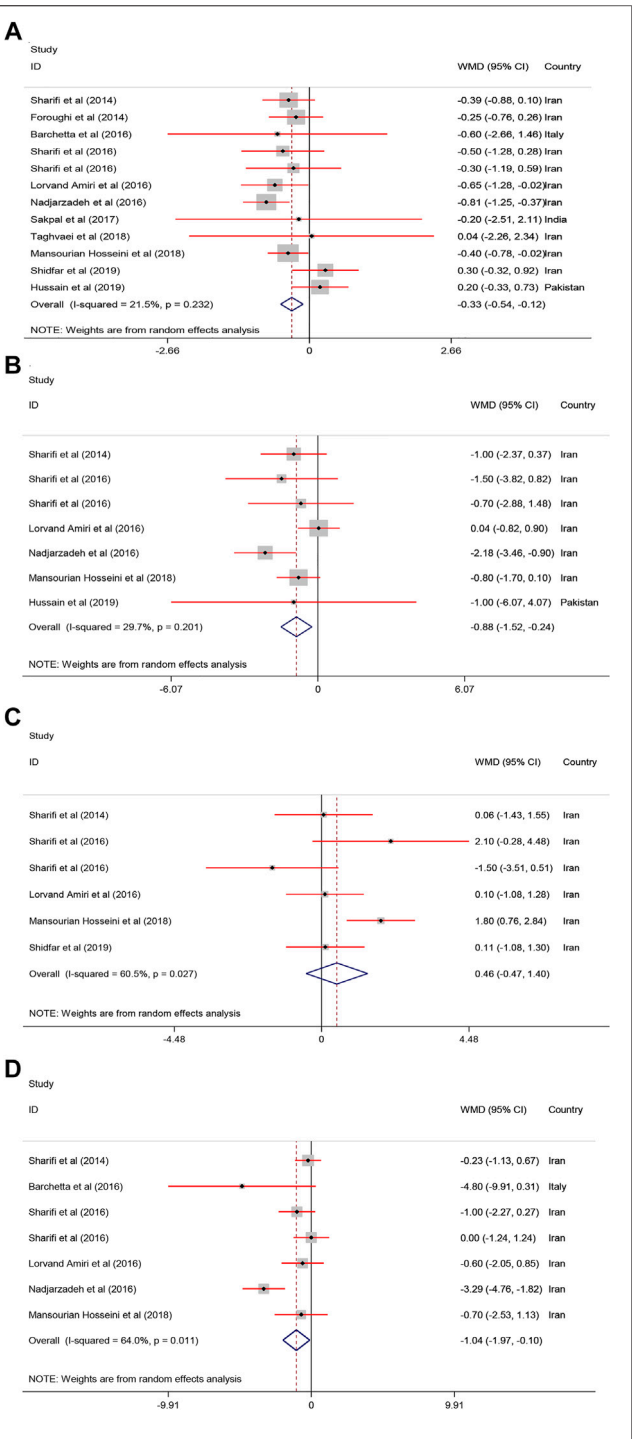


FIGURE 3 | The anthropometric parameters standardized mean differences estimates for **(A)** BMI, **(B)** weight, and **(C)** body fat and **(D)** WC between intervention group (receiving vitamin D supplementation) and placebo groups.

for 12 weeks reduced ALT, AST, LDL-C/HDL-C, TC/HDL-C, and increased non–HDL–C compared with group revived only vitamin D (Shidfar et al., 2019). Moreover, some studies suggested an inverse association between serum 25(OH)-D levels and TG (Chon et al., 2014). The underlying mechanisms of the effects of vitamin D on lipid profile has not been completely yet understood. The low levels of vitamin D can lead to hyperparathyroidism which can lower serum TG. On the other hand, lower vitamin D level can activate microsomal

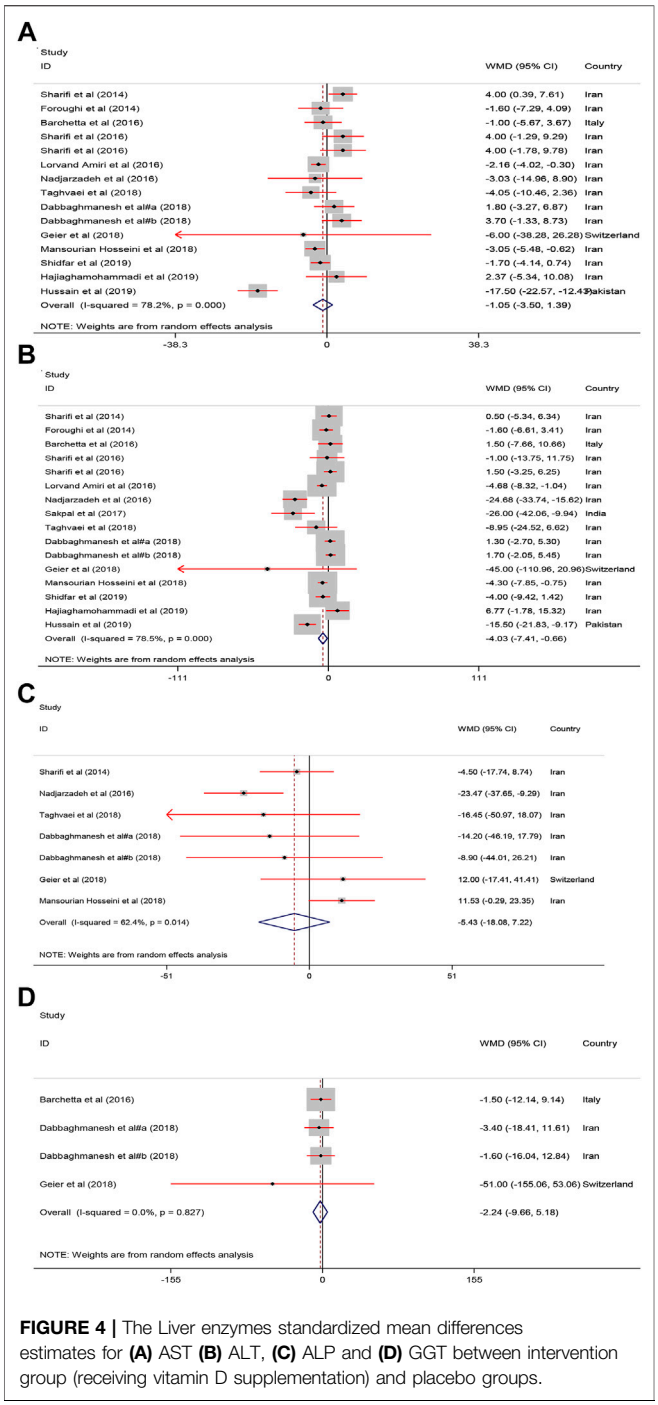


FIGURE 4 | The Liver enzymes standardized mean differences estimates for **(A)** AST **(B)** ALT, **(C)** ALP and **(D)** GGT between intervention group (receiving vitamin D supplementation) and placebo groups.

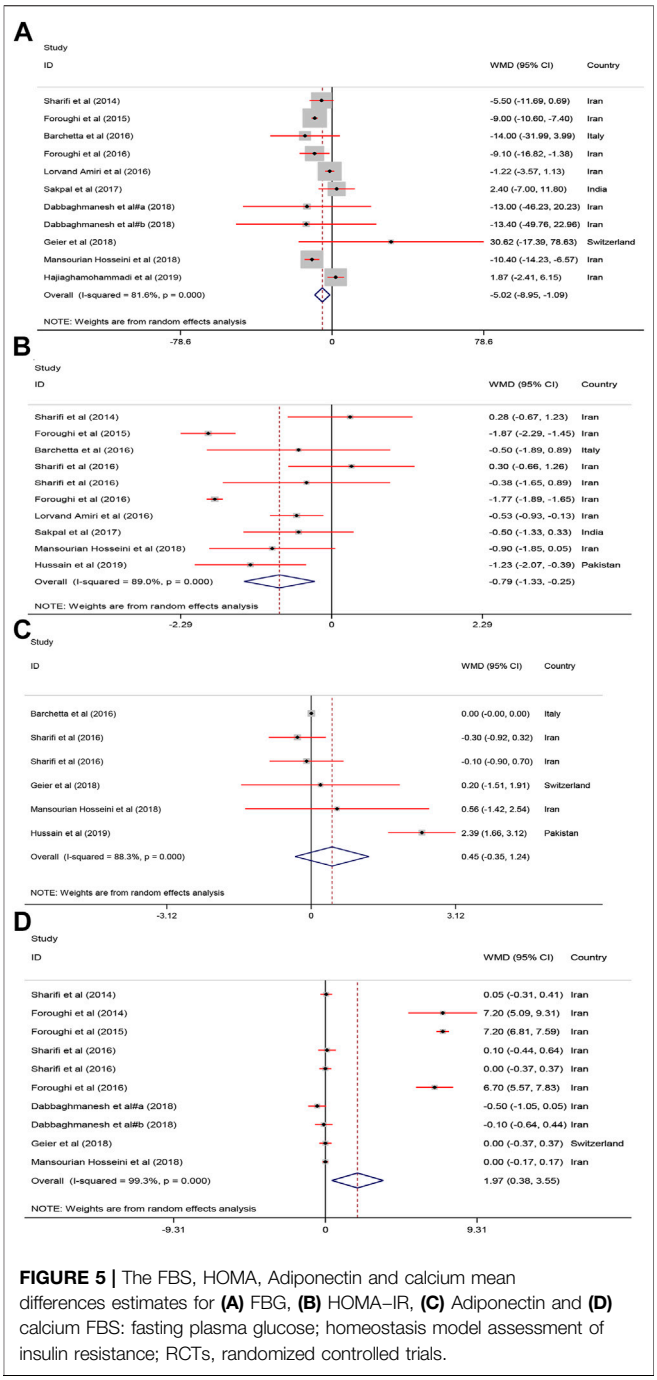


FIGURE 5 | The FBS, HOMA, Adiponectin and calcium mean differences estimates for **(A)** FBG, **(B)** HOMA–IR, **(C)** Adiponectin and **(D)** calcium FBS: fasting plasma glucose; homeostasis model assessment of insulin resistance; RCTs, randomized controlled trials.

TG-transfer protein, which leads to increased TG. Vitamin D also regulates macrophage function in reverse cholesterol transportation and reduces inflammation and insulin resistance (Shidfar et al., 2019).

Regarding to anthropometric measurements, this meta–analysis found that vitamin D reduced body weight, BMI, and WC but no significant change was found in body fat. Hussain et al. investigated the association between vitamin D intake and BMI, body fat, and WC in NAFLD and reported that 50,000 IU vitamin D for 12 weeks had no significant effect on anthropometric indices (Hussain et al., 2019). Another study found that the injection of cholecalciferol (600,000 IU) reduced weight, WC, and BMI (Mansourian Hosseini et al., 2018). Sharifi et al. reported that the intervention group with 50,000 IU vitamin D3 for 4 month had lower weight, WC, and BMI compared with the controls (Sharifi et al., 2016). The reason for these differences may be the differences in doses of vitamin D supplementation and also differences in seum level of vitamin D. Doaei et al. reported that the serum level of vitamin D is inversely associated

TABLE 2 | The results of subgroup analysis.

Subgroups		No. of study	WMD (95% CI)	*p*	Heterogeneity (I^2, *P*)
TG					
Country	Iran	7	−1.73 (−21.01, 17.55)	0.86	41.4%, 0.11
	Other	3	8.29 (−24.32, 40.90)	0.61	57.4%, 0.09
Duration	>12 weeks	4	14.03 (−25.09, 53.15)	0.48	49.7%, 0.11
	≤12 weeks	6	−3.87 (−15.21, 7.47)	0.50	26.0%, 0.23
Dosage	≤25,000 IU	5	1.31 (−34.31, 36.94)	0.94	69.2%, 0.01
	>25,000 IU	5	−0.23 (−7.53, 7.08)	0.95	0.0%, 0.83
TC					
Country	Iran	6	7.19 (−6.90, 21.27)	0.31	75.8%, 0.001
	Other	2	−0.16 (−10.43, 10.10)	0.97	17.9%, 0.27
Duration	>12 weeks	3	11.84 (−16.20, 39.89)	0.40	80.1%, 0.007
	≤12 weeks	5	1.39 (−6.58, 9.36)	0.73	46.1%, 0.11
Dosage	≤25,000 IU	4	7.02 −13.62, 27.66)	0.50	82.6%, 0.001
	>25,000 IU	4	4.45 (−5.80, 14.71)	0.39	0.16
HDL–C					
Country	Iran	6	1.82 (0.51, 3.13)	0.007	0.0%, 0.90
	Other	3	−0.22 (−4.17, 3.72)	0.91	27.3%, 0.25
Duration	>12 weeks	4	0.66 (−1.92, 3.25)	0.61	0.0%, 0.41
	≤12 weeks	5	1.84 (0.51, 3.18)	0.007	0.0%, 0.83
Dosage	≤25,000 IU	5	1.70 (0.25, 3.15)	0.02	0.0%, 0.43
	>25,000 IU	4	1.38 (−0.68, 3.44)	0.18	0.0%, 0.77
BMI					
Country	Iran	9	−0.40 (−0.61, −0.19)	<0.0001	15.1%, 0.30
	Other	3	0.13 (−0.37, 0.64)	0.60	0.0%, 0.73
Duration	>12 weeks	5	−0.40 (−0.77, −0.03)	0.03	0.0%, 0.99
	≤12 weeks	7	−0.29 (−0.61, 0.04)	0.08	56.2%, 0.03
Dosage	≤25,000 IU	7	−0.31 (−0.59, −0.02)	0.03	0.0%, 0.51
	>25,000 IU	5	−0.33 (−0.69, 0.03)	0.07	53.9%, 0.06
Body weight					
Country	Iran	6	−0.90 (−1.60, −0.20)	0.01	41.4%, 0.12
	Other	1	−1 (−6.07, 4.07)	–	–
Duration	>12 weeks	3	−1.03 (−2.07, 0.01)	0.05	0.0%, 0.88
	≤12 weeks	4	−0.89 (−1.94, 0.16)	0.09	62.6%, 0.04
Dosage	≤25,000 IU	4	−0.40 (−1.06, 0.27)	0.23	0.0%, 0.44
	>25,000 IU	3	−1.35 (−2.40, −0.31)	0.01	33.3%, 0.22
ALT					
Country	Iran	12	−2.37 (−5.46, 0.73)	0.13	74.0%, <0.0001
	Other	4	−13.61 (−27.33, 0.10)	0.05	77.6%, 0.004
Duration	>12 weeks	6	−2.41 (−8.67, 3.85)	0.45	59.6%, 0.03
	≤12 weeks	10	−4.69 (−8.79, −0.59)	0.02	83.6%, <0.0001
Dosage	≤25,000 IU	8	−2.72 (−6.67, 1.22)	0.17	56.3%, 0.02
	>25,000 IU	8	−4.98 (−10.41, 0.45)	0.07	87.0%, <0.0001
AST					
Country	Iran	12	0.10 (−1.70, 1.90)	0.91	54.9%, 0.01
	Other	3	−8.77 (−23.21, 5.67)	0.23	90.9%, <0.0001
Duration	>12 weeks	5	2.74 (0.44, 5.04)	0.02	0.0%, 0.46
	≤12 weeks	10	−2.59 (−5.45, 0.27)	0.07	79.9%, <0.0001
Dosage	≤25,000 IU	7	0.53 (−1.86, 2.91)	0.66	60.5%, 0.01
	>25,000 IU	8	−2.76 (−7.44, 1.91)	0.24	84.0%, <0.0001
ALP					
Country	Iran	6	−7.62 (−21.34, 6.09)	0.27	66.2%, 0.01
	Other	1	12.00 (−17.41, 41.41)	—	—
Duration	>12 weeks	2	−1.69 (−13.84, 10.46)	0.78	0.5%, 0.31
	≤12 weeks	5	−9.11 (−27.90, 9.67)	0.34	73.0%, 0.005
Dosage	≤25,000 IU	2	−1.69 (−13.84, 10.46)	0.78	0.5%, 0.31
	>25,000 IU	5	−9.11 (−27.90, 9.67)	0.34	73.0%, 0.005

(Continued on following page)

TABLE 2 | (*Continued*) The results of subgroup analysis.

Subgroups		No. of study	WMD (95% CI)	*p*	Heterogeneity (I^2, *P*)
FBS					
Country	Iran	8	−5.63 (−9.78, −1.48)	0.008	85.5%, <0.0001
	Other	3	−0.85 (−16.87, 15.17)	0.91	51.7%, 0.12
Duration	>12 weeks	4	−3.09 (−11.24, 5.07)	0.45	41.9%, 0.16
	≤12 weeks	7	−5.68 9—-10.34, −1.01)	0.01	87.5%, <0.0001
Dosage	≤25,000 IU	5	−2.20 (−6.33, 1.93)	0.29	31.9%, 0.20
	>25,000 IU	6	−6.87 (−11.81, −1.94)	0.006	78.8%, <0.0001
HOMA–IR					
Country	Iran	7	−0.79 (−1.44, −0.14)	0.01	91.7%, <0.0001
	Other	3	−0.81 (−1.35, −0.26)	0.004	0.0%, 0.43
Duration	>12 weeks	5	−0.12 (−0.58, 0.34)	0.60	0.0%, 0.61
	≤12 weeks	5	−1.30 (−1.88, −0.73)	<0.0001	89.4%, <0.0001
Dosage	≤25,000 IU	6	−0.35 (−0.65, −0.05)	0.02	0.0%, 0.49
	>25,000 IU	4	−1.68 (−1.96, −1.40)	<0.0001	39.0%, 0.17

TABLE 3 | The results of risk of bias.

First author	Country	Random sequence generation (selection bias)	Alloation concealment (selection bias)	Blinding or participants and personnel (performance bias)	Blinding of outcome assessment (detection bias)	Incomplete outcome data addressed (attrition bias)	Selective reporting (reporting bias)	Other sources of bias (e.g. bias of study design, trial stopped early, extreme baseline imbalance and fraudulent)
Sharifi et al. (2014)	Iran	Unclear	Unclear	Low risk	Low risk	Low risk	Low risk	Low risk
Foroughi et al. (2014)	Iran	Unclear	Unclear	Low risk	Low risk	Low risk	High risk	Low risk
Foroughi et al. (2015)	Iran	Unclear	Unclear	Low risk	Low risk	Low risk	Low risk	Low risk
Barchetta et al. (2016)	Italy	Low risk	Low risk	Low risk	Low risk	High risk	Low risk	Low risk
Sharifi et al. (2016)	Iran	Unclear	Unclear	Low risk	Low risk	Low risk	Low risk	Low risk
Foroughi et al. (2016)	Iran	Low risk	Low risk	Low risk	Low risk	Low risk	Low risk	Low risk
Lorvandamiri et al. (2016)	Iran	Low risk	Low risk	Low risk	Low risk	Low risk	Low risk	Low risk
Nadjarzadeh et al. (2016)	Iran	Unclear	Unclear	Low risk	Low risk	Low risk	High risk	Low risk
Sakpal et al. (2017)	India	Unclear	Unclear	Unclear	Low risk	Unclear	Unclear	Low risk
Taghvaei et al. (2018)	Iran	Low risk	Low risk	Low risk	Low risk	Low risk	Low risk	Low risk
Dabbaghmanesh et al. (2018)	Iran	Low risk	Low risk	Low risk	Low risk	Low risk	Low risk	Low risk
Geier et al. (2018)	Switzerland	Unclear	Unclear	Low risk	Low risk	Low risk	Low risk	Low risk
Mansourian Hosseini et al. (2018)	Iran	Low risk	Low risk	Unclear	Low risk	High risk	Low risk	Low risk
Shidfar et al. (2019)	Iran	Low risk	Low risk	Low risk	Low risk	Unclear	High risk	Low risk
Hajiaghamohammadi et al. (2019)	Iran	Unclear	Unclear	Low risk	Low risk	Unclear	High risk	Low risk
Hussain et al. (2019)	Pakistan	Low risk	Low risk	Low risk	Low risk	Low risk	Unclear	Low risk

with obesity. However, short term changes of serum vitamin D was not related to changes in weight (Doaei et al., 2020).

The present study identified that ALT increased and some liver enzymes such as AST, ALP, GGT were not affected following vitamin D supplementation. Vitamin D receptor (VDR) is abundantly expressed on liver cells and this vitamin was reported to have an anti–inflammatory effect on liver (Bozic et al., 2016). One study found that 50,000 IU/wk vitamin D supplementation for 10 weeks reduced AST and ALT in the intervention group compared with the control group (Hajiaghamohammadi et al., 2019). The vitamin D supplementation for 48 weeks decreased liver enzyme in patients with NAFLD (Geier et al., 2018). The difference in the results of the effect of vitamin D on the serum level of liver enzymes may be due to the fact that the levels of liver enzymes is greatly affected by other lifestyle and dietary factors. Sakpal et al. indicated that vitamin D intake along with lifestyle modifications improved serum ALT levels (Jamali et al., 2013). Another placebo–controlled study found that 12–weeks hypocaloric diet combined with calcitriol improved ALT and AST in the intervention group compared with the control group (Amiri et al., 2016).

The levels of FBS and HOMA-IR were improved following vitamin D intake. In line with this study, one study indicated that calcitriol intake (25 mg) for 12 weeks improved HOMA–IR in patients with NAFLD (Amiri et al., 2016). A recent study reported that vitamin D intake increased insulin sensitivity (Inzucchi et al., 1998). Another study found a negative association between vitamin D supplementation and FBS (Pittas et al., 2007). In another study, calcitriol supplementation for a short term increased insulin sensitivity (Foroughi et al., 2016). One meta–analysis suggested that vitamin D administration could improve FBS and insulin resistance in patents with impaired glucose tolerance or HOMA–IR (George et al., 2012). However, the results regarding the effect of vitamin D on serum glucose indices were contradictory. One study reported that vitamin D had no association with FBS (Kitson and Roberts, 2012). Interestingly, Lind et al. found that long–term calcitriol supplementation for 2 years decreased HOMA–IR but had no effect on insulin (Lind et al., 1989). The short–term vitamin D intake was associated with lower FBS in renal disease patients while had no effect on fasting insulin levels (Sarathy et al., 2015). The underlying mechanism of the effect of vitamin D on blood glucose is not yet clear. Vitamin D deficiency increase serum parathyroid hormone levels (PTH) and the PTH plays an important role in NAFLD through increasing insulin resistance (IR) (Foss, 2009).

The results of the present study indicated that the level of adiponectin was not significantly affected by vitamin D supplementation. Some studies reported that patients with NAFLD had lower adiponectin concentration compared with the others and adiponectin can be considered as a predictor of the severity of hepatic steatosis (Targher et al., 2006; Nakano et al., 2011). In line with our study, two previous studies reported that vitamin D intake had no effect on serum adiponectin in people with type 2 diabetes and obese children (Patel et al., 2010; Belenchia et al., 2013). On the other hand, Nakano et al. reported that phototherapy and vitamin D increased adiponectin concentration in rats with NAFLD (Kitson and Roberts, 2012). Adiponectin is secreted from adipose tissue and could influence on metabolism of fat and glucose. Adiponectin increased liver insulin sensitivity and decreased glucose excretion from the liver which can lead to prevent of high blood sugar. It has been suggested that vitamin D regulates adiponectin gene expression in adipose tissue (Hajiaghamohammadi et al., 2019). It seems that many factors may influence the effects of vitamin D on serum adiponectin such as differences in doses of vitamin D supplementation, follow–up duration, and VDR gene polymorphisms. Moreover, the association between vitamin D intake and adiponectin may be influenced by other factors such as calcium intake and body weight. The results of a recent meta–analysis study indicated that vitamin D may promote secretion of adiponectin in subjects with diabetes and this effect may be potentiated if vitamin D intake is on daily basis and in combination with calcium but can be weakened by increasing BMI (Nikooyeh and Neyestani, 2021).

The present study found that vitamin D supplementation improved the level of serum calcium. In contrast with this result, Geier et al. found that adiponectin and calcium levels were not significantly different after vitamin D supplementation (Geier et al., 2018). Sharifi et al. showed that vitamin D supplementation has no effect on serum level of calcium (Sharifi et al., 2016). A recent study of more than 5,000 people found that taking a monthly vitamin D supplement did not alter serum calcium (Malihi et al., 2019). Serum calcium levels play an important role in the cardiovascular and muscular system and are maintained at a certain level by complex mechanisms (Fleet, 2017). Further studies on the effect of vitamin D on serum calcium levels and considering the interaction of various factors on serum calcium levels are needed.

CONCLUSION

The present study showed that Vitamin D supplementation had significant effect on HDL-C, body weight, BMI, WC, serum ALT, serum FBS, HOMA-IR, calcium and no effect on TG, TC, LDL-C, AST, ALP, GGT, and adiponectin. Further studies are needed to identify the underlying mechanisms of the effects of vitamin D supplementation on the anthropometric and biochemical indices in patient with NAFLD.

DATA AVAILABILITY STATEMENT

The raw data supporting the conclusions of this article will be made available by the authors, without undue reservation. Data may be made available upon request.

AUTHOR CONTRIBUTIONS

SR and RT designed the study, and were involved in the data collection, analysis, and drafting of the manuscript. SR, PN-S, MJ, MS-B, SM, SD, and MG were involved in the design of the study, analysis of the data, and critically reviewed the manuscript. All authors read and approved the final manuscript.

FUNDING

Funding for this study was provided by Shiraz University of Medical Sciences, Shiraz, Iran.

ACKNOWLEDGMENTS

This study was conducted at the school of Nutrition and Food Sciences and shahid beheshti University of Medical Sciences, Tehran, Iran.

REFERENCES

Amiri, H. L., Agah, S., Mousavi, S. N., Hosseini, A. F., and Shidfar, F. (2016). Regression of Non–alcoholic Fatty Liver by Vitamin D Supplement: a Double–Blind Randomized Controlled Clinical Trial. *Arch. Iranian Med.* 19 (9), 0.

Barchetta, I., Del Ben, M., Angelico, F., Di Martino, M., Fraioli, A., La Torre, G., et al. (2016). No Effects of Oral Vitamin D Supplementation on Non–alcoholic Fatty Liver Disease in Patients with Type 2 Diabetes: a Randomized, Double–Blind, Placebo–Controlled Trial. *BMC Med.* 14 (1), 92–10. doi:10.1186/s12916–016–0638–y

Belenchia, A. M., Tosh, A. K., Hillman, L. S., and Peterson, C. A. (2013). Correcting Vitamin D Insufficiency Improves Insulin Sensitivity in Obese Adolescents: a Randomized Controlled Trial. *Am. J. Clin. Nutr.* 97 (4), 774–781. doi:10.3945/ajcn.112.050013

Benetti, E., Mastrocola, R., Chiazza, F., Nigro, D., D'Antona, G., Bordano, V., et al. (2018). Effects of Vitamin D on Insulin Resistance and Myosteatosis in Diet–Induced Obese Mice. *PLoS One* 13 (1), e0189707. doi:10.1371/journal.pone.0189707

Bozic, M., Guzmán, C., Benet, M., Sánchez–Campos, S., García–Monzón, C., Gari, E., et al. (2016). Hepatocyte Vitamin D Receptor Regulates Lipid Metabolism and Mediates Experimental Diet–Induced Steatosis. *J. Hepatol.* 65 (4), 748–757. doi:10.1016/j.jhep.2016.05.031

Chalasani, N., Younossi, Z., Lavine, J. E., Diehl, A. M., Brunt, E. M., Cusi, K., et al. (2012). The Diagnosis and Management of Non–alcoholic Fatty Liver Disease: Practice Guideline by the American Association for the Study of Liver Diseases, American College of Gastroenterology, and the American Gastroenterological Association. *Hepatology* 55 (6), 2005–2023. doi:10.1002/hep.25762

Chon, S. J., Yun, B. H., Jung, Y. S., Cho, S. H., Choi, Y. S., Kim, S. Y., et al. (2014). Association between Vitamin D Status and Risk of Metabolic Syndrome Among Korean Postmenopausal Women. *PloS one* 9 (2), e89721. doi:10.1371/journal.pone.0089721

Dabbaghmanesh, M. H., Danafar, F., Eshraghian, A., and Omrani, G. R. (2018). Vitamin D Supplementation for the Treatment of Non–alcoholic Fatty Liver Disease: A Randomized Double Blind Placebo Controlled Trial. *Diabetes Metab. Syndr.* 12 (4), 513–517. doi:10.1016/j.dsx.2018.03.006

Del Ben, M., Polimeni, L., Baratta, F., Pastori, D., Loffredo, L., and Angelico, F. (2014). Modern Approach to the Clinical Management of Non–alcoholic Fatty Liver Disease. *World J. Gastroenterol.* 20 (26), 8341–8350. doi:10.3748/wjg.v20.i26.8341

Doaei, S., Jarrahi, S., Torki, S., Haghshenas, R., Jamshidi, Z., Rezaei, S., et al. (2020). Serum Vitamin D Level May Be Associated with Body Weight and Body Composition in Male Adolescents; a Longitudinal Study. *Pediatr. Endocrinol. Diabetes Metab.* 26 (3), 125–131. doi:10.5114/pedm.2020.97466

Doaei, S., Kalantari, N., Izadi, P., Salonurmi, T., Mosavi Jarrahi, A., Rafieifar, S., et al. (2019). Changes in FTO and IRX3 Gene Expression in Obese and Overweight Male Adolescents Undergoing an Intensive Lifestyle Intervention and the Role of FTO Genotype in This Interaction. *J. Transl Med.* 17 (1), 176–178. doi:10.1186/s12967–019–1921–4

Duval, S., and Tweedie, R. (2000). Trim and Fill: A Simple Funnel–Plot–Based Method of Testing and Adjusting for Publication Bias in Meta–Analysis. *Biometrics* 56 (2), 455–463. doi:10.1111/j.0006–341x.2000.00455.x

Fleet, J. C. (2017). The Role of Vitamin D in the Endocrinology Controlling Calcium Homeostasis. *Mol. Cel Endocrinol* 453, 36–45. doi:10.1016/j.mce.2017.04.008

Foroughi, M., Maghsoudi, Z., and Askari, G. (2016). The Effect of Vitamin D Supplementation on Blood Sugar and Different Indices of Insulin Resistance in Patients with Non–alcoholic Fatty Liver Disease (NAFLD). *Iran J. Nurs. Midwifery Res.* 21 (1), 100–104. doi:10.4103/1735–9066.174759

Foroughi, M., Maghsoudi, Z., Ghiasvand, R., Iraj, B., and Askari, G. (2014). Effect of Vitamin D Supplementation on C–Reactive Protein in Patients with Nonalcoholic Fatty Liver. *Int. J. Prev. Med.* 5 (8), 969–975.

Foroughi, M., Maghsoudi, Z., Ghiasvand, R., Iraj, B., and Askari, G. (2015). The Effect of Vitamin D Supplementation on Insulin Resistance in Patients with Nonalcoholic Fatty Liver. *J. Isfahan Med. Sch.* 33 (342), 1076–1085.

Forouhi, N. G., Luan, J., Cooper, A., Boucher, B. J., and Wareham, N. J. (2008). Baseline Serum 25–hydroxy Vitamin D Is Predictive of Future Glycemic Status and Insulin Resistance: the Medical Research Council Ely Prospective Study 1990–2000. *Diabetes* 57 (10), 2619–2625. doi:10.2337/db08–0593

Foss, Y. J. (2009). Vitamin D Deficiency Is the Cause of Common Obesity. *Med. Hypotheses* 72 (3), 314–321. doi:10.1016/j.mehy.2008.10.005

Geier, A., Eichinger, M., Stirnimann, G., Semela, D., Tay, F., Seifert, B., et al. (2018). Treatment of Non–alcoholic Steatohepatitis Patients with Vitamin D: a Double–Blinded, Randomized, Placebo–Controlled Pilot Study. *Scand. J. Gastroenterol.* 53 (9), 1114–1120. doi:10.1080/00365521.2018.1501091

George, P. S., Pearson, E. R., and Witham, M. D. (2012). Effect of Vitamin D Supplementation on Glycaemic Control and Insulin Resistance: a Systematic Review and Meta–Analysis. *Diabet Med.* 29 (8), e142–50. doi:10.1111/j.1464–5491.2012.03672.x

Gholamalizadeh, M., Jarrahi, A. M., Akbari, M. E., Bourbour, F., Mokhtari, Z., Salahshoornezhad, S., et al. (2020). Association between FTO Gene Polymorphisms and Breast Cancer: the Role of Estrogen. *Expert Rev. Endocrinol. Metab.* 15 (2), 115–121. doi:10.1080/17446651.2020.1730176

Hajiaghamohammadi, A., Shafikhani, A. A., Akbar Shafikhani, A., Bastani, A., and Gaemi, N. (2019). Effect of Vitamin D Replacement on Liver Enzymes in Patients with Non–alcoholic Fatty Liver Disease. *J. Gastroenterol. Hepatol. Res.* 8 (3), 2907–2910. doi:10.17554/j.issn.2224–3992.2019.08.819

Hariri, M., and Zohdi, S. (2019). Effect of Vitamin D on Non–alcoholic Fatty Liver Disease: a Systematic Review of Randomized Controlled Clinical Trials. *Int. J. Prev. Med.* 10, 14. doi:10.4103/ijpvm.IJPVM_499_17

Higgins, J., Thomas, J., Chandler, J., Cumpston, M., Li, T., Page, M., et al. (2019). *Cochrane Handbook for Systematic Reviews of Interventions*. Wiley, NJ, USA, version 6.0(updated July 2019), .

Higgins, J. P., Altman, D. G., Gøtzsche, P. C., Jüni, P., Moher, D., Oxman, A. D., et al. (2011). The Cochrane Collaboration's Tool for Assessing Risk of Bias in Randomised Trials. *BMJ* 343, d5928. doi:10.1136/bmj.d5928

Hussain, M., Iqbal, J., Malik, S. A., Waheed, A., Shabnum, S., Akhtar, L., et al. (2019). Effect of Vitamin D Supplementation on Various Parameters in Non–alcoholic Fatty Liver Disease Patients. *Pak J. Pharm. Sci.* 32, 1343–1348.

Inzucchi, S. E., Maggs, D. G., Spollett, G. R., Page, S. L., Rife, F. S., Walton, V., et al. (1998). Efficacy and Metabolic Effects of Metformin and Troglitazone in Type II Diabetes Mellitus. *N. Engl. J. Med.* 338 (13), 867–872. doi:10.1056/NEJM199803263381303

Jamali, R., Mofid, A., Vahedi, H., Farzaneh, R., and Dowlatshahi, S. (2013). The Effect of helicobacter Pylori Eradication on Liver Fat Content in Subjects with Non–alcoholic Fatty Liver Disease: a Randomized Open–Label Clinical Trial. *Hepat. Mon* 13 (12), e14679. doi:10.5812/hepatmon.14679

Kitson, M. T., and Roberts, S. K. (2012). D–livering the Message: the Importance of Vitamin D Status in Chronic Liver Disease. *J. Hepatol.* 57 (4), 897–909. doi:10.1016/j.jhep.2012.04.033

Kleiner, D. E., Brunt, E. M., Van Natta, M., Behling, C., Contos, M. J., Cummings, O. W., et al. (2005). Design and Validation of a Histological Scoring System for Nonalcoholic Fatty Liver Disease. *Hepatology* 41 (6), 1313–1321. doi:10.1002/hep.20701

Lind, L., Pollare, T., Hvarfner, A., Lithell, H., Sørensen, O. H., and Ljunghall, S. (1989). Long–term Treatment with Active Vitamin D (Alphacalcidol) in Middle–Aged Men with Impaired Glucose Tolerance. Effects on Insulin Secretion and Sensitivity, Glucose Tolerance and Blood Pressure. *Diabetes Res.* 11 (3), 141–147.

Lorvand Amiri, H., Agah, S., Tolouei Azar, J., Hosseini, S., Shidfar, F., and Mousavi, S. N. (2017). Effect of Daily Calcitriol Supplementation with and without Calcium on Disease Regression in Non–alcoholic Fatty Liver Patients Following an Energy–Restricted Diet: Randomized, Controlled, Double–Blind Trial. *Clin. Nutr.* 36 (6), 1490–1497. doi:10.1016/j.clnu.2016.09.020

Ludwig, J., Viggiano, T R., Mcgill, D. B., and Oh, B. J. (1980). "Nonalcoholic Steatohepatitis: Mayo Clinic Experiences with a Hitherto Unnamed Disease," in *Mayo Clinic Proceedings*, 55, 7, 434–438, .

Malihi, Z., Lawes, C. M. M., Wu, Z., Huang, Y., Waayer, D., Toop, L., et al. (2019). Monthly High–Dose Vitamin D Supplementation Does Not Increase Kidney Stone Risk or Serum Calcium: Results from a Randomized Controlled Trial. *Am. J. Clin. Nutr.* 109 (6), 1578–1587. doi:10.1093/ajcn/nqy378

Mansourian, S. H., Aliashrafi, S., and Ebrahimi, M. M. (2018). The Effect of a Single Intramuscular Injection of Cholecalciferol on the Serum Levels of Vitamin D, Adiponectin, Insulin Resistance, and Liver Function in Women with

Non–alcoholic Fatty Liver Disease (NAFLD): A Randomized, Controlled Clinical Trial. *Iranian Red Crescent Med. J.* 20 (10). doi:10.5812/ircmj.60746

Mehrdad, M., Doaei, S., Gholamalizadeh, M., Fardaei, M., Fararouei, M., and Eftekhari, M. H. (2020). Association of FTO Rs9939609 Polymorphism with Serum Leptin, Insulin, Adiponectin, and Lipid Profile in Overweight Adults. *Adipocyte* 9 (1), 51–56. doi:10.1080/21623945.2020.1722550

Moher, D., Liberati, A., Tetzlaff, J., and Altman, D. G. (2009). Preferred Reporting Items for Systematic Reviews and Meta–Analyses: the PRISMA Statement. *BMJ* 339 (4), b2535–9. doi:10.1136/bmj.b2535

Morvaridzadeh, M., Nachvak, S. M., Mohammadi, R., Moradi, S., Mostafai, R., Pizarro, A. B., et al. (2021). Probiotic Yogurt Fortified with Vitamin D Can Improve Glycemic Status in Non–alcoholic Fatty Liver Disease Patients: a Randomized Clinical Trial. *Clin. Nutr. Res.* 10 (1), 36–47. doi:10.7762/cnr.2021.10.1.36

Mouodi, M., Fakheri, H. T., Kashi, Z., Maleki, I., and Mohammadpour, R. (2018). Effects of Vitamin D Supplementation on Patients with Non–alcoholic Fatty Liver Disease (NAFLD). *Acta Med.* 34, 415.

Nadjarzadeh, A., Jani, N., Khoshnevisan, M., Molajaafari, A., Fallahzadeh, H., Khabiri, F., et al. (2016). Effects of Low Caloric Diet with and without Vitamin D Supplementation on Anthropometric Parameters in Patients with Non–alcoholic Fatty Liver. *Tolooebehdasht* 14 (6), 410–422.

Nakano, T., Cheng, Y. F., Lai, C. Y., Hsu, L. W., Chang, Y. C., Deng, J. Y., et al. (2011). Impact of Artificial Sunlight Therapy on the Progress of Non–alcoholic Fatty Liver Disease in Rats. *J. Hepatol.* 55 (2), 415–425. doi:10.1016/j.jhep.2010.11.028

Nikooyeh, B., and Neyestani, T. R. (2021). Can Vitamin D Be Considered an Adiponectin Secretagogue? A Systematic Review and Meta–Analysis. *J. Steroid Biochem. Mol. Biol.* 212, 105925. doi:10.1016/j.jsbmb.2021.105925

Patel, P., Poretsky, L., and Liao, E. (2010). Lack of Effect of Subtherapeutic Vitamin D Treatment on Glycemic and Lipid Parameters in Type 2 Diabetes: a Pilot Prospective Randomized Trial. *J. Diabetes* 2 (1), 36–40. doi:10.1111/j.1753–0407.2009.00057.x

Petta, S., Gastaldelli, A., Rebelos, E., Bugianesi, E., Messa, P., Miele, L., et al. (2016). Pathophysiology of Non Alcoholic Fatty Liver Disease. *Int. J. Mol. Sci.* 17 (12), 2082. doi:10.3390/ijms17122082

Pittas, A. G., Harris, S. S., Stark, P. C., and Dawson, B. H. (2007). The Effects of Calcium and Vitamin D Supplementation on Blood Glucose and Markers of Inflammation in Nondiabetic Adults. *Diabetes care* 30 (4), 980–986. doi:10.2337/dc06–1994

Sakpal, M., Satsangi, S., Mehta, M., Duseja, A., Bhadada, S., Das, A., et al. (2017). Vitamin D Supplementation in Patients with Nonalcoholic Fatty Liver Disease: A Randomized Controlled Trial. *JGH Open* 1 (2), 62–67. doi:10.1002/jgh3.12010

Sarathy, H., Pramanik, V., Kahn, J., Abramowitz, M. K., Meier, K., Kishore, P., et al. (2015). The Effects of Short–Term Vitamin D Supplementation on Glucose Metabolism in Dialysis Patients: a Systematic Review and Meta–Analysis. *Int. Urol. Nephrol.* 47 (3), 537–549. doi:10.1007/s11255–015–0909–0

Schwimmer, J. B., Behling, C., Newbury, R., Deutsch, R., Nievergelt, C., Schork, N. J., et al. (2005). Histopathology of Pediatric Nonalcoholic Fatty Liver Disease. *Hepatology* 42 (3), 641–649. doi:10.1002/hep.20842

Sepidarkish, M., Farsi, F., Akbari, M. F., Namazi, N., Almasi, A. H., Maleki, A. H., et al. (2019). The Effect of Vitamin D Supplementation on Oxidative Stress Parameters: a Systematic Review and Meta–Analysis of Clinical Trials. *Pharmacol. Res.* 139, 141–152. doi:10.1016/j.phrs.2018.11.011

Sharifi, N., Amani, R., Hajiani, E., and Cheraghian, B. (2014). Does Vitamin D Improve Liver Enzymes, Oxidative Stress, and Inflammatory Biomarkers in Adults with Non–alcoholic Fatty Liver Disease? A Randomized Clinical Trial. *Endocrine* 47 (1), 70–80. doi:10.1007/s12020–014–0336–5

Sharifi, N., Amani, R., Hajiani, E., and Cheraghian, B. (2016). Women May Respond Different from Men to Vitamin D Supplementation Regarding Cardiometabolic Biomarkers. *Exp. Biol. Med. (Maywood)* 241 (8), 830–838. doi:10.1177/1535370216629009

Shidfar, F., Mousavi, S. N., Lorvand, H. A., Agah, S., Hoseini, S., and Hajimiresmail, S. J. (2019). Reduction of Some Atherogenic Indices in Patients with Non–alcoholic Fatty Liver by Vitamin D and Calcium Co–supplementation: a Double Blind Randomized Controlled Clinical Trial. *Iran J. Pharm. Res.* 18 (1), 496–505.

Targher, G., Bertolini, L., Rodella, S., Zoppini, G., Scala, L., Zenari, L., et al. (2006). Associations between Plasma Adiponectin Concentrations and Liver Histology in Patients with Nonalcoholic Fatty Liver Disease. *Clin. Endocrinol. (Oxf)* 64 (6), 679–683. doi:10.1111/j.1365–2265.2006.02527.x

Taghvaei, T., Akha, O., Mouodi, M., Fakheri, H. T., Kashi, Z., Maleki, I., Mohammadpour, R., et al. (2018). Effects of Vitamin D Supplementation on Patients with Non-Alcoholic Fatty Liver Disease (NAFLD). *Acta Medica.* 34 (415). doi:10.19193/0393-6384_2018_2_66

Tolman, K. G., Fonseca, V., Dalpiaz, A., and Tan, M. H. (2007). Spectrum of Liver Disease in Type 2 Diabetes and Management of Patients with Diabetes and Liver Disease. *Diabetes care* 30 (3), 734–743. doi:10.2337/dc06–1539

Wang, H., Xia, N., Yang, Y., and Peng, D. Q. (2012). Influence of Vitamin D Supplementation on Plasma Lipid Profiles: a Meta–Analysis of Randomized Controlled Trials. *Lipids Health Dis.* 11 (1), 42–49. doi:10.1186/1476–511X–11–42

Younossi, Z. M. (2019). Non–alcoholic Fatty Liver Disease – A Global Public Health Perspective. *J. Hepatol.* 70 (3), 531–544. doi:10.1016/j.jhep.2018.10.033

Conflict of Interest: The authors declare that the research was conducted in the absence of any commercial or financial relationships that could be construed as a potential conflict of interest.

Publisher's Note: All claims expressed in this article are solely those of the authors and do not necessarily represent those of their affiliated organizations, or those of the publisher, the editors and the reviewers. Any product that may be evaluated in this article, or claim that may be made by its manufacturer, is not guaranteed or endorsed by the publisher.

Copyright © 2021 Rezaei, Tabrizi, Nowrouzi-Sohrabi, Jalali, Shabani-Borujeni, Modaresi, Gholamalizadeh and Doaei. This is an open-access article distributed under the terms of the Creative Commons Attribution License (CC BY). The use, distribution or reproduction in other forums is permitted, provided the original author(s) and the copyright owner(s) are credited and that the original publication in this journal is cited, in accordance with accepted academic practice. No use, distribution or reproduction is permitted which does not comply with these terms.

frontiers | Frontiers in Pharmacology

ORIGINAL RESEARCH
published: 31 May 2022
doi: 10.3389/fphar.2022.677738

Inflammatory-Dependent Bidirectional Effect of Bile Acids on NLRP3 Inflammasome and Its Role in Ameliorating CPT-11-Induced Colitis

Chuyao Liao, Di Wang, Siyuan Qin, Ying Zhang, Jie Chen, Ruijie Xu, Fengguo Xu and Pei Zhang**

Key Laboratory of Drug Quality Control and Pharmacovigilance (Ministry of Education), State Key Laboratory of Natural Medicine, China Pharmaceutical University, Nanjing, China

Irinotecan (CPT-11) in combination with 5-fluorouracil and leucovorin is a first-line chemotherapy regimen for the treatment of colorectal cancer; however, its clinical application is limited by the dose-limiting gastrointestinal toxicity of colitis. In our previous studies, several bile acids (BAs) were found significantly elevated in the colon of the CPT-11-induced rat colitis model. On the other hand, NLRP3 inflammasome has been reported to play important roles in mediating colitis. Interestingly, BA was stated to activate the NLRP3 inflammasome in some studies, while in some other reports, it showed an inhibitory effect. We assumed that the inflammatory status in different circumstances might have contributed to the controversial findings. In this study, we first discovered, under non-inflammatory conditions, that supplementing BA could activate the NLRP3 inflammasome in THP-1-differentiated macrophages and promote inflammation. In lipopolysaccharide (LPS)-induced inflammatory macrophages, however, BA inhibited the NLRP3 inflammasome and reduced inflammation. Further experiments demonstrated that Takeda G protein-coupled receptor 5 (TGR5) is essential in mediating the inhibitory effect of BA, while phospho-SP1 (p-SP1) is key to the activation. Furthermore, we applied the above findings to ameliorate CPT-11-caused colitis in rats by inhibiting SP1 with mithramycin A (MitA) or activating TGR5 using oleanolic acid (OA). Our findings may shed light on the discovery of effective interventions for reducing dose-limiting chemotherapy-induced colitis.

Keywords: bile acid, NLRP3 inflammasome, Sp1, tgr5, CPT-11-induced colitis

OPEN ACCESS

Edited by:
Raquel Abalo,
Rey Juan Carlos University, Spain

Reviewed by:
Michele Biagioli,
University of Perugia, Italy
Changcheng Zhang,
Three Gorges University, China

****Correspondence:***
Pei Zhang
peizhang@cpu.edu.cn
Fengguo Xu
fengguoxu@cpu.edu.cn

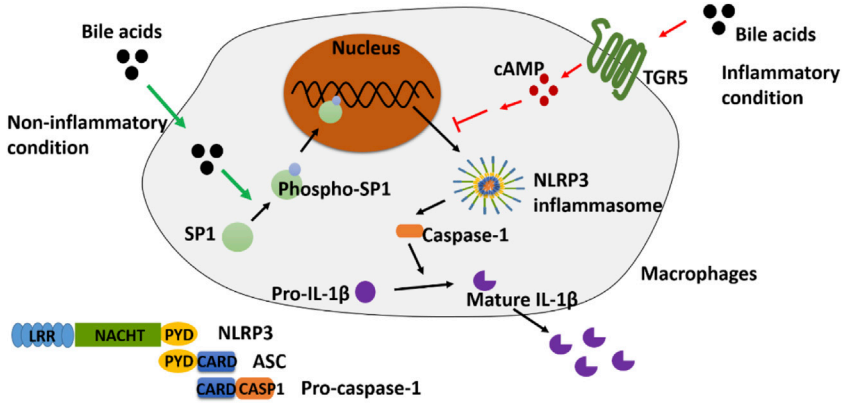
Specialty section:
This article was submitted to Gastrointestinal and Hepatic Pharmacology, a section of the journal Frontiers in Pharmacology

Received: *08 March 2021*
Accepted: *12 April 2022*
Published: *31 May 2022*

Citation:
Liao C, Wang D, Qin S, Zhang Y, Chen J, Xu R, Xu F and Zhang P (2022) Inflammatory-Dependent Bidirectional Effect of Bile Acids on NLRP3 Inflammasome and Its Role in Ameliorating CPT-11-Induced Colitis. Front. Pharmacol. 13:677738. doi: 10.3389/fphar.2022.677738

INTRODUCTION

Bile acids (BAs) are hydroxylated steroids, synthesized from cholesterol in the liver. They play important roles in regulating lipid, glucose, and energy metabolism (McGlone and Bloom, 2019). Disorders in BA homeostasis are associated with cholestatic liver diseases, dyslipidemia, fatty liver diseases, cardiovascular diseases, and diabetes (Chiang, 2013). BA dysregulation is also found closely related to intestinal diseases, such as inflammatory bowel disease and diarrhea (Vítek, 2015; Vijayvargiya and Camilleri, 2019; Sinha et al., 2020). In colitis, the metabolic disorder of BA is an important risk factor for inflammation. These effects of BA are mostly accomplished by simulating its receptors such as BA-activated receptors, especially Farnesoid X receptor (FXR),



GRAPHICAL ABSTRACT |

TGR5, and sphingosine-1-phosphate receptor 2 (S1PR2) (Biagioli and Carino, 2017; Hou et al., 2018; Zhao et al., 2018). For example, it was reported that BA can exacerbate colitis by up-regulating S1PR2 in mice (Zhao et al., 2018). However, there are also studies showing that the activation of TGR5 and FXR can lead to an anti-inflammatory effect (Chávez-Talavera et al., 2017; Hou et al., 2018).

In the interaction between BA and inflammation, the role of NLRP3 inflammasome is widely recognized. However, there are controversies about the effect of BA on the NLRP3 inflammasome. Many studies claimed that BA could activate NLRP3 inflammasome (Gong et al., 2016; Zhao et al., 2016; Hao et al., 2017), while others concluded that BA had an inhibitory effect on NLRP3 inflammasome (Guo et al., 2016a). For example, Wang et al. reported that most BA including cholic acid (CA), glycocholic acid (GCA), chenodeoxycholic acid (CDCA), deoxycholic acid (DCA), ursodeoxycholic acid (UDCA), lithocholic acid (LCA), and taurolithocholic acid (TLCA) could significantly inhibit nigericin-induced NLRP3 inflammasome activation and IL-1β production in macrophages via the TGR5–cAMP–PKA axis (Guo et al., 2016a), while Gonzalez et al. demonstrated that CDCA and DCA promoted NLRP3 inflammasome activation and IL-1β production in various types of macrophages (Hao et al., 2017). The key factors contributing to the opposite effect of BA on NLRP3 inflammasome as well as the underlying mechanism remain elusive.

CPT-11, known as a chemotherapeutic agent, is a selective inhibitor of DNA topoisomerase I. The combination of CPT-11 with 5-fluorouracil and leucovorin is the first-line chemotherapy for the treatment of metastatic colorectal cancer (Sears et al., 1999; Sandmeier et al., 2005). However, CPT-11 could cause severe gastrointestinal toxicity including colitis, which greatly limited its clinical use (Sandmeier et al., 2005; Wang et al., 2020). In our previous metabolomics studies, we found that the metabolism of BA was disturbed in CPT-11-induced colitis in rats, manifested by the significant up-regulated levels of CDCA, DCA, GDCA, and TDCA in the colon tissue (Wang et al., 2015). On the other hand, recent studies indicate that NLRP3 inflammasome plays an essential role in colitis induced by CPT-11, and there is evidence showing that CPT-11 could activate NLRP3 inflammasome and cause inflammation both *in vitro* and *in vivo* (Li et al., 2015; Huang et al., 2020).

In the current study, in light of the vital role of BA in colitis, we investigated the potential mechanism underlying the aforementioned conflicting effect of BA on the NLRP3 inflammasome. As studies have reported, the release of inflammatory factors (for example, TNF-α, IL-6, and IL-1β) can be extensively promoted by LPS stimulation in phorbol 12-myristate 13-acetate (PMA)-differentiated THP-1 cells (Zou et al., 2017; Zhao D. et al., 2019). In the current study, "inflammatory condition" or "non-inflammatory condition" was defined to distinguish the state of THP-1-induced macrophages that receive LPS stimulation or not, respectively. We found that BA could activate NLRP3 inflammasome via promoting p-SP1 under non-inflammatory conditions, while under inflammatory conditions, BA promoted the expression of TGR5 and led to the inhibition of the NLRP3 inflammasome *in vitro*. Utilizing these findings, *in vivo* experiments were designed, and the results showed that the colitis caused by CPT-11 was remarkably ameliorated with the inhibition of SP1 or activation of TGR5. Taken together, our findings may assist in discovering effective interventions for reducing chemotherapy-induced colitis.

MATERIALS AND METHODS

Chemicals and Reagents

DCA, CDCA, GDCA, and PMA were purchased from Sigma-Aldrich (St. Louis, MO, United States). TDCA was purchased from J&K (Manhattan, NY, United States). MitA and SBI-115 were purchased from MedChemExpress (Monmouth Junction, NJ, United States). OA was purchased from Aladdin ® (Los Angeles, CA, United States). Roswell Park Memorial Institute (RPMI) 1640 medium and fetal bovine serum were purchased from Gibco (Grand Island, NY, United States). HEPES buffer was purchased from Boster (Wuhan, China). Anti-NLRP3 (Lot#:

19771-1-AP), anti-caspase-1/p20/p10 (#:22915-1-AP), anti-SP1 (Lot#: 21962-1-AP), anti-β-actin (Lot#: 66009-1-Ig), and HRP-conjugated beta actin monoclonal antibody (Lot#: HRP-60008) were obtained from Proteintech (Chicago, IL, United States). Anti-p-SP1 (Lot#: AF3121) was obtained from Affinity (Affinity Biosciences, United States). Anti-GPBAR1 (Lot#: BS60582) was purchased from Bioworld Technology (MN, United States). Anti-Pro-IL-1β (Lot#: WL02257) and anti-mature-IL-1β (Lot#: WL00891) were purchased from Wanleibio (Shenyang, China). Radioimmunoprecipitation (RIPA) buffer, bicinchoninic acid (BCA) protein assay kit, and loading buffer were purchased from Beyotime Biotechnology (Shanghai, China). Phenylmethylsulfonyl fluoride (PMSF) was purchased from Thermo Fisher Scientific (Waltham, MA, United States). RNAiso Plus and PrimeScript™ RT reagent Kit were purchased from TaKaRa (TaKaRa Biotechnology, Dalian, China). IL-1β, IL-6, and TNF-α enzyme-linked immunosorbent assay (ELISA) kits were purchased from 4A Biotech (Co., Ltd., Beijing, China). ELISA kit for the measurement of cyclic AMP (cAMP) was purchased from GenScript (Nanjing, China).

Cell Culture

THP-1 cells were cultured in RPMI 1640 medium supplemented with 10% fetal bovine serum, 1× HEPES buffer, 100 U/ml of penicillin, and 100 μg/ml of streptomycin. THP-1 monocytes were differentiated into macrophages by stimulating with 100 ng/ml of PMA for 48 h. The cells were then cultured in a serum-free medium for 24 h to enhance the differentiation.

Cell Viability Assay

THP-1 monocytes were seeded into 96-well plates at a density of 3×10^5 cells/well. After differentiation, cells were exposed to BA or cell culture medium as vehicle for 48 h. Cell viability was measured by the 3-(4,5-dimethylthiazol-2-yl)-2,5-diphenyl-2H-tetrazolium bromide (MTT) assay.

Animal Experiments and Sample Collection

Fifty healthy 6–8-week-old male specific-pathogen-free Sprague-Dawley rats weighing 180–200 g were purchased from Vital River Laboratory Animal Technology Co., Ltd. (Pinghu, China, Permission No. SCXK (Zhe) 2019-0001). The animals were housed in a temperature-controlled environment (24 ± 2°C) with a standard rodent diet under a 12 h/12 h-dark/light cycle. All animal studies and procedures were conducted in accordance with the United States National Institutes of Health Guide for the Care and Use of Laboratory Animals and approved by the Animal Ethics Committee of China Pharmaceutical University (License No. SYXK 2018-0019).

After a week of acclimatization, the animals were randomly divided into five groups (n = 10) including the control, model, MitA, OA, and MitA+OA groups. The detailed procedure of the animal experiment can be found in **Supplementary Figure S1**. Briefly, the individuals in the MitA+OA group were injected with MitA (intraperitoneally, 0.15 mg/kg) (Wei et al., 2016) and OA (intragastrically, 100 mg/kg) for five consecutive days from day 1 and CPT-11 (intravenously, 120 mg/kg) each day for two consecutive days from day 2. For the MitA group, the administration was similar to that of the MitA+OA group except that 0.5% CMC-Na (solvent of OA) was given instead of OA. Similarly, normal saline (solvent of MitA) was given to the OA individuals instead of MitA and the rest was in accordance with the MitA+OA group. Individuals in the model group were receiving equivalent 0.5% CMC-Na and normal saline, and CPT-11. In addition, 0.5% CMC-Na, normal saline and the solvent of CPT-11 (Trifan et al., 2002; Mego et al., 2015) were administered to the individuals in the control group as vehicle.

The diarrhea score of each animal was monitored twice a day referring to the scoring criteria in the existing literature (Kurita et al., 2000). The colon tissue was collected on day 6. After being drained of feces, the colon tissue was washed with normal saline, and then a portion of the proximal colon of each rat was fixed in 10% formalin for histological examination and the rest (middle and distal) were stored at −80°C for Western blotting and ELISA analysis.

Enzyme-Linked Immunosorbent (ELISA) Assay

The contents of cAMP, IL-1β, IL-6, and TNF-α in cell culture supernatants or colon tissue homogenates were quantified by ELISA kits according to the manufacturer's instructions.

Western Blotting

Mature-IL-1β, pro-IL-1β, caspase-1, NLRP3, SP1, p-SP1, TGR5 (GPBAR1), and β-actin expression were analyzed using standard Western blotting protocols. Cells and tissues were lysed by RIPA buffer containing 1 mmol/L of PMSF, and total proteins were extracted according to the manufacturer's protocols. Then, the protein concentration was measured using the BCA protein assay kit. Proteins (30 μg) were separated by SDS-polyacrylamide and transferred to polyvinylidene difluoride membranes (0.2 μm, Millipore, MA, United States). The membranes were blocked with 5% (w/v) nonfat milk for 2 h at room temperature and incubated with primary antibodies at 4°C overnight. After being washed three times with PBST, the membranes were incubated with secondary antibodies conjugated to horseradish peroxidase for approximately 1.5 h at room temperature. Then, the immunoreactive bands were visualized using enhanced chemiluminescence (ECL) (Millipore) by a Tanon 5200 chemiluminescent imaging system (Tanon Science and Technology). The relative protein expression was calculated by densitometric analysis using ImageJ software.

mRNA Preparation and qRT-PCR

Total RNA was extracted from THP-1 monocytes using RNAiso Plus Kit. Then, the RNA concentration was measured by a Nano-Drop 2000 (Thermo Fisher Scientific, Waltham, MA, United States). Complementary DNA (cDNA) was obtained by reverse transcription with the PrimeScript™ RT Reagent Kit. Subsequently, qRT-PCR was performed using SYBR Green I Master (Roche Diagnostics, Basel, Switzerland) on a LightCycler 480 (Roche) following the manufacturer's instructions. The sequences of the PCR primers used are as follows: IL-1β forward 5′-ATGATGGCT TATTACAGTGGCAA-3′ and reverse 5′-GTCGGAGATTCGTAG

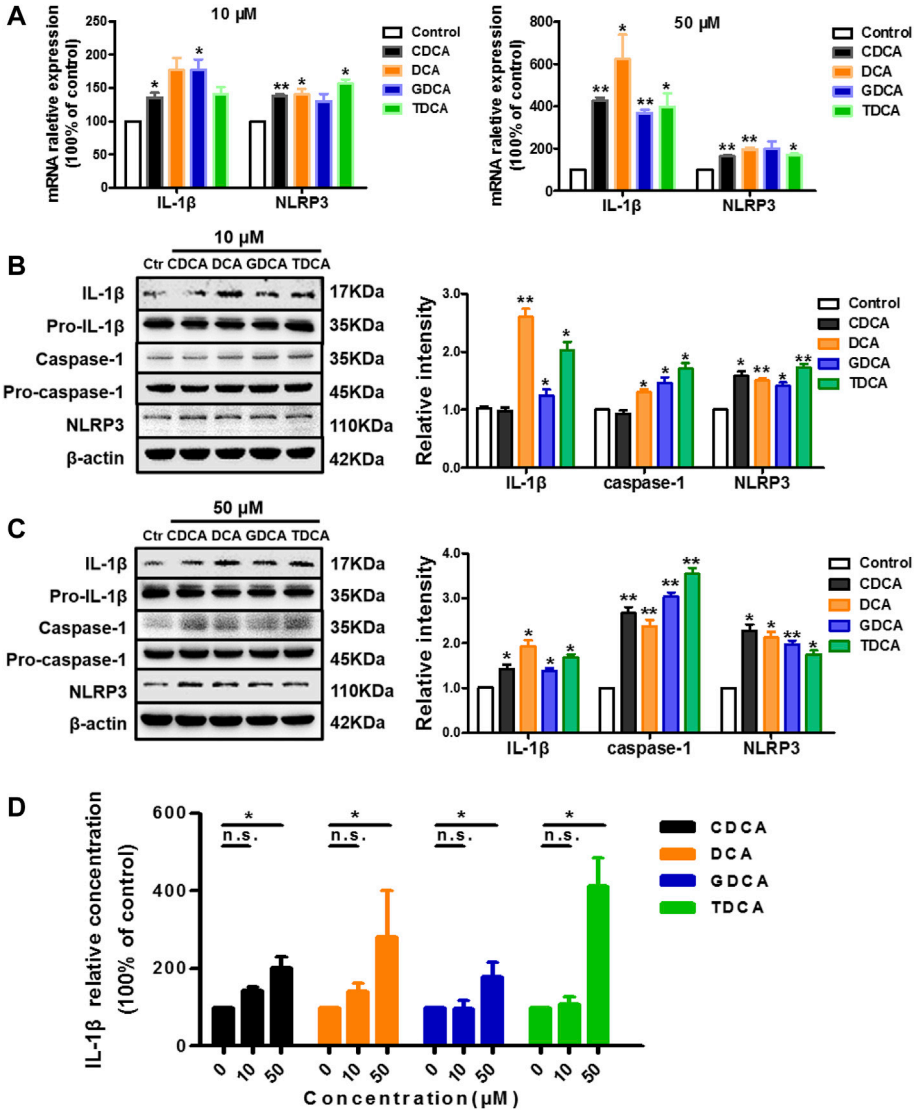


FIGURE 1 | BAs activate NLRP3 inflammasome in non-inflammatory conditions in macrophages. **(A)** Relative mRNA expression of NLRP3 and IL-1β with the treatment of BA at 10 or 50 μM. IL-1β, caspase-1, and NLRP3 protein levels with the treatment of BA at **(B)** 10 μM and **(C)** 50 μM. **(D)** ELISA analysis of IL-1β in culture medium after treating with BAs at 10 and 50 μM. Data are presented as mean ± SD ($n = 3$). Statistical analysis was performed using Student's *t* test (*$p < 0.05$, **$p < 0.01$, and n.s., not significant).

CTGGA-3′; NLRP3 forward 5′-CGTGAGTCCCATTAAGATGGA GT-3′ and reverse 5′-CCCGACAGTGGATATAGAACAGA-3′'; and β-actin forward 5′-ATTGCCGACAGGATGCAGAA and reverse 5′-GCTGATCCACATCTGCTGGAA-3′. Results were normalized to the internal control β-actin, and the expression was calculated by the $2^{-\triangle\triangle CT}$ method (Khan-Malek and Wang, 2017).

Statistical Analysis

Statistical analysis was performed using GraphPad Prism 5.0 software (GraphPad Software Inc., La Jolla, CA, United States). All *in vitro* experiments were repeated at least three times independently with at least three replicates, and the results were presented as mean ± standard deviation (SD) unless otherwise specified. Independent unpaired two-tailed Student's *t*-test was performed to evaluate the differences between two groups, and one-way analysis of variance with Bonferroni correction was performed for multiple comparisons. $p < 0.05$ was considered statistically significant. The survival rate was summarized by Kaplan–Meier survival curves.

RESULTS

BAs Activate NLRP3 Inflammasome in Non-Inflammatory Conditions

To assess the effects of the four BAs on NLRP3 inflammasome in non-inflammatory conditions, we treated macrophages differentiated from THP-1 monocytes for 4 h with 10 and 50 μM of CDCA, DCA, GDCA, or TDCA. The concentrations were selected according to the

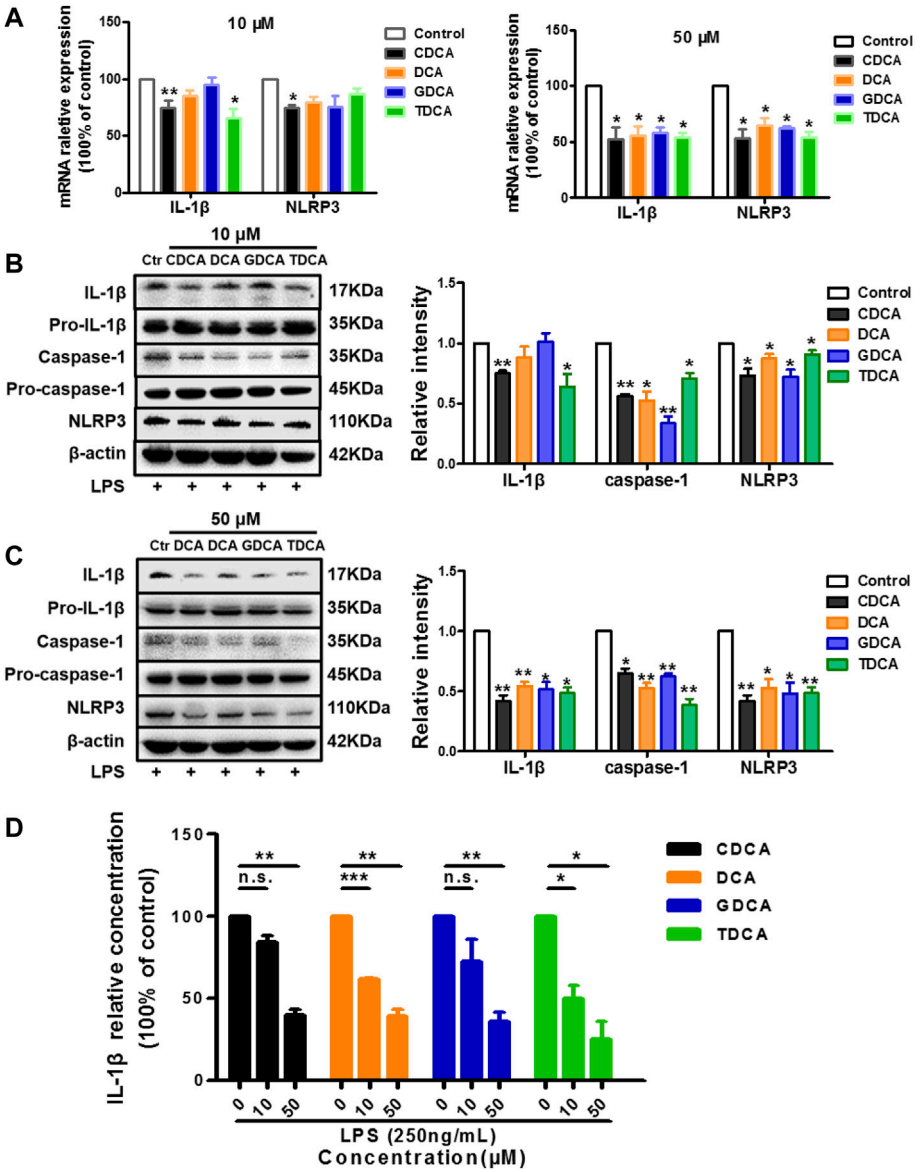


FIGURE 2 | BAs inhibit NLRP3 inflammasome in inflammatory conditions in macrophages. Prior to the BA treatment, cells were pretreated with 250 ng/ml LPS for 1 h. **(A)** Relative mRNA expression of NLRP3 and IL-1β with BAs at 10 or 50 μM. IL-1β, caspase-1, and NLRP3 protein levels after treating with BAs at 10 μM **(B)** and **(C)** 50 μM. **(D)** IL-1β in culture medium after treating with BAs at 10 and 50 μM. Data are presented as mean ± SD ($n = 3$). Statistical analysis was performed using Student's t test (*$p < 0.05$, **$p < 0.01$, ***$p < 0.001$, and n.s., not significant).

published data (Guo et al., 2016a; Hao et al., 2017) and our cell viability assay results (**Supplementary Figure S2A**). At a concentration of 10 μM, CDCA and GDCA activated the mRNA expression of IL-1β; however, DCA, GDCA, and TDCA significantly activated the expression of IL-1β and caspase-1 in protein, while CDCA hardly showed activating effects on it (**Figures 1A,B**). When the concentration was increased to 50 μM, all BAs remarkably increased the mRNA and protein expression of IL-1β, as well as caspase-1 protein expression (**Figures 1A,C**). Little impact on pro-IL-1β and pro-caspase-1 was observed (**Figures 1B,C**). Besides, all BAs activated NLRP3 protein expression at both 10 and 50 μM (**Figures 1B,C**), although GDCA failed to present a significant promoting effect on the mRNA expression of NLRP3 (**Figure 1A**). Moreover, the IL-1β level in the culture medium also increased with the BA treatment, especially at 50 μM (**Figure 1D**). These results suggested that BA can activate the NLRP3 inflammasome and show a pro-inflammatory effect in non-inflammatory conditions.

BAs Inhibit NLRP3 Inflammasome in Inflammatory Conditions

As reported in the existing literature, LPS incubation with macrophages differentiated from THP-1 monocytes could lead to a sharp increase in inflammatory factors (Kuijk et al., 2008; Zhao D. et al., 2019; Zhao W.

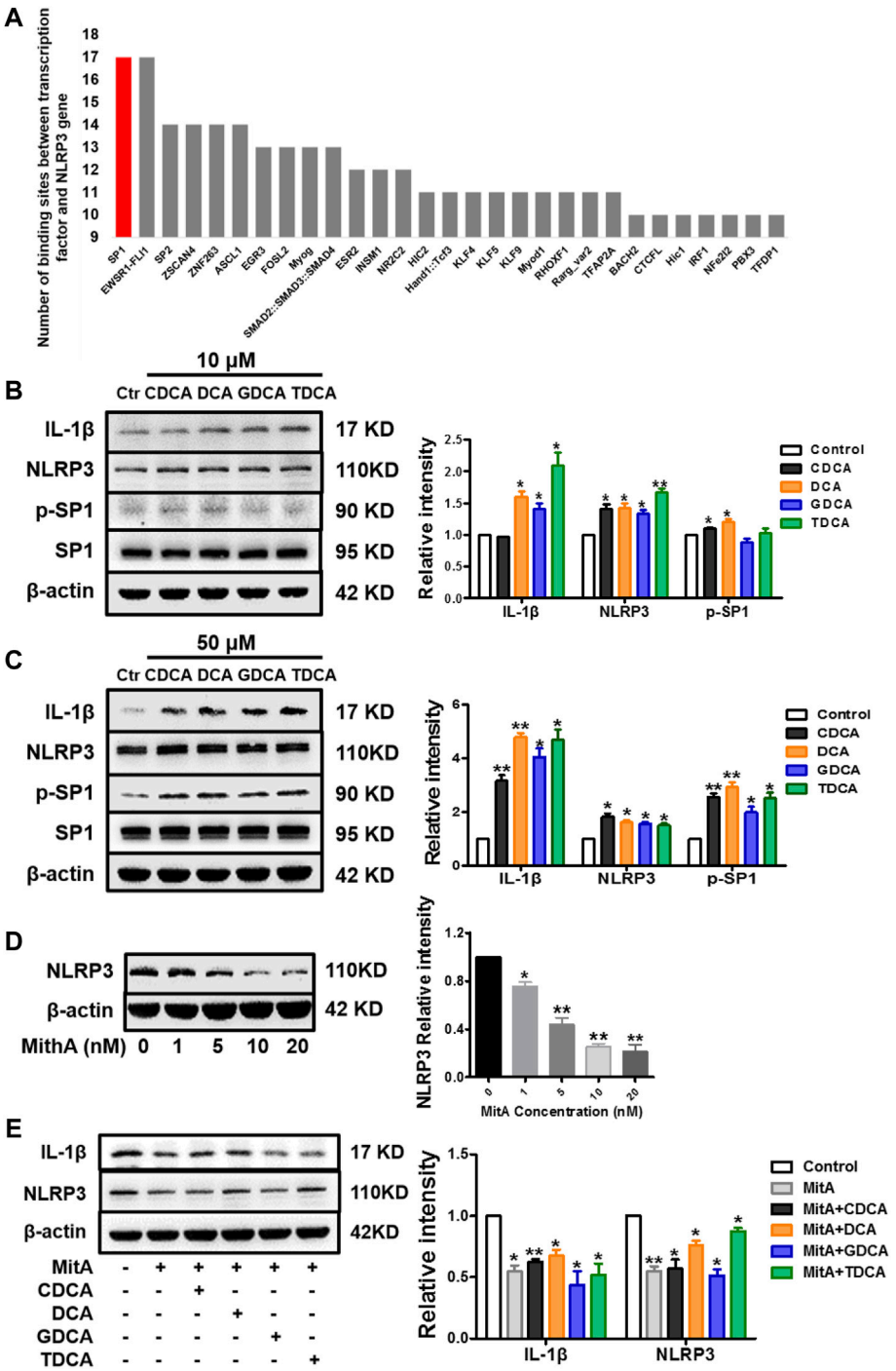


FIGURE 3 | SP1 mediates the activation of NLRP3 inflammasome in non-inflammatory conditions in macrophages. **(A)** Ranking of binding sites between different transcription factors and NLRP3 gene (data were from the eukaryotic promoter database, from −2,000 to 100 bp relative to TSS, and the cut-off was $p = 0.001$) (https://epd.epfl.ch). Western blot analysis of IL-1β, NLRP3, and SP1 in macrophages differentiated from THP-1 monocytes with **(B)** 10 μM and **(C)** 50 μM BA treatments for 4 h. **(D)** NLRP3 expression analyzed by Western blot with different concentrations of MitA for 48 h. **(E)** Western blot analysis of IL-1β and NLRP3 after cells were pretreated with 10 nM of MitA for 48 h prior to the stimulation with BAs at 50 μM for 4 h. Data are presented as mean ± SD ($n = 3$). Statistical analysis was performed using Student's t test (*$p < 0.05$, **$p < 0.01$).

et al., 2019). Our pre-experiments also confirmed this (data not shown). Therefore, to establish an inflammatory condition, we pretreated the macrophages differentiated from THP-1 monocytes with 250 ng/ml of LPS for 1 h before BA stimulation. Opposite to what we observed in non-inflammatory conditions, 10 μM of CDCA and TDCA inhibited IL-1β on mRNA and protein level (**Figures 2A,B**). Although only

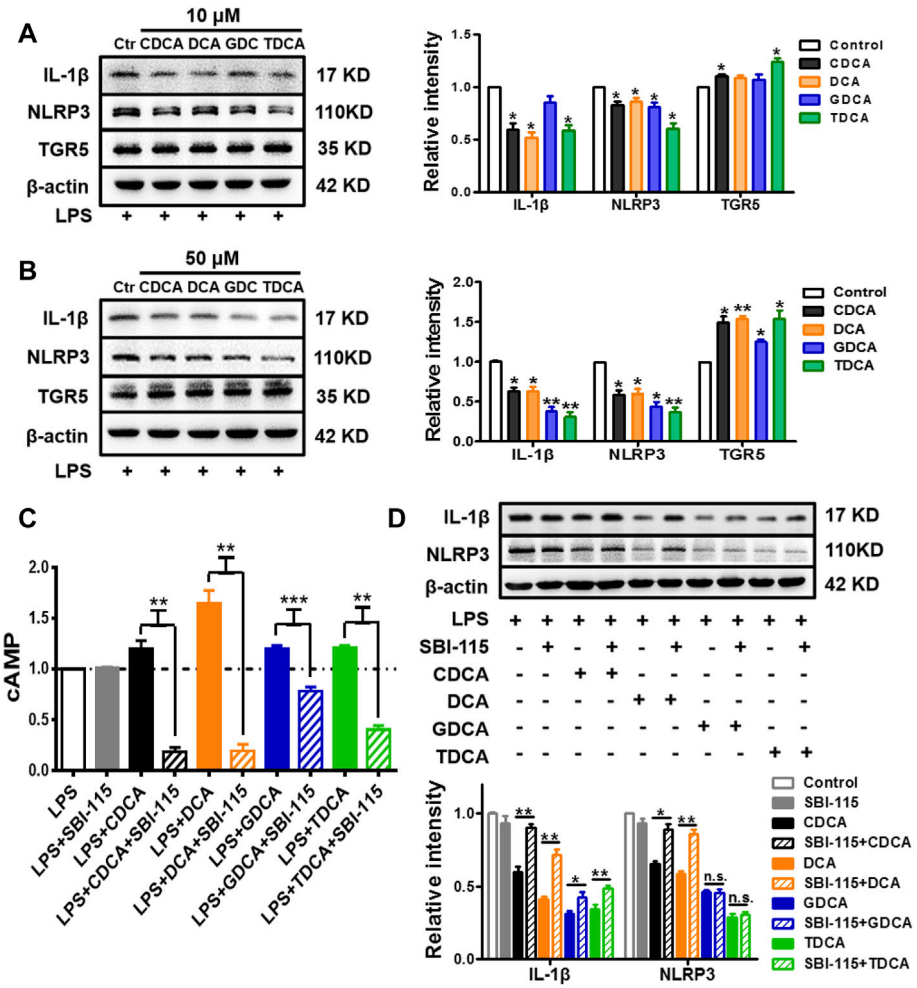


FIGURE 4 | TGR5 participates in the inhibition of NLRP3 inflammasome in inflammatory conditions in macrophages. IL-1β, NLRP3, and TGR5 expressions determined by Western blotting. The cells were pretreated with 250 ng/ml of LPS for 1 h and stimulated with BAs at **(A)** 10 μM and **(B)** 50 μM for 3 h. LPS-pretreated macrophages were treated with 100 μM of SBI-115 and 50 μM of BAs, and the supernatants and lysates were prepared. **(C)** Level of cAMP in the supernatants analyzed by ELISA. **(D)** IL-1β and NLRP3 expression in the lysates. Data are presented as mean ± SD ($n = 3$). Statistical analysis was performed using Student's t test (*$p <$ 0.05, **$p < 0.01$, and ***$p < 0.001$).

CDCA showed a significant inhibitory effect on the NLRP3 mRNA expression, all the BAs significantly inhibited NLRP3 protein at 10 μM (**Figures 2A,B**). At a concentration of 50 μM, all BAs could significantly inhibit the mRNA and protein expressions of IL-1β and NLRP3 (**Figures 2A,C**). Besides, pro-IL-1β and pro-caspase-1 were barely affected, while caspase-1 was inhibited by BA at both 10 and 50 μM (**Figures 2B,C**). Furthermore, all BAs showed a restraint effect on the levels of IL-1β in the culture medium (**Figure 2D**). These results suggest that BA can inhibit the NLRP3 inflammasome and show an anti-inflammatory effect in inflammatory conditions.

SP1 Mediates the Activation of NLRP3 Inflammasome in Non-Inflammatory Conditions

SP1 is one of the transcription factors of the NLRP3 gene with the highest score based on the number of binding sites (**Figure 3A**). Therefore, we investigated whether SP1 is essential in mediating the activation process. Interestingly, we found that p-SP1 was significantly promoted by BA in non-inflammatory conditions, especially at 50 μM, which shared a similar trend with IL-1β and NLRP3. However, there were no obvious changes in SP1 with both 10 and 50 μM of BA (**Figures 3B,C**). Then, we stimulated macrophages with a series of concentrations of MitA (according to **Supplementary Figure S2B**), a selective inhibitor of SP1. The results show that MitA (<10 nM) could inhibit NLRP3 in a dose-dependent manner (**Figure 3D**). Moreover, after 48 h of pretreatment with MitA (Seznec et al., 2011; Liu et al., 2018), the NLRP3 inflammasome activation induced by BA was reversed (**Figure 3E**), indicating that SP1 mediates the activation of NLRP3 by BA in non-inflammatory conditions. We also determined the levels of SP1 and p-SP1 in inflammatory conditions with BA treatment, and a very

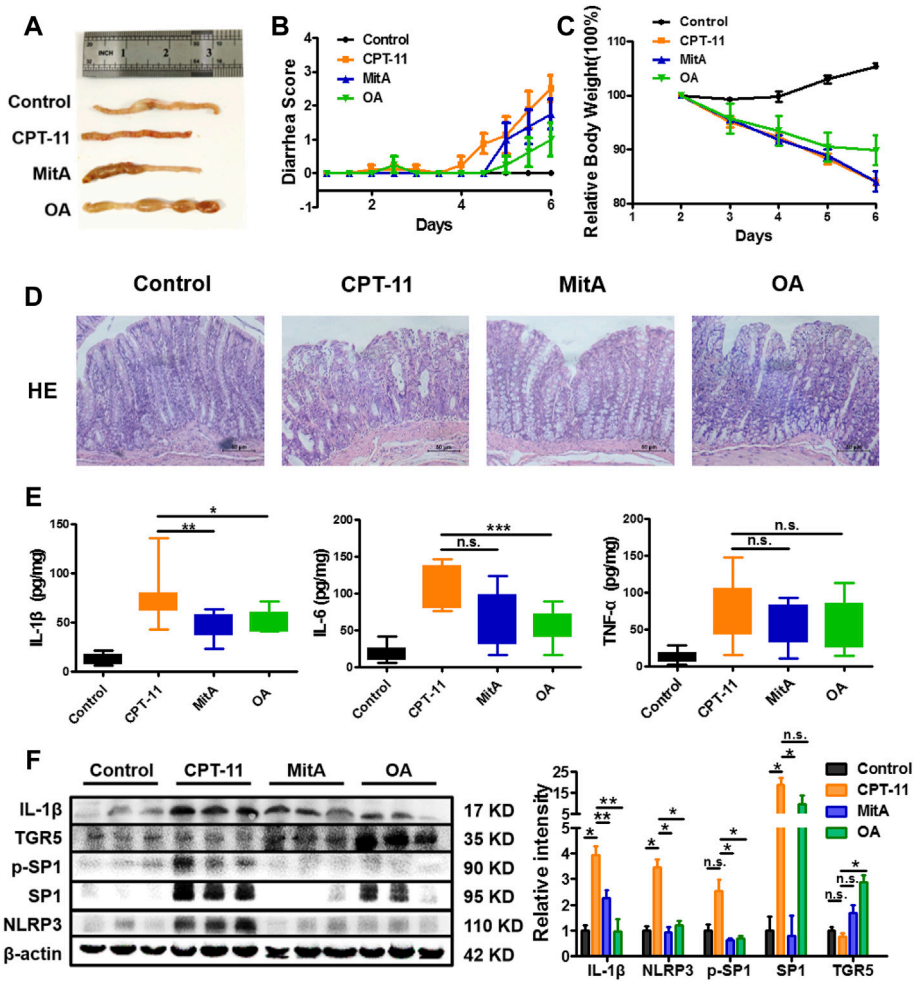


FIGURE 5 | Amelioration of the CPT-11-induced diarrhea in rats. **(A)** Representative images of colon tissues from each group at the last experimental day. **(B)** The diarrhea score of each rat was monitored twice daily and is presented as mean ± SD (n = 8). **(C)** The change of the relative body weight of rats in different groups upon CPT-11 administration. **(D)** HE staining was performed on rat colon after drug administration (at ×200 magnification). **(D)** IL-6, IL-1β, and TNF-a levels in rat colons. **(E)** Expression of IL-1β, NLRP3, TGR5, SP1, and phospho-SP1 in rat colons determined by Western blotting. Data are presented as mean ± SD (n = 3). Statistical analysis was performed using Student's t test (*p < 0.05, **p < 0.01, ***p < 0.001, and n.s., not significant; the statistical analysis results in panels **(B,C)** can be found in **Supplementary Tables S1 and S2**).

mild increase of p-SP1 was observed compared to that in non-inflammatory conditions (**Supplementary Figure S3A**).

TGR5 Participates in the Inhibition of NLRP3 Inflammasome Under Inflammatory Conditions

As previous studies suggested, BA can inhibit the activation of NLRP3 inflammasome via TGR5 signaling (Guo et al., 2016a). In the present study, we confirmed that in inflammatory circumstances induced by 250 ng/ml of LPS, BA promoted the expression of TGR5 and inhibited the expression of IL-1β and NLRP3 at the same time (**Figures 4A,B**). Then, 250 ng/ml of LPS-pretreated macrophages was simultaneously stimulated with BA and SBI-115, an antagonist of TGR5 (Masyuk et al., 2017) (**Supplementary Figure S2C**). As shown in **Figure 4C**, 100 μM of SBI-115 could reverse the increase of the cAMP content in the culture medium caused by BA. It is obvious that among the four BAs, DCA promoted cAMP most remarkably and SBI-115 showed the strongest effect against DCA (**Figure 4C**) as well, which is consistent with the previous findings that TGR5 is differentially activated by BA in the strength order of DCA > LCA > CDCA > CA (Guo et al., 2016b; Wahlström et al., 2016). Antagonizing TGR5 with SBI-115 offsets the inhibitory effect of BA, especially DCA and CDCA, on IL-1β and NLRP3 to some extent (**Figure 4D**), indicating that TGR5 is involved in the inhibition of NLRP3 inflammasome by BA in inflammatory conditions. The level of TGR5 was determined as well in non-inflammatory conditions after BA treatment, and the increase is very limited compared to that in inflammatory conditions (**Supplementary Figure S3B**).

Ameliorating CPT-11-Induced Colitis Utilizing Inflammatory-Dependent Bidirectional Effects of Bile Acids on NLRP3 Inflammasome

Based on what has been found *in vitro*, *in vivo* experiments were designed to confirm whether an anti-inflammatory effect can be achieved in CPT-11-induced colitis (**Supplementary Figure S1**). However, beyond our expectation, the combination of MitA and OA led to a much lower survival rate compared to the MitA or OA group (**Supplementary Figure S4**), making the statistical comparisons between MitA + OA and other groups difficult. Therefore, only the data of control, model, MitA, and OA groups are presented. Inflammation and hemorrhage in colon and watery stool were observed in the model group. Notably, SP1 inhibitor MitA or TGR5 agonist OA dramatically alleviated these adverse symptoms (**Figure 5A**). Besides, OA could significantly ameliorate the weight loss and diarrhea induced by CPT-11, while MitA hardly showed capability in this (**Figures 5B,C**). Histopathological examination showed that MitA and OA improved the colon damage and macrophage infiltration caused by CPT-11 (**Figure 5D** and **Supplementary Figure S5**). Moreover, we found that MitA had a stronger effect on IL-1β, while OA showed a more powerful action on IL-6, and both of them had a relatively weaker effect on TNF-α (**Figure 5E**).

To further clarify whether MitA and OA functioned via inhibiting SP1 or activating TGR5, we detected the expression of SP1, p-SP1, TGR5, IL-1β, and NLRP3 in the rat colons. The results showed that p-SP1 and SP1 were significantly inhibited in the MitA group compared with those in the model group, while TGR5 was significantly promoted in the OA group. Besides, IL-1β and NLPR3 were down-regulated in the groups of MitA and OA (**Figure 5F**). Taken together, our work demonstrated that SP1 and TGR5 could be promising intervention targets for alleviating chemotherapy-induced intestinal toxicity.

DISCUSSION

Emerging evidence has shown a strong association between BA and intestinal diseases. Importantly, almost all inflammatory intestinal diseases are accompanied with BA dysregulation (for example, inflammatory bowel disease (Zhou et al., 2014; Fitzpatrick and Jenabzadeh, 2020) and chemotherapy-induced colitis (Muls et al., 2016; Andreyev et al., 2021)). For example, previous studies have revealed the involvement of disturbed BA metabolism in CPT-11-induced colitis (Fang et al., 2016). On the other hand, inflammasomes, such as NLRP3 and AIM2, have been proved to play crucial roles in CPT-11-induced gastrointestinal toxicity (Li et al., 2015; Lian et al., 2017). Moreover, existing studies suggest that repressing NLRP3 inflammasome can ameliorate intestinal inflammatory injury (Gong et al., 2018; Shao et al., 2019; Cao et al., 2020) as well as CPT-11-induced colitis (Li et al., 2015; Huang et al., 2020). Therefore, it is essential to explore the BA–NLRP3 inflammasome axis in the CPT-11 intestinal injury. However, as mentioned before, there are controversial findings regarding the effect of BA on the NLRP3 inflammasome.

In this study, we discovered that BA could activate NLRP3 inflammasome through promoting the transformation of SP1 into p-SP1 under non-inflammatory conditions. SP1 is a transcription factor that is well known for its significant role in cell growth, differentiation, apoptosis, and carcinogenesis (Beishline and Azizkhan-Clifford, 2015; Vizcaíno et al., 2015). Its encoded proteins are involved in many essential cellular processes such as cell differentiation and immune responses (Vellingiri et al., 2020). According to existing studies, multiple post-translational modifications could mediate SP1 activation (Higuchi et al., 2004; González-Rubio et al., 2015) including phosphorylation, O-linked glycosylation, acetylation, SUMOylation, or ubiquitylation (Beishline and Azizkhan-Clifford, 2015), in which BA might be involved. On the other hand, SP1 also correlates to colorectal cancer (Chen et al., 2018; Yu et al., 2018). MitA, the selective inhibitor of SP1, is reported to inhibit colorectal cancer (Quarni et al., 2019; Li et al., 2020). Therefore, we speculate that the combination of MitA or other SP1 inhibitors and CPT-11 might achieve a startling effect of reducing the side effect and enhancing the anticancer efficacy simultaneously in the treatment of colorectal cancer.

In inflammatory conditions, we show in this study that TGR5 participates in the inhibition of NLRP3 inflammasome by BA *in vitro*, while *in vivo* TGR5 was significantly promoted by OA, but not affected by CPT-11 and MitA treatments. TGR5 is a metabolic regulator involved in glucose tolerance, energy expenditure, and inflammation (Holter et al., 2020). As a member of the G-protein-coupled receptor (GPCR) superfamily, TGR5 can be activated by BA and then elevate intracellular cAMP levels (Guo et al., 2016b; Keitel et al., 2019). Recently, there are studies reporting that TGR5 has an inhibitory effect on NLRP3. For instance, BA could lead to the phosphorylation of NLRP3 via the TGR5–cAMP–PKA axis, which serves as a critical brake on the NLRP3 inflammasome activation (Guo et al., 2016a). In another study, BA reduced the nuclear translocation of the nuclear factor (NF)-κB p65 and lowered the NF-κB transcriptional activity to depress NLRP3 inflammasome through the TGR5–cAMP pathway (Keitel and Häussinger, 2018). In addition, TGR5 has crucial protective functions in augmenting bile composition and cytokine release in cholestasis (Deutschmann et al., 2018; Willis et al., 2020). Moreover, TGR5 is proved to improve colitis by modulating the integrity of intestinal barrier and immune response (Cipriani et al., 2011; Biagioli and Carino, 2017; Sorrentino et al., 2020), indicating its potential in alleviating chemotherapy-induced intestinal toxicity as an intervening target.

In this study, we investigated the interaction between BA and TGR5 or SP1 in inflammatory or non-inflammatory conditions *in vitro*, respectively. Studies manifest that DCA is a more potent ligand of TGR5 than CDCA; it is therefore expected that DCA has a more propounding effect on both NLRP3 and IL-1β than CDCA. However, in our study, we observed that CDCA (50 μM) exhibited a stronger inhibitory effect on NLRP3 and IL-1β. In addition, our results showed that although DCA exhibited a more promotive effect on the transformation of SP1 into active p-SP1 than CDCA, it only more strongly promoted IL-1β but not NLRP3. We speculate that the

ultimate effect of BA on NLRP3 inflammasome is a converged result from the opposite actions of SP1 and TGR5 and potentially other mediators. Besides, since there is no clear borderline between inflammatory and non-inflammatory conditions, at what point BA switches its role from agonist to antagonist needs to be further explored.

In vivo, we proved that MitA and OA are effective against CPT-11-induced colitis. We assumed that the CPT-11-induced colitis is a chronic progress from inflammation initiation to recovery instead of a 100% inflammatory condition. The accumulation of BAs after CPT-11 administration in colon could promote the phosphorylation of SP1 and enhance the inflammation. As the inflammation progresses, BAs could promote the expression of TGR5 and relieve the inflammation reaction to some extent. Our data show that CPT-11 exposure leads to an increased expression of SP1 and p-SP1, while it has no significant effect on the level of TGR5. MitA significantly inhibited SP1 and p-SP1 and ameliorated inflammation, while OA inhibited NLRP3 inflammasome and ameliorated colitis through promoting TGR5. The results indicate that inflammatory and non-inflammatory mechanisms may co-exist in CPT-11-caused colitis.

We also explored whether the combination of MitA and OA was more effective. However, the mortality rate was as high as 70% in the MitA+OA group. MitA is an anticancer antibiotic and has been reported to be effective in various types of cancers, including colorectal cancer, testicular carcinoma, prostate cancer, etc. (Choi and Choi, 2018; Liu et al., 2018; Novakova et al., 2018; Quarni et al., 2019). In our pre-experiments, three different doses of MitA (0.05, 0.15, and 0.25 mg/kg) were administered, and body weight, diarrhea score, pathological changes, and inflammatory factors were recorded or determined. No obvious adverse effect of concern was observed (data not shown). OA belongs to the pentacyclic triterpene family, as a weak agonist of TGR5, and is known for its hepato-protective effect. It has also been reported that OA is effective in relieving dextran sodium sulfate-induced colitis (Kang et al., 2015; Sen, 2020). OA is generally recognized safe in a wide range of dosages to rats; for example, no obvious adverse effect was observed in rats receiving 120 mg/kg of OA for 9 weeks (Pollier and Goossens, 2012; Madlala et al., 2015). In this context, we think there might be two reasons for the unexpected, high mortality of the combination. One is the drug–drug interaction, which can cause changes in the drug concentration in local tissues and alter drug effect or toxicity (Gessner et al., 2019). The other is intervening SP1 and TGR5 at the same time probably over-regulated the NLRP3 inflammasome and caused unknown fatal side effects. Further experiments are needed to explore the actual mechanisms.

In conclusion, we demonstrated that *in vitro* BA could activate NLRP3 inflammasome in non-inflammatory conditions mediated by SP1 and inhibit NLRP3 inflammasome in inflammatory conditions via TGR5. Treating rats receiving CPT-11 with MitA to inhibit SP1 or OA to activate TGR5 can alleviate the colitis. Our findings may shed lights on the discovery of effective interventions for reducing chemotherapy-induced colitis.

DATA AVAILABILITY STATEMENT

The original contributions presented in the study are included in the article/**Supplementary Material**, further inquiries can be directed to the corresponding authors.

ETHICS STATEMENT

The animal study was reviewed and approved by the Animal Ethics Committee of China Pharmaceutical University.

AUTHOR CONTRIBUTIONS

CL designed and performed the experiments, analyzed and interpreted the data, and wrote the manuscript. DW and SQ co-designed the experiments. YZ, JC, BT, and RX performed the animal experiments. FX and PZ designed the study, supervised the experiments, and edited the manuscript.

FUNDING

This work was supported by the NSFC (Nos. 82073812, 81773682, 81773861), the Jiangsu Provincial National Science Foundation for Distinguished Young Scholars (No. BK20180027), the National Science and Technology Major Project (2017ZX09101001), the Fundamental Research Funds for the Central Universities (2632021PY03), Double First-Class University project, the Program for Jiangsu province Innovative Research Team, and a project funded by the Priority Academic Program Development of Jiangsu Higher Education Institutions (PAPD).

ACKNOWLEDGMENTS

The authors would like to thank Meiyu Gao, Siqi Li, Qiwei Liu, and Shaoran Tang from China Pharmaceutical University (Nanjing, China) for their assistance in conducting the animal experiment.

SUPPLEMENTARY MATERIAL

The Supplementary Material for this article can be found online at: https://www.frontiersin.org/articles/10.3389/fphar.2022.677738/full#supplementary-material

REFERENCES

Andreyev, H. J. N., Lalji, A., Mohammed, K., Muls, A. C. G., Watkins, D., Rao, S., et al. (2021). The FOCCUS Study: a Prospective Evaluation of the Frequency, Severity and Treatable Causes of Gastrointestinal Symptoms during and after Chemotherapy. *Support Care Cancer* 29, 1443–1453. doi:10.1007/s00520-020-05610-x

Beishline, K., and Azizkhan-Clifford, J. (2015). Sp1 and the 'hallmarks of Cancer'. *Febs j* 282, 224–258. doi:10.1111/febs.13148

Biagioli, M., Carino, A., Cipriani, S., Francisci, D., Marchianò, S., Scarpelli, P., et al. (2017). The Bile Acid Receptor GPBAR1 Regulates the M1/M2 Phenotype of Intestinal Macrophages and Activation of GPBAR1 Rescues Mice from Murine Colitis. *J. Immunol.* 199, 718–733. doi:10.4049/jimmunol.1700183

Cao, R., Ma, Y., Li, S., Shen, D., Yang, S., Wang, X., et al. (2020). 1,25(OH)2 D3 Alleviates DSS-Induced Ulcerative Colitis via Inhibiting NLRP3 Inflammasome Activation. *J. Leukoc. Biol.* 108, 283–295. doi:10.1002/JLB.3MA0320-406RR

Chávez-Talavera, O., Tailleux, A., Lefebvre, P., and Staels, B. (2017). Bile Acid Control of Metabolism and Inflammation in Obesity, Type 2 Diabetes, Dyslipidemia, and Nonalcoholic Fatty Liver Disease. *Gastroenterology* 152, 1679–e3. e1673. doi:10.1053/j.gastro.2017.01.055

Chen, X., Zeng, K., Xu, M., Hu, X., Liu, X., Xu, T., et al. (2018). SP1-induced lncRNA-ZFAS1 Contributes to Colorectal Cancer Progression via the miR-150-5p/VEGFA axis. *Cell Death Dis* 9, 982. doi:10.1038/s41419-018-0962-6

Chiang, J. Y. (2013). Bile Acid Metabolism and Signaling. *Compr. Physiol.* 3, 1191–1212. doi:10.1002/cphy.c120023

Choi, M. C., and Choi, W. H. (2018). Mithramycin A Alleviates Osteoarthritic Cartilage Destruction by Inhibiting HIF-2α Expression. *Int. J. Mol. Sci.* 19, 1411. doi:10.3390/ijms19051411

Cipriani, S., Mencarelli, A., Chini, M. G., Distrutti, E., Renga, B., Bifulco, G., et al. (2011). The Bile Acid Receptor GPBAR-1 (TGR5) Modulates Integrity of Intestinal Barrier and Immune Response to Experimental Colitis. *PLoS One* 6, e25637. doi:10.1371/journal.pone.0025637

Deutschmann, K., Reich, M., Klindt, C., Dröge, C., Spomer, L., Häussinger, D., et al. (2018). Bile Acid Receptors in the Biliary Tree: TGR5 in Physiology and Disease. *Biochim. Biophys. Acta Mol. Basis Dis.* 1864, 1319–1325. doi:10.1016/j.bbadis.2017.08.021

Fang, Z. Z., Zhang, D., Cao, Y. F., Xie, C., Lu, D., Sun, D. X., et al. (2016). Irinotecan (CPT-11)-Induced Elevation of Bile Acids Potentiates Suppression of IL-10 Expression. *Toxicol. Appl. Pharmacol.* 291, 21–27. doi:10.1016/j.taap.2015.12.003

Fitzpatrick, L. R., and Jenabzadeh, P. (2020). IBD and Bile Acid Absorption: Focus on Pre-clinical and Clinical Observations. *Front. Physiol.* 11, 564. doi:10.3389/fphys.2020.00564

Gessner, A., König, J., and Fromm, M. F. (2019). Clinical Aspects of Transporter-Mediated Drug-Drug Interactions. *Clin. Pharmacol. Ther.* 105, 1386–1394. doi:10.1002/cpt.1360

Gong, Z., Zhao, S., Zhou, J., Yan, J., Wang, L., Du, X., et al. (2018). Curcumin Alleviates DSS-Induced Colitis via Inhibiting NLRP3 Inflammsome Activation and IL-1β Production. *Mol. Immunol.* 104, 11–19. doi:10.1016/j.molimm.2018.09.004

Gong, Z., Zhou, J., Zhao, S., Tian, C., Wang, P., Xu, C., et al. (2016). Chenodeoxycholic Acid Activates NLRP3 Inflammasome and Contributes to Cholestatic Liver Fibrosis. *Oncotarget* 7, 83951–83963. doi:10.18632/oncotarget.13796

González-Rubio, S., López-Sánchez, L., Muñoz-Castañeda, J., Linares, C. I., Aguilar-Melero, P., Rodríguez-Perálvarez, M., et al. (2015). GCDCA Down-Regulates Gene Expression by Increasing Sp1 Binding to the NOS-3 Promoter in an Oxidative Stress Dependent Manner. *Biochem. Pharmacol.* 96, 39–51. doi:10.1016/j.bcp.2015.04.017

Guo, C., Chen, W. D., and Wang, Y. D. (2016b). TGR5, Not Only a Metabolic Regulator. *Front. Physiol.* 7, 646. doi:10.3389/fphys.2016.00646

Guo, C., Xie, S., Chi, Z., Zhang, J., Liu, Y., Zhang, L., et al. (2016a). Bile Acids Control Inflammation and Metabolic Disorder through Inhibition of NLRP3 Inflammasome. *Immunity* 45, 802–816. doi:10.1016/j.immuni.2016.09.008

Hao, H., Cao, L., Jiang, C., Che, Y., Zhang, S., Takahashi, S., et al. (2017). Farnesoid X Receptor Regulation of the NLRP3 Inflammasome Underlies Cholestasis-Associated Sepsis. *Cell Metab* 25, 856–e5. e855. doi:10.1016/j.cmet.2017.03.007

Higuchi, H., Grambihler, A., Canbay, A., Bronk, S. F., and Gores, G. J. (2004). Bile Acids Up-Regulate Death Receptor 5/TRAIL-Receptor 2 Expression via a C-Jun N-Terminal Kinase-dependent Pathway Involving Sp1. *J. Biol. Chem.* 279, 51–60. doi:10.1074/jbc.M309476200

Holter, M. M., Chirikjian, M. K., Govani, V. N., and Cummings, B. P. (2020). TGR5 Signaling in Hepatic Metabolic Health. *Nutrients* 12, 2598. doi:10.3390/nu12092598

Hou, R. G., Fan, L., Liu, J. J., Cheng, Y., Chang, Z. P., Wu, B., et al. (2018). Bile Acid Malabsorption Is Associated with Diarrhea in Acute Phase of Colitis. *Can. J. Physiol. Pharmacol.* 96, 1328–1336. doi:10.1139/cjpp-2018-0017

Huang, H., Wang, X., Zhang, X., Zhang, G., Jinbo, M., Wang, H., et al. (2020). Ganciclovir Reduces Irinotecan-Induced Intestinal Toxicity by Inhibiting NLRP3 Activation. *Cancer Chemother. Pharmacol.* 85, 195–204. doi:10.1007/s00280-019-03996-y

Kang, G. D., Lim, S., and Kim, D. H. (2015). Oleanolic Acid Ameliorates Dextran Sodium Sulfate-Induced Colitis in Mice by Restoring the Balance of Th17/Treg Cells and Inhibiting NF-κB Signaling Pathway. *Int. Immunopharmacol* 29, 393–400. doi:10.1016/j.intimp.2015.10.024

Keitel, V., and Häussinger, D. (2018). Role of TGR5 (GPBAR1) in Liver Disease. *Semin. Liver Dis.* 38, 333–339. doi:10.1055/s-0038-1669940

Keitel, V., Stindt, J., and Häussinger, D. (2019). Bile Acid-Activated Receptors: GPBAR1 (TGR5) and Other G Protein-Coupled Receptors. *Handb Exp. Pharmacol.* 256, 19–49. doi:10.1007/164_2019_230

Khan-Malek, R., and Wang, Y. (2017). Statistical Analysis of Quantitative RT-PCR Results. *Methods Mol. Biol.* 1641, 281–296. doi:10.1007/978-1-4939-7172-5_15

Kuijk, L. M., Mandey, S. H., Schellens, I., Waterham, H. R., Rijkers, G. T., Coffer, P. J., et al. (2008). Statin Synergizes with LPS to Induce IL-1beta Release by THP-1 Cells through Activation of Caspase-1. *Mol. Immunol.* 45, 2158–2165. doi:10.1016/j.molimm.2007.12.008

Kurita, A., Kado, S., Kaneda, N., Onoue, M., Hashimoto, S., and Yokokura, T. (2000). Modified Irinotecan Hydrochloride (CPT-11) Administration Schedule Improves Induction of Delayed-Onset Diarrhea in Rats. *Cancer Chemother. Pharmacol.* 46, 211–220. doi:10.1007/s002800000151

Li, J., Peng, W., Yang, P., Chen, R., Gu, Q., Qian, W., et al. (2020). MicroRNA-1224-5p Inhibits Metastasis and Epithelial-Mesenchymal Transition in Colorectal Cancer by Targeting SP1-Mediated NF-κB Signaling Pathways. *Front. Oncol.* 10, 294. doi:10.3389/fonc.2020.00294

Li, Q., Zhang, X., Wang, W., Li, L., Xu, Q., Wu, X., et al. (2015). CPT-11 Activates NLRP3 Inflammasome through JNK and NF-κB Signalings. *Toxicol. Appl. Pharmacol.* 289, 133–141. doi:10.1016/j.taap.2015.09.025

Lian, Q., Xu, J., Yan, S., Huang, M., Ding, H., Sun, X., et al. (2017). Chemotherapy-induced Intestinal Inflammatory Responses Are Mediated by Exosome Secretion of Double-Strand DNA via AIM2 Inflammasome Activation. *Cell Res* 27 (6), 784–800. doi:10.1038/cr.2017.54

Liu, R., Zhi, X., Zhou, Z., Zhang, H., Yang, R., Zou, T., et al. (2018). Mithramycin A Suppresses Basal Triple-Negative Breast Cancer Cell Survival Partially via Down-Regulating Krüppel-like Factor 5 Transcription by Sp1. *Sci. Rep.* 8, 1138. doi:10.1038/s41598-018-19489-6

Madlala, H. P., Van Heerden, F. R., Mubagwa, K., and Musabayane, C. T. (2015). Changes in Renal Function and Oxidative Status Associated with the Hypotensive Effects of Oleanolic Acid and Related Synthetic Derivatives in Experimental Animals. *PLoS One* 10, e0128192. doi:10.1371/journal.pone.0128192

Masyuk, T. V., Masyuk, A. I., Lorenzo Pisarello, M., Howard, B. N., Huang, B. Q., Lee, P. Y., et al. (2017). TGR5 Contributes to Hepatic Cystogenesis in Rodents with Polycystic Liver Diseases through Cyclic Adenosine monophosphate/Gαs Signaling. *Hepatology* 66 (4), 1197–1218. doi:10.1002/hep.29284

McGlone, E. R., and Bloom, S. R. (2019). Bile Acids and the Metabolic Syndrome. *Ann. Clin. Biochem.* 56 (3), 326–337. doi:10.1177/0004563218817798

Mego, M., Chovanec, J., Vochyanova-Andrezalova, I., Konkolovsky, P., Mikulova, M., Reckova, M., et al. (2015). Prevention of Irinotecan Induced Diarrhea by Probiotics: A Randomized Double Blind, Placebo Controlled Pilot Study. *Complement. Ther. Med.* 23, 356–362. doi:10.1016/j.ctim.2015.03.008

Muls, A. C., Lalji, A., Marshall, C., Butler, L., Shaw, C., Vyoral, S., et al. (2016). The Holistic Management of Consequences of Cancer Treatment by a Gastrointestinal and Nutrition Team: a Financially Viable Approach to an Enormous Problem? *Clin. Med. (Lond)* 16, 240–246. doi:10.7861/clinmedicine.16-3-240

Novakova, R., Núñez, L. E., Homerova, D., Knirschova, R., Feckova, L., Rezuchova, B., et al. (2018). Increased Heterologous Production of the Antitumoral

Polyketide Mithramycin A by Engineered Streptomyces Lividans TK24 Strains. *Appl. Microbiol. Biotechnol.* 102, 857–869. doi:10.1007/s00253-017-8642-5

Pollier, J., and Goossens, A. (2012). Oleanolic Acid. *Phytochemistry* 77, 10–15. doi:10.1016/j.phytochem.2011.12.022

Quarni, W., Dutta, R., Green, R., Katiri, S., Patel, B., Mohapatra, S. S., et al. (2019). Mithramycin A Inhibits Colorectal Cancer Growth by Targeting Cancer Stem Cells. *Sci. Rep.* 9, 15202. doi:10.1038/s41598-019-50917-3

Sandmeier, D., Chaubert, P., and Bouzourene, H. (2005). Irinotecan-induced Colitis. *Int. J. Surg. Pathol.* 13, 215–218. doi:10.1177/106689690501300215

Sears, S., Mcnally, P., Bachinski, M. S., and Avery, R. (1999). Irinotecan (CPT-11) Induced Colitis: Report of a Case and Review of Food and Drug Administration MEDWATCH Reporting. *Gastrointest. Endosc.* 50, 841–844. doi:10.1016/s0016-5107(99)70171-9

Sen, A. (2020). Prophylactic and Therapeutic Roles of Oleanolic Acid and its Derivatives in Several Diseases. *World J. Clin. Cases* 8, 1767–1792. doi:10.12998/wjcc.v8.i10.1767

Seznec, J., Silkenstedt, B., and Naumann, U. (2011). Therapeutic Effects of the Sp1 Inhibitor Mithramycin A in Glioblastoma. *J. Neurooncol.* 101, 365–377. doi:10.1007/s11060-010-0266-x

Shao, B. Z., Wang, S. L., Pan, P., Yao, J., Wu, K., Li, Z. S., et al. (2019). Targeting NLRP3 Inflammasome in Inflammatory Bowel Disease: Putting Out the Fire of Inflammation. *Inflammation* 42, 1147–1159. doi:10.1007/s10753-019-01008-y

Sinha, S. R., Haileselassie, Y., Nguyen, L. P., Tropini, C., Wang, M., Becker, L. S., et al. (2020). Dysbiosis-Induced Secondary Bile Acid Deficiency Promotes Intestinal Inflammation. *Cell Host Microbe* 27, 659–e5. e655. doi:10.1016/j.chom.2020.01.021

Sorrentino, G., Perino, A., Yildiz, E., El Alam, G., Bou Sleiman, M., Gioiello, A., et al. (2020). Bile Acids Signal via TGR5 to Activate Intestinal Stem Cells and Epithelial Regeneration. *Gastroenterology* 159, 956–e8. e958. doi:10.1053/j.gastro.2020.05.067

Trifan, O. C., Durham, W. F., Salazar, V. S., Horton, J., Levine, B. D., Zweifel, B. S., et al. (2002). Cyclooxygenase-2 Inhibition with Celecoxib Enhances Antitumor Efficacy and Reduces Diarrhea Side Effect of CPT-11. *Cancer Res.* 62, 5778–5784.

Vellingiri, B., Iyer, M., Devi Subramaniam, M., Jayaramayya, K., Siama, Z., Giridharan, B., et al. (2020). Understanding the Role of the Transcription Factor Sp1 in Ovarian Cancer: from Theory to Practice. *Int. J. Mol. Sci.* 21, 1153. doi:10.3390/ijms21031153

Vijayvargiya, P., and Camilleri, M. (2019). Current Practice in the Diagnosis of Bile Acid Diarrhea. *Gastroenterology* 156, 1233–1238. doi:10.1053/j.gastro.2018.11.069

Vítek, L. (2015). Bile Acid Malabsorption in Inflammatory Bowel Disease. *Inflamm. Bowel Dis.* 21, 476–483. doi:10.1097/MIB.0000000000000193

Vizcaíno, C., Mansilla, S., and Portugal, J. (2015). Sp1 Transcription Factor: A Long-Standing Target in Cancer Chemotherapy. *Pharmacol. Ther.* 152, 111–124. doi:10.1016/J.pharmthera.2015.05.008

Wahlström, A., Sayin, S. I., Marschall, H. U., and Bäckhed, F. (2016). Intestinal Crosstalk between Bile Acids and Microbiota and its Impact on Host Metabolism. *Cel Metab* 24, 41–50. doi:10.1016/j.cmet.2016.05.005

Wang, J., Fan, H., Wang, Y., Wang, X., Zhang, P., Chen, J., et al. (2015). Metabolomic Study of Chinese Medicine Huang Qin Decoction as an Effective Treatment for Irinotecan-Induced Gastrointestinal Toxicity. *RSC Adv.* 5, 26420–26429. doi:10.1039/c5ra02581h

Wang, L., Wang, R., Wei, G. Y., Zhang, R. P., Zhu, Y., Wang, Z., et al. (2020). Cryptotanshinone Alleviates Chemotherapy-Induced Colitis in Mice with colon Cancer via Regulating Fecal-Bacteria-Related Lipid Metabolism. *Pharmacol. Res.* 163, 105232. doi:10.1016/j.phrs.2020.105232

Wei, C., Zhang, W., Zhou, Q., Zhao, C., Du, Y., Yan, Q., et al. (2016). Mithramycin A Alleviates Cognitive Deficits and Reduces Neuropathology in a Transgenic Mouse Model of Alzheimer's Disease. *Neurochem. Res.* 41, 1924–1938. doi:10.1007/s11064-016-1903-3

Willis, K. A., Gomes, C. K., Rao, P., Micic, D., Moran, E. R., Stephenson, E., et al. (2020). TGR5 Signaling Mitigates Parenteral Nutrition-Associated Liver Disease. *Am. J. Physiol. Gastrointest. Liver Physiol.* 318, G322–g335. doi:10.1152/ajpgi.00216.2019

Yu, Y., Peng, K., Li, H., Zhuang, R., Wang, Y., Li, W., et al. (2018). SP1 Upregulated FoxO3a Promotes Tumor Progression in Colorectal Cancer. *Oncol. Rep.* 39, 2235–2242. doi:10.3892/or.2018.6323

Zhao, D., Jiang, Y., Sun, J., Li, H., Huang, M., Sun, X., et al. (2019). Elucidation of the Anti-Inflammatory Effect of Vanillin in Lps-Activated THP-1 Cells. *J. Food Sci.* 84, 1920–1928. doi:10.1111/1750-3841.14693

Zhao, S., Gong, Z., Zhou, J., Tian, C., Gao, Y., Xu, C., et al. (2016). Deoxycholic Acid Triggers NLRP3 Inflammasome Activation and Aggravates DSS-Induced Colitis in Mice. *Front. Immunol.* 7, 536. doi:10.3389/fimmu.2016.00536

Zhao, S., Gong, Z., Du, X., Tian, C., Wang, L., Zhou, J., et al. (2018). Deoxycholic Acid-Mediated Sphingosine-1-Phosphate Receptor 2 Signaling Exacerbates DSS-Induced Colitis through Promoting Cathepsin B Release. *J. Immunol. Res.* 2018, 2481418. doi:10.1155/2018/2481418

Zhao, W., Ma, L., Cai, C., and Gong, X. (2019). Caffeine Inhibits NLRP3 Inflammasome Activation by Suppressing MAPK/NF-κB and A2aR Signaling in LPS-Induced THP-1 Macrophages. *Int. J. Biol. Sci.* 15, 1571–1581. doi:10.7150/ijbs.34211

Zhou, X., Cao, L., Jiang, C., Xie, Y., Cheng, X., Krausz, K. W., et al. (2014). PPARα-UGT axis Activation Represses Intestinal FXR-FGF15 Feedback Signalling and Exacerbates Experimental Colitis. *Nat. Commun.* 5, 4573. doi:10.1038/ncomms5573

Zou, M., Xi, L., Rao, J., Jing, Y., Liao, F., and Yang, X. (2017). Optimization and Evaluation of an Inflammatory Cell Model in LPS-Stimulated PMA-Differentiated THP-1 Cells. *Xi Bao Yu Fen Zi Mian Yi Xue Za Zhi* 33, 1456–1461.

Conflict of Interest: The authors declare that the research was conducted in the absence of any commercial or financial relationships that could be construed as a potential conflict of interest.

Publisher's Note: All claims expressed in this article are solely those of the authors and do not necessarily represent those of their affiliated organizations, or those of the publisher, the editors, and the reviewers. Any product that may be evaluated in this article, or claim that may be made by its manufacturer, is not guaranteed or endorsed by the publisher.

Copyright © 2022 Liao, Wang, Qin, Zhang, Chen, Xu, Xu and Zhang. This is an open-access article distributed under the terms of the Creative Commons Attribution License (CC BY). The use, distribution or reproduction in other forums is permitted, provided the original author(s) and the copyright owner(s) are credited and that the original publication in this journal is cited, in accordance with accepted academic practice. No use, distribution or reproduction is permitted which does not comply with these terms.

Frontiers in Pharmacology

Explores the interactions between chemicals and living beings

The most cited journal in its field, which advances access to pharmacological discoveries to prevent and treat human disease.

Discover the latest Research Topics

See more →



Frontiers

Avenue du Tribunal-Fédéral 34
1005 Lausanne, Switzerland
frontiersin.org

Contact us

+41 (0)21 510 17 00
frontiersin.org/about/contact